Part B: Publications

This part contains full versions of the 14 publications which comprise the main scientific work. They are arranged according to thematic considerations, and peer-reviewed articles are marked by *****. A complete list of publications by the author is given on his website: http://www.geo.uzh.ch/~mzemp/

P01* **Zemp, M.**, Armstrong, R., Gärtner-Roer, I., Haeberli, W., Hoelzle, M., Kääb, A., Kargel, J.S., Singh Khalsa S.J., Paul, F. & Raup, B. (accepted). Chapter 1: **Global glacier monitoring - a long-term task integrating in-situ observations and remote sensing.** In: Kargel, J.S., Bishop, M.P., Kääb, A. & Raup, B.H. (eds.): Global Land Ice Measurements from Space. Satellite mulitspectral imaging of glaciers. Praxis-Spring.

P02 WGMS (2008b). **Fluctuations of Glaciers 2000-2005** (Vol. IX). Haeberli, W., **Zemp**, **M.**, Kääb, A., Paul, F. & Hoelzle, M. (eds.), ICSU (FAGS) / IUGG (IACS) / UNEP / UNESCO / WMO, World Glacier Monitoring Service, Zurich, Switzerland, 266 pp.

P03 WGMS (2009). **Glacier Mass Balance Bulletin No. 10 (2006–2007)**. Haeberli, W., Gärtner-Roer, I., Hoelzle, M., Paul, F. & **Zemp, M.** (eds.), ICSU(WDS)/IUGG(IACS)/UNEP/UNESCO/WMO, World Glacier Monitoring Service, Zurich, Switzerland, 96 pp.

P04* **Zemp, M.**, Zumbühl, H.J., Nussbaumer, S.U., Masiokas, M.H., Espizua, L.E. and Pitte, P. (subm.). **Extending glacier monitoring into the Little Ice Age and beyond.** PAGES news, 19(2).

P05* Cogley, J.G., Hock, R., Rasmussen, L.A., Arendt, A.A., Bauder, A., Braithwaite, R.J., Jansson, P., Kaser, G., Möller, M., Nicholson, L. & **Zemp, M.** (2011). **Glossary of Glacier Mass Balance and Related Terms**. IHP-VII Technical Documents in Hydrology No. 86, IACS Contribution No. 2, UNESCO-IHP, Paris.

P06* Paul, F., Barry, R.G., Gogley, J.G., Frey, H., Haeberli, W., Ohmura, A., Ommanney, S.C.L., Raup, B., Rivera, A. & **Zemp, M.** (2009). **Recommendations for the compilation of glacier inventory data from digital sources.** Annals of Glaciology, 50(53), 119-126.

P07* Koblet, T, Gärtner-Roer, I., **Zemp, M.**, Jansson, P., Thee, P., Haeberli, W. & Holmlund, P. (2010). **Re-analysis of multi-temporal aerial images of Storglaciären, Sweden (1959-99) - Part 1: Determination of length, area, and volume changes.** The Cryosphere, 4, 333-343.

P08* **Zemp, M.**, Jansson, P., Holmlund, P., Gärtner-Roer, I., Koblet, T., Thee, P. & Haeberli, W. (2010). **Re-analysis of multi-temporal aerial images of Storglaciären, Sweden (1959-99) - Part 2: Comparison of glaciological and volumetric mass balances.** The Cryosphere, 4, 345-357.

P09* **Zemp, M.**, Paul, F., Hoelzle, M. & Haeberli, W. (2008), **Glacier fluctuations in the European Alps 1850–2000: an overview and spatio-temporal analysis of available data.** In: Orlove, B., Wiegandt, E. & Luckman, B. (eds.): The darkening peaks: Glacial retreat in scientific and social context. University of California Press, 152-167.

P10* **Zemp, M.**, Hoelzle, M. & Haeberli, W. (2007). **Distributed modeling of the regional climatic equilibrium line altitude of glaciers in the European Alps.** Global and Planetary Change, 56, 83-100, doi:10.1016/j.gloplacha.2006.07.002.

P11* **Zemp, M.**, Haeberli, W., Hoelzle, M. & Paul, F. (2006). **Alpine glaciers to disappear within decades?** Geophysical Research Letters, 33, L13504, doi:10.1029/2006GL026319.

P12 **Zemp, M.**, Andreassen, L.M., Braun, L., Chueca, J., Fischer, A., Hagen, J.O., Hoelzle, M., Jansson, P., Kohler, J., Meneghel, M., Stastny, P. & Vincent, C. (2010). **Glacier and Ice Caps**. In: Voigt, T., Füssel, H.-M., Gärtner-Roer, I., Huggel, C., Marty, C. & **Zemp, M.** (eds.). **Impacts of climate change on snow, ice, and permafrost in Europe: Observed trends, future projections, and socio-economic relevance.** European Topic Centre on Air and Climate Change, Technical Paper, 2010 (13), 46-65.

P13* WGMS (2008a). **Global Glacier Changes: facts and figures. Zemp, M.**, Roer, I., Kääb, A., Hoelzle, M., Paul, F. & Haeberli, W. (eds.), UNEP, World Glacier Monitoring Service, Zurich, Switzerland: 88 pp.

P14* **Zemp, M.**, Hoelzle, M. & Haeberli, W. (2009). **Six decades of glacier mass balance observations - a review of the worldwide monitoring network.** Annals of Glaciology, 50(50), 101-111.

Publication 1

Zemp, M., Armstrong, R., Gärtner-Roer, I., Haeberli, W., Hoelzle, M., Kääb, A., Kargel, J.S., Singh Khalsa S.J., Paul, F. & Raup, B. (accepted). Chapter 1: **Global glacier monitoring - a long-term task integrating in-situ observations and remote sensing.** In: Kargel, J.S., Bishop, M.P., Kääb, A. & Raup, B.H. (eds.): Global Land Ice Measurements from Space. Satellite mulitspectral imaging of glaciers. Praxis-Spring.

Introduction

Chapter 1: Global Glacier Monitoring – a long-term task integrating in-situ observations and remote sensing

Michael Zemp[1], Richard Armstrong[2], Isabelle Gärtner-Roer[1], Wilfried Haeberli[1], Martin Hoelzle[3], Andreas Kääb[4], Jeff Kargel[5], Siri Jodha Singh Khalsa[2], Frank Paul[1], and Bruce Raup[2]

[1] *World Glacier Monitoring Service, University of Zurich, Zurich, Switzerland*
[2] *National Snow and Ice Data Center, University of Colorado, Boulder, U.S.A.*
[3] *World Glacier Monitoring Service, University of Fribourg, Fribourg, Switzerland*
[4] *Global Land Ice Measurements from Space, University of Oslo, Oslo, Norway*
[5] *Global Land Ice Measurements from Space, University of Arizona, Tucson, U.S.A.*

Glaciers are among the most fascinating elements of nature, an important freshwater resource but also an important contributor to the present sea level rise and a potential cause of serious natural hazards. Because they are close to the melting point and react strongly to small changes in climate, glaciers provide some of the clearest evidence of climate change and constitute key variables for early-detection strategies in global climate-related observations (GCOS 2004).

In this introductory chapter to the GLIMS book, we aim at providing the reader with the relevant background information needed to understand the integration of GLIMS within the framework of the international glacier monitoring and the context of the regional glacier studies presented in this book. This chapter starts with the general definitions and the global coverage of perennial surface-ice on land, followed by a section on the relation between glaciers and climate which covers issues of glacier formation and then reaction to a climatic change. A brief overview on the history of the internationally coordinated glacier monitoring and an overlook on the global monitoring strategy for glaciers and ice caps then lead to a summary of the available data and a discussion of the challenges for the 21st century. Furthermore, the chapter introduces potentials and challenges of satellite remote sensing for glacier monitoring and emphasizes the importance of integrative change assessments. Finally, a synopsis and the organization of the book are provided as well as some concluding remarks on worldwide glacier monitoring.

1 Perennial surface-ice on land

1.1 Definitions

The cryosphere consists of snow, river and lake ice, sea ice, glaciers and ice caps, ice shelves and ice sheets, and frozen ground (IPCC 2007). The different cryospheric components can be categorised as seasonal and perennial ice, or as ice in the sea, in rivers and lakes, in the ground and on land (e.g. UNEP 2007). Talking about perennial surface-ice on land, one usually differentiates glaciers and ice caps from ice sheets and ice shelves (cf. IPCC 2007, UNEP 2007):

Ice sheet: a mass of land ice, of continental size, thick enough to cover the underlying bedrock topography. Its shape is mainly determined by the dynamics of its outward flow. There are only two ice sheets in the modern world, on Greenland and Antarctica; during glacial periods there were others.

Ice shelf: a thick, floating slab of freshwater ice extending from the coast (originating as land ice). Nearly all present ice shelves are found in Antarctica.

Glacier: a mass of surface-ice on land which flows downhill under gravity and is constrained by internal stress and friction at the base and sides. In general, a glacier is formed and maintained by accumulation of snow at high altitudes, balanced by melting at low altitudes or calving into the sea or lakes.

Ice cap: dome-shaped ice mass with radial flow, usually completely covering surface topography. Much smaller than an ice sheet.

In the context of glaciers and ice caps as an essential climate variable (ECV), the term ‘glacier’ is used as a synonym for several glacier types, such as ice fields, valley and mountain glaciers, and glacierets. These general definitions have been extended to more specific classifications that serve the requirements of the corresponding applications and should also be understood and referenced in that context (e.g. Cogley et al. in prep.).

Standards and guidelines for the compilation of an inventory of perennial surface ice on land from aerial photographs, maps and early satellite images, including such detailed classification schemes, have been defined for the compilation of the World Glacier Inventory (WGI; WGMS 1989) and can be found in UNESCO (1970; 1970/73), Müller et al. (1977), Müller (1978), and Scherler (1983). These standards for the classification of glaciers are used also for in-situ fluctuation series (e.g. front variation and mass balance measurements; cf. WGMS 2007, 2008b and earlier issues) and have been revised and updated for satellite based inventories within GLIMS (Rau et al. (2005), Raup and Khalsa (2006)).

1.2 Global coverage

Perennial surface-ice on land presently covers some 10% (or $16x10^6$ km^2) of the earth's land surface and about three times this amount during the ice ages (Paterson 1994, Benn and Evans 1998). An overview on area, volume and sea level equivalent of ice sheets, ice shelves, glaciers and ice caps are given in Table 1, based on IPCC (2007). Glaciers and ice caps, excluding the ones adjacent to the ice sheets of Greenland and Antarctica, cover an estimated area between $0.51x10^6$ km^2 (Ohmura 2004) and $0.54x10^6$ km^2 (Dyurgerov and Meier 2005). Both estimates are mainly based on the WGI (WGMS 1989). If all land ice melted away, sea level would rise by about 64 m, with the Antarctic Ice Sheet contributing 57 m, the Greenland Ice Sheet about 7 m and all other glaciers and ice caps with a few hundred millimetres.

Cryospheric component	Area (10^6 km^2)	Volume (10^6 km^3)	Potential sea level rise (m)
Ice sheets	14.0	27.6	63.7
Ice shelves	1.5	0.7	~0
Glaciers and ice caps	0.51-0.54	0.05-0.13	0.15-0.37

Table 1: Area, volume and sea level equivalent of perennial surface-ice on land components, as published by IPCC (2007). The data for the ice sheet in Greenland come from Bamber et al. (2001), the numbers for the ice sheet in Antarctica and the ice shelves are published by Lythe et al. (2001). The minimum and maximum estimates for glaciers and ice caps are from Ohmura (2004) and Dyurgerov and Meier (2005), respectively, which are both mainly based on the WGI (WGMS 1989), excluding glaciers and ice caps surrounding Greenland and Antarctica.

There are fundamental differences in time-scales and processes involved between the different components of the perennial surface-ice on land. Due to the large volumes and areas, the two continental ice sheets actively influence the global climate over time-scales of months to millennia. Glaciers and ice caps, with their much smaller volumes and areas, react much faster to climatic effects (i.e., time-scales range between months and centuries). They are good indicators of climate change, influencing ecosystems and human activities on a local to regional scale. As the focus of the present book is on glaciers and ice caps, we will concentrate on these two components of land ice below. Furthermore, the term 'glacier' is used in sections 1.2–1.6 to represent both features, since the same measurement principles are applicable. Good overviews on the state of the art concerning ice sheets and ice shelves can be found in Bentley et al. (2007) and in IPCC (2007).

2 Glaciers and climate

2.1 Formation

Glaciers form where snow deposited during the cold/humid season does not entirely melt during warm/dry times. This seasonal snow gradually densifies under the weight of the overlying layers and transforms into perennial firn and finally, after the interconnecting air passages between the grains are closed off, into ice (Paterson 1994). The ice from such accumulation areas then flows under the influence of its own weight and the local slopes down to lower altitudes, where it melts again (ablation areas). Accumulation and ablation areas are separated by the equilibrium line, where the balance between gain and loss in ice mass is exactly zero. Glacier distribution is thus primarily a function of mean annual air temperature and annual precipitation (Fig. 1), modified by the terrain which influences, for example, the amount of incoming solar radiation or the accumulation pattern.

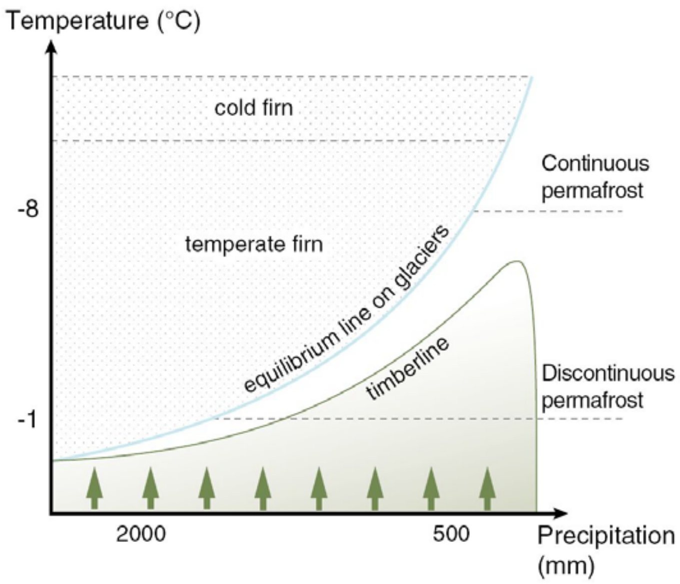

Figure 1. Schematic diagram of glacier, permafrost and forest limits as a function of mean annual air temperature and average annual precipitation. Forests verge on glaciers in humid-maritime climates and grow above permafrost in dry-continental areas. Source: Based on Shumsky (1964) and Haeberli and Burn (2002).

In humid-maritime regions, the equilibrium line is at (relatively low) altitude with warm temperatures and long melting seasons, because of the large amount of ablation required to eliminate thick snow layers (Shumskii 1964, Haeberli and Burn 2002). ‘Temperate’ glaciers with firn and ice at melting temperature dominate these landscapes. Such ice bodies, with relatively rapid flow, exhibit a high mass turnover and react strongly to atmospheric warming by enhanced melt and runoff. The glaciers and ice caps of Patagonia and Iceland, the western Cordillera of North America and in the mountains of New Zealand and Norway are of this type. The lower parts of such temperate glaciers may extend into forested valleys, where summer warmth and winter snow accumulation prevent development of permafrost. In contrast, under dry-continental conditions, such as in northern Alaska, arctic Canada, subarctic Russia, parts of the Andes near the Atacama desert, and in many central-Asian mountain chains, the equilibrium line is usually found at (relatively high) elevation with cold temperatures and short melting seasons. In such regions, glaciers lying far above tree line can contain – or even entirely consist of – cold firn/ice well below melting temperature, have a low mass turnover, and are often surrounded by permafrost (Shumskii 1964).

2.2 Reaction to climate change

The reaction of a glacier to a climatic change involves a complex chain of processes (Nye 1960, Meier 1984). Changes in atmospheric conditions (solar radiation, air temperature, precipitation, wind, cloudiness etc.) influence the mass and energy balance at the glacier surface (cf. Kuhn 1981, Oerlemans 2001). Air temperature thereby plays a predominant role as it is related to the radiation balance, turbulent heat exchange and solid/liquid precipitation. Over time periods of years and decades, changes in mass balance cause volume and thickness changes, which in turn affect the flow of ice via internal deformation and basal sliding. This dynamic reaction finally leads to glacier length changes, the advance or retreat of glacier tongues. In short, the glacier mass balance (i.e., the ‘vertical’ thickness change) is the direct and undelayed signal of annual atmospheric conditions, whereas the advance or retreat of glacier tongues (i.e., the ‘horizontal’ length change) constitutes an indirect, delayed and filtered but also enhanced and easily observed signal of climatic change (Haeberli 1998). The complication involved with the dynamic response disappears if the time interval analysed is sufficiently long, i.e., longer than it takes a glacier to complete its adjustment to a climatic change (Jóhannesson and others 1989, Haeberli and Hoelzle 1995). Over such extended time periods of several decades, cumulative length and mass change can be directly compared (Hoelzle et al. 2003). Exceptions to these rules include heavily debris-covered glaciers with reduced melting and strongly limited ‘retreat’, glaciers ending in deep water bodies causing enhanced melting and calving, and glaciers periodically undergoing mechanical instability and rapid advance (‘surge’) after extended periods of stagnation and recovery. Glaciers that are not influenced by these special problems are widely recognised to be among the best indicators within global climate related monitoring (IPCC 2001, 2007, GCOS 2004, 2006). They are converting a small change in climate, such as for example a temperature change of 0.1°C per decade over a longer time period, into a pronounced length change of several hundred metres or even of kilometres – a signal that is basically understandable by the general public (Fig. 2).

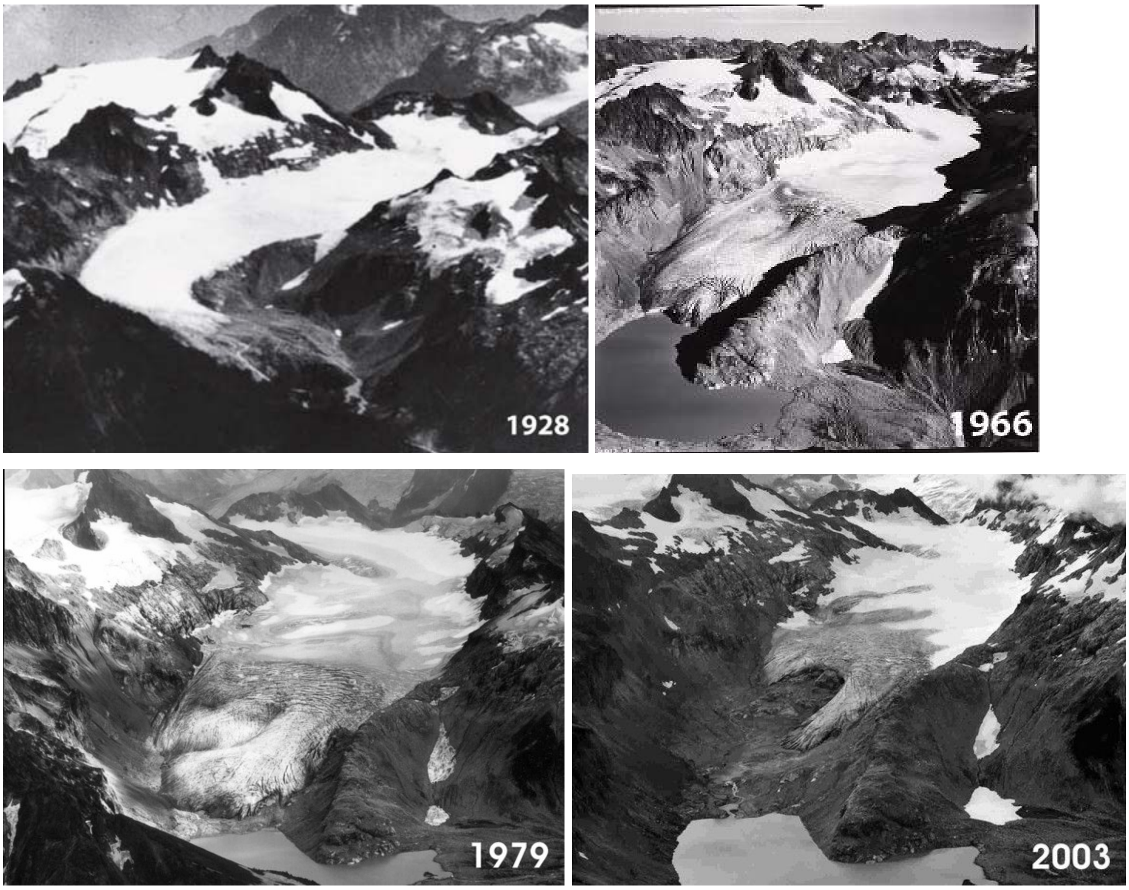

Figure 2. Retreat of South Cascade Glacier, USA: Photographic record of the shrinking of South Cascade Glacier in the North Cascade Mountains of Washington, US. Photos from the US Forest Service (1928) and the US Geological Survey (1966, 1979, 2003). Note the perennial snow banks at the lower right that are more or less unchanged since 1966.

3 International glacier monitoring

Throughout the history of modern science, glaciers have not only been a source of fascination but also a key element in discussions about Earth evolution and climate change. The discovery of the Ice Age in the late 18th and the 19th century significantly contributed to the understanding of the evolutionary development of the Earth; it also demonstrated the possibility of important climate changes involving dramatic environmental effects at global scale (Forel 1895). When systematic glacier observation began in the late 19th century, it was hoped that long-term glacier monitoring would give insight into processes of the formation of the Ice Ages (Agassiz 1840). Since then, the goals of the international glacier monitoring have evolved and multiplied (Haeberli 2004). Today, glaciers are recognized as key indicators of global climate change and as important contributors to global sea level rise, regional water cycle and local hazard situation.

3.1 History of the international glacier monitoring in the 19th and 20th century

Worldwide collection of information about ongoing glacier changes was initiated in 1894 with the foundation of the International Glacier Commission at the 6th International Geological Congress in Zurich, Switzerland. In the beginning, internationally coordinated glacier monitoring focused mainly on glacier fluctuations, i.e. with collection and publication of front variation data and, after the late 1940s, with glacier mass balance series (Haeberli 2007). Summaries of references to the historical data reports are given in Hoelzle et al. (2003) and WGMS (2008a). In the 1970s a world glacier inventory had been planned, resulting in the compilation of detailed and preliminary regional inventories that form a statistical basis for the geography of the world's glaciers (WGI; WGMS 1989). In 1986 the World Glacier Monitoring Service (WGMS; http://www.wgms.ch) started to maintain and continue the collection of standardised information about ongoing glacier changes, when the two former ICSI (International Commission on Snow and Ice) services PSFG (Permanent Service on the Fluctuations of Glaciers) and TTS/WGI (Temporal Technical Secretary for the World Glacier Inventory) were combined (Haeberli 2007). Today the WGMS is a service of the International Association of the Cryospheric Sciences (IACS) within the International Union of Geodesy and Geophysics (IUGG) and of the Federation of Astronomical and Geophysical Data Analysis Services (FAGS) of the International Council for Science (ICSU). It maintains a network of local investigators and national correspondents in all the countries involved in glacier monitoring.

3.2 The Global Terrestrial Network for Glaciers (GTN-G)

In close collaboration with the World Data Center for Glaciology (WDC-G), maintained at the US National Snow and Ice Data Center in Boulder (NSIDC) as well as with the Global Land Ice Measurements from Space (GLIMS) initiative, the WGMS has been in charge of the Global Terrestrial Network for Glaciers (GTN-G) within the Global Climate/Terrestrial Observing System (GCOS/GTOS, cf. Haeberli et al. 2000, Haeberli 2004) since its creation in 1998 (Haeberli et al. 2000). A recently established GTN-G Steering Committee coordinates, supports and advises the three operational bodies (i.e., WGMS, NSIDC, GLIMS) concerning the monitoring of glaciers. This Steering Committee consists of an Executive Board that is responsible for the development and the implementation of the monitoring strategy as well as for the coordination of the operational work, and an Advisory Board under the lead of the IACS/IUGG that is to support, consult, and periodically evaluate the work of the Executive Board and its three bodies.

GTN-G aims at combining (a) in-situ observations with remotely sensed data, (b) process understanding with global coverage, and (c) traditional measurements with new technologies by using an integrated and multi-level strategy (Haeberli 1998, 2004). With this strategy, GTN-G is designed to provide quantitative, comprehensive and easily understandable information in connection with questions about process understanding, change detection, model validation and environmental impacts in an interdisciplinary knowledge transfer to the scientific community as well as to policymakers, the media and the public. A Global Hierarchical Observing Strategy (GHOST) was developed to bridge the gap in scale, logistics and resolution between detailed process studies at a few selected sites and global coverage at pixel resolution using techniques of remote sensing and geo-informatics.

The GTN-G multi-level monitoring strategy following GHOST includes the following main steps or 'tiers':

Tier 1: Multi-component system observation across environmental gradients
The first level of this strategy is a conceptual one that stresses the importance of establishing the multi-component glacier observation system across environmental gradients with primary emphasis on spatial diversity at large (continental) scales or along elevation belts of high-mountain areas. Special attention should be given to long-term measurements. These are to be complemented by new observation series in order to cover large-scale transects such as the American Cordilleras or a profile from the Pyrenees through the Alps and Scandinavia to Svalbard.

Tier 2: Extensive glacier mass balance and flow studies within major climatic zones for improved process understanding and calibration of numerical models
Full parameterisation of coupled numerical energy/mass balance and flow models is based on detailed observations for improved process understanding, sensitivity experiments and extrapolation to regions with less comprehensive measurements. Ideally, sites should be located near the centre of the range of environmental conditions of the zone which they are representing. The actual locations will depend more on existing infrastructure and logistical feasibility rather than on strict spatial guidelines, but there is a need to capture a broad range of climatic zones (such as tropical, subtropical, monsoon-type, mid-latitude maritime/continental, subpolar, polar).

Tier 3: Determination of regional glacier volume change within major mountain systems using cost-saving methodologies
There are numerous sites that reflect regional patterns of glacier mass change within major mountain systems, but they are not optimally distributed. Observations with a limited number of strategically selected index stakes (annual time resolution) combined with precision mapping at about decadal intervals (volume change of entire glaciers) for smaller ice bodies, or with laser altimetry/kinematic GPS for large glaciers constitute optimal possibilities for extending the information into remote areas of difficult access. Repeated mapping and altimetery alone provide important data at a lower time resolution (decades).

Tier 4: Long-term observations of glacier length change data within major mountain ranges for assessing the representativity of mass balance and volume change measurements

At this level, spatial representativity is the highest priority. Locations should be based on statistical considerations concerning climate characteristics, size effects and dynamics (calving, surge, debris cover, etc.). Long-term observations of glacier length change at a minimum of about 10 sites within each of the important mountain ranges should be measured either in-situ or with remote sensing techniques at annual to multi-annual frequencies.

Tier 5: Glacier inventories repeated at time intervals of a few decades by using satellite remote sensing

Continuous upgrading of preliminary inventories and repetition of detailed inventories using aerial photography or – in most cases – satellite imagery should make it possible to attain global coverage and to serve as a validation base of climate models. The use of digital terrain information in geographic information systems (GIS) greatly facilitates automated procedures of image analysis, data processing and modelling/interpretation of newly available information. Preparation of data products from satellite measurements must be based on a long-term program of data acquisition, archiving, product generation, and quality control.

Tiers 2 and 4 mainly represent traditional methodologies which remain fundamentally important for deeper understanding of the involved processes, as training components in environment-related educational programmes and as unique demonstration objects for a wide public. Tiers 3 and 5 constitute wide-open doors for the application of new technologies.

Detailed information on GTN-G and GHOST can be found in Haeberli (2000, 2004) with updates on the present state in several GTOS reports (Haeberli and Barry 2006, Zemp et al. 2008, Zemp et al. in press).

3.3 Available data sets

The WGMS hosts an unprecedented dataset of information about spatial glacier distribution and changes over time which is readily available to the scientific community and the public. At present, the database contains about 36 000 front variation and 3,400 annual mass balance observations for 1,800 and 230 glaciers, respectively. Both, the available length change and mass balance observations are strongly biased towards the Northern Hemisphere and Europe (Fig. 3). The WGI (WGMS 1989) is mainly based on aerial photographs and maps and makes available detailed information on location, classification, area, length, orientation and altitude range for 100 000 glaciers worldwide with a total area of 240 000 km^2 and preliminary estimates of the remaining glacierised regions derived from early satellite imagery (Fig. 3). The detailed inventory corresponds to about 60% of the total number and 35% of the total area of all glaciers worldwide (cf. estimates by Dyurgerov and Meier 2005).

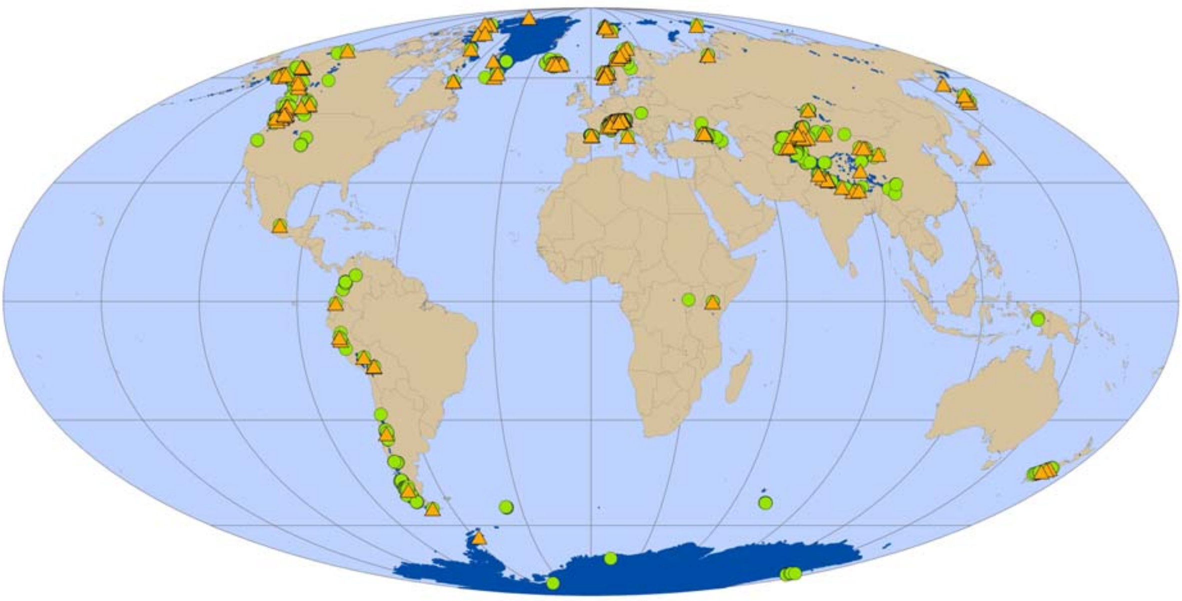

Figure 3: Worldwide Glacier Monitoring. The global distribution of surface ice on land (blue) is shown with locations of glacier front variation (green circles) and mass balance (yellow triangles) measurements. Data sources: locations of glacier observations provided by the WGMS, Zurich, Switzerland; background glacier cover is based on the glacier layer of the Digital Chart of the World, provided by the NSIDC, Boulder, USA.

In 1999, the Global Land Ice Measurements from Space (GLIMS; http://www.glims.org) initiative was established to continue this inventorying task with space-borne sensors (cf. Bishop et al. 2004, Kargel et al. 2005) in close cooperation with the National Snow and Ice Data Center (NSIDC; http://www.nsidc.org) and the WGMS. A GIS, including database and web-interfaces has been designed and implemented at NSIDC to host and distribute both the data from the World Glacier Inventory, i.e., glacier label points with attribute tables, and the new GLIMS data, i.e., glacier outlines with attribute tables (Raup et al. 2007a, b). In addition to the WGI data, the GLIMS database now contains digital outline information on over 83 000 glaciers covering 261 000 km^2 (status of April, 2009; Fig. 4). New projects, such as the International Polar Year (IPY) and the GlobGlacier data user element, by the European Space Agency (cf. Paul et al. 2009), aim at making a major contribution to the current WGMS and GLIMS databases.

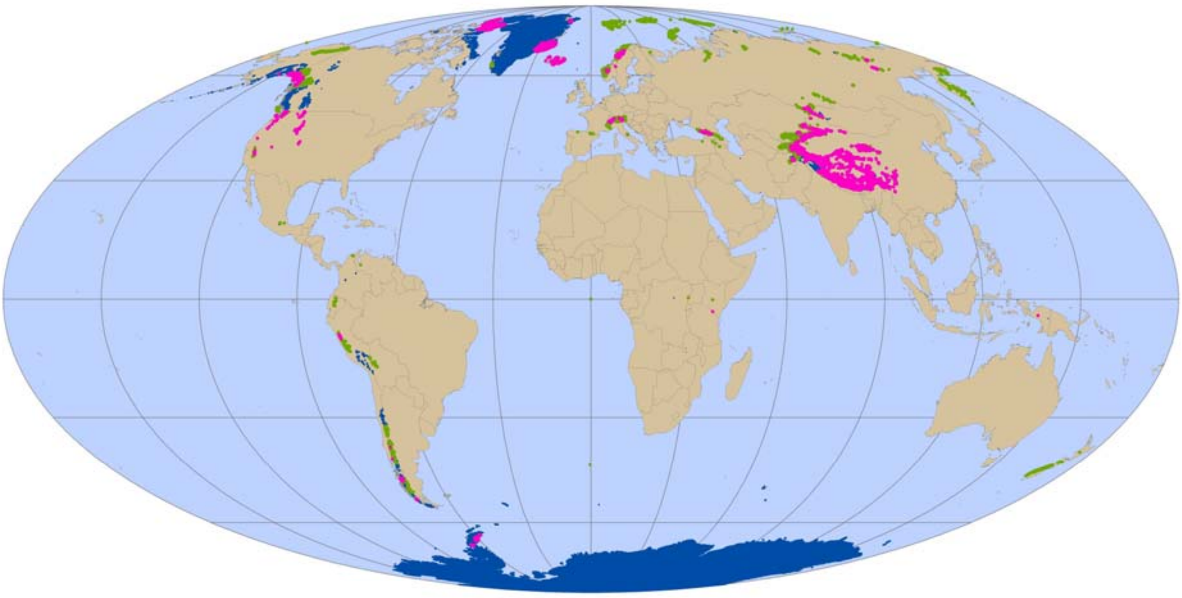

Figure 4. Global distribution of inventoried glaciers. The global distribution of surface ice on land (blue) is shown with the location of glaciers with available digital outlines collected within the GLIMS initiative (pink) and the locations of the point coordinates of glaciers with detailed information of the WGI (WGMS 1989; green). Data sources: WGI data provided by the WGMS, Zurich, Switzerland; glacier layers of GLIMS data and of the Digital Chart of the World provided by NSIDC/GLIMS, Boulder, USA.

Within GTN-G, consistency and interoperability of the different glacier databases is elaborated. A map-based web-interface is currently under implementation (http://www.gtn-g.org). This new one-stop portal is developed to spatially link the different data sets and to provide users with a fast overview of all available data and corresponding meta-information. It will also offer guidance for data submission and request in digital and standardized formats.

3.4 Challenges of the 21st century

Glaciers around the globe have been shrinking dramatically since their Holocene maximum extent towards the end of the Little Ice Age, between the 17th and the second half of the 19th century, with increasing rates of ice loss since the mid-1980s (Zemp et al. 2007, WGMS 2008a). Under the present climate scenarios (cf. IPCC 2007), the ongoing rapid and perhaps accelerating trend of worldwide glacier shrinkage, on the century time-scale, is most likely of non-periodical nature. International monitoring strategies, hence, have to consider extreme perspectives such as the deglaciation of large parts of many mountain ranges within the coming decades (e.g. Zemp et al. 2006, Nesje et al. 2007). In that context, international glacier monitoring has to face major challenges such as:

- the dramatic changes leading to the complete vanishing of some glaciers within the front variation and mass balance monitoring network,
- the downwasting of many glaciers, rather than dynamic retreat, over the past two decades that has decoupled the glacier horizontal extent (i.e., length, area) from current climate, so that glacier length/area change has definitely become a climate proxy of non-linear behaviour,
- the current high rates of ice loss demanding a repetition rate of glacier inventory activities of less than a few decades, which is in strong contradiction with the fact that until now no complete, detailed inventory of the world's glaciers is available,
- regional pilot studies (e.g., from the European Alps) showing that detailed change assessments based on inventories of different time periods and sources (e.g., 1850s based on historical maps and moraine dating, 1970s based on aerial photographs and maps, and 2000 based on satellite images) are very laborious and often hampered by problems with firn-ice-differentiation as well as with disintegration and vanishing of glaciers between the times analysed,
- the limited capacities of a historically grown glacier monitoring system of the 19th and 20th century, which is mainly based on research institutions and funded through time-limited research projects,
- the growing resources needed to manage the exponentially increasing data volume from remote sensing analysis and the often missing corresponding meta-data and quality information,
- the bias of the present monitoring network towards observations in the Northern Hemisphere,
- and the interruption of long-term glacier observation series due to financial, political, warlike and other reasons.

To keep track of fast environmental changes and to assess corresponding impacts on landscape evolution, fresh water supply and natural hazards, the international glacier monitoring will have to make use of the rapidly developing new technologies (remote sensing and geoinformatics) and relate them to the more traditional methods. In order to face such challenges of historical dimension, it is fundamental that the glacier monitoring of the 21st century:

- continues long-term fluctuation series (i.e., front variation and mass balance) in combination with decadal determinations of volume/thickness and length changes from geodetic methods in order to verify these annual in-situ observations,

- re-initiates interrupted long-term series in strategically important regions and strengthens the current monitoring network in the Tropics and the Southern Hemisphere,

- integrates reconstructed glacier states and variations into the present monitoring system in order to extend the historical set of front variation data and to put the measured glacier fluctuations of the last 150 years into context with glacier variations during the Holocene,

- concentrates the extension of the in-situ observation network mainly on (seasonal) mass balance measurements, because they are the direct glacier signal to atmospheric conditions,

- replaces long-term monitoring series of vanishing glaciers by the timely start of parallel observations on larger or higher-reaching glaciers,

- makes use of decadal digital elevation model differencing, and similar techniques, to extend and understand the representativeness of the in-situ mass balance measurements to/for the regional ice volume changes,

- completes one detailed, global glacier inventory, e.g. for the 1970s (cf. WGMS 1989), defines key regions, where the glacier cover is relevant for climate change, sea level rise, hydrological question and natural hazards, in which glacier changes since the end of the Little Ice Age, until the beginning of the 21st century and the coming decades are inventoried on a detailed level,

- and periodically re-evaluates the feasibility and relevance of the monitoring strategy and its implementation.

Glacier monitoring has to overcome national boundaries in terms of observations being coordinated over entire mountain ranges. Glacier observation data are to be provided, via the corresponding data centres, to the scientific community and wider public according to international standards and strategies. This requires the recognition of the importance of monitoring activities, data standards and meta-data by the sponsoring agencies and the research institutions. For this purpose the organisational structure and cooperation of the services involved in the international glacier monitoring (i.e., WGMS, NSIDC, and GLIMS) shall be further strengthened within GTN-G. The professionalized central monitoring services should be coordinated by an international cooperation structure with link to the scientific umbrella organisations, have an adequate financial basis, and strengthen their network to data providers, data users, national agencies and international organisations.

4 Glacier observations from space

Glaciers were one focus of satellite observations from the beginning of the Landsat mission (1972). Although the large regions covered by satellite data were mentioned in most studies as a strong benefit for glacier related applications, mapping of glacier extent was introduced quite late. Early applications focused on the mapping of snowlines (Østrem 1975, Rott 1976) or the analysis of glacier movement and flow (Krimmel and Meier 1975); at that time using contrast enhanced photographic prints rather than digital data. The full potential of working directly with the digital data was delayed until appropriate computers became available. The use of these data for glacier mapping was forwarded by Rundquist et al. (1980) and Howarth and Ommanney (1986) proposed to use Landsat data for creating glacier inventories.

With the availability of higher resolution (30 m) data in six spectral bands from the Thematic Mapper (TM) sensor in 1984, an important step forward was achieved for space-borne glacier monitoring. With this instrument, snow and ice was spectrally distinguishable from clouds and automated glacier mapping at a global scale became feasible. In the following years, a large number of studies used TM data for glaciological applications (e.g. mapping of outlines and terminus changes, snow and ice zones, flow velocities). With the advent of the Terra ASTER and Landsat ETM+ sensors, glaciers were one of the major targets from the beginning (Raup et al. 2000, Bindschadler et al. 2001) and simple but robust techniques were developed to map (debris-free) glaciers automatically (Albert 2002, Paul 2002). In combination with geographic information systems (GIS) and DEM fusion, the automated extraction of detailed glacier inventory data for all glaciers in a satellite scene became feasible (Paul et al. 2002, Kääb et al. 2002).

In parallel, microwave sensors were also increasingly used for glaciological studies, in particular for multi-temporal observations of the firn-line, to derive glacier velocity from interferometric techniques, or changing terminus positions of tidewater glaciers (cf. Bamber 2006). In contrast to optical sensors, clouds are transparent for microwaves which allows the study of glaciers independent of cloud conditions and thus more frequently. Due to the similarity of the microwave backscatter from snow/ice with other surrounding material, mapping of glacier extent from microwave sensors has only rarely been tested (e.g. Hall et al. 2000). Hence, the specific glaciological applications of microwave sensors are different from those of optical sensors.

4.1 Satellite observations in GTN-G

As described above (Section 3.2), the frequent update of glacier inventories from satellite data at time intervals of a few decades is implemented as tier 5 in the GTN-G (e.g. Haeberli 2006). In this regard, Landsat TM/ETM+ data are particularly useful for this task due to the large area covered and the free availability of the scenes stored in the

USGS archive (USGS 2008). To date, two major tasks can be identified for glacier monitoring from satellite data (GCOS 2006): (1) creating a digital two-dimensional (2D) baseline glacier inventory and (2) change assessment from repeat coverage. This is also related to the two main deficits of the former world glacier inventory (WGI) from the 1970s (WGMS 1989): The detailed inventory information in the WGI is not complete and the data are stored as point information. While the former causes large uncertainties for extrapolation of future sea level rise (e.g. Raper and Braithwaite 2006, Rahmstorf 2007), the latter means that change assessment is nearly impossible as the glacier entities which belong to a specific point are generally not known. Moreover, in most countries about 30 years have passed since the last inventory and the time for an update has come. It is a specific aim of the GLIMS initiative to overcome these issues by deriving the required glacier information from satellite data (mainly using the ASTER and TM/ ETM+ sensors) in yet uncovered regions and supplement the WGI with 2D outline information in a digital vector format (Kargel et al. 2005, Raup et al. 2007a).

In principle, this aim is achievable as Landsat TM/ETM+ data of glaciers exist from all around the world and appropriate ASTER data become increasingly available. The developed methods for automated and thus efficient glacier mapping (e.g. band ratios, NDSI, see Chapter XX) are applicable to nearly all multispectral sensors (e.g. ASTER, ETM+, IRS-1C, SPOT) with a band in the shortwave infrared (SWIR) near 1.5 micrometres, which facilitates global application. Under good conditions, the spatial resolution of this band (20-30 m) allows glacier mapping down to 0.05–0.02 km^2, which is sufficient for a detailed glacier inventory of even very small glaciers (Paul 2007, Andreassen et al. 2008). Despite the much smaller area covered per ASTER scene compared to Landsat (1/9), the sensor is particular useful for creating glacier inventories, as a DEM for extraction of topographic glacier data can be derived from its along-track stereo bands (e.g. Toutin 2002, Kääb et al. 2003, Singh-Khalsa et al. 2004). The two-times higher spatial resolution in the visible and near infrared (VNIR) bands (15 m) further facilitates a number of other glaciological applications (Kääb 2005, Racoviteanu et al. 2007, Toutin 2008)

Compared to the traditional glacier mapping from aerial photography (with its much higher spatial resolution), the major advantages of satellite data are: the larger area covered at the same point in time, the possibility of automated mapping using multiple spectral bands, a reduced workload for orthorectification, the potential to convert the raw data to physical units (reflectance/ albedo) and the digital format of the raw data. In principal, glacier outlines derived from high-resolution sensors (1 m or better) can be more precise, but it has to be kept in mind that the accuracy of the derived glacier extent is much more governed by snow conditions (e.g. hiding the glacier perimeter, especially in the accumulation area) and interpretation errors (e.g. debris cover, attached perennial snow fields) than by spatial resolution (Paul and Andreassen 2009). Moreover, due to a lack of contrast, mono- or panchromatic images from high resolution sensors are often much more difficult to interpret than false colour composites from multispectral sensors. An example of the ambiguity related to spatial vs. spectral information is depicted in Fig. 5 for the IRS-1C and Landsat ETM+ sensor. In times of rapid glacier change it might also be more valuable to have a higher update frequency (e.g. 5 years) than a very high precision (meter accuracy) of the outline.

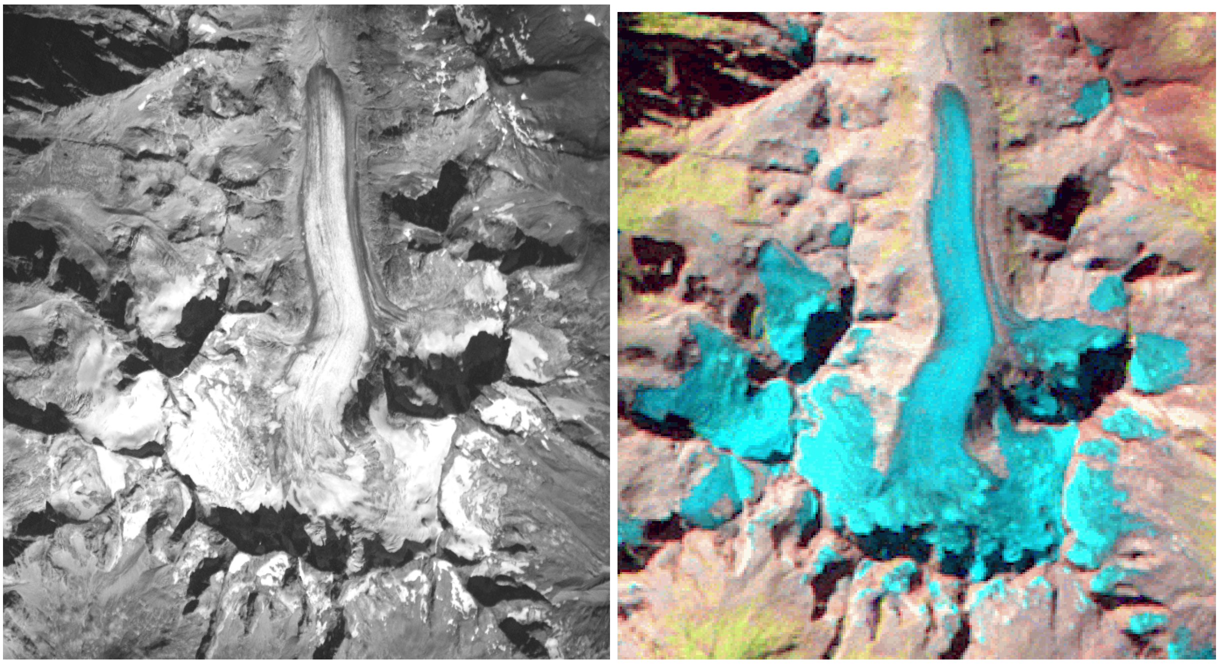

Figure 5. Comparison of spatial resolution vs. spectral information for Forno Glacier in south-western Switzerland. a) Despite the higher spatial resolution (here 10 m) of the the IRS-1C image many glaciers are barely recognizable in the panchromatic band. b) The Landsat TM image has a lower spatial resolution (here 25 m), but all glaciers can be identified clearly in this false colour composite with bands 5, 4, and 3 as RGB. IRS-1C data were obtained from NPOC.

4.2 Possible applications

In principle, the available sensors cover all time scales (minutes to decades) and spatial resolutions (0.5 m to 5000 km), as well as all parts of the spectrum (wavelengths from metres to nanometres). The numerous glaciological applications emerging from this large variety of sensors are not discussed here, but detailed overviews can be found in Williams and Hall (1993 and 1998), Bindschadler (2001), Kargel et al. (2005), Bamber (2006), Rees (2006), and the IGOS cryosphere theme report (IGOS 2007). Moreover, numerous different applications are discussed in the regional Chapters of this book and widely found in the literature (e.g., Haeberli and Hoelzle 1995, Dyurgerov and Meier 2005, Evans 2006, Raper and Braithwaite 2006).

Regarding the monitoring strategy of GTN-G, the prime focus of satellite observations are detailed assessments (individual glaciers) at regional scales (i.e. entire mountain ranges) in typical time periods of 5-10 years. The observations include changes in glacier length, area (repeat inventories) and volume (geodetic mass balance) to allow extrapolation of the related field measurements in space and time and to validate them. Besides the possible extension of the relatively small sample of ground measurements in most regions of the world (cf. WGMS 2008a), a particular useful application at the regional scale is the evaluation of the representativeness of the glaciers selected for field measurements (e.g. mass balance) for an entire mountain range (Paul and Haeberli 2008). Other useful satellite derived products include snow cover extent at the end of the ablation period and glacier velocity fields from repeat-pass data. In principle, all these products can be derived from optical satellite data, but glacier velocities and in particular DEMs (e.g. the SRTM DEM) are also obtained from microwave data (e.g. Rabus et al. 2003, Strozzi et al. 2008).

For precise measurements of glacier elevation changes, laser scanning or altimetry is increasingly applied (Arendt et al. 2006, Geist and Stötter 2008). LIDAR data from space-borne instruments (e.g. ICESat) were also used to test the accuracy of DEMs from other sources (e.g. Kääb 2008) or to determine elevation changes at orbit crossing points (e.g. Slobbe et al. 2008). Value added products can be created when the products mentioned above are combined. For example, glacier outlines and a DEM gives topographic glacier inventory data, or mapped snow extent and glacier outlines gives accumulation area ratios (AARs). Within the framework of the ESA project called GlobGlacier the related methodologies are explored, applied and documented (Paul et al. 2009). In any case, ground observations remain mandatory for calibration and validation of the satellite data (IGOS 2007).

4.3 Challenges

Of course, the use of satellite data for glacier mapping and monitoring purposes has also some challenges. The most important ones are: (a) frequent cloud cover and unfavourable snow conditions, (b) debris-covered glaciers, (c) definition of the glacier entity, and (d) comparison with a former inventory or with field measurements (e.g. length change, mass balance). A recent overview with proposed solutions is given by Racoviteanu et al. (in press) and Paul and Andreassen (2009). Further examples can be found in the regional chapters of this book. The best recommendation to overcome point (a) is to spend considerable time on selecting the best available images for processing and prefer mosaicking of multiple scenes when cloud cover is hiding parts of the glaciers instead of using cloud-free scenes with seasonal snow. For point (b) a number of semi-automated mapping methods have been developed (e.g. Paul et al. 2004), but expert manual delineation on contrast enhanced imagery still provides the best results. The GLIMS guidelines by Raup and Khalsa (2007) provide detailed instructions to define a glacier entity (point c). In most cases, a DEM is needed for a clear separation in the accumulation region. The comparison with previous datasets for change assessment (point d) can only be performed when the same entities or measurements are compared. This generally requires that the respective datasets are available in a digital and georeferenced format.

Despite the magnitude of these hurdles, in view of the ongoing efforts from the GLIMS initiative and ESAs GlobGlacier project, we are confident that most of the challenges can be solved and a more complete data set of global glacier coverage can be realized within the next few years.

5 Integrative glacier change assessments

The numerous length change series together with the positions of the moraines give a rather good qualitative overview on the global and regional glacier changes since their Little Ice Age maximum extents; whereas the mass balance series provide quantitative measures of the ice loss since the late 1940s. However, the relatively few glacier mass balance series cannot truly represent the changes of the global ice cover. Many regions with large amounts of ice cover are strongly underrepresented in the dataset or are even lacking of any observations. As a consequence, the field measurements with a high temporal resolution (but limited in spatial coverage) must be complemented with remotely sensed decadal area and volume change assessment (e.g., Rignot et al. 2003, Larsen et al. 2007, Paul and Haeberli 2008) in order to get a representative view of the climate change impacts.

Examples for such integrative glacier change assessments for entire mountain ranges are given by Molnia (2007) for Alaska, by Casassa and others (2007) for the Andean glaciers, by Kaser and Osmaston (2002) for tropical glaciers, by Andreassen and others (2005) for Norway, by Zemp and others (2007b) and Haeberli and others (2007) for the European Alps, by Kotlyakov (2006) for Russia, and by Chinn (2001) for New Zealand, as well as by Hoelzle and others (2003), Grove (2004), Zemp and others (2007a), and WGMS (2008a) for a global overview.

In addition, numerical modeling studies are encouraged to bridge the gap between local process studies and coverage at the global scale (e.g. Raper and Braithwaite 2006), to link the glacier fluctuations to the climate forcing (e.g. Greuell and Oerlemans 1986), and to downscale GCM/RCM scenarios for the use in local process models (e.g. Machguth et al. subm.).

6 Synopsis and organization of the book

[to be completed as soon as the other book chapters are ready]

Overall it can be concluded that glaciers around the globe have been shrinking dramatically since their Holocene maximum extent towards the end of the Little Ice Age, between the 17th and the second half of the 19th century, with increasing rates of ice loss since the mid-1980s. On a time scale of decades, glaciers in various mountain ranges have shown intermittent re-advances. However, under the present climate scenarios, the ongoing trend of worldwide and fast, if not accelerating, glacier shrinkage on the century time scale is not a periodic change and may lead to the deglaciation of large parts of many mountain regions by the end of the 21st century.

7 Conclusions

Glaciers, in general, form where snow deposited during the cold/humid season does not entirely melt during warm/dry times. As these conditions are widespread over the globe, glaciers are found from the equatorial regions to the poles. International coordinated glacier observation was initiated in 1894 and has resulted in an unprecedented dataset of information about spatial glacier distribution and changes over time. These datasets are readily available to the scientific community and the public, and includes annual front variation observations back to the late 19th century, six decades of annual (seasonal) mass balance measurements and a preliminary world glacier inventory for the 1970s, mainly based on aerial photographs and maps, with detailed information on more than 100 000 glaciers.

The GLIMS initiative, designed to continue this inventorying task in close cooperation with the NSIDC and the WGMS, should give top priority to a) complete the gaps of the detailed inventorying of the WGI (WGMS 1989), b) define key regions of the global glacier cover which are relevant for sea level rise, climate change monitoring, hydrological resources and natural hazards, and c) use these regions for globally representative change assessments since the end of the Little Ice Age (based on trim line mapping and moraine dating), and until the beginning of the 21st century and for the coming decades.

Since the end of the Little Ice Age, glaciers around the globe have been shrinking significantly, with increasing rates of ice loss since the mid-1980s. On a time-scale of decades, glaciers in various mountain ranges have shown intermittent re-advances. However, under current IPCC climate scenarios, the ongoing trend of worldwide and fast, if not accelerating, glacier shrinkage on the century time-scale is most likely of a non-periodic nature, and may lead to the deglaciation of large parts of many mountain ranges by the end of the 21st century.

The challenges of historical dimensions, both with respect to changes in nature and science, can only be faced by a strong, operational monitoring service with an multi-level monitoring strategy integrating reconstructions of glacier states and fluctuations, in-situ observations and remote sensing that has a well organised international structure, a powerful data collection, storing and distribution architecture and a secure financial basis from national and international funding.

Acknowledgments
Our sincere thanks go to the national correspondents and principal investigators of the WGMS and to the GLIMS community for the collection and free exchange of important data over many years. We thank Michael P. Bishop for thorough comments on a first version of the present Chapter.

References

Agassiz, L. (1840): Etudes sur les glaciers, 1. jent & Gassmann, Neuchâtel.
Albert, T. (2002): Evaluations of remote sensing techniques for ice-area classifications applied to the tropical Quelccaya Ice Cap, Peru. Polar Geography, 26: p. 210–226.
Andreassen, L.M., Paul, F., Kääb, A. and Hausberg, J.E. (2008): The new Landsat-derived glacier inventory for Jotunheimen, Norway, and deduced glacier changes since the 1930s. The Cryosphere, 2: p. 131–145.
Arendt, A., Echelmeyer, K., Harrison, W.D., Lingle, G. & Valentine, V. (2002): Rapid wastage of Alaska glaciers and their contribution to rising sea level. Science, 297 (5580): p. 382–386.
Arendt, A., K. Echelmeyer, W. Harrison, C. Lingle, S. Zirnheld, V. Valentine, B. Ritchie and M. Druckenmiller (2006): Updated estimates of glacier volume changes in the western Chugach Mountains, Alaska, and a comparison of regional extrapolation methods. Journal of Geophysical Research, 111, F03019.
Bamber, J.L., R.L. Layberry, and S.P. Gogineni, 2001: A new ice thickness and bed data set for the Greenland ice sheet, 1. Measurement, data reduction, and errors. J. Geophys. Res., 106, 33733–33780.
Bamber, J. (2006): Remote sensing in glaciology. In: Knight, P.G. (Ed.): Glacier Science and Environmental Change, Blackwell Publishing, Oxford: p. 370–382.
Bamber, J.L., and Rivera, A. (2007): A review of remote sensing methods for glacier mass balance determination. Global and Planetary Change, 59 (1–4): p. 138–148.
Benn, D.I. and Evans, D.J.A. (1998): Glaciers and Glaciation. Arnold: 734 pp.
Bentley, C.R., Thomas, R.H. and Velicogna, I. (2007): Ice Sheets. In: UNEP (ed.): Global outlook for ice & snow. UNEP/GRID-Arendal, Norway: 235 pp.
Bindschadler, R., Dowdeswell, J., Hall, D., and Winther, J.-G. (2001), Glaciological applications with Landsat-7 imagery: Early assessments. Remote Sensing of Environment, 78: p. 163–179.
Bishop, M.P., Olsenholler, J.A., Shroder, J.F., Barry, R.G., Raup, B.H., Bush, A.B.G., Coplan, L., Dwyer, J.L., Fountain, A.G., Haeberli, W., Kääb, A., Paul, F., Hall, D.K., Kargel, J.S., Molnia, B.F., Trabant, D.C., and Wessels, R. (2004): Global land ice measurements from space (GLIMS). Remote sensing and GIS investigations of the Earth's cryosphere. Geocarto International, 19(2), p. 57–84.
Cogley, J.G., Arendt, A., Bauder, A., Braithwaite, R., Hock, R., Jansson, P., Kaser, G., Möller, M., Nicholson, L., Rasmussen, A. and Zemp, M. (in prep): Glossary of mass-balance and related terms. Working Group on Mass-balance Terminology and Methods of the International Association of Cryospehric Sciences. Draft 3, 10 July 2009.
Forel, F.A. (1895): Les variations périodiques des glaciers. Discours préliminaire. Extrait des Archives des Sciences Physiques et Naturelles, XXXIV: p. 209–229.
Dyurgerov, M., and M.F. Meier, 2005: Glaciers and the Changing Earth System: A 2004 Snapshot. Occasional Paper 58, Institute of Arctic and Alpine Research, University of Colorado, Boulder, CO, 118 pp.
Evans, I.S. (2006): Local aspect asymmetry of mountain glaciation: A global survey of consistency of favoured directions for glacier numbers and altitudes. Geomorphology 73(1-2): p. 166–184.
GCOS (2004): Implementation plan for the Global Observing System for Climate in support of the UNFCCC. Report GCOS – 92 (WMO/TD No. 1219): 136p.
GCOS (2006): Systematic observation requirements for satellite-based products for climate. Supplemental details to the satellite-based component of the "Implementation Plan for the Global Observing System for Climate in Support of the UNFCCC", Report GCOS-107 (WMO/TD No. 1338), September 2006. 90p.
Geist, T. and J. Stötter (2008): Documentation of glacier surface elevation change with multi-temporal airborne laser scanner data case study: Hintereisferner and Kesselwandferner, Tyrol, Austria. Zeitschrift für Gletscherkunde und Glazialgeologie, 41: p. 77–106.

Greuell, W. and Oerlemans, J. (1986): Sensitivity studies with a mass balance model including temperature profile calculations inside the glacier. Zeitschrift für Gletscherkunde und Glazialgeologie, 22 (2): p. 101–124.

Haeberli, W. and Hoelzle, M. (1995): Application of inventory data for estimating characteristics of and regional climate-change effects on mountain glaciers: a pilot study with the European Alps. Annals of Glaciology, 21: p. 206–212.

Haeberli, W. (1998). Historical evolution and operational aspects of worldwide glacier monitoring. Into the second century of world glacier monitoring: prospects and strategies. UNESCO, Paris, 56, p. 35–51

Haeberli, W., Cihlar, J. & Barry, R.G. (2000): Glacier monitoring within the Global Climate Observing System. Annals of Glaciology, 31: p. 241–246.

Haeberli, W. and Burn, C. (2002): Natural hazards in forests - glacier and permafrost effects as related to climate changes. In: Sidle, R.C. (ed.) Environmental Change and Geomorphic Hazards in Forests. IUFRO Research Series, 9, 167–202.

Haeberli, W. (2004): Glaciers and ice caps: historical background and strategies of world-wide monitoring. In: Bamber, J.L., Payne A.J. (eds.): Mass balance of the cryosphere. Cambridge University Press, Cambridge: p. 559–578.

Haeberli, W. (2006): Integrated perception of glacier changes: a challenge of historical dimen¬sions. In: Knight, P. G. (ed): Glacier Science and Environmental Change. Oxford: Blackwell Publishing: p. 423–430.

Haeberli, W. and Barry, R. (2006): Global Terrestrial Network for Glaciers (GTN-G). In: GTOS (2006): GTOS Biennial Report 2004–2005. GTOS Document 40: p. 30–31.

Haeberli, W. (2007): Changing views of changing glaciers. In: Orlove, B., Wiegandt, E. and B. Luckman (eds.): The darkening peaks: Glacial retreat in scientific and social context. University of California Press: p. 23–32.

Haeberli, W., Hoelzle, M., Paul, F. and Zemp, M. (2007): Integrated monitoring of mountain glaciers as key indicators of global climate change: the European Alps. Annals of Glaciology, 46: p. 150–160.

Hall, D.K., R.S. Williams Jr., J.S. Barton, O. Sigurdsson, L.C. Smith and J.B. Garvin (2000): Evaluation of remote-sensing techniques to measure decadal-scale changes of Hofsjökull ice cap, Iceland. Journal of Glaciology, 46 (154): p. 375–38.

Hoelzle, M., Haeberli, W., Dischl, M. and Peschke, W. (2003): Secular glacier mass balances derived from cumulative glacier length changes. Global and Planetary Change 36(4), p. 77–89.

Howarth, P. and Ommanney, C.S. (1986): The use of Landsat digital data for glacier inventories. Annals of Glaciology, 8: p. 90–92.

IGOS (2007): Integrated Global Observing Strategy Cryosphere Theme Report - For the Monitoring of our Environment from Space and from Earth. Geneva: World Meteorological Organization. WMO/TD-No. 1405: 100 pp.

IPCC (2001): Climate Change 2001: the scientific basis. Contribution of working group I to the Third Assessment Report of the Intergovernmental Panel on Climate Change. Cambridge University Press, Cambridge: 881 pp.

IPCC (2007). Climate Change 2007: The Physical Science Basis. Contribution of Working Group 1 to the Fourth Assessment Report of the Intergovernmental Panel on Climate Change (eds. S. Solomon, D. Qin, M. Manning, Z. Chen, M.C. Marquis, K. Averyt, M. Tignor and H.L. Miller). Intergovernmental Panel on Climate Change, Cambridge and New York.

Johannesson, T., Raymond, C. & Waddington, E. (1989): Time-scale for adjustment of glaciers to changes in mass balance. Journal of Glaciology, 35 (121): p. 355–369.

Kääb, A., Paul, F., Maisch, M., Hoelzle, M. & Haeberli, W. (2002): The new remote-sensing derived Swiss Glacier Inventory: II. First results. Annals of Glaciology, 34: p. 362–366.

Kääb, A., Huggel, C., Paul, F., Wessels, R., Raup, B., Kieffer, H. And Kargel, J. (2003): Glacier monitoring from ASTER imagery: accuracy and applications. In Proceedings of EARSeL- LISSIG-Workshop Observing our Cryosphere from Space, 11 13 March 2002, Bern, Germany, 2: p. 43–53.

Kääb, A. (2005): Remote sensing of mountain glaciers and permafrost creep. Schriftenreihe Physische Geographie. 48: 266 pp.

Kääb, A. (2005): Combination of SRTM3 and repeat ASTER data for deriving alpine glacier flow velocities in the Buthan Himalaya. Remote Sensing of Environment, 94: p. 463–474.

Kääb, A. (in press): Glacier volume changes using ASTER satellite stereo and ICESat GLAS laser altimetry. A test study on Edgeøya, Eastern Svalbard. In: IEEE Transactions on Geosciences and Remote Sensing, 46(10): p. 2823–2830.

Kargel, J.S., M. J. Abrams, M. P. Bishop, A. Bush, G. Hamilton, H. Jiskoot, A. Kääb, H. H. Kieffer, E. M. Lee, F. Paul, F. Rau, B. Raup, J. F. Shroder, D. Soltesz, L. Stearns, R. Wessels and the GLIMS Consortium (2005): Multispectral imaging contributions to Global Land Ice Measurements from Space, Remote Sensing of Environment, 99 (1/2): p. 187–219.
Krimmel, R.M., and Meier, M.F. (1975): Glacier applications of ERTS-1 images. Journal of Glaciology, 15 (73): p. 391– 402.
Kuhn, M., (1981): Climate and glaciers. IAHS, 131: p. 3–20.
Larsen, C.F., R.J. Motyka, A.A. Arendt, K.A. Echelmeyer and P.E. Geissler. 2007. Glacier changes in southeast Alaska and northwest British Columbia and contribution to sea level rise. J. Geophys. Res., 112(F1), F01007. (10.1029/2006JF000586.)
Lythe, M.B., D.G. Vaughan, and the BEDMAP Group, 2001: BEDMAP: A new ice thickness and subglacial topographic model of Antarctica. J. Geophys. Res., 106(B6), 11335–11351.
Machguth, H., F. Paul, S. Kotlarski and M. Hoelzle (submitted): Calculating distributed glacier mass balance for the Swiss Alps from RCM output: a methodical description and interpretation of the results. Journal of Geophysical Research.
Meier, M.F. (1984). The contribution of small glaciers to sea level rise. Science, 226: p. 1418–1421
Müller, F., Caflisch, T. and Müller, G. (Eds.). 1977. Instructions for the compilation and assemblage of data for a world glacier inventory. IAHS(ICSI)/UNESCO report, Temporal Technical Secretariat for the World Glacier Inventory (TTS/WGI), ETH Zurich, Switzerland: 22 pp.
Müller, F. (Ed.). 1978. Instructions for the compilation and assemblage of data for a world glacier inventory; Supplement: Identification/glacier number IAHS(ICSI)/UNEP/UNESCO report, Temporal Technical Secretariat for the World Glacier Inventory (TTS/WGI), ETH Zurich, Switzerland.
Nesje, A., Bakke, J., Dahl, S.O., Lie, Ø. and Matthews, J.A. (2007): Norwegian mountain glaciers in the past, present and future. Global and Planetary Change, 60 (1-2): p. 10–27.
Nye, J.F., (1960): The response of glaciers and ice-sheets to seasonal and climatic changes. Proceedings of the Royal Society of London, A(256), p. 559–584
Oerlemans, J. (2001): Glaciers and climate change. A.A. Balkema Publishers. Lisse, Abingdon, Exton, Tokyo: 148 pp.
Ohmura, A., 2004: Cryosphere during the twentieth century. In: Sparks, R.S.J. and C.J. Hawkesworth (eds.): The State of the Planet: Frontiers and Challenges in Geophysics. Geophysical Monograph 150, International Union of Geodesy and Geophysics, Boulder, CO and American Geophysical Union, Washington, DC, pp. 239–257.
Østrem, G. (1975): ERTS - 1 data in glaciology - an effort to monitor glacier mass balance from satellite imagery. Journal of Glaciology, 15 (73): p. 403–415.
Paterson, W.S.B. (1994). The physics of glaciers. 3rd edition, Pergamon Press, Oxford: 480 pp.
Paul, F. (2002): Changes in glacier area in Tyrol, Austria, between 1969 and 1992 derived from Landsat 5 TM and Austrian glacier inventory data. International Journal of Remote Sensing, 23: p. 787–799.
Paul, F., Kääb, A., Maisch, M., Kellenberger, T. & Haeberli, W. (2002): The new remote sensing-derived Swiss Glacier Inventory: I. Methods. Annals of Glaciology, 34: p. 355–361.
Paul, F., Huggel, C., and Kääb, A. (2004): Combining satellite multispectral image data and a digital elevation model for mapping of debris-covered glaciers. Remote Sensing of Environment, 89: p. 510–518.
Paul, F. (2007): The New Swiss Glacier Inventory 2000 - Application of Remote Sensing and GIS. Schriftenreihe Physische Geographie, Universität Zürich, 52: 210 pp.
Paul, F. and Haeberli, W. (2008): Spatial variability of glacier elevation changes in the Swiss Alps obtained from two digital elevation models. Geophysical Research Letters, 35, L21502.
Paul, F., and Andreassen, L.M. (2009): Creating a glacier inventory for the Svartisen region (Norway) from Landsat ETM+ satellite data: Challenges and results. Journal of Glaciology, 55 (192): p. 607–618.
Paul, F., Kääb, A., Rott, H., Shephard, A., Strozzi, T. and Volden, E. (2009): GlobGlacier: a new ESA project to map the world's glaciers and ice caps from space. EARSeL eProceedings, 8: p. 11–25.
Rabus, B., Eineder, M., Roth, A. and Bamler, R. (2003): The shuttle radar topography mission - a new class of digital elevation models acquired by spaceborne radar. In: ISPRS Journal of Photogrammetry and Remote Sensing, 57 (4): p. 241–262.
Racoviteanu, A.E., Manley, W.F., Arnaud, Y. and Williams, M.W. (2007): Evaluating digital elevation models for glaciological applications: an example from Nevado Coropuna, Peruvian Andes. Global and Planetary Change, 59: p. 110–125.
Racoviteanu, A.E, Paul, F., Raup, B., Khalsa, S.J.S. and Armstrong, R. (in press): Challenges in glacier mapping from space: recommendations from the Global Land Ice Measurements from Space (GLIMS) initiative. Annals of Glaciology, 50 (53).

Rahmstorf, S. (2007): A semi-empirical approach to projecting future sea-level rise. Science, 315 (5810): p. 368–370.
Raper, S.C.B. and R.J. Braithwaite (2006): Low sea level rise projections from mountain glaciers and icecaps under global warming. Nature, 439(7074): p. 311–313.
Rau, F., Mauz, F., Vogt, S., Khalsa, S.J. and Raup, B. (2005): Illustrated GLIMS Glacier Classification Manual. Glacier Classification Guidance for the GLIMS Glacier Inventory: 36 pp.
Raup, B.H., Kieffer, H.H., Hare, T.M., and Kargel, J.S. (2000): Generation of Data Acquisition Requests for the ASTER Satellite Instrument for Monitoring a Globally Distributed Target: Glaciers. IEEE Transactions On Geoscience and Remote Sensing, 38: p. 1105–1112.
Raup, B.H., and Khalsa, J.S. (2007): GLIMS analysis tutorial: 13p. Online from http://www.glims.org/MapsAndDocs/assets/ GLIMS_Analysis_Tutorial_a4.pdf
Raup, Bruce; Andreas Kääb; Jeffrey S. Kargel; Michael P. Bishop; Gordon Hamilton; Ella Lee; Frank Paul; Frank Rau; Deborah Soltesz; Siri Jodha Singh Khalsa; Matthew Beedle; Christopher Helm (2007a). "Remote Sensing and GIS Technology in the Global Land Ice Measurements from Space (GLIMS) Project". Computers and Geosciences 33: p. 104–125. (doi:10.1016/j.cageo.2006.05.015)
Raup, B.H.; A. Racoviteanu; S.J.S. Khalsa; C. Helm; R. Armstrong; Y. Arnaud (2007b). "The GLIMS Geospatial Glacier Database: a New Tool for Studying Glacier Change". Global and Planetary Change 56: p. 101–110. doi:10.1016/j.gloplacha.2006.07.018
Rees, W.G. (2006), Remote sensing of snow and ice. Taylor and Francis, Boca Raton.
Rignot, E., A. Rivera and G. Casassa. 2003. Contribution of the Patagonian icefields of South America to sea level rise. Science, 302(5644), 434–437.
Rott, H. (1976): Analyse der Schneeflächen auf Gletschern der Tiroler Zentralalpen aus Landsat Bildern. Zeitschrift für Gletscherkunde und Glazialgeologie, 12: p. 1–28.
Rundquist, D.C., Collins, S.C., Barnes, R.B., Bussom, D.E., Samson, S.A. and Peake, J.S. (1980): The use of Landsat digital information for assessing glacier inventory parameters. IAHS, 126: p. 321–331.
Scherler, K. (Ed.). 1983. Guidelines for preliminary glacier inventories. IAHS(ICSI)/ UNEP/UNESCO report, Temporal Technical Secretariat for the World Glacier Inventory (TTS/WGI), ETH Zurich, Switzerland.
Shumsky, P.A. (1964): Principles of structural glaciology. Translated from the Russian by D. Kraus. Dover Publications Inc., New York: 497 pp.
Singh Khalsa, S.J., Dyugerov, M.B., Raup, B.H. and Barry, R.G. (2004): Space-based mapping of glacier changes using ASTER and GIS Tools. IEEE Transactions on Geosciences and Remote Sensing, 42: p. 2177–2183.
Slobbe, D.C., Lindenbergh, R.C., Ditmar. P. (2008): Estimation of volume change rates of Green¬land's ice sheet from ICESat data using overlapping footprints. Remote Sensing of Environ¬ment, 112 (12): p. 4204–4213.
Strozzi, T., A. Kouraev, A. Wiesmann, U. Wegmüller, A. Sharov and C. Werner (2008): Estimation of Arctic glacier motion with satellite L-band SAR data. In: Remote Sensing of Environment, 112 (3): p. 636–645.
Toutin, T. (2002): 3D topographic mapping with ASTER stereo data in rugged topography. IEEE Transactions on Geoscience and Remote Sensing, 40: p. 2241–2247.
Toutin, T. (2008): ASTER DEMs for geomatic and geoscientific applications: a review. International Journal of Remote Sensing, 29 (7): p. 1855–1875.
UNEP (2007): Global outlook for ice & snow. UNEP/GRID-Arendal, Norway: 235 pp.
UNESCO (1970): Perennial ice and snow masses – a guide for compilation and assemblage of data for the World Glacier Inventory. Technical Papers in Hydrology No. 1.
UNESCO 1970/73. Combined heat, ice and water balances at selected glacier basins. Part I: A guide for compilation and assemblage of data for glacier mass balance measurements. Part II: Specifications, standards and data exchange. UNESCO/ IAHS Technical Papers in Hydrology 5.
USGS (2008): Opening the Landsat Archive. USGS Factsheet 2008-3091. URL: http:// pubs.usgs.gov/fs/2008/3091/pdf/fs2008-3091.pdf
WGMS (1989): World glacier inventory – status 1988. In: Haeberli, W., Bösch, H., Scherler, K, Østrem, G. and Wallén, C.C. (eds.), IAHS(ICSI)/UNEP/UNESCO, World Glacier Monitoring Service, Nairobi: 458 pp.
WGMS (2007): Glacier Mass Balance Bulletin No. 9 (2004–2005). Haeberli, W., Hoelzle, M. and Zemp, M. (eds.), ICSU(FAGS)/IUGG(IACS)/UNEP/UNESCO/WMO, World Glacier Monitoring Service, Zurich, Switzerland: 100 pp.

WGMS (2008a): Global Glacier Changes: facts and figures. Zemp, M., Roer, I., Kääb, A., Hoelzle, M., Paul, F. and Haeberli, W. (eds.), UNEP, World Glacier Monitoring Service, Zurich, Switzerland: 88 pp.

WGMS (2008b): Fluctuations of Glaciers 2000–2005 (Vol. IX). Haeberli, W., Zemp, M., Kääb, A., Paul, F. and Hoelzle, M. (eds.), ICSU (FAGS) / IUGG (IACS) / UNEP / UNESCO / WMO, World Glacier Monitoring Service, Zurich, Switzerland: 266 pp.

Williams, R.S., Jr. and Hall, D.K. (1993): Glaciers, in: Gurey, R. J., Foster, J. L. and Parkinson, C. L., Atlas of satellite observations related to global change, Cambridge University Press: p. 401–421.

Williams, R.S.,Jr. and Hall, D.K. (1998): Use of remote-sensing techniques, in: Haeberli, W., Hoelzle, M., and Suter, S., Into the second century of worldwide glacier monitoring: pros¬pects and strategies, UNESCO Publishing: p. 97–111.

Zemp, M., Haeberli, W., Hoelzle, M. and Paul, F. (2006): Alpine glaciers to disappear within decades? Geophysical Research Letters, 33, L13504, doi:10.1029/2006GL026319.

Zemp, M., Haeberli, W., Bajracharya, S., Chinn, T.J., Fountain, A.G., Hagen, J.O., Huggel, C., Kääb, A., Kaltenborn, B.P., Karki, M., Kaser, G., Kotlyakov, V.M., Lambrechts, C., Li, Z.Q., Molnia, B.F., Mool, P., Nellemann, C., Novikov, V., Osipova, G.B., Rivera, A., Shrestha, B., Svoboda, F., Tsvetkov D.G. and Yao, T.D. (2007): Glaciers and ice caps. Part I: Global overview and outlook. Part II: Glacier changes around the world. In: UNEP: Global outlook for ice & snow. UNEP/GRID-Arendal, Norway: p. 115–152.

Zemp, M., Haeberli, W., Hoelzle, M. and Paul, F. (2008): Glaciers and ice caps. In: GTOS (2008): GTOS Biennial Report 2006–2007. GTOS Document 50: p. 2–3.

Zemp, M., Roer-Gärtner, I., Haeberli, W., Hoelzle, M. and Paul, F. (in press): ECV T6: Glaciers and Ice Caps. Assessment of the status of the development of standards for the Terrestrial Essential Climate Variables. Global Terrestrial Observing System, 61: 26 pp.

Publication 2

WGMS (2008b). **Fluctuations of Glaciers 2000-2005** (Vol. IX). Haeberli, W., **Zemp**, **M.**, Kääb, A., Paul, F. & Hoelzle, M. (eds.), ICSU (FAGS) / IUGG (IACS) / UNEP / UNESCO / WMO, World Glacier Monitoring Service, Zurich, Switzerland, 266 pp.

Note that the Appendix of WGMS (2008b) is here reduced to one page per data table. A complete version of this publication can be found on the WGMS website: http://www.wgms.ch/fog.html

FLUCTUATIONS

OF

GLACIERS
2000–2005

(Vol. IX)

A contribution to the
Global Terrestrial Network for Glaciers (GTN-G)
as part of the Global Terrestrial/Climate Observing System (GTOS/GCOS),

the Division of Early Warning and Assessment and the Global Environment Outlook
as part of the United Nations Environment Programme (DEWA and GEO, UNEP),

and the International Hydrological Programme (IHP, UNESCO)

Prepared by the
World Glacier Monitoring Service (WGMS)

ICSU (FAGS) – IUGG (IACS) – UNEP – UNESCO – WMO

2008

FLUCTUATIONS OF GLACIERS 2000–2005
with addenda from earlier years

This publication was made possible by support and funds from

the Federation of Astronomical and Geophysical Data Analysis Services (FAGS/ICSU),

the Swiss Academy of Sciences (SCNAT),

the Swiss Federal Office for the Environment (FOEN),

the Swiss National Science Foundation (SNF; WGMS Bridging Credit),

the United Nations Educational, Scientific and Cultural Organisation (UNESCO),

and the University of Zurich, Switzerland (UZH).

This publication is the most
recent volume in the series:

FLUCTUATIONS OF GLACIERS 1959–1965
Paris, IAHS (ICSI) – UNESCO, 1967

FLUCTUATIONS OF GLACIERS 1965–1970
Paris, IAHS (ICSI) – UNESCO, 1973

FLUCTUATIONS OF GLACIERS 1970–1975
Paris, IAHS (ICSI) – UNESCO, 1977

FLUCTUATIONS OF GLACIERS 1975–1980
Paris, IAHS (ICSI) – UNESCO, 1985

FLUCTUATIONS OF GLACIERS 1980–1985
Paris, IAHS (ICSI) – UNEP– UNESCO, 1988

FLUCTUATIONS OF GLACIERS 1985–1990
Paris, IAHS (ICSI) – UNEP– UNESCO, 1993

FLUCTUATIONS OF GLACIERS 1990–1995
Paris, IAHS (ICSI) – UNEP– UNESCO, 1998

FLUCTUATIONS OF GLACIERS 1995–2000
Zurich, IUGG (CCS) – UNEP– UNESCO, 2005

FLUCTUATIONS OF GLACIERS
2000–2005
(Vol. IX)

A contribution to the
Global Terrestrial Network for Glaciers (GTN-G)
as part of the Global Terrestrial/Climate Observing System (GTOS/GCOS),

the Division of Early Warning and Assessment and the Global Environment Outlook
as part of the United Nations Environment Programme (DEWA and GEO, UNEP),

and the International Hydrological Programme (IHP, UNESCO)

Compiled for the
World Glacier Monitoring Service
by Wilfried Haeberli, Michael Zemp,
Andreas Kääb, Frank Paul and Martin Hoelzle

Department of Geography
University of Zurich
Zurich
Switzerland

wgms

International Council for Science
(Federation of Astronomical and Geophysical Data Analysis Services)
and
International Union of Geodesy and Geophysics
(International Association of Cryospheric Sciences)
and
United Nations Environment Programme
and
United Nations Educational, Scientific and Cultural Organisation
and
World Meteorological Organization

2008

Published jointly by the

Federation of Astronomical and Geophysical Data Analysis Services
of the International Council for Science (FAGS/ICSU)
and the
International Association of Cryospheric Sciences
of the International Union of Geodesy and Geophysics (IACS/IUGG)
and the
United Nations Environment Programme (UNEP)
and the
United Nations Educational, Scientific and Cultural Organisation (UNESCO)
and the
World Meteorological Organization (WMO)

Printed by

Staffel Druck AG
8045 Zurich
Switzerland

ISSN 1997-910X (printed issues)
ISSN 1997-9118 (online issues)

For bibliographic and reference purposes this publication should be referred to as:

WGMS (2008): Fluctuations of Glaciers 2000–2005, Volume IX. Haeberli, W., Zemp, M., Kääb, A., Paul, F. and Hoelzle, M. (eds.), ICSU(FAGS)/IUGG(IACS)/UNEP/UNESCO/WMO, World Glacier Monitoring Service, Zurich, Switzerland.

ICSU (FAGS)
IUGG (IACS)
UNEP
UNESCO
WMO

PREFACE by UNEP

Monitoring the changes of glaciers on a year-to-year basis and providing scientifically sound, concise and easy-to-understand information is a critical function in today's world. Consistent trends on glacier changes are one of the most compelling indicators of climate change and its impacts that can be witnessed all around us.

The basic data collection on glaciers from all over the world, as undertaken for many decades by the World Glacier Monitoring Service and its predecessor organisations, is of critical importance to United Nations Environment Programme and the efforts to continuously keep the state of the global environment under review and provide the world community with improved access to meaningful environmental data and information. As a key component of this, the fourth edition of the Global Environment Outlook (GEO-4), published towards the end of 2007, has also benefited from such data on glacier fluctuations – and so have many other reports that are raising awareness on climate change and related environmental issues such as impacts on water availability, land degradation and the health of people and ecosystems.

This ninth volume of the "Fluctuations of Glaciers", the first report of this century and covering the years 2000 to 2005, continues the series of detailed reports on measurements of world-wide glacier fluctuations. It presents the most up-to-date scientific data on individual terrestrial glaciers in many countries of the world, including their length, area, volume and thickness. The report points to a strong acceleration of glacier melting in those years, with a doubling of the rate compared with the two preceding decades. The observations are consistent with recent accelerating global warming and corresponding energy flux towards the surface of the earth.

The five-yearly comprehensive Fluctuation of Glaciers reports are complemented with the bi-annual Glacier Mass Balance Bulletins, which present the data in a summary form for non-specialists through the use of graphic presentations rather than as purely numerical data. A Global Outlook for Ice and Snow was published by UNEP at the occasion of World Environment Day 2007, while a joint UNEP-WGMS illustrative report on "Global Glacier Changes: facts and figures" was released in September 2008.

UNEP looks forward to continued cooperation with the WGMS while supporting efforts to strengthen the scientific base for environment assessment and early warning – a high-priority issue of global climate change.

Peter Gilruth, Dr.

Director
Division of Early Warning and Assessment, UNEP

PREFACE by UNESCO

Many of our headwater catchments around the world accommodate glaciers and they are most vulnerable towards climate change. They contribute to stream flow in terms of quantity, timing and variability. Their role is significant in the light of worldwide increase of freshwater demand and the potential impacts of future climate change. The effect of snow and ice runoff varies between different climatic regions. While in the mid- and high-latitude areas seasonal snow cover exerts a strong control on runoff variations, in low latitudes glaciers provide the most dominant source of water during the dry season. Therefore, the understanding of glacial changes as a response to changing climate is essential for integrated water resources management.

A broad and worldwide public today recognizes glacier changes as a key indication of regional and global climate and environment change. Observational strategies established by expert groups within international monitoring programmes build on advanced process understanding and new strategies. These strategies ensure rapid development of new technologies and relate them to traditional approaches to apply integrated, multilevel concepts enabling a comprehensive view.

Based on important data collected through an international network of glaciologists, the World Glacier Monitoring Service (WGMS) of the International Association of Cryospheric Sciences with their partners, have been providing quantitative and intelligible information about glacial changes. The current Volume IX (2000–2005) of the "Fluctuations of Glaciers" series has been the backbone of the active compilation of glacier fluctuation data since 1967. It comprises information about changes in glacier length, mass, area, volume and thickness from 723 glaciers of 27 countries/regions, as well as 21 special events and 10 glaciological maps. Volume IX elaborates questions about process understanding, change detection, model validation and environmental impacts in transdisciplinary knowledge transfer to the scientific community and the policymakers.

The International Hydrological Programme (IHP) of UNESCO, within its 7th Phase "Water dependences, systems under stress and societal responses", aims to asses the impact and consequences of global climate change on the biophysical environment and socio-economic conditions of mountain people. Therefore UNESCO IHP, under the theme devoted to mountains, undertakes considerable efforts to improve knowledge of glacial changes in various parts of the world.

UNESCO is honored to support this publication and pleased to congratulate the team for their excellent work.

Siegfried Demuth, Prof. Dr.

Chief
Water Sciences Division, UNESCO

FOREWORD by IACS (IUGG)

Glaciers and ice caps, located in the mountains of the world and in both polar regions, are an important part of the global cryosphere. Indeed, the most recent report by the Intergovernmental Panel on Climate Change (IPCC), published in 2007, recognized the particular significance of glaciers and ice caps in contributing to the observed modern sea-level rise of about 3 mm per year. It is likely that glaciers and ice caps will continue to be important contributors to sea-level rise over the coming century. Such ice bodies are also integral to the hydrological cycle in the mountain regions of the world, and changing discharge from them can affect agricultural practice and also influence the frequency of natural hazards.

The long time series of changes in glacier geometry described in the series of volumes, “Fluctuations of Glaciers”, that the WGMS has produced, is also important evidence of the sign and magnitude of the cryospheric response to climate change. Glaciers, taken worldwide, are decreasing in size.

This volume is number IX in the series of publications titled “Fluctuations of Glaciers”. Each one has covered a five-year period and the present volume relates to the period 2000 to 2005.

For many years, the International Commission on Snow and Ice (ICSI) was the parent organization for the WGMS. In 2007, recognizing the increasing importance of cryospheric change in a warming world, the International Union of Geodesy and Geophysics (IUGG) approved a change in the status and title of ICSI and the establishment of the new IUGG International Association of Cryospheric Sciences (IACS). Glacier monitoring now becomes an important part of IACS activity through its role as the new home of the WGMS.

The Bureau of IACS thanks Professor Wilfred Haeberli and his staff at the WGMS for their efforts in putting this new volume together. It is an important addition to the existing series of volumes on the fluctuations of glaciers.

Julian A. Dowdeswell, Prof. Dr.

Head
Division of Glacier and Ice Sheets, IACS/IUGG

PRELIMINARY REMARKS AND THANKS

The present Volume IX of the "Fluctuations of Glaciers" focuses primarily on the time period from 2000–2005. It was prepared by the World Glacier Monitoring Service (WGMS) and is the most recent addition to the continuing series of publications containing internationally collected and standardized data on current changes in glaciers throughout the world, i.e.,

Vol. I	:	Fluctuations of Glaciers 1959–1965 (P. Kasser)
Vol. II	:	Fluctuations of Glaciers 1965–1970 (P. Kasser)
Vol. III	:	Fluctuations of Glaciers 1970–1975 (F. Müller)
Vol. IV	:	Fluctuations of Glaciers 1975–1980 (W. Haeberli)
Vol. V	:	Fluctuations of Glaciers 1980–1985 (W. Haeberli and P. Müller)
Vol. VI	:	Fluctuations of Glaciers 1985–1990 (W. Haeberli and M. Hoelzle)
Vol. VII	:	Fluctuations of Glaciers 1990–1995 (W. Haeberli, M. Hoelzle, S. Suter and R. Frauenfelder)
Vol. VIII	:	Fluctuations of Glaciers 1995–2000 (W. Haeberli, M. Zemp, R. Frauenfelder, M. Hoelzle and A. Kääb)

The World Glacier Monitoring Service was formed in 1986, by the merger of the Permanent Service on the Fluctuations of Glaciers (PSFG) with the Temporary Technical Secretariat for the World Glacier Inventory (TTS/WGI). It is one of the permanent services of the Federation of Astronomical and Geophysical Data Analysis Services of the International Council for Science (FAGS/ICSU) and the International Association of Cryospheric Sciences of the International Union of Geodesy and Geophysics (IACS/IUGG), the former International Commission on Snow and Ice of the International Association of Hydrological Sciences (ICSI/IAHS). The WGMS operates at the University of Zurich, Switzerland, under the auspices of the United Nations Environment Programme (UNEP), the United Nations Educational, Scientific and Cultural Organisation (UNESCO), and the World Meteorological Organization (WMO). The objective of the publication of the "Fluctuations of Glaciers" at 5-yearly intervals is to reproduce a global set of data which

– affords a general view of glacier changes,
– encourages more extensive measurements,
– invites further processing of results,
– facilitates consultation with the other data sources, and
– serves as a basis for research.

In fact, the publication of this standardized data set is the main driver of the active, international data collection and should be regarded as a working tool for the scientific community, especially with regard to the fields of glaciology, climatology, hydrology, and quaternary geology. Thereby, the printing and shipment of the volumes to several hundred of libraries and institutions all over the world is a core element in securing the long-term availability of the collected data and published maps. The following guidelines and instructions are most relevant for the present volume (Vol. IX) of the "Fluctuations of Glaciers":

1. Forel, F.A. (1895): Instructions pour l'observation des variations des glaciers. Discours préliminaire. Archives des Sciences physiques et naturelles, XXXIV, 209-229.

2. Kaser, G., Fountain, A., and Jansson, P. (2003): A manual for monitoring the mass balance of mountain glaciers with particular attention to low latitude characteristics. A contribution from the International Commission on Snow and Ice (ICSI) to the UNESCO HKH-Friend programme. IHP-VI, Technical Documents in Hydrology, No. 59, UNESCO, Paris. 107 p. + Appendices.

3. Østrem, G. and Stanley, A. (1969): Glacier mass balance measurements. A manual for field and office work. Canadian Department of Energy, Mines and Resources, Norwegian Water Resources and Electricity Board. 125 pp.

4. Østrem, G. and Brugman, M. (1991): Glacier mass balance measurements: a manual for field and office work, NHRI Science Report.

5. UNESCO (1969): Variations of Existing Glaciers. A Guide to International Practices for their Measurement. Technical Papers in Hydrology No. 3.

6. UNESCO/IAHS (1970): Perennial Ice and Snow Masses. A Guide for Compilation and Assemblage of Data for the World Glacier Inventory. Technical Papers in Hydrology No. 1, which has been superseded in part by: Müller, F., Caflisch, T. and Müller, G. (1977): Instructions for Compilation and Assemblage of Data for a World Glacier Inventory, and by: TTS/WGI (1983): Guidelines for Preliminary Glacier Inventories, both issued by the former Temporary Technical Secretariat for the World Glacier Inventory, now WGMS, Department of Geography, University of Zurich.

7. UNESCO 1970/73. Combined heat, ice and water balances at selected glacier basins. Part I: A guide for compilation and assemblage of data for glacier mass balance measurements. Part II: Specifications, standards and data exchange. UNESCO/IAHS Technical Papers in Hydrology 5.

These guidelines have in part been superseded and made more specific by: Instructions for Submission of Data for "Fluctuations of Glaciers 2000–2005", issued by the WGMS in September 2006 (cf. also the Appendix in the present volume).

Modern concepts for integrated climate-related glacier observations have been developed for the Global Terrestrial Network for Glaciers (GTN-G) within the Global Terrestrial/Climate Observing Systems (GTOS/GCOS; Haeberli et al. 2000, Haeberli 2004). Such concepts combine in-situ measurements reported primarily in the present volume with results and information obtained from numerical modeling and remote sensing. The Chapters 6 "The Global Land Ice Measurements from Space initiative (GLIMS)" and 7 "The new ESA project GlobGlacier" give overviews on the activities towards the completion of a global glacier inventory based on satellite images. More details on the integrative, tiered monitoring strategy, global glacier changes, and recent developments related to the international glacier monitoring are provided in Chapter 8 "General Comments and Perspectives for the Future".

The data published in the present volume are also available in digital form. The guidelines for data submission and order as well as meta-data on the available fluctuations series are available on the homepage of the WGMS (http://www.wgms.ch).

The present volume was successfully completed thanks to the cooperation and efforts of the national correspondents and their collaborators. In addition to this work of glaciologists all over the world, the main burden of the undertaking had once more to be borne by the staff members of the central service of the WGMS, located at the Department of Geography of the University of Zurich, Switzerland. Philip Woodworth (FAGS/ICSU), Julian A. Dowdeswell and Georg Kaser (IACS/IUGG), Jaap van Woerden (UNEP), Siegfried Demuth (UNESCO) and Stephan Bojinski (WMO) assisted in ensuring proper international administration and coordination. Special thanks are due to Sabine Baumann, Rachel Carr, Luzia Fischer, Susanna Hoinkes, Eva Huintjes, Björn Kröger and Bruno Seiler for their assistance with data collection, and to Susan Braun-Clarke for carefully editing the English.

K. Echelmeyer (Fairbanks), M. Kuhn (Innsbruck), M.F. Meier (Boulder), J. Oerlemans (Utrecht), G. Østrem (Oslo), V.V. Popovnin (Moscow), L. Reynaud (Grenoble) and R.S. Williams (Reston) have accompanied our work through many years as scientific consultants to the WGMS, covering the important fields of energy balance at the glacier surface, glacier dynamics, modelling of glaciers, glacier mass balance, glacier inventories, statistical analysis of glacier fluctuations and remote sensing of perennial surface ice. The discrete but invaluable long-term assistance and help by these internationally recognized experts is greatly appreciated. With the now planned establishment of a steering committee for the Global Terrestrial Network for Glaciers (GTN-G) within the framework of the Global Terrestrial Observing System, the quality controlling and assurance for WGMS is also likely to receive a new structure.

The printing of this volume was made possible by generous grants from the Swiss National Science Foundation (SNF; WGMS Bridging Credit), the Swiss Federal Office for the Environment (FOEN), the United Nations Educational, Scientific and Cultural Organisation (UNESCO), the Federation of Astronomical and Geophysical Data Analysis Services (FAGS/ICSU), and the Department of Geography of the University of Zurich, Switzerland.

TABLE OF CONTENTS

CHAPTER 1 **INTRODUCTION**

1.1 Preparation of Volume IX of "Fluctuations of Glaciers"

The call-for-data for this volume, including revised guidelines and Excel-based data submission forms, was sent out to the national correspondents by the end of September 2006; one year after the end of the observation period 2000–2005, in order to enable the investigators to properly analyse and publish their data before making it available to the scientific community and the wider public. The call-for-data for the "Fluctuations of Glaciers Vol. IX (2000–2005)" coincided with the one for the „Glacier Mass Balance Bulletin No. 9 (2004–2005)". In addition to the material submitted by the national correspondents, completed, revised and updated data series on glacier mass balance and front variation were collected from the literature. A first draft of this volume's data tables was sent out with the press proof of the „Glacier Mass Balance Bulletin No. 9 (2004–2005)" to the national correspondents and principle investigators for double-checking in January 2008, followed by the correction and update of the data series according to the received feedback as well as by the compilation of the maps, prefaces and foreword of the overarching organisations. The final press proof was sent out to all national correspondents in October 2008. Computer work was done using facilities at the Department of Geography of the University of Zurich, Switzerland.

In order to ensure maximum continuity and comparability within the published data series, only minor changes were introduced relating to the format and content of Volume IX. However, as the received meta-data to the submitted glacier fluctuation data was again of moderate extent, the information was summarised in one chapter for all data tables. The digital information in the WGMS database is the most complete and up-to-date of all, more so even than the data printed in the tables of this volume. Updated information on available data can be found and browsed on the WGMS website (http://www.wgms.ch).

The present Volume IX of the "Fluctuations of Glaciers" contains information on 723 glaciers from 27 countries/regions. Data on "Variations in the Positions of Glacier Fronts" during the period 2000–2005 were received for 605 glaciers in 22 countries/regions, with "Addenda from Earlier Years" for 107 glaciers in 11 countries/regions. "Mass Balance Study Results – Summary Data" for the period 2000–2005 were submitted for a total of 112 glaciers in 21 countries with "Addenda from Earlier Years" for 28 glaciers in 10 countries/regions. Detailed information on "Mass Balance versus Altitude" was made available for 58 glaciers in 16 countries/regions and data relating to "Changes in Area, Volume and Thickness" are presented for 41 glaciers in 11 countries/regions.

The Chapter 4 contains three sections on index measurements from three countries as well as information on 21 special events in 10 countries/regions. Following a well-established tradition, 10 special glacier maps from 5 countries/regions are included in the back pocket of this volume with brief comments on each given in Chapter 5 of the present volume. The World Glacier Monitoring Service is again grateful for the donation of all these maps.

1.2 Organisation of the Present Volume

The following types of data are presented in this volume:

Table A	General Information on the Observed Glaciers
Table B	Variations in the Position of Glacier Fronts, 2000–2005
Table BB	Variations in the Position of Glacier Fronts – Addenda from Earlier Years
Table C	Mass Balance Summary Data, 2000–2005
Table CC	Mass Balance Summary Data – Addenda from Earlier Years
Table CCC	Mass Balance versus Altitude for Selected Glaciers
Table D	Changes in Area, Volume and Thickness
Table F	Index Measurements and Special Events presented in Chapter 4

Sources of data and comments can be found in Chapter 2. Within each data table, the glaciers are organised according to the country where they are situated. Table A provides the user with general information on the glaciers of a particular country or region, and also lists which data are available for these glaciers in other tables. An ALPHABETIC INDEX of glaciers is given at the end of this volume to allow easy location of the data for any glacier within the various tables.

The identification system for glaciers consists of:

(1) a name of up to 15 alphabetical and numerical characters,
(2) a PSFG number of five digits with an alphabetical prefix denoting the country.

Although in some cases it was necessary to abbreviate the names of glaciers, it should always be possible to compare data for any particular glacier in the present volume with data in previous volumes. The PSFG number, as provided by the national correspondents, shall help to identify glaciers with the same, unknown or changing names. The number has to remain the same for every glacier through all the volumes of the "Fluctuations of Glaciers". In most cases the numbers were given to glaciers in some historical sequence and may therefore appear to be somewhat unsystematic. Already in the last volume, the alphabetical prefix denoting the country was adapted from a historically evolved one- or two-digit code to the ISO 2-digit-country code (ISO 3166-1-alpha-2), as proposed by the International Organisation for Standardisation (ISO). However, the abbreviation SU has been maintained for C.I.S. in order to facilitate comparison with former volumes of "Fluctuations of Glaciers".

It is strongly recommended that all data tabulated in Tables A to D be used in consultation with the relevant sections in the text; in the case of Table F, the data are given within the text of Chapter 4. Furthermore, when using or citing data from this volume, we strongly suggest to check and refer to the original sources/references of the data – given in the relevant chapters of the text – for full details on measurement methodologies and background.

In contrast to the previously used system in the "Fluctuations of Glaciers" of classifying the countries according to geographical location, the data in the volumes VIII and IX are arranged alphabetically according to (i) country name and (ii) glacier name.

Country/Region	Prefix	Country/Region	Prefix
Antarctica	AQ	Italy	IT
Argentina	AR	Japan	JP
Austria	AT	Kenya	KE
Bolivia	BO	New Zealand	NZ
C.I.S.	SU	Norway	NO
Canada	CA	Peru	PE
Chile	CL	Poland	PL
China	CN	South Georgia	GS
Colombia	CO	Spain	ES
Ecuador	EC	Sweden	SE
France	FR	Switzerland	CH
Heard and McDonald Islands	HM	Tanzania	TZ
Iceland	IS	U.S.A.	US
India	IN		

CHAPTER 2 **INFORMATION ON THE OBSERVED GLACIERS AND SUBMITTED DATA**

The following section provides an overview on the submitted meta-data, principal investigators, national correspondents, and their sponsoring agencies, as well as publications related to glacier data presented in Tables A–F. Full addresses of the sponsoring agencies and organisations holding original data are given in Chapter 3. The information in this chapter is ordered by country/region.

Additional and well illustrated information can be found in the report on "Global Glacier Changes: facts and figures" (WGMS 2008) jointly published by WGMS and UNEP. The report provides a review on the available data up to 2005, the global distribution of glaciers and ice caps, and their changes since the maximum extents of the so-called Little Ice Age. It is available online at: http://www.grid.unep.ch/glaciers/

2.1 Antarctica (AQ)

Data of Glaciar Bahía del Diablo were submitted by P. Skvarca and Y. Yerrmolin (IAA-DNA).

Selected recent publications on glacier fluctuations on the Antarctic Peninsula and adjacent islands are from Rott et al. (2002), Skvarca and De Angelis (2003), Skvarca et al. (2003), Rau et al. (2004) and Cook et al. (2005).

2.2 Argentina (AR)

Data and information were submitted by L. Espizua (IANIGLA).

Reported investigators of glacier front variations are L. Espizua, F. Díaz, L. Ferri Hidalgo, H. Gargantini, P. Lizana, G. Maldonado and P. Pitte (IANIGLA), and V. Popovnin (for Glaciar De Los Tres; MGU).

Reported investigator of glacier mass balances is J.A. Strelin (UNC) for Martial Este.

Front variations of De Las Vacas, Güssfeldt, Tupungato 01/02/03/04, Peñón and Azufre were derived from Landsat 5 TM and Landsat 7 ETM images, georeferenced based on the Earth Science Database Interface image set (cf. Tucker et al. 2004). Glacier outlines were produced by application of a Normal Difference Snow Index (NDSI) using the methodology described by Dozier (1989). Topographic information was obtained from the SRTM Digital Elevation Model.

Selected recent publications related to Argentinean glacier fluctuations are from Leiva (1999), Espizua (2005), Ferri Hidalgo et al. (2006), Espizua and Maldonaldo (2007), Milana (2007) and Strelin and Iturraspe (2007).

2.3 Austria (AT)

Data were submitted by L.N. Braun (CGBAS), B. Hynek (ZAMG), H. Slupetzky (DGGS), as well as by A. Fischer and M. Kuhn (IMGI).

Front variation information was compiled from publications of the Austrian Alpine Club (OEAV) on behalf of G. Patzelt (OEAV). Complete information on investigators of glacier front variations for the observation period 2000–2005 is given in Patzelt (2002, 2003, 2004, 2004, 2006).

Reported investigators of glacier mass balances are A. Fischer, G. Markl and H. Schneider for Hintereisferner, Jamtalferner and Kesselwandferner; H. Slupetzky (DGGS) for Sonnblickkees; L.N. Braun (CGBAS) for Vernagtferner; R. Böhm, W. Schöner, B. Hynek and C. Kroisleitner (ZAMG) for Goldbergkees, Kleinfleisskees, Pasterzenkees and Wurtenkees.

A partly revised mass balance series of Vernagtferner back to 1965 including winter and summer balances is given in Table CC.

Selected recent publications related to Austrian glacier fluctuations are from Schöner et al. (2000), Paul (2002), Hall et al. (2003), Escher-Vetter et al. (2005), Braun et al. (2007), Koboltschnig et al. (2007), Lambrecht and Kuhn (2007), Schöner and Böhm (2007).

2.4 Bolivia (BO)
Data were submitted by J.C. Mendoza Rodríguez (IHH).

Reported investigators are P. Edouard (IRD), J.C. Mendoza Rodríguez (IHH) and B. Francou (CNRS/IRD) for Chacaltaya, Charquini Sur and Zongo.

In 2005, Chacaltaya was reported to have split into parts.

Selected recent publications on Bolivian glacier fluctuations are from Wagnon et al. (2001) and Sicart et al. (2007).

2.5 C.I.S. (SU)
Data were submitted by V.V. Popovnin (MGU).

Reported investigators are A.A. Aleynikov, Ye.A. Zolotaryov and V.V. Popovnin (MGU) for Djankuat; O. Rototayeva and I.F. Khmelevskoy (IGRAN) for Garabashi; Yu K. Narozhniy (TGU) for Dzhelo, Korumdu, Leviy Karagemsk, Praviy Karagemskiy, No. 125 (Vodopadniy), Leviy Aktru and Maliy Aktru; P.A. Cherkasov, N.E. Kasatkin and K.G. Makarevich (IGNANKaz) for Ts. Tuyuksuyskiy.

Selected recent publications on glacier fluctuations in the C.I.S. are from Solomina (2000), Zeeberg and Forman (2001), Hagg et al. (2004), Ananicheva (2006), Kotlyakov (2007), Bolch (2007), Kotlyakov et al. (2008), Shahgedanova et al. (2008).

2.6 Canada (CA)
Data and information were reported by M.N. Demuth (GSC).

Reported investigators are M.N. Demuth (GSC) for Helm, Peyto and Place; G. Cogley (TU/G) for White and Baby; R.M. Koerner (GSC) for Devon Ice Cap.

Natural Resources Canada (at GSC), through an interdepartmental Memorandum of Agreement with Environment Canada on Glaciology, is responsible for the delivery of a National Glacier-Climate Observing System that measures and evaluates changes in glacier mass balance and related glaciological parameters (length, thickness, surface changes and flow regime). The framework for this Earth Observation system is currently based on an in situ network of 12 glaciers and ice caps located in the Cordillera and Arctic Islands. These sites broadly represent the variation in glacier-climate settings that exist in Canada. Aircraft and orbital remote sensing is used to extend these site perspectives to provide estimates of regional glacier-climate behaviour. Each system is maintained through the collaboration of Geological Survey of Canada, Geomatics Canada and university scientists. Site selection was based on the consensus of a formal working group established during the definition of Canada's GCOS plan for the cryosphere (Agnew et al. 1999, 2002).

New glacier research initiatives include:
The "State and Evolution of Canada's Arctic and Alpine Glaciers" is a component activity of Natural Resources Canada's Climate Change Program, attending the documentation and understanding of long-term changes in Canada's glacier-climate system and the impacts of those changes on freshwater resources and fluxes of glacial origin.
Weblink: http://ess.nrcan.gc.ca/ercc-rrcc/

The "Western Canadian Cryosphere Network" (WC2N) is a consortium of six Canadian universities, two American universities and government and private scientists who are examining the links between climatic change and glacier fluctuations in western Canada.
Weblink: http://wc2n.unbc.ca/

The "IP3 Network for Improved Prediction, Measurement and Use of Water in Cold Regions" is a Canada-wide research network devoted to improving the understanding of surface water and weather systems in cold regions, particularly in Canada's Rocky Mountains and western Arctic regions. Weblink: http://www.usask.ca/ip3/

Selected recent literature providing perspectives on glacier changes include Hopkinson et al. (2001), Moore and Demuth (2001), Demuth and Pietroniro (2002), Moore et al. (2002), Wheate et al. (2002), Shea et al. (2004), Fleming and Clarke (2005), Watson and Luckman (2005), Demuth and Keller (2006), Fisher et al. (2006), Hopkinson and Demuth (2006), Stahl and Moore (2006), Larsen et al. (2007) and Demuth et al. (2008) for Western Canada; and Dowdeswell et al. (2003), Mair et al. (2003), Abdalati et al. (2004), Burgess et al. (2005), Koerner (2005), Paul and Kääb (2005) and Short and Gray (2005) for the Canadian Arctic Islands.

2.7 Chile (CL)
Data were submitted by F. Escobar Caceres (DGA).

Reported investigators are C. Garin, J. Quinteros and F. Escobar Caceres (DGA) for Echaurren Norte.

Selected recent publications were published from Rignot et al. (2003), Carrasco et al. (2005) and Rivera et al. (2007).

2.8 China (CN)
Data were submitted by Z. Li and H. Yang (CAREERI).

Reported investigator of glacier front variations is Z. Jin (CAREERI) for Lapate No. 51 and Urumqihe S. No. 1.
Reported investigator of glacier mass balances is H. Yang (CAREERI) for Urumqihe S. No. 1.

An overview of the fluctuations of Urumqihe S. No. 1 was published from Wang et al. (2007). Other selected recent publications on glacier fluctuations in China are by Su and Shi (2002), Xiao et al. (2007) and Li et al. (in press).

2.9 Colombia (CO)
Data (in Tables B and D) were compiled within a Master thesis by S. Baumann at GIUZ with support from J.L. Ceballos Liévando (IDEAM) and J. Ramirez Cadenas (INGEOMINAS).

Selected recent publications on Colombian glacier fluctuations are from Ceballos et al. (2006), Huggel et al. (2007), Ceballos and Tobon (2008).

2.10 Ecuador (EC)
Data and information were submitted by B. Cáceres Correa (INAMHI).

Reported investigators are B. Francou (CNRS/IRD) and B. Cáceres Correa (INAMHI) for Antizana 15 alpha.

In 2006, the glacier inventory of 1998 by Jordan and Hastenrath (1998) was updated based on field observations and aerial photographs. The new inventory of 2006 resulted in an overall Ecuadorian glacier cover of about 70 km^2, and an area loss of 27 km^2 (or 28%) since 1998 (Cáceres et al. 2008). Other recent publications on Ecuadorian glacier fluctuations are by Francou et al. (2000, 2004).

2.11 France (FR)
Data were submitted by C. Vincent (CNRS).

Reported investigators are E. Thibert and D. Richard (CEMAGREF) for Blanc and Sarennes; C. Vincent, M. Vallon and L. Reynaud (CNRS) for Argentière, Bossons, Gébroulaz, Mer de Glace and Saint Sorlin; Pierre René (AM) for Ossoue.

Selected recent publications on French glacier fluctuations are from René (2000), Vincent (2002), Vincent et al. (2004, 2005), and Thibert et al. (2008).

2.12 Germany (DE)
L. Braun (CGBAS) reported that there were no glacier fluctuation data available for the period 2000–2005.

Selected recent publications on the Bavarian glaciers are from Hagg (2006a, b; 2008).

2.13 Heard and McDonald Islands (HM)

Data were submitted by D. Thost (AAD).

General information about glaciers on Heard Islands was updated according to Ruddell (2006). Recent publications on glacier fluctuations on Heard Islands are from Ruddell (2006) and Thost and Truffer (2008).

2.14 Iceland (IS)

Data and information were submitted by F. Pálsson (IES) and O. Sigurðsson (NEAHS).

Reported investigators of glacier mass balances are O. Sigurðsson (NEAHS) for Hofsjökull; H. Björnsson and F. Pálsson (IES) and H. Haraldsson (NPC) for Breidamerkurjökull, Brúarjökull, Dyngjujökull, Eyjabakkajökull, Köldukvíslarjökull, Langjökull S. Dome and Tungnaárjökull.

Reported investigators of glacier front variations are Á. Hjartarson (IGS-NEA) for Gljufurarjökull; Á. Sólbergsson (IGS-NEA) for Leirufj. Jökull; B. Kristinsson (IGS-NEA) for Geitlandsjökull; B. Oddsson (IGS-NEA) for Kvislajökull; B. Skúlason (IGS-NEA) for Satujökull; E.H. Haraldsson (IGS-NEA) for Kirkjujökull, Blagnipujökull and Lodmundarloekul; E. Guðmundsson (IGS-NEA) for Flaajökull and Heinabergsjökull; G. Jóhannesson (IGS-NEA) for Oldufellsjökull; G. Gunnarsson (IGS-NEA) for Falljökull, Skalafellsjökull, Svinafellsjökull and Virkisjökull; H.B. Harðarson (IGS-NEA) for Tungnaarjökull; H. Haraldsson (IGS-NEA) for Hyrningsjökull; H. Jónsson (IGS-NEA) for Sidujökull E M177, Skeidararjökullen W and M, Solheimajökull W; H. Davids (IGS-NEA) for Morsarjökull; H. Björnsson (IES/IGS-NEA) for Breidamjökullen W.A and W.C, Fjallsj. FITJAR, BRMFJ, and G-SEL, Hrutarjökull and Kviarjökull; H.J. Brynjólfsson (IGS-NEA) for Kotlujökull; I. Aðalsteinsson (IGS-NEA) for Kaldalonsjökull; I. Kaldal (IGS-NEA) for Slettjökull; J. Gissurarson (IGS-NEA) for Oldufellsjökull, K.E. Hjartarson (IGS-NEA) for Gljufurarjökull; K.G. Eyþórsdóttir (IGS-NEA) for Jökullkrokur; L. Jónsson (IGS-NEA) for Mulajökull S and Nauthagajökull; O. Sigurðsson (NEAHS/IGS-NEA) for Kotlujökull and Skeidararjökull M; R.F. Kristjánsson (IGS-NEA) for Morsarjökull, Skeidararjökullen E1, E2 and E3; S. Sigurðsson (IGS-NEA) for Rjupnabrekkujökull; S. Þórhallsson (IGS-NEA) for Breidamjökull E.B; T. Theodórsson (IGS-NEA) for Gigjökull, Hagafellsjökullen E and W; Þ. Hjartarson (IGS-NEA) for Gljufurarjökull; Þ. Jóhannesson (IGS-NEA) for Reykjafjardarjökull.

A glacier inventory for Iceland from approximately the year 2000 was submitted to the GLIMS database. Selected recent publications related to Icelandic glacier fluctuations are from Björnsson et al. (2002), Kirkbride (2002), Sigurdsson (2005) and Sigurdsson et al. (2007).

2.15 India (IN)

Data were submitted by C.V. Sangewar (IGS). Mass balances of Chhota Shigri were submitted by P. Wagnon (IRD).

Unfortunately, the involved investigators and institutions were not able to reach a consensus on the origin of the data.

Mass balance measurements and a comparision of mass balance estimates from field and remote sensed data of Chhota Shigri were published by Wagnon et al. (2007) and Berthier et al. (2006), respectively.

2.16 Italy (IT)

Data and information were submitted by M. Meneghel (DGUP).

Reported investigators of glacier front variations are A. Fusinaz (CGI) for Pre de Bar and Toules; A. Borghi (SGL) for Tresero Lingua Mer.; A. Viotti (CGI) for Chavannes; A. Mazza (CGI) for Aurona and Belvedere (Macugnaga); A. Cerutti (CGI) for Brenva; C. Voltolini (CGI) for Vedr. La Mare, Vedr. Rossa and Vedr. Venezia; E. Massa Micon, G. Bosio, R. Miravalle and M. Nicolino (CGI) for Aouille; F. Pollicini (CGI) for Goletta; F. Rodeva (SGL) for Pisgana Occ.; F. Marchetti (SAT) for Amola, Cornisello Mer., Lares, Lobbia, Mandrone, Nardis Occ. and Niscli; F. Rogliardo (CGI) for Bessanese; G. Casartelli (CGI) for Forni and Pizzo Scalino; G. Franchi (CGI) for Malavalle, Neves Or., Pendente, Quaira Bianca; G. Cibin (CGI) for Collalto, Gigante Centr. and Occ.; G. Fontana (SGL) for Dosegu; G. Perini (CGI) for Vedr. Alta, Antelao Inf. Occ. and Sup., Cevedale Principale, Cevedale Forcola and Vedr. Lunga; G. Stella (CGI) for Ventina; G. Catasta (SGL) for Fellaria Occ.; L. Bolognini (SGL) for Tresero Lingua Mer.; L. Carturan (SAT) for Careser; L. Mercalli (SMI) for Basei and Ciardoney; M.Cesco Cancian (CGI) Antelao Inf. Occ., Fradusta and Travignolo; M. Tesoro (CGI) for Grandes Murailles; M. Maggioni (SGL) for Venerocolo; M. Monfredini (SGL) for Pisgana Occ.; M. Pala (SGL) for Pisgana Occ.; M. Pecci (IMONT) for Calderone; M. Tron (CGI) for Agnello Mer.; M. Varotto (CGI) for Marmolada Centr.; M. Meneghel (CGI) for Croda Rossa and Tessa; P. Pagliardi (SGL) for Pisgana Occ. and Venerocolo; R. Ossola (CGI) for Hohsand Sett. (Sabbione Sett.); R. Scotti (SGL) for Fellaria Occ.; R. Bezzi (SAT) for Presanella; R. Garino (CGI) for Rutor; R. Serandrei Barbero (CGI) for Lana, Rosso Destro and Valle del Vento; S. Rossi (CGI) for Sforzellina; S. Alberti (SGL) for Caspoggio; S. Bettola (SGL) for Dosegu; U. Mattana (CGI) for Marmolada Centr., U. Ferrari (CGI) for Rosim, Zai di Dentro, Zai di Mezzo and Zai di Fuori; V. Bertoglio (CGI) for Lauson; W. Monterin (CGI) for Lys and Piode.

Reported investigators of glacier mass balances are R. Seppi (SAT) for Careser; L. Mercalli, D. Cat Berro and F. Fornengo (SMI) for Ciardoney; R. Dinale, C. Oberschmied and M. Munari (UI/HA) for Fontana Bianca; G. Kaser and R. Prinz (DGI) for Verdretta Lunga; G.L. Franchi and G.C. Rossi (CGI) for Malavalle and Pendente; M. Pecci, P. D'Aquila, A. Marino, M. Ciucci and S. Bellagamba (IMONT/ISPESL) for Calderone.

In 2000, Calderone fragmented into two ice aprons which are separated by limestone outcropping for a few metres from the ice. The glacier has been considered as a whole for the calculation of the glacier mass balance (see Table C and CCC). The mass balance calculated by the direct glaciological method is about 30% less negative than the one based on laser GPS measurements (performed in summer 2007 and 2008), which might be explained by intensified ablation along the rock-ice interface not covered by the direct glaciological method.

Winter mass balance at Ciardoney is usually estimated at the end of May or beginning of

June based on snow depth and density measurements at five sites on the glacier. In the first half of September, the summer mass balance is estimated based on snow and ice ablation measurements at five stakes; in addition the glacier front variation is measured.

Selected recent publications related to Italian glacier fluctuations are from D'Orefice et al. (2000), Balerna et al. (2001), D'Alessandro et al. (2001), Pecci (2001, 2005), Pecci et al. (2001), Diolaiuti et al. (2005), Carturan and Seppi (2007), Mercalli and Berro (2007), Citterio et al. (2007), Pelfini et al. (2007) and Piccini et al. (2007).

2.17 Japan (JP)
Data from Hamaguri Yuki perennial snowfield were submitted by K. Fujita (DHAS).

2.18 Kenya (KE)
Data were submitted by S. Hastenrath (UWAOS).

Selected recent publications related to glaciers fluctuations on Mount Kenya are from Hastenrath and Polzin (2004) and Hastenrath (2005a, b), Caukwell and Hastenrath (2006), Rostom and Hastenrath (2007).

2.19 New Zealand (NZ)
Data and information were submitted by T.J. Chinn (APPC).

Reported investigators of glacier front variations are T.J. Chinn (APPC) for Adams, Almer/Salisbury, Andy, Ashburton, Axius, Balfour, Brewster, Butler, Cameron, Classen, Colin Campell, Crow, Dart, Dispute, Donne, Douglas (Kar.), Evans, Fitzgerald, Fox, Freshfield, Godley, Grey and Maud, Gunn, Hooker, Horace Walker, Ivory, Kahutea, La Perouse, Lambert, Lawrence, Leeb-Lornty, Lyell, Marion, Marmaduke Dixon, Mathaias, Mueller, Murchison, Park Pass, Ramsay, Reischek, Sale, Siege, Snow White, Snowball, South Cameron, St. James, Strauchon, Tasman, Tewaewae, Thurneyson, Victoria, Whataroa, Whitbourne, White, Whymper, Wilkinson and Zora; I. Owens (DGUC) for Franz Josef.

Reported investigators of glacier mass balances are B. Anderson (SGEES), N.J. Cullen (DGUO-NZ), S. Fitzsimons (DGUO-NZ), L. George (DGUO-NZ), A. Mackintosh (SGEES) and D. Stumm (DGUO-NZ/GIUZ) for Brewster.

Qualitative glacier front variations are given in Table B. The assessments have been made from oblique aerial photographs taken on annual light aircraft flights made at about 3000 m a.s.l. for annual end-of -summer-snowline (EOSS) surveys on a set of 50 selected glaciers. The full EOSS data series 1977–2005 is given in Chapter 4 'Index Measurements and Special Events'. Full details on these observations are published in Chinn (1995) and Chinn et al. (2005a, 2006).

Over the survey the period (2000–2005), all of the glaciers of New Zealand have averaged near zero mass balances. However, the glacier responses have been been spectacularly contrasting, depending on the glacier reaction time and whether or not a proglacial lake is present.

Three dominant and conflicting processes occur simultaneously:
• The fast response glaciers (which have gained an equilibrium with the climate of the past few decades) are undergoing periodic expansions and retreats from positive balances, best seen in the record of extremely reactive Franz Josef Glacier. All of the other glaciers follow these trends according to their individual response times.

• The slow response glaciers have had perceptible thickening in their upper trunks. In some cases, these pulses enter the collapsing ice of thermokarst tongues, still in readjustment from the climate a century ago. This situation produces a case of simultaneous retreat and advance!

• Most of the large debris-covered valley glaciers are continuing to downwaste from the climate of a century ago and have entered a phase of acceleration and devastatingly spectacular proglacial lake growth. These glaciers have been divorced from the climate signals at their termini, but continue to reflect balance changes in their upper feeders. Observations of the upper feeders to the Tasman, Murchison, Classen and Godley glaciers, well beyond the influence of the lakes, all show evidence that the present ice is lowering from a recent thickening that built moraine lateral.

Current work on New Zealand glaciers is concentrated on direct mass balance measurements, changes in glacier size by remote sensing, and GPS measurements and glacier modelling. In 2004, a new mass balance monitoring programme was started with on-site support by the WGMS on Brewster Glacier. Recent publications related to glacier fluctuations in New Zealand are from Chinn (2001), Clare et al. (2002), Chinn et al. (2005b) and Hoelzle et al. (2007).

2.20 Norway (NO)
Data were submitted by H. Elvehøy (NVE), B. Gadek (SUP), I. Sobota (NCU) and J. Kohler (NPI), under the coordination of J.O. Hagen (DGUO-NO).

Reported investigators of glacier front variations are P. Solnes (NVE) for Austerdalsbreen; K. Åsen (NVE) for Bergsetbreen and Stegholtbreen; S. Winkler (IGUW) for Bødalsbreen, Bøverbreen, Brenndalsbreen, Kjenndalsbreen and Storgjuvbreen; L. Vedaa (NBF) for Bøyabreen; G. Knutsen and J. Flatebø (NVE) for Bondhusbreen; G. Knutsen and J. Flatebø (NVE) for Botnabreen; B. Kjøllmoen, N. Haakensen and O.M. Tøndberg (NVE) for Breidalsblikkbrea; E. Briksdal (NVE) for Briksdalsbreen; M.B. Buer (NVE) for Buarbreen; H. Elvehøy and M. Jackson (NVE) for Engabreen; B. Kjøllmoen, N. Haakensen and O.M Tønsberg (NVE) for Gråfjellsbrea; L. Kolondra (SUP) for Hansbreen; H. Elvehøy, L. Høydal, L.M. Andreassen and M. Jackson (NVE) for Hellstugubreen; I. Soboda (NCU) for Irenebreen and Waldemarbreen; B. Kjøllmoen, C. Nyheim and L.M. Andreassen (NVE) for Koppangsbreen; B. Kjøllmoen, E. Alfnes, N. Haakensen and O.M. Tønsberg (NVE) for Langfjordjøkul; B. Kjøllmoen, L.M. Andreassen and M. Jackson (NVE) for Leirbreen; A. Nesje (DES) for Midtdalsbreen; H. Elvehøy and N. Haakensen (NVE) for Nigardsbreen; H. Elvehøy and S. Villmones (NVE) for Rembesdalsskåka; B. Kjøllmoen and C. Nyheim (NVE) for Steindalsbreen; L.M. Andreassen and N. Haakensen (NVE) for Storbreen; M. Jackson and N. Haakensen (NVE) for Styggedalsbreen; A.L. Brobak, K. Weichart and L. Vedaa (NBF) for Supphellebreen.

Reported investigators of glacier mass balances are J. Kohler (NPI) for Austre Brøggerbreen, Kongsvegen and Midtre Lovénbreen; D. Puczko (PAS), J. Jania (SUP), M. Grabiec (SUP), P. Glowacki (PAS) and L. Kolondra (SUP) for Hansbreen; I. Sobota (NCU) for Irenebreen and Waldemarbreen; R. Engeset and colleagues (NVE) for Ålfotbreen, Austdalsbreen, Breidalblikkbrea, Engabreen, Gråfjelsbrea, Gråsubreen, Hansebreen, Hardangerjøkulen, Hellstugubreen, Langfjordjøkelen, Nigardsbreen, Rundvassbreen, Storbreen and Storglombreen.

An updated front variation series 1897–2005 of Briksdalsbreen is published in Table BB. Full details and methods are published in NVE (2007, Chapter 13-2).

Detailed information on the glaciers investigated through the NVE is published in their annual report series: NVE (2003a, 2003b, 2004, 2005, 2006; and earlier issues). Other selected recent publications related to Norwegian glacier fluctuations are from Jania et al. (2002), Hagen et al. (2003), Pälli et al. (2003), Andreassen et al. (2005), Sobota and Grzes (2006), Kääb (2007), Sobota (2007a, b) and Nesje et al. (2000, 2008).

2.21 Peru (PE)

Data were submitted by A. Raissig (GIUZ) and J. Gómez (INRENA) on behalf of M. Zapata Luyo (INRENA).

Reported investigators for glacier front variations are J. Gómez, A. Cochachin and M. Zapata Luyo (INRENA) for Broggi, Uruashraju, Gajap-Yanacarco, Pastoruri, Yanamarey, Artesonraju and Shallap; J. Gómez, A. Cochachin and M. Zapata Luyo (INRENA) and R. Gallaire (IRD-PE) for Shullcon.

Reported investigators for glacier mass balances are J. Gómez, and A. Cochachin (INRENA) for Yanamarey and Artesonraju.

Selected recent publications related to Peruvian glacier fluctuations are from Kaser et al. (2003), Georges (2004), Racoviteanu et al. (2007, 2008) and Vuille et al. (2007).

2.22 Poland (PL)

Data and information of the glacierets in the Tatra Mountains were submitted by B. Gadek (SUP).

Reported investigators of glacierets in the Tatra Mountains are Z. Kijkowska-Wiślińska, M. Wiśliński, M. Maciejewski and A. Wiśliński (MPG) for Pod Cubryna; A. Wiśliński (MPG) for Mieguszowieckie; Z. Kijkowska-Wiślińska, M. Wiśliński, J. Dzierżek and A. Wiśliński (MPG) for Pod Bula.

Recent related literature are from Wiśliński (1985, 2002) and Ciupak et al. (2005).

2.23 South Georgia (GS)

Data on glacier front variations based on satellite image, aerial photographs, ground photo and field surveys were submitted by J.E. Gordon, V.M. Haynes and A. Hubbard (UASE). Details are published in Gordon et al. (2008).

2.24 Spain (ES)

Data were submitted by A. Pedrero Muñoz (I75SA) on behalf of M. Arenillas (I75SA) and E. Martinez de Pisón (UAM).

Reported investigator of glacier front variations is G. Cobos Campos (MMA) for Alba, Aneto, Balaitus SE, Barrancs, Brecha Latour, Clot de Hount, Coronas, Greguena N and S, Infierno E, W and WW, La Paul, Las Frondellas, Llardana, Llosas, Los Gemelos, Maladeta, Marborecilindro, Perdido Inf. and Sup., Posets, Punta Zarra, Salencas, Tapou and Tempestades.

Reported investigators of glacier mass balances are M. Arenillas and A. Pedrero Muñoz (I75SA) as well as G. Cobos Campos (MMA) for Maladeta.

The front variations in Tables B and BB are derived from Quick-Bird satellite images of 2004 and 2005 as well as from geodetic ground surveys. The following glaciers disappeared during the observation period of 2000–2005: Alba, Balaitus SE, Brecha Latour, Creguena N and S, Infierno WW, Llosas, Salencas and Tapou. Selected recent publications are from Chueca et al. (2005, 2007) and Lopez-Moreno et al. (2006).

2.25 Sweden (SE)

Data were submitted by P. Holmlund (INK).

Reported investigators of glacier front variations are R. Pettersson and P. Holmlund (INK) for Partejekna, Mikkajekna and Storglaciären; H. Grudd and P. Holmlund (INK) for SE Kaskasatj Gl.; P. Holmlund (INK) for Hyllglaciären, Isfallsglaciären, Ruotesjekna, Salajekna, Suottasjekna and Vartasjekna; M. Nyman (INK) for Rabotsglaciär and Riukojietna.

Reported investigators of glacier mass balances are P. Holmlund and P. Jansson (INK) for Mårmaglaciären, Rabotsglaciär, Riukojietna, Storglaciären and Tarfalaglaciären.

Selected recent publications related to Swedish glacier fluctuations are from Schneeberger et al. (2001), Schneider and Jansson (2004), Holmlund and Jansson (2005), Jansson and Linderholm (2005) and Hock et al. (2007).

2.26 Switzerland (CH)

Data and information were submitted by M. Hoelzle (GIUZ/DGUF).

The programme of front variation observations is largely supported by the EKK and operated by the VAW and in collaboration with many Cantonal Forestry Services, hydroelectric power companies, private persons and Universities. The individual observers and their sponsoring agencies involved in this programme are: VAW – A. Bauder (Gries, Silvretta, Rhône, Giétro, Corbassière Grosser Aletsch, Rhône, Findelen, Trift (Gadmen)), VAW – H. Bösch (Schwarzberg, Allalin, Kessjen) – Forestry Service of Canton Valais – U. Andenmatten (Fee), L. Jörger/S. Walther (Gorner), M. Schmidhalter (Kaltwasser), F. Pfammatter (Rossboden), H. Henzen (Lang), M. Barmaz (Zinal, Moming, Moiry), J. Guex (Valsorey, Tseudet, Boveyre, Saleina), S. Seppey (Cheillon, En Darrey), F. Vouillamoz (Grand Dèsert, Mt. Fort), J.D. Brodard (Tsanfleuron), F. Pralong (Ferpècle, Mt. Miné, Arolla, Tsidjiore Nouve), P. Tscherrig (Turtmann, Brunegg, Bella Tola); Forestry Service of Canton Vaud – J. Binggeli (Sex Rouge, Prapio), J.P. Marlètaz (Paneyrosse, Grand Plan Névé); Forestry Service of Canton Bern – C. von Grünigen (Rätzli), R. Straub (Gauli, Stein, Steinlimmi), U. Vogt (Schwarz, Lämmern), R. Descloux (Gamchi), U. Fuhrer (Alpetli, Blümlisalp), R. Zumstein (Eiger, Tschingel); Forestry Service of Canton Glarus – T. Rageth (Sulz); Forestry Service of Canton Obwalden – S. Hess (Firnalpeli), W. Bissig (Griessen); Forestry Service of Canton St. Gallen – A. Hartmann (Pizol, Sardona); Forestry Service of Canton Graubünden – C. Barandun (Porchabella), G. Berchier (Palü, Paradisino, Cambrena), R. Hefti (Vorab), O. Hugentobler (Paradies, Suretta), M. Frei (Punteglias), M. Stadler (Tiatscha), C. Mengelt (Forno), G. Bott (Calderas, Roseg, Tschierva, Morteratsch), B. Riedi (Lenta), G-C. Feuerstein (Sesvenna, Lischana), U. Maissen (Lavaz), M. Maikoff (Verstankla); Forestry Service of Canton Ticino – C. Valeggia (Basòdino, Val Torta, Cavagnoli, Corno, Croslina, Bresciana, Valleggia); Forestry Service of Canton Uri – M. Planzer (Kehlen, Damma, Rotfirn), P. Kläger (Wallenbur), B. Annen (Griess), J. Marx (Brunni, Tiefen, St. Anna), A. Arnold (Hüfi); private investigators – Flotron AG (Oberaar, Unteraar); J.L. Chabloz (Otemma, Mt. Durand, Breney), H. Boss jun. (Ober Grindelwald, Unter Grindelwald), E. Hodel (Ammerten), J. Ehinger (Trient), H.P. Klauser (Biferten, Glärnisch), U. Steinegger (Limmern, Plattalva), A. Wipf (Dungel, Gelten), P. Aschilier (Fiescher);P. Rovina (Ried); B. Teufen (Scaletta); U. Wittdorf (Mutt), C. Theler (Oberaletsch). Glaciers of the front variation programme that were not observed during the observation period are Albigna, Bis, Lötschberg, Martinets, Mittelaletsch, Ofental, Orny, Pierredar, Rosenlaui, Tälliboden, and Zmutt.

The investigators and their sponsoring agencies of glaciers with mass balance series are as follow: A. Bauder and M. Funk (VAW) for Gries and Silvretta; G. Kappenberger (G.K.) and G. Casartelli (G.G.) for Basodino; H. Machguth (GIUZ) and M. Hoelzle (GIUZ/DGUF) for Findelen. Recent comparisons with geodetically derived volume changes have shown that the mass balance measurements of Silvretta (Table C and CCC) have been systematically too positive by several decimetres w.e. per year (cf. Huss et al. in press; A. Bauder pers. comm.). An entirely revised mass balance series with information on corresponding errors and corrections is expected to be published in the next issues of the “Glacier Mass Balance Bulletin” and “Fluctuations of Glaciers” series. For the first time data from Findelengletscher are included in the data sheet. The corresponding data from stake and pit observations are not yet calibrated with geodetic methods. Findelengletscher is situated in the Southern Wallis, Swiss Alps (Mattertal). Process studies focusing on accumulation processes are currently running on this glacier (Machguth et al. 2006b).

The most recent Swiss glacier monitoring data are published in Herren and Bauder (2008). The long-term volume change has been determined for 19 glaciers in the Swiss glacier monitoring network (see Table D, Bauder et al. 2007). The evaluation of these 19 glaciers revealed a total ice volume loss of about 13 km^3 since the 1870s, of which 8.7 km^3 occurred since the 1920s and 3.5 km^3 since the 1980s. Decadal mean net balance rates for the periods 1920–60, 1960–80 and 1980 to present are -0.29, -0.03 and -0.53 m w.e. per year, respectively. The mass balance of Grubengletscher was reconstructed with photogrammetry and by applying a kinematic ice-flow model (Kääb 2001). A study by (Sugiyama et al. 2007) showed the past and future evolution of Rhonegletscher by using a newly developed flowline model, which included the shape effects more accurately than previous models. At Unteraargletscher the thickness distribution was determined by ground penetrating radar measurements (Bauder et al. 2003). Huss et al. (2007a) investigated retreat scenarios for the same glacier by using a combined ice-flow and mass-balance model. The model was validated for the period 1961 to 2005 and showed a good agreement between modelled and measured evolution of surface geometry. Glacier changes were investigated by neural networks using high-resolution multiproxy reconstructions of temperature and precipitation and glacier length variations reconstructed from different sources (Steiner et al. 2005 and 2006, Nussbaumer et al. 2007a and b, Steiner et al. 2008a and b, Zumbühl et al. 2008). Larger glacier ensembles using length change or inventory data were investigated in several studies (e.g. Hoelzle et al. 2003, Paul et al. 2004, Zemp et al. 2006, Haeberli et al. 2007, Hoelzle et al. 2007, Paul et al. 2007a and b, Zemp et al. 2007 and 2008). Automated glacier mapping from multi-spectral satellite data has been used in combination with a digital elevation model (DEM) and geo-informatic techniques to create a new glacier inventory for Switzerland (Paul et al. 2002, Kääb et al. 2002, Paul et al. 2004). Several glacier studies were related to natural hazards, in particular to glacier lake outbursts and ice avalanches (Huggel et al. 2002a and b, 2003, 2004a and b, Raymond et al. 2003, Pralong et al. 2005, Pralong and Funk 2005, Huss et al. 2007b). In addition, many studies focused on the measurement and modelling of glacier energy and mass balance on mainly three glaciers: Arolla (Brock et al. 2000a, Brock et al. 2000b, Hubbard et al. 2000, Strasser et al. 2004, Pellicciotti et al. 2005), Morteratsch (Oerlemans 2000, Oerlemans and Klok 2002, Klok and Oerlemans 2002), and Findelen (Machguth et al. 2006a, Paul et al. 2008).

2.27 Tanzania (TZ)

Ice cover and area changes of Kilimanjaro (see Table D) are taken from Cullen et al. (2006).

2.28 U.S.A. (US)

Data were submitted by W.R. Bidlake (USGS-T).

Reported investigator of glacier front variations is M. Pelto (NCD) for Boulder, Columbia (2057), Daniels, Deming, Easton, Foss, Ice Worm, Lower Curtis, Lynch, Rainbow, Watson and Yawning.

Reported investigators of glacier mass balances are W.R. Bidlake (USGS-T) for South Cascade; D. Trabant (USGS-F) for Wolverine; J. Riedel (NPNC) for Noisy Creek, North Klawatti, Sandalee and Silver; M. Pelto (NCD) for Columbia (2057), Daniels, Easton, Foss, Ice Worm, Lemon Creek, Lower Curtis, Lynch, Rainbow, Sholes and Yawning.

Selected recent publications related to glacier fluctuations in the U.S.A. are from Pelto and Hedlund (2001), Arendt et al. (2002), Meier and Dyurgerov (2002), Krimmel (2002), Bidlake et al. (2004, 2005, 2007), Pelto and Hartzell (2004), Truffer et al. (2005), Pelto (2006, 2007a, b), Josberg et al. (2007), and Larsen et al. (2007).

CHAPTER 3 **SPONSORING AGENCIES AND NATIONAL CORRESPONDENTS FOR THE GLACIER FLUCTUATIONS**

3.1 General Remarks

The information in the present volume was supplied by national correspondents of the WGMS and individual glaciological workers. For operational and efficiency reasons, the number of correspondents per country must be limited to one. In each country, the national correspondent is responsible for coordinating the collection and submission of data with individual investigators. Individual glaciologists are therefore asked to use this “channel” for submitting their data. Only in extraordinary cases can the WGMS accept data which did not arrive via the national correspondent.

The tabulations in Tables A to F are intended to be useful to the glaciological community. However, these data should not be used uncritically; it would be advisable for users to consult WGMS about the existence of extra, unpublished, archival material and to consult with individual investigators and sponsoring agencies. In order to facilitate contacts with the various bodies involved, a key to abbreviations used in the text for sponsoring agencies, together with their addresses and those of the national correspondents is given in the following section. In almost all cases it can be assumed that the data are held by the sponsoring agencies.

3.2 Sponsoring Agencies and Sources of Data for the Various Countries

Antarctica (AN)

IAA-DNA	see IAA-DNA – Argentina (AR)

Argentina (AR)

CADIC-CONICET	Centro Austral de Investigaciones Científicas Casilla de Correo 92 AR-9410 Ushuaia, Tierra de Fuego
CIIN	Centro de Investigaciones Interdisciplinarias de Neuquen Rivadiria 153, 6B AR-8300 Neuquen
UNC	Convenio DNA – UNC Departamento de Geología Básica Facultad de Ciencias Exactas Físicas y Naturales Universidad Nacional de Córdoba Avda. Vélez Sarsfield 1611 AR-X5016 GCA Córdoba

IAA-DNA	Instituto Antártico Argentino Cerrito 1248 AR-1010 Ciudad de Buenos Aires
IANIGLA	Instituto Argentino de Nivología, Glaciología y Ciencias Ambientales CONICET Casilla de Correo 330 AR–5500 Mendoza
UHG	see UHG – Germany

Australia (AU)

AAD	Australian Antarctic Division Antarctic Climate & Ecosystems CRC University of Tasmania Private Bag 80 Hobart, AU-7001 Tasmania

Austria (AT)

CGBAS	see CGBAS – Germany
DGI	Department of Geography University of Innsbruck Innrain 52 AT–6020 Innsbruck
DGGS	Department of Geography and Geology University of Salzburg Hellbrunnerstrasse 34 / III AT–5020 Salzburg
IMGI	Institute for Meteorology and Geophysics University of Innsbruck Innrain 52 AT–6020 Innsbruck
OEAV	Oesterreichischer Alpenverein (Austrian Alpine Club) Wilhelm Greil Strasse 15 AT–6020 Innsbruck

ZAMG	Zentralanstalt für Meteorologie und Geodynamik Hohe Warte 38 AT–1190 Vienna

Bolivia (BO)

CNRS	see CNRS – France
IHH	Instituto de Hidráulica e Hidrología Universidad Mayor de San Andrés P.O. Box 699 BO–La Paz
IRD	see IRD – France
SENAMHI	Servicio Nacional de Meteorología e Hidrología P.O. Box 10993 BO–La Paz

Bulgaria (BG)

DUT	see DUT – Germany

C.I.S. (SU)

IGNANKaz	Institute of Geography National Academy of Sciences of Kazakh Republic Pushkin Str. 99 KZ–480100 Alma Ata
IGNANKir	Institute of Geology National Academy of Sciences of Kirghiz Republic Erkindik Boulevard, 30 KG–720481 Bishkek
IGRAN	Institute of Geography Russian Academy of Sciences Staromonetny, 29 RU–109017 Moscow
IVRAN	Institute of Volcanology Russian Academy of Sciences Piyp Boulevard, 9 RU–683006 Petropavlovsk-Kamchatskiy

KGM	State Agency for Hydrometeorology for the Government of the Krighiz Republic (Kirghizgidromet) Karasuyskaya 1 KG–720017 Bishkek
MGU	Moscow State University Geographical Faculty Leninskiye Gory RU–119992 Moscow, Russia
SANIGMI	Central Asian Regional Research Hydrometeorological Inst. Observatorskaya, 72 UZ–700052 Tashkent
SKGM	North Caucasian Regional Hydrometeorology Department (Sevkavgidromet) Yerevanskaya, 1/7 RU–344025 Rostov/Don
TGU	Tomsk State University Laboratory of Glacioclimatology Lenin Str., 36 RU–634050 Tomsk

Canada (CA)

BCH	British Columbia Hydro Hydrology Department 970 Burrard Street CA–Vancouver, BC, V6Z 1Y3
GSC	Natural Resources Canada Geological Survey of Canada Terrain Sciences Division 601 Booth Street CA–Ottawa, ON, K1A 0E8
MUN/G	Memorial University of Newfoundland Department of Geography CA–Saint John’s, NF, A1B 3X9
NHRI/CGVMAN	National Hydrology Research Institute Canadian Glacier Variations Monitoring and Assessment Network 11 Innovation Boulevard CA–Saskatoon, SK, S7N 3H5

TU/G	Trent University Geography Department P.O. Box 4800 CA–Peterborough, ON, K9J 7B8

Chile (CL)

CECS	Centro de Estudios Científicos Avda. Prat 514 CL–Valdivia
DGA	Dirección General de Aguas Morandé 59 CL–Santiago

China (CN)

CAREERI	Cold and Arid Regions Environment and Engineering Research Institute, Chinese Academy of Sciences (CAS) 260 West Donggang Road CN–730 000 Lanzhou
LIGG	Lanzhou Institute of Glaciology and Geocryology Chinese Academy of Sciences CN–730 000 Lanzhou

Colombia (CO)

IDEAM	Instituto de Hidrología, Meteorología y Estudios Ambientales Subdirección de Geomorfología y Suelos Diagonal 97 No. 17–60, Piso 3 CO–Bogotá
INGEOMINAS	Instituto Colombiano de Geología y Minería Observatorio Vulcanológico y Sismológico de Manizales Grupo de Glaciología Av. 12 de Octubre No. 15–47 CO–Manizales

UCALDAS	Universidad de Caldas Departamento de Geología Calle 65 No. 26–10 CO–Manizales

Ecuador (EC)

INAMHI	Instituto Nacional de Meteorología y Hidrología P.O. Box EC–16 310 Quito
IRD	see IRD – France
CEMAGREF	Snow Division – ETNA Ministry of Agriculture Domaine Universitaire, BP 76 FR–38402 Saint Martin d'Hères, Cedex
CNRS	see CNRS – France

France (FR)

AM	Association Moraine Village FR – 31110 Poubeau
CEMAGREF	Snow Division – ETNA Ministry of Agriculture Domaine Universitaire, BP 76 FR–38402 Saint Martin d'Hères, Cedex
CNRS	Laboratory of Glaciology and Environmental Geophysics (L.G.G.E.) Domaine Universitaire, BP 96 FR–38402 Saint Martin d'Hères, Cedex
IRD	Institut de Recherche pour le Développement P.O. Box 96 FR–38402 St-Martin d'Hères Cedex
PNE	Parc National des Ecrins FR–38740 Entraignes

Germany (DE)

CGBAS	Commission for Glaciology Bavarian Academy of Sciences Alfons-Goppel-Str.11 DE–80539 Munich
DUT	Technische Universität Dresden Institut für Geographie DE–01062 Dresden
FGUT	Fachbereich Geowissenschaften Universität Trier DE–54296 Trier
IGUW	Institut für Geographie Universität Würzburg Am Hubland DE-97074 Würzburg
IPG	Institut für Physische Geographie Universität Freiburg Werderring 4 DE–79085 Freiburg

Greenland (GL)

GEUS	The Geological Survey of Denmark and Greenland (GEUS) Thoravej 8 DK–2400 Copenhagen NV

Heard and McDonald Islands (HM)

AAD	see AAD – Australia

Iceland (IS)

IES	Institute of Earth Sciences University of Iceland Sturlugata 7, Askja IS - 101 Reykjavík

IGS-NEA	Iceland Glaciological Society National Energy Authority Grensásvegi 9 IS-108 Reykjavík
NEAHS	National Energy Authority Hydrological Service Orkustofnun Grensasvegi 9 IS–108 Reykjavik
NPC	National Power Company Háleitisbraut 68 IS – 103 Reykjavík

India (IN)

CNRS	see CNRS – France
IGS	Glaciology Division Geological Survey of India Vasundara Complex, Sector E, Aliganj IN - 226024 Lucknow
IRD	see IRD – France
HIGH-ICE	HIGH-ICE INDIA 409, Slylark Building Nehru Palace IN-110019 New Delhi
RSD-BIT	Remote Sensing Division BIT Extension Centre Jaipur BMBSTC, Statue Circle IN-302005 Jaipur
SES	School of Environmental Sciences Jawaharlal Nehru University INDIA – New Dehli 110067

Indonesia (ID)

TAMU	see TAMU – U.S.A.

Italy (IT)

CGI	Comitato Glaciologico Italiano Via Valperga Caluso 35 IT–10125 Torino
CNR	Consiglio Nazionale delle Ricerche Istituto di Ricerca per la Protezione Idrogeologica, Sezione di Torino Strada delle Cacce, 73 IT–10135 Torino
DGI	see DGI – Austria
DGUP	Department of Geography University of Padua Via del Santo 26 IT–35123 Padova
G.C.	Giacomo Casartelli IT–22032 Albese
IMONT	Italian Mountain Institute Piazza dei Caprettari 70 IT-00186 Roma.
ISPESL	Istituto Superiore per la Prevenzione e la Sicurezza del Lavoro Environmental Department Via Urbana 167 IT-00100 Rome
SAT	Società degli Alpinisti Tridentini Comitato Glaciologico Trentino via Manci, 57 IT-38100 Trento
SGL	Servizio Glaciologico Lombardo Via Alessandro Volta 22 IT-20121 Milano
SMI	Società Meteorologica Italiana Castello Borello IT-10053 Bussoleno (TO)

UI/HA	Ufficio Idrografico / Hydrographisches Amt Provincia Autonoma di Bolzano - Alto Adige Autonome Provinz Bozen - Südtirol via Mendola / Mendelstrasse 33 IT–39100 Bolzano / Bozen

Japan (JP)

DHAS	Department of Hydrospheric-Atmospheric Sciences Graduate School of Environmental Studies Hydrospheric Atmospheric Research Center, Nagoya University JP– 464 8601 Nagoya

Kenya (KE)

UWAOS	see UWAOS – U.S.A.

Mexico (MX)

UNAM	Instituto de Geofísica Universidad Nacional Autónoma de Mexico Circuito Cientifico MX–Coyoacan 04510 D.F.

Nepal (NP)

DHAS	see DHAS – Japan
ICIMOD	International Centre for Integrated Mountain Development P.O. Box 3226 Khumaltar NP–Kathmandu

New Zealand (NZ)

APPC	Alpine and Polar Processes Consultancy 20 Muir Rd. Lake Hawea RD 2 Wanaka NZ–Otago 9382
DGUC	Department of Geography University of Canterbury P.B. 4800 NZ-Christchurch

DGUO-NZ	Department of Geography/Te Ihowhenua University of Otago P.B. 56 NZ-Dunedin
NIWA	National Institute of Water and Atmospheric Research Ltd P.B. 6414 NZ–Dunedin
SGEES	School of Geography, Environment and Earth Science Victoria University of Wellington P.B. 600 NZ-Wellington

Norway (NO)

DES	Department of Earth Sciences University of Bergen Allegaten 41 NO–5007 Bergen
DGUO-NO	Department of Geosciences University of Oslo P.O. Box 1047, Blindern NO–0316 Oslo
IGUW	see IGUW – Germany
NBF	Norsk Bremuseum NO-6848 Fjaerland
NCU	see NCU – Poland
NPI	Norwegian Polar Institute Polar Environmental Centre NO–9296 Tromsø
NVE	Norwegian Water Resources and Energy Administration Hydrology Division – Glacier section P.O. Box 5091 Majorstua NO–0301 Oslo
PAS	see PAS – Poland
SUP	see SUP – Poland

Pakistan (PK)

GCISC	Global Change Impact Studies Center 61/A, 1st Floor, Jinnah Avenue PK - Islamabad

Peru (PE)

EP	Electroperú S.A. Sim Norte, Unidad de Glaciología Av. Confraternidad Internacional s/n PE–Huaraz, Region Chavin
HID	Hidrandina S.A. Av. Confraternidad Internacional s/n PE–Huaraz, Chavin
INRENA	Unidad de Glaciología y Recursos Hídricos Av. Confraternidad Internacional Oeste No. 167 PE–Huaraz, Ancash
IRD-PE	Instituto de Investigación para el Desarrollo (IRD) Jr. Terruel 357, Miraflores PE–Lima

Poland (PL)

MPG	Little Geographical Workshop ul. Wschodnia 19/6 PL–20 015 Lublin
NCU	Department of Cryology and Polar Research Institute of Geography Gagarina 9 PL–87 100 Torun
PAS	Institute of Geophysics Polish Academy of Sciences ul. Ksiecia Janusza 64 PL-01 452 Warsaw
SUP	Department of Geomorphology University of Silesia ul. Bedzinska 60 PL–41 200 Sosnowiec

South Georgia (GS)

UASE	see UASE - United Kingdom

Spain (ES)

I75SA	Ingeniería 75, S.A. C/ Velázquez 87 - 4° Dcha ES–28006 Madrid
MMA	Dirección General del Agua Ministerio de Medio Ambiente Plaza de San Juan de la Cruz s/n. ES-28071 Madrid
UAM	Departamento de Geografía Física Universidad Autónoma Canto Blanco ES–Madrid

Sweden (SE)

INK	Department of Physical Geography and Quaternary Geology Glaciology Section University of Stockholm SE–106 91 Stockholm
SRC	The Swedish Research Council SE–103 78 Stockholm

Switzerland (CH)

DGUF	Department of Geosciences University of Fribourg Chemin de musée 4 CH–1700 Fribourg
EKK	Cryospheric Commission Swiss Academy of Sciences Schwarztorstrasse 9 CH–3007 Bern
G.C.	see G.C. – Italy

G.K.	Giovanni Kappenberger CH–6654 Cavigliano
GIUZ	Department of Geography University of Zurich-Irchel Winterthurerstrasse 190 CH–8057 Zürich
SCNAT	Glaciological Commission Swiss Academy of Sciences Schwarztorstr. 9 CH–3007 Bern
VAW	Versuchsanstalt für Wasserbau, Hydrologie und Glaziologie (VAW) ETH Zürich Gloriastr. 37/39 CH–8092 Zürich

United Kingdom (UK)

UASE	Universities of St Andrews, Stirling and Edinburgh St Andrews, Fife KY16 9AJ UK-Scotland

U.S.A. (US)

NCD	Nichols College 124 Center Road US-Dudley, MA 01571
NPSD	Denali National Park PO Box 9 US–Denali National Park, AK 99755
NPNC	North Cascades National Park Sandalee Marblemount Ranger Station Silver 7280 Ranger Station Rd. US–Marblemount, WA 98267

TAMU	Department of Geography Texas A&M University 810 O&M Bldg College Station US-Texas, TX 77843
UAF	Geophysical Institute University of Alaska Southeast 11120 Glacier Highway US–Juneau, AK 99801
UAS	Geophysical Institute University of Alaska 903 Koyukuk Drive PO Box 757320 US–Fairbanks, AK 99775 7320
USGS-F	U.S. Geological Survey Alaska Science Center, Glaciology 3400 Shell Street US–Fairbanks, AK 99701 7245
USGS-T	U.S. Geological Survey Washington Water Science Center 934 Broadway, Suite 300 US–Tacoma, WA 98402
UW	Geophysics Program University of Washington, AK 50 US–Seattle, WA 98195
UWAOS	Department of Atmospheric and Oceanic Sciences University of Wisconsin-Madison 1225 W. Dayton Street US–Wisconsin, MA 53706

3.3 National Correspondents of WGMS for Glacier Fluctuations

ANTARCTICA	see ARGENTINA and AUSTRALIA
ARGENTINA/ ANTARCTICA	Lydia Espizua Instituto Argentino de Nivología y Glaciología CONICET (IANIGLA) Casilla de Correo 330 AR–5500 Mendoza E-mail: lespizua@lab.cricyt.edu.ar
AUSTRALIA/ ANTARCTICA	Andrew Ruddell 4 Cust Street Rainbow AU– 3424 Victoria E-mail: andrewruddell@bigpond.com
AUSTRIA	Michael Kuhn Institute of Meteorology and Geophysics University of Innsbruck Innrain 52 AT–6020 Innsbruck E-mail: Michael.Kuhn@uibk.ac.at
BOLIVIA	Javier C. Mendoza Rodríguez Instituto de Hidráulica e Hidrología (IHH) and Servicio Nacional de Meteorología e Hidrología (SENAMHI) P.O. Box 699 BO–La Paz E-mail: jmendoza@senamhi.gov.bo E-mail: jcmendoza@umsa.bo
C.I.S./Russia	Victor V. Popovnin Moscow State University Geographical Faculty Leninskiye Gory RU–119 992 Moscow E-mail: begemot@djankuat.msk.ru po@geogr.msu.ru
CANADA	Michael N. Demuth Natural Resouces Canada Geological Survey of Canada 601 Booth Street CA–Ottawa, ON K1A 0E8 E-mail: mdemuth@NRCan.gc.ca

CHILE	Gino Casassa Centro de Estudios Cientificos Av. Prat. 514 CL–Valdivia E-mail: gcasassa@cecs.cl
CHINA	Zhongqin Li Tianshan Glaciological Station / Cold and Arid Regions Environment and Engineering Research Institute (CAREERI) Chinese Academy of Sciences (CAS) 260 West Donggang Road CN–730 000 Lanzhou, Gansu E-mail: lizq@lzb.ac.cn
COLOMBIA	Jair Ramirez Cadenas INGEOMINAS Diagonal 53 No. 34-53 CO–Bogota E-mail: jairamir@ingeominas.gov.co
ECUADOR	Bolivar Cáceres INAMHI and IRD P.O. Box EC–16 310 Quito E-mail: bolivarc@inamhi.gov.ec
FRANCE	Christian Vincent Laboratory of Glaciology and Environmental Geophysics (CNRS) P.O. Box 96 FR–38402 St. Martin d'Hères Cedex E-mail: vincent@lgge.obs.ujf-grenoble.fr
GERMANY	Ludwig N. Braun Commission for Glaciology Bavarian Academy of Sciences Alfons-Goppel-Str. 11 DE–80539 München E-mail: Ludwig.Braun@kfg.badw.de
GREENLAND	Andreas P. Ahlstrøm Department of Quaternary Geology The Geological Survey of Denmark and Greenland (GEUS) Øster Voldgade 10 DK–1350 København K E-mail: apa@geus.dk

ICELAND	Oddur Sigurðsson National Energy Authority Hydrological Service Grensásvegi 9 IS–108 Reykjavik E-mail: osig@os.is
INDIA	Chandrashekhar V. Sangewar Glaciology Division Geological Survey of India Vasundara Complex, Sector E, Aliganj IN–Lucknow 226024 E-mail: cvsangewar@rediffmail.com
INDONESIA	see AUSTRALIA
ITALY	Mirco Meneghel Universita di Padua Dipartimento di Geografi a Via del Santo 26 IT–35123 Padova E-mail: mirco.meneghel@unipd.it
JAPAN	Koji Fujita Department of Hydrospheric-Atmospheric Sciences (DHAS) Graduate School of Environmental Studies c/o Hydrospheric Atmospheric Research Center, Nagoya University JP– 464 8601 Nagoya E-mail: cozy@nagoya-u.jp E-mail: cozy.fujita@gmail.com
KAZAKHSTAN	Igor Severskiy Institute of Geography of the Ministry-Academy of Sciences of the Republic of Kazakhstan Pushkinstreet 99 KZ–480100 Almaty i_severskiy@mail.kz
MEXICO	Hugo Delgado-Granados Instituto de Geofísica Universidad Nacional Autónoma de México Circuito Exterior, C. U. Coyoacán MX–México D. F. 04510 E-mail: hugo@geofisica.unam.mx hugo@tonatiuh.igeofcu.unam.mx

NEPAL	see JAPAN
NEW ZEALAND	Trevor J. Chinn Alpine and Polar Processes Consultancy 20 Muir Rd. Lake Hawea RD 2 Wanaka NZ–Otago 9382 E-mail: t.chinn@xtra.co.nz
NORWAY	Jon Ove Hagen Department of Geosciences Section of Physical Geography P.O. Box 1047, Blindern NO–0316 Oslo E-mail: j.o.m.Hagen@geo.uio.no
PAKISTAN	Ali Ghazanfar Head Water Resources Section Global Change Impact Studies Center (GCISC) 61/A, 1st Floor, Jinnah Avenue PK - Islamabad ghazanfar.ali@gcisc.org.pk
PERU	Marco Zapata Luyo Unidad de Glaciología y Recursos Hídricos INRENA Av. Confraternidad Internacional Oeste No. 167 PE–Huaraz / Ancash E-mail: glaciologia@inrena.gob.pe E-mail: zapataluyomarco@gmail.com
POLAND	Bogdan Gadek University of Silesia Department of Geomorphology ul. Bedzinska 60 PL–41 200 Sosnowiec E-mail: jgadek@us.edu.pl
SPAIN	Eduardo Martínez de Pisón & Miguel Arenillas Parra Ingeniería 75, S.A. Velázquez 87 - 4° derecha ES–28006 Madrid E-mail: ing75@ing75.com E-mail: map@ing75.com

SWEDEN	Per Holmlund Department of Physical Geography and Quaternary Geology University of Stockholm SE–106 91 Stockholm E-mail: pelle@natgeo.su.se
SWITZERLAND	Martin Hoelzle Department of Geosciences University of Fribourg Chemin de musée 4 CH–1700 Fribourg martin.hoelzle@unifr.ch
U.S.A.	William R. Bidlake U.S. Geological Survey Washington Water Science Center 934 Broadway - Suite 300 US–Tacoma, WA 98402 E-mail: wbidlake@usgs.gov
UZBEKISTAN	Andrey Yakovlev Center of Hydrometeorological Service (UzHydromet) 72 K. Makhsumov str. UZ–100 052 Tashkent E-mail: andreyakovlev@mail.ru

This chapter includes information which does not fit into the standard format. The intention is to document:

- index measurements on glacier fluctuations in cases where more complex observations are not possible, especially in relation to remote glaciers and glaciers which are systematically studied using reduced stake networks in combination with statistical considerations or flow calculations.

- information on special events which may pose risks to human activities, such as glacier surges, outbursts of ice-dammed lakes, ice avalanches, drastic retreat of tidal glaciers due to calving instabilities or eruptions of ice-clad volcanoes.

4.1 Index Measurements

It is not without hesitation that WGMS publishes isolated measurements, because they do not always directly relate to the other components (mass balance, length change, inventories) of the integrated and coherent approach used in modern international monitoring strategies. Experience shows that – over longer time periods – index measurements tend to disappear without leading to results of major scientific interest or significance. WGMS is a service to collect standardised information for a coherent observation programme at highest possible scientific levels and – as a consequence – strongly encourages the principal investigators and sponsoring agencies of index measurements to develop a clear concept that relates to the central monitoring strategy and can integrate in prarticular the long-term index observation series. For the same reason, index measurements are published in the “Fluctuations of Glaciers” but not stored in the WGMS database.

JAPAN (JP)

Hamaguri Yuki (JP1)

K. Fujita (DHAS)

Mass balance measurements with the direct glaciological method have been carried out on the Hamaguri Yuki perennial snowfield since 1981. The data for the present observation period are given in Tables A and C. An inventory of perennial snow patches in central Japan was published by Higuchi et al. (1980).

NEW ZEALAND (NZ)

End-of-summer-snowline (EOSS) surveys

T.J. Chinn (APPC)

Since 1977, the end-of-summer-snowline (EOSS) has been surveyed on 50 index glaciers distributed over New Zealand's Southern Alps. The surveys are carried out by hand-held oblique photography taken from a light aircraft (since 2001 also in digital form), where the position of the glacier snowline is recorded at the end of the summer season from a similar viewpoint each year. The flights are generally flown in March at an altitude between 2700 and 3000 m a.s.l. (9000–10000 ft). Back in the office, the snowlines visible on the photographs are sketched onto a map of each glacier and the accumulation and ablation areas are mapped and measured by digitiser. The elevation of the snowline is then accurately read from the glacier area-altitude curve. The data is reported as deviations from a steady-state equilibrium line altitude (ELA_0) which is calculated from the area-altitude curve for each glacier, assuming a steady-state accumulation area ratio (AAR_0) of 0.6. The most recently started mass balance monitoring programme at Brewster Glacier shall help to better link the EOSS data series to on-site measured glacier mass balance. Methods, data and more details are given in Chinn (1995) and Chinn et al. (2005a, 2006); Clare et al. (2002) investigated the inter-annual EOSS in response to patterns of atmospheric circulation and sea surface temperature.

Table 1 Annual EOSS deviations (in m) from assumed ELA_0 (with AAR_0 = 0.6). Number of observations (Obs.) and average (Avg.) are given for years and glaciers.

Source: Chinn et al. (2006)

Table 1

	KAIKOURA	MT. ELLA	MT. FAERIE QUEENE	MT. WILSON	MT. FRANKLI	ROLLESTON	MT. CARRINGTON	MT. AVOCA	MARMADUKE	RETREAT	BROWNING	DOUGLAS	MT. BUTLER
ELA_0	2490	2142	2030	1820	1814	1763	1715	1965	1830	1742	1598	2040	1840
1977				-37		-13			-42.5				-55
1978				-11	-12	5	-45	-55	-35	-4	7	91	112
1979					122	-13			78				55
1980					-54	1	-22		2	38	10	-163	-34
1981				15	-74	-3	-87		-28	-50	-34		-40
1982	5	12	-45			10	25	-15	30	14	7	-18	28
1983				-115	-148	-123	-150		-136	-252	-113	-214	-200
1984	-17			-141		-10	-115	-95	-122			-240	-65
1985				-63		-18		-55	-50	-4	-2	-223	-70
1986				41	-18	13	-10	-5	9	20	17	-128	10
1987				-89	-41	15	45		-5				-9
1988	-5		5	68	35	-1	55	10	65			91	42
1989	50	28	5	93	52	7	5	6	-13	36	-25	172	-34
1990									168				
1991													
1992												-197	-95
1993	-57	-87	-60	-167	-164	-143	-170	-115	-175	-73	-116	-260	-136
1994	-17	-72	-57	-102	-107	-53	-128	-25	-75	-120	-71	-154	-28
1995	-60	-142	-65	-154	-156	-143	-158	-45	-155	-277	-118	-231	-190
1996		-15	-57		-82	-44	-120	12	-82	16	-11	-150	-60
1997				-149		-123	-137	-75	-129	-97	-108	-223	-176
1998	30	17	-50	41	122	49	-39	70	143	47	30	220	68
1999	15	108	145	113	164	87	190	115	164	146		240	98
2000	10	60	160	108	136	97	237	65	153	133		250	148
2001	-15	-22	-55	13	-104	-42	-135	-52	-57	-60	-30	-40	-95
2002	25	46	55	93	121	89	210	88	140	93	62	245	90
2003		-64	-54	-121	-70	-94	-84	-52	-117	-78	-77	-134	-147
2004				-92		-1	-120	-20	-27	18	-28	-35	-80
2005	-25	-77	-60	-82	-106	-55	-137	-53	-130	-132	-110	-163	-176
Obs.	**13**	**13**	**14**	**22**	**20**	**26**	**23**	**20**	**27**	**21**	**19**	**23**	**27**
Avg.	**-5**	**-16**	**-10**	**-34**	**-19**	**-19**	**-39**	**-15**	**-16**	**-28**	**-37**	**-55**	**-38**

Table 1 continued

	DAINTY	KEA	JASPUR	SIEGE	VERTEBRAE #12	VERTEBRAE #25	RIDGE	LANGDALE	TASMAN	SALISBURY	JALF	CHANCELLOR DOME	GLENMARY
ELA_0	1954	1820	1725	1736	1864	1840	2226	2186	1790	1810	1790	1756	2164
1977	-32			-64				12	-10	17	-15	96	
1978	57	65	43	-24	-13	30	79	65	85	17	-10	95	74
1979									-90				
1980	-7	44	63	-76	33	25			20	32	-32	77	-91
1981	-77	-85		-70	-60	-39	2	79	-35	-58	-65	-93	-34
1982	93	134	-15	-70	-33	-8	10	52	-30	17	5	92	17
1983	-96	-230	-155	-268	-73	-62	-15	-1	-80	-92	-230	-211	-29
1984							-141	-236	-95	-51	-78		-144
1985	-81	-120	-105	-94	-67	-50	-32	-96	-90	-76	-146	-147	-56
1986	-73	-82	-42	35	-53	-27	-9	-41	-10	-1	-20	-78	
1987	-84	-83						-69	-29	-35	-51	-28	
1988	-12	-58	-42	-70	-13	3	59	39	50	-81	-32	52	16
1989	-32	-36	-29	-64	-51	-20	51	69	-30	-66	-31	-78	16
1990									310				
1991									-35				
1992	-103			-323	-96	-94		-216	-100	-129	-210		-24
1993	-176	-230	-150	-386	-86	-84	-126	-231	-108	-100	-220	-206	-57
1994	-73	-92	-120	-62	-68	-54	-61	83	-20	-38	-38	-147	-43
1995	-111	-250	-145	-396	-86	-84	-94	-226	-124	-165	-240	-211	-45
1996	-12	80	-92	-72	-68	-54	-88	51	-35	-58	-8	-36	-36
1997	-92	-152	-100	-203	-77	-71	-136	-226	-102	-84	-191	-176	-112
1998	98	78	43	214	-29	-5	9	142	63	42	-3	92	36
1999	176	200		414	226	125	89	114	186	220	260	194	108
2000	74	190		279	129	70	79	89	110	172	265	189	84
2001	-58	-150	-95	-126	-70	-33	-116	-211	-80	-95	-85	-186	-46
2002	126	195	195	239	136	80	74	104	105	50		159	46
2003	-67	-159	-74	-160	-55	-51	-63	-211	-80	-95	-190	-186	-49
2004	-44	-90	-95	-116	-68	-45	2	18	-40	-78	-170	-151	-39
2005	-94	-155	-125	-203	-79	-75	-61	-206	-40	-95	-190	-181	-54
Obs.	**25**	**23**	**19**	**24**	**23**	**23**	**22**	**25**	**29**	**26**	**25**	**24**	**23**
Avg.	**-28**	**-43**	**-55**	**-69**	**-27**	**-23**	**-22**	**-42**	**-12**	**-32**	**-69**	**-45**	**-20**

Table 1 continued

	BLAIR	MT. McKENZIE	JACKSON	JACK	MT. ST. MARY	THURNEYSON	BREWSTER	MT. STUART	LINDSAY	FOG PK	SNOWY CK	MT. CARIA	FINDLAY
ELA_0	1938	1904	2070	1907	1926	1970	1935	1673	1730	1987	2092	1472	1693
1977						-36		-86					
1978	74	46	28	31			25	57	8		64	-30	
1979													
1980	-75	6	-20	23		-44	-89	-23	-78	-71	-68		
1981	-13	-16		-22		-27	-80	-67	-49		66	-59	-89
1982	-51	-2	8	44			36	3	51	35	-54	-48	42
1983	-126	-184	-38	-157		-105	-141	-135	-170		-59	-100	-111
1984	-80	-62	-80	-79	-171	-88	-135			-96	-68		
1985	-85	-124	-56	-32		-65	-139	-53	-64		-72	-49	-64
1986		13		28	-91	-32	-93	-13	38	-57	-56	53	32
1987	-68	-14	-9	-2		-52	-107	5	-115	-85	-67	-50	-71
1988	57			-32	-19	-20			42	35	-55	28	-8
1989	-62	8	10	-9	46	0	-17	-10	34	45	11	-43	-51
1990													
1991													
1992				-90	-76	-36	-84						
1993	15	-122	-78	-142	-141	-60	-185	-138	-175	-93	-34	-97	-118
1994	-73	8	-25	-27	-76	-66	-145	-33	-120	-87	-58	-72	-59
1995	-85	-99	-52	-152	-156	-102	-158	-158	-180	-99	-62	-106	-132
1996	2	6	2	51	-71	-32	27	39	45	-93	-35	-82	-61
1997		-189	-54	-102	-84	-70	-156	-106	-85	-97	-72	-77	-113
1998	34	31	12	33	-37	-5	47	-17	70	111	66	-55	26
1999	152	174	95	101	199	142	345	132	145	135	148	178	197
2000	147	148	63	85	204	162	220	177	140	121	54	188	140
2001	-96	-99	-54	-109	-146	-92	-165	-83	-90	-92	-88	-52	-79
2002	67	56	33	78	189	135	115	142	142	125	28	153	109
2003	-93	-134	-55	-147	-131	-97	-141	-103	-123	-25	-51	-50	-81
2004	-88	-122	-54		-71	-35	-155	-108	-122	-95	-58	-92	-115
2005	-88	-132	-56	-112	-126	-70	-155	-108	-118	-97	-72	-98	-113
Obs.	**22**	**23**	**21**	**24**	**18**	**24**	**24**	**23**	**23**	**20**	**24**	**22**	**21**
Avg.	**-24**	**-35**	**-18**	**-31**	**-42**	**-29**	**-55**	**-30**	**-34**	**-24**	**-25**	**-25**	**-34**

Table 1 continued

	PARK PASS	MT. LARKINS	BRYANT	AILSA MTS.	MT. GUNN	MT. GENDARME	LLAWRENNY PKS.	BARRIER PK.	MT. IRENE	MERRIE	CAROLINE PK.	**Obs.**	**Avg.**
ELA_0	1824	1945	1783	1648	1593	1616	1476	1596	1563	1515	1380	**50**	**1834**
1977			-43		22							**15**	**-19**
1978	79		101	-5	45		4	116	137	140		**40**	**38**
1979												**5**	**30**
1980	-16				-64			-51				**32**	**-22**
1981	-46		-20		-62	-46	-68	-73				**36**	**-42**
1982	34		-3		17	-43	-4	-31				**41**	**9**
1983	-62		-163	-88	-115	-136	-132	-218	-156			**41**	**-131**
1984	-59	-265	-163	-53								**27**	**-109**
1985	-122		-173	-53	-53	-94	-36	-72	-37			**40**	**-77**
1986	39	-53	-13	1		59						**38**	**-16**
1987	19		-20	-23	-38	34	-22	-41	-37			**33**	**-37**
1988		135										**33**	**13**
1989	-30	91	-30	-36	-59	-36	-47	-71	-26	30		**49**	**-3**
1990												**2**	**239**
1991												**1**	**-35**
1992												**15**	**-125**
1993		-275	-27	-84	-108	-114	-116	-168	-156	-135	-160	**49**	**-135**
1994	-41	-95	-55	-52	-64	-64	-68	-118	-51	-95	-47	**50**	**-66**
1995	-214	-315	-153	-93	-122	-198	-176	-236	-163	-165	-150	**50**	**-152**
1996	-64	-163	-113	-64	-86	-100	-15	-126	-65	-90	-78	**48**	**-46**
1997	-134	-312	-113	-55	-73	-126	-155	-132	-103	-130	-130	**45**	**-125**
1998	48	261	-5	-27	-34	32	2	86	49	-70	2	**50**	**44**
1999	138	270	227	182	209	188	194	304	102	173	182	**48**	**171**
2000	119	255	182	137	217	159	181	207	122			**46**	**146**
2001	-154	-280	-118	-55	-78	-131	-71	-108	-125	-103	-105	**50**	**-92**
2002	99	245	87	37	42	34	137	194	165	175	195	**49**	**115**
2003	-163	-205	-117	-65	-68	-96	-100	-148	-109	-100	-89	**49**	**-103**
2004	-159	-255	-108	-58	-108	-133	-96	-131	-93	-110	-110	**45**	**-84**
2005	-154	-285	-118	-68	-108	-129	-76	-131	-123	-105	-125	**50**	**-113**
Obs.	**22**	**17**	**23**	**20**	**22**	**20**	**20**	**21**	**18**	**14**	**12**		
Avg.	**-38**	**-73**	**-42**	**-26**	**-31**	**-47**	**-33**	**-45**	**-37**	**-42**	**-51**		

POLAND (PL)

Pod Bula (PL1617)

A. Wislinski (MPG)

The firn-and-ice patch (glacieret) ‘Pod Bula’ is situated within a flat hollow beneath the north-west wall of ‘Niznie Rysy’ peak (2430 m a.s.l.) and ‘Bula pod Rysami’ (2054 m a.s.l.) in the ‘Czarny Staw pod Rysami’ cirque which is located in the eastern part of Polish Tatra Mountains at an elevation of 1651–1687 m a.s.l. This elevation is in the middle of the subalpine belt of the Polish Tatras. The patch is fed mainly by snow avalanches developing within the ‘Kociol pod Rysami’ cirque from an altitude of about 2000–2300 m a.s.l. Topographical surveys and glaciological observations were started by A. Adamowski (Institute of Meteorology and Water Management, Zakopane) and A. Wiśliński (Maria Curie-Sklodowska University (UMCS), Lublin) in 1978. Since 1980 they have been continued by A. Wislinski (until 1992 UMCS, since 1993 MPG). In September 1978 the glacieret consisted of about 15 ice and firn layers. It was 10 m thick in its rear part and its area was 3.4 x 10^3 m^2. Underneath the firn and ice the glacieret was crossed by a tunnel, which was about 10 m wide and 3–5 m high. On the glacieret’s surface there were several narrow slanting crevices. During the following years the crevices were developing and some new ones occurred. In September 1981 the weakened ceiling of the tunnel fell down completely. Since then the patch has never regained the same state as before the collapse. Each phase of development, which took either a few years or only one year, ended with a collapse of the tunnel ceiling. During the first warm season the new tunnel, establishing itself in new snow, reached 3–4 m in height and 5–10 m in width. The trial to refer the fluctuations of the patch to the meteorological data from ‘Kasprowy Wierch’ (1991 m a.s.l.) proved rather weak statistical correlations.

The data from Pod Bula, as well as of Mieguszowiecki and Pod Cubryna are given in Tables A, B and D. Related references and data sources are Wislinski (1985, 2002) and Ciupak et al. (2005).

4.2 Special Events

ARGENTINA (AR)

Horcones Inferior (AR5006) **glacier surge**

L. Espizua, P. Pitte and L.F. Hidalgo (IANIGLA)

The Horcones Inferior glacier is located at 32º40’S latitude and 70º00’W longitude at the south wall of Cerro Aconcagua (6959 m a.s.l.), the highest peak in the Western Hemisphere. It is a valley glacier covered by debris with thermokarst features, that flows to the southeast. Between 1963 and 1984 the glacier front position did not show significant changes. The glacier surged between 1984 and 1986 and stopped in 1989. It was about 10.5 km long between 1990 and 1997. From 1997 to 1999 the glacier retreated 130 m based on field observations (Happold and Schrott 1993, Unger et al. 2000, 2005). A new surge event started in 2004. The evolution of the surge front was detected through analysis of Landsat images and field observations. We cannot establish the exact start of the surge, but on the image of 13 February, 2003, in the upper part of the glacier at 4175 m a.s.l., a partly debris-covered ice wave advanced 320 m with respect to 10 February, 1999. Between the images of 13 February, 2003, and 8 February, 2004, this ice wave advanced 5140 m with a mean velocity of 14.3 m per day on the debris-covered glacier. It reached an altitude of 3910 m a.s.l., 360 m upstream from the stable front position of the glacier. On the image of 25 January, 2005, the surge advanced another 3000 m with a mean velocity of 8.5 m per day, finally advancing the glacier front position. The satellite image of 28 January, 2006, shows that the surge front advanced another 440 m with a mean velocity of 1.2 m per day. The resulting front variations are given in Tables B and BB.

BOLIVIA (BO)

Chacaltaya (BO5180) **glacier disintegration**

During the observation period (2000–2005) the glaciar lost all the 15 stakes and split into parts.

C.I.S. (SU)

Djankuat (SU3010) **rockfall**

V.V. Popovnin (MGU)

A large rockfall from the crestal part of the Main Caucasus Ridge took place on 1st July 2003, completing a series of similar rockfalls of a smaller extent that had occurred here after the summer of 2001. Recent intensification of rockslide processes was caused by the progressive deglaciation on the crestal revetment of the firn basin due to strongly unfavourable glacier mass balance conditions of the 1999–2001 period. Being devoid of an icy weathering-protective layer, the steep slopes of the axial ridge zone began to be eroded too rapidly, continuing even during the winter months. The deposits from the event of 1st of July, 2003 covered parts of the glacier accumulation area within the 3200–3600 m a.s.l. altitudinal belt, reaching the opposite margin of the glacier and covering the glacier surface with a debris layer approx. 0.7 m thick on average. The volume of the collapsed matter, distributed over an area of about 0.10 km^2, or 4% of the glacier surface, is estimated at about 70000 m^3. The consequent reduction of heat influx to the snow/firn/ice surface distorted the spatial pattern considerably and diminished ablation values greatly. As a result, the surface of the glacier zones, not affected by the rock fall activity, turned out to be 1–2 m lower by the end of the 2002/03 ablation season than those parts of the glacier surface, which are now covered with rockfall debris.

Kolka (SU) **rock-ice avalanche**

V.V. Popovnin (MGU)

A tremendous glacier hazard of a complex nature arose in the Genaldon Valley, North Ossetia Republic in the Caucasus, Russia, on 20 September, 2002. An ice/rock avalanche (or a series of ice avalanches) from the glaciers, hanging on the northern flank of the Main Caucasus Rudge over the Kolka Glacier, provoked a strong mechanical impact upon the glacier body. Most of the valley part of the glacier was pushed away from its original location. A mixture of ice, water and entrapped rocks tumbled about 20 km downvalley at a velocity of up to 180 km/hr until it collided with the narrow entrance of the Karmadon gorge. A huge body of ice/debris conglomerate of 115±10 x 10^6 m^3 piled up there, whereas a mud and debris flow travelled further on for another 17 km downvalley and stopped only 4 km short of the town of Gizel. Depending on the exact definition of the initiation and farthest travel point (initial ice/rock slide, Kolka glacier and ice dam or farthest point of debris flow) the ratio of vertical drop height (H) to horizontal travel distance (L) is 0.08–0.15. The body dammed the right-hand tributary of the Genaldon River, and a number of glacier-dammed lakes were formed. The largest, Saniba Lake, inundated the nearby village and attained a volume of 4.9 x 10^6 m^3 by October 2002, with the maximum depth exceeding 21 m. The catastrophe claimed at least 125 lives. In spite of the fact that similar hazards have been registered here in the past (1834, 1902 A.D.), the 2002 event was extraordinary by the scale of the disaster. The mechanism of hazard origination, extreme initial acceleration, high flow velocity, long travel distance and a huge mass of transported material (130–140 x 10^6 m^3 in total, including 110 x 10^6 m^3 of ice and debris) is still enigmatic and several points of view, some of them mutually contradictory, were published. The principal triggering impulse was explained by at least three groups of possible reasons: meteorological (abundant precipitation and excessive snow/ice masses on the slope), seismic (geological faults, slight earthquake on the eve of the hazard) and volcanic (activation of sub-glacier fumarole activity of Mt. Kazbek, adjacent extinct volcano). The hypothesis of premature glacier surge (after the previous surge of the Kolka Glacier in 1969) was also suggested. Ongoing monitoring of land regeneration and present evolution of the ice/debris conglomerate body in the Karmadon Depression reveals a rather rapid icemelt rate at present, though the ice body could take about 10 years or so to vanish completely.

More details are found in Haeberli et al. (2004), Kotlyakov et al. (2004), Huggel et al. (2005) and Petrakov et al. (2008) as well as in several articles (e.g., Berger, Goncharov et al., Huggel et al., Petrakov et al., Swartz and Ardell) published in the proceedings of the High Mountain Hazard Prevention conference, held in Vladikavkaz-Moscow, June 23–26, 2004 (Polkvoy et al. 2006).

INDIA (IN)

Chhota Shigri (IN) **tectonic event**

P. Wagnon (IRD)

The Pakistan Earthquake was felt by people in the field. Light rockfalls happened on moraines but without consequences on the glacier.

ICELAND (IS)

Reykjafjardar (IS300) **glacier surge**

O. Sigurðsson (NEAHS)

A surge-type activity started at the glacier snout in 2001 and continued during the entire 2001–2005 period.

Skeidarar E3 (IS0117C) **jökulhlaup (flood)**

O. Sigurðsson, Iceland Glaciological Society, National Energy Authority

Many small and one relatively large jökulhlaup occurred in Skeidara (Skeidararjökull E3). The biggest one started on October 29, 2004, and is supposed to have been connected to the triggering of the volcanic eruption of November 1, 2004. Maximum discharge was 3300 m^3/s with a total runoff volume of about 0.8 km^3.

Skeidarar E3 (IS0117C) **volcanic eruption**

O. Sigurðsson (NEAHS)

A small volcanic eruption started on November 1, 2004, in Grimsvötn Volcano within the catchment area of Skeidararjökull and lasted for almost a week.

ITALY (IT)

Malavalle (IT875) **flood**

R. Dinale (UI/HA)

The strong retreat of Malavalle Glacier (Übeltalgletscher) during the past years led to an outburst of the Vogelhütten See. This lake at 2550 m a.s.l. was dammed by the north-eastern part of the glacier tongue. Due to the glacier retreat the lake broke out on July 15, 2005, and drained over the glacier tongue. About 2/3 of the water volume (approx. 1 x 10^6 m^3) drained through a surface channel in the glacier ice into another proglacial lake on the orographic right side. The ice channel reached a size of about 10 m depth and 5 m width. A detailed description and photos of the event can be found in the glacier reports 01/2005 and 03/2006 of the Hydrographical Office, Bolzano, IT, available on the following website: http://www.provincia.bz.it/hydro/glacierreport/index_d.htm.

Belvedere Glacier (IT) **ice avalanche**

L. Fischer (GIUZ)

On 25 August, 2005, an ice avalanche of ca. 1 x 10^6 m^3 volume occurred in the Monte Rosa east face (Italy). The avalanche detached between 3600 and 3900 m a.s.l. and increased its volume further along the runout path by eroding underlying debris and ice. The main part of the material was deposited on the Belvedere Glacier, particularly in the depression of the former lake Effimero that had formed in 2002 and 2003. The powder-part of the avalanche including ice and debris fragments, however, overtopped the lateral moraine of the Belvedere glacier and covered the plain around the Zamboni alpine hut. The runout length was 3.3 km for the main part and 3.9 km for the powder-part of the avalanche with corresponding drop heights of 1750 and 1800 m, respectively. The corresponding ratios of vertical drop height to horizontal travel distance (H/L) were about 0.58 for the solid part and 0.52 for the powder part of the avalanche. Fortunately, this ice avalanche occurred at night when no people were present on the plain around the hut. During the day, when many tourists frequent this morain region, such an ice avalanche would have caused many casualties.

More details are found in Fischer et al. (2006).

Belvedere Glacier (IT) **glacier surge and flood**

A. Kääb (DGUO-NO) and C. Huggel (GIUZ)

Belvedere Glacier has been subject to unusual developments during the past few years. A surge-type flow acceleration started in 2001 and continued a few years with a maximum ice flow speed increase of an entire order of magnitude compared to normal conditions. At the terminal area Belvedere Glacier experienced a strong uplift of the ice causing several hazard and tourist facility problems. In the upper glacier area, at the foot of the Monte Rosa east face, the surge-type development and related changes in the hydraulic system resulted in the formation of a smaller supraglacial lake in 2001, that reformed in 2002 and significantly increased in size with up to 1 x 10^6 m^3 of water. The rapid lake increase and associated serious hazards for the downstream community of Macugnaga prompted a major emergency action by the Italian civil protection authorities, including pumping and detailed monitoring of the lake. In 2003, the lake formed once more and grew to approximately the same size as in 2002. On 18 June, 2003, a subglacial outburst of the supraglacial lake occurred. The duration of the lake outburst was about 3 days with relatively moderate discharge peaks of ca. 25 m^3/s. No damage was caused by the outburst.

The events are described in Haeberli et al. (2002) and Kääb et al. (2004).

Zebrù Glacier (IT490) rock avalanche

C. Huggel (GIUZ)

On September, 18, 2004, a large rock avalanche occurred from the south face of Thurwieser Peak, Ortles-Cevedale region, Italy, in September 2004. The rock mass detached over an elevation range of 3280 to 3 630 m a.s.l., travelled over Zebrù Glacier and further down the moraines, stopping at 2235 m a.s.l. The ratio of vertical drop height to horizontal travel distance (H/L) of the avalanche was 0.47. Estimates of the volume of the avalanche were in the range of 3–5 x 10^6 m^3. The avalanche affected hiking trails and alpine pasture but no one was hurt or killed. The rock slope failure and avalanche was recorded on video by mountaineers. After the slope failure liquid water was observed at the detachment zone. A possible role of permafrost and related degradation was suggested.

More details are found in Cola (2005) and Sosio et al. (2008).

NORWAY (NO)

Blåmannsisen (NO) **flood**

NVE

A subglacial drainage of a glacier-dammed lake occurred at Rundvassbreen, part of Blåmannsisen. On September 5, 2001, 40 x 10^6 m^3 of water drained in 35 hours, with peak discharge of 800–900 m^3 per second. The water level in the hydropower reservoir downstream increased by 2.5 m and was thus financially beneficial to the hydropower station.

The first known jøkulhlaup from the glacier Blåmannsisen in northern Norway occurred on 6^{th} to 7^{th} September, 2001. About 40 x 10^6 m^3 of water drained from a lake (known as Vatn 1051) that was adjacent to and dammed by the glacier. The water drained under the glacier and eventually to the Sisovatn reservoir where the water level rose by 2.5 m. Fortunately, there were no casualties or material damage from the jøkulhlaup; on the contrary, the jøkulhlaup increased the volume of water in the reservoir that is used to supply a hydropower plant operated by Elkem ASA, and was financially beneficial.

On August, 29, 2005, a second subglacial drainage of a glacier-dammed lake occurred. During the event, 35 x 10^6 m^3 of water drained in 36 hours, with peak discharge of ca. 840 m^3 per second. The water level in the hydropower reservoir downstream increased by 2.5 m, and was again financially beneficial to the hydropower station.

Buarbreen (NO21307) **flood**

NVE

A flood event that probably occurred in August 2002 was reported by local inhabitants and the aftermath observed by NVE 10 October, 2002. The estimated volume of water was 1 x 10^6 m^3.

Supphellebreen (NO33014) **flood**

NVE

On 8 May, 2004, a debris flow and flood was caused by the failure in the glacier moraine that dammed water from Flatbreen (part of Supphellebreen). There was significant erosion due to the debris flow. The water volume is unknown but estimated to have been at least 50000 m^3. The debris flow volume was about 240000 m^3. A total of 250000 m^2 of farmland were covered by debris.

PERU (PE)

Pucajirca (PE) **flood**

C. Huggel (GIUZ)

On April 22, 2002, a rock avalanche occurred immediately to the south-west of Laguna Safuna Alta in the Cordillera Blanca. Field mapping indicated that the avalanche deposited 8–20 x 10^6 m^3 of rock into the lake and onto the surface of the frontal section of Glaciar Pucajirca, which flows into the lake. The resulting flood damaged security structures installed to secure the lake, and killed cattle that had been grazing in the area. However, the moraine dam essentially remained intact and the resulting flood was largely contained within a lower lake, Laguna Safuna Baja. The moraine dam cannot be expected to resist a second large displacement wave and mitigation strategies are therefore being developed.

More details are found in Hubbard et al. (2005).

SWITZERLAND (CH)

Bis (CH0107) **ice avalanche**

VAW

A part of Bis Glacier, a hanging glacier on the north-eastern face of Weisshorn, broke off in three parts, with an overall volume of about 460000 m^3, between 23 and 31 March, 2005. No damages were reported because the avalanche did not reach the valley bottom. Already in October 2004, the opening of crevasses pointed to a flow acceleration of the glacier. At the beginning of 2005, a monitoring system based on laser, GPS and geophone measurements was installed to observe the glacier movement and acceleration in order to predict the break-off and, in good time, to close and evacuate the road, railway, and the village Randa (VS) that are located about 3000 m below the glacier.

Bis Glacier has a long history of reported similar events (see Raymond et al. 2003).

U.S.A (US)

Black Rapids (US222) **tectonic event / ice-rock avalanche**

U.S. Geological Survey

South-central Alaska and the Alaska Range were severely shaken on the morning of 3 November, 2002, by an earthquake of magnitude 7.9 with a surface rupture 320 km long and displacements up to 6.9 m. The shaking triggered several rock and ice avalanches on the Black Rapids Glacier. The main rockfall originated from the south walls of the glacier, crossed a medial moraine (~30 m high), and continued across the entire glacier valley (> 2 km). The rock blanket covers an estimated 13 km^2 of the glacier's ablation area. A very crude estimate suggests that the total volume exceeds 10 x 10^6 m^3.

Details are found on the USGS website:
U.S. Geological Survey. http://ak.water.usgs.gov/glaciology/m7.9_quake/

Hubbard (US1290) **flood**

U.S. Geological Survey

Hubbard Glacier dammed Russell Fiord in late June 2002; as a consequence, the ice-dammed Russell Lake grew to a height of 15 m above sea level and to an area of 215 km^2 with a volume of about 3 km^3. Russell Lake outburst took place on August, 14, 2002. Peak flow was about 55000 m^3/s.

More information is found on the USGS website:
http://ak.water.usgs.gov/glaciology/hubbard/

Bering Glacier (US) **ice-rock avalanche**

C. Huggel (GIUZ)

On 14 September, 2005, an exceptionally large rock-ice avalanche occurred from the south face of Mt. Steller between the Bagley Icefield and the Bering Glacier, Alaska. The failure close to the summit of Mt. Steller (3236 m a.s.l.) involved hanging glacier ice and underlying bedrock, with layering sub-parallel to the surface slope. The avalanche with an estimated total volume of 40–60 x 10^6 m^3 travelled for 9 km horizontally with a vertical drop of 2.4 km (resulting in a H/L of 0.27) until the mass was deposited on Bering Glacier. Based on seismic signals recorded at several Alaskan seismic stations, an avalanche velocity of up to 100 m/s could be reconstructed. Reconstruction of mean annual ground surface temperature yielded -10 to -15°C for the failure zone. Modelling results, however, indicated that the failure area was significantly thermally disturbed by warmer overlying firn and glacier ice in the summit region.

More information is found in Huggel et al. (2008).

Red Glacier (US) **ice avalanche**

C. Huggel (GIUZ)

On August, 28, 2000, two large ice-rock avalanches of 11–20 x 10^6 m^3 volume occurred at Iliamna Volcano (3050 m a.s.l.), Cook Inlet Region, Alaska, and travelled down Red Glacier. A second similar avalanche of 12–20 x 10^6 m^3 volume took place on July 25, 2003. The runout length was 8.9 and 8.6 km for the 2000 and 2003 avalanches, respectively, while the corresponding drop height were 1800 and 1760 m, respectively. The ratios of vertical drop height to horizontal travel distance (H/L) were 0.2 in 2000 and 0.21 in 2003. In recent studies, an unusually high frequency of large ice avalanches has been documented at Iliamna Volcano, with avalanches of 10–30 x 10^6 m^3 volume approximately every 4 years. Most of the avalanches descend on Red Glacier and show very similar failure and runout conditions. Iliamna is an active volcano and it is suggested that enhanced geothermal heat flow and fumarolic activity have an impact on glacier stability.

More information is given in Huggel et al. (2007).

CHAPTER 5 **THE ANNEXED MAPS**

The following ten maps can be found in the pocket of the back of the volume. A brief description of the maps with information regarding the purpose of the particular map, its accuracy, and details on the surveying, cartography and reproduction, is added in this chapter. The literature mentioned can be found in the reference chapter. The maps and glaciers concerned are:

1. Granatspitz with Stubacher Sonnblick Kees 1990, Austria (1:5000)
2. Stubacher Sonnblick Kees 2003, Austria (1:10000)
3. Stubacher Sonnblick Kees 2004, Austria (1:10000)
4. Pasterze 2004/05, Austria (1:25000)
5. Zongo 1983–2006, Bolivia (1:10000)
6. Novaya Zemlya 1990–2000, C.I.S.
7. Glaciers of Mount Kenya 1899–2004, Kenya (1:5000)
8. Glaciers of Mount Kenya 2004, Kenya (1:5000)
9. Lewis Glacier 1958, Kenya (1:2500)
10. Wahlenbergfjord, Austfonna, Svalbard, 1987–1998, Norway

GRANATSPITZE WITH STUBACHER SONNBLICK KEES 1990, AUSTRIA, (1:5000)

(Image Line Map)

H. Slupetzky

Department of Geography and Geology, University of Salzburg, AT

The Stubacher Sonnblick Glacier in the Hohe Tauern Range of the Austrian Alps was mapped in 1991 by J. Aschenbrenner, Vienna, and H. Slupetzky, Salzburg. The cartography was done by H. Krottendorfer, Vienna. The presented map is one of a series of five maps of glaciers in the upper Stubach valley. The sheet Granatspitze is derived from the prototype map 'Stubacher Sonnblickkees' (published in Vol. VII, 1998), counted as 'first generation', a preliminary version (Aschenbrenner et al. 1998). The experience gained here was used to produce the other four maps 'Alpinzentrum Rudolfshütte', 'Hohe Riffel', 'Johannisberg', 'Medelzkopf'). Basically, to have the same cartographic design on all five maps and to make further improvements, the sheet Granatspitze covering the Sonnblickkees ('third generation') was developed and printed in 1993 (Aschenbrenner and Slupetzky 1995).

When comparing the two versions of maps, the improvement is obvious. The black plate was reduced to the area of rock by providing enhancement of the rock drawing; even in the previous version the black plate was lightened in order to reduce the darkness in the shade. Three features were additionally depicted by a free-hand line drawing: crevasses, rock and debris. The modulation of contour lines only worked sufficiently well on the glacier surface, so it was not used on the terrain anymore. The production of the orthophoto was entirely done by digital picture processing.

Looking back, it is interesting to note the rapid change in the techniques and methods of surveying and in the way of documentation of glaciers. The main goal of the 'Aschenbrenner maps' was to combine a conventional orthophoto-map with a conventional line map including all characteristics of a topographic map, especially glaciers. The 'Granatspitze' map is an example of the change from classical glacier maps to digital ones. It will, however, be an everlasting question, whether a minimum standard of representing glaciers in digital versions is sufficient (to fulfil scientific demands), or whether a glacier map should be (and not only could be) more sophisticated: a beautiful cartographic-artistic product representing a part of nature in an adequate way.

In terms of glaciological purposes: the Stubacher Sonnblick Kees had an area of 1.504 km² in 1990 compared to 1.772 km² in 1969 (Austrian Glacier Inventory 1969). On all five maps the glacierized area (17 glaciers) was reduced from 7.2 km² in 1969 to 6.5 km² in 1990, which means an area loss of 9% (Slupetzky 1997).

STUBACHER SONNBLICK KEES 2003 AND 2004, AUSTRIA (1:10000)

(Colour Orthophoto Map 2003 and Thematic-Topographic Map 2004)

R. Braunshier[1], W. Gruber[1], H. Slupetzky[1] and H. Wiesenegger[2]

[1]University of Salzburg, AT
[2]Hydrological Service, Regional Government of Salzburg, AT

Within the framework of the long-term glaciological and glacial-hydrological measurement programme carried out on the glacier Stubacher Sonnblick Kees, situated in the Granatspitz Group (Hohe Tauern, Eastern Alps), new maps were produced primarily for mass balance calculation purposes but also to document area changes in the glacier, due to rapid mass loss caused by global warming. The project was carried out by the Department of Geography and Geology at the University of Salzburg in cooperation with the Hydrological Service of Salzburg.

In view of the extraordinary hot summer of 2003 in Central Europe, which resulted in a record mass loss in Alpine glaciers, an aerial photogrammetric survey was initiated just at the right time. It covered the area of the Pasterze, the largest glacier in the Austrian as well as the Eastern Alps, and the surrounding glaciers including the Stubacher Sonnblick Kees (note: this glacier is not to be confused with the famous meteorological observatory on the Hoher Sonnblick, which is situated 30 km to the east). The aerial photographs were taken on August 13, 2003, by Luftbild Fischer, Klagenfurt, and are of excellent quality. The scale of the images is, on average, 1:12000 due to a flight elevation of approx. 4800 m above the Adriatic Sea. In 2004, an ortho-photo using the DTM of the Bundesamt für Eich- und Vermessungswesen, Vienna was produced by students, supervised by B. Zagel and G. Griesebner, Salzburg, of the Department of Geography (now the Department of Geography and Geology).

The map from 2003, with a scale 1:10000, covers the Stubacher Sonnblick Glacier and the catchment area of the Lake Weißsee, which is used as a reservoir for the hydro power plant of the Austrian Federal Railways. It shows the situation of the accumulation area, which is reduced to a few snow patches; by the end of the mass balance year, September 11, 2003, almost no accumulation was left. Therefore, the mean ELA at 3080 m a.s.l. was above the highest point of the glacier and the AAR was only 0.006. Firn layers dating back to the 1960s have melted away since 1982, which was the beginning of an almost continuous mass loss up to the present. The mean specific mass balance was -2.870 m ($B = -4.024 \times 10^6$ m^3). In 2003, the glacier showed the highest yearly mass loss since the beginning of mass balance records in 1964 and probably even exceeded the most extreme year up until now, which was 1947. At the terminus of the glacier, situated at an altitude of 2500 m a.s.l. a proglacial lake developed. On July 27, 2006, the lake drained and the surface level was lowered by 6 m, stabilising at a final elevation of 2499 m a.s.l. according to the outflow situation. After the complete melting of the glaciated basin, the final length of the lake named Unterer Eisboden See, which means the Lower Glacier Basin Lake, will be approx. 400 m.

The basis for producing the 2004 map 1:10000 was elaborated by R. Braunshier in his thesis (2005). A calibrated conventional camera was used to take photos of the Sonnblick-kees from different positions by H. Slupetzky in September 2004. The photos were evaluated by applying the photogrammetric PhotoModeler software, which led then to a DTM. Initially, W. Gruber (2002) used this software, which had originally been developed for architectural purposes, on the Cathedral Massif Glacier, B.C., Canada, and proved it to be an adequate method with satisfactory accuracy. Using the 2003 ortho-photo, the glacier edge was defined and outlined, showing that old snow was covering the ice border at higher altitudes and therefore not yet part to the glacier. The new contour lines were derived from the DTM, the accumulation / ablation patterns and the ELA were determined photogrammetrically.

The map of 2004 shows the areas of old snow, firn and ice and rock islands, which have been melting out more and more in recent years and thus adding considerably to the downwasting of the glacier. The ortho-photo of 2003 was used for the map background. A semi-direct method, derived from a function between the specific mass balance and the AAR, was used to calculate the mass balance for 2004 at the end of the natural balance year (September 9). A net mass budget of +0.011 x 10^6 m^3 was estimated. The ELA was calculated to be at 2755 m a.s.l. Therefore, on small glaciers with a surface area of only a few km^2, it is possible to use amateur photos, apply the PhotoModeler software to them and thus create, with reasonable accuracy, good results for the basic elements needed to produce new glacier maps.

PASTERZE 2004/05, HOHE TAUERN, AUSTRIA (1:25000)

(Mass Balance Map)

Bernhard Hynek[1] , Wolfgang Schöner[1], Christine Kroisleitner[1], Gernot Koboltschnig[2], Daniel Binder[3], Gernot Weyss[4]

[1]Central Institute for Meteorology and Geodynamics (ZAMG), Hohe Warte 38, 1190 Vienna, Austria
[2]University of Natural Resources and Applied Life Sciences (BOKU), Muthgasse 18, 1190 Vienna
[3]Vienna University of Technology Gusshausstrasse 27-29/1282, 1040 Vienna
[4]freelance Civil Engineer, Vienna

The mass balance of Pasterze was monitored during 1980–1997 by the Austrian Electricity Provider Tauernkraft (now VERBUND-AHP). After a break of seven years, measurements of Pasterze mass balance were restarted in 2004 by the Central Institute for Meteorology and Geodynamics (ZAMG). Hence the annexed map of mass balance 2004/2005, obtained by the glaciological method and a fixed date system, is the first complete mass balance after the interruption.

In September 2004, 31 ablation stakes were drilled in the ablation zone of Pasterze. During summer 2005 the stake network was extended by 6 further stakes in the ablation zone, (4 stakes on the debris-covered area) and by 11 stakes on the Oberer Pasterzenboden near the supposed equilibrium line. In sum the ablation data of 48 different stake sites were used to calculate the mass balance of the 2004/05 observation period.

Accumulation was measured by snow depth probing on 88 different points at the end of September 2005. Because of current weather conditions, snow pits could not be dug in 2005. For the calculation of the snow-water equivalent, the snow density values of September 2005 measured on the nearby Goldbergkees and Kleinfleißkees glaciers were used instead (firn: 530 kg/m^3, new snow: 400 kg/m^3). Accumulation measurements in the following years with higher accuracy and spatial resolution (ground penetrating radar, in addition to snow pits and probing, was used to detect horizons from previous years) and led to the estimation that the accumulation in 2005 was obtained with an accuracy of about +/-5%.

Surveying of snow depletion, which was almost the only information of mass balance in the hardly accessible areas in the south-eastern parts of the glacier and the large crevasse zones of Hufeisenbruch, was done at various times during summer 2005; maximum snow depletion was reached in early September 2005. Due to the use of a fixed date system (1.10.2004–30.9.2005) the line of maximum snow depletion (blue line with blue dots for snow in the annexed map) is not identical to the equilibrium line (red-blue border).

Total mass balance 2004/05 was calculated for the glacier area of 2003, which was derived from an ortho-photo taken on the 4th of September 2003 (source: Land Kärnten). The main results of the mass balance measurements are summarised in Table 1. In order to calculate the mass balance for different altitudinal zones (cf. Table 2), a digital elevation model (DEM) from 1998 (Kuhn, 1998) was used. The equilibrium line altitude (ELA) was obtained graphically from the diagram of mass balance versus altitude.

Table 1 Mass balance results for 2004/05 at Pasterze

S (area 2003)	17.7	km^2	B (total net mass balance)	$-15925 \cdot 10^6$	kg
Sc (accumulation area)	10.6	km^2	Bc (total net accumulation)	$5466 \cdot 10^6$	kg
Sa (ablation area)	7.1	km^2	Ba (total net ablation)	$-21391 \cdot 10^6$	kg
Sc/S (AAR)	0.6		b (mean specific mass balance)	-899	mm w.e.
Sc/Sa	1.5		bc (mean specific accumulation)	309	mm w.e.
ELA	2920	m a.s.l.	ba (mean specific ablation)	-1208	mm w.e.

Table 2 Mass balance for 2004/05 at Pasterze versus altitude for the debris-free and the debris-covered areas. Altitudinal zones were calculated from the DEM of 1998 (Kuhn, 1998). Glacier area was derived from the ortho-photo 2003 (source: State of Kärnten).

Altitude	Area S (2003)			Specific Mass Balance b			Mass Balance B		
DEM 98	total	debris-free	debris-covered	total	debris-free	debris-covered	total	debris-free	debris-covered
m a.s.l.	km^2	km^2	km^2	m w.e.	m w.e.	m w.e.	10^6 kg	10^6 kg	10^6 kg
2000 - 2100	0.007		0.007	-1.801		-1.801	-13		-13
2100 - 2200	0.620	0.323	0.298	-4.513	-6.976	-1.846	-2800	-2250	-550
2200 - 2300	1.242	0.678	0.564	-4.413	-6.027	-2.474	-5481	-4085	-1396
2300 - 2400	1.138	0.823	0.316	-4.921	-5.260	-4.040	-5602	-4326	-1276
2400 - 2500	0.543	0.505	0.038	-4.491	-4.474	-4.711	-2440	-2259	-181
2500 - 2600	0.434	0.420	0.015	-3.081	-3.041	-4.223	-1338	-1276	-62
2600 - 2700	0.583	0.582	0.002	-2.000	-1.995	-3.659	-1167	-1161	-6
2700 - 2800	0.853	0.853		-1.536	-1.536		-1310	-1310	
2800 - 2900	1.372	1.372		-0.661	-0.661		-907	-907	
2900 - 3000	2.383	2.383		0.259	0.259		617	617	
3000 - 3100	3.089	3.089		0.634	0.634		1959	1959	
3100 - 3200	2.868	2.868		0.544	0.544		1559	1559	
3200 - 3300	1.679	1.679		0.416	0.416		699	699	
3300 - 3400	0.704	0.704		0.358	0.358		252	252	
3400 - 3500	0.191	0.191		0.242	0.242		46	46	
3500 - 3600	0.003	0.003		0.160	0.160		0	0	
2000 - 3600	17.711	16.471	1.240	-0.899	-0.755	-2.810	-15925	-12442	-3484

ZONGO 1983–2006, BOLIVIA (1:10000)

(Ortho-Photo Map)

A. Soruco[1,2], C. Vincent[2], B. Francou[1], R. Blanc[3], E. Jordan[4],
P. Ginot[1], A. Machaca[5], E. Ramirez[6]

[1]IRD, Institut de Recherche pour le Développement. CP 9214 La Paz, Bolivia.
[2]LGGE, Laboratoire de Glaciologie et de Géophysique de l'Environnement,
BP96-38402 Saint Martin d'Hères, France.
[3]SINTEGRA, Société des Géomètres Experts BP 38241 Meylan, France.
[4]HHU, Heinrich Heine Universität, BP 40225 Düsseldorf – Germany.
[5]IGM, Instituto Geográfico Militar, La Paz – Bolivia.
[6]IHH, Instituto de Hidráulica e Hidrología, Universidad Mayor de San Andrés,
La Paz – Bolivia.

In 1991, the French Institute for Development (IRD) initiated glaciological investigations on tropical glaciers using Zongo (16°S) as the principal monitored glacier in Bolivia. Mass balance calculations require a precise hypsometric map to integrate the mass balance by altitudinal sections along the glacier. In Bolivia, six photogrammetrical flights were carried out over Zongo Gacier, that is, in 1956, 1963, 1975, 1983, 1997 and 2006. Between 1991 and 2001 the glacier mass balance was calculated using a manual digitalization of the cartographic map of the Bolivian Army, based on 1963 photographs (planimetry: UTM – PSAD56 Zone 19S; altimetry: International Geoid, assumed precision between 10 to 15m). Due to the poor quality of the Bolivian Army map, in 2002, IRD has selected the 1983 pictures to carry out another base map of Zongo Glacier. The 1983 picture presents the best contrast quality which allows the photogrametric restitution over snow-covered regions. A digital elevation model was elaborated in an analytical stereoplotter Planicom (Zeiss) with a regular grid of 50 x 50 m (planimetry: UTM – WGS84 Zone 19S; altimetry: EGM96 Geoid), but the accuracy of the model and the number of GCP (Ground Control Points) points were not known. Finally in 2006, IRD in cooperation with their local partners started a program to observe by aerial photogrammetry the evolution of several glaciers around La Paz city. The selected planimetry and altimetry were the UTM-WGS84 and the Ellipsoid-WGS84 respectively, because the geometric leveling of GCP points was not possible in remote areas.

The map aims at describing the new hypsometry and ortho-photo map of Zongo glacier based in 1983 photographs and, moreover, the glacier extension in 2006. The geometric distortion inherent to the corners of aerial images is removed by the ortho re-sampling process also called "ortho-rectification".

The 1983 photogrammetric flight was carried out by the Bolivian cartography army corps on June 20th using a Wild RC10 metric camera. Due to the size of the glacier (less than 2.5 km^2) and the flight height, resulting in a scale of 1:45000, only one stereo-pair (stereo-pair: 0295-0296) was required to generate the digital elevation model. A copy of negatives was scanned using a VEXEL Ultra Scan 5000 with a pixel size of 14 µm, which corresponds to an average ground resolution of 0.70 m. The aero-triangulation process was performed with 20 tie points and 9 GCP points using the Orima DP software. The precision of the model was Sigma0: 9.7 µm; RMSX: 0.75 m; RMSY: 0.97 m; RMSZ: 0.65 m. 12300 points were restituted manually with a 25 x 25 m regular grid in the Stereo Analyst for ArcGIS software and edited using the Terrain Editor of the Leica Photogrammetry Suite software (LPS). The DEM was interpolated linearly to 1m pixel size raster DEM format in ArcGIS. Finally, the ortho-photography (photography 0296) was ortho-rectified using the 1 m pixel size DEM in the LPS software.

In conclusion, the Zongo glacier consists now of six digital elevation models between 1956 and 2006 and in the future the glacier mass balance will be recalculated taking into account the hypsometric variation between 1983 and 2006.

Acknowledgements
The glaciological program was supported by IRD and the LGGE. We are grateful for the assistance received in Bolivia from the IHH (Instituto de Hidráulica e Hidrología) and the SNA (Servicio Nacional de Aerofotogrametría). The Sintegra Society (France) and the Heinrich Heine University (Germany) collaborated in the technical elaboration of this work. The printing of the maps was funded through the Department of Geography of the University of Zurich (GIUZ), Switzerland.

NORTHERN NOVAYA ZEMLYA OUTLET GLACIERS 1990–2000, C.I.S.

(Thematic Satellite Map)

A.V. Kouraev[1,2,*], B. Legrésy[1] and F. Rémy[1],
with the contribution of T. Strozzi[3] and M. Jackson[4]

[1]Laboratoire d'Etudes en Géophysique et Océanographie Spatiales (LEGOS), Toulouse, France
[2]State Oceanography Institute, St. Petersburg, Russia
[3]Gamma Remote Sensing, Gümligen, Switzerland
[4]Norwegian Water Resources and Energy Directorate, Oslo, Norway

[*]Corresponding author, contact: kouraev@legos.cnes.fr

The map based on satellite images shows changes in glacier terminal position of outlet glaciers of the Northern Novaya Zemlya Island. To assess glacier position changes, Landsat TM and ETM+ GeoCover imagery for two periods were used: circa 1990 and circa 2000. By comparing glacier terminal position for the two datasets, assessment of glacier advance/retreat was made for several outlet glaciers: 24 on the western (Barents sea) coast, 12 on the eastern (Kara sea) coast, and for 4 glaciers of the Lednikovoye lake in the southern part of the Northern Novaya Zemlya.

Most of the glaciers retreated during this period, the most pronounced retreat was observed for large Moshniy (-7.76 km^2) and Roze (-6.55 km^2) glaciers on the eastern coast. Only four glaciers of 40 advanced: two of them (Oga and Serp i Molot) on the eastern coast, they advanced very slightly (less than 1 km^2), and two other glaciers (Borzova and Pavlova) on the western coast, whose advance as more pronounced (3.84 and 3.94 km^2, respectively).

Map is made in the UTM (Zone 40) Projection. Glacier boundaries and ice divide line are after a schematic map from Varnakova and Kotlyakov (1978), one of the few available sources of maps for Novaya Zemlya glaciers. Comparison of these boundaries with the ice-surface motion map produced using offset tracking from JERS-1 L-band SAR data (Strozzi et al. 2007) shows that they are generally consistent in the lower parts. However for upper parts, the JERS-1 based map shows significantly larger glacier feeding zones, suggesting potential improvement of the Novaya Zemlya glacier boundaries using remote sensing techniques.

Acknowledgements:
This research was done within the framework of the FP6 EC INTEGRAL (Interferometric Evaluation of Glacier Rheology and Alterations) project (Contract No. SST3-CT-2003-502845). We would like to thank A. Sharov (Joanneum Research, Graz, Austria) for his comment on the Vera glacier state in 2001. Landsat GeoCover imagery is from the MrSID image server (https://zulu.ssc.nasa.gov/mrsid). Map printed by Norwegian Water Resources and Energy Directorate.

GLACIERS OF MOUNT KENYA 1899–2004, KENYA, (1:5000)

(Glaciological Map)

S. Hastenrath

Department of Atmospheric and Oceanic Sciences,
University of Wisconsin, Madison, U.S.A.

The map documents in the context of the century-long history of glacier recession on Mount Kenya. Observations from early expeditions provide evidence from the end of the 19th century to the 1940s, and photogrammetric mappings in 1947, 1963, 1974, 1978, 1982, 1985, 1986, 1987, 1993 and 2004 give quantitative detail for the later decades. Of the eighteen ice entities at the end of the 19th century, one glacier may have disappeared before 1926, five vanished after 1926, one after 1978, and one after 1993. All other glaciers also suffered substantial shrinkage, especially from the 1970s onward. Mount Kenya, right under the Equator, is the mountain with best documentation of glacier recession in all of the tropics. Full documentation on this map is contained in Hastenrath (2005b). Further background information is available in Hastenrath (1984), Caukwell and Hastenrath (2006), Rostom and Hastenrath (2007).

GLACIERS OF MOUNT KENYA 2004, KENYA (1:5000)

(Aerial Photogrammetric Map)

S. Hastenrath

Department of Atmospheric and Oceanic Sciences,
University of Wisconsin, Madison, U.S.A.

The map documents the distribution of glaciers on Mount Kenya in the year 2004. A new glacier inventory was compiled from the map dated September 2004, and the glacier changes during 1993–2004 were evaluated with reference to Rostom and Hastenrath (1994). The map's ground control network is described in Hastenrath et al. (1989). The aerial photograph was flown on 1st of September, 2004, by Photomap International at an average height of 1483 m above the average terrain level of 4800 m a.s.l. The photographs were taken by a Wild 153 mm RC10 camera, and are at an approximante average scale of 1:10000 with 80% forelap and 60% sidelap, to cope with the extreme local relief. Aerial triangulation was conducted to determine the coordinates of control points. In addition to 8 ground control points a further 16 control points established from stereo models were used. Refer to Hastenrath et al. (1989) for a discussion of coordinate systems. Full documentation on this map is contained in Rostom and Hastenrath (2007). Further background information is provided in Hastenrath (1984).

LEWIS GLACIER 1958, KENYA (1:2500)

(Glaciological Map)

S. Hastenrath

Department of Atmospheric and Oceanic Sciences,
University of Wisconsin, Madison, U.S.A.

The present map is a product of the International Geophysical Year (IGY) Mount Kenya Expedition in 1957–1958. Although nearly half a century had passed, this map had not been published and risked being lost to posterity. It is now made accessible to the research community. The IGY Mount Kenya Expedition formed part of the program of the British National Committee for the IGY. The main field program was conducted during December 1957 to January 1958. The expedition established a network of ground control points in local coordinates, which formed the basis for glacier research in later decades. With reference to part of the mentioned network of ground control points, the Lewis Glacier was mapped tacheometrically at scale 1:2500. Full documentation on this map is contained in Caukwell and Hastenrath (2006). Further background information is provided in Charnley (1959).

WAHLENBERGFJORD, AUSTFONNA, SVALBARD, OUTLET GLACIERS: 1987–1998, NORWAY

(Thematic Satellite Map)

A.V. Kouraev[1,2,*], B. Legrésy[1] and F. Rémy[1],
with the contribution of A. Taurisano[3] , J. Kohler[3] and M. Jackson[4]

[1]Laboratoire d'Etudes en Géophysique et Océanographie Spatiales (LEGOS), Toulouse, France
[2]State Oceanography Institute, St. Petersburg, Russia
[3]Norwegian Polar Insitute, Tromsø, Norway
[4]Norwegian Water Resources and Energy Directorate, Oslo, Norway

[*]Corresponding author, contact: kouraev@legos.cnes.fr

The map based on satellite images shows changes of glacier terminal position of several outlet glaciers in the Wahlenbergfjord, North-Western part of Austfonna, Svalbard archipelago. The map is produced in the UTM (Zone 34) projection, glacier boundaries are after Hagen et al. (1993). In order to assess glacier position changes, SPOT-1 to SPOT-4 imagery for various dates between 1987 and 1998 have been used. The images have been georeferenced (using ice-free land and coastal features) based on the NPI vector coastline data, and multi-temporal analysis of glacier terminal position has been done.

For five glaciers (Bodleybreen, Aldousbreen, Frazerbreen, Ericabreen and Palanderbreen) changes between 15 April, 1987 and 28 March, 1998 are provided as (a) color-coded regions of advance/retreat of glacier terminal position and (b) resulting changes in km^2 and change rate (km^2 per year). These changes are rather small (less than 1 km^2). Four of these five glaciers have retreated, and only Ericabreen has slightly advanced.

Etonbreen and the neighbouring Basin 03 glaciers feature more pronounced dynamics. For these glaciers we provide (a) a map of glacier terminus positions for five dates between 1987 and 1988 and (b) corresponding changes in square kilometre and change rate (km^2 per year) for each period. Both glaciers continually retreated between 1987 and 1988, with maximal speed (-1.01 km^2 per year) observed between July 1988 and July 1991. Since then, the retreat gradually slowed down to -0.48 km^2 per year (between July 1993 and March 1998).

Acknowledgements:
This research was done within the framework of the FP6 EC INTEGRAL (Interferometric Evaluation of Glacier Rheology and Alterations) project (Contract No. SST3-CT-2003-502845). SPOT imagery for 1987, 1988, 1991, 1993 and 1998 are from SPOT/ ISIS Program. © CNES, Distribution Spot Image SA. Map printed by Norwegian Water Resources and Energy Directorate.

CHAPTER 6 THE GLOBAL LAND ICE MEASUREMENTS FROM SPACE (GLIMS) INITIATIVE

GLIMS goals

The international GLIMS project is a global consortium of universities and research institutes, coordinated by Jeff Kargel, University of Arizona, Department of Hydrology and Water Resources, whose purpose is to assess and monitor the world's glaciers primarily using data from optical satellite instruments, such as ASTER (Advanced Spaceborne Thermal Emission and reflection Radiometer). Specifically, GLIMS objectives are to ascertain the extent and condition of the world's glaciers so that we may understand a variety of Earth surface processes and produce information for resource management and planning. These scientific, management and planning objectives are supported by the monitoring and information production objectives of the United Nations scientific organizations (Kieffer et al. 2000, Bishop et al. 2004, Kargel et al. 2005, Raup et al. 2006).

A first attempt to obtain an overview of the Earth's glaciers and ice caps was made with the compilation of the World Glacier Inventory (WGMS, 1989), a database of glacier locations and attributes produced mainly on the basis of aerial photographs and topographic maps. In 1999, the GLIMS project was established to, among others, continue this inventorying task based on space technologies and in close cooperation with the National Snow and Ice Data Center (NSIDC; Boulder, USA) and the World Glacier Monitoring Service (WGMS).

GLIMS entails comprehensive satellite multi spectral and stereo-image acquisition of land ice, use of satellite imaging data to measure inter-annual changes in glacier area, boundaries, and snowline elevation, measurement of glacier ice-velocity fields, and development of a comprehensive digital database to inventory the world's glaciers. This work and the global image archive at the EROS Data Center (Sioux Falls, USA) is useful for a variety of scientific and planning applications. The GLIMS glacier database and GLIMS web site are developed and maintained by the NSIDC.

Beside the GLIMS main applications glacier mapping and monitoring, ASTER proved also to be very suitable for assessing glacier hazards and managing related disasters (Kääb et al. 2003). GLIMS is closely collaborating with the international working group on glacier and permafrost hazards in mountains, GAPHAZ, under the International Association for the Cryospheric Sciences (IACS) and the International Permafrost Association (IPA) (http://www.geo.uio.no/remotesensing/gaphaz).

GLIMS technologies

GLIMS primarily utilizes multispectral imaging from the Landsat TM and ETM+ series, and the ASTER sensor. Landsat TM and ETM+ data represent a well-established and robust data source for glacier inventorying and monitoring from space (Kääb et al. 2002, Paul et al. 2002). Capabilities of the ASTER sensor, available since 2000 onboard the NASA Terra spacecraft, include 3 bands in VNIR (visible and near infrared) with 15 m resolution, 6 bands in the SWIR (short-wave infrared) with 30 m, 5 bands in the

TIR (thermal infrared) with 90 m, and a 15 m resolution NIR along-track stereo-band looking backwards from nadir. Of special interest for glaciological studies are the high spatial resolution in VNIR, the stereo-, and the pointing-capabilities of ASTER. With topography being a crucial parameter for the understanding of high-mountain phenomena and processes, such as glacier volume changes, DEMs generated from the ASTER along-track stereo band are especially helpful (Kääb 2005). The nominal ASTER lifetime was designed to be six years, i.e. until 2006. Currently, 2008, in particular the ASTER SWIR bands are deteriorating significantly. The vast archive of ASTER data useful for world-wide glacier mapping already forms, however, an important data source for time series of glacier change between 2000 and the present, and an invaluable baseline data set for comparisons with data from other similar multi spectral satellite missions.

GLIMS database and tools

Currently the GLIMS database at NSIDC holds over 80000 glacier outlines in North and South America, Europe, Asia, Antarctica and is quickly growing (Raup et al. 2007, updated). NSIDC has developed easy-to-use search and extraction tools which allow download of GLIMS data in a variety of geo-information formats. A number of tutorials, documented procedures, specifications, example data and auxiliary tools for data formatting and quality control are available from the GLIMS web site. The GLIMSView software is a free software that facilitates extraction of glacier outlines from optical satellite imagery and their export to GLIMS format. The tool can be used as stand-alone software or in combination with other image processing packages and geo-information systems.

Further information on GLIMS and contacts

GLIMS coordinator: Jeff Kargel, University of Arizona, USA: kargel@hwr.arizona.edu

GLIMS web-page: http://www.glims.org

GLIMS at NSIDC: http://www.nsidc.org/glims/; Richard Armstrong, Bruce Raup

Goals of GlobGlacier

The new ESA project GlobGlacier is a data user element (DUE) activity within ESAs Living Planet program that responds to the needs of a certain number of users and organisations which are actively involved in the project as a user group. The major aim of the GlobGlacier project is to establish a service for glacier monitoring from space, that builds upon, complements and strengthens the existing services and network of global glacier monitoring (e.g. as conducted by the WGMS and GLIMS within the framework of GTN-G). The basic strategy is to apply and document well-established remote sensing techniques to archived satellite data for generating a set of glacier-related products in key regions all over the world (GCOS, 2006). The data products that will be created within the project lifetime consist of (in brackets the foreseen amount): glacier outlines and terminus position (20000 each), snow lines (5000), topography (5000), elevation changes (1000) and flow velocity (200). All data will be provided in a publicly accessible and open digital format through the existing databases at NSIDC and WGMS.

The selection of key regions is mainly driven by places that are not yet covered in the GLIMS database or where detailed glacier inventory data still have to be created. Further selection criteria for the regions include: sea level rise contribution, freshwater resources, climate sensitivity and glacier-related hazards. In order to provide a service that could be widely used, key regions will also cover different sensor types, several validation sites for the individual products, data integration sites (where all or several products will be created) and glaciers/ice caps on all continents. More than ten text documents will describe, among others, the applied methods, workflows, standards, challenges and results. While the target time period for the glacier outlines and topography products is around the year 2000 (driven by the availability of the Landsat ETM+ Geocover and the SRTM DEM), other products will go back in time up to twenty years.

GlobGlacier technologies

The applied technologies will strongly depend on the product and the sensors used for their generation. For a more detailed overview than provided below, see Paul et al. (subm).

Glacier outlines will be created from multispectral sensors (e.g. Landsat TM/ETM+, Terra ASTER, SPOT HRV) using well-established methods (thresholded band ratios) combined with manual editing and GIS-based data fusion at three different levels of detail: Level 0 (L0): outlines enclosing contiguous ice masses that are corrected for misclassification (e.g. debris, shadow, water); L1: individual glaciers that result from combining L0 outlines with hydrologic divides; L2: outlines from L1 combined with DEM data to obtain a detailed glacier inventory. The terminus position will be stored as a glacier specific point with a certain elevation and assigned manually from multispectral sensors or by intersecting a central flowline with the L1 glacier outlines. The snowline will be mapped from multispectral sensors using images from the end of the ablation period combined with L1 outlines and topographic information. Topography will be compiled from already available resources (mostly the SRTM3 DEM) and complemented by satellite-derived DEMs, either from multispectral stereo sensors (e.g. ASTER, SPOT) or interferometric SAR data (e.g. from the ERS1/2 tandem mission). Elevation change will be derived from differencing DEMs from two epochs in time and from time series of airborne or satellite altimetry data (e.g. RADAR, LiDAR). The spatial extrapolation of point measurements to the entire surface will be a special challenge. Velocity fields will be obtained from either feature tracking of repeat pass optical imagery or from microwave sensors using differential SAR interferometry or offset tracking. The time period analyzed will depend on the available satellite data and vary from seasonal to annual means.

GlobGlacier organization

The project started in November 2007 for a duration of three years and is led by the Geography Department, University of Zurich (Switzerland). The designated European consortium further includes Gamma Remote Sensing (Switzerland), Enveo (Austria), and the Universities of Oslo (Norway) and Edinburgh (UK). While the University of Zurich is in charge of the products glacier outlines and terminus position, each of the consortium partners is responsible for one of the other products. The first 16 months of the project (phase 1) are mostly committed to the creation of the text documents and some data examples for the selected key regions. In the second 20 months (phase 2) the data products will be created. The user group members will give feedback on the quality of the generated products and provide data for validation purposes where possible. In a first step data holdings will be compared to the demands for the selected key regions and a strategy will be developed to determine in which regions which products will be created from which sensors. The related compilation will be cross-checked with the user group and currently ongoing activities by the GLIMS community before the products will be created. Where possible, it is also planned to integrate existing results from previous studies (either by the consortium members or other scientists) into the project. A frequently updated meta-information web page will be used for harmonization of the activities within the consortium and to communicate the actual status and results of the project to the public.

Links

ESA: http://dup.esrin.esa.it/projects/summaryp98.asp

GCOS: http://www.wmo.ch/pages/prog/gcos/Publications/gcos-107.pdf

GlobGlacier Project: http://www.globglacier.ch

IGOS cryosphere theme report: http://igos-cryosphere.org/docs/cryos-theme-report.pdf

CHAPTER 8 GENERAL COMMENTS AND PERSPECTIVES FOR THE FUTURE

Strong acceleration of glacier melting characterized the first five-year period of the 21st century (WGMS 2003, 2005a and b, 2007; cf. Zemp et al. 2005). Rates of mass losses (-0.60 m w.e.) of the 30 'reference' glaciers with (almost) continuous measurements since 1976 more than doubled the mean value observed during the two preceding decades 1980–2000 (-0.29 m w.e.). The average annual mass loss of 0.58 m water equivalent (w.e.) for the decade 1996–2005 is more than twice the loss rate during the period 1986–1995 (-0.25 m w.e.), and more than four times the rate of the period 1976–1985 (-0.14 m w.e.). The mean of the 30 'reference' glaciers is influenced by the great number of Alpine and Scandinavian glaciers but closely corresponds to the mean value calculated using only one single (in some places averaged) value for each of the involved mountain ranges and can be considered representative for all measured mass balances according to analyses using various statistic aproaches (Kaser et al. 2006). While 34% of the reference glaciers had an overall positive balance during 1976–1995, only two (7%) of them had an overall mass gain over the past decade (1996–2005). This indicates that glacier shrinkage not only becomes faster but also more spatially uniform. Further analysis requires detailed consideration of such aspects as glacier sensitivity and feedback mechanisms. The cumulative mass balances reported for the individual glaciers not only reflect regional climatic variability but also marked differences in the sensitivity of the observed glaciers.

The past quarter of a century 1980–2005 shows a striking trend of increasingly negative balances with average annual ice thickness losses of decimeters and nearing the meter scale (Braithwaite 2002, Zemp et al. in press). Because unchanged climatic conditions would cause mass balances to approach zero values, constant non-zero mass balances reflect continued climatic forcing. The observed trend of increasingly negative mass balances is consistent with accelerated global warming and correspondingly enhanced energy flux towards the earth surface. In comparison with mass balances, changes in glacier length are strongly enhanced and easily measured but indirect, filtered and delayed signals of climate change. Total retreat of glacier termini during the 20th century is commonly measured in kilometers for larger glaciers and in hundreds of meters for smaller ones. Characteristic long-term average rates of glacier thinning (mass loss) can be calculated from cumulative length change data using a continuity approach over time periods corresponding to the dynamic response time of individual glaciers (Haeberli and Hoelzle 1995, Hoelzle et al. 2003). Assuming negligible changes in precipitation, cumulative glacier length changes can even provide strong independent evidence of global warming at fast rates (Oerlemans 2005). However, the assumption that the mass balance of a glacier is fairly well decoupled from the dynamic response of the glacier and primarily constitutes a direct signal of climatic conditions at the site is reasonable only for relatively steep glaciers with a short response time and/or for slow climate forcing. With accelerating climate change, various feedbacks come into play.

Small and steep glaciers with relatively short dynamic response times can adjust more quickly to changing climatic conditions than large glaciers with lower overall surface slopes. Positive feedbacks between mass balance and altitude, therefore, start playing a predominant role for large glaciers (Raymond et al. 2005) and make direct transfer of mass balance information from small to large glaciers difficult. Cold firn areas may warm up and start losing melt water to the sea, changing their climate sensitivity (Haeberli 2006, Vincent et al. 2007). Independently of size and firn temperature, albedo lowering due to retreating or even disappearing firn areas and to enhanced pollution by soot or dust reinforces melting and mass loss (Paul et al. 2005). Process changes such as widespread appearance of rock outcrops, collapse features at glacier margins, or lake formation further speed up the rate of glacier shrinkage (Paul et al. 2004). The acceleration of negative mass balance and corresponding thickness loss causes increasing disequilibria to develop and glaciers to downwaste and disintegrate rather than to retreat, making length observations as part of long-term glacier monitoring increasingly difficult (Haeberli et al. 2007, Paul et al. 2007). This development could cause the complete vanishing of glaciers which constitute the presently existing in-situ mass balance network. In the European Alps, for instance, several glaciers with long observational series of mass balance could indeed disappear within the first half of our century and three of them (Sarennes, Careser and Sonnblick: Carturan and Seppi 2007, Le Meur et al. 2007) may even not survive more than a decade or two. In order to preserve the continuity of the mass balance network, therefore, mass balance measurements are now being started on still larger and higher reaching glaciers. This is, in fact, an urgent task if sufficient overlap in time is to be assured.

The striking worldwide glacier changes (Ohmura 2006) were accompanied by rapid developments in observational technology. Prominent technologies such as airborne laser altimetry in combination with kinematic GPS (Abdalati et al. 2004), space-borne digital elevation models (DEMs) from SRTM, ASTER or SPOT (e.g. Berthier et al. 2004, Larsen et al. 2007, Rignot et al. 2003, Schiefer et al. 2007, Surazakov and Aizen 2006) and distributed modeling of the climatic accumulation area or the mass and energy balance for individual glaciers (Arnold et al. 2006) or large glacier ensembles (Machguth et al. 2006a, Zemp et al. 2007) open new dimensions for glacier monitoring and data analysis. Correct determination of complex precipitation and accumulation patterns influenced by wind drift and avalanching remains a fundamental problem and a large uncertainty with distributed energy and mass balance modeling (Machguth et al. 2006b), as well as with in-situ measurements of mass balance with networks of stakes and pits (direct glaciological method). Careful validation and calibration with geodetic/photogrammetric volume change determinations is therefore essential. Laser altimetry thereby enables very high precisions to be reached. Differencing of DEMs is much less precise but for the first time helps to establish the extent to which mass balance observations at single glaciers are representative with respect to all glaciers of a mountain range (Paul and Haeberli 2008).

Mountain glaciers are Essential Climate Variables (ECV) in global climate-related observations and assessments (GCOS 2004). The integrated perception and documentation of glacier changes within the framework of such internationally coordinated programmes is a challenge of historical dimensions. Since the initiation in 1894 of a worldwide programme for collection of standardized information about ongoing glacier changes with the foundation of the International Glacier Commission at the 6th International Geological Congress in Zurich, Switzerland (Forel 1895; Haeberli et al. 1998), various related aspects have changed in a most remarkable way:

- It has become obvious that the ongoing trend of worldwide and fast, if not accelerating, glacier shrinkage at the century time scale is of a non-cyclic nature – there is definitely no further question of the originally envisaged “variations périodiques des glaciers”.

- Under the influence of human impacts on the climate system (enhanced greenhouse effect), dramatic scenarios of future developments – including complete deglaciation of entire mountain ranges – must be taken into consideration.

- Such scenarios may lead far beyond the range of historical/holocene variability and most likely introduce processes (extent and rate of glacier vanishing, distance to equilibrium conditions) without precedence in history.

- A broad and worldwide public today recognizes glacier changes as a key indication of regional and global climate and environment change.

- Observational strategies established by expert groups within international monitoring programmes build on advanced process understanding and include extreme perspectives.

- These strategies make use of the rapidly developing new technologies and relate them to traditional approaches in order to apply integrated, multilevel concepts (in-situ measurements to remote sensing, local process oriented to regional and global coverage), within which individual observational components (length, area, volume change) fit together, enabling a comprehensive view.

An international network of glacier observations such as the World Glacier Monitoring Service (WGMS) of the International Association of Cryospheric Sciences (IACS/IUGG) and the Federation of Astronomical and Geophysical Data Analysis Services (FAGS/ICSU), together with its Terrestrial Network for Glaciers (GTN-G; Haeberli et al., 2000, 2002) within the Global Terrestrial Observing System (GTOS) and the Global Climate Observing System (GCOS), is designed to provide quantitative and understandable information in connection with questions about process understanding, change detection, model validation and environmental impacts in a transdisciplinary knowledge transfer to the scientific community as well as to policymakers, the media and the public. A Global Hierarchical Observing Strategy (GHOST) is used to bridge the gap in scale, logistics and resolution between detailed process studies at a few selected sites and global coverage at pixel resolution using techniques of remote sensing and geo-informatics. This tiered system includes

- ***extensive glacier mass balance and flow studies within major climatic zones for improved process understanding and calibration of numerical models:*** Full parameterization of coupled numerical energy/mass balance and flow models is based on detailed – wherever possible, seasonal, or even more frequent – observations for improved process understanding, sensitivity experiments and extrapolation to areas with less comprehensive measurements.

- ***determination of regional glacier volume change within major mountain systems using cost-saving methodologies***: Strategically placed stakes/pits combined with photogrammetric/geodetic mapping of the entire glacier enables annual resolution in time to be combined with exact determination of volume and mass changes for the entire glacier.

- ***long-term observations of numerous glacier length, area and thickness changes within major mountain ranges for assessing the representativeness of continuous mass balance and volume change measurements on single glaciers:*** Documented cumulative glacier length changes allow for worldwide intercomparison of glacier fluctuations, serve as unique demonstration objects concerning long-term climate change, and are the key proxy linking the glacier changes of the 20^{th} century to the past centuries and millennia (Haeberli and Holzhauser 2003, Oerlemans 2005, Sugiyama et al. 2007). However, glaciers in many regions increasingly react with vertical downwasting (instead of dynamical retreat) to the rapid warming since the mid-1980s, and have definitely become a non-linear climate proxy. Here, differentiation of DEMs increasingly assists in these tasks and greatly enhances the potential for regional glacier change assessments (Paul and Haeberli 2008).

- ***glacier inventories repeated at time intervals of a few decades by using (satellite) remote sensing:*** Air- and spaceborn remote sensing is used to compile detailed or preliminary glacier inventories as a basis for quantifying the evolution of large glacier ensembles, for assessing corresponding impacts and for modeling possible future developments at regional to continental scales.

This integrated and multilevel strategy aims at combining in-situ observations with remotely sensed data, process understanding with global coverage and traditional measurements with new technologies. Application of this integrative concept was illustrated for the European Alps (Haeberli et al. 2007), where glaciers can be shown to have lost about half their total volume (roughly -0.5% per year) between 1850 and around 1975, another 25% (or -1% per year) of the remaining amount between 1975 and 2000, and additional 10 to 15% (or -2 to -3% per year) in the first five years of this century. Scenario calculations concerning effects of global atmospheric warming (Nesje et al. 2008, Zemp et al. 2006) clearly confirm earlier regional projections (Haeberli and Hoelzle 1995) that many mountain ranges could lose major parts of their glacier volumes within the 21^{st} century and that the strongest melting in such regions is likely to take place during the coming decades. Impacts are especially severe in relation to the regional water cyle (Huss et al. 2008) and also continue to affect sea level (Meier et al. 2007).

Glacier fluctuation data compiled by the WGMS is widely used in order to analyze regional and global glacier changes as well as theirs impact on hydrology, natural hazards and sea level changes. Since the publication of the last issue of the 'Fluctuations of Glaciers' series (WGMS 2005) several thematic journal volumes (Casassa et al. 2007, International Glaciological Society 2007, Kääb et al. 2007, Kull et al. 2008, International Glaciological Society in prep.) and books (Grove 2004, Bamber and Payne 2004, Knight 2006, Kotlyakov 2007, Orlove et al. 2008, WGMS 2008) have been published on the measurement and modeling of glacier changes and their impacts. In 2007 the ‘4th Assessment Report of the Intergovernmental Panel on Climate Changes’ (IPCC 2007) was released summarizing, among other things, the state-of-knowledge of the research on glaciers and ice caps. In the same year, the ‘Global Outlook for Ice and Snow’ was published by the United Nations Environment Programme (UNEP 2007), written by more than 70 scientists from around the world as a contribution to the International Polar Year 2007–2008, including chapters dedicated to glaciers and ice caps (Zemp et al. 2007) and to ice and sea level change (Church et al. 2007).

Overall it can be concluded that glaciers and ice caps around the globe have been shrinking dramatically since their Holocene maximum extent towards the end of the Little Ice Age, between the 17th and the second half of the 19th century, with increasing rates of ice loss since the mid-1980s. On a time scale of decades, glaciers in various mountain ranges have shown intermittent re-advances. However, under the present climate scenarios, the ongoing trend of worldwide and fast, if not accelerating, glacier shrinkage on the century time scale is not a periodic change and may lead to the deglaciation of large parts of many mountain regions by the end of the 21st century.

In 2006, the WGMS was evaluated through IACS/IUGG. The evaluation, comprising a self-evaluation report, a site visit by the evaluation committee, and a subsequent evaluation report, came to the main conclusions that (i) WGMS is the only organization with an established network able to continue the collection of in-situ data in one database, (ii) the current rapid technological developments require traditional measurements to be related to modern techniques in order to apply integrated, multi level monitoring concepts, which cannot be accomplished by WGMS in its present form, organization and funding structure, and that (iii) WGMS should, therefore, strengthen its cooperation with the World Data Center for Glaciology, at the National Snow and Ice Data Center (NSIDC) in Boulder, USA, and the Global Land Ice Measurements from Space (GLIMS) project. The implementation of the re-organization of the international glacier monitoring has already been started resulting in a Memorandum of Understanding between WGMS and NSIDC as a first step towards a common GTN-G Steering Committee to be established under the umbrella of IACS/IUGG in order to coordinate, consult and support WGMS, NSIDC and GLIMS regarding the monitoring of glaciers and ice caps, facing the challenges of the 21st century.

LITERATURE

This chapter lists literature, cited, collected and submitted by principal investigators and national correspondents.

Abdalati, W., W. Krabill, E. Frederick, S. Manizade, C. Martin, J. Sonntag, R. Swift, R. Thomas, J. Yungel, and R. Koerner (2004): Elevation changes of ice caps in the Canadian Arctic Archipelago. Journal of Geophysical Research, 109, F04007: doi:10.1029/2003JF000045.

Agnew, T., R. Brown, M. Burgess, G. Cogley, M. Demuth, C. Duguay, G. Flato, B. Goodison, R. Koerner, H. Melling, T. Prowse, B. Ramsay, M. Sharp, S. Smith, and A. Walker (1999): Development of a Canadian GCOS Workplan for the Cryosphere: Summary Report of Canadian GCOS Workshop, Victoria, February 24–26. Environment Canada, Meteorological Service of Canada: 37 pp.

Agnew, T., R. Brown, M. Burgess, G. Cogley, M. Demuth, C. Duguay, G. Flato, B. Goodison, R. Koerner, H. Melling, D. O'Neil, T. Prowse (2002): National Plan for Cryospheric Monitoring – A Canadian Contribution to the Global Climate Observing System (Editors: R. Brown and D. O'Neil). Environment Canada, Meteorological Service of Canada: 85 pp.

Ananicheva, M. (2006): Climatically determined glacier fluctuations in the second part of the 20th century – Suntar-Khayata Mountains and Chersky range. In: Kotlyakov et al. (eds.): The glaciarization of Northern and Central Eurasia in present time. Nauka, Moscow: p. 198–204 (in Russian with abstract in English).

Andreassen, L.M., Elvehøy, H., Kjøllmoen, B., Engeset, R.V. and Haakensen, N. (2005): Glacier mass balance and length variations in Norway. Annals of Glaciology, 42: p. 317–325.

Arendt, A.A., Echelmeyer, K.A., Harrison, W.D., Lingle, C.S. and Valentine V.B. (2002): Rapid wastage of Alaska glaciers and their contribution to rising sea level. Science, 297: p. 382–386.

Arnold, N.S., Rees, W.G., Hodson, A.J. and Kohler, J. (2006): Topographic controls on the surface energy balance of a high Arctic valley glacier. Journal of Geophysical Research, 111(F2), F02011: doi:10.1029/2005JF000426.

Aschenbrenner, J. and H. Slupetzky (1995): Granatspitze. Orthophoto-Strichkarte 1:5000. Publ. by the Dept. of Geography and BMLV-Fü/MilGeo, Viennna.

Aschenbrenner, J. and H. Slupetzky (1998): Stubacher Sonnblickkees, Hohe Riffel & Alpinzentrum Rudolfshütte, Austria 1:5000 (Three Image Line Maps). In: WGMS (1998): Fluctuation of Glaciers 1990–1995 Vol. VII: p.71–72.

Balerna, A., Bernieri, E., Esposito, A., Pecci, M. and Smiraglia, C. (2001): Cs-137 gamma peak detection in snow layers on Calderone glacier. In: Visconti, G., Beniston, M., Jannorelli, E. and Barba, D. (eds.): Global change and protected areas. Advances in Global Change Research, Vol. 9, Kluwer Academic Publishers: p. 147–152.

Bamber, J.L. and Payne A.J., eds. (2004): Mass balance of the cryosphere. Cambridge University Press, Cambridge: 662 pp.

Bauder, A., Funk, M. and Gudmundsson, G.H. (2003): The ice-thickness distribution of Unteraargletscher, Switzerland. Annals of Glaciology, 37: p. 331–336.

Bauder, A., Funk, M. and Huss, M. (2007): Ice-volume changes of selected glaciers in

the Swiss Alps since the end of the 19th century. Annals of Glaciology, 46: p. 145–149.
Berthier, E., Arnaud, Y., Baratoux, D., Vincent, C. and Rémy, F. (2004): Recent rapid thinning of the "Mer de Glace" glacier derived from satellite optical images. Geophysical Research Letters, 31 (17), L17401.
Berthier, E., Arnaud, Y., Kumar, R., Ahmad, S., Wagnon, P. And Chevallier, P. (2006): Remote sensing estimates of glacier mass balances in the Himachal Pradesh (Western Himalaya, India). Remote Sensing of Environment: doi:10.1016/j.rse.2006.11.017
Bidlake, W.R., Josberger, E.G., and Savoca, M.E. (2004): Water, ice, and meteorological measurements at South Cascade Glacier, Washington, balance year 2002. U.S. Geological Survey Scientific Investigations Report, 2004-5089: 38 pp.
Bidlake, W.R., Josberger, E.G., and Savoca, M.E. (2005): Water, ice, and meteorological measurements at South Cascade Glacier, Washington, balance year 2003. U.S. Geological Survey Scientific Investigations Report, 2005-5210: 48 pp.
Bidlake, W.R., Josberger, E.G., and Savoca, M.E. (2007): Water, ice, and meteorological measurements at South Cascade Glacier, Washington, balance years 2004 and 2005. U.S. Geological Survey Scientific Investigations Report, 2007-5055: 70 pp.
Bishop, M.P., Olsenholler, J.A., Shroder, J.F., Barry, R.G., Raup, B.H., Bush, A.B.G., Coplan, L., Dwyer, J.L., Fountain, A.G., Haeberli, W., Kääb, A., Paul, F., Hall, D.K., Kargel, J.S., Molnia, B.F., Trabant, D.C., and Wessels, R. (2004): Global land ice measurements from space (GLIMS); remote sensing and GIS investigations of the Earth's cryosphere. Geocarto International, 19 (2): p. 57–84.
Björnsson, H., F. Palsson and H. Haraldsson (2002): Mass balance of Vatnajökull (1991–2001) and Langjökull (1996–2001), Iceland. Jökull, 51: p. 75–78.
Bolch, T. (2007): Climate change and glacier retreat in northern Tien Shan (Kazahkstan/Kyryzstan) using remote sending data. Gobal and Planetary Change, 56 (1–2): p. 1–12.
Braithwaite, R.J. (2002): Glacier mass balance: the first 50 years of international monitoring. Progress in Physical Geography, 26 (1): p. 76–95.
Braun, L.N., Escher-Vetter, H., Siebers, M. and Weber, M. (2007): Water balance of the highly glaciated Vernagt basin, Ötzal Alps. In: Psenner, R. and Lackner, R. (eds.): The water balance of the Alps. Alpine Space – Man & Environment, 3, Innsbruck University Press: p. 33–42.
Braunshier R. (2005): Erstellung eines digitalen Geländemodells zur Erfassung der Ausaperung am Stubacher Sonnblickkees im Jahr 2004 aus Amateurphotos. Thesis. Naturwiss. Fakultät der Universität Salzburg: 101 pp.
Brock, B.W., Willis, I.C. and Sharp, M.J. (2000a): Measurements and parametrization of albedo variations at Haut Glacier d'Arolla, Switzerland. Journal of Glaciology, 46 (155): p. 675–688.
Brock, B.W., Willis, I.C., Sharp, M.J. and Arnold, N.S. (2000b): Modelling seasonal and spatial variations in the surface energy balance of Haut Glacier d'Arolla, Switzerland. Annals of Glaciology, 31: p. 53–62.
Burgess, D.O., Sharp, M.J., Mair, D.W.F., Dowdeswell, J.A. and T.J. Benham, T.J. (2005): Flow dynamics and iceberg calving rates of Devon Ice Cap, Nunavut, Canada. Journal of Glaciology, 51 (173): p. 219–230.

Cáceres, B., Jordan, E., Hastenrath, S. and Francou, B. (2008): Upgrade of the inventory for the glaciers in Ecuador. 4th Alexander Humboldt International Conference, Santiago de Chile, abstract no. AVH4-A-00024.
Carrasco, J.F., Casassa, G. and Quintana, J. (2005): Changes of the 0°C isotherm and the equilibrium line altitude in central Chile during the last quarter of the 10th century. Hydrological Science Journal, 50 (6): p. 933–948.
Carturan, L. and Seppi, R. (2007): Recent mass balance results and morphological evolution of Careser Glacier (Central Alps). Geografia Fisica e Dinamica Quaternaria, 30 (1): p. 33–42.
Casassa, G., Rivera, A., Kaser, G., Ribstein, P. and Schneider, C., eds. (2007): Mass balance of Andean glaciers. Global and Planetary Change, 59 (1–4): 244 pp.
Caukwell, R.A. and Hastenrath, S. (2006): The 1958 map of Lewis Glacier: legacy of the IGY Mount Kenya Expedition. Zeitschrift fur Gletscherkunde und Glazialgeologie, 19: p. 127–132.
Ceballos, J.L., Euscátegui, C., Ramírez, J., Cañon, M., Huggel, C., Haeberli, W. and Machguth, H. (2006): Fast shrinkage of tropical glaciers in Colombia. Annals of Glaciology, 43: p. 194–201.
Ceballos, J.L. and Tobon, E. (2008): Informe de actividades glaciologicas: Sierra Nevada de El Cocuy y Volcan Nevado Santa Isabel. Colombia, 2006–2007. Instituto de Hidrologia, Meteorologia y Estudios Ambientales: 75 pp.
Charnley, F.E. (1959): Some observations on the glaciers of Mount Kenya. Journal of Glaciology, 3 (26): p. 483–492.
Chinn, T.J. (1995): Glacier fluctuations in the Southern Alps of New Zealand determined from snowline elevations. Arctic and Alpine Research, 27 (2): p. 187–198.
Chinn, T.J. (2001): Distribution of the glacial water resources of New Zealand. Journal of Hydrology, 40 (2): p. 139–187.
Chinn, T., Heydenrych, C. and Salinger, M.J. (2005a): Use of ELA as a practical method of monitoring glacier response to climate in New Zealand's Southern Alps. Journal of Glaciology, 51 (172): p. 85–95.
Chinn, T., Winkler, S., Salinger, M.J. and Haakensen, S. (2005b): Recent advances in Norway and New Zealand: a comparison of their glaciological and meteorological causes. Geografisca Annaler, 87A (1): p. 141–157.
Chinn, T.J., Willsman, A. and Salinger, M.J. (2006): Glacier snowline survey. National Institute of Water & Atmospheric Research Client Report, AKL2006-053: 132 pp.
Chueca, J., Julian, A., Saz, M.A., Creus, J. and Lopez, J.I. (2005): Responses to climatic changes since the Little Ice Age of Maladeta Glacier (Central Pyrenees). Geomorphology, 68 (3–4): p. 167–182.
Chueca, J., Julian, A. and Lopez, J.I. (2007): Recent evolution (1981–2005) of the Maladeta glaciers, Pyrenees, Spain: extent and volume losses and their relation with climatic and topographic factors. Journal of Glaciology, 53 (183): p. 547–557.
Citterio, M., Diolaiuti, G., Smiraglia, C., D'Agata, C., Carnielli, T., Stella, G., Siletto, G.B. (2007): The fluctuations of Italian glaciers during the last century: a contribution to knowledge about Alpine glacier changes. Geografiska Annaler, 89 (3): p. 167–184.
Ciupak, M., Maciejewski, M. and Wislinski, A. (2005): Changes of area of the firn-and-

ice patch beneath Bula pod Rysami in years 1978–2004 in reference to the meteorological data from Kasprowy Wierch. In: Kotarba, A. and Borowiec, W. (eds): Tatrzanski Park Narodowy na tle innych gorskich terenow chronionych, V. I, conference papers, Zakopane: p. 119–126. (In Polish, summary in English).

Clare, G.R., Fitzharris, B.B., Chinn, T.J.H. and Salinger, M.J. (2002): Interannual variation in End-Of-Summer-Snowlines of the Southern Alps of New Zealand, in response to changes in Southern Hemisphere atmospheric circulation and sea surface temperature patterns. International Journal of Climatology, 22 (1): p. 121–128.

Cola, G. (2005): The large landslide of the South-East face of Thurwieser Peak (Thurwieser Spitze) 3658 m (Upper Valtellina, Italy). Terra Glacialis, 8: p. 9–45.

Cook, A.J., Fox, A.J., Vaughan, D.G. and Ferrigno, J.G. (2005): Retreating glacier fronts on the Antarctic Peninsula over the past half-century. Science, 308, 5721: p. 541–544.

Cullen, N.J., Mölg, T., Kaser, G., Hussein, K., Steffen, K. and Hardy, D.R. (2006): Kilimanjaro glaciers: Recent areal extent from satellite data and new interpretation of observed 20th century retreat rates. Geophysical Research Letters, 33 L16502: doi:10.1029/2006gl027084.

D'Alessandro, L., D'Orefice, M., Pecci, M., Smiraglia, C., and Ventura, R. (2001): The strong reduction phase of the Calderone Glacier during the last two centuries: reconstruction of the variation and of the possible scenarios with GIS technologies. Advances in Global Change Research, Vol. 9, Global Change and Protected Areas, Kluwer Academic Publishers: p. 425–433.

D'Orefice, M., Pecci, M., Smiraglia, C. and Ventura, R. (2000): Retreat of Mediterranean glaciers since the Little ice Age: Case study of Ghiacciaio del Calderone, Central Apennines, Italy. Arctic, Antarctic and Alpine Research, 32 (2): p. 197–201.

Demuth, M.N. and R. Keller (2006): An assessment of the mass balance of Peyto Glacier 1965–1995 in relation to recent and past-century climate variability. In: Demuth, M.N., Munro, D.S. and Young, G.J. (eds.): Peyto Glacier: One Century of Science. National Hydrology Research Institute Report, 8: p. 83–133.

Demuth, M.N., V. Pinard, A. Pietroniro, B.H. Luckman, C. Hopkinson, P. Dornes and L. Comeau (2008): Recent and past-century variations in the glacier resources of the Canadian Rocky Mountains – Nelson River System. Terra Glacialis, 11 (248): p. 27–52.

Demuth, M.N. and Pietroniro, A. (2002): The impact of climate change on the glaciers of the Canadian Rocky Mountain eastern slopes and implications for water resource adaptation in the Canadian prairies. CCAF - Prairie Adaptation Research Collaborative, Final Report Project P55, plus Technical Appendices: 162pp.

Diolaiuti, G., Kirkbride, M.P., Smiraglia, C., Benn, D.I., D'Agata, C. and Nicholson, L. (2005): Calving processes and lake evolution at Miage glacier, Mont Blanc, Italian Alps. Annals of Glaciology, 40 (1): p 207–214.

Dowdeswell, J. A., T. J. Benham, M. R. Gorman, D. Burgess, and M. J. Sharp (2003): Form and flow of the Devon Island Ice Cap, Canadian Arctic. Journal of Geophysical Research, 109, F02002: doi:10.1029/2003JF000095.

Dozier, J. (1989): Spectral signature of Alpine snow cover from the Landsat Thematic Mapper. Remote Sensing and Environment, 28: p. 9–22.

Escher-Vetter, H., L.N. Braun, M. Siebers and M. Weber (2005): Water balance of the Vernagtferner high alpine basin based on long-term measurements and modelling. In Proceedings of the International Conference on Mountain Hydrology in Berchtesgaden (Sept. 2004). Brunswick, Technical University of Brunswick: p. 19–32.

Espizua, L.E. (2005): Holocene glacier chronology of Valenzuela Valley, Mendoza Andes, Argentina. The Holocene, 15 (7): p. 1079–1085.

Espizua, L.E. and Maldonado, G.I. (2007): Glacier fluctuations in the Central Andes of Mendoza, Argentina from 1894/1896 to 2005. In: Scarpati, O.E. and Jones, A.A. (eds): Environmental change and rational water use. Orientación Gráfica Editora S.R.L. Buenos Aires: p 353–366.

Ferri Hidalgo, L., Espizua, L.E. and Pitte, P. (2006): Glacier fluctuations at Cerro Tupungato. Reconstructing past regional climate variations in South America over the late Holocene: A new PAGES Initiative. International Symposium. Abstracts. Malargüe, Mendoza, Argentina: p. 73.

Fischer, L., Kääb, A., Huggel, C. and Noetzli, J. (2006): Geology, glacier retreat and permafrost degradation as controlling factors of slope instabilities in a high-mountain rock wall: the Monte Rosa east face. Natural Hazards and Earth System Science, 6: p. 761–772.

Fisher, D.A., Wake, C., Kreutz, K., Yalcin, K., Steig, E., Mayewski, P., Anderson, L., Zheng, J., Rupper, S., Zdanowicz, C., Demuth, M.N., Waszkiewicz, M., Dahl-Jensen, D., Goto-Azuma, K., Bourgeois, J.B., Koerner, R.M., Sekerka, J., Osterberg, E., Abbott, M.B., Finney, B.P., Burns, S.J., Carlson, A.E., Jenson, J.W. and Clark, P.U. (2006): Stable isotope records from Mount Logan, Eclipse ice cores and nearby Jellybean Lake. Water cycle of the north Pacific over 2 000 years and over five vertical kilometres: sudden shifts and tropical connections. Geographie physique et Quaternaire, 58 (2–3): p. 337–352.

Flemming, S.W. and Clarke, G.K.C. (2005): Attenuation of high-frequency interannual streamflow variability by watershed glacial cover. ASCE Journal of Hydraulic Engineering, 131 (7): p. 615–618.

Forel, F.A. (1895): Les variations périodiques des glaciers. Discours préliminaire. Archives des Sciences physiques et naturelles, Genève, XXXIV: p. 209–229.

Francou, B., Ramirez, E., Caceres, B. and Mendoza, J. (2000): Glacier evolution in the Tropical Andes during the last decades of the 20th century: Chacaltaya, Bolivia and Antizana, Ecuador. Ambio, 29 (7): p. 416–422.

Francou, B., Vuille, M., Favier, V. and Caceres, B. (2004): New evidence for an ENSO impact on low-latitude glaciers: Antizana 15, Andes of Ecuador, 0°28'S. Journal of Geophysical Research, 109 (18), D18106: doi:101029/2003JD004484.

GCOS (2004): Implementation plan for the Global Observing System for Climate in support of the UNFCCC. Report GCOS-92 (WMO/TD No. 1219): 136pp.

GCOS (2006): Systematic observation requirements for satellite- based products for climate. Supplemental details to the satellite-based component of the "Implementation Plan for the Global Observing System for Climate in Support of the UNFCCC", Report GCOS-107 (WMO/TD No. 1338), September 2006: 90 pp.

Georges, J. (2004): 20th century glacier fluctuations in the tropical Cordillera Blanca, Peru. Arctic, Antarctic and Alpine Research, 36 (1): p. 100–107.
Gordon, J.E., Haynes, V.M. and Hubbard, A. (2008): Recent glacier changes and climate trends on South Georgia. Global and Planetary Change, 60: p. 72–84.
Grove, J.M. (2004): Little Ice Ages: Ancient and modern. Routledge, London and New York.
Gruber W. (2002): Die Neuaufnahme und Visualisierung des Cathedral Massif Gletschers (B.C., Canada). Diplomarbeit an der Naturwissenschaftlichen Fakultät der Universität Salzburg: 60 pp.
Haeberli, W. and Hoelzle, M. (1995): Application of inventory data for estimating characteristics of and regional climate-change effects on mountain glaciers: a pilot study with the European Alps. Annals of Glaciology, 21: p. 206–212.
Haeberli, W., Hoelzle, M. and Suter, S., eds. (1998): Into the second century of worldwide glacier monitoring: prospects and strategies. A contribution to the International Hydrological Programme (IHP) and the Global Environment Monitoring System (GEMS). UNESCO - Studies and Reports in Hydrology, 56.
Haeberli, W., Kääb, A., Paul, F., Chiarle, M., Mortara, G., Mazza, A., Deline, P. and Richardson, S. (2002): A surge-type movement at Ghiacciaio del Belvedere and a developing slope instability in the east face of Monte Rosa, Macugnaga, Italian Alps. Norsk Geografisk Tidsskrift, 56: p. 104–111.
Haeberli, W. and Holzhauser, H. (2003): Alpine glacier mass changes during the past two millennia. Pages News, 1 (11): p. 13–15.
Haeberli,W., Huggel, C., Kääb, A., Oswald, S., Polkvoj, A., Zotikov, I., and Osokin, N. (2004): The Kolka-Karmadon rock/ice slide of 20 September 2002 - an extraordinary event of historical dimensions in North Ossetia (Russian Caucasus). Journal of Glaciology, 50 (171): p. 533–546.
Haeberli, W. (2006): Integrated perception of glacier changes: a challenge of historical dimensions. In: Knight, P.G. (ed.): Glacier Science and Environmental Change. Blackwell, Oxford: p. 423–430.
Haeberli, W., Hoelzle, M., Paul, F. and Zemp, M. (2007): Integrated monitoring of mountain glaciers as key indicators of global climate change: the European Alps. Annals of Glaciology, 46: p. 150–160.
Hagen, J. O., Liestøl, O., Roland, E. and Jørgensen, T. (1993): Glacier atlas of Svalbard and Jan Mayen. NPI, Meddelelser, 129, Oslo, Norway.
Hagen, J.O., Kohler, J., Melvold, K. and Winther, J.G. (2003): Glaciers in Svalbard: mass balance, runoff and fresh water flux. Polar Research, 22 (2): p. 145–159.
Hagg, W. J., Braun, L. N., Uvarov, V. N., and Makarevich, K. G. (2004): A comparison of three methods of mass balance determination in the Tuyuksu glacier region, Tien Shan, Central Asia. Journal of Glaciology, 50 (171): p. 505−510.
Hagg, W. (2006a): Bayerische Gletscher. Akademie aktuell. Zeitschrift der Bayerischen Akademie der Wissenschaften 01/2006: p. 24–28.
Hagg, W. (2006b): Digitale Aufbereitung historischer Gletscherkarten in Bayern. Mitt. d. Geogr. Ges. München 88: p. 67–88.
Hagg, W. (2008): Die Bedeutung kleiner Gletscher am Beispiel der bayerischen Alpen. Geographische Rundschau 3/2008: p. 22–29.
Hall, D.K., Bayr, K.J., Schöner, W., Bindschadler, R.A. and Chien, J.Y.L. (2003): Consideration of the errors inherent in mapping historical glacier positions in Austria

from the ground and space (1893–2001). Remote Sensing of Environment, 86: p. 566–577.

Happoldt, H. and Schrott, L. (1993): Horcones Inferior. In: IAHS/UNESCO (1993): Fluctuations of Glaciers 1985–1990. Volume VI. Haeberli, W. and Hoelzle, M. (eds.), World Glacier Monitoring Service: p. 70.

Hastenrath, S. (1984): The glaciers of equatorial East Africa. Reidel, Dordrecht, Boston, Lancaster: 353 pp.

Hastenrath, S., Rostom, R., Caukwell, R.A. (1989): Variations of Mount Kenya's glaciers 1963–87. Erdkunde, 43: p. 202–210.

Hastenrath, S. and Polzin, D. (2004): Volume decrease of Lewis Glacier, Mount Kenya, 1978–2004. Zeitschrift für Gletscherkunde und Glazialgeologie, 39: p. 133–139.

Hastenrath, S. (2005a): Glaciological studies on Mount Kenya 1971–2005. University of Wisconsin, Madison, USA: 220 pp.

Hastenrath, S. (2005b): The glaciers of Mount Kenya l899-2004. Erdkunde, 59: p. 120–125.

Herren, E. and Bauder, A., eds. (2008): The Swiss Glaciers 2001/02 and 2002/03 Glaciological Report 123/124. Cryospheric Commission (EKK) of the Swiss Academy of Science (SCNAT) and Laboratory of Hydraulics, Hydrology and Glaciology (VAW) at the Swiss Federal Institute of Technology Zurich: 97 pp.

Higuchi, K., Iozawa, T., Fujii, Y. and Kodama, H. (1980): Inventory of perennial snow patches in Central Japan. GeoJournal, 4 (4): p. 303–311.

Hock, R., Radic, V. and De Would, M. (2007): Climate sensitivity of Storglaciären, Sweden: an intercomparison of mass-balance models using ERA-40 re-analysis and regional climate model data. Annals of Glaciology, 46: p. 342–348.

Hoelzle, M., Haeberli, W., Dischl, M. and Peschke, W. (2003): Secular glacier mass balances derived from cumulative glacier length changes. Global and Planetary Change, 36 (4): p. 77–89.

Hoelzle, M., Chinn, T.J., Stumm, D., Paul, F., Zemp, M. and Haeberli, W. (2007): The application of inventory data for estimating characteristics of and regional past climate-change effects on mountain glaciers: a comparision between the European Alps and the New Zealand Alps. Global and Planetary Change, 56: p. 69–82.

Holdsworth, G., Krouse, H.R. and Nosal, M. (1992): Ice core climate signals from Mount Logan, Yukon. In: Bradley, R.S. and Jones, P.D. (eds.): Climate Since A.D.1500. Routledge, London and New York: p. 483–504.

Holmlund, P. and Jansson, P. (2005): A re-analysis of the 58-year mass balance record of Storglaciären, Sweden. Annals of Glaciology, 42 (1): p. 389–394.

Hopkinson, C., Demuth, M.N. Sitar, M. and Chasmer, L. (2001): Applications of LiDAR mapping in a glacierised mountainous terrain. Proceedings of the International Geoscience and Remote Sensing Symposium, Sydney, Australia. July 9–14.

Hopkinson, C. and Demuth, M.N. (2006): Using airborne lidar to assess the influence of glacier downwasting on water resources in the Canadian Rocky Mountains. Canadian Journal of Remote Sensing, 32 (2): p. 212–222

Hubbard, A., Willis, I., Sharp, M., Mair, D., Nienow, P., Hubbard, B. and Blatter, H. (2000): Glacier mass-balance determination by remote sensing and high-resolution modelling. Journal of Glaciology, 46 (154): p. 491–498.

Hubbard, B., Heald, A., Reynolds, J.M., Quincey, D., Richardson, S.D., Zapata-Luyo, M., Santillan-Protilla, N. and Hambrey, M.J. (2005): Impact of a rock avalanche on a moraine-dammed proglacial lake: Laguna Safuna Alta, Cordillera Blanca, Peru. Earth Surface Processes and Landforms, 30: p. 1251–1264.

Huggel, C., Kääb, A., Haeberli, W., Teysseire, P. and Paul, F. (2002a): Remote sensing based assessment of hazards from glacier lake outbursts: a case study in the Swiss Alps, Canadian Geotechnical Journal, 39 (2): p. 316–330.

Huggel, C., Haeberli, W., Kääb, A., Hoelzle, M., Ayros, E. and Portocarrero, C. (2002b): Assessment of glacier hazards and glacier runoff for different climate scenarios based on remote sensing data: a case study for a hydropower plant in the Peruvian Andes. EARSel eProceedings, Berne, 11.–13.03.2002: p. 22–33.

Huggel, C., Kääb, A., Haeberli, W. and Krummenacher, B. (2003): Regional-scale GIS-models for assessment of hazards from glacier lake outbursts: evaluation and application in the Swiss Alps. Natural Hazards and Earth System Sciences, 3 (6): p. 647–662.

Huggel, C., Kääb, A. and Salzmann, N. (2004a): GIS-based modeling of glacial hazards and their interactions using Landsat-TM and IKONOS imagery. Norwegian Journal of Geography, 58: p. 61–73.

Huggel, C., Haeberli, W., Kääb, A., Bieri, D. and Richardon, S. (2004b): Assessment procedures for glacial hazards in the Swiss Alps. Canadian Geotechnical Journal, 41 (6): p. 1068–1083.

Huggel, C., Zgraggen - Oswald, S., Haeberli, W., Kääb, A., Polkvoj, A., Galushkin, I., Evans, S. G. (2005): The 2002 rock / ice avalanche at Kolka / Karmadon, Russian Caucasus: assessment of extraordinary avalanche formation and mobility, and application of QuickBird satellite imagery. Natural Hazards and Earth System Science, 5: p. 173–187.

Huggel, C., Caplan-Auerbach, J., Waythomas, C.F., and Wessels, R. (2007a): Monitoring and modeling ice-rock avalanches from ice-capped volcanoes: a case study of frequent large avalanches on Iliamna Volcano, Alaska. Journal of Volcanology and Geothermal Research, 168: p. 114-136, doi:10.1016/j.jvolgeores.2007.08.009.

Huggel, C., Ceballos, J.L., Ramírez, J., Pulgarín, B. and Thouret, J.C. (2007b): Review and reassessment of hazards owing to volcano-ice interactions in Colombia. Annals of Glaciology 45: p. 128–136.

Huggel, C., Gruber, S., Caplan-Auerbach, J., Wessels, R.L. and Molnia, B.F. (2008): The 2005 Mt. Steller, Alaska, rock-ice avalanche: What does it tell us about large slope failures in cold permafrost? Proceedings of the 9th International Conference on Permafrost 2008, Fairbanks, Alaska, USA: p. 747–752.

Huss, M., Sugiyama, S., Bauder, A. and Funk, M. (2007a): Retreat scenarios of Unteraargletscher, Switzerland, using a combined ice-flow mass-balance model. Arctic, Antarctic and Alpine Research, 39 (3): p. 422–431.

Huss, M., Bauder, A., Werder, M., Funk, M. and Hock, R. (2007b): Glacier-dammed lake outburst events of Gornersee, Switzerland. Journal of Glaciology, 53 (181): p. 189–200.

Huss, M., Farinotti, D., Bauder, A. and Funk, M. (2008): Modelling runoff from a highly glacierized alpine drainage basin in a changing climate. Hydrological Processes, 22 (19): doi:10.1002/hyp.7055.

Huss, M., Bauder, A. and Funk, M. (in press): Homogenization of long term mass balance time series. Annals of Glaciology, 50A053.

IGOS (2007): Integrated global observing strategy cryosphere theme report – for the monitoring of our environment from space and from Earth. Geneva: World Meteorological Organization. WMO/ TD-No. 1405: 100 pp.

International Glaciological Society (2007): The International Symposium on Cryospheric Indicators of Global Climate Change held in the city of Cambridge, England. Annals of Glaciology, 46: 458 pp.

International Glaciological Society (in prep.): Measurements and modelling of glacier mass balance. Annals of Glaciology, 50.

Jania J., Kolondra L., and Aas, H.F. (2002): Werenskioldbreen and surrounding area, Orthophotomap 1:25 000. Wydział Nauk o Ziemi, Uniwersytet Śląski, Sosnowiec and Norsk Polarinstitutt, Tromsø.

Jansson, P. and Linderholm, H. (2005): Assessment of combined glacier and tree-ring studies to constrain latitudinal climate forcing of Scandinavian glacier mass balances. Annals of Glaciology, 42: p. 303–310.

Josberger, E.G., Bidlake, W.R., March, R.S., and Kennedy, B.W. (2007): Glacier mass-balance fluctuations in the Pacific Northwest and Alaska, USA. Annals of Glaciology, 46: p. 291–296.

Kääb, A. (2001): Photogrammetric reconstruction of glacier mass-balance using a kinematic ice-flow model. A 20-year time series on Grubengletscher, Swiss Alps. Annals of Glaciology, 31: p. 45–52.

Kääb, A., Paul, F., Maisch, M., Hoelzle, M. and Haeberli, W. (2002): The new remote sensing derived Swiss glacier inventory: II. First results. Annals of Glaciology, 34: p. 362–366.

Kääb, A., Wessels, R., Haeberli, W., Huggel, C., Kargel, J. and Khalsa, S.J.S. (2003): Rapid ASTER imaging facilitates timely assessment of glacier hazards and disasters. EOS Transactions, American Geophysical Union, 84 (13): p. 117, 121.

Kääb, A., Huggel, C., Barbero, S., Chiarle, M., Cordola, M., Epifani, F., Haeberli, W., Mortara, G., Semino, P., Tamburini, A. and Viazzo, G. (2004): Glacier hazards at Belvedere Glacier and the Monte Rosa east face, Italian Alps: processes and mitigation. Internationales Symposium Interpraevent 2004 - Riva/Trient: p. 67–78.

Kääb, A. (2005): Remote sensing of mountain glaciers and permafrost creep. Schriftenreihe Physische Geographie. Glaziologie und Geomorphodynamik, 48, University of Zurich, Zurich: 264 pp.

Kääb, A. (2007): Glacier volume changes using ASTER optical stereo. A test study in Eastern Svalbard. Geoscience and Remote Sensing Symposium, 2007. IGARSS 2007. IEEE International: p. 3994–3996.

Kääb, A., Chiarle, M., Raup, B. and Schneider, C., eds. (2007): Climate change impacts on mountain glaciers and permafrost. Global and Planetary Change, 56 (3–4): p. 215–416.

Kargel, J.S., Abrams, M.J., Bishop, M.P., Bush, A., Hamilton, G., Jiskoot, H., Kääb, A., Kieffer, H.H., Lee, E.M., Paul, F., Rau, F., Raup, B., Shroder, J.F., Soltesz, D., Stainforth, D., Stearns, L. and Wessels, R. (2005): Multispectral imaging contributions to global land ice measurements from space. Remote Sensing of the Environment, 99 (1–2): p. 187–219.

Kaser, G., Juen, I., Georges, C., Gomez, J. and Tamayo, W. (2003): The impact of glaciers on the runoff and the reconstruction of mass balance history from hydrological data in the tropical Cordillera Blanca, Peru. Journal of Hydrology, 282 (1–4): p. 130–144.

Kaser, G., Cogley, J.G., Dyurgerov, M.B., Meier, M.F. and Ohmura, A. (2006): Mass balance of glaciers and ice caps: Consensus estimates for 1961–2004. Geophysical Research Letters, 33, L19501: doi:10.1029/2006GL027511

Kieffer, H.H. and 41 others (2000): New eyes in the sky measure glaciers and ice sheets. EOS Transactions, American Geophysical Union 81 (24): p. 265, 270–271.

Kirkbride, M.P. (2002): Icelandic climate and glacier fluctuations through the termination of the 'Little Ice Age'. Polar Geography, 26 (2): p. 116–133.

Klein, A.G. and Kincaid, J.L. (2006): Retreat of glaciers on Puncak Jaya, Irian Jaya, determined from 2000 and 2002 IKONOS satellite images. Journal of Glaciology, 52 (176): p. 65–179.

Klein, A.G. and Kincaid, J.L. (2008): On the disappearance of the Puncak Mandala ice cap, Papua. Journal of Glaciology, 54 (184): p. 195–197.

Klok, E.J. and Oerlemans, J. (2002): Model study of the spatial distribution of the energy and mass balance of Morteratschgletscher, Switzerland. Journal of Glaciology, 48 (163): p. 505–518.

Knight, P.G., ed. (2006): Glacier science and environmental change. Blackwell, Oxford: 512 pp.

Koboltschnig, G.R., Schöner, W., Zappa, M. and Holzmann, H. (2007): Contribution of glacier melt to stream runoff: if the climatically extreme summer of 2003 had happened in 1979. Annals of Glaciology, 46: p. 303–308.

Koerner, R.M. (2005): Mass balance of glaciers in the Queen Elizabeth Islands, Nunavut Canada. The International Symposium on Arctic Glaciology, Geilo, Norway 23–27 August 2004. Annals of Glaciology, 42: p. 417–423.

Kotlyakov, V.M., Rototaeva, O.V. and Nosenko, G.A. (2004): The September 2002 Kolka Glacier Catastrophe in North Ossetia, Russian Federation: Evidence and Analysis. Mountain Research and Development, 24 (1): p. 78–83.

Kotlyakov, V.M., ed. (2007): Glaciation in North Eurasia in the recent past and immediate future. Nauka, Moscow: 366 pp. (in Russian with abstracts in English)

Kotlyakov, V.M., Osipova, G.B. and Tsvetkov, D.G. (2008): Monitoring surging glaciers of the Pamirs, Central Asia, from space. Annals of Glaciology, 48 (1): p. 125–134.

Krimmel, R.M. (2002): Water, ice, and meteorological measurements at South Cascade Glacier, Washington, 2000–01 balance years. U.S. Geological Survey Water Resources Investigations Report, 02-4165: 63 pp.

Kuhn, M. (1998): Austrian glacier inventory 1998. Institute for Meteorology und Geophysics, University of Innsbruck.

Kull, C., Solomina, O., Haeberli, W. and Wiles, G., eds. (2008): Historical and Holocene glacier-climate variations. Global and Planetary Change, 60 (1–2): 164 pp.

Lambrecht, A. and Kuhn, M. (2007): Glacier changes in the Austrian Alps during the last three decades, derived from the new Austrian glacier inventory. Annals of Glaciology, 46: p. 177–184.

Larsen, C.F., Motyka, R.J., Arendt, A.A., Echelmeyer, K.A. and Geissler, P.E. (2007): Glacier changes in southeast Alaska and northwest British Columbia and con-

tribution to sea level rise. Journal of Geophysical Research, 112, F101007: doi:10.1029/2006JF000586.
Le Meur, E., Gerbaux, M., Schäfer, M. and Vincent, C. (2007): Disappearance of an Alpine glacier over the 21st Century simulated from modeling its future surface mass balance. Earth and Planetary Science Letters, 261 (3–4): p. 367–374.
Leiva, J.C. (1999): Recent fluctuations of the Argentinian glaciers: Global and Planetary Change, 22 (1): p. 169–177.
Li, X., Cheng, G., Jin, H., Kang, E., Che, T., Jin, R., Zongwu, L., Nan, Z., Wang, J. and Shen, Y. (in press): Distribution and changes of glaciers, snow and permafrost in China. Proceedings of the workshop on 'Assessment of Snow, Glacier and Water Resources in Asia', Almaty, KZ, 2006. UNESCO.
Lopez-Moreno, J.I., Nogues, D., Chueca, J. and Julian, A. (2006): Change of topographic control on the extent of cirque glaciers since the Little Ice Age. Geophysical Research Letters, 33 (24), L24505: doi:10.1029/2006GL028204.
Machguth, H., Paul, F., Hoelzle, M. and Haeberli, W. (2006a): Distributed glacier mass balance modelling as an important component of modern multi level glacier monitoring. Annals of Glaciology, 43: p. 335–343.
Machguth, H., Eisen, O., Paul, F. and Hoelzle, M. (2006b): Strong spatial variability of snow accumulation observed with helicopter-borne GPR on two adjacent Alpine glaciers. Geophysical Research Letters, 33 (L13503): doi:10.1029/2006GL026576.
Mair, D., Burgess, D. andSharp, M. (2003): Thirty-seven year mass balance of Devon Ice Cap, Nunavut, Canada, determined by shallow ice coring and melt modeling. Journal of Geophysical Research, 110, F01011: doi:10.1029/2003JF000099.
Meier, M.F. and Dyurgerov, M.B. (2002): Sea level changes: how Alaska affects the world. Science, 297: p. 350–351.
Meier, M.F., Dyurgerov, M.B., Rick, U.K., O'Neel, S., Pfeffer, W.T., Anderson, R.S., Anderson, S.P. and Glazovsky, A.F. (2007): Glaciers dominate eustatic sea-level rise in the 21st century. Science, 317 (5841): p. 1064–1067.
Mercalli L. and Cat Berro D., eds. (2005): Climi, acque e ghiacciai tra Gran Paradiso e Canavese. SMS, XII: 756 pp.
Milana, J.P. (2007): A model of the Glaciar Horcones Inferior surge, Aconcagua region, Argentina. Journal of Glaciology, 53 (183): p. 565–572.
Moore, G.W.K., G. Holdsworth and K. Alverson (2002): Climate change in the North Pacific region over the last three centuries. Nature, 420: p. 401–403.
Moore, R.D. and Demuth, M.N. (2001): Mass balance and streamflow variability at Place Glacier, Canada, in relation to recent climate fluctuations. Hydrological Processes, 15: p. 3473–3486.
Nesje, A., Lie, O. and Dahl, S.O. (2000): Is the North Atlantic Oscillation reflected in Scandinavian glacier mass balance records? Journal of Quaternary Science, 15 (6): p. 587–601.
Nesje, A., Bakke, J., Dahl, S.O., Lie, O. and Matthews, J.A. (2008): Norwegian mountain glaciers in the past, present and future. Global and Planetary Change, 60 (1–2): p. 10–27.
Nussbaumer, S.U., Zumbühl, H.J. and Steiner, D. (2007b): Fluctuations of the 'Mer de Glace' (Mont Blanc area, France) AD 1500–2050. Part I: The history of the Mer de Glace AD 1500–2003 according to pictoral and written documents.

Zeitschrift für Gletscherkunde und Glazialgeologie, 40: p. 5–140.
Nussbaumer, S.U., Zumbühl, H.J. and Steiner, D. (2007a): Fluctuations of the 'Mer de Glace' (Mont Blanc area, France) AD 1500–2050. Part II: The application of a neural network to the length record of the Mer de Glace. Zeitschrift für Gletscherkunde und Glazialgeologie, 40: p. 141–175.
NVE (2003a): Glaciological investigations in Norway in 2001. Kjøllmoen, B. (ed.), Norwegian Water Resources and Energy Directorate (NVE), Report 1-2003: 103 pp.
NVE (2003b): Glaciological investigations in Norway in 2002. Kjøllmoen, B. (ed.), Norwegian Water Resources and Energy Directorate (NVE), Report 3-2003: 100 pp.
NVE (2004): Glaciological investigations in Norway 2003. Kjøllmoen, B. (ed.), Norwegian Water Resources and Energy Directorate (NVE), Report 4-2004: 97 pp.
NVE (2005): Glaciological investigations in Norway 2004. Kjøllmoen, B. (ed.), Norwegian Water Resources and Energy Directorate (NVE), Report 2-2005: 90 pp.
NVE (2006): Glaciological investigations in Norway 2005. Kjøllmoen, B., Andreassen, L.M., Engeset, R.V., Elvehøy, H., Jackson, M. and Giesen, R.H. (eds.), Norwegian Water Resources and Energy Directorate (NVE), Report 2-2006: 91 pp.
NVE (2007): Glaciological investigations in Norway 2006. Kjøllmoen, B., Andreassen, L.M., Elvehøy, H., Jackson, M., Tvede, A.M., Laumann, T. and Giesen, R.H. (eds.), Norwegian Water Resources and Energy Directorate (NVE), Report 1-2007: 99 pp.
Ohmura, A. (2006): Changes in mountain glaciers and ice caps during the 20th century. Annals of Glaciology, 43: p. 361–368.
Oerlemans, J. (2000): Analysis of a 3-year meteorological record from the ablation zone of Morteratschgletscher, Switzerland: energy and mass balance. Journal of Glaciology, 46 (155): p. 571–579.
Oerlemans, J. and Klok, E.J. (2002): Energy balance of a glacier surface: analysis of AWS data from the Morteratschgletscher, Switzerland. Arctic, Antarctic and Alpine Research, 34 (123): p. 115–123.
Oerlemans, J. (2005): Extracting a climate signal from 169 glacier records. Science, 308 (5722): p. 675–677.
Orlove, B., Wiegandt, E. and Luckman, B. eds. (2008): The darkening peaks: Glacial retreat in scientific and social context. University of California Press: 296 pp.
Pälli A., Moore J. C., Jania J., Kolondra L. and Glowacki P. (2003): The Drainage Pattern of Hansbreen and Werenskioldbreen, two Polythermal Glaciers in Svalbard. Polar Research 22(2): p. 355–371.
Patzelt, G. (2002): Gletscherbericht 2000/2001. Sammelbericht über die Gletschermessungen des Oesterreichischen Alpenvereins im Jahre 2002. Mitteilungen des Oesterreichischen Alpenvereins,. 57 (127), Heft 2/02: p. 6–13.
Patzelt, G. (2003): Gletscherbericht 2001/2002. Sammelbericht über die Gletschermessungen des Oesterreichischen Alpenvereins im Jahre 2002. Mitteilungen des Oesterreichischen Alpenvereins, 58 (128), Heft 2/03: p. 6–13.
Patzelt, G. (2004): Gletscherbericht 2002/2003. Sammelbericht über die Gletschermessungen des Oesterreichischen Alpenvereins im Jahre 2003. Mitteilungen des Oesterreichischen Alpenvereins, 59 (129), Heft 1/04: p. 8–15.
Patzelt, G. (2005): Gletscherbericht 2003/2004. Sammelbericht über die Gletschermes-

sungen des Oesterreichischen Alpenvereins im Jahre 2004. Mitteilungen des Oesterreichischen Alpenvereins, 60 (130), Heft 2/05: p. 24–31.

Patzelt, G. (2006): Gletscherbericht 2004/2005. Sammelbericht über die Gletschermessungen des Oesterreichischen Alpenvereins im Jahre 2005. Bergauf, 2/2006: p. 6–11.

Paul, F. (2002): Changes in glacier area in Tyrol, Austria, between 1969 and 1992 derived from Landsat 5 Thematic Mapper and Austrian Glacier Inventory data. International Journal of Remote Sensing, 23 (4): p. 787–799.

Paul, F., Kääb, A., Maisch, M., Kellenberger, T. and Haeberli, W. (2002): The new remote sensing derived Swiss glacier inventory: I. Methods. Annals of Glaciology, 34: p. 355–361.

Paul, F., Kääb, A., Maisch, M., Kellenberger, T. and Haeberli, W. (2004): Rapid disintegration of Alpine glaciers observed with satellite data. Geophysical Research Letters, 31 (L21402): doi:10.1029/2004GL020816.

Paul, F. and Kääb, A. (2005): Perspectives on the production of a glacier inventory from multispectral satellite data in Arctic Canada: Cumberland Peninsula, Baffin Island. Annals of Glaciology 42 (1): p. 59–66.

Paul, F., Machguth, H. and Kääb, A. (2005): On the impact of glacier albedo under conditions of extreme glacier melt: the summer of 2003 in the Alps. EARSeL Workshop on Remote Sensing of Land Ice and Snow, Berne, 21.–23.2. 2005. EARSeL eProceedings, 4 (2): p. 139–149.

Paul, F., Kääb, A. and Haeberli, W. (2007a): Recent glacier changes in the Alps observed from satellite: Consequences for future monitoring strategies, Global and Planetary Change, 56: p. 111–122.

Paul, F., Maisch, M., Rothenbühler, C., Hoelzle, M. and Haeberli, W. (2007b): Calculation of future glacier extent in the Swiss Alps by means of hypsographic modelling. Global and Planetary Change, 55 (4): p. 343–357.

Paul, F. and Haeberli, W. (2008): Spatial variability of glacier elevation changes in the Alps obtained from two digital elevation models. Geophysical Research Letters: doi:10.1029/2008GL034718.

Paul, F., Machguth, H., Hoelzle, M., Salzmann, N. and Haeberli, W. (2008): Alpine-wide distributed glacier mass balance modelling: a tool for assessing future glacier change? In: Orlove, B., Wiegandt, E. and Luckman, B.H. (eds.): The darkening peaks: Glacial retreat in scientific and social context. University of California Press: p. 111–125.

Paul, F., A. Kääb, H. Rott, A. Shepherd, T. Strozzi, and E. Volden (subm.): GlobGlacier: Mapping the worlds glaciers and ice caps from space. Earsel eProceedings.

Pecci, M. (2001): The historical and iconographic research for the reconstruction of the variation of the Calderone glacier: State of the art and perspectives. In: Visconti, G., Beniston, M., Jannorelli, E. and Barba, D. (eds.): Global change and protected areas. Advances in Global Change Research, Vol. 9, Kluwer Academic Publishers: p. 505–512.

Pecci, M., De Sisti, G., Marino, A. and Smiraglia, C. (2001): New radar surveys in monitoring the evolution of the calderone glacier (Central Apennines, Italy). Convegno Glaciologico Italiano - Risposta dei ghiacciai alpini ai cambiamenti climatici, Bormio 9 - 12 Settembre 1999. in: Suppl. Geogr. Fis. Dinam. Quat., V: p. 145–150.

Pecci, M. (2005): In situ surveys and research on the snow cover in high altitude: case studies in Italian and Himalayan mountain ranges. Suppl. Geogr. Fis. Dinam. Quat., Suppl. VII: p. 253–260.

Pelfini, M., Santilli, M., Geonelli, G. and Bozzoni, M. (2007): Investigating surface movements of debris-covered Miage glacier, Western Italian Alps, using dendroglaciological analysis. Journal of Glaciology, 53 (180): p. 141–152.

Pellicciotti, F., Brock, B.W., Strasser, U., Burlando, P., Funk, M. and Corripio, J. (2005): An enhanced temperature-index glacier melt model including the shortwave radiation balance: development and testing for Haut Glacier d'Arolla, Switzerland. Journal of Glaciology, 51 (175): p. 573–587.

Pelto, M.S. and Hedlund, C. (2001): The terminus behavior and response time of North Cascade glaciers. Journal of Glaciology, 47 (158): p. 497–506.

Pelto, M.S. and Hartzell, P.L. (2004): Change in longitudinal profile on three North Cascades glaciers during the last 100 years. Hydrologic Processes, 18: p. 1139–1146.

Pelto, M.S. (2006): The current disequilibrium of North Cascade Glaciers. Hydrological Processes, 20: p. 769–779.

Pelto, M.S. (2007a): Glacier annual balance measurement, prediction, forecasting and climate correlations, North Cascades, Washington 1984–2006. The Cryosphere, 1: p. 17–39.

Pelto, M.S. (2007b): Western North American glacier mass balance 1984–2005, equilibrium or disequilibrium response? Ice and Climate News (CLIC), 9: p. 14–15.

Petrakov, D.A., Chernomorets, S.S., Evans, S.G. and Tutubalina, O.V. (2008): Catastrophic glacial multi-phase mass movements: a special type of glacial hazard. Advances in Geosciences, 14: p. 211–218.

Piccini P., Mercalli L., Cat Berro D., eds. (2007): Ghiacciai in Valsesia. SMS, X: 133 pp.

Polkvoy, A., Goncharev, V., Haeberli, W., Huggel, C., Berger, M. and Galkina, V., eds. (2006): Proceedings of the International Conference on High Mountain Hazard Prevention, Vladikavkaz-Moscow, June 23-26, 2004, Vladikavkaz: 271 pp.

Pralong, A. and Funk, M. (2005): Dynamic damage model of crevasse opening and application to glacier calving. Journal of Geophysical Research, 110: p. 1–12.

Pralong, A., Birrer, C., Stahel, W.A. and Funk, M. (2005): On the predictability of ice avalanches. Nonlinear Processes in Geophysics, 12: p. 849–861.

Racoviteanu, A., Manley, W.F., Arnaud, Y. and Williams, M. (2007): Evaluating digital elevation models for glaciological applications: an example from Nevado Coropuna, Peruvian Andes. Global and Planetary Change, 59 (1–4): p. 110–125.

Racoviteanu, A., Arnaud, Y., Williams, M.W. and Ordonez, J. (2008): Decadal changes in glacier parameters in the Cordillera Blanca, Peru, derived from remote sensing. Journal of Glaciology, 54 (186): p. 499–510.

Rau, F., Mauz, F., De Angelis, H., Jaña, R., Arigony Neto, J., Skvarca, P., Vogt, S., Saurer, H. and Gossmann, H. (2004): Variations of glacier frontal positions on Northern Antarctic Peninsula. Annals of Glaciology, 39: p. 525–530.

Raup, B., Kääb, A., Kargel, J.S., Bishop, M.P., Hamilton, G., Lee, E., Paul, F., Rau, F., Soltesz, D., Khalsa, S.J.S., Beedle, M. and Helm, C. (2006): Remote sensing and GIS technology in the Global Land Ice Measurements from Space (GLIMS) project. Computers and Geosciences, 33: p. 104–125.

Raup, B., Racoviteanu, A., Khalsa, S.J.S., Helm, C., Armstrong, R. and Arnaud, Y.

(2007): The GLIMS geospatial glacier database: A new tool for studying glacier change. Global and Planetary Change, 56 (1–2): p. 101–110.
Raymond, Ch., Neumann, T.A., Rignot, E., Echelmeyer, K., Rivera, A. and Casassa, G. (2005): Retreat of Glaciar Tyndall, Patagonia, over the last half-century. Journal of Glaciology 51 (173): p. 239–247.
Raymond, M., Wegmann, M. and Funk, M. (2003): Inventar gefährlicher Gletscher in der Schweiz, Zürich: ETH Zürich: 368 pp.
Rene, P. (2000): Etat des lieux des glaciers des Pyrenees francaises. Compte rendu de la campagne de terrain (septembre 1999). Societe Hydrotechnique de France, Grenoble: 16 pp.
Rignot, E., Rivera, A. and Casassa, G. (2003): Contribution of the Patagonia icefields of South America to sea level rise. Science, 302: p. 434–437.
Rivera, A., Benham, T., Casassa, G., Bamber, J. and Dowdeswell, J. (2007): Ice elevation and areal changes of glaciers from the Northern Patagonia icefield, Chile. Global and Planetary Change, 59: p. 126–137.
Rostom, R.S. and Hastenrath, S. (1994): Variations of Mount Kenya's glaciers 1987–1993. Erdkunde, 48: p. 174–180.
Rostom, R.S. and Hastenrath, S. (2007): Variations of Mount Kenya's glaciers 1993–2004. Erdkunde, 61: p. 277–283.
Rott, H., Rack, W., Skvarca, P. and De Angelis, H. (2002): Northern Larsen Ice Shelf – Further retreat after the collapse. Annals of Glaciology, 34: p. 277–282.
Schiefer, E., Menounos, B. and Wheate, R. (2007): Recent volume loss of British Columbian glaciers, Canada. Geophysical Research Letter, 34, L16503: doi:10.1029/2007GL030780.
Schneider, T. and Jansson, P. (2004): Internal accumulation in firn and its significance for the mass balance of Storglaciären. Journal of Glaciology, 50 (168): p. 25–34.
Sigurdsson, O. (2005): Variations of termini of glaciers in Iceland in recent centuries and their connection with climate. In: Caseldine, C., Russell, A., Hardardottir, J. and Knudsen, O. (eds.): Iceland – modern processes and past environments. Amsterdam, Elsevier: p. 241–255.
Sigurdsson, O., Jonsson, T. and Johannesson, T. (2007): Relation between glacier-termini variations and summer temperature in Iceland since 1930. Annals of Glaciology 46 (1): p. 170–176.
Schneeberger, C., O. Albrecht, H. Blatter, M. Wild and R. Hock (2001): Modelling the response of glaciers to a doubling in atmospheric CO2: a case study of Storglaciären. Climate Dynamics, 17 (11): p. 825–834.
Schöner, W., Auer, I. and Böhm, R. (2000): Climate variability and glacier reaction in the Austrian eastern Alps. Annals of Glaciology 31 (1): p. 31–38.
Schöner, W. and Böhm, R. (2007): A statistical mass-balance model for reconstruction of LIA ice mass for glaciers in the European Alps. Annals of Glaciology, 46: p. 161–169.
Shahgedanova, M., Stokes, C.R., Khromova, T., Nosenko, G., Popovnin, V., Narozhny, Y., Aleynikov, A. and Muraveyev, A. (2008): State of glaciers in the Caucasus and southern Siberian mountains and their links with climate oscillations since the 1950s. Geophysical Research Abstracts, Vol. 10, EGU2008-A-10158.
Shea, J.M., Marshall, S.J. and Livingston, J.M. (2004): Glacier distributions and climate in the Canadian Rockies. Arctic, Antarctic and Alpine Research, 36 (2): p.

272–280.
Short, N.H. and Gray, A.L. (2005): Glacier dynamics in the Canadian High Arctic from RADARSAT-1 speckle tracking. Canadian Journal if Remote Sensing, 31 (3): p. 225–239.
Sicart, J.E., Ribstein, P., Francou, B., Pouyaud, B. and Condom, T. (2007): Glacier mass balance of tropical Zongo glacier, Bolivia, comparing hydrological and glaciological methods. Global and Planetary Change, 59 (1–4): p. 27–36.
Skvarca, P. and De Angelis, H. (2003): Impact assessment of regional climatic warming on glaciers and ice shelves of the northeastern Antarctic Peninsula. Antarctic Research Series, 79: p. 69–78.
Skvarca, P., De Angelis, H. and Ermolin, E. (2004): Mass-balance of „Glaciar Bahiá del Diablo", Vega Island, Antarctic Peninsula. Annals of Glaciology, 39: p. 209–213.
Slupetzky, H. (1997): Die Gletscher auf den topographischen Karten 1:5000 im Gebiet der Nationalpark-Forschungsstelle Rudolfshütte (Stubachtal, Hohe Tauern) von 1990. Wissenschaftliche Mitteilungen. Nationalpark Hohe Tauern, 3: p. 137–162.
Slupetzky H. and W. Gruber (2002): Remapping of the Cathedral Massif Glacier (B.C., Canada) – from Traditional Mapping to Digital Techniques. Proceedings of the Mountain Cartography Workshop at Mt. Hood, USA: 5 pp.
Sobota, I. and Grześ, M. (2006): Charakterystyka pokrywy śnieżnej na lodowcach Kaffioyry. Problemy Klimatologii Polarnej, 16: p. 147–159.
Sobota I. (2007a): Mass balance of Kaffiøyra glaciers, Svalbard. Landform Analysis, 5: p. 75–78.
Sobota I. (2007b): Selected methods in mass balance estimation of Waldemar Glacier, Spitsbergen. Polish Polar Research, 28 (4): p. 249–268.
Solomina, O. (2000): Retreat of mountain glaciers of northern Eurasia since the Little Ice Age maximum. Annals of Glaciology, 31: p. 26–30.
Sosio, R., Crosta, G.B. and Hungr, O. (2008): Complete dynamic modeling calibration for the Thurwieser rock avalanche (Italian Central Alps). Engineering Geology, 100 (1–2): p. 11–26.
Stahl, K. and R.D. Moore. (2006): Influence of watershed glacier cover on summer streamflow in British Columbia, Canada. Water Resources Research, 42: W06201, doi:10.1029/2006WR005022.
Steiner, D., Walter, A. and Zumbühl, H.J. (2005): The application of a non-linear back-propagation neural network to study the mass balance of Grosser Aletschgletscher, Switzerland, Journal of Glaciology, 51 (173): p. 313–323.
Steiner, D., Zumbühl, H.J. and Nussbaumer, S.U. (2006): 19th century glacier perception and fluctuations in the central and western European Alps – new methods and results. In: Price, M.F. (ed.): Global Change in Mountain Regions, Sapiens, Duncow: p. 86–88.
Steiner, D., Zumbühl, H.J. and Bauder, A. (2008a): Two Alpine Glaciers over the past two centuries: a scientific view based on pictoral sources. In: Orlove, B., Wiegandt, E. and Luckman, B.H. (eds.): The darkening peaks: Glacial retreat in scientific and social context. University of California Press: p. 83–99.
Steiner, D., Pauling, A., Nussbaumer, S.U., Nesje, A., Luterbacher, J., Wanner, H. and Zumbühl, H.J. (2008b): Sensitivity of European glaciers to precipitation and

temperature – two case studies. Climatic Change: doi:10.1007/s10584-10008-19393-10581.
Strasser, U., Corripio, J., Pellicciotti, F., Burlando, P., Brock, B.W. and Funk, M. (2004): Spatial and temporal variability of meteorological variables at Haut Glacier d'Arolla (Switzerland) during the ablation season 2001: Measurements and simulations. Journal of Geophysical Research, 109: p. 1–18.
Strelin, J. and Iturraspe, R. (2007): Recent evolution and mass balance of Cordon Martial glaciers, Cordillera Fueguina Oriental. Global and Planetary Change, 59 (1–4): p. 17–26.
Strozzi, T., A. Kouraev, A. Wiesmann, U. Wegmüller, A. Sharov, C. Werner (2007): Estimation of Arctic glacier motion with satellite L-band SAR data. Remote Sensing of the Environment: doi:10.1016/j.rse.2007.06.007.
Su, Z. and Shi, Y. (2002): Response of monsoonal temperature glaciers to global warming since the Little Ice Age. Quaternary International, 97: p. 123–131.
Sugiyama, S., Bauder, A., Zahno, C. and Funk, M. (2007): Evolution of Rhonegletscher, Switzerland, over the past 125 years and in the future: application of an improved flowline model. Annals of Glaciology, 46: p. 268–274.
Surazakov, A .B., and Aizen, V.B. (2006): Estimating volume change of mountain glaciers using SRTM and map-based topographic data. IEEE Transactions of Geoscience and Remote Sensing, 44 (10), 2991–2995.
Thiber, E., Blanc, R., Vincent, C. and Eckert, N. (2008): Glaciological and volumetric mass-balance measurements: error analysis over 51 years for Glacier de Sarennes, French Alps. Journal of Glaciology, 54 (186): p. 522–532.
Truffer, M., Harrison, W.D., and March, R.S. (2005): Correspondence – Record negative glacier balances and low velocities during the 2004 heatwave in Alaska, USA: implications for the interpretation of observations by Zwally and others in Greenland. Journal of Glaciology, 51 (175): p. 663–664.
Tucker, C.J., Denelle, M.G. and Dykstra, J.D. (2004): NASA's Global Orthorectified Landsat Data Set. Photogrammetric Engineering and Remote Sensing, 70: p. 313–322.
Unger, C., Espizua, L.E. and Bottero, R. (2000): Untersuchung von Gletscherständen im tal des Río Mendoza (Zentralargentinische Anden) – Kartierung eines Surge-Vorstosses des Horcones Inferior. Zeitschrift für Gletscherkunde und Glazialgeologie, 36: p. 151–157.
Unger, C., Espizua, L.E. and Bottero, R. (2005): Horcones Inferior. In:. IAHS (ICSI) – UNEP – UNESCO (2005): Fluctuations of Glaciers 1995–2000, Volume VIII. Haeberli, W., Zemp, M., Frauenfelder, R., Hoelzle, M., Kääb, A. (eds.), World Glacier Monitoring Service: p. 44.
UNEP (2007): Global outlook for ice and snow. United Nations Environment Programme, EarthPrint: 235 pp.
UNESCO (1970): Perennial ice and snow masses – a guide for compilation and assemblage of data for the World Glacier Inventory. Technical Papers in Hydrology No. 1.
Varnakova, G. M., and Koryakin, V. S. (1978): The catalogue of the USSR glaciers (Katalog lednikov SSSR). Resources of the USSR surface waters (Resoursy poverkhnostnyh vod SSSR), Vol. 3 (Northern Territories), part 2 (Novaya Zemlya) USSR: Leningrad, Hydrometeoizdat publishing: 112 pp., in Russian.

Vincent, C. (2002): Influence of climate change over the 20th century on four French glacier mass balances. Journal of Geophysical Research 107, No. D19, 4375, doi:10.1029/2001JD000832.

Vincent., C., Kappenberger, G., Valla, F., Bauder, A., Funk, M. and Le Meur, E. (2004): Ice ablation as evidence of climate change in the Alps over the 20th century. Journal of Geophysical Research, 109, D10104, doi:10.1029/2003JD003857.

Vincent, C., Le Meur, E., Six, D. and Funk, M. (2005): Solving the paradox of the end of the Little Ice Age in the Alps. Geophysical Research Lettres 32, L09706: doi.10.1029/2005GL022552.

Vincent, C., Le Meur, E., Six, D., Possenti, E., Lefèbre, F. and Funk, M. (2007): Climate warming revealed by englacial temperatures at Col du Dôme (4250 m, Mont Blanc area). Geophysical Research Letters, 34 (L16502): doi:10.1029/2007GL029933.

Vuille, M., Kaser, G. and Juen, I. (2007): Glacier mass balance variability in Cordillera Blanca, Peru and its relationship with climate and large-scale circulation. Global and Planetary Change, 62 (1–2): p. 14–28.

Wagnon, P. Ribstein, B. Francou and Sicart, J.E. (2001): Anomalous heat and mass budget of Glaciar Zongo, Bolivia, during the 1997/98 El Nino year. Journal of Glaciology, 47 (156): p. 21–28.

Wagnon P., Rajesh K., Arnaud Y., Linda A., Sharma P., Vincent C., Pottakal, J. Berthier E., Ramanathan A., Hasnain S.I. and Chevallier P. (2007): Four years of mass balance on Chhota Shigri Glacier (Himachal Pradesh, India), a new benchmark glacier in the Western Himalaya. Journal of Glaciology, 53 (183): p. 603–611.

Wang, N., Jing, Z., Jiao, K., Mikhalenko, V., Li, Z., Han, T. and Yang, H. (2007): Variations of the Glacier No. 1 at the source of the Urumqi River, Tien Shan Mts., China, during the past 40 years. Data of Glaciological Studies, 102: p. 48–51.

WGMS (2003): Glacier Mass Balance Bulletin No. 7 (2000–2001). Haeberli, W., Frauenfelder, R., Hoelzle, M. and Zemp, M. (eds.), IAHS(ICSI)/UNEP/UNESCO/WMO, World Glacier Monitoring Service, University of Zurich: 87 pp.

WGMS (2005a): Glacier Mass Balance Bulletin No. 8 (2002–2003). Haeberli, W., Noetzli, J., Zemp, M., Baumann, S., Frauenfelder, R. and Hoelzle, M. (eds.). IUGG(CCS)/UNEP/UNESCO/WMO, World Glacier Monitoring Service, Zurich: 100 pp.

WGMS (2005b): Fluctuations of Glaciers 1995–2000, Vol. VIII. Haeberli, W., Zemp, M., Frauenfelder, R., Hoelzle, M. and Kääb, A. (eds.). IUGG(CCS)/UNEP/UNESCO, World Glacier Monitoring Service, Zurich: 288 pp.

WGMS (2007): Glacier Mass Balance Bulletin No. 9 (2004–2005). Haeberli, W., Zemp, M. and Hoelzle, M. (eds.). ICSU(FAGS)/IUGG(IACS)/UNEP/UNESCO/WMO, World Glacier Monitoring Service, University of Zurich: 100 pp.

WGMS (2008): Global Glacier Changes: facts and figures. Zemp, M., Roer, I., Kääb, A., Hoelzle, M., Paul, F. and Haeberli, W. (eds.). UNEP, World Glacier Monitoring Service, University of Zurich: 88 pp.

Wislinski, A. (1985): Glacierets in the Vicinity of the Morskie Oko Lake in the Tatra Mts. Annales UMCS (Lublin), B, 40 (4): p. 55–76 (in Polish, summary in English).

Wislinski, A. (2002): About changes within some firn and ice patches in the Morskie Oko basin. In: Borowiec, W., Kotarba, A., Kownacki, A., Krzan, Z. and Mirek, Z. (eds): Changes of the Nature Environment of the Tatra Mountains (Przemiany

srodowiska przyrodniczego Tatr), conference papers, Krakow – Zakopane: p. 71–75 (in Polish, summary in English).
Xiao, C., Liu, S., Zhao, L., Wu, Q., Li, P., Liu, C., Zhang, Q., Ding, Y., Yao, T., Li, Z. and Pu, J. (2007): Observed changes of cryosphere in China over the second half of the 20th century: an overview. Annals of Glaciology, 46: p. 382–390.
Zeeberg, J.J. and Forman, S.L. (2001): Changes in glacier extent on north Novaya Zemlya in the twentieth century. The Holocene, 11 (2): p. 161–175.
Zemp, M., Frauenfelder, R., Haeberli, W. and Hoelzle, M. (2005): Worldwide glacier mass balance measurements: general trends and first results of the extraordinary year 2003 in Central Europe. Data of Glaciological Studies [Materialy glyatsiologicheskih issledovanii, Moscow, Russia], 99: p. 3–12.
Zemp, M., Haeberli, W., Hoelzle, M. and Paul, F. (2006): Alpine glaciers to disappear within decades? Geophysical Research Letters: doi:10.1029/2006GL026319.
Zemp, M., Hoelzle, M. and Haeberli, W. (2007): Distributed modelling of the regional climatic equilibrium line altitude of glaciers in the European Alps. Global and Planetary Change, 56 (1–2): p. 83–100.
Zemp, M., Paul, F., Hoelzle, M. and Haeberli, W. (2008): Glacier fluctuations in the European Alps 1850–2000: an overview and spatio-temporal analysis of available data. In: Orlove, B., Wiegandt, E. and Luckman, B.H. (eds.): The darkening peaks: Glacial retreat in scientific and social context. University of California Press: p. 152–167.
Zemp, M., Hoelzle, M. and Haeberli, W. (in press): Six decades of glacier mass balance observations – a review of the worldwide monitoring network. Annals of Glaciology, 50A018.
Zumbühl, H.J., Steiner, D. and Nussbaumer, S.U. (2008): 19th century glacier representations and fluctuations in the central and western European Alps: an interdisciplinary approach. Global and Planetary Change, 60 (1–2): p. 42–57.

APPENDIX **NOTES ON THE COMPLETION OF THE DATA SHEETS**

This appendix includes the explanatory notes on the completion of the Excel-based data submission forms, sent out with the call-for-data for the observation period 2000–2005 (also valid for Addenda from earlier years):

- Notes on the completion of the data sheet "A GENERAL INFORMATION"
- Notes on the completion of the data sheet "B STATE"
- Notes on the completion of the data sheet "C FRONT VARIATION"
- Notes on the completion of the data sheet "D SECTION"
- Notes on the completion of the data sheet "E MASS BALANCE OVERVIEW"
- Notes on the completion of the data sheet "F MASS BALANCE"
- Notes on the completion of the data sheet "G SPECIAL EVENT"

The notes on the completion of the data sheets A−G describe all attributes compiled during the call-for-data, whereas the Tables A, B, BB, C, CC, CCC and D in this Volume provide a summary of the collected data. The presentation of the data and the corresponding fields are consistent with the Volume VIII of the "Fluctuations of Glaciers". A modification was made in Table D: instead of the mean area for the period of change (AREA MEAN, in thousand square metres), as in the last Volume, the area for the survey year (AREA SY, in square kilometre) is given.

At the beginning of 2005, the WGMS website was revised to simplify the access to information on available data, to procedures for data order and data submission as well as to the addresses of national correspondents. The website can be accessed via:

http://www.wgms.ch

A GENERAL INFORMATION

NOTES ON THE COMPLETION OF THE DATA SHEET

A1 POLITCAL UNIT
Name of country or territory in which glacier is located (For 2 digit abbreviations, see ISO 3166 country code, available at www.iso.org).
Political unit is part of WGI key (positions 1 and 2).
Political unit is part of FoG and MBB key (positions 1 and 2).

A2 WGMS ID
5 digit key identifying glacier in the WGMS data base.

A3 GLACIER NAME
The name of the glacier, written in CAPITAL letters.
Format: Max. 30 column positions.
If neccessary, the name can be abbreviated; in this case, please give the full name under "A16 REMARKS".

A4 HYDROLOGICAL CATCHMENT AREA
Part of WGI key: Position 3 denotes the continent. Positions 4 to 7 denote the drainage basin.

A5 FREE POSITION
Part of WGI number: Positons 8 and 9 are freely chosen identification numbers.

A6 LOCAL CODE
Part of WGI number: Positons 10 to 12

A7 LOCAL PSFG
The local PSFG number is part of FoG and MBB key (positions 3 to 7).
It consists of 4 or, as an exception, 5 numerical digits. Empty spaces should be filled with the digit 0.

A8 GEOGRAPHICAL LOCATION (GENERAL)
Refers to a very large geographical entity (e.g. a large mountain range or large politcal subdivision) which gives a rough idea of the location of the glacier, without requiring the use of a map or an atlas.
Format: max. 30 positions.
Examples: Western Alps, Southern Norway, Polar Ural, Tien Shan, Himalayas.

A9 GEOGRAPHICAL LOCATION (SPECIFIC)
Refers to a more specific geographical location (e.g. mountain group, drainage basin), which can easily be found on a small scale map of the country concerned.
Format: max. 30 positions.

A10 LATITUDE
The geographical coordinates should refer to a point in the upper ablation area; for small glaciers, this point may lie outside the glacier.
Latitude should be given in decimal degrees, positive values indicating the northern hemisphere and negative values indicating the southern hemisphere.
Latitude should be given to a maximum accuracy of 4 decimal places.

A11 LONGITUDE
The geographical coordinates should refer to a point in the upper ablation area; for small glaciers, this point may lie outside the glacier.
Longitude should be given in decimal degrees, positive values indicating east of zero meridian and negative values indicating west of zero meridian.
Longitude should be given to a maximum accuracy of 4 decimal places.

A12 CODE
Classification should be given in coded form, according to "Perennial Ice and Snow Masses" (Technical papers in hydrology, UNESCO/IAHS 1970). The following information should be given:

- Primary Classification Digit 1
- Form Digit 2
- Frontal Characteristcs Digit 3

A12.1 PRIMARY CLASSIFICATION - Digit 1

0	Miscellaneous	Any type not listed below (please explain)
1	Continental ice sheet	Inundates areas of continental size
2	Icefield	Ice masses of sheet or blanket type of a thickness that is insufficient to obscure the subsurface topography
3	Ice cap	Dome-shaped ice masses with radial flow
4	Outlet glacier	Drains an ice sheet, icefield or ice cap, usually of valley glacier form; the catchement area may not be easily defined
5	Valley glacier	Flows down a valley; the catchment area is well defined
6	Mountain glacier	Cirque, niche or crater type, hanging glacier; includes ice aprons and groups of small units
7	Glacieret and snowfield	Small ice masses of indefinite shape in hollows, river beds and on protected slopes, which has developed from snow drifting, avalanhcing, and/or particularly heavy accumulation in certain years; usually no marked flow

pattern is visible; in existence for at least two consecutive years.

8	Ice shelf	Floating ice sheet of considerable thickness attached to a coast nourished by a glacier(s); snow accumultaion on its surface or bottom freezing
9	Rock glacier	Lava-stream-like debris mass containing ice in several possible forms and moving slowly downslope

A12.2 FORM – Digit 2

0	Miscellaneous	Any type not listed below (please explain)
1	Compound basins	Two or more individual valley glaciers issuing from tributary valleys and coalescing (Fig. 1a)
2	Compound basin	Two or more individual accumulation basins feeding one glacier system (Fig. 1b)
3	Simple basin	Single accumulation area (Fig. 1c)
4	Cirque	Occupies a separate, rounded , steep-walled recess which it has formed on a mountain side (Fig. 1d)
5	Niche	Small glacier in a V-shaped gulley or depression on a mountain slope (Fig. 1e); generally more common than genetically further developed cirque glacier.
6	Crater	Occurring in extinct or dormant volcanic craters
7	Ice apron	Irregular, usually thin ice mass which adheres to mountain slope or ridge
8	Group	A number of similar ice masses occurring in close proximity and too small to be assessed individually
9	Remnant	Inactive, usually small ice masses left by a receding glacier

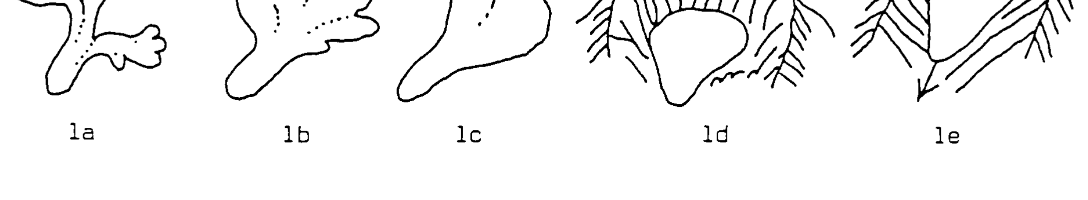

1a 1b 1c 1d 1e

A12.3 FRONTAL CHARACTERISTICS – Digit 3

0	Miscellaneous	Any type not listed below (please explain)
1	Piedmont	Icefield formed on a lowland area by lateral expansion of one or coalescence of several glaciers (Fig. 2a, 2b)
2	Expanded foot	Lobe or fan formed where the lower portion of the glacier leaves the confining wall of a valley amd extends on to a less restricted and more level surface (Fig. 2c)
3	Lobed	Part of an ice sheet or ice cap, disqualified as an outlet glacier (Fig. 2d)
4	Calving	Terminus of a glacier sufficiently extending into sea or lake water to produce icebergs; includes- for this inventory- dry land ice calving which would be recognisable from the “lowest glacier elevation”
5	Coalescing, non-contributing (Fig. 2e)	
6	Irregular, mainly clean ice (mountain or valley glaciers)	
7	Irregular, debris-covered (mountain or valley glaciers)	
8	Single lobe, mainly clean ice (mountain or valley glaciers)	
9	Single lobe, debris-covered (mountain or valley glaciers)	

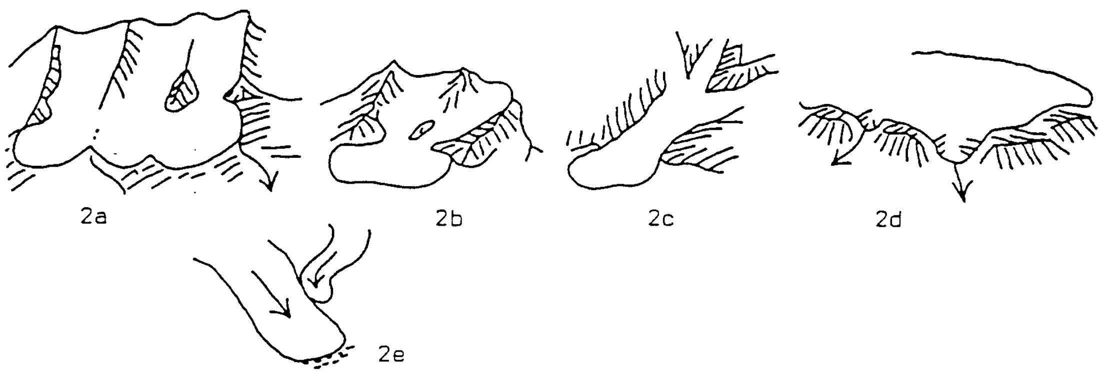

A13 EXPOSITION OF ACCUMULATION AREA
The main orientation of the accumulation area using the 8 cardinal points (8-point compass).

A14 EXPOSITION OF ABLATION AREA
The main orientation of the accumulation area using the 8 cardinal points (8-point compass).

A15 PARENT GLACIER
Links separated glacier parts with former parent glacier, using WGMS ID (see "A2 WGMS ID").

A16 REMARKS
Any important information or comments not included above may be given here. Comments about the accuracy of the numerical data may be made, including quantative comments. Only significant decimals should be given.

B STATE

NOTES ON THE COMPLETION OF THE DATA SHEET

B1 POLITCAL UNIT
Name of country or territory in which glacier is located (cf. “A1 POLITICAL UNIT”).

B2 WGMS ID
5 digit key identifying glacier in the WGMS data base (cf. “A2 WGMS ID”).

B3 GLACIER NAME
The name of the glacier, written in CAPITAL letters. Use the same spelling as in “A3 GLACIER NAME”).

B4 YEAR
Year of present survey.

B5 MAXIMUM ELEVATION OF GLACIER
Altitude of the highest point of the glacier.

B6 MEDIAN ELEVATION OF GLACIER
Altitude of the contour line which halves the area of the glacier.

B7 MINIMUM ELEVATION OF GLACIER
Altitude of the lowest point of the glacier.

B8 ELEVATION ACCURACY
Estimated maximum error of reported elevations.

B9 LENGTH
Maximum length of glacier measured along the most important flowline (in horizontal projection).

B10 LENGTH ACCURACY
Estimated maximum error, in length.

B11 SURVEY DATE
Date of present survey.
For each survey, please indicate the complete date (day, month, year).
Missing data: For unknown day or month, put “01” in the corresponding position(s) and make a note under “B15 REMARKS”

B12 SURVEY METHOD
The survey method should be given using the following alphabetic code:

- A Aerial photography
- B Terrestrial photogrammetry
- C Geodetic ground survey (theodolite, tape, etc.)
- D Combination of a, b or c (please explain under “B15 REMARKS”)
- E Other methods (please explain under “B15 REMARKS”)

B13 INVESTIGATOR
Name(s) of the person(s) or agency doing the field work and / or the name(s) of the person(s) or agency processing the data.

B14 SPONSORING AGENCY
Full name, abbreviation and address of the agency where the data are held.

B15 REMARKS
Any important information or comments not included above may be given here. Comments about the accuracy of the numerical data may be made, including quantative comments. Only significant decimals should be given.

C FRONT VARIATION

NOTES ON THE COMPLETION OF THE DATA SHEET

C1 POLITCAL UNIT
Name of country or territory in which glacier is located (cf. “A1 POLITICAL UNIT”).

C2 WGMS ID
5 digit key identifying glacier in the WGMS data base (cf. “A2 WGMS ID”).

C3 GLACIER NAME
The name of the glacier, written in CAPITAL letters. Use the same spelling as in “A3 GLACIER NAME”).

C4 YEAR
Year of present survey.

C5 FRONT VARIATION
Variation in the position of the glacier front (in horizontal projection) between the previous and present survey.

Signs:

+	Advance
-	Retreat

C6 FRONT VARIATION ACCURACY
Estimated maximum error for front variation.

C7 QUALITATIVE VARIATION
If no quantitative data are available for a particular year, but qualitative data are available, then the front variation should be denoted using the following symbols. They should be positioned in the far left of the data field.

+X	Glacier in advance
- X	Glacier in retreat
ST	Glacier stationary
SN	Glacier front covered by snow making survey impossible.

Qualitative variations will be understood with reference to the previous survey data, whether this data is qualitative or quantitative.

C8 SURVEY DATE
Date of present survey
For each survey, please indicate the complete date (day, month, year).
Missing data : For unknown day or month, put “01” in the corresponding position(s) and make a note under “C13 REMARKS”

C9 SURVEY METHOD
The survey method should be given using the following alphabetic code:

- A Aerial photography
- B Terrestrial photogrammetry
- C Geodetic ground survey (theodolite, tape etc.)
- D Combination of a, b or c (please explain under “C13 REMARKS”)
- E Other methods (please explain under “C13 REMARKS”)

C10 REFERENCE DATE
Date of previous survey
For each survey, please indicate the complete date (day, month, year).
Missing data : For unknown day or month, put “01” in the corresponding position(s) and make a corresponding note under “C13 REMARKS”

C11 INVESTIGATOR
Name(s) of the person(s) or agency doing the fieldwork and / or the name(s) of the person(s) or agency processing the data.

C12 SPONSORING AGENCY
Full name, abbreviation and address of the agency where the data are held.

C13 REMARKS
Any important information or comments not included above may be given here. Comments about the accuracy of the numerical data may be made, including quantative comments. Only significant decimals should be given.

D SECTION

NOTES ON THE COMPLETION OF THE DATA SHEET

D1 POLITCAL UNIT
Name of country or territory in which glacier is located (cf. “A1 POLITICAL UNIT”).

D2 WGMS ID
5 digit key identifying glacier in the WGMS data base (cf. “A2 WGMS ID”).

D3 GLACIER NAME
The name of the glacier, written in CAPITAL letters. Use the same spelling as in “A3 GLACIER NAME”).

D4 YEAR
Year of present survey.

D5 LOWER BOUNDARY
Lower boundary of altitude interval.
If refers to entire glacier, then lower bound = 9999.

D6 UPPER BOUNDARY
Upper boundary of altitude interval
If refers to entire glacier, then upper bound = 9999.

D7 AREA
Area of each altitude interval (in horizontal projection).

D8 AREA CHANGE
Area change for each altitude interval.

D9 AREA CHANGE ACCURACY
Estimated maximum error for area change.

D10 THICKNESS CHANGE
Thickness change for each altitude interval.

D11 THICKNESS CHANGE ACCURACY
Esitmated maximum error for thickness change.

D12 VOLUME CHANGE
Volume change for each altitude interval.

D13 VOLUME CHANGE ACCURACY
Esitmated maximum error for volume change.

D14 SURVEY DATE
Date of present survey
For each survey, please indicate the complete date (day, month, year).
Missing data : For unknown day or month, put “01” in the corresponding position(s) and make a corresponding note under “D19 REMARKS”

D15 SURVEY METHOD
The survey method should be given using the following alphabetic code:

- A Aerial photography
- B Terrestrial photogrammetry
- C Geodetic ground survey (theodolite, tape etc.)
- D Combination of a, b or c (please explain under “D19 REMARKS”)
- E Other methods (e.g., LIDAR, RADAR, map comparison; please explain and add at least one reference under “D19 REMARKS”)

D16 REFERENCE DATE
Date of previous survey.
For each survey, please indicate the complete date (day, month, year).
Missing data: For unknown day or month, put “01” in the corresponding position(s) and make a corresponding note under “D19 REMARKS”

D17 INVESTIGATOR
Name(s) of the person(s) or agency doing the fieldwork and / or the name(s) of the person(s) or agency processing the data.

D18 SPONSORING AGENCY
Full name, abbreviation and address of the agency where the data are held.

D19 REMARKS
Any important information or comments not included above may be given here. Comments about the accuracy of the numerical data may be made, including quantative comments. Only significant decimals should be given.

E MASS BALANCE OVERVIEW

NOTES ON THE COMPLETION OF THE DATA SHEET

E1 POLITCAL UNIT
Name of country or territory in which glacier is located (cf. “A1 POLITICAL UNIT”).

E2 WGMS ID
5 digit key identifying glacier in the WGMS database (cf. “A2 WGMS ID”).

E3 GLACIER NAME
The name of the glacier, written in CAPITAL letters. Use the same spelling as in “A3 GLACIER NAME”).

E4 YEAR
Year of present survey.

E5 TIME MEASUREMENT SYSTEM
The time measurement system should be given using the following 3 digit alphabetic code:

STR	Stratigraphic system
FXD	Fixed data system
COM	Combined system
OTH	Other (please explain under “E22 REMARKS”)

E6 BEGINNING OF SURVEY PERIOD
Date on which survey period began.
For each survey, please give the complete date (day, month, year).
Missing data: For unknown day or month, put “01” in the corresponding position(s) and make a note under “E22 REMARKS”

E7 END OF WINTER SEASON
Date of end of winter season (day, month, year, if known).
Missing data: For unknown day or month, put “01” in the corresponding position(s) and make a note under “E22 REMARKS”

E8 END OF SURVEY PERIOD
Date on which survey period ended.
For each survey, please give the complete date (day, month, year).
Missing data: For unknown day or month, put “01” in the corresponding position(s) and make a note under “E22 REMARKS”

E9 EQUILIBRIUM LINE ALTITUDE (ELA)
Mean altitude (averaged over the glacier) of the (end of mass balanc year) equilibrium line.

E10 EQUILIBRIUM LINE ALTITUDE ACCURACY
Estimated maximum error of ELA.

E11 MINIMUM NUMBER OF MEASUREMENT SITES USED IN ACCUMULATION AREA
The minimum number of different sites at which measurements were taken in the accumulation area. Repeat measurements may be taken for one site, in order to obtain an average value for that site, but the site is still only counted once.

E12 MAXIMUM NUMBER OF MEASUREMENT SITES USED IN ACCUMULATION AREA
The maximum number of different sites at which measurements were taken in the accumulation area. Repeat measurements may be taken for one site, in order to obtain an average value for that site, but the site is still only counted once.

E13 MINIMUM NUMBER OF MEASUREMENT SITES USED IN ABLATION AREA
The minimum number of different sites at which measurements were taken in the ablation area. Repeat measurements may be taken for one site, in order to obtain an average value for that site, but the site is still only counted once.

E14 MAXIMUM NUMBER OF MEASUREMENT SITES USED IN ABLATION AREA
The maximum number of different sites at which measurements were taken in the ablation area. Repeat measurements may be taken for one site, in order to obtain an average value for that site, but the site is still only counted once.

E15 ACCUMULATION AREA
Accumulation area in horizontal projection.

E16 ACCUMULATION AREA ACCURACY
Estimated maximum error for accumulation area.

E17 ABLATION AREA
Ablation area in horizontal projection.

E18 ABLATION AREA ACCURACY
Estimated maximum error for ablation area.

E19 ACCUMULATION AREA RATIO
Accumulation area divided by the total area, multiplied by 100. Given in percent.

E20 INVESTIGATOR
Name(s) of the person(s) or agency doing the fieldwork and / or the name(s) of the person(s) or agency processing the data.

E21 SPONSORING AGENCY
Full name, abbreviation and address of the agency where the data are held.

E22 REMARKS
Any important information or comments not included above may be given here. Comments about the accuracy of the numerical data may be made, including quantative comments. Only significant decimals should be given.

F MASS BALANCE

NOTES ON THE COMPLETION OF THE DATA SHEET

F1 POLITCAL UNIT
Name of country or territory in which glacier is located (cf. “A1 POLITICAL UNIT”).

F2 WGMS ID
5 digit key identifying glacier in the WGMS database (cf. “A2 WGMS ID”).

F3 GLACIER NAME
The name of the glacier, written in CAPITAL letters. Use the same spelling as in “A3 GLACIER NAME”).

F4 YEAR
Year of present survey.

F5 LOWER BOUNDARY OF ALTITUDE INTERVAL
If refers to entire glacier, then lower bound = 9999.

F6 UPPER BOUNDARY OF ALTITUDE INTERVAL
If refers to entire glacier, then lower bound = 9999.

F7 ALTITUDE INTERVAL AREA
Area of each altitude interval (in horizontal projection).

F8 SPECIFIC WINTER BALANCE
Specific means the total value divided by the total glacier area under investigation.
Specific winter balance equals the net winter balance divided by the total area of the glacier.

F9 SPECIFIC WINTER BALANCE ACCURACY
Estimated maximum error for specific winter balance.

F10 SPECIFIC SUMMER BALANCE
Specific means the total value divided by the total glacier area, in this case, it is the net summer balance divided by the total area of the glacier.

F11 SPECIFIC SUMMER BALANCE ACCURACY
Estimated maximum error for specific winter balance.

F12 SPECIFIC NET BALANCE
Net balance of glacier divided by the area of the glacier.

F13 SPECIFIC NET BALANCE ACCURACY
Estimated maximum error for specific net balance.

F14 INVESTIGATOR
Name(s) of the person(s) or agency doing the fieldwork and / or the name(s) of the person(s) or agency processing the data.

F15 SPONSORING AGENCY
Full name, abbreviation and address of the agency where the data are held.

F16 REMARKS
Any important information or comments not included above may be given here. Comments about the accuracy of the numerical data may be made, including quantative comments. Only significant decimals should be given.

G SPECIAL EVENT

NOTES ON COMPLETION OF THE DATA SHEET

This data sheet should be completed in cases of extraordinary events, especially concerning glacier hazards and uncommon changes in glaciers.

G1 POLITCAL UNIT
Name of country or territory in which glacier is located (cf. "A1 POLITICAL UNIT").

G2 WGMS ID
5 digit key identifying glacier in the WGMS database (cf. "A2 WGMS ID").

G3 GLACIER NAME
The name of the glacier, written in CAPITAL letters. Use the same spelling as in "A3 GLACIER NAME").

G4 EVENT DATE
Date of event.
For events lasting for several days, please indicate the date of the main event, and describe the sequence of the event under "G6. EVENT DESCRIPTION."

G5 EVENT TYPE
Indicate the involved event type(s) using 1 = event type involved and 0 = event type not involved for the following event types:

G5.1 GLACIER SURGE
G5.2 CALVING INSTABILITY
G5.3 GLACIER FLOOD (including debris flow, mudflow)
G5.4 ICE AVALANCHE
G5.5 TECTONIC EVENT (earthquake, volcanic eruption)
G5.6 OTHER

G6 EVENT DESCRIPTION
Please give quantitative information wherever possible, for example:

- Glacier surge: Date and location of onset, duration, flow or advance velocities, discharge anomalies and periodicity;

- Calving instability: Rate of retreat, iceberg discharge, ice flow velocity and water depth at calving front;

- Glacier flood (including debris flow, mudflow): Outburst volume, outburst mechanism, peak discharge, sediment load, sediment load, reach and propagation velocity of flood wave or front of debris flow / mudflow;

- Ice avalanche: Volume released, runout distance, overall slope (i.e., ratio of vertical drop height to horizontal travel distance) of avalanche path;

- Tectonic event: Volumes, runout distances and overall slopes of rockslides on glacier surfaces, amount of geothermal melting in craters, etc.

G7 DATA SOURCE
Please indicate at least one reference or source which could help the reader to locate more detailed information, or give the name(s) of contact person(s) who would be able to supply additional information.

G8 REMARKS
Any important information or comments not included above may be given here. Comments about the accuracy of the numerical data may be made, including quantative comments. Only significant decimals should be given.

The amount and/ or kind of possible destruction, particular technical measures taken against glacier hazards, or special studies carried out in connection with the event may be given.

WORLD GLACIER MONITORING SERVICE

GENERAL INFORMATION ON THE OBSERVED GLACIERS 2000-2005

TABLE A

NR	Record number
GLACIER NAME	15 alphabetic or numeric digits
PSFG NUMBER	5 digits identifying glacier with alphabetic prefix denoting country
LAT	Latitude in decimal degrees north or south
LONG	Longitudes in decimal degrees east or west
CODE	3 digits giving “primary classification”, “form” and “frontal characteristics”, respectively
EXP AC	Exposition of accumulation area (cardinal points)
EXP AB	Exposition of ablation area (cardinal points)
ELEVATION MAX	Maximum elevation of glacier in metres
ELEVATION MED	Median elevation of glacier in metres*
ELEVATION MIN	Minimum elevation of glacier in metres*
AREA	Total area of glacier in square kilometres*
LEN	Length of glacier along a flowline from maximum to minimum elevation in kilometres*
TYPE OF DATA	B = Variations in the positions of glacier fronts 2000–2005 or Variations in the position of glacier fronts: addenda from earlier years
	C = Mass balance summary data 2000–2005 or Mass balance summary data: addenda from earlier years
	D = Changes in area, volume and thickness
	F = Index measurements or special events – see Chapter 4

* these are the last reported values which may not correspond to the same survey year

NR	GLACIER NAME	PSFG NR	LAT	LONG	CODE	EXP AC	EXP AB	ELEVATION MAX	ELEVATION MED	ELEVATION MIN	AREA KM²	LEN KM	TYPE OF DATA
	ANTARCTICA												
1	BAHIA DEL DIA.	AQ	63.82 S	57.43 W		NE	E	638		38	14.3		C
	ARGENTINA												
2	AZUFRE	AR	35.29 S	70.55 W	538	E	E	3700	3350	2850	3.87	3.50	B
3	DE LOS TRES	AR	49.33 S	73.00 W	544	SE	SE	1990		1200	0.976	1.70	B
4	GUSSFELDT	AR	32.61 S	70.03 W	526	E	E	5300	4950	4310	14.67	6.57	B
5	HORCONES INF.	AR5006	32.68 S	69.98 W	539	SE	S	4825	4100	3475	6.17	12.15	B F
6	MARTIAL	AR131	54.78 S	68.42 W	143	SE	SE	1170	1050	940	0.33	0.45	B C
7	MARTIAL ESTE	AR	54.78 S	68.40 W	646	SE	SE	1170	1070	970	0.093	0.33	C
8	PENON	AR	35.27 S	70.56 W	525	E	NE	4100	3650	3180	4.42	3.10	B
9	TUPUNGATO 01	AR	33.39 S	69.75 W	507	SE	NE	6600	5300	4380		8.07	B
10	TUPUNGATO 02	AR	33.38 S	69.75 W	507	SE	E	6100	5100	4600		3.34	B
11	TUPUNGATO 03	AR	33.36 S	69.75 W	507	E	NE	6400	5650	4650		2.99	B
12	TUPUNGATO 04	AR	33.34 S	69.75 W	507	NE	NE	6450	6050	4800		3.28	B
13	VACAS	AR	32.55 S	69.99 W	526	E	E	5400	4700	3730	18.32	6.08	B
	AUSTRIA												
14	AEU.PIRCHLKAR	AT229	47.00 N	10.92 E	606	SE	NE	3260	3030	2720	0.94	1.9	B
15	ALPEINER F.	AT307	47.05 N	11.13 E	528	N	NE	3340	2930	2310	3.94	4.6	B
16	BACHFALLEN F.	AT304	47.08 N	11.08 E	608	N	N	3120	2850	2580	2.55	2.9	B
17	BAERENKOPF K.	AT702	47.13 N	12.72 E	624	N	N	3400	3030	2270	2.5	3.1	B
18	BERGLAS F.	AT308	47.07 N	11.12 E	608	E	NE	3290	2990	2490	1.47	2.5	B
19	BIELTAL F. W	AT0105B	46.87 N	10.13 E	646	NW	NW	2810	2680	2540	0.29	0.9	B
20	BIELTAL F.	AT0105A	46.88 N	10.13 E	606	NW	NW	3000	2740	2544	0.73	1.1	B
21	BIELTALF. MITTE	AT	46.88 N	10.13 E	---								B
22	BRENNKOGL K.	AT727	47.10 N	12.80 E	646	N	N	2960	2670	2430	0.59	1.2	B
23	DAUNKOGEL F.	AT0310A	47.00 N	11.10 E	608	NE	NE	3240	2880	2550	2.69	2.9	B
24	DIEM F.	AT220	46.81 N	10.98 E	608	NW	NW	3540	3060	2710	3.5	3.4	B
25	DORFER K.	AT509	47.10 N	12.33 E	628	SE	SE	3600	2790	2270	6.24	4	B
26	EISKAR G.	AT1301	46.62 N	12.90 E	646	N	N	2390	2250	2160	0.151	0.4	B
27	FERNAU F.	AT312	46.98 N	11.13 E	648	NW	N	3310	2850	2380	2.02	2.5	B
28	FREIGER F.	AT320	46.97 N	11.20 E	606	NE	NE	3370	3090	2720	0.59	1.5	B
29	FREIWAND K.	AT706	47.10 N	12.75 E	648	SE	SE	3130	2890	2690	0.35	1.1	B
30	FROSNITZ K.	AT507	47.08 N	12.40 E	636	E	E	3330	2780	2400	4.19	4.4	B
31	FURTSCHAGL K.	AT406	47.00 N	11.77 E	608	NW	NW	3480	2890	2542	1	1.6	B
32	GAISKAR F.	AT325	46.97 N	11.12 E	648	SE	SE	3190	3070	2890	0.75	1.1	B
33	GAISSBERG F.	AT225	46.83 N	11.07 E	528	NW	NW	3390	2850	2460	1.35	3.3	B
34	GEPATSCH F.	AT202	46.85 N	10.77 E	528	NE	N	3536	3057	2060	17.346	8.2	B
35	GOESSNITZ K.	AT1201	46.97 N	12.75 E	647	NW	NW	3060	2690	2520	0.86	1.5	B
36	GOLDBERG K.	AT0802B	47.03 N	12.47 E	648	SE	NE	3080	2680	2310	1.494	2.8	B C
37	GR.GOSAU G.	AT1101	47.48 N	13.60 E	646	NW	NW	2810	2520	2250	1.48	2.2	B
38	GROSSELEND K.	AT1001	47.03 N	13.32 E	636	NW	NW	3140	2720	2410	2.76	2.4	B
39	GRUENAU F.	AT315	46.98 N	11.20 E	648	N	N	3415	2941	2363	1.72	2.24	B
40	GURGLER F.	AT222	46.80 N	10.98 E	528	NW	N	3420	2990	2270		8	B
41	GUSLAR F.	AT210	46.85 N	10.80 E	648	E	SE	3480	3120	2780		2.5	B
42	HABACH K.	AT504	47.15 N	12.37 E	636	N	N	3240	2670	2170	5.03	2.4	B
43	HALLSTAETTER G.	AT1102	47.48 N	13.62 E	608	NE	NE	2910	2560	2080	3.3	2.3	B
44	HINTEREIS F.	AT209	46.80 N	10.77 E	528	E	NE	3727	3011	2400	7.4	7.1	B C
45	HOCHALM K.	AT1005	47.02 N	13.33 E	636	E	E	3350	2880	2540	3.16	2.4	B
46	HOCHJOCH F.	AT208	46.78 N	10.82 E	526	N	NW	3500	3030	2580	7.13	3.8	B
47	HOCHMOOS F.	AT309	47.05 N	11.15 E	609	E	NE	3460	2940	2520	1.74	3	B
48	HORN K.(SCHOB.)	AT1202	46.97 N	12.77 E	648	N	NW	3010	2780	2600	0.46	1.1	B
49	HORN K.(ZILLER)	AT402	47.00 N	11.82 E	538	N	N	3213	2777	2089	3.416	3	B
50	INN.PIRCHLKAR	AT228	47.00 N	10.92 E	656	E	NE	3340	2990	2720	0.62	1.8	B
51	JAMTAL F.	AT106	46.87 N	10.17 E	528	N	N	3120	2780	2370	3.48	2.8	B C
52	KAELBERSPITZ K.	AT1003	47.03 N	13.28 E	608	N	N	2890	2690	2450	0.82	2.2	B
53	KAL.BAERENKOPF	AT	47.11 N	13.60 E	---								B
54	KARLINGER K.	AT701	47.13 N	12.70 E	624	NE	N	3340	2800	2060	4.04	3.6	B
55	KESSELWAND F.	AT226	46.84 N	10.79 E	638	SE	E	3490	3180	2698	3.85	4.25	B C
56	KLEINFLEISS K.	AT801	47.05 N	12.95 E	606	W	W	3080	2840	2510	0.898	2.3	B C

WORLD GLACIER MONITORING SERVICE

VARIATIONS IN THE POSITION OF GLACIER FRONTS 2000-2005

TABLE B

NR	Record number
GLACIER NAME	15 alphabetic or numeric digits
PSFG NUMBER	5 digits identifying glacier with alphabetic prefix denoting country
METHOD	a = aerial photogrammetry b = terrestrial photogrammetry c = geodetic ground survey (theodolite, tape etc.) d = combination of a, b or c e = other methods or no information
1ST SURVEY	Year when first front variation data is available (at WGMS)
LAST SURVEY	Last survey before reported period
VARIATION IN METRES	Variation in the position of the glacier front in horizontal projection expressed as the change in length between the surveys
Key to Symbols	+X: Glacier in advance -X : Glacier in retreat ST : Glacier stationary SN : Glacier front covered by snow

NR	GLACIER NAME	PSFG NR	FIRST	LAST	METHOD	VARIATIONS IN METRES				
			SURVEY			2001	2002	2003	2004	2005
	<u>ARGENTINA</u>									
1	AZUFRE	AR	1963	1997	E				-340	50
2	DE LOS TRES	AR	1996	1998	C			-43		
3	GUESSFELDT	AR	1929	1999	E			30	0	30
4	HORCONES INFERIOR	AR5006	1974	1999	E	-740		0	0	2620
5	MARTIAL	AR131	1943	1984	D		-190	0		
6	PENON	AR	1963	1997	E				-150	10
7	TUPUNGATO 01	AR	1975	1999	E			-140		0
8	TUPUNGATO 02	AR	1975	1999	E			-20		-60
9	TUPUNGATO 03	AR	1975	1999	E			-30		-10
10	TUPUNGATO 04	AR	1975	1999	E			0		0
11	VACAS	AR	1929	1999	E			40	-100	-70
	<u>AUSTRIA</u>									
12	AEU.PIRCHLKAR	AT229	1982	2000	C	-21.3	-6	-4.5	-30.3	
13	ALPEINER F.	AT307	1848	2000	C	-34.8		-X	-X	
14	BACHFALLEN F.	AT304	1892	2000	C	-X	-X	-14.3	-7	-10.4
15	BAERENKOPF K.	AT702	1915	2000	C	-0.1	-13		-6.2	-7.6
16	BERGLAS F.	AT308	1892	2000	C	-5.4	-7	-27.8	-3.5	-69.2
17	BIELTAL F W	AT0105B	1970	2000	C	-4.4	-4.9	-24.1	-2.9	-8.6
18	BIELTAL F.	AT0105A	1924	2000		-2.9	-7.7			
19	BIELTALF. MITTE	AT	1997	2000	C	-2.9	-7.7	-14.2	-1.2	-5.3
20	BRENNKOGL K.	AT727	1988	2000	C	-5.2	-11	-11.7	-0.5	-3.5
21	DAUNKOGEL F.	AT0310A	1891	2000	C	-7.4	-8.5	-25.7	-9.3	-13.9
22	DIEM F.	AT220	1848	2000	C	-6.2	-5	-42.2	-15.1	-11.4
23	DORFER K.	AT509	1891	2000				-X		
24	EISKAR G.	AT1301	1920	2000	C	SN	-1.1	-4.9	0	-10
25	FERNAU F.	AT312	1891	2000	C	-0.1	-7.8	-20.5	-2.1	
26	FREIGER F.	AT320	1899	2000	C			-3.2	-0.7	1.9
27	FREIWAND K.	AT706	1929	2000	C	-4.1	-0.1	-15.3	-2.3	-10.2
28	FROSNITZ K.	AT507	1860	2000	C	-13.5	-13	-32.1	-6.5	-7.5
29	FURTSCHAGL K.	AT406	1897	2000	E	-X	-X	-X	-X	-X
30	GAISKAR F.	AT325	1984	2000	C	-X	-8.7	-22.2	-5	-11.4
31	GAISSBERG F.	AT225	1856	2000	C	-17	-16.8	-32.5	-6.3	-17
32	GEPATSCH F.	AT202	1856	2000	C	-22.9	-26.6	-62.6	-12.6	-20.5
33	GOESSNITZ K.	AT1201	1983	2000	C	-8.6	-7.1	-14.8	-10	-13.3
34	GOLDBERG K.	AT0802B	1850	2000	C	-3.7	-8.5	-10.3	0.9	-21.2
35	GR.GOSAU G.	AT1101	1884	2000	C	-11.7	-4.8	-14.1	-0.6	-0.4
36	GROSSELEND K.	AT1001	1900	2000	C	-4.9	-6.5	-11.4	SN	
37	GRUENAU F.	AT315	1892	2000	C	-5.6	-35	-8.9	SN	-20.8
38	GURGLER F.	AT222	1897	2000	C	-8.8	-X	-X	-8	-16.7
39	GUSLAR F.	AT210	1893	2000	C	-16.9	-16.1	-31.4	-16.9	-21.5
40	HABACH KEES	AT504	1925	1991				-X		
41	HALLSTAETTER G.	AT1102	1848	2000	C	-3.4	-6.6	-13.3	-4.7	-13.4
42	HINTEREIS F.	AT209	1848	2000	C	-19.1	-18.4	-30.4	-14.1	-27.1
43	HOCHALM K.	AT1005	1900	2000	C	-1.2	-9.2	-19.7	-4.9	-12
44	HOCHJOCH F.	AT208	1856	2000	C	-18.5	-25.5	-42.9	-17.9	-22.5
45	HOCHMOOS F.	AT309	1947	1994				-X		
46	HORN K.(SCHOB.)	AT1202	1984	2000	C	-4.8	-7.5	-14.8	-5.7	-6.1
47	HORN K.(ZILLER)	AT402	1882	2000	C	-21	-44	-52	-X	-50
48	INN.PIRCHLKAR	AT228	1982	2000	C	-6.3	-7.4	-24.6	-6.8	-7.2
49	JAMTAL F.	AT106	1892	2000	C	-9	-12.4	-22.4	-4.1	-13.5
50	KAELBERSPITZ K.	AT1003	1927	2000	C	-6.8	-8	-16.2	2.7	-7.5
51	KAL. BAERENKOPF K.	AT	1971	2000	C	-4.5	-0.1	-18.9	1	1.1
52	KARLINGER K.	AT701	1860	2000	E	ST	-X		-X	-X
53	KESSELWAND F.	AT226	1900	2000	C	-17.2	-13	-32.1	-15.3	-17.1
54	KLEINFLEISS K.	AT801	1851	2000	C	-14.5	10.3	-160.5	2	-1.7
55	KLEINEISER K.	AT717	1963	2000	C	-3	-8.3	-12.4	SN	-1.4
56	KLEINELEND K.	AT1002	1900	2000	C	3.4	-4.1	-9	5.8	-5.6
57	KLOSTERTALER M	AT0102B	1969	2000	C	-10.3	-7.3	-17.9	-2	-4.7
58	KLOSTERTALER N	AT0102A	1969	2000	E	SN	-2.2	-X	-X	-X

WORLD GLACIER MONITORING SERVICE

VARIATIONS IN THE POSITION OF GLACIER FRONTS

TABLE BB

ADDENDA FROM EARLIER YEARS

NR	Record number
GLACIER NAME	15 alphabetic or numeric digits
PSFG NUMBER	5 digits identifying glacier with alphabetic prefix denoting country
METHOD	a = aerial photogrammetry b = terrestrial photogrammetry c = geodetic ground survey (theodolite, tape etc.) d = combination of a, b or c e = other methods or no information
1ST SURVEY	Day, month and year of survey
2ND SURVEY	Day, month and year of following survey
VARIATION IN METRES	Variation in the position of the glacier front in horizontal projection expressed as the change in length between the surveys
Key to Symbols	+X : Glacier in advance -X : Glacier in retreat ST : Glacier stationary SN : Glacier front covered by snow

NR	GLACIER NAME	PSFG NR	METHOD	1ST SURVEY D M Y	2ND SURVEY D M Y	VARIATIONS IN METRES
	<u>BOLIVIA</u>					
1	CHACALTAYA	BO5180	C	1999	26.09.2000	-7
2	ZONGO	BO5150	C	15.12.1999	27.10.2000	-12
	<u>CHINA</u>					
3	LAPATE NO.51	CN27	C	19.08.1999	20.08.2000	-4.8
	<u>COLOMBIA</u>					
4	ALFOMBRALES E	CO0013B	A	13.01.1945	10.02.1959	-50
			A	10.02.1959	11.01.1975	-50
			A	11.01.1975	10.12.1985	-80
			A	10.12.1985	19.01.1987	-20
5	AZUFRADO E	CO0005B	A	13.01.1945	10.02.1959	60
			A	10.02.1959	11.01.1975	-20
			A	11.01.1975	10.12.1985	-130
			A	10.12.1985	19.01.1987	ST
6	AZUFRADO W	CO0005A	A	13.01.1945	10.02.1959	-70
			A	10.02.1959	11.01.1975	-20
			A	11.01.1975	10.12.1985	-80
			A	10.12.1985	19.01.1987	ST
7	CENTRAL	CO32	D	1987	01.12.2000	-177
8	CERRO CON-CAVO (7)	CO		26.03.1986	25.03.1991	-157.4
				25.03.1991	22.01.1997	-87
				22.01.1997	20.01.1998	-34
9	CERRO CON-CAVO (8)	CO		26.03.1986	26.03.1991	-136.5
				26.03.1991	15.01.1997	-79.7
				15.01.1997	20.01.1998	-21
10	CERRO TOTI (B)	CO		22.01.1997	21.01.1998	-25.5
11	CERRO TOTI (C)	CO		22.01.1997	21.01.1998	-28
12	DESA S	CO		1961	1989	0
				1989	1995	-810
13	DESA SE	CO		1961	1989	-250
				1989	1995	-575
14	DESA WSW	CO		1961	1989	-1050
				1989	1995	-20
15	EL MAYOR	CO		1961	1965	6.9
				1965	1970	-4.7
				1970	1989	-112.4
				1989	1995	-0.2
16	EL OSO	CO		1961	1965	-33.3
				1965	1989	-136.7
				1989	1995	-221.7
			D	1987	2000	-370
17	EL VENADO	CO		1961	1970	-1.9
				1970	1995	-97
18	GUALI	CO3	D	1987	01.05.2000	-550
19	HOJALARGA 1	CO		21.02.1988	17.03.1991	-64
				17.03.1991	15.01.1997	-49.1
20	LA CABANA	CO7	A	10.02.1959	11.01.1975	-200
			A	11.01.1975	10.12.1985	-200
			A	10.12.1985	19.01.1987	-20
21	LA CONEJERA	CO33	D	1987	01.12.2000	-147
22	LA LISA	CO4	D	1987	01.05.2000	-530
23	LA PLAZUELA	CO6	A	13.01.1945	10.02.1959	-20
			A	10.02.1959	11.01.1975	-30
			A	10.12.1985	19.01.1987	-220
24	LAGUNA AZUL	CO26	D	01.01.1987	01.12.2000	-190
25	LAGUNILLAS	CO8	A	13.01.1945	10.02.1959	0
			A	10.02.1959	11.01.1975	0
			A	11.01.1975	10.12.1985	-50
			A	10.12.1985	19.01.1987	-10

WORLD GLACIER MONITORING SERVICE

MASS BALANCE STUDY RESULTS SUMMARY DATA 2000-2005

TABLE C

NR	Record number
GLACIER NAME	15 alphabetic or numeric digits
PSFG NUMBER	5 digits identifying glacier with alphabetic prefix denoting country
SYS	System of measurement: STR = Stratigraphic FXD = Fixed date COM = Combined System OTH = Other System
FROM	Day, month and year of beginning of balance/measurement year
TO	Day, month and year of end of balance/measurement year
BW	Mean specific winter balance in mm water equivalent
BS	Mean specific summer balance in mm water equivalent
BN/BA	Mean specific net balance or annual balance in mm water equivalent
ELA	Altitude of equilibrium line or annual equilibrium line in metres above sea level
AAR	Ratio of accumulation area to total area of the glacier in percent
AREA	Area of the glacier used for calculation of mean specific quantities

NR	GLACIER NAME	PSFG NR	SYS	FROM	TO	BW	BS	BN/BA	ELA	AAR	AREA
				D M Y	D M Y	MM	MM	MM	M	%	KM²
	ANTARCTICA										
1	BAHIA DEL DIABLO	AQ		2001	2002			-510	440	30	14.3
				2002	2003			-150	410	40	14.3
				2003	2004			-110	380	44	14.3
				2004	2005			-230	400	38	14.3
	ARGENTINA										
2	MARTIAL	AR131		2000	2001			785	1000	100	0.33
				2001	2002			-691	1050	45	
3	MARTIAL ESTE	AR	STR	26.03.2000	02.04.2001	969	-184	785	1045	100	0.093
			STR	21.04.2001	08.04.2002	581	-1263	-682	>1125	0	0.093
			STR	19.05.2002	25.04.2003	675	-877	-202	1095	40	0.093
			STR	01.06.2003	14.04.2004	720	-1976	-1318	>1180	0	0.093
			STR	01.04.2004	31.03.2005			-991	1140	13	0.093
	AUSTRIA										
4	GOLDBERG K.	AT0802B	FXD	01.10.2000	30.09.2001	1788	-2176	-388	2940	18	1.494
			FXD	01.10.2001	30.09.2002	1857	-2468	-612	>3100	20	1.494
			FXD	01.10.2002	30.09.2003	1734	-3540	-1806	>3100	0	1.494
			FXD	01.10.2003	30.09.2004	1737	-1600	137	2925	52	1.425
			FXD	01.10.2004	30.09.2005	1391	-1651	-260	2880	51	1.425
5	HINTEREIS FERNER	AT209	FXD	01.10.2000	30.09.2001			-173	2955	64	7.963
			FXD	01.10.2001	30.09.2002			-647	3050	51	7.906
			FXD	01.10.2002	30.09.2003			-1814	>3750	3	7.817
			FXD	01.10.2003	30.09.2004			-667	3185	32	7.554
			FXD	01.10.2004	30.09.2005			-1061	3225	29	7.47
6	JAMTAL F.	AT106	FXD	01.10.2000	30.09.2001	1418	-1480	-62	2780	61	3.654
			FXD	01.10.2001	30.09.2002	1530	-2220	-671	2910	28	3.62
			FXD	01.10.2002	30.09.2003	1293	-3520	-2229	>3200	0	3.458
			FXD	01.10.2003	30.09.2004	1330	-1560	-228	2870	40	3.458
			FXD	01.10.2004	30.09.2005	850	-1825	-975	>3200	15	3.54
7	KESSELWAND F.	AT226	FXD	01.10.2000	30.09.2001			525	3063	87	4.042
			FXD	01.10.2001	30.09.2002			17	3120	75	4.037
			FXD	01.10.2002	30.09.2003			-1546	>3550	0	3.938
			FXD	01.10.2003	30.09.2004			-189	3157	61	3.905
			FXD	01.10.2004	30.09.2005			-59	3136	66	3.9
8	KLEINFLEISS K.	AT801	FXD	01.10.2000	30.09.2001	1691	-1887	-195	2920	51	0.945
			FXD	01.10.2001	30.09.2002	1332	-2140	-808	3100	13	0.945
			FXD	01.10.2002	30.09.2003	1614	-3056	-1442	>3100	0	0.898
			FXD	01.10.2003	30.09.2004	1417	-1291	125	2820	75	0.872
			FXD	01.10.2004	30.09.2005	1143	-1254	-111	2850	63	0.872
9	PASTERZEN K.	AT704	FXD	1.10.2004	30.9.2005			-899	2920	60	17.71
10	SONNBLICK K.	AT0601A		18.10.2000	31.8.2001			-399	2840	40	1.502
				1.9.2001	15.9.2002			-485	2845	35	1.501
				16.9.2002	10.9.2003			-2870	3080	1	1.402
				11.9.2003	24.9.2004			8	2755	62	1.394
				25.9.2004	30.9.2005			-323	2810	44	1.393
11	VERNAGT FERNER	AT211	FXD	1.10.2000	30.9.2001	1139	-1363	-224	3128	47	8.68
			FXD	1.10.2001	30.9.2002	1013	-1279	-266	3122	53	8.68
			FXD	1.10.2002	30.9.2003	986	-3119	-2133	>3630	0	8.53
			FXD	1.10.2003	30.9.2004	891	-1298	-407	3205	34	8.36
			FXD	1.10.2004	30.9.2005	621	-1144	-523	3224	40	8.36
12	WURTEN K.	AT804	FXD	1.10.2000	30.9.2001	1790	-2090	-300	2985	33	0.972
			FXD	1.10.2001	30.9.2002	1399	-2365	-966	3020	4	0.972
			FXD	1.10.2002	30.9.2003	1732	-3909	-2177	3070	3	0.972
			FXD	1.10.2003	30.9.2004	1501	-1814	-313	2980	28	0.824
			FXD	1.10.2004	30.9.2005	1194	-1642	-448	3020	16	0.824
	BOLIVIA										
13	CHACALTAYA	BO5180	FXD	1.9.2000	31.8.2001	123	33	-350	>5451	0	0.044
			FXD	1.9.2001	31.8.2002	-11	-676	-1827	>5518	0	0.042

WORLD GLACIER MONITORING SERVICE

MASS BALANCE STUDY RESULTS SUMMARY DATA

TABLE CC

ADDENDA FROM EARLIER YEARS

NR	Record number
GLACIER NAME	15 alphabetic or numeric digits
PSFG NUMBER	5 digits identifying glacier with alphabetic prefix denoting country
SYS	System of measurement: STR = Stratigraphic FXD = Fixed date COM = Combined System OTH = Other System
FROM	Day, month and year of beginning of balance/measurement year
TO	Day, month and year of end of balance/measurement year
BW	Mean specific winter balance in mm water equivalent
BS	Mean specific summer balance in mm water equivalent
BN/BA	Mean specific net balance or annual balance in mm water equivalent
ELA	Altitude of equilibrium line or annual equilibrium line in metres above sea level
AAR	Ratio of accumulation area to total area of the glacier in percent
AREA	Area of the glacier used for calculation of mean specific quantities

NR	GLACIER NAME	PSFG NR	SYS	FROM	TO	BW	BS	BN/BA	ELA	AAR	AREA
				D M Y	D M Y	MM	MM	MM	M	%	KM²
	AUSTRIA										
1	HINTEREIS FERNER	AT209	FXD	01.10.1999	30.09.2000			-633	3050	48	8.11
2	JAMTAL F.	AT106	FXD	01.10.1999	30.09.2000	1550	-1631	-80	2765	62	3.67
3	KESSELWAND F.	AT226	FXD	01.10.1999	30.09.2000			140	3120	74	4.16
4	VERNAGT FERNER	AT211	FXD	01.10.1964	30.09.1965			751	2946	92	9.52
			FXD	01.10.1965	30.09.1966	1570	-938	632	2940	93	9.52
			FXD	01.10.1966	30.09.1967	1292	-1209	83	3015	70	9.52
			FXD	01.10.1967	30.09.1968	677	-376	301	2995	86	9.52
			FXD	01.10.1968	30.09.1969	616	-923	-307	3153	56	9.46
			FXD	01.10.1969	30.09.1970	916	-1140	-224	3113	61	9.46
			FXD	01.10.1970	30.09.1971	761	-1185	-424	3155	39	9.46
			FXD	01.10.1971	30.09.1972	878	-741	137	3028	79	9.46
			FXD	01.10.1972	30.09.1973	643	-1103	-460	3185	43	9.30
			FXD	01.10.1973	30.09.1974	851	-621	230	2999	81	9.30
			FXD	01.10.1974	30.09.1975	1131	-960	171	3025	80	9.30
			FXD	01.10.1975	30.09.1976	613	-563	50	3036	74	9.30
			FXD	01.10.1976	30.09.1977	1190	-838	352	2984	88	9.30
			FXD	01.10.1977	30.09.1978	985	-697	288	3004	84	9.55
			FXD	01.10.1978	30.09.1979	993	-949	44	3059	73	9.55
			FXD	01.10.1979	30.09.1980	868	-728	140	3027	77	9.55
			FXD	01.10.1980	30.09.1981	936	-991	-55	3101	72	9.55
			FXD	01.10.1981	30.09.1982	1313	-2158	-845	3418	24	9.35
			FXD	01.10.1982	30.09.1983	1081	-1618	-537	3304	25	9.35
			FXD	01.10.1983	30.09.1984	870	-850	20	3063	71	9.34
			FXD	01.10.1984	30.09.1985	1410	-1522	-112	3102	61	9.34
			FXD	01.10.1985	30.09.1986	870	-1678	-808	3291	18	9.34
			FXD	01.10.1986	30.09.1987	988	-1278	-290	3143	55	9.31
			FXD	01.10.1987	30.09.1988	899	-1396	-497	3230	39	9.09
			FXD	01.10.1988	30.09.1989	949	-1261	-312	3170	50	9.09
			FXD	01.10.1989	30.09.1990	855	-1423	-568	3283	32	9.09
			FXD	01.10.1990	30.09.1991	912	-1991	-1079	>3630	8	9.09
			FXD	01.10.1991	30.09.1992	947	-1805	-858	3268	22	9.09
			FXD	01.10.1992	30.09.1993	895	-1367	-472	3225	37	9.09
			FXD	01.10.1993	30.09.1994	1031	-2059	-1028	>3630	22	9.09
			FXD	01.10.1994	30.09.1995	979	-1377	-398	3226	39	9.09
			FXD	01.10.1995	30.09.1996	486	-899	-413	3225	40	9.09
			FXD	01.10.1996	30.09.1997	928	-1415	-487	3220	41	9.07
			FXD	01.10.1997	30.09.1998	807	-1810	-1003	3280	30	9.07
			FXD	01.10.1998	30.09.1999	1116	-1224	-108	3097	56	8.68
			FXD	01.10.1999	30.09.2000	1079	-1366	-287	3123	48	8.68
	BOLIVIA										
5	CHACALTAYA	BO5180	FXD	01.09.1999	31.08.2000	107	-590	-852	>5383	0	0.04
6	ZONGO	BO5150	COM	01.09.1999	01.09.2000			77	5213	66	1.96
	CANADA										
7	BABY GLACIER	CA205	COM	1989	1990			-313			0.61
			COM	1990	1991			-143			0.61
			COM	1991	1992			-71			0.61
			COM		1993			-594			0.61
			COM		1994			-153			0.61
			COM		1995			-353			0.61
			COM		1996			165			0.61
			COM		1997			-126			0.61
			COM		1998			-21			0.61
			COM		1999			-925			0.61
			COM		2000			-560			0.61
	ECUADOR										
8	ANTIZANA15ALPHA	EC1	FXD	1999	2000			394	4980	80	0.35

WORLD GLACIER MONITORING SERVICE

MASS BALANCE VERSUS ALTITUDE FOR SELECTED GLACIERS

TABLE CCC

NR	Record number
GLACIER NAME	15 alphabetic or numeric digits
PSFG NUMBER	5 digits identifying glacier with alphabetic prefix denoting country
YEAR	Balance year or measurement year
SYS	System of measurement: STR = Stratigraphic FXD = Fixed date COM = Combined System OTH = Other System
ALTITUDE	Altitude interval in metres above sea level
AREA	Area of altitude band and in square kilometres
BW	Mean specific winter balance in mm water equivalent
BS	Mean specific summer balance in mm water equivalent
BN/BA	Mean specific net balance or annual balance in mm water equivalent
SUMMARY	Total and mean specific values computed from data for the individual altitude intervals

NR	GLACIER NAME	PSFG NR	YEAR	SYS	ALTITUDE FROM	ALTITUDE TO	AREA KM²	BW MM	BS MM	BN/BA MM
	ANTARCTICA									
1.1	BAHIA DEL DIABLO	AQ	2002		562	638				-50
					488	562				130
					412	488				50
					338	412				-300
					262	338				-750
					188	262				-750
					112	188				-1550
					38	112				-2800
					38	638	14.3			-510
1.2	BAHIA DEL DIABLO	AQ	2003		562	638				75
					488	562				250
					412	488				140
					338	412				-50
					262	338				-300
					188	262				-225
					112	188				-750
					38	112				-1300
					38	638	14.3			-150
1.3	BAHIA DEL DIABLO	AQ	2004		562	638				125
					488	562				300
					412	488				150
					338	412				-25
					262	338				-250
					188	262				-300
					112	188				-700
					38	112				-1400
					38	638	14.3			-110
1.4	BAHIA DEL DIABLO	AQ	2005		562	638				50
					488	562				225
					412	488				100
					338	412				-100
					262	338				-350
					188	262				-450
					112	188				-900
					38	112				-1700
					38	638	14.3			-230
	ARGENTINA									
2.1	MARTIAL ESTE	AR	2002	STR	1170	1180				81
					1160	1170				78
					1150	1160				38
					1140	1150				36
					1130	1140				31
					1120	1130				30
					1110	1120				25
					1100	1110				-9
					1090	1100				-47
					1080	1090				-101
					1070	1080				-184
					1060	1070				-262
					1050	1060				-331
					1040	1050				-367
					1030	1040				-391
					1020	1030				-398
					1010	1020				-398
					1000	1010				-400
					990	1000				-405

WORLD GLACIER MONITORING SERVICE

CHANGES IN AREA, VOLUME AND THICKNESS

TABLE D

NR	Record number
GLACIER NAME	15 alphabetic or numeric digits
PERIOD FROM TO	Period from ‘reference year’ to ‘survey year’ in which the changes take place
ALTITUDE	Altitude interval in metres above sea level
AREA SY	Area of altitude interval for ‘survey year’ (square kilometres)
AREA CHANGE	Change in area of altitude interval for period of change (thousand square metres)
VOLUME CHANGE	Change in volume of altitude interval for period of change (thousand cubic metres)
THICKNESS CHANGE	Change in thickness of altitude interval for period of change (millimetres)

NR	GLACIER NAME	PERIOD		ALTITUDE		AREA	AREA	VOLUME	THICKNESS
		FROM	TO	FROM	TO	SY	CHANGE	CHANGE	CHANGE
	BOLIVIA								
1.1	CHACALTAYA	1999	2000	5350	5360		0	-0.326	-693
	BO5180			5325	5350		0	-2.193	-693
				5300	5325		-1	-1.873	-482
				5275	5300		0	-1.426	-482
				5250	5275		-1	-2.22	-482
				5225	5250		-2	-8.988	-750
				5200	5225		0	-10.964	-1019
				5175	5200		-1	-9.25	-1029
				5150	5175		0	-7.831	-1253
				5140	5150		0	-1.419	-1325
				5140	5360	0.046	-5	-5	-1698
1.2	CHACALTAYA	2000	2001	5140	5360	0.044	-4	-0.524	-11
	BO5180								
1.3	CHACALTAYA	2001	2002	5140	5360	0.042	-2	-64.627	-1350
	BO5180								
1.4	CHACALTAYA	2002	2003	5140	5360	0.036	-6	-45.987	-1042
	BO5180								
1.5	CHACALTAYA	2003	2004	5140	5360	0.027	-8	-39.825	-902
	BO5180								
1.6	CHACALTAYA	2004	2005	5140	5360	0.01	-17	-50.437	-2635
	BO5180								
2.1	CHARQUINI SUR	2002	2003	5300	5350	0.0025			383
	BO			5250	5300	0.0119			383
				5200	5250	0.0051			383
				5150	5200	0.0741			19
				5100	5150	0.1183			-903
				5050	5100	0.074			-1991
				5000	5050	0.0613			-2053
				4950	5000	0.0051			-2053
				4950	5350	0.3523			
2.2	CHARQUINI SUR	2003	2004	5300	5350	0.002	0	-3	-1228
	BO			5250	5300	0.0155	4	-14.61	-1228
				5200	5250	0.0467	0	-6.26	-1228
				5150	5200	0.0774	3	-101.2	-1366
				5100	5150	0.1171	-1	-178.5	-1509
				5050	5100	0.0729	-1	-125.65	-1698
				5000	5050	0.0616	0	-147.12	-2400
				4950	5000	0.0035	-2	-14.57	-2858
				4950	5350	0.3967	4		
2.3	CHARQUINI SUR	2004	2005	5200	5350	0.0644	0	-63.1	-983
	BO			5150	5200	0.0774	0	-86.76	-1121
				5100	5150	0.1163	-2	-382	-3263
				5050	5100	0.0701	-6	-98.12	-1346
				4950	5050	0.0537	-14	-64.64	-993
				4950	5350	0.3819	-1		
3.1	ZONGO	1999	2000	5900	6000	0.0357			2825
	BO5150			5800	5900	0.078			2825
				5700	5800	0.139			2825
				5600	5700	0.234			2565
				5500	5600	0.262			2305
				5400	5500	0.234			1707

WORLD GLACIER MONITORING SERVICE

ALPHABETIC INDEX

GLACIER NAME	15 alphabetic or numeric digits, names arranged in alphabetic order
PSFG NUMBER	5 digits identifying glacier with alphabetic prefix denoting country
WGMS ID	5 digits, identifying glacier in the WGMS-data base
DATA TABLE AND RECORD NUMBER	Table and record number where data are located

A = General information on the observed glacier
B = Variations in the position of glacier fronts: 2000–2005
BB = Variations in the position of glacier fronts: addenda from earlier years
C = Mass balance summary data: 2000–2005
CC = Mass balance summary data: addenda from earlier years
CCC = Mass balance versus altitude for selected glaciers
D = Changes in area, volume and thickness
F = Index measurements or special events – see Chapter 4

GLACIER NAME	PSFG NR	WGMS ID	DATA TABLE AND RECORD NUMBER							
AALFOTBREEN	NO36204	317	A.479			C.59		CCC.32		
ADAMS	NZ	2923	A.421	B.350	BB.68					
ADI KAILASH	IN	3051	A.274	B.208						
AEU. PIRCHLKAR	AT229	504	A.14	B.12						
AGNELLO MER.	IT29	684	A.288	B.220						
ALBA	ES9010	967	A.539		BB.83					
ALFOMBRALES E	CO0013B	2693	A.154		BB.4					
ALLALIN	CH11	394	A.579	B.484					D.21	
ALLISON	HM1350	2902	A.206		BB.46					
ALMER/SALISBURY	NZ	1548	A.422	B.351						
ALPEINER F.	AT307	497	A.15	B.13						
ALPETLI (KANDER)	CH109	439	A.580	B.485						
ALTA (VEDRETTA)	IT730	632	A.289	B.221						
AMMERTEN	CH111	435	A.581	B.486						
AMOLA	IT644	638	A.290	B.222						
ANDOLLA SETT.	IT336	617	A.291	B.223						
ANDY	NZ	1590	A.423	B.352						
ANETO	ES9030	943	A.540	B.455	BB.84					
ANTELAO INFERIORE (OCC.)	IT967	642	A.292	B.224						
ANTELAO SUP.	IT966	643	A.293	B.225						
ANTIZANA 15 ALPHA	EC1	1624	A.197	B.154	BB.45	C.32	CC.8	CCC.23		
ANZAC PEAK	HM1020	2914	A.207		BB.47					
AOUILLE	IT138	1239	A.294	B.226						
ARGENTIERE	FR00002	354	A.198	B.155		C.33	CC.9			
AROLLA (BAS)	CH27	377	A.582	B.487						
ARTESONRAJU	PE3	3292	A.522	B.439		C.81		CCC.48		
ASHBURTON	NZ	1570	A.424	B.353						
AURONA	IT338	616	A.295	B.227						
AUSTDALSBREEN	NO37323	321	A.480			C.60		CCC.33		
AUSTERDALSBREEN	NO31220	288	A.481	B.408						
AUSTRE BROEGGERBREEN	NO15504	292	A.482			C.61				
AXIUS	NZ	2283	A.425	B.354						
AZUFRADO E	CO0005B	2696	A.155		BB.5					
AZUFRADO W	CO0005A	2697	A.156		BB.6					
AZUFRE	AR	2851	A.2	B.1						
BABY	CA205	1	A.143			C.22	CC.7			
BACHFALLEN F.	AT304	500	A.16	B.14						
BAERENKOPF K.	AT702	567	A.17	B.15						
BAHIA DEL DIABLO	AQ	2665	A.1			C.1		CCC.1		
BALAITUS SE	ES1030	954	A.541		BB.85					
BALFOUR	NZ	1604	A.426	B.355						
BARA SHIGRI	IN	2920	A.275						D.5	
BARRANCS	ES9040	941	A.542	B.456	BB.86					
BASEI	IT64	611	A.296	B.228						
BASODINO	CH104	463	A.583	B.488		C.89		CCC.56	D.22	
BAUDISSIN	HM105	2874	A.208		BB.48					
BEAS KUND	IN	3053	A.276	B.209						
BELLA TOLA	CH21	383	A.584	B.489						
BELVEDERE (MACUGNAGA)	IT325	618	A.297	B.229						F
BERGLAS F.	AT308	496	A.18	B.16						
BERGSETBREEN	NO31013	2290	A.483	B.409						
BERING	US	3336	A.694							F
BESSANESE	IT40	1297	A.298	B.230						
BHAGIRATHI KHARAK	IN	3050	A.277	B.210						
BIELTAL F.	AT0105A	481	A.20	B.18						
BIELTAL F. MITTE	AT	2674	A.21	B.19						
BIELTAL F. W	AT0105B	1452	A.19	B.17						
BIFERTEN	CH77	422	A.585	B.490						
BIS	CH0107	388	A.586							F
BLAAMANNSISEN	NO	2306	A.484							F
BLACK RAPIDS	US222	80	A.695							F

Publication 3

WGMS (2009). **Glacier Mass Balance Bulletin No. 10 (2006–2007)**. Haeberli, W., Gärtner-Roer, I., Hoelzle, M., Paul, F. & **Zemp, M.** (eds.), ICSU (WDS) / IUGG (IACS) / UNEP / UNESCO / WMO, World Glacier Monitoring Service, Zurich, Switzerland, 96 pp.

GLACIER MASS BALANCE BULLETIN

Bulletin No. 10 (2006–2007)

A contribution to

the Global Terrestrial Network for Glaciers (GTN-G)
as part of the Global Terrestrial/Climate Observing System (GTOS/GCOS),

the Division of Early Warning and Assessment and the Global Environment Outlook
as part of the United Nations Environment Programme (DEWA and GEO, UNEP)

and the International Hydrological Programme (IHP, UNESCO)

Compiled by

the World Glacier Monitoring Service (WGMS)

ICSU (WDS) – IUGG (IACS) – UNEP – UNESCO – WMO

2009

GLACIER MASS BALANCE BULLETIN

Bulletin No. 10 (2006–2007)

A contribution to

the Global Terrestrial Network for Glaciers (GTN-G)
as part of the Global Terrestrial/Climate Observing System (GTOS/GCOS),

the Division of Early Warning and Assessment and the Global Environment Outlook
as part of the United Nations Environment Programme (DEWA and GEO, UNEP)

and the International Hydrological Programme (IHP, UNESCO)

Compiled by

the World Glacier Monitoring Service (WGMS)

Edited by

Wilfried Haeberli, Isabelle Gärtner-Roer, Martin Hoelzle, Frank Paul, Michael Zemp

Glaciology, Geomorphodynamics & Geochronology
Department of Geography
University of Zurich

ICSU (WDS) – IUGG (IACS) – UNEP – UNESCO – WMO

2009

Imprint

World Glacier Monitoring Service
c/o Department of Geography
University of Zurich
Winterthurerstrasse 190
CH-8057 Zurich
Switzerland
http://www.wgms.ch
wgms@geo.uzh.ch

Editorial Board

Contributors

Principal Investigators (see pages 85ff): data measurements, submission, and review of press proof
National Correspondents (see pages 93ff): data compilation, submission, and review of press proof
Ursina Gloor (Department of Geography, University of Zurich): data compilation
Dorothea Stumm (Department of Geosciences, University of Fribourg): data quality control, layout, maps and graphics, language editing
Susan Braun-Clarke (Translations & Proof-reading, Eichenau, Germany): language editing

Printed by

Staffel Druck AG
CH-8045 Zurich
Switzerland

ISSN 1997-9088 (printed issues)
ISSN 1997-9096 (online issues)

Citation

WGMS 2009. *Glacier Mass Balance Bulletin* No. 10 (2006-2007). Haeberli, W., Gärtner-Roer, I., Hoelzle, M., Paul, F. and Zemp, M. (eds.), ICSU(WDS)/IUGG(IACS)/UNEP/UNESCO/WMO, World Glacier Monitoring Service, Zurich, 96 pp.

Cover Page

Brewster Glacier with Mt Brewster (2515 m a.s.l.) of the Southern Alps of New Zealand. Photo taken by A. Willsman (Glacier Snowline Survey, NIWA), 14 March 2008.

PREFACE

In-situ measurements of glacier mass balance constitute – and will continue to constitute – a key element in worldwide glacier monitoring as part of global climate-related observation systems. They improve our understanding of the involved processes relating to earth-atmosphere mass and energy fluxes and provide quantitative data at high (annual, seasonal) time resolution, which enables numerical models to be developed for climate-glacier relationships. Together with more numerous observations of glacier length change and air- and space-based spatial information on large glacier samples, this process understanding and quantitative modelling helps to bridge the gap between detailed local studies and global coverage. It also fosters realistic anticipation of possible further developments. The latter includes worst-case scenarios of drastic to even complete deglaciation in many mountain regions of the world as early as the next few decades. On a century time scale, changes in glaciers and ice caps are an easily recognized reflection of rapid if not accelerating changes in the energy balance of the earth's surface and, hence, are also among the most striking indicators in nature of global climate change. The general losses in length, area, thickness and volume of firn and ice can be visually detected and qualitatively understood by everyone. Numeric values and comprehensive analysis, however, must be provided by advanced science: while the initial phases following the cold centuries of the Little Ice Age were most probably related to effects from natural climate variability, anthropogenic influences have increased over the past decades to such an extent that – for the first time in history – continued shrinking of glaciers and ice caps may have become primarily forced by human impacts on the atmosphere.

International assessments such as the periodical reports of the Intergovernmental Panel on Climate Change (IPCC), the Cryosphere Theme Report of the WMO Integrated Global Observing Strategy (IGOS 2007) or various GCOS/GTOS reports (for instance, the implementation plan for the Global Observing System for Climate in support of the UNFCCC; GCOS 2009) clearly recognize glacier changes as high-confidence climate indicators and as a valuable element in early detection strategies. The report on «Global glacier changes – facts and figures» recently published by WGMS under the auspices of UNEP (WGMS 2008) presents a corresponding overview and detailed background information. Glacier changes in the perspective of global cryosphere evolution is treated in the «Global outlook for ice and snow » issued by UNEP (2007).

In order to further document the evolution and to clarify the physical processes and relationships involved, the World Glacier Monitoring Service (WGMS) of the International Association for the Cryospheric Sciences (IACS/IUGG) as one of the permanent services of the World Data System within the International Council of Science (WDS/ICSU) collects and publishes standardized glacier data. This long-term activity is a contribution to the Global Climate/Terrestrial Observing Systems (GCOS/GTOS), to the Division of Early Warning and Assessment and the Global Environment Outlook as part of the United Nations Environment Programme (DEWA and GEO, UNEP), as well as to the International Hydrological Programme (IHP) of the United Nations Educational, Scientific and Cultural Organisation (UNESCO). In close cooperation with the Global Land Ice Measurement from Space (GLIMS) initiative and the National Snow and Ice Data Center (NSIDC) at Boulder, Colorado, an integrated and multi-level strategy within the Global Terrestrial Network for Glaciers (GTN-G) of GTOS is used to combine in-situ observations with remotely sensed data, process understanding with global coverage, and traditional measurements with new technologies. This approach, the Global Hierarchical Observing Strategy (GHOST), applies observations in a system of tiers. Tier 2 includes detailed glacier mass balance measurements within major climatic zones for improved process understanding and calibration of numerical models. Tier 3 uses cost-saving methodologies to determine regional glacier volume change within major mountain systems. The mass balance data compilation of the World Glacier Monitoring Service – a network of, at present, about 110 glaciers in 24 countries/regions, representing tiers 2 and 3 – is published in the form of the bi-annual Glacier Mass Balance Bulletin as well as annually in electronic form. Such a sample of glaciers provides information on presently observed rates of change in glacier mass as well as their regional distribution patterns and acceleration trends as an independent climate proxy.

The publication of standardized glacier mass balance data in the Glacier Mass Balance Bulletin is restricted to measurements which are based on the direct glaciological method and requested to be compared, and if necessary, adjusted to geodetic or photogrammetric surveys repeated at about decadal time intervals. In accordance with an agreement made with the international organizations and countries involved, preliminary glacier mass balance values are made available one year after the end of the measurement period on the WGMS homepage (www.wgms.ch). This internet homepage also contains former issues of and the present Glacier Mass Balance Bulletin, as well as explanations of the monitoring strategy. The following series of reports on the variations of glaciers in time and space has already been published by the WGMS and its predecessor, the Permanent Service on the Fluctuations of Glaciers (PSFG):

- Fluctuations of Glaciers 1959–1965 (Vol. 1, P. Kasser)
- Fluctuations of Glaciers 1965–1970 (Vol. 2, P. Kasser)
- Fluctuations of Glaciers 1970–1975 (Vol. 3, F. Müller)
- Fluctuations of Glaciers 1975–1980 (Vol. 4, W. Haeberli)
- Fluctuations of Glaciers 1980–1985 (Vol. 5, W. Haeberli and P. Müller)
- Fluctuations of Glaciers 1985–1990 (Vol. 6, W. Haeberli and M. Hoelzle)
- Fluctuations of Glaciers 1990–1995 (Vol. 7, W. Haeberli, M. Hoelzle, S. Suter and R. Frauenfelder)
- Fluctuations of Glaciers 1995–2000 (Vol. 8, W. Haeberli, M. Zemp, R. Frauenfelder, M. Hoelzle and A. Kääb)
- Fluctuations of Glaciers 2000–2005 (Vol. 9, W. Haeberli, M. Zemp, A. Kääb, F. Paul and M. Hoelzle)
- World Glacier Inventory – Status 1988 (W. Haeberli, H. Bösch, K. Scherler, G. Østrem and C.C. Wallén)
- Glacier Mass Balance Bulletin No. 1, 1988–1989 (W. Haeberli and E. Herren)
- Glacier Mass Balance Bulletin No. 2, 1990–1991 (W. Haeberli, E. Herren and M. Hoelzle)
- Glacier Mass Balance Bulletin No. 3, 1992–1993 (W. Haeberli, M. Hoelzle and H. Bösch)
- Glacier Mass Balance Bulletin No. 4, 1994–1995 (W. Haeberli, M. Hoelzle and S. Suter)
- Glacier Mass Balance Bulletin No. 5, 1996–1997 (W. Haeberli, M. Hoelzle and R. Frauenfelder)
- Glacier Mass Balance Bulletin No. 6, 1998–1999 (W. Haeberli, R. Frauenfelder and M. Hoelzle)
- Glacier Mass Balance Bulletin No. 7, 2000–2001 (W. Haeberli, R. Frauenfelder, M. Hoelzle and M. Zemp)
- Glacier Mass Balance Bulletin No. 8, 2002–2003 (W. Haeberli, J. Noetzli, M. Zemp, S. Baumann, R. Frauenfelder and M. Hoelzle)
- Glacier Mass Balance Bulletin No. 9, 2004–2005 (W. Haeberli, M. Hoelzle and M. Zemp)

The present Glacier Mass Balance Bulletin reporting the results from the balance years 2005/2006 and 2006/2007 is the tenth issue in a long-term series of publications. It is designed to speed up and facilitate access to information concerning glacier mass balances by reporting measured values from selected reference glaciers at 2-year intervals. The results of glacier mass balance measurements are made more easily understandable for non-specialists through the use of graphic illustrations in addition to numerical data. The Glacier Mass Balance Bulletin complements the publication series ‘Fluctuations of Glaciers’, where the full collection of digital data, including geodetic volume changes and the more numerous observations of glacier length variation, can be found. It should also be kept in mind that this fast and somewhat preliminary reporting of mass balance measurements may require slight correction and updating at a later time. Correspondingly corrected and updated information can be found in the Fluctuations of Glaciers series and are available in digital format from the WGMS.

Special thanks are extended to all those who have helped to build up the database which, despite its limitations, nevertheless remains an irreplaceable treasure of international snow and ice research, readily available to the scientific community as well as to a vast public.

Zurich, 2009

Wilfried Haeberli
Director, World Glacier Monitoring Service

TABLE OF CONTENTS

1 INTRODUCTION

The Glacier Mass Balance Bulletin reports on two main categories of data: basic information and detailed information. Basic information on specific net balance, cumulative specific balance, accumulation area ratio and equilibrium line altitude is given for 111 glaciers. Such information provides a regional overview. Additionally, detailed information such as balance maps, balance/altitude diagrams, relationships between accumulation area ratios, equilibrium line altitudes and balance, as well as a short explanatory text with a photograph is presented for 16 glaciers. These ones were chosen because they had a long and complete series of direct glaciological measurements taken over many years. These long time series, based on high density networks of stakes and firn pits, are especially valuable for analyzing processes of mass and energy exchange at glacier/atmosphere interfaces and, hence, for interpreting climate/glacier relationships. In order to provide broader-based information on glaciers from all regions worldwide, additional selected glaciers with shorter measurement series have been included.

1.1 GENERAL INFORMATION ON THE OBSERVED GLACIERS

The glaciers for which data is reported in the present bulletin are listed below (Table 1.1, Figure 1.1). Additionally, 20 glaciers with long measurement series of 15 years and more are listed.

Table 1.1: General geographic information on the 111 glaciers for which basic information for the years 2006 and/or 2007 is reported. Additionally, 20 glaciers with long measument series of 15 or more years are listed.

No.	Glacier Name[1)]	1st/last survey[2)]	Country	Location	Coordinates[3)]	
1	Bahía del Diablo	2002/2007	Antarctica	Antarctic Peninsula	63.82 S	57.43 W
2	Martial Este	2001/2007	Argentina	Andes Fueguinos	54.78 S	68.40 W
3	Filleckkees	1964/1980	Austria	Eastern Alps	47.13 N	12.60 E
4	Goldbergkees	2001/2007	Austria	Eastern Alps	47.03 N	12.47 E
5	Hintereisferner	1953/2007	Austria	Eastern Alps	46.80 N	10.77 E
6	Jamtalferner	1989/2007	Austria	Eastern Alps	46.87 N	10.17 E
7	Kesselwandferner	1953/2007	Austria	Eastern Alps	46.83 N	10.79 E
8	Kleinfleisskees	2001/2007	Austria	Eastern Alps	47.05 N	12.95 E
9	Pasterzenkees	2005/2007	Austria	Eastern Alps	47.10 N	12.70 E
10	Sonnblickkees	1959/2007	Austria	Eastern Alps	47.13 N	12.60 E
11	Vernagtferner	1965/2007	Austria	Eastern Alps	46.88 N	10.82 E
12	Wurtenkees	1983/2007	Austria	Eastern Alps	47.04 N	13.01 E
13	Chacaltaya	1992/2007	Bolivia	Tropical Andes	16.35 S	68.12 W
14	Charquini Sur	2003/2007	Bolivia	Tropical Andes	16.17 S	68.09 W
15	Zongo	1992/2007	Bolivia	Tropical Andes	16.25 S	68.17 W
16	Baby Glacier	1960/2005	Canada	High Arctic	79.43 N	90.97 W
17	Devon Ice Cap NW	1961/2007	Canada	High Arctic	75.42 N	83.25 W
18	Helm	1975/2007	Canada	Coast Mountains	49.97 N	123.00 W
19	Meighen Ice Cap	1976/2007	Canada	High Arctic	79.95 N	99.13 W
20	Peyto	1966/2007	Canada	Rocky Mountains	51.67 N	116.53 W
21	Place	1965/2007	Canada	Coast Mountains	50.43 N	122.6 W
22	Sentinel	1966/1989	Canada	Coast Mountains	49.90 N	122.98 W
23	White	1960/2007	Canada	High Arctic	79.45 N	90.67 W

No.	Glacier Name[1)]	1st/last survey[2)]	Country	Location	Coordinates[3)]	
24	Echaurren Norte	1976/2007	Chile	Central Andes	33.58 S	70.13 W
25	Urumqihe S.No.1	1959/2007	China	Tien Shan	43.08 N	86.82 E
	Urumqihe E-Branch	1988/2007	China	Tien Shan	43.08 N	86.82 E
	Urumqihe W-Branch	1988/2007	China	Tien Shan	43.08 N	86.82 E
26	La Conejera	2006/2007	Colombia	Cordillera Central	4.48 N	75.22 W
27	Ritacuba Negro	2007/2007	Colombia	Cordillera Oriental	6.45 N	72.3 W
28	Antizana 15 Alpha	1995/2007	Ecuador	Eastern Cordillera	0.47 S	78.15 W
29	Argentière	1976/2007	France	Western Alps	45.95 N	6.98 E
30	Gebroulaz	1995/2007	France	Western Alps	45.30 N	6.63 E
31	Ossoue	2002/2007	France	Pyrenees	42.77 N	0.14 W
32	Saint Sorlin	1957/2007	France	Western Alps	45.17 N	6.15 E
33	Sarennes	1949/2007	France	Western Alps	45.14 N	6.14 E
34	Mittivakkat	2006/2006	Greenland	South-eastern Greenland	65.67 N	37.83 W
35	Brúarjökull	1994/2007	Iceland	Eastern Iceland	64.67 N	16.17 W
36	Dyngjujökull	1994/2007	Iceland	Central Northern Iceland	64.67 N	17.00 W
37	Eyjabakkajökull	1994/2007	Iceland	Eastern Iceland	64.65 N	15.58 W
38	Hofsjökull E	1989/2005	Iceland	Central Iceland	64.80 N	18.58 W
39	Hofsjökull N	1988/2006	Iceland	Central Iceland	64.95 N	18.92 W
40	Hofsjökull SW	1990/2006	Iceland	Central Iceland	64.72 N	19.05 W
41	Koeldukvislarjökull	1995/2007	Iceland	Central Iceland	64.58 N	17.83 W
42	Langjökull S. Dome	1997/2007	Iceland	Central Iceland	64.62 N	20.30 W
43	Tungnaárjökull	1994/2007	Iceland	Central Iceland	64.32 N	18.07 W
44	Chhota Shigri	2003/2006	India	Western Himalaya	32.20 N	77.50 E
45	Hamtah	2001/2006	India	Himachal Pradesh	32.24 N	77.37 E
46	Calderone	2001/2007	Italy	Apennin	42.47 N	13.62 E
47	Caresèr [4)]	1967/2007	Italy	Central Alps	46.45 N	10.70 E
	Caresèr orientale [4)]	2006/2007	Italy	Central Alps	46.45 N	10.70 E
	Caresèr occidentale [4)]	2006/2007	Italy	Central Alps	46.45 N	10.69 E
48	Ciardoney	1992/2007	Italy	Western Alps	45.52 N	7.40 E
49	Fontana Bianca	1984/2007	Italy	Central Alps	46.48 N	10.77 E
50	Lunga (Vedretta)	2004/2007	Italy	Central Alps	46.47 N	10.62 E
51	Malavalle	2002/2007	Italy	Central Alps	46.95 N	11.12 E
52	Pendente	1996/2007	Italy	Central Alps	46.96 N	11.23 E
53	Hamaguri Yuki [5)]	1981/2007	Japan	Northern Japan Alps	36.60 N	137.62 E
54	Igly Tuyuksu	1976/1990	Kazakhstan	Tien-Shan	43.00 N	77.10 E
55	Manshuk Mametova	1976/1990	Kazakhstan	Tien Shan	43.00 N	77.10 E
56	Mayakovskiy	1976/1990	Kazakhstan	Tien Shan	43.00 N	77.10 E
57	Molodezhniy	1976/1990	Kazakhstan	Tien Shan	43.00 N	77.10 E
58	Ordzhonikidze	1976/1990	Kazakhstan	Tien Shan	43.00 N	77.10 E
59	Partizan	1976/1990	Kazakhstan	Tien Shan	43.00 N	77.10 E
60	Shumskiy	1967/1991	Kazakhstan	Dzhungarskiy	45.08 N	80.23 E
61	Ts. Tuyuksuyskiy	1957/2007	Kazakhstan	Tien Shan	43.05 N	77.08 E

No.	Glacier Name[1)]	1st/last survey[2)]	Country	Location	Coordinates[3)]	
62	Visyachiy-1-2	1976/1990	Kazakhstan	Tien Shan	43.00 N	77.10 E
63	Zoya Kosmodemyansk.	1976/1990	Kazakhstan	Tien Shan	43.00 N	77.10 E
64	Golubin	1969/1994	Kirghizstan	Tien-Shan	42.47 N	74.50 E
65	Kara-Batkak	1957/1998	Kirghizstan	Tien-Shan	42.10 N	78.30 E
66	Lewis	1979/1996	Kenya	East Africa	0.15 S	37.30 E
67	Brewster	2005/2007	New Zealand	Tititea Mt Aspiring NP	44.08 S	169.44 E
68	Ålfotbreen	1963/2007	Norway	Western Norway	61.75 N	5.65 E
69	Austdalsbreen	1987/2007	Norway	Western Norway	61.80 N	7.35 E
70	Austre Brøggerbreen	1967/2007	Norway	Spitsbergen	78.88 N	11.83 E
71	Blomstølskardsbreen	2007/2007	Norway	South-western Norway	60.00 N	6.40 E
72	Breidablikkbrea	1963/2007	Norway	South-western Norway	60.10 N	6.40 E
73	Elisebreen	2006/2007	Norway	Spitsbergen	78.64 N	12.25 E
74	Engabreen	1970/2007	Norway	Northern Norway	66.65 N	13.85 E
75	Gråfjellsbrea	1964/2007	Norway	South-western Norway	60.10 N	6.40 E
76	Gråsubreen	1962/2007	Norway	Southern Norway	61.65 N	8.60 E
77	Hansbreen	1989/2007	Norway	Spitsbergen	77.08 N	15.67 E
78	Hansebreen	1986/2007	Norway	Western Norway	61.75 N	5.68 E
79	Hardangerjøkulen	1963/2007	Norway	Central Norway	60.53 N	7.37 E
80	Hellstugubreen	1962/2007	Norway	Southern Norway	61.57 N	8.43 E
81	Irenebreen	2002/2007	Norway	Spitsbergen	78.65 N	12.10 E
82	Kongsvegen	1987/2007	Norway	Spitsbergen	78.80 N	12.98 E
83	Langfjordjøkelen	1989/2007	Norway	Northern Norway	70.12 N	21.77 E
84	Midtre Lovénbreen	1968/2007	Norway	Spitsbergen	78.88 N	12.07 E
85	Nigardsbreen	1962/2007	Norway	Western Norway	61.72 N	7.13 E
86	Storbreen	1949/2007	Norway	Central Norway	61.57 N	8.13 E
87	Svelgjabreen	2007/2007	Norway	South-western Norway	60.00 N	6.40 E
88	Waldemarbreen	1995/2007	Norway	Spitsbergen	78.67 N	12.00 E
89	Artesonraju	2005/2007	Peru	Cordillera Blanca	8.95 S	77.62 W
90	Yanamarey	2005/2007	Peru	Cordillera Blanca	9.65 S	77.27 W
91	Abramov	1968/1998	Tadjikistan	Pamir Alai	39.63 N	71.60 E
92	Djankuat	1968/2007	Russia	Northern Caucasus	43.20 N	42.77 E
93	Garabashi	1984/2007	Russia	Northern Caucasus	43.30 N	42.47 E
94	Kozelskiy	1973/1997	Russia	Kamchatka	53.23 N	158.82 E
95	Leviy Aktru	1977/2007	Russia	Altay	50.08 N	87.72 E
96	Maliy Aktru	1962/2007	Russia	Altay	50.08 N	87.75 E
97	No. 125 (Vodopadniy)	1977/2007	Russia	Altay	50.10 N	87.70 E
98	Maladeta	1992/2007	Spain	South Pyrenees	42.65 N	0.64 E
99	Mårmaglaciären	1990/2007	Sweden	Northern Sweden	68.83 N	18.67 E
100	Rabots Glaciär	1982/2006	Sweden	Northern Sweden	67.90 N	18.55 E
101	Riukojietna	1986/2007	Sweden	Northern Sweden	68.08 N	18.08 E
102	Storglaciären	1946/2007	Sweden	Northern Sweden	67.90 N	18.57 E
103	Tarfalaglaciären	1986/2007	Sweden	Northern Sweden	67.93 N	18.65 E

No.	Glacier Name[1)]	1st/last survey[2)]	Country	Location	Coordinates[3)]	
104	Basòdino	1992/2007	Switzerland	Western Alps	46.42 N	8.48 E
105	Findelen	2005/2007	Switzerland	Western Alps	46.00 N	7.87 E
106	Gries	1962/2007	Switzerland	Western Alps	46.44 N	8.34 E
107	Limmern	1948/1984	Switzerland	Western Alps	46.82 N	8.98 E
108	Plattalva	1948/1984	Switzerland	Western Alps	46.83 N	8.98 E
109	Silvretta	1960/2007	Switzerland	Eastern Alps	46.85 N	10.08 E
110	Blue Glacier	1956/1999	USA	Washington	47.82 N	123.68 W
111	Columbia (2057)	1984/2007	USA	North Cascades	47.97 N	121.35 W
112	Daniels	1984/2007	USA	North Cascades	47.57 N	121.17 W
113	Easton	1990/2007	USA	North Cascades	48.75 N	120.83 W
114	Emmons	2003/2007	USA	Mt Rainier	46.85 N	121.72 W
115	Foss	1984/2007	USA	North Cascades	47.55 N	121.20 W
116	Gulkana	1966/2007	USA	Alaska Range	63.25 N	145.42 W
117	Ice Worm	1984/2007	USA	North Cascades	47.55 N	121.17 W
118	Lemon Creek	1953/2007	USA	Coast Mountains	58.38 N	134.40 W
119	Lower Curtis	1984/2007	USA	North Cascades	48.83 N	121.62 W
120	Lynch	1984/2007	USA	North Cascades	47.57 N	121.18 W
121	Nisqually	2003/2007	USA	Mt Rainier	46.82 N	121.74 W
122	Noisy Creek	1993/2007	USA	Washington	48.67 N	121.53 W
123	North Klawatti	1993/2007	USA	Washington	48.57 N	121.12 W
124	Rainbow	1984/2007	USA	North Cascades	48.80 N	121.77 W
125	Sandalee	1995/2007	USA	Washington	48.42 N	120.80 W
126	Sholes	1990/2007	USA	North Cascades	48.80 N	121.78 W
127	Silver	1993/2007	USA	Washington	48.98 N	121.25 W
128	South Cascade	1953/2007	USA	North Cascades	48.37 N	121.05 W
129	Taku	1946/2007	USA	Coast Mountains	58.55 N	134.13 W
130	Wolverine	1966/2007	USA	Kenai Mtns	60.40 N	148.92 W
131	Yawning	1984/2007	USA	North Cascades	48.45 N	121.03 W

[1)] Countries and glaciers are listed in alphabetical order
[2)] Years of first and most recent survey available to the WGMS
[3)] Coordinates in decimal notation
[4)] In 2005, Caresèr broke into two parts: Caresèr Orientale and Caresèr Occidentale.
[5)] Perennial snowfield or glacieret

1.2 GLOBAL OVERVIEW MAP

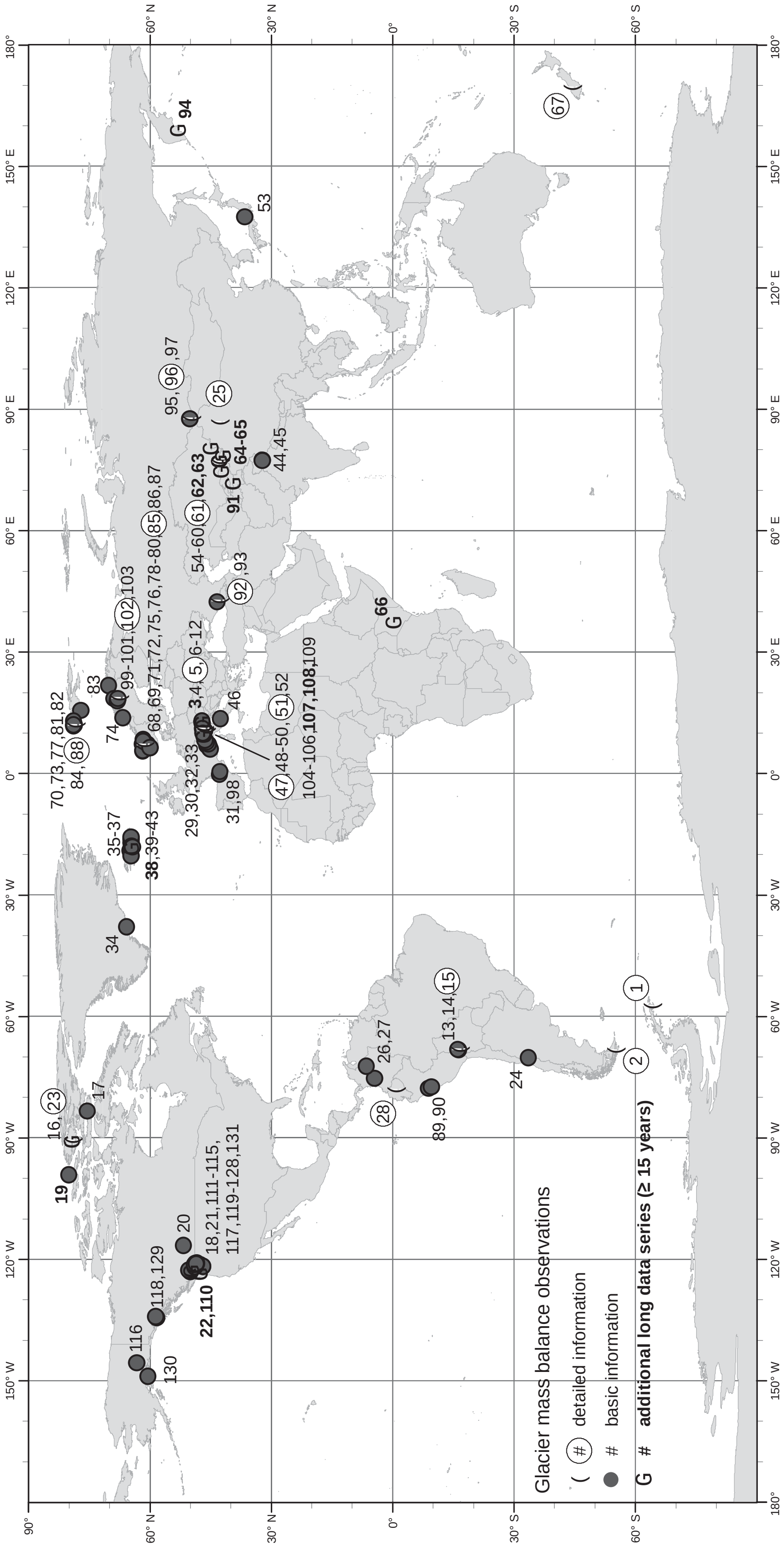

Figure 1.1: Location of the 111 glaciers for which basic information is reported. Additionally, 20 glaciers with interrupted long-term measument series are marked (i.e., 15 or more years).

2 BASIC INFORMATION

Specific net balance (b), equilibrium line altitude (ELA) and accumulation area ratio (AAR) from the balance years 2005/06 and 2006/07 are presented in Part 2.1. ELAs above and below the glacier elevation range are marked with > and <, respectively. In these cases, the ELA value given is supposed to be the glacier max/min elevation. The AAR values are given as integer values only.

Values for ELA_0 and AAR_0 are also given. They represent the calculated ELA and AAR values for a zero net balance, i.e., a hypothetical steady state. All values since the beginning of mass balance measurement-taking were used for this calculation on each glacier. Minimum sample size for regression was defined as six ELA or AAR values. In extreme years some of the observed glaciers can become entirely ablation or accumulation areas. Corresponding AAR values of 0 or 100 % as well as ELA values outside the altitude range of the observed glaciers were excluded from the calculation of AAR_0 and ELA_0 values. For the glaciers with detailed information, the corresponding graphs (AAR and ELA vs. specific net balance) are given in Chapter 3.

The graphs in the second part present the development of cumulative specific net balance over the whole observation period for each glacier where three or more net balances were reported and the years 2005/06 or 2006/07 are included. For each country, the cumulative balances are plotted in a single graph. For countries with more than six glaciers, the cumulative balances were plotted in several graphs, which were split into groups of glaciers from the same region, similar glacier types or alphabetically separated groups. Some of the time series have data gaps and hence have to be interpreted with care. In these cases, the overall ice loss cannot be derived from the cumulative specific net balance graphs and has to be determined by other means, such as geodetic or photogrammetric methods. Generally, for glaciers with data gaps longer than one-fifth of the measurement time series, the cumulative balance has been plotted for the measurements taken after the most recent data gap only.

2.1 SUMMARY TABLE (NET BALANCE, ELA, ELA_0, AAR, AAR_0)

Name	Country	b06 [mm]	b07 [mm]	ELA06 [m a.s.l.]	ELA07 [m a.s.l.]	ELA_0 [m a.s.l.]	AAR06 [%]	AAR07 [%]	AAR_0 [%]
Bahía del Diablo	Antarctica	− 580	− 80	445	360	366	31	49	48
Martial Este	Argentina	− 513	− 99	1096	1072	—	38	62	—
Goldbergkees	Austria	− 1077	− 1106	3020	3000	—	7	24	45
Hintereisferner	Austria	− 1516	− 1797	> 3750	> 3750	2922	11	0	66
Jamtalferner	Austria	− 1293	− 1438	> 3120	> 3120	2760	8	6	58
Kesselwandferner	Austria	− 617	− 837	3233	3280	3114	33	22	69
Kleinfleisskees	Austria	− 655	− 946	3070	3020	2856	10	23	70
Pasterzenkees	Austria	− 1232	− 1355	3000	3025	—	47	49	—
Sonnblickkees	Austria	− 621	− 2175	2860	2990	2740	29	2	59
Vernagtferner	Austria	− 882	− 966	3261	3281	3080	25	19	66
Wurtenkees	Austria	− 778	− 1200	3120	> 3150	2905	17	4	36
Chacaltaya	Bolivia	− 1199	− 1652	5383	> 5400	—	0	0	—
Charquini Sur	Bolivia	− 376	− 482	5132	5157	—	50	38	—
Zongo	Bolivia	− 197	− 173	5191	5271	5231	71	62	67

Name	Country	b06 [mm]	b07 [mm]	ELA06 [m a.s.l.]	ELA07 [m a.s.l.]	ELA$_0$ [m a.s.l.]	AAR06 [%]	AAR07 [%]	AAR$_0$ [%]
Devon Ice Cap NW	Canada	−242	−291	1340	1296	1004	—	—	71 [1]
Helm	Canada	−2750	−210	> 2150	2007	2000	0	12	37
Meighen Ice Cap	Canada	−8	−518	—	—	—	—	—	—
Peyto	Canada	−1650	−1850	3090	3010	2612	10	40	52
Place	Canada	−1900	−150	> 2610	2180	2085	0	26	49
White	Canada	−93	−818	1097	1347	910	61	25	71
Echaurren Norte	Chile	+560	−130	—	—	—	—	—	—
Urumqihe S. No.1	China	−774	−642	4087	4074	4022	28	31	56
Urumqihe E-Branch	China	−920	−696	4086	4060	3949	19	28	65
Urumqihe W-Branch	China	−506	−542	4089	4100	4024	43	36	64
La Conejera	Colombia	−1935	−996	—	—	—	—	—	—
Ritacuba Negro	Colombia	—	−2227	—	—	—	—	—	—
Antizana 15 Alpha	Ecuador	−452	−658	5150	5170	5045	54	53	70
Argentière	France	−1420	−590	—	—	—	—	—	—
Gebroulaz	France	−1000	−910	—	—	—	—	—	—
Ossoue	France	−2710	−1380	> 3200	> 3200	—	0	0	—
Saint Sorlin	France	−1440	−2250	—	—	2863	—	—	—
Sarennes	France	−2380	−2520	—	—	—	—	—	—
Mittivakkat	Greenland	−590	—	—	—	—	—	—	—
Brúarjökull	Iceland	−790	−536	—	—	1183	—	—	60
Dyngjujökull	Iceland	−353	+95	—	—	—	—	—	—
Eyjabakkajökull	Iceland	−1425	−636	—	—	1074	—	—	56
Hofsjökull N	Iceland	−510	—	1325	—	1264	41	—	50
Hofsjökull SW	Iceland	−610	—	1330	—	1266	50	—	46
Koeldukvislarjökull	Iceland	−402	−342	—	—	1289	—	—	60
Langjökull S. Dome	Iceland	−1080	−1412	—	—	975	—	—	57
Tungnaárjökull	Iceland	−1569	−997	—	—	1147	—	—	61
Chhota Shigri	India	−1413	—	5185	—	—	29	—	—
Hamtah	India	−790	—	—	—	—	12	—	—
Calderone	Italy	+1090	−2320	< 2630	> 2830	—	100	0	—
Caresèr [2]	Italy	−2093	−2745	> 3279	> 3279	3094	0	0	44
Caresèr orientale [2]	Italy	−2117	−2769	> 3277	> 3277	—	0	0	—
Caresèr occidentale [2]	Italy	−1911	−2558	> 3279	> 3279	—	0	0	—
Ciardoney	Italy	−2099	−1490	> 3150	> 3150	2977	0	0	57
Fontana Bianca	Italy	−1753	−1607	> 3355	> 3355	3255	0	0	55
Lunga (Vedretta)	Italy	−1456	−1616	3295	> 3390	—	10	0	—
Malavalle	Italy	−1327	−1338	3200	3224	2930	12	9	56
Pendente	Italy	−1740	−2154	> 3075	> 3075	2822	0	0	45
Hamaguri Yuki [3]	Japan	+3289	−609	—	—	—	—	—	—
Ts. Tuyuksuyskiy	Kazakhstan	−969	−915	3980	3885	3746	22	34	52
Brewster	New Zealand	+282	+297	1893	1899	—	72	67	—
Ålfotbreen	Norway	−3190	+1270	> 1382	1000	1199	0	97	57
Austdalsbreen	Norway	−2060	+180	> 1757	1405	1423	0	75	65
Austre Brøggerbreen	Norway	−730	−460	458	427	282	5	10	52
Blomstølskardsbreen	Norway	—	+1880	—	1230	—	—	89	—
Breidablikkbrea	Norway	−2950	+360	> 1659	1410	1473	0	68	—
Elisebreen	Norway	−726	−542	398	392	—	40	40	—
Engabreen	Norway	−1360	+1100	1325	1035	1157	37	84	60
Gråfjellsbrea	Norway	−3150	+750	> 1659	1395	1456	0	80	—
Gråsubreen	Norway	−2080	−710	> 2290	2265	2080	0	1	41
Hansbreen	Norway	+93	−4	300	330	301	61	54	55

Name	Country	b06 [mm]	b07 [mm]	ELA06 [m a.s.l.]	ELA07 [m a.s.l.]	ELA_0 [m a.s.l.]	AAR06 [%]	AAR07 [%]	AAR_0 [%]
Hansebreen	Norway	− 3980	+ 845	> 1327	1042	1158	0	89	56
Hardangerjøkulen	Norway	− 2220	+ 1170	> 1860	1570	1678	0	85	68
Hellstugubreen	Norway	− 2010	− 670	> 2210	1975	1838	0	25	58
Irenebreen	Norway	− 822	− 695	422	454	263	24	20	56
Kongsvegen	Norway	+ 20	− 90	530	555	537	46	39	48
Langfjordjøkelen	Norway	− 2410	− 810	> 1050	870	716	0	42	64
Midtre Lovénbreen	Norway	− 480	− 250	415	376	296	14	26	57
Nigardsbreen	Norway	− 1399	+ 1047	1850	1320	1558	4	91	60
Storbreen	Norway	− 2150	− 390	> 2100	1835	1717	0	30	59
Svelgjabreen	Norway	—	+ 1350	—	1205	—	—	78	—
Waldemarbreen	Norway	− 747	− 771	425	428	270	16	13	47
Artesonraju	Peru	− 1679	− 1522	—	—	—	—	—	—
Yanamarey	Peru	− 1712	− 1532	4888	4868	—	27	36	—
Djankuat	Russia	− 800	− 2010	3290	3500	3189	42	16	56
Garabashi	Russia	− 656	− 633	3950	3910	3794	40	42	60
Leviy Aktru	Russia	− 190	− 320	3230	3250	3161	58	57	61
Maliy Aktru	Russia	− 140	− 300	3250	3270	3154	60	55	70
No. 125 (Vodopadniy)	Russia	− 260	− 270	3240	3240	3201	67	67	69
Maladeta	Spain	− 1787	− 947	> 3200	> 3200	3059	0	0	40
Mårmaglaciären	Sweden	− 1650	− 530	1655	1640	1599	11	13	34
Rabots Glaciär	Sweden	− 1630	—	1505	—	1372	19	—	51
Riukojietna	Sweden	− 1400	− 960	> 1450	> 1450	1332	0	0	55
Storglaciären	Sweden	− 1720	+ 410	1615	1480	1463	17	50	45
Tarfalaglaciären	Sweden	− 2530	+ 210	> 1790	1475	—	0	73	—
Basòdino	Switzerland	− 2501	− 902	> 3300	3100	2878	0	5	50
Findelen	Switzerland	− 1200	− 200	3350	3200	—	40	62	—
Gries [4]	Switzerland	− 1995	− 1473	3325	3324	2818	2	2	56
Silvretta [4]	Switzerland	− 1449	− 916	3071	2877	2760	2	21	55
Columbia (2057)	USA	− 980	− 370	1630	1575	—	40	60	69
Daniels	USA	− 1250	+ 120	—	—	—	34	62	69
Easton	USA	− 790	+ 260	2125	2075	—	50	70	—
Emmons	USA	− 940	− 430	2745	2539	—	40	51	—
Foss	USA	− 1020	− 380	—	—	—	36	54	65
Gulkana	USA	− 330	− 1250	1732	1809	1726	64	53	63
Ice Worm	USA	− 1350	− 620	—	—	—	20	48	70
Lemon Creek	USA	− 170	+ 150	1025	1000	1009	68	72	—
Lower Curtis	USA	− 1060	− 400	1710	1650	—	40	60	64
Lynch	USA	− 1050	+ 70	—	—	—	42	70	69
Nisqually	USA	− 760	− 1400	3000	3000	—	30	29	—
Noisy Creek	USA	− 320	− 360	1889	1825	1806	4	8	50
North Klawatti	USA	− 1140	− 740	2300	2165	2101	18	54	69
Rainbow	USA	− 610	+ 290	1730	1650	—	46	76	67
Sandalee	USA	− 400	− 60	2210	2160	—	40	60	—
Sholes	USA	− 710	− 210	—	—	—	44	72	—
Silver	USA	− 1010	− 650	2565	2560	2298	6	8	47
South Cascade [5]	USA	− 1620	− 210	> 2125	1880	1899	< 10	60	53
Taku	USA	+ 230	+ 480	975	930	976	82	84	—
Wolverine	USA	− 760	− 840	1188	1199	1148	62	61	64
Yawning	USA	− 930	− 130	—	—	—	54	70	—

[1] Based on AAR values from 1961-1980.
[2] In 2005, Caresèr broke into two parts: Caresèr Orientale and Caresèr Occidentale.
[3] Perennial snowfield or glacieret
[4] The direct glaciological mass balance series was compared with the geodetic mass balance, and values of Silvretta from previous years have been adjusted (cf. Huss et al. 2009).
[5] Preliminary data, subject to revision.

2.2 CUMULATIVE SPECIFIC NET BALANCE GRAPHS

Notes:
- missing values are marked by gaps in the plotted data series with graphs restarting with the value of the previous available data point
- y-axis are scaled according to the data range of the cumulative net balance graph

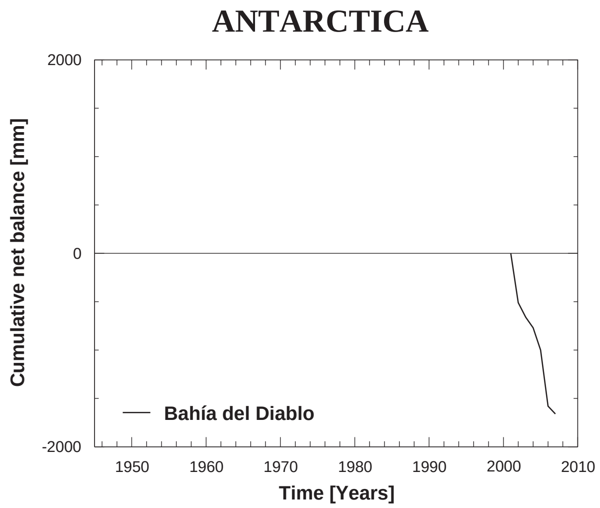

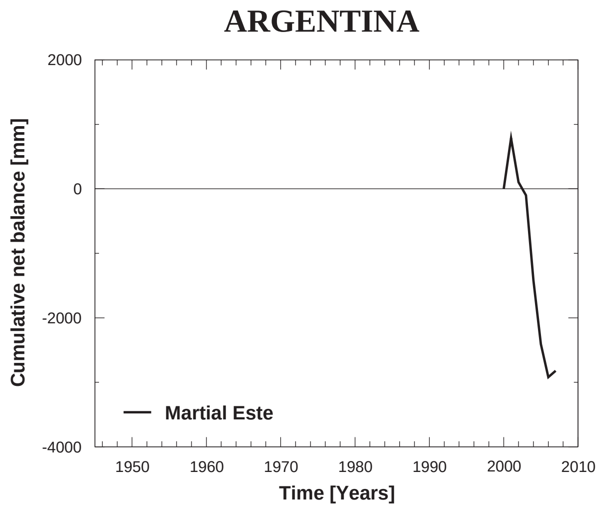

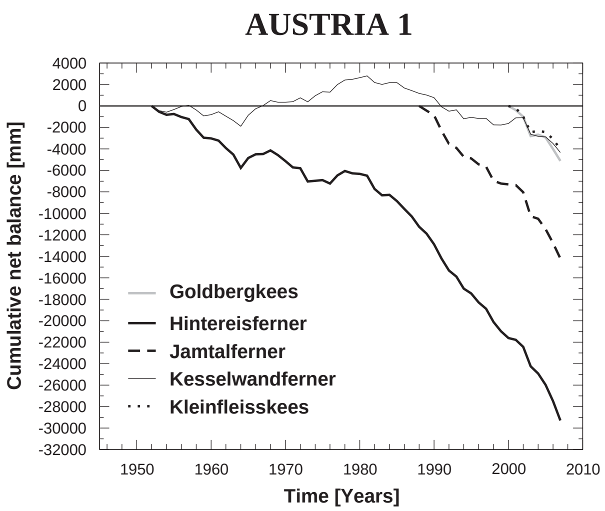

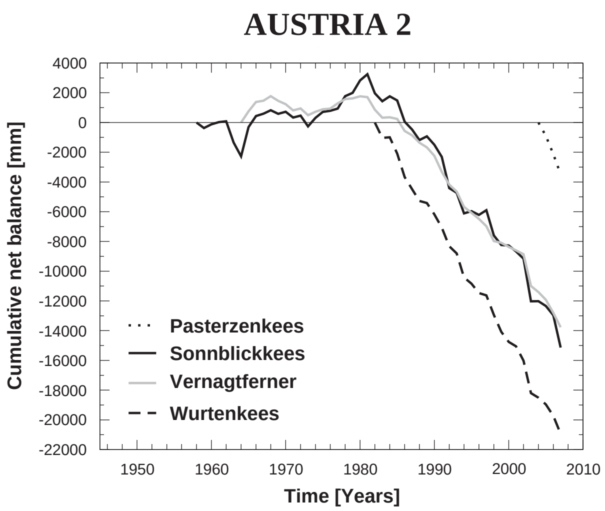

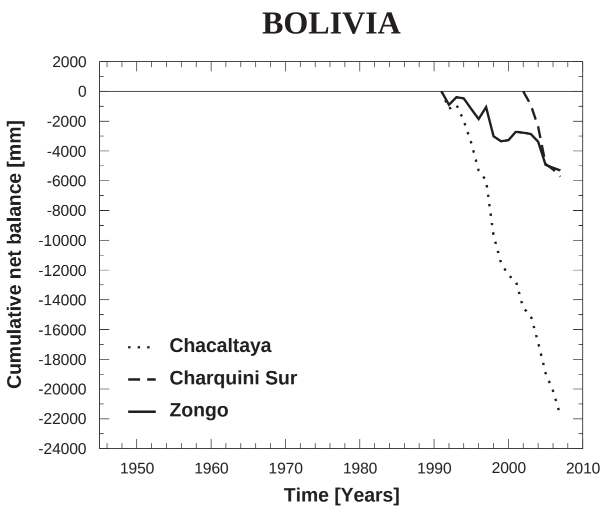

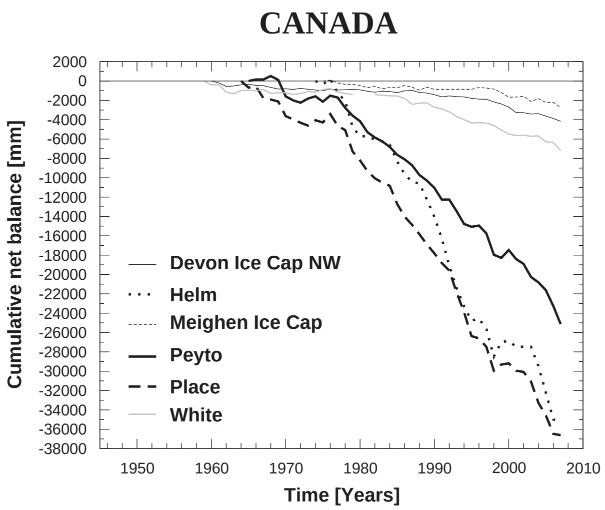

CHILE

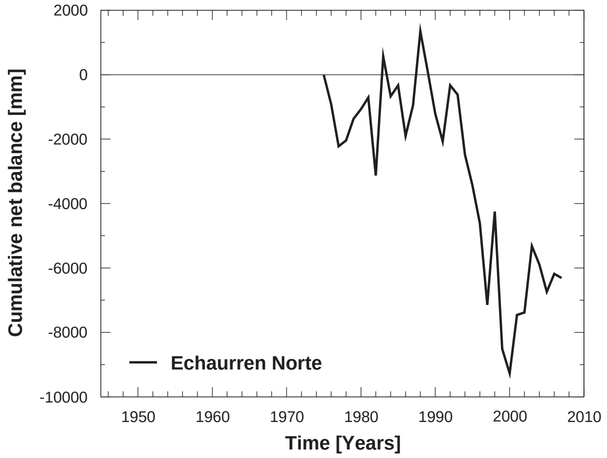

CHINA

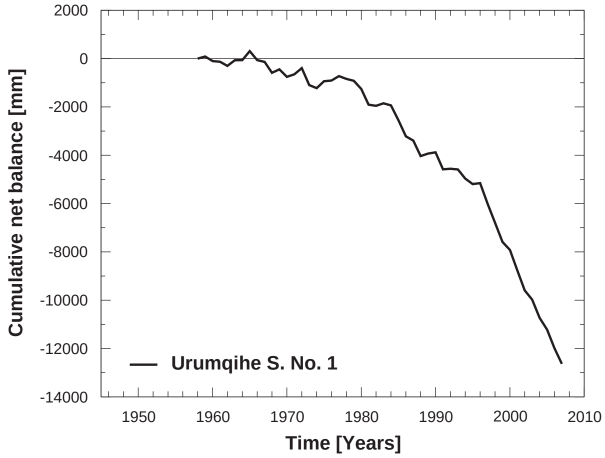

ECUADOR

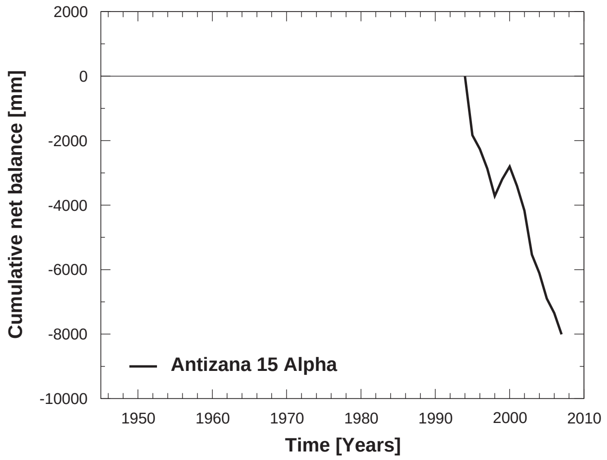

FRANCE

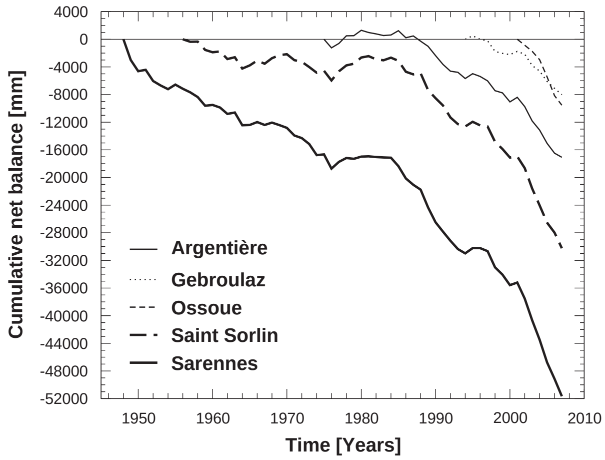

ICELAND 1

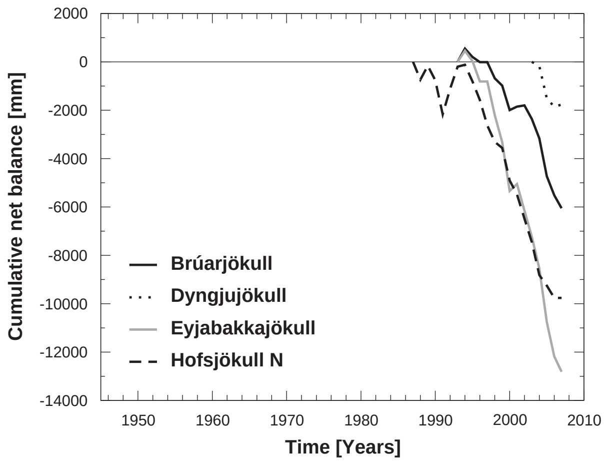

ICELAND 2

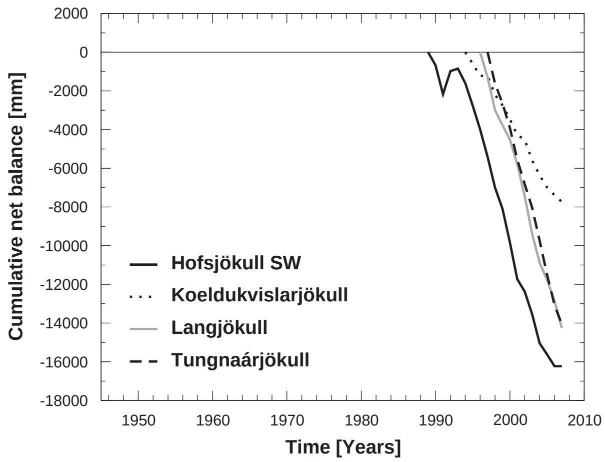

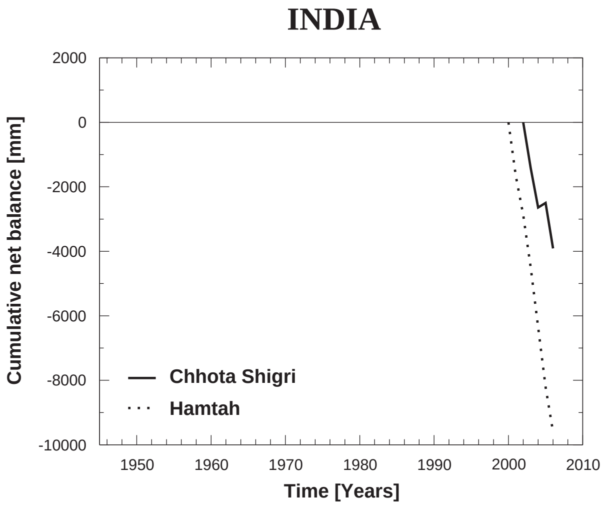
INDIA
Cumulative net balance [mm]
Time [Years]
Chhota Shigri
Hamtah

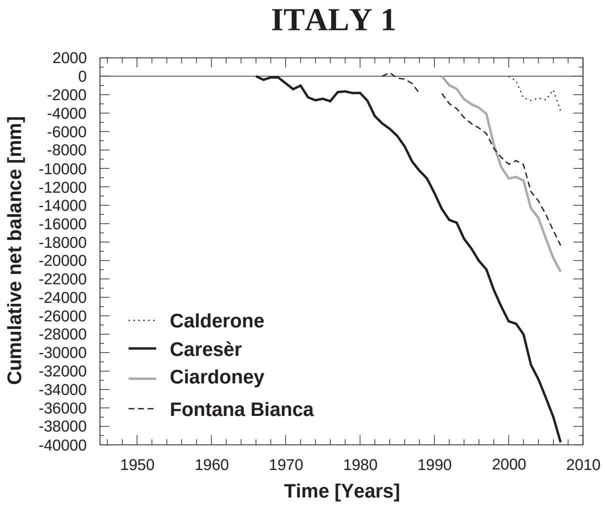
ITALY 1
Cumulative net balance [mm]
Time [Years]
Calderone
Caresèr
Ciardoney
Fontana Bianca

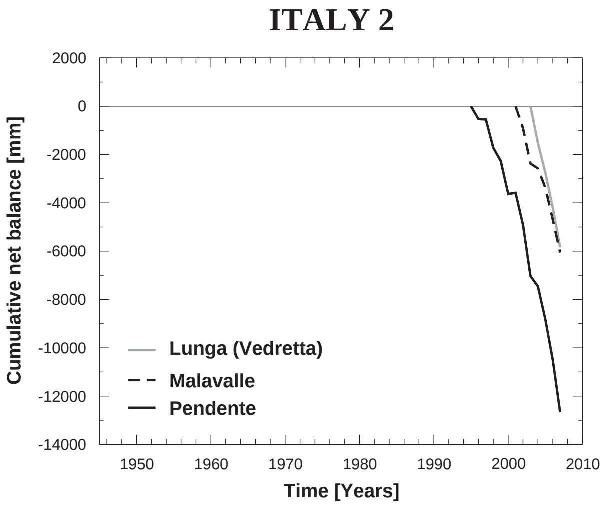
ITALY 2
Cumulative net balance [mm]
Time [Years]
Lunga (Vedretta)
Malavalle
Pendente

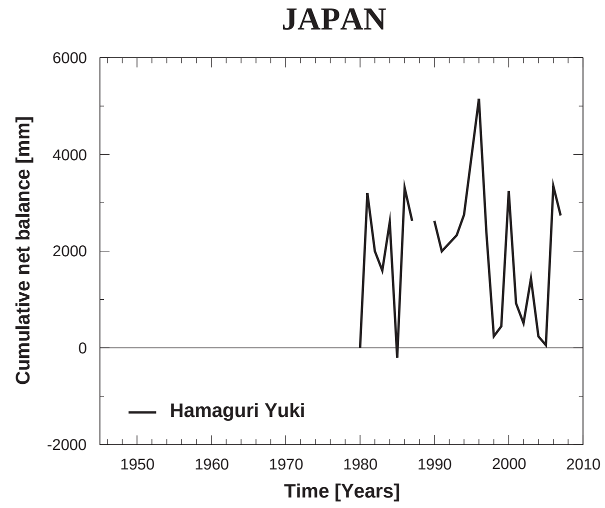
JAPAN
Cumulative net balance [mm]
Time [Years]
Hamaguri Yuki

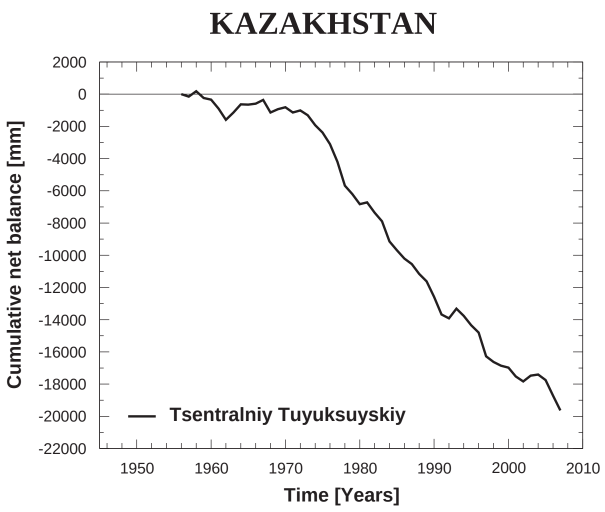
KAZAKHSTAN
Cumulative net balance [mm]
Time [Years]
Tsentralniy Tuyuksuyskiy

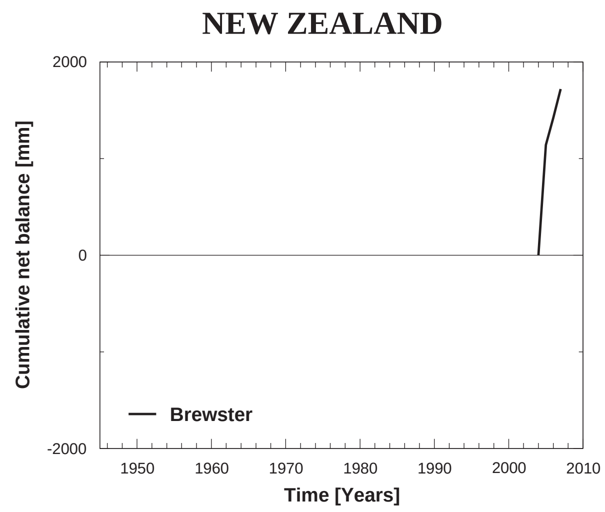
NEW ZEALAND
Cumulative net balance [mm]
Time [Years]
Brewster

NORWAY 1

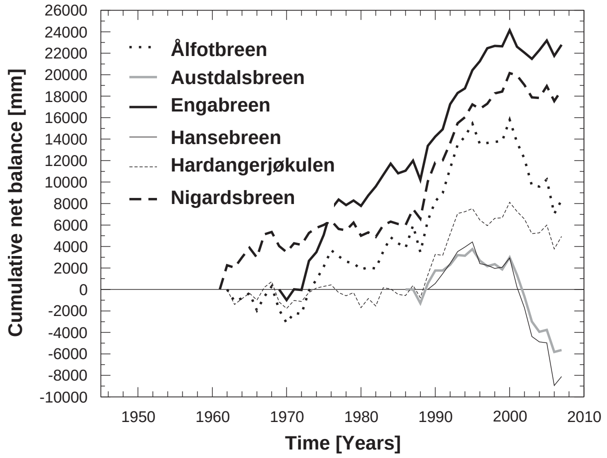

NORWAY 2

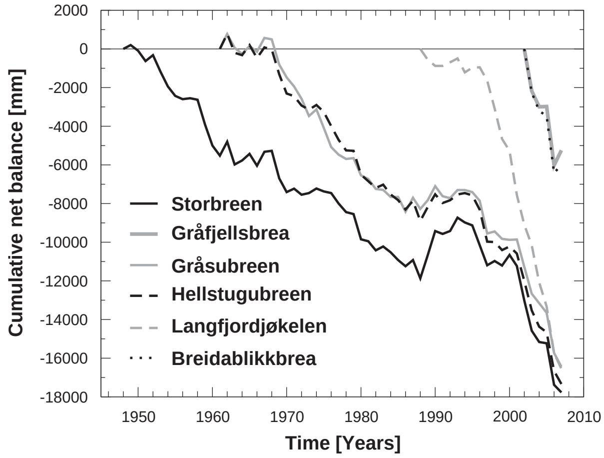

NORWAY (SPITSBERGEN)

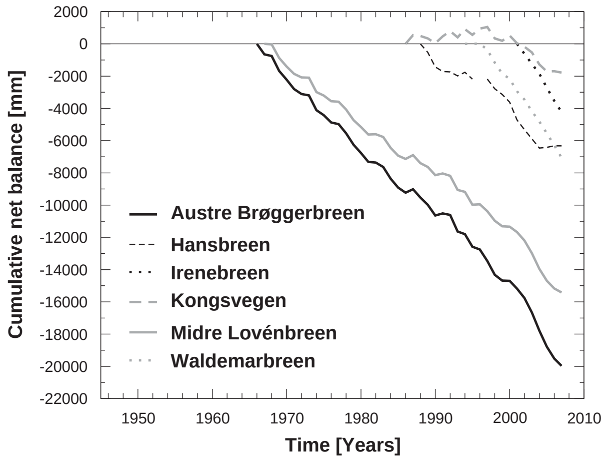

PERU

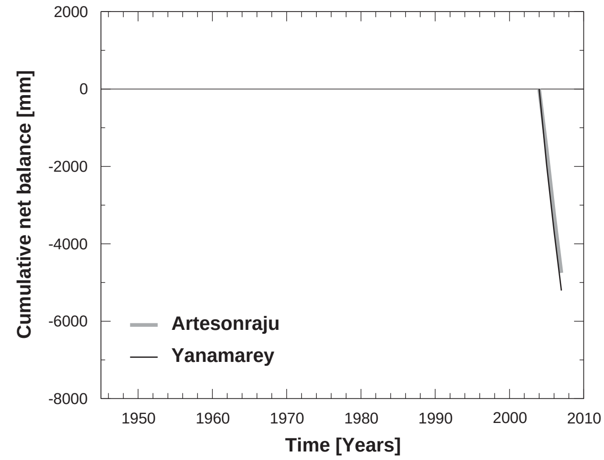

RUSSIA

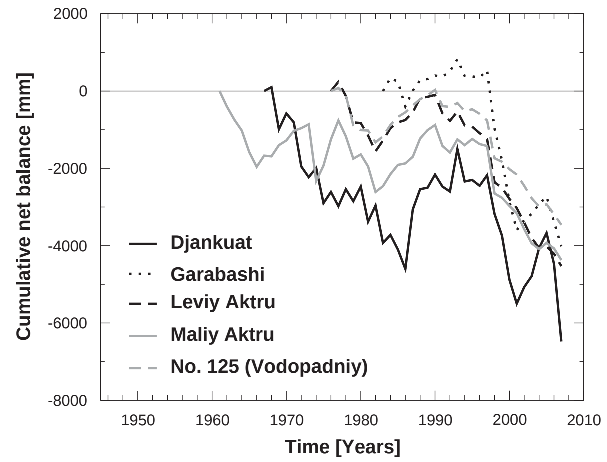

SPAIN

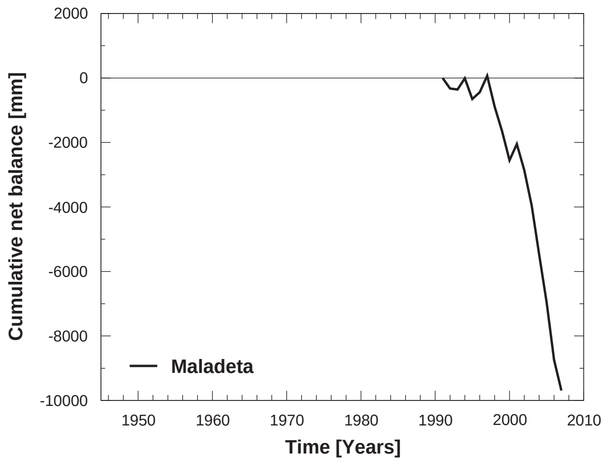

SWEDEN

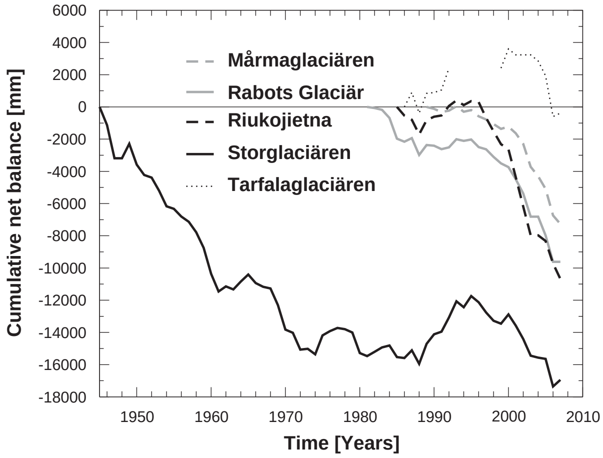

SWITZERLAND

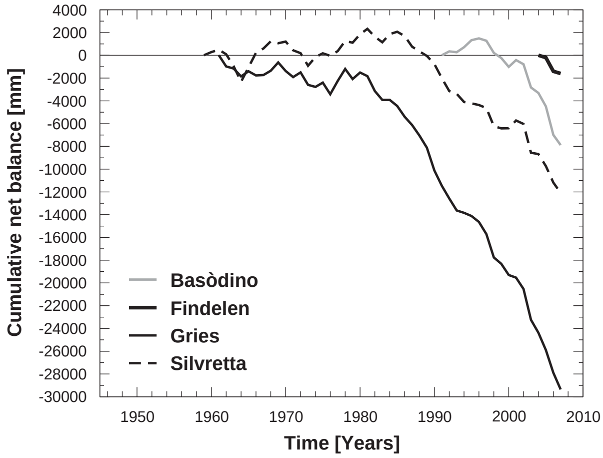

USA (ALASKA)

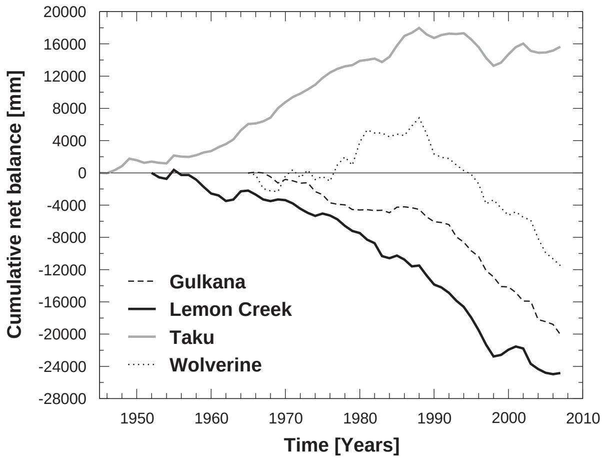

USA (WASHINGTON 1)

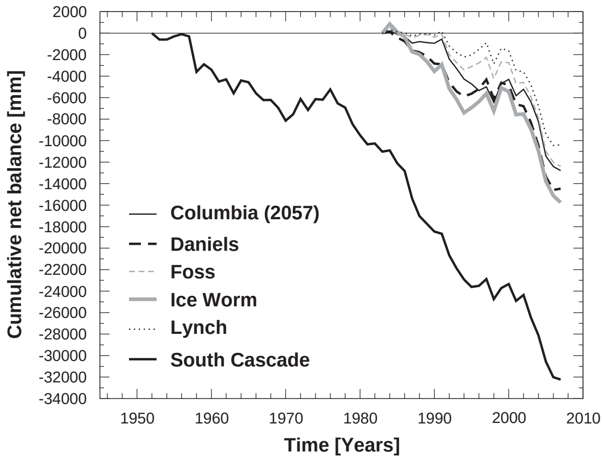

USA (WASHINGTON 2)

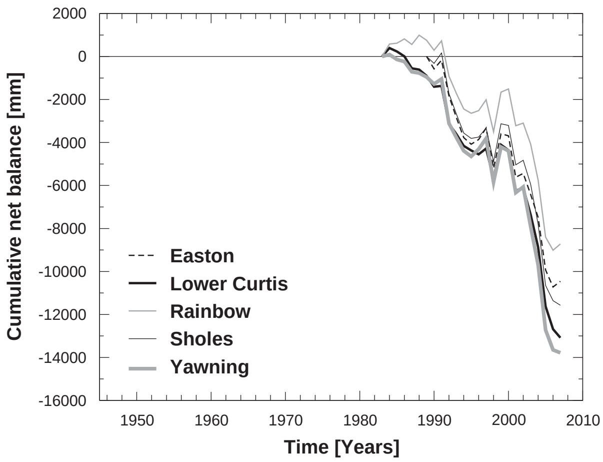

USA (WASHINGTON 3)

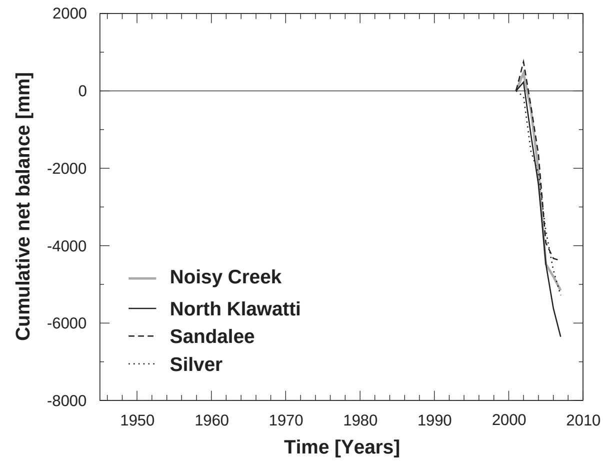

3 DETAILED INFORMATION

More detailed information about selected glaciers in various mountain ranges – with ongoing direct glaciological mass balance measurements – is presented here, in addition to the basic information contained in the previous chapter. In order to facilitate comparison between the individual glaciers, the submitted material (text, maps, graphs and tables) was standardized and rearranged.

The text gives general information on the glacier followed by brief comments on the two reported balance years. General information concerns basic geographic, geometric, climatic and glaciological characteristics of the observed glacier which may help with the interpretation of climate/glacier relationships. An oblique photograph showing the glacier is included.

Three maps are presented for each glacier: the first one, a topographic map, shows the stake, snow pit and snow probing network. This network is basically the same from one year to the next on most glaciers. In cases of differences between the two reported years, the second was chosen, i.e., the network from the year 2006/07. The second and third maps are balance maps from the reported years, illustrating the pattern of ablation and accumulation. The accuracy of such balance maps depends on the density of the observation network, the complexity of the mass balance distribution and the experience of the local investigators.

A graph of net mass balance versus altitude is given for both reported years, overlain with the corresponding glacier hypsography. The relationship between mass balance and altitude – the mass balance gradient – is an important parameter in climate/glacier relationships and represents the climatic sensitivity of a glacier. It constitutes the main forcing function of glacier flow over long time intervals. Therefore, the mass balance gradient near the equilibrium line is often called the 'activity index' of a glacier. The glacier hypsography reveals the glacier elevation bands that are most influential for the specific net balance, and indicates how the specific net balance changes with a shift of the ELA. Some of the elevation bands are irregular, especially the lowest and highests values. The elevation bands represent the submitted altitude intervals.

The last two graphs show the relationship between the specific net balance and the accumulation area ratio (AAR) and the equilibrium line altitude (ELA) for the whole observation period. The regression equation is given at the top of both diagrams. The AAR regression equation is calculated using integer values only (in percent). AAR values of 0 or 100 % as well as corresponding ELA values outside the altitude range of the observed glaciers were excluded from the regression analysis. Such regressions were used to determine the AAR_0 and ELA_0 values (cf. Chapter 2). The points from the two reported balance years (2005/06 and 2006/07) are marked in black. Minimum sample size for regression was defined as 6 ELA or AAR values.

3.1 BAHÍA DEL DIABLO (ANTARCTICA/A. PENINSULA)

COORDINATES: 63.82 S / 57.43 W

Photo taken by P. Skvarca on 1st of March 2005.

This polythermal outlet-type glacier is located on Vega Island, north-eastern side of the Antarctic Peninsula. The glacier is exposed to the north-east, covers an area of 14.3 km^2 and extends from an altitude of 630 m to 75 m a.s.l. The mean annual air temperature at the equilibrium line around 400 m a.s.l. ranges between −7 and −8 °C. The snout of the glacier overrides an ice-cored moraine over a periglacial plain of continuous permafrost.

Detailed mass balance measurements of this glacier began in austral summer 1999/00. A simplified version of combined stratigraphic-annual mass-balance method is applied because the glacier can be visited only once a year. Despite the relatively low mean annual temperature of −5.8 °C, the balance year 2005/06 resulted in −580 mm w.e., the most negative mass budget recorded since the initiation of measurements. This lowest value is probably due to a very high mean summer air temperature of +1.6 °C combined with strong north-westerly warm katabatic winds, which enhanced melting. By contrast, the net budget of only −80 mm w.e. for balance year 2006/07 figures among the lowest in the record because of low mean summer temperature of +0.2 °C, yielding only 96 melt-days. The additional two years of detailed mass balance data further confirm a strong correlation existing in this region between the annual net balance and the mean summer air temperature.

3.1.1 Topography and observation network

Glaciar Bahía del Diablo (ANTARCTICA)

3.1.2 Net balance maps 2005/2006 and 2006/2007

2005/2006

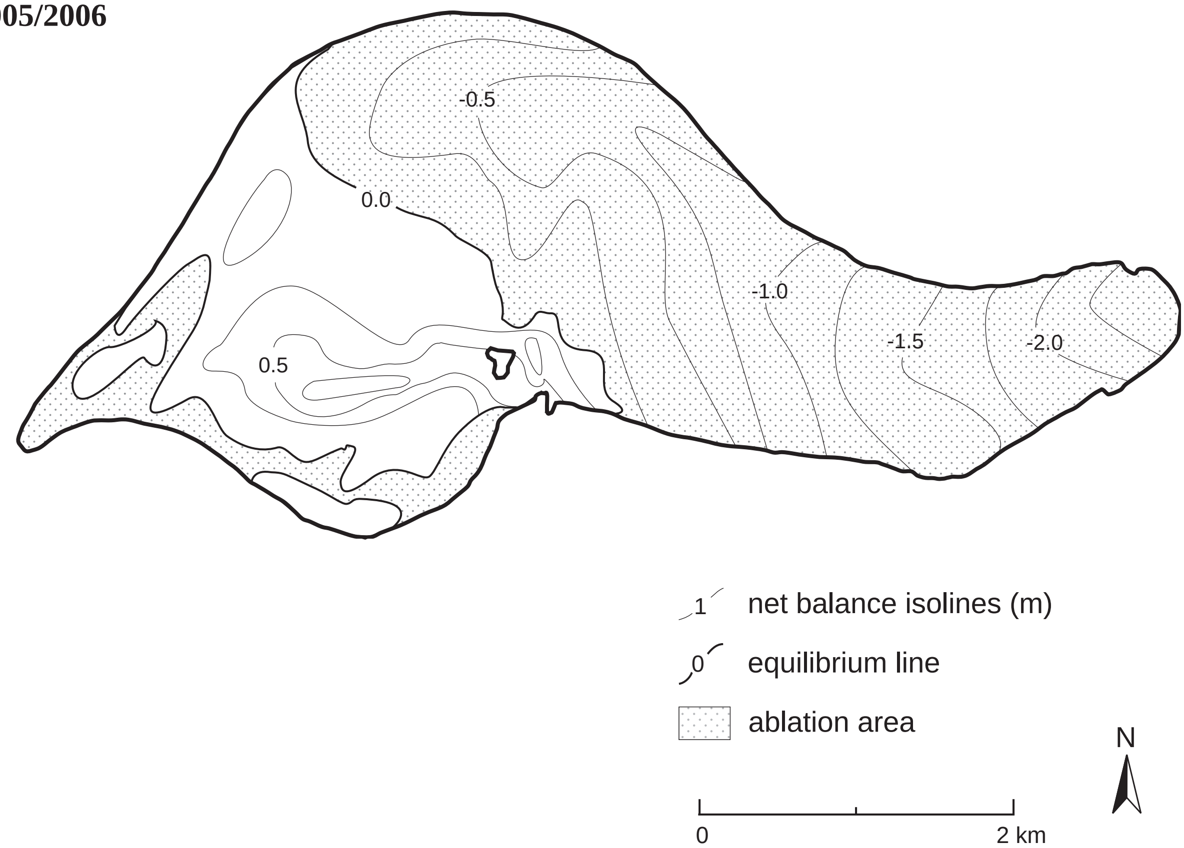

2006/2007

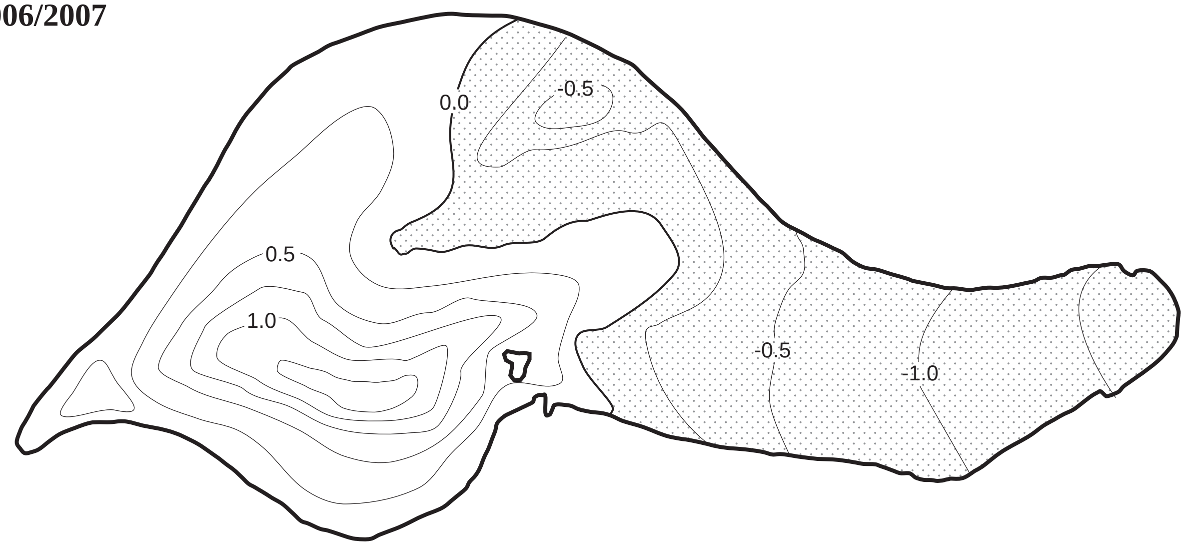

Glaciar Bahía del Diablo (ANTARCTICA)

3.1.3 Net balance versus altitude (2005/2006 and 2006/2007)

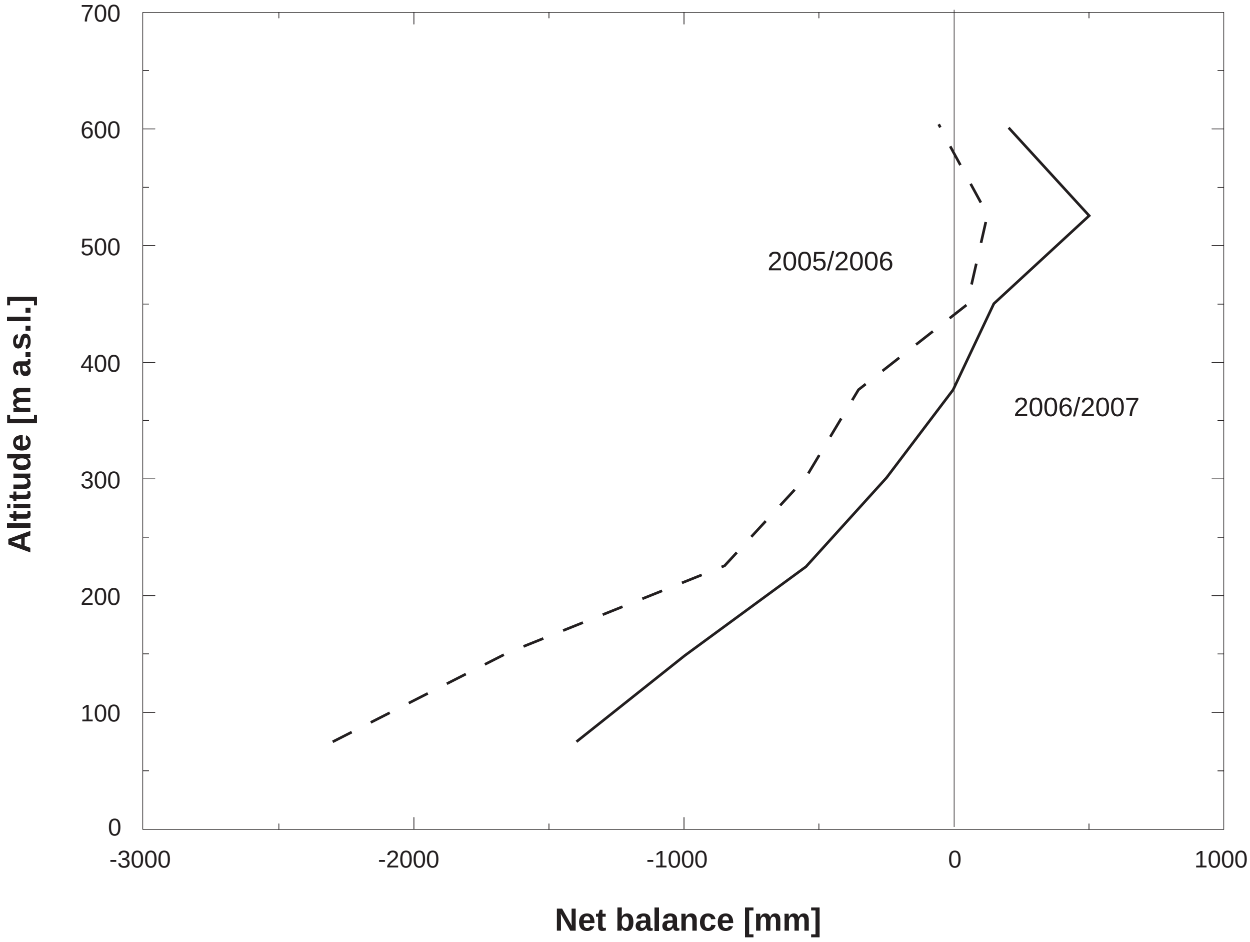

3.1.4 Accumulation area ratio (AAR) and equilibrium line altitude (ELA) versus specific net balance for the whole observation period

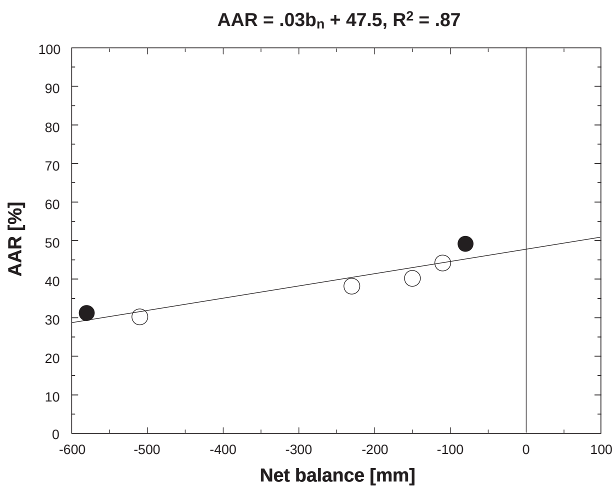

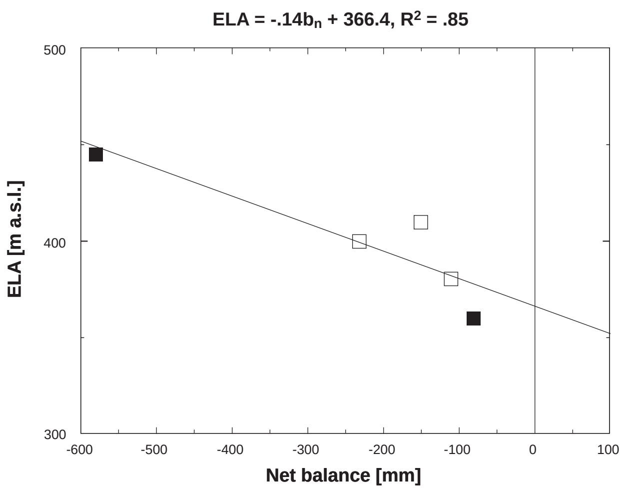

Glaciar Bahía del Diablo (ANTARCTICA)

3.2 MARTIAL ESTE (ARGENTINA/ANDES FUEGUINOS)

COORDINATES: 54.78 S / 68.40 W

Photo taken by R. Iturraspe in February 2006.

The Martial Este is one of the four small glaciers that remain in the well-defined glacial cirque of the Cordon Martial (1319 m a.s.l at Mt Martial) very close to Ushuaia city and to the Beagle channel. Glacier runoff contributes to the water supply of this city. Total ice area on this cirque reaches 0.33 km^2. The Martial Este glacier (the body at the right of the photo) has a surface area of 0.1 km^2 that extends from 1180 m to 970 m a.s.l. with a medium slope of 29° and south-east exposition. It receives less direct solar radiation than the rest of the glaciers on the cirque. Mean annual air temperature at the equilibrium line is −1.5 °C and the average precipitation amounts to 1300 mm, distributed over the whole year. The rain regime has no dry season. The hydrological cycle starts in April and the maximum accumulation on the glacier is reached in October or November. Since the Little Ice Age these glaciers have lost 75 % of their total area. From 1984 to 1998 vertical thinning at the Martial Este Glacier was 7.0 m (450 mm w.e. a^{-1}) based on topographic surveys.

During the hydrological years 2005/06 and 2006/07, the net balance of the Martial Este glacier was more stable than observed in the previous biannual period. In the first year, the deficit was −510 mm w.e., which is close to the computed average from 1984. Precipitation in 2006/07 was the highest in the last 25 years; however that represents just 21 % of the historical average. Snowfalls and cold conditions during the late spring also favored a positive balance, but dry and warm conditions in January and February caused rapid melting. However, the balance was weakly positive (+ 99 mm w.e.) for the first time since 2000/01.

3.2.1 Topography and observation network

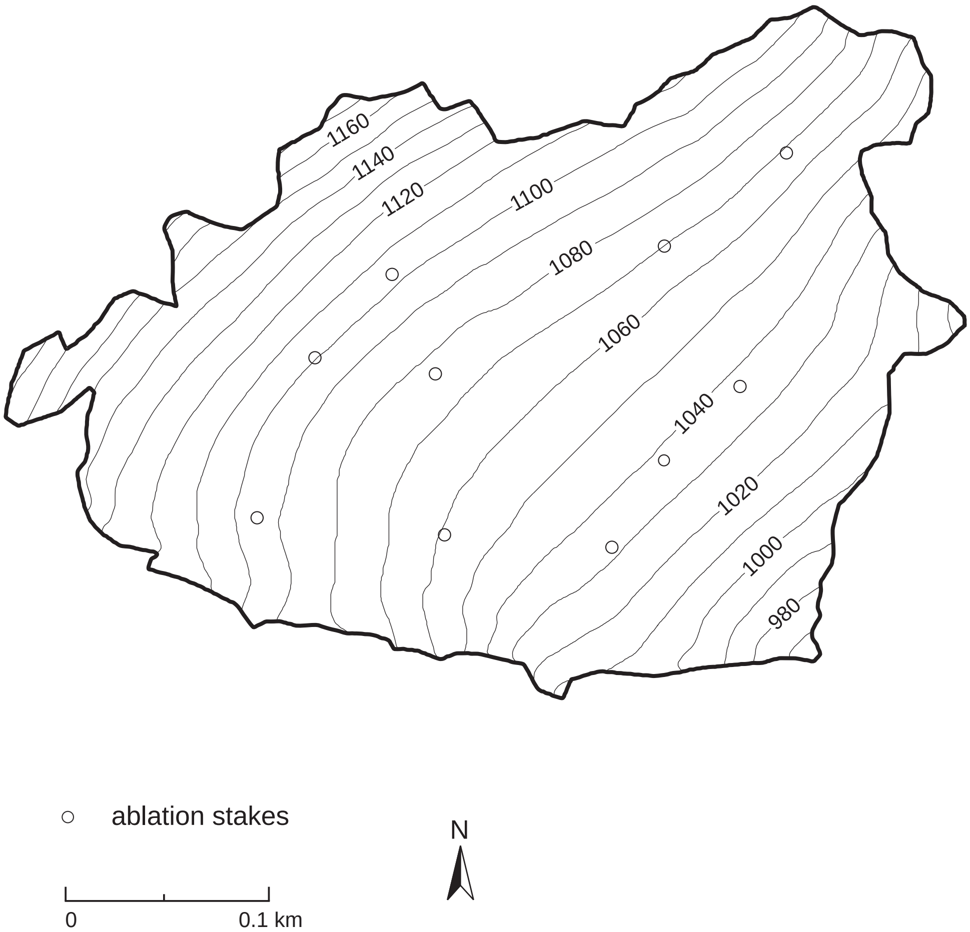

Martial Este (ARGENTINA)

3.2.2 Net balance maps 2005/2006 and 2006/2007

2005/2006

2006/2007

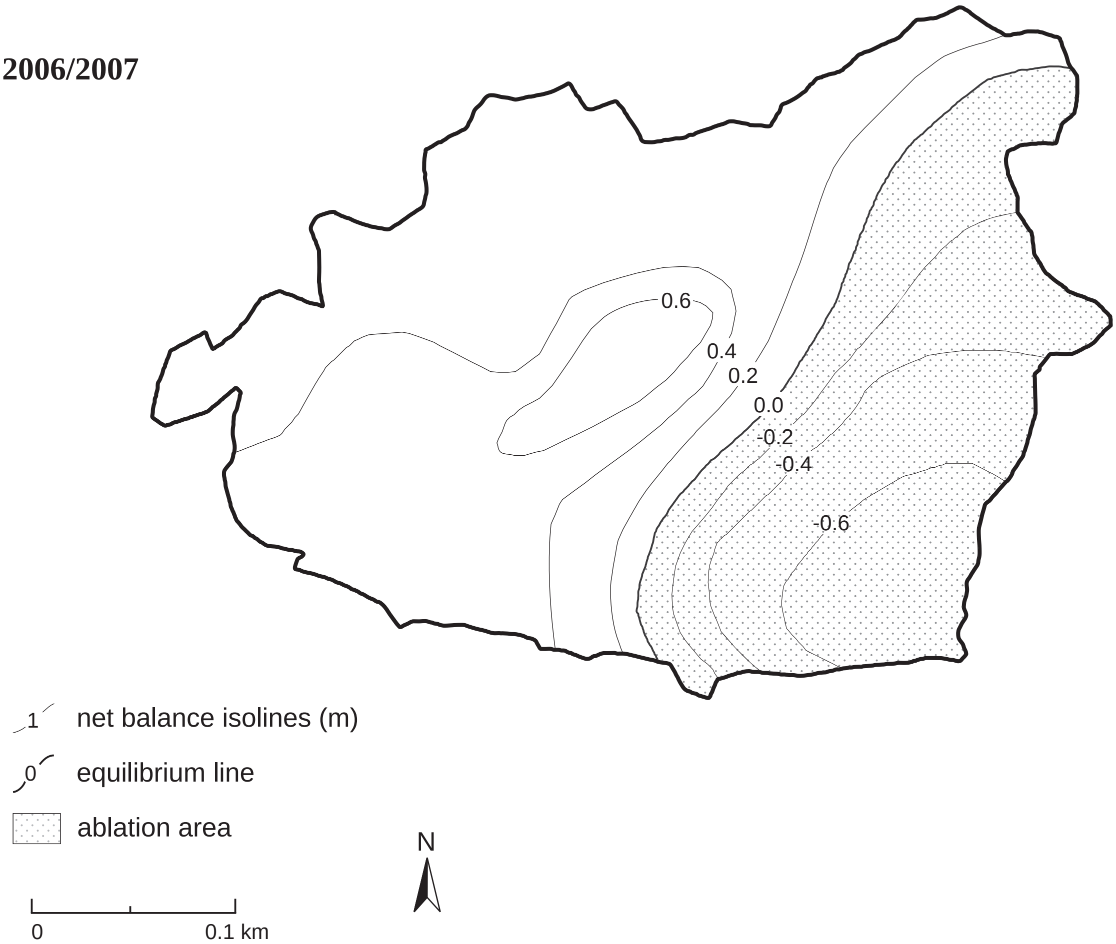

Martial Este (ARGENTINA)

3.2.3 Net balance versus altitude (2005/2006 and 2006/2007)

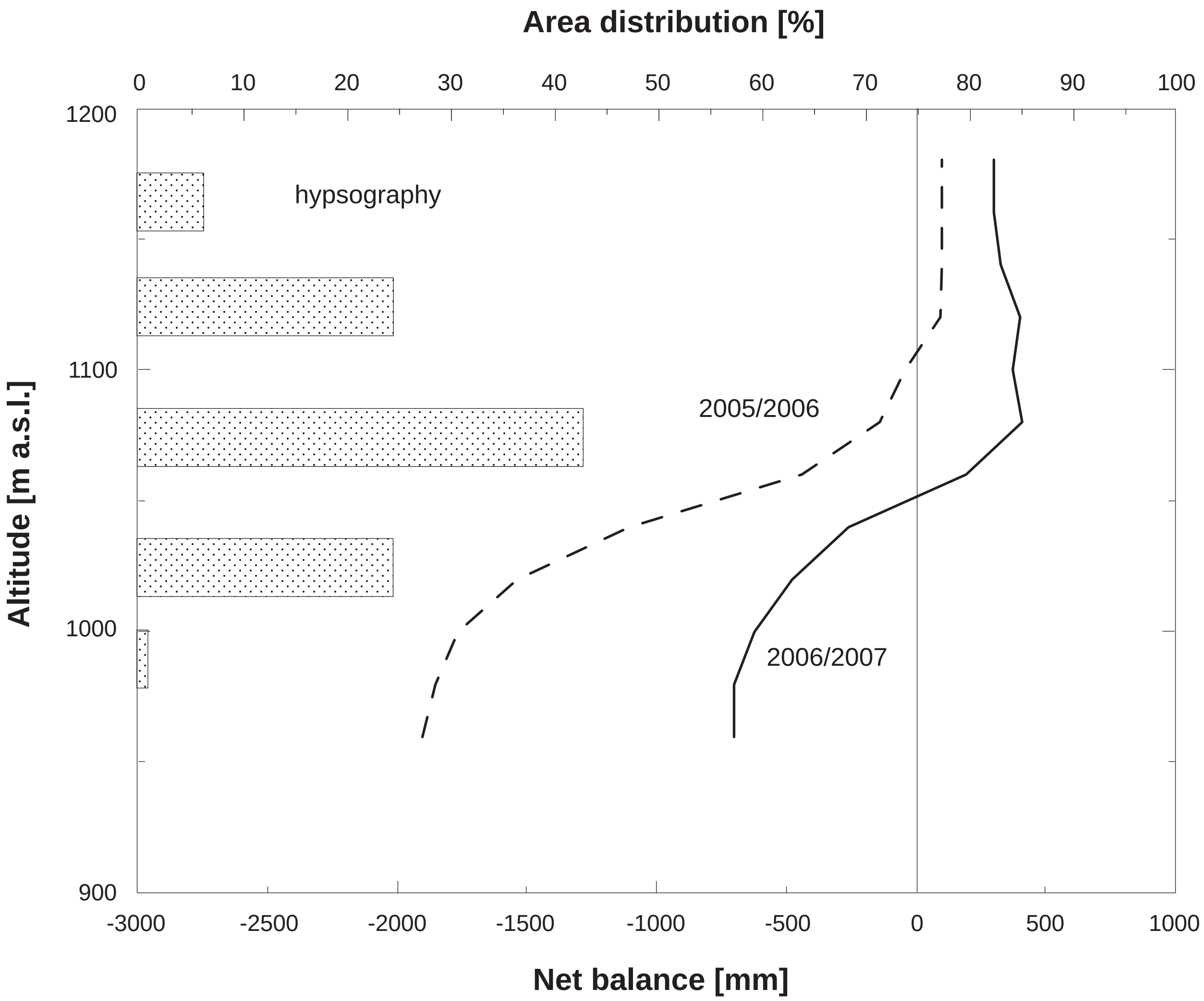

3.2.4 Accumulation area ratio (AAR) and equilibrium line altitude (ELA) versus specific net balance for the whole observation period

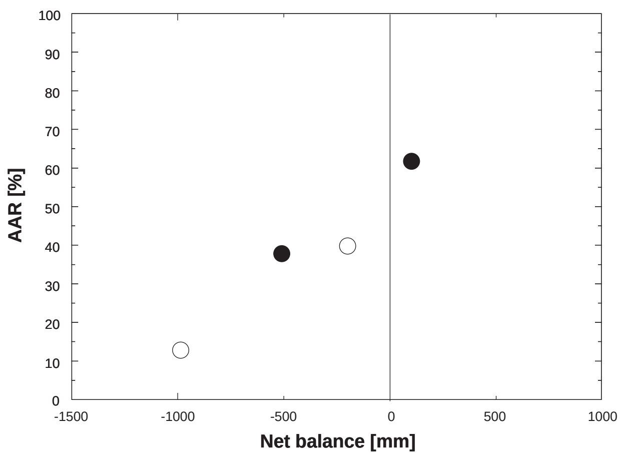

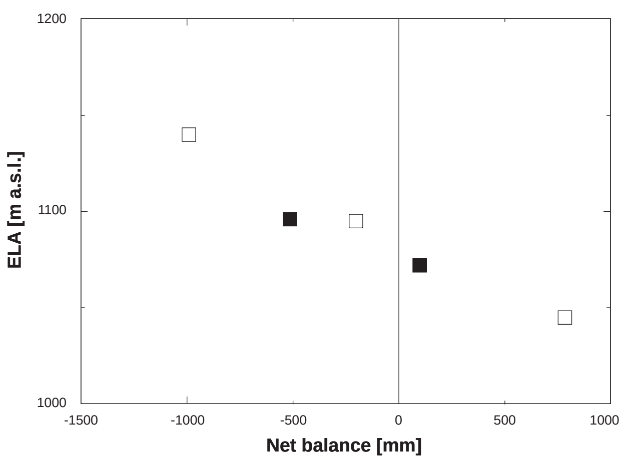

Martial Este (ARGENTINA)

3.3 HINTEREISFERNER (AUSTRIA/EASTERN ALPS)

COORDINATES: 46.80 N / 10.77 W

Photo taken by A. Lambrecht on 12th of September 2006.

The mass balance of Hintereisferner has been measured with the direct glaciological method since 1952/53. Hintereisferner is a valley glacier which had several tributary glaciers in 1953. In the meantime, most of these tributary glaciers have lost connection to the main tongue. The last to separate so far was Langtaufererjochferner in 2000. The glacier area decreased from 10.24 km^2 in 1953 to 7.40 km^2 in 2006 and 7.21 km^2 in 2007. The highest point of Hintereisferner is the Weißkugel/ Pala Bianca peak with an altitude of 3739 m a.s.l. The tongue is located in a north-east orientated valley, the firn area faces north, east and south. The lowest point was 2350 m a.s.l. in 1953 and 2750 m a.s.l. in 2007. The ice thickness losses between 1953 and 2007 exceeded 160 m on parts of the glacier tongue, but were only a few meters in parts of the firn area. In the mass balance year 2002/03 the topographic basis was changed from the DEM of the glacier inventory dating from 1997 to the airborne laser scan DEM of October 2001. In addition to the annual geodetic surveys, several airborne Laser Scan DEMs were compiled between 2001 and 2008. The mean annual air temperature at the ELA_0 is about -4 °C, as estimated from the temperature measurements at the Vent climate station (1906–2005; 1906 m a.s.l.). A mean annual precipitation of 1374 mm was measured at a nearby totalizer (1963–2008; 2970 m a.s.l.).

In 2005/06 the mean air temperature was exactly the long term mean, in 2006/07 it was 3.7 °C. The mean annual lapse rate is assumed to be 0.0057 °C m^{-1}. The specific mass balance was −1516 mm w.e. in 2005/06 and −1798 mm w.e. in 2006/07. The ELA was above the summits in both hydrological years.

3.3.1 Topography and observation network

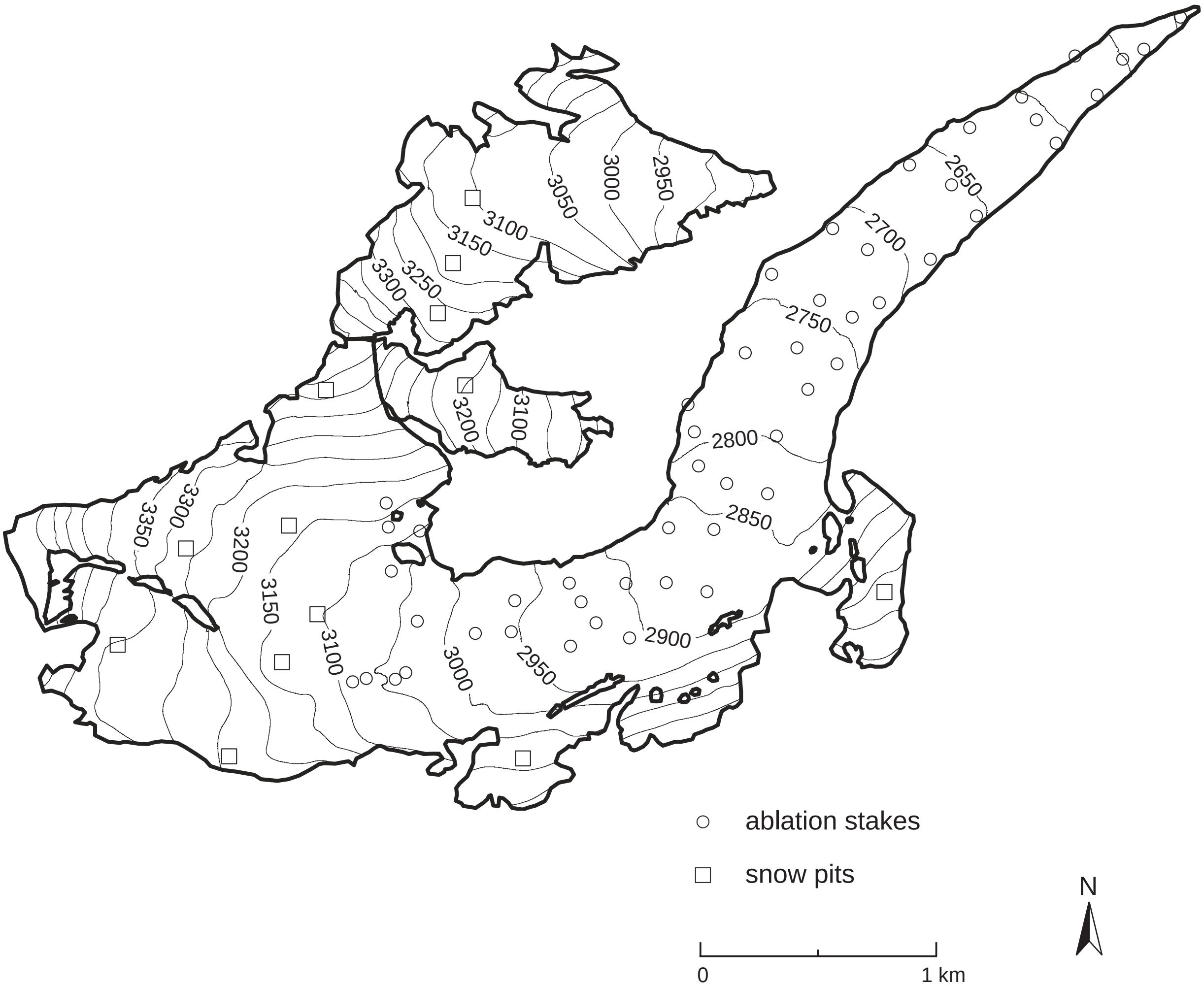

Hintereisferner (AUSTRIA)

3.3.2 Net balance maps 2005/2006 and 2006/2007

2005/2006

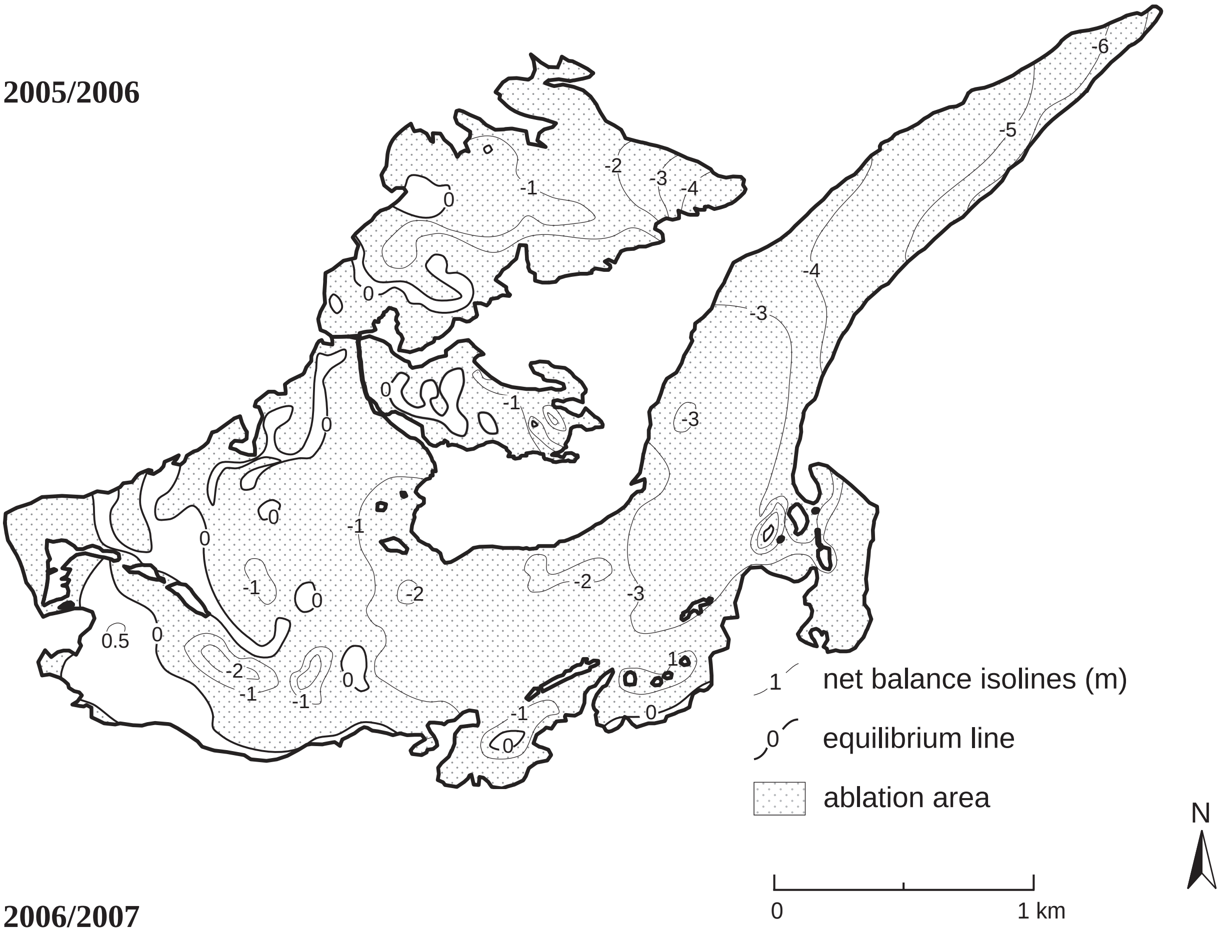

2006/2007

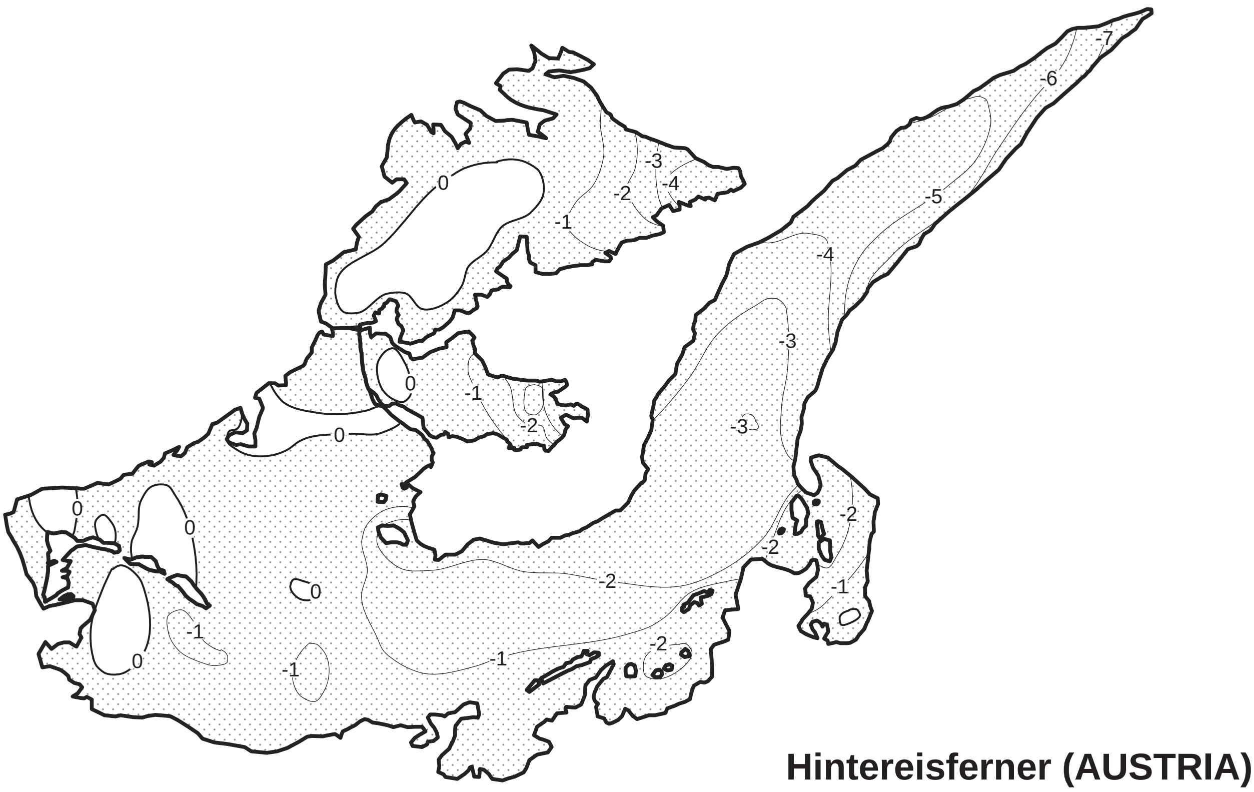

3.3.3 Net balance versus altitude 2005/2006 and 2006/2007

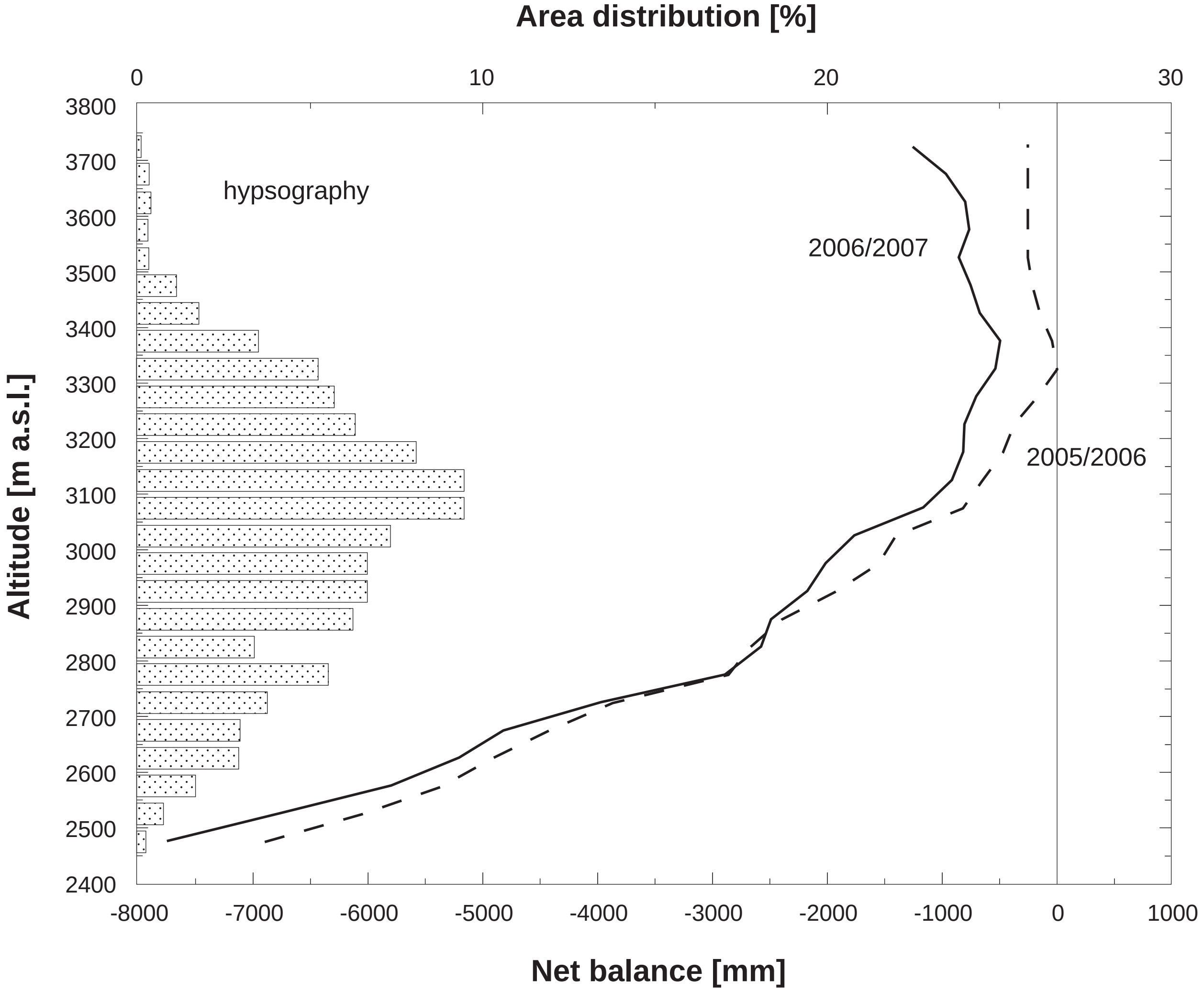

3.3.4 Accumulation area ratio (AAR) and equilibrium line altitude (ELA) versus specific net balance for the whole observation period

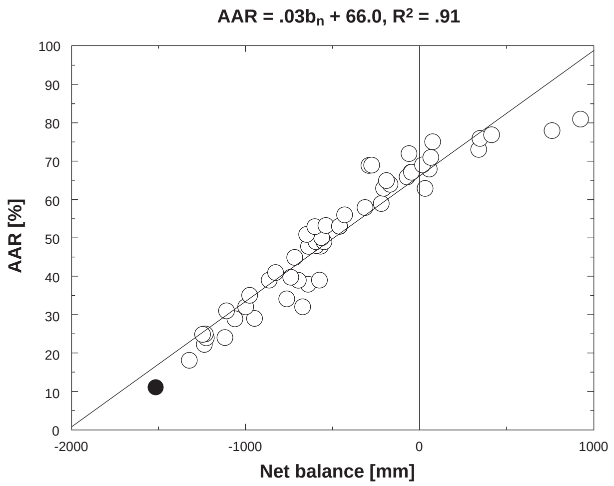

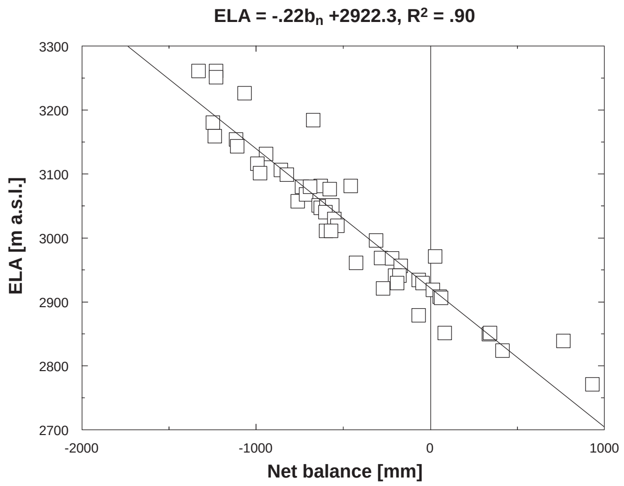

Hintereisferner (AUSTRIA)

3.4 ZONGO (BOLIVIA/TROPICAL ANDES)

COORDINATES: 16.25 S / 68.17 W

Photo provided by P. Ginot in 2007.

Zongo is a small valley glacier located north-east of La Paz, at the headwaters of a large system of power plants supplying the city. It is a glacier 2.2 km long, between 6000 m and 4900 m a.s.l., with an surface area of 1.9 km^2. Exposure is to the south in the upper part and to the east at the lower tongue. The average annual air temperature is −1.5 °C at the ELA (5250 m a.s.l.) and an average annual rainfall of 900 mm (± 150 mm) measured at 4770 m a.s.l. The region has a climate characterized by a dry season and a wet season. The latter occurs in the summer when the ablation reaches its maximum from November to February, with the highest precipitation period from January to March. Like all glaciers in the region, it has generally presented yearly negative mass balances, with few exceptions, with the greatest loss occurring during the 1997–1998 El Niño event (approximately −2000 mm w.e.). The few periods of light positive mass balances have coincided with La Niña events.

The 2005/06 period presents a slightly negative mass balance (−197 mm w.e.). The ENSO index of the observation period was characterized by a weak positive anomaly in the Pacific (Niño phenomenon) at the beginning and negative anomaly (Niña phenomenon) towards the end of the hydrological year. The period 2006/07 presented an almost balanced mass balance (−173 mm w.e.), due to a slightly more humid period with precipitation 7 % above normal.

3.4.1 Topography and observation network

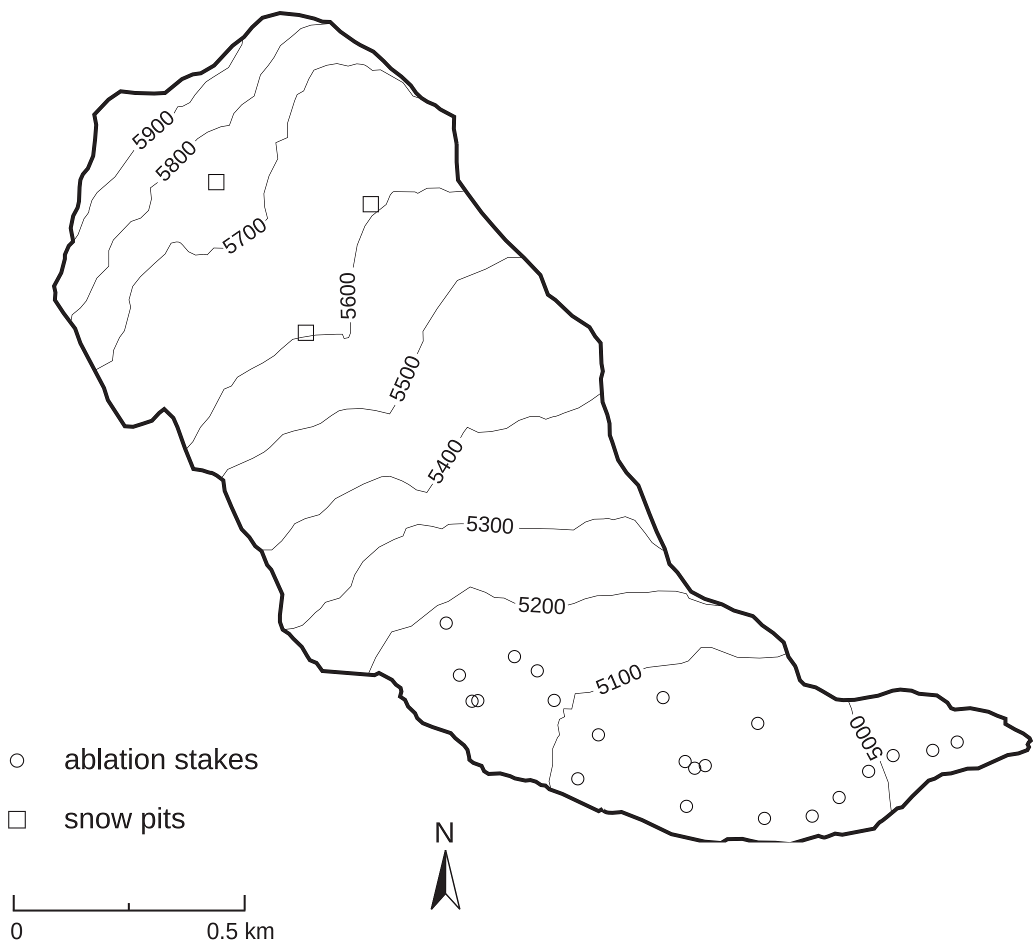

Zongo (BOLIVIA)

3.4.2 Net balance maps 2005/2006 and 2006/2007

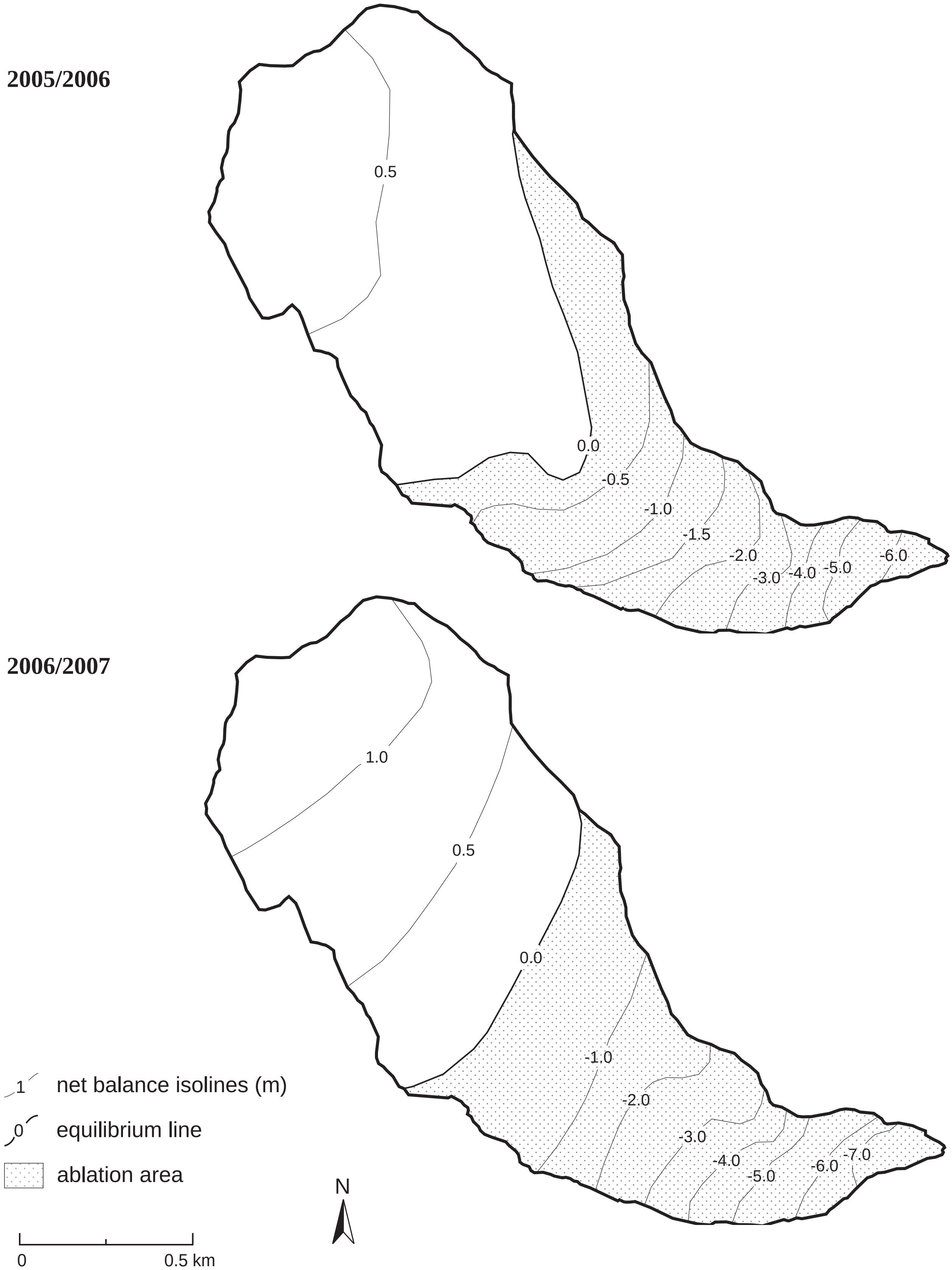

Zongo (BOLIVIA)

3.4.3 Net balance versus altitude (2005/2006 and 2006/2007)

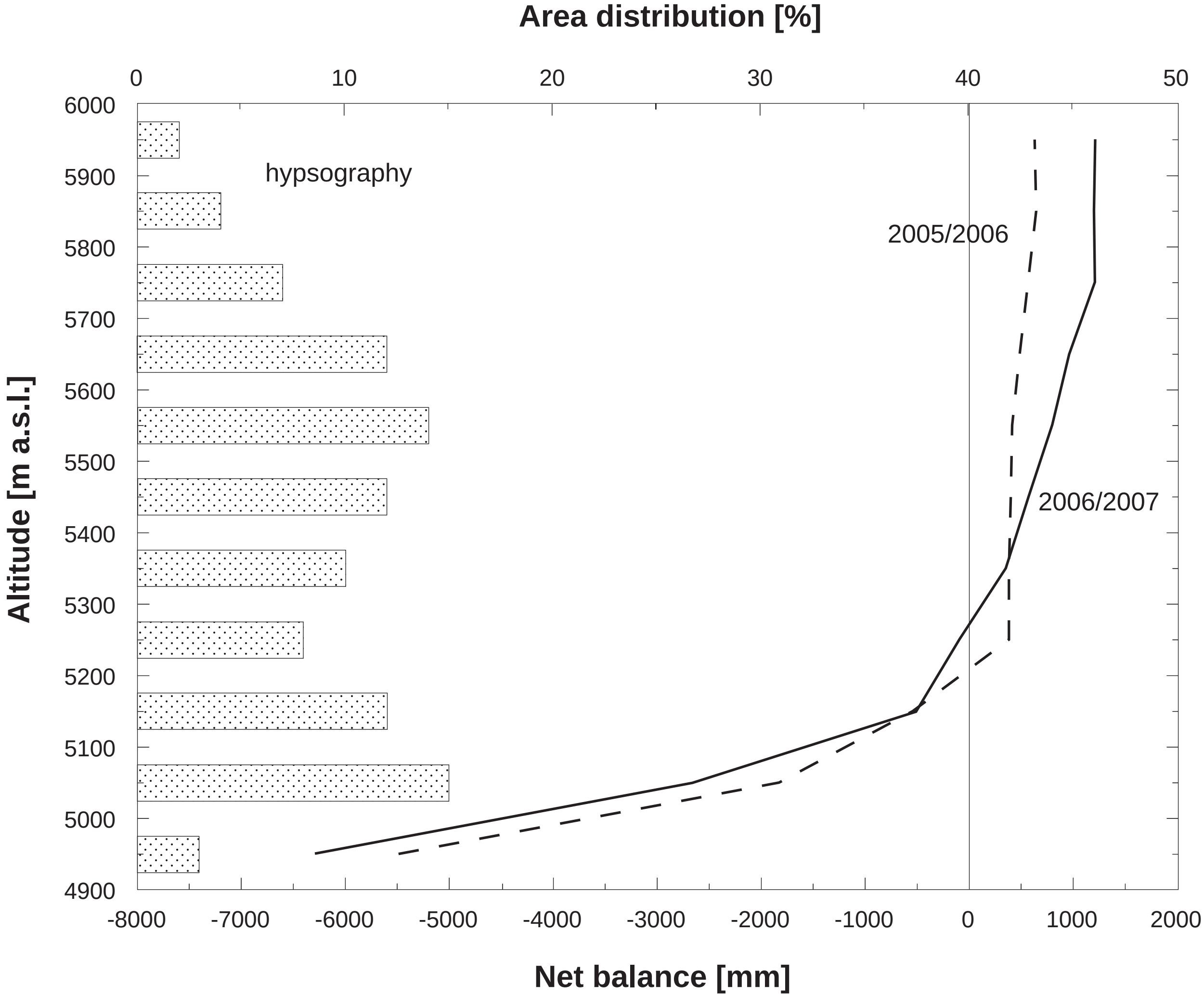

3.4.4 Accumulation area ratio (AAR) and equilibrium line altitude (ELA) versus specific net balance for the whole observation period

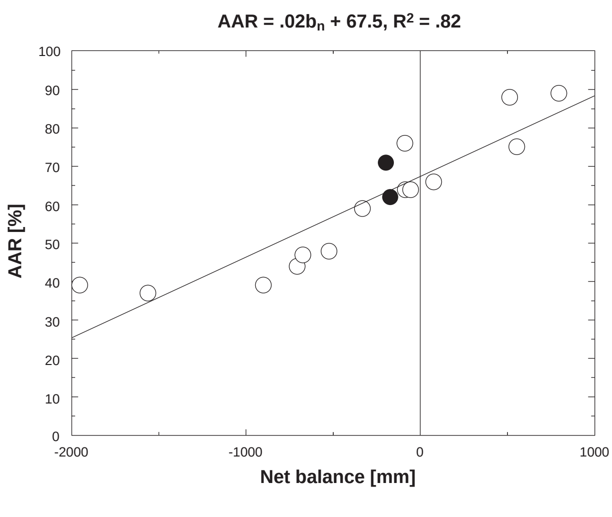

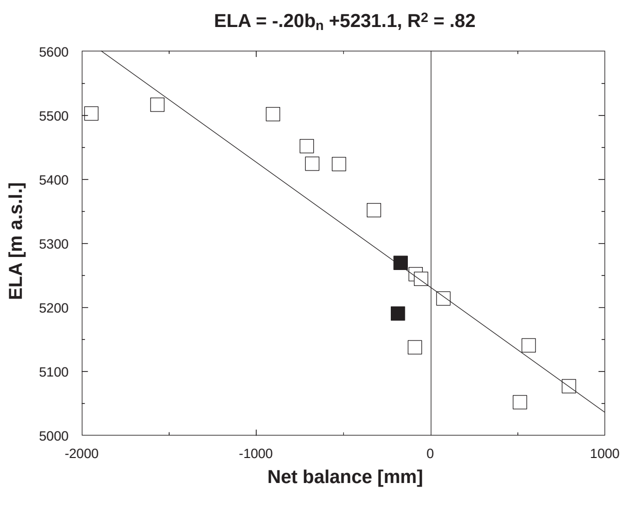

Zongo (BOLIVIA)

3.5 WHITE (CANADA/HIGH ARCTIC)

COORDINATES: 79.45 N / 90.67 W

Aerial view of White Glacier taken on 2 July, 2008. Photo by J. Alean.

White Glacier is a valley glacier in the Expedition Fiord area of Axel Heiberg Island, Nunavut. It extends in elevation from 1782 m to 85 m a.s.l. and at present occupies 39.4 km^2, having shrunk by gradual retreat of its terminus from an extent of 40.2 km^2 in 1960. Sea level temperature in the Expedition Fiord area averages about −20 °C, but the glacier is known to have a bed which is partly unfrozen, at least beneath the valley tongue; ice thickness is typically 200 m, but reaches or exceeds 400 m. Annual precipitation at sea level is very low, about 100 mm, although annual accumulation at higher altitudes is greater. Annual ablation at the terminus of White Glacier ranges between 2000 and 4000 mm w.e. a^{-1}. There is now evidence that the retreat of the terminus, previously about 5 m a^{-1}, is decelerating. However, the advance of Thompson Glacier continues. The terminuses of the two glaciers have been in contact since at least the time of the earliest photographs in 1948, but, while the two terminuses remain distinguishable, White Glacier has become a tributary of Thompson Glacier.

The cumulative mass balance of White Glacier from 1959/60 to 2006/07, with due allowance for three missing years, is −7280 mm w.e. The mass balance for 2005/06, at −93 mm w.e., was slightly negative, but not distinguishable from a state of equilibrium given the uncertainty (±200 to 250 mm w.e.) of the measurement. The mass balance normal for 1960–1991 is −95 mm w.e., also slightly negative but in this case significantly so because it is an average of 29 annual measurements. In contrast to that of 2005/06, the balance for 2006/07, −818 mm w.e., was the most negative ever measured, although it is not statistically distinct from the previous record of −781 mm w.e. in 1961/62. 2006/07 was the first balance year in the history of the measurement programme for which missing stake corrections were necessary. For example, in the 200–300 m elevation band, five out of seven stakes melted out. This may be an omen.

3.5.1 Topography and observation network

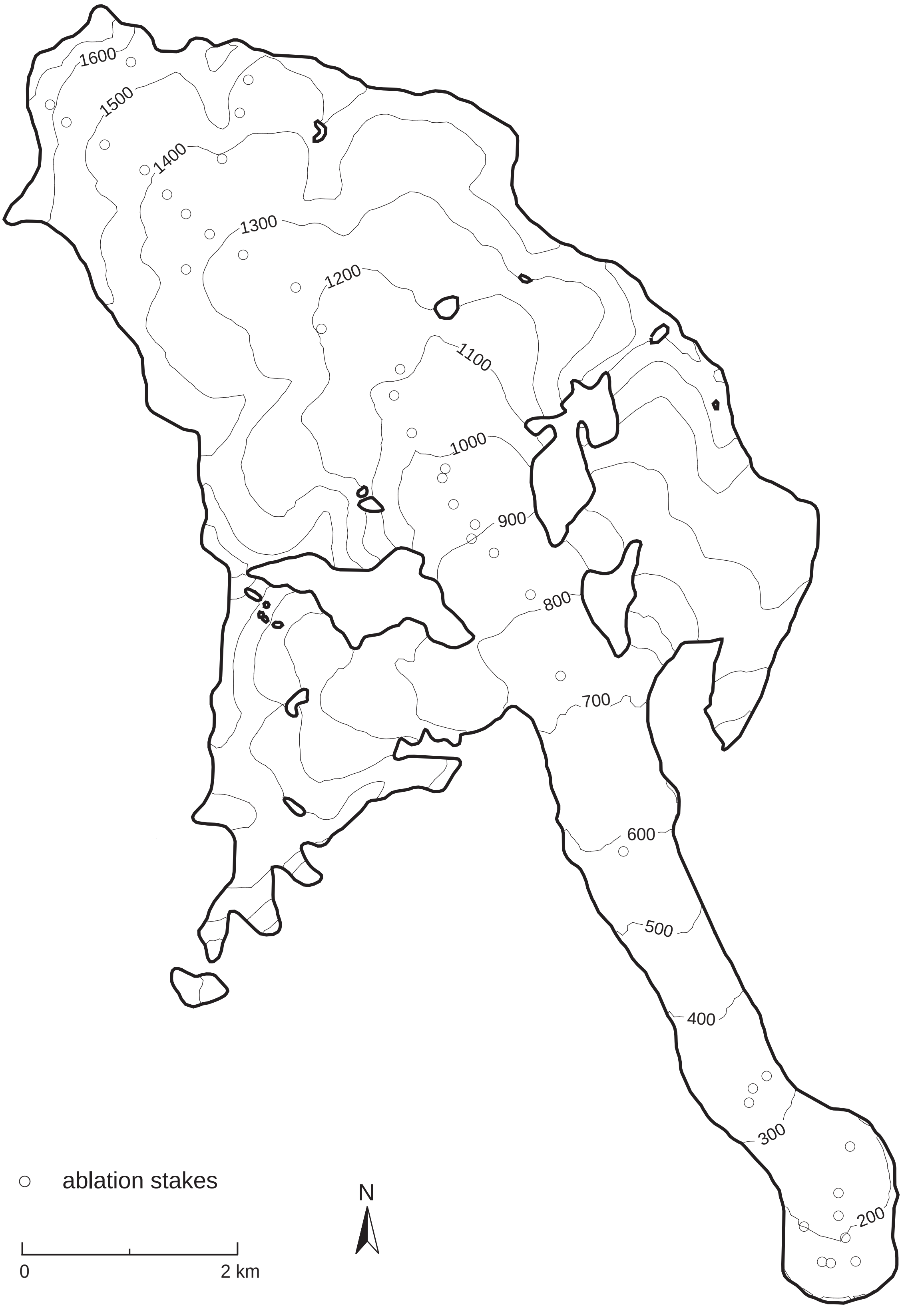

White (CANADA)

3.5.2 Net balance maps 2005/2006 and 2006/2007

2005/2006

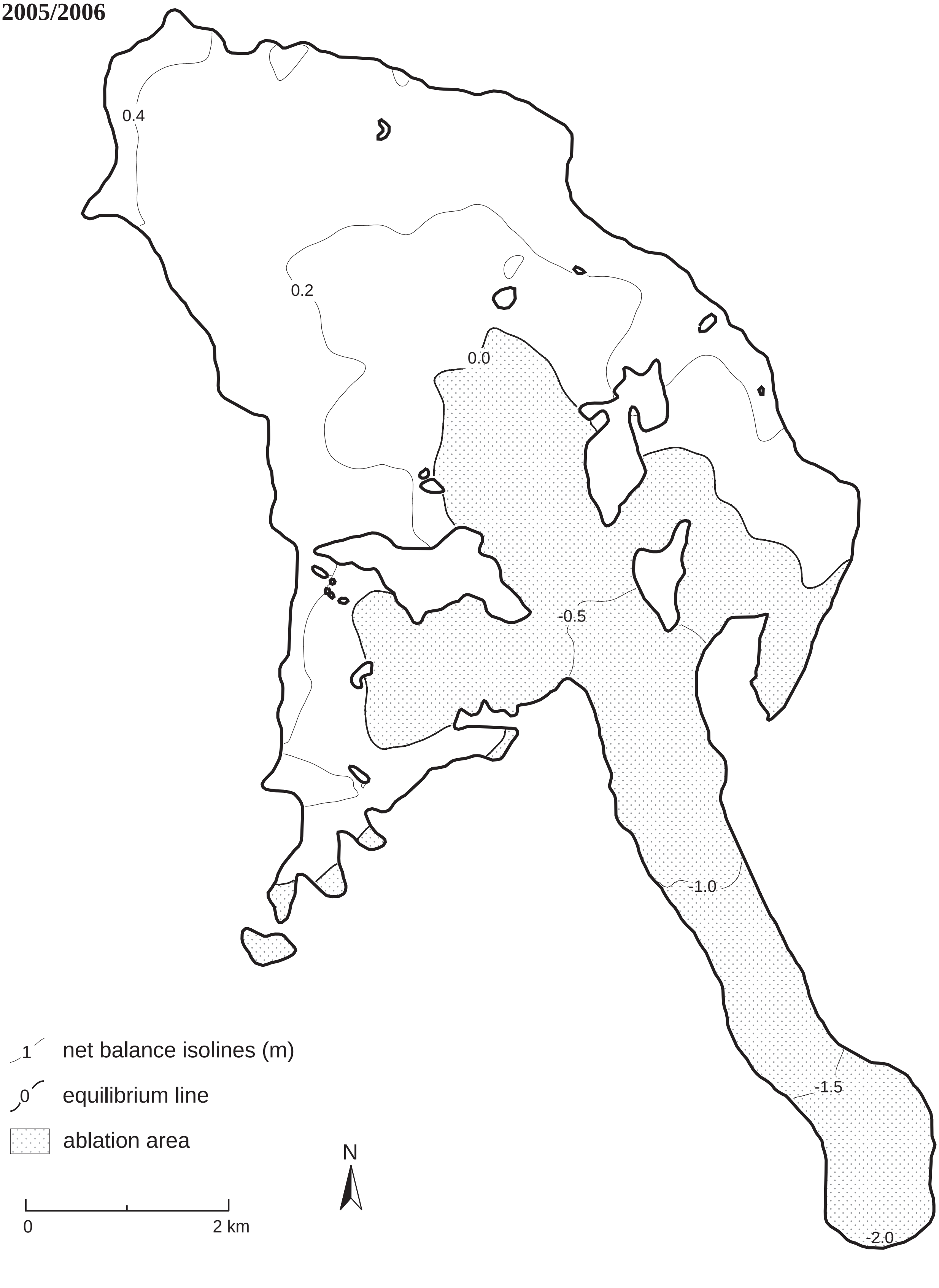

White (CANADA)

2006/2007

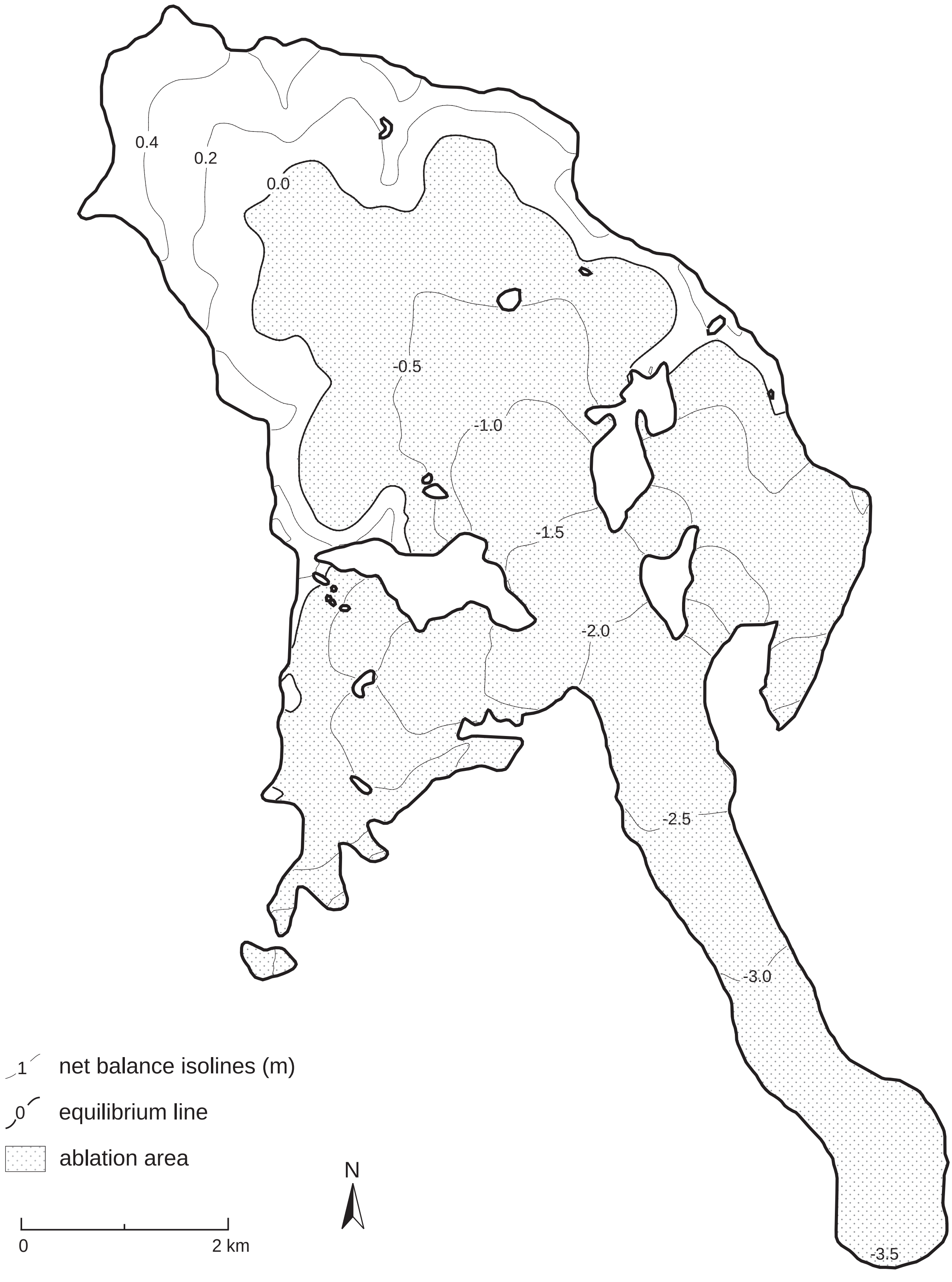

White (CANADA)

3.5.3 Net balance versus altitude (2005/2006 and 2006/2007)

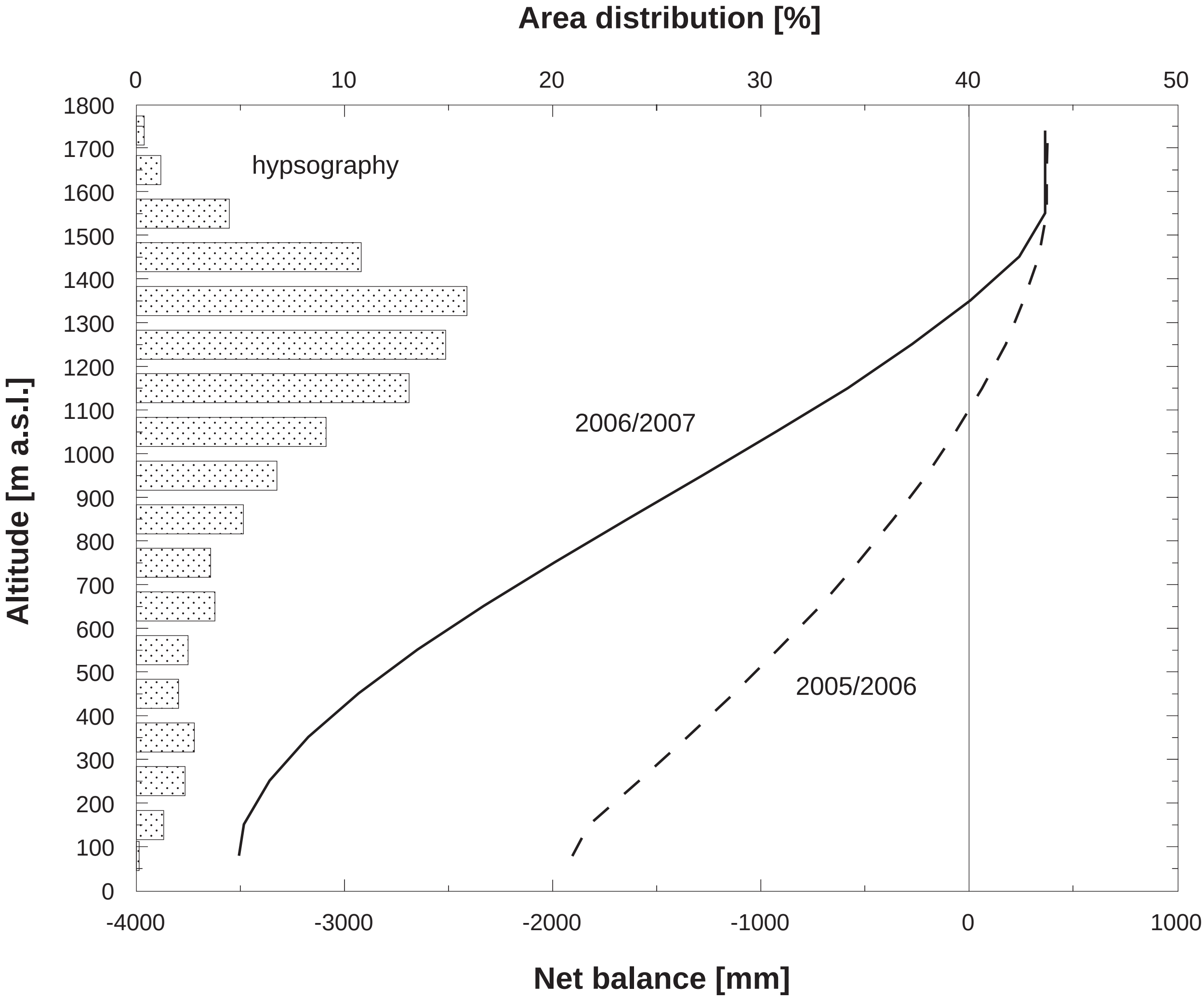

3.5.4 Accumulation area ratio (AAR) and equilibrium line altitude (ELA) versus specific net balance for the whole observation period

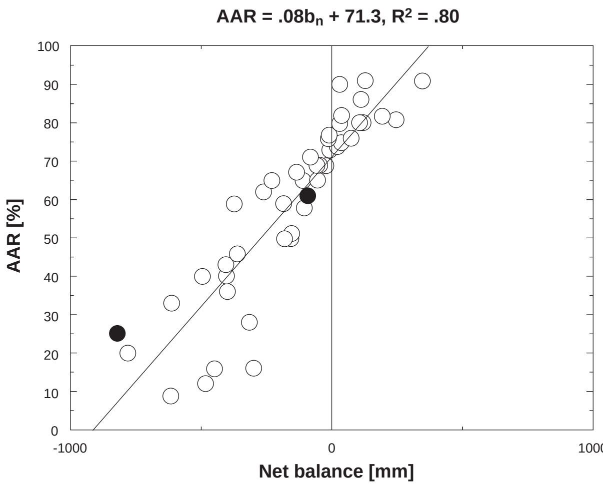

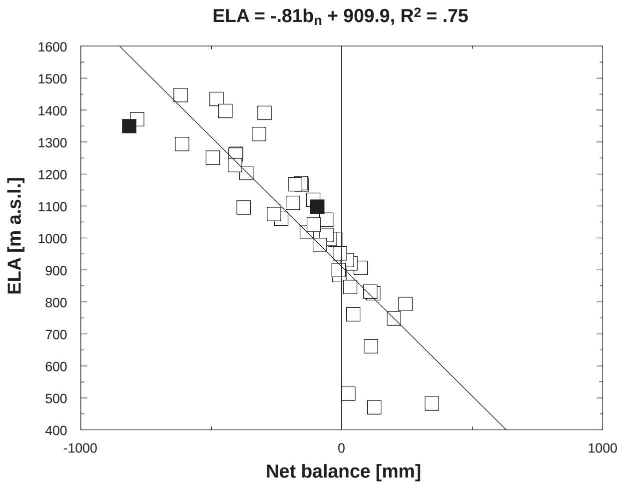

White (CANADA)

3.6 URUMQIHE S. NO 1 (CHINA/TIEN SHAN)

COORDINATES: 43.08 N / 86.82 E

Photo taken by T. Bolch, 2006.

Due to continued glacier shrinkage, the two branches of the former glacier have become two separated small glaciers but are still called East and West branch of Glacier No. 1. The East branch has a total area of 1.1 km^2, the highest and lowest points are at 4267 m and 3742 m a.s.l.; the West branch has a total area of 0.7 km^2, the highest and lowest points are at 4486 m and 3825 m a.s.l. Average annual precipitation measured at the nearby meteorological station at 3539 m a.s.l. is 400 to 500 mm and 600 to 700 mm at the glacier. Mean annual air temperature at the equilibrium line (4022 m a.s.l. for balance years) is estimated at −8.0 to −9.0 °C. The predominantly cold glacier is surrounded by continuous permafrost but reaches melting temperatures over wide areas of the bed. Accumulation and ablation both take place primarily during the warm season and the formation of superimposed ice on this continental-type glacier is important. Since August 2001, a 1:5000 topographic map of the glacier and its forefield has been available for further analysis.

In 2005/06, the mass balance was −920 mm w.e. for the East branch and −506 mm w.e. for the West branch. In 2006/07 , the corresponding values are −696 mm w.e. for the East branch and −542 mm w.e. for the West branch. The calculated mass balance for the entire glacier was −774 mm w.e. in 2005/06 and –642 mm w.e. in 2006/07.

3.6.1 Topography and observation network

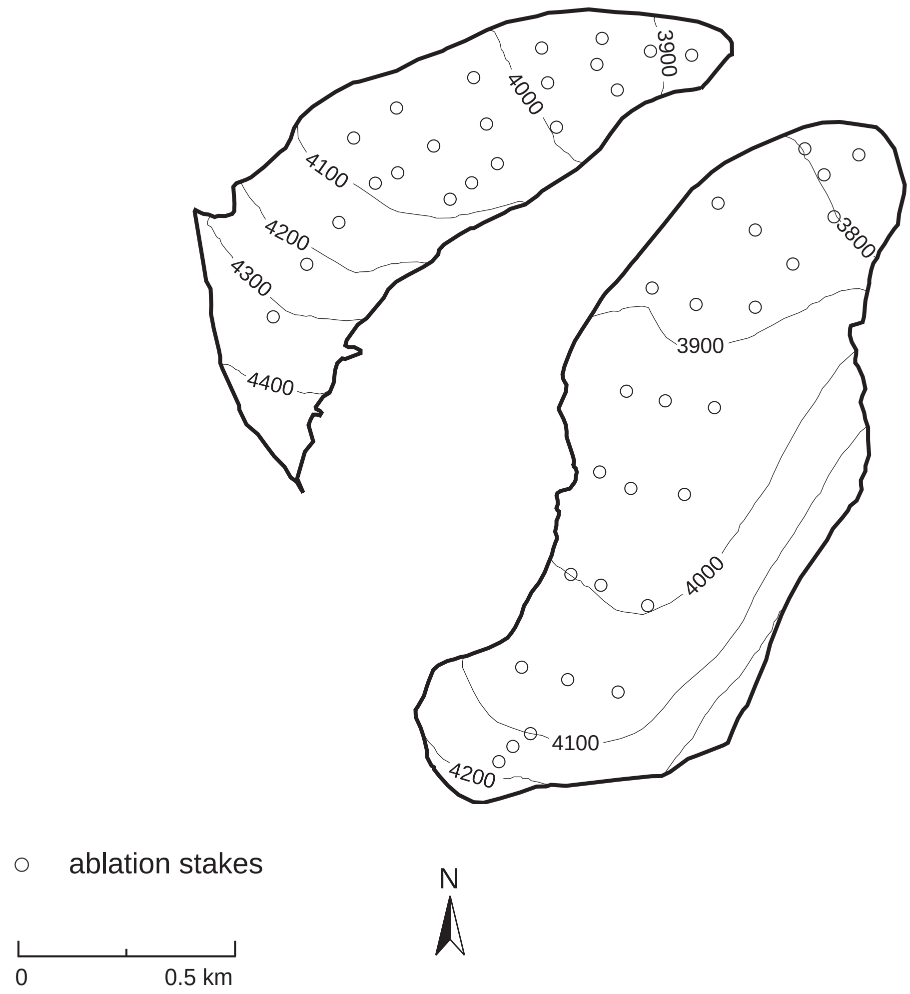

Urumqihe S. No. 1 (CHINA)

3.6.2 Net balance maps 2005/2006 and 2006/2007

2005/2006

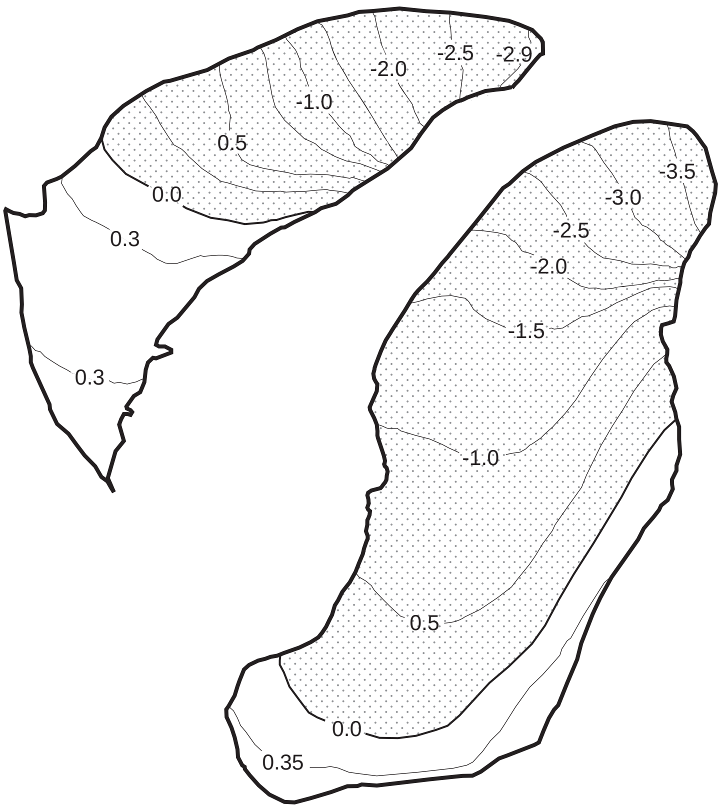

2006/2007

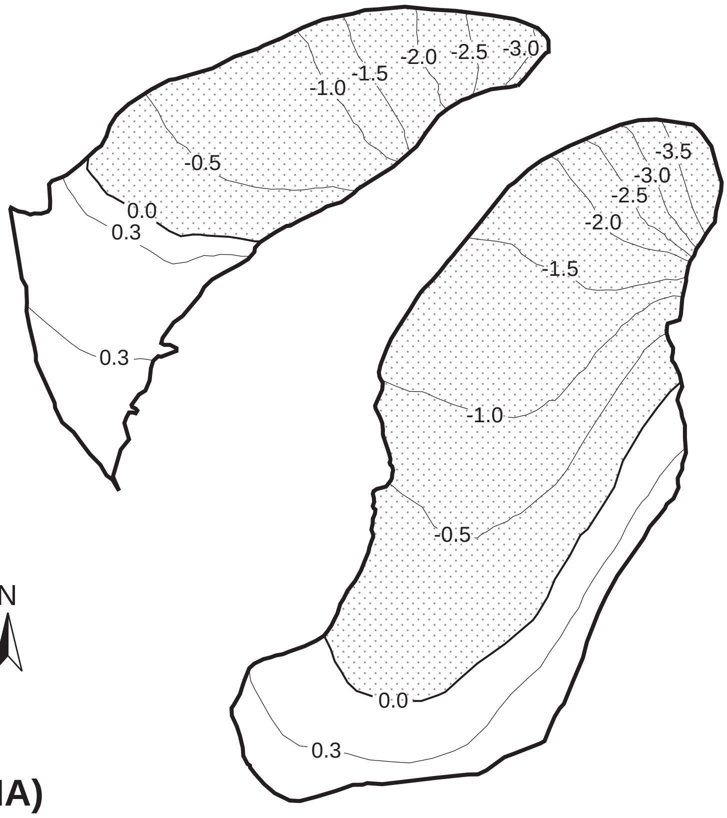

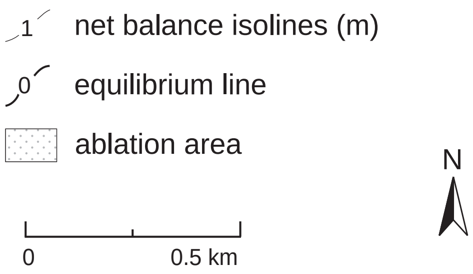

Urumqihe S. No. 1 (CHINA)

3.6.3 Net balance versus altitude (2005/2006 and 2006/2007) of the two branches

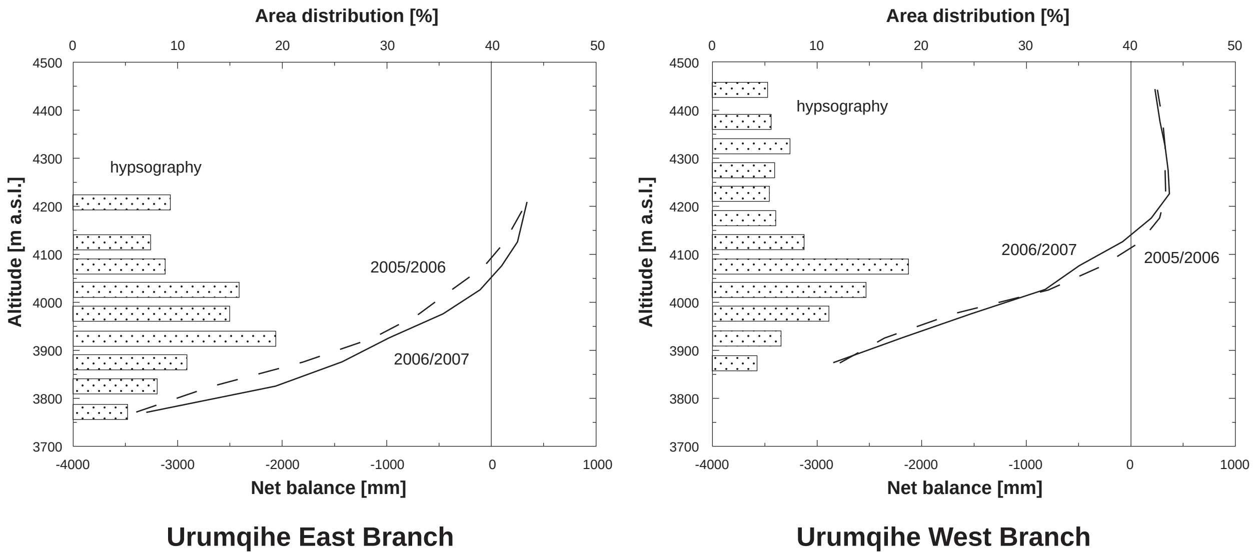

3.6.4 Accumulation area ratio (AAR) and equilibrium line altitude (ELA) versus specific net balance for the whole observation period

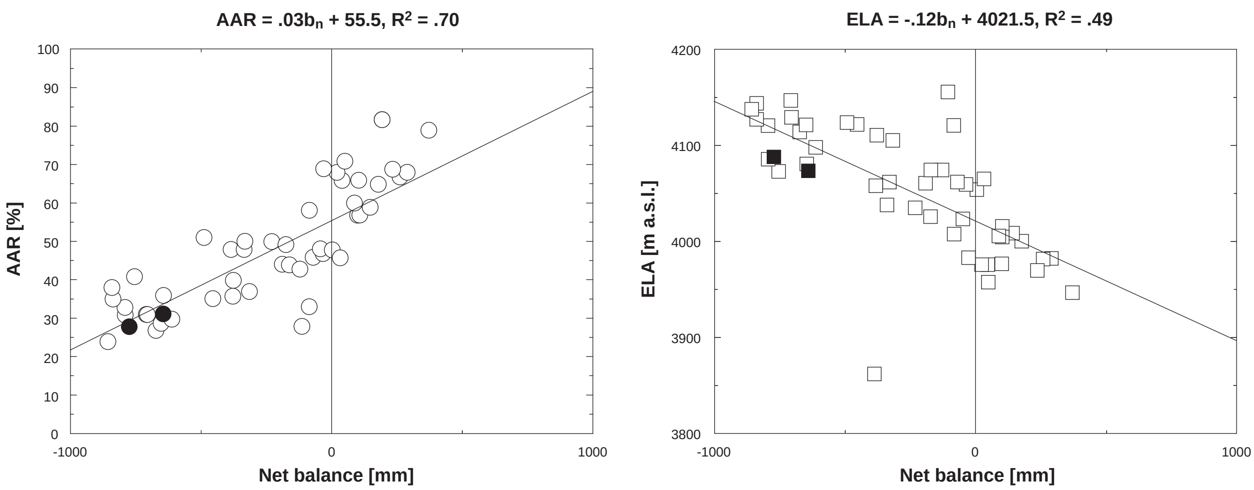

3.7 ANTIZANA 15 ALPHA (ECUADOR/EASTERN CORDILLERA)

COORDINATES: 0.47 S / 78.15 W

Photo taken by B. Cáceres, January 2008.

The 15 Alpha glacier of Antizana (5760 m – 4852 m a.s.l., 0.27 km^2) is the only one situated near the equator in South America providing regular mass balance information to the scientific community. The surface elevations of the glacier have been determined using aerial photogrammetry from the years 1956 and 1997. The first stakes were placed in 1994 to undertake direct measurements in the terminal zone of the glacier. The main exposition of the glacier is to the west and its length is 1.8 km. During the last thirteen years a mean annual average precipitation of 925 mm a^{-1} was measured. In the year 2006/07 a mean annual air temperature of 1.2 °C was recorded at the nearby meteorological station (4820 m a.s.l.), with an annual average of 1.5 °C since 2001.

The 15 Alpha glacier had an average annual mass balance of −615 mm w.e. a^{-1} since 1995. The interannual variation is highly variable. Negative balances were observed during most of the years. Negative records were measured in the years 1995 to 2007. The negative mass balance series was interrupted by two positive balance years in 1999 and 2000. The years 2005/06 and 2006/07 had a negative balance with values of −452 mm w.e. and −658 mm w.e., respectively. The variability of the ENSO (El Niño Southern Oscillation) has been an important factor affecting the climatic conditions and their resulting influence on the mass balance evolution of the Ecuadorian glaciers. Years with favorable conditions for the Ecuadorian glaciers seem to be related to La Niña (cold) events, and for unfavorable conditions to El Niño (warm) events.

3.7.1 Topography and observation network

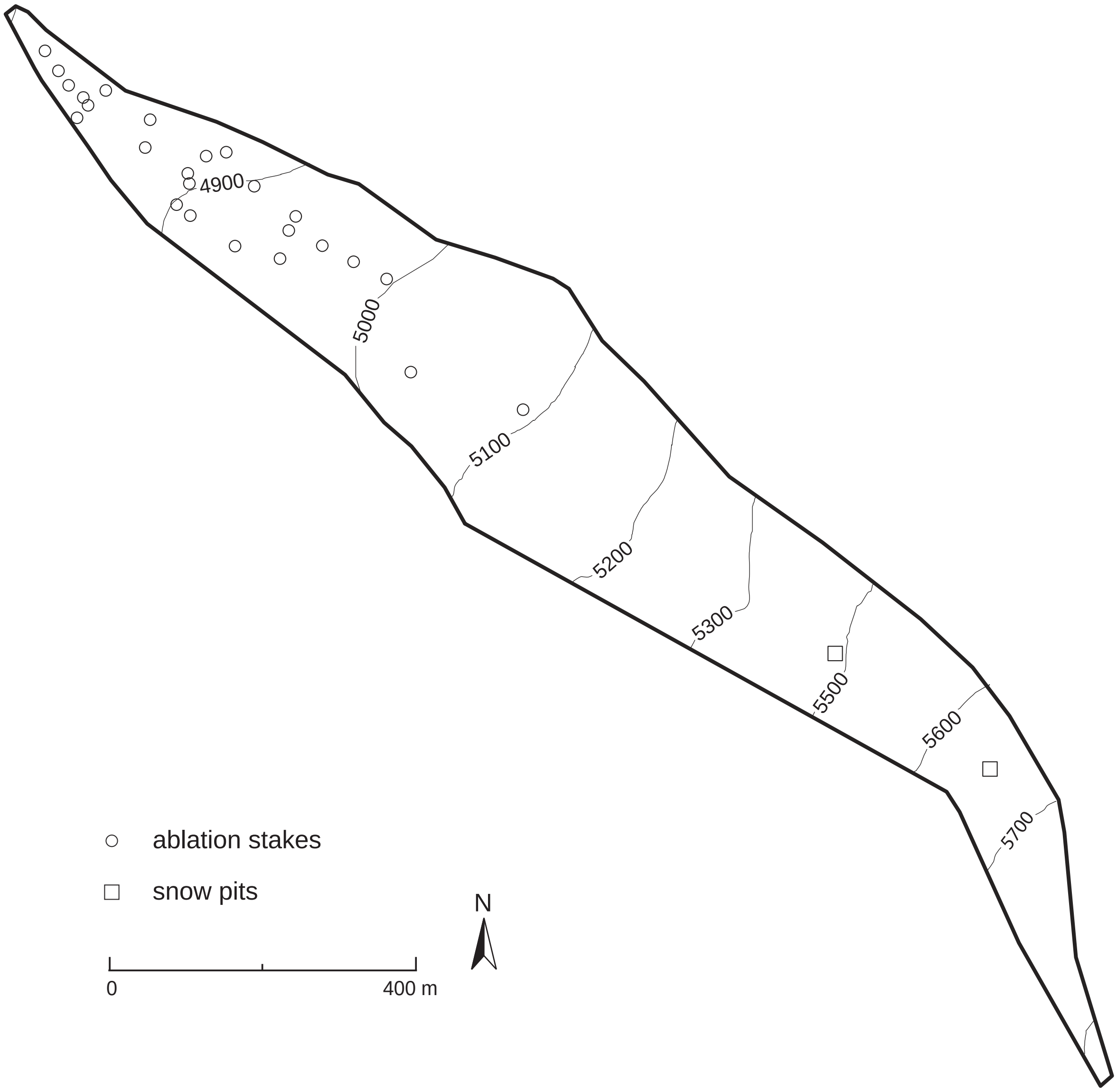

Antizana 15 Alpha (ECUADOR)

3.7.2 Net balance maps 2005/2006 and 2006/2007

2005/2006

2006/2007

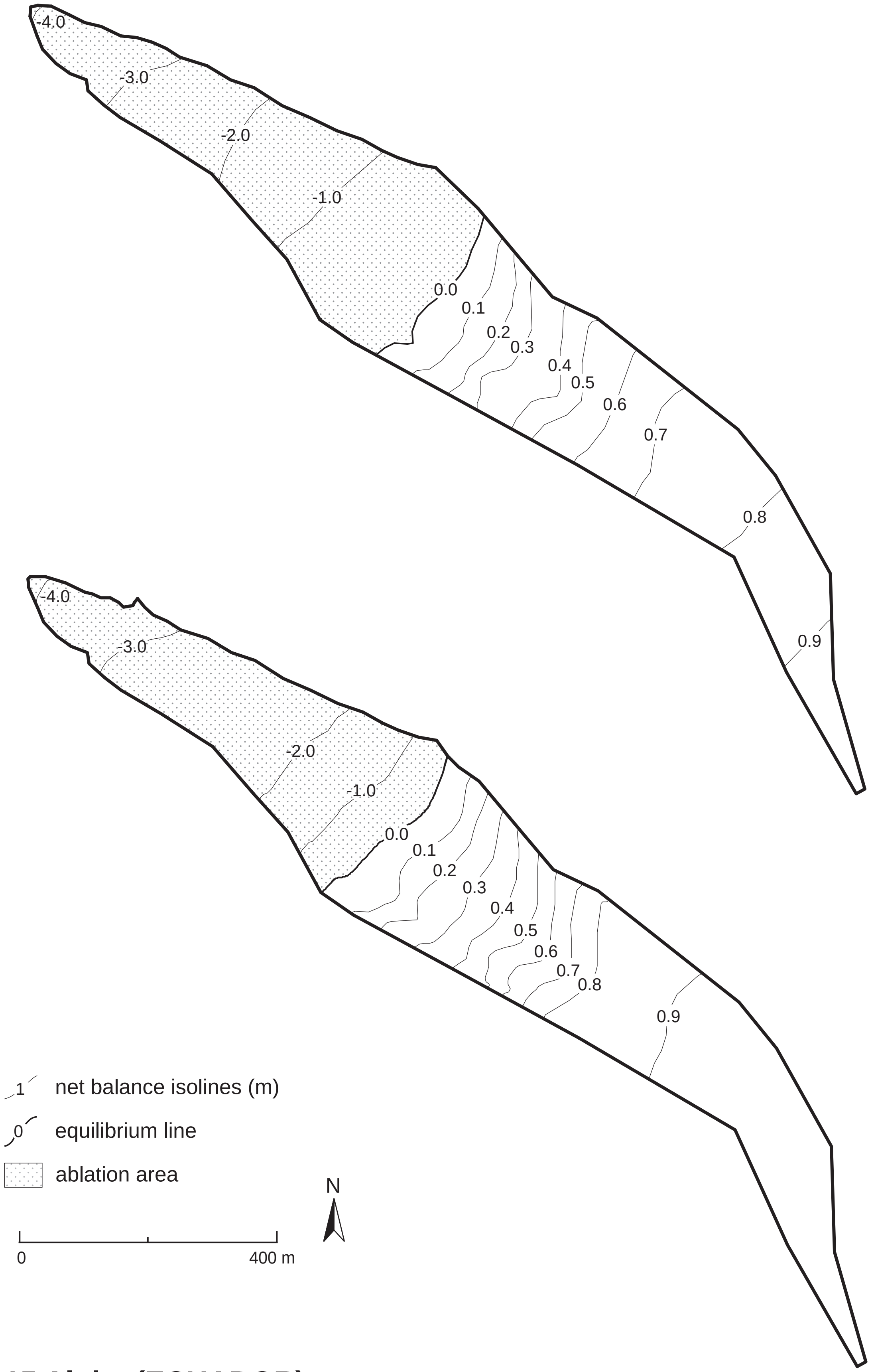

Antizana 15 Alpha (ECUADOR)

3.7.3 Net balance versus altitude (2005/2006 and 2006/2007)

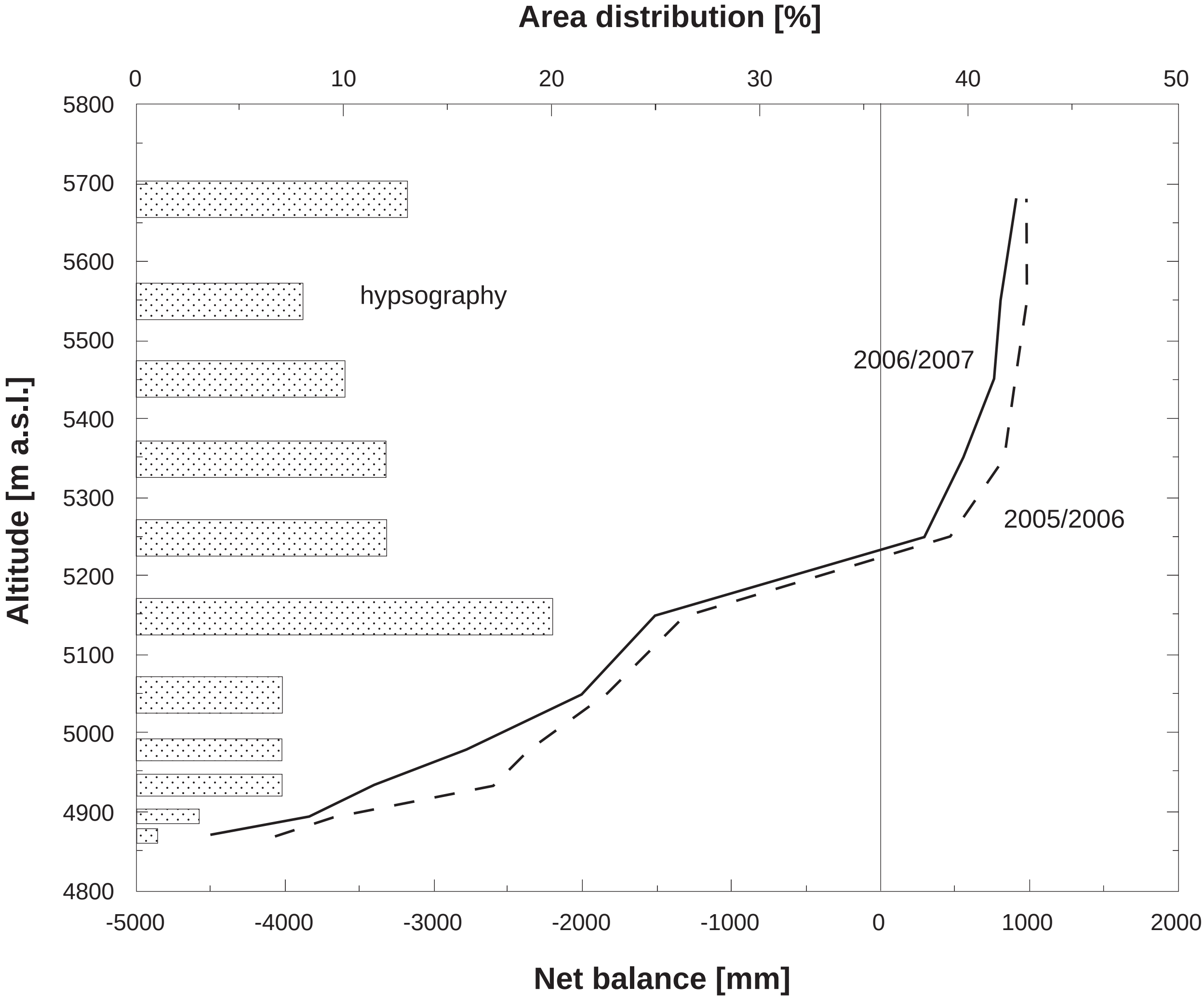

3.7.4 Accumulation area ratio (AAR) and equilibrium line altitude (ELA) versus specific net balance for the whole observation period

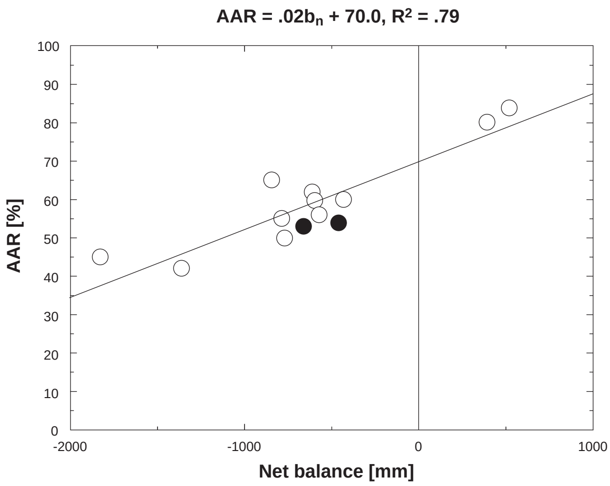

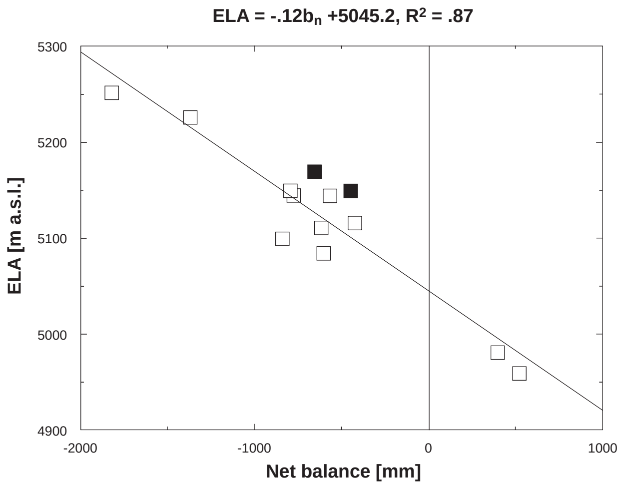

3.8 CARESÈR (ITALY/CENTRAL ALPS)

COORDINATES: 46.45 N / 10.70 E

Photo taken by L. Carturan on 31st of August 2007.

Caresèr Glacier is located in the eastern sector of Ortles-Cevedale group (European Alps, Italy). It occupies an area of 2.4 km^2 and extends from 3279 m to 2869 m a.s.l. The surface is mainly exposed to the south and is quite flat. 75 % of the glacier area lies between 2900 m and 3100 m a.s.l. and the median altitude is 3069 m a.s.l. The mean annual air temperature at this elevation is about −3 to −4 °C and precipitation averages 1450 mm, of which 80 % falls as snow. The mass balance investigations on Caresèr Glacier began in 1967 and extend until present without interruption. The glacier mass balance was near to equilibrium until 1980, but since then it has shown strong mass losses. The mean value of the annual mass balance was −1200 mm w.e. from 1981 to 2002, but decreased to −2350 mm w.e. from 2003 to 2007. This is a result of both warmer ablation seasons and positive feedbacks (albedo and surface lowering). The repeated negative mass balances are causing huge changes in the glacier morphology, with widespread bedrock emersion and rapid fragmentation. The most remarkable event was the detachment of the western portion of the glacier from the main ice body in 2005.

During the hydrological years 2005/06 and 2006/07 the mass balance of Caresèr glacier was strongly negative, reaching the 4th and the 2nd worst values of the entire series of observations with −2093 and −2745 mm w.e., respectively. Warm and long ablation seasons played a dominant role in the observed balance behaviour, but in 2006/07 the winter precipitation was also extremely scarce (40 % of the long-term mean), and ice ablation started abnormally by the end of June.

3.8.1 Topography and observation network

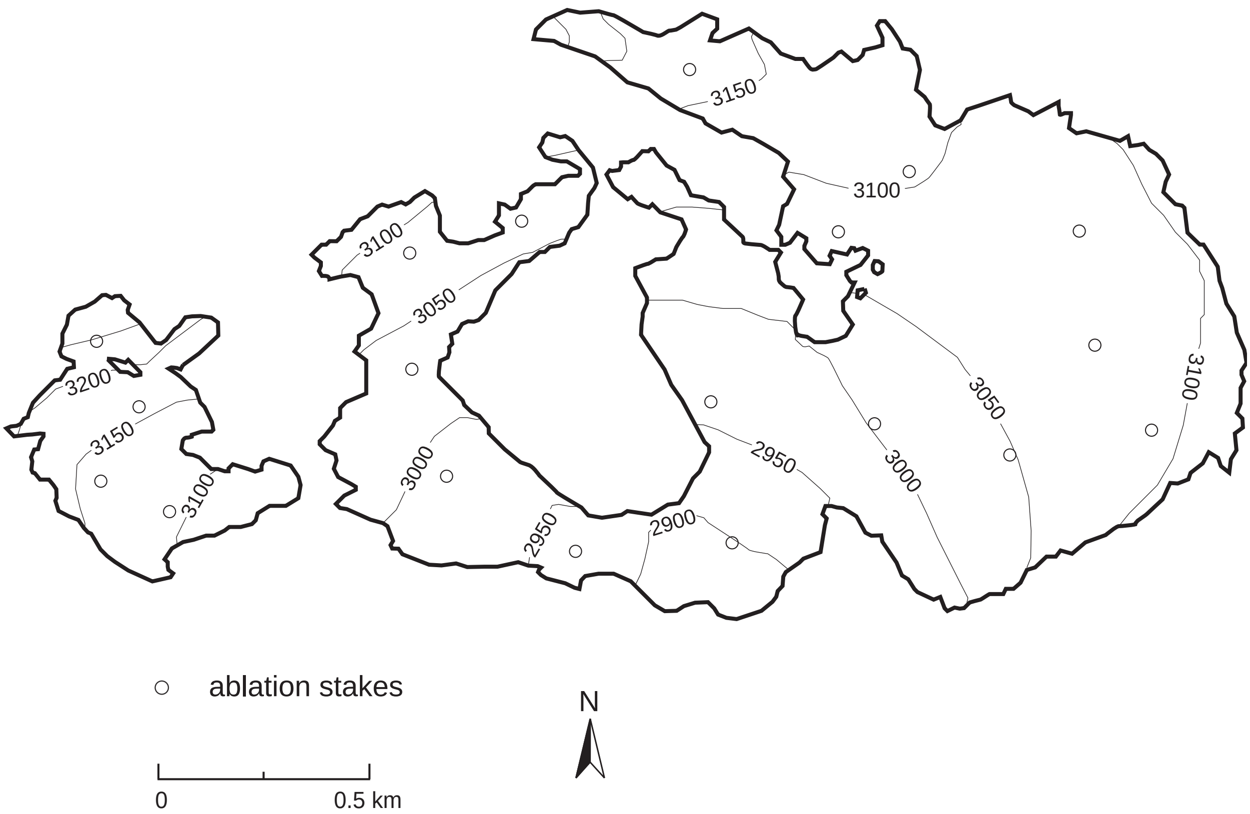

Caresèr (ITALY)

3.8.2 Net balance maps 2005/2006 and 2006/2007

2005/2006

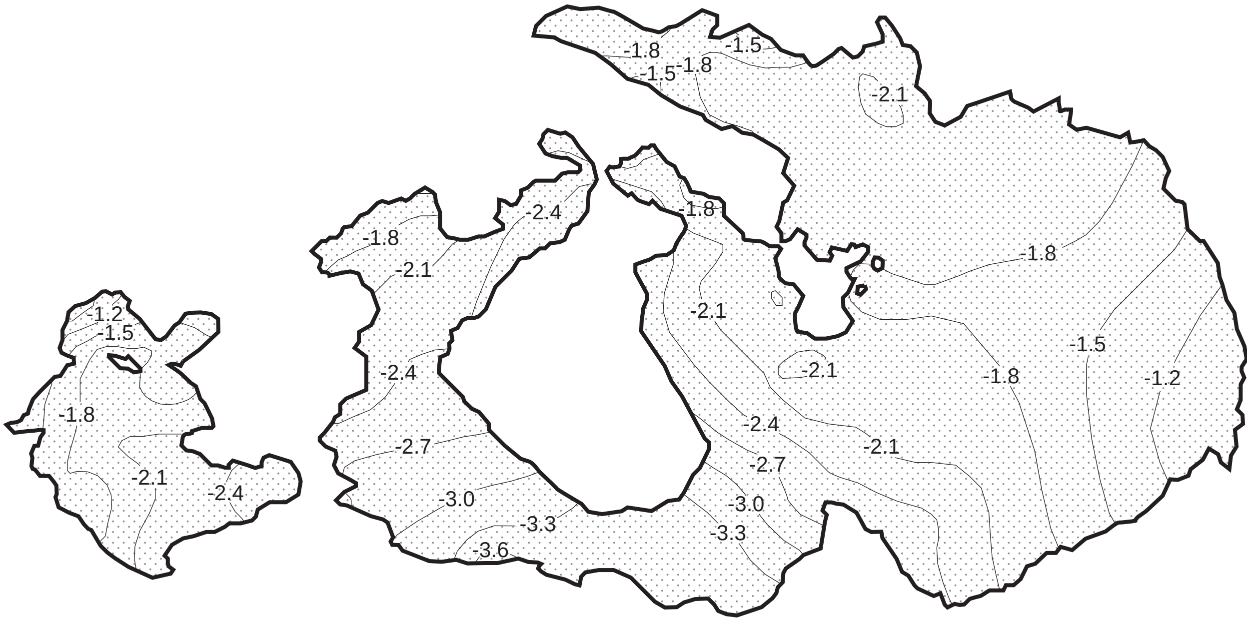

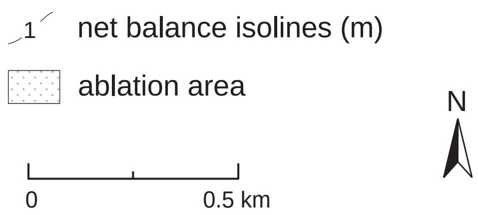

2006/2007

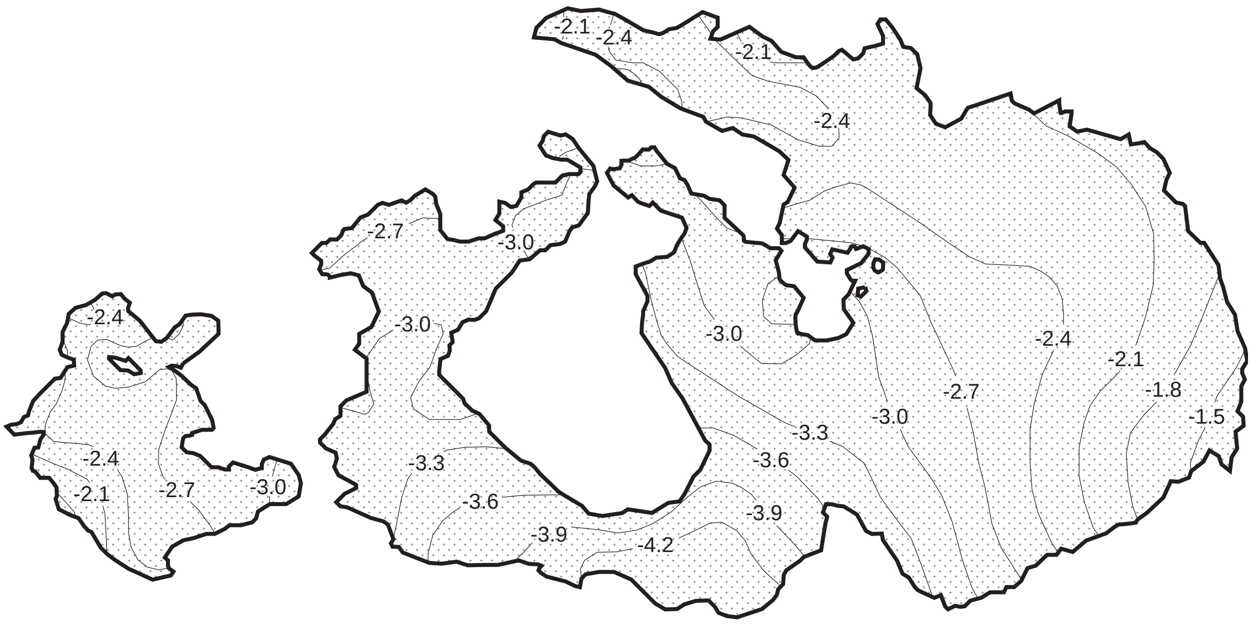

Caresèr (ITALY)

3.8.3 Net balance versus altitude (2005/2006 and 2006/2007) for both parts of the glacier

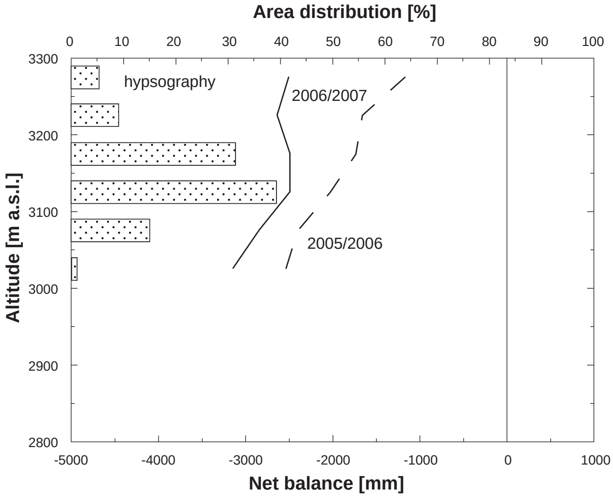

Caresèr Occidentale

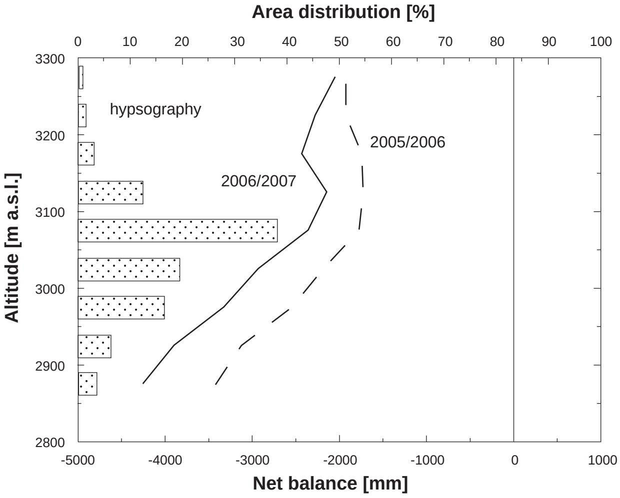

Caresèr Orientale

3.8.4 Accumulation area ratio (AAR) and equilibrium line altitude (ELA) versus specific net balance for the whole observation period

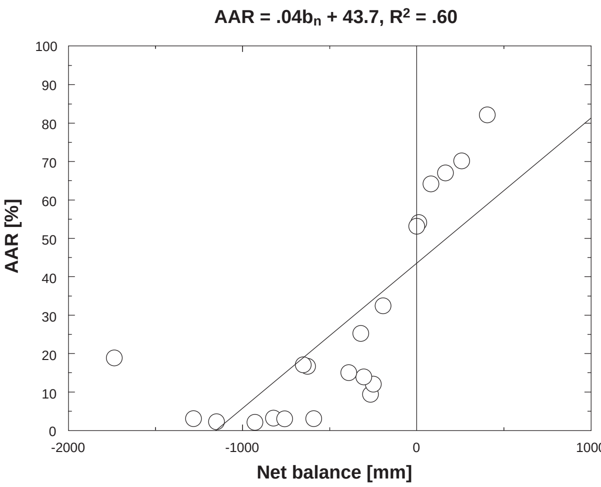

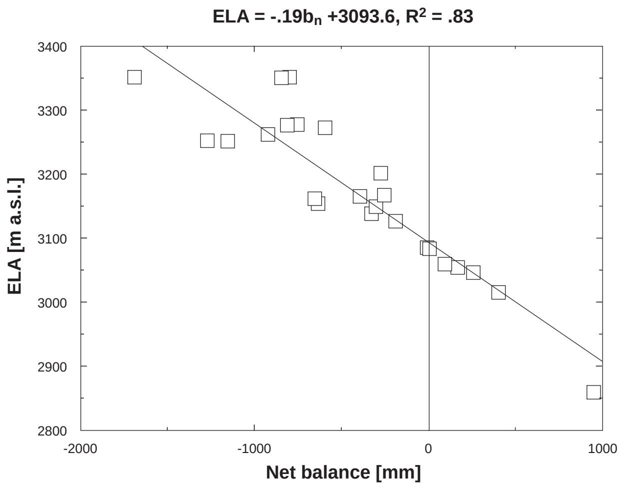

3.9 MALAVALLE (ITALY/CENTRAL ALPS)

COORDINATES: 46.95 N / 11.12 E

Photo taken by M. Kuhn, 22nd September 2007.

The Malavalle Glacier (Übeltalferner) is the widest in the Breonie Alps, an alpine ridge in the Stubai Alps lying in the Italian territory along the Austrian border. The head of the Val Ridanna is shaped like a wide bowl with several levels with different-shaped cirques presenting varying accumulation conditions, depending on aspect and slope. The glacier arms extend from all these cirques and flow into the wide central stream at about 2900 m a.s.l. The front moves down to 2530 m a.s.l. The left side of the glacier stretches along the moraine, which developed between the end of the 18th and the beginning of the 19th century, and ends at a small proglacial lake at about 2500 m a.s.l. The main stream (Fernerbach) originates at the right border of the front, which is on a step above a 300 m drop.

The mass balance measurements began in the year 2001/02, using the fixed date method. In the first three years, the measurements were done annually, and since 2004/05 they have been done on a seasonal basis. In the years 2005/06 and 2006/07, severe mass losses of −1322 mm w.e. and −1358 mm w.e. were measured, respectively. The average mass loss over the six-year period was −1010 mm w.e., resulting in a total ice loss of 6058 mm w.e.. The continuous retreat of the glacier affects both its extension and volume. At the end of the summer season, a new topographic survey was carried out by GPS in order to update the glacial border in the front area, where a 0.4 km^2 tributary glacier is expected to detach in the near future.

3.9.1 Topography and observation network

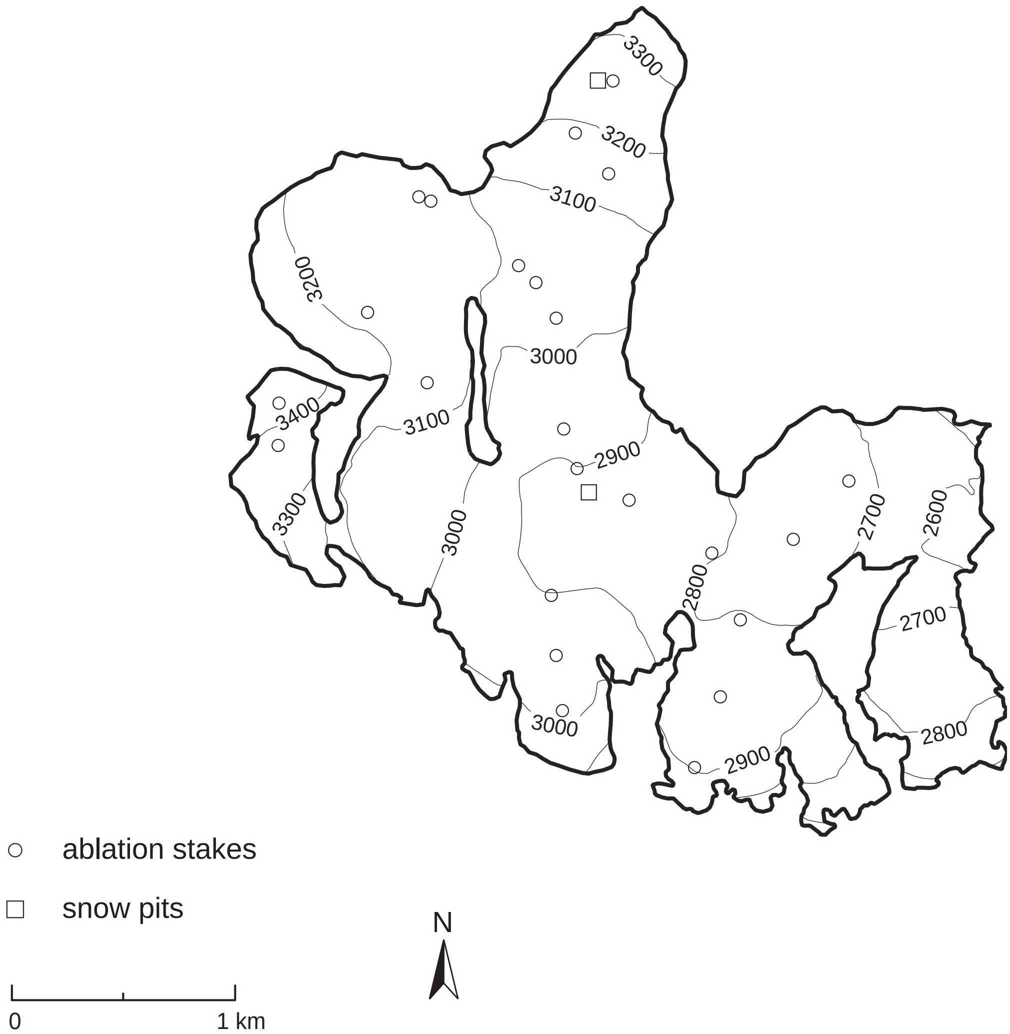

Malavalle (ITALY)

3.9.2 Net balance maps 2005/2006 and 2006/2007

2005/2006

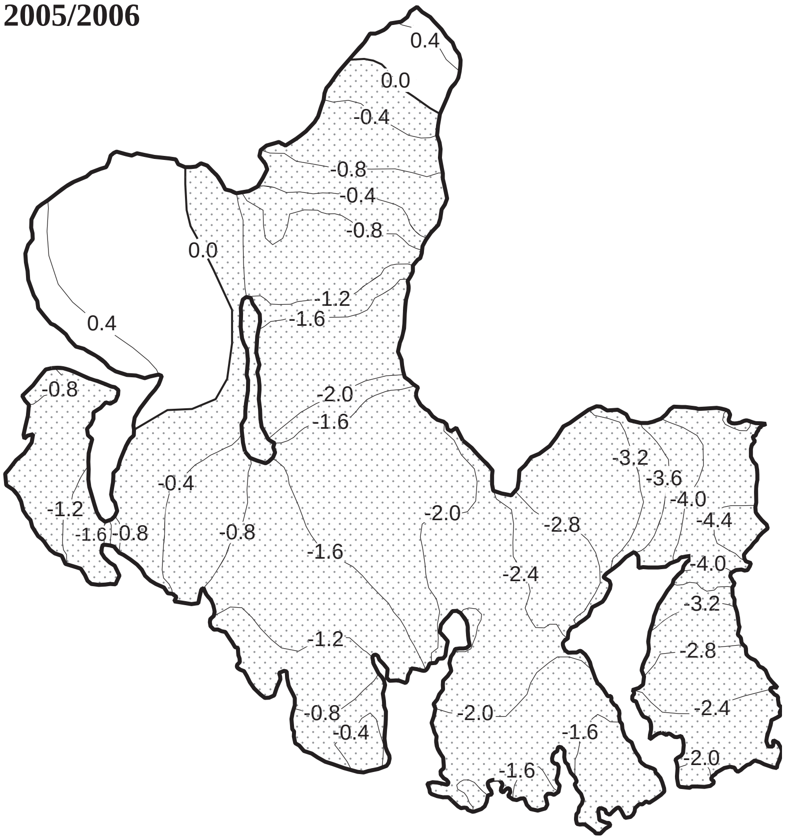

2006/2007

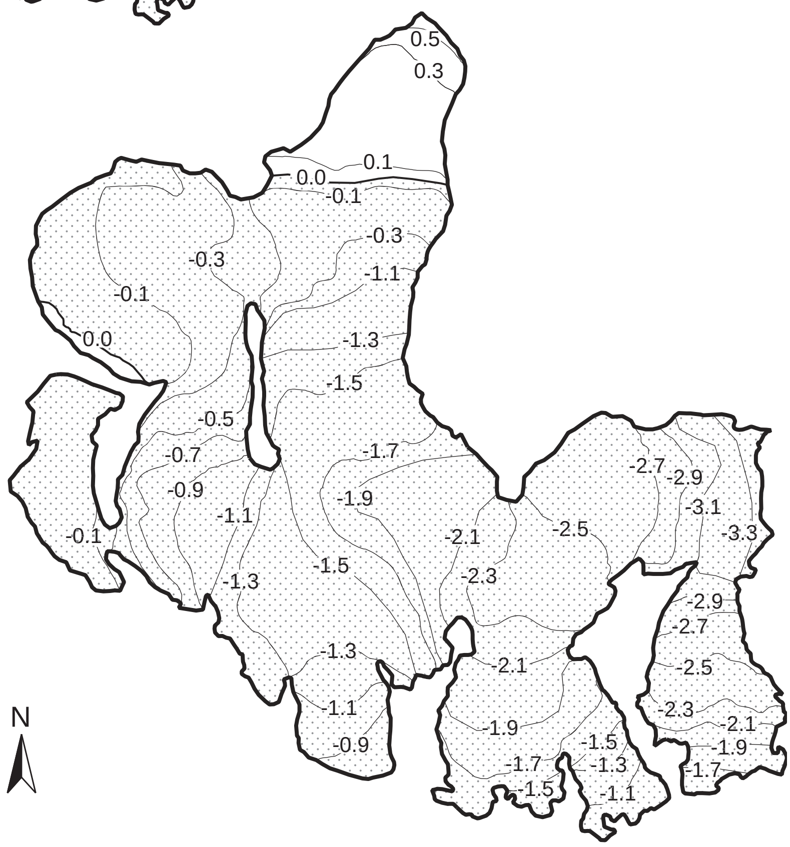

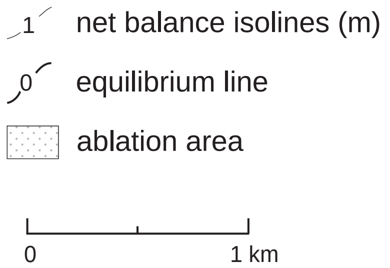

Malavalle (ITALY)

3.9.3 Net balance versus altitude (2005/2006 and 2006/2007)

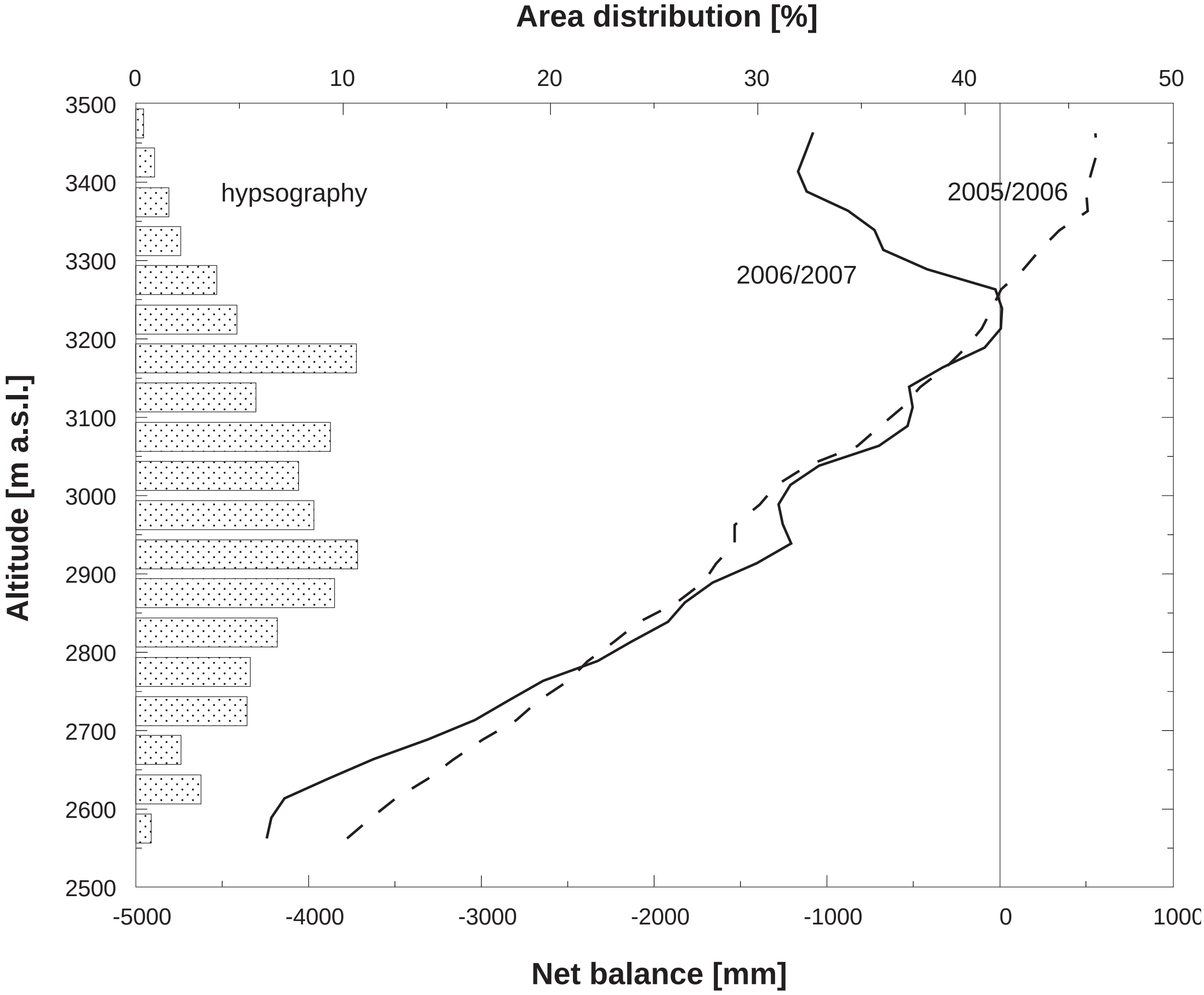

3.9.4 Accumulation area ratio (AAR) and equilibrium line altitude (ELA) versus specific net balance for the whole observation period

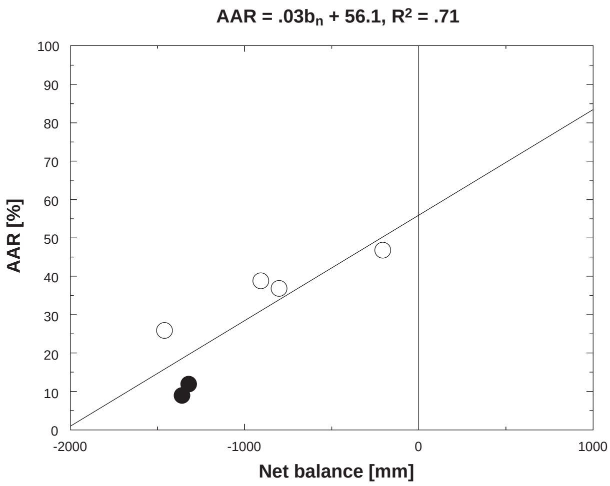

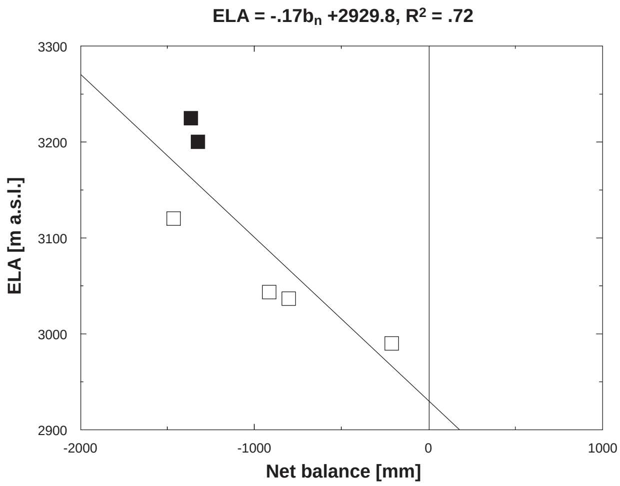

Malavalle (ITALY)

3.10 TSENTRALNIY TUYUKSUYSKIY (KAZAKHSTAN/TIEN SHAN)

COORDINATES: 43.05 N / 77.08 E

Photo taken by V.P. Blagoveshensky in July 2007.

The valley-type glacier in the Zailiyskiy Alatau Range of Kazakh Tien Shan is also called the Tuyuksu Glacier. It extends from 4200 m to 3425 m a.s.l. and has a surface area of 2.51 km^2 (including debris-covered ice) with exposure to the north. Mean annual air temperature at the equilibrium line of the glacier (around 3980 m a.s.l. in 2006 and 3885 m a.s.l. in 2007 for balanced conditions) is between −6 to –7 ºC. The summer precipitation equals 40 % of the annual sum. A characteristic feature of these highly continental climatic conditions is the stable winter anticyclones. The glacier is considered to be cold to polythermal and surrounded by continuous permafrost.

Average annual precipitation as measured with a great number of precipitation gauges for the balance year 2005/06 is equal to 931 mm and 1074 mm for the balance year 2006/07. The summer season of 2006 was 0.4 ºC warmer than the average value for the period 1971/72–2005/06, while precipitation was equal to average. August was 1.8 ºC warmer than the average value. As a result of these conditions the glacier mass balance in 2006 was −969 mm w.e. The summer season of 2007 was 1.1 °C warmer than the average value for the period 1972–2007, while precipitation was 70 mm more than average. As a result of these conditions the glacier mass balance in 2007 was −915 mm w.e.

3.10.1 Topography and observation network

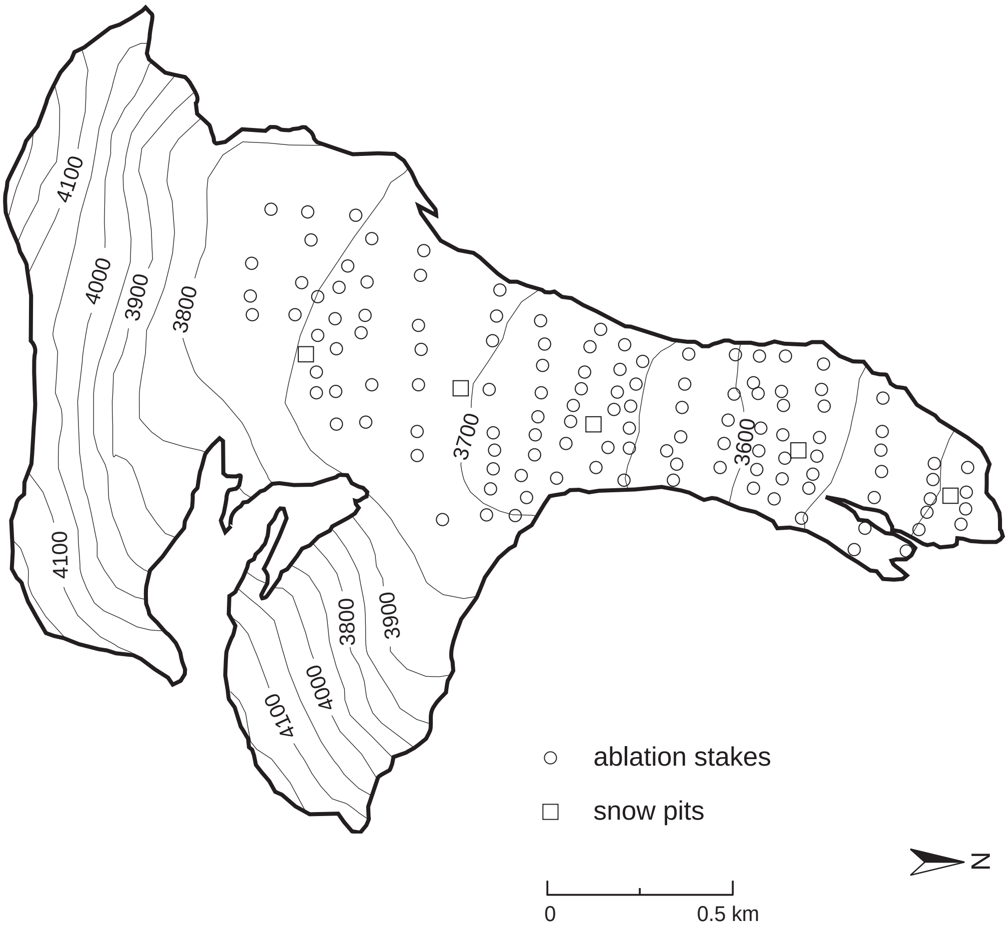

Tsentralniy Tuyuksuyskiy (KAZAKHSTAN)

3.10.2 Net balance maps 2005/2006 and 2006/2007

2005/2006

2006/2007

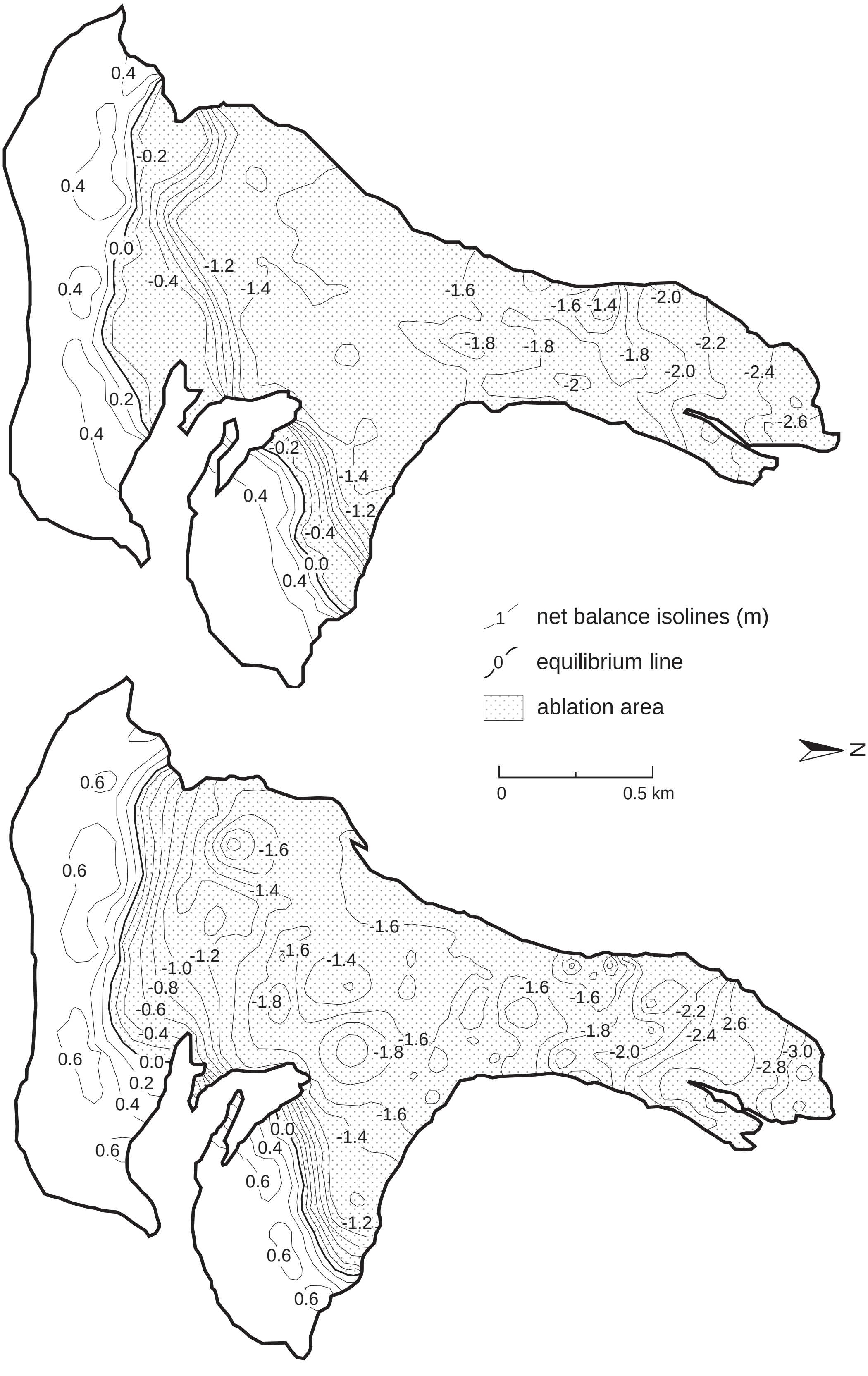

Tsentralniy Tuyuksuyskiy (KAZAKHSTAN)

3.10.3 Net balance versus altitude (2005/2006 and 2006/2007)

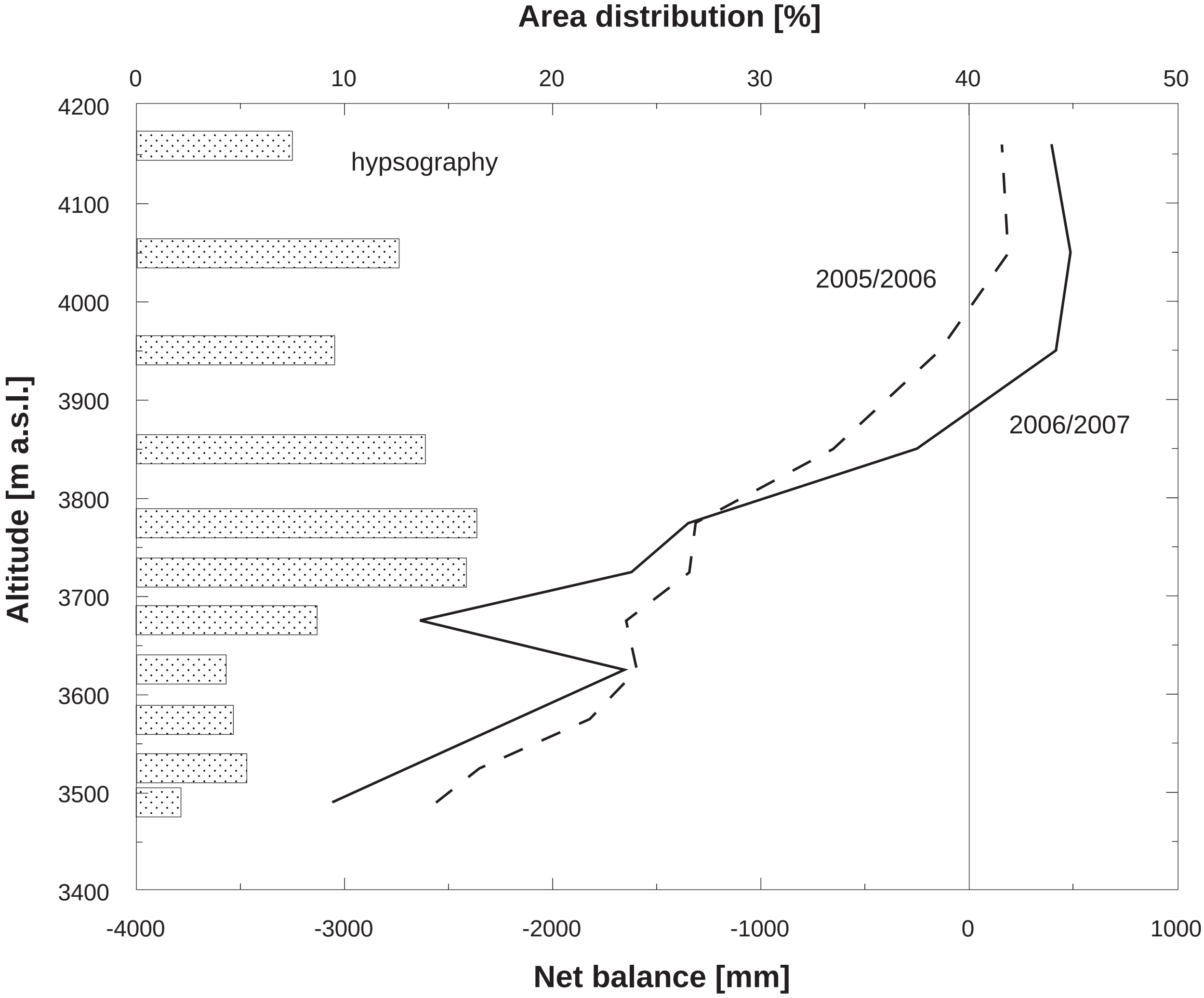

3.10.4 Accumulation area ratio (AAR) and equilibrium line altitude (ELA) versus specific net balance for the whole observation period

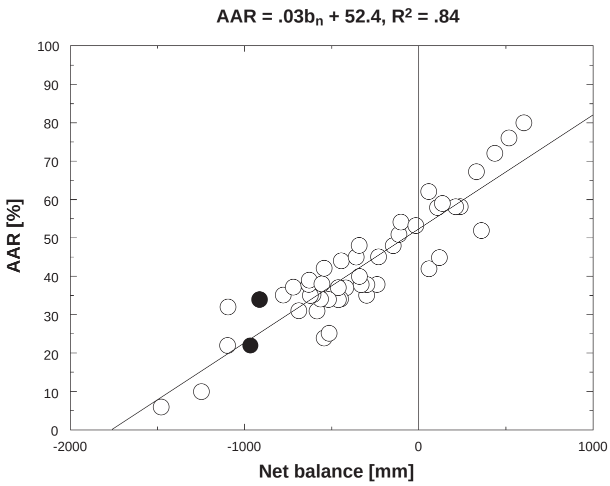

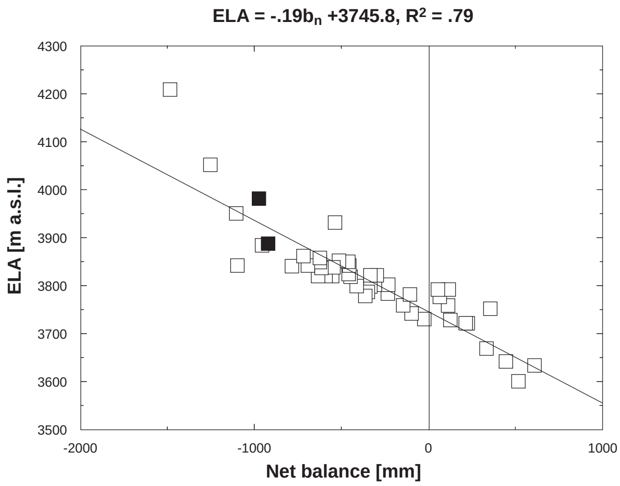

Tsentralniy Tuyuksuyskiy (KAZAKHSTAN)

3.11 BREWSTER (NEW ZEALAND/TITITEA MT ASPIRING NP)

COORDINATES: 44.08 S / 169.44 E

Photo taken by A. Willsman (Glacier Snowline Survey, NIWA), 14 March 2008.

Brewster Glacier is a temperate glacier on the Main Divide of the Southern Alps of New Zealand and lies south of Mt Brewster (2515 m a.s.l.). The glacier has an area of about 2.5 km^2, is about 2.5 km long, and extends over an elevation range of 730 m, from 2390 m to 1660 m a.s.l. The major part of the glacier, up to about 2000 m a.s.l., faces south with an average slope of 11°, and the top 400 m have a south-westerly aspect with a mean slope of 31°. The maximum ice thickness is about 150 m, and a few hundred meters up the snout there is a bed overdeepening. On the western margin of the glacier the valley walls are not clearly confined. The glacier surface is very clean and there is little sedimentation in the glacier forefield. The exposed bedrock is polished and displays abrasion marks from the glacier. These observations, the very few debris delivering rockwalls surrounding Brewster Glacier and very low-frequency measurements by Thiel (1986) suggest minor subglacial sediments, with eroding rather than sedimenting glacier activities. Brewster Glacier is a maritime glacier type with an annual mean precipitation (1951–1980) between 3200–4800 mm and a mean annual air temperature at the ELA (ca. 1900 m a.s.l. for a balanced year) of about 1 °C.

In the years 2005/06 and 2006/07, the mass balances were slightly positive (+282 mm w.e. and +297 mm w.e., respectively) with ELAs at similar altitudes (1893 m a.s.l. and 1899 m a.s.l.). More knowledge about the mass balance above 2000 m a.s.l. and new glacier outlines are needed. Updated glacier outlines would resolve the discrepancies between the mentioned altitude range and the topographical map.

3.11.1 Topography and observation network

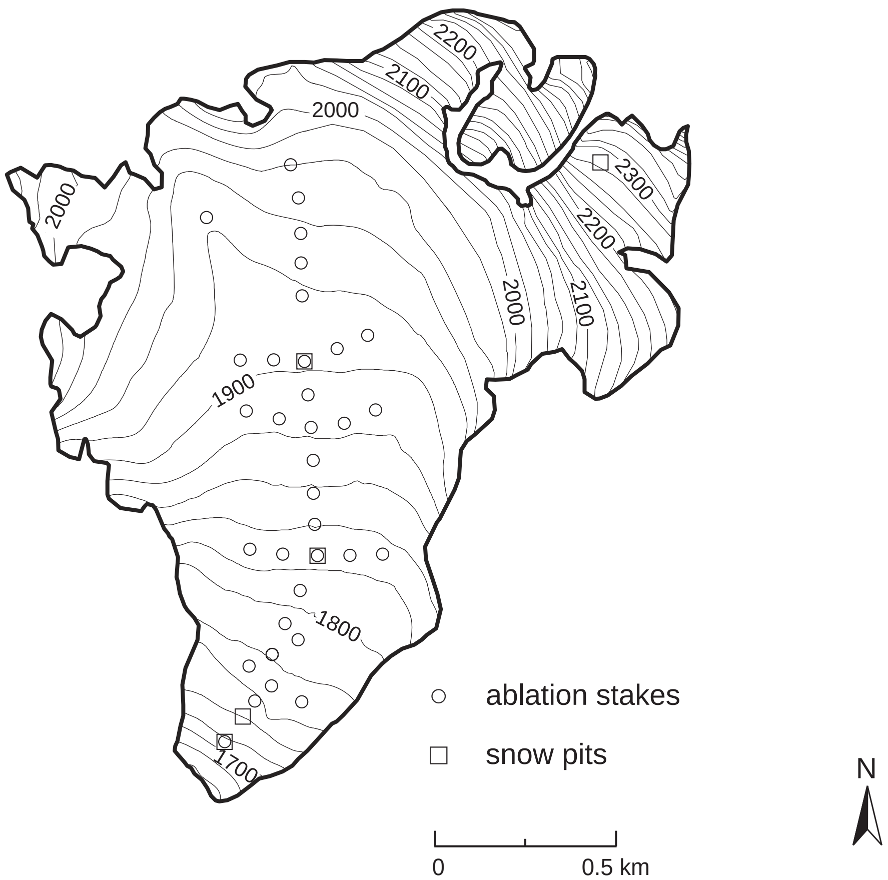

Brewster Glacier (NEW ZEALAND)

3.11.2 Net balance maps 2005/2006 and 2006/2007

2005/2006

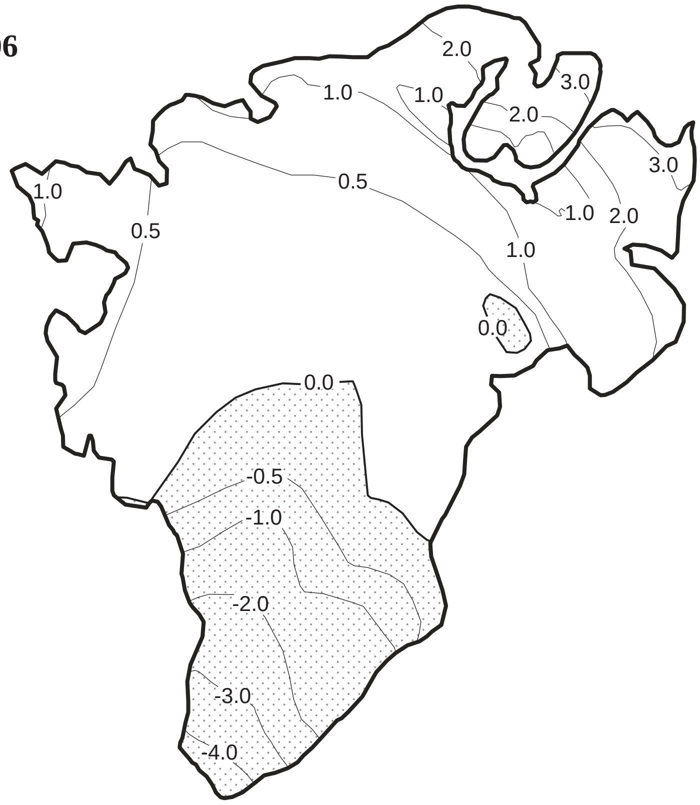

2006/2007

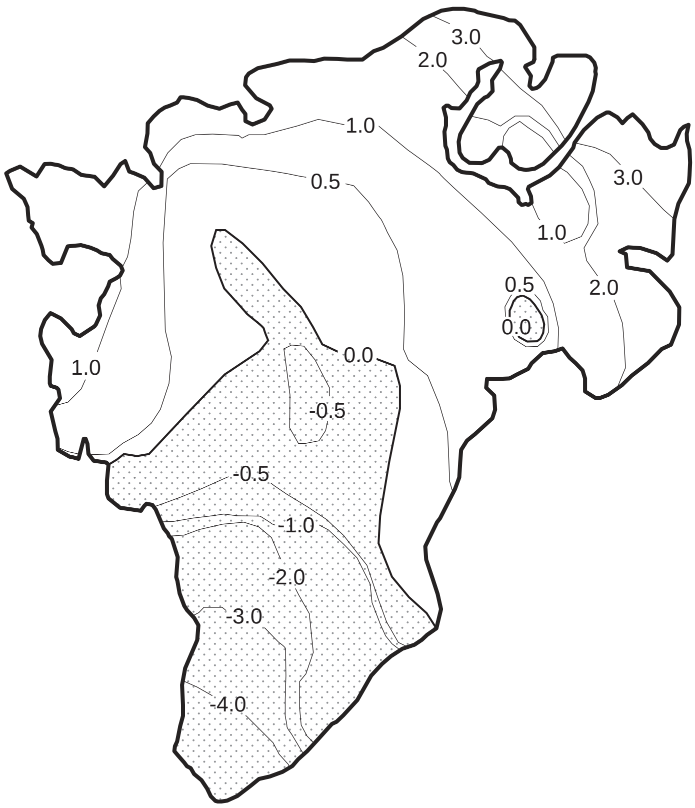

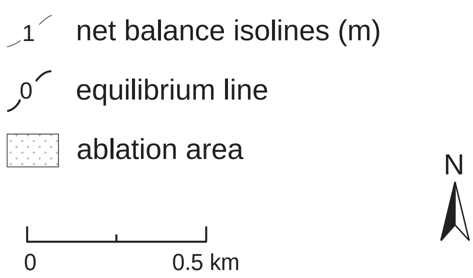

Brewster Glacier (NEW ZEALAND)

3.11.3 Net balance versus altitude (2005/2006 and 2006/2007)

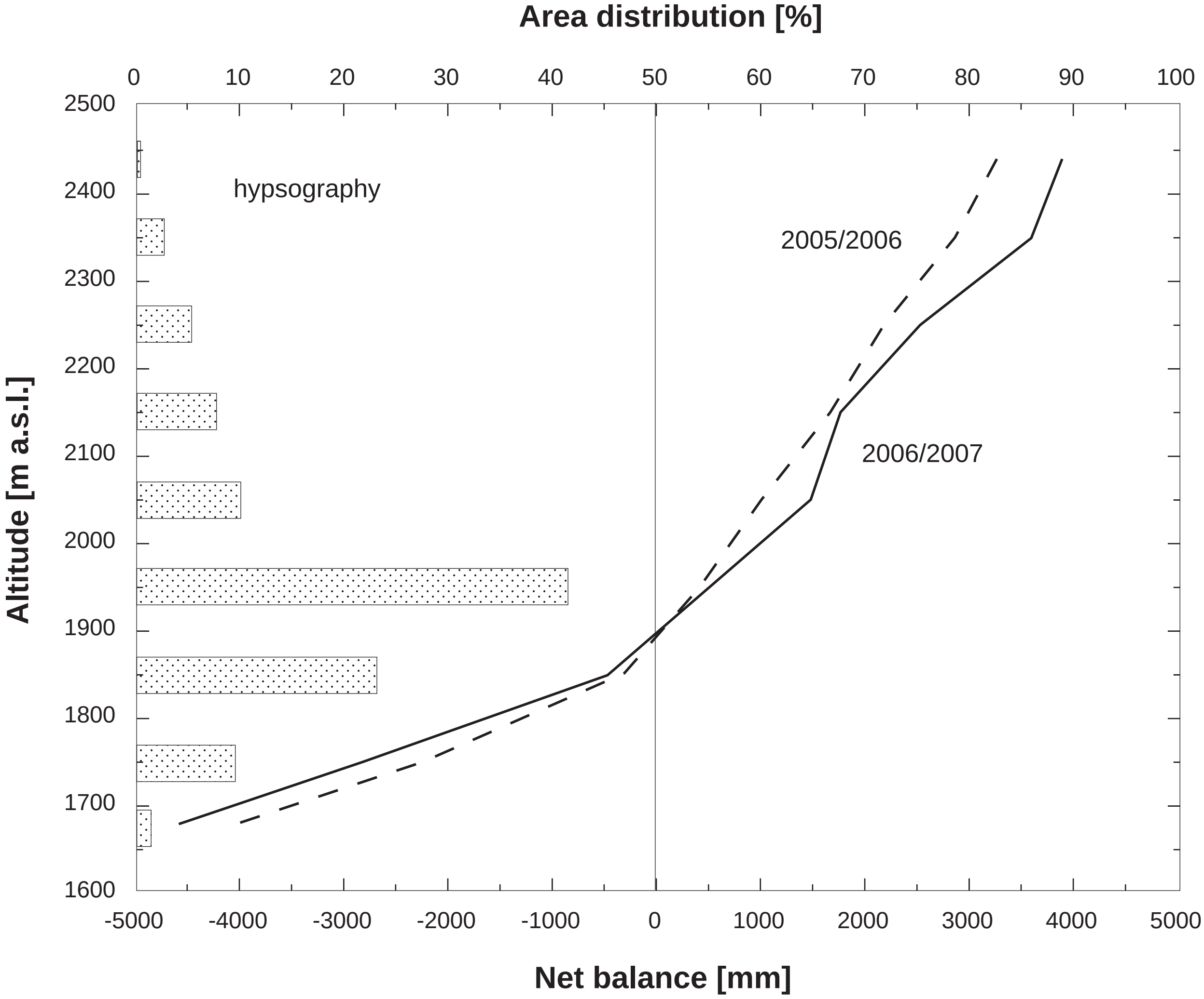

3.11.4 Accumulation area ratio (AAR) and equilibrium line altitude (ELA) versus specific net balance for the whole observation period

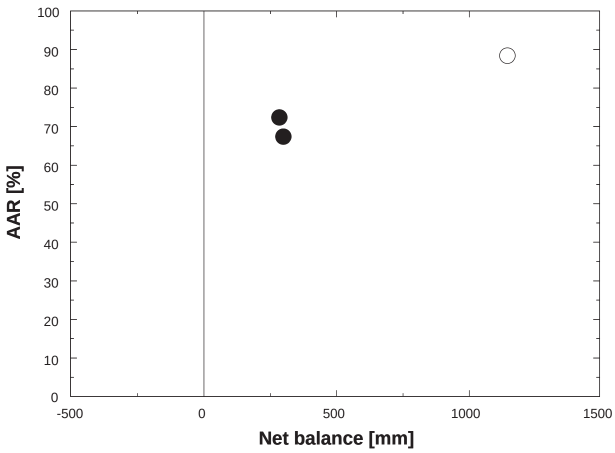

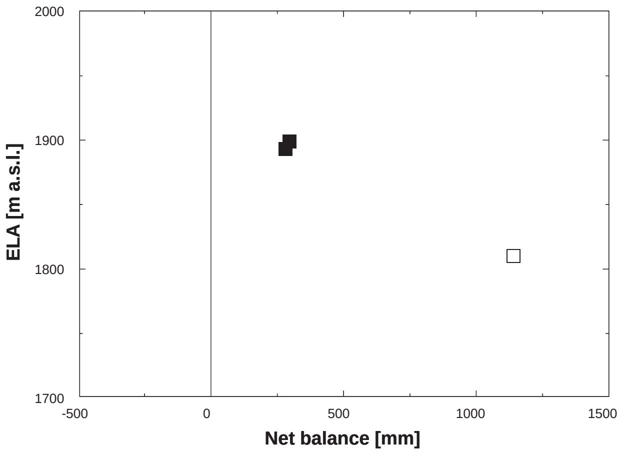

3.12 NIGARDSBREEN (NORWAY/WEST NORWAY)

COORDINATES: 61.72 N / 07.13 E

Photo taken by B. Kjøllmoen, 31st of July 2002.

Nigardsbreen is one of the largest outlet glaciers (47.8 km^2) of the Jostedalsbreen Ice Cap in Southern Norway and reaches from 1960 m to 320 m a.s.l. Its wide accumulation area discharges into a narrow tongue, both being generally exposed to the south-east. The glacier is assumed to be entirely temperate and the periglacial area to be predominantly free of permafrost. Average annual precipitation for the 1961–1990 period is 1380 mm and mean annual air temperature at the equilibrium line is estimated at −3 °C. Since the beginning of detailed mass balance measurements in 1962, glacier thickness has greatly increased, especially after 1988.

In 2005/06, the winter balance was +1750 mm w.e. (73 % of the mean value for the total observation period) and summer balance was −3150 mm w.e. (160 % of the average 1962–2005). The resulting mass balance is −1400 mm w.e. and the calculated equilibrium line altitude is about 1850 m a.s.l. In 2006/07, the winter balance was +3090 mm w.e. (131 % of the average for the period 1962–2006) and summer balance was −2045 mm w.e. (103 % of the long-term mean). The resulting mass balance was +1045 mm w.e. The calculated equilibrium line altitude is about 1320 m a.s.l. Since 1962, the cumulative mass balance has been calculated as 18000 mm w.e.

3.12.1 Topography and observation network

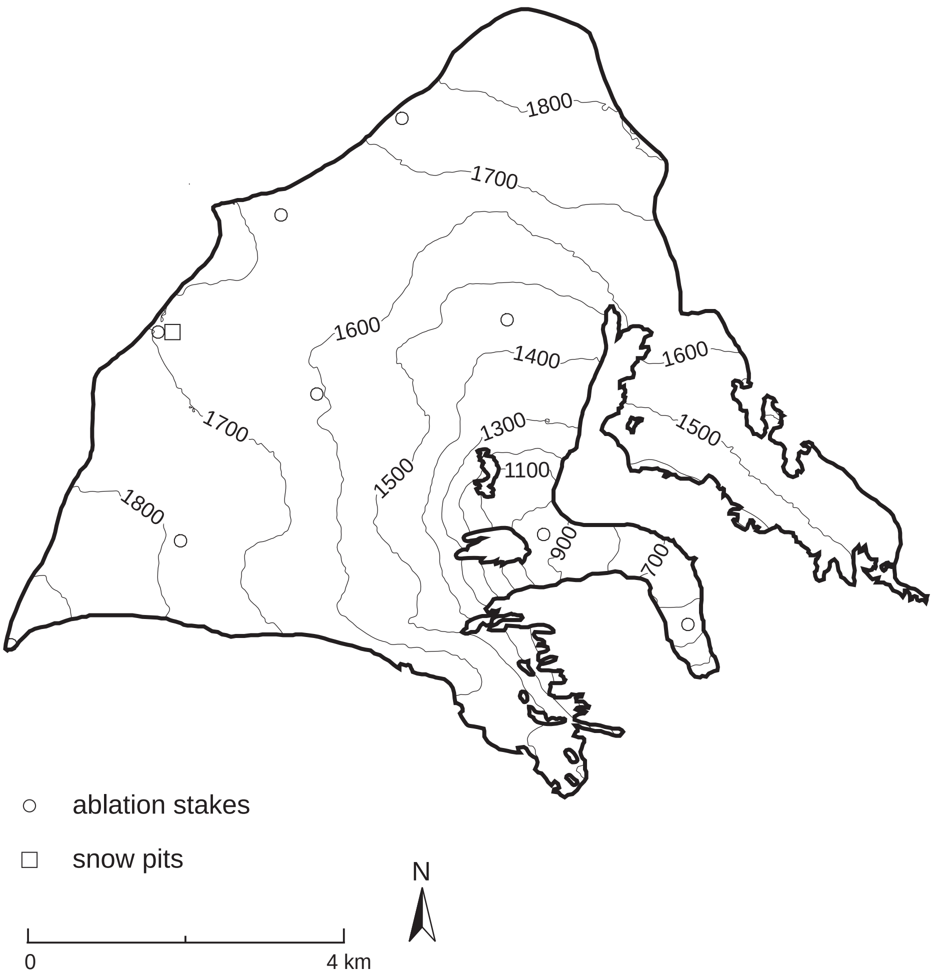

3.12.2 Net balance maps 2005/2006 and 2006/2007

2005/2006

2006/2007

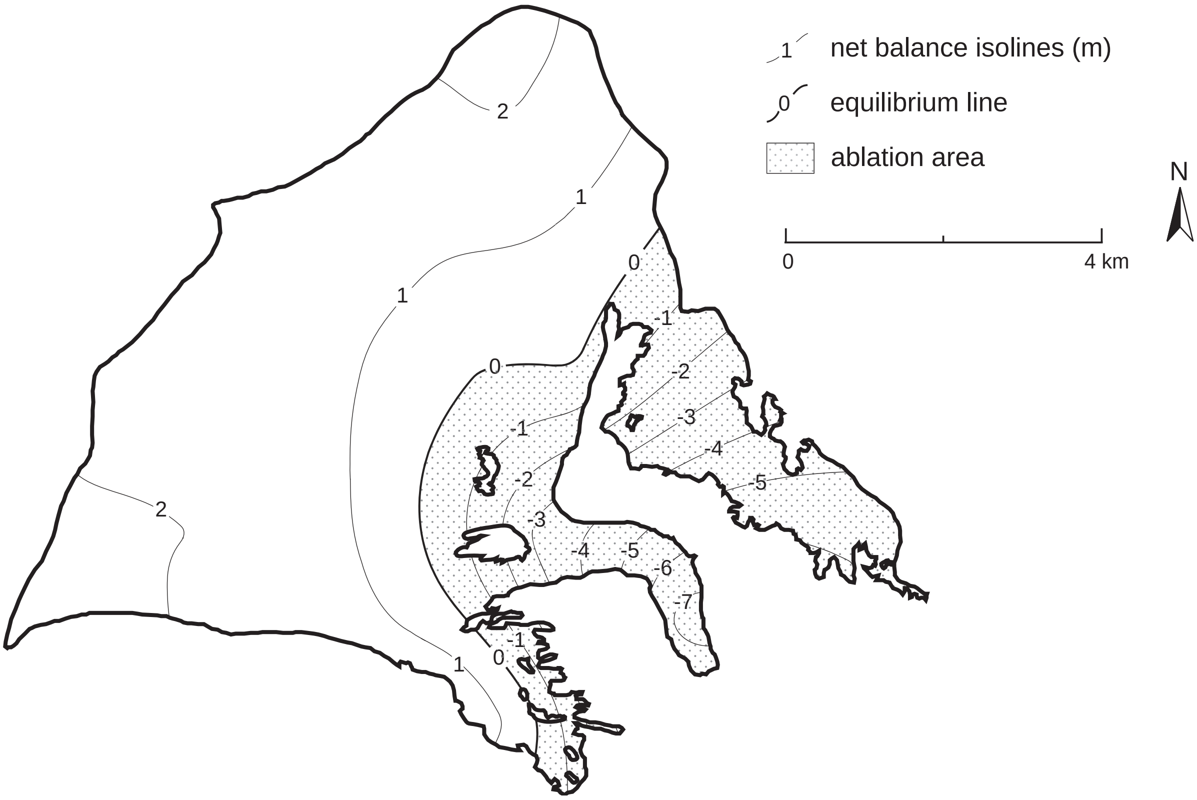

Nigardsbreen (NORWAY)

3.12.3 Net balance versus altitude (2005/2006 and 2006/2007)

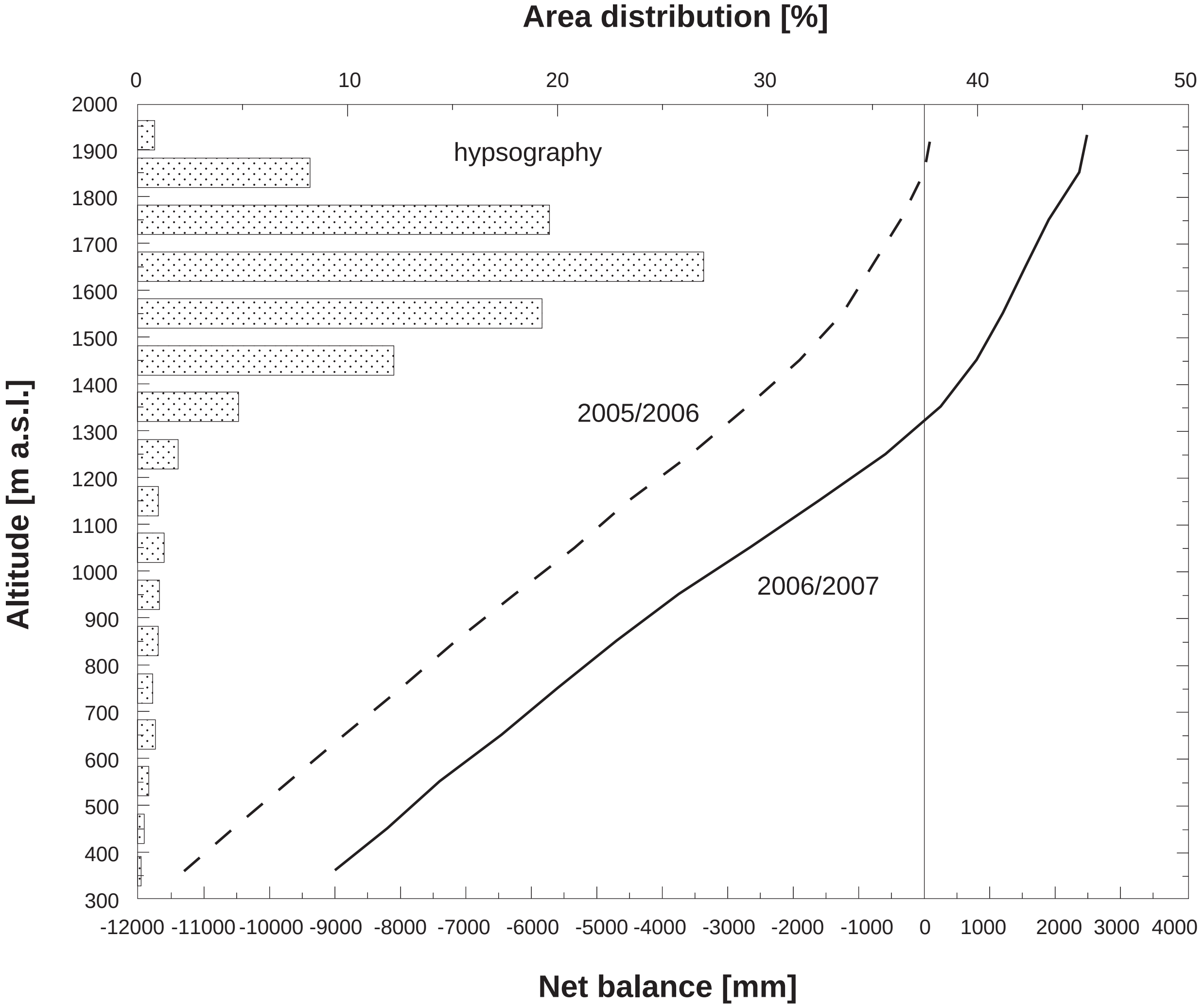

3.12.4 Accumulation area ratio (AAR) and equilibrium line altitude (ELA) versus specific net balance for the whole observation period

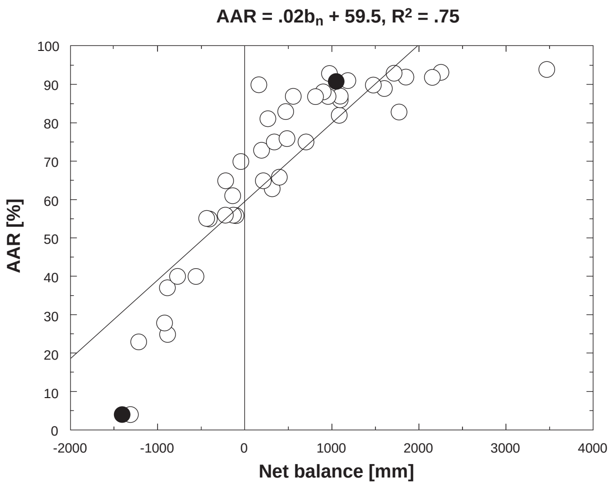

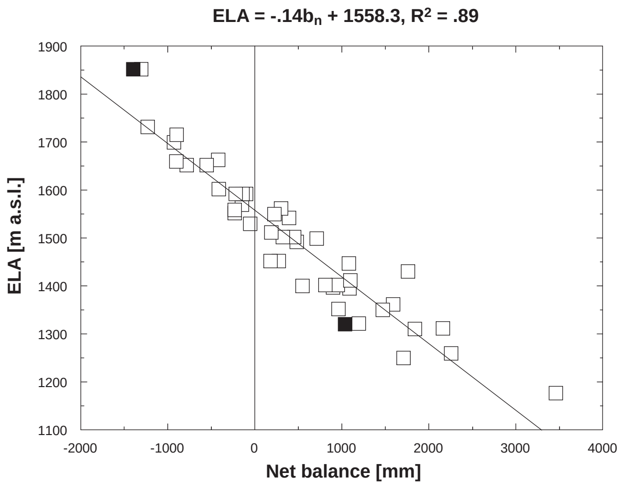

Nigardsbreen (NORWAY)

3.13 WALDEMARBREEN (NORWAY/SPITSBERGEN)

COORDINATES: 78.67 N / 12.00 E

Photo taken by I. Sobota, summer 2007.

Waldemarbreen is located in the northern part of the Oscar II Land, north-western Spitsbergen and flows downvalley to the Kaffiøyra plane. Kaffiøyra is a coastal lowland situated on the Forlandsundet. The glacier is composed of two parts separated by a 1600 m long medial moraine. It occupies an area of 2.5 km^2 and extends from 500 m to 140 m a.s.l. with a general exposure to the west. Mean annual air temperature in this area is about −4 to −5 °C and annual precipitation is generally 300–400 mm. Since the nineteenth century the surface area of the Kaffiøyra glaciers has decreased by approximately 35 %. Recently the Waldemarbreen has been retreating. Detailed mass balance investigations have been conducted since 1995.

The balance in 2005/06 showed a net mass loss of −747 mm w.e., winter accumulation +550 mm w.e. and summer ablation −1297 mm w.e. The ablation in 2006/07 was also higher than normal (−1292 mm w.e.) and the accumulation was +521 mm w.e., resulting in a balance of –771 mm w.e. The mean value of the mass balance for the period 1995–2007 is −587 mm w.e.

3.13.1 Topography and observation network

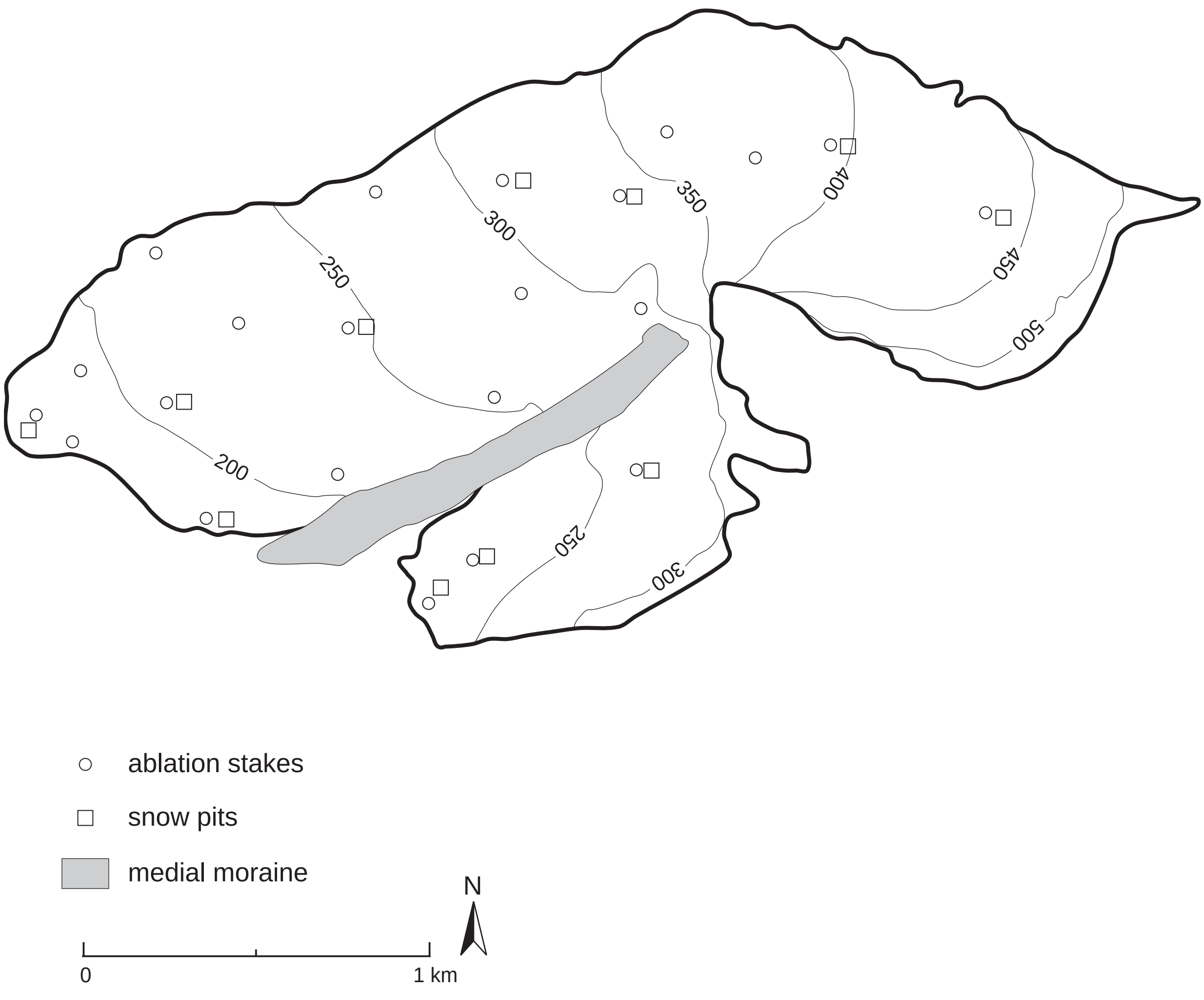

3.13.2 Net balance maps 2005/2006 and 2006/2007

2005/2006

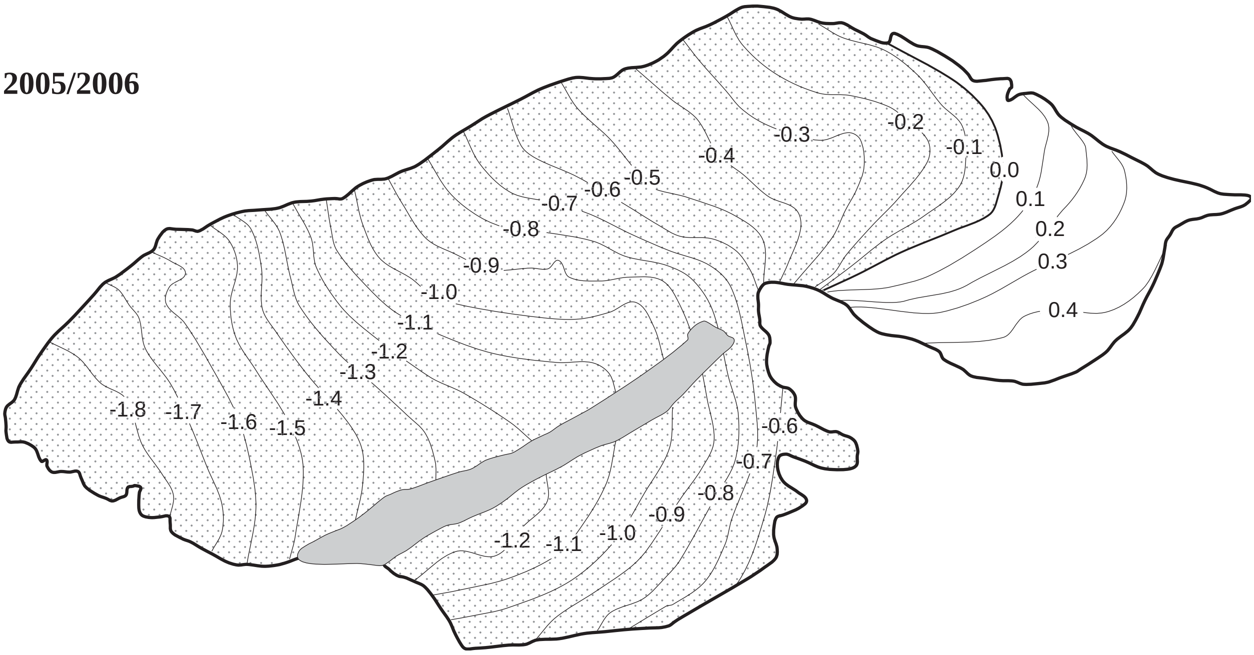

2006/2007

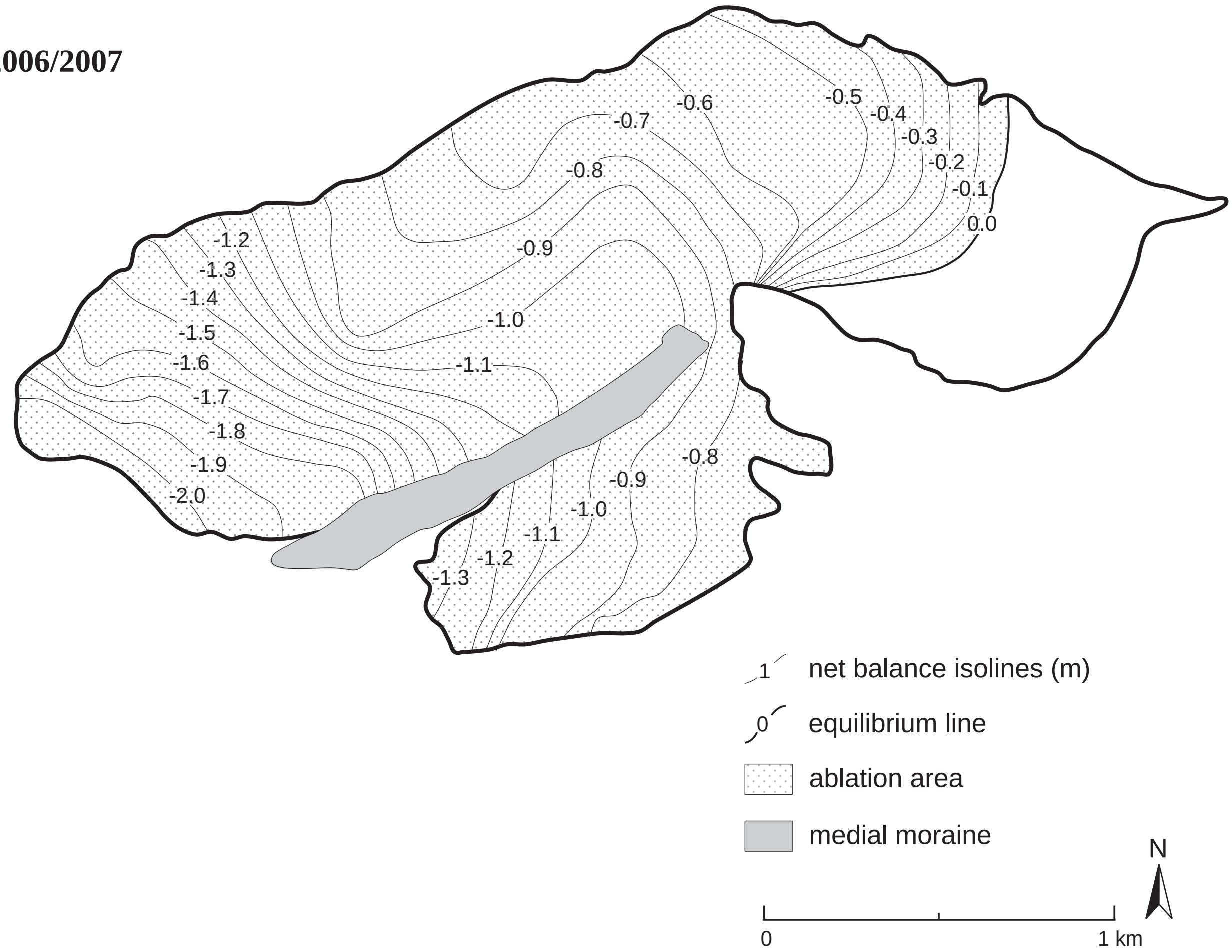

Waldemarbreen (NORWAY)

3.13.3 Net balance versus altitude (2005/2006 and 2006/2007)

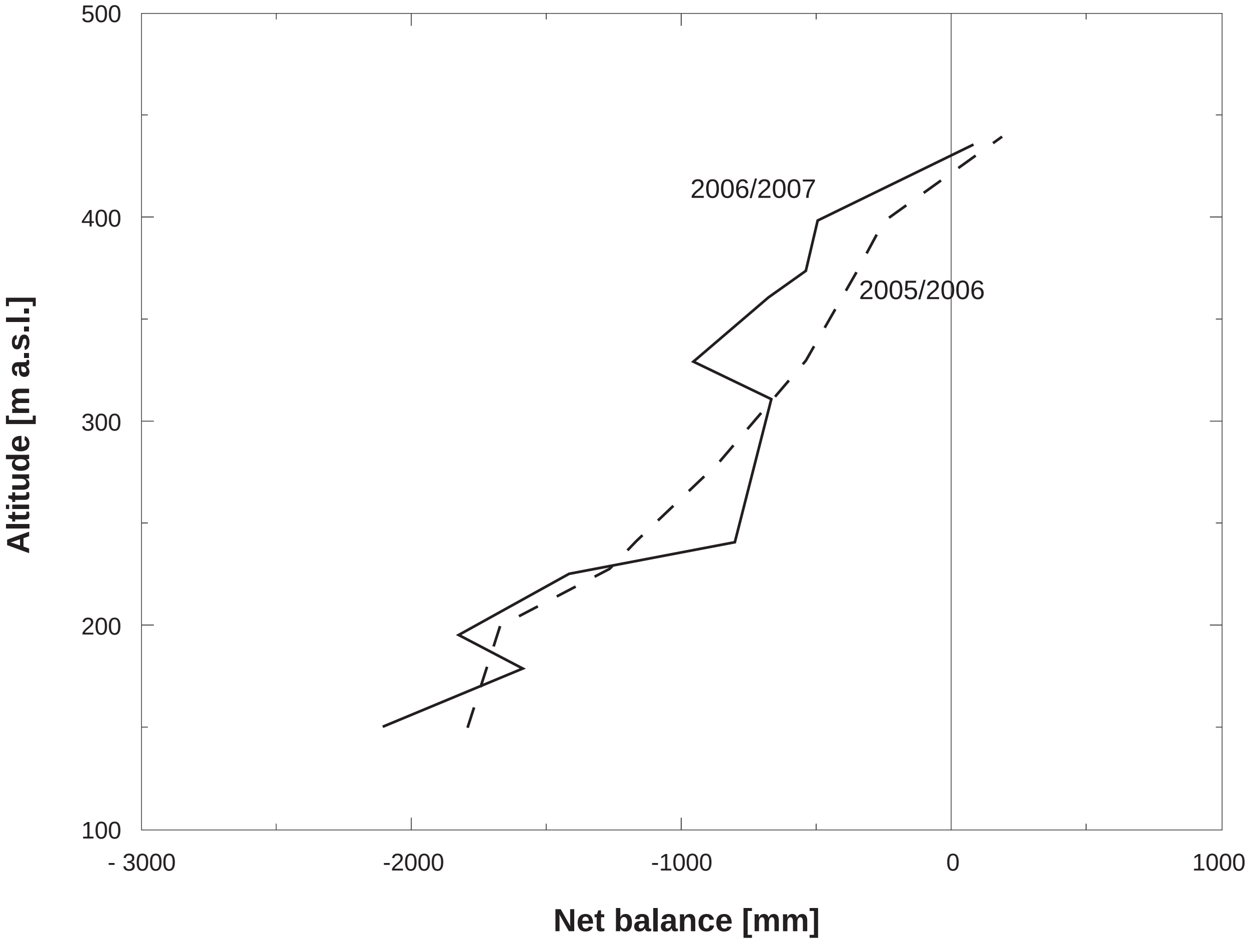

3.13.4 Accumulation area ratio (AAR) and equilibrium line altitude (ELA) versus specific net balance for the whole observation period

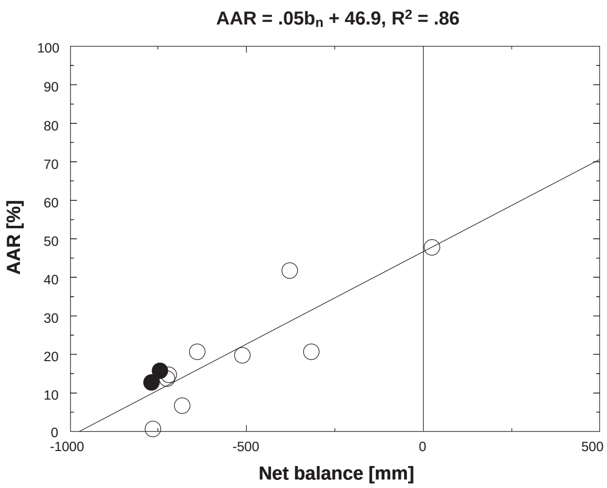

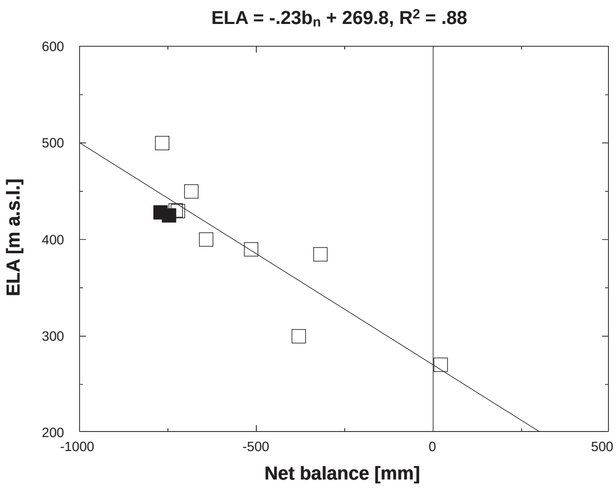

3.14 DJANKUAT (RUSSIA/NORTHERN CAUCASUS)

COORDINATES: 43.20 N / 42.77 E

Photo taken by V. Popovnin in August 2001.

The valley-type glacier is located on the northern slope of the central section of the Main Caucasus Ridge and extends from 3700 m to 2720 m a.s.l. Its surface area is 2.93 km^2 and the exposure is to the north-west. Mean annual air temperature at the ELA (ca. 3200 m a.s.l. for balanced conditions) is −3 to −4.5 °C and the glacier is temperate. Periglacial permafrost is highly discontinuous. Average annual precipitation as measured near the snout is 1100 to 1200 mm, but roughly three times this amount at the ELA. Seven 1:10000 topographic maps (from 1968, 1974, 1984, 1992, 1996, 1999 and 2006) exist at Moscow State University but are not yet published. The peculiarity of the glacier is the migration of the ice divide on the firn plateau of the crest zone, redistributing mass flux between adjacent slopes of the main ridge.

Two reported years were extraordinarily unfavourable for the glacier. Such huge biannual ice loss (−800 mm w.e. and −2010 mm w.e.) has never been registered throughout the 40-year monitoring period. The glacier experienced considerable deficits in winter snow (7 and 26 %), but much more decisive was the unusually high ablation: it exceeded its norm by 20 % in 2005/06 and more than 1.5 times the following year. Ablation (ca. 4000 mm w.e.) and mass balance in 2006/07 broke records, – first of all, owing to an extremely long melt season (at the expense of springtime, particularly) in the lowest altitudinal spans. The probability of the registered ablation value is estimated as once per 70 years. This resulted in a noticeable morphological transformation of the terminal zone of the snout as well as in the icefall zone in the middle course where a long outcrop of the former subglacial barrier emerged from under the ice, partly breaking the continuity of the glacier body and depriving its left debris-covered snout periphery of nourishment from the upper reaches.

3.14.1 Topography and observation network

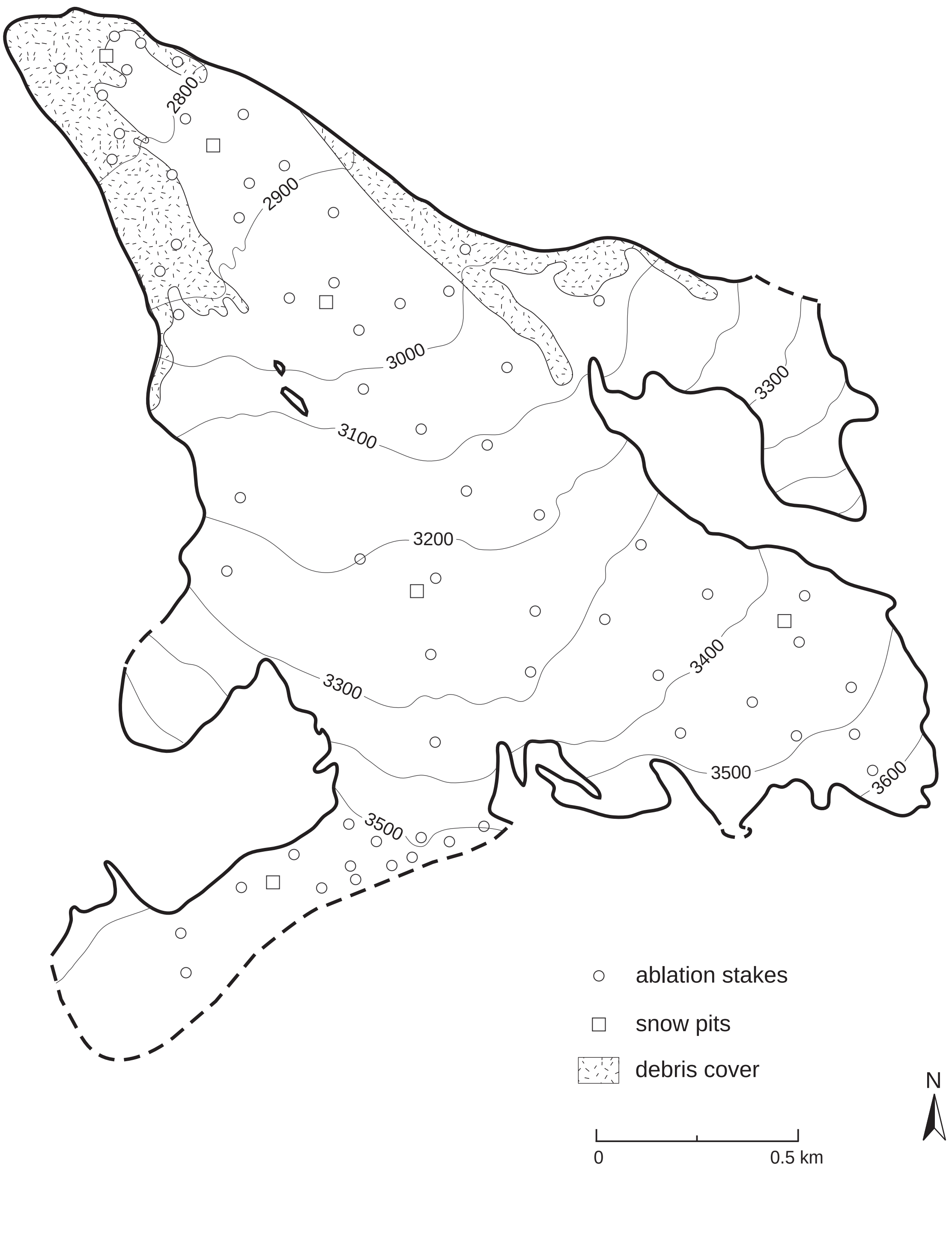

Djankuat (RUSSIA)

3.14.2 Net balance maps 2005/2006 and 2006/2007

2005/2006

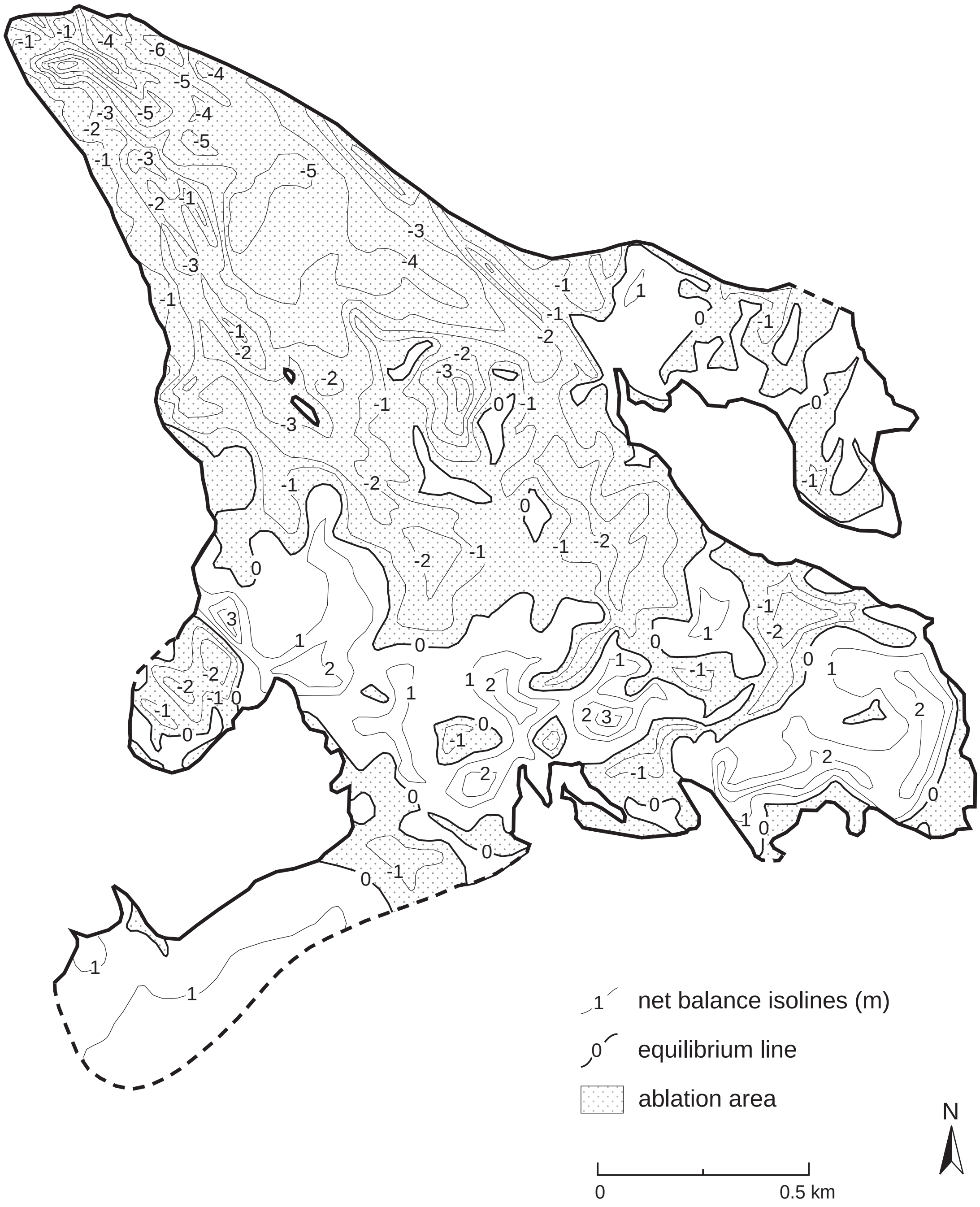

Djankuat (RUSSIA)

2006/2007

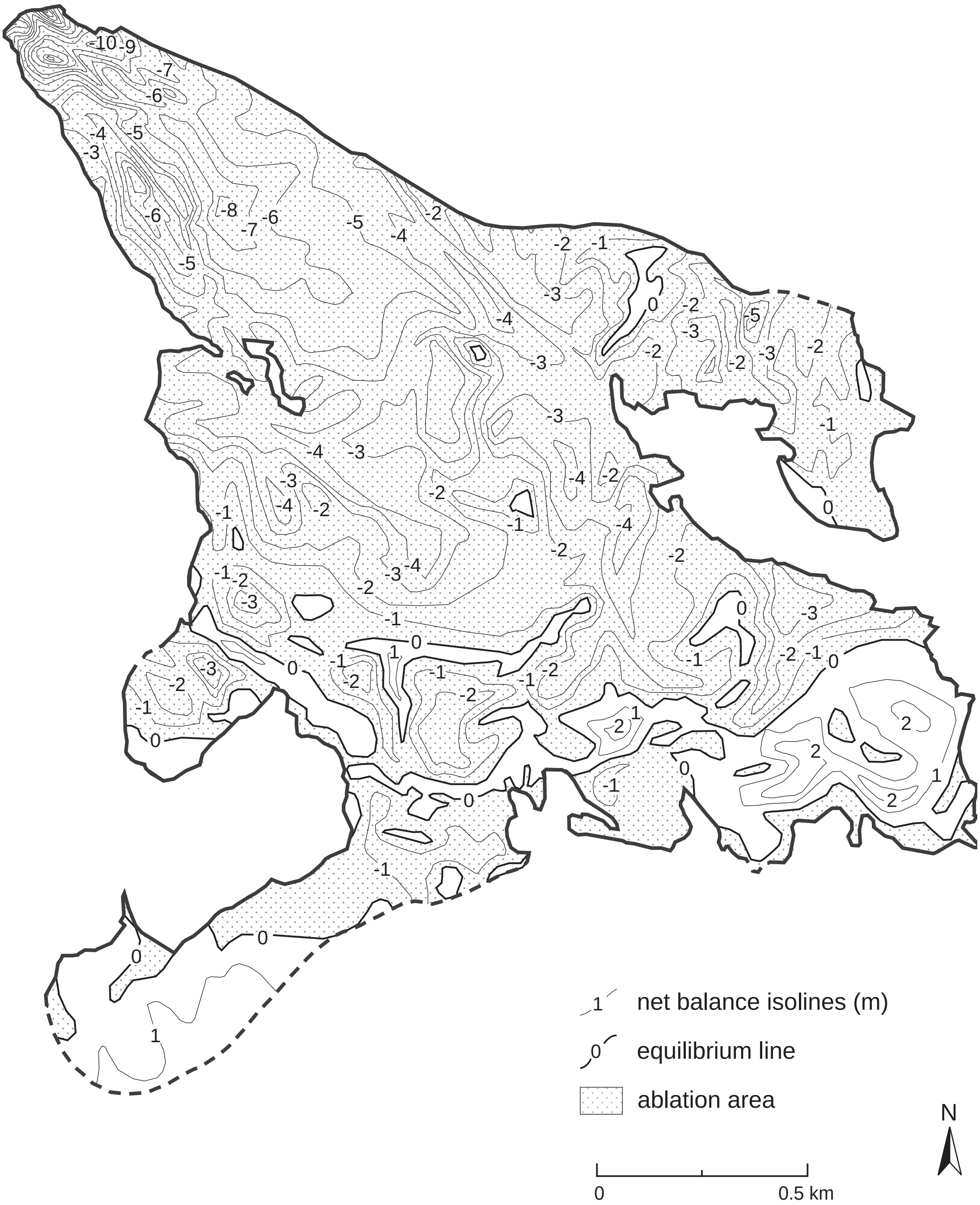

Djankuat (RUSSIA)

3.14.3 Net balance versus altitude (2005/2006 and 2006/2007)

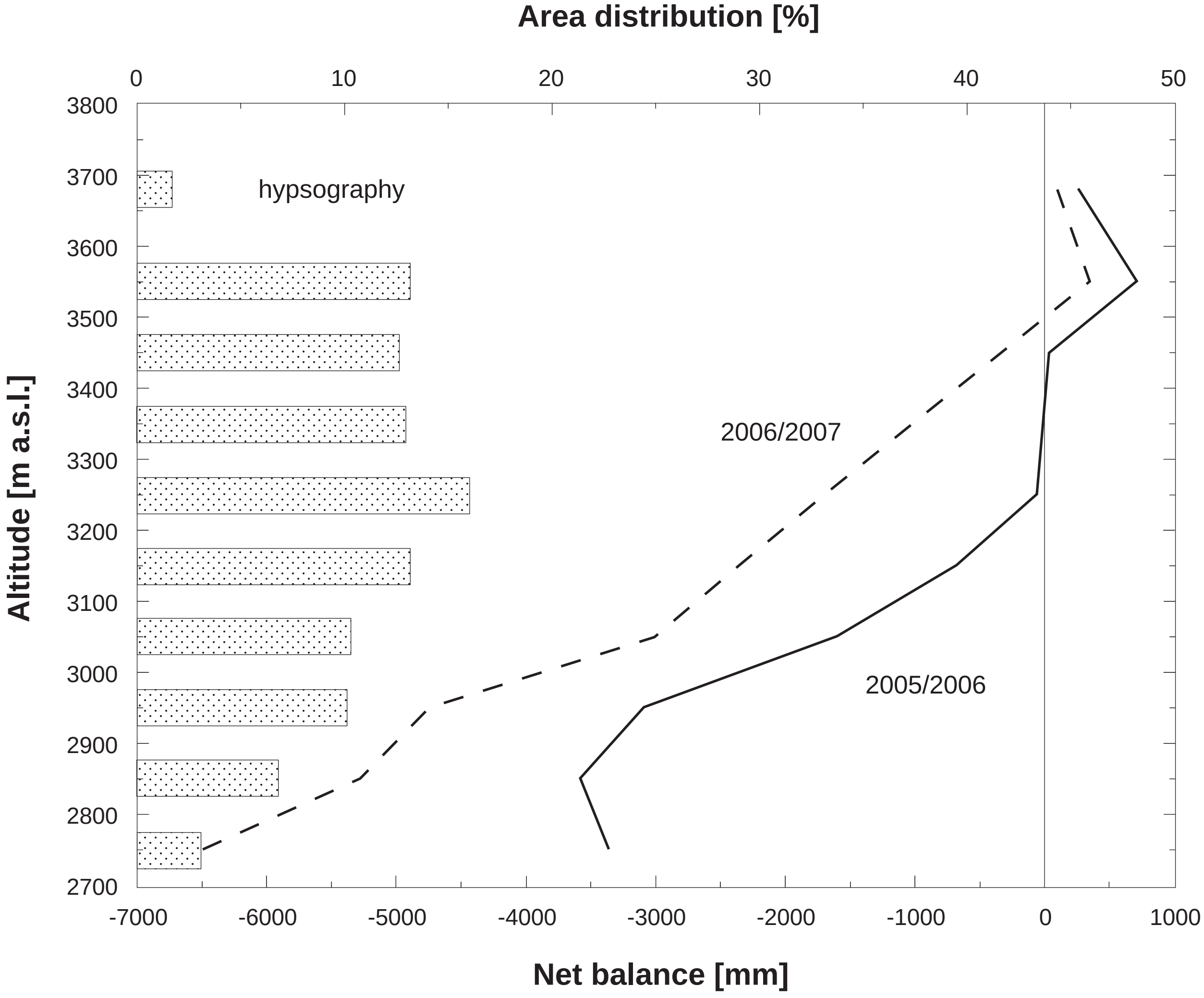

3.14.4 Accumulation area ratio (AAR) and equilibrium line altitude (ELA) versus specific net balance for the whole observation period

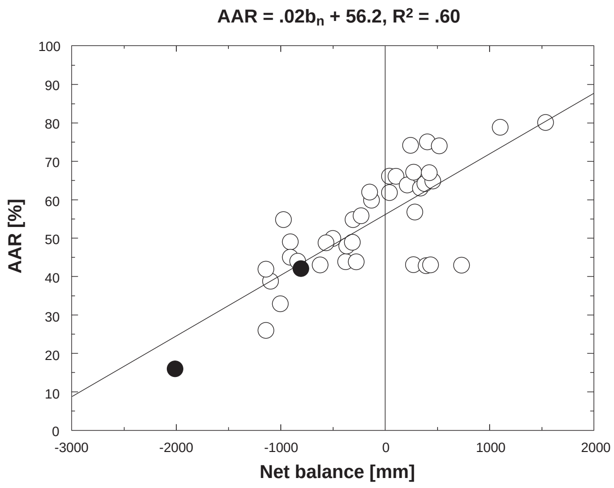

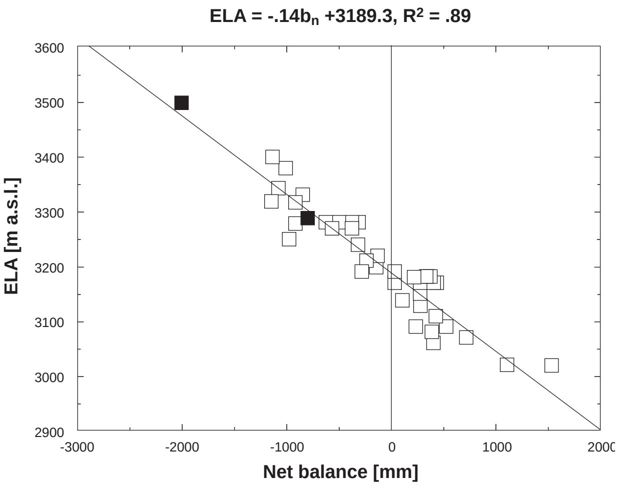

Djankuat (RUSSIA)

3.15 MALIY AKTRU (RUSSIA/ALTAY)

COORDINATES: 50.08 N / 87.75 E

Photo taken by Y.K. Narozhniy, 2nd of July 1992.

The valley-type glacier is located on the northern slope of the North Chuyskiy Range of the Russian Altai Mountains. It extends from 3714 m to 2246 m a.s.l., has a surface area of 2.72 km^2 and is exposed to the east and north. It has an average thickness of 90 m (max. 234 m) and its total volume is estimated to be 0.25 km^3. Mean annual air temperature at the equilibrium line of the glacier (around 3160 m a.s.l. for balanced conditions) is −9 to −10 °C. The glacier is polythermal and surrounded by continuous to discontinuous permafrost. Average annual precipitation, as measured at 2130 m a.s.l., is about 540 mm. Mass balances of three glaciers within the same basin are being determined.

In both reported years, 2005/06 and 2006/07, total accumulation was rather close to its norm (the correspondent deviations were −5 and −8 %), and annual ablation exceeded its long-term mean value by 10 and 14 %, respectively. As a result, mass balance remained negative as in the previous years. However, both the budget parameters and frontal retreat values were influenced considerably by the consequences of earthquakes in 2003–2004. For instance, mass loss due only to ice collapses from the terminal part of Maliy Aktru snout was about 40–60 mm w.e. (averaged over the entire glacier surface), and the terminus retreated at a velocity of 18–25 m a^{-1}, that is, 3–5 times higher than the common rate.

3.15.1 Topography and observation network

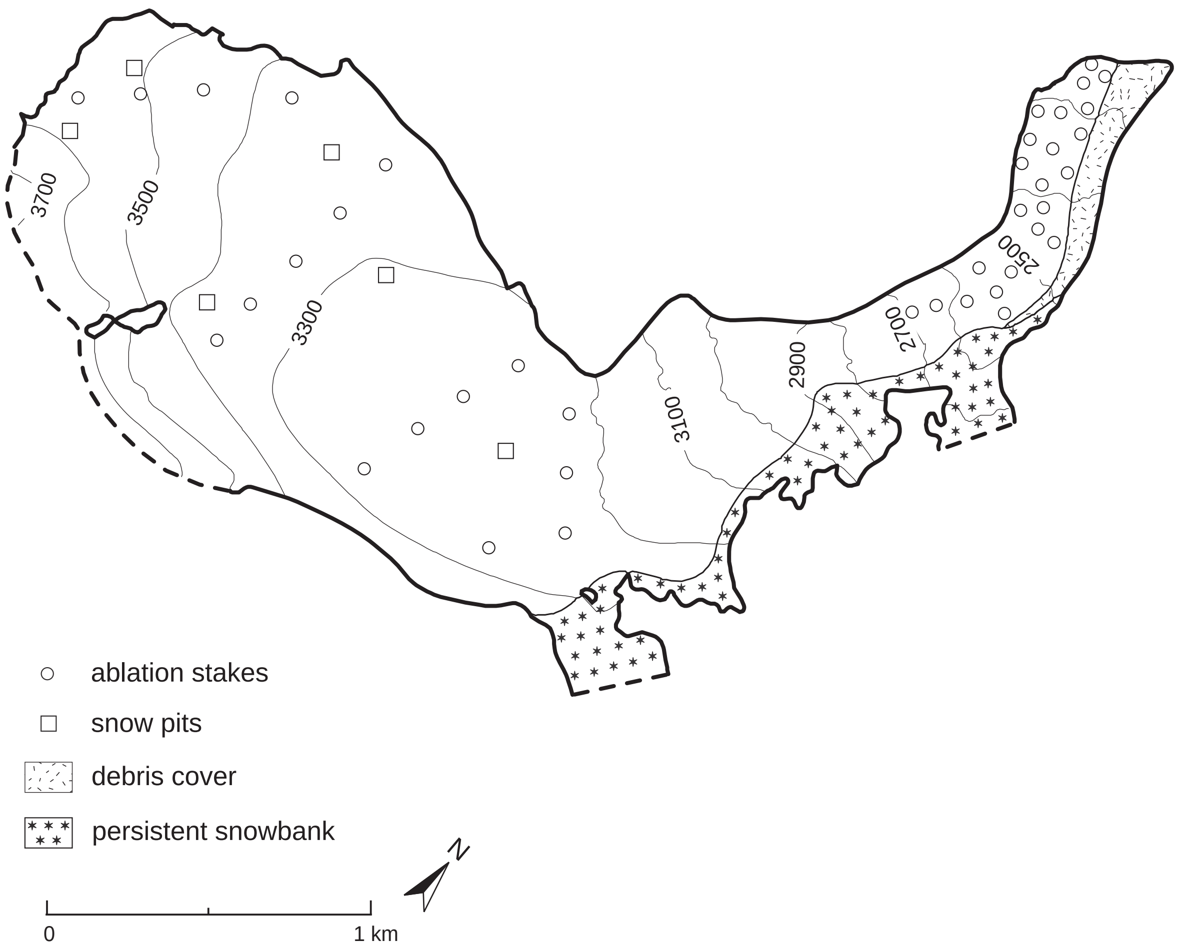

Maliy Aktru (RUSSIA)

3.15.2 Net balance maps 2005/2006 and 2006/2007

2005/2006

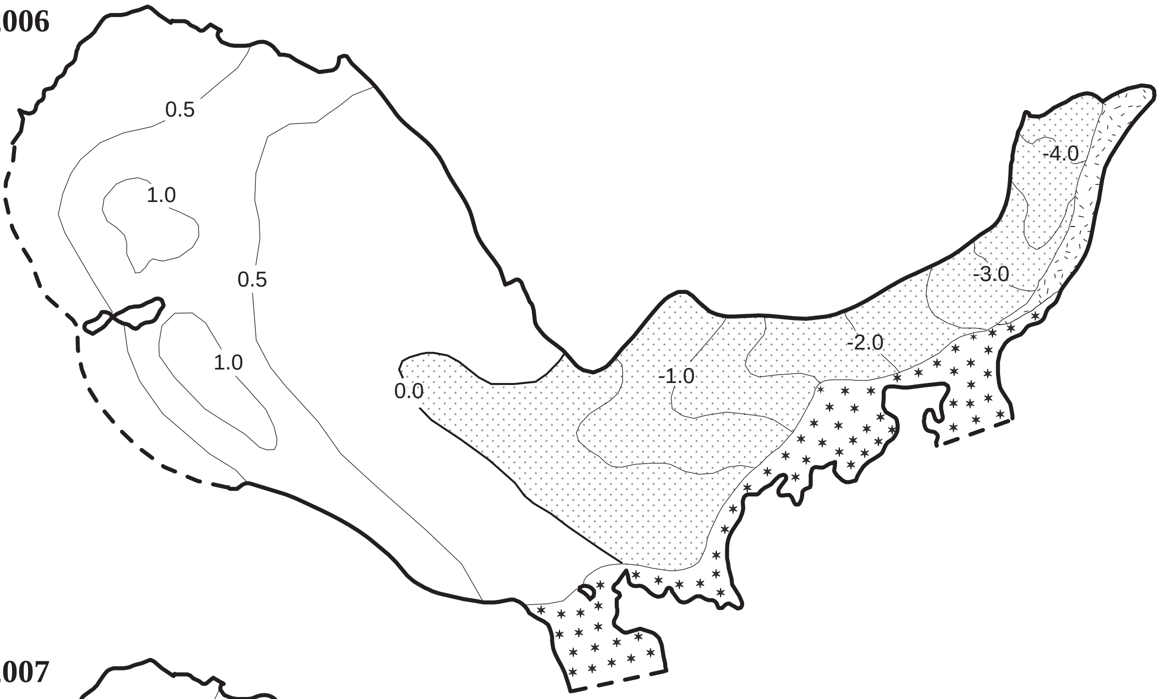

2006/2007

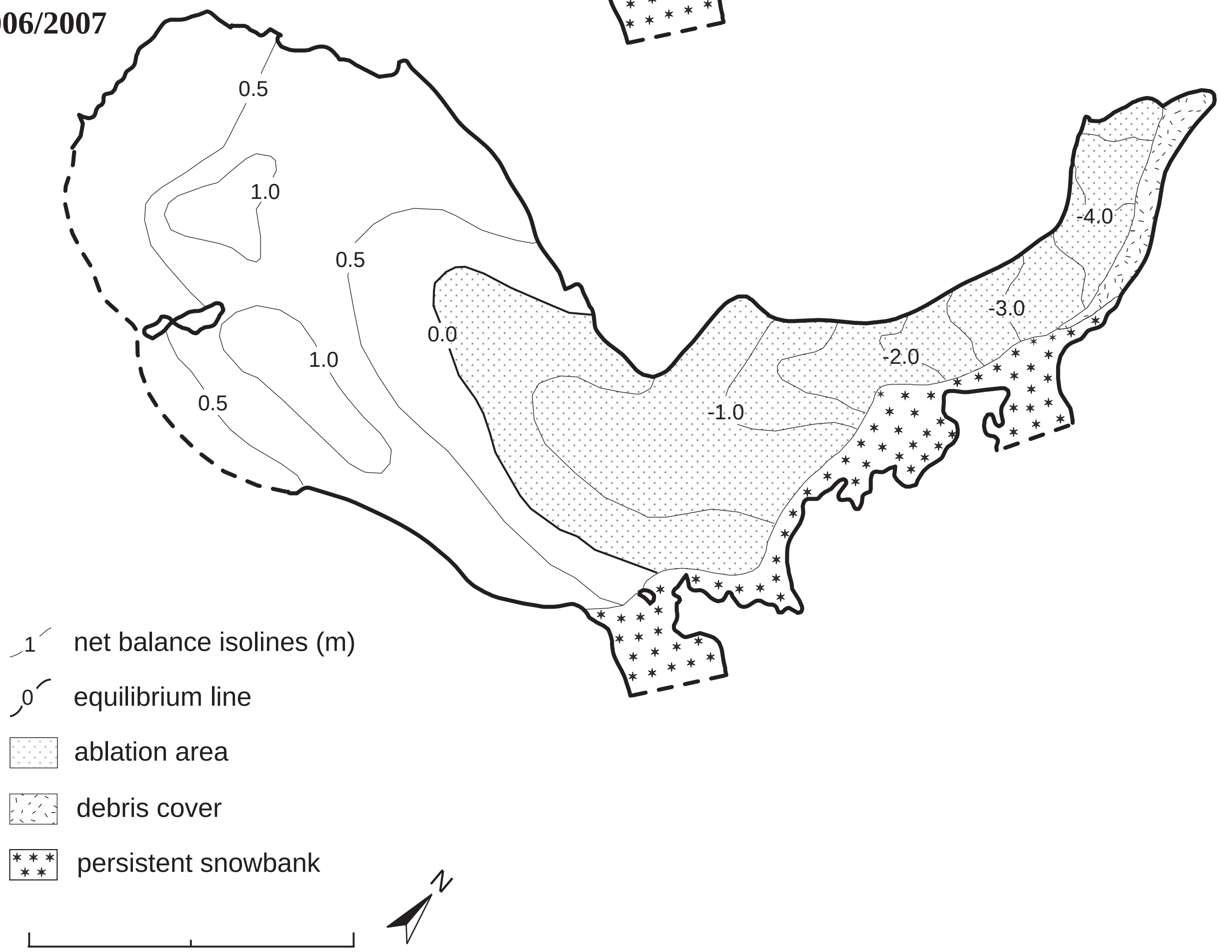

Maliy Aktru (RUSSIA)

3.15.3 Net balance versus altitude (2005/2006 and 2006/2007)

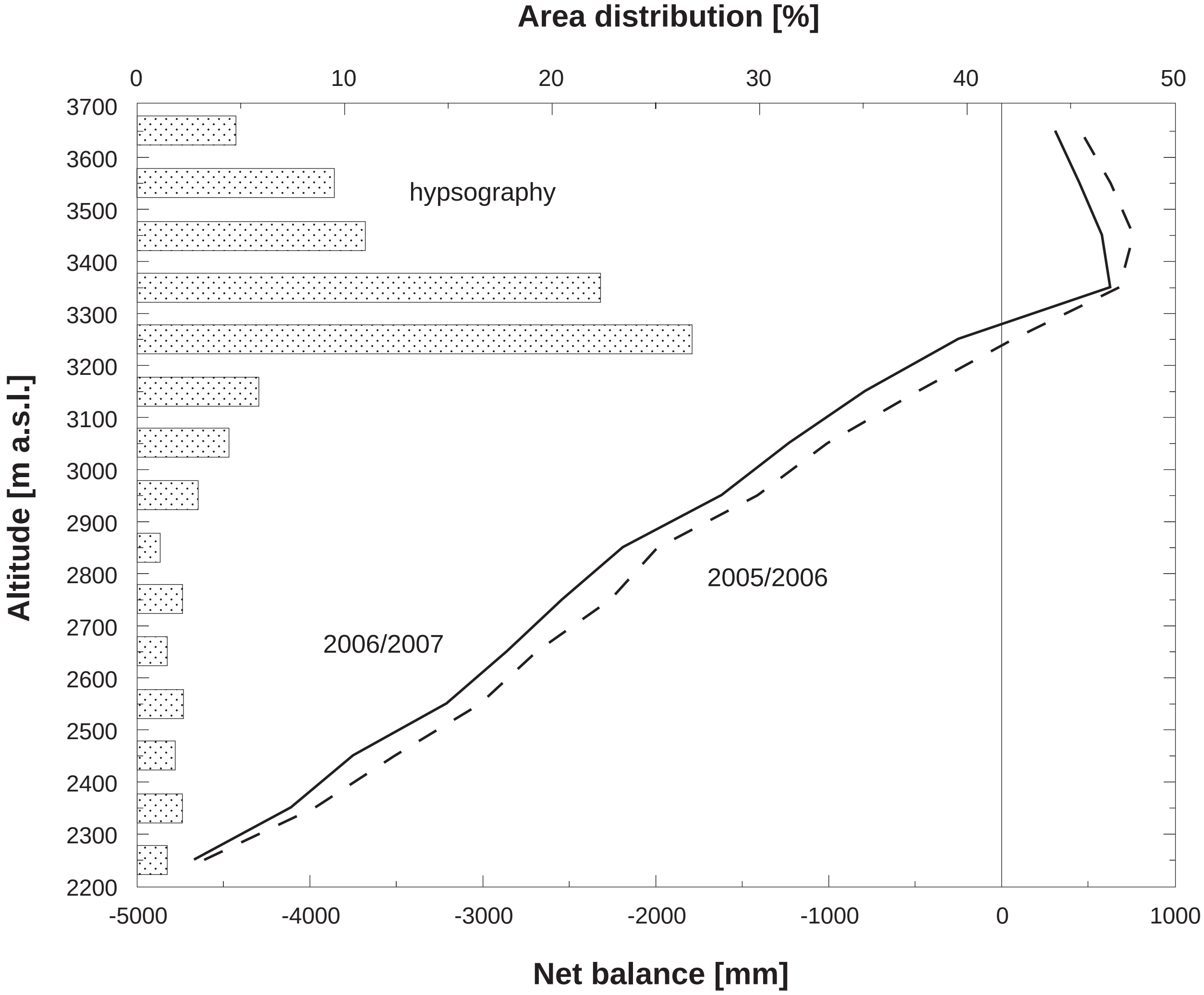

3.15.4 Accumulation area ratio (AAR) and equilibrium line altitude (ELA) versus specific net balance for the whole observation period

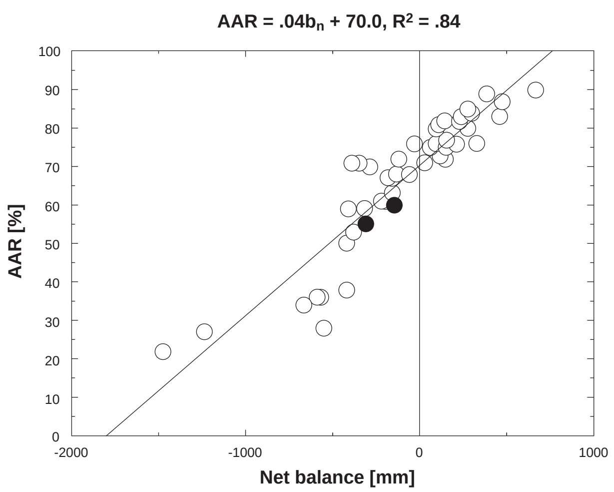

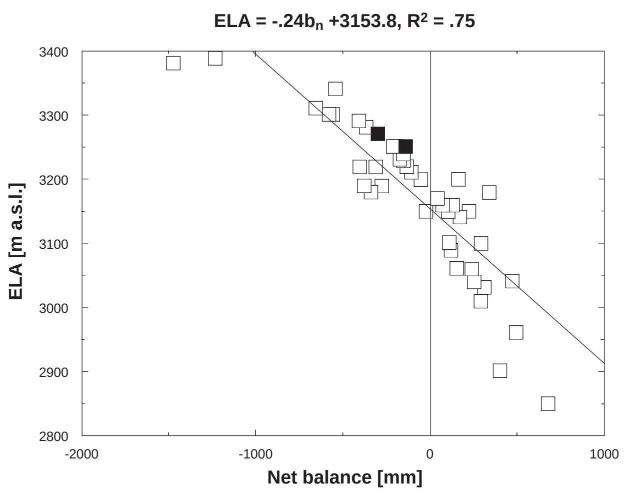

Maliy Aktru (RUSSIA)

3.16 STORGLACIÄREN (SWEDEN/NORTHERN SWEDEN)

COORDINATES: 67.90 N / 18.57 E

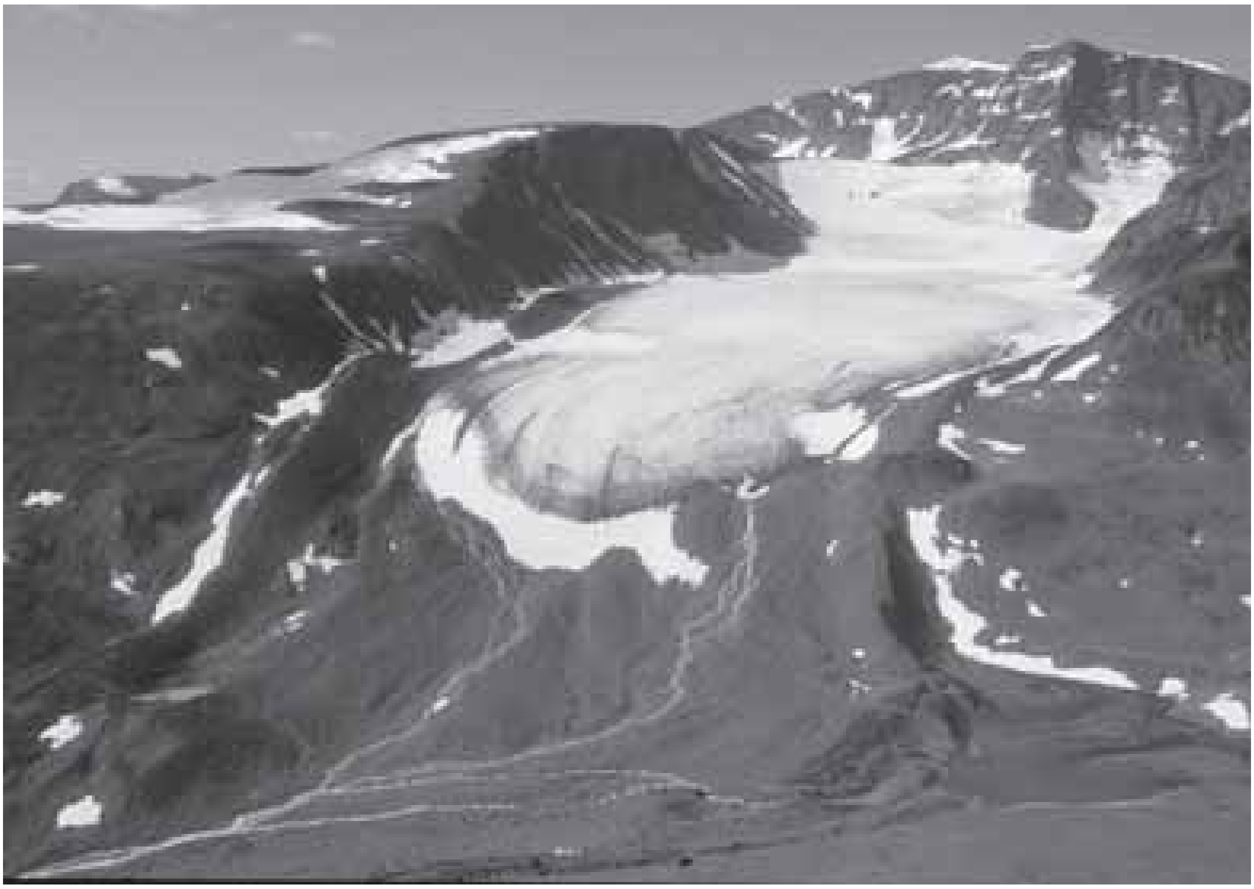

Photo taken by P. Holmlund on 4th of August 2004.

Storglaciären in the Kebnekaise Mountains of northern Sweden is a small valley-type glacier with a divided accumulation area and a smooth longitudinal profile. It is exposed to the east, maximum and minimum elevations are 1750 m and 1130 m a.s.l., surface area is 3.12 km^2, and average thickness is 95 m (maximum thickness is 250 m). Mean annual air temperature at the equilibrium line of the glacier (around 1450 m a.s.l. for balanced conditions) is about −6 °C. Approximately 85 % of the glacier is temperate with a cold surface layer in its lower part (ablation area), and its tongue lying in discontinuous permafrost. Average annual precipitation is about 1000 mm at the nearby Tarfala Research Station.

The net balance in 2005/06 was negative (−1720 mm w.e.) with an ELA at 1615 m a.s.l and a small AAR of 17 %. In 2006/07, the net balance was positive (+410 mm w.e.), which was also reflected in the ELA at 1480 m a.s.l. and the AAR of 50 %. Aerial photographs and corresponding glaciological maps are available for the years 1949/59/69/80/90/99. Recently, diapositives of the original photographs were reprocessed using uniform photogrammetric methods. A comparison of the glaciological mass balance with these new volume changes is in progress.

3.16.1 Topography and observation network

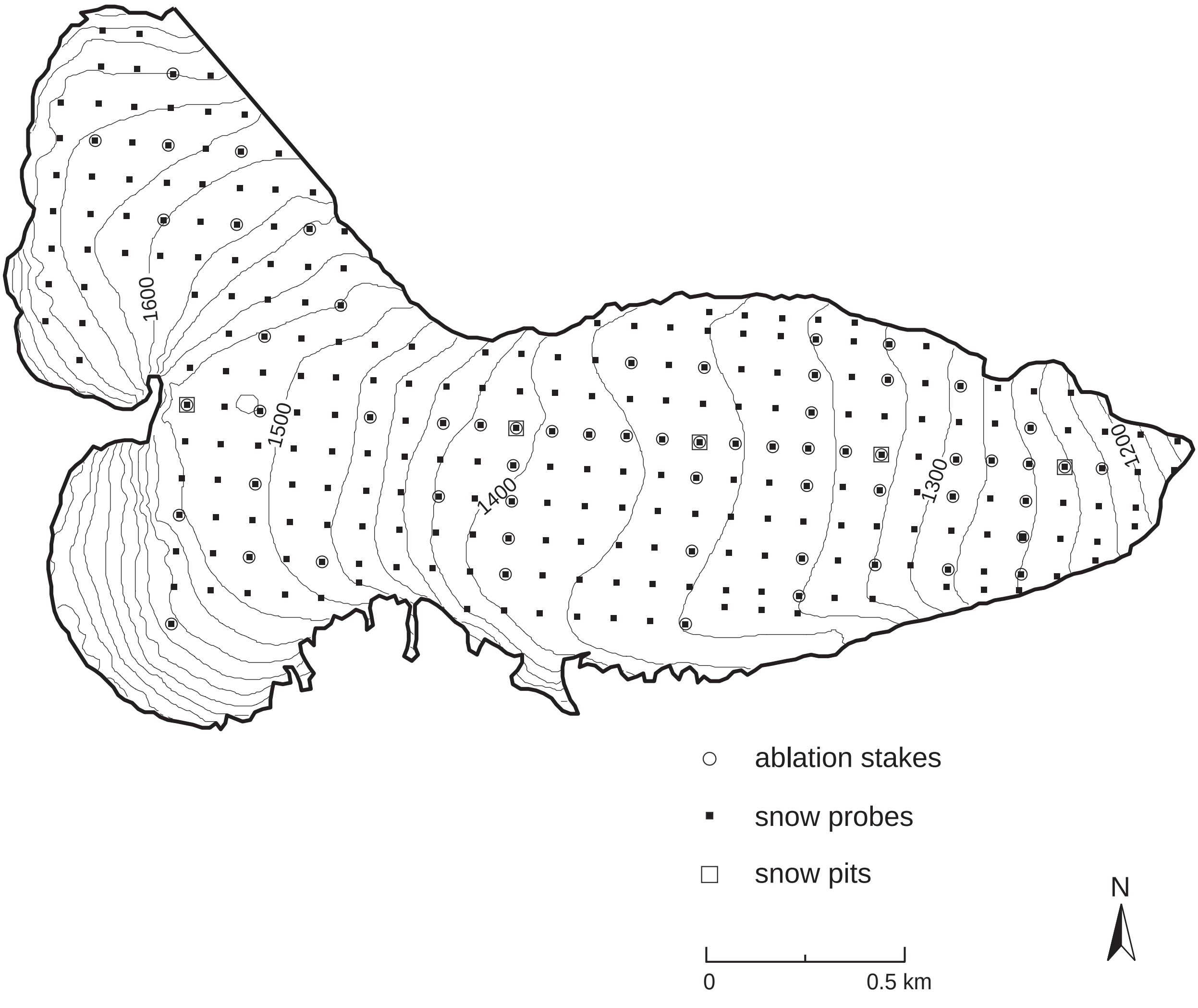

Storglaciären (SWEDEN)

3.16.2 Net balance maps 2005/2006 and 2006/2007

2005/2006

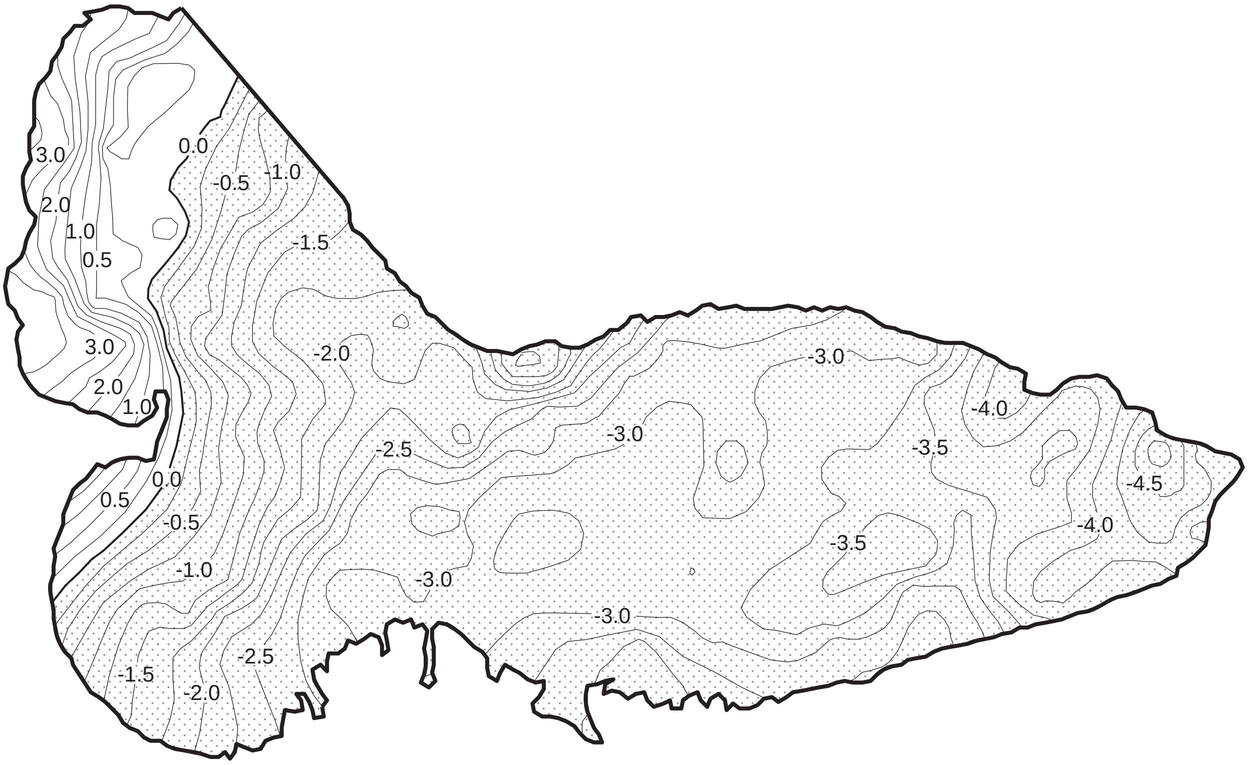

2006/2007

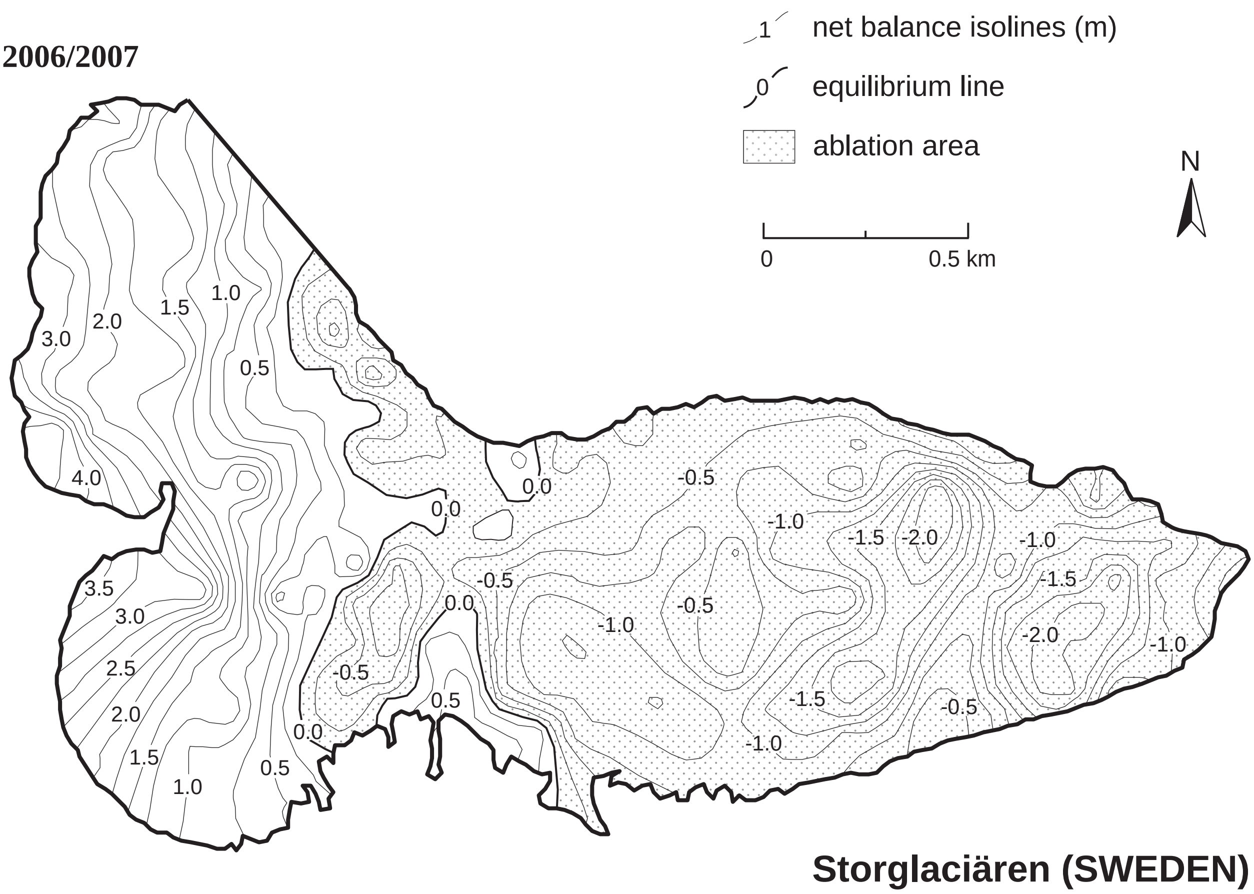

Storglaciären (SWEDEN)

3.16.3 Net balance versus altitude (2005/2006 and 2006/2007)

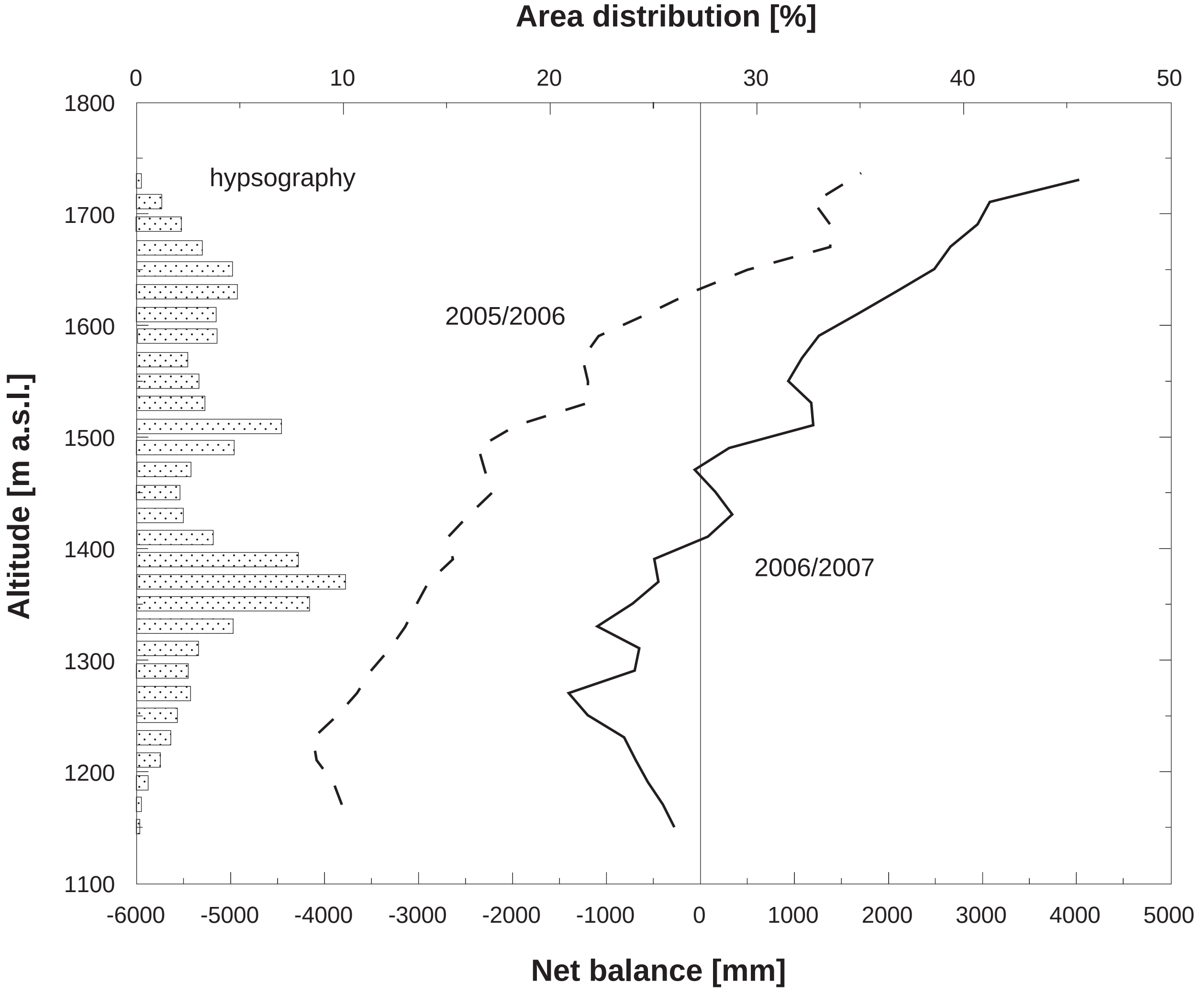

3.16.4 Accumulation area ratio (AAR) and equilibrium line altitude (ELA) versus specific net balance for the whole observation period

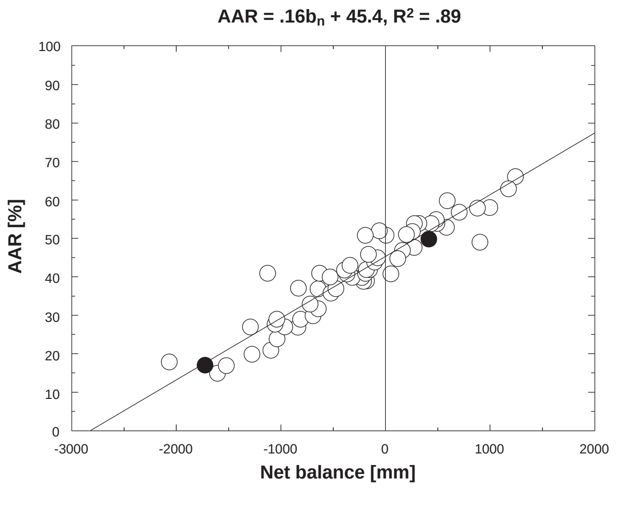

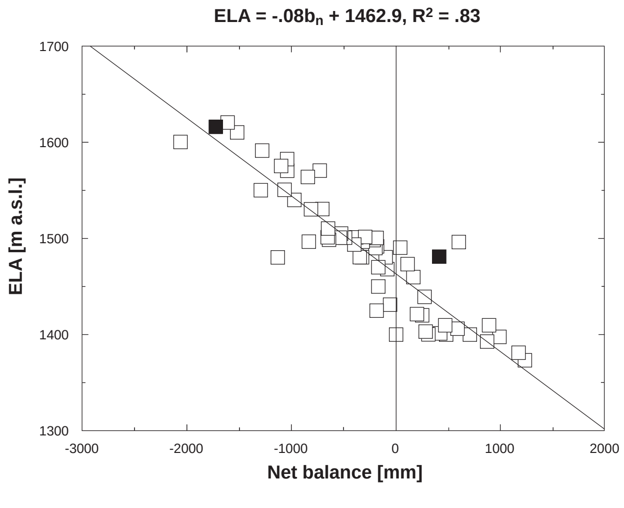

Storglaciären (SWEDEN)

4 FINAL REMARKS AND ACKNOWLEDGEMENTS

Continuous mass balance records for the period 1980–2007 are now available for 30 glaciers from 9 mountain ranges. These glaciers have well-documented, long-term mass balance measurements based on the direct glaciological method (cf. Østrem and Brugman, 1991) and are not dominated by non-climatic drivers such as calving or surge dynamics. Corresponding results from this sample of glaciers in North and South America and Eurasia are summarized in Table 4.1 (all mm values in water equivalent):

Table 4.1: Summarized mass balance data. The mean specific (annual) net balance of 30 glaciers averaged for the years 2000–2007, compared to the mean of the annual means of the last 20 years, is shown in the upper table. A statistical overview of the 30 glaciers during the two reported years is given in the lower table.

		1980–1999			2000–2007	
mean specific (annual) net balance	−	296 mm		−	706 mm	
standard deviation of means	±	257 mm		±	410 mm	
minimum mean value	−	728 mm	(1998)	−	1269 mm	(2003)
maximum mean value	+	107 mm	(1983)	−	61 mm	(2000)
range		835 mm			1208 mm	
positive mean balances		15 %			0 %	
positive balances		32 %			18 %	

		2005/2006			2006/2007	
mean specific (annual) net balance	−	1247 mm		−	676 mm	
standard deviation	±	835 mm		±	1058 mm	
minimum value	−	3190 mm	Ålfotbreen	−	2745 mm	Caresèr
maximum value	+	560 mm	Echaurren Norte	+	1270 mm	Ålfotbreen
range		3750 mm			4015 mm	
positive balances		3 %			17 %	

Taking the two reported years together, the mean mass balance was –962 mm w.e. per year. This represents more than a meter ice thickness loss per year and exceeds by about 35 % the mean mass balance since the turn of the century (2000–2007: –706 mm w.e.), and is more than three times the average of 1980–1999 (–296 mm w.e.). During this most recent time interval, the maximum loss of the 1980–1999 time period (–728 mm w.e. in 1998) was already exceeded for the third time (–1269 mm w.e. in 2003, –744 mm w.e. in 2004, –1247 mm in 2006); the percentage of positive glacier mass balances decreased from an average of 32 % in the 1980s to 18 % and there were no more years with an overall positive mass balance (15 % during 1980–1999). The melt rate and loss in glacier thickness continues to be extraordinary. This development further confirms the accelerating trend in worldwide glacier disappearance, which has become more and more obvious during the past two decades.

The mean of the 30 glaciers included in the analysis is influenced by the large proportion of Alpine and Scandinavian glaciers. A mean value is therefore also calculated using only one single value (averaged) for each of the 9 mountain ranges concerned (Table 4.2). Furthermore, a mean was calculated for all mass balances available, independently of record length. In their general trend and magnitude, all three averages rather closely relate to each other and are in good agreement with the results from a moving-sample-averaging of all available data (cf. Kaser et al., 2006; Zemp et al., 2009).

The evolution with time can be described by means of Figure 4.1:

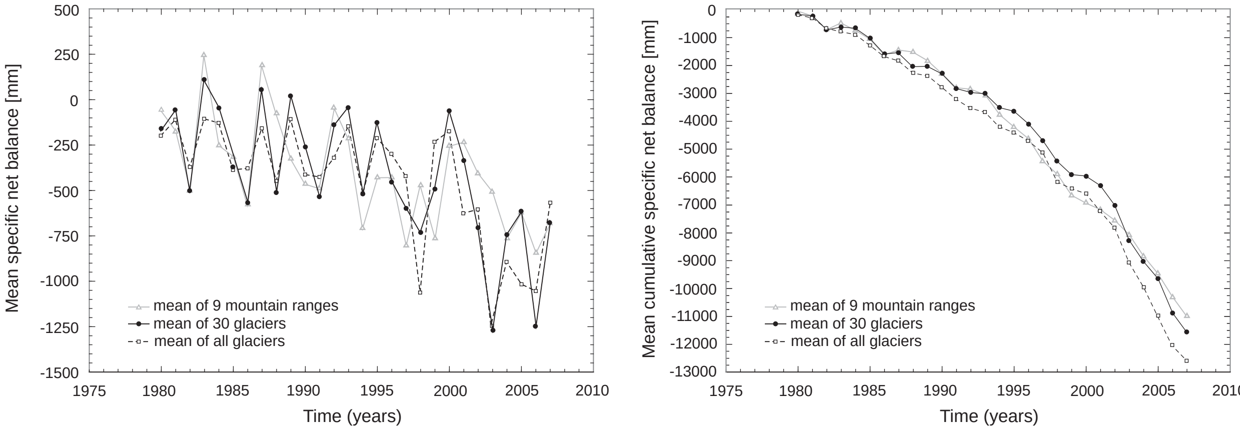

Figure 4.1: Mean specific net balance (left) and mean cumulative specific net balance (right) since 1980.

With their dynamic response to changes in climatic conditions – growth/reduction in area mainly through the advance/retreat of glacier tongues – glaciers readjust to equilibrium conditions of ice geometry with a zero mass balance. Recorded mass balances document the degree of imbalance between glaciers and climate due to the delay in dynamic response caused by the characteristics of ice flow (deformation and sliding); over longer time intervals they depend on the rate of climatic forcing. With constant climatic conditions (no forcing), balances would tend towards and become finally zero. Long-term non-zero balances are, therefore, an expression of ongoing climate change and sustained forcing. Trends towards increasing non-zero balances are caused by accelerated forcing. In the same way, comparison between present-day and past values of mass balance must take the changes of glacier area into account, which have occurred in the meantime (Elseberg et al., 2001; Nemec et al., 2009). Many of the relatively small glaciers, measured within the framework of the present mass balance observation network, have lost large percentages of their area during the past decades. The recent increase in the rates of ice loss over diminishing glacier surface areas, as compared with earlier losses related to larger surface areas, becomes even more pronounced and leaves no doubt about the accelerating change in climatic conditions, even if a part of the observed acceleration trend is likely to be caused by positive feedback processes.

Further analysis requires detailed consideration of aspects such as glacier sensitivity and the mentioned feedback mechanisms. The balance values and curves of cumulative mass balances reported for the individual glaciers (Chapter 2) not only reflect regional climatic variability but also mark differences in the sensitivity of the observed glaciers. This sensitivity has a (local) topographic component: the hypsographic distribution of glacier area with altitude (for the first time reported in selected cases with the present bulletin) and a (regional) climatic component: the change in mass balance with altitude or the mass balance gradient. The latter component tends to increase with increasing humidity and leads to stronger reactions by maritime rather than by continental glaciers. For the same reason, the mean balance values calculated above are predominantly influenced by maritime glaciers rather than by continental ones. Maritme glacier are those found in the coastal mountains of Norway or USA/Alaska, where effects from changes in precipitation may predominate over the influence of atmospheric warming. The modern tool of differencing repeat digital elevation models (DEM) provides excellent possibilities to assess how representative long time series of local mass balance measurements are with respect to large glacier samples (Paul and Haeberli, 2008) and to analyze spatial patterns of glacier thickness/volume changes in entire mountain ranges: DEM differencing, for instance, revealed that average thickness losses in southern Alaska (Larsen et al., 2007) are far higher than the averages reported here from in situ observations on various continents.

Rising snowlines and cumulative mass losses lead to changes in the average albedo and to a continued surface lowering. Such effects cause pronounced positive feedbacks with respect to radiative and sensible heat fluxes.

Table 4.2: Mass balance data for 9 mountain regions 1980–2007

Year	Cascade Mnts.	Alaska	Andes	Svalbard	Scandinavia	Alps	Altai	Caucasus	Tien Shan	Mean
1980	−972	1400	300	−475	−1055	403	−10	380	−483	−57
1981	−967	775	360	−505	194	−11	−213	−910	−271	−172
1982	−337	−245	−2420	−10	−185	−914	−460	420	−338	−499
1983	−606	15	3700	−220	756	−456	197	−970	−220	244
1984	−109	−395	−1240	−705	194	115	307	210	−667	−254
1985	−1541	515	340	−515	−451	−415	200	−380	−581	−314
1986	−1011	−60	−1570	−265	−249	−1031	73	−500	−595	−579
1987	−1703	535	950	230	925	−711	183	1540	−258	188
1988	−1305	395	2300	−505	−1215	−588	333	520	−626	−77
1989	−875	−1440	−1260	−345	1911	−906	117	40	−177	−326
1990	−834	−1555	−1300	−585	1196	−1105	107	340	−454	−466
1991	−595	−260	−860	115	80	−1200	−480	−310	−903	−490
1992	−1400	−210	1740	−120	1161	−1223	−127	−130	−109	−46
1993	−1755	−1170	−290	−955	1174	−556	227	1100	287	−215
1994	−1515	−660	−1860	−140	171	−886	−240	−840	−411	−709
1995	−1588	−765	−950	−785	589	−70	60	40	−408	−431
1996	−61	−950	−1180	−75	−643	−454	−140	−150	−207	−429
1997	−129	−2120	−2530	−570	−470	−400	−123	270	−1160	−804
1998	−2155	−135	2890	−725	221	−1664	−1110	−1000	−575	−473
1999	820	−1095	−4260	−350	−123	−699	−113	−560	−511	−766
2000	255	−490	−760	−25	988	−686	−230	−1140	−222	−257
2001	−1165	−120	1810	−405	−787	53	−190	−620	−698	−236
2002	214	−875	80	−550	−1141	−870	−357	430	−568	−404
2003	−1548	−180	2060	−845	−1392	−2557	−363	280	−13	−506
2004	−1930	−2285	−570	−1045	−161	−1039	−210	730	−347	−762
2005	−1873	−1020	−850	−870	309	−1368	87	390	−414	−623
2006	−1675	−545	560	−605	−2025	−1444	−197	−800	−872	−845
2007	−180	−1045	−130	−355	395	−1742	−297	−2010	−779	−683
Mean	−948	−499	−176	−436	13	−801	−106	−130	−449	−392

Cascade Mtns.	Place, South Cascade
Svalbard	Austre Brøggerbreen, Midtre Lovénbreen
Andes	Echaurren Norte
Alaska	Gulkana, Wolverine
Scandinavia	Engabreen, Ålfotbreen, Nigardsbreen, Gråsubreen, Storbreen, Hellstugubreen, Hardangerjøkulen, Storglaciären
Alps	Saint Sorlin, Sarennes, Silvretta, Gries, Sonnblickkees, Vernagtferner, Kesselwandferner, Hintereisferner, Caresèr
Altai	No. 125 (Vodopadniy), Maliy Aktru, Leviy Aktru
Caucasus	Djankuat
Tien Shan	Ts. Tuyuksuyskiy, Urumqihe S. No. 1

Albedo changes are especially effective in enhancing melt rates and can also be caused by input of dust (Oerlemans et al., 2009). The cumulative length change of glaciers is the result of all effects combined, and constitutes the key to a global intercomparison of decadal to secular mass losses. Surface lowering, thickness loss and the resulting reduction in driving stress and flow, however, increasingly replace processes of tongue retreat with processes of downwasting, disintegration or even collapse of entire glaciers. Moreover, the thickness of most glaciers regularly observed for their mass balance is measured in (a few) tens of meters. From the measured mass losses and thickness reductions, it is evident that several network glaciers with important long-term observations may not survive for many more decades. A special challenge therefore consists in developing a strategy for ensuring the continuity of adequate mass balance observations under such extreme conditions (Zemp et al., 2009).

The volume 50 (50) of the Annals of Glaciology published in 2009 presents recent work from the International Workshop on Mass Balance Measurement and Modelling at Skeikampen, Norway, in 2008. Issues discussed also concern the uncertainty ranges of measured mass balances and the accessibility of information from individual stake/pit measurements in view of energy balance modelling. The ideal measurement accuracy for glacier mass balance is defined as 0.1 m w.e. with a threshold limit of 0.2 m w.e (IGOS 2007). This goal can only be reached by systematic comparison and – in cases of major deviations – adjustment of the direct glaciological with geodetic mass balances (e.g. Thibert et al., 2008; Cogley, 2009; Huss et al., 2009). A corresponding quality ranking may have to be introduced with respect to the internationally reported numbers. Access to point measurements relates to complex questions and may, at first, become possible only in a limited number of cases.

Completion of the present Glacier Mass Balance Bulletin was made possible through the cooperation of the National Correspondents to WGMS and the Principal Investigators of the various glaciers, as listed in Chapter 5. Thanks are due to Ursina Gloor and Dorothea Stumm for their assistance with data collection, quality control and editing of this issue, and to Susan Braun-Clarke for carefully editing the English. Funding is mainly through the WGMS Bridging Credit of the Swiss National Science Foundation and the Department of Geography at the University of Zurich with contributions by FAGS/ICSU, the Federal Office for the Environment (FOEN) and by the Cryospheric Commission of the Swiss Academy of Sciences.

References

Cogley, J.G. (2009): Geodetic and direct mass balance measurements: Comparison and joint analysis. Annals of Glaciology, 50 (50), 96–100.

Elsberg, D.H., W.D. Harrison, K.A. Echelmeyer and R.M. Krimmel (2001): Quantifying the effects of climate and surface change on glacier mass balance. Journal of Glaciology, 47 (159), 649–658.

GCOS (2009): Progress report on the implementation of the Global Observing System for Climate in support of the UNFCCC 2004-2008. GCOS-129. WMO-TD/No.1489, GOOS-173, GTOS-70).

Huss M., Bauder, A. and Funk M. (2009): Homogenization of long-term mass-balance time series, Annals of Glaciology, 50 (50), 198–206.

IGOS (2007): IGOS Cryosphere Theme. A Cryosphere Theme Report for the IGOS Partnership. WMO/TD-No. 1405

Kaser, G., J.G. Cogley, M.B. Dyurgerov, M.F. Meier and A. Ohmura (2006): Mass balance of glaciers and ice caps: consensus estimates for 1961-2004. Geophysical Research Letters, 33, L19501.

Larsen, C.F., Motyka, R.J., Arendt, A.A., Echelmeyer, K.A. and Geissler, P.E. (2007): Glacier changes in southeast Alaska and northwest British Columbia and contribution to sea level rise. Journal of Geophysical Research, 112, F01007.

Nemec, J., Huybrechts, Ph., Rybak, O. and Oerlemans, J. (2009): Reconstruction of the annual balance of Vadret da Morteratsch, Switzerland, since 1865. Annals of Glaciology, 50 (50), 126-134.

Oerlemans, J., Giessen, R.H. and van den Broeke, M.R. (2009): Retreating alpine glaciers: increased melt rates due to accumulatiuon of dust (Vadret da Morteratsch, Switzerland). Journal of Glaciology, 55 (192), 729–736.

Østrem G. and Brugman M. (1991): Glacier mass-balance measurements. A manual for field and office work, Saskatoon, Sask., Environment Canada, National Hydrology Research Institute, NHRI Science Report, 4.

Paul, F. and Haeberli, W. (2008): Spatial variability of glacier elevation changes in the Swiss Alps obtained from two digital elevation models. Geophysical Research Letters, 35, L21502, doi:10.1029/2008/GL034718

Thibert E., Blanc R., Vincent C. and Eckert N. (2008): Glaciological and volumetric mass-balance measurements: error analysis over 51 years for Glacier de Sarennes, French Alps, Journal of Glaciology, 54 (186), 522–532.

UNEP (2007): Global outlook for ice and snow. United Nations Environment Programme, EarthPrint.

WGMS (2008): Global glacier changes: facts and figures (Zemp, M., Roer, I., Kääb, A., Hoelzle, M. Paul, F. and W. Haeberli eds.). UNEP and WGMS, Nairobi and Zurich.

Zemp, M., Hoelzle, M. and Haeberli, W. (2009): Six decades of glacier mass balance observations – a review of the worldwide monitoring network. Annals of Glaciology, 50 (50), 101-111.

5 PRINCIPAL INVESTIGATORS AND NATIONAL CORRESPONDENTS

5.1 PRINCIPAL INVESTIGATORS

ANTARCTICA	Glaciar Bahía del Diablo	Pedro Skvarca and Evgeniy Ermolin División Glaciología Instituto Antártico Argentino Cerrito 1248 ARGENTINA – C1010AAZ Buenos Aires E-mail: glacio@dna.gov.ar ivgen52@yahoo.com
ARGENTINA	Martial Este	Jorge A. Strelin and Rodolfo Iturraspe Convenio DNA – UNC Departamento de Geología Básica Facultad de Ciencias Exactas Físicas y Naturales Universidad Nacional de Córdoba Avda. Vélez Sarsfield 1611 ARGENTINA – X5016 GCA Córdoba E-mail: jstrelin@hotmail.com jstrelin@yahoo.com.ar iturraspe@tdfuego.com
AUSTRIA	Hintereisferner Jamtalferner Kesselwandferner	Andrea Fischer, Gerhard Markl, Michael Kuhn Institute of Meteorology and Geophysics University of Innsbruck Innrain 52 AUSTRIA – 6020 Innsbruck E-mail: andrea.fischer@uibk.ac.at michael.kuhn@uibk.ac.at
	Sonnblickkees	Heinz Slupetzky Department of Geography and Geology University of Salzburg Hellbrunnerstrasse 34 / III AUSTRIA – 5020 Salzburg E-mail: heinz.slupetzky@sbg.ac.at
	Vernagtferner	Ludwig N. Braun Commission for Glaciology Bavarian Academy of Sciences Alfons-Goppel-Str. 11 GERMANY – 80539 München E-mail: ludwig.braun@kfg.badw.de
	Goldbergkees Kleinfleisskees Pasterzenkees Wurtenkees	Reinhard Böhm, Wolfgang Schöner, Bernhard Hynek Zentralanstalt für Meteorologie und Geodynamik (ZAMG) Hohe Warte 38 AUSTRIA – 1190 Wien E-mail: reinhard.boehm@zamg.ac.at wolfgang.schoener@zamg.ac.at bernhard.hynek@zamg.ac.at
BOLIVIA	Chacaltaya Charquini Sur Zongo	Perroy Edouard IRD (Institut de recherche pour le développement) 213, rue La Fayette FRANCE – Paris Cedex 10 (75 480) E-mail: edperroy@yahoo.fr

		Javier C. Mendoza Rodríguez IHH (Instituto de Hidráulica e Hidrología) and SENAMHI (Servicio Nacional de Meteorología e Hidrología) P.O. Box 699 BOLIVIA – La Paz E-mail: jmendoza@senamhi.gov.bo
		Bernard Francou Laboratoire de Glaciologie et de Geophysique de l' Environnement CNRS FRANCE – St-Martin d'Heres E-mail: francou@lgge.obs.ujf-grenoble.fr bernard.francou@ird.fr
CANADA	Devon Ice Cap NW Meighen Ice Cap	Dave O. Burgess and Roy M. Koerner (deceased) Natural Resources Canada Geological Survey of Canada 601 Booth Street CANADA – Ottawa, ON K1A 0E8 E-mail: David.Burgess@NRCan-RNCan.gc.ca
	Helm Peyto Place	Michael N. Demuth Natural Resources Canada Geological Survey of Canada 601 Booth Street CANADA – Ottawa, ON K1A 0E8 E-mail: Mike.Demuth@NRCan-RNCan.gc.ca
	White	Graham Cogley and Miles A. Ecclestone Department of Geography Trent University 1600 West Bank Drive CANADA – Peterborough, Ontario K9J 7B8 E-mail: gcogley@trentu.ca
CHILE	Echaurren Norte	Fernando Escobar and Jorge Quinteros Dirección General de Aguas Morandé 59 CHILE – Santiago E-mail: fernando.escobar@mop.gov.cl
CHINA	Urumqihe S. No. 1	Huilin Li and Huian Yang Cold and Arid Regions Environmental and Engineering Research Institute (CAREERI) Chinese Academy of Sciences (CAS) 260 West Donggang Road P. R. CHINA – 730 018 Lanzhou, Gansu E-mail: lihuilin@lzb.ac.cn
COLOMBIA	La Conejera Ritacuba Negro	Jorge Luis Ceballos Instituto de Hidrología, Meteorología y Estudios Ambientales (IDEAM) Subdirección de Ecosistemas e Información Ambiental Carrera 10 No. 20-30 COLOMBIA – Bogotá Email: jorgec@ideam.gov.co

ECUADOR	Antizana 15 Alpha	Bolívar Cáceres Correa Programa Glaciares Ecuador Instituto Nacional de Meteorología e Hidrología (INAMHI) Iñaquito 700 y Corea ECUADOR – 16 310 Quito E-mail: ernestocaceres2002@yahoo.com.mx bcaceres@inamhi.gov.ec
		Bernard Francou Laboratoire de Glaciologie et de Geophysique de l' Environnement CNRS FRANCE – St-Martin d'Heres E-mail: francou@lgge.obs.ujf-grenoble.fr bernard.francou@ird.fr
FRANCE	Argentière Gebroulaz Saint Sorlin	Christian Vincent and Michel Vallon Laboratoire de Glaciologie et de Geophysique de l' Environnement CNRS P.O. Box 96 FRANCE – 38402 St. Martin d'Hères Cedex E-mail: vincent@lgge.obs.ujf-grenoble.fr
	Ossoue	Pierre René Association Moraine Village FRANCE – 31110 Poubeau E-mail: asso.moraine@wanadoo.fr
	Sarennes	Emmanuel Thibert and Didier Richard CEMAGREF Snow avalanche engineering and torrent control P.O. Box 76 FRANCE – 38402 St. Martin d'Hères Cedex E-mail: didier.richard@cemagref.fr emmanuel.thibert@cemagref.fr
GREENLAND	Mittivakkat	Niels T. Knudsen Department of Earth Science Ny Munkegarde Bg. 1520 DENMARK – 8000 Århus E-mail: ntk@geo.au.dk
		Bent Hasholt Deparment of Geography & Geology University of Copenhagen Øster Voldgade 10 DENMARK – 1350 Copenhagen E-mail: bh@geo.ku.dk
ICELAND	Brúarjökull Dyngjujökull Eyjabakkajökull Köldukvíslarjökull Langjökull S. Dome Tungnaárjökull	Finnur Pálsson and Helgi Björnsson Institute of Earth Sciences University of Iceland Sturlugata 7 ICELAND – 101 Reykjavík E-mail: fp@raunvis.hi.is hb@raunvis.hi.is
		Hannes Haraldsson National Power Company Háleitisbraut 68 ICELAND – 103 Reykjavík E-mail: hannesh@lv.is

	Hofsjökull N Hofsjökull E Hofsjökull SW	Þorsteinn Þorsteinsson Icelandic Meteorological Office Grensásvegi 9 ICELAND – 108 Reykjavík E-mail: thor@vedur.is
INDIA	Chhota Shigri	The data series of 2003-06 was published by Wagnon et. al. (2007): Four years of mass balance on Chhota Shigri Glacier, Himachal Pradesh, India, a new benchmark glacier in the western Himalaya. *Journal of Glaciology*, 53 (183), 603–611.
	Hamtah	C.V. Sangewar Glaciological Division Geological Survey of India Vasundara Complex, Sector E, Aliganj INDIA – Lucknow 226024 E-mail: cvsangewar@rediffmail.com
ITALY	Calderone	Massimo Pecci, Pinuccio D'Aquila, Stefano Pignotti, Luca Lombardi and Thomas Zanoner IMONT (Italian Mountain Institue) Piazza dei Capretteri 70 Italy – 00186 Roma
	Carèser	Luca Carturan SAT-Comitato Glaciologico Trentino Via Manci 57 Italy – 38100 Trento E-Mail: luca.carturan@unipd.it
	Ciardoney	Luca Mercalli, Daniele Cat Berro and Fulvio Fornengo Società Meteorologica Italiana Onlus Castello Borello ITALY – 10053 Bussoleno E-mail: luca.mercalli@nimbus.it d.catberro@nimbus.it
	Fontana Bianca	Robert Dinale, Christoph Oberschmied, Andrea Di Lullo Ufficio Idrografico / Hydrographisches Amt, Provincia autonoma di Bolzano - Alto Adige / Autonome Provinz Bozen - Südtirol, via Mendola / Mendelstrasse 33 ITALY – 39100 Bolzano / Bozen E-mail: hydro@provinz.bz.it
	Lunga (Vedretta)	Rainer Prinz Institute of Geography University of Innsbruck Innrain 52 AUSTRIA – 6020 Innsbruck E-mail: rainer.prinz@uibk.ac.at Ufficio Idrografico / Hydrographisches Amt, Provincia autonoma di Bolzano - Alto Adige / Autonome Provinz Bozen - Südtirol, via Mendola / Mendelstrasse 33 ITALY – 39100 Bolzano / Bozen E-mail: hydro@provinz.bz.it
	Malavalle Pendente	Gian Carlo Rossi Comitato Glaciologico Italiano Via Montello 8 ITALY – 30033 Noale, Venezia E-mail: alvisero@tin.it

		Gian Luigi Franchi Comitato Glaciologico Italiano Via Giardino Giusti 19 ITALY – 37129 Verona E-mail: gianluigifranchi@virgilio.it
		Ufficio Idrografico / Hydrographisches Amt, Provincia autonoma di Bolzano - Alto Adige / Autonome Provinz Bozen - Südtirol, via Mendola / Mendelstrasse 33 ITALY – 39100 Bolzano / Bozen E-mail: hydro@provinz.bz.it
JAPAN	Hamaguri Yuki	Koji Fujita Department of Hydrospheric-Atmospheric Sciences (DHAS) Graduate School of Environmental Studies c/o Hydrospheric Atmospheric Research Center, Nagoya University JAPAN – Nagoya 464 8601 E-mail: cozy@nagoya-u.jp
KAZAKHSTAN	Ts. Tuyuksuyskiy	N.E. Kasatkin and K.G. Makarevich Institute of Geography National Kazakh Academy of Sciences Pushkin Street 99 KAZAKHSTAN – 480 100 Almaty
NEW ZEALAND	Brewster	Dorothea Stumm, Nicolas J. Cullen and Sean Fitzsimons Department of Geography University of Otago Box 56 NEW ZEALAND – Dunedin 9054 E-mail: dorothea.stumm@geo.uzh.ch njc@geography.otago.ac.nz sjf@geography.otago.ac.nz
		Brian Anderson and Andrew Mackintosh School of Geography, Environment and Earth Science Victoria University of Wellington PO Box 600 NEW ZEALAND – Wellington 6140 E-mail: Brian.Anderson@vuw.ac.nz Andrew.Mackintosh@vuw.ac.nz
NORWAY	Ålfotbreen Blomstølskardsbreen Breidalblikkbrea Gråfjellsbrea Hansebreen Langfjordjøkelen Nigardsbreen Svelgjabreen	Bjarne Kjøllmoen Norwegian Water Resources and Energy Directorate (NVE) Section for Glaciers, Snow and Ice P.O. Box 5091, Majorstua NORWAY – 0301 Oslo E-mail: bkj@nve.no
	Austdalsbreen Engabreen Hardangerjøkulen	Hallgeir Elvehøy Norwegian Water Resources and Energy Directorate (NVE) Section for Glaciers, Snow and Ice P.O. Box 5091, Majorstua NORWAY – 0301 Oslo E-mail: hae@nve.no

	Gråsubreen Hellstugubreen Storbreen	Liss M. Andreassen Norwegian Water Resources and Energy Directorate (NVE) Section for Glaciers, Snow and Ice P.O. Box 5091, Majorstua NORWAY – 0301 Oslo E-mail: lma@nve.no
	Austre Brøggerbreen Kongsvegen Midtre Lovénbreen	Jack Kohler Norwegian Polar Institute Polar Environmental Centre NORWAY – 9296 Tromsø E-mail: jack.kohler@npolar.no
	Hansbreen	Piotr Glowacki and Dariusz Puczko Institute of Geophysics Polish Academy of Sciences Ksiecia Janusza 64 POLAND – 01 452 Warsaw E-mail: glowacki@igf.edu.pl
	Elisebreen Irenebreen Waldemarbreen	Ireneusz Sobota Department of Cryology and Polar Research Institute of Geography Gagarina 9 POLAND – 87 100 Torun E-mail: irso@geo.uni.torun.pl
PERU	Artesonraju Yanamarey	Jesús Gómez Unidad de Glaciología y Recursos Hídricos Av. Confraternidad Internacional Oeste No. 167 PERU – Huaraz / Ancash E-mail: glaciologia5@gmail.com rjgomezl@hotmail.com
RUSSIA	Garabashi	O.V. Rototayeva and I.F. Khmelevskoy Russian Academy of Sciences Institute of Geography Staromonetniy 29 RUSSIA – 109 017 Moscow
	Djankuat	Victor V. Popovnin Moscow State University Geographical Faculty Leninskiye Gory RUSSIA – 119 992 Moscow E-mail: po@geogr.msu.ru begemot@djankuat.msk.ru
	Leviy Aktru Maliy Aktru No. 125 (Vodopadniy)	Yu K. Narozhniy Tomsk State University Lenin Str. 36 RUSSIA – 634 010 Tomsk E-mail: aktrunar@ggf.tsu.ru
SPAIN	Maladeta	Miguel Arenillas (Ingeniería 75) Ingeniería 75, S.A. C/ Velázquez 87 - 4° Dcha SPAIN – 28006 Madrid E-mail: map@ing75.com

		Guillermo Cobos Campos Ministerio de Medio Ambiente Planificación Hidrológica y Uso Sostenible del Agua Plaza de San Juan de la Cruz s/n. SPAIN – 28071 Madrid E-mail: gcobos@spesa.es
		Alfonso Pedrero Muñoz E-mail: apedreromu@ing75.com ing75@ing75.com
SWEDEN	Mårmaglaciären Rabots glaciär Riukojietna Storglaciären Tarfalaglaciären	Per Holmlund and Peter Jansson Department of Physical Geography and Quaternary Geology Glaciology University of Stockholm SWEDEN – 106 91 Stockholm E-mail: pelle@natgeo.su.se peter.jansson@natgeo.su.se
SWITZERLAND	Basòdino	Giovanni Kappenberger SWITZERLAND – 6654 Cavigliano E-mail: glkappenberger@hotmail.com
		Giacomo Casartelli ITALY – 22032 Albese, CO
	Findelen	Horst Machguth Department of Geography University of Zurich-Irchel Winterthurerstrasse 190 SWITZERLAND – 8057 Zurich E-mail: horst.machguth@geo.uzh.ch
		Martin Hoelzle Department of Geosciences University of Fribourg Chemin du musée 4 SWITZERLAND – 1700 Fribourg E-mail: martin.hoelzle@unifr.ch
	Gries Silvretta	Martin Funk and Andreas Bauder Laboratory of Hydraulics, Hydrology and Glaciology, VAW ETH Zürich Gloriastrasse 37/39 SWITZERLAND – 8092 Zurich E-mail: funk@vaw.baug.ethz.ch bauder@vaw.baug.ethz.ch
USA	Columbia (2057) Daniels Easton Foss Ice Worm Lower Curtis Lynch Rainbow Sholes Yawning	Mauri Pelto North Cascade Glacier Climate Project (NCGCP) Nicols College USA – Dudley, MA 01571 E-mail: mspelto@nichols.edu

Lemon Creek Taku	Mauri Pelto Juneau Icefield Research Project (JIRP) Nicols College USA – Dudley, MA 01571 E-mail: mspelto@nichols.edu
Emmons Nisqually Noisy Creek North Klawatti Sandalee Silver	Jon Riedel (US National Park Service) North Cascades National Park Marblemount Ranger Station 7280 Ranger Station Rd. USA – Marblemount, WA 98267 E-mail: Jon_Riedel@nps.gov
Gulkana Wolverine	Rod March and Shad O'Neel US Geological Survey Water Resources Division 3400 Shell Street USA – Fairbanks, AK 99701-7245 E-mail: rsmarch@usgs.gov soneel@usgs.gov
South Cascade	William R. Bidlake US Geological Survey Washington Water Science Center 934 Broadway - Suite 300 USA – Tacoma, WA 98402 E-mail: wbidlake@usgs.gov

5.2 NATIONAL CORRESPONDENTS OF WGMS

ARGENTINA/ ANTARCTICA	Lydia Espizua Instituto Argentino de Nivología y Glaciología CONICET (IANIGLA) Casilla de Correo 330 ARGENTINA – 5500 Mendoza E-mail: lespizua@lab.cricyt.edu.ar
AUSTRALIA/ ANTARCTICA	Andrew Ruddell 4 Cust Street Rainbow AUSTRALIA – Victoria 3424 E-mail: andrewruddell@bigpond.com
AUSTRIA	Michael Kuhn Institute of Meteorology and Geophysics University of Innsbruck Innrain 52 AUSTRIA – 6020 Innsbruck E-mail: Michael.Kuhn@uibk.ac.at
BOLIVIA	Javier C. Mendoza Rodríguez IHH (Instituto de Hidráulica e Hidrología) and IRD P.O. Box 9214 BOLIVIA – La Paz E-mail: jmendoza@senamhi.gov.bo
CANADA	Michael N. Demuth Natural Resources Canada Geological Survey of Canada 601 Booth Street CANADA – Ottawa, ON K1A 0E8 E-mail: Mike.Demuth@NRCan-RNCan.gc.ca
CHILE	Gino Casassa Centro de Estudios Cientificos Av. Prat. 514 CHILE – Valdivia E-mail: gcasassa@cecs.cl
CHINA	Li Zhongqin Tianshan Glaciological Station / Cold and Arid Regions Environment and Engineering Research Institute (CAREERI) Chinese Academy of Sciences (CAS) 260 West Donggang Road P. R. CHINA – 730 000 Lanzhou, Gansu E-mail: lizq@ns.lzb.ac.cn lizq@lzb.ac.cn
COLOMBIA	Jair Ramirez Cadenas INGEOMINAS Diagonal 53 No. 34-53 COLOMBIA – Bogota E-mail: jairamir@ingeominas.gov.co

ECUADOR

Bolívar Ernesto Cáceres Correa
Programa Glaciares Ecuador
INAMHI (Instituto Nacional de Meteorología e Hidrología)
Iñaquito 700 y Corea
ECUADOR – 16 310 Quito
E-mail: bcaceres@inamhi.gov.ec

FRANCE

Christian Vincent
Laboratory of Glaciology and Environmental Geophysics (CNRS)
P.O. Box 96
FRANCE – 38402 St. Martin d'Hères Cedex
E-mail: vincent@lgge.obs.ujf-grenoble.fr

GERMANY

Ludwig N. Braun
Commission for Glaciology
Bavarian Academy of Sciences
Alfons-Goppel-Str. 11
GERMANY – 80539 München
E-mail: ludwig.braun@kfg.badw.de

GREENLAND

Andreas Peter Ahlstrøm
Department of Quaternary Geology
The Geological Survey of Denmark and Greenland (GEUS)
Øster Voldgade 10
DENMARK – 1350 Copenhagen K
E-mail: apa@geus.dk

ICELAND

Oddur Sigurdsson
Icelandic Meteorological Office
Grensásvegi 9
ICELAND – 108 Reykjavik
E-mail: osig@sol.vedur.is

INDIA

Chandrashekhar V. Sangewar
Glaciology Division
Geological Survey of India
Vasundara Complex, Sector E, Aliganj
INDIA – Lucknow 226024
E-mail: cvsangewar@rediffmail.com

INDONESIA

see AUSTRALIA

ITALY

Mirco Meneghel
Universita di Padua
Dipartimento di Geografia
Via del Santo 26
ITALY – 35123 Padova
E-mail: mirco.meneghel@unipd.it

JAPAN

Koji Fujita
Department of Hydrospheric-Atmospheric Sciences (DHAS)
Graduate School of Environmental Studies
c/o Hydrospheric Atmospheric Research Center, Nagoya University
JAPAN – Nagoya 464 8601
E-mail: cozy@nagoya-u.jp

KAZAKHSTAN	Igor Severskiy Institute of Geography National Kazakh Academy of Sciences Pushkin Street 99 KAZAKHSTAN – 480 100 Almaty i_severskiy@mail.kz
MEXICO	Hugo Delgado-Granados Instituto de Geofísica Universidad Nacional Autónoma de México Circuito Exterior, C. U. Coyoacán MEXICO – México D. F. 04510 E-mail: hugo@geofisica.unam.mx
NEPAL	see JAPAN
NEW ZEALAND/ ANTARCTICA	Trevor J. Chinn Alpine and Polar Processes Consultancy Rapid 20, Muir Rd. Lake Hawea RD 2 Wanaka NEW ZEALAND – Otago 9382 E-mail: t.chinn@xtra.co.nz
NORWAY	Jon Ove Hagen Department of Geosciences Section of Physical Geography University of Oslo P.O. Box 1047, Blindern NORWAY – 0316 Oslo E-mail: j.o.m.hagen@geo.uio.no
PAKISTAN	Ali Ghazanfar Head Water Resources Section Global Change Impact Studies Center (GCISC) NCP Complex, Quaid-i-Azam University Campus PAKISTAN – Islamabad E-mail: ghazanfar.ali@gcisc.org.pk
PERU	Marco Zapata Luyo Unidad de Glaciología y Recursos Hídricos Av. Confraternidad Internacional Oeste No. 167 PERU – Huaraz / Ancash E-mail: zapataluyomarco@gmail.com
POLAND	Bogdan Gadek University of Silesia Department of Geomorphology ul. Bedzinska 60 POLAND – 41 200 Sosnowiec E-mail: bogdan.gadek@us.edu.pl
RUSSIA	Victor V. Popovnin Moscow State University Geographical Faculty Leninskiye Gory RUSSIA – 119 992 Moscow E-mail: po@geogr.msu.ru begemot@djankuat.msk.ru

SPAIN

Eduardo Martinez de Pisón and Miguel Arenillas
Ingeniería 75, S.A.
Velázquez 87 – 4° derecha
SPAIN – 28006 Madrid
E-mail: ing75@ing75.com
map@ing75.com

SWEDEN

Per Holmlund
Department of Physical Geography and Quaternary Geology
Glaciology
University of Stockholm
SWEDEN – 106 91 Stockholm
E-mail: pelle@natgeo.su.se

SWITZERLAND

Martin Hoelzle
Department of Geosciences
University of Fribourg
Chemin du musée 4
SWITZERLAND – 1700 Fribourg
E-mail: martin.hoelzle@unifr.ch

USA

William R. Bidlake
US Geological Survey
Washington Water Science Center
934 Broadway – Suite 300
USA – Tacoma, WA 98402
E-mail: wbidlake@usgs.gov

UZBEKISTAN

Andrey Yakovlev
The Center of Hydrometeorological Service (UzHydromet)
72, K.Makhsumov str.
UZBEKISTAN – 100 052 Tashkent
E-mail: andreyakovlev@mail.ru

Publication 4

Zemp, M., Zumbühl, H.J., Nussbaumer, S.U., Masiokas, M.H., Espizua, L.E. and Pitte, P. (subm.). **Extending glacier monitoring into the Little Ice Age and beyond.** PAGES news, 19(2).

Extending glacier monitoring into the Little Ice Age and beyond

M. Zemp[1], H. J. Zumbühl[2], S. U. Nussbaumer[1, 2], M. H. Masiokas[3], L. E. Espizua[3] and P. Pitte[3]

[1]World Glacier Monitoring Service, Department of Geography, University of Zurich, Switzerland

[2]Institute of Geography and Oeschger Centre for Climate Change Research, University of Bern, Switzerland

[3]Instituto Argentino de Nivología, Glaciología y Ciencias Ambientales (IANIGLA), CCT-CONICET Mendoza, Argentina

The standardized collection of glacier front variations reconstructed by means of historical evidence and modern dating methods allows a direct comparison between different glaciers and with in situ measurements. Here we present data series from the Alps, Scandinavia, and the southern Andes which extend the direct observations back into the Little Ice Age. These data represent an initial step towards a worldwide compilation and free dissemination of reconstructed glacier fluctuations within the internationally coordinated glacier monitoring system.

Glaciers are among the best natural indicators of climatic changes and, as such, a key variable within the international climate observing system. Glacier changes significantly contribute to global sea level variations, alter the regional hydrology, and can become a serious flood hazard for nearby human settlements. The worldwide monitoring of glacier distribution and fluctuations is well established and has been internationally coordinated for more than a century (WGMS, 2008). Direct measurements of seasonal and annual glacier mass balance, which are available for the past six decades, allow quantifying the reaction of a glacier to changes in atmospheric conditions and can be directly compared among glaciers around the world. The variations of a glacier front position represent an indirect, delayed, filtered and enhanced response to changes in climate over glacier-specific response times spanning up to several decades (Jóhannesson et al., 1989; Haeberli and Hoelzle, 1995; Oerlemans, 2007). Regular observations of glacier front variations have been carried out in Europe and in few other places around the world since the late 19th century. Information on glacier fluctuations before the onset of regular in situ measurements have to be reconstructed from moraines, early photographs, drawings, paintings, prints, maps, written documents. Together with the data of in situ measurements, the positions of the moraines associated with the Little Ice Age (LIA) and other sources of historical information allow the reconstruction of glacier variations back to the 16th–18th centuries. Extensive research has been carried out mainly in Europe and the Americas to reconstruct the fluctuations of glaciers through the LIA and Holocene (e.g., Zumbühl, 1980; Karlén, 1988; Luckman, 1993; Nicolussi and Patzelt, 2000; Holzhauser et al., 2005; Nussbaumer et al., 2007; Masiokas et al., 2009;

Nesje, 2009, Holzhauser, 2010). However, the majority of the data is not available to the scientific community which limits the verification and direct comparison of the results. In this article, we present a first approach towards standardizing reconstructed Holocene glacier front variations while integrating the data series into the database of the World Glacier Monitoring Service (WGMS).

Standardization and database

The standardized compilation of direct glacier front variation measurements is straightforward: The quantitative or qualitative change in glacier front position is determined between two points in time. These basic data are supplemented by information on survey dates, methods and the measurement accuracy. The reconstruction of front positions and their dating is much more complex and often based on multiple evidence. A spatial uncertainty arises from the determination of the exact location of the glacier terminus, while temporal uncertainty is associated with the dating technique used in each case. To take oil paintings as an example, it is important to distinguish between the time of the first draft (e.g. a drawing) in the field and the production of the painting itself which can happen several years later.

The concept for the integration of these reconstructed front variations into the relational glacier database of the WGMS was jointly elaborated and tested by experts of both fields (natural and historical sciences). The standardization of glacier front data is designed to allow direct comparison between the reconstructed and measured front variation series while still providing the most relevant information related to methods and uncertainties of the individual data series. The database storage of the reconstructed front variations is implemented in two data tables: a first one with information on the entire reconstruction series including a figure of the cumulative length changes, name and affiliation of the scientist(s), and reference(s) to published methods and results. Linked to this summary information of the reconstruction series, a second table stores the individual quantitative or qualitative front variations as well as minimum and maximum elevation of the glacier together with metadata related to the reconstruction methods and the uncertainties in space and time. The metadata are stored in a combination of predefined choices of methods and open text fields. This allows a standardized description of the data and leaves extra space for individual and more detailed remarks. The link to related publications guarantees access to full methodological details and background information. Both data tables are linked by a unique numeric glacier identifier to the main table of the WGMS database with general information of the present-day glacier, including name and geographical coordinates. This database relationship allows the direct comparison of reconstructed with directly observed front variations.

The database concept was developed based on reconstruction series of 15 glaciers in Europe (8 in the western/central Alps and 7 in southern Norway) and 11 glaciers in the Argentinean portion of the southern Andes. The glacier reconstructions are based on the evaluation of pictorial, cartographical, and written documents, in accordance with data from preserved moraines (Zumbühl 1980, Zumbühl et al., 1983; Zumbühl and Holzhauser, 1988;

Tribolet, 1998; Nussbaumer et al., 2007 and 2011; Nussbaumer and Zumbühl, 2011), including dendro-geomorphological and radiocarbon dating (Espizua, 2005; Espizua and Pitte, 2009; Masiokas et al., 2009). Among these glaciers, the Unterer Grindelwaldgletscher (central Swiss Alps) contains the best-documented series, with a total number of about 400 historical documents (Zumbühl, 1980; Steiner et al., 2008).

Results and discussion

In addition to the inventory information of about 100,000 glaciers, direct measurements of frontal variations of 1,800 ice bodies and mass balance data of 230 glaciers worldwide, reconstructed frontal variations of the 26 glaciers mentioned above are now readily available in standardized and digital form through the WGMS database (www.wgms.ch). The reconstructed front variation series extend the direct measurements (mainly concentrated to the 20th century) by two centuries in Norway and by four centuries in the Alps and in South America (available are also moraines dated back to the mid-Holocene). Note that, depending on the availability and quality of historical documents and other sources of information, the temporal resolution usually becomes lower whereas the spatial uncertainties increase as we move back in time. Despite these limitations, the now possible direct comparison of long-term reconstructions with recent measurements reveals some striking features (Figure 1).

The investigated glaciers in the western and central Alps show several periods of marked advances during the LIA, similar or even larger than the maximum LIA extent around 1850. The longest records are from the central Swiss Alps (Unterer Grindelwaldgletscher going back to AD 1535) and the French Mont Blanc area (Mer de Glace back to AD 1570 and Glacier des Bossons back to AD 1580). Those reconstructions reveal dramatic glacier advances starting by the end of the 16th century, overrunning cropland and hamlets, and culminating ca. 1600 and 1640 (Zumbühl, 1980; Nussbaumer et al., 2007). Other peaks in glacier extent were reached around 1720, 1780, 1820 and 1850. After this last event, the direct measurement series show an impressive glacier retreat of one to three kilometers, with intermittent periods of minor re-advances in the 1890s, 1920s and between 1965 and 1985. Figure 2 shows an example for the Mer de Glace with the sum of available meta-information stored within the database.

In contrast to the Alps, the historically-based reconstructions for glaciers in southern Norway (Nussbaumer et al., 2011) indicate that the maximum extent of the LIA peaked around 1750 at Jostedalsbreen and in the late 1870s at Folgefonna. The reconstructed front variation series of Nigardsbreen (an outlet glacier of Jostedalsbreen) shows that the maximum LIA extension occurred in 1748, and that it was preceded by a period of strong frontal advance that lasted (at least) 3–4 decades. Other sources report devastation of pastures by neighboring glaciers at that time (Nussbaumer et al., 2011). The retreat from the LIA maximum position was rather gentle until the 1940s, when the rates of frontal retreat accelerated until the mid-1970s. Direct measurements at Nigardsbreen and other glaciers in southern Norway reveal a regional pattern of recent re-advances mainly concentrated during the 1990s. It is worthwhile to note that the extension of Nigardsbreen in the 17th century was similar to the present day extent of the glacier (Nesje et al., 2008), and that the period of glacier re-advances in the 1990s is short both in time and extension considering the overall retreat of one to four kilometers experienced since the LIA maximum.

In southern South America, datable evidence for reconstructing past glacier variations is most abundant in the Patagonian Andes. Despite recent efforts in this region and in other Andean sites to the north (Espizua, 2005; Espizua and Pitte, 2009; Jomelli et al., 2009; Masiokas et al., 2009), the number of chronologies dealing with glacier fluctuations prior to the 20th century is still very limited. In the southern Andes most records indicate that glaciers were generally more extensive prior to the 20th century, with dates of maximum expansion ranging from the 16th to the 19th centuries. Based on the available evidence, Glaciar Frías (northern Patagonian Andes) probably contains the best documented history of fluctuations since the LIA in southern South America, covering the period between 1639 and 2009.

Conclusions and outlook

Reconstructed LIA and Holocene glacier front variations are crucial for understanding past glacier dynamics and allow an objective assessment of the relative significance of recent glacier fluctuations (i.e., 20th and late 19th century changes) in a long term context. The standardized compilation and free dissemination of reconstructed as well as directly measured glacier fluctuation records offer several benefits for both data providers and users. The storage within the international glacier databases guarantees the long-term availability of the data series and increases the visibility of the scientific research which – in historical glaciology – is often the work of a lifetime. The compilation and dissemination of glacier fluctuation records in a standardized and digital format facilitate the comparison between glaciers and between different methods and opens the field for numerous scientific studies and more general applications. The extension of the WGMS databases presented here integrates newly available data series from reconstructed front variations from southern Norway, the western/central Alps and the southern Andes, and represents a first step towards a worldwide compilation and free dissemination of standardized LIA and Holocene glacier fluctuations within the internationally coordinated glacier monitoring community.

The aim of this new initiative is to

- integrate a greater number of time series,
- incorporate records that cover the whole Holocene, and
- include other regions (e.g. the Himalayas, North America).

We believe that this new dataset will grow soon and constitute a major contribution towards the better integration of the glacier monitoring and reconstruction communities. Hopefully this will result in new scientific findings, e.g., related to the climatic interpretation of past and present glacier fluctuations, and become an additional tool for the comparison of present-day to pre-industrial climate changes.

Data request form and submission of data to the international glacier databases:

Worldwide collection of standardized data on the distribution and changes of glaciers has been internationally coordinated since 1894. Today, the World Glacier Monitoring Service (www.wgms.ch) is in charge of the compilation and dissemination of glacier datasets in close collaboration with the US National Snow and Ice Data Center (www.nsidc.org) and the Global Land Ice Measurement from Space initiative (www.glims.org) within the framework of the Global Terrestrial Network for Glaciers (www.gtn-g.org).

For available data or guidelines on data submission please check these websites and/or directly contact: wgms@geo.uzh.ch

Acknowledgements

We are grateful to Wilfried Haeberli and Heinz Wanner for their valuable comments and assistance. This work has been supported by the Swiss National Science Foundation (grant 200021-116354). The collection and processing of data from Argentinean glaciers was supported by Agencia Nacional de Promoción Científica y Tecnológica (grants PICT07-03093 and PICTR02-186), and the Projects CRN03 and CRN2047 from the Inter American Institute for Global Change Research (IAI).

References

Espizua, L. E. (2005): Holocene glacier chronology of Valenzuela Valley, Mendoza Andes, Argentina. *The Holocene* 15 (7), 1079–1085.

Espizua, L. E. and Pitte, P. (2009): The Little Ice Age glacier advance in the Central Andes (35°S), Argentina. *Palaeogeography, Palaeoclimatology, Palaeoecology* 281 (3–4), 345–350.

Haeberli, W. and Hoelzle, M. (1995): Application of inventory data for estimating characteristics of and regional climatic-change effects on mountain glaciers: a pilot study with the European Alps. *Annals of Glaciology* 21, 206–212.

Holzhauser, H. (2010): *Zur Geschichte des Gornergletschers. Ein Puzzle aus historischen Dokumenten und fossilen Hölzern aus dem Gletschervorfeld*. Geographica Bernensia, G 84. Geographisches Institut der Universität Bern, 253 pp.

Holzhauser, H., Magny, M. and Zumbühl, H. J. (2005): Glacier and lake-level variations in west-central Europe over the last 3500 years. *The Holocene* 15 (6), 789–801.

Jóhannesson, T., Raymond, C. and Waddington, E. (1989): Time-scale for adjustment of glaciers to changes in mass balance. *Journal of Glaciology* 35 (121), 355–369.

Jomelli, V., Favier, V., Rabatel, A., Brunstein, D., Hoffmann, G. and Francou, B. (2009): Fluctuations of glaciers in the tropical Andes over the last millennium and palaeoclimatic implications: a review. *Palaeogeography, Palaeoclimatology, Palaeoecology* 281 (3–4), 269–282.

Karlén, W. (2008): Scandinavian glacial and climatic fluctuations during the Holocene. *Quaternary Science Reviews* 7 (2), 199–209.

Luckman, B. H. (1993): Glacier fluctuation and tree-ring records for the last millennium in the Canadian Rockies. *Quaternary Science Reviews* 12 (6), 441–450.

Masiokas, M. H., Rivera, A., Espizua, L. E., Villalba, R., Delgado, S. and Aravena, J. C. (2009): Glacier fluctuations in extratropical South America during the past 1000 years. *Palaeogeography, Palaeoclimatology, Palaeoecology* 281 (3–4), 242–268.

Nesje, A. (2009): Latest Pleistocene and Holocene alpine glacier fluctuations in Scandinavia. *Quaternary Science Reviews* 28 (21–22), 2119–2136.

Nesje, A., Dahl, S. O., Thun, T. and Nordli, Ø. (2008): The 'Little Ice Age' glacial expansion in western Scandinavia: summer temperature or winter precipitation? *Climate Dynamics* 30 (7–8), 789–801.

Nicolussi, K. and Patzelt, G. (2000): Untersuchungen zur holozänen Gletscherentwicklung von Pasterze und Gepatschferner (Ostalpen). *Zeitschrift für Gletscherkunde und Glazialgeologie* 36 (1–2), 1–87.

Nussbaumer, S. U., Nesje, A. and Zumbühl, H. J. (2011): Historical glacier fluctuations of Jostedalsbreen and Folgefonna (southern Norway) reassessed by new pictorial and written evidence. *The Holocene* 21 (3), 455–472.

Nussbaumer, S. U. and Zumbühl H. J. (2011): The Little Ice Age history of the Glacier des Bossons (Mont Blanc area, France): a new high-resolution glacier length curve based on historical documents. *Climatic Change*, in review.

Nussbaumer, S. U., Zumbühl, H. J. and Steiner, D. (2007): Fluctuations of the Mer de Glace (Mont Blanc area, France) AD 1500–2050: an interdisciplinary approach using new historical data and neural network simulations. *Zeitschrift für Gletscherkunde und Glazialgeologie* 40 (2005/2006), 1–183.

Oerlemans, J. (2007): Estimating response times of Vadret da Morteratsch, Vadret da Palü, Briksdalsbreen and Nigardsbreen from their length records. *Journal of Glaciology* 53 (182), 357–362.

Steiner, D., Zumbühl, H. J. and Bauder, A. (2008): Two Alpine glaciers over the past two centuries: a scientific view based on pictorial sources. In Orlove, B., Wiegandt, E. and Luckman, B. H. (eds.), *Darkening peaks: glacier retreat, science, and society*. University of California Press, Berkeley, 83–99.

Tribolet, G. (1998): *Die Schwankungen des Rezli- und des Geltengletschers. Gletschergeschichtliche und glazialmorphologische Untersuchungen*. Unpublished diploma thesis, Universität Bern, 123 pp.

WGMS (2008): *Global glacier changes: facts and figures*. Zemp, M., Roer, I., Kääb, A., Hoelzle, M., Paul, F. and Haeberli, W. (eds.), UNEP, World Glacier Monitoring Service, Zurich, Switzerland, 88 pp.

Zumbühl, H. J. (1980): *Die Schwankungen der Grindelwaldgletscher in den historischen Bild- und Schriftquellen des 12. bis 19. Jahrhunderts. Ein Beitrag zur Gletschergeschichte und Erforschung des Alpenraumes*. Denkschriften der Schweizerischen Naturforschenden Gesellschaft (SNG), Band 92. Birkhäuser, Basel/Boston/Stuttgart, 279 pp.

Zumbühl, H. J., Messerli, B. and Pfister, C. (1983): *Die Kleine Eiszeit: Gletschergeschichte im Spiegel der Kunst*. Katalog zur Sonderausstellung des Schweizerischen Alpinen Museums Bern und des Gletschergarten-Museums Luzern vom 09.06.–14.08.1983 (Luzern), 24.08.–16.10.1983 (Bern), 60 pp.

Zumbühl, H. J. and Holzhauser, H. (1988): Alpengletscher in der Kleinen Eiszeit. Sonderheft zum 125jährigen Jubiläum des SAC. *Die Alpen* 64 (3), 129–322.

Zumbühl, H. J., Steiner, D. and Nussbaumer, S. U. (2008): 19th century glacier representations and fluctuations in the central and western European Alps: an interdisciplinary approach. *Global and Planetary Change* 60 (1–2), 42–57.

Figures

Figure 1: Reconstructed and measured cumulative glacier front variations in the Alps, Norway and southern South America since the LIA (in the y-axis the zero corresponds to the most extensive front position of glaciers during the LIA). The period with direct front measurements is indicated by gray background. The inset bars show the number of dated positions available since the LIA for the selected glaciers. Note the significantly lower number of data points available from the Andes.

Figure 2: Fluctuations of the Mer de Glace, France, during and following the Little Ice Age, reconstructed from a variety of sources (Nussbaumer et al., 2007). Length changes (relative to 1644 = maximum of the LIA) were derived from reliable documentary data shown in the compilation below the x-axis, where small horizontal lines indicate uncertainties concerning the date of the document. Landmarks are indicated beside the y-axis. In situ measurements for the 1911–2003 period were obtained from the Laboratoire de Glaciologie et Géophysique de l'Environnement (LGGE) in Grenoble. Images below: The Mer de Glace (a) in 1804 (presumably) drawn by Jean-Antoine Linck, (b) in 1842 mapped by James David Forbes, (c) in the 1850s photographed by Henri Plaut, and (d) in 2005 (Nussbaumer et al., 2007).

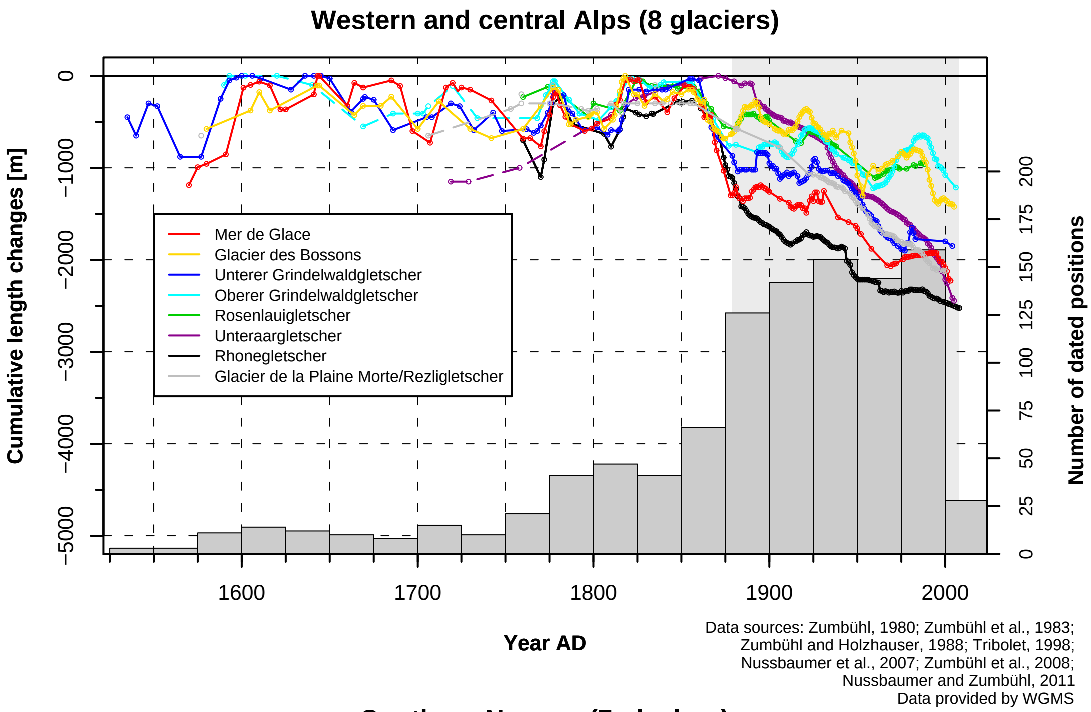
Western and central Alps (8 glaciers)
Cumulative length changes [m]
Number of dated positions
Year AD
Mer de Glace
Glacier des Bossons
Unterer Grindelwaldgletscher
Oberer Grindelwaldgletscher
Rosenlauigletscher
Unteraargletscher
Rhonegletscher
Glacier de la Plaine Morte/Rezligletscher
Data sources: Zumbühl, 1980; Zumbühl et al., 1983; Zumbühl and Holzhauser, 1988; Tribolet, 1998; Nussbaumer et al., 2007; Zumbühl et al., 2008; Nussbaumer and Zumbühl, 2011
Data provided by WGMS

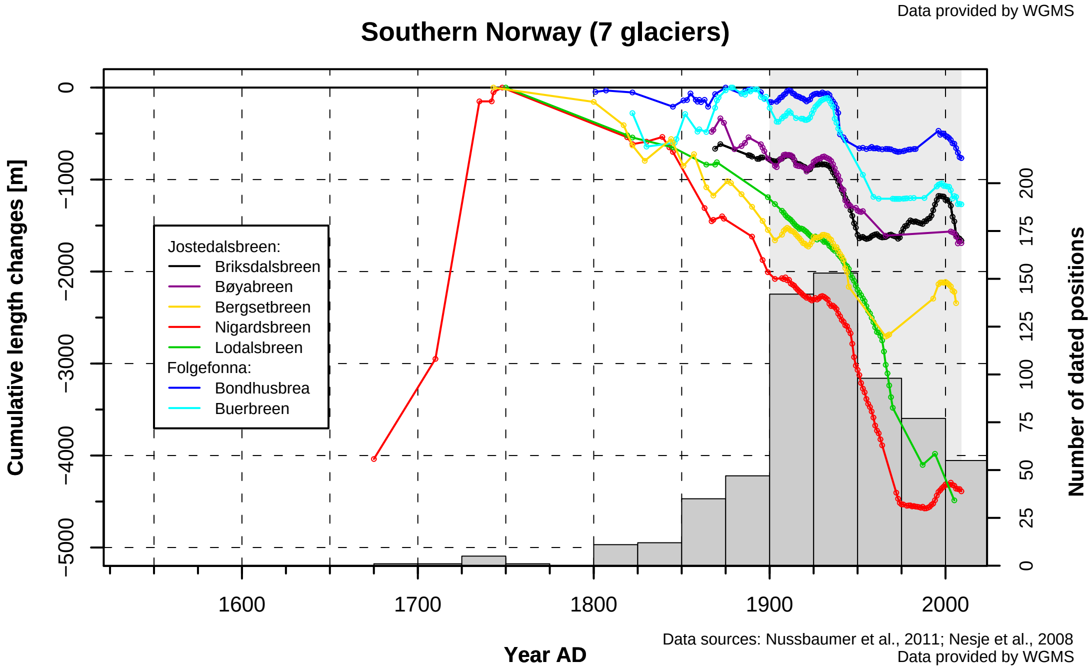
Southern Norway (7 glaciers)
Cumulative length changes [m]
Number of dated positions
Year AD
Jostedalsbreen:
Briksdalsbreen
Bøyabreen
Bergsetbreen
Nigardsbreen
Lodalsbreen
Folgefonna:
Bondhusbrea
Buerbreen
Data sources: Nussbaumer et al., 2011; Nesje et al., 2008
Data provided by WGMS

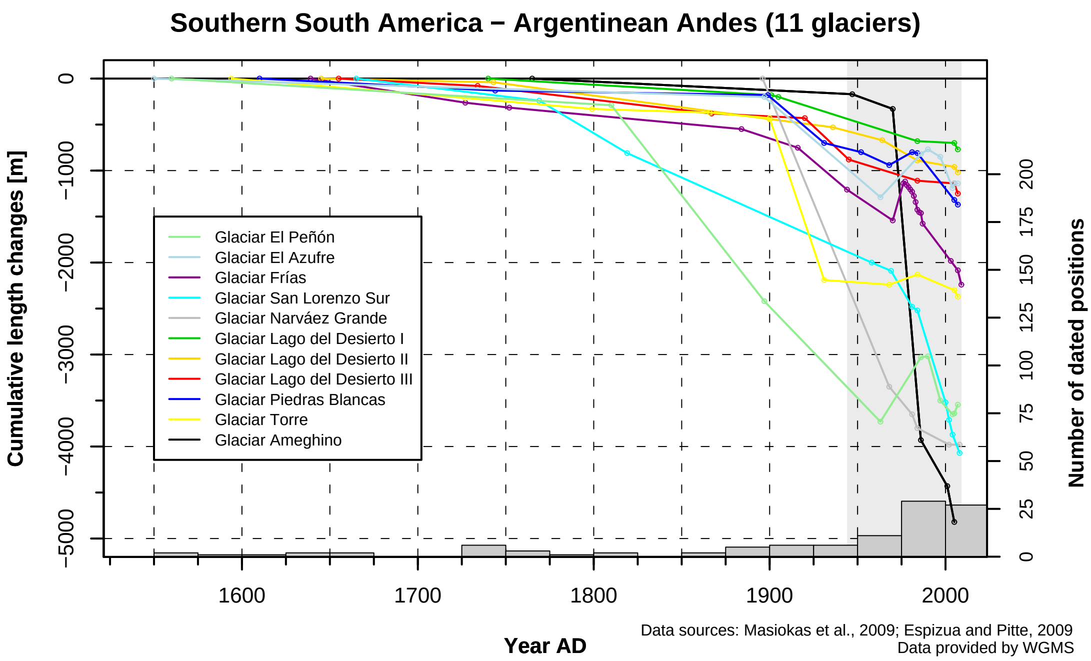
Southern South America − Argentinean Andes (11 glaciers)
Cumulative length changes [m]
Number of dated positions
Year AD
Glaciar El Peñón
Glaciar El Azufre
Glaciar Frías
Glaciar San Lorenzo Sur
Glaciar Narváez Grande
Glaciar Lago del Desierto I
Glaciar Lago del Desierto II
Glaciar Lago del Desierto III
Glaciar Piedras Blancas
Glaciar Torre
Glaciar Ameghino
Data sources: Masiokas et al., 2009; Espizua and Pitte, 2009
Data provided by WGMS

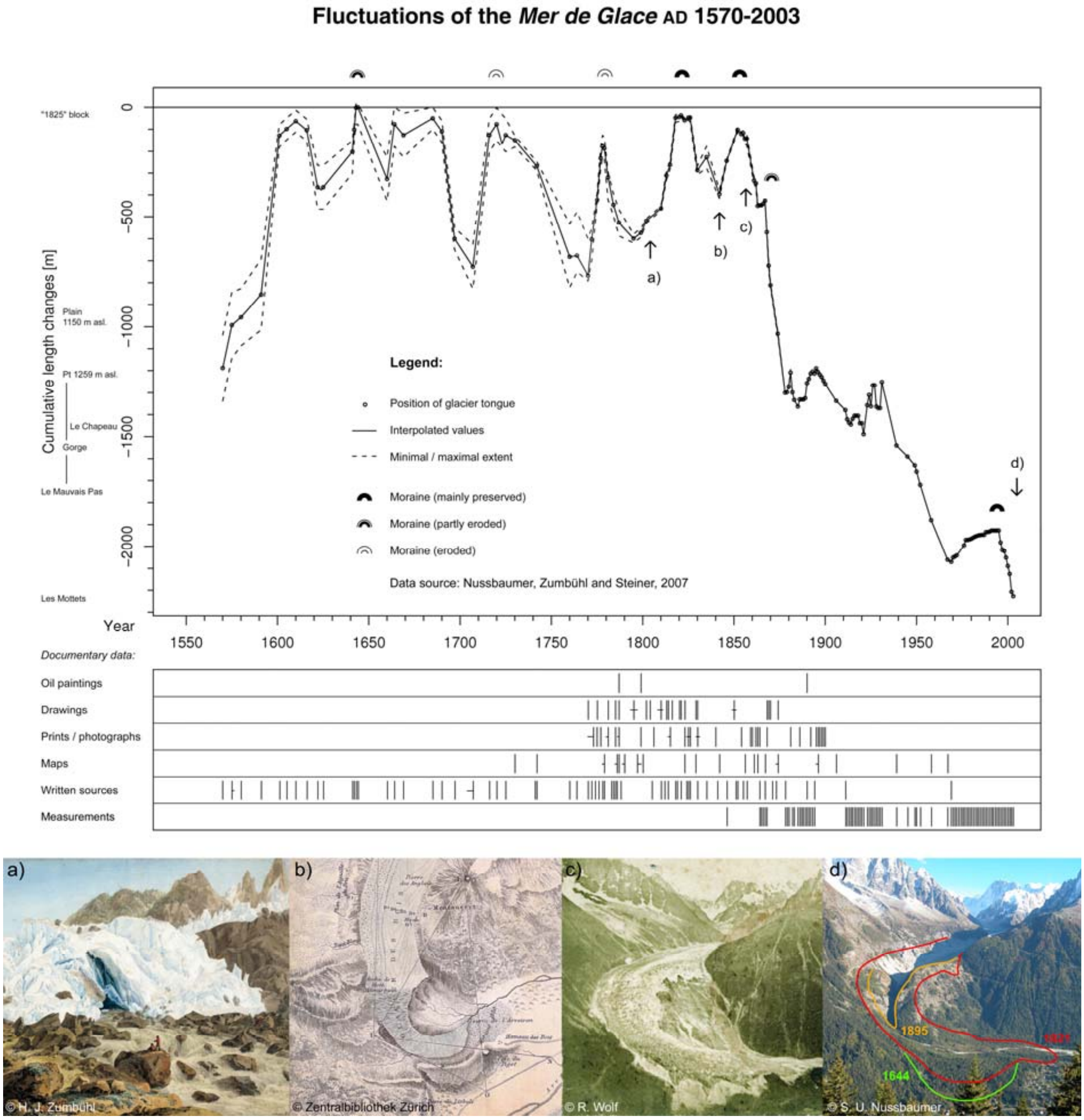

Fluctuations of the Mer de Glace AD 1570-2003
Cumulative length changes [m]
Year
"1825" block
Plain
1150 m asl.
Pt 1259 m asl.
Le Chapeau
Gorge
Le Mauvais Pas
Les Mottets
0
-500
-1000
-1500
-2000
1550
1600
1650
1700
1750
1800
1850
1900
1950
2000
a)
b)
c)
d)
Legend:
Position of glacier tongue
Interpolated values
Minimal / maximal extent
Moraine (mainly preserved)
Moraine (partly eroded)
Moraine (eroded)
Data source: Nussbaumer, Zumbühl and Steiner, 2007
Documentary data:
Oil paintings
Drawings
Prints / photographs
Maps
Written sources
Measurements
© H. J. Zumbühl
© Zentralbibliothek Zürich
© R. Wolf
© S. U. Nussbaumer
1895
1644

Publication 5

Cogley, J.G., Hock, R., Rasmussen, L.A., Arendt, A.A., Bauder, A., Braithwaite, R.J., Jansson, P., Kaser, G., Möller, M., Nicholson, L. & **Zemp, M.** (2011). **Glossary of Glacier Mass Balance and Related Terms**. IHP-VII Technical Documents in Hydrology No. 86, IACS Contribution No. 2, UNESCO-IHP, Paris.

GLOSSARY OF GLACIER MASS BALANCE AND RELATED TERMS

Prepared by the
Working Group on Mass-balance
Terminology and Methods
of the
International Association of Cryospheric Sciences (IACS)

IHP-VII Technical Documents in Hydrology No. 86
IACS Contribution No. 2

Citation:
Cogley, J.G., R. Hock, L.A. Rasmussen, A.A. Arendt, A. Bauder, R.J. Braithwaite, P. Jansson, G. Kaser, M. Möller, L. Nicholson and M. Zemp, 2011, *Glossary of Glacier Mass Balance and Related Terms*, IHP-VII Technical Documents in Hydrology No. 86, IACS Contribution No. 2, UNESCO-IHP, Paris.

Front-cover credits

Left:	Accumulation stake on Vestfonna, Svalbard (Marco Möller)
Middle:	Snow pit on Storglaciären, Sweden (Peter Jansson)
Right::	Transient snowline on Baby Glacier, Axel Heiberg Island, Canada (Jürg Alean)

Back-cover credits

Geodetic survey work on White Glacier, Axel Heiberg Island, Canada (Peter Adams)

Back-cover photo

Foreword

This glossary, produced by a Working Group of the International Association of Cryospheric Sciences (IACS), is the first comprehensive update of glacier mass balance terms for more than 40 years. The mass balance of a glacier is a measure of the change in mass of the glacier, or part of it, over a period of time. Mass balance data help to explain why a particular glacier system may be advancing or retreating and what climate drivers (e.g. decreased snow accumulation; increased surface melt) are responsible for the changes. Fluctuations of the size (most typically length, but also area and/or surface elevation) are monitored for several thousand of the more than 100,000 glaciers distributed globally from equatorial mountains to polar ice sheets. However regular annual mass balance measurements are made on fewer than 200 glaciers. Mass balance information is essential for defining the links between past, present and future climate changes and changes to glaciers in assessments such as those made by the Intergovernmental Panel on Climate Change (IPCC). Having a systematic, concise and unambiguous mass balance terminology is a critical part of this.

The first systematic attempts to define mass balance terminology (UNESCO/IASH, 1970; Anonymous, 1969) were made during the United Nations Educational, Scientific and Cultural Organization (UNESCO) International Hydrological Decade (IHD, 1965-1974). The IHD programme provided an important impetus to international collaboration in hydrology and in 1975, was succeeded by the UNESCO International Hydrological Programme (IHP). IHP has an emphasis on methodologies for hydrological studies, training and education in the water sciences and on the adaptation of the hydrological sciences to cope with the expected changing climate and environmental conditions. It is hence fitting that this glossary is published as part of the IHP series of *Technical Documents in Hydrology*.

This publication is also a crucial early milestone in the work of the International Association of Cryospheric Sciences. IACS is the eighth and newest Association of the International Union of Geodesy and Geophysics (IUGG). Although it has precedents reaching back to the 1894 International Commission on Glaciers, IACS only became a full IUGG Association in 2007. This volume is the first work conceived and completed during the period that IACS has been a full Association. IACS is grateful to the International Hydrological Programme of UNESCO for providing the opportunity to publish the glossary as the second volume in a joint series.

The mass balance definitions and terminologies documented during the IHD have served well for more than 40 years. There are however some ambiguities in current usage, and new technologies (e.g. space-borne altimeters and gravimeters, ground penetrating radars, etc.) are now used for mass balance measurements, particularly of ice sheets. This new glossary addresses these, promotes clarity, and provides a range of useful ancillary material.

IACS, and the glaciological community as a whole, is very grateful to the Chair of the Working Group, Graham Cogley, and his dedicated team of volunteers for producing this volume. It is intended that the Working Group will continue to serve and to produce further reference publications on topics such as mass balance measurement techniques and guidelines for reporting measurement uncertainty.

Ian Allison
President, International Association of Cryospheric Sciences
Hobart, Australia
January 2011

Acknowledgements

The Working Group is very grateful to Garry Clarke, Charles Fierz, Andrew Fountain, Will Harrison, Jo Jacka and Tomas Jóhannesson for careful reviews of the entire Glossary which led to substantial improvements. We also owe a great debt to those colleagues who have commented on the Glossary in whole or in part: Liss Andreassen and colleagues at Norges Vassdrags og Elektrisitetsvesen, Dave Bahr, Andrey Glazovskiy, Barry Goodison, Jon Ove Hagen, Matthias Huss, Wilfried Haeberli and Vladimir Konovalov.

Many thanks also go to colleagues who have assisted in the compilation of the Glossary by discussing mass balance in general and advising on points of detail: Jason Amundsen, Richard Armstrong, Ed Bueler, Howard Conway, Hajo Eicken, Charles Fierz, Ralf Greve, Hilmar Gudmundsson, Jeff Kargel, Ian Joughin, Doug MacAyeal, Roman Motyka, Simon Ommanney, Tad Pfeffer, Bruce Raup, Gina Schmalzle, Ben Smith, Sergey Sokratov, Martin Truffer, Ed Waddington, Mauro Werder and Dale Winebrenner.

Ken Moxham of the International Glaciological Society gave valuable advice about style. Eric Leinberger helped greatly by producing a professional-looking Figure 2 from our hand-drawn drafts.

The advice of these colleagues, and possibly of others whose names we have inadvertently omitted, has improved the Glossary in ways that are many and substantial, and has brought it closer to the ideal of a community-wide consensus than would otherwise have been possible. Nevertheless we owe it to our advisors to note that the Working Group has not been able to agree with them on all points, and that any remaining mistakes are our own fault.

We appreciate very much the willingness of UNESCO, through its International Hydrological Programme (IHP), to publish the *Glossary of Glacier Mass Balance and Related Terms* in its series Technical Documents in Hydrology and as IACS Contribution No. 2. Siegfried Demuth, chief of the IHP section on Hydrological Processes and Climate, and Vincent Leogardo of the IHP Secretariat, have been extremely helpful in seeing the glossary through the process of publication.

Last but not least, we are grateful to the Bureau of the International Association of Cryospheric Sciences (IACS) for its steady and enthusiastic support of the Working Group and the Glossary.

IACS Working Group on Mass-Balance Terminology And Methods

Anthony Arendt
Geophysical Institute, University of Alaska, Fairbanks, AK, **USA**
arendta@gi.alaska.edu

Andreas Bauder
VAW, ETH, Zürich, **Switzerland**
bauder@vaw.baug.ethz.ch

Roger Braithwaite
Environment and Development, University of Manchester, Manchester, **UK**
roger.braithwaite@manchester.ac.uk

Graham Cogley (Chair)
Geography, Trent University, Peterborough, **Canada**
gcogley@trentu.ca

Regine Hock
Geophysical Institute, University of Alaska, Fairbanks, AK, **USA**
regine@gi.alaska.edu

Peter Jansson
Physical Geography and Quaternary Geology, Stockholm University, Stockholm, **Sweden**
peter.jansson@natgeo.su.se

Georg Kaser
Institut für Meteorologie und Geophysik, University of Innsbruck,
Innsbruck, **Austria**
georg.kaser@uibk.ac.at

Marco Möller
Physical Geography and Climatology, RWTH Aachen University, Aachen, **Germany**
marco.moeller@geo.rwth-aachen.de

Lindsey Nicholson
Institut für Meteorologie und Geophysik, University of Innsbruck,
Innsbruck, **Austria**
lindsey.nicholson@uibk.ac.at

Al Rasmussen
Earth and Space Sciences, University of Washington, Seattle, WA, **USA**
lar@ess.washington.edu

Michael Zemp
WGMS, University of Zürich, Zürich, **Switzerland**
michael.zemp@geo.unizh.ch

Contents

GLOSSARY OF GLACIER MASS BALANCE AND RELATED TERMS

IACS Working Group on Mass-balance Terminology and Methods

To enchain syllables, and to lash the wind, are equally the
undertakings of pride, unwilling to measure its desires by its strength.

Samuel Johnson, 1755, *A Dictionary of the English Language*.

1 Introduction

The aim of this *Glossary of Glacier Mass Balance and Related Terms* is to update and revise what has long been the effective standard of mass-balance terminology (Anonymous 1969). Although Anonymous (1969) has served glaciology well for 40 years, there is widespread agreement on the need for a new look at terminology. The new Glossary reflects changes in practice with conventional measurement tools, and also in what is possible with the wide range of new tools which were not available in the 1960s, in particular those now available for the measurement of ice-sheet mass balance. The Glossary includes commentary on usage, particularly problematic usage, with recommendations where appropriate.

Similar publications have appeared in the past. Armstrong et al. (1973) focus strongly on sea ice. Kotlyakov and Smolyarova (1990) is a valuable multi-lingual source but does not cover mass balance as intensively as mass-balance specialists might wish. Nor does the Russian-language dictionary of Kotlyakov (1984). Glaciers Online (undated) is a valuable source for glaciological terms in general, with excellent illustrations. In neighbouring fields, American Meteorological Society (2000), European Avalanche Services (2009) and Canadian Avalanche Association (undated), Fierz et al. (2009), National Snow and Ice Data Center (undated), PhysicalGeography.net (undated), UNESCO (undated) and van Everdingen (2005) are all valuable tools. None of these, however, offers the scope or the kind of detail envisaged for this glossary.

The scope of the glossary extends beyond the measurement of mass balance. There are articles covering such subjects as glacier zonation; the definition of glacier features and morphological types of glaciers; the administrative structures within which mass-balance data are archived once collected; and the modelling of mass balance. We have also included some terms that are mainly of historical interest, and some technical terms from other disciplines that appear in reports of mass-balance measurements by newer methods.

The purpose of the glossary is not to impose awkward constraints on the evolution of glaciological usage, but rather to promote clarity and reduce ambiguity in the communication of information about glacier mass balance, as well as to provide a range of useful ancillary material. The Glossary represents a consensus among a group of practising glaciologists.

We have tried to steer a middle course between being prescriptive, that is, laying down the law about how terms are to be used, and being descriptive, that is, simply recording the facts of current usage. For example we take a firm position on the meanings of “area” and “Julian day number”. The first is sometimes and the second often used in a way which is mistaken. Neither mistake is helpful, the first being harmful, and we think that both ought to be corrected. On the other hand, we accept that a number of technical terms have more than one meaning or sense, and simply record the variants. Examples include “snow” and “firn”. An example of a pair of terms requiring clear understanding, rather than prescriptive or descriptive definitions, is “internal accumulation” and “refreezing”, where we explain the difference of meaning and recommend that it be observed carefully.

2 History

The first measurements of mass balance were made as early as 1874 on Rhonegletscher, Switzerland. Chen and Funk (1990) were able to recover the measurements of annual mass balance for 1884–85 to 1908–09 from the earlier literature (e.g. Mercanton 1916). Unbroken series of measurements at two sites on Claridenfirn, Switzerland, began in 1914 and continue today. Ahlmann (1935, 1939) was a pioneer in the use of what are now regarded as "traditional" mass-balance methods. The longest continuous, modern series of annual measurements of glacier-wide mass balance was begun on the Swedish glacier Storglaciären in 1945–1946, followed by measurements on Taku Glacier in southeastern Alaska, Storbreen in Norway, and a growing number of glaciers in the Alps, western North America and other glacierized regions. As more measurement programs were initiated, it became clear that a uniform approach, as to both methods and terminology, was needed if comparisons were to be accurate and meaningful.

Widely used methods of "traditional" measurement are presented by Østrem and Brugman (1991), which evolved from Østrem and Stanley (1966, 1969), and also by Kaser et al. (2003). Hubbard and Glasser (2005) describe glaciological field methods more generally.

An early proposal for uniform usage in the study of mass balance came from Meier (1962). The terms and the organizing framework of that paper provoked considerable interest and discussion, and evolved into a consensus which was published as UNESCO/IASH (1970), although the source most often cited is Anonymous (1969), a digest of the UNESCO/IASH recommendations which appeared in the *Journal of Glaciology*. Some supplementary material, discussed below, appeared as UNESCO/IASH (1973). Anonymous (1969), while having no formal status, soon became the *de facto* standard for the presentation of mass-balance data.

Anonymous (1969) has been a living, evolving standard over the past four decades. A notable early development appeared in the appendix of UNESCO/IASH (1973), and also as the paper by Mayo et al. (1972). This was a method for combining the stratigraphic and fixed-date "time systems" of Anonymous (1969). The fixed-date system was referred to as the annual system by Mayo et al., who introduced an extensive set of new definitions. Most of these were not adopted, and the main practical result of Mayo et al.'s work was that there are now not two but four recognized time systems, the combined system and the floating-date system being added to the original two.

Today, annual mass balance is measured each year on more than 100 glaciers, and seasonal balances on up to about 40 of those. These measurements are part of an integrated monitoring strategy, described in the Glossary (see *Global Terrestrial Network for Glaciers*). The data are submitted, according to specific guidelines (WGMS 2007b), to the World Glacier Monitoring Service in Zürich, which publishes regular summaries (e.g. WGMS 2007a, 2008a) of the results of mass-balance and other glaciological measurements. A recent survey of available datasets is in WGMS (2008b). The organizational history of mass-balance data management is covered by Radok (1997) and Jones (2008).

Among the important methodological developments of the past 20 years, the emergence of accurate techniques for measurement of the mass balance of ice sheets is particularly notable. The Working Group has made a special effort to cover the terminology of this subject. However, some of the techniques are still emerging (ISMASS Committee 2004), and the time may not be ripe for the specification of guidelines, still less of standards. On the other hand, it is preferable that usage be agreed upon before the terminology becomes fixed in inconsistent and ambiguous ways. Another development is that remotely sensed measurements of mass balance, particularly by geodetic methods, are now a reality. They can be expected to grow in importance, and we have compiled the Glossary with this likelihood in mind, as well as with an eye to the desirability of a common language for the study of glaciers of all sizes (including the ice sheets).

The Bureau of the International Association of Cryospheric Sciences (IACS) approved in principle the creation of a Working Group on Mass-balance Terminology and Methods at its meeting in Perugia in July 2007. The membership of the Working Group was recruited by announcing an invitation to volunteer at the Workshop on Mass Balance Measurements and Modelling held in March 2008 in Skeikampen, Norway. The Working Group was constituted formally at the April 2008 IACS Bureau meeting in Vienna.

The Working Group's activities are organized in terms of a number of themes. Future publications are intended to address subjects such as methods of measurement, guidelines for the reporting of measurement uncertainty, and access to mass-balance data. The present publication, however, is devoted to definitions and terminology.

3 Mass Balance Terminology

3.1 Sign convention

Studies of mass balance are usually not strongly tied to a two- or three-dimensional coordinate frame, especially when the glacier is one in a collection of “boxes” or “control volumes”. In such cases the most common sign convention is “positive inward”, meaning that flows across the boundary of the box are positive when the box gains, and negative when it loses, some of the flowing quantity. This is the main sign convention adopted in this Glossary. *Accumulation* is positive, *ablation* is negative, and balance calculations for the glacier require only additions, but exchanges with other boxes must be managed carefully. After leaving one box, such as a glacier, the sign of the flux must be changed before it enters any other box, such as the ocean.

The main alternative sign convention is that fluxes are positive in the positive coordinate direction. In many systems, a framework of orthogonal coordinates is an obvious way to describe space. This requires careful attention to plus signs and minus signs in algebraic descriptions of the balance of any part of the system. This sign convention is commonly used for glacier flow. For example, one horizontal coordinate may be oriented so that it increases in the downslope (often the down-valley) direction. Then the downslope horizontal component of the velocity vector is positive, and the flux divergence is positive where the flow accelerates and negative where it decelerates.

Whatever sign convention is adopted, reports of mass-balance investigations should state it clearly and use it consistently.

3.2 Notation

It is not possible to standardize all the uses of symbols in mass-balance work, but certain conventions are universally or at least very widely observed. The conventions described here differ from those of Anonymous (1969) in a number of respects.

3.2.1 Variables The variables that appear most often in mass-balance studies are denoted as follows:

a	ablation	c	accumulation	b	mass balance (c+a)
ρ	density	h	glacier thickness		
S	area	V	volume		
AAR	accumulation-area ratio	ELA	equilibrium-line altitude		

The use of h for thickness (a vertical extent) promotes clarity by allowing the symbol z to be reserved for elevations (that is, vertical coordinates). In algebraic expressions, AAR and ELA can be replaced by suitable mnemonic symbols, for example α or z_{eq}.

Calving, a form of ablation, often requires a separate symbol. The Working Group suggests that calving be represented as a horizontal flux $\dot{d}$ or $\dot{D}$ (see *section 3.2.4* for the significance of the overdot). The letter chosen suggests “detachment” rather than discharge. It should be understood that *ice discharge* at the *calving front* and calving itself are only equal at a calving front that neither advances nor retreats (see *Formulations of Mass Balance*, and also *Capitalization*, below).

3.2.2 Subscripts Subscripts are used, among other purposes, for representing parts of the mass-balance year or of the column through the glacier:

a	annual	w	winter	s	summer		
sfc *or* s	surface	i	internal	bed *or* b	basal	f	frontal

The absence of a subscript normally implies “annual”. The subscript n for “net” appears frequently in the literature; see the article *Net mass balance*. If the glacier has a floating portion, subscript g can be used when it is necessary to distinguish the grounding line from the front. Subscripts w and i are also used with density to distinguish water from ice.

3.2.3 Capitalization In the absence of an overriding reason for contrary usage, which should be explained, lower-case symbols refer to quantities at a point on the glacier surface or to the column beneath such a point, and upper-case symbols refer to glacier-wide quantities. By analogy, quantities at points on the glacier outline and along the entire outline may also be distinguished by lower-case and upper-case symbols respectively.

3.2.4 Overdots In studies of mass balance, the function of the overdot is to denote a derivative, usually a partial derivative, with respect to time. That is, if x is any variable, $\dot{x} = \partial x / \partial t$. The overdot signifies that the variable is being expressed as a rate rather than as the equivalent *cumulative* sum, a distinction which is often needed for mass balance because measurements tend to be irregular in duration. There is no implication, as for example in some dynamical studies (Hutter 1983), that the derivative in question is a material derivative within a small volume following the flow (sometimes represented as $Dx / Dt = \partial x / \partial t + \vec{u} \cdot \nabla x$, where $\vec{u}$ is the velocity vector and ∇x is the spatial gradient of x).

3.2.5 Extensions The Working Group recommends that extensions of the notation presented here should follow Anonymous (1969), in which further qualifications are added in parentheses after basic symbols. For example $\dot{a}_{\mathrm{b(fl)}}$ and $\dot{a}_{\mathrm{b(gr)}}$ could be defined to be basal ablation rates beneath floating and grounded portions respectively of the glacier, while surface accumulation as snow and as superimposed ice might be represented as $c_{\mathrm{sfc(sn)}}$ and $c_{\mathrm{sfc(si)}}$ respectively.

4 Formulations of Mass Balance

For convenience, although at the cost of some repetition, we present here a description of the term *mass balance*, which we define as the change of the mass of the *glacier*, or part of the glacier, over a stated span of time. The meaning of "mass balance" depends on the volume within which the mass is changing and on the span of time.

A fundamental question about mass balance is A) whether its dimension is [M] (mass) or [L^3] (volume). There are two possible answers, both internally consistent, but the matter is complicated by the need to answer two further questions: B) whether to treat the balance as a sum (dimension [M], for example) or a rate (dimension [$M\ T^{-1}$]), or in other words whether to divide the change of mass by the span of time; and C) whether to express the balance as a *glacier-wide* total (dimension [M]) or a *specific* quantity (that is, per unit of glacier *area*; dimension [$M\ L^{-2}$]). In this chapter we choose to take mass as the fundamental dimension, and we explain the different ways in which questions B and C can be answered. The recommendations of the Working Group on question A are set out in *section 6.2*.

4.1 Mass balance of a column

We begin with an expression for the *conservation of mass* within a column of square cross-section extending in the vertical direction through the glacier and having mass *m* (expressed here per unit of cross-sectional area; Figure 1). The horizontal dimensions of the column, *ds = dx dy*, are fixed. The mass may change due to the addition or removal of mass either at the surface (that is, to or from a layer the base of which is the *summer surface*), or within the column (referred to as *internal accumulation* or *internal ablation*), or at the bed, or to the *flow* of *ice* into or out of the column. The *mass-balance rate* of the column, in specific units (dimension [$M\ L^{-2}\ T^{-1}$]; see *section 7.1.1*), is

$$\dot{m} = \dot{c}_{\mathrm{sfc}} + \dot{a}_{\mathrm{sfc}} + \dot{c}_{\mathrm{i}} + \dot{a}_{\mathrm{i}} + \dot{c}_{\mathrm{b}} + \dot{a}_{\mathrm{b}} + (q_{\mathrm{in}} + q_{\mathrm{out}}) / ds \ . \tag{1}$$

Equation (1) obeys the positive-inwards sign convention (*section 3.1*). In particular, if $\vec{u}$ is the vertically-averaged horizontal velocity vector, q_{in} and q_{out} are of the form $\bar{\rho}\vec{u}\,h\,dy$, but q_{out} is negative.

Equation (1) is more useful as a checklist than as a guide to how to measure the mass balance. It is not practicable to measure all of its components. Those that are not measured are usually, in practice, either corrected for or assumed (or sometimes shown) to be negligible. For example it may be assumed that *internal accumulation* c_{i} is zero because the glacier is a *temperate glacier*; or *basal ablation* a_{b} may be identified as critical for estimation by modelling because the column is afloat or is in the crater of an active volcano.

For brevity, in what follows the column-average *density* $\bar{\rho}$ is held constant with respect to *t*. Errors can be substantial if this assumption is wrong; see *Sorge's law* in the Glossary.

A special case of (1) is the well-known *continuity equation*

$$\dot{h} = \dot{b} - \nabla \cdot \vec{q}\ , \tag{2}$$

in which, because the average density is constant, changes in *h* are due only to changes in mass. Each term in (2) is expressed in *ice-equivalent* units (dimension [$L\ T^{-1}$]). Thus $\dot{b}$ is equal to $(\dot{c}_{\mathrm{sfc}} + \dot{a}_{\mathrm{sfc}} + \dot{c}_{\mathrm{i}} + \dot{a}_{\mathrm{i}} + \dot{c}_{\mathrm{b}} + \dot{a}_{\mathrm{b}})$ divided by $\bar{\rho}$. The two flow terms on the right in (1) are replaced by the representation of the *flux divergence* that is usual in dynamics. The flow vector $\vec{q}$ is equal to $h\vec{u}$, where $\vec{u}$ is the vertically-averaged ice velocity, and obeys the same sign convention (positive in positive coordinate directions) as $\vec{u}$.

4.2 Climatic mass balance and climatic-basal mass balance

In studies of glacier dynamics, the term $\dot{b}$ in (2) is often called the "mass balance", or more appropriately the "mass-balance rate". In this interpretation, "mass balance" excludes mass changes due to ice flow, which is not consistent with the more general definition of (1). To resolve this ambiguity, we introduce *climatic-basal mass balance* as an appropriate new name for the $\dot{b}$ that appears in the continuity equation (equation 2). This terminology makes it clear that $\dot{b}$ represents mass changes at and near the surface, which are driven primarily by climate, and those at the bed, but not those due to flow dynamics.

Sometimes, with the aim of emphasizing this distinction, $\dot{b}$ is called the “surface mass balance”. The *surface mass balance* is the sum of *surface accumulation* and *surface ablation*, so this usage is accurate if the internal and basal terms in (1) are negligible. However an ambiguity arises because, in some recent studies, the meaning of “surface mass balance” has been extended so that it also includes *internal accumulation*. To avoid confusion the latter usage is better avoided, and instead we recommend the term *climatic mass balance* for the sum of the surface mass balance and the *internal mass balance*.

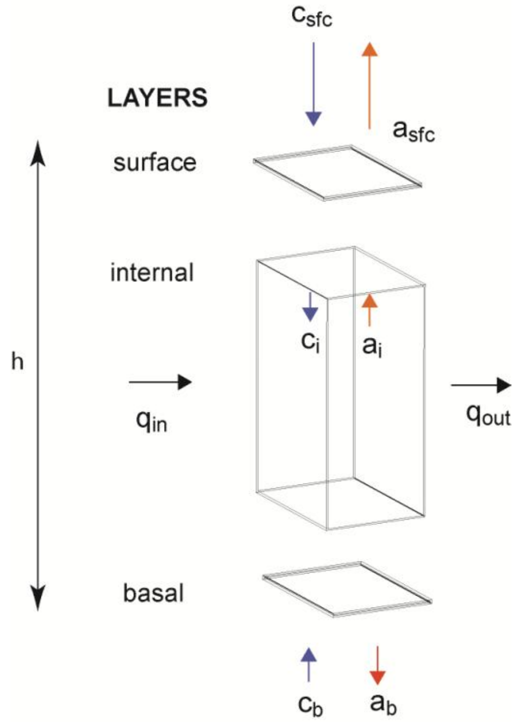

Figure 1. The mass balance of a column of glacier ice, firn and snow. In general, density ρ varies through the thickness $h = m/\bar{\rho}$; h may vary due to changes in either mass m or average density $\bar{\rho}$.

4.3 Mass-balance components

By the convention of section 3.2.3, the lower-case symbols in (1) denote components of the *point mass balance*. Table 1 introduces the equivalent upper-case symbols for the glacier-wide mass balance, which is derived in the next section. It is also convenient to introduce here the simple distinction between the mass-balance rate, in terms of which the formulations above have been cast, and the *mass balance*, which is a mass change rather than a rate. For example the point mass balance Δm for the span of time from t_0 to t_1 is linked to the mass-balance rate by

$$\int_{t_0}^{t_1} \dot{m}(t)\,dt = m(t_1) - m(t_0) = \Delta m\,. \qquad (3)$$

Whether to present the balance as a rate or not will depend on the context of the investigation.

The mass change relative to time t_0, considered as a function of time $m(t) - m(t_0)$, is referred to as the *cumulative mass balance* (see also *Figure 5*).

The mass-balance components in Table 1 are defined in the Glossary. The symbols in the table are for the glacier-wide mass balance; the corresponding lower-case letters denote the mass balance of a column (the point mass balance). Except for the mass balance itself, for which $\dot{M}$ and ΔM are recommended, symbols for the mass-balance rate are the same as for the corresponding mass-balance component but with an overdot. In measurements of the mass balance, and often in models of its short-term evolution, the mass of the glacier is neither known nor needed. However the symbol M for total glacier mass is likely to be in increasing demand in studies of the long-term future of glaciers.

Table 1 Recommended notation for components of the mass balance

Component	*Symbols*	*Constituents*
Surface accumulation	C_{sfc}	
Surface ablation	A_{sfc}	
Surface balance	B_{sfc}	$C_{sfc} + A_{sfc}$
Internal accumulation	C_i	
Internal ablation	A_i	
Internal balance	B_i	$C_i + A_i$
Basal accumulation	C_b	
Basal ablation	A_b	
Basal balance	B_b	$C_b + A_b$
Climatic balance	B_{clim}	$B_{sfc} + B_i$
Climatic-basal balance	B	$B_{clim} + B_b$
Calving	D	
Subaerial frontal melting and sublimation	$A_{f(air)}$	
Subaqueous frontal melting	$A_{f(wtr)}$	
Frontal ablation	A_f	$D + A_{f(air)} + A_{f(wtr)}$
Accumulation	C	$C_{sfc} + C_i + C_b$
Ablation	A	$A_{sfc} + A_i + A_b + A_f$
(Total) mass balance	ΔM	$C + A = B + A_f$

4.4 Glacier-wide mass balance

In what follows, the glacier-wide mass balance is expressed in specific units and as a rate, and the *area S* of the glacier is taken implicitly to be a function of time. Alternative but equivalent formulations are illustrated in section 4.4.1, and Figure 2 illustrates the processes that may contribute to the glacier-wide mass balance.

To obtain the glacier-wide climatic-basal mass-balance rate, we add together the climatic-basal rates of a set of columns (as in Figure 1) over the area S:

$$\dot{B} = \frac{1}{S}\int_S \dot{b}\, ds \quad , \tag{4}$$

but this is not a complete statement of the mass-balance rate because it omits *frontal ablation*, that is, mass loss by calving, subaerial frontal melting and sublimation (above the waterline) and subaqueous frontal melting (below the waterline). (See also Table 1.) Mass loss at the glacier front due to processes other than *calving* can be significant, and even dominant. For simplicity, however, in what follows we assume processes other than calving to be negligible and write the complete glacier-wide mass-balance rate as

$$\dot{M} = \dot{B} + \dot{D} / S \, , \tag{5}$$

where the *calving flux* (dimension [M T^{-1}]) along the perimeter P of the calving margin is

$$\dot{D} = \int_P \dot{d}\; dp \, . \tag{6}$$

and the calving flux per unit of distance along the margin (dimension [M L^{-1} T^{-1}]) is

$$\dot{d} = -\bar{\rho} h \vec{u}_D \quad . \tag{7}$$

Here the *calving velocity* $\vec{u}_D$ averaged over the glacier thickness at any point *p* on the margin is defined as

$$\vec{u}_D = \vec{u} - \dot{L}, \qquad (8)$$

where $\vec{u}$ is the vertically-averaged horizontal velocity and $\dot{L}$ is the rate of advance of the margin, both reckoned normal to the margin; if the flow direction is at right angles to the margin then *L* is the length of the *flowline* that reaches the margin at *p*.

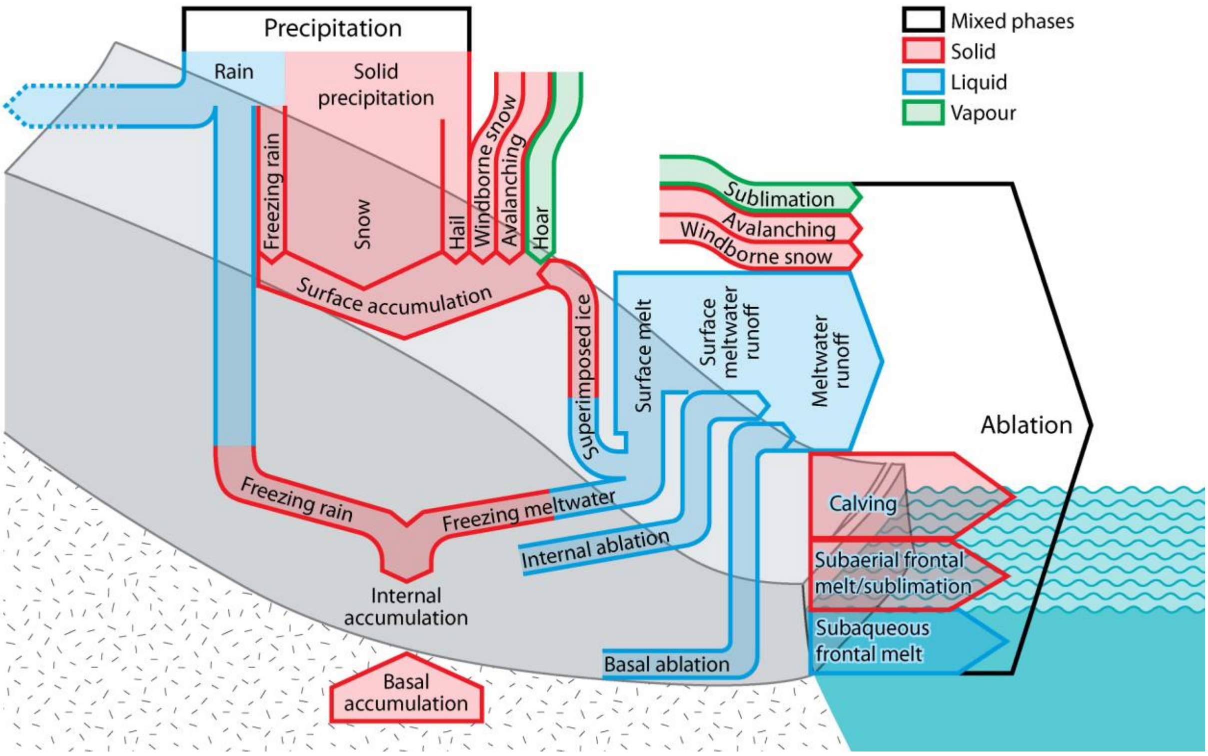

Figure 2. Components of the mass balance of a glacier. The arrows have arbitrary widths and do not indicate physical pathways of mass transfer.

Through (8), equation (7) has two components: the *ice discharge* and the mass "flux" $\bar{\rho}h\dot{L}$ implied by changes in the position of the *calving front*. The ice discharge is defined everywhere on the glacier, not just at the calving front. It can be represented (Figure 3) as $\bar{q} = -\bar{\rho}h\bar{u}$, here in mass units rather than the ice-equivalent units of (2).

The glacier may be delineated such that other mass changes due to flow must be considered, as when separate mass balances are calculated for the grounded and floating portions. The balance is also sometimes calculated for only part of the glacier. In both these cases a term analogous to $\dot{D}$ must be retained in (5) to represent ice flow, inward or outward, across the boundary of the study region. If the boundary itself is mobile, as when a *grounding line* or drainage *divide* migrates, its motion must also be represented. For example migration of the divide results in both inflow and outflow becoming zero on both sides of the new divide and ceasing, in general, to be zero at the old. On each side of the divide, a relation analogous to (7) can be invoked with $\vec{u}_D$ playing the role of "divide velocity", positive in the direction of the growing glacier.

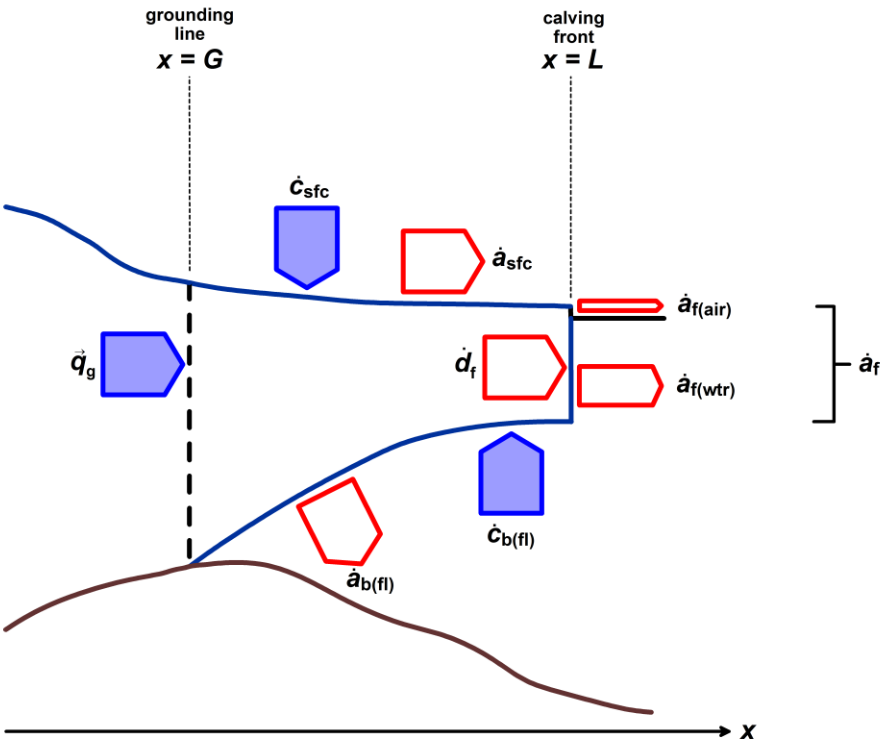

Figure 3. Mass-balance components of a floating tongue or ice shelf; components of the internal mass balance are neglected. Shaded arrows represent gains by accumulation and flow. Unshaded arrows represent ablation. $\dot{d}_f$ is the calving flux, obtained from equations (8) and (7). When frontal ablation other than by calving is significant, the total loss at the front can be represented (Table 1) as $\dot{a}_f$, the sum of the calving flux, subaerial frontal melting and sublimation $\dot{a}_{f(air)}$, and subaqueous frontal melting $\dot{a}_{f(wtr)}$. The diagram is a two-dimensional representation of a flowline with horizontal coordinate *x*, with *x* = *G* at the grounding line and *x* = *L* at the calving front. At the grounding line the inflow to the floating portion is equal to the ice discharge $\vec{q}_g$. For an ice shelf or marine-terminating tongue, the sum of subaqueous frontal ablation and basal ablation is called submarine ablation.

4.4.1 Alternative formulations In (5), $\dot{M}$ is a glacier-wide specific mass-balance rate with dimension [M L^{-2} T^{-1}]. To illustrate our recommended notation, the glacier-wide mass-balance rate with dimension [M T^{-1}] is

$$\begin{aligned}\dot{M} &= \int_S \dot{b}\, ds + \int_P \dot{d}\, dp \\ &= \dot{B} + \dot{D}\end{aligned} \tag{9}$$

with no separate symbol to distinguish, for example, the $\dot{B}$ of (5) from the $\dot{B}$ of (9). This distinction should be made by stating the units of the quantity. The glacier-wide mass balance (dimension [M]) is

$$\begin{aligned}\Delta M &= \int_{t_0}^{t_1}\left[\int_S \dot{b}\, ds + \int_P \dot{d}\, dp\right] dt\ , \\ &= \int_S b\, ds + \int_P d\, dp \quad ,\end{aligned} \tag{10}$$

where in the second line $b = \int_{t_0}^{t_1} \dot{b}\, dt$ is the specific point mass balance (with dimension [M L^{-2}]), implicitly over the columns within *S*, and similarly $d = \int_{t_0}^{t_1} \dot{d}\, dt$ is the calving loss (dimension [M L^{-1}]) along the calving margin *P*, both over the time span from t_0 to t_1. The corresponding glacier-wide specific mass balance (dimension [M L^{-2}]), again with no separate symbol, is

$$\Delta M = \frac{1}{S}\int_S b\, ds + \frac{1}{S}\int_P d\, dp \ . \quad (11)$$

We expect that normally the various qualifying adjectives and nouns will be used only when necessary to eliminate ambiguity.

4.5 Seasonal mass balance

Mass-balance measurements have traditionally spanned either a *year* or a *winter season* or *summer season*, although shorter-term measurements have always played a role in detailed studies, and *multi-annual* measurements by *geodetic methods* have long been used as checks on the accuracy of annual measurements by the *glaciological method*. Recent developments have increased the importance of geodetic methods greatly. Moreover, *gravimetric methods* and mass-balance modelling both promise to make high temporal resolution (days) available routinely.

Nevertheless the traditional focus on the seasonal cycle is as important as ever. The annual and seasonal balances at a point on the glacier are related by

$$b_{\mathrm{a}} = c_{\mathrm{a}} + a_{\mathrm{a}} = b_{\mathrm{w}} + b_{\mathrm{s}} \ . \quad (12)$$

(In the literature, b_{n} often appears in place of b_{a}; see *Net mass balance*.) Seasonal mass balances are usually not expressed as rates. Each of the simple equalities in (12) is a complete description of the climatic-basal mass balance over a period of a year, and for many purposes, especially when only surface quantities need to be considered, no further detail is needed. However it is difficult to measure the *annual accumulation* and *annual ablation*, and indeed impossible with only one or two visits to the glacier each year. This makes the second, seasonal equality in (12) very important, because measurements of *winter balance* and *summer balance* are in practice the only way to isolate the two main climatic forcings. It should be stressed, however, that in general both b_{w} and b_{s} have components of accumulation and ablation, so that, notwithstanding the second equality in (12), $c_{\mathrm{a}} > b_{\mathrm{w}}$ and $a_{\mathrm{a}} < b_{\mathrm{s}}$.

5 Reporting of Mass-balance Data

In a typical mass-balance programme based on the glaciological method, only the two seasonal terms of (12) are measured, and often only the annual term. The minimal requirements for reporting a mass-balance measurement are therefore quite simple: the annual balance, or the winter balance and summer balance if they are known separately, for the whole and possibly for parts of the glacier; the area of the glacier, and when applicable the area-altitude distribution, are also among the minimal data requirements because they are needed for conversion between glacier-wide and specific units. Certain other data are also essential, primarily glacier location, survey dates and the dates to which the measurement refers.

Minimum and maximum glacier elevations, reported separately from the area-altitude distribution, are highly desirable. It is usual to report the accumulation-area ratio and equilibrium-line altitude when they are relevant and the method of measurement allows their determination. Precise dates and spatial details are in general even more important for understanding of the newer methods than of the traditional methods. Other information which is needed for comparison and analysis of mass-balance data, and is often not reported, relates to the treatment of the non-surface terms in (1), and to the time system in which the measurement was made. The latter is discussed in chapter 6.

All glacier mass-balance data should be reported routinely to the World Glacier Monitoring Service, Zürich, which provides guidelines for submission (WGMS 2007b).

6 Departures from Anonymous (1969)

This new set of recommendations departs from the practices recommended in Anonymous (1969), but apart from minor points of detail there are in fact only two departures, described in sections 6.1 and 6.2.

The leading feature of Anonymous (1969) was a set of terms, with accompanying definitions and recommended notation, which is summarized in Appendix A. Two "time systems" were identified, the stratigraphic system and the fixed-date system, for measurements based respectively on the quasi-annual span between successive summer surfaces and on fixed field-survey dates. There was a separate set of terms for each system. Several ancillary observed quantities were defined, all having a connection with the equilibrium line, which has long had a status almost as fundamental as the mass balance itself. Anonymous (1969) also discussed the nature of firn at length, and its suggested definition (in essence, "snow which has survived a summer but is not yet ice") has been adopted widely.

6.1 Time systems

Like other standards, Anonymous (1969) has been extended liberally *ad hoc*. For example "winter and summer seasons are not defined" in the fixed-date system. These two terms refer exclusively to the stratigraphic system, yet fixed-date winter and summer mass balances have been published. More seriously, although the time systems have taken firm root, the separate terminologies for stratigraphic and fixed-date mass balances have become entangled with each other in contemporary usage. For example "net balance" and "total accumulation" are stratigraphic-system terms, and "annual balance" and "annual accumulation" are the corresponding terms in the fixed-date system, but usage in the literature often deviates from these definitions. Phrases such as "net annual balance" appear regularly; "net" and "annual" are often used one for the other; and "total" is used occasionally with the technical meanings given in Anonymous (1969) but more commonly with its plain-English meaning. Evidently glaciologists have found the plain-language meanings of these adjectives more valuable than their technical meanings. In short, in this glossary "net" and "total" are no longer understood as having the meanings assigned to them by Anonymous (1969), and the loss of the connection to the stratigraphic system means that they are often redundant. The situation is made more complicated by the later addition of the combined time system, the name of which is at least self-explanatory, and the floating-date system, which differs from the fixed-date system in that the survey dates are allowed to vary from year to year.

We therefore adopt a different approach to time systems. We retire the terminological distinction drawn by Anonymous (1969) between the stratigraphic and fixed-date systems by the use of the adjectives "net", "annual" and "total". We emphasize strongly that we are not retiring the time systems themselves, and indeed that, by requiring authors to be explicit about which time system is in use and about the dates of observations, the intention is to make the distinctions clearer. (The various time systems are explained in more detail in the body of the Glossary.)

Table 2 seems to suggest that the importance of time-system information is not widely appreciated, or possibly that many of the reported measurements do not fit readily into any of the time systems.

Table 2 Time systems of annual measurements of mass balance reported to WGMS (up to 2008)

No information provided	1519
Fixed-date system	917
Stratigraphic system	931
Combined system	265
Other	188
Total of reported annual measurements	3820

Insufficient information about the dates of field or remote-sensing surveys is an impediment to analysis. For example, very few of the fixed-date measurements listed in Table 2 are accompanied by information on how or whether the field observations, generally made on floating dates, are corrected to the fixed dates. Often, the dates themselves are not reported, making comparison with meteorological and other data difficult or impossible. A more general problem is that measurements in the various systems can differ substantially.

Figure 4 shows that differences between determinations of $\dot{b}_a$ in the floating-date, fixed-date and stratigraphic systems can reach 0.5 m w.e. a^{-1}. Summed over the years, the deviations cancel and the median difference is negligible, but single-year differences of 0.2 m w.e. a^{-1} are typical. Such differences, due solely to differences in time system, are large enough to affect the precision of comparative analyses, and it is essential that the analyst be aware of them.

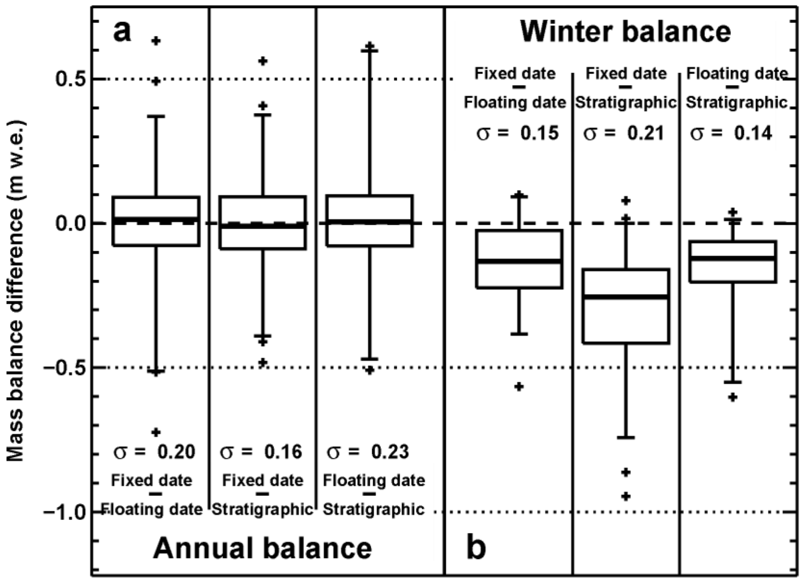

Figure 4. Distributions of differences between (a) annual and (b) winter balance measured in different time systems on two Swiss glaciers during 1960–2007 (after Huss et al. 2009). Bars range from the 2.5 to the 97.5 percentile, with outlying measurements beyond those percentiles represented by plus signs, and boxes cover the 25th to the 75th percentile of each distribution. The central thick line is the median and σ is the standard deviation.

Geodetic measurements of mass balance do not fit into any established time system. Their starting and ending dates do not coincide in general with dates of annual minimum and maximum glacier mass. While this does not affect their status as measurements of "change in the mass of a glacier … over a stated span of time", the amplitude of the annual cycle of mass change may be large by comparison with the measured change and, if the aim is to calculate an annual or seasonal balance, seasonal corrections may be essential if the dates are far enough from the ends of winter or summer. The problem is reduced when the survey dates are an integer number of years apart, but even then the comparability of such measurements with conventional measurements might be in doubt.

It is beyond the present scope to offer solutions in detail for these difficulties with time systems, but some points are clear. The Working Group recommends that:

1. Survey dates, and if different the dates over which the mass balance is reported, be regarded as integral parts of any report of a measurement of mass balance. Each date should be given to the nearest day. Where applicable, ranges of dates should be given. Where, as in the stratigraphic system, a mass-balance survey refers to an epoch that may be unknown or even to a *diachronous* surface, the survey date should be given nevertheless.
2. The method of measurement be described as part of routine metadata. As a minimum this means assigning the measurement to a time system when such an assignment makes sense, and describing seasonal corrections whenever they are made.

3. Reports of measurements include dated glacier area and hypsometric data as well as information on how to obtain maps, including digital elevation models and glacier outlines when available.

These recommendations imply an increase in the burden of reporting. Measurements of mass balance are sometimes made by volunteers, and are often incidental to research campaigns that have other primary purposes.

6.2 Dimensions

A fundamental question about mass balance is related to its dimension: is it [M] (mass) or [L^3] (volume)? Equivalently, when the balance is presented as a rate, is it [M T^{-1}] or [L^3 T^{-1}]? There are two schools of thought, both internally consistent, on this point.

One school holds that the mass in question should be divided immediately by the density of water to yield an equivalent volume of water: if the mass is stated per unit area, for example in kg m^{-2}, dividing by the density in kg m^{-3} yields a length, which is expressed in metres of water equivalent. All subsequent calculations are done in volumetric or "water-equivalent" units.

The other school holds that the division by density is a convenience rather than a fundamental operation. Mass or specific mass units (kg or kg m^{-2} respectively) are the fundamental units, and water equivalents are used for ease of visualization.

Diverging from Anonymous (1969), we have accorded primacy to mass units rather than volumetric units. This means that, although we do not discourage use of the metre and millimetre water equivalent, we consider that usage and understanding would be the better for a stronger emphasis on the difference between mass and volume. Geodetic measurements of mass balance most commonly consist of a volume-balance measurement coupled with an assumption about density, and gravimetric measurements are direct measurements of mass change. Thus the difference between mass and volume will grow in importance as geodetic and gravimetric methods become more widely used.

However we do not suggest that the metre or millimetre water equivalent should be discarded, nor do we expect that they will be. On the contrary, we suggest that the units metre water equivalent and metre ice equivalent be accorded the status of extensions of the SI. See the next section, and see also the articles in the body of the Glossary on *ice equivalent*, *mass-balance units* and *water equivalent*.

7 Units of Measurement

With three exceptions (see section 7.2), the units in which mass-balance quantities are reported are those of the Système International d'Unités or SI (BIPM 2006a, with a summary in BIPM 2006b).

7.1 Essentials of the Système International d'Unités (SI)

7.1.1 Base quantities The fundamental concept in the SI is that of a quantity. Each quantity has its own dimension, and a unit is associated with it. There are seven base quantities. The four base quantities which are used in studies of glacier mass balance are listed in Table 3 with their units.

Table 3 Some base quantities of the SI

Quantity	*Symbol for dimension*	*Base unit*	*Abbreviation for unit*
length	L	metre	m
mass	M	kilogram	kg
time, duration	T	second	s
thermodynamic temperature	Θ	kelvin	K

7.1.2 Derived quantities The SI defines a large number of derived quantities with corresponding derived units which are products of powers of the base units. Some derived units have special names and symbols (abbreviations). Table 4 gives some examples of derived quantities used in mass-balance work and closely related subjects.

Table 4 Some derived quantities of the SI

Quantity	*Units*	*Special name*	*Symbol*
area	m^2		
volume	m^3		
speed	$m\ s^{-1}$		
acceleration	$m\ s^{-2}$		
density	$kg\ m^{-3}$		
surface density	$kg\ m^{-2}$		
force	$kg\ m\ s^{-2}$	newton	N
energy	$kg\ m^2\ s^{-2}$; N m	joule	J
power	$kg\ m^2\ s^{-3}$; $J\ s^{-1}$	watt	W
pressure, stress	$kg\ m^{-1}\ s^{-2}$; $N\ m^{-2}$	pascal	Pa
Celsius temperature	K	degree Celsius	°C
frequency	s^{-1}	hertz	Hz
plane angle	$m\ m^{-1}$	radian	rad
solid angle	$m^2\ m^{-2}$	steradian	sr

Plane angle and solid angle, being ratios of base quantities and derived quantities respectively, are examples of dimensionless quantities. They have the dimension "1".

7.1.3 Multiples and submultiples Decimal multiples and submultiples of SI units may be distinguished when convenient by selecting from a set of SI prefixes. Some that arise in mass-balance studies are given in Table 5. Stylistic rules for combining prefixes with units, and prefix symbols with unit abbreviations, are explained in BIPM (2006b). When base units and derived units are used with no prefixes, the resulting set of units is said to be *coherent*. The adjective "coherent" appears to have been chosen to stress that, when only coherent units are used, conversion factors between units are never needed. Otherwise, however, there is no implication that coherent units are superior to "non-coherent" units.

The Working Group recommends that the prefixes centi-, deci-, deka- and hecto- be used sparingly in reports of mass balance, preferably only in units such as the decibel and hectopascal which have an unshakeable place in usage for historical reasons. The centimetre and the gram are not recommended. They introduce an avoidable risk of numerical error.

Table 5 Some SI prefixes

Factor	*Prefix*	*Symbol*	*Factor*	*Prefix*	*Symbol*
10^{-9}	nano-	n	10^{6}	mega-	M
10^{-6}	micro-	μ	10^{9}	giga-	G
10^{-3}	milli-	m	10^{12}	tera-	T
10^{3}	kilo-	k	10^{15}	peta-	P

7.1.4 Non-SI units The SI also recognizes a number of non-SI units. Those in Table 6 are some that are "accepted for use with the International System of Units". Of those that are "used by special interest groups for a variety of purposes", only the bar (a unit of pressure; 1 bar = 10^5 N m^{-2}) and the atmosphere (1 atm = 101 325 N m^{-2}) need to be mentioned here.

Table 6 Accepted non-SI units

Quantity	*Unit*	*Symbol*	*Value in SI Units*
time, duration	minute	min	1 min = 60 s
time, duration	day	d	1 d = 86 400 s
plane angle	degree	°	1° = (π/180) rad
plane angle	minute	′	1′ = (π/10 800) rad
plane angle	second	″	1″ = (π/648 000) rad
mass	tonne	t	1 t = 1000 kg

7.2 Extensions of the SI in glaciological usage

7.2.1 The year The year is not an SI unit. In the form of the "tropical year 1900", it was once the basis for the definition of the second, but fell into disfavour because of the ability of modern physics to supply more precise measures of time based on atomic phenomena. The duration of a single orbit of the Earth around the Sun is intrinsically a variable and not a constant, and it can be defined in more than one astronomically plausible way. A definition of the year, therefore, cannot be both precise and general.

Yet the annual cycle is a fundamental attribute of the terrestrial environment. In the study of mass balance, the year is synchronized not directly with the Earth's orbit but rather with the local hydrological cycle as it affects each glacier, or alternatively with the civil calendar. We define the mass balance as a "change in mass ... over a stated span of time". It can be treated as a sum, with dimension [M]. Often, however, the most fitting interpretation is that the mass balance is a rate, with dimension [M T^{-1}], and in this interpretation the appropriate unit of time is the year.

The year is also firmly established in other branches of glaciology, particularly dynamic glaciology, in which it is natural to express rates of motion, such as speed and velocity (m a^{-1}), and of deformation or strain rate (a^{-1}), as rates per year.

Of the three kinds of glaciological year – the mass-balance year in the stratigraphic system, the fixed-date system and the floating-date system – none is specifiable exactly in terms of the SI base unit of time, the second, although two are specifiable exactly (with due allowance for leap years) in terms of the day, which is an accepted non-SI unit.

The Working Group recommends that the year be considered to be a practical extension of the SI, with the symbol “a”. Normally the duration of the year need not be specified more precisely than as under *Year* in the Glossary. In accurate work the time coordinate is best represented in terms of the *Julian date* or the *Day of the year*.

7.2.2 The metre water equivalent The Working Group recommends that the metre water equivalent, abbreviated as “m w.e.” and defined in the Glossary, be considered an extension of the SI. The metre water equivalent is oriented parallel to the local vertical axis at the Earth’s surface and is connected tightly by definition to the unit kg m^{-2} (surface density).

7.2.3 The metre ice equivalent The metre ice equivalent, abbreviated “m ice eq.” and defined in the Glossary, is also considered to be an extension of the SI.

8 Format of the Glossary

Each article in the body of the Glossary begins with a bold-font head term – the word or phrase that is about to be defined. The head term may be qualified to explain what part of speech (adjective, noun, verb, ...) it is. In a few cases a recommended algebraic symbol, selected with the aim of increasing clarity, is given after the head term.

The head term is followed by a definition paragraph, consisting usually of a single noun phrase or sentence giving the essence of the meaning of the head term. The definition paragraph may be followed by one or more paragraphs of commentary or background information.

When the head term has more than one distinct meaning, the distinct definitions are numbered. Some head terms, for example "**Mass balance**" and "**Microwave remote sensing**", have nested subheadings for closely related terms.

Italicized words or phrases are cross-references to other articles in the Glossary.

GLOSSARY

Acronyms

AAR
Accumulation-area ratio.

CIG
International Glacier Commission.

DAS
Data Analysis Services.

DEM
Digital elevation model.

DTM
Digital terrain model. See *digital elevation model*.

DGPS
Differential *Global Positioning System*.

ELA
Equilibrium-line altitude.

FoG
Fluctuations of Glaciers.

GCOS
Global Climate Observing System.

GIA
Glacial-isostatic adjustment.

GLIMS
Global Land Ice Measurements from Space.

GLONASS
See *global navigation satellite system*.

GNSS
Global navigation satellite system.

GPR
Ground-penetrating radar.

GPS
Global Positioning System.

GRACE
Gravity Recovery and Climate Experiment. See *gravimetric method*.

GTN-G
Global Terrestrial Network for Glaciers.

GTOS
Global Terrestrial Observing System.

IACS
International Association of Cryospheric Sciences.

ICESat
Ice, Cloud and land Elevation Satellite. See *laser altimeter*.

ICSI
International Commission on Snow and Ice.

ICSIH
International Commission on Snow and Ice Hydrology.

ICSU
International Council for Science.

IGS
International Glaciological Society.

InSAR
Interferometric synthetic aperture radar.

IUGG
International Union of Geodesy and Geophysics.

LIA
Little Ice Age.

NSIDC
National Snow and Ice Data Center.

PDD
Positive degree-day.

PGR
Post-glacial rebound. See *glacial isostatic adjustment*.

PSFG
Permanent Service on the Fluctuations of Glaciers.

RES
Radio-echo sounding. See *ground-penetrating radar*.

SAR
Synthetic aperture radar. See *InSAR*.

SLE
Sea-level equivalent.

SRTM
Shuttle Radar Topography Mission.

SSC
Seasonal sensitivity characteristic.

SWE
Snow water equivalent. See *passive-microwave sensor*.

TTS/WGI
Temporary Technical Secretariat for the World Glacier Inventory.

WDC
World Data Centres.

WDS
World Data System.

WGI
World Glacier Inventory.

WGMS
World Glacier Monitoring Service.

A

Ablation *a* (point), *A* (glacier-wide)
1. All processes that reduce the mass of the *glacier*.

2. The mass lost by the operation of any of the processes of sense 1, expressed as a negative number (see *mass-balance units*).

The main processes of ablation are *melting* and *calving* (or, when the glacier nourishes an *ice shelf*, *ice discharge* across the *grounding line*). On some glaciers *sublimation*, loss of *windborne snow* and *avalanching* are significant processes of ablation.

"Ablation", unqualified, is sometimes used as if it were a synonym of *surface ablation*, although *internal ablation*, *basal ablation*, and *frontal ablation*, especially *calving*, can all be significant in some contexts.

Ablation area
Same as *ablation zone*.

Ablation season
A time span extending from a seasonal maximum of *glacier* mass to a seasonal minimum.

The ablation season is the same as the *summer season* on most glaciers, which are of *winter-accumulation type*. Special cases include glaciers of *summer-accumulation type* and *year-round ablation type*, and glaciers that have more than one ablation season during the year.

Ablation zone
The part of the *glacier* where *ablation* exceeds *accumulation* in magnitude, that is, where the *cumulative mass balance* since the start of the *mass-balance year* is negative.

Unless qualified, for example by giving a date within the year, references to the ablation zone refer to its extent at the end of the mass-balance year. The extent of the ablation zone can vary strongly from year to year. See *zone*.

Ablatometer
A device installed at the *glacier* surface for the measurement, during the *ablation season*, of changes in *elevation* of the glacier surface relative to a fixed elevation, such as that of the top of a mass-balance *stake*, in the ice beneath the surface.

A star ablatometer is an array of rigid metal arms that can be attached to a stake and levelled. A graduated rod is lowered through holes in the arms to measure changes in the surface elevation, yielding a considerably larger sample than that obtained from readings of the stake alone.

Sometimes an ablatometer is actually a *sonic ranger*.

Accreted ice
Ice formed by the *freezing* of water at the base of an *ice body*.

See *basal accumulation*, *marine ice*.

Accumulation *c* (point), *C* (glacier-wide)
1. All processes that add to the mass of the *glacier*.

2. The mass gained by the operation of any of the processes of sense 1, expressed as a positive number (see *mass-balance units*).

The main process of accumulation is *snowfall*. Accumulation also includes deposition of *hoar*, *freezing rain*, *solid precipitation* in forms other than *snow*, gain of *windborne snow*, *avalanching* and *basal accumulation* (often beneath floating ice). See also *internal accumulation*.

Unless the *rain* freezes, *rainfall* does not constitute accumulation, nor does the addition of debris by avalanching, ashfall or similar processes.

Accumulation area
Same as *accumulation zone*.

Accumulation-area ratio AAR
The ratio, often expressed as a percentage, of the area of the *accumulation zone* to the area of the *glacier*.

The AAR is bounded between 0 and 1. On many glaciers it correlates well with the *climatic mass balance*. The likelihood that the climatic mass balance will be positive increases as the AAR approaches 1.

Unless qualified by a different adjective, references to the AAR refer to the *annual AAR*.

Annual AAR
The AAR at the end of the *mass-balance year*.

Annual AARs can vary greatly from year to year, but an average over a number of years, when compared with the *balanced-budget AAR*, gives a measure of the *health* of the glacier. If the difference is large and in the same direction over a considerable time, a prolonged period of non-zero mass balance can be expected as the glacier seeks *equilibrium*.

Balanced-budget AAR
The AAR, sometimes denoted AAR_0, of a glacier with a mass balance equal to zero.

Glaciers do not in general have mass balances equal to zero. The balanced-budget AAR is usually estimated as the AAR at which a curve (often linear) fitted to an observed relation between AAR and the annual surface mass balance B_{sfc}, measured over a number of years, crosses the axis $B_{sfc} = 0$.

The $AAR_{\mathbf{0}}$ of non-calving glaciers has been found to vary roughly between 0.5 and 0.6 on average, although the range of variation is substantial. On calving glaciers it is typically larger, approaching 1.0 on the Antarctic Ice Sheet. AAR_0 can exceed 0.8 on tropical glaciers of *year-round ablation type*. The balanced-budget AAR may differ from the *steady-state AAR* because it summarizes observations made in conditions that may not approximate to *steady state*

Equilibrium AAR
A synonym of *balanced-budget AAR*.

Steady-state AAR
The AAR of a *glacier* in *steady state*.

The steady-state AAR is difficult to estimate because glaciers are seldom if ever in steady state. In practice, it must be estimated by modelling. To emphasize that the balanced-budget AAR and steady-state AAR are distinct concepts, the steady-state AAR should be given a distinctive symbol, perhaps AAR_0'.

Transient AAR
The AAR at any instant, particularly during the *ablation season*.

Accumulation season
A time span extending from a seasonal minimum of *glacier* mass to a seasonal maximum.

The accumulation season is the same as the *winter season* on most glaciers, which are of *winter-accumulation type*. Special cases include glaciers of *summer-accumulation type* and *year-round ablation type*, and glaciers that have more than one accumulation season during the year.

Accumulation zone
The part of the glacier where *accumulation* exceeds *ablation* in magnitude, that is, where the *cumulative mass balance* since the start of the *mass-balance year* is positive.

Unless qualified, for example by giving a date within the year, references to the accumulation zone refer to its extent at the end of the mass-balance year. The extent of the accumulation zone can vary strongly from year to year. The term is not the same as *firn area*. See *zone*.

Active-microwave sensor
See article *Active-microwave sensor* under *Microwave remote sensing*.

Activity index
The *mass-balance gradient* at the *balanced-budget ELA*.

Advance
Increase of the length of a *flowline*, measured from a fixed point.

In practice, when the advance is of a land-terminating glacier *terminus*, the fixed point is usually downglacier from the *glacier margin*, and the quantity reported is the amount of advance rather than the length itself.

Retreat is the opposite of advance, that is, retreat of the terminus.

Albedo
The ratio of the reflected flux density to the incident flux density, usually referring either to the entire spectrum of solar radiation (broadband albedo) or just to the visible part of the spectrum.

The broadband albedos of *glacier* surfaces exceed 0.8 for freshly fallen *snow*, are less for aged snow and *firn*, and are significantly less for exposed *glacier ice*. Snow and ice that are sediment-laden or covered by debris can have albedos still lower. The difference between the albedos of snow and glacier ice is significant in the seasonal evolution of the *energy balance* and therefore of the rate of *surface ablation*; see *degree-day factor*.

Spectral albedo is the albedo at a single wavelength or, more loosely, over a narrow range of wavelengths.

Alpine glacier
See *mountain glacier*.

Altimetry
A *remote-sensing* technique in which surface *altitudes* (*elevations*) are estimated as a function of the travel time of a pulse of electromagnetic radiation transmitted from and received by a precisely located altimeter.

Altimeters are mounted on either satellite or aircraft. Satellite altimeters use on-board *Global Positioning System* (GPS) instruments and star trackers to determine orbital position and altimeter pointing angles. Aircraft systems measure the altimeter trajectory using GPS and Inertial Navigation Systems. Accurate altimetry measurements, especially those acquired from space, require corrections for variations in atmospheric and ionospheric conditions, and for variations in orbital position of the sensor.

Altimeters are either *laser altimeters* or *radar altimeters*. Each of the two radiation bands has strengths and weaknesses with respect to footprint size and ability to sample through atmospheric obstructions such as clouds.

Altimetry measurements are compared with surface elevations obtained at identical points in horizontal space at an earlier time to calculate *elevation changes* which can then be used to compute volume changes. The earlier elevation measurement is commonly obtained from a previous altimetry pass, but can also be derived from other sources such as topographic maps. A mass balance is obtained from knowledge of the ice-column *density* usually supplied by *Sorge's law*.

Altitude
The vertical distance of a point above a datum.

The vertical datum is usually an estimate of mean sea level. Older measurements were often determined in a local coordinate system and were not tied to a global reference frame. Some were made not with surveying instruments but with barometers, in reliance on the decrease of atmospheric pressure with altitude. It is now usual to measure altitude or elevation using the *Global Positioning System* or an equivalent *global navigation satellite system*.

Altitude and *elevation* are synonyms in common usage, although altitude is less ambiguous. The unqualified word “elevation” can also refer, for example, to the act of elevating or to angular distance above a horizontal plane.

Annual (*adj.*)
Descriptive of a period equal or approximately equal in duration to a calendar year, such as a *hydrological year* or *mass-balance year*.

“Annual” often has a meaning equivalent to “end-of-summer”, which is more explicit but longer and also depends on summer being a well-defined season.

Formerly (Anonymous 1969; *Appendix A*) “annual mass balance” was a technical term in the *fixed-date system*, to be distinguished from “net mass balance” in the *stratigraphic system*, but this distinction is no longer recommended.

Annual AAR
See article *Annual AAR* under *Accumulation-area ratio.*

Annual ablation a_a (point), A_a (glacier-wide)
See article *Annual ablation* under *mass balance.*

Annual accumulation c_a (point), C_a (glacier-wide**)**
See article *Annual accumulation* under *mass balance.*

Annual ELA
See article *Annual ELA* under ***equilibrium-line altitude.***

Annual equilibrium line
See article *Annual equilibrium line* under *Equilibrium line*.

Annual exchange
See article *Annual exchange* under mass *balance*.

Annual mass balance b_a (point), B_a (glacier-wide)
See article *Annual mass balance* under *mass balance.*

Annual snowline
See article *Annual snowline* under *snowline.*

Area *S*
Extent in two spatial dimensions, always understood in *mass-balance* work (when the two dimensions are horizontal) to be map area, that is, the extent of the *glacier* or part thereof when the *glacier outline* is projected onto the surface of an ellipsoid approximating the surface of the Earth or onto a planar (horizontal) approximation to that ellipsoid.

In mass-balance studies, except for *ice discharge* and for the special case of *frontal ablation*, lengths such as layer thicknesses are always measured parallel to the vertical axis and not normal to the glacier surface. When calculating volumes within a specified outline, the area to be used is therefore the integral of ds (an element of projected area) and not the integral of $\sec\theta\,ds$, the so-called “true” area (where θ is the slope of the glacier surface).

The glacier area excludes *nunataks* but includes debris-covered parts of the glacier. However, delineating the glacier where it is debris-covered can be very difficult, because the debris may cover *stagnant ice* and there may be no objective way to distinguish between the debris-covered glacier and contiguous ice-cored moraine.

Area-altitude distribution
The frequency distribution of glacier area with surface *altitude* (or *elevation*), generally presented as a *hypsometric curve* or table giving the *area* of the *glacier* within successive *altitude* intervals. See *hypsometry*.

Area-averaged (*adj*.)
Descriptive of a quantity that has been averaged over part or all of the *area* of the *glacier*.
The "area-averaged" *mass balance* is simply the *specific* mass balance of the region under consideration. The adjective has sometimes been used to emphasize that the specific mass balance is that of the whole glacier and not of a "specific" location (see *point mass balance*). "Mean specific mass balance" has been used in the same sense.

Avalanche
A slide or flow of a mass of *snow*, *firn* or *ice* that becomes detached abruptly, often entraining additional material such as snow, debris and vegetation as it descends.
The duration of an avalanche is typically seconds to minutes.

Avalanching
Mass transfer by *avalanches* which redistribute *snow*, *firn* and *ice*.
Avalanching from a valley wall to the *glacier* surface constitutes *accumulation*. Avalanching from the *glacier margin* constitutes *ablation*.

Azimuth
1. The horizontal angle, in radians or degrees, measured at any point between a line heading in a reference direction and a line heading in a particular direction.
In geography and navigation, azimuths are measured clockwise from geographical north.

2. The along-track coordinate in the coordinate frame of an airborne or orbiting *radar*, a usage deriving from the azimuth (in sense 1) of the direction of travel of the radar. See *range*.

B

Balance (*adj.*)
For most terms in which "balance" is used as an adjective, see the equivalent entry under "mass-balance". In ordinary usage the prefix "mass-" is omitted when there is no risk of confusion.

Balanced-budget (*adj.*)
Descriptive of a *glacier* with a *mass balance* equal to zero on average over a number of years. See *steady state*.

Balanced-budget AAR
See article *Balanced-budget AAR* under *Accumulation-area ratio*.

Balanced-budget ELA
See article *Balanced-budget ELA* under *Equilibrium-line altitude*.

Balance flux
The hypothetical horizontal *mass flux* (dimension [M T^{-1}]) through a vertical cross-section that would be equal to the *mass balance* (usually the *climatic mass balance*) over the region upglacier from the cross-section.

Comparison of balance flux and actual mass flux at the same cross-section gives an indication of the *health* of the *glacier*. If the mass balance of the glacier is zero it follows that at the *terminus* the balance flux and mass flux are equal, and if there is also no *calving* that they are equal to zero. If the two are equal at all cross-sections the glacier is in *steady state*.

Volumetric balance flux
The balance flux divided by average *density*.

Balance velocity
The *volumetric balance flux* divided by the *area* of the vertical cross-section through which it passes.

Comparison of balance velocity to actual velocity, that is, to the actual volumetric flux (*mass flux* divided by average *density*) divided by the area of the vertical cross-section, gives an indication of the *health* of the glacier. See *balance flux*.

Balance year
The *mass-balance year*.

Basal ablation a_b (point), A_b (glacier-wide)
The removal of *ice* by *melting* at the base of a *glacier*. See *mass-balance units*.

At the base of grounded *temperate ice*, melting is either fuelled by the geothermal heat flux and the conversion of the kinetic energy of basal sliding to heat, or results from variations of the *pressure-melting point*. Pressure melting, however, tends to be balanced by *regelation*.

Typical continental geothermal heat fluxes G of 0.05–0.15 W m^{-2} imply potential basal ablation G/L_f of 5–14 mm w.e. a^{-1}, where L_f is the *latent heat of fusion*. Much greater geothermal heat fluxes are found in areas of active volcanism. If all of the energy of basal sliding is converted to heat, basal ablation $u_b\tau_b/L_f$ at rates of 3–30 mm w.e. a^{-1} is implied by sliding velocities u_b of 10–100 m a^{-1} and basal shear stress τ_b of 10^5 Pa. Basal ablation rates tens or hundreds of times greater are implied beneath *ice streams*.

At the base of an *ice shelf* or *floating tongue*, melting occurs because of convection of warmer sea water to the ice-water interface, supplying the required latent heat of fusion. The rate of melting depends on the temperature of the sea water and the efficiency of the heat transfer between the sea water and the base of the ice shelf. Basal ablation rates beneath ice shelves or floating tongues can reach tens of m w.e. a^{-1}, equivalent to heat transfer at hundreds of W m^{-2}.

Basal accumulation c_b (point), C_b (glacier-wide)
The *freezing* of water to the base of the *glacier* as *accreted ice*, increasing its mass and raising its basal temperature. See *mass-balance units*.

Basal accumulation is typically observable in ice cores or at *glacier margins* as basal ice that is relatively clear, often, in the case of grounded ice, with some concentration of dispersed sediments incorporated during freezing. Furthermore, basal ice can usually be distinguished from *glacier ice* by differences in isotopic content of the water, geochemical composition and optical properties. Hence there are both visual and analytical ways to distinguish and quantify basal accumulation.

Accreted ice at the base of an *ice shelf* is referred to as *marine ice*.

From a practical *mass-balance* point of view, basal accumulation is indistinguishable from *internal accumulation* in that both represent addition of mass to the glacier that goes unaccounted for by surface observations.

Basal accumulation, although typically a small contribution to mass change, is systematically positive.

Basal mass balance b_b (point), B_b (glacier-wide)
The change in the mass of the *glacier* due to *basal accumulation* and *basal ablation* over a stated period. See *mass-balance units*, *climatic-basal mass balance*.

Benchmark glacier
In the monitoring strategy of the United States Geological Survey, a *glacier* on which detailed measurements of seasonal glacier mass changes, meteorological environment, and streamflow variations are collected on a continuing basis.

See *reference glacier*, *tier*.

Bergschrund
A *crevasse* at the head of a *glacier* that separates flowing *ice* from *stagnant ice*, or from a rock headwall.

From an ice-dynamical point of view the bergschrund is the headward boundary of the glacier, while for hydrological and other purposes, including *glacier inventory*, the stagnant ice above the bergschrund is part of the glacier.

Bergschrund is an anglicized word of German origin.

Blowing snow
Snow entrained, suspended and transported by the wind at heights greater than 2 m above the surface.

The height of 2 m is a convenient separator between blowing snow, which reduces horizontal visibility significantly, and *drifting snow*.

Blue ice
Dense *glacier ice* with a blue appearance accounted for by lack of air bubbles.

The crystal structure absorbs all colours except the blue part of the visible spectrum. Strictly, blue ice is ice that has originated by *recrystallization* upglacier and, having followed a trajectory through the interior of the *glacier*, becomes exposed at the surface downglacier, a locally zero or negative *surface mass balance* being implied. The term is used loosely, however, to refer to all exposed ice on the Antarctic Ice Sheet; again, the absence of *snow* and *firn* implies a locally negative surface mass balance.

Bomb horizon
A horizon of enhanced radioactivity in *snow*, *firn* or *ice*, originating from fallout from atmospheric nuclear tests.

The bomb horizon originating from nuclear tests during the 1950s and 1960s has been detected on *glaciers*. The maximum rate of production of radioactive isotopes is datable to 1963, which makes the bomb horizon a useful *marker horizon*. A similar horizon is that due to the accident at the Chernobyl nuclear power station in 1986.

Bomb layer
See *bomb horizon*.

Boundary
The surface separating the *glacier* from its surroundings.

The term is often simply a synonym of *glacier margin* or *glacier outline*, but it can be useful to have a separate word that is understood to encompass the glacier surface and the glacier bed as well.

Brightness temperature
The conventional measure of the intensity of microwave emission from a natural medium, defined as $T_B = \varepsilon T - T_{sky}$, where ε is the emissivity of the medium (on *glaciers*, a mixture of *ice*, air, and possibly water), T is its physical (thermodynamic) temperature and $T_{sky} \approx 3$ K (and therefore often neglected) is an equivalent measure of downwelling emission from the sky; the temperatures are expressed in kelvins, the emissivity being dimensionless.

In dry snow, the emissivity is determined by volume scattering at interfaces such as grain boundaries and larger structures such as layers of *depth hoar*. Grain growth rate depends on both temperature and *accumulation* rate, and this behaviour is exploited to estimate the accumulation rate as a function of T_B and T.

Scattering at air-water interfaces is much more effective than at air-ice interfaces. When *meltwater* appears at the surface, subsurface scattering ceases to be significant and the emissivity approaches unity. T_B changes abruptly as meltwater comes and goes, and continued monitoring of these changes yields reliable estimates of the *melt extent* and duration of *melting*. Analogous phenomena – abrupt changes in the intensity of backscattered radiation – are also seen by *scatterometers* and imaging *radars*.

C

Calving *d*, *D*
The component of *ablation* consisting of the breaking off of discrete pieces of *ice* from a *glacier margin* into lake or sea water, producing icebergs, or onto land in the case of *dry calving*.

Calving excludes frontal *melting* and *sublimation*, although in practice it may be difficult to measure the phenomena separately. For example subaqueous frontal melting may lead to the detachment of icebergs by undercutting or by encouraging the propagation of crevasses.

Calving flux
The *mass flux*, with dimension [M T^{-1}], of *ice* by *calving* from a *glacier margin*.

Volumetric calving flux
The calving flux divided by average glacier *density* (dimension [L^3 T^{-1}]).

Calving front
A *glacier margin* from which discrete pieces of *ice* calve or break off, to become icebergs if the margin stands or floats in sea or lake water.

Calving rate
Either the *calving flux* or the *calving velocity*, depending on the context.

Calving velocity
The *volumetric calving flux* divided by the *area* of projection of the calving *glacier margin* onto a vertical plane normal to the mean direction of the ice flow. See *calving*.

Denoting horizontal components of velocity in the direction of the ice flow as *u*, the calving velocity u_{calv} can be determined by application of the principle of *conservation of mass* at the *glacier margin*:

$$u_{\mathrm{calv}} = u_{\mathrm{bal}} + u_{\mathrm{thin}} - \dot{L} \,,$$

where u_{bal} is the *balance velocity*, u_{thin} is the *thinning velocity* and $\dot{L}$ is the rate of change of the glacier's length reckoned from a fixed point upglacier from the margin.

Cartographic method
Like *topographic method*, a synonym of *geodetic method* in the context of measurement of *mass balance*.

Chionosphere
The part of the Earth's surface lying above the *regional snowline*.

Though useful, the term, due originally to Kalesnik, is in fact confined to the Russian literature. "Chion" is a Greek word for snow.

Cirque glacier
A *glacier* occupying a cirque.

A cirque is a rounded recess with steep sides and back wall, formed on a mountainside by glacial erosion.

Cirque is an anglicized French word that has displaced the synonyms "corrie" (from Scots Gaelic) and "cwm" (from Welsh) of early glaciological usage.

Climatic-basal mass balance *b* (point), *B* (glacier-wide)
The sum of the *climatic mass balance* and the *basal mass balance*.

The expression

$$b = c_{\mathrm{sfc}} + a_{\mathrm{sfc}} + c_{\mathrm{i}} + a_{\mathrm{i}} + c_{\mathrm{b}} + a_{\mathrm{b}}$$

states that the climatic-basal mass-balance b is the sum of *surface accumulation* c_{sfc}, *surface ablation* a_{sfc}, *internal accumulation* c_i, *internal ablation* a_i, *basal accumulation* c_b and *basal ablation* a_b.

The sum of c_b and a_b is the *basal mass balance*. The sum of c_i and a_i is the *internal mass balance*. The sum of c_{sfc} and a_{sfc} is the *surface mass balance*. The sum of the surface mass balance and internal mass balance (the first four quantities on the right of the expression) is the *climatic mass balance*. The sum of the six quantities on the right (that is, of the climatic mass balance and the basal mass balance) is the climatic-basal mass balance.

The climatic-basal mass balance includes all those components of mass change that do not arise from glacier *flow* or *calving*. The qualifier "basal" does not exclude a role for the climate, for example through interactions between the atmosphere and the ocean.

Climatic mass balance b_{clim} (point), B_{clim} (glacier-wide)
The sum of the *surface mass balance* and the *internal mass balance*; see also *climatic-basal mass balance*.

The term is introduced to preserve the distinction between its two components, which is compromised if surface mass balance is redefined to include *internal accumulation*.

The qualifier "climatic" reflects the fact that the surface and internal balances both depend strongly on interaction between the glacier, the hydrosphere and the atmosphere.

Climatic snowline
See *snowline*.

Coffee-can method
A means of measuring the *submergence velocity* or *emergence velocity* of the glacier surface by anchoring a stand for a *global navigation satellite system* (GNSS; usually a *Global Positioning System*) receiver to the body of the *glacier*, using a suitable object (such as a coffee can) as an anchor connected to the surface by a cable under tension.

The essence of the method is that measured changes in the exposed length of the cable (or equivalent measurements of the local *surface mass balance*), and in the surface *elevation* (measured by the GNSS receiver), yield two of the three terms in the *continuity equation* and allow the third term, the submergence or emergence velocity (that is, the *flux divergence*) to be determined.

Corrections may be needed for the *densification* (that is, settling) of *firn* beneath the anchor and for downslope advection of the anchor. The coffee-can method has been used mainly in the *accumulation zones* of *ice sheets*, where the surface mass balance can be obtained by *ice-core stratigraphy*. However in the *ablation zone* the emergence of cables emplaced for other reasons, such as the measurement of temperature profiles, can serve a similar purpose.

Cold-based glacier
A *glacier* whose bed is below its *pressure-melting point*, implying that there is no liquid water at the bed. Same as *dry-based glacier*.

Cold content
The amount of energy required to raise the temperature of a body of frozen water to the *freezing point*.

The cold content γ of a layer between the surface and depth Z is usually expressed per unit of vertically projected horizontal area, in J m^{-2}:

$$\gamma = C_p \int_0^Z \rho(z)[T_f - T(z)]\, dz$$

where C_p is the heat capacity of *ice* (*Table B2*), and ρ and T are density and temperature respectively at depth z. Sometimes the cold content is expressed as the equivalent depth $\gamma/(\rho_w L_f)$, where L_f is the *latent heat of fusion*, of refreezing water (with temperature equal to the freezing point) that would yield the required energy.

Cold firn zone
See *infiltration-recrystallization zone*.

Cold glacier
A *glacier* consisting of *cold ice*, except possibly in a surface layer up to 10–15 m thick that might warm to the *melting point* seasonally, and possibly right at the bed.
See *polythermal glacier*, *temperate glacier*, *dry-based glacier*, *warm-based glacier*.

Cold ice
Ice at a temperature below its *pressure-melting point*; see *temperate ice*.

Cold infiltration-recrystallization zone
See *infiltration-recrystallization zone*.

Combined system
A combination of two *time systems* of *mass-balance* measurement, usually of the *stratigraphic system* with either the *fixed-date system* or the *floating-date system*.
As originally defined (Mayo et al. 1972), the combined system accounted rigorously for differences between the stratigraphic and fixed-date systems, but this rigorous accounting has been found impractical in most measurement programmes and various simplifications have been adopted.

Condensation
The process by which a vapour changes phase into a liquid; see *latent heat of vaporization*.

Congelation
1. The *freezing* of liquid water in the absence of pre-existing *ice*; see *infiltration ice*, *recrystallization*.

2. Addition of *ice* to the base of *sea ice* by freezing.
If new and young ice are not deformed into rafts or ridges, they will continue to grow by congelation. Congelation ice has distinctive columnar crystal texture due to the downward growth of the crystals into the water. It is very common in Arctic pack ice and fast ice. In limnology it is called “black ice”. Congelation derives from “congeal”, meaning freeze or thicken, increase in viscosity.

Conservation of mass
The principle that mass in a system is neither created nor destroyed, expressed by the relation: the rate of change of mass in an element of the system equals the rate at which mass enters the element minus the rate at which mass leaves the element.
The definition rests on the convention that all flows are positive in the positive coordinate direction. With the commonest alternative convention, that inward flows are positive and outward flows are negative, the definition would be read with “plus” replacing “minus”.

Continuity equation
The mathematical expression of the conservation of mass or (*ice-equivalent*) volume, the principle being that the rate of change of storage of material in an element is the rate of flow of material into the element minus the rate of flow of material out of the element; in ice-equivalent units:

$$\dot{h} = \dot{b} - \nabla \cdot \vec{q} \ ,$$

where $\dot{h}$ is the rate of change of glacier thickness, $\dot{b}$ is the *climatic-basal mass-balance rate* and $\nabla \cdot \vec{q}$ is the volumetric *flux divergence*. (The rates are positive in the positive coordinate direction.) To determine $\dot{b}$, the element is taken to be a vertical column through the glacier, and the equation is rearranged as

$$\dot{b} = \dot{h} + \nabla \cdot \vec{q} \ .$$

When the flux divergence $\nabla \cdot \vec{q}$ is positive, it is called the *submergence velocity*; when it is negative, it is called the *emergence velocity*.

Each of the terms in the continuity equation entails approximations in practical use. The term $\dot{h}$ assumes that the mean *density* is constant, the *point mass-balance* is usually approximated by the *surface mass balance*, while the calculation of the flux divergence nearly always requires an assumption about the unknown vertical profile of the horizontal component of ice velocity.

Conventional balance
The *mass balance* of a *glacier*, the term having been introduced by Elsberg et al. (2001) to distinguish the mass balance from the *reference-surface balance*, which is the balance the glacier would have if the glacier surface geometry were fixed in time.

Conventional balances are obtained when point measurements over a particular time interval are extrapolated to the glacier *area* and *hypsometry* measured during the same time interval. Calculations of conventional balance require repeated mapping of glacier hypsometry at intervals appropriate to the rate of change of the surface geometry. However, maps are often re-calculated at longer time intervals, the reported balances being a combination of conventional and reference-surface balances.

Conventional balances are relevant for hydrological applications because they represent the actual mass change of a glacier. Conventional balances are not simply correlated to variations in climate because they incorporate both climate forcing and changes in glacier hypsometry. For glacier/climate investigations the *reference-surface balance* is a more relevant quantity.

Crater glacier
A *glacier* contained in or overflowing from a volcanic crater.

Crevasse
A crack formed in *glacier ice* when tensile stresses exceed the tensile strength of the ice.

The tensile stresses, and the tensile strength of the ice, are variable, and compressive stress at depth is believed to play a role in limiting the depth to which surface crevasses propagate. This depth can be up to a few tens of metres, or more if the crevasse is filled with water.

Crevasses are conduits for the transfer of water, including surface *meltwater*, to the glacier interior and sometimes the glacier bed; see *moulin*. When crevasses in floating ice fill with surface meltwater, they may propagate to the base, causing the *ice shelf* or *floating tongue* to disintegrate. The fragments may contribute to an ice *melange*.

Crevasse stratigraphy
The observation of annual and other layer thicknesses in the walls of *crevasses* and similar nearly vertical exposures.

See *ice-core stratigraphy*.

Cryoconite
Dark, fine-grained debris on the *glacier* surface, often forming small, roughly circular patches. See *cryoconite hole*.

The word was introduced by Nordenskiöld in 1872.

Cryoconite hole
A small cylindrical hole on the surface of a *glacier*, formed by patches of *cryoconite* that absorb more short-wave radiation than the surrounding ice, melting downwards at a faster rate and adding to sub-metre-scale spatial variability in *ablation*. See also *weathering crust*.

Cumulative (*adj.*)
Descriptive of a quantity that has been summed over a span of time.

Cumulative mass balance
The mass of the *glacier*, or part of the glacier, at a stated time relative to its mass at some earlier time t_0, considered as a function of time, $M(t) - M(t_0)$. See Figure 5, and *section 4.3*.

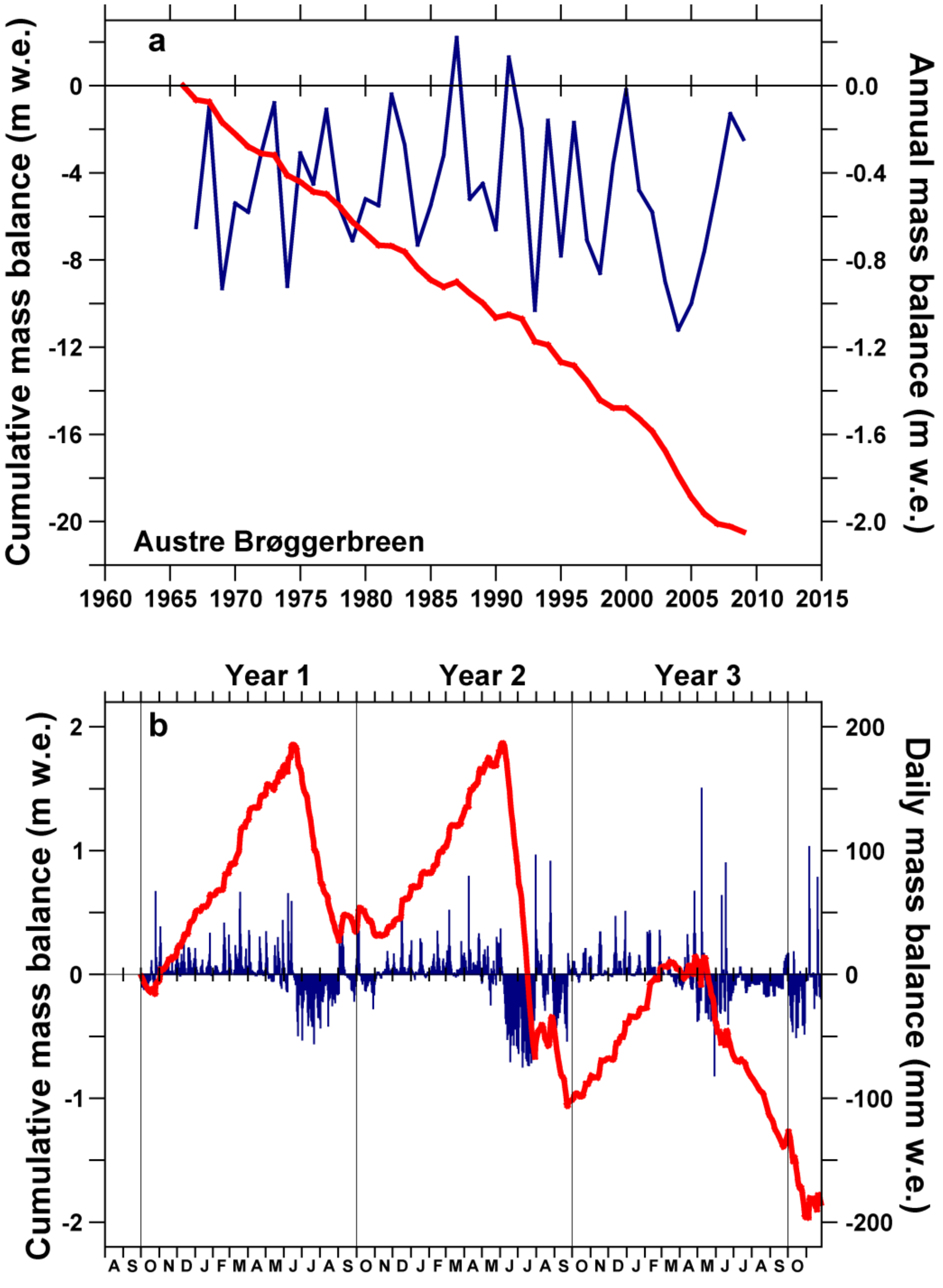

Figure 5. a: Cumulative mass balance relative to 1966 (red, left axis) and annual mass balance for 1966 to 2009 (blue, right axis) of Austre Brøggerbreen, Svalbard. b: Cumulative mass balance relative to 1 October of Year 1 (red left axis) and daily mass balance (blue, right axis) over three mass-balance years of a representative northern-hemisphere glacier; after Huss et al. 2009.

D

Data Analysis Services (DAS)
A series of services for the storage, analysis and dissemination of scientific data under the sponsorship of the *International Council for Science (ICSU).*

In 2009, the Data Analysis Services and the *World Data Centres (WDC)* were reorganized within ICSU's new *World Data System (WDS).*

Day of the year
One plus the number of days elapsed since 00 hours on 1 January of a given calendar *year*.

The day of the year is not the same as the *Julian day number* or the *Julian date*.

Dead ice
Any part of a *glacier* that does not flow at a detectable rate. Same as *stagnant ice*.

Debris-covered glacier
A *glacier* that supports a layer of rock, dust or ash detritus on most or all of the surface of its *ablation zone*.

In the *accumulation zone* any deposited debris is buried by later *snowfalls*, but in the ablation zone debris remains at the surface and *englacial* debris is added to the surface layer from beneath as ice ablates away.

The debris cover affects the rate of *ablation*, with very thin debris resulting in accelerated *melt* and debris thicker than a few tens of millimetres reducing the melting rate.

Degree-day
The name of a derived unit, the K d, equal in magnitude to a departure of temperature above or below a reference temperature averaging 1 K over a period of 1 day.

Different choices of the reference temperature lead to different kinds of degree-day, such as the heating degree-day and freezing degree-day. The kind that is relevant in studies of *mass balance* is the *positive degree-day* (above the reference temperature 0 ºC).

Degree-day factor
In a *positive degree-day* model, the coefficient of proportionality $f = -a/\varphi$ between *surface ablation* a (which is negative) and the *positive degree-day sum* φ over any period.

The degree-day factor parameterizes all of the details of the *energy balance* that results in ablation by *melting* and possibly *sublimation*, and is therefore a simplification. It is usually treated as one or more constants; in particular, it is different for *snow* and for *glacier ice*, because the ice is generally less reflective than snow. It is usually expressed in mm w.e. K^{-1} d^{-1} or kg m^{-2} K^{-1} d^{-1}.

Densification
The conversion of *snow* to *firn* and then *glacier ice*.

Newly fallen snow (*Table B6*) has a variable *density* depending on the meteorological conditions of its formation and deposition. The density of dry snow increases rapidly at first, by the conversion of snowflakes to grains. Then, usually under the pressure of an increasing overburden of newer snow, density increases more slowly by settling of the grains to about 550 kg m^{-3}, representing the maximum practically attainable packing. Snow becomes *firn* (in the structural sense) over a range of density beginning at about 400 kg m^{-3}.

Beyond the maximum packing density, even slower mechanisms of densification – sintering and plastic deformation of the grains, and *recrystallization* – become dominant. When the firn reaches a density of about 830 kg m^{-3}, the pore spaces between crystals are closed off, air can no longer flow (as opposed to diffusing through the lattice), and the substance is deemed to be *glacier ice*.

When there has been no *melting*, densification rarely proceeds beyond 400 kg m^{-3} over the course of a typical mid-latitude winter. Depending on the *accumulation* (that is, loading) rate, glacier ice may be produced in times from a few years to a few centuries. Melting followed by *refreezing* can yield bulk densities near that of pure *ice* in times shorter than a day.

Density ρ

The ratio of the mass of any substance to the volume that it occupies.

Density is expressed in kg m^{-3}. The density of the matter constituting the *glacier* can range from as low as 10 kg m^{-3}, at the surface in unusual weather, to the density of pure *ice* at depths at which all air has been squeezed out of bubbles. See *Table B6*, and *densification*.

It is very common to assume that the bulk density of the glacier is 900 kg m^{-3}. This reduced density is a rough-and-ready allowance for the presence of *snow* and *firn*, large voids (*crevasses*, *moulins* and subglacial cavities) and sediment. Where a large proportion of the glacier thickness consists of snow and firn, a bulk density even lower than 900 kg m^{-3} is appropriate. Where there is relatively little snow or firn, and the temperature is very low, a higher density, approaching or even exceeding the conventional 917 kg m^{-3}, may be appropriate.

In studies of *mass balance*, however, densities are never known with the accuracy of laboratory measurements of pure ice, which are made by measuring the lattice parameters of single crystals. Typical field instruments are hand-held corers and spring balances, and inaccuracies of the order of 4–8% are usual. Better accuracy is possible in principle with advanced devices such as neutron-scattering probes, but these are not in routine use.

In some circumstances, such as when a load of low-density snow produces compensating densification at depth, the density of the mass gained or lost by the glacier may be assumed equal to the bulk density. See *Sorge's law*.

Deposition

The process by which a vapour changes phase directly into a solid; *resublimation* is a synonym. See *latent heat of sublimation*.

Depth hoar

A layer of *ice* crystals, usually cup-shaped and facetted, formed by vapour transfer (sublimation followed by deposition) within dry *snow* beneath the snow surface.

Depth hoar is associated with very fast crystal growth under large temperature gradients. Sometimes a layer of depth hoar forms just above, and may assist in identifying, the *summer surface*. The low *density* and low strength of depth hoar can make it difficult to retrieve unbroken core sections during coring, and can complicate estimates of *accumulation* by *microwave remote sensing* . Layers of depth hoar also increase the likelihood of *avalanching*.

Diachronous (*adj*.)

Of a surface or layer, spanning time.

The word diachronous is needed most commonly when the surface or layer did not form instantaneously. The *summer surface* may be diachronous, forming at different times over a span of days or weeks, but it is assumed to be instantaneous. In a record of a *ground-penetrating radar* traverse, a *marker horizon* may be valuable in the determination of *mass balance* if it is an *isochrone*, but not if it is diachronous.

Diamond dust

An optically and physically thin layer of ground-level cloud composed of small *ice* crystals that settle slowly.

Typically diamond dust forms by the mixing of relatively moist air from aloft into a low-level *inversion* layer in which the temperature is −40 °C or lower, so that, upon saturation, vapour is deposited as ice crystals and not water droplets. It can be the most significant form of *precipitation*, and therefore of *accumulation*, in the interior of Antarctica, but is difficult to measure with accuracy.

Dielectric constant

See *relative dielectric constant*.

Digital elevation model (DEM)
An array of numbers representing the *elevation* of part or all of the Earth's surface as samples or averages at fixed spacing in two horizontal coordinate directions.

Digital elevation models are now the preferred means of representing the *elevation changes* on which *mass-balance* measurements by *geodetic methods* are based. The elevation change is calculated by subtracting an earlier DEM from a later DEM. See *Finsterwalder's method*.

A "triangulated irregular network" or TIN is a particular, more sophisticated data structure for the representation of surfaces. A "digital terrain model" is a set of arrays of numbers, including arrays not just of elevations but also of variables derived from elevation such as slope and orientation; this term, however, is often used as a synonym of "digital elevation model".

Direct method
See *glaciological method*.

Discharge
The rate of *flow* of *ice* or water through a vertical section perpendicular to the direction of the flow.

Care is needed because discharge can refer to either *ice discharge* or *meltwater discharge*, as well as being used in hydrology to refer to water flow from basins in which there are no *glaciers*.

Ice discharge
Mass flux or volumetric flux of ice through a glacier cross-section or "gate".

The gate can be anywhere on the glacier, but is often at or close to the *terminus*. If the terminus is a *calving front*, ice discharge is usually in discrete pieces that, when discharged into a body of water, become icebergs, and the ice discharge is equivalent to the *calving flux* plus the flux due to *advance* (positive) or *retreat* (negative) of the calving front.

Avalanching, for example from the margin of a hanging glacier, may constitute ice discharge; see also *dry calving*.

Meltwater discharge
The rate of flow through a cross-section, usually a stream cross-section, of water produced by melting of *glacier ice*, *firn* or *snow* that is removed from the glacier in surface, englacial or subglacial flows. See *runoff*.

The measured discharge may include a contribution from *rainfall* on the glacier, and typically includes contributions from unglacierized parts of the drainage basin.

Meltwater discharge is always reported as volume per unit time.

Divide
A line separating two contiguous *glaciers*, the horizontal *flow* of ice diverging on each side of the line. See *glacier margin*, *glacier outline*.

Downwasting
Thinning of the *glacier* due to *ablation*. See *dynamic thinning*.

Drifting snow
Snow entrained and transported within 2 m of the surface by the wind.

The height of 2 m is a convenient separator between drifting snow, which does not reduce sensibly the horizontal visibility at eye level, and *blowing snow*.

Dry-based glacier
A *glacier* whose bed is below its *pressure-melting point*, implying that there is no liquid water at the bed. Same as *cold-based glacier*.

Dry calving
Ice discharge from a *glacier margin* onto land, usually in discrete pieces.

Dry-snow line
The set of points on a *glacier* separating the *dry-snow zone* from the *percolation zone*. See *zone*.

Dry-snow zone
Region of the *glacier* where there is neither surface *melting* nor *rainfall*. See *zone*.

Dust
An accumulation of aerosol that, when deposited on the surface of a *glacier*, modifies the *mass balance* through its effect on surface albedo.

Saharan dust, for instance, sometimes has a substantial impact on the mass balance of European glaciers. Volcanic eruptions can deliver dust and ash to nearby, and sometimes to distant, glaciers. In extreme cases the added material can turn the glacier into a *debris-covered glacier*.

Dust can help to define the *summer surface*, and a dateable dust layer in *firn* or *glacier ice* can be useful as a *marker horizon*.

Dynamic thinning
The reduction of *glacier* thickness, in excess of that due to *ablation*, that results when the *flux divergence* is positive, that is, when more mass flows out of the thinning region than flows in. See *downwasting*.

Dynamic thinning, when not compensated by thickening in a downstream part of the glacier, implies an enhanced *calving flux* at the glacier *terminus*, or an advance of the terminus, or both. See also *calving velocity*.

E

Elevation
See *altitude*.

Elevation change
Vertical change in *glacier* surface *elevation* (i.e. *altitude*), typically derived from two elevation measurements, adjusted if necessary for the difference of their respective datum surfaces, at the same (or nearly the same) horizontal coordinates.

The elevation of the surface can change due to: (i) *ablation* and *accumulation* at the surface and bottom of the glacier; (ii) compaction (*densification*) of *snow* and *firn*; (iii) emergence and submergence resulting from ice flow; (iv) changes in subglacial water pressure; (v) tectonic and isostatic movements of the glacier bed; and (vi) geomorphic processes (abrasion, plucking; lodgement of sediment) at the bed. Changes due to (iv) and (vi) can usually be neglected in mass-balance studies, although a correction is sometimes applied for *glacial isostatic adjustment (GIA)*.

Surface elevation change is usually similar to *thickness change*, but (iv–vi) above produce elevation changes without changes of the thickness or glacier mass, while (ii) above produces a decrease of thickness with no accompanying change of mass. See *continuity equation*, *geodetic method*.

In turn, large changes of glacier thickness lead to isostatic changes of the bed elevation.

Emergence velocity
The vertical component, when it is directed upward, of the glacier-flow velocity vector at the *glacier* surface, at a point fixed in space.

When the component is directed downward, it is called the *submergence velocity*. The emergence velocity is related through the *continuity equation* to the *mass balance* and the rate of *thickness change*.

The component is typically upward in the *ablation zone* and downward in the *accumulation zone*.

End-of-summer (*adj.*)
See *annual*.

End-of-summer snowline
See article *Annual snowline* under *Snowline*.

Energy balance
A relation describing the change in the amount of energy stored within a defined volume owing to flows of energy across the boundary of the volume.

A change in the amount of stored energy, due for example to the advection or conduction of heat or the absorption or emission of radiation, will result in a change in the temperature or the phase, or both, of the material in the volume. Phase changes, in particular *melting* and *freezing* but also *sublimation* and *deposition*, couple the energy balance strongly to the *mass balance*. For example they determine the amount of *ablation* by melting and sublimation, and so the energy balance must be determined using either an *energy-balance model* or a *temperature-index model* in any attempt to model ablation.

The surface energy balance is that of an interface or degenerate volume, the thickness of which approaches zero, at the surface of the *glacier*. Glaciers also have internal and basal energy balances. In *cold glaciers* and some *polythermal glaciers*, the largest component of the internal energy balance is usually the heat source due to *refreezing*. In both the internal and basal energy balances, friction is a mechanical source of heat and heat is conducted (or advected) between adjacent volumes that are not isothermal. The geothermal heat flux is usually a significant term in the basal energy balance and *basal mass balance* of grounded ice, but the resulting contribution to the *climatic-basal mass balance* is generally small. Exchanges of heat with sea or lake water must be considered where the ice is afloat.

Energy-balance model
A model of *mass balance* in which *ablation* by *melting* and *sublimation* is estimated by solving the surface *energy balance*.

Energy balance models require more input information than *temperature-index models*, but are preferred for being based on a more complete description of processes, and for superior accuracy when the input information can be supplied accurately.

Energy of glacierization
A less-used synonym of *activity index*, appearing mainly in the Russian-language literature.

Englacial
Pertaining to the interior of the *glacier*, between the *summer surface* and the bed.

Equilibrium
A state in which the *mass balance* is equal to zero over one or more years.

Equilibrium may hold for a single column, for an entire *flowline*, or for an entire *glacier*. See *steady state*.

Equilibrium AAR
See article *Equilibrium AAR* under *Accumulation-area ratio.*

Equilibrium line
The set of points on the surface of the *glacier* where the *climatic mass balance* is zero at a given moment (Figure 6).

The equilibrium line separates the *accumulation zone* from the *ablation zone*. It coincides with the *snowline* only if all mass exchange occurs at the surface of the glacier and there is no *superimposed ice*.

Unless qualified by a different adjective, references to the equilibrium line refer to the *annual equilibrium line*. See also *equilibrium-line altitude, firn line*, *snowline*, *transient equilibrium line*, *zone*.

Annual equilibrium line
The equilibrium line at the end of the *mass-balance year*.

At the annual equilibrium line, *annual ablation* balances *annual accumulation* and the *annual mass balance* is zero.

Transient equilibrium line
The equilibrium line at any instant, where cumulative *ablation* balances cumulative *accumulation* since the start of the *mass-balance year*.

See *snowline, firn line*.

Figure 6. The transient snowline, which happens to coincide with the transient equilibrium line, on Baby Glacier, Axel Heiberg Island, August 1977. The *terminus* is at 715 m and the transient equilibrium line at about 900 m above sea level. The annual ELA for 1976–77 was at about 980 m. Photo courtesy of J. Alean.

Equilibrium-line altitude *ELA*
The spatially averaged *altitude* of the *equilibrium line*.

The ELA may be determined by direct visual observation, but is generally determined, in the context of *mass-balance* measurements, by fitting a curve to data representing *surface mass balance* as a function of atitude (see *mass-balance profile*). This is often an idealization, because the equilibrium line tends to span a range of altitudes. Many approximations of the ELA have been suggested; *glaciation level* and *mid-range altitude* are examples.

The ELA is understood to be the *annual ELA* unless it is qualified as the *transient ELA*.

Annual ELA
The ELA at the end of the *mass-balance year*.

The annual ELA is not in general the same as the average altitude of the *annual snowline*. The *superimposed ice zone* lies below the annual snowline and above the annual ELA. However, if there is no *superimposed ice*, the annual snowline can be used as proxy for the annual ELA.

Balanced-budget ELA
The ELA, sometimes denoted ELA_0, of a *glacier* with a *climatic mass balance* equal to zero on average over a number of years.

The balanced-budget ELA is usually estimated as the altitude at which a curve fitted to an observed relation between annual ELA and annual mass balance B_a crosses the axis $B_a = 0$. The uncertainty in such estimates can be substantial, especially when mass-balance sampling is sparse or the *equilibrium zone* occupies a large fraction of the glacier surface.

The balanced-budget ELA may differ from the *steady-state ELA* because it is estimated from observations made in conditions that may not approximate to *steady state*. In particular, most measurements of mass balance published over the past several decades have been negative.

Steady-state ELA
The ELA of a glacier in *steady state*.

The steady-state ELA is difficult to estimate because glaciers are seldom if ever in steady state. It must usually be estimated by modelling. To emphasize that the balanced-budget ELA and steady-state ELA are distinct concepts, the steady-state ELA should be given a distinctive symbol, perhaps ELA_0'.

Transient ELA
The ELA at any instant, particularly during the *ablation season*.

The transient ELA is not in general the same as the average altitude of the *transient snowline*. The *superimposed ice zone* lies below the transient snowline and above the transient ELA.

Equilibrium zone
Part of a *glacier* bounded by two contours of surface *elevation*, within which the *equilibrium line* lies.

Evaporation
The process by which a liquid changes phase into a vapour. See *latent heat of vaporization*, *Table B1*.

Evapotranspiration
The process by which a liquid changes phase into a vapour, explicitly including the transpiration that happens at the stomata of the leaves of plants. See *evaporation*.

Expanded foot
The fan of *glacier ice* formed when a *valley glacier* or *outlet glacier* flows beyond its constricting valley walls onto lowland terrain and expands laterally.

Expanded-foot glacier
A glacier with an *expanded foot*, the lateral expansion of which is too limited to justify calling the glacier a *piedmont glacier*.

F

Facies
A collection of attributes serving to distinguish one part of the *glacier* from others; by extension, the part of the glacier so distinguished.

The term, originally Latin for "face, outward appearance", was borrowed from geology. Examples of diagnostic attributes include ice lenses in the *firn*, indicating *refreezing* and therefore the "percolation facies"; the absence of such lenses, possibly suggesting the "dry snow facies"; or the seasonal exposure of *glacier ice*, indicating the "ablation facies".

In glaciology the term *zone* is equivalent and is now more common.

Feature tracking
A method for estimating *glacier* surface velocities by measurement of the positions of easily distinguishable features on repeated images of known date. See *speckle tracking*.

Surface debris and *crevasses* are the most commonly measured features.

Finsterwalder's method
A method for the measurement of *elevation change* by comparison of contours on maps of two dates.

The area between the later and the earlier instance of each contour is measured. The average elevation change of the region between any two contours is the sum of the area changes (later minus earlier) of the two contours, divided by the sum of the earlier and later areas of the region and multiplied by the difference of the contour elevations.

The method, described by Finsterwalder (1953), is now less used, having been superseded by the preparation and subtraction of *digital elevation models*.

Firn
1. *Snow* that has survived at least one *ablation season* but has not been transformed to *glacier ice*.

This sense prevails in the study of *mass balance*. Snow becomes firn, by definition, at the instant when the *mass-balance year* ends. See *zone*.

2. Structurally, the metamorphic stage intermediate between *snow* and *ice*, in which the pore space is at least partially interconnected, allowing air and water to circulate; typical densities are 400–830 kg m^{-3} (*Table B6*).

In this sense, the firn is generally up to a few tens of metres thick on a *temperate glacier* that is close to a *steady state*, and up to or more than 100 m thick in the *dry snow zone* on the *ice sheets*.

Firn area
The *zone* of the *glacier* where the *summer surface* is underlain by *firn* instead of *glacier ice*.

Changes in extent of the firn area, and thickness of the firn, complicate *mass-balance* calculations by the *geodetic method* since *Sorge's law* no longer applies.

The firn area is not the same as the *accumulation zone*.

Firn-ice zone
See *infiltration zone*.

Firn line
The set of points on the surface of a *glacier* delineating the *firn area* and, at the end of the *mass-balance year*, separating *firn* (usually above) from *glacier ice* (usually below).

In *steady state* and *equilibrium*, and in the absence of *superimposed ice*, the firn line coincides with the *equilibrium line*. However, the equilibrium line will generally be above the firn line in a year of negative *mass balance*; in a year of positive mass balance it will in general be below the firn line of the previous year (see *Figure 15*).

Firn limit
A synonym of *firn line*.

Fixed-date system
The *time system* in which *mass balance* is determined by conducting field surveys on fixed calendar dates.

The fixed date representing the start of the *mass-balance year* is usually at the start of the local *hydrological year*. To determine seasonal balances, a fixed date is chosen to represent the mean date of the end of the *accumulation season*. Due to logistical constraints it is often impossible to conduct field surveys on these exact dates. Therefore the data need to be corrected, which is often done by estimating *ablation* and *accumulation* between the survey date and the fixed date using meteorological data from a nearby weather station or a database of upper-air measurements.

See also *measurement year*, *stratigraphic system*, *floating-date system*, *combined system*.

Floating-date system
The *time system* in which *mass balance* is determined by conducting field surveys on floating calendar dates.

Annual field surveys are usually carried out close to the beginning of the *hydrological year*. For the determination of seasonal mass balances, a survey is carried out close to the end of the *accumulation season*, without interpolation or extrapolation to a fixed date.

The duration of the *mass-balance year* varies in the floating-date system. See also *measurement year*, *stratigraphic system*, *fixed-date system*, *combined system*.

Floating tongue
The terminal part of a *glacier*, the weight of which is partially or entirely supported by lake or sea water.

Lateral stress from valley walls, and possibly from *ice rises* and other grounded parts of the glacier, supports a significant part of the weight of the floating ice, in which respect floating tongues generally differ from *ice shelves*.

Flotation
The transition from being grounded to being afloat, made when the pressure $\rho_w gd$ exerted by water of depth d on adjacent *ice* of thickness $h = d + h_{flot}$ becomes just equal to the weight $\rho_i gh$ of the ice; ρ_w is the density of the water, ρ_i is the depth-averaged *density* of the ice (allowing for example for *crevasses* and possibly *snow* or *firn*) and h_{flot} is the *freeboard*, that is, the *elevation* of the ice surface above the water level.

The definition neglects tidal flexure and some other lesser phenomena. It represents mutual hydrostatic equilibrium of the column of water and the adjacent column of ice: the water below d supports the weight of both columns, which are at rest with respect to each other. If the two densities are known, a measurement of the freeboard of floating ice is a measurement of ice thickness, which is required for the calculation of *ice discharge*.

The condition for flotation is $d = h \rho_i / \rho_w$. A condition for being afloat is $d \geq h \rho_i / \rho_w$.

The spellings “flotation” and “floatation” are equally acceptable, although the former is more common.

Flow
Motion of an *ice body* by a combination of internal deformation, rigid displacement over the bed and deformation of bed material.

Rigid displacement over the bed is called basal sliding, and implies that the *ice* at the bed is at its *pressure-melting point*.

The speed and direction of the flow are determined by a balance of forces. In the momentum balance, acceleration terms are negligible. Typically, gravity is balanced by pressure and frictional forces.

Flowline

1. A sequence of columns of infinitesimal cross section, each extending vertically from base to surface of the *glacier*, arranged so that each column but the first gains mass by *flow* from an upglacier neighbour and each column except possibly the last loses mass by flow to a downglacier neighbour.

2. The trace of such a sequence on the glacier surface.

Ideally, the upglacier and downglacier walls of all the columns would be at right angles to the local horizontal velocity vector. It is assumed that flow through the other two walls of the columns may be neglected, by allowing an implicit relative width of the flowline to vary and thus to account for transverse straining. In practice, velocity measurements are usually sparse or lacking and it is necessary to construct the flowline from the surface topography. The topography is averaged within a radius of the order of the glacier thickness, to suppress the effect on calculations that might be exerted by short-wavelength topographic features that are not due to the glacier flow.

The definitions may be extended to accommodate *interrupted glaciers*, in which part of the "flow" is by *avalanching* from an upper part to a lower part.

Fluctuations of Glaciers (FoG)

A database containing information on *glacier* changes, such as in length, *area*, mass, *mass balance* and volume, archived and published by the *World Glacier Monitoring Service* and its predecessor organisations since 1895.

Flux divergence

The divergence $\nabla \cdot \vec{q}$ of the horizontal flux vector $\vec{q}$, which is the integral through the glacier thickness *h* of the vertical profile of the horizontal *mass flux* vector $\rho\vec{u}$ or velocity vector $\vec{u}$.

For one-dimensional flow, for example along a *flowline*, the divergence reduces to the derivative $\partial\vec{q} / \partial x$ of the vertically integrated mass flux or volumetric flux with respect to horizontal distance *x*.

The integrated horizontal mass flux vector (dimension [M L^{-1} T^{-1}]), where ρ is the *density*, is

$$\vec{q} = \int_0^h \rho(z)\vec{u}(z)\,dz \quad .$$

When it is reasonable to assume incompressibility of the medium, that is, when *snow* and *firn* occupy only a small fraction of the total thickness, a simpler definition of the volumetric flux vector (dimension [L^2 T^{-1}]) is

$$\vec{q} = \int_0^h \vec{u}(z)\,dz \quad .$$

Because the vertical profile of the velocity is generally not known, an approximation is usually made: in volumetric units, with *h* the *ice-equivalent* thickness, $\vec{q} \approx h\gamma\vec{u}_{\mathrm{sfc}}$. Here γ is the ratio of the mean velocity through the glacier thickness to the surface velocity and ranges from $\gamma = 1$ for pure sliding motion down to $\gamma \approx 0.8$ or lower for motion due solely to deformation.

See *emergence velocity*, *submergence velocity*.

Flux-divergence method

Application of the *continuity equation* to determine *mass balance* at a point using measurements on the *glacier* surface or remotely of thickness, *thickness change* and surface velocity.

The required data may be obtained:

(1) for thickness, from boreholes or *radar*,

(2) for thickness change, from repeated optical surveying, *laser altimetry*, *radar altimetry*, *photogrammetry*, or *GPS* determinations of altitude,

(3) for surface velocity, from repeated optical surveying or *GPS* determinations of *stake* locations or *feature tracking*.

In the case of several repeated thickness change and velocity determinations, thickness can also be obtained as the solution of a problem in geophysical inverse theory.

Forbes band
See *ogive*.

Forefield
See *glacier forefield*.

Freeboard
The *elevation* of the surface of a floating *ice body* above the surface of the water in which it is afloat. See *flotation*.

Freezing
The process by which a liquid changes phase into a solid; a synonym of *solidification*.

Freezing point T_m or T_f
The temperature, T_m = 273.15 K = 0 ºC, at which pure water freezes, releasing an amount of energy known as the *latent heat of fusion* (*Table B1*), when the pressure is equal to a standard pressure of 101 325 Pa. *Melting point* is a synonym.

Strictly the freezing point is the (temperature, pressure) pair of numbers, but the variation of pressure at the surface of the *glacier* has negligible effect and the term is applied to the temperature alone.

See *pressure-melting point*, *ice point*.

Freezing rain
Rain that freezes upon impact, forming a surface coating of *glaze*, or after percolating below the *glacier* surface.

Front
See *glacier front*.

Frontal ablation a_f, A_f
Loss of mass from a near-vertical *glacier margin*, such as a *calving front*.

The processes of mass loss can include *calving*, subaerial *melting* and subaerial *sublimation*, and subaqueous frontal melting.

Fusion
The process by which a solid changes phase into a liquid; a synonym of *melting*. See *latent heat of fusion, Table B1*.

G

Geodetic method
Any method for determining *mass balance* by repeated mapping of *glacier* surface *elevations* to estimate the *volume balance*; *cartographic method* and *topographic method* are synonyms.

The conversion of *elevation change* to *mass balance* requires information on the *density* of the mass lost or gained, or an assumption about the time variations in density (see *Sorge's law*). Elevation changes are commonly measured using repeated *altimetry*, *photogrammetry* or ground surveys. In the past, glacier mapping relied on ground surveying with theodolites and similar instruments, but *global navigation satellite system* receivers are now usual, offering more rapid and more accurate coverage. The entire glacier surface may be mapped, but more sparse elevation measurements, generally along a central glacier *flowline*, are often extrapolated to the full glacier surface.

Glacial isostatic adjustment (GIA)
A change of *glacier* surface *elevation* due to vertical motion of the glacier bed under the influence of mass redistribution in the underlying solid Earth.

Present-day mass redistribution in the Earth's interior is dominated by continuing adjustment to the redistribution of surface water at the end of the most recent ice age. Corrections are also required for vertical motions of tectonic origin in some regions, such as the Karakoram.

Glaciated
Covered by *glacier ice* in the past, but not at present. See *glacierized*, which refers to present-day coverage.

Glaciation level
In any small *glacierized* region, the average of the *elevations* of the highest unglacierized peak and the lowest glacierized peak.

The glaciation level has been used as a regional-scale proxy for the *steady-state ELA*, although a correction is required for this purpose because the glaciation level is known to be systematically higher by about 200 m. See *mid-range altitude*.

Glaciation limit
A less-used synonym of *glaciation level*.

Glacier
A *perennial* mass of *ice*, and possibly *firn* and *snow*, originating on the land surface by the *recrystallization* of snow or other forms of *solid precipitation* and showing evidence of past or present *flow*.

For *mass-balance* purposes glaciers are delineated, when possible, by outlines across which there is no flow, so that transfer of mass as ice across those outlines is zero. Any change of the outline during the study period must be allowed for appropriately. If part of the outline fails the no-flow test, such as at a *grounding line*, the *ice discharge* must be included as a component of the mass balance.

In contrast to what is natural in dynamic glaciology and glacial geomorphology, for mass-balance purposes the glacier consists only of frozen water. Sediment carried by the glacier is deemed to be outside the glacier. Meltwater in transit or in storage, for example in supraglacial lakes or subglacial cavities, is also regarded as being outside the glacier.

Glaciers may contain or consist of other glaciers. The more generic term *glacier complex* is available for objects that may be divisible into more than one glacier, and the term *ice body* is available for any object that is made mainly of ice and may or may not be a glacier.

Glacier complex
A number of contiguous *glaciers*; a generic term for all collections of glaciers that meet at *divides*.

Glacieret
A very small *glacier*, typically less than 0.25 km^2 in extent, with no marked *flow* pattern visible at the surface.

To be termed a glacieret, an *ice body* must persist for at least two consecutive *years*.

Glacierets can be of any shape, and usually occupy sheltered parts of the landscape. *Drifting snow* and *avalanches* can be dominant contributors to the *accumulation* of glacierets.

Glacier fluctuations
Glacier changes with time, such as changes of length, *area*, *thickness*, volume and mass.

Glacier forebay
The water in front of a *calving* glacier into which icebergs are discharged.

Glacier forefield
An unglacierized area abutting on a *glacier margin*.

Glacier front
The *terminus* of the glacier.

Glacier ice
1. *Ice* that is part of a *glacier*, as opposed to other forms of frozen water such as ground ice and *sea ice*.
2. *Ice* that is part of a *glacier*, having formed by the compaction and *recrystallization* of *snow* to a point at which few of the remaining voids are connected and having survived at least one *ablation season*.

In this sense, the term refers to the body of the glacier, excluding not only snow and *firn* but also *superimposed ice*, *accreted ice* and *marine ice*. See *zone*.

The *density* at which voids cease to form a connected network, that is, the density at which *firn* becomes glacier ice, is conventionally taken to be near to 830 kg m^{-3} (*Table B6*).

Glacier inventory
A detailed record of the attributes of the *glaciers* in a region. See *World Glacier Inventory*.

Glacierized
Of a region or terrain, containing *glaciers* or covered by *glacier ice* today. See *glaciated*, which refers to past coverage.

Glacier margin
The line separating the *glacier* from unglacierized terrain. See *divide*, *glacier outline, terminus*.

Glacier outline
The line in horizontal space separating the *glacier* from unglacierized terrain or, at *divides*, from contiguous glaciers. See *glacier margin*.

Glacier table
A rock that rests on a pedestal of *ice* formed when *ablation* of the ice beneath the rock is less than ablation of the surrounding bare ice.

Glacier terminus
See *terminus*.

Glacier tongue
See *tongue*.

Glacier-wide (*adj*.)
Descriptive of a quantity that, whether or not it is expressed in *specific* units, has been measured or estimated over the entire *glacier*.

The adjective is used to emphasize that the *mass balance* is that of the entire glacier and not that at a "specific" location (for which the recommended term is *point mass balance*).

Glaciological method
A method of determining *mass balance* in-situ on the *glacier* surface by measurements of *accumulation* and *ablation*, generally including measurements at *stakes* and in *snow pits*; *direct method* has long been a synonym.

The measurements may also rely on depth probing and *density* sampling of the *snow* and *firn*, and coring. They are made at single points, the results from a number of points being extrapolated and integrated to yield the *surface mass balance* over a larger *area* such as an elevation band or the entire *glacier*. The *internal mass balance* and *basal mass balance*, and *ice discharge* if any, are treated separately.

Glaciological noise
In an ice core, fluctuations in layer thicknesses that are due not to variations in the rate of spatially averaged *annual accumulation* but to redistribution of *snow* by the wind, including the migration of snow dunes and *zastrugi* across the core site.

Glaze
1. A solid surface deposit formed by the *freezing* of supercooled raindrops or possibly of condensed water vapour, distinguished from *rime* by having a *density* near that of *ice*. See also *hoar*.

In this sense, glaze represents *accumulation*.

2. A surface deposit of ice formed by a short episode of *melting* that results only in *recrystallization* and not in *percolation* and is followed by a return to sub-freezing temperatures.

In this sense, glaze is largely responsible for the creation of the *summer surface*.

Global Land Ice Measurements from Space (GLIMS)
An initiative launched during the 1990s to monitor the world's *glaciers*, relying primarily on optical satellite imagery.

GLIMS (Rau et al. 2005; Raup et al. 2007a, 2007b) is a leading source of information about glacier extent, as described by digitized *glacier outlines*, and *glacier fluctuations*. It involves a large number of investigators distributed around the world. It is coordinated at the University of Arizona, Tucson, and its database is developed and maintained at the *National Snow and Ice Data Center*, Boulder, Colorado, U.S.A.

Global navigation satellite system (**GNSS**)
Any satellite navigation system that provides positioning information to suitable receivers located anywhere on the Earth or in its vicinity.

The United States' *Global Positioning System* was the only fully operational GNSS until September 2010, when the Russian GLONASS achieved full global coverage. The Galileo system under development by the European Union is scheduled to become operational in 2013.

Global Positioning System (GPS)
A constellation of satellites, currently 24 to 32 in number, orbiting at an *altitude* of 20 200 km, the pattern of the orbits being designed so that, in principle, at least six satellites transmitting timing and orbital-position information are above the horizon at any point on the Earth's surface at any time; the satellites constitute the "space segment", and the system is completed by a "control segment", monitoring and synchronizing the satellites from ground stations, and a "user segment" or GPS receiver.

A GPS receiver converts the transit time of each transmitted message to the distance of the transmitting satellite, and uses the resulting distances and the transmitted information about satellite positions to determine its own position by trilateration. A minimum of four satellites must be observed to solve for the three-dimensional position (x,y,z) of the receiver's antenna.

The Global Positioning System, developed by the United States Department of Defense, has transformed the practice of positioning, both for ground and airborne surveys and for positioning of Earth-monitoring satellites in orbits lower than those of the GPS constellation. Accuracies better than a few metres are readily attainable in ground surveys. Accuracy improves with observing time.

In differential GPS or DGPS operations, a receiver is installed at a base station the location of which is known precisely. The location deduced from signals received by the base receiver is compared with the known location, and the difference is used to correct the locations of a mobile receiver, sometimes called a "rover". Absolute positions in an appropriate coordinate frame can be determined with accuracies better than 0.1 m.

Global Terrestrial Network for Glaciers (GTN–G)

Part of two related systems, the Global Terrestrial Observing System (GTOS) and the Global Climate Observing System (GCOS), for the detection and management of global and regional environmental change in support of the United Nations Framework Convention on Climate Change and the work of the Intergovernmental Panel on Climate Change.

Since its creation in 1998 the GTN–G has been managed by the *World Glacier Monitoring Service* (WGMS) in close collaboration with the US *National Snow and Ice Data Center* (NSIDC) and the *Global Land Ice Measurements from Space* initiative (GLIMS). GTN–G implements an integrated, multi-*tier* monitoring strategy, and is responsible for providing data on *mass balance* (kg m^{-2} a^{-1}), length change (m) and area (km^2) of *glaciers* other than the *ice sheets*, defined as Essential Climate Variables, to GCOS and GTOS.

GRACE

The Gravity Recovery and Climate Experiment. See *gravimetric method*.

Gravimetric method

A technique in which *glacier* mass variations are calculated via direct measurements of Earth's gravity field.

Satellite gravimetry is at present the most feasible method for determining glacier *mass balance* from changes in gravity. The Gravity Recovery and Climate Experiment (GRACE) consists of two polar-orbiting satellites separated by about 200 km along-track, and is the primary mission for this work to date. Precise measurements of *range* and range rate are used to construct local gravity fields after correcting for non-gravitational accelerations. Suitable models are used to remove gravity variations resulting from atmospheric, hydrospheric and lithospheric mass variations, leaving a time series that represents the glacier *mass balance* (usually summed and shown as the *cumulative mass balance*). GRACE spatial and temporal resolutions as good as 2 arc degrees and 10 days have been achieved. Satellite gravimetry is limited by the quality of observations used to constrain the models of non-glacial mass variations, and at present it can resolve only large and rapidly changing *glacier complexes* or glacierized regions. A distinctive advantage of the method is that it yields a direct measure of mass and does not require *density* corrections such as those required for *geodetic methods*.

Glacier mass balance has also been estimated using ground-based gravimeters. Measurements at two or more times yield the change in absolute gravity that results from the change in vertical position of a sensor on the glacier surface or at a fixed position above it, and from changes in glacier mass. This technique may become more widely developed as gravimeter resolution, precision and portability improve.

Gravity Recovery and Climate Experiment (GRACE)

See *gravimetric method*.

Ground-penetrating radar (GPR)
A *radar*, usually a pulsed system with one transmitting and one receiving antenna, operating at a frequency suitable for imaging the subsurface.

In glaciology, low frequencies (2–220 MHz) are suitable for *ice* thickness measurements whereas higher frequencies of several hundred MHz are suitable for *snow* thickness measurements, including detection of the current *summer surface* and older annual layering (see *radar method*). Higher frequencies yield better resolution but may not allow very deep penetration; lower frequencies exhibit the reverse properties. Choice of frequency is therefore paramount.

Radar imaging of the subsurface relies on accurate determination of the two-way travel time of the radar wave, which depends on the *density*. Reflections are caused by contrasts in the (complex) *relative dielectric constant* at interfaces between layers. Illustrative values of the real part of the relative dielectric constant, at frequencies used by ground-penetrating radars, are 1 for air, ~3.15 for pure ice, ~10 for bedrock and 88 for water at 0 ºC. Interfaces between these media tend to be identifiable readily. More subtle contrasts between layers, due to variations in density, water content, salinity or the concentration of solid impurities, can also be identified. See *marker horizon*, and also *bomb horizon*.

The term ground-penetrating radar is now used more often than the synonymous and more descriptive *radio-echo sounding*. Sometimes the term "tomography" is used with the same meaning.

Grounding line
The set of points separating the floating part of a *glacier* from the grounded part. See *flotation*.

Usually the floating part is downstream and the grounded part is upstream. However, the "shorelines" of subglacial lakes are grounding lines.

Growth time
The time scale for a glacier to attain steady state from an initial state of zero mass. See *response time*.

H

Hanging glacier
A *glacier*, usually small, that clings to a steep slope, or a glacier that terminates abruptly at the top of a cliff.

Health
The extent to which the *mass balance*, usually averaged over a period of some years, differs from zero, growth or *equilibrium* representing “good health” and a negative mass balance representing “poor health”.

The term is generally used only informally.

Hoar
A surface deposit of interlocking *ice* crystals formed by the deposition of water vapour. See also *glaze*, *rime*; *depth hoar*.

Homogenization
A procedure to correct measurement time series for artefacts and biases that are not natural variations of the signal itself but originate from changes in instrumentation or changes in observational or analytical practice.

Systematic artefacts can distort or even hide the true signal. Homogenization may lead to the detection and removal of measurement errors. Gaps in the time series may be filled by interpolation or modelling at the same time as the homogenization procedure.

The uncorrected measurements should remain available after the homogenized measurements have been published.

See *reanalysis*.

Hydrological method
A method of determining the *mass balance* indirectly by solving the *water balance* for the change in storage ΔW in a drainage basin:

$$\Delta W = P - E - Q \ ,$$

with P the *precipitation*, E the *evapotranspiration* and Q the *discharge*, each of these quantities being a total over a stated span of time.

In practical work the hydrological method can be applied only to an entire drainage basin. It does not provide any information on the spatial distribution or gradients. The quantity ΔW will include changes in storage in lakes, seasonal *snowpatches*, soil and aquifers as well as in the *glacier*. Each of these changes must be accounted for to isolate the mass balance of the *glacierized* part of the catchment, but the changes in storage other than in the glacier and the snow cover are often assumed to be negligible over annual periods.

Hydrological year
A period of one *year*, synchronized with the natural progression of the hydrological seasons by specifying the calendar date of its first day.

Generally in glaciology the hydrological year is found to be convenient because it begins near the start of the *accumulation season* and ends near the end of the *ablation season*. For example the appropriate dates are 1 October to 30 September in the mid-latitudes of the Northern Hemisphere and 1 April to 31 March in the mid-latitudes of the Southern Hemisphere. The concept of the hydrological year is most useful where the accumulation and ablation seasons are well differentiated, as on mid-latitude *glaciers* and most high-latitude glaciers, but it is less well suited to those regions in which there are more than two hydrological seasons, as in the tropics, or in which most of the *accumulation* occurs in the same season as most of the *ablation*, as in monsoon climates (see *summer-accumulation type*.).

Hypsometric curve
A graph of the *area-altitude distribution*. See Figure 7.

Also called hypsographic curve. Shows the area-altitude distribution by plotting *area* on the horizontal axis versus *altitude* on the vertical axis. Intervals on the altitude axis are commonly 25, 50 or 100 metres.

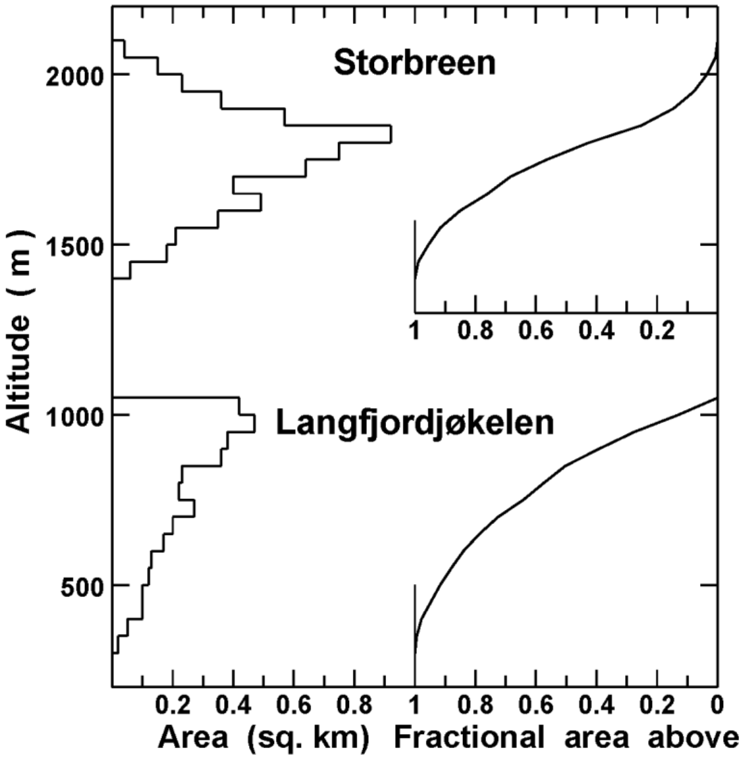

Figure 7. Hypsometric curves (left) and *cumulative* hypsometric curves (right) for two glaciers in Norway.

Hypsometry
The measurement of the distribution of glacier area with surface *altitude* (or *elevation*), or more loosely the result of such measurement.

Hypsometric and topographic data are essential for converting measurements of the *mass-balance profile* to *glacier-wide* estimates of the *mass balance*.

Hypsography is a synonym. See *area-altitude distribution*, *hypsometric curve*.

I

Ice
Water substance in the solid phase.

Ice can occur in many forms. At and near the Earth's surface, ice always crystallizes in the hexagonal system. This phase is designated ice Ih, the Roman numeral I distinguishing it from more than a dozen other phases and the letter h distinguishing it from the metastable cubic phase ice Ic.

See, among other articles, *glacier ice* and *diamond dust*.

Ice apron
1. A synonym of *mountain apron glacier*.

2. A conglomerate of snow, refrozen meltwater and blocks of ice resulting from *dry calving*, found fringing the base of a steep *terminus*, typically that of a *cold glacier*.

Ice body
Any continuous mass of *ice*, possibly including *snow* and *firn*, at or beneath the Earth's surface.

Glaciers, *ice shelves*, ice floes, icebergs, a continuous cover of *sea ice*, ice wedges in permafrost, and accumulations of ice in caves are all examples of ice bodies.

Ice cap
A dome-shaped *ice body* with radial *flow*, largely obscuring the subsurface topography and generally defined as covering less than 50 000 km^2 (see *ice sheet*).

The flow pattern is less influenced by the subsurface topography than is true of *icefields* and *valley glaciers*. The definition embraces small as well as large ice bodies.

The usage "(polar) ice cap" for the *sea-ice* cover of the Arctic Ocean or Southern Ocean is confusing and best avoided.

Ice-core stratigraphy
The determination of layering, usually identifiable as annual or seasonal, in an ice core by visual, chemical, or isotopic methods; more loosely, the result of such determination.

After correction for thinning due to ice *flow*, the resulting layer thicknesses are measures of *climatic mass balance*. If there is no *ablation*, they are measures of *accumulation*.

While some information can be obtained from cores even when the ice is not cold, ice-core stratigraphy is usually done on cores through *cold ice*, such as in Greenland or Antarctica.

Ice discharge
See article *Ice discharge* under *Discharge*.

Ice equivalent
A unit, in full the "metre [of] ice equivalent", that is an extension of the SI for describing *glacier* mass in *specific* units as the thickness (in "m ice eq.") of an equal mass having the *density* of *ice*.

Ice equivalents can be converted to kg m^{-2} by multiplying by the density of ice, and to *water equivalents* (m w.e.) by multiplying by the density of ice and dividing by the density of water (with sufficient accuracy, 1000 kg m^{-3}).

Icefield
A large *ice body* that covers mountainous terrain but is not thick enough to obscure all of the subsurface topography, its flow therefore not being predominantly radial as is that of an *ice cap*.

Icefall
A steep reach of a *glacier* where the *ice* becomes heavily crevassed, commonly when flowing over a bedrock step.

Ice flux
See *mass flux*, *flux divergence*.

Ice melange
See *melange*.

Ice-penetrating radar
Ground-penetrating radar when it is used to penetrate *ice*.

Ice mass
A synonym of *ice body*.

Ice piedmont
An expanse of *glacier ice* covering a lowland, nourished by two or more upland tributary *glaciers*.

Ice plain
Part of an *ice stream* extending upglacier from the *grounding line* and having a surface slope so small as to suggest that it is not far from the transition to being afloat. See *flotation*.

The upglacier limit of the ice plain may be marked by a measurable break of surface slope, or may be indistinct. Ice plains are documented from several of the ice streams of Antarctica.

Ice point T_{m} or T_{f}
The narrowly correct name of what in everyday usage is called the *melting point* or *freezing point* of water. See *pressure-melting point*.

Ice raft
Part of an *ice stream* raised slightly higher, and flowing slightly more slowly, than surrounding *ice*.

The attributes that define the ice raft suggest that basal shear stress is relatively enhanced at its bed, and therefore that it might represent a persistent "sticky spot".

Ice rise
An area of grounded ice surrounded or almost surrounded by *shelf ice* or the ice of a *floating tongue*.

Currently the largest ice rise, with an area of 44 000 km^2, is Berkner Island in the Ronne-Filchner Ice Shelf.

Ice rumple
A small *ice rise*, generally of irregular outline, or a group of small ice rises.

Ice sheet
An *ice body* that covers an area of continental size, generally defined as covering 50 000 km^2 or more.

Currently there are only two ice sheets, the Greenland Ice Sheet and the Antarctic Ice Sheet. The latter is sometimes subdivided into the East Antarctic Ice Sheet and the West Antarctic Ice Sheet.

See *ice cap*.

Ice shelf
A thick and extensive *ice body* attached to a coast and floating on the sea, gaining mass by *flow* from grounded *glacier ice*. See *floating tongue*, *shelf ice*.

Ice shelves are much thicker than *sea ice*. Currently, nearly all are located in Antarctica. The *mass balance* of an ice shelf may have significant components of both gain and loss at the base.

Ice stream
A part of an *ice sheet* or *ice cap* with strongly enhanced *flow*, often separated from surrounding *ice* by strongly sheared, crevassed margins.

“Pure” ice streams are bounded by ice on either side and lack significant non-glacial topographic control, while “topographic” ice streams are constrained by the topography. An ice stream of the latter type is similar to an *outlet glacier*, but outlet glaciers do not necessarily have strongly enhanced flow velocity.

Infiltration
The entry of a liquid such as water into a permeable solid such as *snow* or *firn,* and, more loosely, the *percolation* of the liquid through the void spaces of the solid.

In general, two forces govern infiltration: gravity and capillary tension. The latter allows the solid to draw in the liquid and is determined by adhesive molecular forces, which can be substantial in materials with very small pores. The rate of infiltration of a liquid into a permeable solid is determined by the *porosity* and liquid content of the solid and by its hydraulic conductivity.

Infiltration ice
In Russian-language usage, *ice* derived from the *refreezing* of *meltwater* that has saturated the void spaces in *snow* or *firn*. See *congelation, recrystallization, superimposed ice*.

Infiltration zone
In the Russian-language literature, part of the lower *percolation zone* where *meltwater* is abundant in the *snow* and *firn,* but the firn is either a survival from previous years of more positive *mass balance* or is advected by the glacier *flow* from higher elevations. See *zone*.

The infiltration zone is sometimes also referred to as the “firn-ice zone”.

Infiltration-congelation zone
In the Russian-language literature, a synonym of *superimposed ice zone*. See *zone*.

Infiltration-recrystallization zone
A term in Russian-language usage referring to the lower *percolation zone,* where enough *meltwater* is produced at the surface to percolate out of the *snow* and into the *firn*. See *zone*.

In the *cold infiltration-recrystallization zone,* generally at higher elevation and sometimes called the “cold firn zone”, the meltwater refreezes in the firn because the temperature is below the *freezing point*. This *refreezing* is the dominant mechanism for the formation of *glacier ice*. In the *warm infiltration-recrystallization zone*, generally at lower elevation and sometimes called the “warm firn zone”, the temperature is at or near the freezing point and refreezing makes a lesser contribution to the formation of ice.

The *runoff limit* may lie within the warm firn zone, or within the cold firn zone where slopes are steep.

Inland ice
A translation, seen infrequently in earlier English-language literature, of “inlandsis”, an originally Danish word which is the word for *ice sheet* in several European languages.

InSAR
An acronym for interferometric synthetic aperture *radar,* an instrument (and by extension a method) for *microwave remote sensing* of the topography, velocity field and other characteristics of a surface.

A synthetic aperture radar (SAR) consists of a side-looking radar system that takes advantage of the forward motion of the radar platform to synthesize a very long antenna, enabling a much higher ground resolution than ordinary *radar altimetry*. Each SAR acquisition contains information on the amplitude and phase of the radiation reflected from the target and received at the antenna.

Interferometric SAR requires the calculation of differences in phase between two co-registered SAR images obtained with slightly different viewing geometries, either at the same time from two antennae, or at two different times from one antenna. These phase differences yield fringe patterns (interferograms) that are an expression of both surface topography and surface motion.

If the surface is not in motion, or the time between images is sufficiently short, phase differences can be converted to surface *elevations* with knowledge of the attitude and orbital position of the interferometer; more specifically, the baseline length, or distance between the two orbital positions, must be known. Using InSAR to detect motion of the surface requires imagery from two different epochs (repeat-pass interferometry). In this case topographic effects are removed using an independently derived digital elevation model.

Interferometer
An instrument that relies on the interference of waves, particularly electromagnetic waves, from a common source such as a *radar* to measure the length or displacement of a target with an ambiguity that is an integer multiple of the wavelength. See *InSAR*.

Interferometry
Measurement of the interference of waves, particularly electromagnetic waves, from a common source such as a *radar*, with the aim of obtaining information about the topography, velocity field and other characteristics of the *glacier* surface. See *InSAR*.

Internal ablation a_i (point), A_i (glacier-wide)
Loss of mass from a *glacier* by melting of *ice* or *firn* between the *summer surface* and the bed. See *mass-balance units*.

Internal ablation can occur due to strain heating of *temperate ice* as the ice deforms. However, the largest heat sources for internal ablation are likely to be the potential energy released by downward motion of the ice and of meltwater. The magnitude of the former is equivalent to a few mm w.e. a^{-1}, and of the latter, which occurs mainly in conduits transferring water from the glacier surface to the bed, to up to a few tens of mm w.e. a^{-1}. (These rates are expressed over the extent of a typical *valley glacier*.)

Internal accumulation c_i (point), C_i (glacier-wide)
Refreezing of water within a *glacier*, between the *summer surface* and the bed, which goes undetected by measurements of *surface mass balance*.

See *mass-balance units*, *zone*.

Internal accumulation is the refreezing of surface *meltwater* (or *freezing* of *rain*) that is in transit and otherwise would have left the glacier as *runoff*. In the case of meltwater, it may be regarded as redistributing mass within the glacier. This may require careful accounting in the calculation of mass balance.

Internal accumulation proceeds by the freezing of water that percolates early in the *ablation season* into *firn* that is still cold, heating the firn in the process, or by the freezing of retained pore water during the *accumulation season*, also releasing latent heat and thus slowing the downward advance of the winter cold wave.

The term is reserved for refreezing beneath the *summer surface*, that is, within the firn or the *ice*. *Meltwater* that refreezes within the *snow* does not constitute internal accumulation since it is accounted for by end-of-season *density* measurements as part of conventional *mass-balance* measurements. Internal accumulation may be small in magnitude, and negligible on *temperate glaciers*, but if not accounted for it constitutes a bias towards overestimation of mass loss.

In *remote-sensing* studies, it is not always possible to detect the summer surface. In addition *surface mass balance* models do not always distinguish between internal accumulation and refreezing within the snow. To avoid confusion, it is advisable to use “internal accumulation” only in the sense given above and to use the more inclusive “*refreezing*” only for “internal accumulation plus refreezing within the snow”. Refreezing within the snow should be described as such explicitly.

Internal mass balance b_i (point), B_i (glacier-wide)
The change in the mass of the *glacier* due to *internal accumulation* and *internal ablation* over a stated period.

See *mass-balance units*, *climatic mass balance*.

International Association of Cryospheric Sciences (IACS)
A body of the International Union of Geodesy and Geophysics (IUGG) founded in 2007 to encourage and promote research in cryospheric sciences and to facilitate the standardisation of measurement or collection as well as analysis, archiving and publication of data on cryospheric systems.

The IACS is the successor of the *International Commission on Snow and Ice (ICSI)*.

International Council for Science (ICSU)
A non-governmental organisation, founded in 1931, representing a global membership that includes both national scientific bodies and international scientific unions, and coordinating interdisciplinary research to address major issues of relevance to science and society.

The name International Council for Science was adopted by the International Council of Scientific Unions in 1998, but the acronym ICSU was deliberately retained.

International Commission on Snow and Ice (ICSI)
A former body of the International Association of Hydrological Sciences of the International Union of Geodesy and Geophysics (IUGG).

The ICSI can be traced back to the merger in 1939 of the International Commission on Snow with the *International Glacier Commission*. It became the *International Association of Cryospheric Sciences*, which is a full member of the International Union of Geodesy and Geophysics, in 2007. Concurrently, a new commission of the International Association of Hydrological Sciences, the International Commission for Snow and Ice Hydrology (ICSIH), was formed to maintain and promote contacts between the cryospheric and the hydrological sciences.

International Commission on Snow and Ice Hydrology (ICSIH)
A commission of the International Association of Hydrological Sciences (IAHS) launched in 2005.

The goal of ICSIH is to promote the scientific study of the processes of snow, permafrost and ice dynamics, the interactions between snow, permafrost and ice and ecosystems, and the impact of snow, permafrost and ice on runoff generation, rivers and lakes.

International Glacier Commission (CIG)
A body founded in 1894 to coordinate the monitoring of glacier fluctuations.

Data collected under the auspices of the International Glacier Commission were mostly about fluctuations of glacier length. The work begun by the International Glacier Commission is traceable continuously to that coordinated by the present-day *World Glacier Monitoring Service*.

Interrupted glacier
A *glacier* consisting of two or more parts between which mass transfer or "*flow*" to the lower part is by *avalanching*.

Whether to regard the parts as separate entities is a matter of convenience. See *regenerated glacier*.

Inversion
A layer of the atmosphere in which temperature increases with height.

An inversion develops above a *glacier* surface when the air transfers heat to the surface, for example because the air is warmer than the *snow* or *ice* (which cannot have a temperature above the *freezing point*) or because of strong radiative cooling from the surface. The inversion in the temperature profile makes the atmosphere strongly stable, such that vertical motions of air parcels, whether convective or orographic, are retarded or suppressed.

Isochrone
A surface that formed at the same time over its entire extent. See *marker horizon*.

J

Julian date
The number of days elapsed since noon (12.0 h UTC) on 1 January 4713 BC in the proleptic Julian calendar, or 24 November 4714 BC in the proleptic Gregorian calendar.

The Julian date is a real number, not an integer. At 0.0 h UTC on 1 January 2000 AD it was 2451544.5. The Julian date is not the same as the *day of the year*.

Properly implemented, as for example by Press et al. (1992), an algorithm to convert between calendar dates and Julian dates is the best way to ensure that the time coordinate is represented correctly when studying the long-term evolution of *mass balance* in calendar time.

A proleptic calendar is one that is extended to dates before its first historical use.

Julian day number
The integer part of the *Julian date*.

K

Kinematic method

Any method of determining the *mass balance* that involves measurement or calculation of glacier *flow*, including the *flux-divergence method*, the *kinematic-equation method* and methods in which the mass balance is determined as the sum of the *discharge* through a cross-section and the *surface mass balance* of the region upglacier from the cross-section.

Information about *density* is needed to convert the volumetric fluxes obtained by kinematic methods to *mass fluxes*.

Kinematic-equation method

A method of determining the spatial distribution of the *mass balance* by solving the equation of the kinematic boundary condition at the surface for the *ice-equivalent mass-balance rate* $\dot{b}$ as a function of the rate of change $\dot{h}$ of the ice-equivalent thickness, the spatial gradient of the thickness ∇h (usually approximated by the inclination of the surface), and the velocity at the surface $\vec{u}$:

$$\dot{b} = \dot{h} + \vec{u}_H \cdot \nabla h - \vec{u}_V \ ,$$

where subscripts H and V denote horizontal and vertical vector components respectively of $\vec{u}$. It is assumed that the basal ice velocity is zero, for example because the *ice* is frozen to the bed.

L

Lake-terminating glacier
A *glacier* the *terminus* of which stands or floats in a lake.
See *calving*, *tidewater glacier*.

Laser altimeter
An instrument for *altimetry*, and in *mass-balance* studies for the measurement of *elevation change* by repeated altimetry, that uses pulses of laser radiation, for example at 532 nm (green) or 1024 nm (near infrared) wavelengths.

There are both profiling and scanning laser altimeters. A profiling system is nadir-pointing, while a scanning system uses a rotating mirror, or a series of sensors arrayed in a parallel (pushbroom) configuration, to obtain a swath rather than a linear profile of measurements.

The Ice, Cloud and land Elevation Satellite (ICESat, 2003–2010) measured surface *elevations* with approximately 70 m footprint and 170 m along-track spacing. Adjacent tracks are separated by a few to a few tens of kilometres, the lesser separations being found at the polar extremities of the orbit. Sources of error include sensor saturation, atmospheric scattering effects, and inaccurate knowledge of the laser pointing angles. Aircraft altimeters have footprints of 1 m or smaller and along-track spacing on the order of 1 to 3 m, and are less affected by atmospheric and pointing errors. Laser altimeters are unable to obtain measurements through clouds.

Laser is an acronym standing for light amplification by stimulated emission of radiation. A related term, lidar (light detection and ranging), applies more generally to the measurement of scattered light from distant targets.

Laser altimetry
The measurement of surface *elevation* (*altitude*) with a *laser altimeter*.

Particularly when used to measure *elevation change*, laser altimetry has become a leading source of data for the measurement of *mass balance* by the *geodetic method*. If, for logistical or financial reasons, it is not possible to survey the whole *glacier* by airborne laser altimetry, it is necessary to extrapolate to obtain a glacier-wide geodetic *mass balance*.

Latent heat
The energy taken up or released per unit mass by a system in a reversible change of phase at constant temperature and pressure.

In glaciology and meteorology, the latent heats of *evaporation* (*condensation*), *fusion* (*solidification* or *freezing*), and *sublimation* (*deposition* or *resublimation*) of water phases are of importance. See *Table B1*, *Table B4*.

Latent heat of evaporation L_v
See *latent heat of vaporization*

Latent heat of fusion L_f
The energy taken up by a substance as it changes phase from solid to liquid, or released as it changes from liquid to solid.

The amount of energy taken up in the *fusion* or released in the *freezing* of water is 333.5 kJ kg^{-1} at 0° C. See *Table B1*.

Latent heat of sublimation L_s
The energy taken up by a substance as it changes phase from solid to vapour, or released as it changes from vapour to solid.

The amount of energy taken up in the *sublimation* or released in the *deposition* (*resublimation*) of water is 2834.2 kJ kg^{-1} at 0° C. See *Table B1*.

Latent heat of vaporization L_v

The energy taken up by a substance as it changes phase from liquid to vapour, or released as it changes phase from vapour to liquid. A synonym of *latent heat of evaporation*.

The amount of energy taken up in the *evaporation* or released in the *condensation* of water is 2500.8 kJ kg^{-1} at 0° C. See *Table B1*.

Lidar

Light detection and ranging. See *laser altimeter*.

Little Ice Age (LIA)

A period of greater *glacier* mass and extent, relative to the preceding and following periods, with increased glacier thickness and extension to lower *altitudes*.

In different regions of the Earth, in both hemispheres, the Little Ice Age began and ended at different times, beginning as early as about AD 1300 and ending as late as about AD 1900, with one or more glacier advances distinguishable during that period. In many regions the LIA maximum glacier extent was also the maximum extent of the entire Holocene (the past 10 000 years). Gain of mass usually resulted from both enhanced *accumulation* and reduced *ablation*. See *trimline*.

M

Margin
See *glacier margin*.

Marine ice
Ice formed by the *freezing* of sea water at the base of an *ice shelf*.

The formation of marine ice can contribute substantially to ice-shelf *mass balance* (see *basal accumulation*), and marine ice can be a substantial component of the ice shelf itself. See also *accreted ice*.

Marker horizon
A distinctive, datable layer in *ice*, *firn* or *snow*; see *isochrone*.

Ice-core stratigraphy relies on an uninterrupted series of annual marker horizons. Volcanic eruptions and nuclear tests (see *bomb horizon*) yield marker horizons which allow the measurement of average *accumulation* rates. Marker horizons with *relative dielectric constants* that contrast strongly enough allow the mapping of accumulation with *ground-penetrating radar*.

Mascon
The mass of a thin layer of uniform thickness added to or subtracted from a reference model of the solid and liquid Earth over a specified region, particularly a *glacierized* region, during a specified period. See *GRACE*, *gravimetric method*.

Mascon is an abbreviation by geodesists of “mass concentration”, coined originally to stand for a large positive gravitational anomaly. In modern usage the mascon itself is a number representing the mass of the layer as a *surface density* (kg m^{-2}), although the word is often used loosely to refer to the “mascon region”, that is, the region over which the mass is added or subtracted. The “mascon parameters” are sets of coefficients describing the difference of gravitational potential that arises due to the mascon.

Mass balance Δm (point), ΔM (glacier-wide)
The change in the mass of a *glacier*, or part of the glacier, over a stated span of time; the term *mass budget* is a synonym. See *mass-balance units* for recommended units.

The span of time is often a year or a season. A seasonal mass balance is nearly always either a *winter balance* or a *summer balance*, although other kinds of season are appropriate in some climates, such as those of the tropics. The definition of *year* depends on the method adopted for measurement of the balance. See *time system*.

The reference in the definition to a glacier means that a particular volume of space is being studied. A properly delineated glacier has no mass transfer of *ice* across its boundary other than as *ice discharge*. However, the mass balance is often quoted for volumes other than that of the whole glacier, for example a column through the glacier, the part of the glacier upglacier or downglacier from the *grounding line*, or a band defined by two contours of surface *elevation*. It is necessary in such cases to make clear that the study volume is something other than the whole glacier, and also to make clear which components of the mass balance are being reported. The quantity reported may be the *climatic mass balance* or the *climatic-basal mass balance*, but will often be the *surface mass balance*. In all cases the need for a defined study volume is fundamental because without it the principle of *conservation of mass* cannot be invoked.

The study volume may change over the study period. The surface and bed elevations may change, and the areal extent is unlikely to be the same at the end of the period as it was at the beginning. Whether these changes are significant will depend not just on their magnitude and the accuracy with which they can be determined but on the purpose of the investigation. See *conventional balance*, *reference-surface balance*.

Annual ablation a_a (point), A_a (glacier-wide)
Ablation integrated over the *mass-balance year*.

Annual ablation is the sum of *winter ablation* and *summer ablation* where winter and summer are well-differentiated. Formerly it was referred to as "total ablation" when working in the *stratigraphic system* (Anonymous 1969; *Appendix A*).

Annual accumulation c_a (point), C_a (glacier-wide)
Accumulation integrated over the *mass-balance year*.

Annual accumulation is the sum of *winter accumulation* and *summer accumulation* where winter and summer are well-differentiated. Formerly it was referred to as "total accumulation" when working in the *stratigraphic system* (Anonymous 1969; *Appendix A*).

Annual exchange
Annual accumulation minus *annual ablation*.

Ablation is defined to be negative, so the annual exchange may also be regarded as the sum of the absolute values of accumulation and ablation. It is a possible measure of the amplitude of mass exchange between the *glacier* and its environment, but the *mass-balance amplitude* is more often used for that purpose.

Formerly annual exchange was defined only in the *fixed-date system* and *total exchange* was defined as its equivalent in the *stratigraphic system* (Anonymous 1969; *Appendix A*).

Annual mass balance b_a (point), B_a (glacier-wide)
The sum of *accumulation* and *ablation* over the *mass-balance year*, equivalent to the sum of *annual accumulation* and *annual ablation*, and also to the sum of *winter mass balance* and *summer mass balance* where winter and summer are well-differentiated; that is,

$$b_a = c_a + a_a = b_w + b_s \,.$$

For reasons explained more fully under *Net mass balance*, the term annual mass balance replaces the formerly distinct terms "annual balance" and "net balance", which were used in the *fixed-date system* and the *stratigraphic system* respectively (Anonymous 1969; *Appendix A*). The adjective "annual" describes the time span of the mass-balance measurement more adequately than the adjective "net", which does not refer to a time period but rather to the mass that is remaining after all deductions (here ablation) have been made.

Net ablation
The sum, if negative, of *accumulation* and *ablation* over any time period; if the sum is positive then net ablation is zero.

In the *ablation zone* the net ablation is equal to the *mass balance*.

Net accumulation
The sum, if positive, of *accumulation* and *ablation* over any time period; if the sum is negative then net accumulation is zero.

In the *accumulation zone* the net accumulation is equal to the *mass balance*. The term appears often in ice-core studies, where the layer thickness is related to the mass balance.

Net mass balance b_n (point), B_n (glacier-wide)
According to Anonymous (1969), the sum of *accumulation* and *ablation* over the *mass-balance year* in the *stratigraphic system*.

In common usage, "net balance" has a number of meanings inconsistent with that of Anonymous (1969; *Appendix A*). It is used for the balance over approximately one year, regardless of the *time system* (see *fixed-date system*, *floating-date system*), and for balances over other periods than the mass-balance year. In these usages "net" has its plain-language meaning, referring to the change of mass after all deductions (here ablation) have been made.

To resolve this ambiguity, it is recommended that the original definition of "net mass balance" be retired, and that i) *annual mass balance* be used instead for the mass balance over a mass-balance year in any time system; and ii) explicit information about the time system be given as metadata whenever it is relevant (as it is for all measurements by the *glaciological method*). The adjective “net” thus becomes a plain-language word, and in many cases becomes redundant because the meaning of “balance” includes the meaning of “net”.

Point mass balance
Mass balance at a particular location on the *glacier*, for example at an ablation *stake* or a *snow pit*.

The point referred to is at the top of a vertical column through the glacier. Most measurements of point mass balance are actually measurements of *surface mass balance*. That is, they exclude the *internal mass balance* and *basal mass balance*, which are either assumed to be negligible or corrected for later, and the *flux divergence* of the column.

In the absence of an overriding reason for a different notation, point balances are indicated by lower-case letters, e.g. b_w for the winter balance, while glacier-wide balances are denoted by upper-case letters, e.g. B_w.

Specific mass balance
Mass balance expressed per unit area, that is, with dimension [M L^{-2}] or [M L^{-2} T^{-1}]; see *specific*.

The prefix “specific” is not necessary in general. The units in which a quantity is reported make clear whether or not it is specific. Specific mass balance may be reported for a point on the surface, a column of unit cross-section, or a larger volume such as an entire *glacier* or a collection of glaciers. In the latter two cases the term “mean specific mass balance” has been used, although the adjective “mean” is also not necessary.

The definition of “specific” apparently offered by Meier (1962) has led to some confusion. He wrote:

> ... quantities measured at a point will first be discussed. [They] should all be prefaced by the word *specific* ... . Specific budget terms have dimensions of [length] or [length]/[time].

The confusion arises because of the primacy given by Meier to *water-equivalent* dimensions (“[length]”). The adjective “specific” indicates that the quantity has dimension [M L^{-2}] or [M L^{-2} T^{-1}], not that it is being measured at a point.

The adjective “point”, as in *point mass balance*, should be used when clarity is needed.

The unit of *area* lies in the horizontal plane, not a plane parallel to the glacier surface. For mass-balance purposes this rule applies even when the surface is vertical. For example, at a *calving front* the *ablation* is equal to the mass of the entire calved volume. If quoted as a specific quantity it is divided by the horizontal area over which the balance is to be stated, such as that of the entire glacier for a *glacier-wide mass balance*.

The glaciological usage is not that which prevails in some other sciences, where often a specific quantity is either a dimensionless ratio of the value of a property of a given substance to the value of the same property of some reference substance, or is a quantity expressed per unit mass.

Summer ablation a_s (point), A_s (glacier-wide)
Ablation integrated over the *summer season*.

Summer ablation is not the same as *summer mass balance*. It is generally more negative because some of the lost mass may be offset by *accumulation*. *Mass-balance* measurements by the *glaciological method* generally measure *summer mass balance* and not summer ablation.

Summer accumulation c_s (point), C_s (glacier-wide)
Accumulation integrated over the *summer season*.

Part or all of summer accumulation may be lost by *ablation* before the end of the summer season.

Summer mass balance b_s (point), B_s (glacier-wide)
The sum of *accumulation* and *ablation* over the *summer season*.

Surface ablation a_{sfc} (point), A_{sfc} (glacier-wide)
Ablation at the surface of the *glacier*, generally measured as the lowering of the surface with respect to the *summer surface*, corrected for the increase in *density* of any residual snow and firn and multiplied by the density of the lost mass.

Surface accumulation c_{sfc} (point), C_{sfc} (glacier-wide)
Accumulation at the surface of the glacier, generally measured as the rise of the surface with respect to the *summer surface* multiplied by the *density* of the added mass.

Surface mass balance b_{sfc} (point), B_{sfc} (glacier-wide)
The sum of *surface accumulation* and *surface ablation*.

This is the sense in which the term is understood in descriptions of measurements by the *glaciological method*, in which the *internal mass balance* is treated separately. Recently, in estimates of ice-sheet mass balance by modelling, the term has been extended to include *internal accumulation*. This extended meaning is discouraged. The unambiguous term *climatic mass balance* is recommended for the sum of the surface mass balance and the internal mass balance.

Winter ablation a_w (point), A_w (glacier-wide)
Ablation integrated over the *winter season*.

Winter accumulation c_w (point), C_w (glacier-wide)
Accumulation integrated over the *winter season*.

Winter accumulation is not the same as *winter mass balance*. It is generally larger because some of the accumulated mass may be lost by *ablation*. *Mass-balance* measurements by the *glaciological method* generally measure *winter mass balance* and not winter accumulation.

Winter mass balance b_w (point), B_w (glacier-wide)
The sum of *accumulation* and *ablation* over the *winter season*.

Mass-balance amplitude
One half of the difference between *winter mass balance* and *summer mass balance*, $(B_w – B_s)/2$.

Note that summer mass balance is generally negative because *ablation* dominates in the *summer season*.

A more general definition, $(C_a – A_a)/2$ or one half of the *annual exchange*, could be offered in terms of *annual accumulation* and *annual ablation*, but these quantities are so seldom measured that a calculation from seasonal balances is more practicable.

The balance amplitude tends to be large in maritime climates, in which *accumulation* is large, and small in continental climates, in which accumulation is small. In consequence the mean balance amplitude is well correlated with the interannual variability of *annual mass balance*, and, when it can be estimated from climatological information, has been used as an estimator of the magnitude of the annual mass balance itself.

Mass-balance gradient
The rate of change of *mass balance* with *altitude*, that is, the derivative db/dz of the *mass-balance profile* $b(z)$.

If mass balance varies linearly with altitude, the mass-balance gradient will be constant with z; if not, the gradient will vary with z.

The mass-balance gradient at the *equilibrium-line altitude* is called the *activity index*.

Mass-balance index
The rate of change db/dx of *mass balance* with horizontal distance from the upper end of a *flowline*.

The term has also been used informally for a variety of measures of the mass balance.

Mass-balance profile
The variation $b(z)$ of *mass balance* with *altitude* (Figure 8).

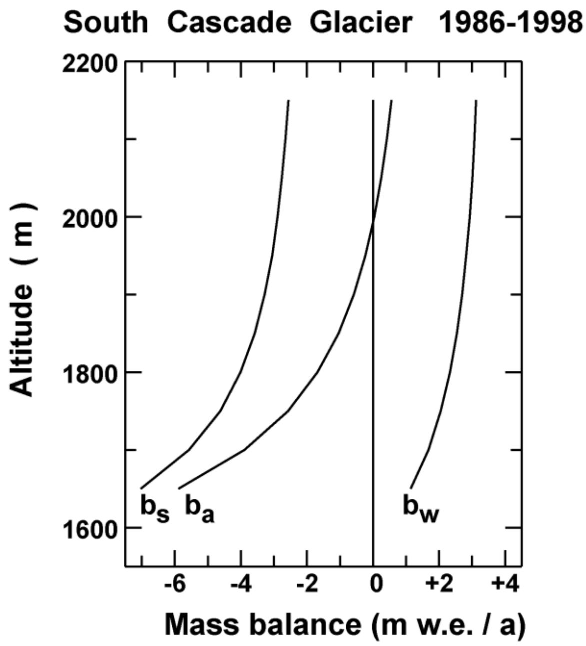

Figure 8. *Multi-annual* average mass-balance profiles, South Cascade Glacier, U.S.A.

Mass-balance rate
The change of mass per unit of time as the interval of mass change approaches zero, obtained in practice by dividing the *mass balance* by the duration over which it is measured or modelled. See *mass-balance units*.

The qualifiers "instantaneous" and "average" can be used to distinguish between the rate in the mathematical sense and the rate as obtained in practice. For example, the average mass-balance rate $\bar{\dot{M}}$ over interval Δt is related to the *mass balance* ΔM by $\bar{\dot{M}} = \Delta M / \Delta t$.

Mass-balance ratio
The ratio of the *mass-balance gradient* in the *ablation zone* to the mass-balance gradient in the *accumulation zone*, each of these gradients being assumed constant and that in the accumulation zone also being assumed non-zero.

Mass-balance sensitivity
The change in *mass balance* due to a change in a climatic variable such as air temperature or precipitation.

Sensitivities to temperature and precipitation are often expressed as changes in response to a 1 K warming or a 10% precipitation increase, resulting in a negative sensitivity to temperature and a positive sensitivity to precipitation.

Sensitivities are generally derived from mass-balance modelling, that is, from the difference in mass balance between model runs with and without climate perturbation, but they have also been estimated from mass-balance and climate observations.

Mass balance does not vary linearly with the climate in general. That is, dB/dT and dB/dP are not constant, but may be assumed constant as a good approximation for small changes of the climatic variable.

The "dynamic" mass-balance sensitivity changes as the extent and *area-altitude distribution* of the glacier or glacierized region evolve. In contrast, the "static" sensitivity neglects these geometric changes, although it may still vary with, for example, components of the surface *energy balance*.

Mass-balance units

The dimension of *mass balance* is [M] (mass). The dimension of the *mass-balance rate* is [M T^{-1}] (mass per unit time). When the mass balance is presented per unit *area*, it is called *specific mass balance* and its dimension becomes [M L^{-2}], while the dimension of the mass-balance rate becomes [M L^{-2} T^{-1}]. When *water-equivalent* units are adopted (see below), the dimension becomes [L^3] or [L^3 T^{-1}], the corresponding specific units being [L] or [L T^{-1}].

The unit for expressing mass or change of mass numerically is the kilogram (kg). When more convenient the petagram (Pg) or gigatonne (Gt; 1 Gt = 1 Pg = 10^{12} kg) can be substituted. When mass balance is expressed per unit area, its unit is kg m^{-2}.

The unit kg m^{-2} is usually replaced by the millimetre *water equivalent*, mm w.e. This substitution is convenient because 1 kg of liquid water, of *density* 1000 kg m^{-3}, has a thickness of exactly 1 mm when distributed uniformly over 1 m^2. The units kg m^{-2} and mm w.e. are therefore numerically identical. More formally, the metre water equivalent (m w.e.) is an extension of the SI that is obtained by dividing a particular mass per unit area by the density of water, ρ_w:

$$1 \text{ m w.e.} = 1000 \text{ kg m}^{-2} / \rho_w .$$

Because of the risk of confusion with the metre *ice equivalent*, or with ordinary lengths, it is important that the qualifier “w.e.” not be omitted.

Mass balances can also be stated in m^3 w.e. (1 m^3 w.e. = 1 m w.e. distributed uniformly over 1 m^2) or km^3 w.e. Note that 1 km^3 w.e. is numerically identical with 1 Gt.

For the mass-balance rate, appropriate units are kg a^{-1} or kg m^{-2} a^{-1} (or m^3 w.e. a^{-1} or mm w.e. a^{-1}) when the time span is an integer multiple of 1 year. Over shorter intervals the unit of time should be the second or the day.

Mass units (kg or m^3 w.e.) are useful for hydrological and oceanographic purposes, while specific mass units (kg m^{-2}, mm w.e., m w.e.) are needed when comparing the mass balances of different glaciers and for studying glacier-climate relations.

To convert, with sufficient accuracy for many purposes, to the frequently needed *sea-level equivalent* (SLE), mass balance in kg m^{-2} is first converted to kg by multiplying by the area of the glacier, and then divided by the product of ρ_w and the area of the ocean (362.5 × 10^{12} m^2; *Table B5*). The sign of SLE is opposite to that of glacier mass balance, a loss from the ice being deemed to be an equivalent gain for the ocean.

Mass-balance year

The time span, equal or approximately equal in duration to one calendar *year*, to which the *annual mass balance* in any *time system* refers.

In the *stratigraphic system* the annual mass balance refers to the period between formation of two successive mass-balance minima in the sequence of annual cycles of mass growth and decline. These minima are usually reached at different times in successive years, and the duration of the mass-balance year may therefore vary strongly. *Point mass balances* can be determined unambiguously in the stratigraphic system, but *glacier-wide* determinations require the assumption that the *diachronous* character of the *summer surface* can be neglected.

In the *fixed-date system* the first day of the mass-balance year is always on the same calendar date, which is typically chosen to coincide with the start of the local *hydrological year*, for example 1 October in the mid-latitudes of the Northern Hemisphere, or sometimes with the average date of minimum annual mass. The mass-balance year is 365 (or 366) days long.

In the *floating-date system* the mass-balance year is defined by the calendar dates of the two successive surveys, which may vary from year to year and may or may not be 365 (or 366) days apart.

Formerly (Anonymous 1969; *Appendix A*) the mass-balance year was defined only in the *stratigraphic system*.

Mass budget

A synonym of *mass balance*.

Mass budget is a more correct term than mass balance, but is used less often. While *water balance* and *energy balance* refer to equations in which the change in storage is only one of the terms, common glaciological usage equates mass balance with the change in storage (in other words, with the mass *im*balance). It is unlikely that this usage will change.

Mass conservation
See *conservation of mass*.

Mass flux
1. The horizontal rate of flow of mass through a plane normal to the direction of the horizontal velocity vector.

Depending on the context, the flux may be through an element of *area* at a given position in the vertical plane, through a unit of width extending from the glacier bed to the surface, or through an entire glacier cross-section.

2. The vertical rate of *flow* of mass at the *glacier* surface or bed.

In sense 2, the flux at the surface is equal to the sum of *surface accumulation* and *surface ablation*, or in other words to the *surface mass balance*. Equivalently the flux at the bed is equal to the *basal mass balance*.

Mass turnover
The renewal of the mass of a *glacier* by *mass-balance* processes.

Mass turnover is measured most usefully by the mass-turnover time, which is the mass of the glacier divided by the *mass-balance amplitude*, with the latter expressed as an annual rate. Mass-turnover times range from several decades for *glacierets* to tens of thousands of years for *ice sheets*.

See *response time*.

Measurement year
The time span, equal or approximately equal in duration to one calendar *year*, between two surveys constituting a measurement of *annual mass balance* in any *time system*.

Formerly (Anonymous 1969; *Appendix A*) the measurement year was defined only in the *fixed-date system*.

Melange
A floating agglomerate of icebergs and larger fragments of *sea ice* that forms when a *glacier* calves icebergs more quickly than they melt or are evacuated by wind or ocean currents.

The melange may be strong enough to retard the accelerated discharge of grounded ice that would otherwise be expected (from the elimination of back-stress) after a *calving* event.

The word, originally French, means “mixture”. In tectonics and petrology it refers to a body of deformed rocks characterized by the inclusion of native and exotic blocks in a pervasively sheared, commonly fine-grained, matrix.

Melt
1. (*v.*) To undergo *fusion*, or (when used transitively) to cause to undergo fusion.

2. (*n.*) The liquid produced by the process of *fusion* (see *meltwater)*.

Melt extent
The spatial extent (dimension [L^2]) of *melting* on the surface of the *glacier*.

The melt extent can be measured by *microwave remote sensing* of the *brightness temperature* with a *passive-microwave sensor*, or equivalent analysis of *radar* or *scatterometer* imagery. The spatial resolution of passive-microwave radiometers and scatterometers being low at present (several km or coarser), the method is mainly exploited on *ice sheets* and large *ice caps*.

Melting
The process by which a solid changes phase into a liquid; a synonym of *fusion*. See *ablation*.

Melting index
A measure, with dimension [L^2 T] and units such as km^2 d, of the spatiotemporal extent of surface *melting*.

The melting index, usually obtained by *remote sensing*, is the integral over a defined region and time span of the time-varying melt extent, and is approximated in practice as a regional sum of products at local scale (such as that of the pixels of a *passive-microwave sensor*) of the *melt extent* and the duration of melting. The accuracy of the duration is principally determined by the frequency of imaging, which tends to be high at high latitudes because most orbital sensors are in polar orbits. The melting index is a valuable proxy indicator in the absence of more direct measures of *melting*.

The melting index is sometimes called the melt index or the surface-melt index, and is formulated in slightly different ways by different authors.

Melting point
The temperature, T_m = 273.15 K = 0 ºC, at which *ice* undergoes *fusion* when the pressure is equal to a standard pressure of 101 325 Pa and the *latent heat of fusion* is made available to fuel the change of phase. *Freezing point* is a synonym.

Strictly the melting point is the (temperature, pressure) pair of numbers, but the variation of pressure at the surface of the *glacier* has negligible effect and the term is applied to the temperature alone.

See *pressure-melting point*, *ice point*.

Meltwater
The liquid resulting from *melting* of *ice*, *firn* or *snow*.

Meltwater discharge
See article *Meltwater discharge* under *Discharge*.

Meltwater runoff
See article *Meltwater runoff* under *Runoff*.

Microwave remote sensing
Remote sensing with an *active-microwave sensor* or a *passive-microwave sensor*.

At frequencies between about 1 GHz and 40 GHz, microwaves are capable of penetrating clouds, and orbiting sensors can measure surface properties in all atmospheric conditions. Corrections must be made for scattering resulting from atmospheric and ionospheric variations. At frequencies below 1 GHz, the depth of penetration into the solid earth becomes great enough to permit active-microwave imaging of the subsurface from the surface or from aircraft.

The terms microwave and *radar* are often used interchangeably. This is mainly because the boundary between the lower-frequency radio and higher-frequency microwave regions of the electromagnetic spectrum is fixed differently, between 0.3 and 300 GHz (wavelengths of 1 m to 1 mm), by different authorities.

Active-microwave sensor
A sensor transmitting radiation and receiving reflections in the radio or microwave regions of the electromagnetic spectrum; in glaciological applications, either an imaging *radar* or a radar configured as a *scatterometer* or *radar altimeter*.

Frequencies from about 1–2 MHz up to about 15 GHz have various applications in the study of *mass balance* with active-microwave sensors. See *ground-penetrating radar*, *InSAR*, *Shuttle Radar Topography Mission*.

Passive-microwave sensor
A radiometer sensing the emission of radiation at microwave frequencies from a medium.

Frequencies from about 5 GHz up to 37 GHz are used in the study of quantities related to *mass balance* with passive-microwave sensors. The intensity of emission depends on the temperature of the medium and its emissivity. See *brightness temperature*.

Microwave radiometers in orbit have resolutions of a few to a few tens of kilometres, so that they are best suited to monitoring of extensive ice and snow covers. All are in polar, sun-synchronous orbits, and offer daily near-global coverage. At high latitudes, coverage is available at least twice daily, that is, from an ascending (south to north) pass, typically in the afternoon or evening, and a descending (north to south) pass, typically in the morning.

SMMR, the Scanning Multi-channel Microwave Radiometer, operated from 1978 to 1987. SSM/I, the Special Sensor Microwave Imager, was first launched in 1987 and has operated on several different satellites since. AMSR-E, the Advanced Microwave Scanning Radiometer for the Earth Observing System, has operated since 2002.

In snow hydrology, passive-microwave radiometers are operational tools for the estimation of snow water equivalent (“SWE”).

Mid-range altitude

The average of the minimum *altitude* and maximum altitude of the *glacier*.

The mid-range altitude is of interest in itself as a measure of the vertical location of the glacier, but has also been shown to be (to within the accuracy of measurements) an unbiased estimator of the *balanced-budget ELA*. See *glaciation level*.

Moulin

A deep shaft, nearly vertical and of roughly circular cross-section, formed when surface *meltwater* enlarges a crack in the *ice* by transferring kinetic and thermal energy to its walls.

Moulins connect to the *englacial* drainage network, facilitating transfer of surface meltwater to the bed. The meltwater resulting from enlargement of the moulin is an instance of *internal ablation*. Moulins may play a significant role in supplying lubricant to the bed.

The word is French for mill, referring to the swirling motion of the water as it descends the shaft.

Mountain apron glacier

A small *glacier* of irregular outline, elongate along slope, in mountainous terrain.

Mountain glacier

1. A *glacier* that is confined by surrounding mountain terrain, also called an alpine glacier.

2. A glacier in mountainous terrain that is a *cirque glacier*, a *niche glacier*, a *crater glacier*, or a *mountain apron glacier*. See also *valley glacier*.

Sense 2 is that in which the term is used in the *World Glacier Inventory*, but the more general sense 1 is also widely used.

Multi-annual (*adj*.)

Spanning more than one year, but referring to duration, e.g. of a measurement, rather than to persistence; see *perennial*.

N

National Snow and Ice Data Center (NSIDC)
An organization that manages and distributes data and supports research about all aspects of the cryosphere and, notably for studies of *glacier fluctuations*, houses the databases of the *Global Land Ice Measurements from Space* initiative and the *World Glacier Inventory*.

NSIDC is part of the Cooperative Institute for Research in Environmental Sciences at the University of Colorado, Boulder, U.S.A., and is the site of one of the *World Data Centers* for Glaciology.

Net (*adj*.)
Descriptive of a quantity that is the final result of a series of additions and subtractions, especially, in the context of *mass balance*, of mass-balance components.

Formerly (Anonymous 1969; *Appendix A*) net mass balance was a technical term in the *stratigraphic system*, to be distinguished from “annual mass balance” in the *fixed-date system*, but this usage is no longer recommended (see article *Annual mass balance* under *mass balance*).

Net ablation
See article *Net ablation* under *mass balance*.

Net accumulation
See article *Net accumulation* under *mass balance*.

Net mass balance
See article *Net mass balance* under *mass balance*.

Névé
1. A synonym of *firn*, of French origin, now little used.

2. A little-used synonym of *snowfield*, or sometimes of *accumulation zone*.

Niche glacier
A small *glacier* in a gully or depression, elongate downslope.

Nunatak
A mountain, or any exposed ground, projecting from and surrounded by *glacier ice*.

The word is a 19th-century borrowing from the Greenlandic language.

O

Ogive
Arcuate bands or waves, convex downglacier, that develop in an *icefall*.

Alternating light and dark bands are called banded ogives or Forbes bands. Each pair of bands, that is, one crest (light) and one trough (dark), represents a year's movement through the icefall. It can be shown that, to yield visible banding, *ice* must flow through the icefall in a time shorter than the duration of the *ablation season* or *accumulation season*.

James Forbes was the first to describe ogives, in 1843.

Orographic snowline
See *snowline*.

Outlet glacier
A *glacier*, usually of *valley-glacier* form, that drains an *ice sheet*, *icefield* or *ice cap*.

In the *accumulation zone* the *glacier outline* may not be well-defined because of the subdued relief.

Outline
See *glacier outline*.

P

Passive-microwave sensor
See article *Passive-microwave sensor* under *Microwave remote sensing*.

Penitente
A spike-like irregularity of the *glacier* surface, significantly taller than wide and on occasion reaching heights as great as a few metres.

Penitentes are an extreme form of the metre-scale roughness which must be accounted for in all *ablation* measurements using *stakes*. They are usually found together in large numbers when low temperature and intense solar radiation favour ablation by *sublimation* and the consequent amplification of small surface irregularities.

The word is Spanish and is generally not anglicized; the final *e* is retained (and pronounced).

Percolation
The movement of a liquid such as water through the void spaces of a permeable solid such as *snow* or *firn*, the rate of movement being governed by the *porosity* and liquid content of the solid, the geometric attributes of the pores, including their diameter and tortuosity, and the response of the pore walls to wetting. See *infiltration*.

Percolation zone
The part of the *glacier* where water from surface *melting* or *rainfall* percolates into the subsurface; see *percolation*, *zone*.

In the upper percolation zone, above the *wet-snow line*, water percolates only into the *snow*. In the lower percolation zone, also called the *wet-snow zone*, water percolates into the *firn* below the *summer surface*. The lower percolation zone contains the *slush zone*.

If, having percolated, the water refreezes, it warms its surroundings by releasing latent heat. If it refreezes in the firn, the result is *internal accumulation*. If it refreezes as a layer immediately above the *summer surface*, it forms *superimposed ice*. If this superimposed ice becomes exposed by continued surface *ablation*, the resulting *superimposed ice zone* is conventionally regarded as distinct from the percolation zone.

Perennial (*adj*.)
Persisting for an indefinite time longer than one *year*.

Perennial refers to the persistence of an object rather than, e.g., the duration of a measurement. See *multi-annual*.

Permanent Service on the Fluctuations of Glaciers (PSFG)
The immediate precursor, established in 1962, of the present-day *World Glacier Monitoring Service*.

The name of the Permanent Service on the Fluctuations of Glaciers survives in the form of the “PSFG number” which is assigned to *glaciers* in the *Fluctuations of Glaciers* database of the World Glacier Monitoring Service.

Permittivity
See *relative dielectric constant*.

Photogrammetry
Quantitative analysis of photographs, usually vertical aerial photographs but also aerial oblique or terrestrial oblique photographs, to determine the coordinates in a specified coordinate system of features visible in the photographs.

Photogrammetry, or “measurement of photographs”, is now understood to embrace measurements of images in general, including negative images on film, diapositives (positive images on film) and digital images, and images obtained by sensors on orbiting satellites as well as by airborne sensors.

Piedmont glacier
A *glacier* the lower *tongue* of which is fan-shaped and significantly wider than the upper tongue.
The lateral expansion of a piedmont glacier is markedly greater than that of an *expanded-foot glacier*. In some classifications piedmont glaciers are distinguished from expanded-foot glaciers by requiring that a piedmont glacier have two or more coalescing tributaries. See the related but not synonymous *ice piedmont*.

Point mass balance
See article *Point mass balance* under *Mass balance*.

Polar glacier
An obsolete term, due to Ahlmann (1935), originally in the form “high-polar glacier”, describing a *glacier* with an *accumulation zone* in which there is little or no *melting* and the temperature is below the *freezing point* to depths of at least 200 m. See *cold glacier*, *polythermal glacier* for rough equivalents in modern terminology.

Polythermal glacier
A *glacier* containing some *cold ice* and some *temperate ice*.
Classically, as first described, a polythermal glacier has a basal layer of *temperate ice* overlain by a layer of *cold ice* (panel a in Figure 9), above which there may be a surface layer up to about 10–15 m thick that warms to the *melting point* seasonally. See *cold glacier*, *temperate glacier*.

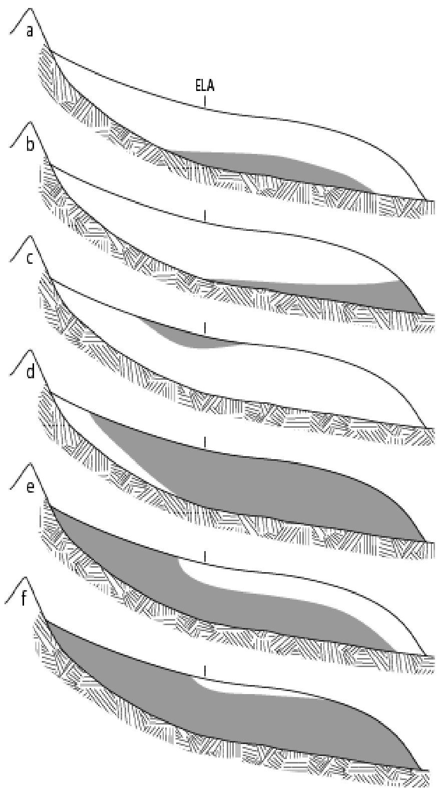

Figure 9. Schematic view of different polythermal structures encountered in glaciers. The temperate ice is shaded grey and the cold ice white (Pettersson, 2004).

Different types of polythermal glacier are found in different regions depending on the climate and the glacier geometry (Figure 9).

Porosity
The fraction of any given volume not occupied by solid matter, and therefore available for occupation by fluids such as air and water.
In *snow* and *firn* the porosity is nearly equal to $1 - \rho/\rho_i$, where ρ is the *density* of the dry snow or firn and ρ_i the density of *ice*.

Positive degree-day

The name of a derived unit, the K d, equal in magnitude to a 1 K excess of temperature above the *melting point* (273.15 K, 0 ºC) averaged over a period of 1 day.

See *positive degree-day sum.*

Positive degree-day sum

The integral, in K d (kelvin days), of the excess of temperature T above the *melting point* T_m (273.15 K, 0 ºC) over a span of time:

$$\varphi = \int_{t_1}^{t_2} \max[0, T(t) - T_m]\, dt \ ,$$

where the span extends from t_1 to t_2 and t is measured in days. In practical work, the temperature is available over the span in degrees Celsius as a series of averages over some time step Δt, or as instantaneous values at intervals Δt, of near-surface air temperature T_i (i=1,n), and the expression becomes:

$$\varphi = \Delta t \sum_{i=1}^{n} \max(0, T_i) \ ,$$

Δt being expressed in days.

The T_i are often mean daily temperatures, in which case Δt = 1, but positive degree-day sums can also be accumulated over intervals such as an hour or a month. The latter have also been referred to as positive degree-month sums. The quantity “positive degree-day sum” is often abbreviated PDD and shortened to “positive degree-days”, which can lead to confusion because the latter is the name of the unit in which the former is measured.

At temperatures near T_m, the positive degree-day sum becomes inaccurate as the time step Δt becomes large, each mean temperature T_i representing a distribution of instantaneous temperatures of which some are opposite in sign to T_i. Mean temperatures slightly below T_m are wrongly estimated to contribute nothing to the positive degree-day sum while mean temperatures slightly above T_m contribute too little.

Positive degree-day models, in which a *degree-day factor* represents the proportionality between *surface ablation* and the positive degree-day sum, are a leading form of *temperature-index model*.

Precipitation

Liquid or solid products of the *condensation* of water vapour that fall from clouds or are deposited from the air onto the surface.

Pressure-melting point

The temperature at which *ice* and water are in thermodynamic equilibrium at a given pressure.

The pressure-melting temperature is 273.15 K when the pressure is 101 325 Pa, changing, when the water is saturated with air, at –9.8 × 10^{-8} K Pa^{-1} or, in ice of *density* 900 kg m^{-3}, about –0.86 × 10^{-3} K m^{-1}. This means, for example, that beneath 4000 m of such ice the pressure-melting temperature is 269.75 K. For pure water and ice the corresponding rates are –7.4 × 10^{-8} K Pa^{-1} and about –0.65 × 10^{-3} K m^{-1} (see *Table B3*).

Factors other than pressure can alter the melting point; see *temperate ice*.

The pair (273.15 K, 101 325 Pa) is known in thermodynamics as the *ice point*. The specified pressure is the sea-level pressure of the standard atmosphere defined by the International Civil Aeronautical Organization (1993). See also *triple point*.

Proglacial

Pertaining to an object in physical contact with, or close to, the *glacier margin*.

R

Radar
A method of, and by extension an instrument for, detecting and locating objects by sensing radiation transmitted by the instrument and reflected from the objects. See *active-microwave sensor*.

The depth to which a radio or microwave signal is likely to penetrate *ice* or *snow* before being absorbed or scattered depends on the frequency (or equivalently the wavelength). In the case of scattering, the penetration depth also depends on the size of any inhomogeneities in the ice; those smaller than the wavelength of the signal cause less scattering. In glaciology, the lower frequencies (about 2 to several hundred MHz) are the basis for *ground-penetrating radar* (see also *radar method*), while frequencies of 1 to 15 GHz, at which effective penetration depths can still reach some metres, are used in *radar altimeters* mounted on aircraft or satellites (see also *InSAR*, *Shuttle Radar Topography Mission*).

Radar is an acronym standing for radio detection and ranging.

Radar altimeter
An instrument for *altimetry* that transmits and receives pulses of microwave radiation.

Satellite radar altimeters (including ERS-1 and 2, Envisat and others) typically operate in the Ku band (13.5 GHz; 22 mm wavelength) and were designed primarily for oceanographic monitoring. Because of their relatively large footprint (several km), they are best suited for measuring *elevations* of gently-sloping regions of the *ice sheets*. Steep or undulating terrain produces complex waveforms and difficulties in achieving accurate estimates of *range* (i.e. distance). Surface and volume scattering also affect the radar pulse and create uncertainty in the effective depth of the reflecting horizon. Surface dielectric properties and roughness that cause scattering are time-varying and introduce errors in calculations of elevation change.

Recent radar altimeters use synthetic aperture processing (see *InSAR*) that increases resolution and decreases slope errors relative to earlier radar altimeters. The *Shuttle Radar Topography Mission (SRTM)* used a C-band radar (5.6 GHz; 54 mm wavelength) and synthetic aperture processing to obtain an accurate map of surface elevations with near-global coverage. CryoSat-2, launched in April 2010, will also use InSAR to map *glaciers* and ice sheets.

Radar altimetry
See *radar altimeter*.

Radar method
A method of determining *net accumulation* by interpreting a subsurface horizon detected by *ground-penetrating radar*, either from the surface or remotely, as an *isochrone*.

The thickness of the layer between the isochrone and the surface, multiplied by its *density*, is the net accumulation since the date of the isochrone. With a suitable choice of radar frequency, the isochrone may be as recent as the *summer surface*, allowing the measurement of *snow depth*. The dates of older isochrones are obtained by *ice-core stratigraphy* in one or more nearby boreholes, from which the density profile can also be obtained. In creating the depth-age scale from which the date is derived, changes of layer thickness caused by ice *flow* are considered. The density profile enables conversion to *water-equivalent* or *ice-equivalent* units.

Radio-echo sounding
See *radar*, *ground-penetrating radar*.

Rain
Precipitation other than dew that falls from the air as liquid.

Rainfall
The amount of *rain* that falls during a stated period.

Rammsonde
A device for measuring the penetration hardness (also called the ram resistance) of *snow* or *firn*, a quantity formerly believed to be a reliable guide to the *density*, and still commonly used in assessments of the risk of snow *avalanches*.

Range
1. (*n*.) The distance to a target such as a *glacier* surface from an active sensor such as a *sonic ranger* or a *radar*.

2. (*n*.) The cross-track coordinate in the coordinate frame of an airborne or orbiting radar. See *azimuth*.

3. (*v*.) Of an active sensor, to measure the distance to, that is, to “range to”, a target.

Senses 2 and 3 have evolved from sense 1, which originated in gunnery but has become common in several branches of *remote sensing*.

Reaction time
The time required for a change in forcing of *mass balance* to result in an observable response of the geometry, particularly the length, of the *glacier*.

The reaction time is not a physical property of the glacier. Estimates of the reaction time depend on, among other things, the precision of observation and the extent to which the glacier is out of equilibrium. See *response time*.

Reanalysis
Re-examination and possible modification of a series of measurements of *mass balance* in the light of methods or data not available when the measurements were made.

The modifications, in addition to the correction of processing and other errors, often include correction of biases identified by comparison of annual measurements by the *glaciological method* with one or more multi-annual measurements by *geodetic methods* covering the same time span. These corrections are made only when one or other of the two types of measurement can be shown clearly to be more accurate than the other. The uncorrected measurements should remain available after the corrections have been made and published.

The glaciological meaning of reanalysis is only roughly comparable to its meaning in meteorology, where a reanalysis is a recalculation of variations of the state of the atmosphere over periods of decades using a uniform system of data assimilation and analysis.

See *homogenization*.

Reconstructed glacier
A synonym of *regenerated glacier*.

Recrystallization
1. The metamorphosis, without *melting* but not necessarily without advection in the vapour phase, of an assemblage of grains of *snow* and old crystals of *ice* to a new assemblage of crystals of ice, generally resulting in changes of mean crystal size and orientation (fabric) and, of most significance for *mass-balance* purposes, an increase of *density*.

See *congelation*, *infiltration ice, glacier*.

2. The formation of a new assemblage of crystals from an old assemblage.

Sense 1 is the meaning of the term in studies of the *densification* of *snow*, while sense 2 is its everyday meaning.

Recrystallization zone
In the Russian-language literature, where it is sometimes also referred to as the “snow zone”, a synonym of *dry-snow zone*. See *zone*.

Recrystallization-regelation zone
In the Russian-language literature, where it is sometimes also referred to as the “snow-firn zone”, a term for the upper *percolation zone*. See *zone*.

In this context the Russian word “regelatsiya” refers to *refreezing*, not to *regelation*.

Reference glacier
In the monitoring strategy of the *Global Terrestrial Network for Glaciers*, a *glacier* with a long-term, continuous, continuing programme of *mass-balance* observations.

See *benchmark glacier*, *tier*.

Reference-surface balance
The *glacier-wide mass balance* that would have been observed if the *glacier* surface topography had not changed since a reference date.

The time-invariant surface is called the “reference surface”, and is defined at some convenient time within a mass-balance programme, often at the start (Elsberg et al. 2001). The reference-surface balance is obtained when point measurements are extrapolated from their actual altitude to the *altitude* of the reference surface at the same horizontal position, and then extrapolated over the reference area. The reference surface is likely to differ from the actual surface in both *area* and *area-altitude distribution*.

Differences in area and area-altitude distribution feed back on the magnitude of glacier response to climate. The reference-surface balance does not incorporate any of these feedback effects and is therefore more closely correlated to variations in climate than is the *conventional balance*.

Refreezing
The *freezing* of *meltwater* generated at the *glacier* surface, or of *rain*, that percolates to some depth at which the temperature is below the *freezing point*.

Refreezing below the *summer surface* represents *internal accumulation*. Percolating water may also refreeze at the base of *snow* overlying impermeable *glacier ice*, in which case it is called *superimposed ice*. See *zone*.

The release of *latent heat* heats the layer within which the water freezes.

Regelation
The *freezing* of *meltwater* due to a change in pressure alone.

The term is often used for “pressure melting and regelation”. Regelation happens because the *pressure-melting point* of *ice* varies inversely with pressure. Water in equilibrium with ice will freeze, releasing the *latent heat of fusion*, 333.5 kJ kg^{-1}, if there is a decrease of pressure, as on the downglacier face of a bump in the bed of a *temperate glacier*. Ice in equilibrium with water will melt if there is an increase of pressure, as on the upglacier face of the bump. However, the latent heat of fusion must be supplied for this change of phase. A natural source is the latent heat released by regelation on the downglacier face. If pressure melting and regelation are unequal, there will be a contribution to *basal ablation* or *basal accumulation*.

Smaller bumps are more favourable to pressure melting and regelation than larger ones.

The Russian word “regelatsiya” refers to *refreezing* rather than to regelation.

Regenerated glacier
The lower part of an *interrupted glacier*.

Regional snowline
See article *Regional snowline* under *Snowline*.

Relative dielectric constant
The ratio ε_r of the electric displacement (electric flux per unit area) at any point in a dielectric (that is, non-conducting) medium to the displacement that an identical electric field would produce in a vacuum, measured at the same point.

The relative dielectric constant, which is not in fact a constant and is more properly called the relative permittivity, is a complex number. Its imaginary part, ε_r'', is sensitive to attenuation of microwaves by absorption and other phenomena; it is sometimes called the dielectric loss. *Ice*, however, is generally assumed to be a low-loss medium, and its dielectric loss is approximated as $\varepsilon_r'' = 0$. The real part of ε_r, denoted ε_r', depends on frequency and temperature, and more subtly on variations in crystalline fabric and the presence of impurities. It determines the geometry of wave propagation, including refraction at and reflection from interfaces between layers within the medium.

See *ground-penetrating radar*.

Remote sensing
Measurement of surface properties with a sensor distant from the surface, such as on an airplane or satellite, or of subsurface properties with a sensor on or distant from the surface, either with a signal emitted by the sensor (active remote sensing) or a signal emitted or reflected by the surface (passive remote sensing).

See *active-microwave sensor*, *feature tracking*, *ground-penetrating radar*, *InSAR*, *laser altimeter*, *microwave remote sensing*, *passive-microwave sensor*, *photogrammetry*, *radar altimeter*, *scatterometer*, *Shuttle Radar Topography Mission*.

Response time
The *e*-folding time scale for the transition of a *glacier*, following a step change in *mass balance*, from one *steady state* to another.

Response times have been formulated for various attributes of the glacier such as volume and length. They can be confused easily with the *mass-turnover* time; the *reaction time*; and the *growth time*.

The volumetric response time is the most commonly seen formulation. Here the glacier changes from an initial volume V_1 to a later volume V_2, and the response time is the time needed for the volume to change by $(V_2 - V_1)(1 - e^{-1})$, where $e = 2.71828...$ is the base of natural logarithms. The response time is much shorter than the time required to attain volume V_2. Indeed, in this formulation the time to attain volume V_2 is infinite. The change between state 1 and state 2 is assumed to be “small”.

The response time for volume is somewhat shorter than that for length, that is, for the length to change by $(L_2 - L_1)(1 - e^{-1})$.

The response time is an idealization. The essence of the idea is that the glacier “remembers” its earlier steady state because it adjusts its size and shape by *flow*. The volume response time τ is often estimated with an expression due to Jóhannesson et al. (1989)

$$\tau = H' / (-\dot{b}_T)$$

in which H' is a representative glacier thickness and $\dot{b}_T$ (< 0) a representative mass-balance rate, in ice-equivalent units, in the vicinity of the *terminus*. H' is somewhat larger than the mean ice thickness, and approaches the maximum thickness where the bed geometry is simple (no troughs). These two variables are rather easy to estimate but should be considered as scales rather than exact quantities. The expression has been used widely, but not always with the caution due to its generalized nature.

Resublimation
The process by which a vapour changes phase directly into a solid; *deposition* and desublimation are synonyms. See *latent heat of sublimation*.

Retreat
Decrease of the length of a *flowline*, measured from a fixed point.

In practice, when the retreat is of a land-terminating glacier terminus, the fixed point is usually downglacier from the terminus, and the quantity reported is the amount of retreat rather than the length itself.

Advance is the opposite of retreat, that is, advance of the terminus.

Rime
A solid surface deposit formed by the rapid *freezing* of supercooled water, distinguished from *glaze* by being less dense (Figure 10). See also *hoar*.

Figure 10. Rime, or possibly *hoar*, recently dislodged from an accumulation stake by solar heating (foreground) and still coating meteorological instruments (background), on Vestfonna, Svalbard.

.

Rock glacier
A mass of rock fragments and finer material in a matrix of *ice*, showing evidence of past or present *flow*.

Runoff
1. *Discharge* of water divided by the *area* of the drainage basin contributing water to the measurement cross-section, expressed in *specific* units such as mm w.e. d^{-1} or kg m^{-2} s^{-1}.

2. The flux of water leaving the *glacier*.

Sense 2 is common in *mass-balance* studies, especially in studies of *ice-sheet* mass balance.

See *mass-balance units*; it is useful to have one word for total flux and a different word for specific flux, so the distinction between discharge and runoff is to be encouraged. Runoff includes *meltwater discharge* but also water from other sources than *melt*, such as *rainfall*.

Meltwater runoff
The component of runoff (in sense 2) produced by *melting* of *glacier ice*, *firn* or *snow* that is removed in surface, *englacial* or *subglacial* flows.

Meltwater runoff is not the same as *surface ablation* by melting, because surface meltwater may refreeze in the *glacier* (see *refreezing, internal accumulation*), and part of the meltwater runoff may originate from *basal ablation* or *internal ablation*. Nor is it usually the same as the total runoff, which is likely to include contributions from unglacierized parts of the drainage basin, and may include a contribution from *rainfall* on the glacier.

Runoff limit
The *altitude* above which all *rainfall* and surface *melt*, if any, *refreezes* in the *snow* or *firn*, and below which part or all of it runs off the *glacier*. See *zone*.

S

Sastrugi
A variant spelling of *zastrugi*.

Scatterometer
A *radar* designed to measure microwave backscattering, quantified as the scattering coefficient or normalized radar cross-section, σ^0, from natural media.

Exposed *glacier ice* in the *ablation zone* lacks a distinctive *mass-balance*-related signature at microwave wavelengths. In the *percolation zone*, subsurface ice lenses are strong scatterers, but there is a sharp reduction in backscattering when *meltwater* appears at the surface. When wet, the surface becomes a more nearly specular (forward) reflector and appears "radar-dark" instead of "radar-bright". In the *dry snow zone* radar returns are unaffected by liquid water, which is absent, and the scattering coefficient contains information on *snow* grain size and possibly on the *accumulation* rate.

Scatterometers have relatively poor spatial resolution (several to some tens of kilometres), which can be improved by temporal averaging, but they compensate by offering wide and frequent coverage. SeaWinds, on the polar-orbiting QuikSCAT satellite (1999-2009) has been a productive scatterometer. Intended for the measurement of ocean-surface wind speeds, it has also proved valuable for measuring the extent and duration of *melting* on *ice caps* and *ice sheets*. See also *brightness temperature*.

Sea ice
Ice formed at the sea surface by the *freezing* of sea water.

Except where it forms ridges, sea ice is up to a few metres thick, in which respect it differs from *shelf ice*. See also *marine ice*.

Sea-level equivalent
The change in mean global sea level that would result if a mass of water were added to or removed from the ocean; in glaciology, the mass added or removed is usually equal respectively to the mass removed from or added to a *glacier*.

Sea-level equivalent is usually abbreviated as SLE, and customary units are m SLE (for large masses), mm SLE or mm a^{-1} SLE. The sign of glacier *mass balance* is opposite to that of SLE, a loss from the glacier being deemed to be an equivalent gain for the ocean.

SLE is often estimated by dividing the mass by the product of the *density* of (fresh) water, ρ_w = 1000 kg m^{-3}, and the area of the ocean, 362.5×10^{12} m^2, with a change of sign when necessary.

More accurate estimates of SLE must account for shoreline and *grounding-line* migration, altering ocean area; isostatic adjustment of the land surface and ocean floor to changing patterns of loading by water and ice; and flow of *meltwater* into aquifers and enclosed basins rather than to the ocean. It is also necessary to differentiate between floating and grounded *ice*. The SLE of grounded ice is $h\,(\rho_i / \rho_w) - d$, where h is the total thickness of the ice, ρ_i its density, and d the depth (possibly zero) of the sea water in which it stands. The subtraction of d accounts for the fact that some of the grounded ice is already displacing sea water. Apart from a small effect on sea water density due to reduction of salinity upon melting, any ice body floating in the sea has $d \geq h\,(\rho_i / \rho_w)$, and therefore its SLE is zero.

Seasonal sensitivity characteristic (SSC)
A set of sensitivities, $C_{T,k}$ (in m w.e. K^{-1}) and $C_{P,k}$ (in m w.e.), of *annual mass balance B* to changes in monthly mean temperature T_k and monthly precipitation P_k, , where k = 1, ..., 12 is the month index and *precipitation* is normalized by $P_{\mathrm{ref},k}$, the monthly precipitation averaged over a reference period.

The SSC, which is estimated either from observations or from model calculations, was introduced by Oerlemans and Reichert (2000). It consists of two sets of 12 numbers each:

$$C_{T,k} = \frac{\partial B}{\partial T_k} \quad ; \quad C_{P,k} = \frac{\partial B}{\partial (P_k / P_{\mathrm{ref},k})}$$

There is no reason other than convenience for describing seasonal sensitivity with a resolution of 1 month.

Serac
A tower or block of *glacier ice* bounded by intersecting *crevasses*.
The term is of French origin.

Shelf ice
Ice forming part of an *ice shelf*, whether *glacier ice*, *marine ice* or ice originating from *accumulation* on the surface of the ice shelf.

Shuttle Radar Topography Mission (SRTM)
A flight of the space shuttle Endeavour in February 2000 which yielded an interferometric *digital elevation model*, with ~90 m horizontal resolution (~30 m for the conterminous United States), of the Earth's land surfaces roughly between latitudes 54° S and 60° N. See *InSAR*.
The effective penetration depth of the *radar* pulse into *snow* can be of the order of metres at the 5.6 GHz frequency of the shuttle radar. This, and the boreal mid-winter date of the mission, are leading contributors to uncertainty in SRTM data for *mass-balance* applications.

Slush
Snow or *firn* mixed with an amount of liquid water equalling or exceeding that required to fill the voids; soaked snow.
Slush *avalanches* ("slushflows") can be a significant means of downslope transfer of mass, and hence of accelerating *ablation* by *melting* because of the increase of temperature with decreasing *altitude*.

Slush limit
A synonym of *runoff limit*. See *zone*.

Slush zone
The part of the *glacier* between the *snowline* and the *runoff limit*, that is, the lowest part of the *percolation zone*. See *zone*.

Snow
1. *Solid precipitation* in the form of *ice* crystals, chiefly in complex branched hexagonal form and often agglomerated into snowflakes; or an accumulation of the same on the Earth's surface.

2. Solid precipitation that has accumulated on the *summer surface* on a *glacier* and that transforms to *firn* at the end of the *mass-balance year*. See *zone*.
In this sense, which prevails almost universally in the study of *mass balance*, snow may contain *ice* in the form of lenses or pipes which are the result of *refreezing* of *meltwater*.

3. An accumulation of solid precipitation on a glacier that has not yet attained a *density* through compaction sufficient to restrict the circulation of air and water significantly.
In this structural sense, the dividing line between snow and *firn* is diffuse but is conventionally taken to be near to a density of 400 kg m^{-3} (see *Table B6*).

Snow classification
The systematic description of a snow cover, usually seasonal rather than *perennial*, recording morphological, process-related and other attributes.
Guidelines for the classification of snow are given by Colbeck et al. (undated [1990?]) and by Fierz et al. (2009),

Snowfall
The depth of *snow* that falls from the air and accumulates on the surface during a stated period.
Snowfall excludes the deposition of *windborne snow*.

Snow depth
In the *firn area*, the vertical distance between the glacier surface and the *summer surface*; outside the firn area, the vertical distance between the glacier surface and the ice surface (which may be *superimposed ice* or *glacier ice*) at the time of observation.

Snowfield
A more or less extensive and persistent mass of *snow*.

Snowfields are more extensive than *snowpatches*, but the distinction is not made precisely in common usage. A snowfield that is *perennial* may be difficult to distinguish from a *glacier*.

Snowline
A set of points forming the lower limit of a snow-covered area; on a *glacier*, the line separating snow surfaces from ice or firn surfaces, and also separating the *percolation zone* from either the *superimposed ice zone* or the *ablation zone* (see also *zone*).

The set of points need not form a continuous curve. The snow-covered area of the glacier may include outliers (isolated patches of *snow* surrounded by *firn* or *ice*) and may exclude inliers (isolated patches of exposed firn or ice).

The snowline is usually easy to see, because the snow above it is brighter than the firn or ice below it. It may therefore be mapped by analysis of suitable imagery. When, and only when, there is no *superimposed ice*, the snowline coincides with the *equilibrium line*.

Unless qualified by a different adjective, references to the snowline are understood to refer to the annual snowline. It is common for “snowline” to be used as an abbreviation of “average altitude of the snowline”.

Annual snowline
The snowline at the end of the *ablation season*, usually representing the highest position of the snowline during the *mass-balance year*; *end-of-summer snowline* is a synonym.

The snowline of any given balance year is established at the end of that balance year. If this newly established snowline is lower than the previous year’s *firn line,* it also becomes the new firn line.

Climatic snowline
Same as *regional snowline*.

End-of-summer snowline
Same as *annual snowline*.

Orographic snowline
The imaginary line formed by the generalized lower limit of *perennial* snowpatches on the terrain surface between *glaciers* at the end of the *ablation season*.

The orographic snowline is so called (originally by Ratzel in 1886) because its *altitude* is predominantly defined by local topography and exposure.

Regional snowline
The mean *orographic snowline* on a regional scale; *climatic snowline* is a synonym.

Transient snowline
The snowline at any instant, particularly during the *ablation season*.

Snowpatch
A mass of *snow* of restricted extent, especially one that persists through most or all of the *ablation season*.

Snowpatches are less extensive than *snowfields*, but the distinction is not made precisely in common usage. A snowpatch that is *perennial* may be difficult to distinguish from a *glacieret*.

Snow pit
A hole dug into *snow* or *firn* to facilitate observation and sampling of *density*, snow and firn structure and associated grain sizes, layering and other attributes.

Snow-pit measurements are part of the basis of the *glaciological method* of measuring glacier mass balance (see *stake*).

A snow pit (Figure 11) can be excavated by hand using shovels (common on most smaller *glaciers*) or by trenching using a larger machine such as a tracked vehicle or caterpillar (now common in work on *ice sheets*). Coring by means of a barrel corer is a much less labour-intensive alternative to, and can to some extent replace, snow pits in determining bulk density of the snow and firn. Cores, however, are not well suited for detailed observations of stratigraphy because of their small size relative to what can be observed on a snow-pit wall (Figure 12).

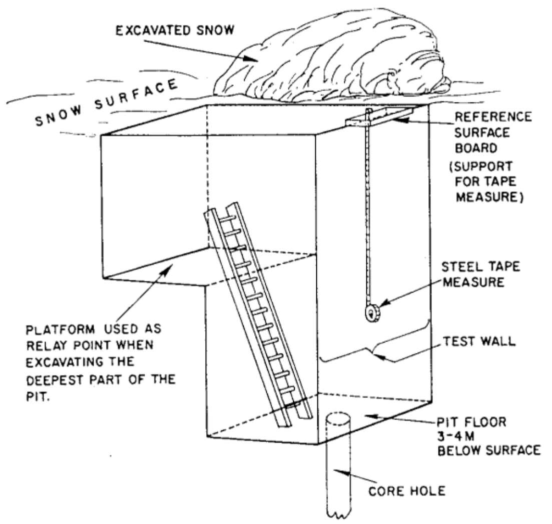

Figure 6. Sketch of a typical test pit.

Pits were dug in places undisturbed by foot or vehicle traffic. Waste snow was not thrown over the test wall and no one walked within several feet of its edge. Test walls, located on the south side to avoid direct sunshine, were made clean and vertical. A board on the snow surface served as a mount for the steel tape measure and also as a radiation shield for thermometers in the snow (see also Fig. 7a).

Figure 11. A diagram of a snow pit from a classical early study of snow stratigraphy in Greenland (Benson 1959, 1962).

Figure 12. A snow pit for mass-balance observations (Holmlund and Jansson 2002).

Snow zone
See *recrystallization zone*.

Snow-firn zone
See *recrystallization-regelation zone*.

Solidification
The process by which a liquid changes phase into a solid; a synonym of *freezing*.
See *latent heat of fusion*.

Solid precipitation
Precipitation that falls in a solid state, such as sleet, *snow* or hail.

Sonic ranger
A device that measures the distance to a target, such as the *glacier* surface, by timing the return of echoes from acoustic (typically ultrasonic) pulses emitted by the device itself.

A sonic ranger mounted on a suitable support can yield a continuous record of relative change of surface height and, if information on changes of *density* can also be obtained, can therefore contribute to the monitoring of *accumulation* or *ablation*.

Knowledge is required of the speed of sound in the medium traversed by the pulse and its echo, which may in turn require knowledge of the temperature of the medium. The medium is usually air.

Sorge's law
The proposition that a *glacier* with a constant *accumulation* rate and no *melting* has a constant profile of *density* as a function of depth beneath the surface; by extension, and more loosely, the proposition that an unchanging density profile is sustained by the *climatic mass balance*.

It follows from Sorge's law that a *thickness change* can be converted to an equivalent change of mass by multiplying by the density of *glacier ice*. This approach has been used in most *mass-balance* calculations by *geodetic methods*.

Sorge's law was originally introduced to describe *densification* of high polar snowpacks where *melt* is negligible. When Sorge's law is invoked in its looser sense, the constancy of the density profile is usually assumed rather than measured.

The name was given by Bader (1954) in recognition of Ernst Sorge's observations in Greenland in 1930–1931. The German name Sorge is pronounced as two syllables, the first stressed, with *s* as English *z* and with hard *g*.

Specific (*adj*.)
Descriptive of a quantity expressed as mass per unit area (dimension [M L^{-2}]), and therefore in units such as kg m^{-2} (which is numerically equivalent to mm *water equivalent*).

In mass-balance studies, the prefix "specific" is not necessary in general. The units in which a quantity is reported make clear whether or not it is specific. See *specific mass balance*.

The glaciological usage is not that prevailing in some other sciences, where often a specific quantity is either a dimensionless ratio of the value of a property of a given substance to the value of the same property of some reference substance, or is a quantity expressed per unit mass.

Specific mass balance
See article *Specific mass balance* under *Mass balance*.

Speckle tracking
The measurement of surface velocity as the rate of displacement of correlated patterns of speckle, or noise, in successive radar-interferometric images of the *glacier*.

The speckle originates from large numbers of statistically independent scatterers in the scene. Small "chips" or windows from a later image are matched to a similar chip from an earlier image. Measured from the earlier chip, the distance to and bearing of the later chip that exhibits the greatest correlation with the earlier chip is taken to be the vector displacement that has accumulated between the dates of the images. Speckle tracking (e.g. Gray et al. 2001) is less precise than interferometric measurement of velocity but, relying only on image intensity rather than on both the intensity and the phase of the complex radar signal, is more robust.

See *feature tracking*.

Stagnant ice
Any part of a *glacier* that does not flow at a detectable rate; a synonym of *dead ice*.

Stake
A pole or rod that has been emplaced in a vertical hole drilled into the *glacier* surface; may also be referred to as a *mass-balance* stake, or as an *accumulation* stake or *ablation* stake as appropriate**.**

The length of the stake exposed above the glacier surface measured at successive times is used to record changes in height of the glacier surface relative to the top of the stake as a measure of the sum of accumulation and ablation (that is, of *surface mass balance*) over the measurement interval (Figure 13).

Such measurements are reliable only when the stake can be assumed neither to have sunk into the *ice* or *firn* nor to be floating in water contained within the drill hole. Additionally, settling of firn between the *summer surface* and the bottom of the stake (a change in the height of the summer surface that is due only to a change in *density*) must be corrected for. If the stake is not protruding vertically from the ice, but at an inclination to the vertical, or if it is bent, geometric corrections are required so as to yield the correct exposed length. If the surface is rough, as for example in a field of *penitentes*, measurements are made to a plane that approximates the average surface. If heat transfer from the stake has enhanced ablation in its immediate surroundings, the resulting surface depression is compensated for by measuring from the stake top to the maximum surface height of the surroundings.

Stake measurements are part of the basis of the *glaciological method* of measuring glacier mass balance (see *snow pit*). Stakes can be made of many materials, bamboo, aluminium and polyvinylchloride (PVC) being most common.

The *surface mass balance* is calculated as the change in height of the surface below the top of the stake, multiplied by the vertically-averaged density of the matter added or removed. The result is a *point mass balance*.

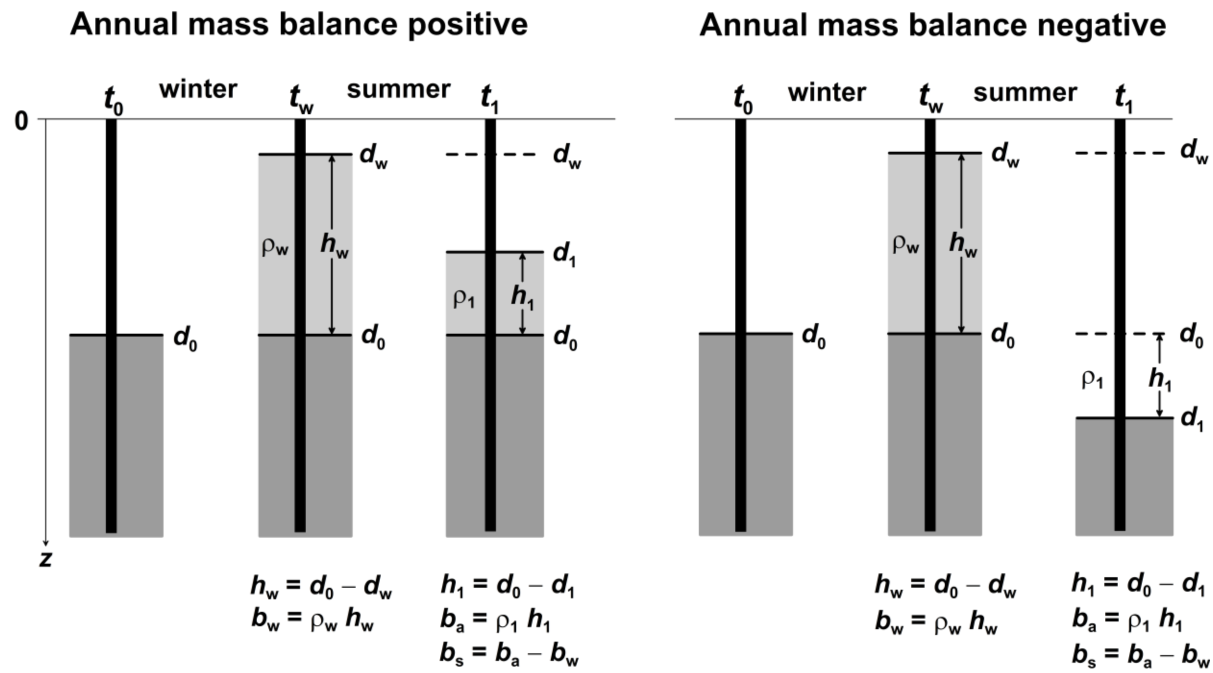

Figure 13. Stake measurements of seasonal mass balances in a year of positive (left) and a year of negative (right) *surface mass balance*, with no *superimposed ice*. The vertical coordinate is positive downwards, and all distances are measured from the origin $z = 0$ at the top of the stake. Light shading represents *snow*; dark shading represents *firn* or *glacier ice*. Measurements are made at t_0, the start of the *accumulation season*; at t_w, the start of the *ablation season*; and at t_1, the end of the mass-balance year. The *winter balance* b_w is the change of mass between t_0 and t_w. The *summer balance* b_s is the change of mass between t_w and t_1. The five quantities measured are: at t_0, when by definition there is

no snow, the distance d_0 from the stake top to the *summer surface*; at t_w, the distance d_w from the stake top to the surface and (in a nearby *snow pit* or with a coring device) the mean density ρ_w of the snow (if any; the winter balance is not necessarily positive); and at t_1, the distance d_1 from the stake top to the surface and the mean density ρ_1 of the snow (if any). The layer thicknesses h_w and h_1 are obtained by subtraction, as beneath the figure; note that in the right part of the figure the annual balance is negative because the thickness h_1 is negative. When the balance is positive the stake measurements are often supplemented by digging or probing to sample local variability. It is not possible to measure the density of mass that is lost between any two survey dates. For example the summer balance is commonly evaluated as $b_a – b_w$; and when h_1 is negative an appropriate value (usually, outside the firn area, the density of ice) must be assumed for ρ_1. At the instant following t_1, any residual snow is deemed to become firn and the glacier surface, at d_1, becomes the summer surface d_0 of the next balance year.

Stake farm
A group of *stakes* placed within a small area on the surface of a *glacier*, serving to improve estimates of the small-scale variability, and therefore of the sampling uncertainty, of *surface mass balance*.

Steady state
A state of the *glacier* in which over many years the thickness at the end of each *mass-balance year* remains unchanged, that is, $dh/dt = 0$ at every point.

It follows from the definition that the *glacier-wide mass balance*, including *calving*, is zero, because the glacier must *flow* at just the rate required to eliminate *thickness changes* due to the *climatic-basal mass balance*.

Steady state is a valuable idealization, and may be realized roughly when the climate is constant, or changes only slowly, over periods considerably longer than the *response time* of the glacier.

See *equilibrium*, *balanced-budget*.

Steady-state AAR
See *accumulation-area ratio*.

Steady-state ELA
See *equilibrium-line altitude*.

Stratigraphic system
The *time system* in which the determination of *mass balance* is based on the identification of successive annual minima, and for seasonal balances annual maxima also, in the mass of the *glacier* or a part of the glacier.

In field work, *annual mass balance* is determined by the detection of two successive *summer surfaces*, usually at individual observation sites. In the *ablation zone*, the earlier summer surface has disappeared by the time the later one is observed, but its vertical position is known from earlier observations. For seasonal balances, it is not possible to determine the annual maximum of mass with a single field survey that can be scheduled to coincide only roughly with the expected date of the maximum. Thus, in the stratigraphic system, seasonal balances by the *glaciological method* are actually measured in a *combined system*.

Continuously recording sensors, such as snow pillows and *sonic rangers*, can yield accurate stratigraphic-system estimates of seasonal balances at single points, but they are not in wide use.

The annual extrema of mass may be reached at different times at different sites on the glacier. *Glacier-wide* balances in the stratigraphic system can be determined rigorously only by accurate spatially distributed modelling or by *gravimetric methods*. Determinations based on field measurements require the assumption that the *diachronous* character of the summer surface can be neglected.

The duration of the *mass-balance year* varies in the stratigraphic system. See also *measurement year*, and *fixed-date system*, *floating-date system*, *combined system*.

Subglacial
Pertaining to the *glacier* bed or to the material below the bed.

Sublimation
The process by which a solid changes phase directly into a vapour without *melting*. See *latent heat of sublimation*, *Table B1*.

Submergence velocity
The vertical component, when it is directed downward, of the glacier-flow velocity vector at the *glacier* surface, at a point fixed in space.

When the component is directed upward, it is called the *emergence velocity*. The submergence velocity is related through the *continuity equation* to the *climatic-basal mass balance* and the rate of *thickness change*.

The component is typically upward in the *ablation zone* and downward in the *accumulation zone*.

Sub-polar glacier
An obsolete term, due to Ahlmann (1935), describing a *glacier* with an *accumulation zone* in which, except for possible seasonal warming and *melting* near the surface, the temperature is below the *freezing point* to depths of 100 m or more.

The term is sometimes used as if it were a synonym of *polythermal glacier*.

Summer ablation a_s (point), A_s (glacier-wide)
See article *Summer ablation* under *Mass balance*.

Summer accumulation c_s (point), C_s (glacier-wide)
See article *Summer accumulation* under *Mass balance*.

Summer-accumulation type
A type of *glacier* on which the regional seasonality results in extrema of *ablation* rate and *accumulation* rate at roughly the same time.

On a glacier of summer-accumulation type, *mass balance* remains relatively stable throughout the *year*. This is typical of high-altitude, low-latitude glaciers with a summer *precipitation* maximum.

Summer mass balance b_s (point), B_s (glacier-wide)
See article *Summer mass balance* under *Mass balance*.

Summer season
The time span from the end of the *winter season* to the end of the *mass-balance year*.

The length of the summer season may vary greatly from year to year. The term is best suited to *glaciers* of *winter-accumulation type*. See *accumulation season*.

In the *stratigraphic system* the summer season starts when the glacier has attained maximum mass and ends when the glacier has attained minimum mass. In the *floating-date system* and the *fixed-date system*, the mass is not necessarily at its annual maximum or minimum when the summer season starts or ends.

Summer surface
The surface formed at the time of minimum annual mass at each point on the *glacier*, marking (in the *stratigraphic system*) the end of one *mass-balance year* and the start of the next. See *zone*.

In general the summer surface is *diachronous*. For example, when the higher reaches of a glacier start to gain mass, the lower parts may still be ablating.

The summer surface is the surface on which the first *snow* of the new balance year falls. It is easily detectable when it consists of *glacier ice*, which now includes *superimposed ice* added during the previous balance year. In the *firn area* it is recognizable as a well-marked crust, that is, a thin, relatively strong layer with a *density* near that of ice, and sometimes also (or instead) as a layer of *depth hoar* at the base of the current year's *accumulation*.

The crust typically originates by *recrystallization* of the surface snow in late summer to form *glaze*. It may also be marked by an accumulation of sediment or wind-blown *dust*. It can be difficult to detect when *melting* and *snowfall* alternate during the transition between the *ablation season* and the *accumulation season*. In some *mass-balance* programmes the summer surface is "labelled" in the vicinity of *stakes* with a distinctive material, such as sawdust, during a visit late in the ablation season.

Superimposed ice
Ice accumulated on the current *summer surface*, during the current *mass-balance year*, by the *refreezing* there of *rain* or *meltwater*. See *zone*.

Superimposed ice is not the same thing as *internal accumulation*, which represents refreezing below the summer surface.

Superimposed ice requires special attention in conventional *mass-balance* programmes. In a pair of *stake* measurements, one at the beginning and one at the end of the *ablation season*, accumulation of superimposed ice causes a decrease of the distance from the top of the stake to the *ice* surface (regardless of any overlying *snow*). This decrease is real and not, for example, due to faulty book-keeping.

Superimposed ice zone
The part of the *glacier* where *superimposed ice* is exposed. See *zone*.

The superimposed ice zone occupies the range of *elevations* below the *snowline* and above the *equilibrium line*. Superimposed ice may also be found beneath *snow* of the current year at elevations above the snowline. Whether exposed or beneath the surface, it requires special attention in *mass-balance* measurements.

Supraglacial
Pertaining to the surface of the *glacier* or to features on the surface.

Surface ablation a_{sfc} (point), A_{sfc} (glacier-wide)
See article *Surface ablation* under *mass balance.*

Surface accumulation c_{sfc} (point), C_{sfc} (glacier-wide)
See article *Surface accumulation* under *mass balance.*

Surface mass balance b_{sfc} (point), B_{sfc} (glacier-wide)
See article *Surface mass balance* under *mass balance.*

Surface density
The SI name of the derived unit kg m^{-2}, mass per unit area. See *section 7.1.2*.

It can be helpful to regard the product of a thickness and a *density* as a surface density. For example *mass balance*, when expressed in *specific* units, is a surface density.

Surge (*n*.; also *v*.)
Abnormally fast *flow* of a *glacier* over a period of a few months to years, during which the *glacier margin* may advance substantially.

A *surge-type glacier* exhibits quiescent phases, typically lasting some decades, during which velocities are lower than in a "normal", non-surge-type glacier. The ice discharge is thus too small to maintain the longitudinal profile of the glacier, which thickens in its upper reaches and thins in its lower reaches. Surges recur at quasi-periodic, glacier-specific intervals, and transfer large quantities of ice from the thickened upper part to the thinned lower part. Velocities during the surge are often greater by an order of magnitude than those during the quiescent phase.

A surge-type glacier will almost always be out of balance. That is, a surge-type glacier cannot be in *steady state*. Surge-type glaciers may end on land or in water, and the proportion of glaciers that are of surge type varies from region to region. The mechanism of surging is poorly understood. Surges seem, however, to be related to changes in the subglacial hydrological regime and not primarily to climatic fluctuations. Although surging is best documented on smaller glaciers, many larger *outlet glaciers* of *ice caps* have been observed to surge, and there may be a connection with the unsteady behaviour exhibited by some *ice streams*.

Surge-type glacier
A *glacier* that has been observed to *surge*, or is inferred from evidence such as contorted medial moraines to have surged in the past.

Synthetic Aperture Radar Interferometry
See *InSAR*.

T

Temperate glacier
A *glacier* consisting of *temperate ice* over its entire thickness and extent, except for a surface layer of the order of 10–15 m thick which may experience seasonal cooling.
By definition a temperate glacier is a *wet-based glacier*. See *cold glacier, polythermal glacier*.

Temperate ice
1. *Ice* that contains a liquid phase of no more than moderate salinity with which it is in thermodynamic equilibrium at the solid–liquid phase boundaries.

2. Less precisely, ice that is at its *pressure-melting point*.

Other factors, notably the salinity of water inclusions, can be of comparable importance to the hydrostatic pressure for determination of the *melting point*. Sense 2 is adequate for simple purposes, but the details illuminated by Lliboutry (1971) and Harrison (1972) are likely to be of practical importance in detailed work.

Temperature-index model
A model of *mass balance* in which *surface ablation* is estimated as a function of temperature, usually near-surface air temperature measured either on the glacier or at the nearest weather station; temperatures may also be taken from upper-air soundings, meteorological reanalyses or climate models.
A leading form of temperature-index model is the *positive degree-day* model, in which a *degree-day factor* represents the dependence of ablation on temperature. Temperature-index models are valuable because they require only simple input variables and perform well when suitably calibrated, for example by allowing for the differences in reflectivity between surfaces of ice and snow by choosing a smaller *degree-day factor* for *snow* than for *ice*.
See *energy-balance model*.

Temporary Technical Secretariat for the World Glacier Inventory (TTS/WGI)
A body established in 1975 to prepare guidelines for the compilation of a world glacier inventory and to collect inventories from different countries.
In 1986, the Temporary Technical Secretariat for the World Glacier Inventory was merged with the *Permanent Service on the Fluctuations of Glaciers* to form the *World Glacier Monitoring Service*.

Terminus
The lowest end of a *glacier,* also called glacier snout, *glacier front* or glacier toe.
The term is applicable primarily to glaciers with well-defined *tongues,* and to *ice streams*. See *glacier margin*.
The plural is either “terminuses” or “termini”.

Thickness
The vertical distance between any two surfaces, and in particular between the *glacier* surface and the *summer surface*, or the glacier surface and the bed.
Glacier thickness is measured ideally by interpolating from a dense array of point measurements, constructed for example from *ground-penetrating radar* traverses. However the measurement density is often less than ideal, as when the array consists of a single traverse or even just a small number of boreholes. On most glaciers there are no thickness measurements at all and the thickness must be estimated, for example by *volume-area scaling* or as a function of surface slope and estimated basal shear stress.

The definition of thickness as a vertical distance is adopted almost invariably in studies of *mass balance*, but not in all branches of cryospheric science. For example Fierz et al. (2009) define thickness as the coordinate normal to the slope, measured from the base of a layer of snow.

Thickness change
The change in the *thickness* of the *glacier* at a defined horizontal location.

Thickness can change at a point due to *ablation* and *accumulation* at the surface and bottom of the glacier, compaction of *snow* and *firn*, or a non-zero *emergence velocity* or *submergence velocity* (see *continuity equation*). Thickness change is often used interchangeably with *elevation change*, but the two are not necessarily the same. For example, elevation can change due to *glacial isostatic adjustment* or vertical tectonic motions, without a change in glacier thickness. The thickness change at a point is not equivalent to the *climatic-basal mass balance* at that point because the thickness change may be due in part to emergence or submergence (see *continuity equation*). Thickness change at a point is therefore not a direct indicator of the local climate.

The *glacier-wide* mean thickness change Δh is the volume change of the entire glacier divided by the mean glacier *area* during the time span of the measurements:

$$\Delta h = 2(V_2 - V_1)/(S_2 + S_1) \ ,$$

where V is volume, S is area, and subscripts 1 and 2 refer to measurements at an earlier and later time, respectively. The quantity $(V_2 - V_1) = \Delta V$ is the volume change. Usually the two volumes are not known separately, and ΔV is obtained from measurements of Δh by *geodetic methods*.

The mean thickness change, if multiplied by the *density* of the mass gained or lost, is equal to the glacier-wide *mass balance* over the period of the thickness change.

The mean thickness change is not the same as the change of mean thickness. The latter is $V_2/S_2 - V_1/S_1$.

Thinning flux
The *mass flux* through a vertical cross-section corresponding to the decrease of mass upglacier from the cross-section (that is, the integral of *density* through the thickness of the *glacier* and over the upglacier area).

Volumetric thinning flux
The thinning flux divided by average *density*.

Thinning velocity
The *volumetric thinning flux* divided by the *area* of the vertical cross-section through which it passes.

Tidewater glacier
A *glacier* that terminates in the sea, with *terminus* either floating or grounded below sea level. See *floating tongue*, *tidewater instability*.

The adjective “tidewater” indicates geographical setting and does not imply a role for tides in the *mass balance*.

Tidewater instability
Unsteady, perhaps quasi-periodic, behaviour (Meier and Post 1987) of a *tidewater glacier* that undergoes alternating episodes of slow advance and rapid retreat.

The conditions permitting advance to the advanced position in the first place, and the triggers for subsequent unstable retreat, are both poorly understood, although they may involve variations in basal water pressure and probably involve variations of the *climatic mass balance*.

Once retreat has begun, however, observation and numerical simulation (Schoof 2007) agree that, if the bed is grounded below sea level but has a slope opposed to that of the surface, the retreat will continue until the *calving front* (or the *grounding line* if there is a *floating tongue* or *ice shelf*) reaches a part of the bed that slopes in the same direction as the surface. During this unstable retreat, enhanced *calving* leads to a positive feedback in which accelerated flow and *dynamic thinning* extend far upglacier from the part that is grounded below sea level. Mass loss is far greater than, and essentially independent of, the climatic mass balance.

Tier

One of the levels in the multi-level monitoring strategy of the *Global Terrestrial Network for Glaciers*.

Tier 1 is a conceptual level that integrates monitoring studies at lower levels into large-scale transects across environmental gradients.

Tier 2 consists of *glaciers* on which extensive *mass-balance* measurements are made and research is conducted to improve process understanding and model calibration.

A Tier-3 glacier is one on which mass balance is measured using cost-saving methodologies.

On Tier-4 glaciers measurements, for example of length changes and volume changes, are made with the aim of assessing the spatial representativeness of more detailed measurements on nearby Tier-2 and Tier-3 glaciers.

A Tier-5 glacier is a glacier included in a *glacier inventory*, the latter ideally repeated at intervals of a few decades.

See *benchmark glacier*, *reference glacier*.

Time system

A protocol for identifying stages in the evolution of the *mass balance* of the *glacier* over the *mass-balance year*, making it possible to quantify the mass change during each stage objectively.

Four time systems are recognized. Figure 14 illustrates the differences between the original two. See *combined system*, *fixed-date system*, *floating-date system*, *stratigraphic system*.

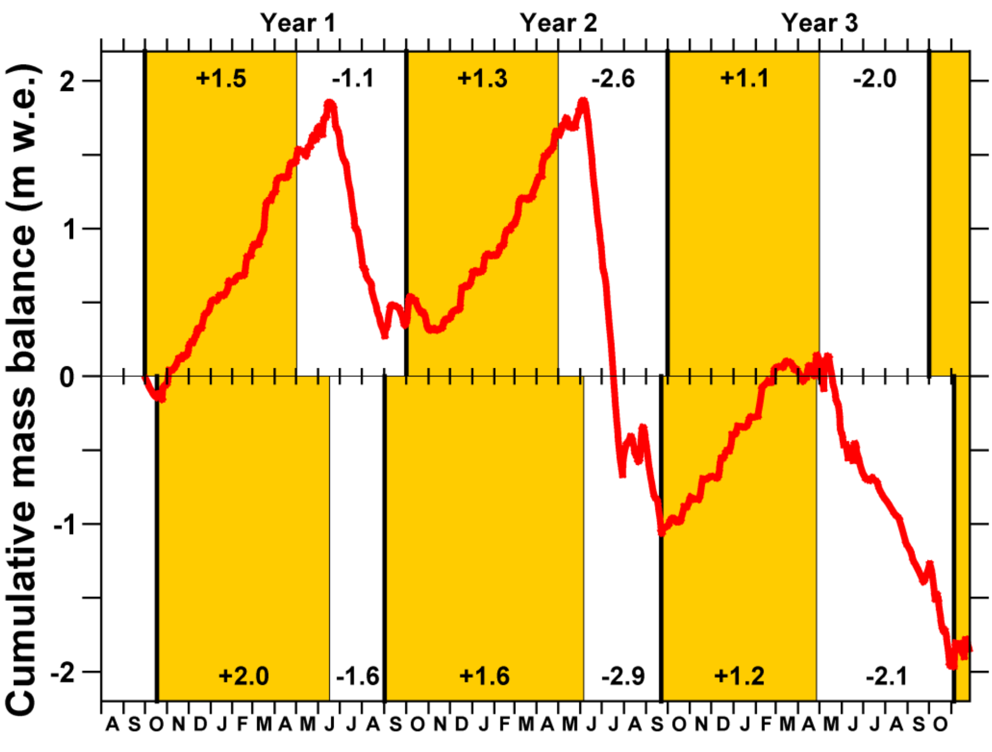

Figure 14. The *cumulative mass balance* over three mass-balance years, relative to 1 October of Year 1, of a representative northern-hemisphere glacier. In the upper half of the graph the *winter seasons* of the fixed-date system (1 October to 1 May) are shaded. In the lower half the winter seasons of the stratigraphic system (annual minimum of mass to annual maximum of mass) are shaded. For each time system the *winter balance* and *summer balance* are given for each season. After Huss et al. 2009.

Tongue
1. The lower, elongate part of a *valley glacier* or *outlet glacier*.

2. A floating extension of a *glacier* or *ice stream*, laterally unconfined but markedly longer than wide.

Topographic method
Like *cartographic method*, a synonym of *geodetic method* in the context of measurement of *mass balance*.

Total ablation
A term formerly used in the *stratigraphic system* (Anonymous 1969; *Appendix A*) for *annual ablation*.

Total accumulation
A term formerly used in the *stratigraphic system* (Anonymous 1969; *Appendix A*) for *annual accumulation*.

Total exchange
A term formerly used (Anonymous 1969; *Appendix A*) for the difference between *annual accumulation* and *annual ablation*, c_a minus a_a, in the *stratigraphic system*.

Note that *ablation* is defined to be negative. See *annual exchange*.

Total mass balance
The sum of the *climatic-basal mass balance* and *frontal ablation*, or equivalently the sum of *accumulation* and *ablation*; a synonym of *mass balance*.

The adjective "total" was formerly a technical term in the *stratigraphic system* (Anonymous 1969; *Appendix A*). It is now needed only when it is important to emphasize that all the components of the mass balance are being studied.

Transient *(adj.)*
Of a state or entity, changing with time or persisting for only a short time.

Transient AAR
See article *Transient AAR* under *Accumulation-area ratio*.

Transient ELA
See article *Transient ELA* under *Equilibrium-line altitude*.

Transient equilibrium line
See article *Transient equilibrium line* under *Equilibrium line*.

Transient snowline
See article *Transient snowline* under *Snowline*.

Trimline
A line separating tracts of unglacierized terrain of strikingly different appearance, the appearance of one of the tracts being interpretable as due to recent deglaciation.

The trimline usually separates terrain with more mature vegetation, deglaciated in the more distant past or never glaciated at all, from terrain exposed during the retreat of *glaciers* from their *Little Ice Age* maximum extents. The separation may also be marked in part by terminal moraines. The trimline can be used to reconstruct former glacier extent and volume. Reliably dated trimlines have been used in this way to estimate long-term average *mass balance*.

Triple point
The temperature, 273.16 K by definition, and pressure, 611.657 Pa, at which *ice*, water and water vapour are in thermodynamic equilibrium.

The term “point” derives from the practice in thermodynamics of choosing temperature and pressure as the coordinates of a two- or higher-dimensional phase diagram.

V

Valley glacier
A *glacier* flowing down a valley and in consequence having a distinct *tongue*.
The *glacier outline* is well-defined.

Volume–area scaling
A method of relating *glacier* volume or volume changes to glacier *area* or area changes, based on a tendency for glacier *thickness* to be well correlated (to "scale") with glacier area.
Glacier volume V is the product of area S and mean thickness H. Measured mean thicknesses are well described by a relation of the form $H = cS^{\gamma-1}$, which is the basis for the volume-area relation $V = cS^{\gamma}$. Here c and γ are parameters estimated from samples of glaciers with measured thicknesses. There is good evidence, as shown by Bahr et al. (1997), that estimates of γ from observations are nearly consistent with theoretical expectation. Mean thickness is also sometimes estimated as a function of average surface slope and basal shear stress.
Volume–area scaling is both a way of estimating regional and global glacier volumes from abundant data on glacier area, and a possible way of estimating (with large random uncertainty) the *volume balance* of single glaciers from successive measurements of area S_1 and S_2, for example as $\Delta V \simeq c(S_2^{\gamma} - S_1^{\gamma})$. It can also be used, as a practical alternative to ice-flow modelling, to estimate glacier area changes in attempts to model the response of glaciers to climatic change.
Glacier volume is also expected, and found, to scale with glacier length, particularly when the length is that of a *flowline*.

Volume balance
The change in the volume of a *glacier*, or part of a glacier, over a stated span of time.
A volume balance contains no information about the *density* of the matter within the volume gained or lost. It is meaningful in itself, but is often an intermediate product in the determination of *mass balance* by *geodetic methods*.
Balances expressed in *ice-equivalent* or *water-equivalent* units, such as m^3 w.e. a^{-1}, are not volume balances but mass balances.

Volumetric balance flux
See article *Volumetric balance flux* under *Balance flux*.

Volumetric calving flux
See article *Volumetric calving flux* under *Calving flux*.

Volumetric thinning flux
See article *Volumetric thinning flux* under *Thinning flux*.

W

Warm-based glacier
A *glacier* whose bed is at its *pressure-melting point*. Same as *wet-based glacier*,

Warm firn zone
See *infiltration-recrystallization zone*.

Warm infiltration-recrystallization zone
See *infiltration-recrystallization zone*.

Water balance
A relation describing the change in the amount of water stored within a defined volume owing to transfers of water across the boundary of the volume.

The general water balance equation is:

$$\Delta W = P - E - Q,$$

where P is *precipitation*, E is *evapotranspiration*, Q is *runoff* and ΔW is the change in storage.

The water balance is the basis of the *hydrological method* of determination of glacier *mass balance*. Typically in glaciological research the defined volume is a drainage basin tributary to a *discharge* measurement station near to the glacier *margin*, and not all of the basin is *glacierized*. Transfers of water by precipitation and evapotranspiration will include transfers not passing through the boundary of the *glacier*, and stores of water will include lakes, seasonal *snowpatches*, soil and aquifers as well as the glacier. Changes in each of the non-glacial stores must be accounted for to isolate the glacier mass balance.

It can be convenient in glacier hydrology to distinguish between *meltwater runoff* from *glacier ice* and *firn* and runoff from the basin-wide snowpack, the latter including the snow on the glacier. Denoting these stores by I and N respectively, and assuming that changes in other stores are negligible,

$$\Delta I = \Delta N - E_i - Q_i \ ,$$
$$\Delta N = P_n - E_n - Q_n \ .$$

Snowfall P_n that does not evaporate or run off must accumulate, contributing to the ice balance ΔI as ΔN. The total runoff is the sum of runoff from snow Q_n, runoff from ice and firn Q_i and runoff of liquid-water inputs.

Water equivalent
A unit, in full the "metre [of] water equivalent", that is an extension of the SI for describing *glacier* mass in *specific* units as the thickness of an equal mass having the *density* of water.

1 kg of liquid water, of density $\rho_w = 1000$ kg m^{-3}, has a thickness of exactly 1 mm when distributed uniformly over 1 m^2. More formally, the metre water equivalent (m w.e.) is obtained by dividing a particular mass per unit area by the density of water:

$$1 \text{ m w.e.} = 1000 \text{ kg m}^{-2} / \rho_w \ .$$

Water equivalents (m w.e.) can be converted to kg m^{-2} by multiplying by the density of water, and to *ice equivalents* (m ice eq.) by multiplying by the density of water and dividing by the density of *ice*.

Water year
The *hydrological year*.

Weathering crust
A friable surface layer, of reduced density, that develops due to small-scale variations of the melting rate of *ice* in the presence of *cryoconite*.

Short-term measurements of surface lowering are unreliable as estimates of *surface ablation* when there is a weathering crust. The crust may reach a *thickness* of the order of 100–200 mm over several days, only to be removed abruptly by *rain* or strong winds.

Wet-based glacier
A *glacier* the bed of which is at its *pressure-melting point*. *Warm-based glacier* is a synonym.

Wet-snow line
The set of points on a *glacier* separating the upper *percolation zone*, at higher elevation, from the lower percolation zone or *wet-snow zone*. See *zone*.

The wet-snow line has no surface expression, but is significant as the upper limit of the region where *internal accumulation* may happen.

Wet-snow zone
The part of the *accumulation zone* of a *cold glacier* or *polythermal glacier* where all of the *snow* reaches the *melting point* during the *ablation season*.

The wet-snow zone is sometimes referred to as the lower *percolation* zone.

See *zone*.

Wind ablation
Mass loss, local or *glacier-wide*, by *wind scour*.

Snow lost to wind ablation on one part of the *glacier* surface is often re-deposited in more sheltered parts of the glacier surface, making no contribution to glacier-wide ablation.

Windborne snow
Blowing snow or *drifting snow*.

Windborne snow may be redistributed from one part of the glacier to another. It contributes to the *glacier-wide mass balance* only when it is carried across a lateral boundary of the glacier, either inward or outward; or when it suffers *sublimation* instead of being redeposited.

Wind scour
The entrainment and removal of surface *snow* by the wind.

The resulting *windborne snow* may be re-deposited elsewhere in more sheltered parts of the glacier surface, or may be transported off the glacier.

Winter ablation a_w (point), A_w (glacier-wide)
See article *Winter ablation* under *Mass balance*.

Winter accumulation c_w (point), C_w (glacier-wide)
See article *Winter accumulation* under *Mass balance*.

Winter-accumulation type
A type of *glacier*, typically at mid-latitudes or high latitudes, on which the regional seasonality leads to *accumulation* predominating in the *winter season* and *ablation* predominating in the *summer season*.

Winter mass balance b_w (point), B_w (glacier-wide)
See article *Winter mass balance* under *Mass balance*.

Winter season
The time span from the start of the *mass-balance year* to the time of maximum glacier mass (see *zone*).

The term is best suited to *glaciers* of *winter-accumulation type*. See *accumulation season*.

In the *stratigraphic system* the winter season ends when the glacier has attained maximum mass. In the *floating-date system* and the *fixed-date system*, the mass is not necessarily at its annual minimum or maximum when the winter season starts or ends.

World Data Centres (WDC)
A set of centres for the storage and dissemination of scientific data under the sponsorship of the *International Council for Science (ICSU)*.

The three World Data Centres for Glaciology are at the *National Snow and Ice Data Center*, University of Colorado, Boulder, U.S.A.; the Scott Polar Research Institute, University of Cambridge, Cambridge, England; and the Cold and Arid Regions Environmental and Engineering Research Institute (CAREERI), Lanzhou, China.

World Data System (WDS)
A body, founded in 2009, that provides an operational framework for the *World Data Centres* and *Data Analysis Services* of the *International Council for Science (ICSU)*.

World Glacier Inventory (WGI)
A cooperative project, organized during the International Hydrological Decade (1965–1974) on the basis of suggestions first made in the 1950s, for the collection of morphometric and other basic information about all of the world's *glaciers*.

The *World Glacier Monitoring Service* (WGMS 1989) reported on the status of the WGI in the late 1980s. In 1998 the World Glacier Monitoring Service and the US *National Snow and Ice Data Center*, having pooled their data sources, made an enlarged version of the WGI available online at the NSIDC website. This version is incomplete. Completion of the WGI is the aim of collaborative efforts by many investigators under the auspices of WGMS, NSIDC and the *Global Land Ice Monitoring from Space* initiative.

World Glacier Monitoring Service (WGMS)
The leading organization for the collection, storage and dissemination of information about *glacier fluctuations*.

The WGMS, formed in 1986 by merging the *Permanent Service on the Fluctuations of Glaciers* and the *Temporary Technical Secretariat for the World Glacier Inventory*, is based in Zürich, Switzerland. It coordinates the work of local investigators through a network of national correspondents in countries involved in glacier monitoring. WGMS runs the *Global Terrestrial Network for Glaciers* (GTN–G) in close collaboration with the *National Snow and Ice Data Center* and the *Global Land Ice Measurements from Space* initiative.

Y

Year
The duration of the Earth's revolution round the Sun, forming a natural but slightly variable unit of time.

In glaciology, as in other disciplines concerned with the natural progression of the seasons, the year may vary in length for reasons of necessity or convenience, and depending on whether the particular investigation requires precise treatment of calendar time. For the latter, see *Julian date*.

In *mass-balance* practice the year is always either exactly or approximately 365 calendar days long (the duration of a calendar year which is not a leap year; see *hydrological year*, *mass-balance year*). However the sidereal year is very nearly equal to 365.2564 mean solar days. In turn, the mean solar day is very nearly equal to 86 400 seconds, and 1 day is defined in the Système International d'Unités as an accepted non-SI unit equal to 86 400 seconds exactly.

The practice when brevity is desirable, regardless of hemisphere, is to identify the hydrological year, mass-balance year or *measurement year* by the calendar year in which it ends. For example the mass-balance year 2000 began in calendar year 1999 and ended in calendar year 2000.

Year-round ablation type
A type of *glacier* on which *ablation* by *melting* or *sublimation* occurs throughout the *year*.

Year-round ablation is typical of glaciers in the inner tropics, where there are two seasonal temperature maxima each year, and seasonal temperature variations are smaller than diurnal temperature variations. The seasonal variation of *mass balance* is affected more by variation of *accumulation* rates between wet and dry seasons than by variation of ablation rates between winter and summer. Year-round ablation is also observed at low altitude on glaciers in some warm maritime climates, as in Norway, and on high-latitude glaciers where ablation is predominantly by sublimation, as in the Dry Valleys of Antarctica.

Z

Zastrugi
Ridges of hard *snow* alternating with wind-eroded furrows parallel to the wind direction, with typical lengths of metres and heights less than a metre.

The word is the plural of Russian “zastruga”, and alludes to the result of planing a wooden surface with a jack plane.

Zone
A part of the *glacier*, and especially of the glacier surface, distinguished from other parts by the prominence or predominance of a particular *mass-balance* process.

The *temperate glacier* of Figure 15 and the *cold glacier* of Figure 16 are end members of a continuum. Many glaciers have attributes, including patterns of zonation, that are intermediate between these end members.

The conventional system of zones in the English-language literature diverges in part from that in Russian-language work (Shumskiy 1955). For the latter, which is based on the relative magnitudes of *accumulation*, *melting* and *cold content*, see *infiltration zone*, *infiltration-congelation zone*, *infiltration-recrystallization zone*, *recrystallization zone*, *recrystallization-regelation zone*.

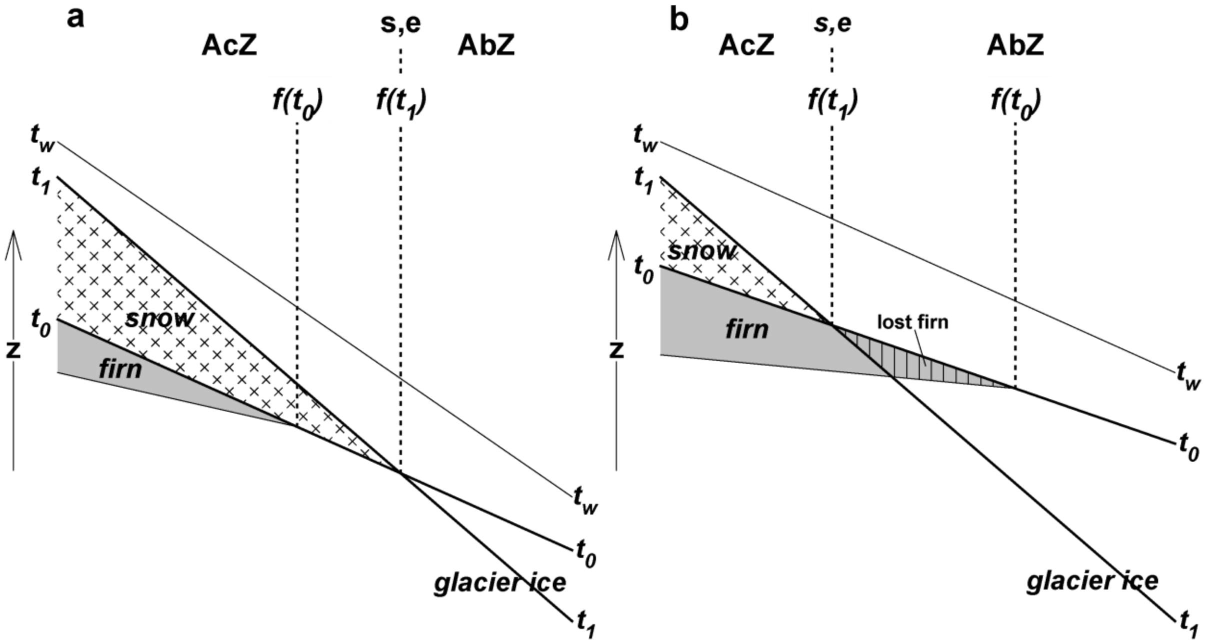

Figure 15. Glacier zonation on a representative *temperate glacier* during a) a year of more positive and b) a year of more negative *mass balance* than the previous year. At the start of each *mass-balance year* the glacier surface is at the line $t_0 - t_0$, the *summer surface*. It evolves (schematically, the effects of ice flow being neglected) to $t_w - t_w$ at the end of the *accumulation season*, when the mass of the glacier reaches its annual maximum, and then to $t_1 - t_1$ at the end of the *ablation season*, when it becomes the summer surface of the next balance year. e: *equilibrium line*; s: *snowline*; *f*: *firn line* at the start and end of the balance year; AbZ: *ablation zone* (the zone below e); AcZ: *accumulation zone* (the zone above e).

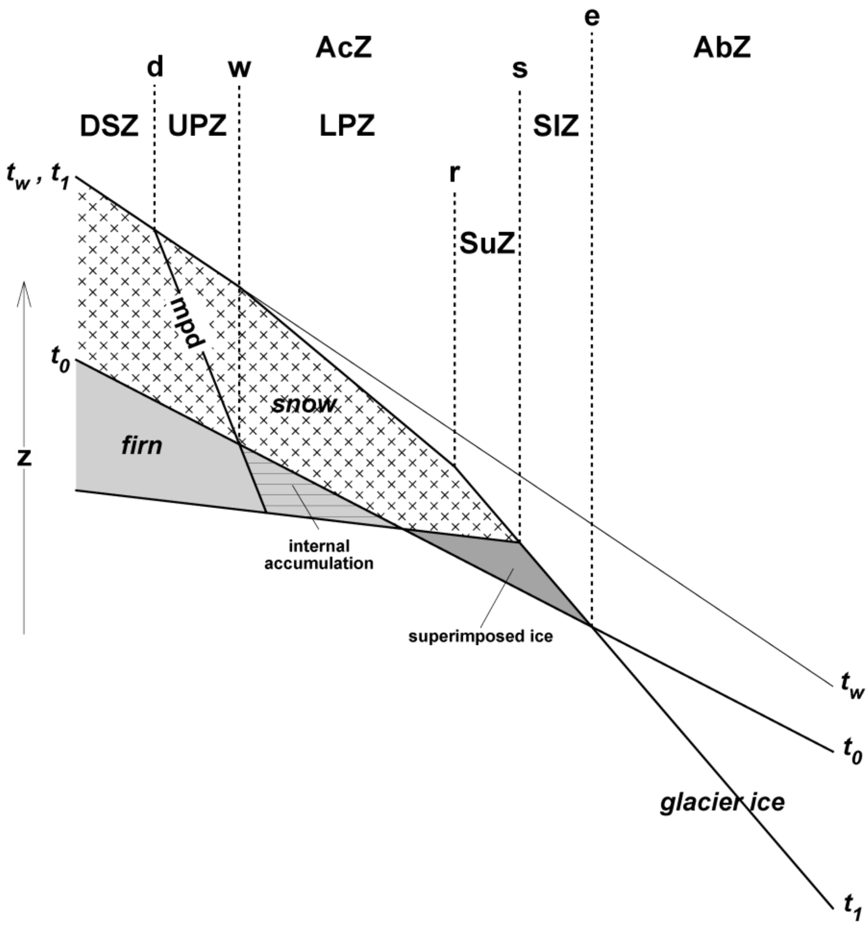

Figure 16. Glacier zonation and its balance-related aspects on a representative *cold glacier* or *polythermal glacier*. At the start of each *mass-balance year* the glacier surface is at the line $t_0 – t_0$, the *summer surface*. It evolves (schematically, the effects of ice flow being neglected) to $t_w – t_w$ at the end of the *accumulation season*, when the mass of the glacier reaches its annual maximum, and then to $t_1 – t_1$ at the end of the *ablation season*, when it becomes the summer surface of the next balance year. “mpd” is the maximum depth to which meltwater percolates before *refreezing*.

The zones are: AbZ: *ablation zone* (the zone below e); AcZ: *accumulation zone* (all the zones above e); SIZ: *superimposed ice zone*; SuZ: *slush zone*, a part of LPZ; UPZ: upper *percolation zone*; LPZ: lower *percolation zone* or *wet-snow zone*; DSZ: *dry-snow zone*.

The zones are separated by the lines: e: *equilibrium line*; s: *snowline*; r: *runoff limit* or *slush limit* (position variable, depending especially on the surface slope); w: *wet-snow line* (intercept of mpd on summer surface, separating UPZ and LPZ); d: *dry-snow line* (surface outcrop of mpd).

Appendix A – Terms Defined in Anonymous (1969)

Term	*Symbol*[1]	*Definition*
STRATIGRAPHIC SYSTEM		MEASUREMENT SYSTEM BASED ON EXISTENCE OF AN OBSERVABLE SUMMER SURFACE
Summer surface		Surface formed at time of minimum annual mass at each point, marking end of one balance year and start of next (NB: may be diachronous over the extent of the glacier)
Balance year		Time span between formation of two successive summer surfaces
Winter season		Time span from start of balance year to time of maximum glacier mass
Summer season		Time span from time of maximum glacier mass to end of balance year
Winter accumulation	c_w	Integral of accumulation $c(t)$ over winter season
Summer accumulation	c_s	Integral of accumulation $c(t)$ over summer season
Total accumulation	c_t	Integral of accumulation $c(t)$ over balance year
Winter ablation	a_w	Integral of ablation $a(t)$ over winter season
Summer ablation	a_s	Integral of ablation $a(t)$ over summer season
Total ablation	a_t	Integral of ablation $a(t)$ over balance year
Winter balance	b_w	Change in mass during winter season
Summer balance	b_s	Change in mass during summer season
Net balance	b_n	$c_t + a_t$; also $b_w + b_s$
Total exchange	e_t	$c_t - a_t$; also $b_w - b_s$
FIXED-DATE SYSTEM		MEASUREMENT SYSTEM BASED ON SPECIFIC CALENDAR DATES
Measurement year		Time between start and end of measurement
Annual accumulation	c_a	Integral of accumulation $c(t)$ over measurement year
Annual ablation	a_a	Integral of ablation $a(t)$ over measurement year
Annual balance	b_a	$c_a + a_a$
Annual exchange	e_a	$c_a - a_a$
OTHER		
Transient equilibrium line		Locus of points where balance $b(t)$ is zero
Equilibrium line		Locus of points where b_n is zero
Annual equilibrium line		Locus of points where b_a is zero
Accumulation area	S_c	Area above equilibrium line
Ablation area	S_a	Area below equilibrium line
Accumulation-area ratio	AAR	$S_c /(S_c + S_a)$
Transient snow line		Line separating snow from ice or firn at any time t
Firn line		Transient snow line at time of minimum snow cover
Firn		Snow which has passed through (at least) one summer

1: Lower-case symbols are for point mass-balance quantities, and the corresponding upper-case symbols are for areal, including glacier-wide, mass-balance quantities.

The terminology in this Glossary diverges at several points from that summarized above.

Appendix B – Constants and Properties

Table B1 Physical properties of water substance

Property	*Expression*	*Remarks*
Ice point[1]	(T_m = 273.15 K = 0 ºC, p = 101 325 Pa)	Commonly called the melting point or freezing point
Triple point[1,2]	(T = 273.16 K, p = 611.7 Pa)	Temperature and pressure at which ice, water and water vapour are in thermodynamic equilibrium
Mean molecular weight[1]	0.018015 kg mol^{-1} ≅18 g mol^{-1}	Vienna Standard Mean Ocean Water (VSMOW)
Thermal conductivity[3]	$K = 2.238 - 0.0107\,T$ W m^{-1} K^{-1}	Pure ice, T in ºC
Effective thermal conductivity of dry snow[4]	$K_{eff} = 0.06 + 2.69 \times 10^{-6}\,\rho^2$	At –5 ºC; includes heat transfer by diffusion of vapour
Latent heat of vaporization[2]	L_v = 2500.8 kJ kg^{-1}	At 0 ºC
Latent heat of fusion[2]	L_f = 333.5 kJ kg^{-1}	Decreases nearly linearly to 289 kJ kg^{-1} at –20 ºC
Latent heat of sublimation[2]	L_s = 2834.2 kJ kg^{-1}	At 0 ºC; equal to $L_v + L_f$
Relative dielectric constant[5]	$\varepsilon_r' = 1$	Air
Relative dielectric constant[6]	$\varepsilon_r' = 88$	Water (0 ºC, below 500 MHz; decreases to 68 at 5 GHz and 42 at 10 GHz)
Relative dielectric constant[5]	$\varepsilon_r' \approx 3.15$	Ice of density 917 kg m^{-3}
Relative dielectric constant[5]	$\varepsilon_r' = (1 + 0.000845\,\rho)^2$	Firn of density ρ

1: BIPM 2006a; 2: Murphy and Koop 2005; 3: Pounder 1965; 4: Pitman and Zuckerman 1967; 5: real part only, Kovacs et al. 1995; 6: real part only, Ulaby et al. 1986.

Table B2 Temperature-dependent properties of pure ice (and supercooled water)

T (ºC)	ρ_i (kg m^{-3})	α_V ($\times 10^{-6}$ K^{-1})	κ ($\times 10^{-12}$ Pa^{-1})	e_{i*} (Pa)	e_{w*} (Pa)	K (W m^{-1} K^{-1})	C_p (J kg^{-1} K^{-1})
0	916.7	159	130	611.15	611.21	2.24	2114
−10	918.7	155	128	259.89	286.45	2.34	2036
−20	920.3	149	127	103.25	125.50	2.45	1958
−40	922.8	137	124	12.84	18.91	2.65	1806
−80	927.4	105	119	0.05	0.11	3.10	1517

T Temperature
ρ_i Density (Chemical Rubber Company 2008–09)
α_V Volumetric coefficient of thermal expansion (Chemical Rubber Company 2008–09)
κ Adiabatic compressibility (Chemical Rubber Company 2008–09)
e_{i*} Equilibrium vapour pressure (Murphy and Koop 2005)
e_{w*} Equilibrium vapour pressure over supercooled water (Murphy and Koop 2005)
K Thermal conductivity (Pounder 1965)
C_p Heat capacity at constant pressure (Murphy and Koop 2005)

Table B3 Pressure dependence of the melting point of ice (after Wagner et al. 1994)

Thickness of ice *h (m)*	*Pressure* *p (MPa)*	*Equilibrium temperature T_m (°C)*
200	1.80	–0.1
500	4.50	–0.3
1000	9.00	–0.7
2000	17.99	–1.3
5000	44.98	–3.3

The pressure is $\rho_i\, g\, h$, with density ρ_i = 917 kg m^{-3} and g acceleration due to gravity (*Table B5*). The equilibrium temperature is that of pure ice and water, changing with pressure at -7.4×10^{-8} K Pa^{-1}.

Table B4 Properties of water at 0 °C and 1000 hPa

Property		*Magnitude*
Density[1]	ρ_w =	999.84 kg m^{-3}
Heat capacity at constant pressure[2]	C_p =	4211 J kg^{-1} K^{-1}
Equilibrium vapour pressure[2]	e_{w*} =	611.2 Pa
Latent heat of vaporization[2]	L_v =	2500.8 kJ kg^{-1}
Thermal conductivity[1]	K_w =	0.561 W m^{-1} K^{-1}
Viscosity[1]	ν =	1793 μPa s

1: Chemical Rubber Company 2008–09; 2: Murphy and Koop 2005.

Table B5 Selected physical constants and reference values

Constant	*Magnitude*	*Remarks*
Speed of electromagnetic waves in a vacuum[1]	c = 299 792 458 m s^{-1}	≈ 3 × 10^{8} m s^{-1}
Gravitational constant[1]	$G = 6.67428 \times 10^{-11}$ m^3 kg^{-1} s^{-2}	
Gas constant[1]	R = 8.3145 J mol^{-1} K^{-1}	
Stefan-Boltzmann constant[1]	$\sigma = 5.6704 \times 10^{-8}$ W m^{-2} K^{-4}	
Reference value		
Mean radius of the Earth[2]	R_E = 6371007 m	Radius of a sphere of area equal to that of WGS84 reference ellipsoid
Acceleration due to gravity[3]	g = 9.81 m s^{-2}	"Standard acceleration due to gravity" is exactly 9.80665 m s^{-2}, but the acceleration at sea level varies with location within a range of about 0.5%
Sea-level pressure[4]	p_0 = 101 325 Pa	Pressure at sea level in the ICAO standard atmosphere
Area of the ocean[5]	$S_O = 362.5 \times 10^6$ km^2	Includes 1.555 × 10^6 km^2 beneath ice shelves

1: Mohr et al. 2006; 2: NIMA 2000; 3: BIPM 2006a; 4: International Civil Aviation Organization 1993. 5: from data of Wessel and Smith 1996, Fox and Cooper 1994.

Table B6 Density of frozen water in various forms

Material		*Density (kg m^{-3})*
SURFACE SNOW[1,2]		
	Newly fallen snow in cold, calm conditions	10 – 65
	Newly fallen snow near the *freezing point*	100 – 300
	Settled snow	200 – 300
	Wind-packed snow	350 – 400
DEPTH HOAR[2]		100 – 300
FIRN[1]		
	Firn	400 – 650
	Thawed and refrozen firn, and "firn-ice"	600 – 830
GLACIER ICE[2]		830 – 917
PURE MONOCRYSTALLINE ICE[3]		
	0 ºC	916.7
	–10 ºC	918.7
	–20 ºC	920.3
	–40 ºC	922.8
	–80 ºC	927.4

1: Seligman 1936 and others; 2: Paterson 1994; 3: Chemical Rubber Company, 2008–09.

Bibliography

Ahlmann, H.W., 1939, Scientific results of the Swedish-Icelandic investigations 1936–37–38. Chapter VII. The regime of Hoffellsjökull, *Geografiska Annaler*, **21**, 177–188.

Ahlmann, H.W., 1935, Scientific results of the Norwegian-Swedish Spitsbergen Expedition 1934. Part V. The Fourteenth of July Glacier, *Geografiska Annaler*, **17**, 167–218.

American Meteorological Society, 2000, *Glossary of Meteorology*. 2nd edition, ed. T.S. Glickman. American Meteorological Society, Boston, MA. 850p.

Anonymous, 1969, Mass-balance terms, *Journal of Glaciology*, **8**(52), 3–7.

Armstrong, T., B. Roberts and C. Swithinbank,1973, *Illustrated Glossary of Snow and Ice*. Special Publication 4, Scott Polar Research Institute, Cambridge. 2nd ed. 60p., photographs.

Bader, H., 1954, Sorge's Law of densification of snow on high polar glaciers, *Journal of Glaciology*, **2**(15), 319–323.

Bahr, D.B., M.F. Meier and S.D. Peckham, 1997, The physical basis of glacier area-volume scaling, *Journal of Geophysical Research*, **102**(B9), 20355–20362.

Benson, C.S., 1959, Physical Investigations on the Snow and Firn of Northwest Greenland 1952, 1953 and 1954, *Research Report 26*, Snow Ice and Permafrost Research Establishment, U.S. Army Corps of Engineers, Hanover, NH. 62p., appendices.

Benson, C.S., 1962, Stratigraphic Studies in the Snow and Firn of the Greenland Ice Sheet, *Research Report 70*, Snow Ice and Permafrost Research Establishment, U.S. Army Corps of Engineers, Hanover, NH. 93p., appendices.

BIPM, 2006a, *Le Système International d'Unités (SI)*. 8th edition, French and English texts. Bureau International des Poids et Mesures, Paris. 180p.

BIPM, 2006b, *A Concise Summary of the International System of Units, the SI*. Bureau International des Poids et Mesures, Paris. 4p.

Canadian Avalanche Association, undated, *Glossary*. Canadian Avalanche Association, Revelstoke, BC, Canada.

Chemical Rubber Company, 2008–2009, *Handbook of Chemistry and Physics*, 89th ed.

Chen, J., and M. Funk, 1990, Mass balance of Rhonegletscher during 1882/83–1986/87, *Journal of Glaciology*, **36**(123), 199–209.

Colbeck, S.C., E. Akitaya, R. Armstrong, H. Gubler, J. Lafeuille, K. Lied, D. McClung and E. Morris, undated [1990?], *The International Classification for Seasonal Snow on the Ground*. Working Group on Snow Classification, International Commission on Snow and Ice of the International Association of Scientific Hydrology. 29p.

Elsberg, D.H., W.D. Harrison, K.A. Echelmeyer and R.M. Krimmel, 2001, Quantifying the effects of climate and surface change on glacier mass balance, *Journal of Glaciology*, **47**(159), 649–658.

European Avalanche Services, 2009, *Glossary Snow and Avalanches*, Working Group, European Avalanche Forecasting Services.

Fierz, C., R.L. Armstrong, Y. Durand, P. Etchevers, E. Greene, D.M. McClung, K. Nishimura, P.K. Satyawali and S.A. Sokratov, 2009, The International Classification for Seasonal Snow on the Ground, *Technical Documents in Hydrology*, **83**. UNESCO-IHP, Paris. 90p.

Finsterwalder, R. (Richard), 1953, Photogrammetry and glacier research with special reference to glacier retreat in the eastern Alps, *Journal of Glaciology*, **2**(15), 306–313.

Fox, A.J., and A.P.R. Cooper, 1994, Measured properties of the Antarctic ice sheet derived from the SCAR Antarctic digital database, *Polar Record*, **30**(174), 201–206.

Glaciers Online, undated, *Photoglossary: Illustrated Glossary of Glaciological Terms*.

Gray A.L., N. Short, K.E. Mattar and K.C. Jezek, 2001, Velocities and ice flux of the Filchner Ice Shelf and its tributaries determined from speckle tracking interferometry, *Canadian Journal of Remote Sensing*, **27**(3), 193–206.

Harrison, W.D., 1972, Temperature of a temperate glacier, *Journal of Glaciology*, **11**(61), 15–29.

Holmlund, P., and P. Jansson, 2002, *Glaciologi*. Stockholm University/Swedish Research Council, Stockholm.

Hubbard, B., and N. Glasser, 2005, *Field Techniques in Glaciology and Glacial Geomorphology*. Wiley, Chichester. 400p.
Huss, M., A. Bauder and M. Funk, 2009, Homogenization of long-term mass-balance time series, *Annals of Glaciology*, **50**(50), 198–206.
Hutter, K., 1983, *Theoretical Glaciology*. Reidel, Dordrecht. 510p.
International Civil Aviation Organization, 1993, *Manual of the ICAO Standard Atmosphere: extended to 80 kilometres (262 500 feet)*, Doc 7488-CD. 3rd edition.
ISMASS Committee, 2004, Recommendations for the collection and synthesis of Antarctic Ice Sheet mass balance data, *Global and Planetary Change*, **42**, 1–15.
Jóhannesson, T., C. Raymond and E. Waddington, 1989, Time-scale for adjustment of glaciers to changes in mass balance, *Journal of Glaciology*, **35**(121), 355–369.
Jones, H.G., 2008, From Commission to Association: the transition of the International Commission on Snow and Ice (ICSI) to the International Association of Cryospheric Sciences (IACS), *Annals of Glaciology*, **48**, 1–5.
Kaser, G., A.G. Fountain and P. Jansson, 2003, A Manual for Monitoring the Mass Balance of Mountain Glaciers, *Technical Documents in Hydrology*, **59**, UNESCO, Paris. 107+20p.
Kotlyakov, V.M., ed., 1984, *Glyatsiologicheskiy Slovar'*. Gidrometeoizdat, Leningrad. 527p. [*Glaciological Dictionary*. In Russian.]
Kotlyakov, V.M., and N.A. Smolyarova, 1990, *Elsevier's Dictionary of Glaciology in Four Languages*. Elsevier, Amsterdam. 336p.
Kovacs, A., A.J. Gow and R.M. Morey, 1995, The in-situ dielectric constant of polar firn revisited, *Cold Regions Science and Technology*, **23**(3), 245–256.
Mayo, L.R., M.F. Meier and W.V. Tangborn, 1972, A system to combine stratigraphic and annual mass-balance systems – a contribution to the International Hydrological Decade, *Journal of Glaciology*, **11**(61), 3–14.
Lliboutry, L., 1971, Permeability, brine content and temperature of temperate ice, *Journal of Glaciology*, **10**(58), 15–29.
Meier, M.F., 1962, Proposed definitions for glacier mass budget terms, *Journal of Glaciology*, **4**(33), 252–263.
Meier, M.F., and A. Post, 1987, Fast tidewater glaciers, *Journal of Geophysical Research*, **92B**, 9051-9058.
Mercanton, P.L., 1916, Vermessungen am Rhonegletscher: 1874-1915, *Neue Denkschriften der Schweizerischen Naturforschenden Gesellschaft*, **52**. 189p.
Mohr, P.J., B.N. Taylor and D.B. Newell, 2006, *CODATA Recommended Values of the Fundamental Physical Constants*. National Institute of Standards and Technology, Gaithersburg, Maryland, U.S.A. 105p.
Murphy, D.M., and T. Koop, 2005, Review of the vapour pressures of ice and supercooled water for atmospheric applications, *Quarterly Journal of the Royal Meteorological Society*, **131**, 1539–1565.
NIMA, 2000, *Department of Defense World Geodetic System 1984: Its Definition and Relationships with Local Geodetic Systems*, Technical Report 8350.2, 3rd edition, Amendment 1. National Imagery and Mapping Agency, Bethesda, Maryland.
NSIDC, undated, *Glossary*. National Snow and Ice Data Center, Boulder, CO.
Oerlemans, J., and Reichert, B.K., 2000, Relating glacier mass balance to meteorological data using a Seasonal Sensitivity Characteristic (SSC), *Journal of Glaciology*, **46**(152), 1–6.
Østrem, G., and M.M. Brugman, 1991, *Glacier Mass-balance Measurements: A Manual for Field and Office Work*, Report 4, National Hydrology Research Institute, Environment Canada, Saskatoon. 224p.
Østrem, G., and A. Stanley 1969, *Glacier Mass-balance Measurements: A Manual for Field and Office Work*, Energy, Mines and Resources Canada, Ottawa, and Norwegian Water Resources and Electricity Board, Oslo. 129p.
Østrem, G., and A. Stanley 1966, *Glacier Mass-balance Measurements: A Manual for Field Work*, Department of Mines and Technical Surveys, Ottawa. 81p.
Paterson, W.S.B., 1994, *The Physics of Glaciers*. 3rd edition, Elsevier Science, Tarrytown, N.Y. 480p.

Pettersson, R., 2004, Dynamics of the cold surface layer of polythermal Storglaciären, Sweden, Ph.D. thesis, Department of Physical Geography and Quaternary Geology, Stockholm University.
Pitman, D., and B. Zuckerman, 1967, Effective thermal conductivity of snow at −88º, −27º, and −5ºC, *Journal of Applied Physics*, **38**(6), 2698−2699.
PhysicalGeography.net, undated, *Glossary of Terms*.
Pounder, E.R., 1965, *The Physics of Ice*. Pergamon Press, Oxford. 151p.
Press, W.H., S.A. Teukolsky, W.T. Vetterling and B.P. Flannery,1992, *Numerical Recipes in Fortran*. 2nd ed., Cambridge University Press.
Radok, U., 1997, The International Commission on Snow and Ice (ICSI) and its precursors, 1894–1994, *Hydrological Sciences Journal*, **42**(2), 131–140.
Rau, F., F. Mauz, S. Vogt, S.J. Singh Khalsa and B. Raup, 2005, *Illustrated GLIMS Glacier Classification Manual: Glacier Classification Guidance for the GLIMS Inventory*. Version 1. GLIMS Regional Center "Antarctic Peninsula", Institut für Physische Geographie, Albert-Ludwigs-Universität, Freiburg. 36p.
Raup, B., A. Racoviteanu, S.J.Singh Khalsa, C. Helm, R. Armstrong and Y. Arnaud, 2007, The GLIMS geospatial glacier database: a new tool for studying glacier change, *Global and Planetary Change*, **56**(1–2), 101–110.
Raup, B., and S.J. Singh Khalsa, 2007, *GLIMS Analysis Tutorial*. 15p.
Schoof, C., 2007, Ice sheet grounding line dynamics: steady states, stability, and hysteresis, *Journal of Geophysical Research*, **112**, F03S28, doi:10.1029/2006JF000664.
Seligman, G., 1936, *Snow Structures and Ski Fields*. Macmillan, London.
Shumskiy, P.A., 1955, *Osnovy Strukturnogo Ledovedeniya*. Izdatel'stvo Akademii Nauk SSSR, Moscow. 492p. Translated by D. Kraus, 1964, as *Principles of Structural Glaciology*, Dover, New York. 497p.
Ulaby, F.T., R.K. Moore and A.K. Fung, 1986, *Microwave Remote Sensing: Active and Passive. Volume III: From Theory to Applications*. Artech House, Norwood, MA.
UNESCO, undated, *International Glossary of Hydrology*.
UNESCO/IASH, 1973, Combined Heat, Ice and Water Balances at Selected Glacier Basins, Part II: Specifications, Standards and Data Exchange, *Technical Papers in Hydrology*, **5**. UNESCO/IASH, Paris. 32p.
UNESCO/IASH, 1970, Combined Heat, Ice and Water Balances at Selected Glacier Basins: A Guide for Compilation and Assemblage of Data for Glacier Mass Balance Measurements, *Technical Papers in Hydrology*, **5** ["Part I"]. UNESCO/IASH, Paris. 20p.
van Everdingen, R., ed., 2005, *Multi-language glossary of permafrost and related ground-ice terms*. National Snow and Ice Data Center/World Data Center for Glaciology, Boulder, CO.
Wagner, W., A. Saul and A. Pruss, 1994, International equations for the pressure along the melting and along the sublimation curve of ordinary water substance, *Journal of Physical and Chemical Reference Data*, **23**, 515−527.
Wessel, P., and W.H.F. Smith, 1996, A global, self-consistent, hierarchical, high-resolution shoreline database, *Journal of Geophysical Research*, **101**(B4), 8741–8743.
WGMS, 2008a, *Global Glacier Changes: Facts and Figures*, Zemp, M., I. Roer, A. Kääb, M. Hoelzle, F. Paul and W. Haeberli, eds., UNEP, World Glacier Monitoring Service, Zürich. 88p.
WGMS, 2008b, *Fluctuations of Glaciers 2000-2005 (Vol. IX)*, Haeberli, W., M. Zemp, A. Kääb, F. Paul and M. Hoelzle, eds., ICSU (FAGS)/IUGG (IACS)/UNEP/ UNESCO/WMO, World Glacier Monitoring Service, Zürich. 266p.
WGMS, 2007a, *Glacier Mass Balance Bulletin No. 9 (2004-2005)*, Haeberli, W., M. Zemp and M. Hoelzle, eds., ICSU (FAGS)/IUGG (IACS)/UNEP/UNESCO/WMO, World Glacier Monitoring Service, Zürich. 100p.
WGMS, 2007b, *Submission of Glacier Fluctuation Data to the World Glacier Monitoring Service – General Guidelines and Attribute Descriptions*. World Glacier Monitoring Service, Zürich. 18p.

WGMS, 1989, *World Glacier Inventory: Status 1988*, Haeberli, W., H. Bösch, K. Scherler, G. Østrem and C.C. Wallén, eds., IAHS (ICSI)/UNEP/UNESCO, World Glacier Monitoring Service, Zürich. 458 p.

Publication 6

Paul, F., Barry, R.G., Gogley, J.G., Frey, H., Haeberli, W., Ohmura, A., Ommanney, S.C.L., Raup, B., Rivera, A. & **Zemp, M.** (2009). **Recommendations for the compilation of glacier inventory data from digital sources.** Annals of Glaciology, 50(53), 119-126.

Recommendations for the compilation of glacier inventory data from digital sources

F. PAUL,[1] R. BARRY,[2] G. COGLEY,[3] H. FREY,[1] W. HAEBERLI,[1] A. OHMURA,[4] S. OMMANNEY,[5] B. RAUP,[2] A. RIVERA,[6] M. ZEMP[1]

[1]*Department of Geography, University of Zürich-Irchel, Winterthurerstrasse 190, CH-8057 Zürich, Switzerland*
E-mail: fpaul@geo.unizh.ch
[2]*National Snow and Ice Data Center/World Data Center for Glaciology, CIRES, University of Colorado, Boulder, CO 80309-0449, USA*
[3]*Department of Geography, Trent University, Peterborough, Ontario K9J 7B8, Canada*
[4]*Institute for Atmospheric and Climate Science, ETH Zürich, CH-8092 Zürich, Switzerland*
[5]*56 Spinney Road, PO Box 730, R.R. #1, Glenwood, Yarmouth County, Nova Scotia B0W 1W0, Canada*
[6]*Centro de Estudios Cientificos, Av. Arturo Prat 514, Casilla 1469, Valdivia, Chile*

ABSTRACT. Modern geoinformatic techniques allow the automated creation of detailed glacier inventory data from glacier outlines and digital terrain models (DTMs). Once glacier entities are defined and an appropriate DTM is available, several possibilities exist to derive the inventory data (e.g. minimum, maximum and mean elevation; mean slope and aspect) for each glacier from digital intersection of both datasets. Compared to the former manual methods, the new grid-based statistical calculations are very fast and reproducible. The major aim of this contribution is to help in standardizing the related calculations to enhance the integrity of the Global Land Ice Monitoring from Space (GLIMS) database. The recommendations were prepared by a working group and also contribute to the European Space Agency project GlobGlacier. The document follows the former UNESCO manual for the production of the World Glacier Inventory published in 1970, identifies the potential pitfalls, and describes the differences from the former methods of compilation. The online background material for this paper (see http://www.glims.org) contains example scripts for calculation of each parameter and will be updated when required.

1. INTRODUCTION

The guidelines outlined here are designed to help in the efficient compilation of glacier inventory data from digital sources (vector outlines, digital terrain models (DTMs)) according to the standards set in the former UNESCO manual (UNESCO/IASH, 1970). This idea was suggested by A. Ohmura at the Workshop on World Glacier Inventory that took place in Lanzhou, China, in September 2008. A small group of experts involved in former and current glacier-inventory efforts was nominated to draft the recommendations. The initial focus is on the basic glacier parameters to be compiled. The importance of such compilations is growing in response to the need for regional to global assessments of climate-change impacts, today involving new approaches and advanced technologies. Where more detailed information is available (e.g. the primary classification of glacier type), those data should be included.

In this context, the term 'glacier' refers to all types of glaciers (e.g. valley, mountain, cirque) as well as to ice caps and icefields. The two continental ice sheets Antarctica and Greenland, their outlet glaciers and ice shelves are not considered here. Certain parts of the original recommendations (UNESCO/IASH, 1970; Müller and others, 1977) no longer apply, as techniques have changed (e.g. punch cards are no longer in use), the source material is now digital and the focus is now on climate-change impacts. This has motivated the decision to compile a new set of recommendations.

The most important changes in this document, compared to the former UNESCO manual for the production of the World Glacier Inventory (WGI), are due to the availability of modern data-generation techniques, such as Geographic Information Systems (GIS). In part, the applied methods result in parameters that differ from those obtained previously and thus cannot be compared directly (Manley, 2008). The second important difference is that two-dimensional (2-D) glacier outlines in a digital vector format are now used in addition to the point information available in the former inventory (WGMS, 1989). The related format specifications have been developed within the framework of the Global Land Ice Measurements from Space (GLIMS) initiative (Raup and others, 2007), and a database that stores the information is maintained at the US National Snow and Ice Data Center (NSIDC) in Boulder, CO, USA.

While the 2-D outlines strongly facilitate assessment of glacier changes, rules have to be applied that allow the clear identification of glacier entities independent of the geographic region or the data source (e.g. aerial photography or satellite imagery). These rules have been compiled in the 'GLIMS Analysis Tutorial' (B. Raup and S.J.S. Khalsa, www.glims.org/MapsAndDocs/guides.html) and thus are not discussed here. Further documents describing methods for the automated mapping of glacier outlines from optical satellite data are in preparation. Practical recommendations for glacier mapping are given by Racoviteanu and others (2009). A comprehensive overview of the World Glacier Monitoring Service (WGMS) database was given by WGMS (2008), and a review of the available WGI data is given by Cogley (2009).

2. PERENNIAL SNOW AND ICE MASSES TO BE REGISTERED

In principle, all perennial snow and ice masses should be compiled for a glacier inventory irrespective of size, debris cover, type or other factors. This implies that imagery acquired at the end of the ablation period or dry season is preferred, i.e. without seasonal snow outside the glaciers. To achieve this, every effort should be made to screen the available images and select only the best scenes for glacier mapping, even when parts of them are cloud-covered. However, in some regions it might be difficult to find even a single scene that is free of seasonal snow outside the glaciers. From a practical point of view, it can be very difficult to discriminate between seasonal and perennial snow on a single (satellite) image. As errors are large when seasonal snow is mapped instead of perennial snow or glaciers, a first general recommendation is to identify and mark all snowfields that do not show any bare ice at all. When possible, multitemporal analysis is recommended to separate seasonal snow from perennial snow or glaciers.

It has been recognized from previous studies that human, as opposed to automated, delineation of glacier outlines tended to digitize only a part of all glaciers in a region, in general the largest ones. This can lead to biased size class distributions and may hide important information about ongoing changes, as in many regions the smallest glaciers may exhibit the strongest changes and can make a significant contribution to the total change (e.g. Paul and others, 2004b). The second recommendation is to use one of the many simple, but robust, automated mapping techniques (e.g. band ratios) to map the entire glacier sample and then use manual delineation to correct this classification (e.g. for water bodies, debris cover, shadow, snowfields, and ice on water). Further details are given by Raup and Khalsa (www.glims.org/MapsAnd
Docs/guides.html) as well as Racoviteanu and others (2009). A manual deselection of seasonal snowfields or any unclear region should also be performed.

The minimum size of the glaciers was not defined consistently for the existing inventories. For example, the inventory of glaciers in Svalbard recorded only ice bodies larger than 1 km^2 (WGMS, 1989). In the Alps, with a different size distribution, 90% of the glaciers would have been left out according to this rule. On the other hand, a size of 0.01 km^2 could be seen as a practical lower limit, as entities smaller than this can be very numerous and their status as glaciers is likely to be doubtful. This is also the minimum size that can be identified with certainty under good conditions from satellite sensors operating at 15–30 m spatial resolution (e.g. Terra Advanced Spaceborne Thermal Emission and Reflection Radiometer (ASTER), SPOT High Resolution Visible (HRV), Landsat Thematic Mapper (TM)/Enhanced TM Plus (ETM+)). It is thus recommended that 0.01 km^2 be used as the minimum size to be registered when conditions permit. This small size is also important for following temporal developments. Entities that were much larger in a previous inventory might have shrunk to this size or to several patches of this size. In the latter case, the total size of the remaining ice bodies could again be larger than 0.01 km^2. Also, from a statistical point of view, it is necessary to make the comparison against some value rather than none.

3. SOURCE MATERIAL

For the application of the methods presented here, we assume that digital glacier outlines (i.e. individual entities including their debris-covered parts rather than contiguous ice masses) and a DTM are available. While the sources of the outlines and DTM are not prescribed, both should have been acquired within the same decade, and the spatial resolutions of both datasets should be comparable. The metadata of the source material are stored separately in the GLIMS database (B. Raup and S.J.S. Khalsa, 'A method for transferring GLIMS analysis products from regional centers to NSIDC. Version 1.2', www.glims.org/MapsAndDocs/). Within the framework of the Global Terrestrial Network for Glaciers (GTN-G), the use of satellite data is highly recommended for the compilation of glacier inventory data. This has the advantage of covering large areas at the same time, of permitting automated mapping from multispectral sensors and of an appropriate spatial resolution for the target. However, glacier outlines digitized from topographic maps of sufficient quality and detail can also be used.

For a thorough description of the related digitizing work, refer to Fountain and others (2007). When working with satellite data at 15–30 m resolution, the DTM should optimally have the same resolution. However, a DTM with 100 m resolution can still be used for glaciers at least 0.1 km^2 in size, which corresponds to 10 pixels at 100 m. In regions with rapid and strong glacier changes, the DTM should be no more than 5–10 years older than the satellite scene to avoid wrong topographic parameters such as minimum elevation. In any case, inclusion of the date of the DTM will be mandatory.

For a global glacier inventory it would be ideal to use the same satellite sensor, year of data acquisition, DTM, mapping method and classification guidelines for all countries. Because this is not feasible, it is difficult to make general recommendations. However, as some countries might be able to follow a common guideline in this regard, we summarize a few points (input data, method, date) that should help create a more consistent global glacier inventory.

In view of the free availability of Landsat data from the US Geological Survey archive, the Shuttle Radar Topography Mission 3 (SRTM3) DTM from 2000 at about 90 m resolution (void filled from http://srtm.csi.cgiar.org/), the new ASTER global DEM (GDEM) and the well-established automated mapping methods such as band ratios with a threshold, the following recommendations can be made:

Landsat ETM+ or TM data from the year 2000 (±5 years) should be used. In regions with tiny glaciers, ASTER scenes may be preferable.

The void-filled version of the SRTM3 DTM version 4 (A. Jarvis and others, http://srtm.csi.cgiar.org/PDF/Jarvis4.pdf) or the new global ASTER GDEM (Hayakawa and others, 2008) should be used.

A thresholded band ratio (e.g. TM3/TM5 or ASTER 2/4) with an additional threshold in band 1 of each sensor for improved shadow mapping should be used for automated glacier delineation (clean ice). Regions of misclassification (lakes, debris cover, shadow, seasonal snow, ice on water) should be corrected manually. For mapping of lakes and debris cover, semi-automated methods have been proposed in the literature (e.g.

Huggel and others, 2002; Paul and others, 2004a; Bolch and others, 2007), which can help with the correction.

The published guidelines for determining glacier entities (Raup and Khalsa, www.glims.org/MapsAndDocs/guides.html) and calculation of glacier parameters as given in this document should be followed.

In view of the rapid technological developments (new sensors or data sources), it is expected that the global picture of glaciers and ice caps will become more and more complete. In particular, updated glacier inventories and related change assessments will increasingly become available for different parts of the world. In this respect, it is paramount to have methodological coherence in the derived datasets. Future sensors might permit calculation of additional relevant glacier parameters or the development of operational glacier monitoring. Such opportunities will be described in forthcoming documents.

4. DATA ORGANIZATION

In order to accomplish a global glacier inventory quickly (Casey, 2003), a restriction to a minimum set of glacier parameters that can usually be generated automatically is recommended. This minimum set should be included in each compilation and consists of 12 elements: identification (ID), coordinates, date, surface area, length, minimum, maximum, mean and median elevation, as well as mean orientation and slope (see below for details). For the GLIMS database, the date of each dataset analysed (e.g. related to the acquisition date of a satellite scene) is a mandatory part of the submission and can automatically be transferred to all analysed glaciers. Their surface area is also calculated automatically in the database. Apart from length, the values for all parameters can be derived with automated GIS-based calculations which are assumed to be precise and objective. A general rule for the records in a database is that only quantities are stored that are not derived from the entries in the database. For example, the midpoint elevation, calculated as minimum plus maximum elevation divided by two, will not be reported, while the mean elevation as derived from DTM statistics will be included. Elevation range is minimum minus maximum elevation and thus is also not included in the database.

Apart from this minimum set, a large number of additional items are useful, but not mandatory for fast delivery; some require manual work, while others can be derived automatically. The former group includes: glacier name, national inventory code, former WGI code or hydrologic unit, debris-free surface area, primary classification (glacier type) and elevation of the snowline. The latter group includes: local ID, country code, hypsography in 100 m elevation bins, and elevations for certain area ratios. The latter are frequently used for modelling purposes (e.g. Haeberli and Hoelzle, 1995; Maisch and others, 2000; Hoelzle and others, 2007; Paul and others, 2007) because the elevation referring to a certain ratio (e.g. a 2 : 1 or 67% accumulation-area ratio (AAR)) can be used as a proxy for the steady-state equilibrium-line altitude (ELA_0) (e.g. Gross and others 1977). A recent study by Bahr and others (2009) indicates that a 1 : 1.5 ratio (57% AAR) fits better to the global mean value (59%).

Elevations can be derived automatically for each glacier using the original DTM, and one of the elevations can be used to separate a glacier in an accumulation and ablation region to derive some quantities (e.g. length, aspect) specifically for these regions, as in the former WGI. Thus, apart from the median elevation or 1 : 1 area ratio, the elevation corresponding to the 2 : 1 area ratio should also be reported. This would cover the typical range of measured values (e.g. WGMS, 2008) around a mean, and facilitate upper/lower bound modelling. In the end, it will be up to the analyst to decide which additional items are included in the submission. The data formats for most of the parameters are prescribed by the GLIMS data transfer specification (Raup and Khalsa, www.glims.org/MapsAndDocs/).

In this regard it is important to note that the elevation of the snowline as visible on the satellite imagery is only a proxy for the ELA of that specific year and only when image acquisition was close to the end of the ablation period. In Arctic regions, there is often a considerable difference between the elevation of the snowline and the ELA, as the superimposed ice zone is difficult to distinguish from bare ice on satellite imagery. This kind of annually highly variable information thus belongs to a fluctuation data series rather than to an inventory. Indeed, transient snowline positions were listed in the former WGI and have been used to derive further quantities. However, as detailed above, the quantities relevant for modelling with inventory data should be based on hypsographic area ratios which are more characteristic for the long-term status of glaciers (e.g. Furbish and Andrews, 1984).

A special topic is accuracy. The GLIMS glacier database allows the assignment of two accuracy values for each outline segment of a glacier. One is related to the overall positional accuracy of the input dataset (e.g. the root-mean-square error of x and y coordinates of the orthorectification), and the other to the accuracy of the outline delineation. The latter could be much lower in regions with debris cover compared to clean ice, shadow or for ice–ice divides in flat accumulation areas. As the compilation of this information is time-consuming for individual glacier segments, it is recommended that a fixed accuracy value be applied (e.g. size of one or two image pixels) to all glaciers as a first step for fast data submission. When time permits, further details can be added later to the accuracy item.

All meta-information required for clear identification of the dataset is submitted with the mandatory GLIMS files. These data files include among others information about the satellite scene used (date, path, row, sensor), the classification method applied, the name of the analyst and the date/region of the analysis, as well as the date/source/spatial resolution of the DTM. Of course, references to be cited, acknowledgements and any other important meta-information can also be submitted (see Raup and Khalsa, www.glims.org/MapsAndDocs/). In the case of a multitemporal composite for a specific region, the acquisition dates for each glacier entity are particularly important.

5. ADDITIONAL INFORMATION

There are several parameters of great practical use that can be calculated from the basic inventory entries and would thus not be part of the database. However, to ensure some consistency in the calculation, we also include the calculation for the orientation in eight sectors here. For a few glaciers, mean thickness values are available from extrapolated field measurements. They can be listed in the

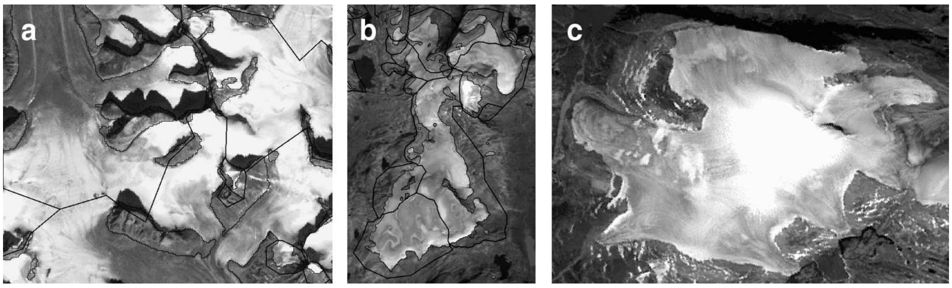

Fig. 1. (a) Uncertain drainage divides (estimated by straight lines) in the accumulation area of glaciers due to a missing DTM. The region is located near Penny Ice Cap, Baffin Island, Canada, and acquired by Landsat ETM+ (17-13) on 13 August 2000. (b) A compound glacier (Harbardsbreen) near Jostedalsbreen, Norway, as seen with Landsat TM (201-17) on 16 September 2006. Individual glaciers have been separated using a DTM. (c) A small ice cap with radial flow on Baffin Island as seen with Landsat ETM+ (21-11) on 30 July 2002. In this case the entire ice mass will be treated as one entity. Seasonal snow hides a part (<5%) of the perimeter.

'point_measurements' table of the GLIMS database. As part of the GTN-G database integration, it is planned to provide a joint map interface and a corresponding look-up table which link the available data from the WGMS, WGI, GLIMS and NSIDC photograph collection. This should allow easy access to mass-balance data or volume/length-change measurements.

A further point suggested here for the first time is a new 'remarks' item in the GLIMS database that gives a unique four-digit code for rapid identification of specific glacier characteristics (Table 1). This allows for an efficient selection or deselection of such special glaciers in global assessments. The numbering scheme follows that used in the WGI for the morphological classification of glaciers with one digit per item and considers the items snow conditions, calving, surging and ice divides. A basic intention of the reduced number of codes is to keep the scheme simple in order to facilitate its wide application. The digit 0 indicates that none of the criteria apply to a specific glacier and everything is normal, 8 is assigned to indicate that special remarks are given elsewhere for this item, and 9 is given as the default when the item is not classified. The unused numbers for each item are reserved for later extensions. Hence, in the default case, the remarks item has the code 9999 and if everything is normal 0000 which is equivalent to 0. If the code is larger than 0 but less than 10, something is special about the basin divides, and so forth. For example, a tidewater glacier with signs of surging (e.g. looped moraines) and uncertain drainage divides would receive the code 0121 (numerically equal to 121); or a (mainly) dry-calving ice cap where 20% of the perimeter is covered by seasonal snow would get the code 1303.

In Figure 1 some examples for glaciers which would be coded 1, 2 or 3 in the remarks column (i.e. special ice divides) are illustrated. Code 1, 'uncertain', is depicted in Figure 1a showing digitized straight lines in the snow-covered accumulation area of several adjacent glaciers. In this case, a DTM was not available and a lack of contrast prevents the location of the divide from being identified (Paul and Kääb, 2005). Similarly, a poor-quality DTM might not reveal the location properly and code 1 can be assigned to the related glaciers. A compound glacier (code 2) is an ice mass that is a composite of several individual glaciers (Fig. 1b) without the radial flow required for an ice cap. It is divided into individual entities, although the location of the divides might not be certain (Andreassen and others, 2008). On the other hand, an ice cap (code 3) has some sort of radial flow from one or more centres and is treated as one entity without divides (Fig. 1c).

When codes for the second and third digits are given, the derived topographic parameters (e.g. minimum or mean elevation) might be very different from those of neighbouring glaciers and should be excluded from the related statistical calculations. Problems related to glacier identification due to snow cover can be indicated with the first digit. Apart from debris cover, seasonal snow introduces the most serious problem for correct glacier delineation and thus has the highest number (1000 and larger). Whether a snowfield is seasonal or perennial can only be determined by multitemporal image analysis.

Table 1. Codes for the four digits of the new remarks column in the GLIMS glacier database. Abbreviations: perim.: perimeter, spec. rem.: see specific remarks, not spec.: not specified.

Code	1: Snow	2: Calving	3: Surging	4: Divides
0	normal	normal	normal	normal
1	hides 5–50% of perim.	tidewater	reported	uncertain
2	hides >50% of perim.	freshwater	signs	compound
3	perennial snowfield	dry	signs &reported	ice cap
4	seasonal snowfield	regenerated		
8	spec. rem.	spec. rem.	spec. rem.	spec. rem.
9	not spec.	not spec.	not spec.	not spec.

6. BASIC PARAMETERS

6.1. General remarks

In the compilation below, a description and a definition of each parameter is provided, including the description of the GIS-based method of calculation. Differences from the previous inventory guidelines are also given. In Table 2, all parameters are listed including a link to their calculation as given in the appendix of the online background material for this paper. The source codes are only given in that document to exemplify and better illustrate the manner of calculation. In the following, it is assumed that the newly created glacier inventory is the first one. The comparison of data from repeat inventories from two or more points in time and the related calculation of changes in any of the parameters will be addressed in forthcoming documents.

6.2. Identification/code

Each glacier entity must have a unique identification code. In the former guide this code was related to the political state and hydrological unit of major and lower-order streams. In the GLIMS database a unique code is generated (GLIMS-ID) from the geographic coordinates of the glacier. Automated scripts for generating the code from the geographic coordinates (latitude, longitude) of the glacier exist (see appendix 1 in the online background material). A point to consider is that a coordinate transformation must be applied to convert the coordinates of the finally assigned glacier entities from the projected coordinate system (e.g. Universal Transverse Mercator (UTM)) used for the analysis to geographic coordinates with the World Geodetic System 1984 (WGS84) datum before they can be converted to the GLIMS-ID. Also, all glacier outlines are stored in longitude/latitude coordinates in the GLIMS glacier database.

6.3. Coordinates

The coordinates should describe the location of a glacier as accurately as possible. In the former WGI it was recommended to place this point *in the upper part of the ablation area near the centre of the main stream*. This recommendation is still valid for manual assignment of the coordinates. Considering the available GIS-based methods, it is also acceptable to create a label point inside a glacier polygon automatically, and add the x-y coordinates of this point to the attribute table of the respective glacier (see example script in appendix 1 of the online background material). While this automated assignment is fast, it has to be noted that internal polygons might also receive a label point (depending on the software used) and these have to be replaced with the ID of the surrounding glacier. In general, the label point will be located somewhere inside the polygon, maybe very close to the outline of the glacier. As long as the number of digits for each geographical coordinate is sufficient to separate the labels of two adjacent glaciers, this is in general straightforward. The number of digits for the GLIMS ID is fixed.

In regions where glacier changes are small and the coordinates from a former glacier inventory are available, it should be determined whether the former coordinates are still within the current outlines. If they have been stored with a sufficient number of digits, it is possible that only a few label points have to be shifted slightly. This way of assigning label points is preferable in order to establish a link to the former inventory.

6.4. Date

Each glacier outline has to be associated with the date of its acquisition, if possible day, month and year. This can be done automatically for all glacier entities under consideration in a GIS. Special care is required when multitemporal data are used in the same region. For submission of results to the GLIMS database, the date of the analysed glacier outlines is a mandatory part in a separate file and is automatically linked to each outline.

6.5. Total surface area

The surface area of a glacier is an important parameter because it is used in many applications including global upscaling of glacier properties. It is thus recommended that the Raup and Khalsa tutorial (www.glims.org/MapsAndDocs/guides.html) be followed for defining individual glacier entities. Once this has been done, a GIS can automatically write the area and perimeter of the glacier polygon to the attribute table. It is important that glacier area is measured in an appropriate metric projection. The value should be recorded in square kilometres with three digits after the decimal point. This precision facilitates sorting glaciers into logarithmic (base 2) size classes in subsequent analysis.

For the transfer to the GLIMS database it is important that all polygons which are internal to a specific outer polygon are labelled as 'intrnl_rock' and that they have the same GLIMS-ID as the surrounding glacier, and are not simply represented as 'holes' in the outer polygon. On the other hand, rock outcrops shared by more than one glacier (called shared polygons) have no GLIMS-ID (Raup and Khalsa, www.glims.org/MapsAnd
Docs/guides.html), as they are not internal to any glacier polygon. There is a so-called flattening tool available on the GLIMS website that can be used to convert polygon holes that represent internal rock outcrops to polygons with appropriate GLIMS glacier IDs (http://glims.colorado.edu/tools/).

Table 2. Basic glacier parameters that should be provided with each GLIMS submission. For the scripts that describe the calculation of each parameter refer to appendixes 1 and 2 of the online background material **[[AUTHOR: shall we italicize as** x**,**y**,** l_{max}, etc. , in column 3 and capitalize as initial A in automatic in column 4 or leave as is?]

Name	Item	Symbol	Script
Code (GLIMS-ID)	ID	ID	App. 1
Coordinates	x_coord, y_coord	x,y	automatic
Acquisition date	Date	date	automatic
Surface area	Area_km2	S	automatic
Length (max.)	Length	l_{max}	Manual
Minimum elevation	Min	h_{min}	App. 2
Maximum elevation	Max	h_{max}	App. 2
Mean elevation	Mean	h_{mean}	App. 2
Median elevation	Median	h_{medi}	App. 2
Mean slope	Slope_deg	a	App. 2
Mean aspect	Aspect_360	ϕ_{360}	App. 2
Aspect sector	Aspect_sec	ϕ_{sec}	App. 2

6.6. Length

Glacier length is the most demanding parameter regarding additional manual work and uncertainty. The definitions used in the former guide are:

> *Mean length: The average of the lengths of each tributary along its longest flowlines to the glacier snout.*

and

> *Maximum length: The longest flowline of the whole glacier.*

These definitions still apply and it is recommended that initially only the maximum length be determined, as this reduces the workload considerably. The mean length could be added in a later step. When a DTM of sufficient quality is available, automated techniques can be used to identify the highest glacier point and then follow the steepest downward gradient until the curvature of the glacier surface changes from concave to convex. In this region – in general, the ablation area – manual digitization close to the central flowline of the main trunk might be more efficient. For manual digitization of the length, the flowline should cross contours perpendicularly. Uncertainty of the result is thereby reduced if flowline digitization starts at the lower end of the glacier.

6.7. Elevation (max, min, mean, median)

Highest, mean and lowest glacier elevation are also basic entries in the former WGI. It is recommended that they be derived from glacier-specific statistical analysis using the elevation information from the DTM and a local glacier ID as an identifier for the respective glacier or zone. The related script for calculation is given in appendix 2 of the online background material for this paper. It has to be noted that in the former inventory mean elevation was defined as the elevation of 'The contour line which divides the glacier surface in half', which is identical with the hypsographic 1 : 1 area ratio or median elevation. The mean value derived from zone statistics will represent a different value: the sum of all elevation values divided by the number of all cells used for the sum. This is different from the midpoint elevation and should thus be included in the inventory. The median elevation as calculated from area statistics represents the correct 1 : 1 elevation and should also be included.

6.8. Mean aspect

The aspect or orientation of a glacier is a useful parameter for all kinds of modelling (e.g. Evans, 2006). In the former UNESCO guidelines this variable was restricted to eight directions: 'Orientation of the down-glacier direction according to the eight cardinal points ... should be given.' The mean aspect as derived from a DTM allows one to consider the value of all individual cells covered by the glacier and to derive a mean value in the full 0–360° range. It must be taken into account that aspect is a circular parameter, which means that mean values must be derived by a decomposition in the respective sine and cosine values (Paul, 2007; Manley, 2008). A script that calculates the correct mean values is given in appendix 2 of the online background material. Apart from the improved detail and the objectivity of its calculation, the DTM-derived value also has a slightly different meaning than in the former inventory (e.g. main flow direction vs mean value of individual cells). The value could also be calculated separately for the accumulation and ablation region once they are defined and transformed to the eight cardinal directions.

6.9. Mean slope from the DTM

Mean slope is a value that could be derived from elevation range and glacier length and was thus not listed in the guidelines by UNESCO/IASH (1970). Mean slope as derived for each glacier from the DTM with zone statistics is independent of the glacier length and refers to all individual cells of the DTM (Manley, 2008). As mean slope is a good proxy for other parameters like mean thickness (Haeberli and Hoelzle, 1995) it is recommended that the DTM-derived mean slope value be included in the basic inventory.

6.10. Derived quantities

A large number of further parameters characterizing individual glaciers (e.g. driving stress, slope-dependent thickness, volume, thermal conditions, response and reaction times) can be derived or estimated from the basic parameters described above and in combination with climatic data as demonstrated in the case study for the European Alps by Haeberli and Hoelzle (1995). For details of their calculation the reader is referred to that publication.

7. FURTHER PARAMETERS

As mentioned in section 4, several further parameters exist that could be included in a glacier inventory, but their compilation is time-consuming and the entries are not mandatory for a fast submission. These parameters are briefly described in the following.

7.1. Glacier name

The glacier name facilitates discussion of the glacier, but is not unique. Where an official name of the main glacier is available, it should be provided. If no official name has been assigned, only a well-established unofficial name should be given. Meaningful abbreviations are allowed for very long names. The spelling of the name should be in the Latin alphabet without special characters. The local word for 'glacier' (e.g. Firn, Kees, Gletscher in the Alps) should be retained where it is an integral part of the name such as in Storbreen and Storglaciaeren**[AUTHOR: please confirm spelling: we normally have Storglaciaren]]**. If a glacier has more than one common name, a list of names may be provided, separated by commas.

7.2. WGI code or hydrologic unit

All glaciers with an entry in the former WGI should have a WGI code as a unique identifier. Where available, this code should be transferred to the new inventory. Moreover, major hydrological units and river systems have been identified on all continents (WGMS, 1989) and can be applied to previously unregistered units. The recommended clockwise numbering of the entities should be maintained. Problems of identifying the correct WGI code for more recent entities are related to:

the former assignment of glacier groups (only one code available for several glaciers, partly located in different drainage basins),

separate codes having been given to tributaries still connected to the main glacier,

only one code being available for a contiguous ice mass that should be separated into parts,

glaciers having no code at all as they were excluded in the former inventory (e.g. due to snow conditions or clouds),

codes having been given to seasonal rather than perennial snowfields.

All these issues can only be resolved if the generally analogue base maps from the former inventory are available for inspection. In many cases it will be necessary to assign the former code to more than one entity, as many glaciers have split into two or more parts in the past 30 years. When this can be done properly, it will help considerably in change assessment. In the GLIMS glacier database the relation to formerly connected glacier entities is addressed by the parent ice-mass code (see Raup and Khalsa, www.glims.org/MapsAndDocs/).

7.3. Exposed area

In general, optically thick (in respect to the averaged spectral information of one image pixel) debris cover is not mapped by the spectrally based automated methods. This implies that the debris-free surface area is available from the automated classification and the total area is given after manual correction of the debris-covered parts. Both values could be given when multispectral classification is used for glacier mapping.

7.4. Local ID

For practical reasons it is useful to work with a unique local ID for each glacier entity. This code should be a simple four- or five-digit number which could be assigned automatically to all glaciers. The local ID is particularly helpful when attribute items from external computations have to be joined with the main dataset and when statistics are calculated for each glacier zone.

7.5. Primary classification (glacier type)

The primary classification (WGMS, 1989) helps to characterize a glacier sample in more detail. Apart from the fact that the former key has to be extended when polar ice masses are classified (e.g. Cogley, 2008; F. Rau and others, 'Illustrated GLIMS glacier classification manual: glacier classification for the GLIMS inventory. Version 1', www.glims.org/MapsAndDocs/guides.html), little is known about the practical value of the classification. In particular, the classes are often not unique and different analysts might arrive at different types. When glaciers change rapidly (e.g. due to the formation of proglacial lakes), certain parts of the classification may also change in a short time, so updating the database might become a continuous effort. For this reason, it is recommended that the taxonomical classification be postponed to a later date. Of course, if the classification is available already, it should be submitted as well.

7.6. Elevation of the end-of-summer snowline

This parameter is mentioned here because it was compiled in many regions for the WGI. However, in most cases the transient snowline (TSL) was mapped in the WGI, which is of little relevance in glaciologic terms. Only when data are acquired at the end of the ablation period can the elevation of the snowline or the area covered by snow compared to the entire surface area (AAR) be used as a proxy for the mass balance or to assess local differences in accumulation. In this regard, snowlines can be considered as glacier fluctuation data (with strong changes from year to year) that must not be a part of an inventory but can be submitted to the WGMS. From this point of view it is recommended that time be spent on deriving the other parameters first.

7.7. Hypsography in 100 m bins

A new possibility, easily obtained by combining glacier outlines with the DTM, is the calculation of glacier-specific area–elevation distribution or hypsography. Such information would greatly improve the calculation of future glacier response to climate change, as glacier melt as well as precipitation is largely elevation-dependent. A 100 m binning (or sub-multiple thereof for very small glaciers) is recommended to maintain some consistency in the database and to cover the large range of possible values without losing relevant information for smaller glaciers. While the database transfer specification allows a designation of how elevations of bins are registered, it is recommended that the value for a specific elevation band (e.g. 3800 m) should refer to the range of the following 100 m (here 3800–3900 m). This would strongly facilitate the comparability of the created datasets and hence global applications. The GLIMS glacier database includes two tables that store the information about the hypsometry dataset as a whole (bin width, etc.) and another that stores the area (in km^2) in each elevation bin (for details see Raup and Khalsa, www.glims.org/MapsAndDocs/). A script for calculating a 100 m hypsography automatically for each glacier can be found in Paul (2007).

8. CONCLUSIONS

We have presented recommendations on how glacier parameters should be calculated for a detailed glacier inventory when digital glacier outlines and a DTM are available. The focus is on parameters that can be compiled automatically for each glacier. Most time-consuming is the manual digitizing of glacier length. Besides the basic parameters, other useful parameters are added for practical purposes. Considering the rapid technological development and the explosion of freely available datasets in the recent past, it is assumed that parts of the recommendations will have to be updated regularly. The online background material for this paper (available at http://www.glims.org) includes example source codes for calculation and will be updated when required.

ACKNOWLEDGEMENTS

The study was supported by a grant from the European Space Agency project GlobGlacier (21088/07/I-EC). Feedback from the GLIMS community as well as from the GlobGlacier user group and consortium is gratefully acknowledged.

REFERENCES

Andreassen, L.M., F. Paul, A. Kääb and J.E. Hausberg. 2008. Landsat-derived glacier inventory for Jotunheimen, Norway, and deduced glacier changes since the 1930s. *Cryosphere,* **2**(2), 131–145.

Bahr, D.B., M. Dyurgerov and M.F. Meier. 2009. Sea-level rise from glaciers and ice caps: a lower bound. *Geophys. Res. Lett.,* **36**(3), L03501. (10.1029/2008GL036309.)

Bolch, T., M.F. Buchroithner, A. Kunert and U. Kamp. 2007. Automated delineation of debris-covered glaciers based on ASTER data. *In* Gomarasca, M.A., *ed. GeoInformation in Europe. Proceedings of the 27th EARSeL Symposium, 4–6 June 2007, Bolzano, Italy.* Rotterdam, Millpress, 403–410.

Casey, A., *ed.* 2003. *Papers and recommendations: Snow Watch 2002 Workshop and Workshop on Assessing Global Glacier Recession, 31 October–1 November 2002, Camp Spring, MD.* Boulder, CO, National Snow and Ice Data Center. World Data Center A for Glaciology. (Glaciological Data GD-32.)

Cogley, J.G. 2008. *Extended format for the World Glacier Inventory. Revised edition.* Peterborough, Ont., Trent University. (Trent Technical Note 2005-1.)

Cogley, J.G. 2009. A more complete version of the World Glacier Inventory. *Ann. Glaciol.,* **50**(53), 32–38.

Evans, I.S. 2006. Local aspect asymmetry of mountain glaciation: a global survey of consistency of favoured directions for glacier numbers and altitudes. *Geomorphology,* **73**(1–2), 166–184.

Fountain, A.G., M.J. Hoffman, K.M. Jackson, H.J. Basagic, T.H. Nylen and D. Percy. 2007. Digital outlines and topography of the glaciers of the American West. *USGS Open File Rep.* 2006-1340.

Furbish, D.J. and J.T. Andrews. 1984. The use of hypsometry to indicate long-term stability and response of valley glaciers to changes in mass transfer. *J. Glaciol.,* **30**(105), 199–211.

Gross, G., H. Kerschner and G. Patzelt. 1977. Methodische Untersuchungen über die Schneegrenze in alpinen Gletschergebieten. *Z. Gletscherkd. Glazialgeol.,* **12**(2), 223–251.

Haeberli, W. and M. Hoelzle. 1995. Application of inventory data for estimating characteristics of and regional climate-change effects on mountain glaciers: a pilot study with the European Alps. *Ann. Glaciol.,* **21**, 206–212.

Hayakawa, Y.S., T. Oguchi and Z. Lin. 2008. Comparison of new and existing global digital elevation models: ASTER G-DEM and SRTM-3. *Geophys. Res. Lett.,* **35**(17), L17404. (10.1029/2008GL035036.)

Hoelzle, M., T. Chinn, D. Stumm, F. Paul and W. Haeberli. 2007. The application of glacier inventory data for estimating past climate change effects on mountain glaciers: a comparison between the European Alps and the Southern Alps of New Zealand. *Global Planet. Change,* **56**(1–2), 69–82.

Huggel, C., A. Kääb, W. Haeberli, P. Teysseire and F. Paul. 2002. Remote sensing based assessment of hazards from glacier lake outbursts: a case study in the Swiss Alps. *Can. Geotech. J.,* **39**(2), 316–330.

Maisch, M., A. Wipf, B. Denneler, J. Battaglia and C. Benz. 2000. *Die Gletscher der Schweizer Alpen. Gletscherhochstand 1850, Aktuelle Vergletscherung, Gletscherschwund-Szenarien.* Zürich, vdf Hochschulverlag AG ETH. (Schlussbericht NFP 31.)

Manley, W.F. 2008. Geospatial inventory and analysis of glaciers: a case study for the eastern Alaska Range. *In* Williams, R.S., Jr and J.G. Ferrigno, *eds. Satellite image atlas of glaciers of the world.* Denver, CO, United States Geological Survey, K424–K439. (USGS Professional Paper 1386-K.)

Müller, F., T. Caflisch and G. Müller. 1977. *Instructions for the compilation and assemblage of data for a world glacier inventory.* Zürich, ETH Zürich. Temporary Technical Secretariat for the World Glacier Inventory.

Paul, F. 2007. The new Swiss glacier inventory 2000: application of remote sensing and GIS. *Schr. Phys. Geogr. Univ. Zürich* 52.

Paul, F. and A. Kääb. 2005. Perspectives on the production of a glacier inventory from multispectral satellite data in Arctic Canada: Cumberland Peninsula, Baffin Island. *Ann. Glaciol.,* **42**, 59–66.

Paul, F., C. Huggel and A. Kääb. 2004a. Combining satellite multispectral image data and a digital elevation model for mapping debris-covered glaciers. *Remote Sens. Environ.,* **89**(4), 510–518.

Paul, F., A. Kääb, M. Maisch, T. Kellenberger and W. Haeberli. 2004b. Rapid disintegration of Alpine glaciers observed with satellite data. *Geophys. Res. Lett.,* **31**(21), L21402. (10.1029/2004GL020816.)

Paul, F., M. Maisch, C. Rothenbühler, M. Hoelzle and W. Haeberli. 2007. Calculation and visualisation of future glacier extent in the Swiss Alps by means of hypsographic modelling. *Global Planet. Change,* **55**(4), 343–357.

Racoviteanu, A.E., F. Paul, B. Raup, S.J.S. Khalsa and R. Armstrong. 2009. Challenges and recommendations in mapping of glacier parameters from space: results of the 2008 Global Land Ice Measurements from Space (GLIMS) workshop, Boulder, Colorado, USA. *Ann. Glaciol.,* **50**(53) (see paper in this issue).

Raup, B., A. Racoviteanu, S.J.S. Khalsa, C. Helm, R. Armstrong and Y. Arnaud. 2007. The GLIMS geospatial glacier database: a new tool for studying glacier change. *Global Planet. Change,* **56**(1–2), 101–110.

UNESCO/International Association of Scientific Hydrology (IASH). 1970. *Perennial ice and snow masses: a guide for compilation and assemblage of data for a world inventory.* Paris, UNESCO/IASH. (Technical Papers in Hydrology 1.)

World Glacier Monitoring Service (WGMS). 1989. *World glacier inventory: status 1988, ed.* Haeberli, W., H. Bösch, K. Scherler, G. Østrem and C.C. Wallén. IAHS(ICSI)–UNEP–UNESCO, World Glacier Monitoring Service, Zürich.

WGMS. 2008. *Global glacier changes: facts and figures, ed.* Zemp, M., I. Roer, A. Kääb, M. Hoelzle, F. Pau, and W. Haeberli. Geneva, World Glacier Monitoring Service/United Nations Environment Programme.

Publication 7

Koblet, T, Gärtner-Roer, I., **Zemp, M.**, Jansson, P., Thee, P., Haeberli, W. & Holmlund, P. (2010). **Re-analysis of multi-temporal aerial images of Storglaciären, Sweden (1959-99) - Part 1: Determination of length, area, and volume changes.** The Cryosphere, 4, 333-343.

The Cryosphere, 4, 333–343, 2010
www.the-cryosphere.net/4/333/2010/
doi:10.5194/tc-4-333-2010

The Cryosphere

Reanalysis of multi-temporal aerial images of Storglaciären, Sweden (1959–99) – Part 1: Determination of length, area, and volume changes

T. Koblet[1], **I. Gärtner-Roer**[1], **M. Zemp**[1], **P. Jansson**[2], **P. Thee**[3], **W. Haeberli**[1], **and P. Holmlund**[2]

[1]Department of Geography, University of Zurich, Winterthurerstrasse 190, 8057 Zürich, Switzerland
[2]Department of Physical Geography and Quaternary Geology, 106 91 Stockholm, Sweden
[3]Swiss Federal Institute for Forest, Snow and Landscape Research, Zürcherstrasse 111, 8903 Birmensdorf, Switzerland

Received: 1 March 2010 – Published in The Cryosphere Discuss.: 25 March 2010
Revised: 4 August 2010 – Accepted: 4 August 2010 – Published: 8 September 2010

Abstract. Storglaciären, located in the Kebnekaise massif in northern Sweden, has a long history of glaciological research. Early photo documentations date back to the late 19th century. Measurements of front position variations and distributed mass balance have been carried out since 1910 and 1945/46, respectively. In addition to these in-situ measurements, aerial photographs have been taken at decadal intervals since the beginning of the mass balance monitoring program and were used to produce topographic glacier maps. Inaccuracies in the maps were a challenge to early attempts to derive glacier volume changes and resulted in major differences when compared to the direct glaciological mass balances. In this study, we reanalyzed dia-positives of the original aerial photographs of 1959, -69, -80, -90 and -99 based on consistent photogrammetric processing. From the resulting digital elevation models and orthophotos, changes in length, area, and volume of Storglaciären were computed between the survey years, including an assessment of related errors. Between 1959 and 1999, Storglaciären lost an ice volume of $19\times10^6\,m^3$, which corresponds to a cumulative ice thickness loss of 5.69 m and a mean annual loss of 0.14 m. This ice loss resulted largely from a strong volume loss during the period 1959–80 and was partly compensated during the period 1980–99. As a consequence, the glacier shows a strong retreat in the 1960s, a slowing in the 1970s, and pseudo-stationary conditions in the 1980s and 1990s.

Correspondence to: T. Koblet
(thomas.koblet@gmail.com)

1 Introduction

Glacier volume change is of major concern when estimating the effects of climate change on factors such as sea level change and water resources in mountainous terrain (e.g., Lemke et al., 2007). With data from glacier change measurements spanning from century to decadal scales, techniques for measuring and processing data have evolved with developing technologies. Thus, it is important to carefully assess older data sets and homogenize these to remove any bias introduced by changing methods or processing. Homogenization of data series has become a standard for instrumental climate data series (e.g., Böhm et al., 2001) and is gaining importance as available glaciological data series increase in length (e.g., Thibert et al., 2008; Huss et al., 2009; Fischer, 2010).

Glaciological research at Storglaciären has a long tradition reaching back to the late 19th century, when early photo documentations were compiled in the Tarfala Valley (Holmlund et al., 1996). In 1910, the first detailed documentation with photographs and terrestrial photogrammetry was carried out (Holmlund, 1996) and continuous length change measurements were initiated. Systematic in-situ mass balance studies based on the direct glaciological method (cf. Østrem and Brugman, 1991) began in 1945/46 by the Swedish glaciologist Valter Schytt, when the Tarfala Research Station (Stockholm University) was constructed. Based on these continuous long-term observation series, a wealth of scientific studies has been produced, especially related to glacier mass balance measurements (e.g., Schytt, 1981; Holmlund and Jansson, 1999; Jansson, 1999; Schneider and Jansson, 2004; Holmlund et al., 2005; Jansson and Pettersson; 2007) and reconstructions (e.g., Holmlund, 1987; Raper et al., 1996; Linderholm et al., 2007), modelling (e.g., Hock, 1999; Albrecht et al., 2000; Hock and Holmgren, 2005), hydrology (e.g., Hock and Noetzli, 1997), and ice temperature (e.g., Pettersson et al., 2003, 2007).

In addition to the field observations, aerial photographs have been taken in decadal intervals since the beginning of the mass balance monitoring program. The resulting data were used to produce topographic glacier maps for the years 1949, -59, -69, -80, and -90, as well as for early, qualitative volume change assessments as summarized in Holmlund (1996). A first quantitative computation of glacier volume changes was done by Holmlund (1987). The author superimposed the maps of 1949, -59, -69, and -80, calculated changes in thickness at contour lines intersections and contoured at 5 m intervals, finally obtaining volume changes by planimetering. A first comparison with the glaciological mass balances showed large differences that were assumed to come from errors in the datum level of the maps (Holmlund, 1987). Albrecht et al. (2000) repeated the calculation of volume changes, this time based on digitized contour maps of 1959, -69, -80, and -90, interpolated to a regular grid for comparison with the glaciological mass balances. Again, major differences were attributed to inaccuracies in the maps and an error in the datum level. Also, the mapped glacier outlines and related area changes vary between different authors (cf. Holmlund, 1987; Holmlund et al., 2005), probably due to different interpretations of the glacier margins, where determining snow and shadow conditions present challenges. To complicate matters further, each map has its own history of basic data and assumptions, methods, revisions, and related errors (Holmlund, 1996). In order to reduce the errors of the maps and the related digitization processes, it is necessary to go back to the original aerial images and process them with consistent standard techniques.

In this study, we reanalyze the original aerial photographs of 1959, -69, -80, -90, and -99, applying a consistent photogrammetric processing strategy for all survey years. The resulting digital elevation models (DEMs) and orthophotos are used to determine and analyse length, area, and volume changes of Storglaciären. The main objective of the present study is to find out whether a thorough reanalysis of existing aerial photographs allows for a more accurate quantification of glacier changes. Given the limited number of long volumetric mass balance series, the quality control of existing data is very important. Therefore, the results are discussed including a qualitative and quantitative assessment of related uncertainties, in view of results from this and earlier studies as well as resulting consequences for future research. In a second paper (Zemp et al., 2010) the photogrammetrically derived volume changes of the present paper are compared to the in-situ mass balance measurements.

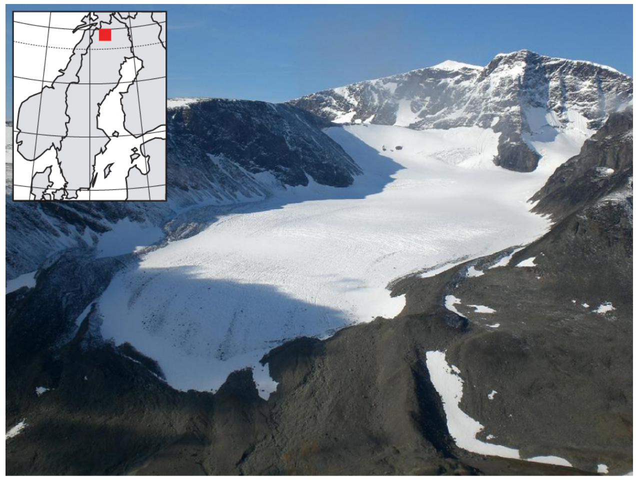

Fig. 1. Storglaciären in northern Sweden with Kebnekaise Mountain in the background. View to the west. Photo taken by T. Koblet in September 2008.

2 Study site

Storglaciären (67°55′ N, 18°35′ E) is located in the Kebnekaise massif in northern Sweden. As described by Schytt (1959) and Østrem et al. (1973), Storglaciären is classified as a small valley glacier of about 3 km^2 (cf. Table 6) with an elevation range from 1130 to 1700 m a.s.l. and is characterized by a branched accumulation area (Fig. 1). Based on its thermal regime the glacier is described as a polythermal glacier with a perennially cold surface layer in the ablation area (Hooke et al., 1983; Holmlund and Eriksson, 1989; Pettersson et al., 2003). Based on radio-echo sounding maps of the bed topography and the 1959 surface map, the ice volume of Storglaciären is approximately 300×10^6 m^3 (Björnsson, 1981; Eriksson et al., 1993; Albrecht et al., 2000). Based on these data the average ice thickness amounts to 100 m, with maximum values of 250 m (Björnsson, 1981). The mean annual air temperature (1965–2008) at the Tarfala Research Station (1130 m a.s.l.) is -3.5 ± 0.9°C; the average summer temperature (1946–2008) is 5.9 ± 1.2°C with maximum temperatures up to 20–25°C; the mean winter temperature (1965–2008) is -6.6 ± 1.1°C with minimum temperatures of c. -25°C (Grudd and Schneider, 1996, updated with unpublished data of Tarfala Research Station). The mean annual precipitation amounts to 1000 mm a^{-1} (Holmlund and Jansson, 2002; based on data from Tarfala Research Station since 1989) which must be considered as a minimum estimate with respect to Storglaciären.

3 Data and methods

3.1 Photogrammetric DEM computation

Repeated aerial photographs of the Storglaciären/Tarfala Valley had been taken by the Swedish Air Force in 1949 and by the Swedish mapping, cadastral, and land registration authority (Lantmäteriet) in the years 1959, -69, -80, -90, and -99 (Holmlund, 1996). Aside from the photographs of 1949, which were not available, the data from the years 1959–99 built the substantial database for the determination of length, area, and volume changes in this study. Since the original negatives of the aerial photographs were not available, copies of the positives were used for the photogrammetric analysis. Each survey consisted of three to four photographs with an overlap of 65% and therefore allowed for processing the images photogrammetrically. The mean scale of the aerial images is 1:30 000 (1:22 000 for the 1960 survey). An overview of the available data sets, including scales and survey dates, is given in Table 1.

For the photogrammetric DEM computation, a combination of analytical and digital photogrammetry was applied. The analytical work was performed on a WILD BC2000S plotter. The interior orientation was calculated from the fiducial marks given in the photographs and the camera calibration files, which were partly available at the Lantmäteriet. The 1999 survey was chosen as the master survey, since camera information and corresponding calibration files were identified clearly for 1999. This information was also available for 1990. Due to missing camera information on the earlier photographs, the corresponding parameters had to be assumed based on the available calibration files from Lantmäteriet.

The digital calculation of the DEMs was conducted within the photogrammetry software SocetSet (BAE Systems version 5.4.1). For this purpose the scanned photographs (resolution 12 µm) were used in combination with the interior orientation from the analytical step. To optimize the quality, an additional 53 tie points were identified for the relative orientation. Finally, the absolute orientation was performed by the implementation of 21 Ground Control Points (GCPs) from field surveys (Jansson and Pettersson, 1997, Tarfala Research Station, unpublished data). The pixel size of the resulting DEMs is 5 m. Based on these DEMs, orthophotos of each survey data were created within SocetSet.

3.2 Differential GPS survey (reference data)

In order to quantify the DEM accuracy by the comparison with independent reference data, 26 points were measured in the field with a TRIMBLE 4600LS differential global positioning system (dGPS). A first dGPS survey had been conducted already in the 1990s (Bomark and Lundberg, 1995; Jansson and Pettersson, 1997), but as only a few of the points are within reasonable distance of Storglaciären, additional reference points were surveyed in September 2008 and added to the data set. The theoretical accuracy of the measurements lies in the range of 0.02 m in the horizontal and about 0.04 m in the vertical. Due to long baselines, the actual positioning is approximately 0.05 m in the horizontal and 0.1 m in the vertical. Bomark and Lundberg (1995) as well as Pettersson and Jansson (2005) give comprehensive information on technical details and precision of the dGPS system used at the Tarfala Research Station. Fig. 2 shows the spatial distribution of the reference points. They are concentrated in the Tarfala Valley and on the mountain ridge on the southern side of Storglaciären since they had to be placed in non-moving terrain and ideally on bedrock.

Table 1. Orthophoto information. The survey dates are based on information from Lantmäteriet and are also labelled on the image margins of the original photographs for 1980/90/99. The mean scale of the images is calculated from the average flight altitude. The fraction of areas influenced by snow and shadow is determined within a bounding box around Storglaciären (cf. Fig. 2). The contrast at the glacier surface is qualitatively estimated from the orthophotos.

Date	Scale	No of images	Snow cover [%]	Shadow [%]	Contrast
23 Sep 1959	1:30 000	3	87	27	medium
14 Sep 1969	1:22 000	3	49	18	low
18 Aug 1980	1:30 000	3	12	13	high
04 Sep 1990	1:30 000	3	36	17	low
09 Sep 1999	1:30 000	4	35	22	medium

3.3 Glacier mapping and calculation of changes in length, area and volume

Glacier mapping serves as an important basis for determining glacier geometry and its changes and is influenced by the available data as well as by the operator's knowledge and experience. In this study, mapping was conducted by stereoscopic interpretation of the orthophotos as well as by geomorphometric analysis of the DEMs (e.g., shaded reliefs, profiles). Visualizations and spatial calculations were performed using ESRI ArcGIS Desktop 9.3.

The glacier outline was mapped and digitized for every survey date by the interpretation of the orthophotos and the DEMs. Based on experiences reported from previous studies (Albrecht et al., 2000; Holmlund et al., 2005) and discussions (Hock et al., 2008), it was assumed that the real changes of the areal extent of the accumulation area are smaller than the differences due to the interpreter. Hence, outlines of the glacier tongue were digitized for all the survey years, keeping the outline of the accumulation area consistent (based on the 1990 image). Length changes were calculated on the basis of the corresponding orthophoto (Fig. 3). Thereto, a band of stripes with 50 m distance was drawn parallel to the main flow direction of the glacier (i.e. W–E). Length change was

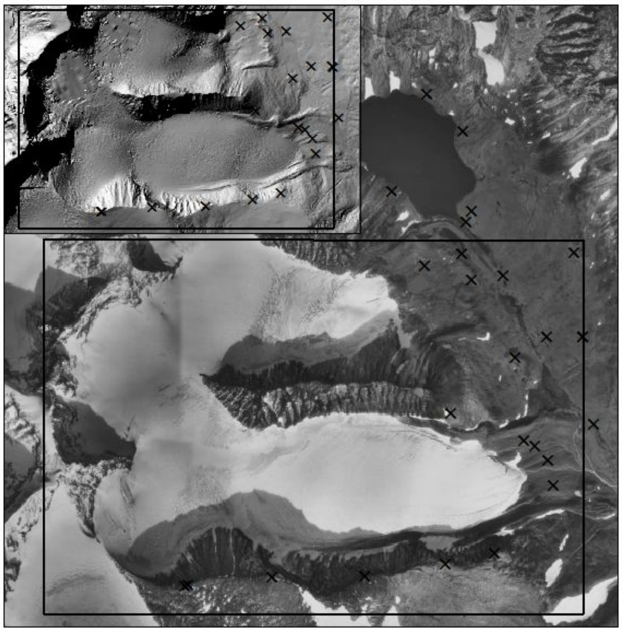

Fig. 2. Orthophoto and hill-shading of the corresponding DEM as computed from the aerial photographs of 1999. In addition, the locations of the 26 dGPS reference points and the bounding box used for the shadow and snow cover statistics (cf. Table 1) are shown.

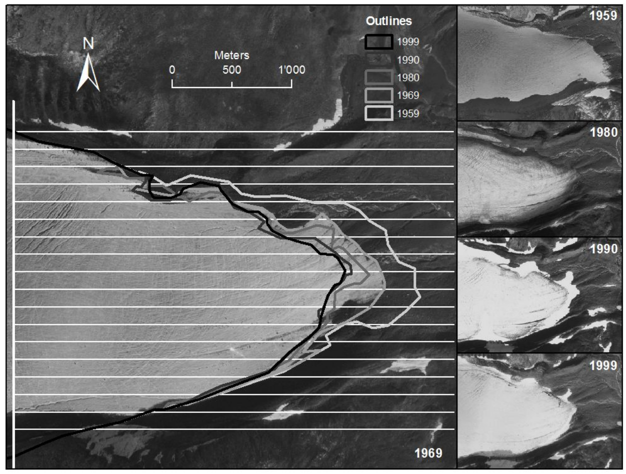

Fig. 3. Frontal retreat of Storglaciären as derived from the orthophotos. The average retreat rates are derived from the intersection of the glacier outlines with the band of stripes. Note the perennial snow banks in front of the glacier in the images of 1990 and 1999.

calculated as the average length from the intersection of the stripes with the glacier outlines (cf. Kappeler 2006). Based on the outlines of the different survey years, corresponding areas and area changes were calculated. The changes in ice thickness were quantified by subtracting the DEM at the earlier date from the DEM at the later date. Volume change was calculated by adding the thickness changes between two survey years within the outline at the time of the bigger extent and multiplied by the cell size (i.e. 25 m).

4 DEM and volume change accuracies

Probable sources of errors in the final DEMs are the quality of the raw data, technical information on the surveys (camera calibration files, dates), as well as ground control points. In addition, topography (steep slopes) and meteorological conditions (snow cover) influence the accuracy of a DEM. If a DEM represents the reality insufficiently, calculations based on DEMs are not reliable (Wood and Fisher, 1993; Temme et al., 2007). It is therefore essential that the accuracy, which is regarded as the difference between a recorded value and the true value, is specified (Jones, 1997). Many publications have examined the different methods to evaluate the accuracy of DEMs (e.g. Heuvelink, 1998; Kääb 2005; Fisher and Tate, 2006; Kraus, 2004; Kraus et al., 2006; Thibert et al., 2008). The range of methods varies from qualitative evaluation of shaded reliefs to complex error propagation modelling (e.g. Li et al., 2005). Thibert et al. (2008) present a sound and comprehensive error compilation approach for photogrammetric analysis of glacier volume changes. Such a detailed approach cannot be conducted within this study, as not all parameters are known for the early survey dates (due to missing camera calibration files) and because analogue and digital steps are combined in the photogrammetric processing.

In the following, we qualitatively evaluate the new DEMs and orthophotos and use three different approaches to quantitatively assess the uncertainty of the DEMs and derived elevation changes: (a) a comparison of the DEM values with an independent set of dGPS points in non-glacierized terrain and statistical significance testing of the glacier changes (signal) versus the elevation changes in non-glacierized terrain (noise), using (b) T-Test and (c) Monte-Carlo simulation approaches. The first two methods (a, b) are used to interactively estimate systematic and stochastic uncertainties of the glacier thickness and volume changes.

4.1 Qualitative evaluation of DEMs and orthophotos

The aerial photographs available for Storglaciären are well suited for the computation of DEMs and orthophotos, even though a lower accuracy must be expected in areas with steep terrain or low contrast (e.g., due to shadow, snow cover). A review of the different photographs (see Table 1) shows good contrast on the glacier surface in 1959, 1980, and 1999. An extract of the orthophoto of the year 1999 and the corresponding shaded relief are shown in Fig. 2. The hill-shading of the DEM shows a very plausible representation of the real terrain. Regional artefacts in the accumulation areas of Storglaciären and Isfallsglaciären correspond to areas with snow

Table 2. Validation of DEMs against 26 independent dGPS points. For the statistics given, the elevation of the dGPS points is subtracted from the elevation of the DEMs. The spatial distribution of the dGPS points is shown in Fig. 2.

Year	Mean [m]	RMSE [m]	STDV [m]	SE [m]
1959	−2.85	3.35	1.74	0.34
1969	−3.19	2.11	1.17	0.23
1980	−4.08	4.85	5.05	0.99
1990	−3.23	1.54	0.98	0.19
1999	−2.74	3.01	1.02	0.20

cover and a discoloration in the orthophoto. In 1959, the whole area is covered by a thin snow cover and a large part of the glacier is lying in shadow, which is again represented as artefacts in the hill-shading of the DEM. In 1969, some prominent artefacts show up in steep and shadowed terrain. In 1990, most of the glacier area has a good contrast but a lot of snow is lying in concavities such as in front of the glacier tongue. This signal is reflected in local artefacts, where snow cover, shadow, and steep terrain occur in parallel. The best contrast is given in 1980, where most of the area is free of snow and only few shadows occur. However, analyzing the corresponding shaded relief, a striking rugged topography occurs in the area northwest of Storglaciären, indicating a general tilt in the DEM. In addition, a linear artefact is visible in the orographic right part of the accumulation area of the glacier, which seems to be a vertically small but systematic step in the DEM.

4.2 Comparison with dGPS reference points

Common methods to compare the elevation of a set of independent reference points with the elevation at the corresponding coordinates in a DEM are the calculation of (a) the mean value (MEAN), (b) the root mean square error (RMSE), (c) the standard deviation (STDV), and (d) the standard error (SE) (Kääb, 2005; Fisher and Tate, 2006). Obviously, the comparison of precise point data with pixels (in our case with side lengths of 5 m) imports certain inexactness in the analysis. All statistical values for each survey date are given in Table 2. While the mean values indicate a general shift of about 3 m, the root mean square errors show a wider spread between 1.5 and 4.9 m. The standard deviations amount to values around 1 m, apart for the year 1980 (5 m). Also the standard errors give relatively consistent values around 0.2 m, apart for the year 1980 (1 m).

The validation with dGPS data was used as an estimate of systematic and stochastic uncertainties for the glacier thickness change within an observation period (T0–T1) as follows:

$$\sigma_{\mathrm{dGPS.sys}} = \frac{\sum_{1}^{n}(z_{\mathrm{DEM.T0}} - z_{\mathrm{dGPS}})}{n} - \frac{\sum_{1}^{n}(z_{\mathrm{DEM.T1}} - z_{\mathrm{dGPS}})}{n} \quad (1)$$

$$\sigma_{\mathrm{dGPS.stoc}} = \sqrt{\mathrm{SE}_{\mathrm{T0}}^2 + \mathrm{SE}_{\mathrm{T1}}^2} \quad (2)$$

where n is the number of dGPS points, z the elevation, and SE the standard error of DEM and dGPS elevation differences. The resulting uncertainties are given in Table 3.

4.3 Elevation changes in glacierized vs. non-glacierized area

As a standard method, a Student's T-test was performed in order to test if the ice changes (signal) on the glacier are significantly different from the error (noise) in the non-glacierized area which is assumed to be stable between two surveys. Separate evaluations were conducted for the accumulation area, the ablation area, and the total area and give overall p-values below 0.001 so therefore can be considered to be significant. The only exception was a p-value of 0.36 for the total glacier area in the comparison of 1990–1999. This can be explained by the small thickness change that occurred in that period.

From the analysis of elevation differences in non-glaciated terrain, the mean difference between two DEMs can be considered as the systematic uncertainty for the volume changes of the corresponding time period.

$$\sigma_{\mathrm{DEM.non-glac.sys}} = \frac{\sum_{1}^{n}(z_{\mathrm{DEM.T0}} - z_{\mathrm{DEM.T1}})}{n} \quad (3)$$

where n is the number of non-glacierized DEM grid cells.

The related standard error provides a measure for the corresponding stochastic uncertainty:

$$\sigma_{\mathrm{DEM.non-glac.stoc}} = \frac{\mathrm{STD}}{\sqrt{n}} \quad (4)$$

where STD is the standard deviation of the non-glacierized elevation differences of the two DEMs and n the number of DEM grid cells. Note that for the calculation of the latter (i.e., the standard error) the elevation differences of the grid cells in the sample have to be independent. Due to the photogrammetric auto-correlation this is not given when using all grid cells. We addressed this issue by reducing the sample of n grid cells by applying a nearest neighbor re-sampling in ESRI ArcGIS Desktop 9.3. Under the assumption that the auto-correlation of pixels with 100 m (or 20 pixels) distance is negligible, we used an n of 523. The resulting uncertainties are given in Table 3.

4.4 Slope dependency of errors

The accuracy in DEMs varies due to their dependence on good contrast. Possible problems during the photogrammetric process may occur in areas with steep slopes or strong relief (e.g. Gousie, 2005; Temme et al., 2007). A T-test as performed above simply compares glacierized and non-glacierized area and does not consider this slope dependency

Table 3. Systematic and stochastic uncertainties of the ice thickness changes at Storglaciären. The uncertainties (in meter ice thickness) are based on a comparison with 26 independent dGPS measurements and a comparison of DEM changes in non-glacierized terrain ($n = 523$). For details see text.

observation period	dGPS systematic	dGPS stochastic	non-glacierized systematic	non-glacierized stochastic
1959–1969	+0.344	± 0.413	−0.746	± 0.356
1969–1980	+0.896	± 1.022	+0.436	± 0.482
1980–1990	−0.850	± 1.010	+2.285	± 0.390
1990–1999	−0.494	± 0.276	−0.804	± 0.195
1959–1999	−0.115	± 0.390	+0.873	± 0.253

Table 4. Statistical analysis of the Monte-Carlo Simulation. The p-values show the probability that random error in the DEMs and the calculated thickness changes (signal) are equal. The results are separated into entire glacier, accumulation area, and ablation area. For details see text.

Time period	Parameter α	Entire glacier		Accumulation area		Ablation area	
		p-value	Signal [m]	p-value	Signal [m]	p-value	Signal [m]
1959–69	0.384	0.0677	6.076	0.1246	6.453	0.0336	5.805
1969–80	0.644	0.1867	6.044	0.2349	6.525	0.1488	5.683
1980–90	0.681	0.2533	5.297	0.2978	6.972	0.2175	4.813
1990–99	0.199	0.0713	3.790	0.1029	4.598	0.0576	3.186
1959–99	0.385	0.0341	6.974	0.1361	6.213	0.0102	7.482

of the error. To account for this circumstance and to quantify the inaccuracies that accumulate in the results of numerical modelling, a Monte-Carlo Simulation was performed (Burrough and Mc-Donnell, 1998). It is assumed that the error in a DEM has a Gaussian (normal) probability distribution function with known mean μ and standard deviation σ. As the error is normally distributed μ is 0, σ varies through the DEM depending on the slope of the terrain and hence σ increases in steeper slopes.

A linear relationship between the (absolute) differences in elevation of two DEMs in terrain where no changes are assumed (the glaciated areas are masked out) and the slope of the terrain can be calculated. Based on this relationship, $\sigma$is estimated performing a Maximum Likelihood Analysis. Summarized, the distribution of the error in a DEM is

$$\mathrm{N}\left(0, a \cdot [\mathrm{slope}]\right) \tag{5}$$

where a indicates the relationship between slope and error. Table 4 gives an overview of the used parameter for all time periods.

The Monte-Carlo Simulation was then performed on the area of Storglaciären. With 10 000 iterations a random error was calculated for every pixel following the Gaussian probability distribution of the error (Eq. 5); following Burrough & McDonnell (1998) at least 100 iterations are required. In a next step the mean error was calculated for each iteration.Then the statistical comparison of the artificial data sets (noise) with the calculated thickness changes (signal) between two years showed the probability that the real changes on the glacier are equal from the random error in the DEMs.

Table 4 specifies the coefficient between slope and error (a), as well as the probabilities for accumulation, ablation, and total glacier area of all time periods. The coefficient a shows that the dependence of the error on slope is higher in the periods including the DEM of 1980. The probability that the thickness change over the entire glacier equals the random error in the DEMs is 0.03 for the entire period of investigation, and can thus be rejected based on a significance level of 0.05. It is striking how the p-values for the periods 1969–1980 and 1980–1990 are considerably higher than in the remaining time steps, although the signal is relatively strong. Splitting the results of the Monte-Carlo Simulation into accumulation area and ablation area, the p-value is notably higher in the accumulation area. Thus the probability that thickness change is indistinguishable from random error is higher in the accumulation area. Otherwise the p-values in the ablation area are lower than calculated for the complete glacier area. Again it is clearly visible that the periods including the DEM of 1980 have higher p-values.

Table 5. Length, area, thickness, and volume changes at Storglaciären for given time periods.

Time period	Length change [m]	Area change [km^2]	Thickness change [m]	Volume change [10^6 m^3]
1959–69	−104	−0.07	−4.57	−15.22
1969–80	−44	−0.03	−3.30	−10.78
1980–90	−30	−0.01	+1.51	+4.88
1990–99	0.00	0.00	+0.68	+2.18
1959–99	−178	−0.11	−5.69	−18.95

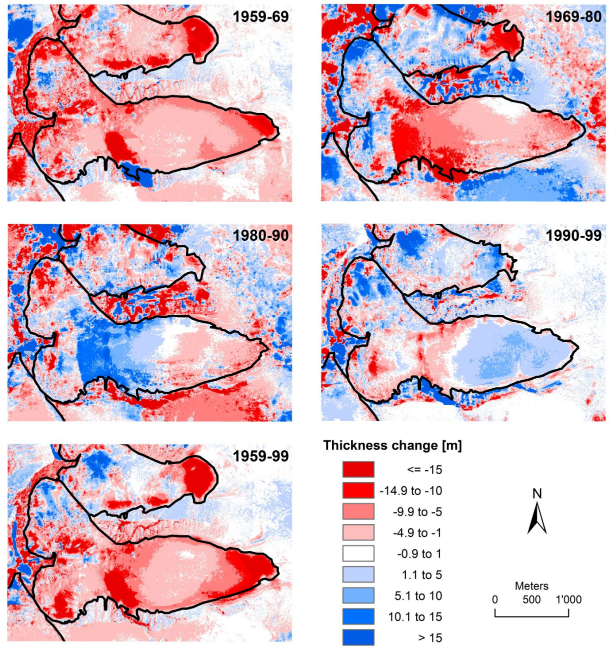

Fig. 4. DEM differences within and outside the outlines of Storglaciären (in the centre), Isfallsglaciären (adjacent to the north) and the northern edge of Björlings glaciär (south-west of Storglaciären) (black lines). The extent of the five figures corresponds to the bounding box as shown in Fig. 2. The differences are calculated by subtracting the earlier from the later DEM. The overall thickness loss (1959–99) originates from the strong ice loss in the first two decades, which was only slightly compensated for in the last two decades. Note the increased noise in the non-glacierized sections (i.e., upper left, upper right, and lower right corners) especially of the two images including the DEM of 1980.

4.5 Accuracies used for change assessment

We used different statistical methods in order to assess the accuracy of the multi-temporal DEMs. In general it was shown that the signal-to-noise ratio (glacier changes vs. changes in non-glacierized terrain) is appropriate. Two different analyses were performed for the quantification of systematic and stochastic uncertainties: the comparison with independent dGPS measurements and the comparison of glacierized and non-glacierized regions in the data sets. The latter approach integrates all errors, such as general shifts, included in the DEMs, since no independent data set, such as a master DEM, is available. Therefore we decided to use the comparison with dGPS reference points, providing an independent validation, as appropriate measure to assess the quality of our data. Hence, the resulting values (Table 2) are implemented as integrative estimates in the comparison of volume changes with in-situ mass balance measurements (Zemp et al., 2010).

5 Length, area, and volume changes

Changes of Storglaciären in length, area, thickness and volume are given in Table 5. Variations at the glacier snout between 1959 and 1999 are illustrated in Fig. 3. During the first two decades the retreat of the glacier is clearly visible. After 1980 only small changes in glacier length occur and between 1990 and 1999 no length change could be measured. The retreat over the whole period of investigation amounts to about 180 m.

The area changes between 1959 and 1999 amount to -0.11 km^2 or -3.3% (Table 5). Again most of the changes occur in the first two decades. After 1980, the area loss is only 0.01 km^2 whereas between 1959 and 1980 the loss is 0.10 km^2. An exact determination of the position of the glacier front after 1980 is hampered by perennial snow patches (see Fig. 3).

During the first decade (1959–69) the thickness change is -4.57 m which results in a volume change of -15.22×10^6 m^3. The thickness and volume loss continues in the following decade (1969–80) although it is slightly smaller. The second half of the investigation period (1980–99) is characterized by a general volume gain. Between 1980 and 1990 the increase of thickness is 1.51 m. During the last decade the increase of thickness amounts to 0.68 m. For the entire period results a volume loss of 18.95×10^6 m^3. Hence, according to the available DEMs, the volume loss at Storglaciären between 1959 and 1999 originates from the beginning of the period of investigation (1959–80) and particularly from the first decade.

The spatial distribution of thickness changes at Storglaciären is shown in Fig. 4, giving the pattern for the different time steps as well as for the entire period. The elevation changes are shown for an entire bounding box around the glacier in order to provide an idea of the signal to noise ratio. Note that the non-glacierized terrain is located in the upper right corner, as well as on the left and lower sides of the bounding box (Fig. 2). The intense volume loss between 1959 and 1969 is the result of a thickness reduction over the entire glacier area. The highest values of thickness loss are achieved at the snout of the glacier and at a small patch at the southern edge in the middle of the glacier. On large parts of the glacier tongue there is a moderate thickness loss. In the accumulation area the distribution of gain and loss looks rather random. During the following decade (1969–80) the dominant component is again thickness loss in the ablation area and again the highest values occur at the snout of the glacier and in the upper part of the ablation area whereas the accumulation zone experiences a thickness increase. In contrast to the first decade the accumulation area is dominated by thickness increase. A noticeable edge divides the ablation area from the accumulation area. The same edge appears again from 1980 to 1990. The overall increasing thickness between 1980 and 1990 results from the thickness gain in the upper part of the ablation area. During the last decade there is a trend to thickness gain on the entire glacier. Particularly in the lower part of the ablation area, the thickness increase is clearly visible. Comparing the single periods, it becomes apparent that the thickness increase that occurs in the accumulation zone between 1969 and 1980 seems to flow towards the snout of the glacier in the following two decades (Fig. 4).

The combined analysis of length and area changes, representing the changing shape of the entire glacier as a reaction to volumetric changes, provides an integrative impression of glacier reaction to a change in climatic forcing. The change from a distinct loss in thickness/volume of the first two decades (1959–80) to a gain in the third and fourth decades (1980–99) results in a delayed reaction of the glacier extent in the form of a slowing down of the retreat over the entire four decades. The regional thickness gain of the 1980s in the lower accumulation area is about to reach the glacier tongue in the fourth decade. This does not lead to a glacier re-advance because of continued negative mass balances after 1995, as apparent from in-situ measurements.

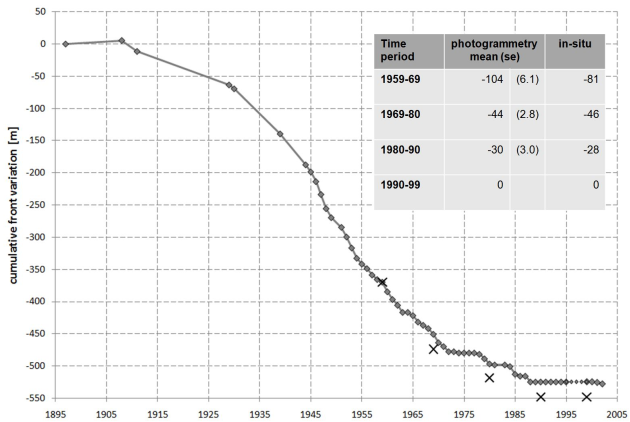

Fig. 5. Length change of Storglaciären 1897–2002. The cumulative front variations are shown, based on the in-situ observations (grey line and diamonds) and as derived from the orthophotos (black crosses). All values are given in meters. Note that in the figure, the in-situ value of 1959 was used as a common reference point.

6 Discussion

During the photogrammetric processing of DEMs and orthophotos of the survey years, inaccuracies appeared due to missing raw data, as well as shadows and snow cover on the photographs. The 1980 DEM in particular shows a rugged topography and large elevation differences compared to DEMs of 1969 and 1990 in the non-glacierized areas northwest of Storglaciären, even if the contrast in the original data is very good and the fractions of snow cover and shadow are lower than in the other images. A possible explanation is that the DEM is partly tilted, which is supported by the results from the comparison with the dGPS points and leads to the poor performance in the uncertainty assessment. The comparison with the independent dGPS points indicates that all the DEMs seem to be systematically too low by a few meters, which must be attributed to an elevation bias in the GCPs (used in the photogrammetric processing), as already noted by Bomark and Lundberg (1995). Apart from the DEM of 1980, the corresponding standard deviations and standard errors of below 1.8 m and 0.4 m, respectively, are quite reasonable for comparing elevations of point measurements with 5×5 m pixels. Taking this into account, and also considering that the original photographs as well as some of the basic photogrammetric parameters were not available, the quality of the DEMs is in general well suited for deriving glacier changes. The "lesson learnt" in this context is that there is a need for (a) a proper documentation of all available data sets and their acquisition (including survey dates, raw data and processing steps), (b) the maintenance of existing networks such as the ground control points around Storglaciären, and (c) the compilation of a new high resolution dataset that provides a reference DEM and allows for an improved quality assessment (Kääb, 2005).

The photogrammetrically derived glacier length changes are compared with the in-situ front variation measurements as available from the WGMS (2008 and earlier issues; Fig. 5). The in-situ observations of the glacier snout are based on tape measuring from four to five points across the snout to a single fixed point (1959–78) and with the use of a theodolite with a distance meter from one single fixed point (1979–99). The results from the in-situ observations and the photogrammetry agree well in the three periods between 1969 and 1999. In the first period (1959–69), the cumulative annual in-situ measurements result in a retreat of 81 m, which is 24 m less than calculated from the orthophoto. The larger value of the remote sensing method comes from the measurement stripes on the northern half of the glacier tongue that intersect at a low angle with the glacier outlines. This opens the door to a larger discussion on the most appropriate method for determining heterogeneous front variations along complex glacier terminus geometries (cf. Kappeler, 2006), which cannot be followed here. As already mentioned earlier, the determination of the glacier area and corresponding changes depends to a certain degree on the interpretation and generalization of the interpreter. This is especially true when the relative changes are small, as in the case for Storglaciären. The comparison with glacier areas as mapped

Table 6. Areal extent of Storglaciären as published in different studies.

Year	Holmlund (1987)	Holmlund et al. (2005)	this study
1949	3.30	n.a.	n.a.
1959	3.27	3.38	3.33
1969	3.15	3.09	3.27
1980	3.12	3.15	3.23
1990	n.a.	3.21	3.22
1999	n.a.	n.a.	3.22

by Holmlund (1987) and as used for the calculation of specific mass balances by Holmlund et al. (2005) does confirm this (see Table 6). Whereas the absolute differences are relatively small, the outlines by Holmlund et al. (2005) show a stronger area loss between 1959 and 1969 followed by a growing glacier extent until 1990, which contradicts the present study. The differences come from the different interpretations of the glacier outlines in the accumulation area and – due to the small absolute values – only has a minor influence on the calculation of the mass balance (Zemp et al., 2010). However, with the continuation of glacier changes this issue must be addressed in future.

The computed volume changes are compared to the results from earlier studies as shown in Table 7. The only good agreements are in first decade (1959–69) with the original result by Holmlund (1987) and in the second decade (1969–80) with the corrected one by the same author. Note that the corrected volume changes by Holmlund (1987) are adjusted to better fit the glaciological mass balance measurements and, hence, a direct comparison might not be appropriate. The comparison with the volume changes 1959–69–80–90 as calculated by Albrecht et al. (2000) shows large differences: whereas they find only half the volume change from this study in the first decade, their results are twice and almost four times our values in the second and third decade, respectively. The different reference areas – as discussed above – can only explain a small portion of these deviations. The major deviation is best explained by an error in the datum level (Morgner and Hock unpublished data) and the different methodologies applied. Hence, all studies based on data from Albrecht et al. (2000) need to be reanalysed and conclusion need to be revised. Holmlund (1987) and Albrecht et al. (2000) computed the volume changes from interpolating contour lines of the topographic glacier maps using both analogue and digital approaches. The use of these maps, instead of the original aerial photographs, is an intermediate production step that introduces additional errors. Additionally, all these maps were produced at different points in time by different operators using different methodologies (Holmlund, 1996). A sound quantification of these errors – e.g. by analyzing the changes in non-glacierized terrain – is not possible, as the corresponding data is not (digitally) available (Holmlund, 1996; Albrecht et al., 2000). The results of this study, based on dia-positives of the original aerial photographs using consistent photogrammetric processing by the same operator, allow for a sound uncertainty assessment. We therefore consider the volume changes presented here – including estimates for systematic and stochastic errors – as the most consistent dataset, which is now ready for comparison with the results from the direct glaciological mass balances (cf. Zemp et al., 2010).

7 Conclusions

The presented approach of reanalyzing dia-positives of original aerial photographs of 1959, -69, -80, -90, and -99 with standard photogrammetric techniques resulted in a complete and consistent dataset of DEMs and orthophotos of the Tarfala Valley. Based on this new dataset, changes of Storglaciären in length, area, and volume are computed for the time periods between these surveys. The glacier lost 15 and 11×10^6 m^3 from 1959–69 and 1969–80, respectively. In the following two decades (1980–90, 1990–99) a partial regain of the lost ice volume of 5 and 2×10^6 m^3 was found. Over the entire period from 1959–99, Storglaciären lost an ice volume of 19×10^6 m^3. Averaged over the glacier area, this corresponds to a total ice thickness loss of 5.7 m, or to a mean annual ice loss of 0.14 m. The glacier reacted to this volume change with a slowing of its retreat, finally to pseudo-stationary conditions in the last observation period (1990–99).

The uncertainty assessment shows that elevations of all the DEMs are systematically too low by a few meters, but with standard errors of below one meter. Thereby, the DEM of 1980 performed worse than the other DEMs. Statistical comparisons of the glacier changes with the "noise" in non-glacierized terrain prove the general significance of the results, with ablation areas performing better than accumulation areas. Again, the results including the DEM of 1980 perform poorer than the others. From the first to the last observation period, the absolute signal decreases and challenges the basic dataset and methodology.

The resulting length changes fit well to the cumulative in-situ observations. Only in the first decade (1959–69) do larger differences occur, which are probably due to the different measurement approaches. The absolute changes in area are small, but the relative changes differ between this and earlier studies. This is attributed to different interpretations of the glacier margins, especially in regions with shadow and/or snow cover. The major differences from earlier studies, however, are in the resulting volume changes of the glacier. Although difficult to quantify, we see the major cause as the heterogeneous methodology of earlier studies, which derived volume changes indirectly from topographic glacier maps of various origins. The resulting volume changes from

Table 7. Comparison of the volume change [10^6 m^3] at Storglaciären from the results of Holmlund (1987), Holmlund (1996) and Albrecht et al. (2000), and this study. The results by Holmlund (1996) and Albrecht et al. (2000) are probably based on the glacier areas described in Holmlund et al. (2005).

Time period	Holmlund (1987) (original data)	Holmlund (1987) (adjusted data)	Holmlund (1996) and Albrecht (2000)	This study
1949–59	+9.5	−16.5	n.a.	n.a.
1959–69	−15.5	−11.21	−7.7	−15.23
1969–80	−8.6	−10.99	−22.97	−10.78
1980–90	n.a.	n.a.	+18.11	+4.88
1990–99	n.a.	n.a.	n.a.	+2.18

the present study – although not free of errors – are based on a consistent re-processing of the original material, come with a sound uncertainty assessment, and allow a comparison with the in-situ mass balance measurements (cf. Zemp et al., 2010).

The resulting data promote the importance of aerial photographs in glacier research, especially for quantifying length, area, and volume changes as well as for cross-checking in-situ measurements. Beyond that, the available DEMs and orthophotos can be used for investigations on the surrounding glaciers and for geomorphological mapping purposes in the Tarfala Valley. Looking into the (scientific) future, we would like to stress the importance of such decadal flight campaigns. We highly recommend compiling a new, high-resolution and high-precision data set that serves as a master data set for a new accuracy assessment, including independent spatial data. In this context, the spatial distribution and visibility of the ground control points around Storglaciären have to be improved and the date of the survey should be as close as possible to the in-situ annual mass balance measurements. With such a data set, glacier changes since 1959 can be quantified with higher accuracy and reliability. In addition, more analyses using the multi-temporal DEMs in combination with reference data and glaciological field measurements should be performed at the test site Storglaciären. By the application of modern techniques such as airborne laser scanning, problems related to shadows and snow cover, influencing the final data product, can be reduced.

Acknowledgements. We are indebted to the staff of the Tarfala Research Station for their hospitality and Dominik Heinzmann (University of Zurich) for statistical support. We thank Betsy Armstrong for polishing the English. We gratefully acknowledge the constructive comments of two anonymous referees and the editor that helped to improve the paper. The present study was supported by the Universities of Zurich and Stockholm, and by the GLACIAS project (SNF-Nr. 200021–116354).

Edited by: I. M. Howat

References

Albrecht, O., Jansson, P., and Blatter, H.: Modelling glacier response to measured mass-balance forcing, Ann. Glaciol., 31, 91–96, 2000.

Björnsson, H.: Radio-echo sounding maps of Storglaciären, Isfallsglaciären and Robots Glaciär, northern Sweden, Geogr. Ann., 63A(3–4), 225–231, 1981.

Böhm, R., Auer, I., Brunetti, M., Maugeri, M., Nanni, T., and Schöner, W.: Regional temperature variability in the European Alps: 1760-1998 from homogenized instrumental time series, Int. J. Climatol., 21, 1779–1801, 2001.

Bomark, M. and Lundberg, C.: GPS-Mätning i Tarfala 1994, Master's thesis, Institutionen för Geodesi och Fotogrammetri Kungliga Tekniska Högskolan, Stockholm, 1995.

Burrough, P. A. and McDonnell, R. A.: Principles of geographic information systems, Oxford University Press, New York, 1998.

Eriksson, M. G., Björnsson, H., Herzfeld, U. C., and Holmlund, P.: The bottom topography of Storglaciären, Department of Physical Geography, Stockholm University, Stockholm, 1993.

Fischer, A.: Glaciers and climate change: Interpretation of 50 years of direct mass balance of Hintereisferner, Global Planet. Change, 71, 13–26, 2010.

Fisher, P. F. and Tate, N. J.: Causes and consequences of error in digital elevation models, Progr. Phys. Geogr., 30(4), 467–489, 2006.

Gousie, M. B.: Digital elevation model error detection and visualization, The 4th Workshop on Dynamic & Multi-dimensional GIS, 42–46, 2005.

Grudd, H. and Schneider, T.: Air temperature at Tarfala Research Station 1946–1995, Geogr. Ann., 78A(2–3), 115–120, 1996.

Haeberli, W.: Glaciers and ice caps: historical background and strategies of world-wide monitoring, in: Mass balance of the cryosphere, edited by: Bamber, J. L. and Payne, A. J., 559–578, Cambridge University Press, Cambridge, 2004.

Heuvelink, G. B. M.: Error propagation in environmental modelling with GIS, Taylor & Francis Ltd, London, 1998.

Hock, R.: A distributed temperature-index ice- and snowmelt model including potential solar radiation, J. Glaciol., 45(149), 101–111, 1999.

Hock, R. And Noetzli, C.: Areal melt and discharge modelling of Storglaciären, Sweden. Ann. Glaciol., 24, 211–216, 1997.

Hock, R. and Holmgren, B.: A distributed surface energy-balance model for complex topography and its application to Stor-

glaciären, Sweden. J. Glaciol., 51(172), 25–36, 2005.
Hock, R., Hulth, J., and Pettersson, R.: Mass balance of Storglaciären, Sweden - re-evaluation and error assessment. Abstract, Workshop on mass balance measurements and modelling, Skeikampen, Norway, 2008.
Holmlund, P.: Mass balance of Storglaciären during 20th Century, Geogr. Ann., 69, 439–447, 1987.
Holmlund, P.: Maps of Storglaciären and their use in glacier monitoring studies, Geogr. Ann., 78A(2–3), 193–196, 1996.
Holmlund, P. and Eriksson, M.: The cold surface layer on Storglaciären, Geogr. Ann., 71A, 241–244, 1989.
Holmlund, P. and Jansson, P.: The Tarfala Mass Balance Programme, Geogr. Ann., 81A, 621–631, 1999.
Holmlund, P. and Jansson, P.: Glaciological research at Tarfala Research Station. Stockholm University, Stockholm, 48 pp., 2002.
Holmlund, P., Karlén, W., and Grudd, H.: Fifty years of mass balance and glacier front observations at the Tarfala Research Station, Geografiska Annaler, 78A(2–3), 105–114, 1996.
Holmlund, P., Jansson, P., and Pettersson, R.: A re-analysis of the 58 year mass-balance record of Storglaciären, Sweden, Ann. Glaciol., 42, 389–394, 2005.
Hooke, R. L., Gould, J. E., and Brzozowski, J.: Near-surface temperatures near and below the equilibrium line on polar and subpolar glaciers, Z. Gletscherkd Glazialgeol., 19(1), 1–25, 1983.
Huss M., Bauder, A., and Funk M.: Homogenization of long-term mass balance time series, Ann. Glaciol., 50(50), 198–206, 2009.
Jansson, P.: Effect of uncertainties in measured variables on the calculated mass balance of Storglaciären. Geogr. Ann., 81(4), 633–642, 1999.
Jansson, P. and Pettersson, R.: Fixed points and co-ordinate systems in the Tarfala valley, Tarfala Research Station Annual Report 1995–96: 26–29, 1997.
Jansson, P. and Pettersson R.: Spatial and temporal characteristics of a long mass balance record, Storglaciären, Sweden, Arct., Ant. Alp. Res., 39(3), 432–437, 2007.
Jones, C. B.: Geographical information systems and computer cartography, Longmann, 1997.
Kääb, A.: Remote Sensing of mountain glaciers and permafrost creep. Schriftenreihe Physische Geographie 48, 266, 2005.
Kappeler, S. : Längenänderungsmessungen an ausgewählten Gletschern der Schweizer Alpen unter Verwendung von GIS. Diploma thesis, Department of Geography, University of Zurich, 80 pp., unpublished, 2006.
Kraus, K.: Photogrammetrie. Band 1: Geometrische Informationen aus Photographien und Laserscanneraufnahmen, Walter de Gruyter, Berlin, 7. edn., 2004.
Kraus, K., Karel, W., Briese, C., and Mandlburger, G.: Local accuracy measures for digital terrain models, The Photogrammetric Record, 21(116), 342–354, 2006.
Lemke, P., Ren, J., Alley, R. B., et al.: Climate change 2007: the physical science basis. Contribution of Working Group I to the Fourth Assessment report of the Intergouvernmental Panel on Climate Change, edited by: Solomon, S., Qin, D., Manning, M., Chen, Z., Marquis, M., Averyt, K. B., Tignor, M., and Miller, H. L., Cambridge University Press, Cambridge, UK , 2007.
Li, Z., Zhu, Q., and Gold, C.: Digital terrain modeling – principles and methodology, CRC Press, Boca Raton, Florida, 2005.
Linderholm, H. W., Jansson, P., and Chen, D.: A high-resolution reconstruction of Storglaciären mass balance back to 1780/81 using tree-ring data and circulation indices, Quat. Res., 67, 12–20, 2007.
Østrem, G. and Brugman, M.: Mass balance measurement techniques. A manual for field and office work, Environment Canada, Saskatoon, 1991.
Østrem, G., Haakensen, N., and Melander, O.: Atlas over breer I Nordskandinavia. Glacier atlas of Northern Scandinavia, Meddelande nr. 46 från Naturgeografiska Institutionen, 1973.
Pettersson, R., Jansson, P., Huwald, H., and Blatter, H.: Spatial pattern and stability of the cold surface layer of Storglaciären, Sweden. J. Glaciol., 53(180), 99–109, 2007.
Pettersson, R. and Jansson, P.: Quick manual for measurement and processing of kinematic GPS data, Department of Physical Geography and Quaternary Geology Stockholm University, Stockholm, 2005.
Pettersson, R., Jansson, P., and Holmlund, P.: Cold surface layer thinning on Storglaciären, Sweden, observed by repeated ground penetrating radar surveys, J. Geophys. Res., 108(F1), doi.10.1029/2003JF000024, 2003.
Raper, S. C. B., Briffa, K. R., and Wigley, T. M. L.: Glacier change in northern Sweden from AD 500: a simple geometric model of Storglaciären, J. Glaciol., 42, 341–351, 1996.
Schneider, T. and Jansson, P.: Internal accumulation in firn and its significance for the mass balance of Storglaciären, Sweden. J. Glaciol., 50(168), 25–34, 2004.
Schytt, V.: Glaciers of the Kebnekaise-Massif, Geogr. Ann., 41, 213–227, 1959.
Schytt, V.: The net mass balance of Storglaciären, Kebnekaise, Sweden, related to the height of the equilibrium line and to the height of the 500 mb surface. Geogr. Ann., 63(3–4), 219–223, 1981.
Temme, A. J. A. M., Schoorl, J. M., and Claessens, L.: Geostatistical simulation and error propagation in geomorphometry, in: Geomorphometry: concepts, software, applications, edited by: Hengl, P. and Reuter, H. I., chap. 5, pp. 93–108, Office for Official Publications of the European Communities, Luxembourg, 2007.
Thibert, E., Blanc, R., Vincent, C., and Eckert, N.: Glaciological and volumetric mass-balance measurements: error analysis over 51 years for Glacier de Sarenne, French Alps, J. Glaciol., 54, 522–532, 2008.
WGMS: Fluctuations of Glaciers 2000–2005 (Vol. IX), edited by: Haeberli, W., Zemp, M., Kääb, A., Paul, F., and Hoelzle, M., ICSU(FAGS)/IUGG(IACS)/UNEP/UNESCO/WMO, World Glacier Monitoring Service, Zurich, 266 pp., 2008.
Wood, J. D. and Fisher, P. F.: Assessing interpolation accuracy in elevation models, IEEE Computer Graphics and Applications, 13, 48–56, 1993.
Zemp, M., Jansson, P., Holmlund, P., Gärtner-Roer, I., Koblet, T., Thee, P., and Haeberli, W.: Reanalysis of multi-temporal aerial images of Storglaciären, Sweden (1959–99) – Part 2: Comparison of glaciological and volumetric mass balances, The Cryosphere, 4, 345–357, doi:10.5194/tc-4-345-2010, 2010.

Publication 8

Zemp, M., Jansson, P., Holmlund, P., Gärtner-Roer, I., Koblet, T., Thee, P. & Haeberli, W. (2010). **Re-analysis of multi-temporal aerial images of Storglaciären, Sweden (1959-99) - Part 2: Comparison of glaciological and volumetric mass balances.** The Cryosphere, 4, 345-357.

The Cryosphere, 4, 345–357, 2010
www.the-cryosphere.net/4/345/2010/
doi:10.5194/tc-4-345-2010

The Cryosphere

Reanalysis of multi-temporal aerial images of Storglaciären, Sweden (1959–99) – Part 2: Comparison of glaciological and volumetric mass balances

M. Zemp[1], **P. Jansson**[2], **P. Holmlund**[2], **I. Gärtner-Roer**[1], **T. Koblet**[1], **P. Thee**[3], **and W. Haeberli**[1]

[1]Department of Geography, University of Zurich, Winterthurerstr. 190, 8057 Zürich, Switzerland
[2]Department of Physical Geography and Quaternary Geology, 106 91 Stockholm, Sweden
[3]Swiss Federal Institute for Forest, Snow and Landscape Research, Zürcherstr. 111, 8903 Birmensdorf, Switzerland

Received: 18 March 2010 – Published in The Cryosphere Discuss.: 25 March 2010
Revised: 4 August 2010 – Accepted: 4 August 2010 – Published: 8 September 2010

Abstract. Seasonal glaciological mass balances have been measured on Storglaciären without interruption since 1945/46. In addition, aerial surveys have been carried out on a decadal basis since the beginning of the observation program. Early studies had used the resulting aerial photographs to produce topographic glacier maps with which the in-situ observations could be verified. However, these maps as well as the derived volume changes are subject to errors which resulted in major differences between the derived volumetric and the glaciological mass balance. As a consequence, the original photographs were re-processed using uniform photogrammetric methods, which resulted in new volumetric mass balances for 1959–69, 1969–80, 1980–90, and 1990–99. We compared these new volumetric mass balances with mass balances obtained by standard glaciological methods including an uncertainty assessment considering all related previous studies. The absolute differences between volumetric and the glaciological mass balances are 0.8 m w.e. for the period of 1959–69 and 0.3 m w.e. or less for the other survey periods. These deviations are slightly reduced when considering corrections for systematic uncertainties due to differences in survey dates, reference areas, and internal ablation, whereas internal accumulation systematically increases the mismatch. However, the mean annual differences between glaciological and volumetric mass balance are less than the uncertainty of the in-situ stake reading and stochastic error bars of both data series overlap. Hence, no adjustment of the glaciological data series to the volumetric one is required.

Correspondence to: M. Zemp
(michael.zemp@geo.uzh.ch)

1 Introduction

Changes in glacier mass are a key element of glacier monitoring, providing important information for assessing climatic changes, water resources, and sea level changes (Kaser et al., 2006, Zemp et al., 2009). The available dataset of in-situ glacier mass balance measurements covers the past six decades (Sect. 2). The majority of these data series consists of just a few observation years. There are only 12 mass balance programs with continuous observations back to 1960 or earlier (Zemp et al., 2009), including Storglaciären with the longest record of glacier mass balance and one of the densest observation networks. The homogenization of these observations is gaining importance with increasing time length of the data series (e.g., Thibert et al., 2008; Huss et al., 2009; Fischer, 2010).

Annual glacier mass balance measurements based on the direct glaciological method (cf. Østrem and Brugman, 1991) are, hence, ideally combined with decadal volume-change assessments from geodetic surveys in order to assess random and systematic errors of both methods (Hoinkes, 1970; Haeberli, 1998, Fountain et al., 1999). Storglaciären has been surveyed by aerial photography about every decade (Holmlund, 1996). Maps had been constructed from these aerial photographs to determine the glacier area needed for mass balance calculations (Holmlund et al., 2005, Tarfala Research Station data) and to analyze the changes in surface topography (Holmlund, 1987, 1996). However, the comparison of volumetric mass balances derived from these digitized topography maps (of 1959, -69, -80, -90) with cumulative mass balance measurements shows major discrepancies, with maximum differences of half a meter per year (1969–80), as already noted by Albrecht et al. (2000).

Published by Copernicus Publications on behalf of the European Geosciences Union.

In order to overcome the problems related to the various existing maps and the methods used for deriving volume changes of Storglaciären, we re-processed dia-positives of the original aerial photographs of 1959, -69, -80, -90, and -99 based on a consistent photogrammetric processing for all survey years. Details on the study site, methodology, resulting digital elevation models (DEMs) and orthophotos, and derived changes in length, area, and volume are published in Koblet et al. (2010). In this paper, we compare the new volumetric mass balances with the glaciological mass balances for the periods of the aerial surveys. In addition, we summarize uncertainties related to both methods under consideration of all related previous studies and conclude with some recommendations for the mass balance monitoring program.

2 Historical background of mass balance measurement

Early observations of point mass balance date back to the end of the 19th and beginning of the 20th century, for example at Grosser Aletsch Gletscher (Aellen, 1996), Clariden Firn (Kasser et al., 1986; Müller and Kappenberger, 1991), Rhône Gletscher (Mercanton, 1916), and Silvretta Gletscher (Aellen 1996; Huss et al., 2008) in Switzerland. In the 1920s and 1930s, short-term observations (up to one year) were carried out at various glaciers in Nordic countries (e.g., Ahlmann 1929, 1935, 1939, 1942). After a detailed glacio-meteorological observation program at Kårsaglaciären, northern Sweden, in the early 1940s (Wallén 1948), Storglaciären in the Kebnekaise massif, northern Sweden, was chosen due to its relative accessibility and simple geometry for a long-term observation program (Schytt, 1947; Ahlmann, 1951). The mass balance work on Storglaciären started with winter-balance measurements in May 1946 (Karlén and Holmlund, 1996) and still continues today. In North America, early mass balance work started in the second half of the1940s as well (Meier, 1951; Pelto and Miller, 1990). Meanwhile, mass balance observations have been carried out on more than 300 glaciers worldwide (Cogley and Adams, 1998; Dyurgerov and Meier, 2005), of which about 230 data series are available from the World Glacier Monitoring Service (WGMS 2008).

3 Review of data and methods

A sound comparison of volumetric and glaciological mass balance data requires an uncertainty assessment of the major potential sources of error, such as in-situ and remote sensing methods applied, density assumptions, differences in survey dates and reference areas, internal ablation and accumulation, superimposed ice, and flux divergence. In this section, we aim at providing estimates for related uncertainties based on new data and/or earlier related studies.

3.1 Glaciological mass balances

Glacier surface mass balance at Storglaciären is measured following the direct glaciological method as described by Østrem and Brugman (1991). Measurements of winter and summer balances are carried out from late April to early May and around mid-September, respectively. Between 1945 and 1965, winter balance was measured by manual snow probing in fixed profiles across the glacier. Ablation was measured from a network of stakes along the same profiles. Since 1966, winter balance measurements have been made using a fixed system of probing points arranged in a 100×100 m grid covering the entire glacier (3 km^2; $\sim$100 data points km^{-2}). Snow density is determined from a varying number of pits or by core drillings. In recent years a depth-density function was fitted to the latter data and used to calculate density for each of the snow depth probings. Summer balance is measured from traditional stake readings. The observation network typically comprises 40–50 stakes distributed across the entire glacier ($\sim$15 stakes km^{-2}), and reaches up to 90 measurement points in some years. The stake network is less dense in crevassed and steep areas such as the headwalls of the glacier. Traditionally, the linear ablation gradient (cf. Haefeli, 1962) is used to extrapolate ablation in these areas. The number of stake and snow depth measurements has never been smaller than about half the modern values but have varied from year to year, especially before 1966 (Jansson and Pettersson, 2007).

Until 1993/94, the accumulation and ablation measurements were inter-/extrapolated manually by drawing contour lines. Areas between adjacent contour lines were integrated using a planimeter and assigning a constant balance value to each of these areas. Since 1994/95, the data have been interpolated on a 10 m resolution grid using the commercial PC software SURFER from Golden Software Inc. and more recently a MATLAB based toolbox implementing GSlib kriging (Deutch and Journel, 1998), applying the default parameter set of ordinary kriging (no nugget effect considered). Specific winter and summer balances are then obtained from averaging all grid cell values. In both the early and the new system, annual mass balance results from the sum of (negative) summer and (positive) winter balances.

Overviews on the Tarfala mass balance program and specifically on Storglaciären are given by Holmlund et al. (1996) and by Holmlund and Jansson (1999). The latter provide details on winter and summer balance measurement, whereas descriptions of inter-/extrapolation methods are found in Hock and Jensen (1999) and Jansson and Pettersson (2007). In the (old) official dataset as published by Holmlund and Jansson (1999), there are considerable time lags between the mass balance data and the reference area (from the most recent topographic map) used for calculating specific mass balances. This issue – inherent to all operational mass balance programs – is addressed by Holmlund

Table 1. Aerial and field survey dates, positive degree day sums (PDDS), related melt factors and resulting absolute melt corrections. The volumetric mass balance of 1969–80, for example, requires additional melt of 0.210 m w.e. in order to fit the field survey period. A corresponding correction for the beginning of the period is not required as there are no positive degree days recorded between the surveys. For more details see text.

aerial survey	field survey			PDDS		degree day	
date	end winter	end summer	summer balance [m w.e.]	summer survey [K d]	between surveys [K d]	factor [m w.e. K^{-1} d^{-1}]	correction [m w.e.]
23 Sep 1959	15 May 1959	15 Sep 1959	−1.80	501.5	7.3	0.0036	0.026
14 Sep 1969	15 May 1969	15 Sep 1969	−1.93	531.2	0.0	0.0036	0.000
18 Aug 1980	27 May 1980	21 Sep 1980	−2.16	607.5	59.2	0.0036	0.210
04 Sep 1990	24 May 1990	10 Sep 1990	−1.65	429.3	16.6	0.0038	0.064
09 Sep 1999	05 May 1999	15 Sep 1999	−1.52	434.0	27.2	0.0035	0.095

et al. (2005) by re-processing the data series (1945/46–2002/03) based on refined topographic maps. The authors do not re-evaluate the field data but digitize the old water equivalent contour maps, interpolate them onto a surface grid (20×20 m), and recalculate the seasonal and annual mass balances based on glacier areas (from the maps) corresponding to the years of the aerial surveys. Up until present, Holmlund et al. (2005) has been used as the new official dataset and was updated with Tarfala Research Station data, using the glacier area of the 1990 survey as reference for the calculation of specific mass balances since 1985/86.

3.2 Volumetric mass balances

Recurring aerial surveys have been carried out since the very beginning of the mass balance monitoring program at Storglaciären. The resulting vertical photographs had been used to produce several topographic glacier maps which are described in detail by Holmlund (1996). Based on these maps, early volume change assessments had been carried out challenged by inaccuracies in maps and methodologies (Holmlund, 1987, 1996; Albrecht et al., 2000). Koblet et al. (2010) re-analyze dia-positives of the original aerial photographs of 1959, -69, -80, -90, and -99 using a combination of analytical and digital photogrammetry. This results in a complete and consistent dataset of DEMs and orthophotos of the glacier. Based on this new dataset, the authors compute changes in length, area, and volume for the time periods between the aerial surveys. In this study, we now used these volume changes, including estimates for systematic and stochastic errors, for comparison with the glaciological mass balances.

3.3 Uncertainty assessments

3.3.1 Glaciological mass balance: field measurements and interpolation method

Jansson (1999) investigates uncertainties related to the in situ mass balance measurements at Storglaciären. Jansson empirically evaluates the influence of errors in stake reading and snow probing, snow density information, interpolation between observations, and extrapolation to areas not probed, as well as effects on reduced probing networks on the glacier mass balance results. Due to the dense observation network and the stochastic character of most of the errors related to point observations, the mean specific mass balance of Storglaciären is not very sensitive to errors in the investigated factors and can roughly be estimated to an overall uncertainty of $\pm$ 0.1 m w.e. a^{-1} (Jansson 1999). The re-analysis of the mass balance series by Holmlund et al. (2005) confirms this value for data after about 1960 and shows some larger errors in the early data. We, hence, set the overall stochastic uncertainty related to the field measurements to $\pm$ 0.2 m w.e. a^{-1} for the years 1959–65 and to $\pm$ 0.1 m w.e. a^{-1} for the years after 1965. Systematic errors related to the field measurements, such as the sinking of stakes in the accumulation area or the false determination of the last year's summer surface, might be an issue for individual survey years, but cannot be quantified due to the lack of corresponding information. Hock and Jensen (1999) demonstrate that different parameter settings of the kriging interpolation method have a strong influence on the spatial distribution pattern but little impact on the mean specific mass balances. They estimate the error (on the latter) introduced by the interpolation method to about $\pm$ 0.1 m w.e a^{-1}.

Table 2. Cumulative glaciological mass balances and related stochastic and systematic uncertainties with regard to field measurements (σ_{field}), interpolation methods (σ_{krig}), reference areas (σ_{ref}), internal ablation (σ_{intAbl}) and accumulation (σ_{intAcc}). Overall uncertainties are calculated based on the law of error propagation for the stochastic estimates ($\sigma_{\text{total.stoc}}$) and as sums for the systematic estimates ($\sigma_{\text{total.sys}}$); the latter including and excluding uncertainties for internal accumulation. All values are cumulated over the corresponding observation period with units in meter water equivalent (m w.e.). Note that the observation periods refer to the start and end year of the corresponding first and last field surveys, respectively, e.g., the period 1959–99 covers the hydrological years from 1959/60 to 1998/99.

observation period (# years)	cum. glac. mass balance	$\sigma_{\text{field.stoc}}$	$\sigma_{\text{krig.stoc}}$	$\sigma_{\text{ref.stoc}}$	$\sigma_{\text{ref.sys}}$	$\sigma_{\text{intAbl.sys}}$	$\sigma_{\text{intAcc.sys}}$	$\sigma_{\text{total.stoc}}$	$\sigma_{\text{total.sys}}$ excl. intAcc	$\sigma_{\text{total.sys}}$ incl. intAcc
1959–69 (10)	−3.110	± 0.529	± 0.316	± 1.009	+0.048	−0.110	+0.484	± 1.182	−0.062	+0.422
1969–80 (11)	−2.540	± 0.332	± 0.332	± 0.984	+0.133	−0.121	+0.642	± 1.090	+0.012	+0.654
1980–90 (10)	1.000	± 0.316	± 0.316	± 0.378	−0.007	−0.110	+0.646	± 0.585	−0.117	+0.529
1990–99 (9)	0.720	± 0.300	± 0.300	± 0.059	−0.001	−0.099	+0.588	± 0.428	−0.100	+0.488
1959–99 (40)	−3.930	± 0.632	± 0.632	± 1.460	+0.173	−0.440	+2.360	± 1.712	−0.267	+2.093

Table 3. Volumetric mass balances and related stochastic and systematic uncertainties with regard to density assumptions (σ_{density}), survey dates (σ_{survey}), and to the photogrammetric processing of the DEMs based on independent dGPS measurements (σ_{dGPS}). Overall uncertainties are calculated based on the law of error propagation for the stochastic estimates ($\sigma_{\text{total.stoc}}$) and as sums for the systematic estimates ($\sigma_{\text{total.sys}}$). All values are cumulated over the corresponding observation period with units in meter water equivalent (m w.e.). Note that the observation periods refer to the years of the corresponding aerial surveys.

observation period(# years)	volumetric mass balance	$\sigma_{\text{density.stoc}}$	$\sigma_{\text{dGPS.stoc}}$	$\sigma_{\text{dGPS.sys}}$	$\sigma_{\text{survey.sys}}$	$\sigma_{\text{total.stoc}}$	$\sigma_{\text{total.sys}}$
1959–69 (10)	−3.932	± 0.274	± 0.353	+0.292	−0.026	± 0.447	+0.266
1969–80 (11)	−2.841	± 0.198	± 0.874	+0.765	−0.210	± 0.896	+0.555
1980–90 (10)	1.299	± 0.091	± 0.867	−0.731	+0.146	± 0.872	−0.585
1990–99 (9)	0.582	± 0.041	± 0.237	−0.421	−0.031	± 0.241	−0.452
1959–99 (40)	−4.891	± 0.350	± 0.339	−0.095	−0.121	± 0.487	−0.216

The uncertainties related to field measurements and interpolation method cumulated over the survey periods were calculated following the law of error propagation:

$$\sigma_{\text{field.stoc}} = \sqrt{\sum_{i=1}^{n} \sigma^2_{\text{field.stoc.i}}} \tag{1}$$

$$\sigma_{\text{krig.stoc}} = \sqrt{\sum_{i=1}^{n} \sigma^2_{\text{krig.stoc.i}}} \tag{2}$$

where $\sigma_{\text{field.stoc}}$ and $\sigma_{\text{krig.stoc}}$ are the uncertainties of field measurements and interpolation method, respectively, cumulated over n years of the survey periods. The resulting estimates for the stochastic errors of field measurements and interpolation method are given in Table 2.

3.3.2 Volumetric mass balances: photogrammetry

A sound quantitative assessment of the photogrammetry-related uncertainties is nicely demonstrated for Sarennes glacier, French Alps, by Thibert et al. (2008). Such a detailed analysis would be difficult to conduct in our case, as not all parameters are known for the early survey dates and because analogue and digital steps are combined in the photogrammetric processing (cf. Koblet et al., 2010).

As a consequence, Koblet et al. (2010) qualitatively evaluate the resulting DEMs and orthophotos and use two different approaches to assess the systematic and stochastic uncertainties of the volumetric mass balance derived from DEM-differencing. A set of 26 reference points located with a differential global-positioning system (dGPS) provides an independent validation of the digital elevation models (DEMs) and corresponding volume changes. The analysis of elevation differences in non-glacierized terrain allows investigating the significance of computed glacier thickness changes, the slope dependency of errors, and quantifying the integrative errors of the photogrammetry. Full details and equations are given in Koblet et al. (2010). In this study we used their results from the comparison with independent dGPS points as integrative estimates of stochastic and systematic uncertainties of the photogrammetric processing of the volume changes (Table 3).

3.3.3 Density assumptions

Density information is required in order to convert the change of a snow/firn/ice volume into a mass change. Most studies assume a constant density profile in the accumulation area and, hence, use glacier ice density for the conversion. This, however, may only be valid under steady-state conditions and for glaciers with a constant accumulation rate and no melting in that zone (Sorge 1935; Bader 1954). In reality, the density of the volume change is determined by the quantity of melted/newly formed snow, firn, and ice. Corresponding three-dimensional measurements are not available. We, hence, based our density assumptions on maximum and minimum estimates. Using the density of ice (917 kg m^{-3}) for the entire volume change will likely overestimate mass changes during periods of changing snow and firn layers and was thus regarded as a maximum estimate. As a minimum estimate we used a density of 800 kg m^{-3}, which is calculated as the zonal average of 700 (917) kg m^{-3} above (below) the balanced-budget equilibrium line altitude (ELA$_0$) of Storglaciären. ELA$_0$ and the corresponding accumulation area ratio (AAR$_0$) are derived from the linear regressions of ELA and AAR versus mass balance data (1946–2007) resulting in an ELA$_0$ at 1450 m a.s.l. and an AAR$_0$ of 45%. We hence used the (rounded) average of the two density assumptions (860 kg m^{-3}) for the conversion of the volumetric changes into water equivalent and the difference to maximum/minimum estimates (60 kg m^{-3}) as an uncertainty measure (Table 3, $\sigma_{\text{density.stoc}}$).

3.3.4 Survey dates

Comparison of glaciological with geodetic mass balance requires a correction because the field and aerial surveys are not carried out on the same date. The related error corresponds to the mass balance of that period and, hence, depends on the time span between the two surveys, the season, and the glacier mass turn over. The dates for the aerial surveys are based on information from Lantmäteriet and for 1980, -90, and -99, also labelled on the image frames. Exact dates of the winter and summer balance field work are available for 1980 and 1990 from the WGMS database. Corresponding meta-data for the surveys of the other years are not readily available. Assumptions for these other dates of mass balance field work are based on information from the Tarfala Station (Table 1).

For the mass balance correction we applied a classical degree-day model that relates glacier melt M, expressed in mm w.e., during a period of n time intervals, Δt, to the sum of positive air temperatures of each time interval, T^+, during the same period:

$$\sum_{i=1}^{n} M = \mathrm{DDF} \sum_{i=1}^{n} T^{+} \cdot \Delta t \tag{3}$$

The degree-day factor, DDF, is expressed in mm w.e. K^{-1} d^{-1} for Δt expressed in days and temperature in °C (Braithwaite, 1995; Hock, 2003). We used the daily air temperature series from the Tarfala meteorological station (1138 m a.s.l.; Grudd and Schneider, 1996), which are available since 1965, and a temperature lapse rate of 0.55 K 100 m^{-1}(Hock and Holmgren, 2005) to calculate positive degree-day sums at the balanced-budget equilibrium line altitude (ELA$_0$) of Storglaciären. The degree-day factor was calculated from summer balances and positive degree-day sums for every (aerial) survey year separately, with resulting values of 3.5, 3.6, and 3.8 mm K^{-1} d^{-1}. For 1959, positive degree-day sums were derived from averaging the cumulative positive degree-day profiles of the years 1969, -80, -90, and -99 as air temperature had only been measured during daytime in the summer months (JJA) prior to 1965. The largest difference between field and aerial surveys is found for 1980 with 34 days and a corresponding positive degree day sum of 59.2 K d resulting in an absolute melt correction of 0.21 m w.e. (see Table 1). For the uncertainty assessment in Sect. 3.3, the melt corrections for the beginning and the end of the survey periods are required in order to correct the volumetric mass balance to the dates of the field surveys (Table 3, $\sigma_{\text{survey.sys}}$). As such, the volumetric mass balance of the period from 18 August 1980 to 4 September 1990 needs to be corrected by +0.210 m w.e. and −0.064 m w.e., in order to fit the field survey period from 21 September 1980 to 10 September 1990.

The present approach does neglect the influence of snow fall events (and related albedo effects) during the summer period. This might lead to a systematic underestimation of the positive degree-day factor and to an overestimation of the melt correction in case of major snow fall events between the aerial and the field surveys. As there is no solid precipitation record available covering the entire period of interest, we used hourly temperature and precipitation data from 1989 to 2007 measured at the Tarfala Research Station to at least estimate the relevance of ignoring summer snow fall events. We used the summer data (15 May to 15 September) and skipped the years with more than 35 data gaps or implausible values (i.e., 1989, 1994, 1998, 2000, 2004). Solid precipitation was estimated from hourly precipitation at temperatures below 1.5 °C (Rohrer, 1989). Thereto, temperature at ELA$_0$ was calculated from the average of available sensors and a lapse rate of 0.55 K 100 m^{-1} (see above). Precipitation, measured with a Campbell tipping bucket rain gauge (0.16 mm per tip), was increased by 35% to account for the gauge undercatch error and then extrapolated assuming a 10% increase per 100 m elevation (Hieltala, 1989, Hock and Holmgren, 2005) to the ELA$_0$ of Storglaciären. However, a multiple linear regression model showed that solid precipitation does not significantly contribute to the summer mass balance whereas the positive degree-day sums explain a high percentage of its variance. Furthermore, there had been no major events of solid precipitation (i.e., daily sum >3 mm, cf. Fischer, 2010) during the days between the aerial and the field surveys in 1990 and in 1999 that would argue against a melt correction.

3.3.5 Reference areas

The calculation of "conventional" mass balances (Elsberg et al., 2001) actually requires an update of glacier extent (and elevation) for every survey year. However, the required information is only available after the decadal geodetic surveys and hence a lagged step-function of the real changes. Holmlund et al. (2005) address the time lag by recalculating the glaciological mass balance series on the basis of time periods with (constant) glacier extents centered on the years (1949, -59, -69, -80, -90) when the aerial photos were taken. However, they do not address the step change in reference area. The geodetic volume changes (1959–69, 1969–80, 1980–90, 1990–99) by Koblet et al. (2010) are calculated based on glacier extents on the orthophotos. Their outlines are congruent in the accumulation area for all years. In each period, the (larger) area of the first survey year is used as a reference extent. As a consequence, the reference area differs by up to 8% between the glaciological and the volumetric mass balances of a year (Koblet et al., 2010).

We assessed the related systematic uncertainty by correcting the glaciological mass balances to the reference areas of the aerial surveys. Thereto, the specific annual balances were multiplied by the glacier area of the glaciological dataset and divided by the extent in the volumetric dataset which was linearly interpolated between the aerial surveys in order to avoid step changes. As a result, the absolute values of the cumulated, glaciological mass balance decrease (Table 2, $\sigma_{\text{ref.sys}}$) due to the generally larger glacier areas as determined by Koblet et al. (2010).

The chosen approach does, however, not take into account that the relation between the specific mass balance and differences in glacier extent is not linear – local area differences at the glacier tongue (headwall) have a much more negative (positive) influence than those close to the ELA. The related possible error range can be estimated as the product of the above determined annual area differences ΔS and half the range of the annual mass balance within the glacier elevation boundaries $\mathrm{M}_{\text{range}}$, resulting in the following stochastic uncertainty related to differences in reference areas:

$$\sigma_{\text{ref.stoc}} = \sqrt{\sum_{i=1}^{n} (0.5 \cdot \mathrm{M}_{\text{range.i}} \cdot \Delta S_i)^2} \tag{4}$$

As the mass balance data for individual elevation boundaries are not readily available for all the years, we used an average mass balance range for all years (4.6 m w.e.; based on available data since 1971). The stochastic uncertainty was cumulated over the number of years n of the aerial survey periods according to the law of error propagation (Table 2, $\sigma_{\text{ref.stoc}}$).

3.3.6 Internal ablation and accumulation

Internal ablation due to ice motion, geothermal heat, and heat-conversion of gravitational potential energy loss from water flow through and under the glacier are other potential systematic biases not accounted for by standard measurements. The ice motion of the poly-thermal glacier (Pettersson et al., 2004) was considered to be small and corresponding internal ablation, thus, to be negligible (cf. Hooke et al., 1989 and Albrecht et al., 2000). The contribution of basal melting by geothermal heat was estimated according to Östling and Hooke (1986) as about 0.001 m w.e. a^{-1}. The internal melting by released potential energy in descending water was estimated on the order of 0.01 m w.e. a^{-1}, using an average drop of 200 m and a total annual discharge of $7\times10^6\,\mathrm{m}^3$ (Holmlund, 1987). Finally, the total systematic uncertainty due to internal ablation (0.011 m w.e. a^{-1}) was cumulated over the number of years of the aerial survey periods (Table 2, $\sigma_{\text{intAbl.sys}}$).

Internal accumulation as described by Trabant and Mayo (1985) is usually not accounted for by traditional glaciological methods (Østrem and Brugman, 1991). Its influence on mass balance may be small in magnitude or even negligible on temperate glaciers, but if not accounted for can result in a systematic underestimation of the mass balance. As a consequence, internal accumulation needs to be considered for a poly-thermal glacier such as Storglaciären (Petterson et al., 2003). Based on data from 1997/98 and 1998/99, Schneider and Jansson (2004) estimate the internal accumulation due to re-freezing of percolating water in cold snow and firn as well as the freezing of water trapped by capillary action in snow and firn by the winter cold. They find that these two factors account for 30% and 70%, respectively, of the annual internal accumulation and that the significance of internal accumulation for the glacier mass balance depends on the areal extent of the accumulation area, the thickness of the active layer, and the winter temperature. Based on measured temperature profiles as well as physical characteristics and water content of firn, they obtaine values for internal accumulation of 0.04–0.06 m w.e. a^{-1}, or 3–5% of the winter balance of the entire glacier. Hence, we assumed the underestimation of the glaciological mass balance due to internal accumulation to 4% of the winter balances (Table 2, $\sigma_{\text{intAcc.sys}}$).

3.3.7 Superimposed ice

Superimposed ice accumulates on the current summer surface by refreezing of rain or melt-water produced during the current mass balance year. It forms above the previous year's surface and can be accounted for during standard stake readings (Østrem and Brugman, 1991). On Storglaciären, Schytt (1949) measured a maximum of about 0.1–0.2 m w.e. of superimposed ice formation in the ablation zone. The thickness can be substantial larger at the glacier margins and at the glacier terminus. The total amount of superimposed ice remaining at the end of the ablation season depends on the elevation of the snow line and is, hence, larger for positive balance years. We assumed the error of its determination to be covered with the uncertainty estimate for the field observations (Sect. 3.3.1).

3.3.8 Flux divergence

According to the principal of mass conservation, the mass balance should be balanced by the ice flux divergence and the thickness change, as long as integrated over the entire glacier (Paterson, 1994) and was not treated separately in this study. Note that any analysis dealing with mass balance at points or along profiles needs to consider the flux divergence.

3.3.9 Overall uncertainties

A direct comparison of glaciological and volumetric mass balances requires a correction for related uncertainties. Thereto, the glaciological mass balance were cumulated over the aerial survey periods and corrected for systematic errors due to uncertainties related to reference areas, internal ablation and accumulation (Table 2, $_{.sys}$). Besides the conversion from volume to mass balance (Sect. 3.3.3), the systematic corrections of the volumetric mass balances include the melt-correction due to differences in survey dates and elevation differences in the DEMs as derived from independent dGPS measurements (Table 3, $_{.sys}$). The systematic uncertainties are of positive and negative signs depending on whether they are to be added or subtracted from the glaciological/volumetric mass balance to fit the one based on the other method. Overall stochastic uncertainties are cumulated for the glaciological ($\sigma_{\text{glac.stoc}}$) and the volumetric ($\sigma_{\text{vol.stoc}}$) mass balances separately, both according to the law of error propagation:

$$\sigma_{\text{glac.stoc}} = \sqrt{\sigma^2_{\text{field.stoc}} + \sigma^2_{\text{krig.stoc}} + \sigma^2_{\text{ref.stoc}}} \quad (5)$$

$$\sigma_{\text{vol.stoc}} = \sqrt{\sigma^2_{\text{density.stoc}} + \sigma^2_{\text{dGPS.stoc}}} \quad (6)$$

where $\sigma_{\text{field.stoc}}$, $\sigma_{\text{krig.stoc}}$, and $\sigma_{\text{ref.stoc}}$ are the stochastic uncertainties related to the field measurements, interpolation method, and reference areas (Table 2, $_{.stoc}$) and where $\sigma_{\text{density.stoc}}$ and $\sigma_{\text{dGPS.stoc}}$ are the stochastic uncertainties related to density assumptions and to the DEMs (Table 3, $_{.stoc}$).

4 Results

The cumulative glaciological mass balances and related uncertainties are given in Table 2. The first two periods are negative followed by two periods of ice gain. The mass balance over the entire period covered is also negative. Annual stochastic uncertainties related to the field measurements ($\sigma_{\text{field.stoc}}$) were estimated to 0.2 and 0.1 m w.e. a^{-1} until and after the year 1965, respectively. Cumulated over the observation periods according to the law of error propagation, they result in errors of about $\pm$ 0.5 m w.e. for the first period, $\pm$ 0.3 m w.e. for the other decadal periods, and $\pm$ 0.6 m w.e. for the entire period from 1959–99. The annual stochastic uncertainties related to the interpolation methods ($\sigma_{\text{krig.stoc}}$) were estimated to $\pm$ 0.1 m w.e. a^{-1}, and hence result in the same cumulative errors as for field measurements, with exception of the first period. The correction of the glaciological mass balance to the reference areas and corresponding changes of the glacier in the new orthophotos lead to a systematic decrease of the absolute values of the glaciological mass balance ($\sigma_{\text{ref.sys}}$) of below 0.2 m w.e. and stochastic uncertainties ($\sigma_{\text{ref.stoc}}$) which are greatest in the first two periods with values of of below $\pm$ 1.0 m w.e. The overestimation of the mass balance due to ignoring the internal ablation ($\sigma_{\text{intAbl.sys}}$) was estimated to be small, with values of about -0.01 m w.e. a^{-1}. Cumulated over the aerial survey periods this leads to corrections for the decadal and the entire period of about -0.1 and -0.4 m w.e., respectively. The rough estimate of the internal accumulation ($\sigma_{\text{intAcc.sys}}$) shows an underestimation of the glaciological mass balance by between 0.5 and 0.7 m w.e. for the four decadal periods and by 2.4 m w.e. for the 40 years between the first and the last aerial survey. Overall systematic uncertainties ($\sigma_{\text{total.sys}}$) including internal accumulation are positive for all periods with decadal values of about 0.5 m w.e. When excluding corrections for internal accumulation, absolute decadal corrections are about 0.1 m w.e. or smaller and negative in all but the second period. Overall stochastic uncertainties ($\sigma_{\text{total.stoc}}$) are about $\pm$ 1.0 m w.e. in the first two decadal periods, roughly $\pm$ 0.5 m w.e. in the second two, and $\pm$ 1.7 m w.e. for the entire period of 1959–99.

The volumetric mass balances, based on Koblet et al. (2010) and an assumed density of 860 kg m^3, show the same trend in mass loss over the first two decades followed by two decades of mass regain. The mass balances and corresponding systematic and stochastic uncertainties are given in Table 3. The uncertainty related to the density assumption ($\sigma_{\text{density.stoc}}$) is below $\pm$ 0.4 m w.e. The comparison of the DEM with independent dGPS points provides a rough idea of the systematic and stochastic uncertainties related to the photogrammetry ($\sigma_{\text{dGPS.sys}}$ and $\sigma_{\text{dGPS.stoc}}$). Both show that the uncertainties of the volume changes related to the DEM of 1980 are about twice as large as the ones from the other periods. Systematic corrections of the volumetric mass balance to fit the field survey dates ($\sigma_{\text{survey.sys}}$) require additional melt in all but the third period (1980–90). Overall systematic uncertainties ($\sigma_{\text{total.sys}}$) are positive in the first two periods and negative in the others with absolute values between 0.2 and 0.6 m w.e. and with stochastic uncertainties ($\sigma_{\text{total.stoc}}$) between $\pm$ 0.2 and $\pm$ 0.9 m w.e. (Table 3.)

A summary of the above results is given in Fig. 2 which compares the cumulated official glaciological (Holmlund et al. (2005), Tarfala Research Station data) and the volumetric

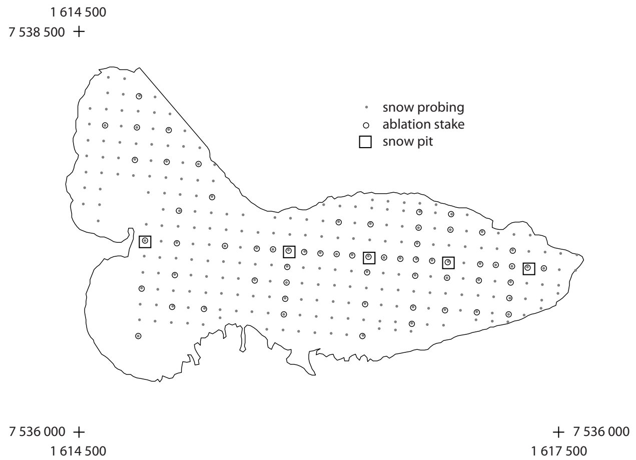

Fig. 1. Observation network on Storglaciären in 2006/07. Snow observations and ablation stakes are used for the determination of the winter and summer mass balance, respectively. Glacier outlines from the 1990 map (Holmlund, 1996). Map coordinates are in the Swedish coordinate system RT 90 2.5 gon V.

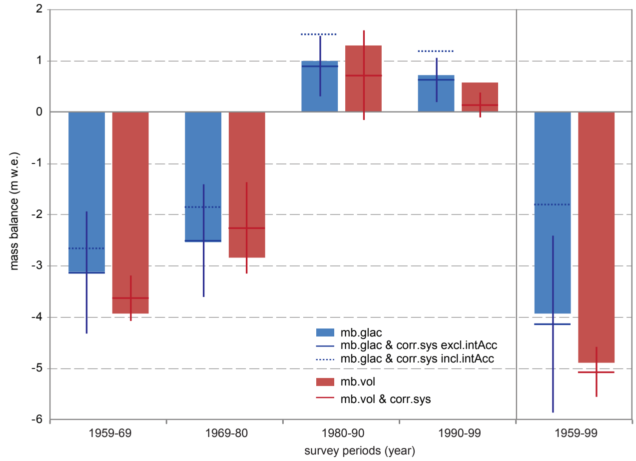

Fig. 2. Decadal glaciological and volumetric mass balances of Storglaciären. The "official" glaciological mass balances by Holmlund et al. (2005; blue bars) and the volumetric mass balances by Koblet et al. (2010; red bars) are shown for the periods of the aerial surveys. Corrections for systematic and stochastic uncertainties are indicated by horizontal and vertical lines, respectively. For the glaciological mass balances, the systematic uncertainties including corrections for internal accumulation (intAcc) are shown by dotted horizontal lines.

mass balances (Koblet et al., 2010). Corresponding overall systematic and stochastic errors are indicated by horizontal and vertical lines, respectively. Overall systematic corrections of the glaciological mass balance including internal accumulation are given separately (dotted horizontal line) as they offset clearly from the other results. The absolute values of the glaciological mass balance are smaller than the ones of the volumetric mass balance in all but the last period (1990–99). Systematic uncertainties are relatively small for the glaciological data and mostly negative when excluding internal accumulation. Including the latter, however, leads to clearly positive corrections. Stochastic uncertainties of the glaciological data are largest in the first two periods (about ± 1 m w.e.) mainly due to corrections related to reference areas. Absolute corrections for systematic uncertainties are 0.6 m w.e. or smaller and reduce the absolute volumetric mass balances in all but the overall time period (1959–99). Overall stochastic uncertainties are ± 0.9 m w.e. for the changes including the DEM of 1980 and half or less for the other periods.

5 Discussion

Based on the "official" glaciological mass balance series (Holmlund et al. (2005), Tarfala Research Station data), Storglaciären experienced a strong cumulative ice loss of about 13 m w.e. from the initiation of measurements in 1945 to the first half of the 1970s, followed by 15 years of small cumulative mass balance variations (Fig. 3). Between 1988 and 1995, the glacier increased its specific mass by some 4 m w.e. and subsequently lost 6 m w.e. from 1995–2007. The volumetric mass balances by Koblet et al. (2010) based on the available aerial photographs from 1959, -69, -80, -90, and -99 can only roughly trace these variations due to the decadal resolution. The cumulative changes (of the glaciological mass balance) between 1959 and 1999 account for just 4 m w.e. ice loss, of which 3 m w.e. were already lost by 1969. As a consequence, the decadal signal as derived from the photogrammetric surveys after 1969 is in the same order of magnitude or even smaller than the sub-decadal variations of the glaciological mass balances. The absolute glacier changes based on the photogrammetric surveys are larger than the corresponding changes from the glaciological in-situ measurements in three of the four decadal periods as well as over the entire observation period (1959–99).

The uncertainty assessment as described in Sects. 3 and 4 was an attempt to quantify the major sources of potential errors to be addressed in order to compare the glaciological with the volumetric mass balances. All estimates and assumptions taken to address stochastic and systematic uncertainties comprise additional sources of potential errors. The melt correction due to the different observation dates in 1959, for example, inherits the errors from the degree-day model (temperature data series, summer balance, melt factor, ELA_0-determination) as well as from the determination of the dates of the field survey and of the aerial survey (reporting), and neglects the effect of summer snow fall events. We waive the attempt to quantify all these potential errors of the uncertainty estimates since a corresponding overall value would represent a statistical exercise rather than a real-world uncertainty.

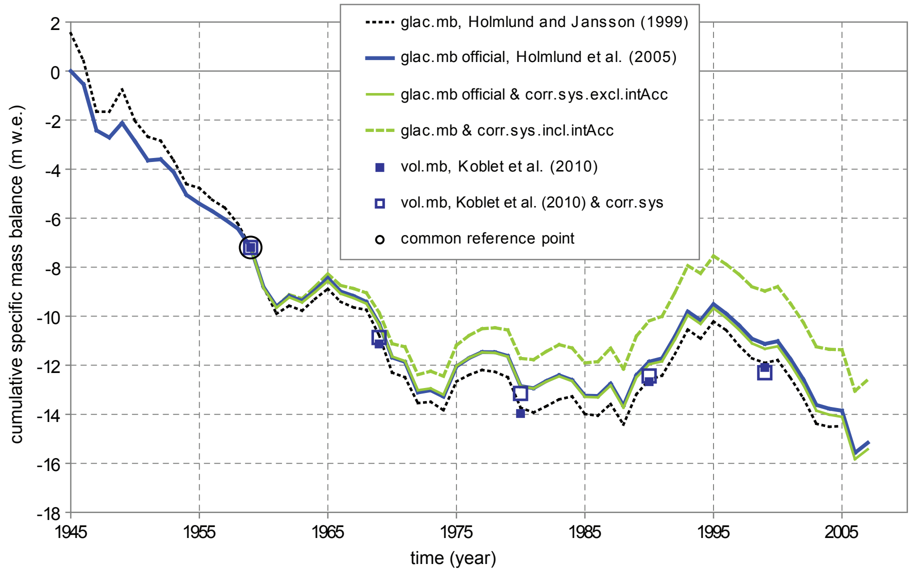

Fig. 3. Cumulative glaciological and volumetric mass balance series of Storglaciären. The official glaciological mass balance series (Holmlund et al. (2005), Tarfala Research Station data) is compared to the new volumetric mass balance data by Koblet et al. (2010; 1959-69-80-90-99). In addition, two glaciological mass balance series are shown which are based on the official one but corrected for directional uncertainties including/excluding internal accumulation (for details see text) as well as the old official series by Holmlund and Jansson (1999). In order to have a common reference point, all changes are relative to the value of 1959 of the "official" glaciological data series (Holmlund et al. (2005), Tarfala Research Station data; −7.2 m w.e.).

However, we applied the systematic uncertainties including corrections for reference areas, internal ablation, and internal accumulation to the official mass balance series (Holmlund et al. (2005), Tarfala Research Station data) in order to produce a "best estimate" glaciological mass balance series to compare with the volumetric changes by Koblet et al. (2010) which were converted to mass balance and corrected for systematic uncertainties in survey periods and photogrammetric processing. In principle, this should reduce the differences between the glaciological and the volumetric mass balance. In fact, this is true for most of the corrections and periods; but the systematic bias from the internal accumulation clearly increases the deviations in all periods. This effect becomes most prominent in Fig. 3, where the changes are cumulated with reference to the year of the first aerial survey (i.e., 1959).

The estimate of internal accumulation by Schneider and Jansson (2003; 0.04–0.06 m w.e. a^{-1}) is larger than earlier ones for Storglaciären by Östling and Hooke (1986; 0.02 m w.e. a^{-1}) and by Holmlund (1987; 0.03 m w.e. a^{-1}), which do both not consider refreezing capillarity water, but smaller than other estimates, e.g., for Alaskan glaciers by Trabant and Mayo (1985). Miller and Pelto (1999) note on Lemon Creek Glacier, Alaska, that a part of the observed internal accumulation could represent a redistribution rather than a net mass gain and that during warm winters there was no internal accumulation. However, Schneider and Jansson (2003) consider their results from 1997/98 and 1998/99 as representative for Storglaciären, at least with regard to winter temperatures and winter balances for the period 1965–99. Even if we assume that the findings by Schneider and Jansson (2003) are maximum estimates and set the average annual systematic error due to internal accumulation to half their absolute values, a systematic error of 0.82–1.23 m w.e. cumulates over the 40-year observation period. The systematic uncertainties of the volumetric mass balance as derived from independent dGPS measurements (cf. Koblet et al., 2010) do not provide an explanation for these differences and suggest that either the long-term effect of internal accumulation at Storglaciären is overestimated significantly, or another systematic error of the glaciological or the volumetric mass balance is not yet (correctly) accounted for.

At first glance, the comparison of the different data series as cumulative changes from 1959 might look unsatisfactory. The best agreements with the volumetric mass balances by Koblet et al. (2010) are the "old" glaciological series by Holmlund and Jansson (1999), followed by the official one (Holmlund et al. (2005), Tarfala Research Station data), and finally the "best estimates" (excl. and incl. internal accumulation) of the present study (Fig. 3). The systematic uncertainties applied to the volumetric mass balance by Koblet et al. (2010) cannot provide a final answer to these questions but show that the official glaciological series is within the range of uncertainty, whereas our "best estimate" is only within when ignoring internal accumulation. However, the mean annual deviations from the official glaciological mass balance series (Holmlund et al. (2005), Tarfala Research Station data) are below 0.1 m w.e. a^{-1} for all data series. This holds

Table 4. "Official" glaciological mass balance (Holmlund et al. (2005), Tarfala Research Station data) in comparison with other glaciological (glac.) and volumetric (vol.) mass balance (mb) series of Storglaciären. The table shows cumulative mass balances of the "official" glaciological data series for the observation periods and corresponding mean annual differences of the other series. Note that the observation periods refer to the start and end year of the corresponding first and last field surveys, respectively, e.g., the period 1959–99 covers the hydrological years from 1959/60 to 1998/99.

Obs. period	glac. mb by Holmlund et al. (2005), Tarfala Research Station data	glac. mb by Holmlund and Jansson (1999)	glac. mb this study, "best estimate", $\sigma_{\text{total.sys}}$ excl. intAcc	glac. mb this study, "best estimate", $\sigma_{\text{total.sys}}$ incl. intAcc	vol. mb by Koblet et al. (2010)	vol. mb by Koblet et al. (2010), $\sigma_{\text{total.sys}}$
(#) years	m w.e.	m w.e. a^{-1}	m w.e. a^{-1}	m w.e. a^{-1}	m w.e. a^{-1}	m w.e. a^{-1}
1959–69 (10)	−3.110	−0.047	−0.006	+0.042	−0.082	−0.056
1969–80 (11)	−2.540	−0.037	0.001	+0.059	−0.027	+0.023
1980–90 (10)	1.000	+0.014	−0.012	+0.053	+0.030	−0.029
1990–99 (9)	0.720	−0.003	−0.011	+0.054	−0.015	−0.066
1959–99 (40)	−3.930	−0.019	0.007	+0.052	−0.024	−0.029

for all the four observation periods as well as over the entire period of 1959–99 (Table 4). These mean annual deviations (Table 4) are then within or even smaller than the estimated uncertainty of a single stake or snow pit reading (cf. Thibert et al., 2008; Huss et al., 2009).

Over the past decades, it has become a standard procedure to check the (annual) glaciological with (decadal) volumetric mass balance methods, utilizing techniques such as topographic map comparison (e.g., Andreassen 1999; Conway et al. 1999; Kuhn et al. 1999; Hagg et al., 2004; Østrem and Haakensen, 1999), photogrammetry (e.g., Krimmel, 1999; Cox and March, 2005; Thibert et al., 2008; Haug et al., 2009; Huss et al., 2009; Fischer, 2010), global positioning systems (e.g., Hagen et al. 1999, Miller and Pelto 1999), or laser altimetry (e.g., Conway et al., 1999; Fischer, 2010; Echelmeyer et al., 1996; Sapiano et al., 1998; Geist and Stötter, 2007), the latter three references without direct comparison. It has become evident that a sound validation ideally is based on consistent data and procedures, and includes a sound assessment of stochastic and systematic uncertainties. In cases of major deviations between the results of the different methods, it is recommended that the (annual) glaciological data series be adjusted to the (decadal) volumetric changes (cf. Thibert et al., 2008; Huss et al., 2009). The decisive factor thereby is provided by the uncertainty assessment: if the stochastic error bars of the glaciological and volumetric mass balances, both corrected for systematic errors, do not overlap, an adjustment over the corresponding period is required. Large uncertainties in the volumetric mass balance might require a correction of the basic DEMs to a high-precision and high-resolution reference DEM (cf. Kääb, 2005) prior to the homogenization of the mass balances. In the case of Storglaciären, corresponding error bars do overlap in all periods (cf. Fig. 2) when ignoring systematic corrections for internal accumulation and, hence, an adjustment is not required. The inclusion of present systematic (over-) corrections for internal accumulation would, however, require such an adjustment for at least the overall period from 1959–99. Further research and the next aerial survey will have to re-address this issue.

6 Conclusions

Storglaciären has a continuous glacier mass balance record back to 1945/46 with a network density of about 100 observations per square kilometer for winter balance and 15 observations per square kilometer for summer balance. It is hence the longest glacier mass balance record with probably the greatest observation density available from the WGMS. As recommended by international monitoring standards, regular aerial surveys have been carried out on a decadal base since the beginning in order to validate the glaciological in-situ measurements with results from the geodetic method. For the first time, dia-positives of the original aerial photographs of 1959, -69, -80, -90, and -99 are used by Koblet et al. (2010) to directly produce volumetric changes based on uniform photogrammetric methods. In the present study we compared these volumetric with the official glaciological mass balances by Holmlund et al. (2005) including a sound analysis of potential uncertainties.

The volumetric mass balances are in good agreement with the glaciological data. The absolute differences between volumetric and the glaciological mass balances are 0.8 m w.e. in the first and 0.3 m w.e. or less in the other three decadal survey periods. These deviations can be reduced in most periods by applying corrections for systematic uncertainties such as differences in survey dates and reference areas or accounting for internal ablation. In contrast, accounting for internal accumulation based on the study by Schneider and Jansson (2004) systematically increases the mismatch. This suggests that either the effect of the internal accumulation is overestimated or that there is another systematic error not yet considered. However, the mean annual differences between such a "best estimate" glaciological mass balance, which corrects the official series by all directional uncertainties, and the volumetric mass balance, corrected for systematic uncertainties, are less than about 0.1 m w.e. a^{-1} and as such are within the order of magnitude of the stake and pit reading error.

From the present study we conclude that the new volumetric mass balances fit well overall with the glaciological ones and confirm the excellent quality of this data series. Excluding the systematic deviations due to the issue with the internal accumulation, there is an overlap of stochastic error bars of volumetric and glaciological mass balances and, hence, no need for an adjustment of the glaciological data series. Thanks to the very dense observation network of Storglaciären, the cumulative glaciological series fits well to the decadal volumetric data in spite of the low mass balance signal. Further investigations should, however, address the better quantification of systematic error sources, such as internal accumulation, as well as the issue of the (changing) reference areas used for mass balance calculations. The present study shows the importance of systematic and ideally uniform data processing as well as a sound uncertainty assessment in order to detect – and if necessary correct – systematic errors in the measurements. A next aerial survey is, therefore, overdue and should provide a new high-precision and high-resolution reference DEM.

Acknowledgements. We are indebted to all the investigators and field assistants involved in the long-term monitoring of Storglaciären and also thank the staff of the Tarfala Research Station for their hospitality during field seasons. Sincere thanks go to the two anonymous referees, Mauri Pelto and the editor for their constructive comments that helped to improve the paper, to Stefanie Gubler for fruitful discussions on statistical issues, and to Betsy Armstrong for polishing the English. The present study was supported by the Universities of Zurich and Stockholm, and by the GLACIAS project (SNF-Nr. 200021–116354).

Edited by: I. M. Howat

References

Ahlmann, H. W.: Projet d'un programme de recherché glaciaire, Geogr. Ann., 2(3–4), 313–320, 1929.

Ahlmann, H. W.: Scientific results of the Norwegian-Swedish Spitsbergen Expedition 1934. Part V. The Fourteenth of July Glacier, Geogr. Ann., 17, 167–218, 1935.

Ahlmann, H. W.: Scientific results of the Swedish-Icelandic investigations 1936-37-38. Chapter VII. The regime of Hoffellsjökull, Geogr. Ann., 21, 177–188, 1939.

Ahlmann, H. W.: Studies on north-east Greenland. Part III. Accumulation and ablation on the Fröya glacier; its regime in 1938–39 and 1939–40. Geogr. Ann., 24(1–2), 1–50, 1942.

Ahlmann, H. W.: Scientific investigations in the Kebnekajse Massif, northern Sweden. I. General outline of the investigations in 1946–51, Geogr. Ann., 24(1–2), 90–94, 1951.

Aellen, M.: Glacier mass balance studies in the Swiss Alps. Z. Gletscherkd. Glazialgeol., 31(1–2), 159–168, 1996.

Albrecht, O., Jansson, P., and Blatter, H.: Modelling glacier response to measured mass balance forcing, Ann. Glaciol., 31, 91–96, 2000.

Andreassen, L. M.: Comparing traditional mass balance measurements with long-term volume change extracted from topographic maps: a case study of Storbreen glacier in Jotunheimen, Norway, for the period 1940–1997, Geogr. Ann., 81A(4), 467–476, 1999.

Bader, H.: Sorge's law of densification of snow on high polar glaciers, J. Glaciol., 2(15), 319–323, 1954.

Braithwaite, R. J.: Positive degree-day factors for ablation on the Greenland ice sheet studied by energy-balance modeling, J. Glaciol., 41(137), 153–160, 1995.

Cogley, J. G. and Adams, W. P.: Mass balance of glaciers other than the ice sheets, J. Glaciol., 44(147), 315–325, 1998.

Conway H., Rasmussen, L. A., and Marshall, H.-P.: Annual mass balance of Blue Glacier, USA: 1955–97, Geogr. Ann., 81A(4), 509–520, 1999.

Cox, L. H. and March, R. S.: Comparison of geodetic and glaciological mass balance techniques, Gulkana Glacier, Alaska, U.S.A., J. Glaciol., 50(170), 363–370, 2004.

Deutch, C. and Journel, A.: GSLIB: Geostatistical Software Library and User's Guide, Oxford University Press, New York, 369, 1998.

Dyurgerov, M. B. and Meier, M. F.: Glaciers and the changing Earth system: a 2004 snapshot, Institute of Arctic and Alpine Research (INSTAAR) Occasional Paper, Boulder, 58, 117 pp., 2005.

Echelmeyer, K. A., Harrison, W. D., Larsen, C. F., Sapiano, J. J., Mitchell, J. E., DeMallie, J., Rabus, B., Adalgeirsdóttir, G., and Sombardier, L.: Airborne surface profiling of glaciers: a case-study in Alaska. J. Glaciol., 42(142), 538–547, 1996.

Elsberg, D. H., Harrison, W. D., Echelmeyer, K. A., and Krimmel, R. M.: Quantifying the effects of climate and surface change on glacier mass balance, J. Glaciol., 47(159), 649–658, 2001.

Fischer, A.: Glaciers and climate change: Interpretation of 50 years of direct mass balance of Hintereisferner, Global Planet. Change, 71, 13–26, 2010.

Fountain, A. G., Jansson, P., Kaser, G., and Dyurgerov, M.: Summary of the workshop on methods of mass balance measurements and modelling, Tarfala, Sweden, August 10–12, 1998, Geogr. Ann., 81A(4), 461–465, 1999.

Geist, T. and Stötter, J.: Documentation of glacier surface elevation change with multi-temporal airborne laser scanner data – case study: Hintereisferner and Kesselwandferner, Tyrol, Austria. Z. Gletscherk. Glazialgeol., 41, 2007.

Grudd, H. and Schneider, T.: Air temperature at Tarfala Research Station 1946–1995, Geogr. Ann., 78, 115–120, http://www.ink.su.se/pub/jsp/polopoly.jsp?d=6787&a=23702, last access: 28 May 2009, 1996.

Haeberli, W.: Historical evolution and operational aspects of worldwide glacier monitoring, in: Into the Second Century of World Glacier Monitoring – Prospects and Strategies, edited by: Haeberli, W., Hoelzle, M., and Suter, S., UNESCO publishing, Paris, 35–51, 1998.

Haefeli, R.: The ablation gradient and the retreat of a glacier tongue, Union Géodésique et Géophysique Internationale, Association Internationale d'Hydrologie Scientifique, Commissions des Neiges et Glaces, Colloque d'Obergurgle, 49–59, 1962.

Hagg, W. J., Braun, L. N., Uvarov, V. N., and Makarevich, K. G.: A comparison of three methods of mass balance determination in the Tuyuksu glacier region, Tien Shan, Central Asia, J. Glaciol., 50(171), 505–510, 2004.

Hagen, J. O., Melvold, K., Eiken, T., Isaksson, E., and Lefauconnier, B.: Mass balance methods on Kongsvegen, Svalbard. Geogr. Ann., 81A(4), 593–601, 1999.

Haug T., Rolstad C., Elvehøy H., Jackson, M., and Maalen-Johansen, I.: Geodetic mass balance of the western Svartisen ice cap, Norway, in the periods 1968–1985 and 1985–2002, Ann. Glaciol., 50(50), 119–125, 2009.

Hieltala, M.: En utvärdering av areella nederbördsmetoder och mätardplaceringar I Tarfaladalen, Master thesis, Stockholm University, Sweden, unpublished, 1989.

Hock, R.: Temperature index melt modelling in mountain areas, J. Hydrol., 282, 104–115, 2003.

Hock, R. and Jensen, H.: Application of kriging interpolation for glacier mass balance computations, Geogr. Ann., 81A, 611–619, 1999.

Hock, R. and Holmgren, B.: A distributed surface energy-balance model for complex topography and its application to Storglaciären, Sweden. J. Glaciol., 51(172), 25–36, 2005.

Hoinkes, H.: Methoden und Möglichkeiten von Massenhaushaltsstudien auf Gletschern: Ergebnisse der Messreihe Hintereisferner (Ötztaler Alpen) 1953–1968. Z. Gletscherkd. Glazialgeol., 6(1–2), 37–90, 1970.

Holmlund, P.: Mass balance of Storglaciären during the 20th century, Geogr. Ann., 69A(3–4), 439–447, 1987.

Holmlund, P.: Maps of Storglaciären and their use in glacier monitoring studies, Geogr. Ann., 78A(2–3), 193–196, 1996.

Holmlund, P., Karlén, W., and Grudd, H.: Fifty years of mass balance and glacier front observations at the Tarfala Research Station, Geogr. Ann., 78A(2–3), 105–114, 1996.

Holmlund, P. and Jansson, P.: The Tarfala mass balance programme, Geogr. Ann., 81A(4), 621–631, 1999.

Holmlund, P., Jansson, P., and Pettersson, R.: A re-analysis of the 58 year mass balance record of Storglaciären, Sweden, Ann. Glaciol., 42, 389–394, 2005.

Hooke, L. R., Calla, P., Holmlund, P., Nilsson, M., and Stroeven, A.: A 3 year record of seasonal variation in surface velocity, Storglaciären, Sweden, J. Glaciol., 35(120), 235–247, 1989.

Huss, M., Bauder, A., Funk, M., and Hock, R.: Determination of the seasonal mass balance of four Alpine glaciers since 1865, J. Geophys. Res., 113(F1), F01015, doi:10.1029/2007JF000803, 2008.

Huss, M., Bauder, A., and Funk, M.: Homogenization of long-term mass balance time series, Ann. Glaciol., 50(50), 198–206, 2009.

Jansson, P.: Effect of uncertainties in measured variables on the calculated mass balance of Storglaciären, Geogr. Ann., 81A, 633–642, 1999.

Jansson, P. and Pettersson, R.: Spatial and temporal characteristics of a long mass balance record, Storglaciären, Sweden, Arct., Ant. Alp. Res., 39(3), 432–437, 2007.

Kääb, A.: Remote sensing of mountain glaciers and permafrost creep. Schriftenreihe Physische Geographie, University of Zurich, 48, 266 pp. ISBN3855432449, 2005.

Karlén, W. and Holmlund, P.: Tarfala Research Station, 50 years of activity, Geogr. Ann. 78A(1–2), 101, 1996.

Kaser, G., Cogley, J. G., Dyurgerov, M. B., Meier, M. F., and Ohmura, A.: Mass balance of glaciers and ice caps: consensus estimates for 1961–2004, Geophys. Res. Lett., 33(19), L19501, doi:10.1029/2006GL027511, 2006.

Kasser, P., Aellen, M., und Siegenthaler, H.: Die Gletscher der Schweizer Alpen 1977/78 und 1978/79. 99. und 100. Bericht, Jahrbuch der GK/SNG, 288 pp., 1986.

Koblet, T., Gärtner-Roer, I., Zemp, M., Jansson, P., Thee, P., Haeberli, W., and Holmlund, P.: Reanalysis of multi-temporal aerial images of Storglaciären, Sweden (1959–99) – Part 1: Determination of length, area, and volume changes, The Cryosphere, 4, 333–343, doi:10.5194/tc-4-333-2010, 2010.

Krimmel, R. M.: Analysis of difference between direct and geodetic mass balance measurements at South Cascade Glacier, Washington, Geogr. Ann., 81A(4), 653–658, 1999.

Kuhn, M., Dreiseitl, E., Hofinger, S., Markl, G., Span, N., and Kaser, G.: Measurements and models of the mass balance of Hintereisferner, Geogr. Ann., 81A(4), 659–670, 1999.

Meier, M. F.: Glaciers of the Gannett Peak-Fremont Peak Area, Wyoming, M.Sc. thesis, State University of Iowa, USA, 159 pp., 1951.

Meeus, J.: Astronomical algorithms, 2nd edition, Willmann-Bell, Richmond, 477 pp., 1999.

Mercanton, P. L.: Vermessungen am Rhonegletscher/Mensuration au glacier du Rhône: 1874–1915, Neue Denkschr. Schweiz. Naturforsch. Ges., 52, 1916.

Miller, M. M. and Pelto, M. S.: Mass balance measurements on the Lemon Creek Glacier, Juneau Icefield, Alaska 1953–1998, Geogr. Ann., 81A(4), 671–681, 1999.

Müller, H. und Kappenberger, G.: Claridenfirn – Messungen 1914–1984. Züricher Geogr. Schr., 40, 79 pp., 1991.

Östling, M. and Hooke, R. LeB.: Water storage in Storglaciären, Kebnekaise, Sweden, Geogr. Ann. 68A(4), 279–290, 1986.

Østrem, G. and Brugman, M.: Glacier mass balance measurements. A manual for field and office work, Saskatoon, Sask., Environment Canada, National Hydrology Research Institute, NHRI Science Report, 4, 1991.

Østrem, G. and Haakensen, G.: Map comparison or traditional mass-balance measurements: which method is better? Geogr. Ann., 81A, 703–711, 1999.

Paterson, W. S. B.: The physics of glaciers, 3rd edition, Pergamon Press, Oxford, 480 pp, 1994.

Pelto, M. S. and Miller, M. M.: Mass balance of the Taku Glacier, Alaska from 1946 to 1986, Northwest Science, 64(3), 121–130, 1990.

Pettersson, R., Jansson, P., and Blatter, H.: Spatial variability in water content at the cold-temperate transition surface of the polythermal Storglaciären, Sweden, J. Geophys. Res., 109, F02009, doi:10.1029/2003JF000110, 2004.

Pettersson, R., Jansson, P., and Holmlund, P.: Cold surface layer thinning on Storglaciären, Sweden, observed by repeat ground penetrating radar surveys, J. Geophys. Res., 108, F16004, doi:10.1029/2003JF000024, 2003.

Roher, M.: Determination of the transition air temperature from snow to rain and intensity of precipitation, in: Instruments and observing methods, edited by: Sevruk, B., Geneva, World Meteorological Organization, Technical Report, 48, 475–482, 1989.

Sapiano, J. J., Harrison, W. D., and Echelmeyer, K. A.: Elevation, volume and terminus changes of nine glaciers in North America. J. Glaciol., 44(146), 119–135, 1998.

Schneider, T. and Jansson, P.: Internal accumulation in firn and its significance for the mass balance of Storglaciären, Sweden, J. Glaciol., 50(168), 25–34, 2004.

Schytt, V.: Glaciologiska arbete i Kebnekaise, Ymer, 67(1), 18–42, 1947.

Schytt, V.: Re-freezing melt-water on the surface glacier ice, Geogr. Ann., 31, 222–227, 1949.

Sorge, E.: Glaziologische Untersuchungen in Eismitte. In: Wissenschaftliche Ergebnisse der Deutschen Groenland-Expedition Alfred Wegener 1929 und 1930/31, Leipzig, F.A. Brockhaus, 3, 270 pp., 1935.

Thibert, E., Blanc, R., Vincent, C., and Eckert, N.: Glaciological and volumetric mass balance measurements: error analysis over 51 years for Glacier de Sarennes, French Alps, J. Glaciol., 54(186), 522–532, 2008.

Trabant, D. C. and Mayo, L. R.: Estimation and effects of internal accumulation on five glaciers in Alaska, Ann. Glaciol., 6, 113–117, 1985.

Wallén, C. C.: Glacial-meteorological investigations on the Kårsa Glacier in Swedish Lappland, Geogr. Ann., 30(3–4), 451–672, 1948.

WGMS: Global Glacier Changes: facts and figures, edited by: Zemp, M., Roer, I., Kääb, A., Hoelzle, M., Paul, F., and Haeberli, W., UNEP, World Glacier Monitoring Service, Zurich, Switzerland, 88 pp., 2008.

Zemp, M., Hoelzle, M., and Haeberli, W.: Six decades of glacier mass balance observations – a review of the worldwide monitoring network, Ann. Glaciol., 50, 101–111, 2009.

Publication 9

Zemp, M., Paul, F., Hoelzle, M. & Haeberli, W. (2008), **Glacier fluctuations in the European Alps 1850–2000: an overview and spatio-temporal analysis of available data.** In: Orlove, B., Wiegandt, E. & Luckman, B. (eds.): The darkening peaks: Glacial retreat in scientific and social context. University of California Press, 152-167.

11

Glacier Fluctuations in the European Alps, 1850–2000

AN OVERVIEW AND A SPATIOTEMPORAL ANALYSIS OF AVAILABLE DATA

Michael Zemp, Frank Paul,
Martin Hoelzle, and Wilfried Haeberli

Fluctuations of mountain glaciers are among the best natural indicators of climate change (Houghton et al. 2001). Changes in precipitation and wind lead to variations in accumulation, while changes in temperature, radiation fluxes, and wind, among other factors, affect the surface energy balance and thus ablation. Disturbances in glacier mass balance, in turn, alter the flow regime and, consequently, after a glacier-specific delay, result in a glacier advance or retreat such that the glacier geometry and altitude range change until accumulation equals ablation (Kuhn et al. 1985). Hence, mass balance is the direct and undelayed signal of annual atmospheric conditions, whereas changes in length are an indirect, delayed, and filtered but enhanced signal (Haeberli 1998).

The modern concept of worldwide glacier observation is an integrated and multilevel one; it aims to combine in-situ observations with remotely sensed data, understanding of process with global coverage, and traditional measurements with new technologies. This concept uses detailed mass and energy balance studies from just a few glaciers, together with length change observations from many sites and inventories covering entire mountain chains. Numerical models link all three components over time and space (Haeberli 2004). The European Union–funded ALP-IMP Project focuses on multicentennial climate variability in the Alps on the basis of instrumental data, model simulations, and proxy data. It represents a unique opportunity to apply this glacier-monitoring concept to the European Alps, where by far the most concentrated amount of information about glacier fluctuations over the past century is available. The World Glacier Monitoring Service (WGMS) has compiled, within the framework of the ALP-IMP Project, an unprecedented data set containing inventory data (i.e., area, length, and altitude range) from approximately 5,150 Alpine[1] glaciers and fluctuation series from more than 670 of them (i.e., more than 25,350 observations of annual front variation and 575 of annual mass balance) dating back to 1850.

In this chapter we offer an overview of the available glacier data sets from the European Alps and analyze glacier fluctuations between

1850 and 2000. To achieve this, we analyze glacier size characteristics from the 1970s, the only time period for which a complete Alpine inventory is available, and extrapolate Alpine glaciation in 1850 and in 2000 from size-dependent area changes from Switzerland. We go on to examine mass balance and front variation series for the insight they provide into glacier fluctuations, the corresponding acceleration trends, and regional distribution patterns at an annual resolution. Finally, we discuss the representativeness of these recorded fluctuation series for all the Alpine glaciers and draw conclusions for glacier monitoring.

BACKGROUND

The worldwide collection of information about ongoing glacier changes was initiated in 1894 with the founding of the International Glacier Commission at the Sixth International Geological Congress in Zurich, Switzerland. At that time, the Swiss limnologist F. A. Forel began publishing the periodical *Rapports sur les variations périodiques des glaciers* on behalf of the commission (Forel 1895). Up until 1961, data compilations constituting the main source of length change data worldwide were published in French, Italian, German, and English. Since 1967, the publications have all been in English. The first reports contain mainly qualitative observations except for the glaciers of the European Alps and Scandinavia, many of which have had extensive documentation and quantitative measurements recorded from the very beginning. After World War I, P. L. Mercanton edited the publications, which began to appear less than annually. From 1933 to 1967 they were published on behalf of the International Commission on Snow and Ice (ICSI), part of the International Association of Hydrological Sciences (IAHS). Since then they have been published at five-year intervals under the title *Fluctuations of Glaciers*, at first by the Permanent Service on the Fluctuations of Glaciers (PSFG [Kasser 1970]) and then, after the merger of the PSFG with the Temporary Technical Secretariat for the World Glacier Inventory (TTS/WGI) in 1986, by the WGMS. An extensive overview of the corresponding literature is given by Hoelzle et al. (2003).

The need for a worldwide inventory of perennial snow and ice masses was first considered during the International Hydrological Decade declared by the United Nations Educational, Scientific, and Cultural Organization (UNESCO) from 1965 until 1974 (UNEP/GEMS 1992). Preliminary results and a thorough discussion of the techniques and standards employed in glacier inventorying were given in IAHS (1980). A status report and the corresponding national literature of all national glacier inventories compiled at that time was published by Haeberli et al. (1989a). More detailed reports on glacier area changes for specific regions or countries, often with special emphasis on developments since 1850, can be found in CGI/CNR (1962) for Italy, Gross (1988a) for Austria, Maisch et al. (2000) for Switzerland, Vivian (1975) for the Western Alps, Maisch (1992) for the Grisons (Switzerland), Böhm (1993) for the Goldberg region (Hohe Tauern, Austria), and Damm (1998) for the Rieserferner group (Tyrol, Austria).

THE DATA

The Alpine glacier information available is of three types: the World Glacier Inventory (WGI), the Swiss Glacier Inventory 2000 (SGI2000), and Fluctuations of Glaciers (FoG). The geographical distribution of the different data sets is shown in Figure 11.1.

THE WORLD GLACIER INVENTORY

The WGI contains attribute data on glacier area, length, orientation, and elevation as well as a classification of morphological types and moraines linked to the glacier coordinates. The inventory entries are based upon specific observation times and can be viewed as snapshots of the spatial glacier distribution. The data are stored in the WGI database (part of the WGMS database) and are published in Haeberli et al. (1989*a*), which summarizes the national inventories for the entire Alps.

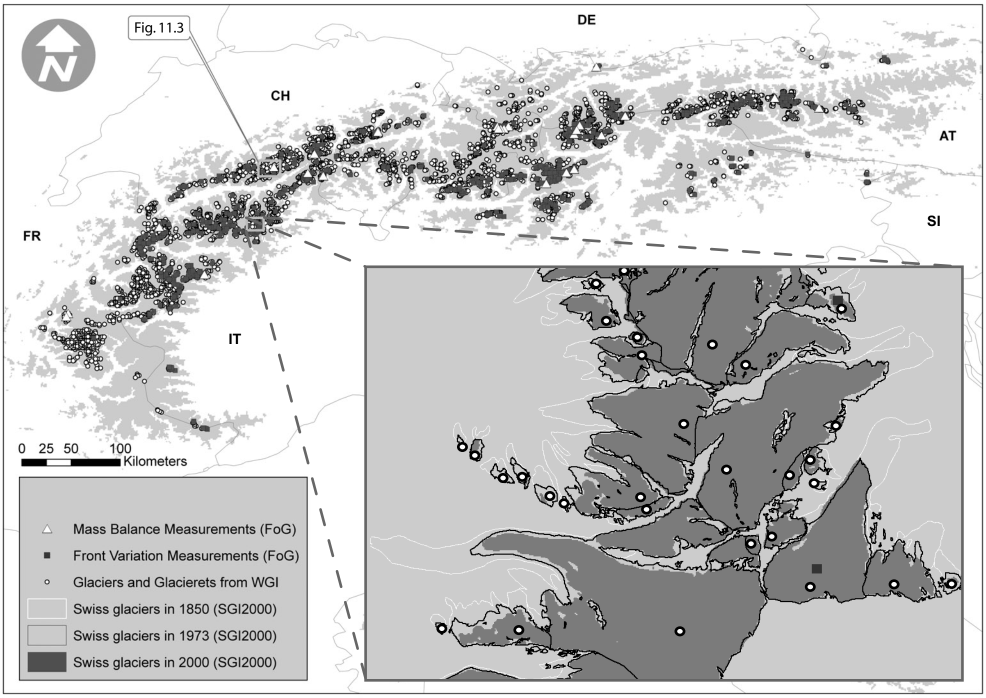

FIGURE 11.1. Geographical distribution of available glacier information in the Alps: WGI data (*white circles*) and mass balance (*white triangles*) and front variation (*dark gray squares*) data from the FoG database. Elevations above 1,500 m a.s.l. are in light gray. *AT*, Austria; *FR*, France; *DE*, Germany; *IT*, Italy; *SI*, Slovenia; and *CH*, Switzerland. The inset shows Swiss glacier polygons for 1850, 1973, and 2000 from the SGI2000.

Complete national inventories for the European Alps are available for Austria (1969), France (1967–71), Switzerland (1973), Germany (1979), and Italy (1975–84). The inventories for Austria, Switzerland, and Germany refer to a single reference year, while the records of France and Italy are compiled over a longer period of time to achieve total coverage (Figure 11.2). However, in every inventory there is a certain percentage of glaciers for which no data from the corresponding reference period/year could be obtained and information from earlier years has been substituted. For example, in the Swiss inventory, data from only 1,550 glaciers date from 1973, while the information for the remaining 274 glaciers refers to earlier years. Glacier identification, assignment, and partitioning (due to glacier shrinkage) are the main challenges for comparisons of inventories overlapping in space or time. Therefore, the total number and areas of glaciers may vary in different studies. Haeberli et al. (1989*a*) sum the area of the 5,154 Alpine glaciers from Austria (542 km^2), France (417 km^2), Switzerland (1,342 km^2), Germany (1 km^2), and Italy (607 km^2) as 2,909 km^2. Because of the inconsistencies just mentioned, the data set used in this study differs slightly from these numbers; the Italian inventory sums up to only 602 km^2 and the number of Alpine glaciers to 5,167. These differences, however, are smaller than 0.3% and therefore negligible.

THE SWISS GLACIER INVENTORY 2000

The SGI2000 has been compiled from multispectral Landsat Thematic Mapper (TM) data acquired in 1998–99 (path-row 194/5-27/8). Glacier information (e.g., area, slope, aspect) was obtained from a combination of glacier outlines with a digital elevation model and the related analysis by a Geographic Information

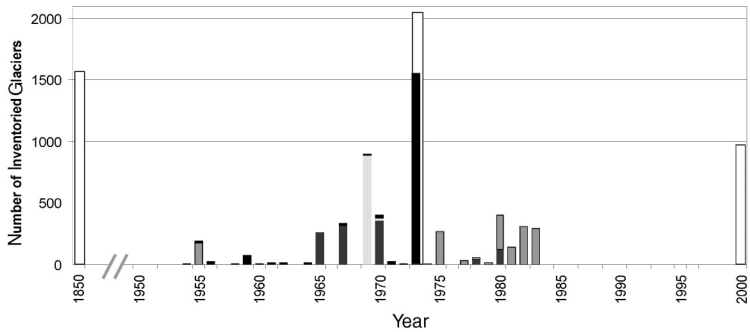

FIGURE 11.2. Numbers of inventoried glaciers in the Alps by year, country, and data source. (For 1973, for example, there are data in the WGI from 6 Italian, 2 Austrian, and 1,550 Swiss glaciers and data in the SGI2000 from 2,057 Swiss glaciers.)

System (Kääb et al. 2002; Paul et al. 2002; Paul 2004). Several glaciers were not properly identified because of cast shadow, snow cover, and debris and were excluded from the statistical analysis. New areas for 938 glaciers were obtained for 2000 and the related topographical information extracted. The glacier inventories from 1850 and 1973 were digitized from the original topographic maps and are now a major part of the SGI2000 (Figure 11.3). The 1973 outlines are also used to define the hydrological basins of individual glaciers in the satellite-derived inventory, in particular the ice-ice divides. However, because different identification codes were used in the inventories of Müller, Caflisch, and Müller (1976), Maisch et al. (2000), and the SGI2000, a direct comparison of glacier areas is not yet possible. Moreover, glacier retreat has caused severe changes in glacier geometry (tongue separation, disintegration, etc.) that prevent direct comparison. For this reason our analysis of glacier changes was based on different samples. The major results of this study have been summarized by Paul et al. (2004).

FLUCTUATIONS OF GLACIERS

The FoG database contains attribute data on glacier changes over time—front variations, mass balance, and changes in area, thickness, and volume—linked to glacier coordinates. The data are stored in the FoG database (part of the WGMS database) and published in the *Fluctuations of Glaciers* series at five-year intervals (latest edition, Haeberli et al. 2005*b*) and biannually in the *Glacier Mass Balance Bulletin* (latest edition, Haeberli et al. 2005*a*).

Regular glacier front variation surveys in the Alps started around 1880. The number of glaciers surveyed and the continuity of series changed over time because of world history and the perceptions of the glaciological community (Haeberli and Zumbühl 2003; Haeberli, this volume). Direct measurements of glacier mass balance in the Alps started at Limmern (Switzerland) and Plattalva (Switzerland) in 1948, followed by Sarennes (France) in 1949, Hintereis (Austria) and Kesselwand (Austria) in 1953, and others. In the last reporting period (1995–2000) 297 glacier front measurements were made, along with measurements of the mass balance of 18 Alpine glaciers (Haeberli et al. 2005*b*). For the analysis here only front variation series with more than nine survey years and mass balance series longer than three years have been considered (Figure 11.4).

There are some reconstructed front variation series for several Alpine glaciers, spanning time periods from centuries to millennia (e.g., Holzhauser and Zumbühl 1996; Holzhauser 1997; Nicolussi and Patzelt 2000; Holzhauser,

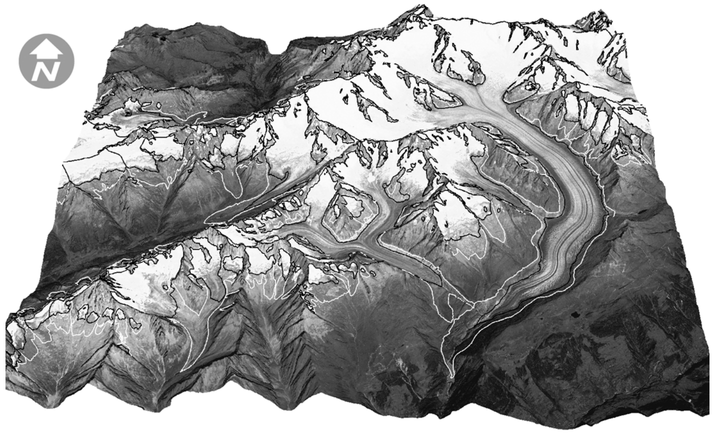

FIGURE 11.3. Synthetic oblique-perspective of the Aletsch Glacier region, Switzerland, generated from a digital elevation model (DEM25; reproduced by permission of swisstopo, BA057338) overlaid with a fusion of satellite images from Landsat TM (1999) and IRS-1C (1997) in a grayscale rendition. The Grosser Aletsch Glacier retreated about 2,550 m from 1850 (*white lines*) to 1973 (*black lines*) and another 680 m by 2000.

Magny, and Zumbühl 2005). In addition, there are some studies that estimate secular mass balance trends from cumulative glacier length changes (e.g., Haeberli and Holzhauser 2003; Hoelzle et al. 2003) or from glacier surfaces reconstructed from historical maps (cf. Haeberli 1998; Steiner et al., this volume). These studies, however, have not been prepared within an international framework, and most of the data are not publicly available, so we have not considered them here.

ANALYSIS AND RESULTS

ALPINE GLACIERIZATION IN THE 1970s

The only complete Alpine inventory available is from the 1970s, with 5,154 glaciers and an area of 2,909 km^2 (Haeberli et al. 1989*a*). Paul et al. (2004) have estimated the total ice volume to be about 100 km^3, much lower than the 130 km^3 suggested earlier by Haeberli and Hoelzle (1995). The latter estimated the total ice volume from the total Alpine glacier area and an averaged thickness from all the glaciers (in accordance with semielliptical cross-sectional glacier geometry). Paul et al. (2004) calculated the total volume loss (-25 km^3) for the period 1973–1998/99 from the mean Alpine glacier area (2,753 km^2) and the average cumulative mass balance for eight Alpine glaciers (-9 m water equivalent). Assuming that the relative change in volume is likely to have been larger than the corresponding relative change in area (for geometric reasons), the estimated relative volume loss is roughly -25% and, therefore, the total Alpine ice volume in the 1970s was about 100 km^3.

Eighty-two percent of Alpine glaciers are smaller than 0.5 km^2 and cover 21% of the total glaciated area (Figure 11.5). Glacierets and névés (perennial snowbanks) do not normally show dynamic reactions and therefore are usually excluded from glacier studies. However, neglecting these small glaciers in inventories could introduce significant errors in the assessment of regional glacier change. Only seven glaciers (Grosser Aletsch, Gorner, Fiescher, Unteraar, Unterer Grindelwald, and Oberaletsch in Switzerland and Mer de Glace in France) are larger than 20 km^2 but represent 10% of the total area. Glaciers between 1 and 10 km^2 account for 46% of the Alpine glacier area.

The regional distribution of numbers and areas of Alpine glaciers can be calculated for each Alpine country. Most of the glaciers are located in Switzerland (35%), followed by Italy (27%), France (20%), and Austria (18%). Regarding total glacier area, the majority of European ice is located in Switzerland (46%) and Italy (21%). Austria ranks third, with 19% of the Alpine glacier area, followed by France with

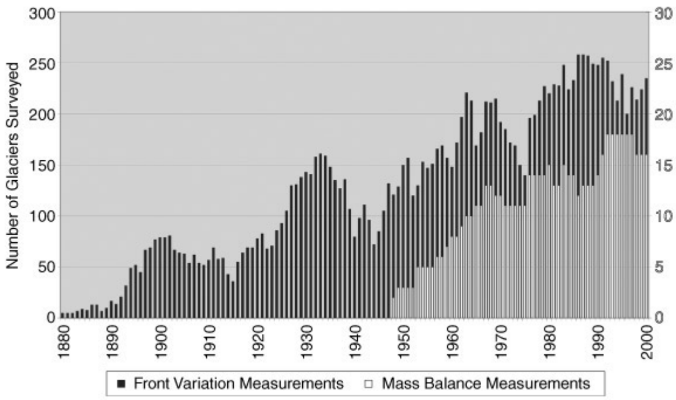

FIGURE 11.4. Frequency of front variation (*black bars, left axis*) and mass balance (*white bars, right axis*) measurements in the Alps, 1880–2000. Only glaciers with more than 18 front variations or three mass balance surveys are considered.

14%. The five German glaciers, with a total area of 1 km^2, and the two small Slovenian glaciers are not considered in the tables.

Tables 11.1 and 11.2 show the glacier size characteristics in the 1970s. The numbers of glaciers in each area-class are very similar in all countries except for France, where 50% of the glaciers are smaller than 0.1 km^2. The area distribution in Austria and Italy is dominated equally by small- and middle-sized glaciers. Mer de Glace, with an area of 33 km^2, corresponds to almost 8% of the French glacierization. In Switzerland the 22 largest glaciers (> 10 km^2) account for 37% of the total glacier area.

ALPINE GLACIERIZATION IN 1850 AND 2000

Using the Alpine inventory of the 1970s, the Alpine glacier areas in 1850 and in 2000 can be extrapolated by applying the relative area changes (1850–1973, 1973–2000) of the seven glacier size classes from the SGI2000 to the corresponding Alpine glacier areas in the 1970s (Table 11.3). The estimated Alpine glacier areas amount to 4,474 km^2 in 1850 and to 2,272 km^2 in 2000. This corresponds to an overall glacier area loss from 1850 until the 1970s of 35% and almost 50% by 2000—or an area reduction of 22% between the 1970s and 2000. Dividing the total area loss by time provides estimates of area change per decade of 2.9% between 1850 and 1973 and 8.2% between 1973 and 2000. Several methods exist for calculating glacier volume from other variables, based either on statistical relationships (e.g., Müller, Caflisch, and Müller 1976), empirical studies (e.g., Maisch et al. 2000), or physical parameters (e.g., Haeberli and Hoelzle 1995). However, all of them employ glacier size as a scaling factor, and the deviations between individual methods are large. As the individual glacier sizes for the year 2000 are not yet available for all glaciers, we have not attempted to present glacier volume evolution over time. However, a current estimate of Alpine glacier volume in 2000 indicates that approximately 75 km^3 remain (Paul et al. 2004).

ALPINE FRONT VARIATIONS

Large valley glaciers have retreated continuously since the Little Ice Age maximum around 1850. Smaller mountain glaciers show marked periods of intermittent advances in the 1890s, the 1920s, and the 1970–80s. The front variations of the smallest glaciers have a high annual variability. In Figure 11.6 front variation series with more than 18 measurement years are plotted and sorted according to glacier size. The advance periods of the 1920s and the 1970–80s and the retreat periods in between and after 1990 show up very clearly. However, on the individual level the climate signal from variations in the front position of glaciers is much more complex. This noise prevails even when the data set is sorted according to

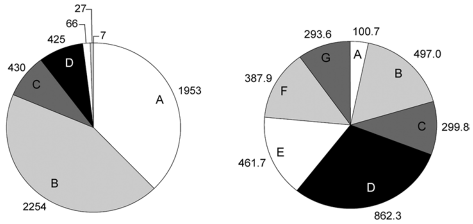

FIGURE 11.5. Distribution of glaciers by number (*left*) and size (*right*) in the Alps for the 1970s. Pie charts give percentages with absolute values indicated. (A) < 0.1 km^2; (B) 0.1–0.5 km^2; (C) 0.5–1.0 km^2; (D) 1.0–5.0 km^2; (E) 5.0–10.0 km^2; (F) 10.0–20.0 km^2; (G) > 20.0 km^2. The five German and two Slovenian glaciers are not considered in this figure.

response time (see Johannesson, Raymond, and Waddington 1989; Haeberli and Hoelzle 1995) or analyzed in geographical subsamples. Figure 11.6 is dominated by the smaller mountain glaciers, and therefore the signals of the large valley glaciers and the smallest glaciers (including absolute retreat values) are more visible in the graphs of individual cumulative front variation (e.g., Haeberli et al. 1989*b*; Hoelzle et al. 2003).

ALPINE MASS BALANCES

Fifty years of direct mass balance measurements show a clear trend of mass loss. Although some of the glaciers measured gained mass from the 1960s to the 1980s, ice loss has accelerated in the past two decades (Figure 11.7). With respect to the geographical distribution, years with a uniformly positive (e.g., 1965, 1977, 1978) or negative (e.g., 1964, 1973, 1983) Alpine mass balance signal, as well as years with a clear spatial gradient in net balance (e.g., 1963, 1976) or with heterogeneous signals, can be found mainly before 1986. After 1981, uniformly negative mass balance years dominate. Nine Alpine reference glaciers (Careser in Italy, Gries and Silvretta in Switzerland, Hintereis, Kesselwand, Sonnblick, and Vernagt in Austria, and Saint Sorlin and Sarennes in France) with continuous mass balance series over more than 30 years show a mean annual loss of ice thickness close to 37-cm water equivalent per year, resulting in a total thickness reduction of about 13 m water equivalent between 1967 and 2001. The corresponding values for the period 1980–99 are 60 cm water equivalent and 12.3 m water equivalent per year, respectively (Table 11.4).

DISCUSSION

DATA COVERAGE

Glacier studies have a long tradition in the Alps that began with the establishment of systematic observation networks in the 1890s (Haeberli, this volume). In comparison with the rest of the world, the European Alps have the densest and most complete spatial glacier inventory over time (Haeberli et al. 1989*a*). Thus, the inventory data contain information on spatial glacier distribution at certain times, whereas the fluctuation series provides high-resolution temporal information for specific locations. Interestingly, the 1970s is the only period in which an Alpine inventory with total spatial coverage can be compiled, most glaciers being relatively close to steady-state conditions (Figure 11.7; Patzelt 1985). The reconstructed glacier extents at the end of the Little Ice Age (around 1850) and the glacier outlines derived from multispectral satellite data around 2000 from the SGI2000 cover the major parts and the full range of area-classes of Swiss glaciation. Thus, they can be used to extrapolate Alpine glaciation in 1850 and 2000 on the assumption that the relative losses of the different area-classes in Switzerland are representative of other Alpine countries as well. This, of course, is not necessarily the case. The fluctuation series are numerous and well distributed over the Alps, with a minimum number of front variation series in the southwestern part of the Alps. For the fluctuation series, length and completeness of the time series are most relevant.

GLACIER SHRINKAGE

The inventory for the 1970s and the extrapolated area estimates for 1850 and 2000 show dramatic shrinkage of the Alpine glaciers. Despite the high degree of variability in individual glaciers, the European Alps have experienced a 50% decrease

TABLE 11.1

Distribution of Glaciers by Number and Area (Absolute Values) in the Alps in the 1970s

AREA-CLASS (KM^2)		ALPS WGI	AT WGI	CH WGI	FR WGI	IT WGI	ALPS FOG, FV	ALPS FOG, MB
0.0–0.1	Number	1,953	287	636	522	508	16	0
	Area (km²)	100.7	16.2	29.4	24.5	30.5	1.0	0.0
0.1–0.5	Number	2,254	416	826	361	651	130	3
	Area (km²)	497.0	92.3	185.5	77.0	142.2	36.2	0.9
0.5–1	Number	430	112	156	73	89	92	4
	Area (km²)	299.8	77.6	108.4	51.4	62.5	64.0	2.8
1–5	Number	425	95	152	79	99	198	13
	Area (km²)	862.3	213.2	294.8	153.6	200.7	446.6	35.2
5–10	Number	66	10	32	7	17	56	3
	Area (km²)	461.7	71.8	223.0	51.0	115.9	392.1	24.6
10–20	Number	27	5	16	2	4	27	2
	Area (km²)	387.9	71.2	240.1	26.1	50.5	396.0	33.0
>20	Number	7	0	6	1	0	7	0
	Area (km²)	293.6	0.0	260.5	33.1	0.0	293.5	0.0
Total	Number	5,162	925	1,824	1,045	1,368	526	25
	Area (km²)	2,902.9	542.2	1,341.7	416.6	602.4	1,629.3	96.5

NOTE: *AT*, Austria, *CH*, Switzerland, *FR*, France, *IT*, Italy; *FV*, front variation surveys (more than nine measurements); *MB*, mass balance surveys (more than three measurements).

in ice coverage over the past 150 years. The area loss over each decade (in percent) between the 1970s and 2000 is almost three times greater than the related loss of ice between 1850 and the 1970s. Variations in glacier front position provide a higher-resolution assessment of the glacier retreat over the past 150 years. Though glaciers have generally been retreating since 1850, there have been several periods of documented readvances—in the 1890s, the 1920s, and the 1970s and 1980s (Patzelt 1985; Müller 1988; Pelfini and Smiraglia 1988; Reynaud 1988; Haeberli et al. 1989b). The area reduction after the 1970s occurred mainly after 1985 (see also Paul et al. 2004), and therefore the acceleration of the glacier retreat in the past two decades was even more pronounced. Mass balance measurements are available only for the past five decades and confirm the general trend of glacier shrinkage. While some glaciers gained mass between 1960 and 1980, ice loss has accelerated in the past two decades. The mean specific (annual) net balance of the 1980s is 18% below the average of 1967–2001, and the value for the 1990s doubles that average ice loss. The most recent mass balance data show a continuation of the acceleration trend after 2000, with a peak in the extraordinary year of 2003, when the ice loss of the nine Alpine reference glaciers was about 2.5-m water equivalent—exceeding the average of 1967–2000 by a factor of nearly seven. Estimated total glacier-volume loss in the Alps in 2003 corresponds to 5–10% of the remaining ice volume (Zemp et al. 2005). The acceleration of glacier shrinkage after 1985 indicates a transition toward rapid down-wasting rather than a dynamic glacier response to a changed climate (cf. Paul et al. 2004).

The general glacier retreat since 1850 corresponds well with the observed warming trend in

TABLE 11.2

Distribution of Glaciers by Number and Area (Percentage) in the Alps in the 1970s

AREA-CLASS (KM^2)		ALPS WGI	AT WGI	CH WGI	FR WGI	IT WGI	ALPS FOG, FV	ALPS FOG, MB
0.0–0.1	Number (%)	37.8	31.0	34.9	50.0	37.1	3.0	0.0
	Area (%)	3.5	3.0	2.2	5.9	5.1	0.1	0.0
0.1–0.5	Number (%)	43.7	45.0	45.3	34.5	47.6	24.7	12.0
	Area (%)	17.1	17.0	13.8	18.5	23.6	2.2	0.9
0.5–1	Number (%)	8.3	12.1	8.6	7.0	6.5	17.5	16.0
	Area (%)	10.3	14.3	8.1	12.3	10.4	3.9	2.9
1–5	Number (%)	8.2	10.3	8.3	7.6	7.2	37.6	52.0
	Area (%)	29.7	39.3	22.0	36.9	33.3	27.4	36.5
5–10	Number (%)	1.3	1.1	1.8	0.7	1.2	10.6	12.0
	Area (%)	15.9	13.2	16.6	12.2	19.2	24.1	25.5
10–20	Number (%)	0.5	0.5	0.9	0.2	0.3	5.1	8.0
	Area (%)	13.4	13.1	17.9	6.3	8.4	24.3	34.2
>20	Number (%)	0.1	0.0	0.3	0.1	0.0	1.3	0.0
	Area (%)	10.1	0.0	19.4	7.9	0.0	18.0	0.0
Total	Number (%)	100.0	100.0	100.0	100.0	100.0	100.0	100.0
	Area (%)	100.0	100.0	100.0	100.0	100.0	100.0	100.0

NOTE: *AT*, Austria, *CH*, Switzerland, *FR*, France, *IT*, Italy; *FV*, front variation surveys (more than nine measurements); *MB*, mass balance surveys (more than three measurements).

this period (e.g., Oerlemans 1994, 2001: 110–11; Maisch et al. 2000; Zemp, Hoelzle, and Haeberli 2007). However, the onset of the Alpine glacier retreat after 1850 may have been triggered by a negative winter precipitation anomaly (relative to the mean of 1901–2000) during the second half of the nineteenth century (Wanner et al. 2005). The intermittent periods of glacier advances in the 1890s, the 1920s, and the 1970s and 1980s can be explained by earlier wetter and cooler periods, with reduced sunshine duration and increased winter precipitation (Patzelt 1987; Schöner, Auer, and Böhm 2000; Laternser and Schneebeli 2003). Schöner, Auer, and Böhm (2000) concluded from the study of a homogenized climate data set and mass balance data from the Austrian part of the eastern Alps that the more positive mass balance periods show a high correlation with winter accumulation and a lower correlation with summer temperature, while more negative mass balance periods are closely correlated with summer temperature and show no correlation with winter accumulation. In addition they found that the positive mass balance period between 1960 and 1980 was characterized by negative winter North Atlantic Oscillation index values, which caused an increase of the meridional circulation mode and a more intense northwesterly to northerly precipitation regime (see Wanner et al. 2005). The observed trend of increasingly negative mass balances since 1980 is consistent with accelerated global warming and correspondingly enhanced energy flux toward the earth's surface (Haeberli et al. 2005*b*).

REPRESENTATIVENESS OF THE SGI2000 AND THE FLUCTUATION SERIES

When analyzing national inventories or individual fluctuation series, the question of representativeness often arises. Are the subsample

TABLE 11.3

Alpine Glaciation, 1850, 1970s, and 2000

	SWITZERLAND (SGI2000)								ALPS			
	1850		1973		2000		1850–1973[a]	1973–2000[a]	1970s		1850[b]	2000[b]
AREA-CLASS (KM^2)	*Number*	*Area (km^2)*	*Number*	*Area (km^2)*	*Number*	*Area (km^2)*	*Area Change (%)*	*Area Change (%)*	*Number*	*Area (km^2)*	*Area (km^2)*	*Area (km^2)*
$<$ 0.1	297	17.3	1,022	40.1	164	3.6	–55.4	–64.6	1,953	100.7	225.5	35.6
0.1–.5	715	181.3	673	153.9	448	60.3	–52.9	–45.6	2,254	497.0	1,055.0	270.4
0.5–1	249	172.5	151	104.1	131	63.5	–44.3	–29.1	430	299.8	538.0	212.6
1–5	253	524.4	157	296.0	141	217.1	–33.2	–17.9	425	862.3	1,291.1	707.9
5–10	26	195.5	35	249.4	36	232.6	–19.7	–10.8	66	461.7	574.8	412.1
10–20	18	259.9	14	216.3	13	192.8	–14.8	–8.2	27	387.9	455.1	356.1
$>$ 20	9	270.5	5	225.9	5	213.0	–12.3	–5.7	7	293.6	334.8	276.9
Total	1,567	1,621.4	2,057	1,285.7	938	982.9	–27.1	–16.1	5,162	2,902.9	4,474.3	2,271.6

[a]The relative area changes in Switzerland are calculated from the comparable subsamples: 1,567 glaciers for 1850–1973 and 938 glaciers for 1973–2000, respectively.

[b]Alpine glacier area in 1850 and 2000 is extrapolated from the glacier area in the 1970s (WGI) and relative area changes of the seven glacier area-classes in Switzerland (SGI2000).

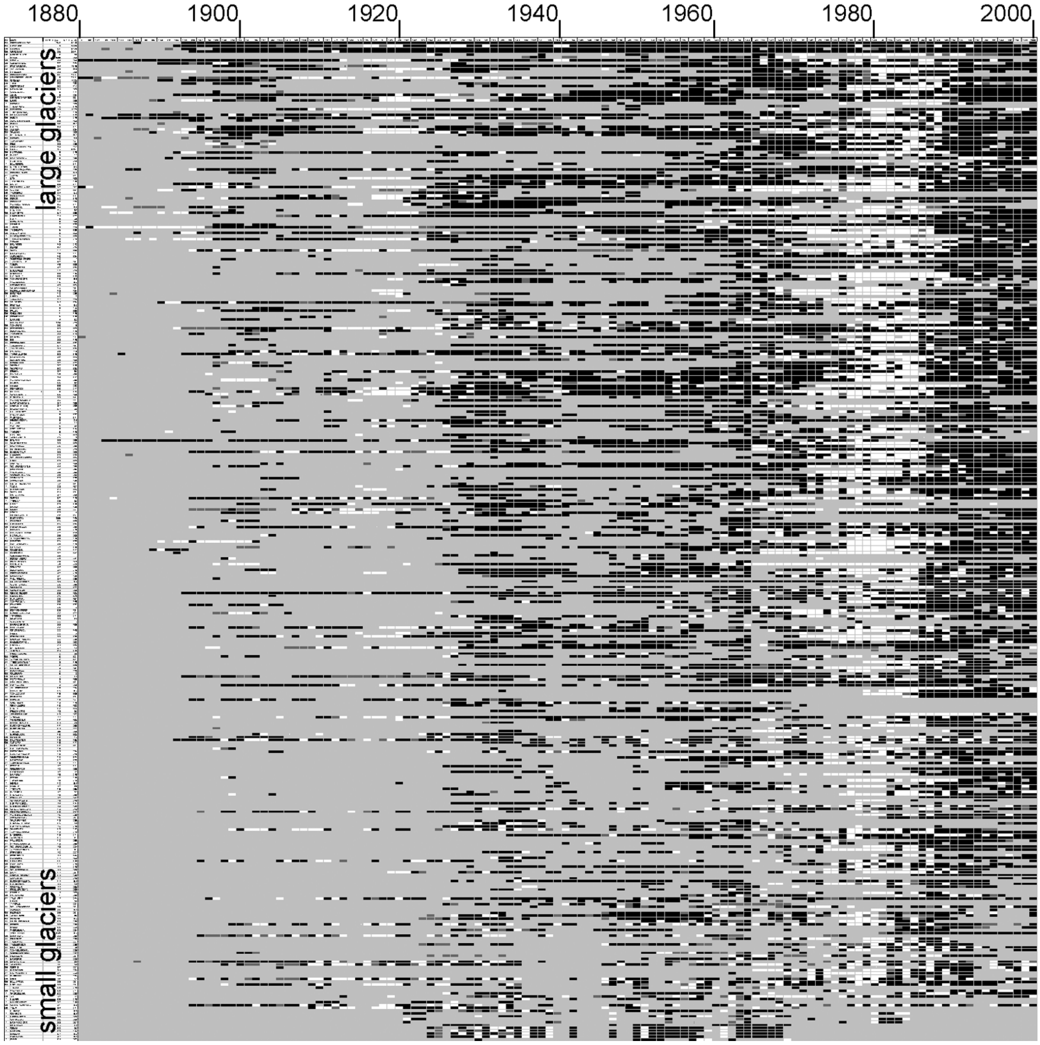

FIGURE 11.6. Alpine front variation series, 1880–2000. Annual front variation values from glaciers with more than 18 measurements are colored white after an advance, black after a retreat; dark gray indicates no apparent variation and light gray no data. Each row represents one glacier. The glaciers are sorted according to length in the 1970s (*y*-axis).

investigated and the glaciers surveyed representative of the entire glacierization? Comparison of the area characteristics of the 1850 and 2000 subsamples of the SGI2000 (on which the extrapolation of the Alpine areas of 1850 and 2000 is based) with the complete Swiss inventory in the WGI shows that the distributions of the area-classes are similar. Nevertheless, small glaciers (<0.1 km^2) are underrepresented, and glaciers in northeastern Switzerland are poorly represented (Paul et al. 2004). However, the SGI2000 subsamples for 1850 and 2000 include 86% of the Swiss glaciers covering 88% of the total area and 51% of the Swiss glaciers covering 87% of the total area, respectively. Thus, the SGI2000 can be considered a representative subsample of Swiss glaciation, which is very similar to the glaciation of the other Alpine countries. The ice coverage of the European countries is equally distributed with respect to the number of glaciers in each area-class, with the largest glaciers being overrepresented in the area distribution. Therefore, the different area-classes were considered when the

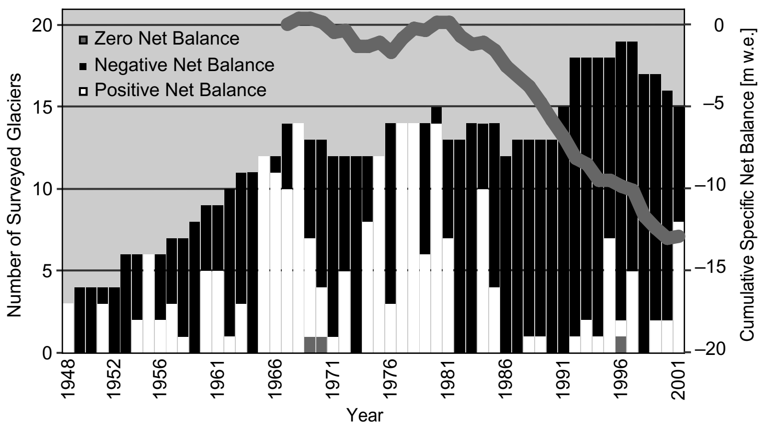

FIGURE 11.7. Alpine mass balance measurements, 1948–2001, showing annual numbers of glaciers (*left axis*) with a zero net balance (*dark gray*), positive net balance (*white*), or negative net balance (*black*) and the mean cumulative specific net balance of the nine Alpine reference glaciers from 1967 to 2001 (*right axis*).

extrapolation was applied to all Alpine glaciers. The large relative area change of the smaller glaciers leads to a more pronounced area change in the entire Alps than in Switzerland (assuming a uniform climate change across the region) because of the greater frequency of large glaciers in the latter.

Front variations are measured mainly on middle-sized and large glaciers, while glaciers smaller than 0.5 km^2 are underrepresented. This is to be expected because glacierets and névés are often unsuitable for this kind of measurement in terms of their limited accessibility and their low dynamic response. Front variation series with more than nine measurement years exist for about 10% of all Alpine glaciers, which cover more than 50% of the total glacier area. The dynamic response to climatic forcing of glaciers with variable geometry results in striking differences in the recorded curves, reflecting the considerable effects of size-dependent filtering, smoothing, and enhancing of the delayed tongue response with respect to the input (mass balance) signal (Oerlemans 2001). Dynamic response time depends mainly on glacier length, slope, and mass balance gradient (Johanneson, Raymond, and Waddington 1989; Haeberli and Hoelzle 1995). As a consequence, large valley glaciers with a dynamic response time of several decades show the secular climate trend, while smaller mountain glaciers show marked periods of intermittent advances and retreats on a decadal scale. The smallest, somewhat static, low-shear-stress glaciers (cirque glaciers) have altitude ranges that are comparable to or smaller than the interannual variation in equilibrium line altitude and hence, in general, reflect yearly changes in mass balance without any delay (Hoelzle et al. 2003).

Mass balance measurements are labor-intensive and are therefore available from only 25 glaciers, mainly from 0.5 to 10 km^2 in size, covering only 3% of the glacier area. In spite of their small number, they are geographically well distributed over the entire Alps. Mass balance is the direct and undelayed response signal to annual atmospheric conditions. It documents degrees of imbalance between glaciers and climate due to the delay in dynamic response caused by the characteristics of ice flow (deformation and sliding). Over long time intervals mass balance variations indicate trends of climatic forcing. With constant climatic conditions (no forcing), balances would tend toward zero. Long-term nonzero balances are therefore an expression of ongoing climate change (Haeberli et al. 2005). Summer and winter balance even provide intraannual climate information and should therefore be surveyed on all mass balance glaciers (Dyurgerov and Meier 1999; Vincent 2002). In general, fluctuation series are well distributed across the Alps and represent the range of area-classes quite well. In view of the large contribution of

TABLE 11.4
Mean Specific (Annual) Net Balance of the Alpine Reference Glaciers

TIME PERIOD	NUMBER OF REFERENCE GLACIERS	NET BALANCE (MM W.E.)
1950–59	1–5	–536
1960–69	6–9	–26
1970–79	9	–69
1980–89	9	–437
1990–99	9	–767
1949–2001	1–9	–412
1967–2001	9	–369

glaciers smaller than 1 km^2 to glacier shrinkage in the past and the prediction of ongoing global warming (e.g., Schär et al. 2004; Beniston 2005), future work should include studies on the influence of atmospheric warming on small glaciers and on current down-wasting processes (see also Paul et al. 2004). However, the climatic sensitivity of glaciers depends not only on glacier size but also on sensitivity to variations in regional climate versus local topographic effects, which potentially complicates the extraction of a regional or global climate signal from glacier fluctuations (Kuhn et al. 1985; Vincent et al. 2004). Mass balance and ice flow models calibrated with available fluctuation data are needed to quantify these effects (Oerlemans et al. 1998; Oerlemans 2001; Paul et al., this volume).

CONCLUSIONS

In the European Alps the growth of the glacier monitoring network over time has resulted in an unprecedented glacier data set with excellent spatial and temporal coverage. The WGMS has compiled information on spatial glacier distribution from approximately 5,150 Alpine glaciers and fluctuation series (front variation and mass balance) from more than 670 of these glaciers. National inventories provide complete Alpine coverage for the 1970s, when the glaciers covered an area of 2,909 km^2. This inventory, together with the SGI2000, is used to extrapolate Alpine glacier-covered areas in 1850 and 2000 of about 4,470 km^2 and 2,270 km^2, respectively. This corresponds to an overall glacier area loss from 1850 of 35% by the 1970s and almost 50% by 2000.

Annual mass balance and front variation series provide a better time resolution of glacier fluctuations over the past 150 years than the inventories. During the general retreat, intermittent periods of glacier advances in the 1890s, the 1920s, and the 1970s and 1980s can still be seen. Increasing mass loss, rapidly shrinking glaciers, and disintegrating and spectacular tongue retreats are clear warnings of the atmospheric warming observed in the Alps during the past 150 years and the acceleration observed over the past two decades.

While inventory data contain information on spatial glacier distribution at certain times, fluctuation series provide temporal information at specific locations. Continuity and representativeness of fluctuation series are thus essential for the planning of glacier monitoring. Furthermore, modeling should be enhanced and integrated into monitoring strategies. It is very important to continue with long-term fluctuation measurements and to extend the series back in time with reconstructions of former glacier geometries. Additionally, it is necessary to integrate glacier monitoring and reconstruction activities into the framework of the Global Land Ice Measurements from Space (GLIMS) project and the WGMS.

ACKNOWLEDGMENTS

We are indebted to the numerous people who have provided the WGMS with data over the years. In particular, we thank all the national correspondents of the WGMS and G. Rossi and W. Schöner for their collaboration in the revision of the Italian and the Austrian data sets. Special thanks go to S. Baumann, M. Dischl, A. Hinterberger, J. Meilwes, W. Peschke, C. Rothenbühler, and A. Stolz for their contribution to the correction and formatting of the data and to I. Woodhatch for editing this report. We gratefully acknowledge the constructive comments of G. Pederson, an anonymous referee, and the scientific editors. Last but not least, we thank R. Frauenfelder and other colleagues from the WGMS for their daily efforts and teamwork. This study was mainly funded by the ALP-IMP Project of the European Community's Environment/Global Change program (BBW. No. 01.0498-2) and the Department of Geography of the University of Zurich.

REFERENCES CITED

Beniston, M. 2005. Warm winter spells in the Swiss Alps: Strong heat waves in a cold season? A study focusing on climate observations at the Saentis high mountain site. *Geophysical Research Letters* 32: L01812, doi: 10.1029/2004GL021478.

Böhm, R. 1993. Kartometrische Daten der Vergletscherung der Goldberggruppe in den Hohen Tauern. *Zeitschrift für Gletscherkunde und Glazialgeologie* 29:133–52.

CGI/CNR (Consiglio Nazionale delle Ricerche/Comitato Glaciologico Italiano). 1962. *Catasto dei ghiacciai italiani*. 4 vols. Varese.

Damm, B. 1998. Der Ablauf des Gletscherrückzuges in der Rieserfernergruppe (Tirol) im Anschluss an den Hochstand um 1850. *Zeitschrift für Gletscherkunde und Glazialgeologie* 34:141–59.

Dyurgerov, M., and M. Meier. 1999. Analysis of winter and summer glacier mass balances. *Geografiska Annaler* 81A:541–54.

Forel, F. A. 1895. Les variations périodiques des glaciers: Discours préliminaire. *Extrait des Archives des Sciences Physiques et Naturelles* 34:209–29.

Gross, G. 1988. Der Flächenverlust der Gletscher Österreichs 1850–1920–1969. *Zeitschrift für Gletscherkunde und Glazialgeologie* 23:131–41.

Haeberli, W. 1998. Historical evolution and operational aspects of worldwide glacier monitoring. In *Into the second century of worldwide glacier monitoring: Prospects and strategies*, ed. W. Haeberli, M. Hoelzle, and S. Suter, 35–51. Paris: UNESCO.

———. 2004. Glaciers and ice caps: Historical background and strategies of world-wide monitoring. In *Mass balance of the cryosphere*, ed. J. L. Bamber and A. J. Payne, 559–78. Cambridge, UK: Cambridge University Press.

Haeberli, W., H. Bosch, K. Scherler, G. Østrem, and C. Wallén, eds. 1989*a*. *World glacier inventory: Status 1988*. Nairobi: IAHS(ICSI)/UNEP/UNESCO/ World Glacier Monitoring Service.

Haeberli, W., and M. Hoelzle. 1995. Application of inventory data for estimating characteristics of and regional climate-change effects on mountain glaciers: A pilot study with the European Alps. *Annals of Glaciology* 21:206–12.

Haeberli, W., and H. Holzhauser. 2003. Alpine glacier mass changes during the past two millennia. *PAGES News* 11(1):13–15.

Haeberli, W., P. Müller, P. Alean, and H. Bösch. 1989*b*. Glacier changes following the Little Ice Age: A survey of the international data basis and its perspectives. In *Glacier fluctuations and climatic change: Proceedings of the Symposium on Glacier Fluctuations and Climatic Change, held in Amsterdam, 1–5 June 1987*, ed. J. Oerlemans, 77–101. Dordrecht, Boston, and London: Kluwer Academic Publishers.

Haeberli, W., J. Noetzli, M. Zemp, S. Baumann, R. Frauenfelder, and M. Hoelzle, eds. 2005*a* *Glacier mass balance bulletin. 8, 2002–2003*. Zurich: World Glacier Monitoring Service/IUGG(CCS)/ UNEP/UNESCO/WMO.

Haeberli, W., M. Zemp, R. Frauenfelder, M. Hoelzle, and A. Kääb, eds. 2005*b*. *Fluctuations of glaciers 1995–2000*. Vol. 8. Zurich: World Glacier Monitoring Service/IUGG (CCS)/UNEP/UNESCO.

Haeberli, W., and H. Zumbühl. 2003. Schwankungen der Alpengletscher im Wandel von Klima und Perzeption. In *Welt der Alpen: Gebirge der Welt*, ed. F. Jeanneret, D. Wastl-Walter, U. Wiesmann, and M. Schwyn, 77–92. Bern: Haupt.

Hoelzle, M., W. Haeberli, M. Dischl, and W. Peschke. 2003. Secular glacier mass balances derived from cumulative glacier length changes. *Global and Planetary Change* 36:295–306.

Holzhauser, H. 1997. Fluctuations of the Grosser Aletsch Glacier and the Gorner Glacier during the last 3200 years: New results. In *Glacier fluctuations during the Holocene*, ed. B. Frenzel, 35–58. Paläoklimaforschung/Palaeoclimate Research 24.

Holzhauser, H., M. Magny, and H. J. Zumbühl. 2005. Glacier and lake-level variations in west-central Europe over the last 3500 years. *The Holocene* 15:789–801.

Holzhauser, H., and H. J. Zumbühl. 1996. To the history of the Unterer Grindelwald Glacier during the last 2800 years: Palaeosols, fossil wood and historical pictorial records, new results.

Zeitschrift für Geomorphologie, n.s., suppl. 104:95–127.
Houghton, J. T., et al. 2001. *Climate change 2001: The scientific basis. Contribution of Working Group 1 to the third assessment report of the Intergovernmental Panel on Climate Change*. Cambridge, UK: Cambridge University Press.
IAHS (International Association of Hydrological Sciences). 1980. *World glacier inventory: Proceedings of the Riederalp Workshop, September 1978*. IAHS publication 126. Paris: International Association of Hydrological Sciences.
Jóhanneson, T., C. Raymond, and E. Waddington. 1989. Time-scale for adjustment of glaciers to changes in mass balance. *Journal of Glaciology* 35:355–69.
Kääb, A., F. Paul, M. Maisch, M. Hoelzle, and W. Haeberli. 2002. The new remote-sensing-derived Swiss glacier inventory. 2. First results. *Annals of Glaciology* 34:362–66.
Kasser, P. 1970. Gründung eines "Permanent Service on the Fluctuations of Glaciers." *Zeitschrift für Gletscherkunde und Glazialgeologie* 6:193–200.
Kuhn, M., G. Markl, G. Kaser, U. Nickus, and F. Obleitner. 1985. Fluctuations of climate and mass balance: Different responses of two adjacent glaciers. *Zeitschrift für Gletscherkunde und Glazialgeologie* 2:409–16.
Laternser, M., and M. Schneebeli. 2003. Long-term snow climate trends of the Swiss Alps (1931–1999). *International Journal of Climatology* 23:733–50.
Maisch, M. 1992. Die Gletscher Graubündens: *Rekonstruktion und Auswertung der Gletscher und deren Veränderungen seit dem Hochstand von 1850 im Gebiet der östlichen Schweizer Alpen (Bündnerland und angrenzende Regionen)*. Physische Geographie 33. Zurich: Geographisches Institut der Universität Zürich.
Maisch, M., A. Wipf, B. Denneler, J. Battaglia, and C. Benz. 2000. *Die Gletscher der Schweizer Alpen: Gletscherhochstand 1850, Aktuelle Vergletscherung, Gletscherschwund Szenarien*. 2d ed. Zurich: VdF Hochschulverlag.
Müller, F., T. Caflisch, and G. Müller. 1976. *Firn und Eis der Schweizer Alpen: Gletscherinventar*. Geographisches Institut der ETH Zürich publ. 57. Zürich: Versuchsanstalt für Wasserbrau, Hydrologie und Glaziologie der ETH Zürich.
Müller, P. 1988. *Parametrisierung der Gletscher-Klima-Beziehung für die Praxis: Grundlagen und Beispiele*. Mitteilungen der Versuchsanstalt für Wasserbau, Hydrologie und Glaziologie 95.
Nicolussi, K., and G. Patzelt. 2000. Untersuchungen zur holozänen Gletscherentwicklung von Pasterze und Gepatschferner (Ostalpen). *Zeitschrift für Gletscherkunde und Glazialgeologie* 36:1–87.
Oerlemans, J. 1994. Quantifying global warming from the retreat of glaciers. *Science* 264:243–45.
———. 2001. *Glaciers and climate change*. Lisse, Abingdon, Exton, and Tokyo: A. A. Balkema.
Oerlemans, J., B. Anderson, A. Hubbard, P. Huybrechts, T. Johannesson, W. H. Knap, M. Schmeits, A. P. Stroeven, R. S. W. Van de Wal, J. Wallinga, and Z. Zuo. 1998. Modelling the response of glaciers to climate warming. *Climate Dynamics* 14:267–74.
Patzelt, G. 1985. The period of glacier advances in the Alps, 1965 to 1980. *Zeitschrift für Gletscherkunde und Glazialgeologie* 21:403–7.
———. 1987. Gegenwärtige Veränderungen an Gebirgsgletschern im weltweiten Vergleich. *Verhandlungen des Deutschen Geographentages* 45:259–64.
Paul, F. 2004. The new Swiss glacier inventory 2000: Application of remote sensing and GIS. Ph.D. diss., University of Zurich.
Paul, F., A. Kääb, M. Maisch, T. Kellenberger, and W. Haeberli. 2002. The new remote-sensing-derived Swiss glacier inventory. 1. Methods. *Annals of Glaciology* 34:355–61.
———. 2004. Rapid disintegration of Alpine glaciers observed with satellite data. *Geophysical Research Letters* 31: L21402, doi: 10.1029/2004GL020816.
Pelfini, M., and C. Smiraglia. 1988. L'evoluzione recente del glacialismo sulle Alpi Italiani: Strumenti e temi di ricerca. *Bollettino della Società Geografica Italiana* No. 1–3:127–54.
Reynaud, L. 1988. Alpine glacier fluctuations and climatic changes over the last century. *Mitteilungen der Versuchsanstalt für Wasserbau, Hydrologie und Glaziologie* 94:127–46.
Schär, C., P. L. Vidale, D. Lüthi, C. Frei, C. Häberli, M. Liniger, and C. Appenzeller. 2004. The role of increasing temperature variability in European summer heat waves. *Nature* 427:332–36.
Schöner, W., I. Auer, and R. Böhm. 2000. Climate variability and glacier reaction in the Austrian eastern Alps. *Annals of Glaciology* 31:31–38.
UNEP/GEMS. 1992. *Glaciers and the environment*. UNEP/GEMS Environmental Library 9. Nairobi: UNEP.
Vincent, C. 2002. Influence of climate change over the 20th century on four French glacier mass balances. *Journal of Geophysical Research* 107(D19):4375, doi: 10.1029/2001JD000832.
Vincent, C., G. Kappenberger, F. Valla, A. Bauder, M. Funk, and E. Le Meur. 2004. Ice ablation as evidence of climate change in the Alps over the

20th century. *Journal of Geophysical Research* 109: D10104, doi: 10.1029/2003JD003857.

Vivian, R. 1975. *Les glacier des Alpes occidentales*. Grenoble: Allier.

Wanner, H., C. Casty, J. Luterbacher, and A. Pauling. 2005. 500 Jahre Klimavariabilität im europäischen Alpenraum: Raumzeitliche Strukturen und dynamische Interpretation. *Rundgespräche der Kommission für Ökologie, Klimawandel im 20. und 21. Jahrhundert* 28:33–52.

Zemp, M., R. Frauenfelder, W. Haeberli, and M. Hoelzle. 2005. Worldwide glacier mass balance measurements: General trends and first results of the extraordinary year 2003 in Central Europe. *Materialy Glyatsiologicheskikh Issledovaniy* 99:3–12.

Zemp, M., M. Hoelzle, and W. Haeberli. 2007. Distributed modelling of the regional climatic equilibrium line altitude of glaciers in the European Alps. *Global and Planetary Change* 56:83–100.

Publication 10

Zemp, M., Hoelzle, M. & Haeberli, W. (2007). **Distributed modeling of the regional climatic equilibrium line altitude of glaciers in the European Alps.** Global and Planetary Change, 56, 83-100, doi:10.1016/j.gloplacha.2006.07.002.

Available online at www.sciencedirect.com
ScienceDirect
Global and Planetary Change 56 (2007) 83 – 100
GLOBAL AND PLANETARY CHANGE
www.elsevier.com/locate/gloplacha

Distributed modelling of the regional climatic equilibrium line altitude of glaciers in the European Alps

Michael Zemp *, Martin Hoelzle, Wilfried Haeberli

Glaciology and Geomorphodynamics Group, Department of Geography, University of Zurich, Winterthurerstr. 190, CH-8057 Zurich, Switzerland

Received 9 August 2005; accepted 21 July 2006
Available online 11 September 2006

Abstract

Glaciers are among the key indicators of ongoing climate change. The equilibrium line altitude is a theoretical line which defines the altitude at which annual accumulation equals the ablation. It represents the lowest boundary of the climatic glacierisation and, therefore, is an excellent proxy for climate variability. In this study we introduce a simple approach for modelling the glacier distribution at high spatial resolution over entire mountain ranges using a minimum of input data. An empirical relationship between precipitation and temperature at the steady-state equilibrium line altitude (ELA_0), is derived from direct glaciological mass balance measurements. Using geographical information systems (GIS) and a digital elevation model, this relationship is then applied over a spatial domain, to a so-called distributed modelling of the regional climatic ELA_0 ($rcELA_0$) and the climatic accumulation area (cAA) of 1971–1990 over the entire European Alps. A sensitivity study shows that a change in $rcELA_0$ of ±100 m is caused by a temperature change of ±1 °C or a precipitation decrease of 20% and increase of 27%, respectively. The modelled cAA of 1971–1990 agrees well with glacier outlines from the 1973 Swiss Glacier Inventory. Assuming a warming of 0.6 °C between 1850 and 1971–1990 leads to a mean $rcELA_0$ rise of 75 m and a corresponding cAA reduction of 26%. A further rise in temperature of 3 °C accompanied by an increase in precipitation of 10% leads to a further mean rise of the $rcELA_0$ of about 340 m and reduces the cAA of 1971–1990 by 74%.

Keywords: glacier; climate at equilibrium line altitude; climate change; geographical information systems

1. Introduction

Fluctuations of mountain glaciers are among the best natural indicators of climate change (IPCC, 2001). Glacier mass balance is the direct and undelayed signal of annual atmospheric conditions, i.e., temperature, precipitation and radiation balance (Haeberli, 2004). The equilibrium line altitude (ELA) on a glacier is a theoretical line which defines the altitude at which annual accumulation equals the ablation. It represents the lowest boundary of climatic glacierisation — that is, where glacierisation can begin. Thus, climatic variability can be inferred from variations in the ELA (Kuhn, 1981; Ohmura et al., 1992; Lie et al., 2003a).

To understand the climate at the ELA the processes of accumulation and ablation can be examined, the latter based on the energy balance principle. Another approach is to search for relationships between the relevant parameters for the ELA and the glacier accumulation or ablation (Ahlmann, 1924; Shumsky, 1964; Ohmura et al., 1992).

Physical models describing the relationship between glacier behaviour and climate change can be very

* Corresponding author.
E-mail address: mzemp@geo.unizh.ch (M. Zemp).

0921-8181/$ - see front matter © 2006 Elsevier B.V. All rights reserved.
doi:10.1016/j.gloplacha.2006.07.002

sophisticated (Greuell, 1989; Klok and Oerlemans, 2002), in particular those which include the mechanics of glacier flow, driven by the mass balance (e.g., Leysinger Vieli and Gudmundsson, 2004). These models require detailed input data from various sources. Because of their complexity, they facilitate a deeper understanding of physical glacier behaviour (Kerschner, 2002). However, due to the large amount of required input data, they can be applied only to recent glacier states and to single glaciers or glacierised catchments. Other studies use correlations between glacier energy balance, ablation and meteorological parameters to complete and extend mass balance series in time (e.g., Hoinkes and Steinacker, 1975; Braithwaite, 1981; Letréguilly and Reynaud, 1990).

Our aim is a) to present a simple approach that is able to model the glacier distribution at high spatial resolution (about 100 m) over entire mountain ranges, b) to investigate the sensitivity of the Alpine[1] glacierisation to changes in temperature and precipitation, and c) to demonstrate the possible impact of a climate scenario on Alpine glacierisation in the decades to come. To achieve this, an empirical relationship between precipitation and temperature at the steady-state equilibrium line altitude (ELA_0) is derived from direct glaciological mass balance measurements. GIS techniques and a DEM are then used to apply this relationship over a spatial domain to a so-called distributed modelling of the regional climatic ELA_0 ($rcELA_0$), and the climatic accumulation area (cAA) of 1971–1990 over the entire European Alps. Different sources of model errors and the order of magnitude of their amounts are discussed. In conclusion, a sensitivity study demonstrates the potential of this distributed modelling approach for the reconstruction of historical $rcELA_0$ and future scenarios.

2. Previous studies

In the relevant literature, and in the various languages used there, no consistent terminology can be found for the equilibrium line altitude. Gross et al. (1978) gave an overview of definitions of glacier snowline, firn line, equilibrium line and different approaches for estimating these. In this study we use the original terms cited in the literature. In addition, we distinguish between equilibrium line altitude (ELA), steady-state equilibrium line altitude (ELA_0), regional climatic equilibrium line altitude ($rcELA_0$) and local topographic equilibrium line altitude ($ltELA_0$).

[1] In this article 'Alps' or 'Alpine' refer explicitly to the European Alps, the terms 'alps' or 'alpine' are purely generic.

Haeberli (1983) presented a schematic diagram of glacier limits after Shumsky (1964), describing the distribution of glaciers primarily as a function of mean annual air temperature and annual precipitation. As a general rule, in humid-maritime regions, the ELA is at low altitude because of the great amount of ablation required to eliminate the deep snowfall. Temperate glaciers dominate these landscapes. Such ice bodies, with relatively rapid flow, exhibit a high mass turnover and react strongly to atmospheric warming by enhanced melt and runoff. Under dry continental conditions the ELA is at high elevation. In such regions, glaciers are polythermal or cold and feature a low mass turnover.

The basic idea of discovering an empirical relationship between precipitation or temperature and the snowline goes back to Ahlmann (1924). Krenke (1975) pursued a similar concept for estimating precipitation in high mountain areas in the former Soviet Union. Ananicheva and Krenke (2005) used such relationships to investigate the evolution of the climatic snowline and the ELA in north-eastern Siberia Mountains. Gross et al. (1978) suggested a steady-state Accumulation Area Ratio (AAR_0) of 0.67 for glaciers in the Alps as an approximation of the ELA_0 and zero mass balance and compared it to the eight most frequently applied methods for the estimation of the snowline. Furthermore they used the AAR_0 to estimate the snowline depression of Late-Würm (20,000–10,000 years BP) glacier readvances. With the AAR_0 method, the ELA_0 of past glaciers is fairly easy to determine from topographical glacier maps and hence often applied in palaeo-climatic studies (e.g., Kerschner, 1985; Maisch, 1992; Kerschner et al., 2000; Maisch et al., 2000). However, AAR_0 values obtained from worldwide mass balance measurements vary between 0.22 and 0.72 (IUGG(CCS)/UNEP/UNESCO/WMO, 2005). Therefore, the AAR_0 method should not be used uncritically.

Multivariate regression models, relating the change in the dependent variable (ELA) to the changes in the independent variables (climate data) were presented by Ohmura et al. (1992), Kerschner (1996) and Greene et al. (1999). The results of the multivariate regression analysis are difficult to interpret from a physical point of view and, for statistical reasons, are of only limited value for extrapolation beyond the spatial and temporal limits of the independent variables in the original data set (Kerschner, 1996).

Shea et al. (2004) modelled a simple cell-based climatology of the Canadian Rockies from temperature, precipitation and snowfall lapse rates constructed from climate normal, and elevation attributes extracted from a 1-km DEM for the period 1961–1990. Fractional

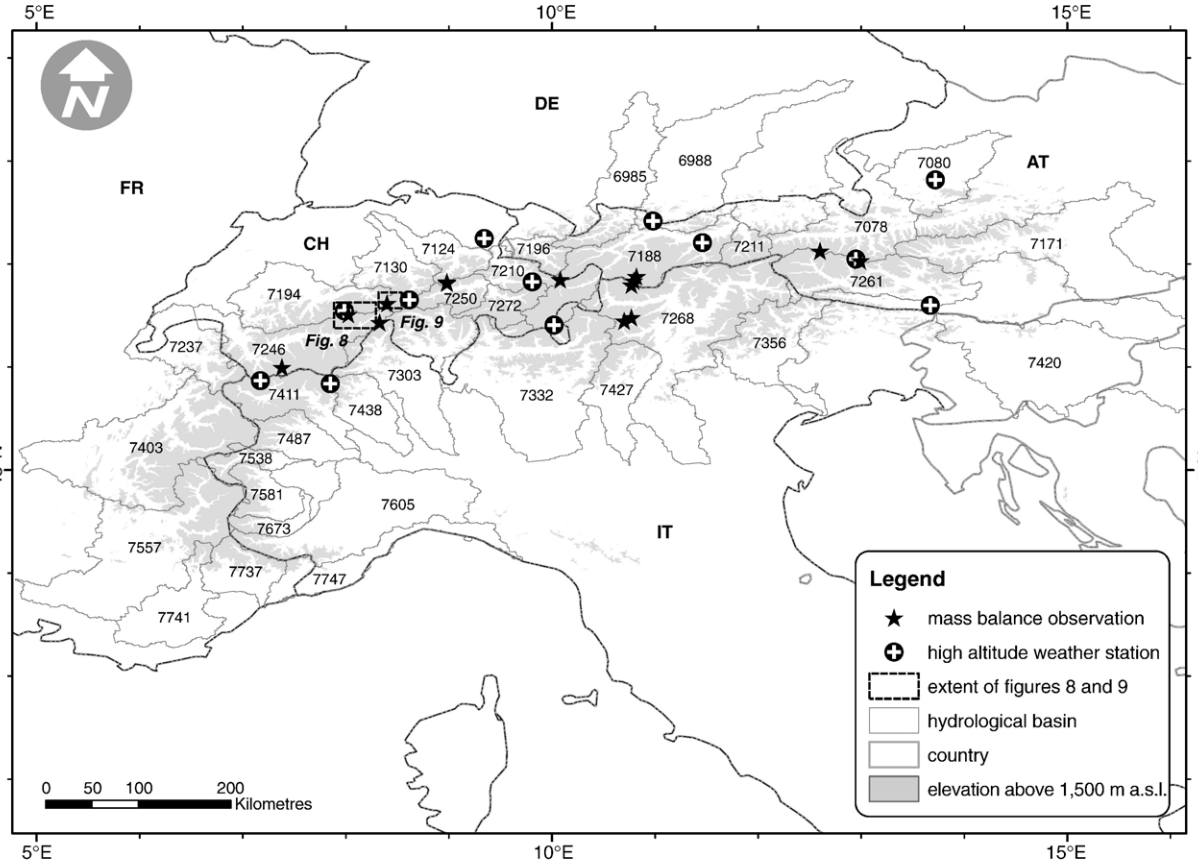

Fig. 1. Alpine mountain range (shaded in grey) with available mass balance observations (glaciers from west to east: Giétro, Grosser Aletsch, Gries, Rhone, Limmern, Plattalva, Silvretta, Caresèr, Fontana Bianca, Hintereis, Kesselwand, Vernagt, Sonnblick and Wurten) and high altitude weather stations (from west to east: Gr. St. Bernhard, Lago Gabiet, Junfraujoch, Gütsch ob Andermatt, Säntis, Weissfluhjoch, Bernina Hospiz, Zugspitze, Patscherkofel, Sonnblick, Villacher Alpe and Feuerkogel). Hydrological basins from the HYDRO1k DEM (http://LPDAAC.usgs.gov) are labelled with the corresponding basin IDs. The spatial extent of Fig. 8 and 9 is indicated by dashed black lines.

glacierised areas were calculated from a digital glacier inventory for the 0.25°×0.5° model cells. Single and multivariate statistical analysis was then performed to determine the climatic variables controlling the spatial distribution of glaciers in the Rockies.

Lie et al. (2003a) presented an exponential relationship between mean ablation season temperature and winter precipitation at the ELA of ten Norwegian glaciers. Using interpolated precipitation and temperature data for the period of 1961–1990 and a DEM of southern Norway, they modelled the altitude of instantaneous glacierisation (AIG) and the corresponding glacier accumulation areas, with a spatial resolution of 5° min (Lie et al., 2003b).

The approach presented in this study is based on the concept of Haeberli (1983) and Shumsky (1964). We present an empirical relationship between 6-month summer temperature and annual precipitation at the ELA_0, based on the period of 1971–1990. Rather than applying the often-used AAR_0 method, we determine the ELA_0 from direct glaciological mass balance measurements. Implementing the approach from Lie et al. (2003a), we then apply the obtained empirical relationship, using GIS techniques, to

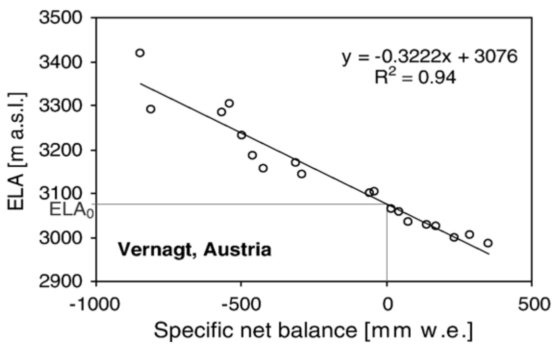

Fig. 2. Linear relationship between ELA and specific net balance of Vernagt Glacier (Austria) for the period 1971–1990. The ELA_0 of 3076 m a.s.l. represents the calculated ELA value for a zero net balance, i.e., a hypothetical steady-state.

model the AIG, the rcELA_0 and the cAA with a spatial resolution of 3 arc sec (approx. 100 m) over the entire European Alps.

3. Methods

In Fig. 1 an overview is given of all the elements mentioned later in the article, such as locations of mass balance observations, high altitude weather stations, hydrological basins and extent of the Alpine mountain range.

3.1. Precipitation and temperature at the ELA_0

To set up an empirical relationship between precipitation and temperature at the ELA_0 we focus on the period of 1971–1990. In this period, mass balance series from 14 Alpine glaciers as well as Alpine-wide temperature and precipitation data are available. The ELA_0 is calculated for each glacier from the relation between the specific net balance and the ELA, as compiled by the World Glacier Monitoring Service (http://www.wgms.ch) and published in the Glacier Mass Balance Bulletin series (e.g. IUGG(CCS)/UNEP/UNESCO/WMO, 2005). ELA values outside the glacier altitude range (i.e., when the entire glacier is an accumulation or ablation area) are excluded in this regression analysis. Fig. 2 shows the example of Vernagt Glacier (Austria) with an ELA_0 of 3076 m a.s.l. The regression analysis of the 14 glaciers shows coefficients of determination (R^2) ranging from 0.74 to 0.99, with a mean of 0.89.

Precipitation values at the glacier ELA_0 were obtained from the Alpine precipitation climatology (1971–1990) published by Frei and Schär (1998) and Schwarb et al. (2001). Based on a comprehensive database with observations from 5831 conventional rain gauges and 259 totalisators (i.e. cumulative precipitation gauges), this gridded data set provides mean monthly precipitation (1971–1990), as well as monthly precipitation–elevation gradients on a spatial resolution of 1.25 arc min (approx.

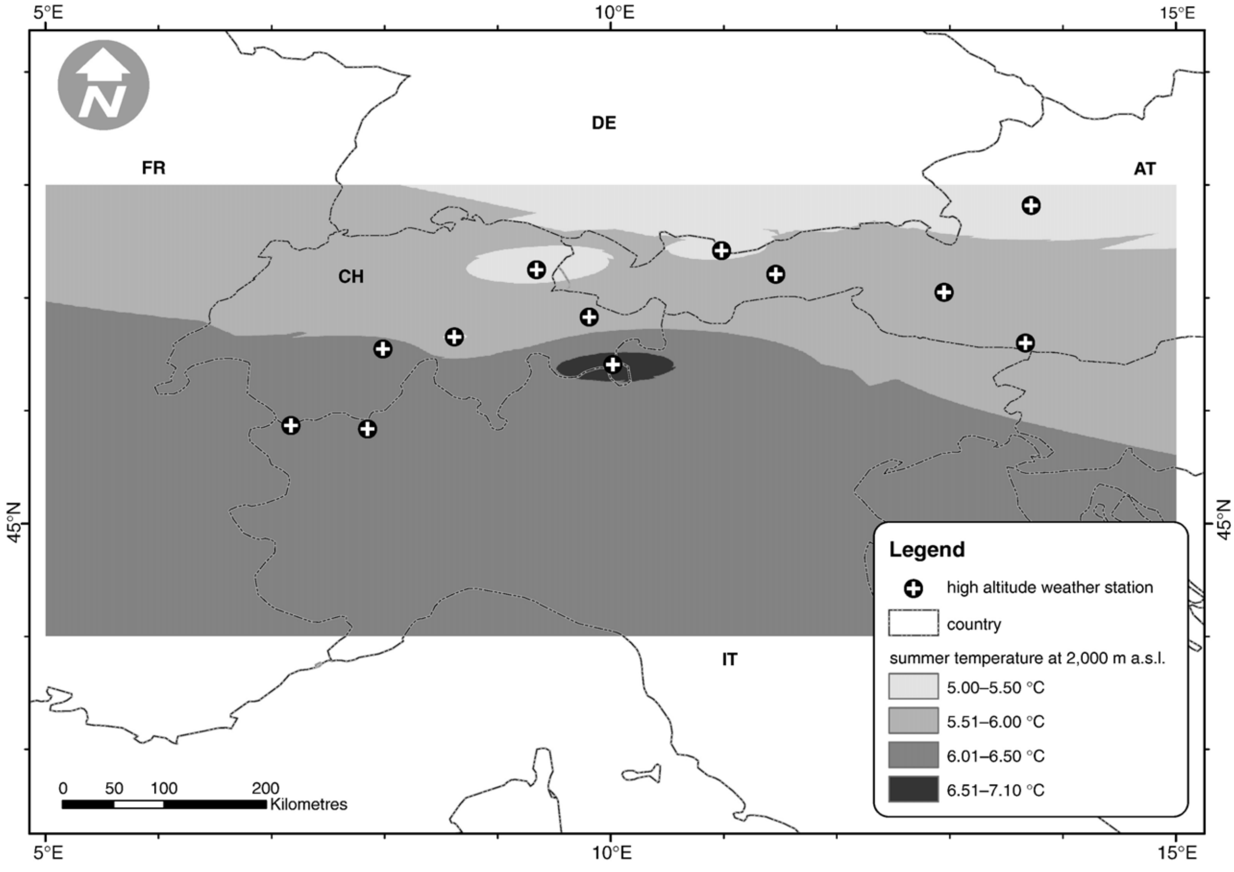

Fig. 3. The 6-month summer temperature field at 2000 m a.s.l. (1971–1990) as interpolated from 12 high altitude weather stations. A seasonal lapse rate of 0.67 °C per 100 m was used to altitude-adjust the seasonal mean temperature at weather stations to 2000 m a.s.l. The IDW (Watson and Philip, 1985) method was used for the interpolation.

2 km). Frei and Schär (1998) and Schwarb et al. (2001) calculated a regression between precipitation and altitude for each grid cell. Station data is weighted differently according to the extent to which they are representative of conditions at that grid cell. The weighting takes into account factors such as distance and difference in altitude from the grid cell, as well as varying aspect. However, in this study we find that the DEM that underlies the precipitation climatology differs significantly in altitude from the ELA_0, i.e., the altitude assigned to a grid cell in the precipitation climatology is significantly different from the measured ELA_0 (mean absolute difference of 161 m, with a maximum absolute difference of 655 m). Therefore, we use the precipitation–elevation gradients (ranging at ELA_0 locations from −2 to 78% per 100 m) to correct the precipitation of each grid cell in the glacier accumulation area to the corresponding ELA_0. Not knowing the exact location of the ELA_0 (only the location of the glacier boundaries and the altitude value of the ELA_0 are known) and of the uncertainties of the precipitation climatology, the precipitation at the ELA_0 is calculated as the mean of all precipitation grid cells covering the glacier accumulation area.

The variations in precipitation are complex and, in contrast to temperature variations, can be poorly correlated with altitude. Auer et al. (2005) show that the spatial mean decorrelation distances (R^2 decreasing below 0.5) of temperature (annual: 993 km, seasonal: 765 km, monthly: 722 km) are much larger than those of precipitation (annual: 149 km, seasonal: 120, monthly: 105 km). Hence, many fewer stations are needed to interpolate temperature at glacier locations. However, Oerlemans (2001, p. 37–38) demonstrates for the Morteratsch Glacier (Switzerland) that temperature at a nearby valley station may tend to become decoupled from the temperature measured at an automatic weather station located on the glacier surface (e.g., due to atmospheric inversions in the flat valley during winter), whereas the correlation with a high altitude weather station remains high. Therefore, we use temperature from 12 Alpine high altitude weather stations with continuous data series between 1971 and 1990, provided by MeteoSwiss,

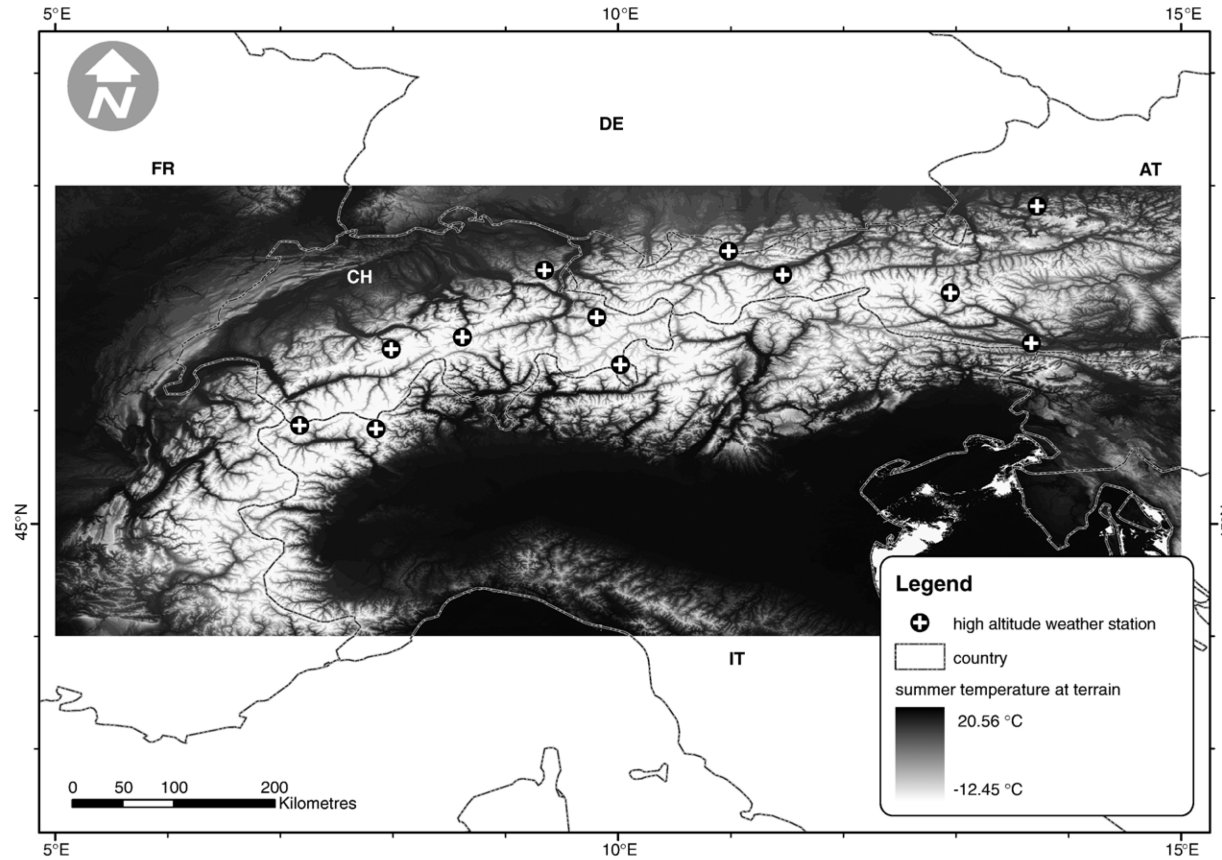

Fig. 4. The 6-month summer temperature on terrain (1971–1990). The data set was produced by extrapolating the temperature field at 2000 m a.s.l. (Fig. 3) to the altitude of the terrain (SRTM3, competed with SRTM30) using a seasonal lapse rate of 0.67 °C per 100 m.

Table 1
Precipitation and temperature at the ELA_0 for the period of 1971–1990. ELA_0 is calculated from the linear relationship between ELA and the specific net balance. Annual precipitation (P_a, sum) and 6-month winter precipitation ($P_{O–M}$, sum) are derived from the Alpine precipitation climatology by Frei and Schär (1998) and Schwarb et al. (2001). Annual temperature (T_a, average), 6-month summer temperature ($T_{A–S}$, average) and 3-month summer temperature (T_{JJA}, average) are interpolated at 2000 m a.s.l. from high altitude weather stations (see Fig. 1) and extrapolated to the ELA_0

Glacier name	Lat	Lon	ELA_0	P_a	$P_{O–M}$	T_a	$T_{A–S}$	T_{JJA}
	(°)	(°)	(m a.s.l.)	(mm)	(mm)	(°C)	(°C)	(°C)
Fontana Bianca (IT)	46.48	10.77	3177	1125	417	−5.43	−1.58	1.20
Gietro (CH)	46.00	7.38	3174	1250	604	−5.52	−1.63	1.21
Kesselwand (AT)	46.83	10.80	3106	1270	480	−5.19	−1.52	1.12
Careser (IT)	46.45	10.70	3088	1111	401	−4.86	−0.91	1.91
Vernagt (AT)	46.88	10.82	3076	1100	428	−5.03	−1.35	1.28
Gr. Aletsch (CH)	46.50	8.03	[a]2961	2926	1327	−4.18	−0.23	2.40
Hintereis (AT)	46.80	10.77	2933	1228	466	−4.13	−0.33	2.35
Rhone (CH)	46.62	8.40	2918	2031	1094	−4.04	−0.44	2.26
Gries (CH)	46.43	8.33	2852	2226	1036	−3.58	0.34	3.07
Plattalva (CH)	46.83	8.98	2772	1968	839	−3.14	0.64	3.34
Wurten (AT)	47.03	13.00	2770	2518	1063	−3.61	0.73	3.47
Silvretta (CH)	46.85	10.08	2755	1443	530	−2.93	0.89	3.56
Sonnblick (AT)	47.13	12.60	2731	2726	1135	−3.26	0.89	3.59
Limmern (CH)	46.82	8.98	2677	2012	857	−2.57	1.27	3.99

[a] The ELA_0 of Grosser Aletsch Glacier is calculated from mass balance data from the hydrological method, and ELA values interpolated from snow pits in the accumulation area of the glacier (Jungfraufirn) and aerial photographs.

Zurich, and the Central Institute for Meteorology and Geodynamics, Vienna. The 12 stations are all located above 2000 m a.s.l., with the exception of Feuerkogel (Austria) at 1618 m a.s.l. Monthly lapse rates are empirically derived from temperature and elevation values of the 12 stations. All of these linear regression analyses show high correlations (R^2 above 0.9) and range from 0.54 °C per 100 m in December to 0.71 °C per 100 m in July. Seasonal mean temperatures and lapse rates are calculated. With these empirically derived lapse rates, seasonal temperatures are altitude-adjusted to 2000 m a.s.l. Using the inverse distance weighted (IDW; Watson and Philip, 1985) interpolation method, temperatures are interpolated over the entire Alps. Anisotropy is taken into account by specifying a lower power along and a higher power against the Alpine ridge (specifying a lower value for power will provide more influence to surrounding points farther away). Fig. 3 shows the altitude-adjusted 6-month summer temperature field at 2000 m a.s.l. over the greater Alpine region. Temperature ranges from 5.0–7.1 °C. At glacier locations the empirical lapse rates are used again to extrapolate temperatures at 2000 m a.s.l. to the ELA_0. The same principle is applied to produce an Alpine-wide data set of temperature on terrain, with a resolution of 3 arc sec (approx. 100 m), by extrapolating the temperature field at 2000 m a.s.l. with the seasonal lapse rate to the altitude of a DEM (Fig. 4). As already mentioned, the exact location of the ELA_0 is not known and it might also differ from the elevation of the corresponding grid cell of the DEM. For the estimation of temperature and precipitation at the ELA_0, used to derive the empirical relationship, we consider, therefore, the ELA_0 instead of the corresponding altitude of the DEM. Hence, temperature and precipitation values at the location of the mass balance observations might differ from the values at the corresponding locations in the gridded precipitation and temperature climatologies.

Annual and 6-month winter precipitation, and annual and 6- and 3-month summer temperatures at the ELA_0

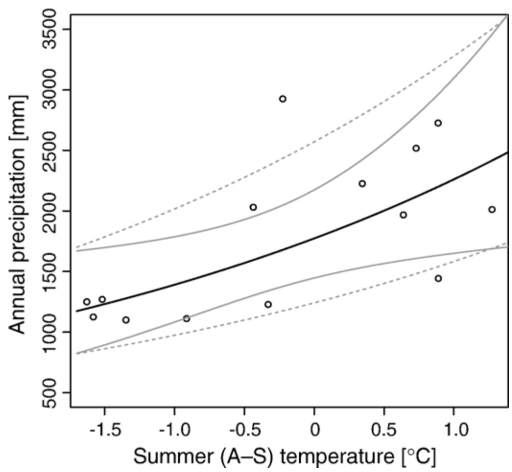

Fig. 5. Annual precipitation and 6-month summer temperature at the ELA_0 for the period 1971–1990 (cf. Table 1). The exponential regression model (Eq. (1); black line) performs with a R^2 of 0.49. The boundaries of the 95% confidence interval (Eq. (2); grey line) are conservatively approximated by shifting the regression model (Eqs. (3) and (4); dashed grey lines).

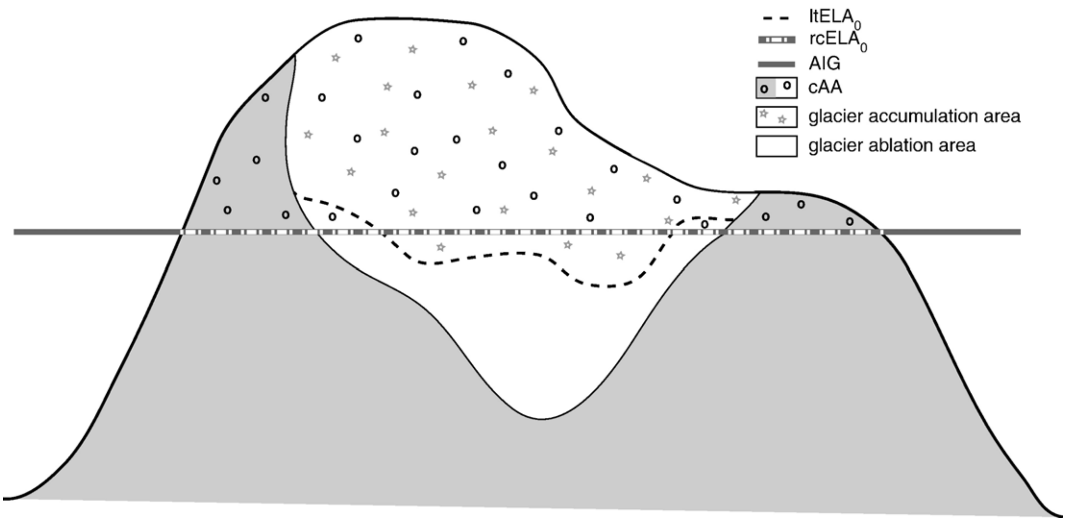

Fig. 6. Diagram to explain the concept of the AIG and its association with ltELA$_0$, rcELA$_0$ and cAA. Figure modified after Lie et al. (2003a).

of the 14 Alpine glaciers are shown in Table 1. The empirical relationship between annual precipitation (P_a) and the 6-month summer temperature (T_{A-S}) at the ELA$_0$ performs best with an R^2 of 0.49 on a 1% significance level (p-value of 0.0052) and can be expressed by the regression equation:

$$P_a = 1773 \cdot e^{0.2429 \cdot T_{A-S}} \tag{1}$$

Eq. (1) is plotted in Fig. 5 together with the upper and lower boundaries of the 95% confidence interval which can be formulated as:

$$P_a = 1773 \cdot e^{0.2429 \cdot T_{A-S}^{\pm 0.1985 \cdot \sqrt{(1+(T_{A-S}+0.2301)^2}}} \tag{2}$$

These boundaries describe the possible range of annual precipitation, at a 5% significance level, for a given 6-month summer temperature at the ELA$_0$.

The 95% confidence interval boundaries can be approximated by a shift of Eq. (1) in such a manner that the new equations for the lower boundary, Eq. (3), and upper boundary, Eq. (4), describe a confidence interval greater than 95% within the temperature data range and lower than 95% outside the temperature data range, respectively.

$$P_a = 0.7 \cdot 1773 \cdot e^{0.2429 \cdot T_{A-S}} \tag{3}$$

$$P_a = 1.45 \cdot 1773 \cdot e^{0.2429 \cdot T_{A-S}} \tag{4}$$

3.2. Distributed modelling of the regional climatic ELA$_0$

To apply Eq. (1) in space, we implement the approach from Lie et al. (2003a). Along with this, we introduce temperature lapse rate and precipitation–elevation gradient to derive temperature and precipitation at the AIG. Temperature at the AIG (T_{AIG}) can be derived from the temperature at a known altitude (T_0), the lapse rate (ΔT) in degrees Celsius per 100 m and the height of the AIG above the terrain (h, in 100 m units):

$$T_{AIG} = T_0 - (\Delta T \cdot h) \tag{5}$$

The precipitation at the AIG (P_{AIG}) can be derived from the precipitation at a known altitude (P_0), the precipitation–elevation gradient (ΔP) in percent per 100 m and the height of the AIG above the terrain (h, in 100 m units):

$$P_{AIG} = P_0 \cdot (1 + \Delta P)^h \tag{6}$$

By combining Eqs. (5) and (6) with Eq. (1), the expression becomes:

$$P_0 \cdot (1 + \Delta P)^h = 1773 \cdot e^{0.2429 \cdot (T_0 - (\Delta T \cdot h))} \tag{7}$$

Solving Eq. (7) with respect to the only unknown parameter h, the AIG is:

$$\begin{aligned} \mathrm{AIG} &= \mathrm{ALT_{DEM}} + (h \cdot 100) = \mathrm{ALT_{DEM}} \\ &\quad + \left(\frac{\ln(1773) + 0.2429 \cdot T_0 - \ln(P_0)}{\ln(1 + \Delta P) + 0.2429 \cdot \Delta T} \cdot 100 \right) \end{aligned} \tag{8}$$

where ALT$_{DEM}$ is the altitude of the terrain. The rcELA$_0$ can now be computed from the intersection of the DEM with the AIG, where ALT$_{DEM}$ is equal to AIG (or: $h = 0$).

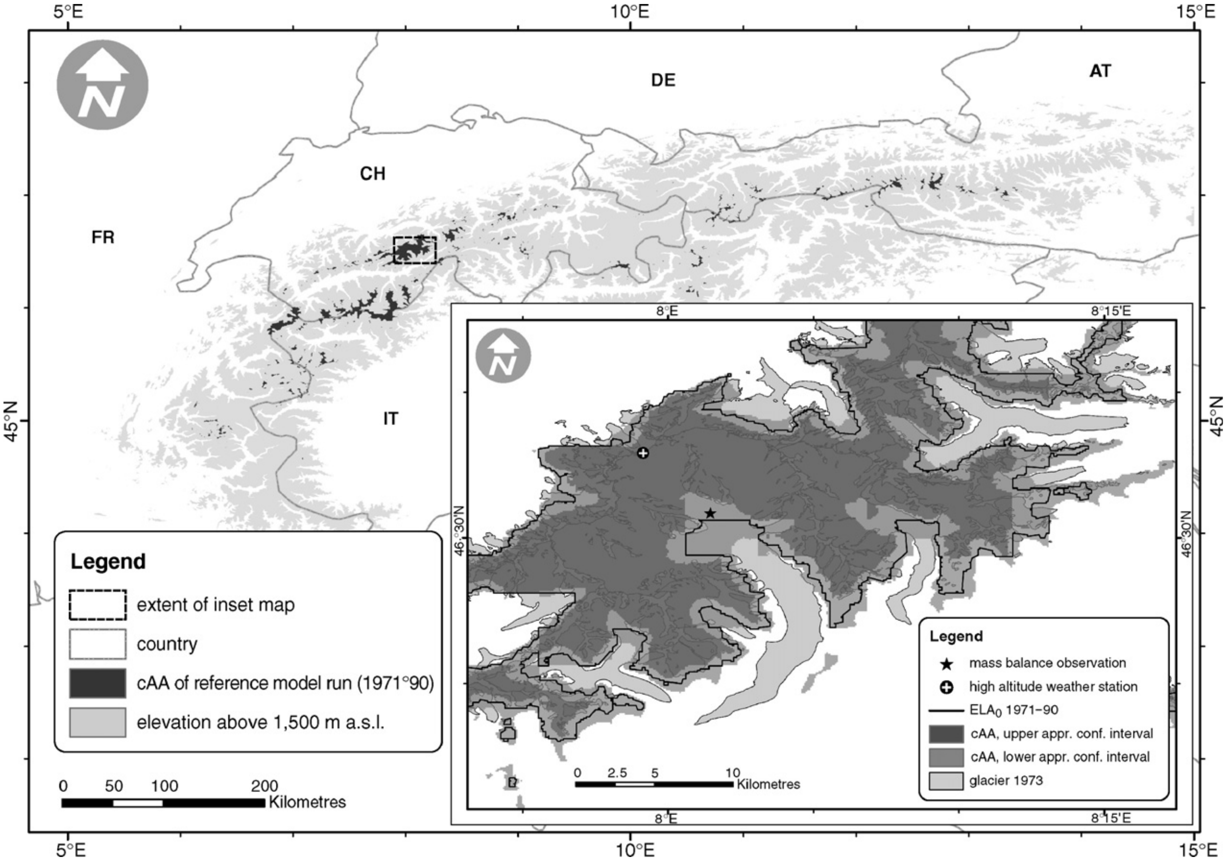

Fig. 7. cAA of the reference model run (1971–1990). The inset map shows the ELA_0 of the reference model run (black line) and the cAAs of the corresponding lower (grey) and upper (dark grey) boundaries of the approximated confidence interval. Glacier extents of 1973 from the Swiss Glacier Inventory are shown in light grey.

The climatic accumulation area (cAA) corresponds to the regions where the ALT_{DEM} is above the AIG (or: $h<0$):

$$\mathrm{AIG}\begin{cases} < & \mathrm{ALT_{DEM}} \rightarrow \mathrm{cAA} \\ = & \mathrm{ALT_{DEM}} \rightarrow \mathrm{rcELA_0} \\ > & \mathrm{ALT_{DEM}} \rightarrow \mathrm{no.cAA} \end{cases} \tag{9}$$

A schematic representation of the AIG and its association with $ltELA_0$, $rcELA_0$ and cAA appears in Fig. 6.

The AIG, $rcELA_0$ and cAA are modelled in space using the annual precipitation data (in mm) and the corresponding annual precipitation–elevation gradients (in percent per 100 m) from Frei and Schär (1998) and Schwarb et al. (2001) and 6-month summer lapse rate (0.67 °C per 100 m) and 6-month summer temperature on terrain as input raster data sets. The summer temperature data set is extrapolated with the summer lapse rate from the altitude-adjusted temperature field at 2000 m a.s.l. (Fig. 3) to the altitude of the DEM (Fig. 4). The latter is the 3 arc sec version created by the Shuttle Radar Topography Mission (SRTM3; spatial coverage from 61° N to 57° S) and resampled to 100 m spatial resolution for our purposes. The data can be downloaded for free from a NASA ftp-server (ftp://e0mss21u.ecs.nasa.gov/srtm/) and are described in Rabus et al. (2003). Larger gaps in the SRTM3 data set have been filled by resampled 30 arc sec SRTM30 elevation data, and can be obtained from the

Table 2
Overview of the seven model runs. Deviations in temperature and precipitation of the six sensitivity runs from the reference model run ($MR_{1971–1990}$)

	MR 1971–1990	MR T+1	MR T−1	MR P+25	MR P−25	MR T−0.6	MR T+3/ P+10
ΔT [°C]	0	+1	−1	0	0	−0.6	+3
ΔP [%]	0	0	0	+25	−25	0	+10

same source. The distributed modelling is implemented and automated using the ESRI software ArcGIS 9.0. A model run takes a few minutes of computing time.

In Fig. 7 the modelled cAA is shown for the reference period 1971–1990, and the maximum spatial extent of the investigation area (6–14° E, 44–48° N) is defined by the data set with the minimum spatial extent (precipitation data). By combining Eqs. (5) and (6) with Eqs. (3) and (4), AIG, rcELA$_0$ and cAA of the boundaries of the approximated confidence interval can be applied in space as well (Fig. 7, inset map).

3.3. Sensitivity study

In addition to the model run for the reference period 1971–1990, six more model runs were carried out to study the sensitivity of the ELA$_0$ to changes in temperature and precipitation. Temperature and/or precipitation are altered by a uniform deviation over the entire investigation area (i.e., the entire gridded climatologies). Table 2 gives an overview on the seven model runs.

MR$_{T+1}$ and MR$_{T-1}$ as well as MR$_{P+25}$ and MR$_{P-25}$ are sensitivity studies with deviations only in temperature or

Table 3
Basin mean ELA$_0$ of the reference model run (MR$_{1971-1990}$) and ELA$_0$ deviations of the six sensitivity runs. Zonal borders come from the HYDRO1k DEM (http://LPDAAC.usgs.gov). In addition, zonal means within the 1973 outlines of the Swiss Glacier Inventory (Kääb et al., 2002; Paul et al., 2002) for glaciers larger than 1 km^2 are given

Hydrological basin (no.)	MR$_{1971-1990}$ (m a.s.l.)	MR$_{T+1}$ (m)	MR$_{T-1}$ (m)	MR$_{P+25}$ (m)	MR$_{P-25}$ (m)	MR$_{T-0.6}$ (m)	MR$_{T+3/P+10}$ (m)
Lech (6985)	#	#	*	*	#	*	#
Isar (6988)	2592	+190	−137	−130	#	−60	#
Enns (7078)	2772	+131	−124	−110	+148	−78	+319
Traun (7080)	#	#	*	*	#	*	#
Linth (7124)	2784	+135	−134	−125	+149	−80	+340
Reuss (7130)	2784	+154	−131	−124	+167	−82	+366
Mur (7171)	2716	+130	−47	−47	+130	+18	#
Inn (7188)	3102	+118	−154	−142	+152	−95	+375
Aare (7194)	2795	+137	−125	−117	+150	−72	+310
Ill (7196)	#	#	*	*	#	#	#
Landquart (7210)	2807	+119	−80	−73	+113	−32	#
Ziller (7211)	2873	+150	−128	−121	+174	−83	+359
Arve (7237)	2895	+141	−120	−112	+170	−64	+360
Rhone (7246)	2966	+130	−132	−122	+147	−73	+315
Hinterrhein (7250)	2805	+126	−116	−103	+144	−71	+302
Drau (7261)	2810	+118	−96	−86	+145	−62	+309
Adige (7268)	3110	+135	−128	−114	+151	−80	+296
Vorderrhein (7272)	2896	+163	−44	−42	+168	−24	+327
Toce (7303)	2878	+161	−145	−134	+192	−92	+414
Adda (7332)	3144	+121	−194	−188	+171	−116	+351
Piave (7356)	2981	#	−83	−62	#	−66	#
Isere (7403)	3154	+131	−154	−142	+166	−90	+368
Aosta (7411)	3001	+112	−118	−107	+124	−65	+283
Drava (7420)	#	#	*	*	#	*	#
Chiese (7427)	3079	+137	−119	−110	+184	−91	#
F. Sesia (7438)	2980	+116	−117	−104	+113	−66	+295
Oreo (7487)	3159	+138	−135	−134	+165	−82	+325
D. Riparia (7538)	3144	+114	−138	−130	+190	−78	#
Durance (7557)	3183	+127	−193	−166	+169	−116	+344
Chisone (7581)	3148	+184	−83	−79	+184	−91	+368
Po basin (7605)	2987	#	−123	−108	#	−76	#
Po fount (7673)	#	#	*	*	#	*	#
Var (7737)	3077	#	−201	−172	#	−131	#
Argens (7741)	#	#	*	#	#	#	#
Liguria (7747)	#	#	*	*	#	*	#
All hydro basins	2951	+137	−125	−114	+157	−75	+336
Swiss glaciers	2946	+126	−118	−107	+140	−65	+308

* The calculation of an rcELA$_0$ difference from the reference run is not possible, since for one model run the #AIG is above the highest peaks in of the corresponding hydrological basin.

precipitation. $MR_{T-0.6}$ represents a summer temperature cooling of 0.6 °C, as assumed by Maisch et al. (2000) for the year 1850. $MR_{T+3/P+10}$ applies a warming of the summer temperature of 3 °C and a concurrent rise in precipitation by 10%. This corresponds to a moderate climate change scenario as published by OcCC (2004), commissioned by the Swiss Federal Office of Energy (SFOE). This study is based on IPCC (2001) and estimates a summer (JJA) temperature rise of 0.8–5.1 °C by 2050 for the northern and 1.0–5.6 °C for the southern slope of the Swiss Alps, respectively. It estimates precipitation to decrease in summer and increase in winter. For winter (DJF) precipitation a rise of 5–23% is indicated by 2050.

Reference and sensitivity model runs are analysed for individual glacier regions, within the hydrological basins, as derived from the HYDRO1k DEM (provided by the Land Processes Distributed Active Archive Centre located at the U.S. Geological Survey's EROS Data Centre: http://LPDAAC.usgs.gov), and within the 1973 outlines of the Swiss Glacier Inventory (Kääb et al., 2002; Paul et al., 2002) for glaciers larger than 1 km^2.

4. Results

4.1. Empirical relationship between precipitation and temperature at the ELA_0

Precipitation at the glacier ELA_0 (Eq. (1), Table 1) shows a non-linear increase with increasing temperature. The differences in R^2 between the applied exponential trends and linear trends range from 0.06–0.08, i.e., 6–8% of the explained variance. The empirical relationships with annual precipitation perform better than the ones with 6-month winter precipitation, with R^2 differences of 0.10–0.12. For the distributed modelling of the AIG, the $rcELA_0$ and the cAA the relationship between annual precipitation and 6-month summer temperature is used (Eq. (1)), as it performs best with an R^2 of 0.49 on a 1% significance level (p-value of 0.0052).

4.2. Modelled glacierisation of the reference run (1971–1990)

The AIG of the reference model run (1971–1990), shows two culminations with AIG values above 3100 m a.s.l.; one ranging from the southern Valaisan Alps, Switzerland, to the south-western Alps and another one between the Rhaetian Alps, Switzerland, over the South Tyrol, Italy, to the Upper Tauern, Austria. There is an AIG depression over the Ticino Alps, Switzerland, and a generally lower AIG on the northern Alpine slope.

Table 3 lists the $rcELA_0$ averaged within the hydrological basins and within the Swiss glacier outlines. As the $rcELA_0$ represents the intersection of the AIG with the DEM, it reproduces the general image of the AIG. It ranges from 2591 m a.s.l. (Isar) to 3183 m a.s.l. (Durance) with a mean value of 2951 m a.s.l. However, some hydrological basins show an average, caused by local topographic effects, that does not correspond to the $rcELA_0$ of the sub-regions. The most pronounced example is the Rhone basin in the Valais, Switzerland. It has an average ELA_0 of 2966 m a.s.l. with a standard deviation of 161 m. This is produced by $rcELA_0$ values below 2800 m a.s.l. in the northern Valais and above 3100 m a.s.l. in the southern Valais.

Over the entire Alps the cAA covers an area of 3059 km^2. As the cAA is simply the terrain above the $rcELA_0$, it does not distinguish between glacier surface and ice-free rock walls. In a first order approach this can be taken into account by applying a slope-dependent glacier fraction to the modelled cAA. Table 4 shows the slope-area distribution (derived from the SRTM3) within the cAA and within the parts of the 1973 outlines of the Swiss Glacier Inventory inside the cAA of a test area (Canton Valais, Switzerland, corresponding approximately to the Rhone basin). From these parameters, glacier fractions are calculated for the nine slope classes and applied to the slope-area distribution of the Alpine cAA. These empirical glacier fractions are dependent on quality and resolution of the DEM used and therefore have to be re-evaluated when using other DEMs. The corrected cAA equals 1950 km^2 and corresponds to an AAR_0 of 0.67 of the measured total Alpine glacier area in the 1970s, which was 2909 km^2 (Zemp et al., in press).

4.3. Model validation

The model error can be described by the deviations of the modelled AIG values of the 14 glaciers from the measured ELA_0. The mean absolute difference is 66.7 m with a standard deviation of 55.4 m. The greatest deviations are found for Silvretta Glacier, where the measured ELA_0 is 214 m below the modelled AIG, and for Grosser Aletsch Glacier, where the ELA_0 is 127 m above the AIG. To get an estimation of the possible deviation of the $ltELA_0$ from the $rcELA_0$ (as modelled), Eq. (1) is substituted by the two approximations of the confidence interval boundaries, Eqs. (3) and (4), to calculate a spatial confidence zone. This results in average deviations of −177 m and +209 m from the reference $rcELA_0$, based on Eq. (1).

The resulting cAA is checked in a qualitative manner by comparison with the outlines from the 1973 Swiss

Table 4
Slope-area distribution (in km^2) within the cAA (1971–1990) and within the 1973 outlines of the Swiss Glacier Inventory inside the cAA (1971–1990), computed in the Canton Valais, Switzerland (corresponding approximately to the Rhone basin). The glacier fraction of each slope class (in %) is calculated based on this distribution

Data set	0–10°	11–20°	21–30°	31–40°	41–50°	51–60°	61–70°	71–80°	81–90°
cAA	220.0	370.7	290.3	171.7	70.8	13.4	1.5	<0.1	0
Glacier area within cAA	196.3	288.7	169.8	67.7	22.8	3.8	0.4	0	0
Glacier fraction	89	78	58	39	32	29	29	0	0

Glacier Inventory and with LandsatTM images dating from the 1990s. The modelled cAA corresponds well overall to the real accumulation areas of Alpine glaciers and there are minor quantities of cAA cells in regions with no glacierisation. A general overestimation of the accumulation areas on SE–SW slopes and underestimation on NE–NW slopes can be found.

4.4. Sensitivity study

The $rcELA_0$ deviations of the sensitivity model runs from the reference run (1971–1990) within the hydrological basins are shown in Table 3. A temperature change of ±1 °C leads to an average $rcELA_0$ deviation of +137/−125 m, ranging from +112 m (Aosta) to +190 m (Isar) and from −44 m (Vorderrhein) to −201 m (Var), respectively. A precipitation change of ±25% leads to an average $rcELA_0$ deviation of −114/+157 m, with a range similar to the 1° temperature deviation. $MR_{T-0.6}$ results in an average $rcELA_0$-decrease of 75 m, ranging from 24 m to 131 m. The increase of 18 m within the Mur basin is an undesired side-effect caused by the very small number of cAA cells. The occurrence of an additional glacierised peak in the $MR_{T-0.6}$ run leads to an average

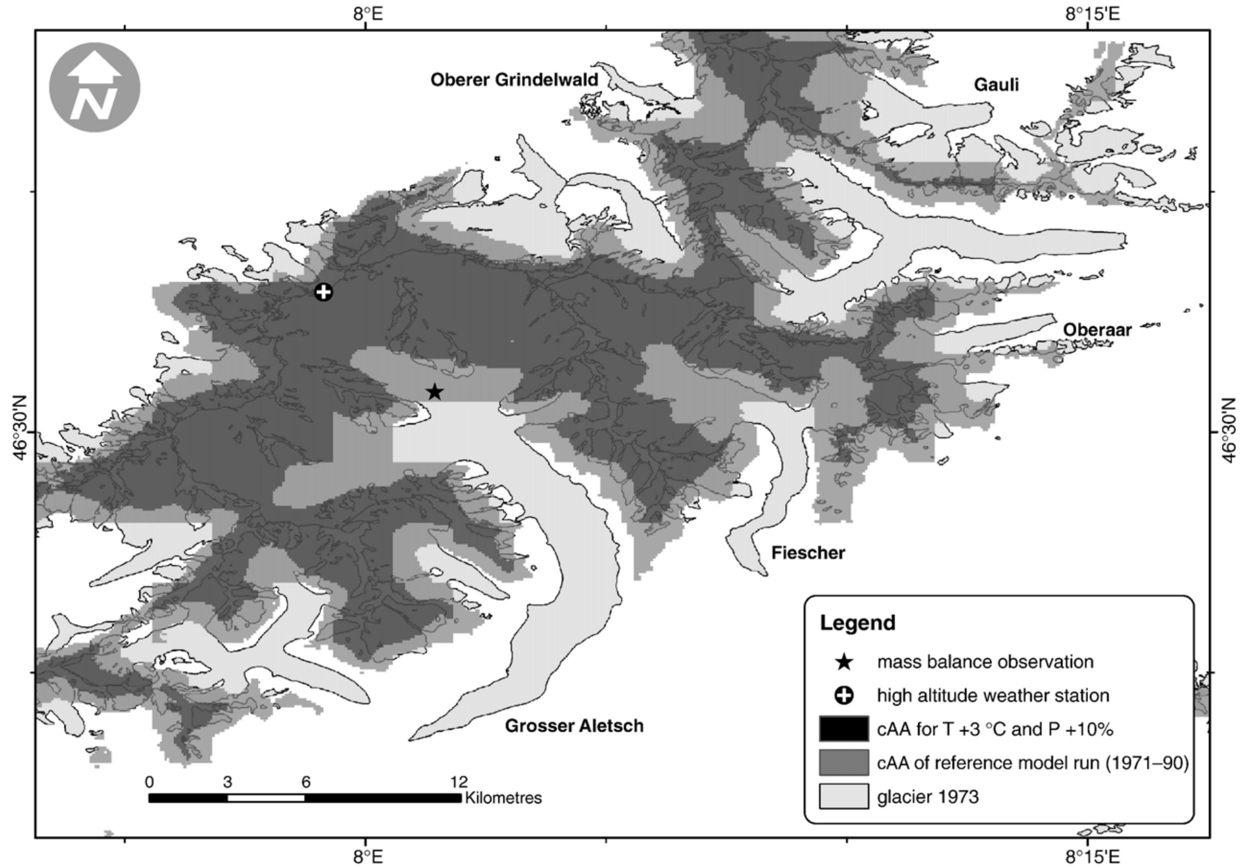

Fig. 8. cAA of the reference model run (1971–1990, grey) and cAA of the $MR_{T+3/P+10}$ (dark grey) in the region of Grosser Aletsch glacier, Switzerland. Glacier extents in 1973 from the Swiss Glacier Inventory are shown in light grey.

$rcELA_0$ higher than the one from the reference model run (1971–1990). The total cAA of the $MR_{T-0.6}$ run amounts to 4157 km^2. $MR_{T+3/P+10}$ leads to an average $rcELA_0$ rise of 336 m and the disappearance of glaciers in eight out of 28 basins. The corresponding total cAA over the entire Alps shrinks to 812 km^2. When the slope-dependent glacier fraction (Table 4) is applied, the cAA of the $MR_{T-0.6}$ and the $MR_{T+3/P+10}$ amounts to 2650 km^2 and 504 km^2, respectively. The average $rcELA_0$ and the deviations corresponding to the sensitivity runs, calculated within the 213 Swiss glacier outlines, represent a $rcELA_0$ subset of the hydrological basins Aare, Adda, Hinterrhein, Inn, Landquart, Linth, Reuss, Rhone, Toce and Vorderrhein. The deviations within the glacier outlines are slightly more moderate than those of the corresponding basin. The $MR_{T-0.6}$ induced a $rcELA_0$ lowering of 65 m.

Fig. 8 and 9 show the modelled cAA of the reference run (1971–1990) and of $MR_{T+3/P+10}$ for the regions of Grosser Aletsch Glacier and Rhone Glacier. To facilitate a qualitative check, the outlines of the 1973 Swiss Glacier Inventory are shown as well. The modelled cAA of the reference run (1971–1990) covers the accumulation areas of the Swiss glacier outlines of 1973 reasonably well. In flat areas (e.g., upper tongue of Grosser Aletsch Glacier, Fig. 8) the coarser resolved precipitation data may determine the $rcELA_0$ (i.e., long, sharp boundaries), whereas on steeper terrain, the temperature data set with higher resolution (20 times) is the determining factor. In general, cAA is overestimated on SE–SW slopes and underestimated on NE–NW slopes. The $rcELA_0$ rise between the reference run and $MR_{T+3/P+10}$ leads to a much more pronounced cAA reduction in flat regions compared to steep slopes.

In regions where the glacier outlines are available, the rise of the $rcELA_0$ can be derived for individual glaciers. In Fig. 8, the rise of the $rcELA_0$ between the two model runs amounts to 249 m for Grosser Aletsch Glacier, 315 m for Fiescher Glacier, 314 m for Oberaar Glacier, 310 m for Gauli Glacier and 353 m for the Oberer

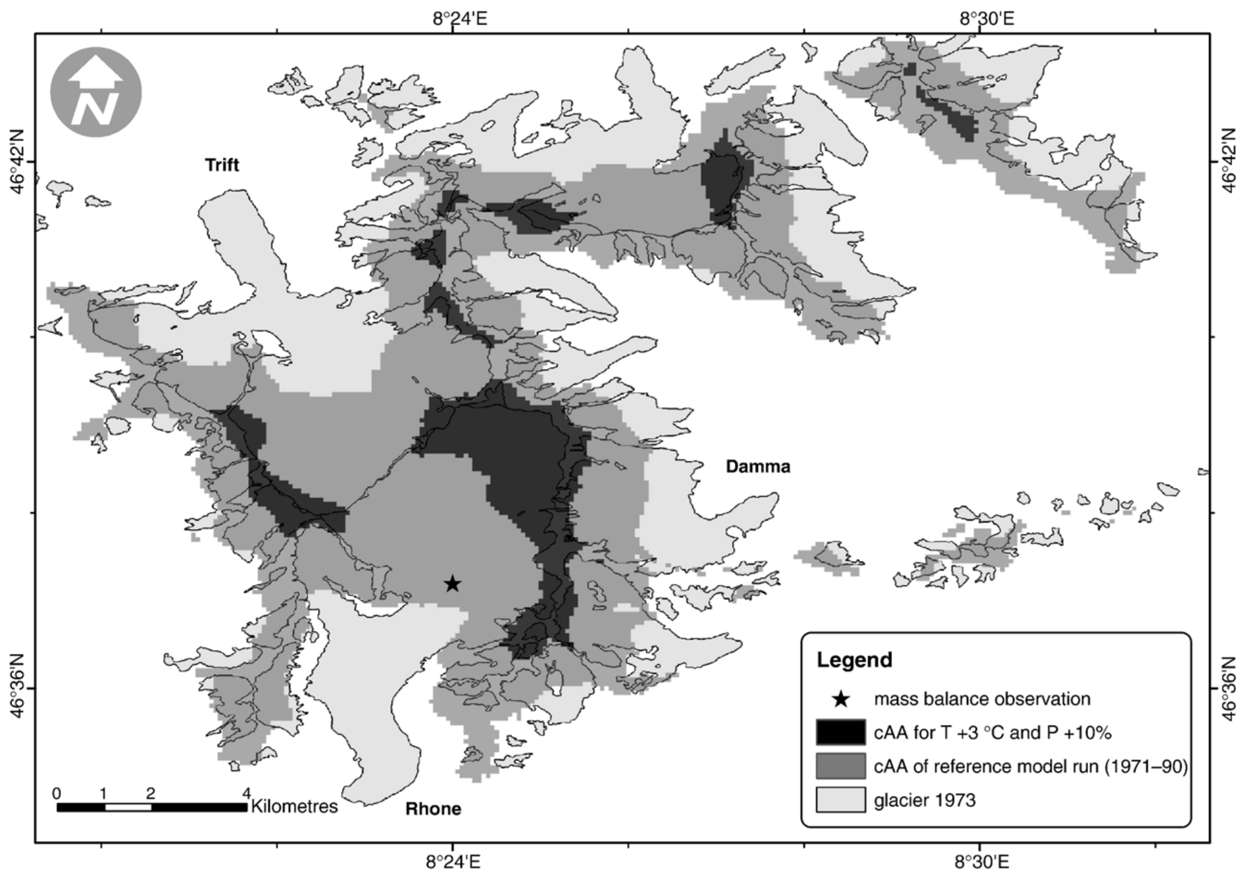

Fig. 9. cAA of the reference model run (1971–1990, grey) and cAA of the $MR_{T+3/P+10}$ (dark grey) in the region of Rhone glacier, Switzerland. Glacier extents in 1973 from the Swiss Glacier Inventory are shown in light grey.

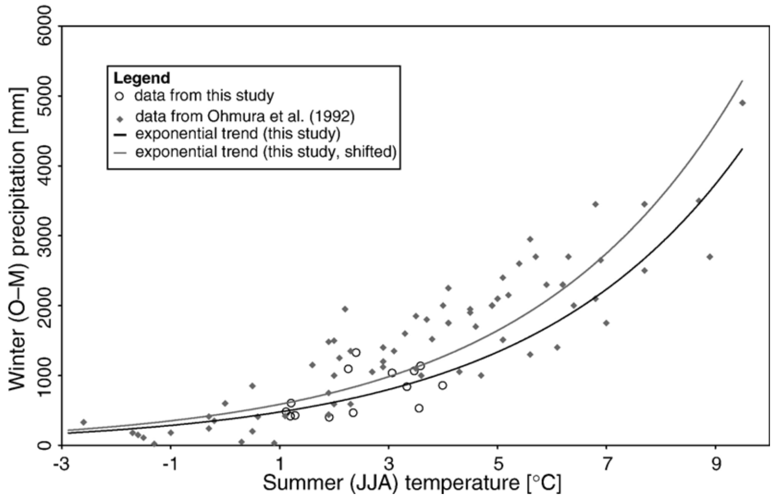

Fig. 10. The 6-month winter precipitation and the 3-month summer temperature at the ELA_0. Comparison between the data set presented in this study (black circles) and the one by Ohmura et al. (1992; grey diamonds). The exponential model (black line) based on the 12 data points from this study is shown together with a shifted exponential curve assuming a systematic precipitation measurement error of 23% (grey line).

Grindelwald Glacier. In Fig. 9 the $rcELA_0$ rises by 384 m at Rhone Glacier, 381 m at Damma Glacier and 374 m at Trift Glacier. In this region the temperature rise of the $MR_{T+3/P+10}$ leads to a strong reduction and disintegration of the cAA.

5. Discussion

5.1. Error estimations and model uncertainties

The 14 glaciers, on which the relationship between precipitation and temperature at the ELA_0 is based, are geographically and climatologically well-distributed over the Alps. Only the south-western Alps between France and Italy lack temperature and mass balance data. In this region, temperature measurements from high altitude weather stations began only after 1990. Mass balance data from Saint Sorlin (45° 11′ N, 6° 10′ E) and Sarennes (45° 7′ N, 6° 10′ E) exist, but ELA values are not available.

The precipitation data set by Frei and Schär (1998) and Schwarb et al. (2001) is based on more than 6000 data points and is currently the best available data set at this resolution covering the entire Alps. The applied interpolation method takes into account the fact that the precipitation–elevation gradients can vary considerably from one region to another (Schwarb et al., 2001). Approaches using a constant precipitation–elevation gradient for the precipitation extrapolation to the ELA may work in regions dominated by orographic precipitation due to frontal cyclones flowing perpendicular to the orientation of the mountain ridge (e.g., western side of the Canadian Rockies, western mountains in southern Norway), but will not include the effects of the complex gradient-patterns of the European Alps. However, in the precipitation climatology used, the data are not adjusted to the systematic precipitation measurement error, since the data needed to do this (wind, aspect of the station) are not available. Sevruk (1985) estimates this error for mean annual precipitation at 15–30% above 1500 m a.s.l. Hence, Eq. (1) has to be adapted if it is applied or compared to precipitation data with corrected systematic measurement error.

As already mentioned in Section 3: Methods, the spatial decorrelation distance is much greater for temperature than for precipitation. Together with the high coefficients of determination ($R^2 > 0.9$) of the derived temperature lapse rates, this justifies the interpolation of the general high altitude temperature field (at 2000 m a.s.l.) over the Alps based on the data from only 12 stations. Comparisons of the applied IDW interpolation method (considering anisotropy) with IDW (not considering anisotropy) and KRIGING (Oliver and Webster, 1990) show a mean temperature difference of 0.04 °C (with a standard deviation of 0.16 °C) and −0.03 °C (with a standard deviation of 0.35°), respectively. Assuming a temperature lapse rate of 0.67 °C per 100 m this corresponds to a mean ELA difference of about 5 m. In a test area of about 42 km × 34 km in the southern Valaisan Alps, Switzerland, comparisons of the SRTM3 (used to extrapolate temperature at 2000 m a.s.l. to the terrain) with the

DEM25L2 (a high-quality Swiss DEM with a resolution of 25 m) show a mean altitude difference between the two DEMs of 7.7 m with a standard deviation of 53.7 m. In the regions where the SRTM3 gaps had to be filled with the SRTM30, the DEM difference amounts to 100 m with a standard deviation of 158 m. This shows that the temperature error due to the applied interpolation method is of the same order of magnitude as the one due to errors in the DEM. However, in the presented distributed model the step from a non-cAA grid cell to a cAA grid cell is dominated by the parameter with the greatest variability from one cell to its immediate neighbours. The mean absolute difference from a grid cell to its eight neighbours of the used DEM is 15.9 m, whereas that of temperature at 2000 m a.s.l. is 0.0003 °C (corresponding to 0.04 m). This means that the altitude of the terrain is the decisive factor determining in the spatial distribution of the rcELA$_0$, superimposed by the precipitation field and the temperature field at 2000 m a.s.l. over the Alps.

The non-linearity of the empirical relationship between precipitation and temperature at the ELA$_0$, Eq. (1), is physically sound since, with increasing temperature, the rise of the ELA leads to a longer ablation season. Hence the influence of the temperature lapse rate becomes more dominant and the mass balance gradient increases. An additional amount of solid precipitation is needed to compensate the melting. Eq. (1) includes an uncertainty of about 500 mm precipitation for a given temperature at the ELA$_0$. The corresponding confidence zone is a conservative approximation of the 95% confidence interval (Eq. (2), Fig. 5). By applying this confidence zone in space, an uncertainty buffer with an average deviation of about ±190 m from the rcELA$_0$ of the reference run can be modelled, that accounts for measurement errors and for deviations of the ltELA$_0$ from the modelled rcELA$_0$ due to influences not included in the model (e.g., snow drift, avalanches, solar radiation). The general overestimation of the cAA on SE–SW slopes and underestimation on NE–NW slopes can be interpreted as differences, for example in solar radiation. Distributed mass balance models are needed (e.g., Klok and Oerlemans, 2002; Paul et al., in press) in order to account for these topographic effects. The influence of the uncertainty in rcELA$_0$ on the cAA is indirectly proportional to the slope of the terrain, i.e., the steeper the terrain, the smaller the corresponding error of the cAA.

Beyond the range of precipitation and temperature values, used for the derivation of Eq. (1) the uncertainties increase non-linearly. However, a comparison with worldwide data from Ohmura et al. (1992) shows that the empirical relationship derived from the 14 Alpine glaciers is also plausible for strongly continental and strongly maritime regions in the world. In Fig. 10, the 3-month summer temperature and the 6-month winter precipitation at the ELA$_0$ are plotted for the 14 Alpine glaciers in this study as well as for 69 glaciers worldwide as published in Ohmura et al. (1992). In addition, the exponential relationship derived only from the 14 Alpine glaciers is drawn, together with a shifted exponential curve that assumes a systematic precipitation measurement error of 23% (i.e., mean of the estimated measurement error of 15–30% for altitudes above 1500 m a.s.l.; Sevruk, 1985). We have not combined these two data sets in order to derive a worldwide valid relationship between precipitation and temperature at the ELA$_0$, as they are not based on the same methodology, and in particular because the precipitation figures for Alpine glaciers existing in both data sets differ significantly. However, it is a future aim to extend the range of validity of the relationship, towards both more continental and more maritime regions. We recommend the determination of monthly, seasonal or at least annual precipitation and temperature at the ELA$_0$ of all glaciers with mass balance measurements. The determination of these two parameters together with the calculation of the ELA should become a standard for mass balance measurements.

The qualitative check of the cAA with the 1973 Swiss Glacier Inventory and with LandsatTM images dating from the 1990s, as well as the resulting AAR of 0.67 (calculated from the modelled cAA and the measured glacier area of the 1970s), confirm the overall accuracy of the modelled rcELA$_0$ and cAA. This can be quantitatively validated using a classification error matrix (Lillesand and Kiefer, 1994: 612–618) as soon as glacier outlines for the entire Alps are available and the real Alpine AAR value(s) are known. In addition, distributed mass balance values can be used to quantify the deviations of the ltELA$_0$ from the rcELA$_0$.

5.2. Findings from the distributed modelling in comparison with other studies

For the first time, rcELA$_0$ and cAA have been modelled at reasonable spatial resolution over the entire European Alps. Qualitative comparisons show that the modelled cAA of the reference model run (1971–1990) corresponds well overall to the real accumulation areas of Alpine glaciers. The cAA is clearly underestimated only between the Silvretta group and the Bernina group, in the eastern part of Switzerland, or only exists when the lower confidence boundary, Eq. (3), is used instead of the reference run, based on Eq. (1). In this region, the AIG is above many peaks, i.e. there is no cAA. The reason for this is found in the underestimation of the precipitation in that region. To decrease the AIG at the location of Silvretta Glacier to the terrain (so that the AIG becomes a rcELA_0), an increase in annual precipitation of 757 mm (+53%) would be needed. To sustain a glacier at that location another decrease in the rcELA_0 by 200 m is required, which would result in a total precipitation increase of about 1800 mm (+125%). The probable cause of the underestimation of precipitation in the Silvretta region is the climatology by Frei and Schär (1998) and Schwarb et al. (2001). This is also supported by the fact that the Hydrological Atlas of Austria (2003) differs in this part by about 1600 mm from the precipitation climatology by Frei and Schär (1998) and Schwarb et al. (2001).

The sensitivity model runs show that a temperature change of ±1 °C would be compensated by a precipitation increase/decrease of 25%. The relative precipitation change corresponds to a mean absolute change over the greater Alpine region of about 300 mm. This is in agreement with Oerlemans (2001) and Braithwaite and Zhang (2000), who showed from mass balance modelling that a 25% increase in annual precipitation is typically needed to compensate for the mass loss due to a uniform warming of 1 °C. Kuhn (1981) calculated a rise of the ELA by 100 m if either the winter accumulation decreases by 400 mm or if the summer free air temperature increases by 0.8 °C. $\mathrm{MR}_{T-0.6}$ leads to an average ELA_0-decrease of 75 m over the entire Alps and of 65 m within the 1973 outlines of the Swiss Glacier Inventory larger than 1 km^2. This corresponds well to the reconstructed ELA rise of 69 m between 1850 and 1973 presented by Maisch et al. (2000). The cAA difference of −26% between $\mathrm{MR}_{T-0.6}$ and $\mathrm{MR}_{1971-1990}$ is somewhat lower than the loss in glacier area (35%) between 1850 and the 1970s as estimated from inventories by Zemp et al. (in press). This suggests that either the model is not perfectly able to reproduce the area loss between 1850 and the 1970s, or that a rise in temperature by 0.6 °C cannot completely explain the corresponding glacier shrinkage. In the $\mathrm{MR}_{T+3/P+10}$ the 10% increase in precipitation compensates for only a small amount of the ELA_0 rise caused by the temperature rise of 3 °C. The average rise of the rcELA_0 of 336 m clearly exceeds the upper boundary of the approximated confidence interval, based on Eq. (4). As a consequence, many areas become ice-free. The cAA of the reference run is reduced by 74%. This relative area loss clearly indicates the dimension of such a change. These results correspond well with other studies that are based on different methods. Maisch et al. (2000) quote a glacier area loss in Switzerland of 75% for an ELA rise of 300 m. Haeberli and Hoelzle (1995) applied a parameterisation scheme to glacier inventory data to simulate potential climate change effects on Alpine glaciers. They expect a reduction of glacier area and volume to a few percent of the values estimated for the 1850 glacierisation by the second half of the 21st century.

5.3. Potential applications

The presented approach is a valuable complement to current distributed mass balance models (e.g., Klok and Oerlemans, 2002; Paul et al., in press). Since the distributed ELA_0-model needs only a minimum of input data, it is able to compute the rcELA_0 and the cAA over the entire Alps. Distributed mass balance models are (currently) not able to be applied to such large areas, but can be used for individual glaciers or within glacierised catchments to account for further important components of the energy balance (e.g., solar radiation, albedo, turbulent fluxes, mass balance–altitude feedback) and local, topographic effects (e.g., shading, avalanches, snow drift).

Eq. (1) has the potential to estimate precipitation at glacier locations when the glacier ELA_0 and the temperature at the ELA_0 are known. The example of Silvretta Glacier demonstrates that the presented approach is a promising tool for estimating precipitation in high altitude terrain. However, in doing so, one has to take into account the uncertainties, both of the model and of the reconstruction of the ELA_0. In addition, Eq. (1) seems to be plausible beyond the range of the parameters on which it is based (Fig. 10), but a future aim must be to enlarge this data set on an identical methodological basis. Here, availability and quality of the precipitation data at glacier ELA_0 will be the decisive element.

Regional climate models (RCM) have a horizontal resolution of about 20–50 km. These models use static glacier masks which indicate whether a specific grid cell is covered completely by ice or is totally ice-free. These glacier masks remain constant throughout the model simulation. Potential changes in the ice cover, their feedback to the atmosphere and their effects (e.g., enhanced summer runoff due to glacier melting) are not accounted for. Current efforts are undertaken to represent mountain glaciers in RCMs on a subgrid scale (Kotlarski and Jacob, 2005). Here, information on altitude-area distribution of glaciers for the initialisation of time-slice experiments and for model validation is urgently needed. Hence, quality and resolution of the approach presented here would definitely be good enough to provide an approximation of glacier altitude-area distribution for past and present states as well as for future climate scenarios.

6. Conclusions

Based on direct glaciological mass balance measurements for the period of 1971–1990, this study presents an empirical relationship between 6-month summer temperature and annual precipitation at the glacier ELA_0. Using GIS techniques and a DEM (SRTM3), this relationship is applied for the first time to a distributed modelling of the $rcELA_0$ and the cAA over the entire Alps at a spatial resolution of 3 arc sec (approx. 100 m). It is shown that the altitude of the terrain is the decisive factor determining the spatial distribution of the $rcELA_0$, and hence also of the cAA, superimposed by the precipitation field and the temperature field at 2000 m a.s.l. The empirical relationship is able to explain about 50% of the variance in precipitation at the glacier ELA_0 by the variance in temperature at that location. Hence, the uncertainties in the prediction of precipitation based on a given temperature and the ELA_0 at a single location are rather large. Nevertheless, it represents a promising tool for the estimation of precipitation in high altitude terrain based on a large number of ELA_0 values. The empirical relationship is used as a boundary condition for the distributed modelling of the $rcELA_0$. The mean absolute difference between modelled $rcELA_0$ and measured ELA_0 amounts to about 70 m. The uncertainties of the $rcELA_0$ are restricted to its location, and affect the cAA only in flat terrain. Under the assumption that local, topographic effects and components of the energy balance not included in the model do not change, the distributed modelling approach presented here is an adequate tool for studies of glacier sensitivity to changes in temperature and/or precipitation.

A sensitivity study shows that a summer temperature deviation of ±1 °C results in an average deviation of the $rcELA_0$ of +137/−125 m. An annual precipitation deviation of ±25% (an order of magnitude of 300 mm) leads to a deviation of the $rcELA_0$ of −114/+157 m. A summer temperature decrease of 0.6 °C lowers the ELA_0 by 75 m on the Alpine average and by 65 m within the outlines (>1 km^2) of the 1973 Swiss Glacier Inventory. A summer temperature rise of 3 °C combined with an increase in annual precipitation of 10% results in an average rise in the $rcELA_0$ of 336 m and a reduction in the cAA in the order of 74%.

To enhance the statistical basis and to extend the range of validity of the empirical relationship, we recommend the determination of monthly, seasonal or at least annual precipitation and temperature at the ELA_0 of all glaciers with mass balance measurements. These two parameters together with the calculation of the ELA values should become a standard component of mass balance measurement series.

The presented approach is an excellent complement to distributed mass balance models. As the distributed $rcELA_0$-model requires only a minimum amount of input data to compute the $rcELA_0$ over the entire Alps, distributed mass balance models can then be used to account for further important components of the energy balance (e.g., solar radiation, albedo, turbulent fluxes, mass balance–altitude feedback) and local, topographic effects (e.g., shading, avalanches, snow drift) within individual catchments.

In conclusion, distributed modelling of the $rcELA_0$ can potentially contribute to the current efforts to include glacier altitude-area distribution of past, present and future glacier states in regional climate models.

Acknowledgements

We are indebted to the following institutes and organisations that placed their data at our disposal: Central Institute for Meteorology and Geodynamics in Vienna (temperature data), Institute for Atmospheric and Climate Science at the ETH in Zurich (precipitation data), Land Processes Distributed Active Archive Centre located at the U.S. Geological Survey in Sioux Falls (HYDRO1k), MeteoSwiss in Zurich (temperature data), National Aeronautics and Space Administration in Washington (SRTM3 and SRTM30), Swisstopo in Bern (DEM25L2), and World Glacier Monitoring Service in Zurich (mass balance measurements). Sincere thanks are given to the following colleagues for fruitful discussions and helpful comments in their research fields: Christoph Frei and Manfred Schwarb (precipitation and precipitation gradients in the European Alps), Sven Kotlarski (regional climate models), Frank Paul (DEM production and mass balance modelling), Max Maisch (Swiss glaciers), Nadine Salzman (climate modelling and interpolation techniques), Dominic Schuhmacher and the BABS group (statistical analysis). We gratefully acknowledge the constructive comments of Andrew G. Fountain, an anonymous referee and of the guest editor in charge Bruce Raup. Thanks go to Karen Hames and Susan Braun-Clarke for editing the English. The present study is funded mainly by the Swiss Federal Office of Education and Science (BBW-Contract 901.0498-2) within the EU programme ALP-IMP (Contract EVK2-CT-2002-00148).

References

Ahlmann, H.W., 1924. Le niveau de glaciation comme fonction de l'accumulation d'humidité sous forme solide. Geografisk Annaler VI, 223–272.

Ananicheva, M.D., Krenke, A.N., 2005. Evolution of climatic snow line and equilibrium line altitudes in the north-eastern Siberia mountains (20th century). Ice and Climate News 6, 3–6.

Auer, I., Böhm, R., Jurkovic, A., Orlik, A., Potzmann, R., Schöner, W., Ungersböck, M., Brunetti, M., Nanni, T., Maugeri, M., Briffa, K., Jones, P., Efthymiadis, D., Mestre, O., Moisselin, J.M., Begert, M., Brazdil, R., Bochnicek, O., Cegnar, T., Gajic-Capka, M., Zaninovic, K., Majstorovic, Z., Szalai, S., Szentimrey, T., 2005. A new instrumental precipitation data set in the greater alpine region for the period 1800–2002. International Journal of Climatology 25/2, 139–166.

Braithwaite, R.J., 1981. On glacier energy balance, ablation and air temperature. Journal of Glaciology 27 (97), 381–391.

Braithwaite, R.J., Zhang, Y., 2000. Sensitivity of mass balances of five Swiss glaciers to temperature changes assessed by tuning a degree-day model. Journal of Glaciology 46 (152), 7–14.

Frei, C., Schär, C., 1998. A precipitation climatology of the Alps from high-resolution rain-gauge observations. International Journal of Climatology 18, 873–900.

Greene, A.M., Broecker, W.S., Rind, D., 1999. Swiss glacier recession since the Little Ice Age: reconciliation with climate records. Geophysical Research Letters 26 (13), 1909–1912.

Greuell, W., 1989. Glaciers and climate: energy balance studies and numerical modelling of the historical front variations of the Hintereisferner (Austria). Ph.D. Thesis, Utrecht University, Netherlands, 178 pp.

Gross, G., Kerschner, H., Patzelt, G., 1978. Methodische Untersuchungen über die Schneegrenze in alpinen Gletschergebieten. Zeitschrift für Gletscherkunde und Glazialgeologie 12 (2), 223–251.

Haeberli, W., 1983. Permafrost–glacier Relationships in the Swiss Alps Today and in the Past. Proceedings of the Fourth International Conference on Permafrost, Fairbanks AK. National Academy of Sciences, Washington, D.C., pp. 415–420.

Haeberli, W., 2004. Glaciers and ice caps: historical background and strategies of world-wide monitoring. In: Bamber, J.L., Payne, A.J. (Eds.), Mass Balance of the Cryosphere. Cambridge University Press, Cambridge, pp. 559–578.

Haeberli, W., Hoelzle, M., 1995. Application of inventory data for estimating characteristics of and regional climate-change effects on mountain glaciers: a pilot study with the European Alps. Annals of Glaciology 21, 206–212.

Hoinkes, H.C., Steinacker, R., 1975. Zur Parametrisierung der Beziehung Klima-Gletscher. Rivista Italiana di Geofisica e Scienze Affini 1, 97–104 (Speciale).

Hydrological Atlas of Austria, 2003. Bundesministerium für Land-und Forstwirtschaft, Umwelt und Wasserwirtschaft. Österreichischer Kunst-und Kulturverlag, Wien, Plate, vol. 2.2.

IPCC, 2001. Climate change 2001: the scientific basis. Contribution of working group I to the Third Assessment Report of the Intergovernmental Panel on Climate Change. Cambridge University Press, Cambridge, UK, 881 pp.

IUGG(CCS)/UNEP/UNESCO/WMO, 2005. In: Haeberli, W., Noetzli, J., Zemp, M., Baumann, S., Frauenfelder, R., Hoelzle, M. (Eds.), Glacier Mass Balance Bulletin No. 8 (2002–2003). World Glacier Monitoring Service, Zurich, 100 pp.

Kääb, A., Paul, F., Maisch, M., Hoelzle, M., Haeberli, W., 2002. The new remote-sensing-derived Swiss Glacier Inventory: II. First results. Annals of Glaciology 34, 362–366.

Kerschner, H., 1985. Quantitative paleoclimatic inferences from late glacial snowline, timberline and rock glacier data, Tyrolean Alps, Austria. Zeitschrift für Gletscherkunde und Glazialgeologie 21, 363–369.

Kerschner, H., 1996. Multivariate statistical modelling of equilibrium line altitudes. Hintereisferner (Ötztal)-Stubacher Sonnblickkees (Hohe Tauern). Zeitschrift für Gletscherkunde und Glazialgeologie 32, 119–127.

Kerschner, H., 2002. Mountain glaciers as sources of palaeoclimatic information — an alpine perspective. WMO Bulletin 51 (1), 29–35.

Kerschner, H., Kaser, G., Sailer, R., 2000. Alpine Younger Dryas glaciers as palaeo-precipitation gauges. Annals of Glaciology 31, 80–84.

Klok, E.J., Oerlemans, J., 2002. Model study of the spatial distribution of the energy and mass balance of Morteratschgletscher, Switzerland. Journal of Glaciology 48 (163), 505–518.

Kotlarski, S., Jacob, D., 2005. Development of a subgrid scale parameterization of mountain glaciers for use in regional climate modelling. WGNE Blue Book, WMO, pp. 4–13.

Krenke, A.N., 1975. Climatic conditions of present-day glaciation in Soviet Central Asia. IAHS-AISH 104, 30–41.

Kuhn, M., 1981. Climate and glaciers. IAHS 131, 3–20.

Letréguilly, A., Reynaud, L., 1990. Space and time distribution of glacier mass-balance in the northern hemisphere. Arctic and Alpine Research 22 (1), 43–50.

Leysinger Vieli, G.J., Gudmundsson, G.H., 2004. On estimating length fluctuations of glaciers caused by changes in climatic forcing. Journal of Geophysical Research 109, F01007, doi:10.1029/2003JF000027.

Lie, O., Dahl, S.O., Nesje, A., 2003a. A theoretical approach to glacier equilibrium-line altitudes using meteorological data and glacier mass balance records from southern Norway. The Holocene 13.3, 365–372.

Lie, O., Dahl, S.O., Nesje, A., 2003b. Theoretical equilibrium-line altitudes and glacier buildup sensitivity in southern Norway based on meteorological data in Geographical Information System. The Holocene 13.3, 373–380.

Lillesand, T.M., Kiefer, R.W., 1994. Remote Sensing and Image Interpretation, 3rd edition. Wiley & Sons, Inc., New York, 750 pp.

Maisch, M., 1992. Die Gletscher Graubündens. Rekonstruktion und Auswertung der Gletscher und deren Veränderungen seit dem Hochstand von 1850 im Gebiet der östlichen Schweizer Alpen (Bündnerland und angrenzende Regionen). Teil A: Grundlagen-Analysen-Ergebnisse. Physische Geographie, vol. 33. Geographisches Institut der Universität Zürich, Zurich, 324 pp.

Maisch, M., Wipf, A., Denneler, B., Battaglia, J., Benz, C., 2000. Die Gletscher der Schweizer Alpen. Gletscherhochstand 1850, Aktuelle Vergletscherung, Gletscherschwund Szenarien, Schlussbericht NFP31, 2nd edition. VdF Hochschulverlag, Zurich, 373 pp.

OcCC, 2004. Klimaentwicklung in der Schweiz bis 2050. Ein kurzer Überblick. Studie im Rahmen des Forschungsprogramms Energiewirtschaftliche Grundlagen des Bundesamts für Energie BFE, durchgeführt durch das Organe consultatif pour le Changement Climatique (OcCC), Bern, 7 pp.

Oerlemans, J., 2001. Glaciers and Climate Change. A.A. Balkema Publishers, Lisse, 148 pp.

Ohmura, A., Kasser, P., Funk, M., 1992. Climate at the equilibrium line of glaciers. Journal of Glaciology 38, 397–411.

Oliver, M.A., Webster, R., 1990. Kriging: a method of interpolation for Geographical Information Systems. International Journal of Geographical Information Systems 4 (3), 313–332.

Paul, F., Kääb, A., Maisch, M., Kellenberger, T.W., Haeberli, W., 2002. The new remote-sensing-derived Swiss Glacier Inventory: I. methods. Annals of Glaciology 34, 355–361.

Paul, F., Machguth, H., Hoelzle, M., Salzmann, N., Haeberli, W., in press. Alpine-wide distributed glacier mass balance modelling: a tool for assessing future glacier change? In: Orlove, B., Wiegandt, E., Luckmann, B. (Eds.), The darkening peaks: Glacial retreat in scientific and social context. University of California Press.

Rabus, B., Eineder, M., Roth, A., Bamler, R., 2003. The shuttle radar topography mission — a new class of digital elevation models acquired by spaceborne radar. ISPRS Journal of Photogrammetry and Remote Sensing 57 (4), 241–262.

Schwarb, M., Daly, C., Frei, C., Schär, C., 2001. Mean annual and seasonal precipitation throughout the European Alps 1971–1990. Hydrological Atlas of Switzerland. Plates 2.6, 2.7.

Sevruk, B., 1985. Systematischer Niederschlagsfehler in der Schweiz. Beiträge zur Geologie der Schweiz. Hydrologie, vol. 31. Kuemmerly and Frey, Bern, pp. 65–75.

Shea, J.M., Marshall, S.J., Livingston, J.L., 2004. Glacier distributions and climate in the Canadian Rockies. Arctic, Antarctic and Alpine Research 36 (2), 272–279.

Shumsky, P.A., 1964. Principles of structural glaciology. Translated from the Russian by D. Kraus. Dover Publications, Inc., New York, 497 pp.

Watson, D.F., Philip, G.M., 1985. A refinement of inverse distance weighted interpolation. Geo-Processing 2, 315–327.

Zemp, M., Paul, F., Hoelzle, M., Haeberli, W., in press. Glacier fluctuations in the European Alps 1850–2000: an overview and spatio-temporal analysis of available data. In: Orlove, B., Wiegandt, E., Luckmann, B. (Eds.), The darkening peaks: Glacial retreat in scientific and social context. University of California Press.

Publication 11

Zemp, M., Haeberli, W., Hoelzle, M. & Paul, F. (2006). **Alpine glaciers to disappear within decades?** Geophysical Research Letters, 33, L13504, doi:10.1029/2006GL026319.

GEOPHYSICAL RESEARCH LETTERS, VOL. 33, L13504, doi:10.1029/2006GL026319, 2006

Click Here for Full Article

Alpine glaciers to disappear within decades?

Michael Zemp,[1] Wilfried Haeberli,[1] Martin Hoelzle,[1] and Frank Paul[1]

Received 21 March 2006; revised 11 May 2006; accepted 22 May 2006; published 15 July 2006.

[1] Past, present and potential future glacier cover in the entire European Alps has been assessed from an integrated approach, combining in-situ measurements, remote sensing techniques and numerical modeling for equilibrium line altitudes. Alpine glaciers lost 35% of their total area from 1850 until the 1970s, and almost 50% by 2000. Total glacier volume around 1850 is estimated at some 200 km^3 and is now close to one-third of this value. From the model experiment, we show that a 3°C warming of summer air temperature would reduce the currently existing Alpine glacier cover by some 80%, or up to 10% of the glacier extent of 1850. In the event of a 5°C temperature increase, the Alps would become almost completely ice-free. Annual precipitation changes of ±20% would modify such estimated percentages of remaining ice by a factor of less than two. **Citation:** Zemp, M., W. Haeberli, M. Hoelzle, and F. Paul (2006), Alpine glaciers to disappear within decades?, *Geophys. Res. Lett.*, *33*, L13504, doi:10.1029/2006GL026319.

1. Introduction

[2] Impacts on cold mountain ranges from ongoing climate change are especially pronounced in regions above the timberline where effects related to perennial surface ice reflect increasing atmosphere/earth energy fluxes with extraordinary clarity [*Royal Swedish Academy of Sciences*, 2002]. Many mountain ranges have lost a significant proportion of their glacierization during the past 150 years with strong acceleration occurring in the past two decades [e.g., *Haeberli et al.*, 2005a, 2005b]. The shrinking of mountain glaciers is indeed the most obvious indication in nature of fast if not accelerating climate change on a worldwide scale. The predicted global temperature increase [*Intergovernmental Panel on Climate Change (IPCC)*, 2001] is likely to induce dramatic scenarios of future glacier developments including complete deglaciation of entire mountain ranges. Such future scenarios of glacier vanishing have thus far not been assessed quantitatively from spatial climatologies on an Alpine-wide scale, but are likely to affect landscape appearance, slope stability, the water cycle, sediment loads in rivers and natural hazards far beyond the range of historical and Holocene variability [*Watson and Haeberli*, 2004; *Barnett et al.*, 2005].

[3] In this study we apply an integrated approach, combining in-situ measurements, remote sensing techniques and numerical modeling to the European Alps. These techniques allow to quantitatively assess past as well as potential evolutions of area and volume of a glacier ensemble within an entire mountain chain. Glacier cover in the entire European Alps has been computed for different climate-change scenarios using satellite-derived glacier changes and a digital terrain model (DTM) together with a distributed model for equilibrium line altitudes (ELA). We thereby demonstrate the possibility of fast glacier disappearance within the European Alps, as well as the potential of new technologies to use information from glacier monitoring in mountain regions for quantification of global climate-change scenarios (Figure S1[1]).

2. Glacier Fluctuations From 1850–2000

[4] Information on glacier fluctuations in the European Alps is available from earlier and recent glacier inventories [*Haeberli et al.*, 1989; *Maisch et al.*, 2000; *Kääb et al.*, 2002; *Paul et al.*, 2002] (Figure S2) together with data compilations on past glacier fluctuations [*Zemp et al.*, 2006a] (Figure S2). National glacier inventories in the 1970s yield a total glacier area of 2909 km^2 [*Haeberli et al.*, 1989]. During the mid-1970s, glacier mass balances were close to zero or slightly positive [*Patzelt*, 1985] (Figure S3), many shorter glacier tongues slightly re-advanced and, hence, most glaciers were probably quite close to equilibrium conditions. The fact that the time basis for the corresponding inventory data is not uniform (Austria 1969, France 1967–71, Germany 1975, Italy 1975–84 and Switzerland 1973, cf. *Zemp et al.* [2006a]), therefore, plays a minor role: the center point of the corresponding time interval is thus defined as 1975. Detailed reconstructions of glacier areas around AD 1850 – the maximum extent for most glaciers in the European Alps at the end of the Little Ice Age – are available for the Swiss [*Maisch et al.*, 2000] and Austrian Alps (unpublished). The latest glacier inventory data based on satellite images is again available for most of the Swiss Alps in 1998/99 [*Kääb et al.*, 2002; *Paul et al.*, 2002], hereafter attributed to the year 2000 for the sake of simplicity. The Alpine glacier area in 1850 and 2000 is extrapolated by applying relative area changes for individual glacier size classes from the Swiss Alps to the corresponding entire Alpine glacier sample from 1975 (Table S1). This extrapolation reveals an overall loss in Alpine glacier area of 35% from 1850 up until 1975 (−2.8% per decade) and almost 50% by 2000 (−3.3% per decade). The area reduction between 1975 and 2000 is about 22% (−8.8% per decade), mainly occurring after 1985 (i.e., −14.5% per decade) as glacier fluctuation measurements and satellite-derived data have clearly shown [*Paul et al.*, 2004; *Zemp et al.*, 2006a] (Figure S3). Disintegration and

[1]Glaciology and Geomorphodynamics Group, Department of Geography, University of Zurich, Zurich, Switzerland.

0094-8276/06/2006GL026319$05.00

[1]Auxiliary material is available at ftp://ftp.agu.org/apend/gl/2006gl026319.

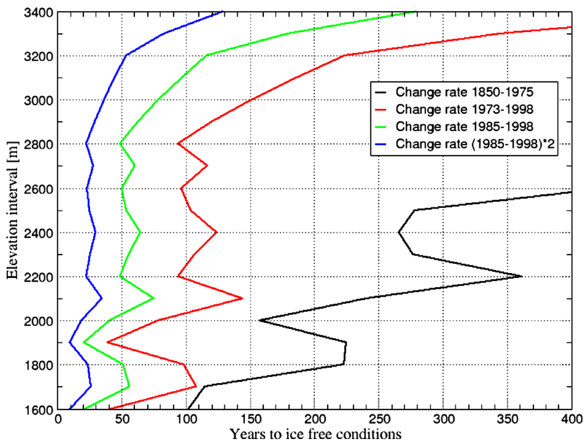

Figure 1. Years to ice-free elevation bands as obtained from the observed change in hypsography for two glacier samples (1850–1973 and 1973–1998, Figure S4). The glacier covered area in 1973 (1998) has been divided by the respective area loss per elevation band and multiplied with the number of years in the respective period (125, 25, 13, 6). Compared to the 1850–1973 period, there is not really a dependence of the change on elevation up to 2800 m a.s.l. for the more recent period.

'down-wasting' have been predominant processes of glacier decline during the most recent past [*Paul et al.*, 2004].

3. Assessment of Glacier Area Loss During the 21st Century

[5] Potential future area changes for the entire Alps are estimated by two independent methods. The first method is a purely empirical one that relates documented changes in glacier hypsography (i.e., rates of area change for altitudinal bands; see Figure S4) to scenarios of glacier shrinking, ranging from 'continued loss' (area reduction for the period 1850–1975), 'accelerated loss' (loss from 1975–2000), 'strongly accelerated loss' (period 1985–2000) and 'extreme loss' (using a doubled 1985–2000 loss rate). These scenarios cover the range of documented glacier shrinking rates and are related to a 20th-century warming of about 1°C in the European Alps [*Böhm et al.*, 2001]. The scenarios of future area losses (Figure 1) illustrate that the scenario of 'accelerated loss' would drastically reduce Alpine glacier areas within this century and that the scenario of extreme ice loss would cause most of the presently existing glaciers in the Alps to disappear within decades as large parts of the ice is located below 3000 m a.s.l. The 'extreme loss' scenario should be seen as an upper limit assumption but may not be unrealistic: hot-dry conditions like in the summer of 2003, which could occur at shorter and shorter intervals [*Schär et al.*, 2004] and involve strong reinforcing effects (albedo feedback, mass balance/altitude feedback, glacier down-wasting and collapse) could indeed soon bring about such a situation.

[6] The second method is based on the fact that, glacier health is primarily influenced by air temperature, while precipitation is the second most important climatic factor affecting their condition [*Kuhn*, 1981; *Oerlemans*, 2001]. The ELA on a glacier is a theoretical line which defines the altitude at which annual accumulation equals ablation. It represents the lowest boundary of climatic glacierization – that is, where the glacierization can begin. Hence, the second approach is a statistically calibrated and distributed model of ELA after *Lie et al.* [2003] that utilizes an empirical relation between 6-month summer air temperature (T_{A-S}, in degree Celsius) and annual precipitation (P_a, in millimeter) at the steady-state ELA (ELA_0) [*Zemp et al.*, 2006b]:

$$P_a = 1773 \cdot e^{0.2429 \cdot T_{A-S}}$$

The relation is obtained from long-term mass balance data from 14 Alpine glaciers [*Haeberli et al.*, 2005a] in combination with gridded precipitation [*Frei and Schär*, 1998; *Schwarb et al.*, 2001] and temperature (interpolated from twelve high-altitude weather stations, cf. [*Zemp et al.*, 2006b]) climatologies of the period 1971–1990 and a DTM of 100 m cell size, resampled from the DTM of the Shuttle Radar Topography Mission [cf. *Rabus et al.*, 2003]. Its application to the entire European Alps enabled distributed modeling of the regional climatic ELA for zero mass balance ($rcELA_0$) and the corresponding climatic accumulation area (cAA) above it (see Figure S5 for a diagram explaining this concept and *Zemp et al.* [2006b] for methodological details). The accumulation area over the entire Alps obtained from the reference model run (1971–1990) is 1950 km^2 and agrees well with accumulation areas of mapped glaciers (Figure S6).

[7] The impact on glacier areas as related to scenarios of temperature and precipitation change is illustrated in Figure 2. Atmospheric warming of 3°C in summer accompanied by an increase of 10% in annual precipitation would,

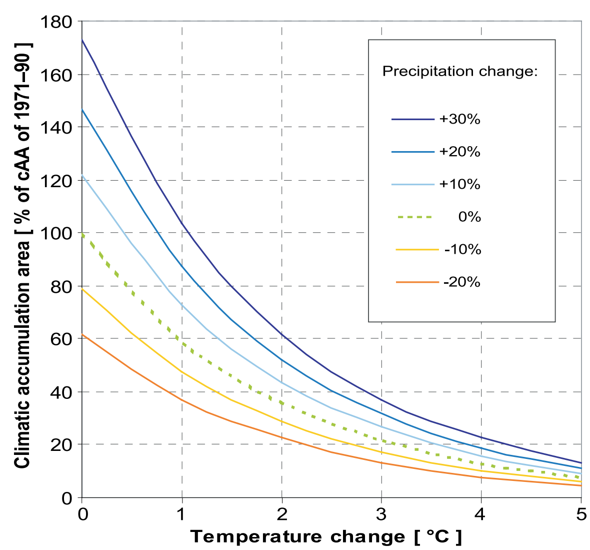

Figure 2. Modeled climatic accumulation area (cAA) according to changes in 6-month summer temperature and/or annual precipitation. The total of 100% refers to the cAA of the reference model run (1971–1990) and amounts to 1950 km^2. The changes in temperature and precipitation cover the range of the IPCC-scenarios [*IPCC*, 2001]. The dotted line refers to pure summer temperature changes (order of the lines correspond to legend).

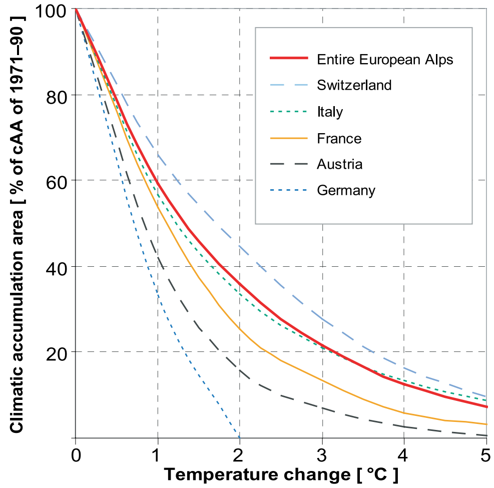

Figure 3. Modeled remains of Alpine glacierization as a consequence of a 1–5°C warming of the 6-month summer temperature. The total of 100% refers to the cAA of the reference model run (1971–1990) and amounts to 1950 km^2 for the entire European Alps. The 100%-marks of the other lines refer to the fraction of glacierization of the corresponding Alpine country.

for instance, raise the rcELA$_0$ by 340 m and reduce the cAA by 75% compared to the 1971–1990 reference period. Depending on the climate scenario chosen, this could take place toward the middle or the end of this century [*IPCC*, 2001]. Due to the strong warming in the past two decades, more than one-third of this glacier area reduction has already been taking place [*Paul et al.*, 2004; *Zemp et al.*, 2006a]. An increase in summer air temperature of 5°C would reduce the glacier cover by more than 90% as compared to the reference period. Precipitation changes of ±20% would modify such estimated percentages of remaining ice by a factor of less than two. Many individual mountain ranges within the Alps would become ice-free under such conditions and only rather small glacier remnants would persist in a few regions with the highest mountain peaks (Figure 3 and Figure S6). Because Alpine glaciers were close to equilibrium conditions during the reference period (1971–1990), the model is able to compute plausible rises of the rcELA$_0$ and corresponding cAA for the range of climate change scenarios for the 21st century. Present ablation areas, however, will respond with a certain delay to such fast changes and glacier mass balance will be far away from steady-state conditions. The presented results confirm earlier (independent) estimates from modeling of statistical glacier data [*Haeberli and Hoelzle*, 1995; *Maisch et al.*, 2000] and show that the calculation is robust.

4. Estimations of Past, Present, and Future Ice Volumes

[8] Changes in glacier volume are calculated by multiplying representative mass balance values with the average surface area (the mean of the areas at the beginning and end) of a given time period. Mean mass balance of nine Alpine glaciers between 1975 and 2000 was almost −0.5 m water equivalent (w.e.) per year (Figure S3). This is about twice the loss rate reconstructed from cumulative length change for the time period after 1850 [*Haeberli and Hoelzle*, 1995; *Hoelzle et al.*, 2003; *Steiner et al.*, 2005] and characteristic long-term mass changes during the past 2000 years [*Haeberli and Holzhauser*, 2003]. The cumulative balance of −12 m w.e. over a mean glacier area of 2590 km^2 during the same time interval (1975–2000) indicates a lower limit of the corresponding volume loss of 30 km^3. As average slope and ELA have increased, but glacier size (as well as altitudinal extent, mass flux and driving stress) decreased, the percentage of volume loss must be even greater than the calculated area loss of 22% (see remarks on volume estimations in auxiliary material). Based on this assumption, the estimated volume loss (30 km^3) corresponds to 25–30% of the total Alpine ice volume in the 1970s. This estimates show that the glaciers in the Alps have lost an average of 1% of their volume per year since 1975. On the same basis, total Alpine ice volumes can be estimated roughly as 105 ± 15 km^3 in 1975, and 75 ±10 km^3 at the turn of the century [*Paul et al.*, 2004], that is, considerably lower than the 130/100 km^3 estimated earlier [*Haeberli and Hoelzle*, 1995]. Total glacier volume for the end of the Little Ice Age (around 1850) with an extrapolated total glacierized area of 4475 km^2 is estimated at some 200 km^3 or more, and is now close to one-third of this value.

[9] Mean ice depth over the entire remaining glacier area of the Alps, calculated as the quotient of ice volume and area in 2000, is only about 30–35 meters. The average mass balance of −2.5 m w.e. in the extreme year 2003, therefore, eliminated an estimated 8% of the remaining Alpine ice volume within one single year [*Haeberli et al.*, 2005a; *Zemp et al.*, 2005]. The following year 2004 with an average mass balance of −1 m w.e. reduced an additional 3%, leading to about 10% volume loss in only two years. Extremely hot and dry summers such as 2003 thus not only induce strong positive feedbacks, but also eliminate increasing percentages of shrinking total ice volume. It is likely that five rather than ten repetitions within the coming decades of conditions as in 2003, would bring out this scenario of widely deglaciated Alps. As 90% of all Alpine glaciers are smaller than 1 km^2, the probability that most glaciers in the European Alps will disappear within the coming decades (Figure 3) is indeed not insignificant. The few largest valley glaciers with maximum ice thicknesses of several hundred meters will be able to resist such warming effect for somewhat longer. However, reinforcing mechanisms such as the mass balance/altitude feedback or the development of glacier lakes will also increasingly enhance their wasting.

5. Discussion and Conclusions

[10] The major sources of error and corresponding consequences for the three methods (a: scenarios for changes in glacier hypsography, b: distributed ELA model, c: volume estimations) are: for a), the representativity of the analyzed sub samples for the entire Alpine glacierization, which might bias the rates of ice loss due to regional peculiarities, for b), the neglect of topographic effects (e.g., snow drift, avalanches, radiation) leading to differences between the modeled rcELA$_0$ and the local topographic ELA$_0$, and the assumption of a constant accumulation area ratio, resulting in an uncertainty in the extrapolation of glacier changes

from the modeled cAA to the total glacier area, and for c) the representativity of average reconstructed/measured mass balance values from the used glacier samples for the entire Alpine glacierization in 1850/1975/2000, resulting in estimated thickness changes biased by mid-size glaciers [cf. *Zemp et al.*, 2006a].

[11] Glaciers in the European Alps lost almost 50% in area from 1850 to 2000. The area reduction between the 1970s and 2000 is about 22%, mainly occurring after 1985. Total glacier volume around 1850 is estimated at some 200 km^3 and is now close to one-third of this value. From the model experiment, we show that the probability of Alpine glaciers disappearing within the coming decades is far from slight.

[12] Modern strategies of glacier observations established within international monitoring programs make use of fast-developing new technologies and relate them to traditional approaches in order to apply integrated, multilevel concepts [*Haeberli*, 2004]. The combination of in-situ measurements with remote sensing, digital terrain information and numerical models thereby allows for comprehensive views by assimilating individual observational components over different scales in space and time. Glacier changes as a function of climate change are not only easily observed, they are also comprehensible, in their basic physical principles, to a large public. By simply looking at the evolution of glaciers in the mountain ranges of the world, coming generations will be able to define and to physically see whether and at what rate climate change has taken place.

[13] **Acknowledgments.** We are indebted to the following institutes and organizations that placed their data at our disposal: Central Institute for Meteorology and Geodynamics in Vienna (temperature data), Institute for Atmospheric and Climate Science at the ETH in Zurich (precipitation data), MeteoSwiss in Zurich (temperature data), National Aeronautics and Space Administration in Washington (SRTM3 and SRTM30), Swisstopo (DEM25), National Point of Contact (satellite data) and World Glacier Monitoring Service in Zurich (glacier data). We thank all national correspondents, principal investigators and contributing institutes who have been providing the World Glacier Monitoring Service with data for many years! Thanks go to Susan Braun-Clarke for editing the English. We gratefully acknowledge the constructive comments of the two anonymous referees and of the editor in charge, James E. Saiers. This study is funded mainly by the Swiss Federal Office of Education and Science (BBW-Contract 901.0498-2) within the EU program ALP-IMP (Contract EVK2-CT-2002-00148).

References

Barnett, T. B., J. C. Adam, and D. P. Lettenmaier (2005), Potential impacts of a warming climate on water availability in snow-dominated regions, *Nature*, *438*, 303–309.
Böhm, R., I. Auer, M. Brunetti, M. Maugeri, T. Nanni, and W. Schöner (2001), Regional temperature variability in the European Alps: 1760–1998 from homogenized instrumental time series, *Int. J. Climatol.*, *21*, 1779–1801.
Frei, C., and C. Schär (1998), A precipitation climatology of the Alps from high-resolution rain-gauge observations, *Int. J. Climatol.*, *18*, 873–900.
Haeberli, W. (2004), Glaciers and ice caps: Historical background and strategies of world-wide monitoring, in *Mass Balance of the Cryosphere*, edited by J. L. Bamber and A. J. Payne, pp. 559–578, Cambridge Univ. Press, New York.
Haeberli, W., and M. Hoelzle (1995), Application of inventory data for estimating characteristics of and regional climate-change effects on mountain glaciers: A pilot study with the European Alps, *Ann. Glaciol.*, *21*, 206–212.
Haeberli, W., and H. Holzhauser (2003), Alpine glacier mass changes during the past two millennia, *Pages News*, *11*(1), 13–15.
Haeberli, W., H. Bösch, K. Scherler, G. Østrem, and C. C. Wallén (Eds.) (1989), *World Glacier Inventory–Status 1988*, 458 pp., Int. Assoc. of Hydrol. Sci., Int. Comm. on Snow and Ice, Nairobi.
Haeberli, W., , J. Noetzli, M. Zemp, S. Baumann, R. Frauenfelder, and M. Hoelzle (Eds.) (2005a), Glacier mass balance bulletin, *Bull. 8 (2002–2003)*, 100 pp., World Glacier Monit. Serv., Zurich, Switzerland.
Haeberli, W., M. Zemp, R. Frauenfelder, M. Hoelzle, and A. Kääb (Eds.) (2005b), Fluctuations of glaciers 1995–2000, Volume VIII, report, 288 pp., World Glacier Monit. Serv., Zurich, Switzerland.
Hoelzle, M., W. Haeberli, M. Dischl, and W. Peschke (2003), Secular glacier mass balances derived from cumulative glacier length changes, *Global Planet. Change*, *36*, 295–306.
Intergovernemental Panel on Climate Change (IPCC) (2001), *Climate Change 2001: The Scientific Basis: Contribution of Working Group I to the Third Assessment Report of the Intergovernmental Panel on Climate Change*, edited by J. T. Houghton et al., 881 pp., Cambridge Univ. Press, New York.
Kääb, A., F. Paul, M. Maisch, H. Hoelzle, and W. Haeberli (2002), The new remote-sensing-derived Swiss Glacier Inventory: II. First results, *Ann. Glaciol.*, *34*, 362–366.
Kuhn, M. (1981), Climate and glaciers, *Int. Assoc. Hydrol. Sci. Publ. 131*, pp. 3–20, Int. Assoc. Hydrol. Sci., Geneva, Switzerland.
Lie, O., S. O. Dahl, and A. Nesje (2003), A theoretical approach to glacier equilibrium-line altitudes using meteorological data and glacier mass balance records from southern Norway, *Holocene*, *13*(3), 365–372.
Maisch, M., A. Wipf, B. Denneler, J. Battaglia, and C. Benz (Eds.) (2000), *Die Gletscher der Schweizer Alpen. Gletscherhochstand 1850, Aktuelle Vergletscherung, Gletscherschwund Szenarien*, 2nd ed., 373 pp., VdF Hochschulverlag, Zurich, Switzerland.
Oerlemans, J. (2001), *Glaciers and climate change*, 148 pp., A. A. Balkema Publishers, Brookfield, Vt.
Patzelt, G. (1985), The period of glacier advances in the Alps, 1965 to 1980, *Z. Gletscherkd. Glazialgeol.*, *21*, 403–407.
Paul, F., A. Kääb, M. Maisch, T. W. Kellenberger, and W. Haeberli (2002), The new remote-sensing-derived Swiss Glacier Inventory: I. Methods, *Ann. Glaciol.*, *34*, 355–361.
Paul, F., A. Kääb, M. Maisch, T. Kellenberger, and W. Haeberli (2004), Rapid disintegration of Alpine glaciers observed with satellite data, *Geophys. Res. Lett.*, *31*, L21402, doi:10.1029/2004GL020816.
Rabus, B., M. Eineder, A. Roth, and R. Bamler (2003), The shuttle radar topography mission–a new class of digital elevation models acquired by spaceborne radar, *ISPRS J. Photogramm. Remote Sens.*, *57*, 241–262.
Royal Swedish Academy of Sciences (2002), The Abisko Agenda: Research for mountain area development, *Ambio. Spec. Rep. 11*, 105 pp., Stockholm, Sweden.
Schär, C., P. L. Vidale, D. Lüthi, C. Frei, C. Häberli, M. A. Liniger, and C. Appenzeller (2004), The role of increasing temperature variability in European summer heatwaves, *Nature*, *427*, 332–336.
Schwarb, M., C. Daly, C. Frei, and C. Schär (2001), Mean annual precipitation throughout the European Alps 1971–1990, *Hydrol. Atlas of Switzerland plate 2.6*, Geogr. Inst. der Univ. Bern, Bern.
Steiner, D., A. Walter, and H. J. Zumbühl (2005), The application of a nonlinear backpropagation neural network to study the mass balance of the Great Aletsch Glacier, *J. Glaciol.*, *51*, 131–324.
Watson, R. T., and W. Haeberli (2004), Environmental threats, mitigation strategies and high-mountain areas, *Ambio*, *13*, 2–10.
Zemp, M., R. Frauenfelder, W. Haeberli, and M. Hoelzle (2005), Worldwide glacier mass balance measurements: General trends and first results of the extraordinary year 2003 in Central Europe, *Data Glaciol. Stud.*, *99*, 3–12.
Zemp, M., F. Paul, M. Hoelzle, and W. Haeberli (2006a), Glacier fluctuations in the European Alps 1850–2000: an overview and spatiotemporal analysis of available data, in *The Darkening Peaks: Glacial Retreat in Scientific and Social Context*, edited by B. Orlove, E. Wiegandt, and B. Luckman, Univ. Calif. Press, Berkeley.
Zemp, M., M. Hoelzle, and W. Haeberli (2006b), Distributed modeling of the regional climatic equilibrium line altitude of glaciers in the European Alps, *Global Plant. Change*, special issue on climate change impacts on glaciers and permafrost.

W. Haeberli, M. Hoelzle, F. Paul, and M. Zemp, Glaciology and Geomorphodynamics Group, Department of Geography, University of Zurich, Winterthurerstr. 190, CH-8057 Zurich, Switzerland. (mzemp@geo.unizh.ch)

Publication 12

Zemp, M., Andreassen, L.M., Braun, L., Chueca, J., Fischer, A., Hagen, J.O., Hoelzle, M., Jansson, P., Kohler, J., Meneghel, M., Stastny, P. & Vincent, C. (2010). **Glacier and Ice Caps**. In: Voigt, T., Füssel, H.-M., Gärtner-Roer, I., Huggel, C., Marty, C. & **Zemp, M.** (eds.). **Impacts of climate change on snow, ice, and permafrost in Europe: Observed trends, future projections, and socio-economic relevance.** European Topic Centre on Air and Climate Change, Technical Paper, 2010 (13), 46-65.

Impacts of climate change on snow, ice, and permafrost in Europe: Observed trends, future projections, and socio-economic relevance

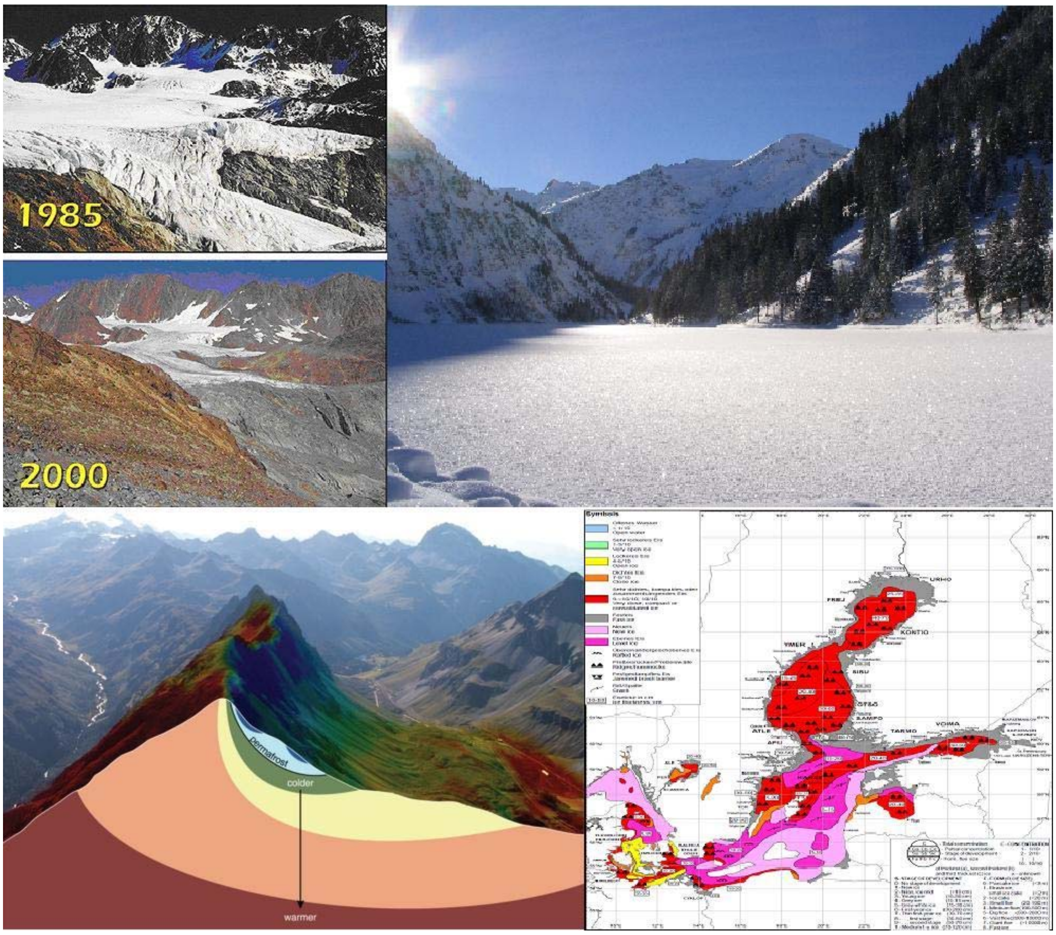

ETC/ACC Technical Paper 2010/13
December 2010

Thomas Voigt, Hans-Martin Füssel, Isabelle Gärtner-Roer, Christian Huggel, Christoph Marty, Michael Zemp

European Topic Centre on Air and Climate Change

The European Topic Centre on Air and Climate Change (ETC/ACC)
is a consortium of European institutes under contract of the European Environment Agency
PBL UBA-D UBA-V NILU AEAT AUTh CHMI MET.NO ÖKO TNO REC

4.2 Glaciers and ice caps

Key messages

- Due to their proximity to melting conditions, glaciers are one of the most reliable natural indicators for climatic changes.
- In the second half of the 20th century, European glaciers and ice caps (outside Greenland) covered a total of about 54,000 km^2 distributed in Svalbard (68%), Iceland (21%), Scandinavian Peninsula (6%), Alps (5%), and the Pyrenees (<1%).
- The total volume of glaciers can only be roughly approximated. Current estimates based on the above (area) data come to an ice volume of about 15,500 km^3. This corresponds to a potential sea level rise of about 40 mm, of which the vast majority is located in Svalbard (26 mm) and Iceland (12 mm).
- The Little Ice Age moraines that formed between the mid 18th and the mid 19th century mark the maximum glacier extents during the past 11,000 years (the Holocene).
- The strong centennial retreat of glaciers from these Little Ice Age moraines is well documented and apparent in all European regions. In some regions, there have been intermittent periods of reduced glacier melting or even of glacier re-advance such as in the late 1970s in the Alps and Iceland and in the 1990s in coastal Scandinavia.
- Glacier melt seems to be strongest in the European Alps. There, more than half of the ice-covered area and probably two third of the ice volume disappeared since 1850; the average annual ice thickness loss since 2000 has been above one meter.
- European glacier changes since the Little Ice Age have been driven mainly by increased summer air temperatures with secondary effects from variations in winter precipitation. Both are influenced by atmospheric and oceanic circulation patterns. Further factors for increasingly negative mass balances in most regions are most probably the (re-) brightening of the atmosphere, extension of the ablation period, and reinforcing effects such as dust-related darkening or melt-induced elevation lowering of glacier surfaces.
- Climate change scenarios for the 21st century suggest a continued increase in global mean air temperature by 1.4–5.8°C and 2.0–6.3°C in Europe (without policy measures). Corresponding projections of precipitation patterns show a more varied picture with seasonal change rates of 1-5% per decade. Under such scenarios, glaciers will continue to melt and may totally disappear in some mountain ranges in the coming decades.
- Available numerical model experiments of glaciers in Iceland, Scandinavia and in the Alps indicate that a further increase of regional summer air temperature by 2° C will reduce glacier area and volume by half or more of their present extents. The impact of a 1°C warming could only be offset if precipitation would increase by 20% or more. Potential re-growth of glaciers in these regions would require decades of cooler and wetter conditions.
- Glaciers changes in Europe already influence the local hazard situation, the runoff from alpine catchments, tourism and landscape, and – to a limited extent – global sea level. The anticipated marked changes for the 21st century might lead to impacts that are unprecedented during the last 11,000 years (the Holocene).

Key graphs

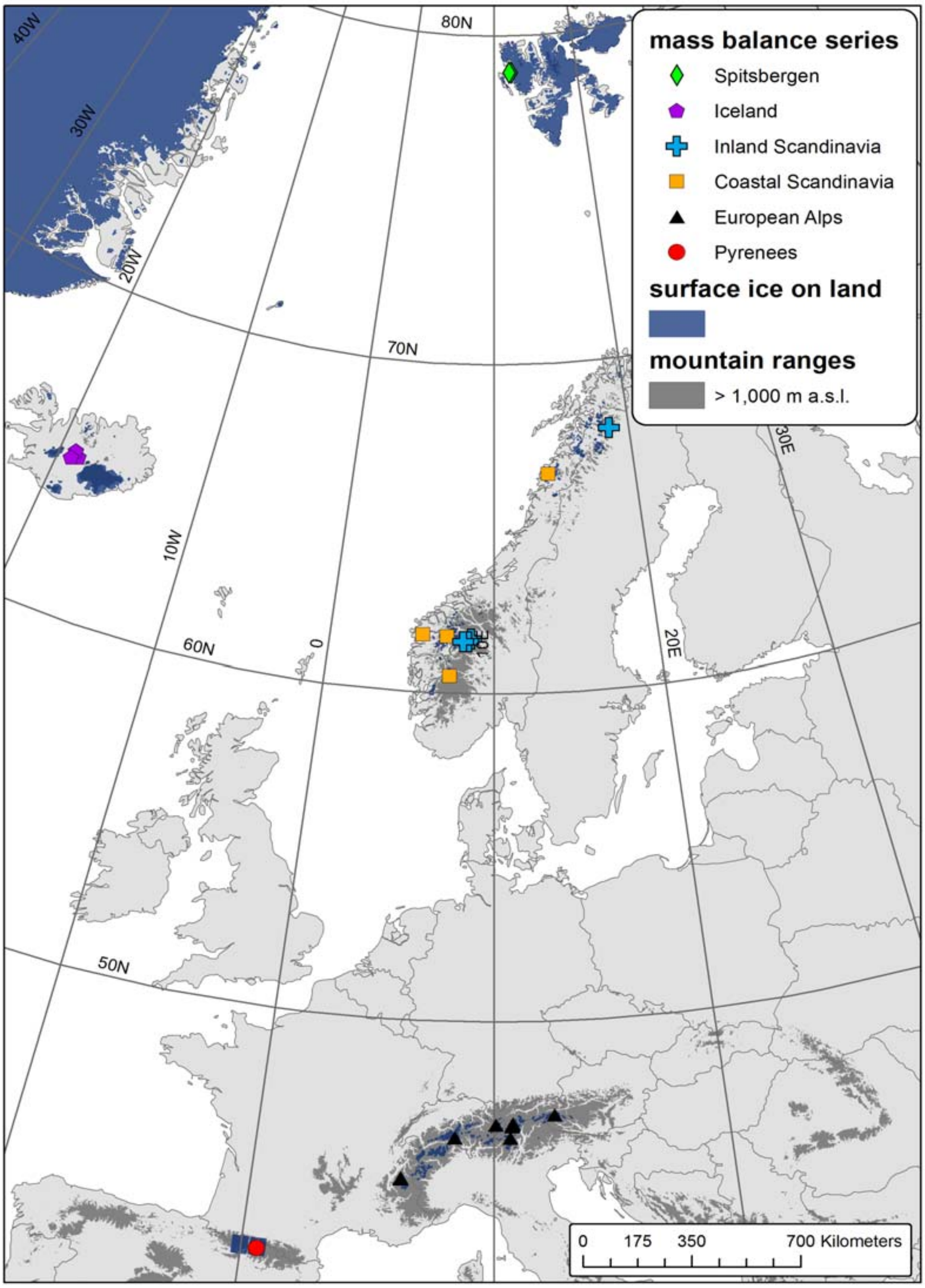

Figure 4.5: Glacier distribution in Europe. The map shows the distribution of glacier and ice caps as well as the Greenland Ice Sheet (upper left corner) together with the locations of long-term glacier mass balance observation programs (cf. Fig. 4.6). Note that the location of glaciers in the Pyrenees is marked with oversized squares which do not represent their real extents.

Source : Glacier information from the World Glacier Monitoring Service; country outlines and surface ice on land cover from ESRI's Digital Chart of the World.

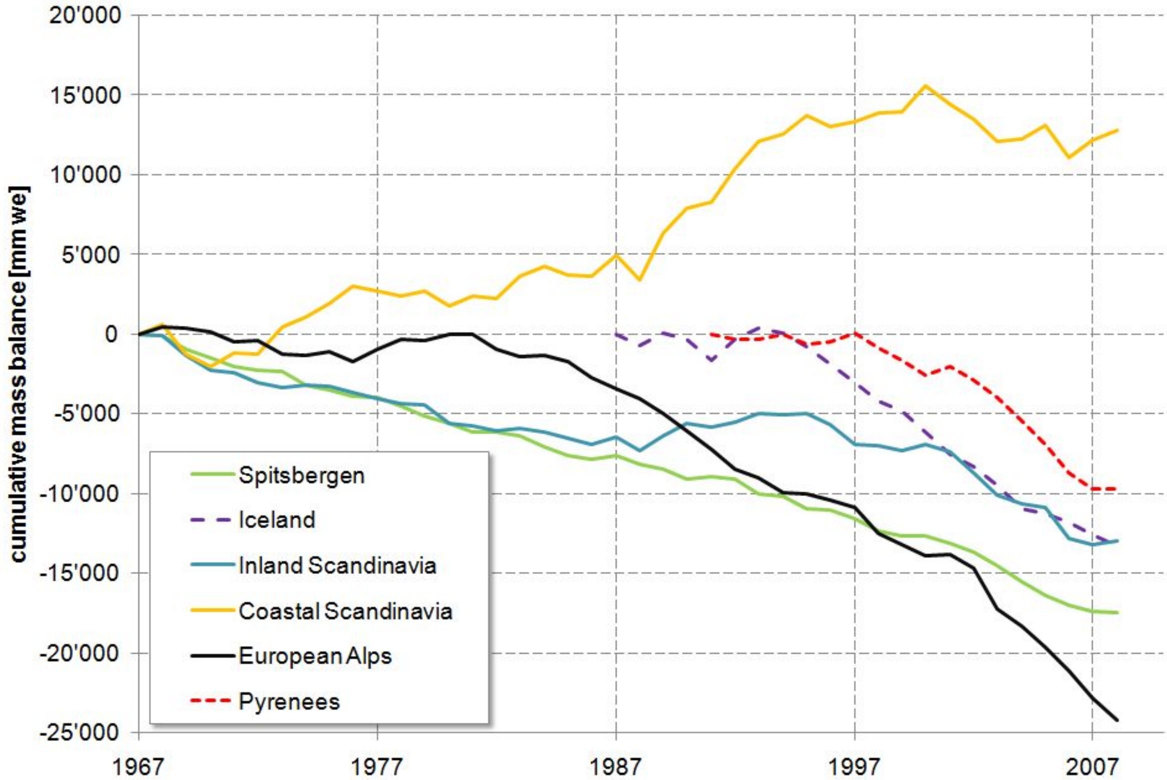

Figure 4.6: Glacier mass balance results in Europe. Long-term and continuous mass balance series are an excellent index of regional glacier changes. The absolute values might, however, not be representative for the total ice changes of the corresponding region. The index shows a cumulative loss in ice thickness from 1967 to 2008 in all regions except for coastal Scandinavia where glaciers gained mass until 2000. Note that data series from Iceland and the Pyrenees start later and, hence, their absolute values cannot directly be compared to the ones of the other series. The graph is based on data from the following glaciers: Spitsbergen: Midtre Lovénbreen, Austre Brøgerbreen; Iceland Hofsjökull E, N, ans SW; Inland Scandinavia: Gråsubreen, Hellstugubreen, Storbreen, Storglaciären; Coastal Scandinavia: Nigardsbreen, Engabreen, Hardangerjøkullen, Ålfotbreen; European Alps: Gries, Silvretta, Vernagtferner, Hintereisferner, Kesselwandferner, Sonnblickkees, Caresèr, Saint Sorlin, Sarennes; Pyrennes: Maladeta.

Source : World Glacier Monitoring Service.

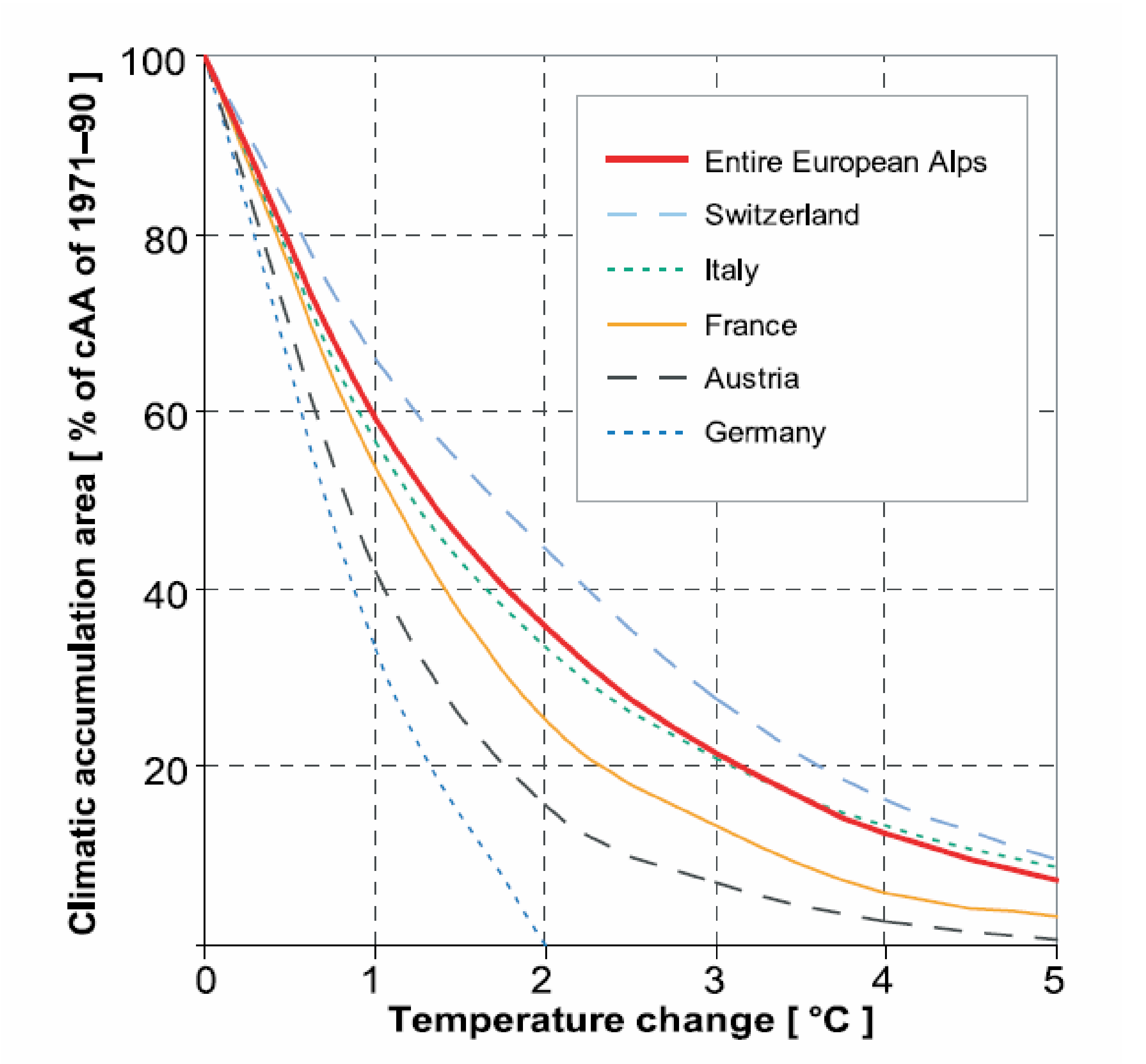

Figure 4.7: Alpine glacier scenarios for 21st century. The figure shows the estimated relative changes in glacier extent compared to the reference period (1971–90) for an increase in regional summer air temperature.

Source : Zemp et al. (2006).

Relevance

Glaciers are an inherent component of the culture, landscape and environment in Alpine and Nordic countries of Europe. They represent a unique resource of fresh water for domestic, agricultural and industrial use, an important economic component of tourism and hydro-power production, and a potential source of serious natural hazards. Glacier melt during summer is an important component of the hydrological water cycle in mountain areas and contributes to the discharge of river systems (BOX 4.2). In today's Norway, 15% of the used runoff comes from glacierized basins and 98% per cent of the electricity is generated by hydropower production (Andreassen et al. 2005). Globally, glaciers are one of the main contributors of present sea level rise. Their contribution has more than doubled over the past decades and is currently estimated to about one millimetre per year (Meier et al. 2007, Kaser et al. 2009). Moreover, glacier changes are recognized as high-confident indicators and as valuable elements in early detection strategies within the international climate monitoring programmes (GCOS 2004, GTOS 2008).

Box 4.1: Glacier contribution to the Alpine runoff

The Alps are widely known as the 'water towers' of Europe. The capacity to export water to the adjoining lowlands of its rivers is more dependable and specific runoff is higher than that of similar-sized lowland basins (Weber et al., 2010). Thereby, glacier ice-melt further enhances water yield from high mountain regions during dry and hot summer periods. Since 1973, the runoff from Vernagtferner in the Austrian Oetz Valley has been recorded continuously at the gauging station Vernagtbach at 2,635 m a.s.l. The runoff from this head watershed with an area of 11.4 km² and a present glacier area fraction of about 70% can be set in relation to basin precipitation and change in glacier storage. A recent analysis by Weber et al. (in press) shows that for the past decade that in glacierized head watersheds there is about an equal amount of runoff originating from ice-melt, snow-melt and rain (about 33% each). Further downstream the portion of ice-melt decreases sharply with the effect that ultimately 2% of annual runoff is of glacial origin in Passau/Achleiten (basin area of about 77,000 km², current glaciation 0.5 %), and about three quarter originates from rain and one quarter from snowmelt. Using climate scenarios from regional climate models (SRES A1B, cf. BOX 2.2) revealed that the contribution from ice-melt in the glaciated head watersheds will decrease sharply after some decades, the proportion of snowmelt will be about the same, and rain contribution will increase to about half of the annual runoff. In Passau, the portion from ice-melt will be negligible, and 80% of runoff will be from rain and 20% from snowmelt. With the anticipated warming over the whole year and the drying out of the summer season the Alps' capacity to export water will diminish, and water availability will be reduced mainly through the loss of summer precipitation and increased evaporation, and not so much due to the loss of glacier-melt.

Data compilation and process understanding

The observation of glaciers has been internationally coordinated since 1894 and is today lead by the World Glacier Monitoring Service (WGMS 2008; BOX 4.3). The fluctuations of a glacier, which is not influenced by thick debris covers, calving or surge instabilities, are a reaction to climatic forcing. Thereby, the glacier length change (i.e., the advance or retreat) is a delayed reaction to climatic changes over the past years to decades, or even centuries. The glacier mass balance (i.e., the change in thickness) is a more direct and un-delayed reaction to the annual atmospheric conditions (Haeberli and Hoelzle 1995). The mass balance variability of glaciers is well correlated over distances of several hundred kilometres and with air temperature (Lliboutry 1974, Letréguilly and Reynaud 1990, Schöner et al. 2000, Greene 2005). Glacier mass balance change provides an integrative climatic signal, however, and the quantitative attribution of the forcing to individual meteorological parameters is not straight forward. The energy and mass balance at the glacier surface is influenced by changes in atmospheric conditions (e.g., solar radiation, air temperature, precipitation, wind, cloudiness). Air temperature thereby plays a predominant role as it is related to the radiation balance, turbulent heat exchange and solid/liquid precipitation ratio (Kuhn 1981, Ohmura 2001). The climatic sensitivity of a glacier not only depends on regional climate variability but also on local topographic effects and the distribution of the glacier area with elevation, which can result in two adjacent glaciers featuring different specific mass balance responses (Kuhn et al. 1985).

Box 4.2: International Glacier Monitoring
Glacier research and monitoring have a long tradition in Europe. Already in 1894, the internationally coordinated collection of information about ongoing glacier changes was initiated at the 6th International Geological Congress in Zurich, Switzerland. Today, the World Glacier Monitoring Service (www.wgms.ch), in close collaboration with the US National Snow and Ice Data Center (www.nsidc.org) and the Global Land Ice Measurements from Space initiative (www.glims.org), continues the compilation and dissemination of standardised data and information on distribution and ongoing changes in glaciers worldwide (WGMS 2008). Together, these three bodies run the Global Terrestrial Network of Glaciers (www.gtn-g.org) which aims to combine field observations with remotely sensed data, process understanding with global coverage, and traditional measurements with new technologies within the global climate observation systems as a contribution to the United Nations Framework Convention on Climate Change (www.unfccc.int).
(details of the World Glacier Monitoring Service and its National Correspondents in Europe are given in Annex 6.4.).

Past Trends

20th century distribution in Europe

In Europe[1], glaciers (outside Greenland) are found on Svalbard, in Iceland, on the Scandinavian Peninsula, in the Alps, and in the Pyrenees. A few small glacierets and perennial snow fields are also found in the Apennines, the Tatras between Slovakia and Poland, and in the mountains of Albania, Bulgaria, and Slovenia. For the second half of the 20th century, an almost complete detailed inventory of Europe's glaciers and ice caps was compiled mainly based on topographic maps and aerial photographs for the World Glacier Inventory (WGMS 1989, Table 4.1). The largest ice masses are found on the Svalbard Archipelago which is situated in the Arctic Ocean north of mainland Europe. Its topography is more than half covered by ice (36,612 km^2), and is characterized by plateau mountains and fjords. Iceland is covered by 15 major ice caps and a few hundred other glaciers with a total area of 11,260 km^2. Icelandic ice caps and glaciers are often influenced by volcanic activities. Due to the combination of high latitude and the moisture from the North Atlantic, many glaciers and ice caps with an overall area of 3,058 km^2 developed on the Scandinavian Peninsula, all within 180 km of the west coast. The Alps host a total glacier cover of 2,909 km^2 distributed along the entire mountain range from the peaks above 4,000 m a.s.l. in France and western Switzerland, over Italy and Germany to Austria. The glaciers of the Pyrenees are situated in the Maladeta massif in Spain and around the peak Vignemale in France and sum up to about 12 km^2. All together, these inventories sum up to a total glacier cover of about 54,000 km^2 in Europe. Based on rough estimates by Radic and Hock (2010) this corresponds to an ice volume of about 15,500 km^3, or about 40 mm potential sea level rise, of which the vast majority is located in Svalbard (26 mm) and Iceland (12 mm).

[1] The European region covered in this report includes all member countries of the EEA

Table 4.1: Glacier distribution in Europe

Region	Glacier area [km^2]	Time period and standard deviation of data in WGI	Original sources
Svalbard total	**36,612**		
- Spitsbergen	21,871	1966 ±5	Hagen et al. 1993
- Nordaustlandet	11,309	1971 ±3	Hagen et al. 1993
- Edgeöya/Barentsöya	2,705	1971 ±3	Hagen et al. 1993
- Kong Karls Land	22	1970 ±0	Hagen et al. 1993
- Kvitöya	705	1977 ±0	Hagen et al. 1993
Iceland total	**11,260**		
- Vatnajökull	8,300	1960/73/77	Björnson 1980, Williams 1986
- Langjökull	953	1960/73/77	Björnson 1980, Williams 1986
- Hofsjökull	925	1960/73/77	Björnson 1980, Williams 1986
- Myrdalsjökull	596	1960/73/77	Björnson 1980, Williams 1986
- Drangajökull	160	1960/73/77	Björnson 1980, Williams 1986
- Eyjafjallajökull	78	1960/73/77	Björnson 1980, Williams 1986
- others	247	1960/73/77	Björnson 1980, Williams 1986
Scandinavian Peninsula	**3,058**		
- Northern Norway and Sweden	1,441	1961 ±6	Østrem et al. 1973
- Southern Norway	1,617	1966 ±1	Østrem et al. 1969
Alps total	**2,909**		
- Switzerland	1,342	1973 ±0	Müller et al. 1976
- Italy	607	1977 ±9	various, cf. WGMS 1989
- Austria	543	1969 ±0	Gross 1983, 1988; Patzelt 1980
- France	417	1971 ±4	Edouard and Vivian 1980
- Germany	1	1970/71	Finsterwalder and Rentsch 1973
Pyrenees total	**12**	1975 ±5	Höllermann 1968
Total Europe	**53,851**		

Source: WGMS (1989)

Changes from the Little Ice Age to present

The LIA moraines that were formed between the mid 18th and the mid 19th century mark a Holocene (i.e., the past 11,000 years) maximum extent of glaciers in Europe, as well as in many other regions of the world (Grove 2004, Solomina et al. 2008). The strong centennial retreat of glaciers from these moraines is apparent in all European regions and well documented in a wealth of studies. The following section on regional changes is based on WGMS (2008) and updated with a selection of more recent studies.

-Svalbard

During the LIA, most glaciers were close to their late Holocene maximum extents and remained there until the onset of the 20th century (Svendsen and Mangerud 1997). The western part of Svalbard is quite well represented with glacier observations. Front variation series span most of the 20th century and continuous mass balance measurements are available since the end of the 1960s from Austre Brøggerbreen and Midtre Lovénbreen. Annual mass balance records of small glaciers in western Spitsbergen indicate a negative mass balance regime since at least the mid 1960s (Jania and Hagen 1996, Hagen et al. 2003a,b, Sobota 2007; Fig. 4.6).In that region, comparisons of photogrammetric maps/DEMs, dating back to 1936, show substantial decreases of glacier area and volume (Nuth et al., 2007) with enhanced thinning rates after 1990 when compared to recent airborne LiDAR (Bamber et al. 2005, Kohler et al. 2007) and ICESat altimetry (Nuth et al. 2010). This 20th century mass loss has even been documented in an accelerated uplift of the rocky margins of the Island as indicated by high-precision global positioning system located in western Spitsbergen (Kierulf et al. 2009, Jiang et al. 2010). The mass balance of northeastern Spitsbergen glaciers has been less negative than the western ones (Bamber et al. 2005, Nuth et al. 2010). The Nordaustlandet ice caps, Austfonna and Vestfonna, have been close to balance over the last two decades (Pinglot et al. 2001, Moholdt et al. 2010, Nuth et al. 2010) if the calving front retreat losses are ignored (Dowdeswell et al. 2008). Based on repeat-track ICESat altimetry from 2003 to 2008, Moholdt et al. (in press) find that most glaciers have experienced low-elevation thinning combined with high-elevation thickening. Thereby, the largest ice losses have occurred in the west and south, while north-eastern Spitsbergen and the Austfonna Ice Cap have gained mass.

The climate and as such the fluctuations of glaciers and ice caps are much influenced by the extent and distribution of sea ice which in turn depends on ocean current and on the Arctic and North Atlantic Oscillations. Furthermore, dynamic processes such as calving and surges might dominate the fluctuations of some glaciers. About 60% of glacierized areas drain into tidewater glaciers (Blaszczyk et al. 2009), and surge activities have been observed over most of Svalbard (e.g., Lefauconnier and Hagen 1991; Hamilton and Dowdeswell 1996; Sund et al. 2009).

-Iceland

Most glaciers in Iceland reached their maximum postglacial extent around 1890 (Björnsson 1979, Kirkbride 2002, Sigurðsson 2007). During the first quarter of the 20th century, retreat was notable but not rapid (Björnsson 1998). The abrupt increase in temperature that occurred about 1925 was accompanied by a rapid retreat of glacier fronts all over Iceland (Eyþórsson 1931, 1963, Sigurðsson 1998). Regular front variation observations were started in 1930 (Eyþórsson 1931) and document the periods of glacier retreat (1930–60, after 1990) and intermittent re-advances (1970–85; Sigurdsson et al. 2007). Continuous glacier mass balance measurements started in 1988 (Björnsson et al. 2002, Sigurðsson et al. 2007; Fig. 4.6). Mass-balance measurements show alternating positive and negative mass balance of glaciers during the period 1987–95, but the mass balance has been predominantly negative since 1996 (Sigurdsson et al. 2007). As in Svalbard, the 20th century mass loss of the major ice caps, such as Vatnajøkull, has been documented in an accelerated uplift of the rocky margins of the Island (Jiang et al. 2010). The outlines of all 276 identified glaciers have been digitized using mainly satellite images, but also aerial photographs and direct field observations, for approximately the year 2000 (Sigurdsson et al. 2007). The total glacier area in 2000 was found to be 11,048 km^2 which is about 2% less than the area reported in the inventory of the 1970s (see Table 1). Changes in summer temperature seem to have been the predominant driving factor in variations of the mass balance of the non-surg-type glaciers in Iceland (Sigurðsson et al. 2007). However, some of the rapid glacier advances might have been related to volcanic activities and surges rather than to climatic events.

-Scandinavian Peninsula

After having probably disappeared in the early/mid Holocence (Nesje et al. 2008), Norwegian glaciers and ice caps reached their maximum extents in the mid-18th century (Grove 2004). These advanced glacier states are attributed both to lower summer temperatures and higher winter precipitation, due to a positive NAO-index, in the first half of the 18th century (Nesje and Dahl 2003). Blomsterskardsbreen, an outlet glacier of Folgefonna, is one of the known exceptions in southern Norway, reaching its maximum extent in the 20th century (Tvede and Liestøl 1977). In Lyngen in northern Norway the LIA glacier maximum is suggested to be about 1900–1910 (Ballantyne 1990, Bakke et al. 2005). In the Kebnekaise Mountains, Swedish Lapland, glaciers had their greatest Holocene extents probably in the period of 17th century and beginning of 18th century (Karlén 1973, 1988). Most glaciers in northern Sweden reached positions close to their Holocene maximum at the beginning of the 20th century (Holmlund and Jansson 1999).

At the turn to the 20th century, annual observations of glacier front variations began in Sweden (Holmlund 1996) and Norway (Andreassen et al. 2005). These observations reveal that Scandinavian glaciers experienced a general recession during the 20th century with intermittent periods of re-advances around 1910 and 1930, in the second half of the 1970s, and around 1990; the last advance stopped at the beginning of the 21st century (Grove 2004, Andreassen et al. 2005).Mass balance measurements began in 1946 at Storglaciären (Sweden; Schytt 1981, Jansson and Pettersson 2007) and in 1949 at Storbreen (Norway, Liestøl 1967,Andreassen et al. 2005), providing long and continuous series of winter and summer balances. In the 1960s and 1970s measurements began at many other glaciers in Scandinavia (e.g., Holmlund and Jansson 1999, Andreassen et al. 2005). In addition to the field observations, aerial photographs have been taken in about decadal intervals and are used for comparison of the glaciological and the geodetic mass balances (e.g., Andreassen 1999, Østrem and Haakensen 1999, Haug et al. 2009, Zemp et al. 2010). Results reveal cumulative mass surplus at the maritime glaciers (e.g., Hardangerjøkulen, Nigardsbreen, Ålfotbreen, Engabreen), whereas the more continental glaciers (e.g. Storglaciären, Gråsubreen, Hellstugubreen, Storbreen) continued their ice loss. All glaciers in Norway, except Langfjordjøkelen, had a transient mass surplus in the period 1989 to 1995 which was mainly a result of increased winter accumulation. Since 2001, all monitored glaciers have experienced an overall mass deficit (Kjøllmoen et al. 2010).

To gain an updated overview of the present state of overall glacier cover and its changes since the previous inventories, glaciers have been mapped in recent years based on Landsat data. Whereas glaciers in the Svartisen region in northern Norway showed an area reduction close to zero from 1968 to 1999 (Paul and Andreassen 2009), the glacier area reduced by 10% from about 1980 to 2003 in Jotunheimen, southern Norway (Andreassen et al. 2008). Analysis of aerial photographs from 1968 1985, and 2002 of the western Svartisen Ice Cap confirmed the limited glacier area reduction in that region and suggest a volume loss for the drainage basin of Engabreen (Haug et al. 2009). The latter is in contrast to mass gain over the same periods reported from direct glaciological measurements at Engabreen and might be caused by changing ice divides of the ice cap (Elvehøy et al 2009).

The mass balance of Scandinavian glaciers is strongly influenced by atmospheric and oceanic circulation changes over the North Atlantic (Hanssen-Bauer and Førland 1998, Chen and Hellström 1999, Nesje et al. 2000, Wanner et al. 2001, Uvo 2003). Summer air temperature – and thus glacier ablations – is strongly related to the position of the jet stream and the strength of high pressure areas as the corresponding circulation pattern determines the relative contribution of incoming air masses from the North Atlantic (wet and cold), the Arctic (dry and cold) or from the East (dry and warm). Winter precipitation – and thus glacier accumulation – is strongly related to the North Atlantic Oscillation (NAO) index: a positive index with strong westerly winds and increased cyclonic frequency across the North Atlantic leads to high amounts of winter precipitation, especially in the coastal areas of Southern Norway. Pronounced south-easterly airflows bring moisture from the Baltic Sea to glaciers east of the drainage divide of the Scandinavian mountain chain.

-Alps

The Alps are probably the densest populated mountain range with glaciers. It is hence not surprising that here the greatest number of available information about distribution and changes of glaciers as well as scientific studies are found. For several Alpine glaciers, fluctuations spanning time periods from centuries to millennia were reconstructed based on geomorphological and archaeological evidences, dendrochronology, as well as from historical documents and pictorial sources (Zumbühl 1976, Holzhauser and Zumbühl 1996, Pelfini 1999, Nicolussi and Patzelt 2000, Holzhauser et al. 2005, Nussbaumer et al. 2007, Nussbaumer and Zumbühl in press). Three main glacier advances are reported during the LIA period, i.e., in the 14th century, in the 17th century, and the last one culminating around 1850 in which most glaciers reached their Holocene maximum extent and destroyed earlier moraines (Gross 1987, Maisch et al. 2000, Grove 2004). However, in some regions the moraines from 1820 mark this maximum extent (e.g., Wetter 1987, Holzhauser and Zumbühl 2003).

From detailed repeat inventories in Switzerland (1850: Maisch et al. 2000; 1973: Müller et al. 1976; 1998/99: Kääb et al. 2002, Paul et al. 2002), the overall Alpine glacier cover is estimated to have reduced by 35% from 1850 to the 1970s (Paul et al. 2004; Zemp et al. 2008) and by another 22% from the 1970s to 1998/99 (Zemp et al. 2008). A second complete Alpine inventory was derived from Landsat scenes for 2003 and reveals another 9% since 1998/99 (Paul et al. in prep.). Analysis of early inventories in Austria (Gross 1987) and recent regional repeated inventories (Abermann 2009) confirm these estimates.

Annual front variation observations started in the second half of the 19th century. They document a general trend of glacier retreat over the past 150 years with intermittent Alpine glacier re-advances in the 1890s, 1920s, and 1970–1980s (Patzelt 1985, Pelfini and Smiraglia 1988, Citterio et al. 2007, Zemp et al. 2008).

Mass balance measurements show an accelerated ice loss after 1980 (Vincent 2002, Huss et al. 2008) culminating in an annual loss of 5 to 10 per cent of the estimated remaining ice volume (cf. Haeberli and Hoelzle 1995, Zemp et al. 2006, Farinotti et al. 2009) in the extraordinarily warm year of 2003 (Zemp et al. 2005). The mean annual mass balances of available long-term measurement series were slightly negative in the 1970s, roughly -0.5 m w.e. a^{-1} in the 1980s, about -0.75 m w.e. a^{-1} in the 1990s, and exceeded -1.0 m w.e. a^{-1} after the turn of the century (Fig 2). The measured rates of mass loss since 1980 are similar to modelled ones in the 1940s (Huss et al. 2008, Huss and Bauder 2009) but about two to four times the loss rates reconstructed from cumulative length changes for the time period after 1850 (Hoelzle et al. 2003, Steiner et al. 2005) and characteristic long-term mass changes during the past 2,000 years (Haeberli and Holzhauser 2003). Decadal volume changes back to the late 19th century from geodetic surveys confirm these change rates (Lang and Patzelt 1971, Kuhn et al. 1999, Bauder et al. 2007, Abermann et al. 2009) and are used to homogenize, validate and calibrate the direct mass balance measurements (Thibert et al. 2008, Huss et al. 2009, Fischer 2010).

The general centennial glacier retreat from the LIA moraines corresponds well with the observed warming trend over this period (e.g., Oerlemans 1994, Vincent et al. 2005). However, the onset of the retreat in the decades after 1850 might have been triggered by a negative winter precipitation anomaly (relating to the mean of 1901-2000; Wanner et al. 2005, Vincent et al. 2005). The intermittent periods of glacier re-advances in the 1890s, 1920s and 1970-1980s can be explained by earlier wetter and cooler periods, with reduced sunshine duration and increased winter precipitation (Patzelt 1987, Schöner et al. 2000, Laternser and Schneebeli 2003). In addition, the positive mass balance period between 1960 and 1980 was characterised by negative winter North Atlantic Oscillation index values, which caused an increase of the meridional circulation mode and more intense north-westerly to northerly precipitation regime (Hoinkes 1969, Wanner et al. 2005, Huss et al. 2010). The high mass loss rates of the 1940s are attributed to enhanced solar radiation whereas the dimming of solar radiation from the 1950s until the 1980s is in line with reduced melt rates and advancing glaciers (Ohmura et al. 2007, Huss et al. 2009). The observed trend of increasingly negative mass balances since 1980 seems to be consistent with strong warming (Schöner et al. 2000, Vincent et al. 2004, Bocchiola and Diolaiuti 2009), (re-) brightening of the atmosphere (Ohmura et al. 2007), extension of the ablation period (Vincent et al. 2004, Bocchiola and Diolaiuti 2009), and reinforcing effects such as dust-related darkening of glacier surfaces and corresponding surface albedo reduction (Paul et al. 2005, Oerlemans et al. 2009).

-Pyrenees

The moraines that mark the LIA maximum extension of glaciers in the Pyrenees are dated to around 1820–30 (Chueca and Julián 1996). At that time, overall glacier extent in the nine main Pyrenean mountainous massifs both in Spanish and French regions (Balaitús, Infiernos, Vignemale, Monte Perdido/Gavarnie, Pic Long, La Munia, Posets, Perdiguero and Maladeta) summed up to over 20 km^2 (Chueca et al. 2005). The continuous glacier retreat since then has been analyzed in several works (Martínez de Pisón and Arenillas 1988, Gellatly et al. 1995, Copons and Bordonau 1997, Julián and Chueca 1998, René 2000, Chueca and Julián 2002, Chueca et al. 2002, 2003) and revealed an overall loss of about two third of the LIA extent until the end of the 20th century. Extensive studies based on dated moraines, iconographic sources, topographic maps, aerial and terrestrial photographs have been carried out on the evolution of Maladeta Glacier in the central Spanish Pyrenees (Chueca et al. 2005, and references therein). Based on these works, the glacier lost about 36% of its LIA area (c. 1.5 km^2) until the year 2000, with an increase of its equilibrium line altitude of 255 m. The continuous glacier retreat was more pronounced in the second half of the 19th century and in the last two decades of the 20th century. Continuous mass balance measurements since 1991/92 show a close to zero balance until 1997 followed by a mean annual loss of about 1 m w.e. a^{-1} until present (Fig. 2). The glacier retreat since the LIA is generally attributed to the increase in (summer) temperature over this period and scarce (winter) precipitation during periods of accelerated glacier ice loss (Chueca et al. 2005, López Moreno 2005).

-Others, e.g. Apennines & Tatra Mountains

Small glaciers of the (French-Italian) Southern Maritime Alps (Gellatly et al. 1994a, Pappalardo 1999), the Central Apennines in Italy with the Ghiacciaio del Calderone (Gellatly et al. 1994b, D'Orefice et al. 2000), and of the Spanish Sierra Nevada with the Corral del Veleta Glacier (Messerli 1980, Gómez Ortiz and Salvador 1997) are reported to showing observed trends of constant retreat during the 19th and 20th century associated with prolonged periods of negative mass balances similar to the ones of glaciers in the Pyrenees (cf. Chueca et al. 2005). Perennial snow patches in the Tatra Mountains have been mentioned already back in the early 17th century with detailed descriptions and measurements starting in the early 20th century (Gadek 2008, and references therein). In the Slovak Tatras, the largest glacieret is situated in Medená Kotlina and is strongly influenced by avalanche accumulation and shading of the surrounding peaks (Gadek and Kotyrba 2007). From three of glacierets in the Polish Tatras (Mięguszowiecki, Pod Bulą and Pod Cubryną), annual measurements of their extents have been carried out since 1980 (Wiśliński 1985, 2002, Ciupak et al 2005). From these analyses, it was concluded that the fluctuations of these three mainly avalanche and snow-drift fed glacierets were usually not synchronous and do not show any trend, that changes in their dimensions are strongly connected to the destruction of subglacial tunnes, and that these inter-annual variations cannot be explained by changes in air temperature. Gadek (2008) showed that the fluctuations of these firn-ice patches depend most of all on the weather regime of the winter season and local topographic conditions. Unlike the firn-ice patches in the Tatras, the inter-annual fluctuations of the two investigated glacierets (Snezhnika and Banski suhodol) in the Bulgarian Pirin Mountains seem to be mainly related to variations in (summer) temperature, and precipitation (Gachev et al. 2009).

Projections *(21st century)*

Over the 20th century, glaciers have dramatically retreated from their LIA moraines which mark Holocene maximum extents in all European regions. Today, glaciers are close to the 'short end' of the Holocene variability, and may have already passed it in some regions of the Alps and in the Pyrenees. While coastal glaciers on the Scandinavian Peninsula were able to regain some mass in the last decade of the 20th century, the vast ice loss over the past few decades has already led to the disintegration of many glaciers (e.g., Carèser, IT) within the Alpine observation network (Carturan and Seppi 2007, Paul et al. 2007). The massive downwasting of many glaciers, rather than dynamic retreat, has decoupled the horizontal extent (i.e., length, area) of these glaciers from current climate. Under present climate change scenarios for the 21st century (IPCC 2007, Chapter 3.7), the ongoing trend of rapid, if not accelerated, glacier melting on the century time scale may lead to the deglaciation of large parts of many mountain ranges in the coming decade. However, while the process understanding of glacier reaction to (further) climatic changes is well developed, most available analysis are rather sensitivity studies of selected glaciers and forcing scenarios than standardised glacier ensemble projections for entire Europe.

From degree-day model and worldwide glacier samples (e.g., Oerlemans and Fortuin 1992, Gregory and Oerlemans 1998, Braithwaite and Zhang 1999), it is shown that the (static) sensitivity of mass balance to a +1°C temperature increase shows a global mean sensitivity of about -0.35 m w.e. a^{-1} K^{-1} (e.g., Raper and Braithwaite 2006) with a wide range from decimetres to a few meter water equivalent. Thereby, sub-polar glaciers (e.g., in Svalbard and northern Scandinavian Peninsula) have lower temperature sensitivities and more maritime (e.g., in Iceland and coastal Norway) and tropical glaciers have higher sensitivities.

De Woul and Hock (2005) use such a degree-day approach to investigate the sensitivity of 42 Arctic glaciers and ice caps. The authors confirm earlier findings (see above) and show that on average an increase in precipitation of about 20% is needed in order to offset the effect of a one degree warming. Thereby, much higher percentage increases in precipitation are needed for continental than for maritime glaciers. The mean (static) mass balance sensitivities to a one degree warming (and corresponding contributions to sea level rise) of investigated glaciers are -0.45 m w.e. a^{-1} (0.045 mm a^{-1}) for Svalbard, -0.74 m w.e. a^{-1} (0.006 mm a^{-1}) for the Scandinavian Peninsula, and -1.63 m w.e. a^{-1} (0.049 mm a^{-1}) for Iceland.

The sensitivity of the Vatnajökull Ice Cap to a warming over the 21st and 22nd centuries is examined by Flowers et al. (2005) using spatially distributed coupled models of ice dynamics and hydrology. For a prescribed warming rate of 2°C per century, simulated area and volume of the ice cap are reduced by 12–15% and 18–25%, respectively, by the end of the 21st century. As a consequence, glacier discharge from northern and northwestern Vatnajökull (distal from the coast) appears to be the most robust to climate warming, while discharge from Vatnajökull's southern margin (proximal to the coast) is particularly vulnerable and has implications for glacier flood routing and frequency. With a similar modelling experiment, Aðalgeirsdóttir et al. (2006) found an ice volume reduction by half of Hofsjökull and southern Vatnajökull by the first half of the 22nd century forcing their transient model with a warming rate of 1.5 and 3.0 °C per century in midsummer and midwinter, respectively.

The (flat) ice caps on the Scandinavian Peninsula are especially vulnerable to a rise in the equilibrium line altitude (ELA) due to their relatively small altitudinal difference between the present-day ELA and the maximum elevation of the individual (outlet) glacier. Oerlemans (1997) used a dynamic ice-flow model of Nigardsbreen and showed that a continued warming rate of 2°K a^{-1} would reduce the ice volume of this outlet glacier from Jostedalsbreen ice cap by more than 90%. Nesje et al. (2005) show that an increase in summer temperature of 2.3°C and an increase in winter precipitation of 16% by the end of the 21st century would cause the steady-state ELA to rise 260 m. As a result, about 98% of glaciers in Norway (including seven of the 34 largest) are likely to disappear and the overall glacier area may be reduced by c. 34%. The Hardangerjøkulen in southern Norway is expected to disappear for a linear temperature increase of 3°C until the end of the 21st century based on a spatially distributed mass balance model coupled to a vertically integrated ice-flow model by Giesen and Oerlemans (2010).

For Storglaciären in the Swedish Kebnekaise massif, typical (static) mass balance sensitivities to changes in temperatures and precipitation (see above) are found by Brugger (1997), Schneeberger et al. (2001), and Radic and Hock (2008). According to the latter, projections of volume change in the 21st century driven by the B2 emission scenario (cf. CHAPTER) from statistically downscaled regional and global climate model outputs result in a volume loss of 50–90% of the glacier's initial volume by end of the 21st century. From a model comparison, Hock et al. (2007) suggest that the total ice loss might be underestimated by temperature-index models as compared to detailed energy-balance approaches.

For the Alps, Zemp et al. (2006, 2007) used a distributed model of the ELA to simulate the glacierisation over the entire mountain range for the reference period of 1971-90 and climate change scenarios for the 21st century. They find that a summer temperature increase of +3°C (which corresponds to about +2°C from present days) would reduce the total Alpine glacier area of the reference period by 80% (Fig. 4.7). In the event of a 5°C warming, the Alps would become almost completely ice-free with only the thickest and highest reaching glaciers being able to survive into the 22nd century. In order to offset a 1°C warming, a precipitation increase of more than 25% would be needed. Earlier simple but robust estimates (Haeberli and Hoelzle 1995) as well as recent more sophisticated modeling approaches of individual glaciers (Huss et al. 2007, Le Meur et al. 2007, Jouvet et al. 2009, Huss et al. 2010b) and glaciated drainage basins (Huss et al. 2008) generally confirm these results, with some differences in the individual glacier melt rates. The processes of glacier ablation are modeled with high accuracy in most simple and more complex approaches, whereas the spatial distribution of glacier accumulation and spectral albedo require still improvement (Machguth et al. 2006, 2009).

References

Abermann, J., Lambrecht, A., Fischer, A. and Kuhn, M. (2009): Changes in glacier area and volume in the Austrian Ötztal Alps. The Cryosphere, 3: 205-215.

Aðalgeirsdóttir, G., T. Jóhannesson, H. Björnsson, F. Pálsson, and O. Sigurðsson (2006), Response of Hofsjökull and southern Vatnajökull, Iceland, to climate change, J. Geophys. Res., 111, F03001, doi:10.1029/2005JF000388.

Andreassen, L.M. , F. Paul, A. Kääb, and J.E. Hausberg (2008): Landsat-derived glacier inventory for Jotunheimen, Norway, and deduced glacier changes since the 1930s. The Cryosphere, 2, 131-145.

Andreassen, L.M., Elvehøy, H., Kjøllmoen, B., Engeset, R.V. and Haakensen, N. (2005): Glacier mass balance and length variations in Norway. Annals of Glaciology, 42: p. 317–325.

Andreassen, L.M. (1999): Comparing traditional mass balance measurements with long-term volume change extracted from topographic maps: a case study of Storbreen glacier in Jotunheimen, Norway, for the period 1940–1997, Geogr. Ann., 81A(4), 467–476.

Bakke, J., Dahl, S.O., Paasche, Ø., Løvlie, R. and Nesje, A. (2005): Glacier fluctuations, equilibrium-line altitudes and palaeoclimate in Lyngen, northern Norway, during the Lateglacial and Holocene. The Holocene, 15 (4): p. 518-540.

Ballantyne, C.K. (1990), The Holocene glacial history of Lyngshalvöya, northern Norway: chronology and climatic implications. Boreas, 19: 93–117.

Bamber, J.L., Krabill, W., Raper, V., Dowdeswell, J.A., & Oerlemans, J. (2005). Elevation changes measured on Svalbard glaciers and ice caps from airborne laser data. Annals of Glaciology, 42, 202-208.

Bauder, A., Funk, M. and Huss, M., 2007, Ice-volume changes of selected glaciers in the Swiss Alps since the end of the 19th century. Annals of Glaciology, 46, pp. 145-149.

Baumann, S., S. Winkler and L.M. Andreassen, 2009. Mapping glaciers in Jotunheimen, South-Norway, during the 'Little Ice Age' maximum. The Cryosphere, 3, 231-243.

Blaszczyk, M., J. A. Jania and J. O. Hagen. 2009. Tidewater glaciers of Svalbard: Recent changes and estimates of calving fluxes. Polish Polar Research, Vol. 30, no. 2, pp. 85–142.

Björnsson, H., Palsson, F. and Haraldsson, H. (2002): Mass balance of Vatnajökull (1991-2001) and Langjökull (1996-2001), Iceland. Jökull, 51: p. 75-78.
Björnsson, F. 1998. Samtíningur um jökla milli Fells og Stadherfjalls. Jökull, 46, 49–61.
Björnson, H. (1980): The surface area of glaciers in Iceland. Jökull, 28: 31 pp.
Björnsson, H. 1979. Glaciers in Iceland. Jökull, 29, 74–80.
Bocchiola, D., and Diolaiuti, G. (2009): Evidence of climate change within the Adamello Glacier of Italy. Theoretical and Applied Climatology, doi 10.1007/s00704-009-0186-x.
Braithwaite, R.J. & Zhang, Y., 1999. Modelling changes in glacier mass balance that may occur as a result of climate changes. Geogr. Ann. 81A (4): 489–496.
Braithwaite, R.J. & Zhang, Y., 1999. Relationships between interannual variability of glacier mass balance and climate. J. Glaciol. 45 (151): 456–462.
Brugger, K.A. 1997. Predicted response of Storglacia¨ren, Sweden, to climatic warming. Ann. Glaciol., 24, 217–222.
Carturan, L. and Seppi, R. (2007): Recent mass balance results and morphological evolution of Carèser Glacier (Central Alps). Geografia Fisica e Dinamica Quaternaria, 30 (1): p. 33-42.
Chen, D. and Hellström, C., 1999. The influence of the North Atlantic Oscillation on the regional temperature variability in Sweden: spatial and temporal variations. Tellus 51A, 505-516.
Chueca, J., Julian, A., Saz, M.A., Creus, J. and Lopez, J.I. (2005): Responses to climatic changes since the Little Ice Age on Maladeta Glacier (Central Pyrenees). Geomorphology, 68 (3–4): p. 167–182.
Chueca, J., Julián, A. and López-Moreno, J.I. (2003): Variations of Glaciar Coronas, Pyrenees, Spain, during the 20th century. Journal of Glaciology, 49 (166): 449-455.
Chueca, J. and Julian, A. (2002): Los glaciares pirenaicos aragoneses: estudio de su evolución desde el final de la Pequeña Edad del Hielo hasta la actualidad a través de documentación fotográfica. Diputación de Huesca, Huesca: 323 pp.
Chueca, J., Julián, A., Peña, J.L. (2002): Comparación de la situación de los glaciares del Pirineo español entre el final de la Pequeña Edad del Hielo y la actualidad. Bol. Glaciol. Aragon. 3, 13– 41.
Chueca, J. and Julián, A. (1996): Datación de depósitos morrénicos de la Pequeña Edad del Hielo: macizo de la Maladeta. In: Pérez Alberti, A., Martini, P., Chesworth, W., Martínez Cortizas, A. (Eds.), Dinámica y Evolución de Medios Cuaternarios. Xunta de Galicia, Santiago de Compostela, p. 171–182.
Citterio, M., Diolaiuti, G., Smiraglia, C., D'Agata, C., Carnielli, T., Stella, G., and Siletto, G.B. (2007): The fluctuations of Italian glaciers during the last century: a contribution to knowledge about Alpine glacier changes. Geografiska Annaler, 89, A3, p. 164-182.
Ciupak, M., Maciejewski, M. and Wiśliński, A. (2005), Zmiany powierzchni płata firnowo-lodowego pod Bulą pod Rysami w latach 1978–2004 w nawiązaniu do danych meteorologicznych z Kasprowego Wierchu [Changes of area of the firn and ice patch beneath Bula pod Rysami in years 1978–2004 in reference to the meteorological data from Kasprowy Wierch] , in Kotarba, A. and Borowiec, W. (eds.), Przyroda Tatrzańskiego Parku Narodowego a Człowiek, Tom 1 [The Nature of the Tatra National Park and Man, Volume 1], Tatrzański Park Narodowy, Zakopane; Polskie Towarzystwo Przyjaciół Nauk o Ziemi, Kraków, 119–126.
Copons, R., Bordonau, J. (1997): El registro glaciar correspondiente a la Pequeña Edad del Hielo en la península Ibérica. In: Ibáñez, J.J., Valero, B.L., Machado, C. (Eds.), El paisaje mediterráneo a través del espacio y del tiempo. Implicaciones en la desertificación. Geoforma Ediciones, Logroño, pp. 295–310.
D'Orefice, M., Pecci, M., Smiraglia, C., Ventura, R. (2000): Retreat of Mediterranean glaciers since the Little Ice Age: case study of Ghiacciaio del Calderone, Central Apennines, Italy. Arct. Antarct. Alp. Res. 32 (2), 197– 201.
Dowdeswell J.A., T.J. Benham, T. Strozzi, and J.O. Hagen, 2008. Iceberg calving flux and mass balance of the Austfonna ice cap on Nordaustlandet, Svalbard, Journal of geophysical research, Vol. 113, F03022.
Edouard, J.L. and Vivian, R. (1980): The French glacier inventory. In: World Glacier Inventory – Proceedings of the Riederalp Workshop. IAHS Publ., 126: 195 pp.

Elvehøy, H., M. Jackson, and L.M. Andreassen. 2009. The influence of drainage boundaries on specific mass balance results, a case study of Engabreen, Norway. Annals of Glaciology, 50, 135-140.
Eyþórsson, J. 1931. On the present position of the glaciers in Iceland: some preliminary studies and investigations in the summer 1930. Vísindafélag Isl. Rit. 10.
Eyþórsson, J. 1963. Variations of Iceland glaciers, 1931–1960. Jökull, 13, 31–33.
Kirkbride, M.P. (2002): Icelandic climate and glacier fluctuations through the termination of the 'Little Ice Age'. Polar Geography, 26 (2): p. 116-133.
Farinotti, D., Huss, M., Bauder, A. and Funk, M., 2009, An estimate of the glacier ice volume in the Swiss Alps. Global and Planetary Change, 68, pp. 225-231.
Fischer, A. (2010): Glaciers and climate change: Interpretation of 50 years of direct mass balance of Hintereisferner. Global and Planetary Change, 71, p. 13–26.
Finsterwalder, R. and Rentsch, H. (1973): Das Verhalten der bayerischen Gletscher in den letzten zwei Jahrzehnten. Zeitschrift für Gletscherkunde und Glazialgeologie, 9 (1-2): p. 59-72.
Flowers, G. E., Marshall, S. J., Björnsson, H., and Clarke, G. K. C.: Sensitivity of Vatnajökull ice cap hydrology and dynamics to climate warming over the next 2 centuries, J. Geophys. Res., 110, F02011, doi:10.1029/2004JF000200, 2005.
Gachev, E., Gikov, A., Zlatinova, C. and Blagoev, B. (2009): Present state of Bulgarian glacierets. Landform Analysis, 11: p. 16-24.
Gądek, B. (2008): The Problem of Firn-ice Patches in the Polish Tatras as an Indicator of Climatic Fluctuations. Geographia Polonica, 81 (1): p. 41-52.
GCOS (2004): Implementation plan for the Global Observing System for Climate in support of the UNFCCC. Report GCOS – 92 (WMO/TD No. 1219): 136 pp.
Gellatly, A.F., Grove, J.M., Bücher, A., Latham, R., Whalley, W.B., 1995. Recent historical fluctuations of the Glacier du Taillon, Pyrénées. Phys. Geogr. 15 (5), 399–413.
Gellatly, A.F., Grove, J.M., Latham, R., Parkinson, R.J., (1994a): Observations of the glaciers in the Southern Maritime Alps (Italy). Rev. Géomorphol. Dyn. 43 (3), 93–107.
Gellatly, A.F., Smiraglia, C., Grove, J.M., Latham, R. (1994b): Recent variations of Ghiacciaio del Calderone, Abruzzi, Italy. J. Glaciol. 40 (136), 486–490.
Giesen, R. and Oerlemans, H. (2010): Response of the ice cap Hardangerjøkulen in southern Norway to the 20th and 21st century climates. The Cryosphere, 4: p. 191-213.
Gómez Ortiz, A., Salvador, F. (1997): El glaciarismo de Sierra Nevada, el más meridional de Europa. In: Gómez Ortiz, A., Pérez Alberti, A. (Eds.), Las huellas glaciares de las montañas españolas. Universidade de Santiago de Compostela, Santiago de Compostela, pp. 385– 430.
Greene, A.M. (2005): A time constant for hemispheric glacier mass balance. Journal of Glaciology 51 (174): p. 353–362.
GregoryJ, .M. and Oerlemans J,. , 1998: Simulated future sea-level rise duet o glacier melt based on regionally and seasonally resolved temperature changes. Nature, 391: 474-476.
Gross, G. (1988): Der Flächenverlust der Gletscher in Österreich 1850–1920–1969. Zeitschrift für Gletscherkunde und Glazialgeologie 23 (2): p. 131–141.
Gross, G. (1983): Die Schneegrenze und die Altschneelinie in den österreichischen Alpen. Innsbrucker Geographische Studien, 8: p. 59-83.
Grove, J.M. (2004): Little Ice Ages: Ancient and modern. Vol. I + II, 2nd edition. Routledge, London and New York.
GTOS (2008): Terrestrial essential climate variables for climate change assessment, mitigation and adaptation. GTOS-52. http://www.fao.org/gtos/doc/pub52.pdf
Haeberli, W. and Hoelzle, M. (1995): Application of inventory data for estimating characteristics of and regional climate-change effects on mountain glaciers: a pilot study with the European Alps. Annals of Glaciology, 21: p. 206–212.
Hagen, J.O., Kohler, J., Melvold, K. and Winther, J.G. (2003a): Glaciers in Svalbard: mass balance, runoff and fresh water flux. Polar Research 22 (2): p. 145–159.
Hagen, J.O., Melvold, K., Pinglot, F., & Dowdeswell, J.A. (2003b). On the net mass balance of the glaciers and ice caps in Svalbard, Norwegian Arctic. Arctic, Antarctic, and Alpine Research, 35, 264-270.
Hamilton, G.S., & Dowdeswell, J.A. (1996). Controls on glacier surging in Svalbard. Journal of Glaciology, 42, 157-168.

Hanssen-Bauer, I. and E.J. Førland. 1998. Annual and seasonal precipitation trends in Norway 1896-1997. DNMI Report KLIMA, 27/98, Norwegian Meteorological Institute, 37 pp.
Hagen, J.O., O.Liestøl, E. Roland and T. Jørgensen 1993: Glacier Atlas of Svalbard and Jan Mayen. Norsk Polarinstitutt Meddelelser, no 129, 141 pp.
Haug, T., Rolstad, C.; Elvehøy, H. Jackson, M. Maalen-Johansen, I. 2009. Geodetic mass balance of the western Svartisen ice cap, Norway, in the periods 1968-1985 and 1985-2002. Annals of Glaciology, 50, 119-125.
Hock, R., Radíc, V., and de Woul, M. 2007. Climate sensitivity of Storglaciären – An intercomparison of mass balance models using ERA-40 reanalysis and regional climate model data. Ann. Glaciol. 46. 342—348.
Hoinkes, H.C. 1968. Glacier variations and weather. JOUI'naL oj' Glaciology, Vol. 7, No. 49, p. 3-19.
Höllermann, P. (1968): Die rezenten Gletscher der Pyrenäen. Geographica Helvetica 23 (4), p. 157-168.
Holmlund, P. and Jansson, P. (1999): The Tarfala mass balance programme, Geogr. Ann., 81A(4), 621–631.
Holmlund, P. (1996): Maps of Storglaciären and their use in glacier monitoring studies, Geogr. Ann., 78A(2–3), 193–196.
Holzhauser, H., Zumbühl, H.J., 1996: To the history of the Lower Grindelwald Glacier during the last 2800 years – palaeosols, fossil wood and historical records – new results. Z. Geomorph. N.F. Suppl.-Bd. 104, 95-127.
Huss, M., Hock, R., Bauder, A. and Funk, M., 2010, 100-year glacier mass changes in the Swiss Alps linked to the Atlantic Multidecadal Oscillation. Geophysical Research Letters, 37, p. doi:10.1029/2010GL042616.
Huss, M., Jouvet, G., Farinotti, D. and Bauder, A., 2010b, Future high-mountain hydrology: a new parameterization of glacier retreat. Hydrology and Earth System Sciences, 14, pp. 815-829.
Huss, M. and Bauder, A., 2009, Twentieth century climate change inferred from four long-term point observations of seasonal mass balance. Annals of Glaciology, 50, pp. 207-214.
Huss, M., Bauder, A. and Funk, M., 2009, Homogenization of long-term mass-balance time series. Annals of Glaciology, 50, pp. 198-206.
Huss, M., Funk, M. and Ohmura, A., 2009, Strong Alpine glacier melt in the 1940s due to enhanced solar radiation. Geophysical Research Letters, 36, p. doi:10.1029/2009GL040789.
Huss, M., Bauder, A., Funk, M., and Hock, R. (2008): Determination of the seasonal mass balance of four Alpine glaciers since 1865. Journal of Geophysical Research, 113, F01015, doi: 10.1029/2007JF000803.
Huss, M., Farinotti, D., Bauder, A. and Funk, M. 2008. Modelling runoff from highly glacierized alpine drainage basins in a changing climate, Hydrological Processes, 22(19), 3888–3902, doi:10.1002/hyp.7055.
Huss, M., Sugiyama, S., Bauder, A. and Funk, M., 2007, Retreat scenarios of Unteraargletscher, Switzerland, using a combined ice-flow mass-balance model. Arctic, Antarctic and Alpine Research, 39, pp. 422-431.
Jania, J., and Hagen, J.O. (1996). Mass Balance of Arctic Glaciers. Report No. 5. Sosnowiec-Oslo: International Arctic Science Committee: 62 pp.
Jansson, P. and Pettersson, R. (2007): Spatial and temporal characteristics of a long mass balance record, Storglaciären, Sweden, Arct., Ant. Alp. Res., 39(3), 432–437.
Jiang, Y., T.H. Dixon and S. Wdowinski. 2010. Accelerating uplift in the North Atlantic region as an indicator of ice loss. Nature Geoscience 3, 404 - 407 (2010) doi:10.1038/ngeo845
Jouvet, G., Huss, M., Blatter, H., Picasso, M. and Rappaz, J. (2009): Nuermical simulation of Rhonegletscher from 1874 to 2100. Journal of Computational Physics, 228 (17): p. 6426-6439.
Julián, A., Chueca, J., 1998: Le Petit Âge Glaciaire dans les Pyrénées Centrales Méridionales: estimation des paléotempératures à partir d'inférences géomorphologiques. Sud-Ouest Eur. 3, 79– 88.
Karlén, W. (1988): Scandinavian glacial and climatic fluctuations during the Holocene. Quaternary Science Reviews, Volume 7, Issue 2: p. 199-209.
Karlén, W., 1973. Holocene glacier and climatic variations, Kebnekaise mountains, Swedish Lapland. Geogr. Ann. 55A (1): 29–63.

Kaser, G., J.G. Cogley, M.B. Dyurgerov, M.F. Meier and A. Ohmura. 2006. Mass balance of glaciers and ice caps: consensus estimates for 1961–2004. Geophys. Res. Lett., 33(19), L19501. (10.1029/2006GL027511.)

Kierulf, H.P., H.-P. Plag & J. Kohler. 2009. Surface deformation induced by present-day ice melting in Svalbard. Geophys. J. Int. 179, 1-13 doi: 10.1111/j.1365-246X.2009.04322.x

Kjøllmoen, B., Andreassen, L. M., Elvehøy, H., Jackson, M. and Giesen, R.H. (2010): Glaciological investigations in Norway in 2009, NVE Report No 2, NorwegianWater Resources and Energy Directorate, Oslo: 85 pp.

Kohler, J., T. D. James, T. Murray, C. Nuth, O. Brandt, N. E. Barrand, H. F. Aas, & A. Luckman. 2007. Acceleration in thinning rate on western Svalbard glaciers, Geophys. Res. Lett., 34, L18502, doi:10.1029/2007GL030681.

Gądek, B. and Kotyrba, A. (2007): Contemporary and fossil metamorphic ice in Medena kotlina (Slovak Tatras), as mapped by ground-penetrating radar, Geomorphologia Slovaca et Bohemica, 1: p. 75–81.

Kuhn, M., Dreiseitl, E., Hofinger, S., Markl, G., Span, N., and Kaser, G.: Measurements and models of the mass balance of Hintereisferner, Geogr. Ann. A, 81A, 659–670, 1999.

Kuhn, M., Markl, G., Kaser, G., Nickus, U. and Obleitner, F. (1985): Fluctuations of climate and mass balance. Different responses of two adjacent glaciers. Zeitschrift für Gletscherkunde und Glazialgeologie 2: p. 409–416.

Kuhn, M. (1981): Climate and glaciers. IAHS, 131: p. 3–20.

Lang, H. and Patzelt, G.: Die Volumenänderungen des Hintereisferners (O¨ tztaler Alpen) im Vergleich zur Massen¨anderung im Zeitraum 1953–64, Z. Gletscherk. Glazialgeol., 7(1–2), 20 229–238, 1971.

Lefauconnier, B., & Hagen, J.O. (1991). Surging and calving glaciers in Eastern Svalbard. Meddelelser (130 pp). Oslo: Norwegian Polar Institute.

Letréguilly, A. and Reynaud, L., 1990. Space and time distribution of glacier mass balance in the Northern hemisphere. Arctic and Alpine Research, 22(1): 43-50.

Le Meur, E., Gerbaux, M., Schäfer, M. and Vincent, C. (2007): Disappearance of an Alpine glacier over the 21st Century simulated from modeling its future surface mass balance. Earth and Planetary Science Letters 261: p. 367–374.

Liestøl, O. 1967. Liestøl, O. 1967. Storbreen glacier in Jotunheimen, Norway. Norsk Polarinstitutt Skrifter, 141: 63 p.

Lliboutry, L. (1974): Multivariate statistical analysis of glacier annual balance. Journal of Glaciology 13: p. 371–392.

López-MorenoJ.L (2005) - Recent variations of snowpack depth in the central Spanish Pyenees. Artic, Ant. Alp. Research, 37(2), pp.253-260.

Machguth, H., F. Paul, S. Kotlarski and M. Hoelzle (2009): Calculating distributed glacier mass balance for the Swiss Alps from RCM output: A methodical description and interpretation of the results. J. Geophys. Res., 114: D19106, doi:10.1029/2009JD011775.

Machguth, H., Eisen, O., Paul, F. and Hoelzle, M. 2006: Strong spatial variability of snow accumulation observed with helicopter-borne GPR on two adjacent Alpine glaciers. Geophysical Research Letters 33, 1-5.

Maisch, M., Wipf, A., Denneler, B., Battaglia, J. and Benz, C. (2000): Die Gletscher der Schweizer Alpen. Gletscherhochstand 1850, Aktuelle Vergletscherung, Gletscherschwund Szenarien. Schlussbericht NFP31. 2. Auflage, VdF Hochschulverlag, Zürich.

Martínez de Pisón, E. and Arenillas, M. (1988): Los glaciares actuales del Pirineo español. In: MOPU (Ed.), La nieve en el Pirineo español. Ministerio de Obras Pu´ blicas y Urbanismo, Madrid, pp. 29– 98.

Matthews, J.A. 2005. ‘Little Ice Age’ glacier variations in Jotunheimen, southern Norway: a study in regionally-controlled lichenometric dating of recessional moraines with implications for climate and lichen growth rates. The Holocene 15: 1-19.

Meier, M.F., Dyurgerov, M.B., Rick, U.K., O’Neel, S., Pfeffer, W.T., Anderson, R.S., Anderson, S.P. and Glazovsky, A.F. (2007): Glaciers dominate eustatic sealevel rise in the 21st century. Science, 317(5841), 1064–1067.

Messerli, B. (1980): Mountain glaciers in the Mediterranean area and in Africa. World Glacier Inventory Workshop Publication, vol. 126, pp. 197–211.

Moholdt, G.. J. O. Hagen, T. Eiken, and T. V. Schuler. 2010. Geometric changes and mass balance of the Austfonna ice cap, Svalbard. The Cryosphere, 4, 21-34, 2010.
Moholdt, G., Nuth, C., Hagen, J.O. and Kohler, J. (subm.): Recent elevation changes of Svalbard glaciers derived from ICESat laser altimetry. Remote Sensing of Environment, RSE-D-10-00159R1.
Müller, F. Caflisch, T. and Müller, G. (1976): Firn und Eis der Schweizer Alpen. Gletscherinventar. Dept. of Geography, ETH Zurich, Publ. No. 57: 174 pp.
Nesje, A., Bakke, J., Dahl, S.O., Lie, O. and Matthews, J.A. (2008): Norwegian mountain glaciers in the past, present and future. Global and Planetary Change 60 (1–2): p. 10–27.
Nesje, A. and S.O. Dahl. 2003. The 'Little Ice Age' - only temperature? The Holocene, 13, 1, 139-145.
Nesje, A., Ø. Lie, and S.O. Dahl. 2000. Is the North Atlantic Oscillation reflected in Scandinavian glacier mass balance records? Journal of Quaternary Science, 15 (6), 587-501.
Nussbaumer, S. U., A. Nesje, and H. J. Zumbühl (in press): Historical glacier fluctuations of Jostedalsbreen and Folgefonna (southern Norway) reassessed by new pictorial and written evidence. The Holocene.
Nuth, C., J. Kohler, H.F. Aas, O. Brandt and J.O. Hagen. 2007. Glacier geometry and elevation changes on Svalbard (1936–90): a baseline dataset. Annals of Glaciology 46, 106-116.
Nuth, C., Moholdt, G., Kohler, J., Hagen, J. O. and Kääb, A. 2010: Svalbard glacier elevation changes and contribution to sea level rise, J. Geophys. Res., Vol. 115. doi:10.1029/2008JF001223, 2010.
Oerlemans, H., Giesen, R.H. and Van Den Broeke, M.R. (2009): Retreating alpine glaciers: increased melt rates due to accumulation of dust (Vadret da Morteratsch, Switzerland). Journal of Glaciology, 55 (192): p. 729-736.
Oerlemans 1997: A flow-line model for Nigardsbreen: projection of future glacier lenth based on dynamic calibration with the historic record. Ann. Glaciol. 24: p. 382-389.
OerlemansJ, . and Fortuin,J .P.F., 1992:S ensitivityo f glaciers ands malli ce capst o Greenhouswe armingN. ature,2 58:115-117.
Ohmura, A., A. Bauder, H. Müller, and G. Kappenberger (2007), Long-term change of mass balance and the role of radiation, Ann. Glaciol., 46(1), 367– 374.
Ohmura, A. (2001): Physical basis for the temperature-based melt-index method. Journal of Applied Meteorology 40: p. 753–761.
Østrem, G. and Haakensen, G. (1999): Map comparison or traditional mass-balance measurements: which method is better? Geogr. Ann., 81A, 703–711.
Østrem, G., Selvig, K.D. and Tandberg, K. (1988): Atlas over breer i Sør-Norge. Oslo, Norges Vassdrags-og Energiverk Vassdragsdirektoret.
Østrem, G., Haakensen, M., and Melander, O. (1973): Atlas over breer i Nord-Skandinavia. Hydrologisk avdeling, Norges Vassdrags-og Energiverk, Meddelelse, 22: 315 pp.
Pappalardo, M. (1999): Remarks upon the present-day condition of the glaciers in the Italian Maritime Alps. Geogr. Fis. Din. Quat. 22, 79– 82.
Paul, F., H. Frey, and R. LeBris (in prep.): A new glacier inventory for the European Alps derived from ten Landsat TM scenes acquired in 2003. Annals of Glaciology, 52 (59).
Paul, F. and L.M. Andreassen. 2009. A new glacier inventory for the Svartisen region (Norway) from Landsat ETM+ data: Challenges and change assessment. Journal of Glaciology, 55 (192), 607-618.
Paul, F., Machguth, H. and Kääb, A., 2005. On the impact of glacier albedo under conditions of extreme glacier melt: the summer of 2003 in the Alps. EARSeL eProceedings, 4: 139-149.
Paul, F., Kääb, A., Maisch, M., Kellenberger, T. W. and Haeberli, W. (2004): Rapid disintegration of Alpine glaciers observed with satellite data. Geophysical Research Letters 31, L21402, doi:10.1029/2004GL020816.
Patzelt, G. (1985): The period of glacier advances in the Alps, 1965 to 1980. Zeitschrift für Gletscherkunde und Glazialgeologie 21: p. 403–407.
Patzelt, G. (1980): The Austrian glacier inventory: status and first results. In: World Glacier Inventory – Proceedings of the Riederalp Workshop. IAHS Publ. No. 126: p. 181-183.
Pelfini., M. (1999): Dendrogeomorphological study of glacier fluctuations in the Italian Alps during the Little Ice Age. Annals of Glaciology, 28, p. 123-128.

Pelfini, M. and Smiraglia, C. (1988): L'evoluzione recente del glacialismo sulle Alpi Italiani: strumenti e temi di ricerca. Bollettino della Societa Geografica Italiana, 1–3: p. 127– 154.

Pinglot, J.F., Hagen, J.O., Melvold, K., Eiken, T., & Vincent, C. (2001). A mean net accumulation pattern derived from radioactive layers and radar soundings on Austfonna, Nordaustlandet, Svalbard. Journal of Glaciology, 47, 555-566.Svendsen, J.I. and Mangerud, J. (1997): Holocene glacial and climatic variations on Spitsbergen, Svalbard. Holocene 7: p. 45–57.

Radic, V. and Hock, R. (2006): Modeling future glacier mass balance and volume changes using ERA-40 reanalysis and climate models: A sensitvity study at Storlgaciären, Sweden. Journal of Geophysical Research, 111, F03003, doi:10.1029/2005JF000440.

Raper, S.C.B. and Braithwaite, R. (2006): Low sea level rise projections from mountain glaciers and icecaps under global warming. Nature, 439: p. 311-313.

René, P. (2000): Etat des lieux des glaciers des Pyrénées françaises. Compte rendu de la campagne de terrain (septembre 1999). Société Hydrotechnique de France, Grenoble (16 pp.).

Schneeberger, C. Albrecht, O., Blatter, H., Wild, M., & Hock, R., 2001. Modelling the response of glaciers to a doubling of CO2: a case study on Storglaciären, northern Sweden. Climate Dyn. 17 (119): 825–834.

Schöner, W., Auer, I. and Böhm, R. (2000): Climate variability and glacier reaction in the Austrian eastern Alps. Annals of Glaciology 31 (1): p. 31–38.

Schytt, V. (1981): The net mass balance of Storglaciären, Kebnekaise, Sweden, related to the height of the equilibrium line and to the height of the 500 mb surface. Geogr. Ann., 63(3–4): p. 219–223.

Sigurðsson, O. 1998. Glacier variations in Iceland 1930–1995: from the database of the Iceland Glaciological Society. Jökull, 45, 3–25.

Sigurðsson, O., Jónsson, T. and Jóhannesson, T. (2007): Relation between glacier-termini variations and summer temperature in Iceland since 1930. Annals of Glaciology 46 (1): p. 170–176.

Sobota, I. (2007): Mass balance of Kaffiøyra glaciers, Svalbard. Landform Analysis, 5: p. 75-78.

Solomina, O., Haeberli, W., Kull, C. and Wiles, G. (2008): Historical and Holocene glacier-climate variations: General concepts and overview. Global and Planetary Change 60 (1-2): p. 1–9.

Steiner, D., A. Walter and H.J. Zumbühl. 2005. The application of a non-linear back-propagation neural network to study the mass balance of Grosse Aletschgletscher, Switzerland. J. Glaciol., 51(173), 313–323.

Sund, M., Eiken, T., Hagen, J.O., & Kääb, A. (2009). Svalbard surge dynamics derived from geometric changes. Annals of Glaciology, 50, 50-60.

Svendsen, J.I. and Mangerud, J. (1997): Holocene glacial and climatic variations on Spitsbergen, Svalbard. Holocene, 7: p. 45-57.

Thibert, E., Blanc, R., Vincent, C. and Eckert, N. (2008): Glaciological and volumetric mass-balance measurements: error analysis over 51 years for Glacier de Sarennes, French Alps. Journal of Glaciology, 54, 186, p. 522-532.

Tvede, A.M. and Liest¢l, O. (1977). Blomsterskardbreen, Folgefonni, mass balance and recent fluctuations. Norsk Polarinstitutt Årbok 1976, 225-234.

Uvo, C.B., 2003. Analysis and regionalization of northern European winter precipitation based on its relationship with the North Atlantic Oscillation. Int. J. Climatol. 23, 1185-1194.

Vincent, C., E. Le Meur, D. Six, and M. Funk (2005): Solving the paradox of the end of the Little Ice Age in the Alps, Geophys. Res. Lett., 32, L09706, doi:10.1029/2005GL022552.

Vincent, C., G. Kappenberger, F. Valla, A. Bauder, M. Funk, and E. Le Meur (2004): Ice ablation as evidence of climate change in the Alps over the 20th century. J. Geophys. Res., 109, D10104, doi:10.1029/2003JD003857.

Vincent, C. (2002): Influence of climate change over the 20th century on four French glacier mass balances. Journal of Geophysical Research 107, No. D19, 4375, doi:10.1029/2001JD000832.

Wanner, H., Brönnimann, S., Casty, C., Dimitrios, G., Luterbacher, J., Schmutz, C., Stephenson, D.B. and Xoplaki, E. (2001): North Atlantic Oscillation – concept and studies. Surveys in Geophysics 22: p. 321-382.

Weber, M., Braun, L., Mauser, W. and Prasch, M. (2010): Contribution of rain, snow- and icemelt in the Upper Danube discharge today and in the future. Geografia Fisica e Dinamica Quaternaria, 33, p.221-230.

Wehren, B., Weingartner, R., Schädler, B. and Viviroli, D. (2010): General Characteristics of Alpine Waters. In: Bundi, U. (ed.): Alpine Waters, Hdb Env Chem (2010) 6: 17-58, DOI 10.1007/978-3-540-88275-6_2, Springer-Verlag Berlin Heidelberg 2010.

WGMS (1989): World glacier inventory - Status 1988. Haeberli, W., Bösch, H., Scherler, K., Østrem, G. and Wallén, C. C. (eds.), IAHS (ICSI) / UNEP / UNESCO, World Glacier Monitoring Service, Zurich, Switzerland: 458 pp.

WGMS (2008): Global Glacier Changes: facts and figures. Zemp, M., Roer, I., Kääb, A., Hoelzle, M., Paul, F. and Haeberli, W. (eds.), UNEP, World Glacier Monitoring Service, Zurich, Switzerland: 88 pp.

Williams, R.S. (1986): Glacier inventory of Iceland: evaluation and use of sources data. Annals of Glaciology, 8: p. 184-191.

Wiśliński, A. (1985), Lodowczyki otoczenia Morskiego Oka w Tatrach [Glacierets in the vicinity of the Morskie Oko tarn in the Tatra Mts.], Annales Universitatis Mariae Curie-Skłodowska, 40: 55–76.

Wiśliński, A. (2002), O zmianach zasięgu niektórych płatów firnu i lodu w zlewni Morskiego Oka [On the changes within some firn and ice patches in the Morskie Oko basin], in Kotarba A. (ed.), Przyroda Tatrzańskiego Parku Narodowego a Człowiek, Tom 1 [The Nature of the Tatra National Park and Man, Volume 1], Tatrzański Park Narodowy, Zakopane; Polskie Towarzystwo Przyjaciół Nauk o Ziemi, Kraków, 71–75.

de Woul, M. & Hock, R., 2005. Static mass balance sensitivity of Arctic glaciers and ice caps using a degree-day approach. Ann. Glaciol. 42, 217–244.

Zemp, M., Jansson, P., Holmlund, P., Gärtner-Roer, I., Koblet, T., Thee, P. and Haeberli, W. (2010): Reanalysis of multi-temporal aerial images of Storglaciären, Sweden (1959-99) - Part 2: Comparison of glaciological and volumetric mass balances. The Cryosphere, 4: p. 345-357.

Zemp, M., Paul, F., Hoelzle, M. and Haeberli, W. (2008): Glacier fluctuations in the European Alps 1850–2000: an overview and spatio-temporal analysis of available data. In: Orlove, B., Wiegandt, E. and B. Luckman (eds.): The darkening peaks: Glacial retreat in scientific and social context. University of California Press: p. 152–167.

Zemp, M., Hoelzle, M. and Haeberli, W. (2007): Distributed modelling of the regional climatic equilibrium line altitude of glaciers in the European Alps. Global and Planetary Change, 56: p. 83–100,

Zemp, M., Haeberli, W., Hoelzle, M. and Paul, F. (2006): Alpine glaciers to disappear within decades? Geophysical Research Letters, 33, L13504, doi:10.1029/2006GL026319.

Zemp, M., Frauenfelder, R., Haeberli, W. and Hoelzle, M. (2005): Worldwide glacier mass balance measurements: general trends and first results of the extraordinary year 2003 in Central Europe. Data of Glaciological Studies [Materialy glyatsiologicheskih issledovanii], 99, Moscow, Russia: p. 3–12.

Zumbühl, H.J. 1976: Die Schwankungen des Unteren Grindelwaldgletschers in den historischen Bild- und Schriftquellen des 12. bis 19. Jahrhunderts. In: MESSERLI, B., ZUMBÜHL, H.J., AMMANN, K., KIENHOLZ, H., OESCHGER, H., PFISTER, C. und ZURBUCHEN, H.: Die Schwankungen des Unteren Grindelwaldgletschers seit dem Mittelalter. Zeitschrift für Gletscherkunde und Glazialgeologie XI, 1, 12-50, Innsbruck.

Publication 13

WGMS (2008a). **Global Glacier Changes: facts and figures. Zemp, M.**, Roer, I., Kääb, A., Hoelzle, M., Paul, F. & Haeberli, W. (eds.), UNEP, World Glacier Monitoring Service, Zurich, Switzerland: 88 pp.

Note that the Appendix of WGMS (2008a) is here reduced to one page. A complete version of this publication can be found on the UNEP website: http://www.grid.unep.ch/glaciers/

UNEP

Global Glacier Changes: facts and figures

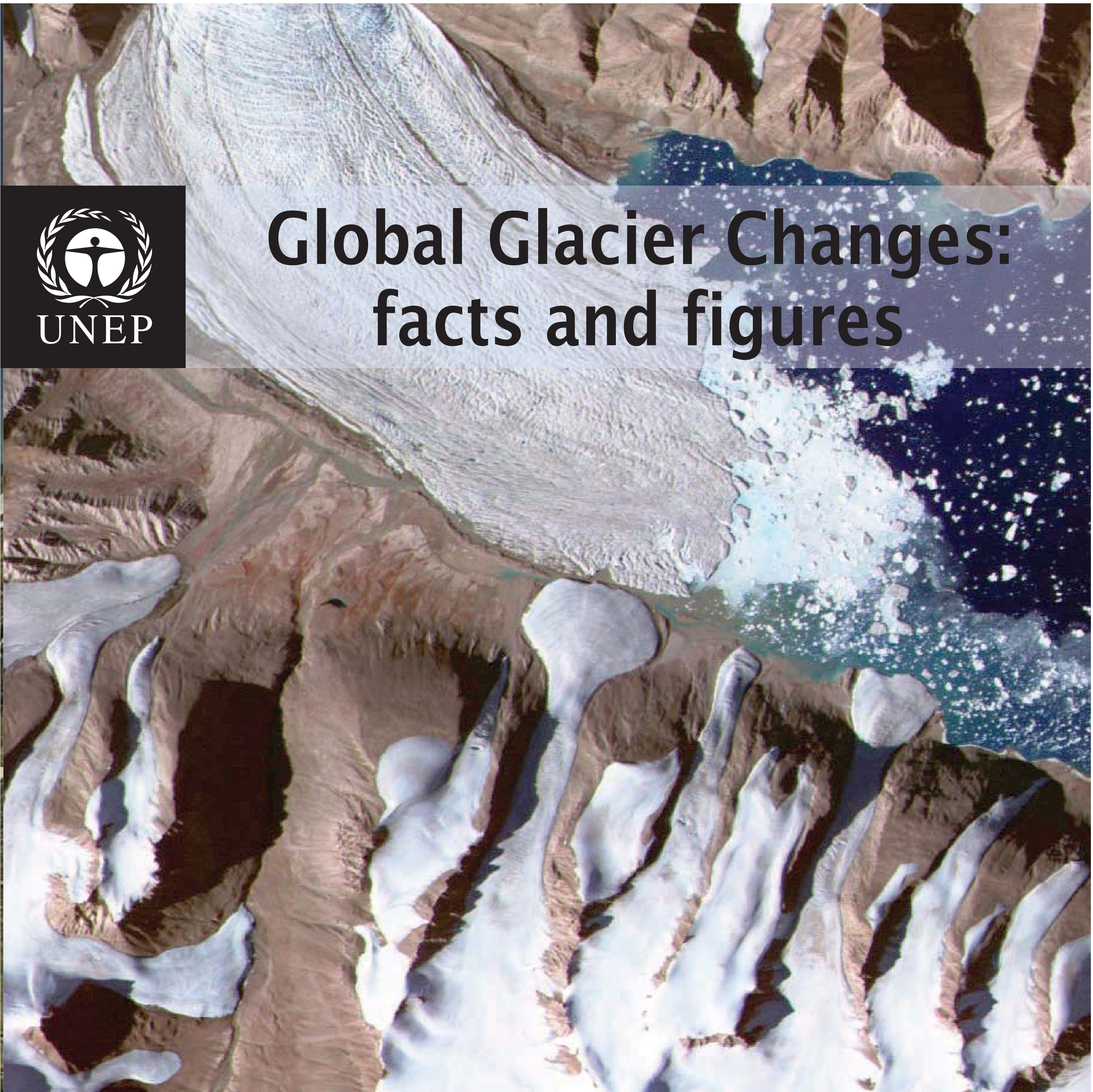

wgms
World Glacier Monitoring Service

The **United Nations Environment Programme (UNEP)**, as the world's leading intergovernmental environmental organisation, is the authoritative source of knowledge on the current state of, and trends shaping, the global environment. The mission of UNEP is to provide leadership and encourage partnership in caring for the environment by inspiring, informing, and enabling nations and peoples to improve their quality of life without compromising that of future generations.

The **World Glacier Monitoring Service (WGMS)** compiles, analyses, and publishes standardised information on the distribution and ongoing changes in the world's glaciers and ice caps. The WGMS works under the auspices of ICSU (FAGS), IUGG (IACS), UNEP, UNESCO, and WMO and maintains a collaborative network of local investigators and national correspondents in all countries involved in glacier monitoring.

ISBN: 978-92-807-2898-9
Job N°: DEW/1027/GE

Project management and editing:
Michael Zemp (*University of Zurich*)
Jaap van Woerden (*UNEP/DEWA/GRID-Europe*)

Scientific authors:
Michael Zemp (*University of Zurich*)
Isabelle Roer (*University of Zurich*)
Andreas Kääb (*University of Oslo*)
Martin Hoelzle *(University of Fribourg)*
Frank Paul (*University of Zurich*)
Wilfried Haeberli (*University of Zurich*)

Language editing:
Susan Braun-Clarke (Munich)

Design, layout, maps and graphics:
Diana Rizzolio (*UNEP/DEWA/GRID-Europe*)

The chapters on regional glacier changes and a first manuscript of the report were reviewed by glaciologists associated with the WGMS collaborative network as listed in the acknowledgements.

UNEP and the Department of Geography of the University of Zurich have provided financial support for the assessment, preparation, and publication of this report.

The front cover shows:
- an ASTER satellite image (62 x 61 km) of glaciers in Dobbin Bay on eastern Ellesmere Island, Canadian Arctic, 31 July 2000;
- Briksdalsbreen, an outlet glacier of Jostedalsbreen, Norway, in a photo comparison of the years 1995 and 2007 (Source: S. Winkler, University of Würzburg, Germany); and
- the length change curve of Briksdalsbreen, Norway (Source: WGMS).

Contents

Foreword by UNEP Executive Director

Climate change is now clearly at the top of the world's agenda. This momentum was generated in large part by the *Intergovernmental Panel on Climate Change* (IPCC), which made clear that climate change is already happening and accelerating. As a result of the remarkable efforts of last year, the international community is armed with a powerful combination of authoritative and compelling science, a far-reaching and rising tide of public concern, and powerful declarations of political will voiced at the Bali *Climate Change Conference* held in December 2007.

The *United Nations Development Programme* (UNDP) *2007/2008 Human Development Report* highlighted the devastating effects climate change is already having on the poorest and most vulnerable, making the achievement of the *Millennium Development Goals* more challenging. UNEP's flagship *Global Environment Outlook* report (GEO-4), published in October 2007, concludes that: "Tackling climate change globally will demand political will and leadership, and strong stakeholder engagement. Adaptation to the changes expected is now a global priority. Improved monitoring is needed, and it is urgent to enhance our scientific understanding of the potential tipping points beyond which reversibility is not assured."

Glaciers are a critical component of the earth' system and the current accelerated melting and retreat of glaciers have severe impacts on the environment and human well-being, including vegetation patterns, economic livelihoods, natural disasters, and the water and energy supply. Monitoring glacier changes and providing scientifically-sound, consistent and illustrative facts and figures on glaciers are therefore critical functions in today's world. Glaciers and ice caps are now also one of the *Essential Climate Variables*, a set of core variables in support of the work of organizations such as the *United Nations Framework Convention on Climate Change* (UNFCCC) and the IPCC.

Under the auspices of the *International Council for Science* (FAGS/ICSU), the *International Union of Geodesy and Geophysics* (IACS/IUGG), the *United Nations Educational, Scientific and Cultural Organisation* (UNESCO), the *World Meteorological Organisation* (WMO), and the UNEP, the *World Glacier Monitoring Service* (WGMS) collects and compiles the basic glacier data from all parts of the world and provides information on the state and trends of glaciers in almost all mountain regions. The current publication follows the *Global Outlook for Ice and Snow* that was published by UNEP at the occasion of *World Environment Day* 2007 and complements regular reports by WGMS on *Fluctuations of Glaciers* and *Glacier Mass Balances*. It presents basic information on a range of glaciers and ice caps throughout the world in a concise and illustrative format, serving as a miniature atlas on global glacier changes for a wide range of audiences.

UNEP commends the work of WGMS and partners on this very important global issue and is grateful to all those who contributed to this current comprehensive and illustrative publication on the dramatic changes affecting so many glaciers in so many parts of the world.

Achim Steiner
United Nations Under-Secretary-General and
Executive Director, United Nations Environment Programme

Foreword by WGMS Director

In 2006, a new record annual mass loss was measured on the reference glaciers under observation, whose mass balance has been recorded since the late 1940s as part of internationally coordinated glacier observation programmes. The average annual melting rate of mountain glaciers appears to have doubled after the turn of the millennium in comparison with the already accelerated melting rates observed in the two decades before. The previous record loss in the year 1998 has already been exceeded three times, i.e., in the years 2003, 2004 and 2006, with the losses in 2004 and 2006 being almost twice as high as the previous 1998 record loss. Glaciers and ice caps are indeed key indicators and unique demonstration objects of ongoing climate change. Their shrinkage and, in many cases, even complete disappearance leaves no doubt about the fact that the climate is changing at a global scale and at a fast if not accelerating rate. Anyone can see the changes in glacier extent and understand the basic physical principle of snow and ice melting as temperatures continue to rise: as the glaciers and ice caps on earth grow smaller, the energy content in the climate system and in the environment on which we depend becomes greater.

The task of scientific glacier monitoring networks is to coordinate the worldwide collection of standardised data in order to quantify the rate of change, to compare its magnitude with the range of variability during the pre-industrial times of the Holocene period, to validate projections of possible future climate change based on general circulation and regional climate models, and to anticipate and assess impacts on the environment, the economy and on society. By looking at glaciers or what is left of them, future generations will be able to discern clearly which climate scenario is being played out at the present time. The consequences of snow and ice disappearance for landscape characteristics and natural hazards in high mountain areas will be felt at local to regional scales, while the changes in the water cycle will also affect continental-scale water supply and global-scale sea levels. The degree of glacier vanishing indeed reflects the increasing distance from dynamic equilibrium conditions of the climate system.

Glaciers and ice caps constitute *Essential Climate Variables* (ECV) within the *Global Climate Observing System* (GCOS) and its terrestrial component, the *Global Terrestrial Observing System* (GTOS), as related to the *United Nations Framework Convention on Climate Change* (UNFCCC). The corresponding *Global Terrestrial Network for Glaciers* (GTN-G) is run by the *World Glacier Monitoring Service* (WGMS) at the *University of Zurich*, Switzerland, in cooperation with the *National Snow and Ice Data Center* (NSIDC) at Boulder, Colorado, and the *Global Land Ice Measurement from Space* (GLIMS) initiative. The collected data form the basis for international assessments such as IPCC, or UNEP's recent *Global Outlook for Ice and Snow*. They are frequently analysed and discussed at scientific conferences and in related publications.

It is the task and responsibility of the WGMS to collect and disseminate standardised data on glacier changes worldwide. The standards are documented in the periodical WGMS publications (*Fluctuations of Glaciers* at 5-yearly intervals and the biennial *Glacier Mass Balance Bulletin*) as well as by the corresponding forms and requests for data submission through the national correspondents and principal investigators. The present publication aims at providing a commented and illustrated overview of the distribution and development of glaciers and ice caps based on the currently available database and selected satellite imagery. It was compiled in collaboration with the WGMS network of national correspondents and principal investigators and reviewed by regional glacier experts.

Our sincere thanks go to all the colleagues and friends who generously provided materials, ideas and expertise. It is with their help and with the support of the sponsoring agencies at national and international levels that the glacier community has been able to build up, for more than a century now, a unique treasury of information on the fluctuations in space and time of glaciers and ice caps on earth.

Wilfried Haeberli
Director, World Glacier Monitoring Service

Summary

Changes in glaciers and ice caps provide some of the clearest evidence of climate change, and as such they constitute key variables for early detection strategies in global climate-related observations. These changes have impacts on global sea level fluctuations, the regional to local natural hazard situation, as well as on societies dependent on glacier meltwater. Internationally coordinated collection and publication of standardised information about ongoing glacier changes was initiated back in 1894. The compiled data sets on the global distribution and changes in glaciers and ice caps provide the backbone of the numerous scientific publications on the latest findings about surface ice on land. Since the very beginning, the compiled data has been published by the *World Glacier Monitoring Service* and its predecessor organisations. However, the corresponding data tables, formats and meta-data are mainly of use to specialists.

It is in order to fill the gaps in access to glacier data and related background information that this publication aims to provide an illustrated global view of the available data sets related to glaciers and ice caps, their distribution around the globe, and the changes that have occurred since the maximum extents of the so-called Little Ice Age (LIA).

International glacier monitoring has produced a range of unprecedented data compilations including some 36 000 length change observations and roughly 3 400 mass balance measurements for approximately 1 800 and 230 glaciers, respectively. The observation series are drawn from around the globe; however, there is a strong bias towards the Northern Hemisphere and Europe. A first attempt to compile a world glacier inventory was made in the 1970s based mainly on aerial photographs and maps. It has resulted to date in a detailed inventory of more than 100 000 glaciers covering an area of about 240 000 km^2 and in preliminary estimates, for the remaining ice cover of some 445 000 km^2 for the second half of the 20th century. This inventory task continues through the present day, based mainly on satellite images.

The moraines formed towards the end of the Little Ice Age, between the 17th and the second half of the 19th century, are prominent features of the landscape, and mark Holocene glacier maximum extents in many mountain ranges around the globe. From these positions, glaciers worldwide have been shrinking significantly, with strong glacier retreats in the 1940s, stable or growing conditions around the 1920s and 1970s, and again increasing rates of ice loss since the mid 1980s. However, on a time scale of decades, glaciers in various mountain ranges have shown intermittent re-advances. When looking at individual fluctuation series, one finds a high rate of variability and sometimes widely contrasting behaviour of neighbouring ice bodies.

In the current scenarios of climate change, the ongoing trend of worldwide and rapid, if not accelerating, glacier shrinkage on the century time scale is most likely of a non-periodic nature, and may lead to the deglaciation of large parts of many mountain ranges in the coming decades. Such rapid environmental changes require that the international glacier monitoring efforts make use of the swiftly developing new technologies, such as remote sensing and geo-informatics, and relate them to the more traditional field observations, in order to better face the challenges of the 21st century.

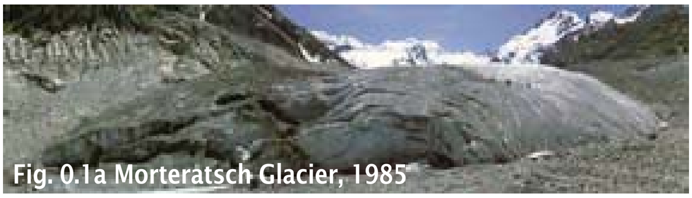

Fig. 0.1a—b Recession of Morteratsch Glacier, Switzerland, between 1985 and 2007. Source: J. Alean, *SwissEduc* (www.swisseduc.ch) / *Glaciers online* (www.glaciers-online.net).

1 Introduction

Glaciers, ice caps and continental ice sheets cover some ten per cent of the earth's land surface at the present time, whereas during the ice ages, they covered about three times this amount (Paterson 1994, Benn and Evans 1998). The present ice cover corresponds to about three-quarter of the world's total freshwater resources (Reinwarth and Stäblein 1972). If all land ice melted away, the sea level would rise by almost 65 m, with the ice sheets of Antarctica and Greenland contributing about 57 and 7 metres, respectively, and all other glaciers and ice caps roughly half a metre to this rise (IPCC 2007). Glaciers are an inherent component of the culture, landscape, and environment in high mountain and polar regions. They represent a unique source of freshwater for agricultural, industrial and domestic use, an important economic component of tourism and hydro-electric power production, yet they can also constitute a serious natural hazard. Because they are close to the melting point they react strongly to climate change, and thereby provide some of the clearest evidence of climate change and are essential variables within global climate-related monitoring programmes (GCOS 2004).

The cryosphere, derived from the Greek word *kryo* for cold, consists of snow, river and lake ice, sea ice, glaciers and ice caps, ice shelves and ice sheets, and frozen ground (Fig. 1.1). The different cryospheric components can be categorised in a) seasonal and perennial ice, b) surface and subsurface ice c) ice in the sea, in

Box 1.1 Perennial surface ice on land

Ice sheet: a mass of land ice of continental size, and thick enough to cover the underlying bedrock topography. Its shape is mainly determined by the dynamics of its outward flow. There are only two continental ice sheets in the modern world, on Greenland and Antarctica; during glacial periods there were others.

Ice shelf: a thick, floating slab of freshwater ice extending from the coast, nourished by land ice. Nearly all ice shelves are located in Antarctica.

Glacier: a mass of surface-ice on land which flows downhill under gravity and is constrained by internal stress and friction at the base and sides. In general, a glacier is formed and maintained by accumulation of snow at high altitudes, balanced by melting at low altitudes or discharge into lakes or the sea.

Ice cap: dome-shaped ice mass with radial flow, usually covering the underlying topography.

Note that drawing a distinction between ice sheets on one hand, and glaciers and ice caps on the other, is in accordance with the definition of the *Essential Climate Variables* as put forth by GCOS (2004). The term 'glacier' is used in this context as a synonym for different types of surface land ice masses including outlet glaciers, valley glaciers, mountain glaciers and glacierets.

Sources: WGMS 1989, WGMS 2005a,b, IPCC 2007, UNEP 2007.

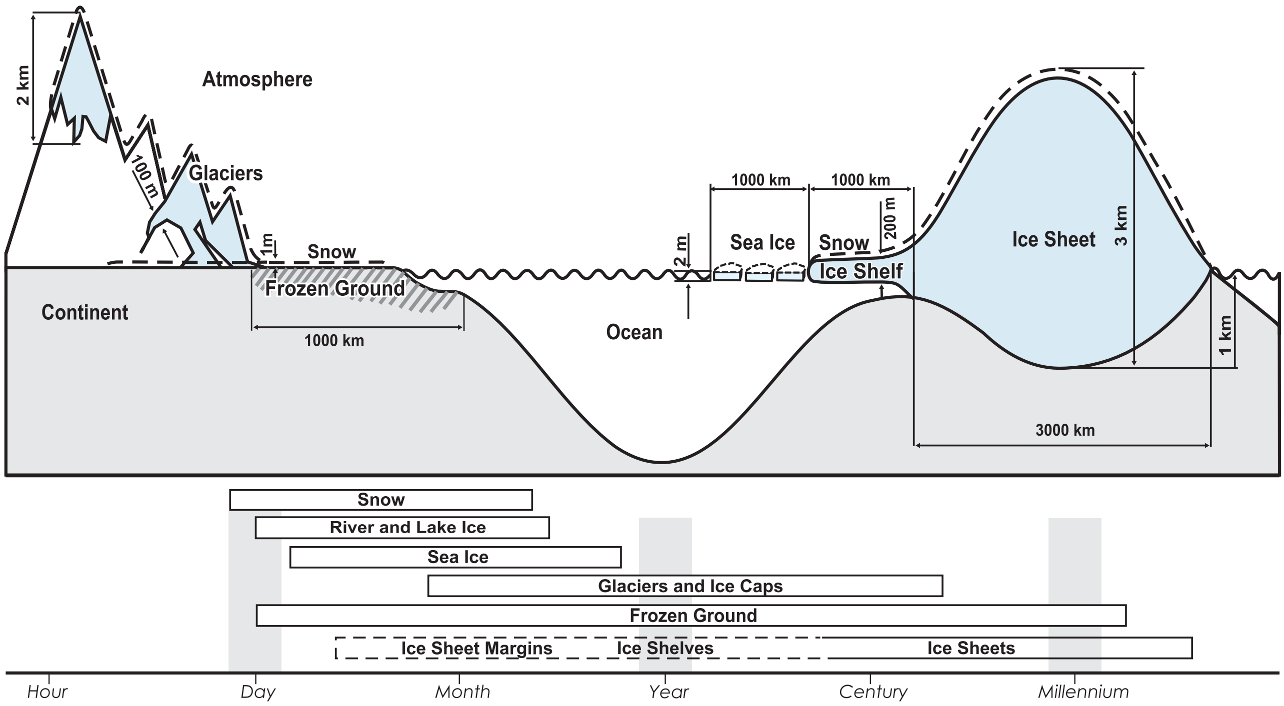

Fig. 1.1 Components of the cryosphere and their typical time scales. Source: Fig. 4.1 of IPCC (2007).

rivers, in lakes and on land. When referring to perennial surface ice on land, one usually differentiates between ice sheets, ice shelves, glaciers and ice caps (Box 1.1). There are fundamental differences in time-scales and processes involved between the different components of the perennial surface-ice on land. Due to the large volumes and areas, the two continental ice sheets actively influence the global climate over time scales of months to millennia. Glaciers and ice caps, with their smaller volumes and areas, react to climatic forcing at typical time scales from years to centuries. The focus of the present publication is on glaciers and ice caps. Good overviews on the state of knowledge concerning all cryospheric components can be found in IGOS (2007), IPCC (2007) and UNEP (2007).

Internationally coordinated glacier monitoring was initiated already as early as 1894 (Box 1.2). To the present day, the active international compilation and publication of standardised glacier data has resulted in unprecedented data sets on the distribution and changes of glaciers and ice caps. These data derived from field measurements and remote sensing provide a fundamental basis for the scientific studies which constitute the present state of knowledge on glacier changes in time and space. Usually, scientific articles report on the methods and main results of glacier investigations. The raw data and meta-data are compiled, published in standardised formats and made readily available in printed and digital form by the World Glacier Monitoring Service (WGMS) and its cooperation partners. These are the US National Snow and Ice Data Center (NSIDC), which is one of the World Data Centers for Glaciology, and the Global Land Ice Measurements from Space (GLIMS) initiative. So far, a status report on the World Glacier Inventory (WGI) was published in 1989 (WGMS 1989) whereas detailed information on glacier fluctuations has been compiled every five years (WGMS 2008, and earlier volumes) and on glacier mass balance every other year (WGMS 2007, and earlier volumes). With the exception of the latter, these products present the data in tabular form with related meta-data, usually comprehensible to specialists.

The aim of this publication is to provide an illustrated global view of (a) the available data basis related to the monitoring of glaciers and ice caps, (b) their worldwide distribution, and (c) their changes since the maximum extents of the Little Ice Age (LIA).

Box 1.2 International glacier monitoring

Worldwide collection of information about ongoing glacier changes was initiated in 1894 with the foundation of the *Commission Internationale des Glaciers* at the *6th International Geological Congress* in Zurich, Switzerland. Today, the *World Glacier Monitoring Service* (WGMS) continues the collection and publication of standardised information on distribution and ongoing changes in glaciers and ice caps. The WGMS is a service of the *International Association of the Cryospheric Sciences* of the *International Union of Geodesy and Geophysics* (IACS, IUGG) and the *Federation of Astronomical and Geophysical Data Analysis Services* of the *International Council for Science* (FAGS, ICSU) and maintains a network of local investigators and national correspondents in all the countries involved in glacier monitoring. In cooperation with the *US National Snow and Ice Data Center* (NSIDC) in Boulder and the *Global Land Ice Measurements from Space* (GLIMS) initiative, the WGMS is in charge of the *Global Terrestrial Network for Glaciers* (GTN-G) within the *Global Climate/Terrestrial Observing System* (GCOS/GTOS). GTN-G aims to combine (a) field observations with remotely sensed data, (b) process understanding with global coverage, and (c) traditional measurements with new technologies by using an integrated and multi-level monitoring strategy.

More information on the history of international glacier monitoring is found in Haeberli (2007). The GTN-G monitoring strategy is discussed in detail in Haeberli et al. (2000) and Haeberli (2004), with updates on the present state in the biennial GTOS reports (GTOS 2006, GTOS 2008), and illustrated using the example of the European Alps in Haeberli et al. (2007).

Federation of Astronomical and Geophysical Data Analysis Services: www.icsu-fags.org

Global Land Ice Measurements from Space: www.glims.org

Global Terrestrial Network for Glaciers: www.fao.org/gtos/gt-netGLA.html

Global Climate Observing System: www.wmo.ch/pages/prog/gcos/

Global Terrestrial Observing System: www.fao.org/gtos/

International Association of Cryospheric Sciences: www.cryosphericsciences.org

United Nations Environment Programme: www.unep.org

United Nations Educational, Scientific and Cultural Organization: www.unesco.org

US National Snow and Ice Data Center: www.nsidc.org

World Glacier Monitoring Service: www.wgms.ch

World Meteorological Organization: www.wmo.ch

2 Glaciers and climate

Glaciers generally form where snow deposited during the cold/humid season does not entirely melt during warm/dry times. Temperate glaciers not influenced by thick debris cover, calving or surge instabilities are recognised as being among the best climate indicators as their reaction or change provide a signal that is easily understandable to a wider public.

Glaciers form where snow is deposited during the cold/humid season and does not entirely melt during warm/dry periods. This seasonal snow gradually densifies and transforms into perennial firn and finally, after the interconnecting air passages between the grains are closed off, into ice (Paterson 1994). The ice from such accumulation areas then flows under the influence of its own weight and the local slopes down to lower altitudes, where it melts again (ablation areas). Accumulation and ablation areas are separated by the equilibrium line, where the balance between gain and loss of mass is exactly zero. Glacier distribution is thus primarily a function of mean annual air temperature and annual precipitation sums modified by the terrain which influences, for example, the amount of incoming net radiation or the accumulation pattern.

In humid-maritime regions, the equilibrium line is at (relatively) low altitude with warm temperatures and long melting seasons, because of the large amount of ablation required to eliminate thick snow layers (Shumskii 1964, Haeberli and Burn 2002). 'Temperate' glaciers with firn and ice at melting temperature dominate these landscapes. Such ice bodies, with relatively rapid flow, exhibit a high mass turnover and react strongly to atmospheric warming by enhanced melt and runoff. Features of this type are the Patagonian Icefields and the ice caps of Iceland, as well as the glaciers of the western Cordillera of North America, the western mountains of New Zealand (Fig. 2.1) and Norway. The lower parts of such maritime-temperate glaciers may extend into forested valleys, where summer warmth and winter snow accumulation prevent development of permafrost. In contrast, under dry-continental conditions, such as in parts of Antarctica (Fig. 2.2), northern Alaska, Arctic Canada, subarctic Russia, parts of the Andes near the Atacama desert, and in many Central Asian mountain chains, the equilibrium line may be at (relatively) high elevation with cold temperatures and short melting seasons. In such regions, glaciers lying far above the tree line can have polythermal as well as cold firn/ice well below melting temperature, also a low mass turnover, and are often surrounded by permafrost (Shumskii 1964).

The reaction of a glacier to a climatic change involves a complex chain of processes (Nye 1960, Meier 1984). Changes in atmospheric conditions (solar radiation, air temperature, precipitation, wind, cloudiness, etc.) influence the mass and energy balance at the glacier surface (see Kuhn 1981, Oerlemans 2001). Air temperature thereby plays a predominant role as it is related to the long-wave radiation balance, turbulent heat exchange and solid/liquid precipitation. Over time periods of years to several decades, cumulative changes in mass

Fig. 2.1 Franz-Josef Glacier, New Zealand, is a temperate valley glacier in a maritime climate descending into rain forest. Source: M. Hambrey, *SwissEduc* (www.swisseduc.ch).

Fig. 2.2 Commonwealth Glacier, Taylor Valley, Antarctica, is a cold glacier in a continental climate (10 January 2007). In the background Canada Glacier and frozen Lake Fryxell are shown. Source: D. Stumm, *University of Otago*, New Zealand.

Fig. 2.2 Commonwealth Glacier, 2007

balance cause volume and thickness changes, which in turn affect the flow of ice via altered internal deformation and basal sliding. This dynamic reaction finally leads to glacier length changes, the advance or retreat of glacier tongues. In short, the advance or retreat of glacier tongues (i.e., the 'horizontal' length change) constitutes an indirect, delayed and filtered but also enhanced and easily observed signal of climatic change, whereas the glacier mass balance (i.e., the 'vertical' thickness change) is a more direct and undelayed signal of annual atmospheric conditions (Haeberli 1998). The described complication involved with the dynamic response disappears if the time interval analysed is sufficiently long, i.e., longer than it takes a glacier to complete its adjustment to a climatic change (Jóhannesson et al. 1989, Haeberli and Hoelzle 1995). Cumulative length and mass change can be directly compared over such extended time periods of decades (Hoelzle et al. 2003). Different behaviours are encountered at heavily debris-covered glaciers with reduced melting and strongly limited 'retreat', glaciers ending in deep water bodies causing enhanced melting and calving, and glaciers periodically undergoing mechanical instability and rapid advance ('surge') after extended periods of stagnation and recovery. Glaciers (those not affected by these special conditions) are recognised to be among the best indicators within global climate related monitoring (Box 2.1). They gradually convert a small change in climate, such as a temperature change of 0.1°C per decade over a longer time period, into a pronounced length change of several hundred metres or even kilometres.

Box 2.1 Glaciers as climate indicator

Glacier changes are recognised as high-confident climate indicator and as a valuable element in early detection strategies within the international climate monitoring programmes (GCOS 2004, GTOS 2008). Fluctuations of a glacier, which are not influenced by thick debris covers, calving or surge instabilities, are a reaction to climatic forcing. Thereby, the glacier length change (i.e., the advance or retreat) is the indirect, delayed, filtered but also enhanced signal to a change in climate, whereas the glacier mass balance (i.e., the change in thickness/volume) is the direct and un-delayed response to the annual atmospheric conditions (Haeberli and Hoelzle 1995). The mass balance variability of glaciers is well correlated over distances of several hundred kilometres and with air temperature (Lliboutry 1974, Schöner et al. 2000, Greene 2005). However, the glacier mass balance change provides an integrative climatic signal and the quantitative attribution of the forcing to individual meteorological parameters is not straight forward. The energy and mass balance at the glacier surface is influenced by changes in atmospheric conditions (e.g., solar radiation, air temperature, precipitation, wind, cloudiness). Air temperature thereby plays a predominant role as it is related to the radiation balance, turbulent heat exchange and solid/liquid precipitation ratio (Kuhn 1981, Ohmura 2001). The climatic sensitivity of a glacier not only depends on regional climate variability but also on local topographic effects and the distribution of the glacier area with elevation, which can result in two adjacent glaciers featuring different specific mass balance responses (Kuhn et al., 1985). As a consequence, the glacier sensitivity to a climatic change is much related to the climate regime in which the ice is located. The mass balance of temperate glaciers in the mid-latitudes is mainly dependent on winter precipitation, summer temperature and summer snow falls (temporally reducing the melt due to the increased albedo; Kuhn et al. 1999). In contrast, the glaciers in the low-latitudes, where ablation occurs throughout the year and multiple accumulation seasons exist, are strongly influenced by variations in atmospheric moisture content which affects incoming solar radiation, precipitation and albedo, atmospheric longwave emission, and sublimation (Wagnon et al. 2001, Kaser and Osmaston 2002). In the Himalaya, influenced by the monsoon, most of the accumulation and ablation occurs during the summer (Ageta and Fujita 1996, Fujita and Ageta 2000). Cold glaciers in high altitude and the polar regions can receive accumulation in any season (Chinn 1985). As described in the text, strongly diverse mass balance characteristics also exist between glaciers under dry-continental conditions and in maritime regions. As a consequence, analytical or numerical modelling is needed to quantify the above mentioned topographic effects as well as to attribute the glacier mass changes to individual meteorological or climate parameters (e.g., Kuhn 1981, Oerlemans 2001). Modelling is further needed in combination with measured and reconstructed glacier front variations, to compare the present mass changes with the (pre-) industrial variability (e.g. Haeberli and Holzhauser 2003).

3 Global distribution of glaciers and ice caps

A first attempt to compile a world glacier inventory started in the 1970s based mainly on aerial photographs and maps. Up to now, it resulted in a detailed inventory of more than 100 000 glaciers covering an area of about 240 000 km², and in preliminary estimates for the remaining ice cover of some 445 000 km². Today the task of inventorying glaciers worldwide is continued for the most part based on satellite images.

The need for a worldwide inventory of existing perennial ice and snow masses was first considered during the *International Hydrological Decade* declared by UNESCO for the period of 1965–1974 (Hoelzle and Trindler 1998, UNESCO 1970). The *Temporal Technical Secretariat for the World Glacier Inventory* (TTS/WGI) was established in 1975 to prepare guidelines for the compilation of such an inventory and to collect available data sets from different countries (WGMS 1989). These tasks were continued by its successor organisation, the WGMS, after 1986. In 1989, a status report on the WGI was published including detailed information on about 67 000 glaciers covering some 180 000 km² and preliminary estimates for the other glacierised regions, both based on aerial photographs, maps, and satellite images (WGMS 1989). The detailed inventory includes tabular information about geographic location, area, length, orientation, elevation and classification of morphological type (a selection of different types is shown in Figures 3.2–3.5, and more in the other chapters) and moraines, which are related to the geographical coordinates of glacier label points. Due to the different data sources, the entries of the WGI do not refer to one specific year but can be viewed as a snapshot of the glacier distribution around the 1960s. The average map year is 1964 with a standard deviation of eleven years, and a time range from 1901 to 1993. In 1998, the WGMS and the NSIDC agreed to work together, pooled their data sources and made the inventory available online in 1999 via the NSIDC website (Box 3.1). Since then, several plausibility checks, subsequent data corrections and updates of the inventory have been carried out, including updates and new data sets from the former Soviet Union and China. At present the database contains information for over 100 000 glaciers throughout the world with an overall area of about 240 000 km² (NSIDC 2008). This corresponds to about half of the total number and roughly one-third of the global ice cover of glaciers and ice caps, which are estimated at 160 000 and 685 000 km², respectively, by Dyurgerov and Meier (2005) based mainly on the WGI (WGMS 1989) and additional estimates from the literature.

In 1995, the GLIMS initiative was launched, in close collaboration with the NSIDC and the WGMS, to continue the inventorying task with space-borne sensors as a logical extension of the WGI and storing the full complement of the WGMS-defined glacier characteristics (see Kääb et al. 2002, Bishop et al. 2004, Kargel et al. 2005). GLIMS is designed to monitor the world's glaciers primarily using data from optical satellite instruments, such as the *Advanced Spaceborne Thermal Emission and reflection Radiometer* (ASTER), an instrument that is required on board of Terra satellite (Box 3.2). A geographic infor-

Box 3.1 Online data access to the WGI and GLIMS databases

The ***World Glacier Inventory*** **(WGI)** currently has detailed information on over 100 000 glaciers throughout the world. Parameters within the inventory include coordinates (latitude and longitude) per glacier, together with tabular information about geographic location, area, length, orientation and elevation, as well as classifications of morphological type and moraines. The entire database can be searched by entering attributes and geographical location. The data sets thus selected or the entire database can be downloaded via the websites of the NSIDC, the WGMS, or of the *GLIMS glacier database.*

The ***GLIMS Glacier Database*** stores some 62 000 digital glacier outlines together with tabular information such as glacier area, length and elevation. The database can be queried using a text or mapping search interface. Glacier outlines with the related information can be downloaded from the GLIMS website in several formats used by geographic information system software products.

WGI at NSIDC: http://nsidc.org/data/glacier_inventory/index.html
WGI at WGMS: http://www.wgms.ch/wgi.html
GLIMS Glacier Database: http://glims.colorado.edu/glacierdata/

Box 3.2 ASTER satellite images

Satellite data are an important resource for global-scale glacier monitoring. They enable the observation of land ice masses over large spatial scales using a globally uniform set of data and methods, and independent of monitoring obstacles on the ground such as access problems and financial limitations on institutional levels. On the other hand, space-aided glacier monitoring relies on a small number of space agencies, the financial resources and political willingness of which are thus crucial for the maintenance of the monitoring system. Typical glaciological parameters that can be observed from space are glacier areas and their changes over time, snow lines, glacier topography and glacier thickness changes, and glacier flow and its changes over time (Kääb 2005).

The satellite images in this publication were taken by the *US/Japan Advanced Thermal Emission and Reflection Radiometer* (ASTER) onboard the *NASA Terra* spacecraft. They were acquired within the *Global Land Ice Measurements from Space* (GLIMS) initiative and obtained through the *US Geological Survey/NASA EOS* data gateway. The ASTER sensor includes two spectral bands in the visible range (green and red), one band in the near-infrared, six bands in the short-wave infrared, and five bands in the thermal infrared. The most important bands for glaciological applications are the visible, near- and short-wave infrared bands (Fig. 3.1 a–d). They allow for automatic mapping of ice and snow areas. This technique exploits the large difference in ice and snow reflectivity between the visible, near- and short-wave infrared spectrum, and enables the fast compilation of a large number of glacier outlines and their changes over time. In addition to the above-mentioned nadir bands, ASTER has also a back-looking stereo sensor that, together with the corresponding nadir image, allows for the photogrammetric computation of glacier topography and its changes over time (Kääb 2005).

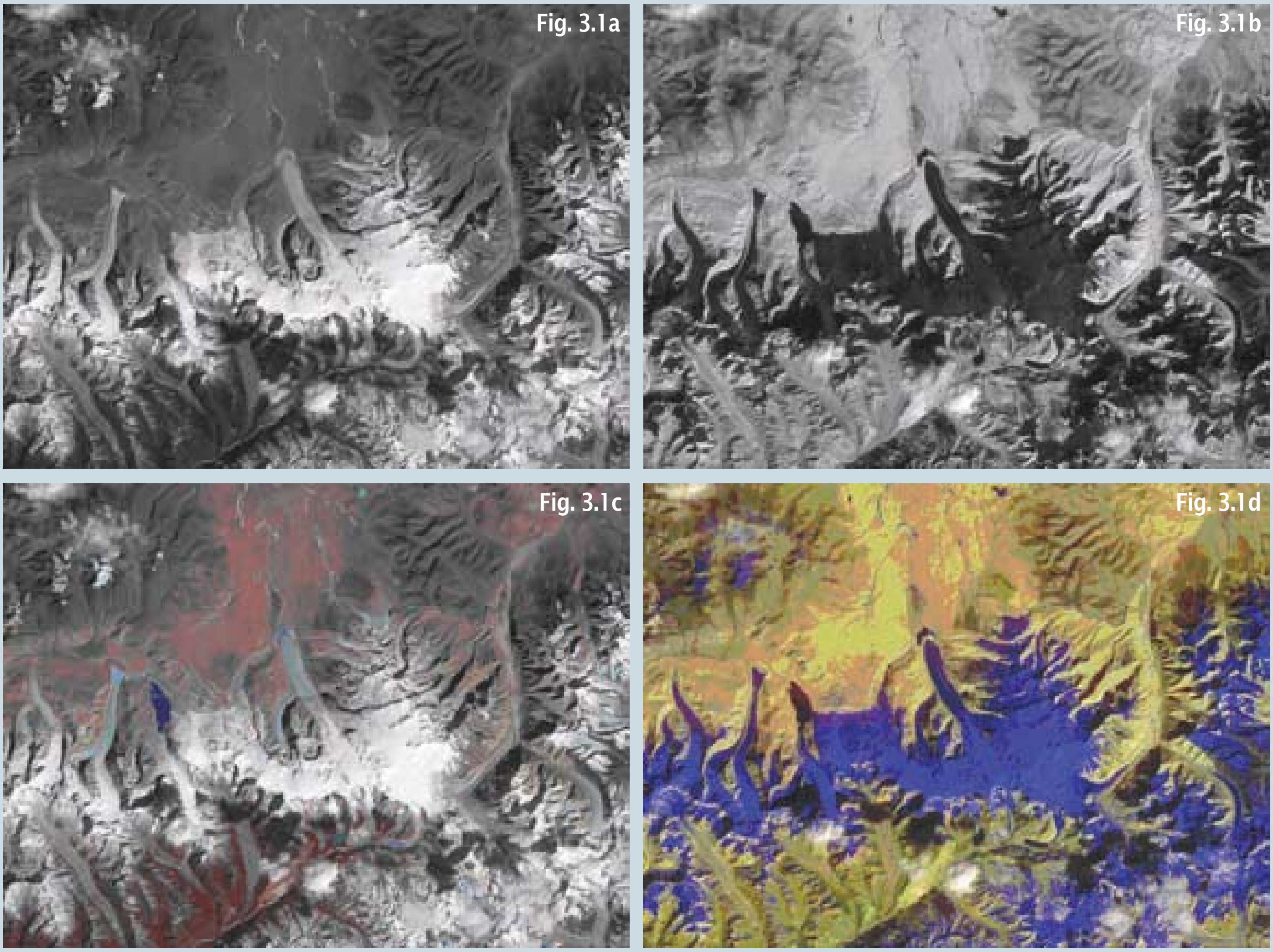

Fig. 3.1 a—d Glaciers in Bhutan, Himalayas (57x42 km): a) green ASTER band, b) shortwave-infrared, c) colour composite of the green, red and near-infrared bands, and d) colour composite of red, near-infrared and short-wave infrared bands.


Fig. 3.2 Gaisberg- and Rotmoosferner


Fig. 3.3 Piedmont glaciers


Fig. 3.4 Jostedalsbreen (ice cap) with outlet glaciers


Fig. 3.5 Balfour Glacier

mation system, including database and web interfaces, has been designed and implemented at the NSIDC in order to host and distribute the information from the WGI and the new GLIMS databases (Raup et al. 2007). In addition to the point information of the WGI, the GLIMS database now contains digital outlines on over 62 000 glaciers (status as of May, 2008). A global overview of the distribution of glaciers and ice caps as well as available datasets is given in Figure 3.6. New projects, such as the *International Polar Year* (IPY; www.ipy.org) and the *GlobGlacier* project, a data user element activity within the *European Space Agency* (Volden 2007), aim at making a major contribution to the current WGMS and GLIMS databases.

At first glance it might be surprising to find that after more than three decades of cryosphere observation from space (see IGOS 2007) there is still no complete detailed inventory of the world's glaciers and ice caps. Glacier mapping techniques from threshold ratio satellite images have been developed and automated to a high degree (Paul et al. 2002). However, fully automated inventorying of individual glaciers is hampered by challenges encountered with topographic shadowing effects, debris-covered and calving glaciers, clouds and snow separation as well as with the location of ice divides. A high quality inventory of glaciers and ice caps from both aerial photographs and satellite images still needs to be operated by a well-trained glaciologist. Empirical values of completed glacier inventories based on satellite images (e.g., Paul and Kääb 2005), indicate average operation times of five minutes per glacier for the semi-automatic detection of ice outlines as well as manual correction of errors due to shading and debris cover, and another five minutes per glacier for the delineation of individual glacier catchments, neither including the compilation of useful satellite images nor the rectification and restoration of the scenes (see Lillesand and Kiefer 1994).

The latest assessment report of IPCC (2007) quotes the total area of land ice and corresponding potential sea level rise at 510 000–540 000 km^2 and at 150–370 mm, respectively (Table 3.1). These estimates – as noted in IPCC (2007) – do not include ice bodies around the ice sheets in Greenland and Antarctica. Preliminary rough

Fig. 3.2 Gaisbergferner (left) and Rotmoosferner (right), Austria (July 2002). These typical valley glaciers were connected during the last ice age (transfluence zone in the centre of the photograph). Source: I. Roer, *University of Zurich*, Switzerland.

Fig. 3.3 Piedmont glaciers in southern Axel Heiberg Island, Canadian Arctic. Aerial photograph (1977). Source: J. Alean, *SwissEduc* (www.swisseduc.ch) / *Glaciers online* (www.glaciers-online.net).

Fig. 3.4 Jostedalsbreen, Norway, is a typical ice cap with several outlet glaciers, e.g., Nigardsbreen in the centre of the aerial photography of 1982. Source: Photo of unknown photographer provided by the archive of the *Norwegian Water Resources and Energy Directorate* (NVE).

Fig. 3.5 Debris-covered tongue of Balfour Glacier, New Zealand. Source: M. Hoelzle, *University of Zurich*, Switzerland.

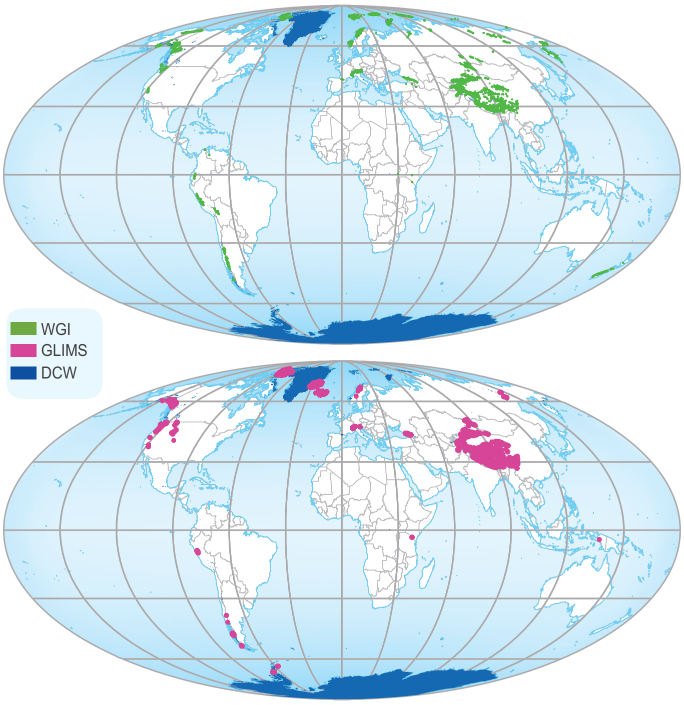

Fig. 3.6 Global glacier inventories

Table 3.1 Ice sheets, ice shelves, glaciers and ice caps

Cryospheric Component	Area (mio km²)	Ice volume (mio km³)	Potential sea level rise (m) [e]
Glaciers and ice caps			
- smallest estimate [a]	0.51	0.05	0.15
- largest estimate [b]	0.54	0.13	0.37
Ice shelves [c]	1.50	0.70	~0
Ice sheets			
- Greenland [d]	1.7	2.9	7.3
- Antarctica [c]	12.3	24.7	56.6

Notes:
[a] Ohmura (2004); glaciers and ice caps surrounding Greenland and Antarctica are excluded; [b] Dyurgerov and Meier (2005); glaciers and ice caps surrounding Greenland and Antarctica are excluded; [c] Lythe et al. (2001); [d] Bamber et al. (2001); [e] Assuming an oceanic area of 3.62 × 100 mio km², an ice density of 917 kg/m³, a seawater density of 1 028 kg/m³, and seawater replacing grounded ice below sea level.

Source: IPCC (2007), Table 4.1

estimates of the ice cover of glaciers and ice caps, surrounding the continental ice sheets, are 70 000 km² in Greenland based on Weidick and Morris (1998) and ranges between 70 000 km² (Weidick and Morris 1998) and 169 000 km² (Shumsky 1969) for Antarctica. Hence the values indicated in the table (Table 3.1) of the IPCC report (2007), represent minimum values of the global area of glaciers and ice caps as well as their potential contribution to sea level rise.

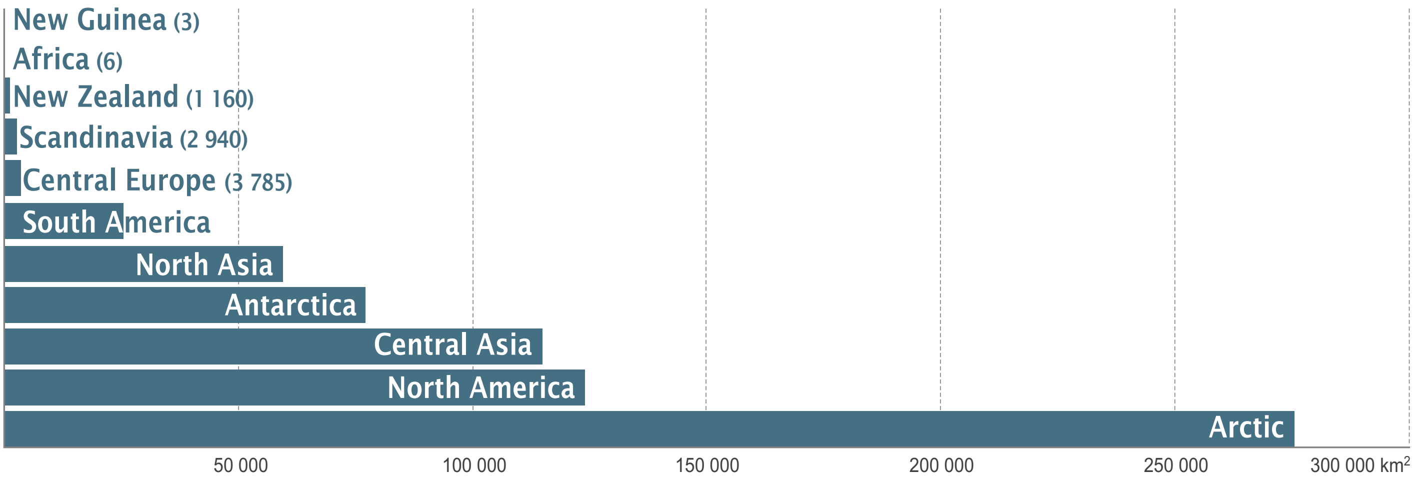

Fig. 3.7 Regional overview of the distribution of glaciers and ice caps

Fig. 3.6 Worldwide distribution of perennial surface ice on land. The map shows the approximate distribution of glaciers, ice caps and the two ice sheets from ESRI's Digital Chart of the World (DCW), overlaid by the point layer of the *World Glacier Inventory* (WGI) and the polygons of the *Global Land Ice Measurements from Space* (GLIMS) databases (status June 2008).

Fig. 3.7 Regional overview of the distribution of glaciers and ice caps. Source: Dyurgerov and Meier (2005).

Table 3.1 Area, volume and sea level equivalent of glaciers and ice caps, ice shelves and the two continental ice sheets as given in the latest report of the Intergovernmental Panel on Climate Change. The values for glaciers and ice caps denote the smallest and largest estimates, excluding the ice bodies surrounding the ice sheets on Greenland and Antarctica. Source: IPCC (2007), Table 4.1

4 Glacier fluctuation series

The internationally coordinated collection of information on glacier changes has resulted in unprecedented compilations of data including some 36 000 length change observations and roughly 3 400 mass balance measurements for about 1 800 and 230 glaciers, respectively. The observation series are located around the globe, with a bias towards the Northern Hemisphere and in particular Europe.

Since the very beginning of the internationally coordinated glacier monitoring activities in 1894, the collected data on glacier fluctuations has been published in written reports. The Swiss limnologist François-Alphonse Forel started the periodical publishing of the *Rapports sur les variations périodiques des glaciers* (Forel 1895) on behalf of the then established *Commission Internationale des Glaciers*, which later developed into the *International Commission on Snow and Ice*, and in 2007 into the *International Association of Cryospheric Sciences* (see Radok 1997, Jones 2008). Up to 1961, the data compilations constituting the main source of glacier length change (Box 4.1) data worldwide were published in French, Italian, German, and English; since 1967, all publications appear in English (Haeberli 1998). The first reports contain mainly qualitative observations, with the exception of the glaciers in the Alps and Scandinavia, which have been well documented by quantitative measurements right from the start (Forel and Du Pasquier 1896, 1897; Richter 1898, 1899, 1900; Finsterwalder and Muret 1901, 1902, 1903; Reid and Muret 1904, 1905, 1906; Brückner and Muret 1908, 1909, 1910, 1911; Rabot and Muret 1911, 1912, 1913; Rabot and Mercanton 1913; Hamberg and Mercanton 1914). After the First World War, Mercanton edited the publications which appeared less frequently (Mercanton 1930, 1934, 1936, 1948, 1952, 1954, 1958, 1961). Starting with 1967, the data have been published in five-yearly intervals under the Fluctuations of Glaciers series, first by the *Permanent Service on the Fluctuations of Glaciers* (PSFG 1967, 1973, 1977, 1985) and, after the merger of the PSFG with the *Temporal Technical Secretariat* (TTS)/WGI in 1986, by the WGMS (1988, 1993a, 1998, 2005a, 2008). In 1945, annual

Fig. 4.1 Sketch explaining the measurement of the glacier front position as published by Forel (1895).

Fig. 4.2 Length change measurement at Steinlimmi Glacier, Switzerland. An investigator determines the direction from a marked boulder in the forefield to the glacier terminus. Source: S. Kappeler, Switzerland.

Box 4.1 Measurement of glacier length changes

The basic principle behind the measurement of horizontal changes in the position of the glacier terminus is very simple and was already illustrated in the *Instruction pour l'observation des variations des glaciers* by Forel (1895).

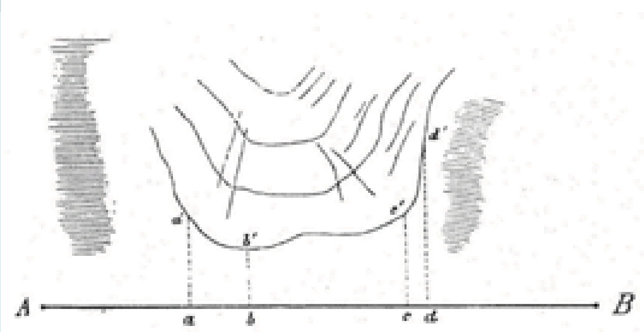

Fig. 4.1 Front position measurement (Forel 1895)

The distance and direction from fixed positions in the glacier forefield (such as landmarks, cairns and boulders) to the ice front are measured in metres and compared to the values of the previous year(s). Historically the measurements have been carried out using tape and compass, and over the past years increasingly by means of universal surveying instruments and global positioning systems. Ideally the cumulative annual length change measurements of a glacier are compared with decadal length changes as derived from aerial photographs or satellite images.

Fig. 4.2 Length change measurement at Steinlimmi Glacier

Fig. 4.3 Drilling of an ablation stake

Box 4.2 Measurement of glacier mass balance

The WGMS collects and publishes mass balance data of glaciers and ice caps from direct glaciological and geodetic methods. The direct glaciological method is based on field measurements of the change in glacier surface elevation between two dates at a network of ablation stakes, snow pits and snow probings. The differences in elevation, i.e. gain or loss, are multiplied by (measured or estimated) density of snow, firn or ice to units in metre water equivalent (m w.e.) and then interpolated over the entire glacier by a set of methods. The mass change calculated in this way corresponds to the total meltwater runoff in cubic m w.e. of the measurement period. Division of the total mass change by the glacier area yields the specific glacier mass balance which corresponds to the mean glacier thickness change in m w.e. and can be compared directly between different glaciers. The measurement and calculation of glacier mass balance contains various sources of systematic and random errors and uncertainties (see Gerbaux et al. 2005 and references therein). This requires checking against the independent geodetic methods which derive decadal volume changes from repeated mapping of the glacier topography.

Detailed explanations on how to measure glacier mass balance are found in the manuals of Østrem and Stanley (1969), Østrem and Brugman (1991), and Kaser et al. (2003).

mass balance measurements (Box 4.2) over an entire glacier with the direct glaciological method (cf. Østrem and Brugman 1991), based on an extensive net of ablation stakes, snow pits and snow probing, were initiated on Storglaciären, Sweden (Holmlund and Jansson 2005). This new type of data has been included, together with detailed meta-data in tabular form, in the *Fluctuations of Glaciers* series since the very first volume (PSFG 1967). As a consequence of the rising interest in and in order to accelerate the access to the glacier mass balance information, preliminary values on the specific annual mass balance as well as on the equilibrium line altitude and the accumulation area ratio have been published in the bi-annual *Glacier Mass Balance Bulletin* (WGMS 1991, 1993b, 1994, 1996, 1999, 2001, 2003, 2005b,

Fig. 4.4 Accumulation measurements in a snow pit

Fig. 4.3 Drilling of an ablation stake. Source: D. Vonder Mühll, *University of Zurich*, Switzerland.

Fig. 4.4 Accumulation measurements in a snow pit. Source: M. Hoelzle, *University of Zurich*, Switzerland.

2007). Based on an agreement with the Terrestrial Observation Panel for Climate of GCOS/GTOS, preliminary glacier mass balance results have been made available annually on the WGMS website since 1999, as of one year after the end of the measurement period.

In 1989, an initial attempt was made to set up a glaciological database with the data collected and published in the WGI and in the *Fluctuations of Glaciers* series as well as those compiled from the literature (Hoelzle and Trindler 1998, Hoelzle et al. 2003). Nowadays, all data is available digitally, either directly from the website or on email request (Box 4.3). Online meta-data browsers provide an overview of the location of glaciers with available data and corresponding attributes. Table 4.1 gives an overview of the number of length change and mass balance series carried out in 11 macro-regions (see Fig. 6.0.1). Global maps of available length change and mass balance data series are given in Figures 4.6 and 4.7, respectively. A temporal overview of the reported fluctuation data is shown in Figure 4.8.

Length change measurements have been reported to WGMS from 1 803 glaciers worldwide, including a total 36 240 observations. At the global level, the average measurement series covers a time range of 47 years with 20 observations. Of all the glacier tongues observed, 85 per cent are located on the northern hemisphere and 42 per cent in Central Europe. On the global average, there are between two and three glaciers with available length change data per 1 000 km^2 of glacierised area. Highest observation densities are found in Central Europe with over 200 series per 1 000 km^2, followed by New Zealand (85 series per 1 000 km^2), Scandinavia (23 series per 1 000 km^2), and South America (three series per 1 000 km^2). The other macro-regions do have less dense observation networks with fewer than three series per 1 000 km^2. The virtual high observation densities in Africa and New Guinea are due to the minimal ice area in these regions. Earliest field observations of glacier length changes started in the late 19th century and often extended with measured distances from the glacier termini to the LIA moraines. The best temporal observation coverage is again found in Central Europe with an average time range of 65 years and a mean of 35 observations per data series, and in Scandinavia with 53 years and 30 observations. The length change data from the Arctic amount also to a mean of over 30 observations per series, which is mainly thanks to the long-term programmes reported from Iceland, whereas the corresponding numbers from

Box 4.3 Submission and request for glacier fluctuation data

The WGMS regularly collects data on changes in glacier length, area, thickness and volume for publication in the *Fluctuations of Glaciers* and the *Glacier Mass Balance Bulletin* series. Corresponding calls-for-data are sent out through the national correspondents of WGMS who organise the collection and submission of the glacier data in line with the WGMS standards. Apart from the official calls-for-data, the WGMS welcomes any information on glacier changes that is submitted according to the standards described in the submission guidelines on the WGMS website. All data hosted by the WGMS is available on request in digital form and at no charge. In addition to the review of collected data sets presented here, online meta-data browsers on the WGMS website provide updated overviews of the available information.

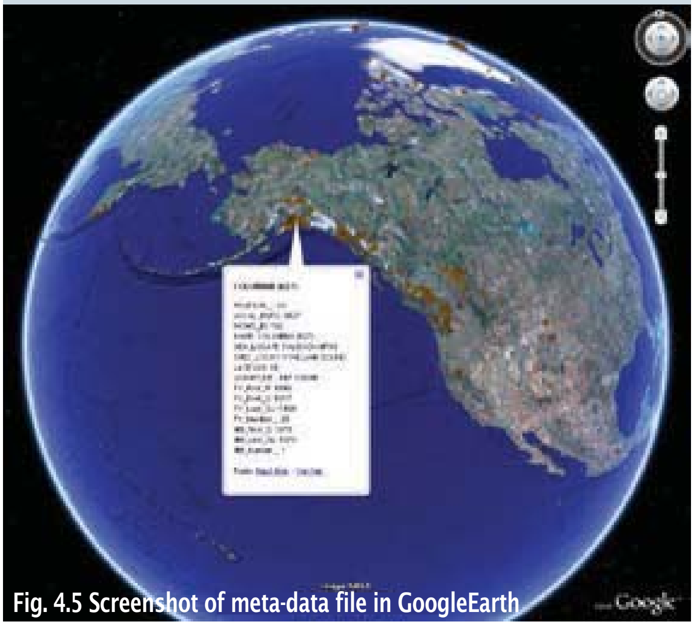

Fig. 4.5 Screenshot of meta-data file in GoogleEarth

Fig. 4.5 Screenshot of meta-data file in GoogleEarth. Meta-data file with information about available glacier fluctuation data displayed in Google Earth application.

Table 4.1 Global and regional overview of the distribution of glaciers and ice caps as well as of reported length change and mass balance observation series. Source: Macroregions and ice cover areas (in sq km) after Dyurgerov and Meier (2005); information on glacier fluctuations from WGMS.

Table 4.1 Global and regional overview of the available length change and mass balance observations

Macroregion	Area	FRONT VARIATION								MASS BALANCE						
		NoSer	NoSer 21th	First RY	First SY	Last SY	AvTR	AvNo Obs	SerDens	NoSer	NoRef Ser	NoSer 21st	First SY	Last SY	AvNo Obs	Ser Dens
New Guinea	3	3	0	1936	1941	1990	46.3	4.7	1000.0	0	0	0				0.0
Africa	6	14	11	1893	1899	2004	71.4	6.1	2333.3	1	0	0	1979	1996	18.0	166.7
New Zealand	1160	99	70	1879	1892	2005	14.4	6.2	85.3	3	0	1	1959	2005	2.7	2.6
Scandinavia	2940	67	45	1896	1899	2005	53.2	30.2	22.8	39	8	23	1946	2005	16.3	13.3
Central Europe	3785	764	417	1730	1815	2005	65.1	35.3	201.8	43	10	29	1948	2005	19.6	11.4
South America	25500	160	49	1830	1888	2005	36.4	4.1	6.3	11	1	9	1976	2005	8.1	0.4
Northern Asia	59600	24	11	1833	1895	2005	55.2	14.1	0.4	14	3	5	1962	2005	13.5	0.2
Antarctica	77000	48	7	1882	1883	2004	30.4	2.8	0.6	1	0	1	2002	2005	4.0	0.0
Central Asia	114800	310	16	1850	1893	2005	21.5	4.5	2.7	35	2	6	1957	2005	13.1	0.3
North America	124000	221	15	1720	1885	2005	36.9	5.2	1.8	45	4	24	1953	2005	15.8	0.4
Arctic	275500	93	49	1840	1886	2005	52.4	30.5	0.3	34	2	20	1960	2005	12.6	0.1
Worldwide	684294	1803	690	1720	1815	2005	46.7	20.1	2.6	226	30	118	1946	2005	15.0	0.3

Notes:
NoSer: number of series; NoSer21th: number of series with last survey after 1999; FirstRY: first reference year; FirstSY: first survey year; LastSY: last survey year; AvTR: average time range per series; AvNoObs: average number of observations per series; SerDens: number of series per 1 000 square kilometre; NoRefSer: number of 'reference' mass balance series with continuous measurements since 1976.

the Canadian Arctic and Greenland are much lower. The 24 series from Northern Asia on average comprise 14 measurements. The temporal observation density is rather limited in other macro-regions with an average of six or fewer observations per series. A striking feature is the breakdown of the field monitoring network towards the end of the 20th century in North America as well as in Central Asia. A general cause for this interruption is not easy to provide, as each glacier observation series has its own history and is often strongly linked to the activity and situation of its investigators. However, the dissolution of the former Soviet Union might at least partly explain the situation in Asia. In North America the reasons are rather to be found in budget cuts, retirement of dedicated investigators and maybe in the belief that remote sensing can replace the field measurements.

Initial surface mass balance measurements at individual stakes were already carried out on a few glaciers around the beginning of the 20th century, e.g., on Rhone (1885), Clariden (1912), Silvretta (1915) and Aletsch (1921) in Switzerland (Huss et al. 2008). Most of these series have some lengthy data gaps, with the exception of the continuous measurement series at two stakes in the accumulation area of Claridenfirn (Müller and Kappenberger 1991, Ohmura et al. 2007). Mass balance measurements on entire glaciers have been carried out since after the Second World War, with first data available from Scandinavia (Storglaciären, SE) in 1946, Plattalva (CH) and Limmern (CH) in 1948, Storbreen (NO) and Sarennes (FR) in 1949, South Cascade (US), Hintereis (AT), Kesselwand (AT) and Lemon Creek (US) in 1953, and others following later. For the period 1946–2005 there are 3 383 annual mass balance results from 226 glaciers available through the WGMS. The highest observation density is once more found in Scandinavia and Central Europe with 13 and 11 observation series per 1 000 km^2, respectively, and a total of 39 and 43 glaciers under observation. North America has the most reported series (45) overall. In Central Asia and the Arctic, mass balance programmes were carried out on 36 and 35 glaciers, respectively. Mass balance observations from South America have been available since 1976 with recent data reported from nine glaciers. Globally, there is an average of 15 observation years per data series, with 39 glaciers having more than 30 years of measurements. From the 226 available data series, 118 provide information from the 21st century, and there are only 30 'reference' glaciers with continuous measurements since 1976. Additional information related to mass balance data, such as seasonal balances, equilibrium line altitudes and accumulation area ratio are also available for many of these.

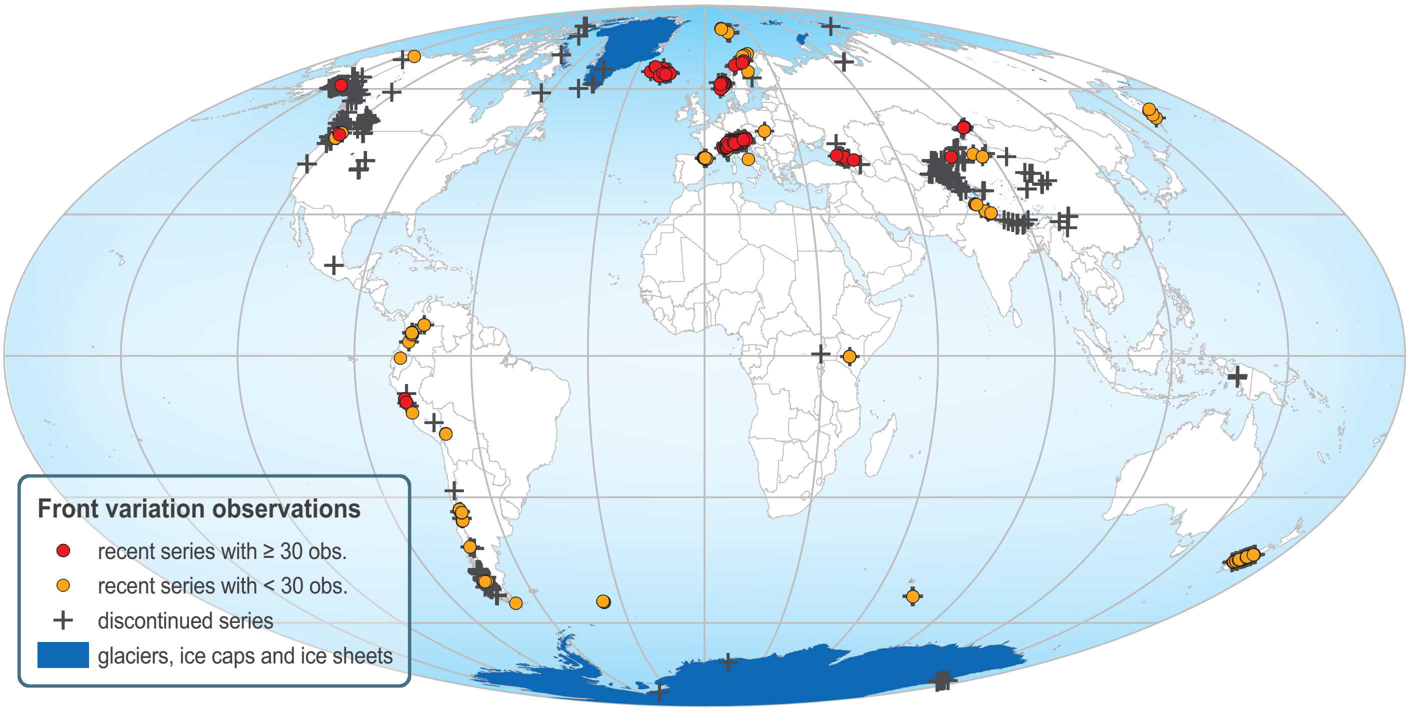

Fig. 4.6 Worldwide length change observations

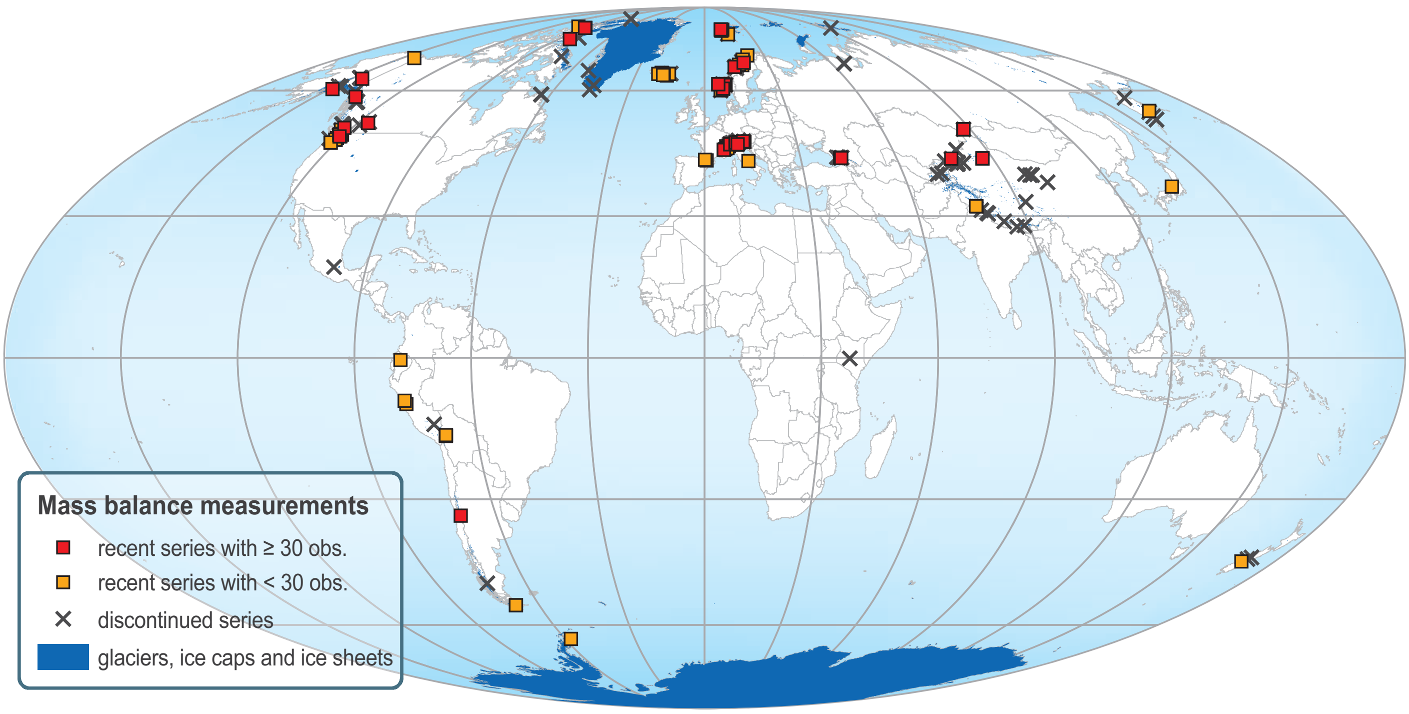

Fig. 4.7 Worldwide mass balance measurements

Fig. 4.6 Worldwide length change observations. The map shows the location of glaciers with reported information on length changes. Data series with surveys after 1999 are plotted as red and orange circles when having more or equal and less than 30 observations, respectively. The locations of observation series which were discontinued before 2000 are shown as black crosses. Data source: glacier information from WGMS; country outlines and surface ice on land cover from *ESRI's Digital Chart of the World*.

Fig. 4.7 Worldwide mass balance measurements. The map shows the location of ice bodies with reported measurements of the glacier mass balance. Data series with surveys after 1999 are plotted as red and orange squares when having more or equal and less than 30 observation years, respectively. The locations of observation series discontinued before 2000 are shown as black crosses. Data source: glacier information from WGMS; country outlines and surface ice on land cover from *ESRI's Digital Chart of the World*.

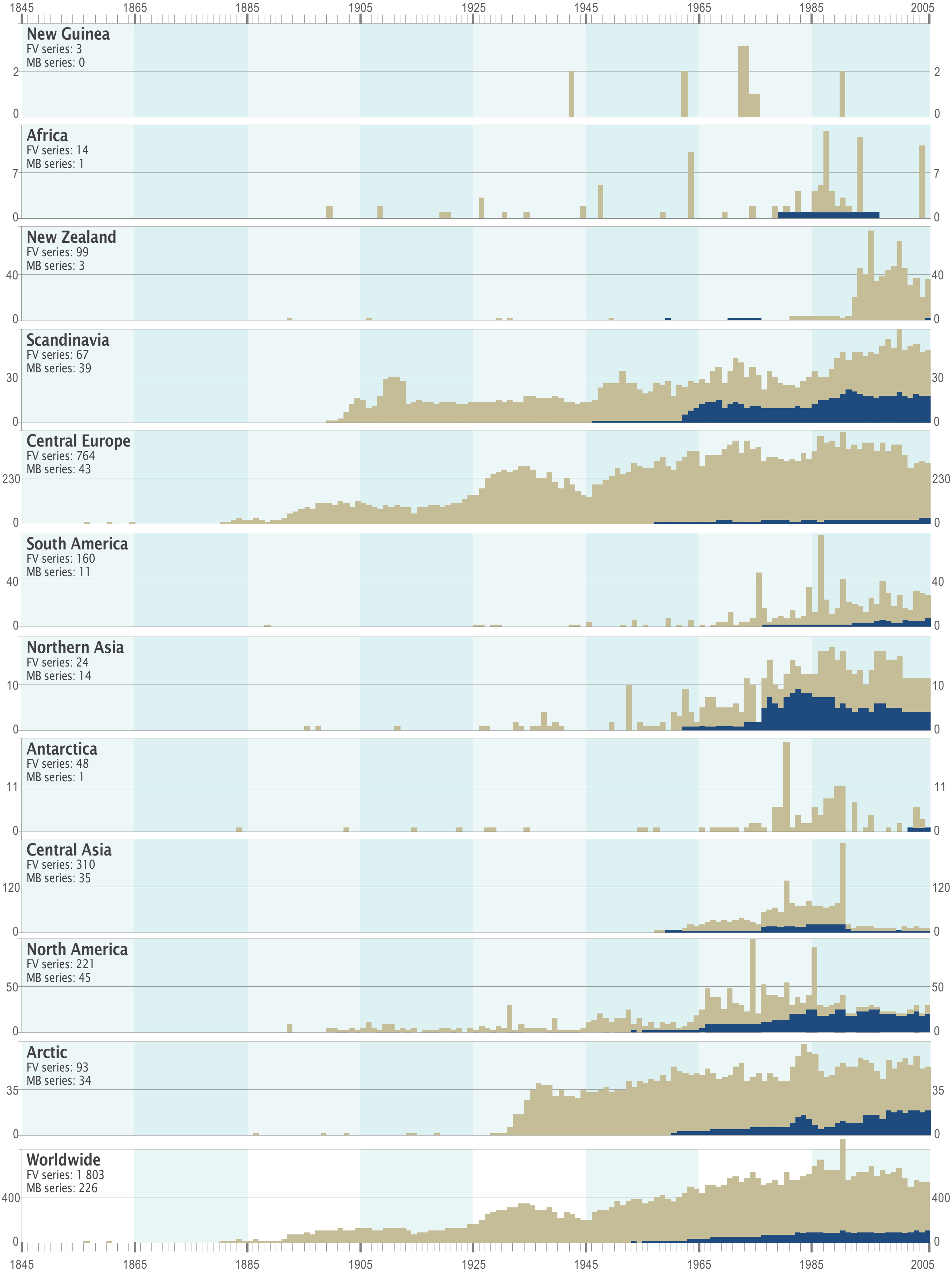

Fig. 4.8 Length change and mass balance surveys - Temporal overview on the number of reported length change (light brown bars) and mass balance surveys (dark blue bars). Note that the scaling of the number of observations on the y-axis changes between the regions. The total number of length change (FV) and mass balance (MB) series are listed below the name of the region. Source: Data from WGMS.

5 Global glacier changes

The moraines from the Little Ice Age mark maximum Holocene glacier extents in many mountain ranges. From these positions, glaciers around the world show a centennial trend of ice wastage which has been accelerating since the mid 1980s. On a decadal time scale, glaciers in various regions have shown intermittent re-advances.

At the peak of the last ice age about 21 000 years ago, about one-third of the land on earth was covered by ice (Paterson 1994, Benn and Evans 1998). Glacier fluctuations can be reconstructed back to that time using a variety of scientific methods. General warming during the transition from the Late Glacial period (between the Late Glacial Maximum and about 10 000 years ago) to the early Holocene (about 10 000 to 6 000 years ago) led to a drastic general ice retreat with intermittent periods of re-advances (Maisch et al. 2000, Solomina et al. 2008). About 11 000 to 10 000 years ago, the pronounced warming reduced the glaciers in most mountain ranges to extents comparable with conditions at the end of the 20th century (Grove 2004). Northern Europe and western North America were still influenced by the remnants of the great ice sheets and the major retreat was delayed until about 6 000 to 4 000 years ago (Solomina et al. 2008). During the Holocene (the past 10 000 years) there were periods of glacier advances on a centennial time scale, peaking in the late Holocene in the Northern Hemisphere and in the early Holocene in the Southern Hemisphere (Koch and Clague 2006). Glaciers in the tropics were rather small or even absent in the early to mid Holocene and gradually re-advanced from about 4 000 years ago (Abbott et al. 2003). Also in Scandinavia, glaciers seem to have largely disappeared during that time (Nesje et al. 2008). The moraines that were formed during the LIA (early 14th to mid 19th century) mark a Holocene maximum extent of glaciers in many regions of the world (Grove 2004, Solomina et al. 2007). However, the timing of these last maximum states is not really synchronous around the globe, but extends from the 17th to the second half of the 19th century. A detailed review of LIA glacier maximum extents around the globe is provided by Grove (2004).

Length change measurements have been available since the late 19th century (Fig. 5.1). These observations show a general glacier recession from the positions of the LIA moraines worldwide. The overall retreat of the glacier termini is commonly measured in kilometres for larger glaciers, and hundreds of metres for smaller glaciers (Hoelzle et al. 2003). Within this general trend, strong glacier retreat was observed in the 1920s and 1940s, followed by stable or advancing conditions around the 1970s, and again drastic glacier retreats after the mid 1980s. On shorter timescales, deviations from these global trends are found in many regions. Looking at the individual data series, one finds a high variability in glacier fluctuations. Large, flat valley glaciers with centennial response times are too long to react dynamically to decadal mass variations, but exhibit a continuous retreat from their LIA moraines, while medium-sized steeper glaciers reacted with re-advances to intermittent wetter and cooler periods. Small cirque glaciers are able to react in a much more direct manner to annual mass changes. Their length changes exhibit a high interannual variability. Surge-type glaciers (Box 5.1) have extreme advances on the short term, followed by a rapid decay of the glacier tongue after the event (Kamb et al. 1985, Kamb 1987). The length change of glaciers calving into a lake or into the sea (Box 5.2) is strongly controlled by the relation between ice velocity and calving rates, as influenced primarily by water depth (Benn et al. 2007). Once they lose contact with their end moraines, such glaciers have to retreat into shallow waters or onto land before being able to advance again on a new frontal moraine. Heavy debris cover acts as an insulator of the glacier ice which, hence, becomes decoupled from climatic changes (Box 5.3). Glaciers in contact with lakes (Box 5.4) or volcanoes (Box 5.5) can feature peculiar behaviours, and be hazardous in populated areas. From the large variety of glacier types and their different sensitivities and reactions to climatic changes it becomes evident that the signal derived from a set of length change series depends strongly on the chosen observation sites. Climate related analysis will have to select the data series of glaciers not influenced by thick debris cover, calving or surge instabilities. Furthermore such studies have to consider the whole spectrum of glacier response characteristics in order to obtain optimal information on secular, decadal and annual developments and its causes (Box 5.6).

Mass balance measurements on entire glaciers have been available for the past six decades. Glacier mass

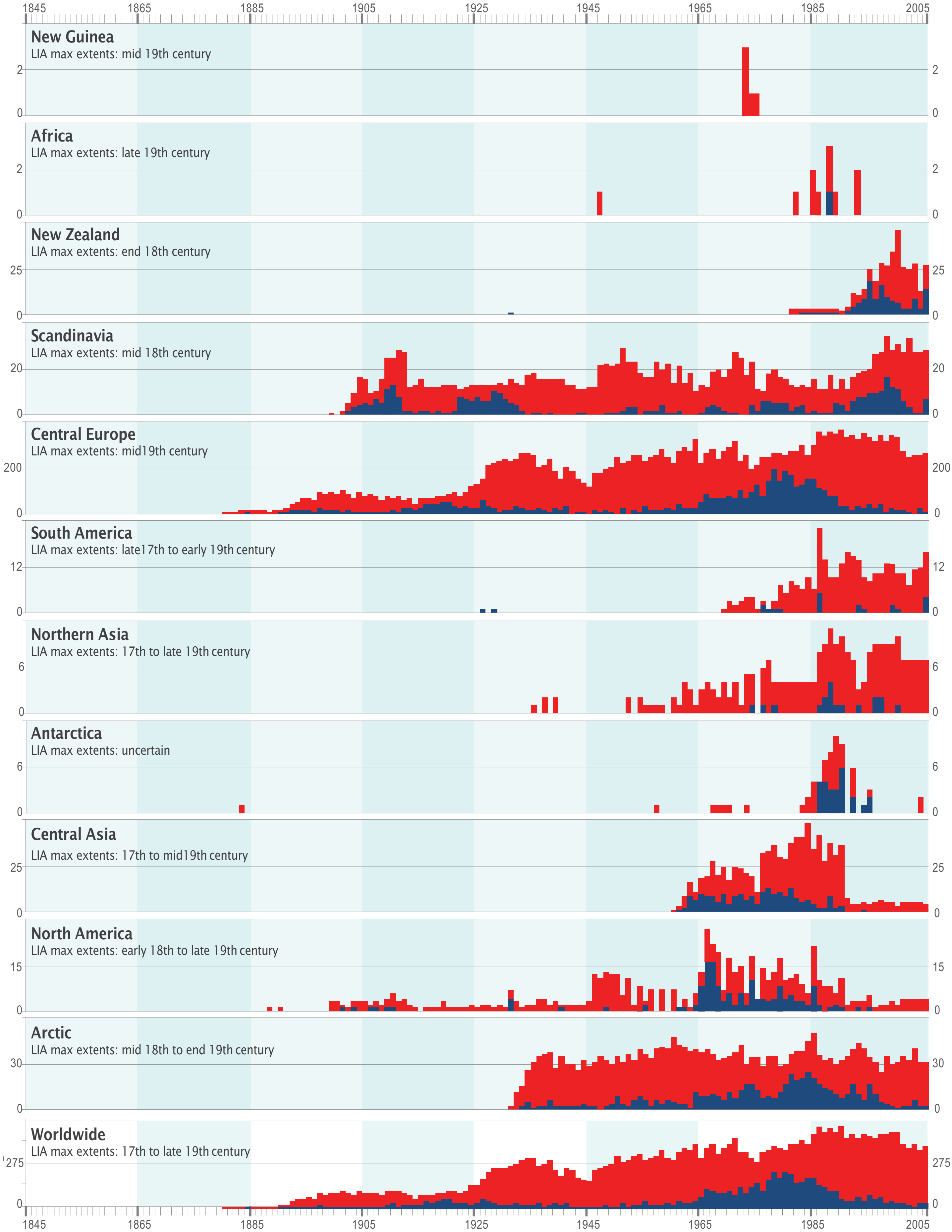

Fig. 5.1 Glacier length changes - Temporal overview on short-term glacier length changes. The number of advancing (blue) and retreating (red) glaciers are plotted as stacked columns in the corresponding survey year. This figure shows 30 420 length change observations with a time range of less than 4 years (between survey and reference year). This corresponds to almost 85 per cent of the reported data which in addition include observations covering a longer time scale and/or stationary conditions. The time period of glacier LIA maximum extents is given according to the regional information in Chapter 6. Note that the scaling of the number of glaciers on the y-axis changes between the regions. Source: figure based on data analysis by R. Prinz, *University of Innsbruck*, Austria; data from WGMS.

Box 5.1 Surging glaciers

Glacier surges are short-term, often periodic, events where a glacier suddenly begins to flow with velocities up to 100 times faster than normal and substantially advances expressed in kilometres per month (Benn and Evans 1998). Typically, the surge starts in the upper part and propagates in a wave down the glacier. The basal motion seems to be restricted to a thin layer at the ice/bed interface. During and after the surge, the glacier surface is characterised by deep crevasses and jagged pinnacles. Most of the glaciers indicating surge behaviour are found in Svalbard, Arctic Islands and Alaska, but some have also been reported from Patagonia and Central Asia. The mechanisms of glacier surges are widely discussed and still not understood completely. In any case, the drainage system underneath and within the glacier seems to play a key role in surge cycles. Lingle and Fatland (2003) investigated temperate glacier surges and suggest that the fundamental driving force is englacial storage of water, combined with gravity-driven movement of stored water to the bed. When crossing a certain threshold, the drainage system collapses and forces failure of the subglacial till – or, alternatively, widespread and rapid basal sliding – and thus initiates the surge (Lingle and Fatland 2003).

Fig 5.2 Variegated Glacier

change is a direct, undelayed reaction to atmospheric conditions. The specific mass balance can be compared directly between different glaciers. This makes it easier to establish a link to climate data, as compared to length changes. However, the limited number of long-term observations – only 30 'reference' glaciers have continuous data series since 1976 – renders global analysis much more complicated. As a consequence

Box 5.2. Calving glaciers

Calving glaciers typically terminate into a lake or the ocean, and in the latter case are also known as tidewater glaciers. Calving occurs when pieces of glacier ice break off and fall into the water. Calving is the most efficient way for these glaciers to lose ice. For the world's oceans, the gain of water by melting of icebergs plays an important role (Van der Veen 1996). Most of the tidewater glaciers are found in high latitudes such as on Svalbard, in Alaska, on the Arctic- and Antarctic Islands. In Patagonia or New Zealand many glaciers calve into lakes. In Alaska a few large calving glaciers are currently in the process of increasing in volume and advance, in strong contrast to the majority of glaciers in that region (Molnia 2007). Hubbard Glacier, at the head of Disenchantment Bay near Yakutat, is one of these advancing glaciers and is the largest calving glacier on the North American continent. Its advance began shortly before 1895 and has periodically been newsworthy, for example, when it blocked the entrance to Russell Fiord, creating a 60 km long glacier-dammed lake, once in 1986 and again in 2002 (Trabant et al. 2002). The accumulation area of Hubbard Glacier is 95 per cent of the entire glacier area and, like the other advancing glaciers, is far from being in equilibrium with climate on the positive mass balance side. The sometimes catastrophic retreat of calving glaciers after losing contact with their frontal moraine and the related production of huge icebergs can threaten nearby ship passages, as in the case of Columbia Glacier in the Chugach Mountains of Alaska (Molnia 2007). While fluctuations of land-based glaciers are generally driven by climate forcing, the behaviour of calving glaciers is often dominated by the calving processes where water depth plays an important role.

Fig. 5.3 Perito Moreno

Fig. 5.2 Variegated Glacier, Alaska, during a surge (photograph taken in 1983). Source: J. Alean, *SwissEduc* (www.swisseduc.ch) / *Glaciers online* (www.glaciers-online.net).

Fig. 5.3 Perito Moreno, Argentina, is a prime example of a calving glacier (photograph taken in December 2005). Source: J. Nötzli, *University of Zurich*, Switzerland.

Fig. 5.4 a—b Luana, Bhutan Himalayas (17 x 13 km). Details from a Landsat image of 1990 (left) and an ASTER image of 2001 (right). Most of the lakes have increased in area between 1990 and 2001, either due to retreat of the calving front, or from growing and connecting supra- and pro-glacial ponds. On October 7, 1994, the lake to the right of the images, Lugge Tsho, burst out and caused a major flood (see deposits in the valley (circle)). Source: A. Kääb, *University of Oslo*, Norway.

Fig. 5.5 High angle view of Mount St. Helens' crater, USA, with new dome and glacier (photograph taken on September 21, 2005). Source: J. Ewert, J. Vallance, *US Geological Survey*.

Box 5.3 Debris-covered glaciers

Debris-covered glaciers occur in every mountain chain with ice-free steep slopes, but are particularly common in the Himalaya, Alaska and New Zealand. In general, the debris appears on the glacier surface below the equilibrium line by medial moraines converging downglacier and forming a continuous debris cover, or by rock falls from the surrounding slopes. A general increase in debris cover over time was observed in Central Asia by several studies (e.g. Ageta et al. 2000, Shroder et al. 2006). The debris cover partially or completely masks the ablation zone of a glacier and therefore significantly influences the energy balance. It also partially controls the ablation rate and the discharge of melt water (Nakawo et al. 2000). When melting, the glaciers waste down or back where they have clean ice, while changes in the debris-covered part are significantly smaller. Therefore, the behaviour of heavily debris-covered glaciers – such as Imja Glacier in the Himalaya or Tasman Glacier in New Zealand – are limited in terms of their use as climatic indicators.

Box 5.4 Lake formation and glacier lake outburst floods

Lakes can form underneath (subglacial-), within (englacial-), on top of (supraglacial-) or in front of (proglacial) a glacier. The lake formation process can occur permanently, periodicly or infrequently. Their formation and also their draining are in most cases controlled by changes in the glacial drainage system (Benn and Evans, 1998). Thus, lake drainage occurs slowly or in a catastrophic manner when a certain threshold is crossed. Other processes such as earthquakes, subglacial volcanic eruptions and rock avalanches or debris flows reaching the lake may cause breaching of ice or moraine dams and lead to sudden glacier lake outburst floods (Kääb et al. 2006). Parallel to the worldwide glacier retreat, numerous glacier lakes have been forming at a rapid rate – especially on the surface of debris-covered glaciers (e.g. in the Himalaya) (Reynolds 2000). Therefore, the number of hazardous glaciers, where outburst floods endangers human life and resources, is rising.


Fig. 5.4a Bhutan Himalaya, 1990


Fig. 5.4b Bhutan Himalaya, 2001

Box 5.5 Glaciers and Volcanoes

Active volcanoes are typically associated with the boundaries of tectonic plates and often reach sufficient heights to sustain the occurrence of glaciers, even in tropical climates. The concurrence of glaciers and volcanoes occurs noticeably in South America (e.g., Nevado del Ruiz), in Mexico (e.g., Popocatépetl), in North America (e.g., Mt. St. Helens) and in Iceland (e.g., Hofsjøkull). Geothermal activity beneath a glacier can strongly enhance the glacier motion, as investigated on Vatnajøkull ice cap in Iceland (Björnsson et al. 2001). More intense processes like volcanic eruptions or pyroclastic flows directly influence the glacier by melting of the ice. The meltwater can trigger catastrophic floods or lahars when incorporating ice and debris from the volcano's flanks. Such an event occurred on Nevado del Ruiz Volcano in Colombia in 1985, where pyroclastic flows caused surface melting of 10 per cent of the ice cap, leading to floods and lahars which claimed at least 25 000 lives (Naranjo et al. 1986). For this reason, glacier-covered volcanoes pose a very serious potential hazard in populated areas (Huggel et al. 2007).


Fig. 5.5 Mount Saint Helens

Box 5.6 Causes of global glacier changes

The reasons for the cyclical nature of the ice ages, so-called Milankovitch cycles, with dominant periods of 23 000, 41 000, 100 000 and 400 000 years (Milankovitch 1930), are mainly to be found in the variation of the earth rotational parameters. Further influences include the variability of solar activity, the latitudinal position of the earth's continents, the chemical composition of the atmosphere, the internal dynamics of the climate system, as well as volcanic eruptions and impacts of meteorites of extreme dimensions (Imbrie and Imbrie 1979, Ruddiman 2000). The overall glacier retreat after the Last Glacial Maximum and extending to the early Holocene is very much in line with the global warming (Solomina et al. 2008). The major glacier re-advances around 8 200 years ago were related possibly to a change in the thermohaline circulation of the ocean in the North Atlantic and North Pacific, and a subsequent cooling, due to the outburst of the Lake Agassiz on the North American continent (Solomina et al. 2008). By contrast, the gradual re-advance of tropical glaciers from their small extents, or even absence, in the early to mid Holocene was probably a result of increasing humidity (Abbott et al. 2003). The periods of simultaneous glacier advances around the world, peaking in the late Holocene in the Northern Hemisphere and in the early Holocene in the Southern Hemisphere, as well as the glacier maximum extents towards the end of the LIA are attributed to changes in solar irradiance, in dependence on the sun's activity and the earth's orbit, and also to the effects of volcanic eruption, internal dynamics of the climate system (Grove 2004, Solanki et al. 2004, Koch and Clague 2006) and possible initial large-scale anthropogenic changes in land use (Ruddiman 2003).

The overall shrinking of glaciers and ice caps since their LIA maximum extents is well correlated with the increase in global mean air temperature of about 0.75 °C since the mid 19th century, which is most likely man-induced since the second half of the 20th century (IPCC 2007). On decadal or regional scales, changes in snow accumulation may have dominated glacier response in maritime climates (IPCC 2007). As such, the onset of the post LIA retreat and the later periods of intermittent re-advances in the European Alps are attributed to changes in winter precipitation rather than temperature (Vincent et al. 2005, Zemp et al. 2007b). Increased precipitation is also seen as the main reason for the glacier advances in the early 18th century and the 1990s in Norway (Andreassen et al. 2005), in the 1990s in New Zealand (Chinn et al. 2005), and for the 20th century advances and/or thickening of some glaciers in central Karakoram (Hewitt 2005). Such glacier changes are striking features in photo comparisons as shown in Figures 0.1, 5.6, 5.7 and 7.1.

The period in which glaciers were close to steady state or even advancing, which occurred worldwide around the 1970s, might be explained, at least in part by diminished incoming solar radiation due to the increase of atmospheric pollution after the mid 20th century (Wild et al. 2007). Recent studies have shown that the atmosphere cleared up again in the mid 1980s, probably as a result of the implementation of industrial filters and the breakdown of industry in the former Soviet Union, which increased the amount of incoming solar radiation and, as such, of glacier melting (Ohmura 2006, Padma Kumari et al. 2007). Analyses of mass balance data have shown a moderate increase in mean winter accumulation and a substantially increased low-altitude summer melting (Ohmura 2004, Dyurgerov and Meier 2005, Greene 2005). This is consistent with the observed increase in the mass turnover rate which is derived from field measurements in the Northen Hemisphere (Dyurgerov and Dwyer 2000) and remote sensing studies in Alaska (Arendt et al. 2002), the Canadian Arctic Archipelago (Abdalati et al. 2004) and Patagonia (Rignot et al. 2003).

In addition to climate changes on the global level, altered atmospheric circulation patterns can have a great impact on the glacier behaviour of entire mountain ranges. Examples are the accelerated glacier retreat in continental USA and southwest Canada which are attributed to a shift in atmospheric circulation in approximately 1976/77 (Bitz et al. 1999, McCabe et al. 2000), the mass balance variations of glaciers in the tropical Andes which are strongly influenced by the El Niño-Southern Oscillation (ENSO; Wagnon et al. 2001, Francou et al. 2004, Sicart et al. 2005), and the North Atlantic Oscillation that has an effect on glaciers in the European Alps and Scandinavia (Schöner et al. 2000, Nesje et al. 2000).

Fig. 5.6a 1989 b 1995 c 2001 d 2007

Fig. 5.7.a Peyto Glacier, 1966

Fig. 5.7.b Peyto Glacier, 2001

there are three main approaches to calculating global average mass balances which are independent of climate, hydrology or climate indicator data. These are by (i) using the (arithmetic) mean value of the few continuous measurement series, (ii) averaging the moving sample of all available data series, and (iii) using regionally weighted samples (cf. Kaser et al. 2006). However, when cumulated over the past six decades, the results of these approaches are consistent. The global averages (i, ii, iii) reveal strong ice losses in the first decade after the start of the measurements in 1946, slowing down in the second decade (1956–65), followed by a moderate mass loss between 1966 and 1985, and a subsequent acceleration of ice loss until present (Fig. 5.8 a—f). The mean of the 30 continuous 'reference' series yields an annual mass loss of 0.58 m water equivalent (m w.e.) for the decade 1996–2005, which is more than twice the loss rate of the previous decade (1986–95: 0.25 m w.e.), and over four times the rate for the period 1976–85 (0.14 m w.e.).

Overall, the cumulative average ice loss over the past six decades exceeds 20 m w.e. (Fig. 5.9), which is a dramatic ice wasting when compared to the global average ice thickness, which is estimated (by dividing estimated volume by area) to be between 100 m (IPCC 2007) and about 180 m (Ohmura, personal comm.). The average ice loss over that period of about 0.35 m w.e. per year exceeds the loss rates reconstructed from worldwide cumulative length changes for the time since the LIA (see Hoelzle et al. 2003) and is of the same order of magnitude as characteristic long-term mass changes during the past 2 000 years in the Alps (Haeberli and Holzhauser 2003). Based on the mass balance measurements, the annual contribution of glaciers and ice caps to the sea level rise is to be estimated at one-third of a millimetre between 1961 and 1990, with a doubling of this rate in the period from 1991 to 2004 (Kaser et al. 2006), and passing the one millimetre per year limit for the period 2000 to 2006. However, these values are to be considered first order estimates due to the rather small number of mass balance observations and their probably limited representativeness for the entire surface ice on land, outside the continental ice sheets. The vast ice loss over the past decades has already led to the splitting or disintegration of many glaciers within the observation network, e.g., Lower Curtis and Columbia 2057 (US), Chacaltaya (BO), Carèser (IT), Lewis (KE), Urumqihe (CN), and presents one of the major challenges for glacier monitoring in the 21st century (Paul et al. 2007). The massive downwasting of many glaciers over the past two decades, rather than dynamic retreat, has decoupled the glaciers horizontal extent (i.e. length, area) from current climate, so that glacier length or area change has definitely become a diminished climate indicator of non-linear behaviour. Under the present climate change scenarios (IPCC 2007), the ongoing trend of global and rapid, if not accelerating, glacier shrinkage on the century time scale is of non-periodic nature and may lead to the deglaciation of large parts of many mountain ranges in the coming decades (e.g., Zemp et al. 2006, Nesje et al. 2008).

For a temperate glacier, a step-change in climatic conditions would cause an initial mass balance change followed by a return to zero values, due to the glacier's adaptation of its size (surface area) to the new climate

Fig. 5.6 a—d Advance and retreat of Briksdalsbreen, an outlet glacier of Jostedalsbreen, Norway, in a photo series of the years 1989, 1995, 2001 and 2007. Source: S. Winkler, *University of Würzburg*, Germany.

Fig. 5.7 a—b Retreat of Peyto Glacier, Canadian Rockies, between 1966 and 2001. Source: W.E.S. Henoch and M.N. Demuth, Canada.

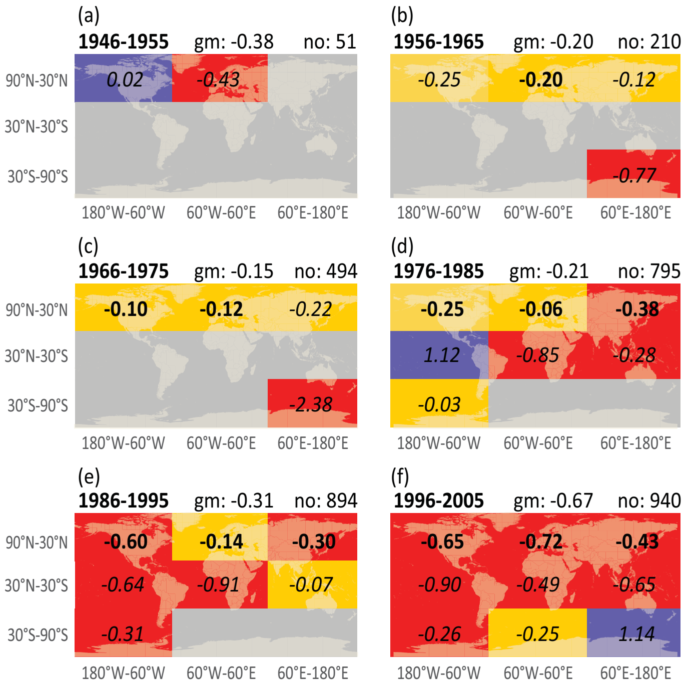

Fig. 5.8 Spatio-temporal overview on glacier mass changes

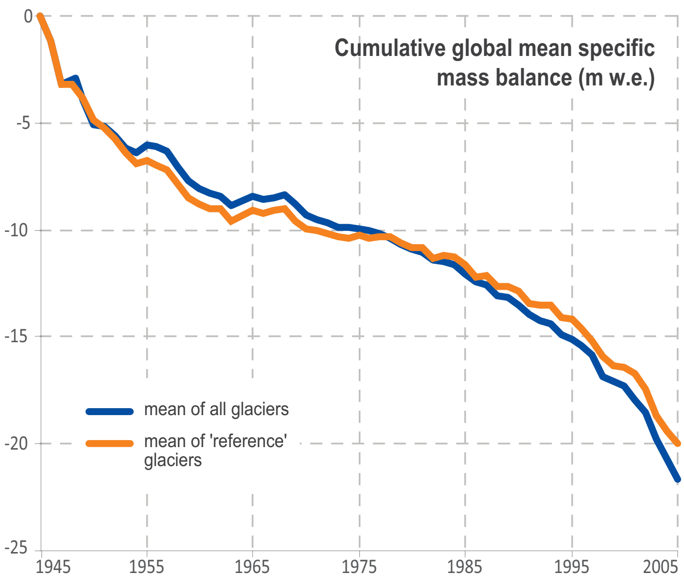

Fig. 5.9 Cumulative specific mass balance

(Jóhannesson et al. 1989). The observed trend of increasingly negative mass balance over reducing glacier surface areas thus leaves no doubt about the ongoing climatic forcing resulting from the change in climate and possible enhancement mechanisms such as mass balance / altitude feedback, altered turbulent and long-wave radiation fluxes due to the size and existence of rock outcrops or changes in the surface albedo (Paul et al. 2007). The specific mass balance data can be directly compared between different glaciers of any size and elevation range. The data series provide a combined hydrological and climatic signal. Runoff can be calculated by multiplying the specific mass balance with the corresponding glacier area, whereas a climatic interpretation needs to consider the geometric changes. In order to derive a real climate signal, it is required to relate the mass changes to a reference extent of the glacier (Elsberg et al. 2001, WGMS 2007 and earlier issues).

The numerous length change series together with the positions of moraines from the LIA provide a good qualitative overview on the global and regional glacier changes; while the mass balance series provide quantitative measures of the ice loss since the late 1940s. However, the about 230 glacier mass balance series are less representative for the changes in the global ice cover. Many regions with large ice cover are strongly underrepresented in the data set or are even lacking in observations. Data from south of 30° N has only been reported since 1976. As a consequence, the field measurements with a high temporal resolution but limited in spatial coverage should be complemented by remotely-sensed decadal area and volume change assessment in order to obtain a representative view of the climate change impact on the glacierisation. Examples for such integrative analysis for entire mountain ranges are given by Molnia (2007) for Alaska, by Casassa et al. (2007) on the Andean glaciers, by Kaser and Osmaston (2002) for tropical glaciers, by Andreassen et al. (2005) for Norway, by Zemp et al. (2007b) for the European Alps, by Kotlyakov et al. (2006) for Russia, and by Chinn (2001) and Hoelzle et al. (2007) for New Zealand, as well as by Hoelzle et al. (2003), Grove (2004), Zemp et al. (2007a) and USGS (in prep.) for a global overview.

Fig. 5.8 a—f Spatio-temporal overview on glacier mass changes. The average annual mass balance for nine sectors of the globe are shown for the decades (a) 1946–55, (b) 1956–65, (c) 1966–75, (d) 1976–85, (e) 1986–95, and (f) 1996–2005. Sectors with measurements are coloured according to the mean annual specific mass balance in metre w.e. with positive balances in blue, ice losses up to 0.25 m w.e. in orange and above that in red; sectors without data in grey. Average decadal mass balance values based on less than 100 observations (marked in italics) are less representative for the entire sector. For each decade, the global mean (gm) annual mass balance in m w.e. and the number of observations (no) are indicated. Source: Data from WGMS.

Fig. 5.9 The cumulative specific mass balance curves are shown for the mean of all glaciers and 30 'reference' glaciers with (almost) continuous series since 1976. Source: Data from WGMS.

6 Regional glacier changes

The following sections provide an overview on the glacier changes after the Little Ice Age (LIA) in eleven glacierised macroregions (Fig. 6.0.1). Sections 6.1-6.11 are ordered according to the extent of the glacier cover in the macroregions (see Table 4.1). A classification of the world's glaciers and ice caps into geographical macroregions is based on the purpose of the particular investigation as well as on the spatial resolution of the data set and, hence, is somewhat arbitrary. The regional attributions, names and ice cover information used in this publication are based on Dyurgerov and Meier (2005). Each section includes a brief statistic of the glacier fluctuation data as reported to the WGMS. The sections summarise the characteristics of the mountain ranges and its ice covers, followed by a brief discussion of the available fluctuation series, the timing of the LIA maximum extents and the subsequent regional glacier changes based on the available field series and some key publications. Selected long-term length change and mass balance series are plotted as cumulative graphs. A complete overview of the data series reported to, and available from, the WGMS as well as a list of the National Correspondents are given in the Appendix. Detailed information on the Principal Investigators and Sponsoring Agencies of the reported data is published in the *Fluctuations of Glaciers* series (WGMS 2008, and earlier volumes). In order to provide an impression of the glacier characteristics, false-colour satellite images from ASTER, including close-up to interesting glaciological features, as well as terrestrial, oblique aerial photographs are shown for each region.

Figure 6.0.1 gives an overview of the distribution of the global ice cover and indicates the location of the eleven macroregions. Figure 6.0.2 a—f details the available fluctuation series (WGMS glacier data) and those presented in the following regional sections 6.1 to 6.11. Note that the two-digit country code assigned to the glaciers in the following sections and the appendix table is given according to the information submitted to the WGMS and as such might not correspond to present political territories.

Fig. 6.0.1 The selected eleven glacierised macroregions.
Details on the mountain ranges, its glacier covers and changes are presented in detail in the sections 6.1 – 6.11. Source: glacier outlines from *ESRI's Digital Chart of the World* (DCW).

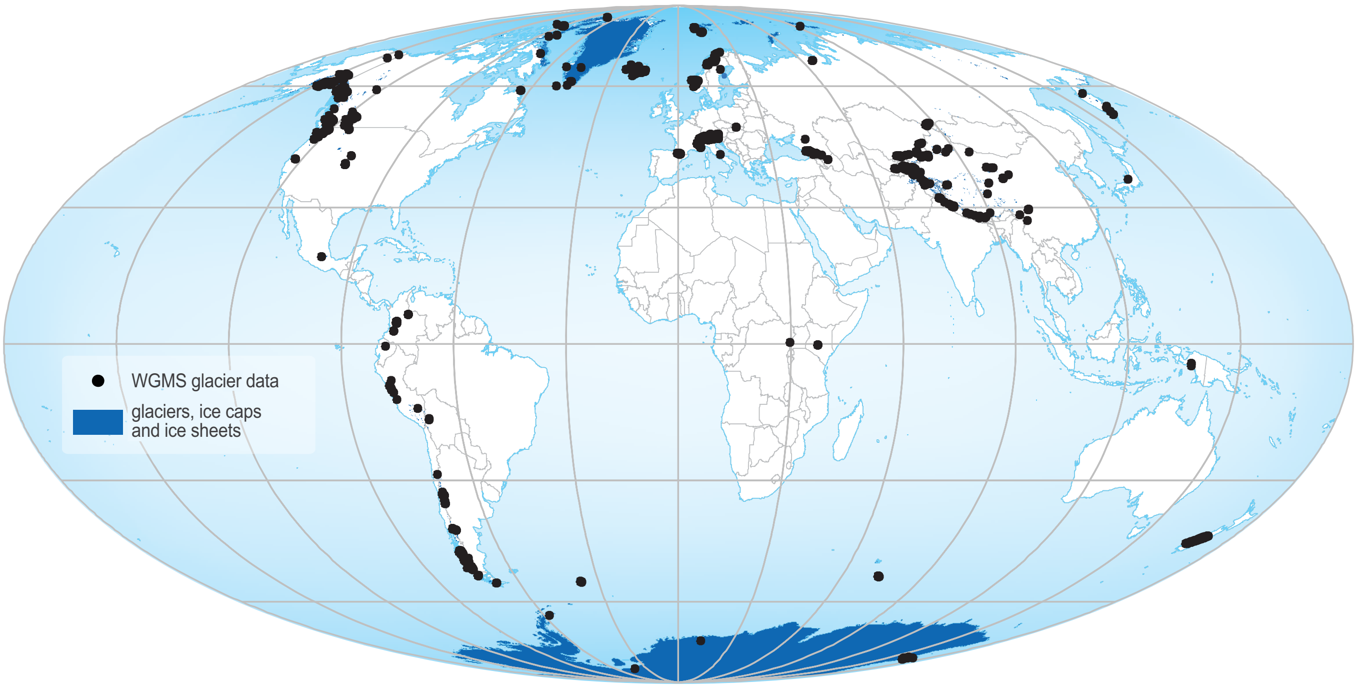

Fig. 6.0.2a WGMS glacier data

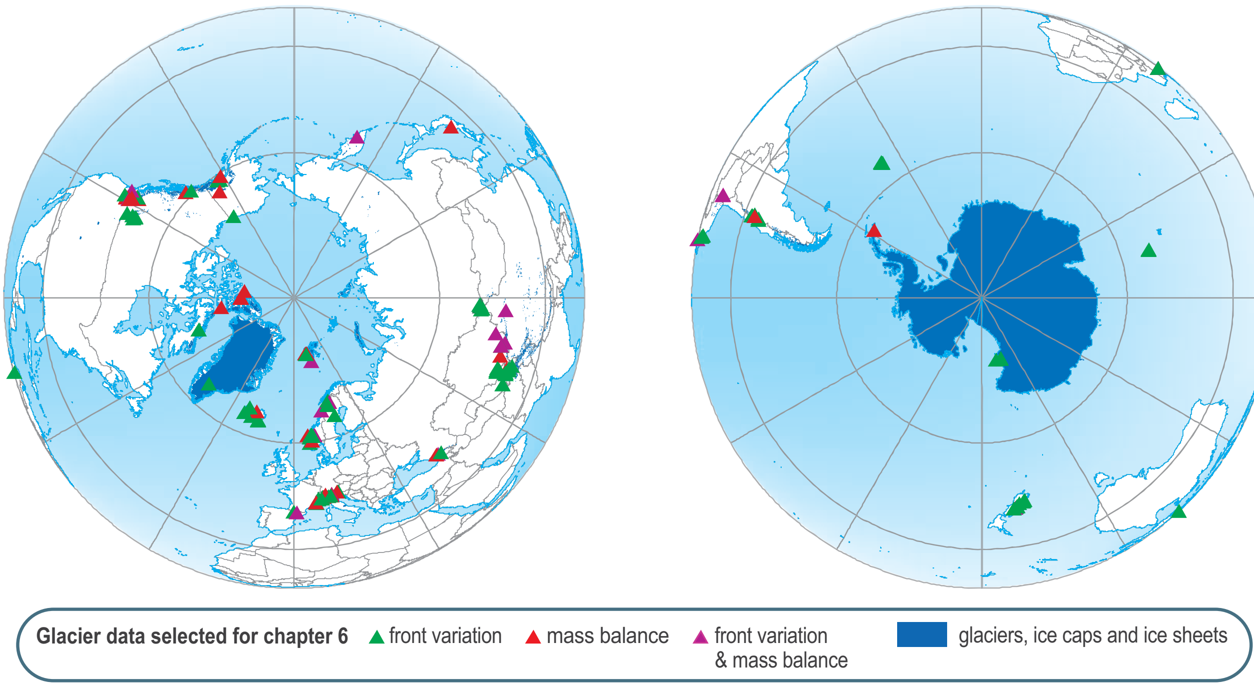

Fig. 6.0.2b—c Selected front variation and mass balance data

Fig. 6.0.2 Global distribution of glaciers, ice caps and ice sheets are shown with (a) the available fluctuations data and (b-f) selected mass balance and front variation series shown in sections 6.1-11. Sources: glacier outlines from *ESRI's Digital Chart of the World* (DCW), fluctuation series from WGMS.

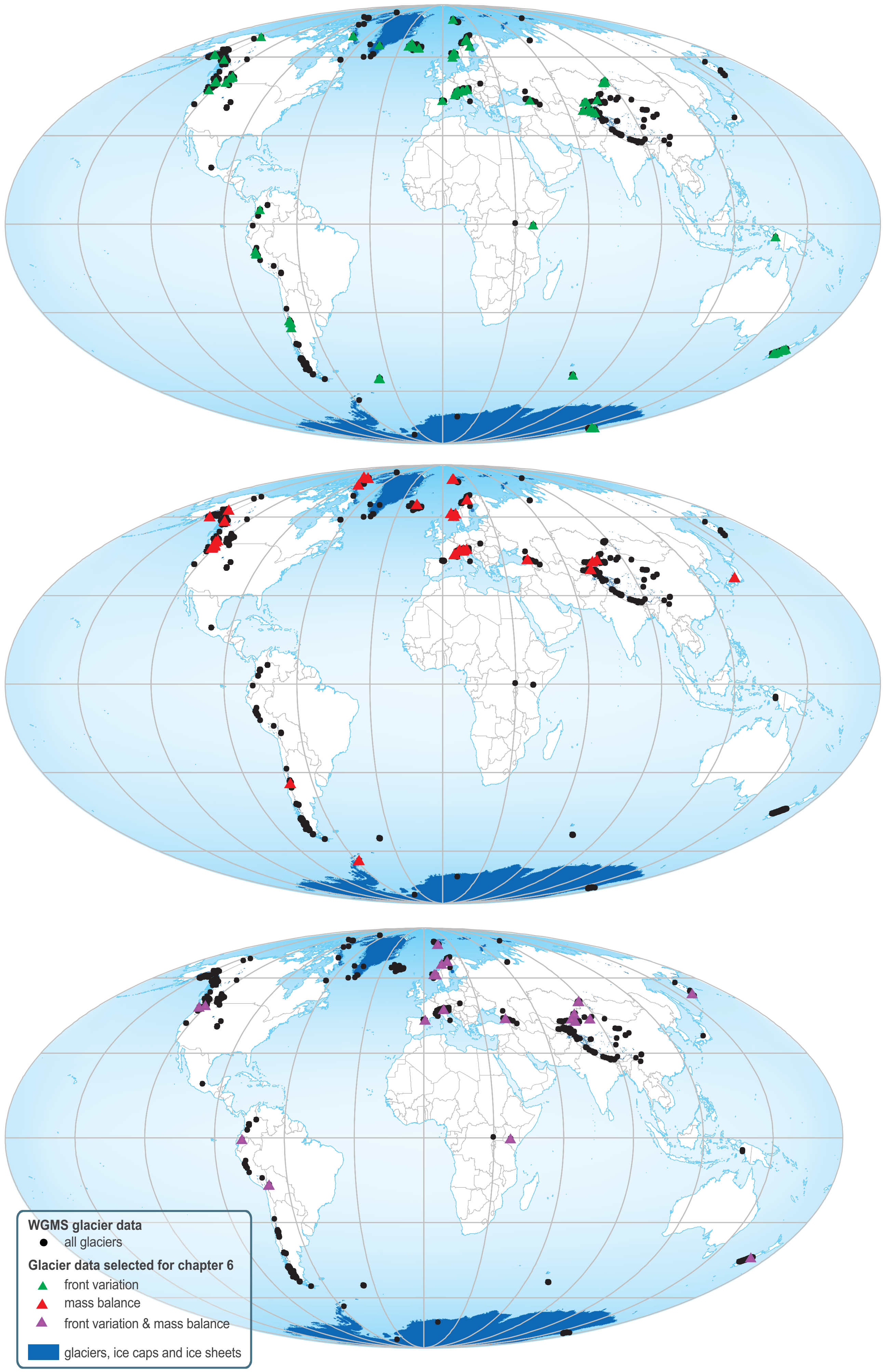

Fig. 6.4d—f Selected front variation and mass balance series

6.1 New Guinea

The few glaciers of Papua (formerly Irian Jaya, Indonesia) and Papua New Guinea are located on the peaks of the great Cordillera of the island of New Guinea. Direct observations are sparse, but historical documents, aerial photographs and satellite images offer insight into the historical glacier changes.

FRONT VARIATION

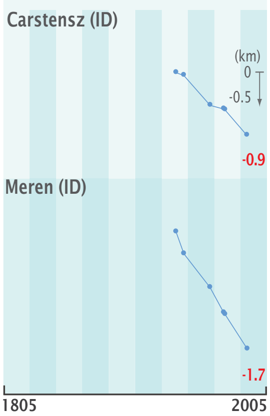

The only tropical glaciers of Asia are located on the mountains of New Guinea. In the 20th century glaciers were found on Puncak Mandala (Juliana 4 640 m asl), Ngga Pilimsit (Idenburg 4 717 m asl) and Puncak Jaya (Carstenz 5 030 m asl), three peaks in Papua, Indonesia, located in the western part of the great Cordillera of New Guinea (Grove 2004). A small ice cap existed on Puncak Trikora (Wilhelmina 4 730 m asl) in Papua New Guinea (Grove 2004). The LIA maximum extent was reached in the mid 19th century (Allison and Peterson 1976).

Regular series of direct measurements of front variation or mass balance are not available. The glacier changes have been traced from information on glacier extents derived from historical records, dated cairns erected during several expeditions, aerial photographs, satellite images as well as from some in-situ measurements carried out during Australian expeditions in the 1970s (Allison and Peterson, 1989). Most observations focused on the glaciers on Puncak Jaya, namely the North Wall Firn; two valley glaciers, Meren and Carstenz; and the Southwall Hanging Glacier. All have undergone extensive retreat since the LIA maximum extent (Peterson et al. 1973) reducing the entire Puncak Jaya ice cover from almost 20 km^2 around 1850 to less than 3 km^2 in 2002, with highest retreat rates around 1940 and in the early 1970s (Klein and Kincaid 2006). All ice masses except some on Puncak Jaya have now disappeared. The isolated ice caps vanished from Puncak Trikora between 1939 and 1962; from Ngga Pilimsit between 1983 and 2003 (Klein and Kincaid, 2006); and from Puncak Mandala between 1989 and 2003 (Klein and Kincaid, 2008). The larger Meren Glacier on Puncak Jaya melted away between 1992 and 2000 (Klein and Kincaid, 2006).

Fig. 6.1.1 Punca Jaya

Fig. 6.1.1 Oblique aerial photograph looking east at Northwall Firn, Meren Glacier and Carstensz Glacier (left to right) on Puncak Jaya. Source: Photograph of 1936 by J.J. Dozy, provided by the *United States Geological Survey* (Allison and Peterson 1989).

Ice covered area (km^2):	3
Front variation	
number of series:	3
average number of observations:	5
average time length (years):	46
Mass balance	
number of series:	0
average number of observations:	0

6.2 Africa

The few tropical ice bodies in East Africa are located on Ruwenzori, Mount Kenya and Kilimanjaro. Their recession since the late 19th century has been well documented.

African glaciers are found near the equator in East Africa, situated on three mountains: Ruwenzori (5,109 m asl), Mount Kenya (5 199 m asl) and Kilimanjaro (5 895 m asl), of which the latter are volcanoes (Grove 2004). The glaciers are situated in the tropical climate zone. The processes governing accumulation and ablation are thus different from mid-latitude or polar climates. The glaciers reached their LIA maximum extents towards the late 19th century (Hastenrath 2001).

Fig. 6.2.2 Lewis Glacier

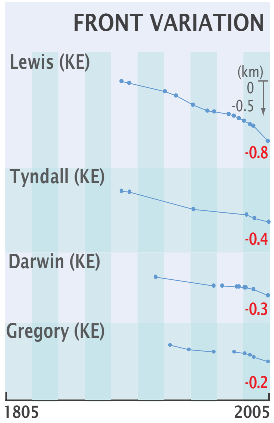

Glaciological studies on Ruwenzori, Mount Kenya and Kilimanjaro have a long history and are summarised in Hastenrath (1984, 2005), Kaser and Osmaston (2002), and Cullen et al. (2006). Several front variation series document the glacier changes on Mount Kenya where also the only African mass balance measurements were carried out on Lewis Glacier between 1978 and 1996 (Hastenrath 2005).

The ice cover on Ruwenzori has retreated continuously since the late 19th century, became strongly fragmented and on some peaks has completely vanished (Kaser and Osmaston 2002). The ice bodies on Kilimanjaro have shrunk continuously from about 20 km² just before 1880 to about 2.5 km² in 2003 (Cullen et al. 2006). The plateau glaciers thereby showed a linear retreat, whereas the glaciers on the slopes of the mountain had higher loss rates in the first half of the 20th century. Front variation measurements and repeated mapping provide documentation of the century-long history of glacier recession on Mount Kenya, with eight (out of 18) glaciers vanishing in the 20th century (Hastenrath 2005). The ice volume of Lewis Glacier decreased from about 7.7 km³ in 1978 to about 0.3 km³ in 2004 (Hastenrath and Polzin 2004) with an average thickness loss of almost one metre ice per year.

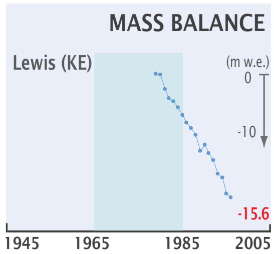

Fig. 6.2.1.a Mount Kilimanjaro, 1950

Fig. 6.2.3 Kilimanjaro

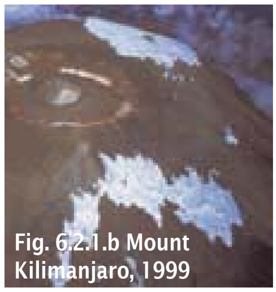

Fig. 6.2.1.b Mount Kilimanjaro, 1999

Ice covered area (km²):	6
Front variation	
number of series:	14
average number of observations:	6
average time length (years):	71
Mass balance	
number of series:	1
average number of observations:	18

Fig. 6.2.1 a—b Mount Kilimanjaro, Tanzania, northern icefield. Source: Upper photograph taken in the early 1950s by J. West, lower photograph taken in 1999 by J. Jafferji.

Fig. 6.2.2 Lewis Glacier, Mount Kenya, in the mid 1990s. Source: S. Ardito.

Fig. 6.2.3 Mount Kilimanjaro, Tanzania. Space view of the glaciers around the crater (center) and typical surrounding clouds. Source: ASTER satellite image (50 x 45 km), 19 August 2004.

6.3 New Zealand

Most glaciers are situated along the Southern Alps, with a few more on Mount Ruapehu Volcano on the Northern Island. The country has a long tradition of glacier observation; however, the majority of the available data series are of qualitative type and start in the 1980s.

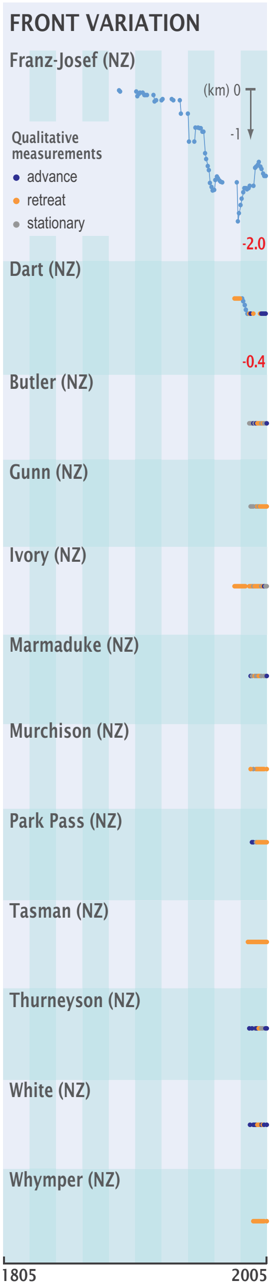

The topography of New Zealand is characterised by evidence of the collision of the Indio-Australian Plate with the Pacific Plate and the resulting tectonic uplift, seismic activity and volcanism. Apart from a few glaciers on Mount Ruapehu Volcano on the North Island, the majority of glaciers are located along the Southern Alps spanning the length of the South Island between 42° and 46° south. Their climatic regime is characterised by high precipitation with extreme gradients. Annual average values amount to 4500 mm on the west side (Whataroa) of the Alps and maximum values of up to 15 000 mm (Chinn 1979, Griffiths and McSaveney 1983, Tomlinson and Sansom 1994). Mount Cook is the highest peak at 3 754 m asl. Below its flank, the Tasman Glacier – the largest glacier in New Zealand – is located. In total, the inventory of 1978 reported 3 144 glaciers covering an area of about 1 160 km^2 with an estimated total ice volume of about 53 km^3 at that time (Chinn 2001). Glacier runoff is used for irrigation east of the main divide of the Southern Island and for hydro-electric power production, which accounts for over two-thirds of the nation's total generating outputs.

The LIA maximum extent of New Zealand's glaciers occurred towards the end of the 18th century, with only minor retreats until the end of the 19th century (Gellatly et al. 1988, Anderson 2003, Winkler 2004). New Zealand has a long tradition of glacier observation going as far back as the 19th century and focusing on glacier front variations. The most comprehensive series is a detailed history of frontal positions of the Franz-Josef Glacier with the first survey made in 1893 (Harper 1894, Anderson and Mackintosh 2006).


Fig. 6.3.1 Franz-Josef Glacier

However, the majority of the data series start in the 1980s and provide qualitative data only (advance, retreat, stationary). Glacier extents have been mapped for an inventory

Fig. 6.3.1 Oblique aerial photograph showing the west coast of the South Island with Franz-Josef Glacier and Mount Cook (photograph taken on March 27, 2006). Source: M. Hoelzle, *University of Zurich*, Switzerland.

Fig. 6.3.2 Brewster Glacier (on left) with almost no accumulation area. The oblique aerial photograph was taken during the end-of-summer snowline survey on 14 March, 2008. Source: A. Willsman (NIWA), as part of *New Zealand Foundation of Research, Science and Technology* contract C01X0701.

Fig. 6.3.3 Tasman (left) and Murchison (right) Glaciers region. Source: ASTER satellite image (23 x 31 km) and close-ups, 29 April 2000.

Ice covered area (km²): 1 160

Front variation	
number of series:	99
average number of observations:	6
average time length (years):	14

Mass balance	
number of series:	3
average number of observations:	3

Fig. 6.3.2 Brewster Glacier

in 1978 (Chinn 1996), revealing an overall retreat from the moraines of the LIA extents. Since 1977 annual end-of-summer snowline surveys have been carried out by taking aerial photographs of 50 glaciers (Chinn et al. 2005). Limited mass balance data are available from two glaciers only, the Tasman and Ivory. Most recently a new mass balance monitoring program has been started with on-site support by the WGMS on Brewster Glacier.

Overall, New Zealand's glaciers lost between one-quarter (Chinn 1996) and almost half of their area (Hoelzle et al. 2007) between the timing of their LIA maximum extents and the 1970s. After the mid 1980s many glaciers on the west coast have gained mass and advanced noticeably. Since the beginning of the 21st century, the number of retreating glaciers has increased again. A net ice volume loss between 1977 and 2005 of about 11 per cent has been reported in a recent study (Chinn pers. comm.). This mass loss was attributed mainly to the downwasting of the 12 largest glaciers and the minor contributions from their calving into lakes, as well as from negative mass balances of smaller glaciers.

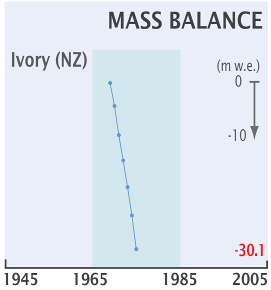

Fig. 6.3.3 Tasman and Murchison Glaciers

Fig. 6.3.3a

Fig. 6.3.3b

Fig. 6.3.3c

6.4 Scandinavia

The majority of the ice on the Scandinavian Peninsula is located in southern Norway. Some glaciers and ice caps are also found in northern Norway and the Swedish Kebnekaise mountains. Scandinavia is one of the regions with the most and longest reported observation series.

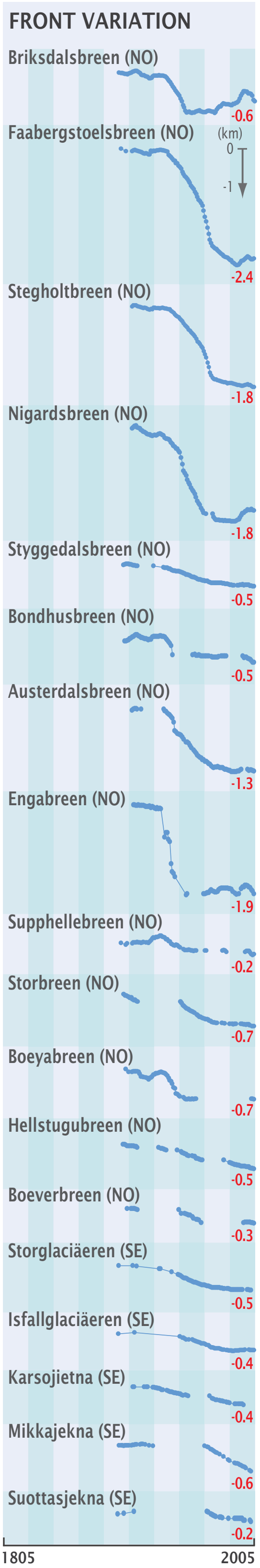

The Scandinavian Peninsula is located between 60° and 71° north. Galdehøpiggen (2469 m asl) in southern Norway is the highest peak on the Peninsula, and Kebnekaise (2104 m asl) is the highest summit in northern Sweden. Due to the combination of high latitude and the moisture from the North Atlantic, many glaciers and ice caps developed, mainly in Norway, all within 180 km of the west coast (Grove 2004). The greater part of the ice cover is concentrated in southern Norway, namely in Folgefonna, Hardangerjøkulen, Breeheimen, Jotunheimen, and Jostedalsbreen, which is the largest ice cap of mainland Europe (Østrem et al. 1988, 1993). In northern Norway there are the Okstindan and Svartisen ice caps, glaciers in Lyngen and Skjomen (Østrem et al. 1973), as well as in the adjacent Kebnekaise region in Sweden (Holmlund and Jansson 2005). The relevance of glaciers and their changes to the lives of the Scandinavian people is reflected in the extensive observation record. Farms and farmland buried by ice, resettlements and reduced taxes due to the Little Ice Age glacier advances are reported in historical documents (Grove 2004). In today's Norway, 15 per cent of the used runoff comes from glacierised basins and 98 per cent of the electricity is generated by hydropower production (Andreassen et al. 2005).

After having probably disappeared in the early/mid Holocene (Nesje et al. 2008), most of the Scandinavian glaciers and ice caps reached


Fig. 6.4.1 Nigardsbreen

their maximum extent in the mid-18th century (Grove 2004). Blomsterskardsbreen, the southern outlet glacier of Folgefonna, is one of the exceptions, reaching its maximum extent at the beginning of the 20th century (Grove 2004). Annual front variation measurements began in Norway and Sweden at the turn to the 19th century. Several glaciers have been observed on a regular basis for more than a century. A total of over 60 Scandinavian front variation series are available. Storglaciären in Sweden provides the longest existing mass balance record for an entire glacier with continuous seasonal measurements since 1946. Mass balance measurements in Norway started at Storbreen (Jotunheimen) in 1949. Overall mass balance measurements have been reported from 39 glaciers, with 8 continuous series since 1970.

After their enlarged state in the 18th century and the minor retreat trend with small fron-

Fig. 6.4.1 View toward the proglacial lake and the tongue of Nigardsbreen, Norway, Jostedalsbreen Ice Cap in the background (photograph taken in July 2005). Source: I. Roer, *University of Zurich*, Switzerland.

Fig. 6.4.2 Tarfala research station in the Kebnekaise region (Sweden), with Isfallsglaciären in the background (photograph taken in August 2007). Source: P. Jansson, *University of Stockholm*, Sweden.

Fig. 6.4.3 Svartisen Ice Caps, Norway, with Engabreen outlet glacier to the middle left. Source: ASTER satellite image (35x21 km) and close-ups, 11 August 2006.

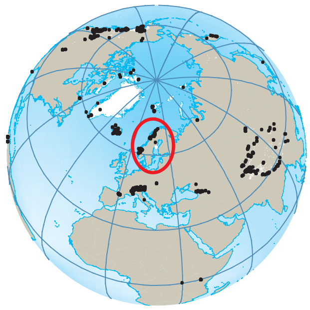

Ice covered area (km²): 2 940

Front variation		**Mass balance**	
number of series:	65	number of series:	39
average number of observations:	30	average number of observations:	16
average time length (years):	53		

Fig. 6.4.2 Kebnekaise region

tal oscillations up until the late 19th century, Scandinavian glaciers experienced a general recession during the 20th century with intermittent periods of re-advances around 1910 and 1930, in the second half of the 1970s, and around 1990; the last advance stopped at the beginning of the 21st century (Grove 2004, Andreassen et al. 2005). Local precipitation variances superimposed on these generally coherent patterns, cause variations to occur on individual glaciers. The maritime glaciers (e.g. Hardangerjøkulen, Nigardsbreen, Ålfotbreen, Engabreen) with large annual mass turnover started to gain mass after the early 1960s, whereas the more continental glaciers (e.g. Storglaciären, Gråsubreen, Hellstugubreen, Storbreen) continued their ice loss. Since 2001 all monitored glaciers have experienced a distinct mass deficit (Andreassen et al. 2005).

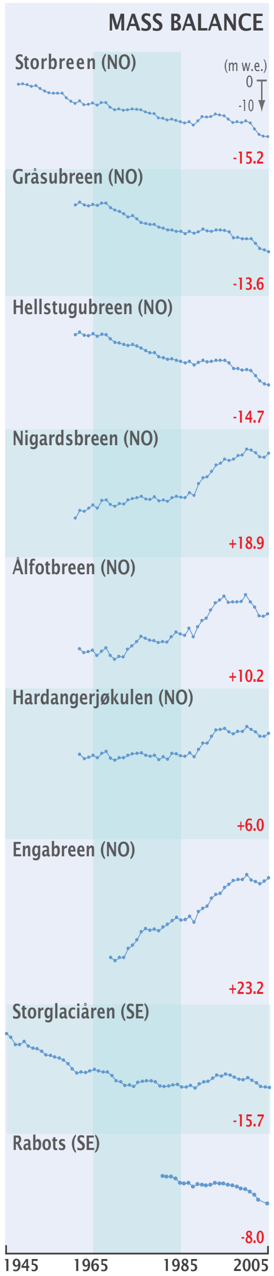

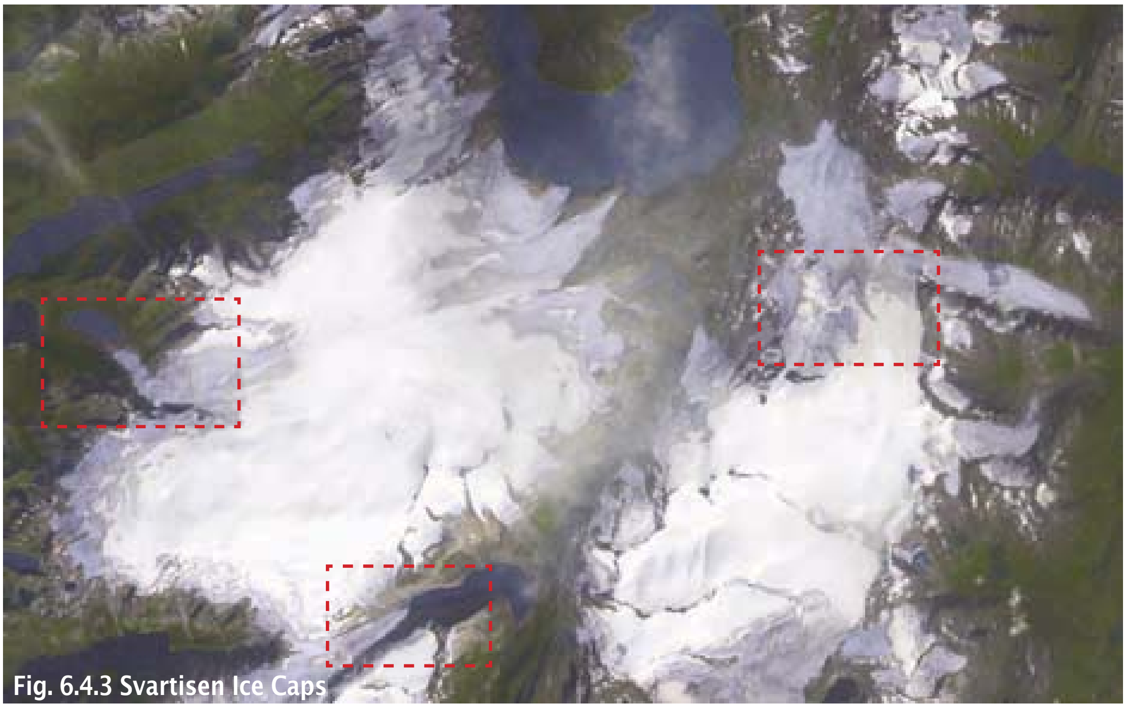

Fig. 6.4.3 Svartisen Ice Caps

Fig. 6.4.3a

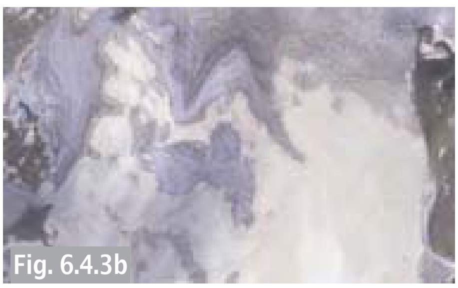

Fig. 6.4.3b

Fig. 6.4.3c

6.5 Central Europe

Glaciers are found in the European Alps, the Pyrenees, and the Caucasus Mountains. Central Europe has the greatest number available of length change and mass balance measurements, with many long-term data series.

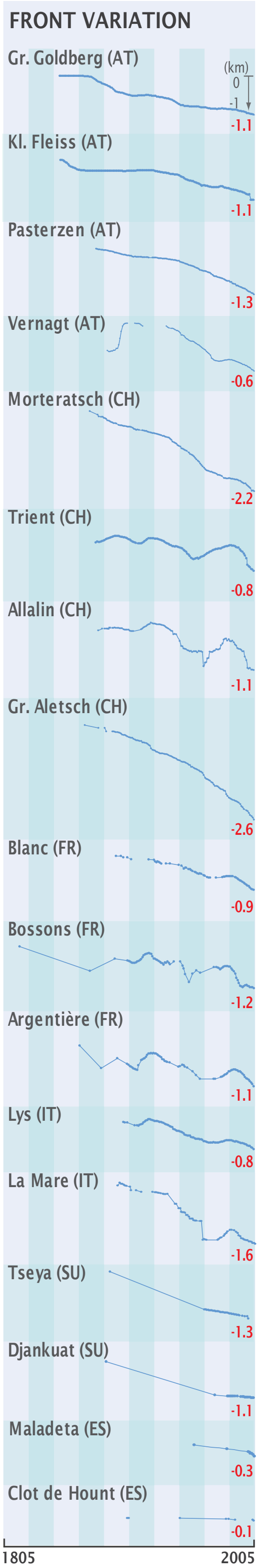

In Central Europe, almost two-thirds of the perennial surface ice cover is located in the Alps with Aletsch Glacier as their greatest valley glacier. The Alps represent the 'water tower' of Europe and form the watershed of the Mediterranean Sea, the North Sea/North Atlantic Ocean, and the Black Sea. The highest peak is Mont Blanc, at 4 808 m asl, near the Italian-French border. About one-third of the region's ice cover is represented by glaciers in the Caucasus Mountains which are situated between the Black Sea and the Caspian Sea. Most glaciers are located in the northern part known as the Ciscaucasus with Mount Elbrus (5 642 m asl) considered as the highest peak in Europe. Some smaller glaciers are found in the Pyrenees – a mountain range in southwest Europe. It extends from the Bay of Biscay to the Mediterranean Sea. The glaciers are situated in the Maladeta massif in Spain with the highest peak of the Pyrenees, Pico d'Aneto (3 404 m asl), and around the peak Vignemale (3 298 m asl) in France. A few more perennial ice fields are found e.g. in the Appennin, Italy, as well as in Slovenia and Poland. In the densely populated Alps, glaciers are a unique resource of freshwater for domestic, agricultural, and industrial use, an important economic component of tourism and hydro-electric power production, but also a source of natural hazards. One of the largest historical glacier disasters occurred in 2002 in North Ossetia, in the Caucasus. An ice-rock avalanche in the Kazbek region resulting from a slope failure sheared off almost the entire Kolka Glacier and devastated the Genaldon valley, causing the death of about 140 people (Huggel et al. 2005).

In the Alps as well as in the Pyrenees and in the Caucasus most glaciers reached their LIA maximum towards mid 19th century (Gross 1987, Maisch et al. 2000, Grove

Fig. 6.5.1 Aerial view toward the Maladeta Massif, Spain, with Pico d'Aneto (left), Aneto Glacier (center) as well as Maladeta Glacier (right) from September 2002. Source: M. Arenillas, *Ingeniería 75*, Spain.

Fig. 6.5.2 Mount Elbrus, seen from the north (photograph taken in September 2007). Source: A. Kääb, *University of Oslo*, Norway.

Fig. 6.5.3 Bernese Alps with Grosser Aletsch Glacier in the center, Swiss Alps. Source: ASTER satellite image (32 x 44 km) and close-ups, 21 July 2006.

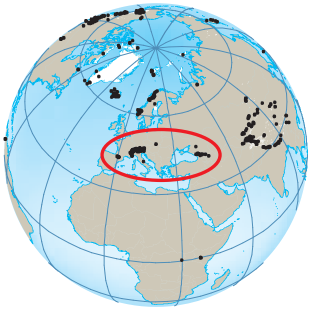

Ice covered area (km²): 3 785

Front variation
number of series: 764
average number of observations: 35
average time length (years): 65

Mass balance
number of series: 43
average number of observations: 20

2004). Annual observations of glacier front variations started in the second half of the 19th century in Austria, Switzerland, France and Italy resulting in more than 680 data series, distributed over the entire Alpine mountain range. There are over 40 front variation series available for the Caucasus, mostly starting in the 2nd half of the 20th century and a few going back to the 1930s. There are two glaciers in the Pyrenees with length change data, one starting in the 1980s and a second one covering the 20th century, though with a few observation points. Mass balance measurements started in 1949 in the Alps, in 1968 in the Caucasus, and in 1992 on Maladeta Glacier in the Pyrenees. Overall mass balance data is available for 43 glaciers, with 10 continuous series since 1968.

The front variations show a general trend of glacier retreat over the past 150 years with intermittent Alpine glacier re-advances in the 1890s, 1920s, and 1970-1980s (Patzelt 1985, Pelfini and Smiraglia 1988, Zemp et al. 2007b). The Alpine glacier cover is estimated to have diminished by about 35 per cent from 1850 to the 1970s and another 22 per cent by 2000 (Paul et al. 2004, Zemp et al. 2007b). Mass balance measurements show an accelerated ice loss after 1980 (Vincent 2002, Huss et al. 2008) culminating in an annual loss of 5 to 10 per cent of the remaining ice volume in the extraordinarily warm year of 2003 (Zemp et al. 2005). In the Caucasus, glacier retreat since the end of the LIA is also widespread, with a certain amount of mass gain in the late 1980s and the early years of the 21st century. The recent retreat was associated with an increase in debris cover and glacier lake development (Stokes et al. 2007). Since the first half of the 19th century, about two-thirds of the ice cover was lost in the Pyrenees with a marked glacier shrinking after 1980 (Chueca et al. 2005).

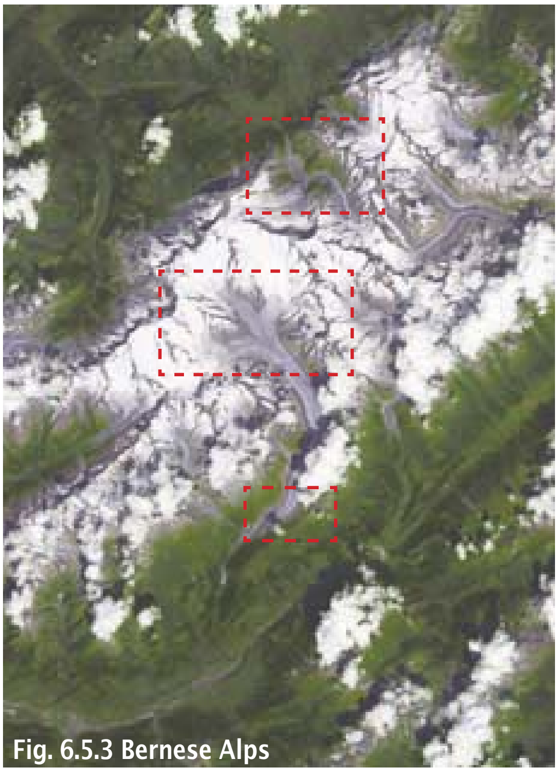

Fig. 6.5.3 Bernese Alps

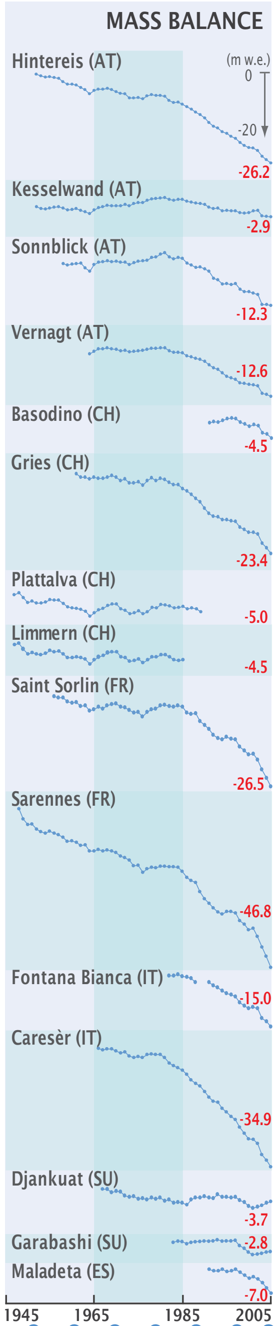

Fig. 6.5.3a

Fig. 6.5.3b

Fig. 6.5.3c

6.6 South America

Glaciers are widespread along the Andes from the tropical ice bodies in the north to the Patagonian Icefields and the Tierra del Fuego in the south. The available fluctuation series cover the time period since the 1960s.

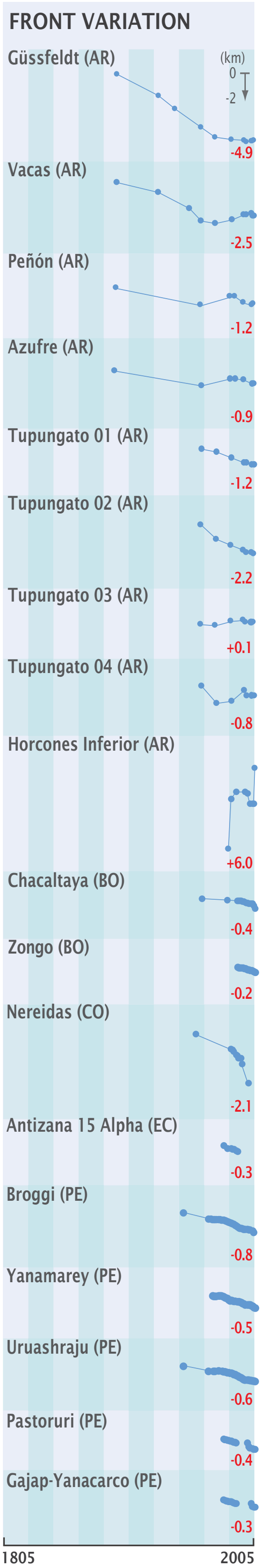

The Andes, stretching over 7 000 km, is the world's longest continental mountain range and a distinct feature of South America, forming a continuous chain of mountains in a north-south direction along the entire west coast. In the north-central portion of South America the Andes are divided into several ridges which span some hundred km in width, whereas to the south the Andes form a narrower and more concentrated chain. The highest peak is the Aconcagua (6 962 m asl), situated in Argentina close to the border with Chile. The climate of the Andes varies greatly depending on latitude, altitude and proximity to the sea. This is found for example in the snowline altitude, which is at 4 500 – 4 800 m asl in the tropical Andes of Ecuador, Colombia, Venezuela, and northern Peru, rises to 5 000–6 500 m asl in the Atacama desert (northern Chile), then descends to 4 500 m asl on Aconcagua at 32˚ S, 2 000 m asl at 40˚ S, 650–1 000 m asl at 50˚ S, and only 300 m asl at 55˚ S (Troll 1973).

Approximate glacier areas for tropical South America are: 1.8 km² for Venezuela, 87 km² for Colombia, 90 km² for Ecuador, 1 780 km² for Peru and 534 km² for Bolivia (Kaser and Osmaston 2002). By far the largest ice cover at about 23 000 km² is found in Chile and Argentina, with more than 85 per cent located in the Northern and Southern Patagonian Icefields and in the Cordillera Darwin Icefield in Tierra del Fuego (Naruse 2006). Glaciers in South America are critically important as a water resource for domestic, agricultural and industrial uses, particularly in equatorial, tropical and subtropical latitudes (Casassa et al. 2007). Andean glaciers also pose a natural hazard, for example, in the form of lahars related to volcanic eruptions, rock/ice avalanches, debris flows and glacier floods related to gravity, climatic processes and ice dynamics (Casassa et al. 2007).

In the southern Andes, most glaciers reached their LIA maximum between the late 17th and early 19th centuries (Villalba 1994). The Peruvian glaciers were in advanced positions in the 1870s, followed by a rapid retreat (Grove 2004). Of the available in-situ mass balance measurements from the Andes only a dozen cover more than a decade, with earliest observations starting at the end of the 1960s. Mass balance is currently being

Fig. 6.6.1 Glaciarised volcanoes in Colombia

Fig. 6.6.1 Glacierised volcanoes in Colombia. The view to the north shows the active volcanos Nevado del Tolima (foreground) and Nevado del Ruiz (background, right) as well as the the inactive Santa Isabel (background, center). The photograph was taken in 2002. Source: J. Ramírez Cadena, *INGEOMINAS*, Colombia.

Fig. 6.6.2 Zongo Glacier and downstream hydroelectric power station located north-east of La Paz city, Bolivia. Photograph taken in July 2006. Source: B. Francou, *IRD*, Bolivia.

Fig. 6.6.3 San Quintín Glacier, Northern Patagonian Icefield. Source: ASTER satellite image in artificial natural colors (35 x 28 km) and close-ups, 2 May 2000.

Ice covered area (km²): 25 500

Front variation

number of series:	160
average number of observations:	4
average time length (years):	36

Mass balance

number of series:	11
average number of observations:	8

Fig. 6.6.2 Zongo Glacier

measured on 28 glaciers from which eleven series have been reported. Long-term series comes from Echaurren Norte in central Chile with more than 30 years of continuous mass balance measurements, as well as from Zongo and Chacaltaya in Bolivia (14 years), and Antizana 15 Alpha in Ecuador (11 years). The observations thus include the glacier shrinkage of the past decades. There have been a few cases of surging glaciers, the most recent being Horcones Inferior in Argentina, with two major surge events starting in 1984 and in 2004 (Milana 2007). The small number of available data series indicates the problems encountered when conducting such measurements under difficult logistical conditions and with unreliable financial support (Casassa et al. 2007). Except for a few cases in Patagonia and Tierra del Fuego, glaciers in South America have shown a general retreat and wasting since the LIA maximum extent with an enhanced retreat trend in recent decades (Casassa et al. 2007).

The Northern Patagonian Icefield lost about 3.4 per cent (140 km²) of its area between 1942 and 2001, whereby the frontal tongues of calving glaciers were observed to be an important source of recession and area change (Rivera et al. 2007). Thinning rates of up to 30 m/y have been observed recently in the Southern Patagonian Icefield, with a relevant contribution to sea level rise (Rignot et al. 2003).

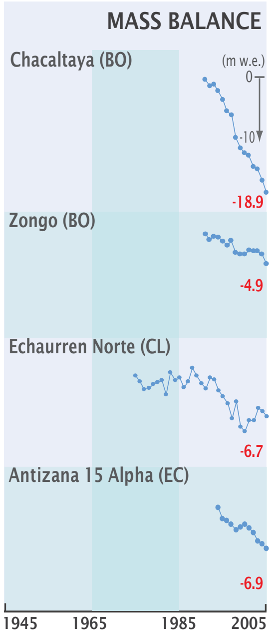

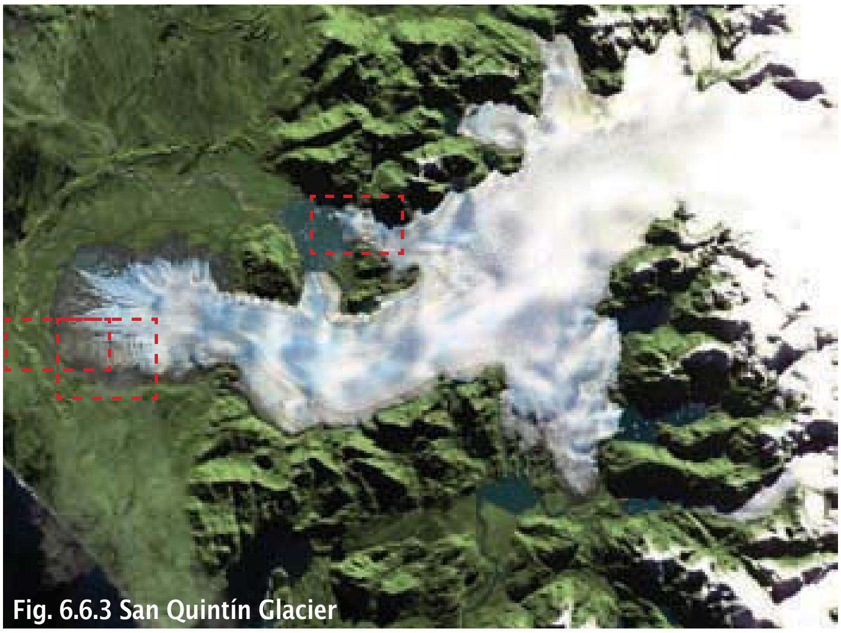

Fig. 6.6.3 San Quintín Glacier

Fig. 6.6.3.a

Fig. 6.6.3.b

Fig. 6.6.3.c

6.7 Northern Asia

The majority of land surface ice in Northern Asia is located on the East Arctic Islands such as Novaya Zemlya, Severnaya Zemlya and Franz Josef Land, as well as distributed in the mountain ranges from the Ural to the Altay, in the east Siberian mountains and Kamchatka. The available data series are sparse and most of the few measurements were discontinued in latter decades of the 20th century.

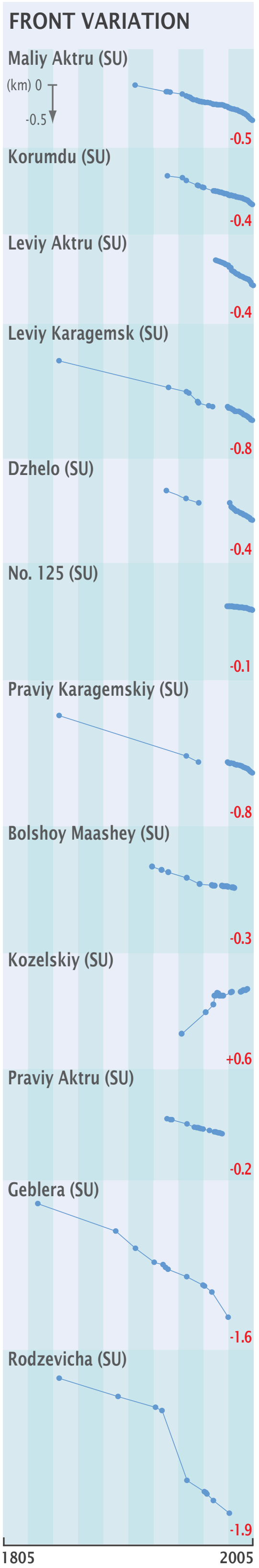

Most of the glacier ice in Northern Asia is concentrated on the East Arctic Islands (total ice cover of about 56 000 km²) such as Novaya Zemlya (23 645 km²), Severnaya Zemlya (18 325 km²) and Franz Josef Land (13 735 km²). In addition, glaciers occur in the mountain ranges from the Ural to the Altay, and Kamchatka with a total area of about 3 500 km² (Dyurgerov and Meier 2005). The glaciers on the East Arctic Islands are not well investigated due to their remote location in the Barents and Kara Sea. They are very much influenced by the extent of sea ice and the North Atlantic oscillations, and some of them are tidewater glaciers. Dated moraines suggest LIA maxima around or after 1300 for some glaciers, and the late 19th century for others on Novaya Zemlya (Zeeberg and Forman 2001). The Altay extends over about 2 100 km from Kazakhstan, China, Russia to Mongolia, reaching its highest elevation of 4 506 m asl on Belukha Mountain in the Russian Altay. Until recently, investigations in the Altay failed to disclose evidence of early LIA advances (Kotlyakov et al. 1991). New studies based on lichenometry indicate extended glacier states in the late 14th and mid 19th century (Solomina 2000). The east Siberian Mountains, such as Cherskiy Range, Suntar-Khayata, and Kodar Mountains, show only small amounts of glacier ice and the knowledge on these glaciers is limited. Gurney et al. (2008) mapped more than 80 glaciers in the Buordakh Massif, in the Cherskiy Range (northeast Siberia), a region with a total glacierised area of about 70 km². The LIA maximum extents have also been delineated and have been dated to 1550–1850 AD (Gurney et al. 2008). The topography of Kamchatka is characterised by numerous volcanoes with heights up to 5 000 m asl. Therefore, some of the glaciers are strongly influenced by volcanic activities. Here, the maximum stage of the LIA was reached in the mid to late 19th century (Grove 2004), with advances of similar magnitudes in the 17th, 18th century (Solomina 2000).


Fig. 6.7.1 Maliy Aktru Glacier

The few available fluctuation series mainly come from the Russian Altay, with half a dozen front variation series covering the entire 20th century and three continuous mass balance series extending back to 1977, from Leviy Aktru and No. 125 (Vodopadniy), and to 1962 from Maliy Aktru. Some information is available from Kamchatka with front variation and mass balance measurements from 1948–2000 and 1973–1997, respectively, and a few short-term series from the Northern Ural and Severnaya Zemlya. Most of the observation series were discontinued at the end of the 20th century. A particular challenge in this region, as well as in parts of Central Asia, has been the breakdown

Fig. 6.7.1 Maliy Aktru Glacier located in the Russian Altay (photograph taken in July 2007). Source: W. Hagg, *LMU Munich*, Germany.
Fig. 6.7.2 Kozelskiy Glacier on Kamchatka in September 2007. Source: A.G. Manevich, *Russian Academy of Sciences*.
Fig. 6.7.3 Ice caps on Severnaya Zemlya, Russian Arctic. ASTER satellite image (63 x 47 km) and close-ups, 19 August 2003.

Ice covered area (km²): 59 600

Front variation

number of series:	24
average number of observations:	14
average time length (years):	55

Mass balance

number of series:	14
average number of observations:	14

Fig. 6.7.2 Kozelskiy Glacier

of the Soviet system in 1989 and the related loss in expertise in and capacities for glacier monitoring. In Japan, mass balance measurements have been carried out since 1981 on Hamaguri Yuki, a perennial snow patch at 2 750 m asl in the Tateyama Mountain, Central Japan (Higuchi et al. 1980).

In the Arctic islands a slight reduction in the glacierised area by little more than one per cent over the past 50 years has been found (Kotlyakov et al. 2006). Tidewater calving glaciers in north Novaya Zemlya underwent a rapid retreat in the first half of the 20th century, half of them being stable during 1952 to 1964, with a more moderate retreat occurring up to 1993 (Zeeberg and Forman 2001). A study based on satellite images shows that from 40 outlet glaciers on north Novaya Zemlya, 36 retreated and only four advanced between 1990 and 2000 (Kouraev et al. 2008). Russian studies show that in the Urals, some glaciers have disappeared completely, while in the Altay, glaciers have been shrinking continuously since the mid 19th century (Kotlyakov et al. 2006) accelerating from seven per cent ice loss between 1952 and 1998 to four per cent between 1998 and 2006 (Shahgedanova et al. 2008). Comparisons with Landsat satellite images of 2003 have shown that the glacier extent of Suntar-Khayata has diminished by 19 per cent since 1945, and in the Cherskiy Range by 28 per cent since 1970 (Ananicheva 2006). On average, the scale of glacier shrinkage was much smaller in continental Siberia than in central Asia and along the Pacific margins (Solomina 2000). On Kamchatka both retreats and advances have occurred on glaciers influenced by volcanoes, whereas a general retreat was found on glaciers located in the coastal area (Kotlyakov et al. 2006).

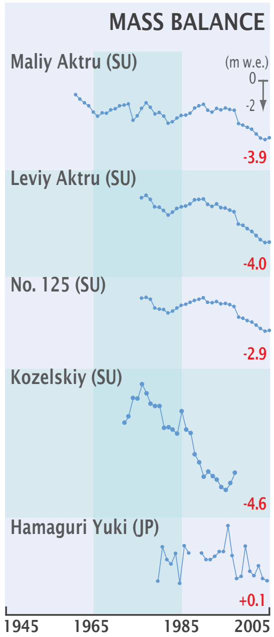

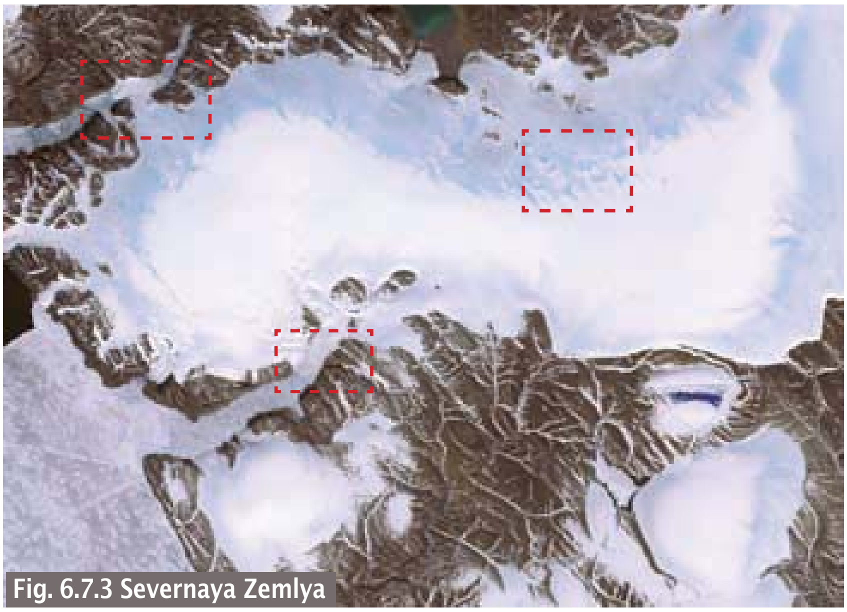

Fig. 6.7.3 Severnaya Zemlya

Fig. 6.7.3a

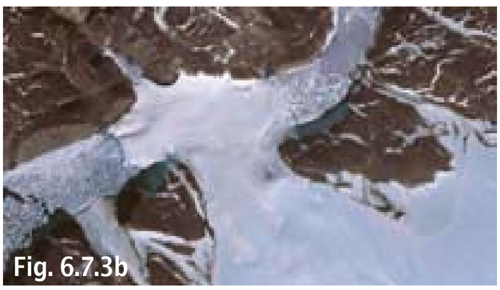

Fig. 6.7.3b

Fig. 6.7.3c

6.8 Antarctica

Mainly due to the remoteness and the immense size of the ice masses, little is known about the distribution and changes in the large number of glaciers and ice caps around the continental ice sheet in Antarctica and on the Subantarctic Islands.

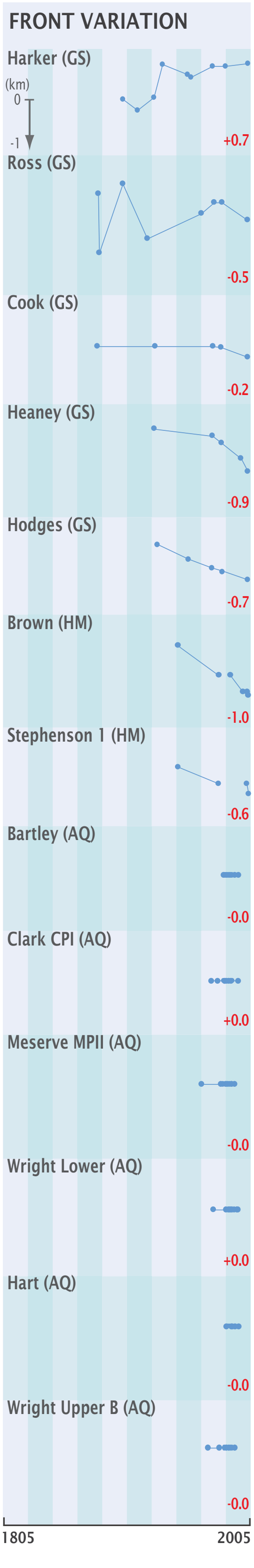

The vast majority of glaciers and ice caps in the Antarctica are located on the Antarctic Peninsula and around the Antarctic Ice Sheet, with an overall estimated area ranging from 70 000 km² (Dyurgerov and Meier 2005) to 169 000 km² (Shumsky 1969). This large uncertainty results from the difficulty to differentiate clearly between the various glaciers and ice caps, and the ice bodies closely linked to the continental ice sheet. Weidick and Morris (1998) describe three categories of local glaciers outside the ice sheet: coastal glaciers, ice streams which are discrete dynamic units attached to the ice sheet, and isolated ice caps. Coastal local glaciers are most obvious in the McMurdo Dry Valleys within Victoria Land and on the Antarctic Peninsula. The latter is covered by a long, relatively narrow and thin ice field nourishing valley glaciers, which cut through the coastal mountains and terminate in ice cliffs at sea level. Ice streams range from smaller ones on the southern part of the Antarctic Peninsula to larger ones flowing from the central Antarctic Plateau down to the Ross or Filchner-Ronne ice shelves. Examples of the third type are the ice rises on the Larsen and Filchner-Ronne ice shelves. Berkner Island, the largest ice rise in the world, is located on the latter (Swithinbank 1988). Evidence of the timing of LIA glacier maxima south of the Antarctic Circle (66° 30' S) is sparse due to the lack of organic material for dating (Grove 2004).

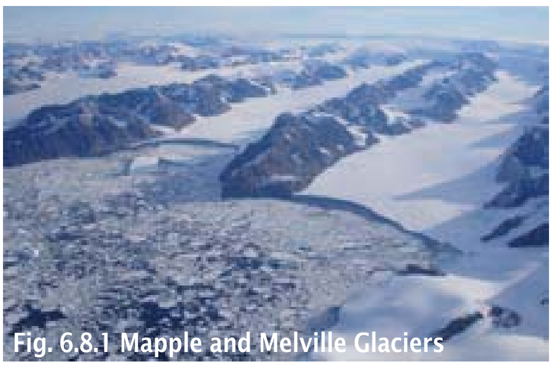

In addition to Antarctica, glaciers and ice caps are situated on Subantarctic Islands such as the South Shetland Islands, South Georgia, Heard Island and Kerguelen, with a total estimated ice cover of roughly 7 000 km² (Dyurgerov and Meier 2005). On the South Shetland Islands, at least ten glacial events were found to have occurred between 1240 and 1991 (Birkenmajer 1998, Clapperton 1990). South Georgia is located about 1 400 km east-southeast of the Falkland / Malvinas Islands. More than half of it is ice covered, with most of the glaciers extending to the sea (Clapperton et al. 1989a, b). Clapperton et al. (1989a, b) described LIA advances beginning after the late 13th century and culminating in the 18th, 19th and 20th centuries. Heard Island is situated in the Southern Indian Ocean, 1 650 km north of the Antarctic continent. The island is characterised by two volcanoes; the larger and still active one, Big Ben, reaching 2 750 m asl. Some 21 glaciers are identified on the volcanic cone (Ruddell 2006); typically, they widen and steepen toward the sea, and terminate in ice cliffs (Grove, 2004). A total of 70 per cent of the island is ice covered (Ruddell 2006, Thost and Truffer 2008).

Fig. 6.8.1 Oblique aerial photograph with Antarctic Peninsula plateau in the background (March 11, 2007). From north to south (right-left) the Mapple and Melville Glaciers, which are calving at present into the Larsen B embayment. Both glaciers nourished formerly the Larsen B ice shelf, which collapsed within a few weeks in February–March 2002, during the warmest summer ever recorded in the region. Source: P. Skvarca, *Instituto Antártico Argentino.*

Fig. 6.8.2 Wright Lower Glacier with Lake Brownworth, Dry Valleys in Antarctica (January 14, 2007). The Wright Lower Glacier is fed from the Wilson-Piedmont Glacier. The Onyx River dewaters from Lake Brownworth into the drainless Lake Vanda. The nunatak is called King Pin (820 m) and at the far back Mt Erebus (3794 m), the most southern active volcano, is visible. Source: D. Stumm, *University of Otago,* New Zealand.

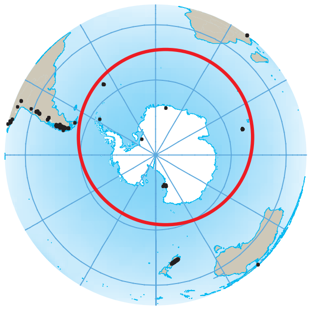

Ice covered area (km²): 77 000

Front variation

number of series:	48
average number of observations:	3
average time length (years):	30

Mass balance

number of series:	1
average number of observations:	4

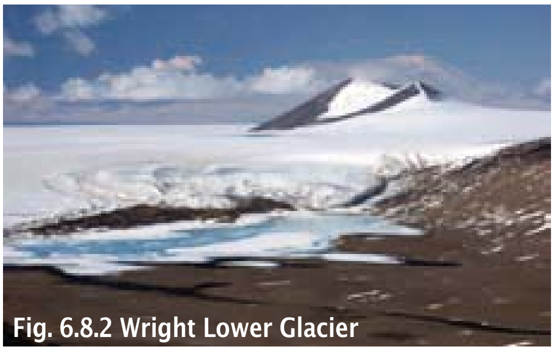

Fig. 6.8.2 Wright Lower Glacier

A number of front variation series as derived from expedition reports, aerial photographs and satellite images are available from the Dry Valleys in Antarctica extending back to the 1960s, as well as from South Georgia, back to the late 19th century, and from Heard Island back to 1947. In summer 1999–2000, a detailed mass balance monitoring program was initiated on Glaciar Bahía del Diablo, a glacier on Vega Island, at the northeastern side of the Antarctic Peninsula (Skvarca and De Angelis 2003, Skvarca et al. 2004). Additional reconstructions and measurements are reported in the literature, e.g. from Kerguelen (e.g., Frenot et al. 1993) and South Shetland Islands (e.g., Hall 2007), with no data having been reported to the WGMS.

Cook et al. (2005) mapped 244 glaciers on the Antarctic Peninsula and adjacent islands, most of them terminating in the sea. Their analyses of aerial photographs and satellite images showed that 87 per cent of the glaciers have retreated over the last six decades. A general glacier recession trend of different spatial pattern on the Antarctic Peninsula was previously reported by Rau et al. (2004), who investigated the ice-front changes north of 70° S over the period 1986–2002. Large retreat and thinning rates over the past two decades have been reported from glaciers terminating on land on Vega and James Ross Islands, as well as strong glacier acceleration, surges and retreats subsequent to the collapse of the Larsen Ice Shelf A and B sections (De Angelis and Skvarca 2003, Rott et al. 2002, Skvarca and De Angelis 2003). Glaciers on South Georgia receded overall by varying amounts from their more advanced positions in the 19th century, with large tidewater glaciers showing a more variable behavior and remaining in relatively advanced positions until the 1980s. Since then, however, most glaciers have receded; some of these retreats have been dramatic and a number of small mountain glaciers are about to disappear (Gordon et al. 2008). According to expedition records, little or no change occurred on glaciers at Heard Island during the first decades of the 20th century (Grove 2004). However, in the second half, recession of glaciers has been widespread. A recent study yields a reduction in the overall ice extent of about 29 per cent from 1947 to 2003 (Thost and Truffer 2008), interrupted by a re-advance of some glaciers in the 1960s (Radok and Watts 1975).

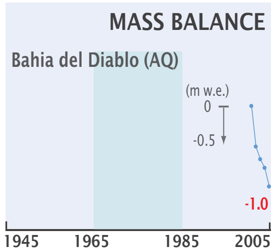

Fig. 6.8.3a

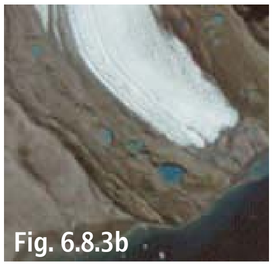

Fig. 6.8.3b

Fig. 6.8.3c

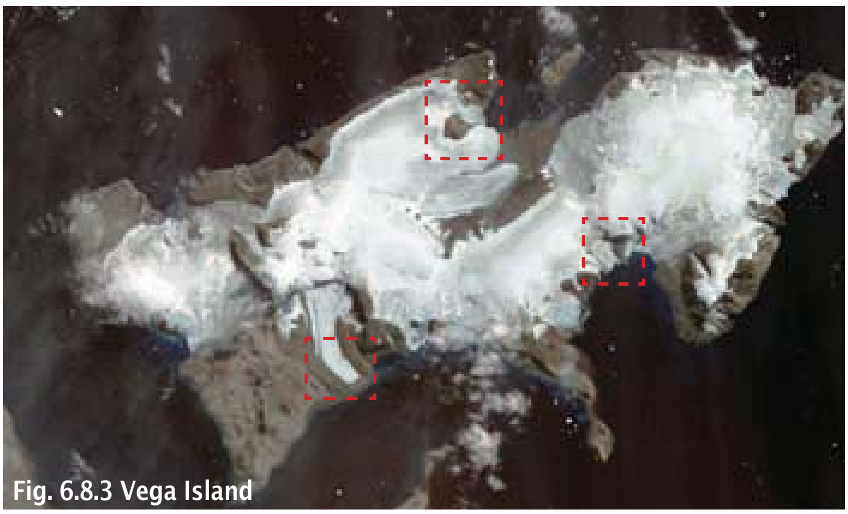

Fig. 6.8.3 Vega Island

Fig. 6.8.3 Bahía del Diablo on Vega Island, at the northeastern side of the Antarctic Peninsula. Source: ASTER satellite image (37 x 20 km) and close-ups, 27 January 2006.

6.9 Central Asia

The main mountain range of Central Asia is the Himalaya and its adjacent mountain ranges such as Karakoram, Tien Shan, Kunlun Shan and Pamir. The sum of its glacierised area corresponds to about one sixth of the global ice cover of glaciers and ice caps. The available observations are distributed well over the region but continuous long-term fluctuations series are sparse.

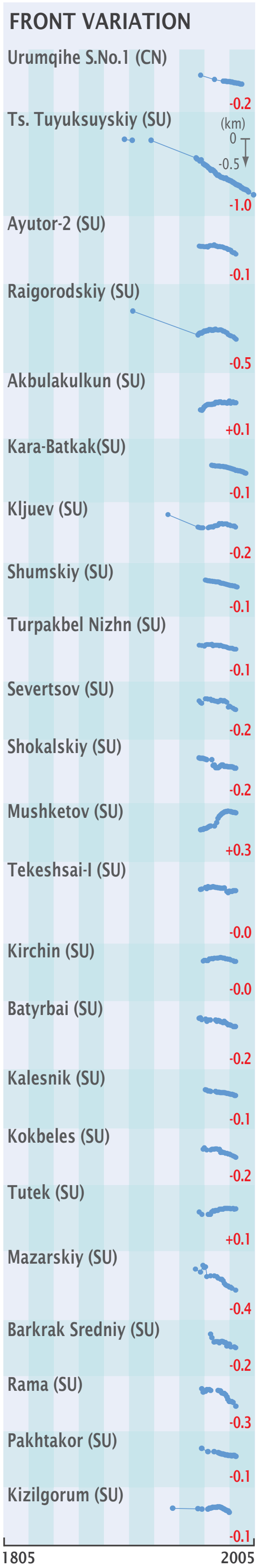

Central Asia with an estimated total ice cover of 114 800 km² has as its dominant mountain range the Himalaya, where most of the glaciers occur (33 050 km²) and its adjacent mountain ranges (with corresponding ice areas): Karakoram (16 600 km²), Tien Shan (15 417 km²), Kunlun Shan (12 260 km²) and Pamir (12 260 km²) mountains (Dyurgerov and Meier 2005). The Himalaya is the highest mountain range of the world and extends from the Nanga Parbat (8 126 m asl) in the NW over 2 500 km to the Namcha Barwa (7 782 m asl) in the SE with a north-south extent of 180 km (Burga et al. 2004). The climate, and the precipitation in particular, is characterised by the influence of the South Asian monsoon in summer and the mid-latitude westerlies in winter. In Central Asia, glacier degradation is accompanied by increasing debris cover on many glacier termini and the formation of glacier lakes (Ageta et al. 2000). Such lakes, sometimes also dammed due to glacier surges (Kotlyakov et al. 2008), have the potential to threaten downstream areas with outburst floods (Wessels et al. 2002). The mountain ranges of Central Asia function as water towers for millions of people. Glacier runoff thereby is an important freshwater resource in arid regions as well as during the dry seasons in monsoonal affected regions (Barnett et al. 2005).

Fig. 6.9.1 Ts. Tuyuksuyskiy Glacier

The LIA is considered to have lasted until the mid or late 19th century in most regions (Grove 2004) with glacier maximum extents occurring between the 17th and mid 19th century (Solomina 1996, Su and Shi 2002, Kutuzov 2005). The available 310 front variation series are distributed over most of the region, and the first observations started early in the 20th century. About 10 per cent of the series extend back to the first half of the 20th century but only 24 data series, located in Pamir and Tien Shan, consist of more than 15 observation series. Unfortunately, 90 per cent of the observations series were discontinued before 1991 and only about a dozen series have reported information in the 21st century. The distribution of mass balance series in space and time shows a similar pattern. Just six (out of 35) series consist of more than 15 observation years and only

Fig. 6.9.2 Baltoro Glacier in the Karakoram

Fig. 6.9.1 Tsentralniy Tuyuksuyskiy, Kazakh Tien Shan, in September 2003. Source: V.P. Blagoveshchenskiy.

Fig. 6.9.2 Panoramic view with direction NNE to the confluence of the Godwin Austen Glacier, flowing south from K2 (8 611 m asl), with the Baltoro Glacier in the Karakoram. Source: C. Mayer, *Commission for Glaciology of the Bavarian Academy of Sciences.*

Fig. 6.9.3 Himalaya main ridge between Bhutan and Tibet. Source: ASTER satellite image (56 x 32 km) and close-ups, 20 January 2001.

Ice covered area (km²): 114 800

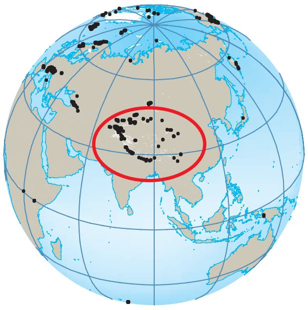

Front variation	
number of series:	310
average number of observations:	5
average time length (years):	22

Mass balance	
number of series:	35
average number of observations:	13

two of them, Ts. Tuyuksuyskiy (Kazakh Tien Shan) and Urumqihe South No.1 (Chinese Tien Shan) are still surveyed every year. As in Northern Asia, the breakdown of the Soviet System in 1989 might partly explain the breakdown of the observation network in the 1990s. Within Central Asia, the Himalaya is strongly underrepresented in terms of front variation and mass balance observations, and most series are comparably short.

Regional studies based on remote sensing data help to provide a better overview on the recent changes in the Central Asian ice cover. Glacier retreat was dominant in the 20th century, except for a decade or two around 1970, when some glaciers gained mass and even reacted with re-advances of a few hundred metres. After 1980 ice loss and glacier retreat was dominant again. In Bhutan, Eastern Himalaya, an eight per cent glacier area loss was observed between 1963 and 1993 (Karma et al. 2003). Berthier et al. (2007) used remote sensing data to investigate glacier thickness changes in the Himachal Pradesh, Western Himalaya. They found an annual ice thickness loss of about 0.8 m w.e. per year between 1999 and 2004 – about twice the long-term rate of the period 1977–1999. In China, the overall glacier area loss is estimated at about 20 per cent since the maximum extent in the 17th century (Su and Shi 2002). The area loss since the 1960s is estimated to about 6 per cent, and is more pronounced in the Chinese Himalaya, Qilian Mountains and Tien Shan, but with rather small recessions in the hinterland of the Tibetan plateau (Li et al. in press). Over the 20th century, glacier area is estimated to have decreased by 25–35 per cent in the Tien Shan (Podrezov et al. 2002, Kutuzov 2005, Narama et al. 2006, Bolch 2007), by 30–35 per cent in the Pamirs (Yablokov 2006), and by more than 50 per cent in northern Afghanistan (Yablokov 2006).

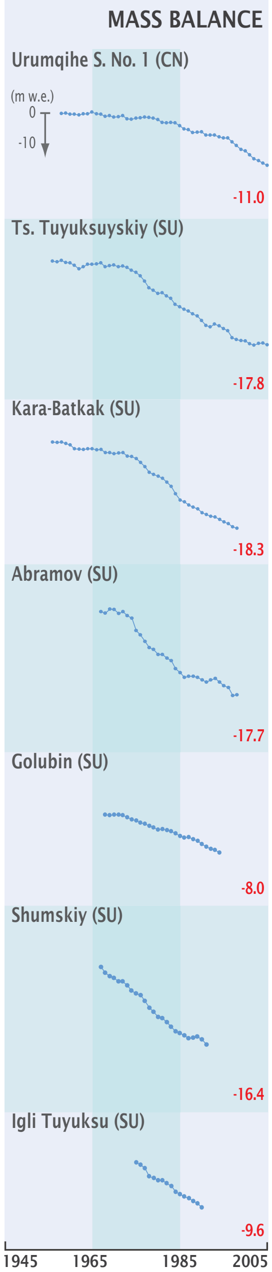

Fig. 6.9.3 Himalaya main ridge

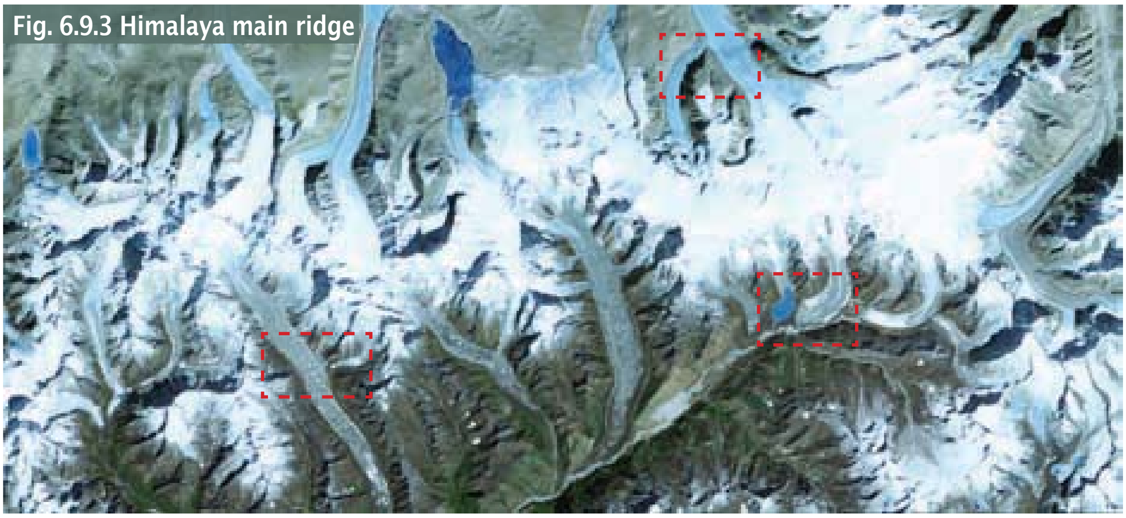

Fig. 6.9.3a

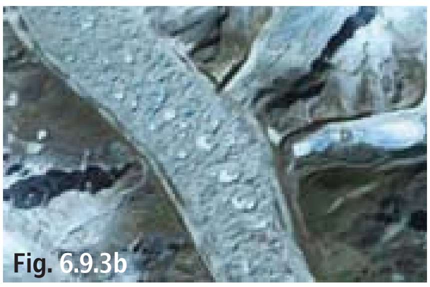

Fig. 6.9.3b

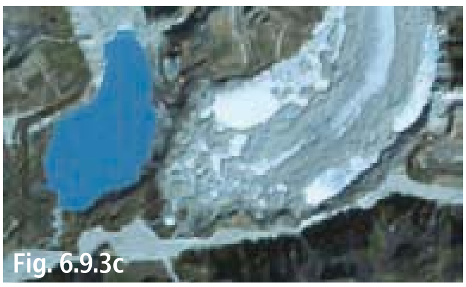

Fig. 6.9.3c

6.10 North America

North American glaciers are located on mountains in the west of the continent from Alaska down to the Canadian and US Rockies, and on volcanoes in Mexico. A lot of the length change observations were discontinued at the end of the 20th century, but there still are several long-term mass balance series.

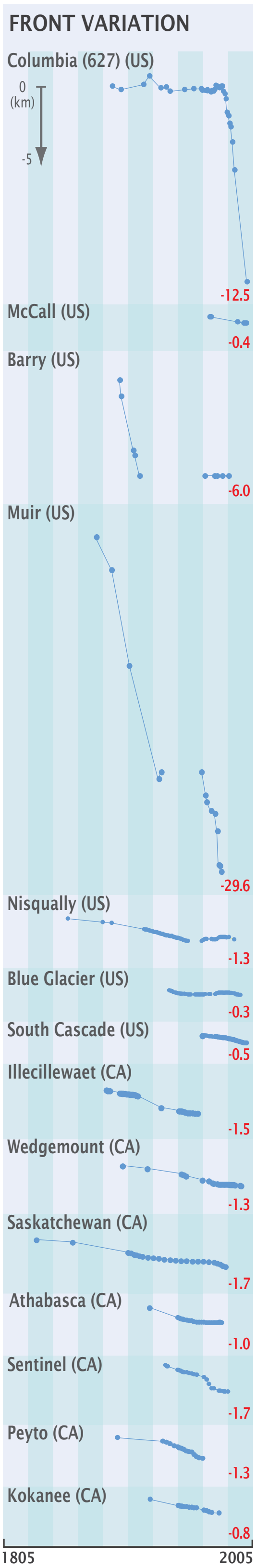

Most of the mountain ranges in North America are found on the west of the continent, parallel to the coastline. Prominent are the "Rocky Mountains", which spread over more than 3 000 km from the Mexican border through the United States and into Canada and eastern Alaska. To the north they extend into the Alaska Range and the Brooks Range. The highest peak of the continent is Mount McKinley / Denali (6 193 m asl), which is situated in the Alaska Range. Glaciers and ice fields in the region presented here cover almost as much area as in the Canadian Archipelago (see section 6.11 Arctic Islands) with about 75 000 km^2 in Alaska and about 49 000 km^2 in the conterminous USA and western Canada. In the latter, glaciers are situated in the Rocky Mountains and Interior Ranges, and along the coast of the Pacific Ocean, where they are in some regions continuous with Alaskan Glaciers (Williams and Ferrigno 2002). In general, the climate of the mountain ranges shows strong variations depending on latitude, altitude and proximity to the sea. Therefore, the glaciers in the south are much smaller and occur at higher elevations than in the higher latitudes, where some glaciers extend down to the shore. In Mexico, small glaciers occur on the peaks of three volcanoes, namely on Pico de Orizaba, Iztaccíhuatl, and Popocatépetl (White 2002).

In conterminous USA and Canada glaciers reached their LIA maximum extent in the mid to late 19th century (Kaufmann et al. 2004). In Alaska, the LIA maxima were attained at various times; for the northeast Brooks Range it was the late 15th century, and for the Kenai Mountains, the mid 17th century (Grove 2004). However, most of the Alaskan glaciers reached the LIA maximum extent between the early 18th and late 19th centuries (Molnia 2007). Although several dozen front variation observations exist for the 20th century, most of the series were discontinued in the 1980s or 1990s. Half of the 45 reported mass balance series cover ten or more measurement years. Among these there are seven with 39 or more years of observations, including for example Peyto Glacier in the Canadian Rockies, Place and South Cascade Glacier in the Cascade Mountains, as well as Lemon Creek, Gulkana and Wolverine Glacier in Alaska, with some extending as far back as the early 1950s. Half of the mass balance series were not continued into the 21st century.

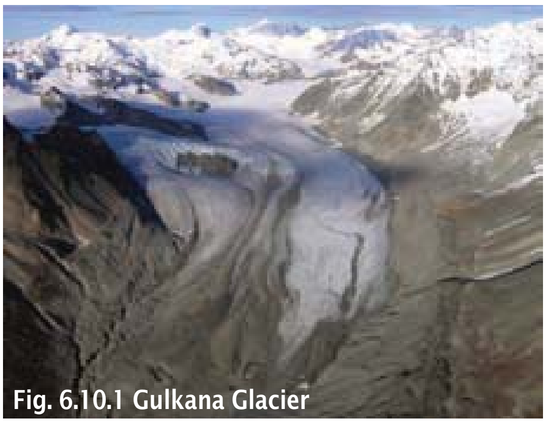
Fig. 6.10.1 Gulkana Glacier

Fig. 6.10.1 Gulkana Glacier in the Alaska Range, USA. Photograph was taken October 5, 2003. Source: R. March, *United States Geological Survey.*

Fig. 6.10.2 South Cascade Glacier in the Canadian Rockies. Photograph was taken in 2001. Source: M.N. Demuth, *Natural Resources Canada.*

Fig. 6.10.3 Section of Kenai Mountains, Alaska, USA, with Wolverine Glacier to the middle bottom. Source: ASTER satellite image (37 x 48 km) and close-ups, 8 September 2005.

Ice covered area (km²): 124 000

Front variation
number of series: 221
average number of observations: 5
average time length (years): 37

Mass balance
number of series: 45
average number of observations: 16

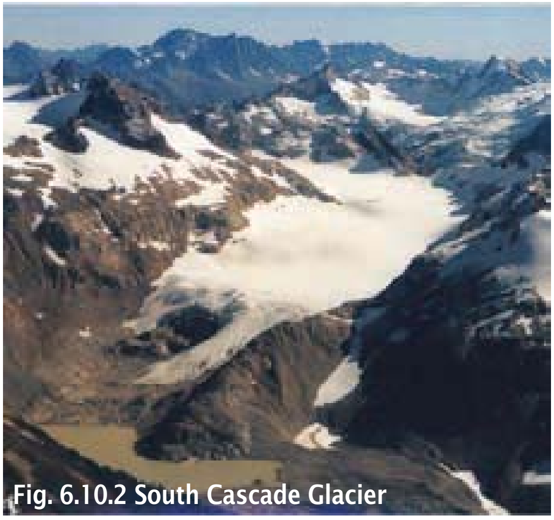

Fig. 6.10.2 South Cascade Glacier

The glacier observations show a general retreat after the LIA maximum, particularly at lower elevations and southern latitudes (Molnia 2007), which slowed down somewhat between the 1950s and 1970s (La Chapelle 1960) and accelerated again after the 1970s. Distinct exceptions to this overall trend are found in the fluctuations of certain tidewater glaciers such as Muir (Saint Elias Mountains), Columbia 627 (Chugach Mountains), or Taku Glacier (Alaskan Panhandle). Mass balance measurements show strong accelerating ice losses since the mid 1970s (Demuth and Keller 2006, Josberg et al. 2007, Moore and Demuth 2001) which was confirmed by remote sensing studies in Alaska and Canada (Arendt et al. 2002, Demuth et al. 2008, Larsen et al. 2007). In the Western Cordillera of the Rocky Mountains the glacier area loss since the LIA is estimated at about 25 per cent (Fountain et al. 2006, Luckman 2000, Luckman 2006). Small glacier diminution appears to be a distinct feature of the past century and a half of ice observation in some regions (Canadian Rocky Mountain eastern slopes: Demuth et al. 2008; North Cascades: Granshaw and Fountain 2006). It is recognised in both instances however, that topographic controls and glacier dynamics can be the source of significant local and regional variability (e.g., DeBeer and Sharp 2007).

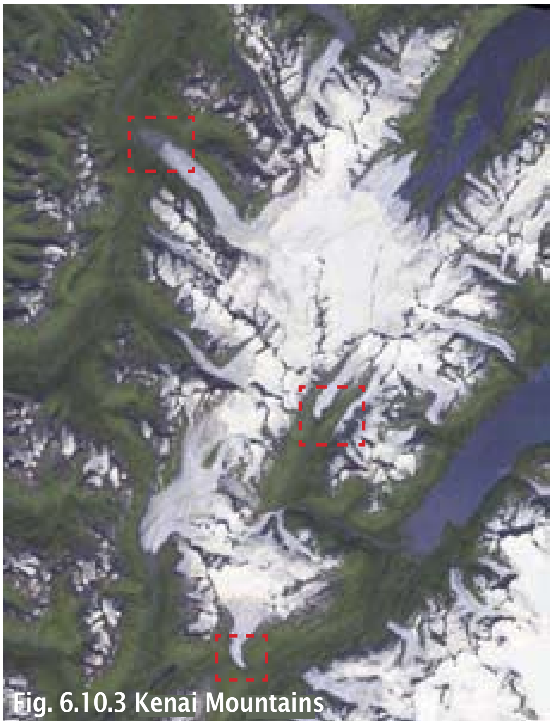

Fig. 6.10.3 Kenai Mountains

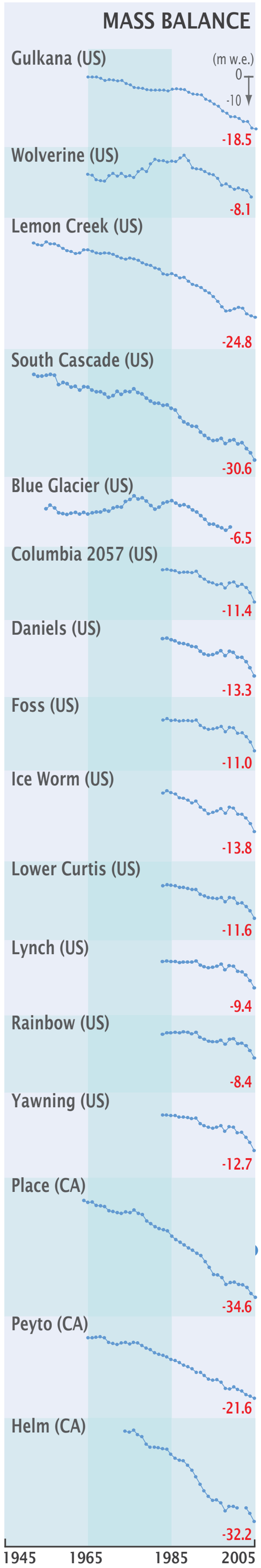

Fig. 6.10.3a

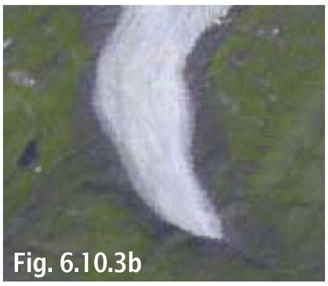

Fig. 6.10.3b

Fig. 6.10.3c

6.11 Arctic Islands

Glaciers and ice caps are found on the Canadian Arctic Archipelago and around the Greenland Ice Sheet, as well as on the West Arctic Islands, Iceland, and Svalbard. The majority of the fluctuation measurements have been reported from the latter two regions.

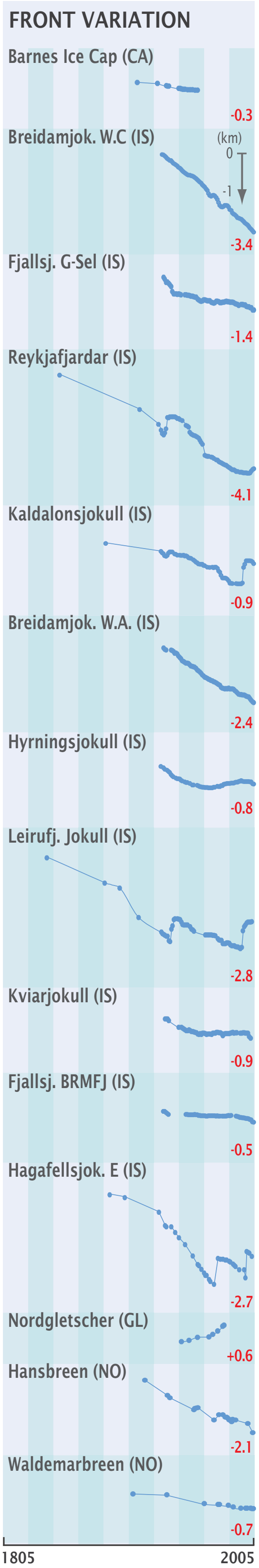

The Arctic Islands consist of Greenland, the Canadian Arctic Archipelago to the west, Iceland, Svalbard and the West Arctic Islands, as well as the East Arctic Islands (see section Northern Asia) to the east. More than half of the area covered by glaciers and ice caps (~ 150 000 km^2) is located on the Canadian Arctic Archipelago, which is a group of more than 36 000 islands (e.g. Baffin, Devon, Ellesmere, and Axel Heiberg Island), and another quarter is found around the Greenland ice sheet. Iceland is located on the Mid-Atlantic Ridge, the boundary of the European and the American plates, with its ice cover dominated by six large ice caps, with Vatnajökull as the largest. The Svalbard Archipelago is situated in the Arctic Ocean north of mainland Europe. Its topography is more than half covered by ice, and is characterized by plateau mountains and fjords. The climate and as such the fluctuations of glaciers and ice caps of the Arctic Islands are very much influenced by the extent and distribution of sea ice which in turn depends on ocean current and on the Arctic and North Atlantic Oscillations. The large variability in ice thickness of Arctic glaciers and ice caps as well as different ice temperatures is expected to result in different responses to climatic changes. In addition, some of the rapid glacier advances might have been related to volcanic activities (in Iceland), glacier surges or calving processes rather than to climatic events.

The timing of the LIA maximum extent of glaciers and ice caps differs between the regions. It is estimated to the mid 18th century for Iceland and the end of the 19th century for the Canadian Arctic Archipelago (Grove 2004). The few investigations from Greenland indicate that many glaciers and ice caps (e.g. on Disko Island) reached their maximum extents before the 19th century (Weidick 1968). In the LIA the glaciers on Svalbard were close to their late Holocene maximum extent and remained there until the onset of the 20th century (Svendsen and Mangerud 1997).

Iceland and the western part of Svalbard are quite well represented in glacier observation series. Front variation series span most of the 20th century. Continuous mass balance measurements are available since the end of the 1960s from Svalbard (Austre Brøggerbreen, Midtre Lovénbreen) and since 1988 from Iceland (Hofsjökull North). Available fluctuation series from glaciers and ice caps of Greenland and the Canadian Arctic Archipelago are sparse and most of them were interrupted in the 20th century. The only long-term mass balance series, starting in the early 1960s, are available from White and Baby Glacier (Axel Heiberg Island), as well as from the

Fig. 6.11.1 Waldemarbreen in the western part of Svalbard (summer of 2006). Source: I. Sobota, *Nicolaus Copernicus University*, Poland.

Fig. 6.11.2 The Hofsjökull Ice Cap, Iceland. Source: ASTER satellite image (50 x 51 km), 13 August 2003.

Fig. 6.11.3 Glaciers draining the Grinnell Land Icefield on Ellesmere Island, Canadian Arctic. Source: ASTER satellite image (62 x 61 km) and close-up, 31 July 2000.

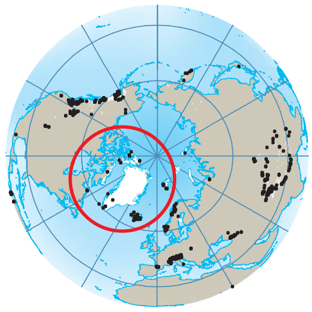

Ice covered area (km²): 275 500

Front variation

number of series:	93
average number of observations:	31
average time length (years):	52

Mass balance

number of series:	34
average number of observations:	13

Devon Ice Cap (Koerner 2005). Archaeological findings, historical documents, trim lines together with the fragmentary measurement series, give evidence of a general retreating trend of the Arctic glaciers and ice caps since the time when of their LIA extent which slowed down somewhat during the middle of the 20th century (Dowdeswell et al. 1997, Grove 2004, ACIA 2005). Glaciers on Cumberland Peninsula, Baffin Island, yield an area loss of 10–20 per cent between the LIA maximum extent and 2000 (Paul and Kääb 2005). However, there are several regional or glacier specific variations found in this overall trend such as the mass gain of Kongsvegen (Svalbard) in the early 1990s (Hagen et al. 2003) and periods of glacier retreat (1930–1960, after 1990) and advance (1970–1985) in Iceland (Sigurdsson et al. 2007).

Fig. 6.11.2 Hofsjökull

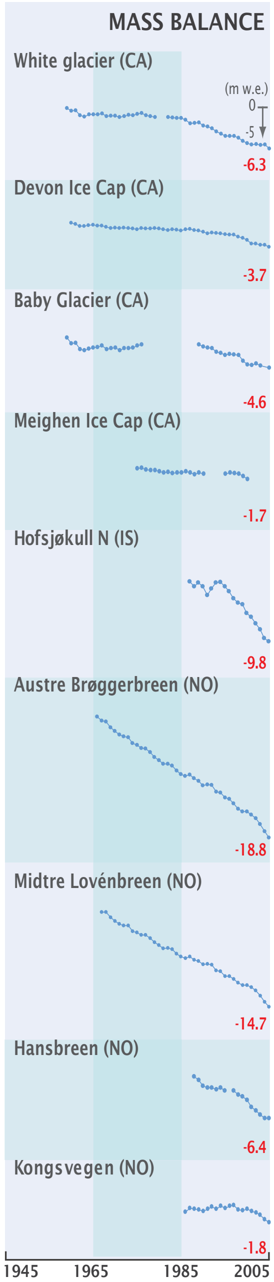

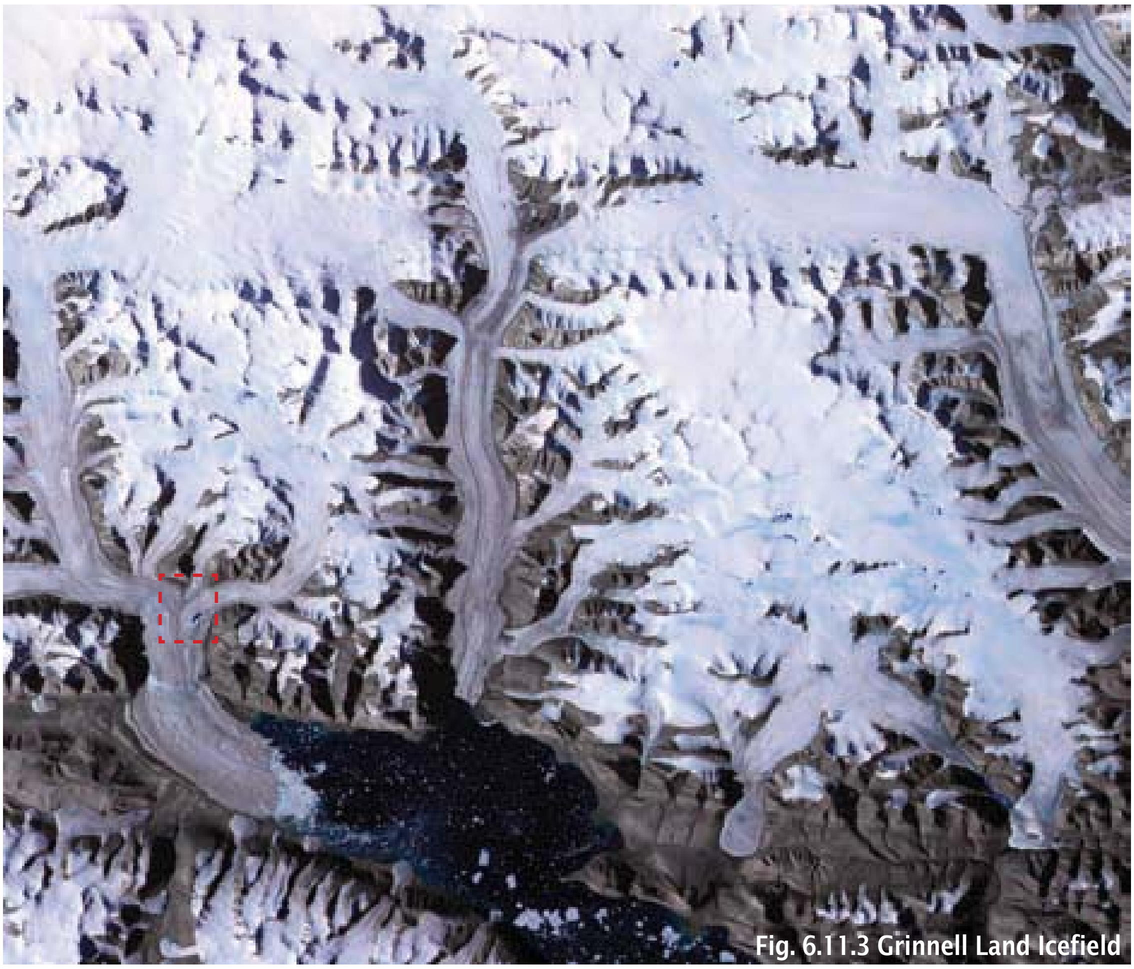

Fig. 6.11.3 Grinnell Land Icefield

Fig. 6.11.3a

7 Conclusions

The internationally coordinated collection of information about ongoing glacier changes since 1894 and the efforts towards the compilation of a world glacier inventory have resulted in unprecedented data sets. Several generations of glaciologists around the world have contributed with their data to the present state of knowledge. For the second half of the 20th century, preliminary estimates of the global distribution of glaciers and ice caps covering some 685 000 km^2, are available, including detailed information on about 100 000 glaciers, and digital outlines for about 62 000 glaciers. The database on glacier fluctuations includes 36 240 length change observations from 1803 glaciers as far back as the late 19th century, as well as about 3 400 annual mass balance measurements from 226 glaciers covering the past six decades. All data is digitally made available by the WGMS and its cooperation partners, the NSIDC and the GLIMS initiative.

The glacier moraines formed during the end of the LIA, between the 17th and the second half of the 19th century, mark Holocene maximum extents of glaciers in most of the world's mountain ranges. From these positions, glaciers around the globe have been shrinking significantly, with strong glacier retreats in the 1940s, stable or growing conditions around the 1970s, and again increasing rates of ice loss since the mid 1980s. On a shorter time scale, glaciers in various mountain ranges have shown intermittent re-advances. Looking at individual fluctuation series, a high variability and sometimes contradictory behaviour of neighbouring ice bodies are found which can be explained by the different glacier characteristics. The early mass balance measurements indicate strong ice losses as early as the 1940s and 1950s, followed by a moderate ice loss between 1966 and 1985, and accelerating ice losses until present. The global average annual mass loss of more than half a metre water equivalent during the decade of 1996 to 2005 represents twice the ice loss of the previous decade (1986–95) and over four times the rate of the decade from 1976 to 1985. Prominent periods of regional mass gains are found in the Alps in the late 1970s and early 1980s and in coastal Scandinavia and New Zealand in the 1990s. Under current IPCC climate scenarios, the ongoing trend of worldwide and rapid, if not accelerating, glacier shrinkage on the century time scale is most likely to be of a non-periodic nature, and may lead to the deglaciation of large parts of many mountain ranges by the end of the 21st century.

In view of the incompleteness of the detailed inventory of glaciers and ice caps and the spatio-temporal bias of the available fluctuation series towards the Northern Hemisphere and Europe, it is of critical importance that glacier monitoring in the 21st century:

- continues long-term fluctuation series (i.e., length change and mass balance) in combination with decadal determinations of volume/thickness and length changes from geodetic methods in order to verify the annual field observations,
- re-initiates interrupted long-term series in strategically important regions and strengthens the current monitoring network in the regions wich are currently sparsely covered (e.g. Tropics, South America, Asia, and the polar regions),
- integrates reconstructed glacier states and variations into the present monitoring system in order to extend the historical set of length change data and to put the measured glacier fluctuations of the last 150 years into context with glacier variations during the Holocene,
- replaces long-term monitoring series of vanishing glaciers with timely starting parallel observations on larger or higher-reaching glaciers,
- concentrates the extent of the field observation network mainly on (seasonal) mass balance measurements, because they are the most direct indication of glacier reaction to climate changes,

- makes use of decadal digital elevation model differencing, and similar techniques, to extend and understand the representativeness of the field measurements to/for the regional ice changes,

- completes a global glacier inventory, e.g., for the 1970s (cf. WGMS 1989),

- defines key regions, where the glacier cover is relevant to climate change, sea level rise, hydrological issues and natural hazards, and in which repeated detailed inventories assess glacier changes (e.g., from the trim lines of the LIA) around 2000, and of the coming decades, with respect to the global baseline inventory, and

- periodically re-evaluates the feasibility and relevance of the monitoring strategy and its implementation.

The potentially dramatic climate changes, as sketched for the 21st century by IPCC (2007) refer to glacier changes of historical dimensions with strong impacts on landscape evolution, fresh water supply, natural hazards and sea level changes. This requires that international glacier monitoring makes use of the rapidly developing new technologies (remote sensing and geo-informatics) and relate them to the more traditional field observations, in order to face the challenges of the 21st century.


Fig. 7.1a Muir Glacier, 1941


Fig. 7.1b Muir Glacier, 2004

Fig. 7.1a—b Photo comparison of Muir Glacier, Alaska, which is a typical tidewater glacier. The photo 7.1a was taken on 13 August 1941 by W. O. Field; the photo 7.1b was taken on 31 August 2004 by B. F. Molnia of the *United States Geological Survey*. Source: *US National Snow and Ice Data Center*.

References

Abbott, M.B., Wolfe, B.B., Wolfe, A.P., Seltzer, G.O., Aravena, R., Mark, B.G., Polissar, P.J., Rodbell, D.T., Rowe, H.D. and Vuille, M. (2003): Holocene paleohydrology and glacial history of the central Andes using multiproxy lake sediments studies. *Palaeogeography, Palaeoclimatology, Palaeocology*, 194: p. 123–138.

Abdalati, W., Krabill, W., Frederick, E., Manizade, S., Martin, C., Sonntag, J., Swift, R., Thomas, R., Yungel, J. and Koerner, R. (2004): Elevation changes of ice caps in the Canadian Arctic Archipelago. *J. Geophys.* Res., 109, F04007, doi:10.1029/2003JF000045.

ACIA (2005): *Arctic Climate Impact Assessment*, Cambridge University Press: 1047 pp.

Ageta, Y. and Fujita, K (1996): Characteristics of mass balance of summer-accumuation type glaciers in the Himalayas and Tibetan Plateau. *Zeitschrift für Gletscherkunde und Glazialgeologie*, 32 (2): p. 61–65.

Ageta, Y., Iwata, S., Yabuki, H., Naito, N., Sakai, A., Narama, C. and Karma (2000): Expansion of glacier lakes in recent decades in the Bhutan Himalayas. In: Nakawo, M., Raymond, C.F. and Fountain, A. (eds.): *Debris-Covered Glaciers*, IAHS Publications, 264: p. 165–175.

Allison, I. and Peterson, J.A. (1976): Ice areas on Puncak Jaya – their extent and recent history. In: Hope, G.S., Peterson, J.A., Radok, U. and Allison, I. (eds.): The equatorial glaciers of New Guinea – results of the 1971–1973 Australian Universities' expeditions to Irian Jaya: survey, glaciology, meteorology, biology and paleoenvironments. Rotterdam, A.A. Balkema: p. 27–38.

Allison, I. and Peterson, J.A. (1989): Glaciers of Irian Jaya, Indonesia. In: USGS (in prep.): Satellite Image Atlas of Glaciers. Williams, R.S.Jr. and Ferrigno, J.G. (eds.), *U.S. Geological Survey Professional Paper* 1386-H: H1–H20.

Ananicheva, M. (2006): Climatically determined glacier fluctuations in the second part of the 20th century - Suntar-Khayata Mountains and Chersky range. In: Kotlyakov et al. (eds.): *The glaciarization of Northern and Central Eurasia in present time.* Nauka, Moscow: p. 198–204 (in Russian with abstract in English).

Anderson, B. (2003): *The Response of Franz Josef Glacier to Climate Change.* University of Canterbury, Christchurch: 129 pp.

Anderson, B. and Mackintosh, A. (2006): Temperature change as the major driver of late-glacial and Holocene glacier fluctuations in New Zealand. Geology, 34 (2): 121-124.

Andreassen, L.M., Elvehøy, H., Kjøllmoen, B., Engeset, R.V. and Haakensen, N. (2005): Glacier mass balance and length variations in Norway. *Annals of Glaciology*, 42: p. 317–325.

Arendt, A., Echelmeyer, K., Harrison, W.D., Lingle, G. and Valentine, V. (2002): Rapid wastage of Alaska glaciers and their contribution to rising sea level. *Science*, 297 (5580): p. 382–386.

Bamber, J.L., R.L. Layberry, and Gogineni, S.P. (2001): A new ice thickness and bed data set for the Greenland ice sheet, 1. Measurement, data reduction, and errors. *Journal of Geophysical Research*, 106: p. 33733–33780.

Barnett, T.P., Adam, J.C. and Lettenmaier, D.P. (2005): Potential impacts of a warming climate on water availability in snow-dominated regions. Nature, 438(17): p. 303–309.

Benn, D.I. and Evans, D.J.A. (1998): *Glaciers and Glaciation.* Arnold: 734 pp.

Benn, D.I., Warren, C.R. and Mottram, R.H. (2007): Calving processes and the dynamics of calving glaciers. *Earth-Science Reviews*, 82(3–4): p. 143–179.

Berthier, E., Arnaud, Y., Kumar, R., Ahmad, S., Wagnon, P. and Chevallier, P. (2007): Remote sensing estimates of glacier mass balances in the Himachal Pradesh (Western Himalaya, India). *Remote Sensing of Environment*, 108: p. 327–338.

Birkenmajer, K. (1998): Quaternary geology at Potter Peninsula, King George Island (South Shetland Islands, West Antarctica). *Bulletin of the Polish Academy of Sciences*, Earth Sciences 46: p. 9–20.

Bishop, M.P., Olsenholler, J.A., Shroder, J.F., Barry, R.G., Raup, B.H., Bush, A.B.G., Coplan, L., Dwyer, J.L., Fountain, A.G., Haeberli, W., Kääb, A., Paul, F., Hall, D.K., Kargel, J.S., Molnia, B.F., Trabant, D.C., and Wessels, R. (2004): Global land ice measurements from space (GLIMS). Remote sensing and GIS investigations of the Earth's cryosphere. Geocarto International, 19(2): p. 57–84.

Björnsson, H., Rott, H., Gudmundsson, S., Fischer, A., Siegel, A. and Gudmundsson, M.T. (2001): Glacier-volcano interactions deduced by SAR interferometry. *Journal of Glaciology*, 47, 156: p. 58–70.

Bolch, T. (2007): Climate change and glacier retreat in northern Tien Shan (Kazakhstan/Kyrgyzstan) using remote sensing data. *Global and Planetary Change*, 56: p. 1–12.

Brückner, E. and Muret, E. (1908): Les variations périodiques des glaciers. XIIème Rapport, 1906. *Zeitschrift für Gletscherkunde und Glazialgéologie II*: p. 161–198.

Brückner, E. and Muret, E. (1909): Les variations périodiques des glaciers. XIIIème Rapport, 1907. *Zeitschrift für Gletscherkunde und Glazialgéologie III*: p. 161–185.

Brückner, E. and Muret, E. (1910): Les variations périodiques des glaciers. XIVème Rapport, 1908. *Zeitschrift für Gletscherkunde und Glazialgéologie IV*: p. 161–176.

Brückner, E. and Muret, E. (1911): Les variations périodiques des glaciers. XVème Rapport, 1909. *Zeitschrift für Gletscherkunde und Glazialgéologie V*: p. 177–202.

Burga, C., Klötzli, F. and Grabherr, G. (2004): *Gebirge der Erde – Landschaft, Klima, Pflanzenwelt.* Ulmer, Stuttgart: 504 pp.

Casassa, G., Haeberli, W., Jones, G., Kaser, G., Ribstein, P., Rivera, A. and Schneider, C. (2007): Current status of Andean glaciers. Global and Planetary Change, doi:10.1016/j.gloplacha.2006.11.013

Chinn, T.J. (1979): How wet is the wettest of the wet West Coast. New Zealand. *Alpine Journal*, 32: p. 85–88.

Chinn, T.J. (1985): Structure and equilibrium of the dry valley glaciers. *New Zealand Antarctica Records*, 6: p.73–88.

Chinn, T.J. (1996): New Zealand glacier responses to climate change of the past century. *New Zealand Journal of Geology and Geophysics* 39 (3): p. 415–428.

Chinn, T.J. (2001): Distribution of the glacial water resources of New Zealand. *Journal of Hydrology New Zealand* 40 (2): p. 139–187.

Chinn, T.J., Heydenrych, C. and Salinger, M.J. (2005): Use of the ELA as a practical method of monitoring glacier response to climate in New Zealand's Southern Alps, *Journal of Glaciology*, 51 (172): 85-95.

Chueca, J., Julian, A., Saz, M.A., Creus, J. and Lopez, J.I. (2005): Responses to climatic changes since the Little Ice Age on Maladeta Glacier (Central Pyrenees). *Geomorphology*, 68 (3–4): p. 167–182.

Clapperton, C.M., Sugden, D.E., Birnie, J. and Wilson, M.J. (1989a): Late-Glacial and Holocene glacier fluctuations and environmental change in South Georgia, Southern Ocean. *Quaternary Research* 32: p. 210–228.

Clapperton, C.M., Sugden, D.E. and Pelto, M. (1989b): The relationship of land terminating and fjord glaciers to Holocene climatic change, South Georgia, Antarctica. In: Oerlemans, J. (ed.): *Glacier Fluctuations and Climatic Change*. Dordrecht, Kluwer Academic Publishers: p. 57–75.

Clapperton, C.M. (1990): Quaternary glaciations in the Southern Ocean and Antarctic Peninsula area. Quaternary Science Reviews 9: p. 229–252.

Cook, A.J., Fox, A.J., Vaughan, D.G. and Ferrigno, J.G. (2005): Retreating glacier fronts on the Antarctic Peninsula over the past half-century. *Science*, 308, 5721: p. 541–544.

Cullen, N.J., Mölg, T., Kaser, G., Hussein, K., Steffen, K. and Hardy, D.R. (2006): Kilimanjaro glaciers: Recent areal extent from satellite data and new interpretation of observed 20th century retreat rates. *Geophysical Research Letters*, 33(L16502), doi:10.1029/2006gl027084.

De Angelis, H. and Skvarca, P. (2003): Glacier surge after ice shelf collapse. *Science*, 299, 5612: p. 1560–1562.

De Beer, C.M. and Sharp, M. (2007): Recent changes in glacier area and volume within the southern Canadian Cordillera. *Annals of Glaciology* 46: p. 215–221.

Demuth, M.N. and Keller, R. (2006): An assessment of the mass balance of Peyto Glacier (1966 1995) and its relation to recent and past century climatic variability. In: Demuth, M.N., Munro, D.S. and Young, G.J. (eds.): Peyto Glacier: One Century of Science. National Hydrology Research Institute Science Report 8: p. 83–132.

Demuth, M.N., Pinard, V., Pietroniro, A., Luckman, B.H., Hopkinson, C., Dornes, P. and Comeau, L. (2008): Recent and past-century variations in the glacier resources of the Canadian Rocky Mountains – Nelson River System. *Terra Glacialis*, 11(248): p. 27–52.

Dowdeswell, J.A., Hagen, J.O., Björnsson, H., Glazovsky, A.F., Harrison, W.D., Holmlund, P., Jania, J., Koerner, R.M., Lefauconnier, B., Ommanney, C.S.L. and Thomas, R.H. (1997): The mass balance of circum-Arctic glaciers and recent climate change. *Quaternary Research*, 48: p. 1–14.

Dyurgerov, M. and Dwyer, J. (2000): The steepening of glacier mass balance gradients with Northern Hemisphere warming. *Zeitschrift für Gletscherkunde und Glazialgeologie*, 36: p. 107–118.

Dyurgerov, M., and Meier, M.F. (2005): *Glaciers and the Changing Earth System: A 2004 Snapshot*. Occasional Paper 58, Institute of Arctic and Alpine Research, University of Colorado, Boulder, CO: 118 pp.

Elsberg, D.H., Harrison, W.D., Echelmeyer, K.A. and Krimmel, R.M. (2001): Quantifying the effect of climate and surface change on glacier mass balance. *Journal of Glaciology*, 47 (159): p. 649–658.

Finsterwalder, S. and Muret, E. (1901): Les variations périodiques des glaciers. VIme Rapport, 1900. Extrait des *Archives des Sciences physiques et naturelles* 106/4 (12): p. 118–131.

Finsterwalder, S. and Muret, E. (1902): Les variations périodiques des glaciers. VIIme Rapport, 1901. Extrait des *Archives des Sciences physiques et naturelles* 107/4 (14): p. 282–302.

Finsterwalder, S. and Muret, E. (1903): Les variations périodiques des glaciers. VIIIme Rapport, 1902. Extrait des *Archives des Sciences physiques et naturelles* 108/4 (15): p. 661–677.

Forel, F.A. (1895): Les variations périodiques des glaciers. Discours préliminaire. Extrait des *Archives des Sciences physiques et naturelles* XXXIV: p. 209–229.

Forel, F.A. and Du Pasquier, L. (1896): Les variations périodiques des glaciers. Ier Rapport, 1895. Extrait des *Archives des Sciences physiques et naturelles* 101/4 (2): p. 129–147.

Forel, F.A. and Du Pasquier, L. (1897): Les variations périodiques des glaciers. IIme Rapport, 1896. Extrait des *Archives des Sciences physiques et naturelles* 102/4 (4): p. 218–245.

Fountain, A.G., Basagic, H.J., Hoffman, M.J. and Jackson, K. (2006): Glacier response in the American West to climate change during the past century. In: Millar, C.I. (ed.): Mountain climate 2006. Government Camp, Oregon.

Francou, B., Vuille, M., Favier, V. and Cáceres, B. (2004): New evidence for an ENSO impact on low-latitude glaciers: Antizana 15, Andes of Ecuador, 0°28'S. *Journal of Geophysical Research* 109, D18106, doi:10.1029/2003JD004484.

Frenot, Y., Gloaguen, J.-C., Picot, G., Bougère, J. and Benjamin, D. (1993): Azorella selago Hook used to estimate glacier fluctuations and climatic history in the Kerguelen Islands over the last two centuries. Oecologia 95: p. 140–144.

Fujita, K., and Ageta, Y. (2000): Effect of summer accumulation on glacier mass balance on the Tibetan Plateau revealed by mass-balance model. *Journal of Glaciology*, 46 (153): p. 244–252.

GCOS (2004): Implementation plan for the Global Observing System for Climate in support of the UNFCCC. Report GCOS – 92 (WMO/TD No. 1219): 136 pp.

Gellatly, A.F., Chinn, T.J.H. and Röthlisberger, F. (1988): Holocene glacier variations in New Zealand: a review. *Quaternary Science Reviews* 7: p. 227–242.

Gerbaux, M., Genthon, C., Etchevers, P., Vincent, C. and Dedieu, J.P. (2005): Surface balance of the glaciers in the French Alps: distributed modeling and sensitivity to climate change, *Journal of Glaciology* 51 (175): p. 561–572.

Gordon, J.E., Haynes, V.M. and Hubbard, A. (2008): Recent glacier changes and climate trends on South Georgia. *Global and Planetary Change*, 60: p. 72–84.

Granshaw, F.D. and Fountain, A.G. (2006): Glacier change (1958–1998) in the North Cascades National Park Complex, Washington, USA. *Journal of Glaciology*, 52 (177): p. 251–256.

Greene, A.M. (2005): A time constant for hemispheric glacier mass balance. *Journal of Glaciology* 51 (174): p. 353–362.

Griffiths, G.A. and McSaveney, M.J. (1983): Distribution of mean annual precipitation across some steepland regions of New Zealand. *New Zealand Journal of Science* 26: p. 197–209.

Gross, G. (1987): Der Flächenverlust der Gletscher in Österreich 1850–1920–1969. *Zeitschrift für Gletscherkunde und Glazialgeologie* 23 (2): p. 131–141.

Grove, J.M. (2004): *Little Ice Ages: Ancient and modern*. Vol. I + II, 2nd edition. Routledge, London and New York.

GTOS (2006): *Global Terrestrial Observing System Biennial Report* 2004–2005. GTOS-40.

GTOS (2008): Terrestrial essential climate variables for climate change assessment, mitigation and adaptation. *GTOS-52*.http://www.fao.org/gtos/doc/pub52.pdf

Gurney, S.D., Popovnin, V.V., Shahgedanova, M. and Stokes, C.R. (2008): A glacier inventory for the Buordakh Massif, Cherskiy Range, Northeast Siberia, and evidence for recent glacier recession. *Arctic, Antarctic and Alpine Research* 40 (1): p. 81–88.

Haeberli, W. and Hoelzle, M. (1995): Application of inventory data for estimating characteristics of and regional climate-change effects on mountain glaciers: a pilot study with the European Alps. *Annals of Glaciology*, 21: p. 206–212.

Haeberli, W. (1998): *Historical evolution and operational aspects of worldwide glacier monitoring. Into the second century of world glacier monitoring: prospects and strategies*. UNESCO, Paris, 56: p. 35–51.

Haeberli, W., Cihlar, J. and Barry, R.G. (2000): Glacier monitoring within the Global Climate Observing System. *Annals of Glaciology* 31: p. 241–246.

Haeberli, W. and Burn, C. (2002): Natural hazards in forests – glacier and permafrost effects as related to climate changes. In: Sidle, R.C. (ed.): Environmental Change and Geomorphic Hazards in Forests. *IUFRO Research Series* 9: p. 167–202.

Haeberli, W. and Holzhauser, H. (2003): Alpine glacier mass changes during the past two millennia. *PAGES News* 11, No 1: p. 13–15.

Haeberli, W. (2004): Glaciers and ice caps: historical background and strategies of world-wide monitoring. In: Bamber, J.L. and Payne, A.J. (eds.): Mass balance of the cryosphere. *Cambridge University Press*, Cambridge: p. 559–578.

Haeberli, W. (2007): Changing views on changing glaciers. In: Orlove, B., Wiegandt, E. and Luckman, B. (eds.): The darkening peaks: Glacial retreat in scientific and social context. *University of California Press*: p. 23–32.

Haeberli, W., Hoelzle, M., Paul, F. and Zemp, M. (2007): Integrated monitoring of mountain glaciers as key indicators of global climate change: the European Alps. *Annals of Glaciology* 46: p. 150–160.

Hagen, J.O., Kohler, J., Melvold, K. and Winther, J.G. (2003): Glaciers in Svalbard: mass balance, runoff and fresh water flux. *Polar Research* 22 (2): p. 145–159.

Hall, B. (2007): Late-Holocene advance of the Collins Ice Cap, King George Island, South Shetland Islands. *The Holocene*, 17: p. 1253–1258.

Hamberg, A. and Mercanton, P.L. (1914): Les variations périodiques des glaciers. XIXme rapport 1913, *Zeitschrift für Gletscherkunde und Glazialgeologie*, 9: 42-65.

Harper, A.P. (1894): The Franz Josef Glacier. Appendix to the *Journal of the House of Representatives of New Zealand* 1, C1, Appendix No 6: p. 75–79.

Hastenrath, S. (1984): *The glaciers of equatorial East Africa*. Reidel, Dordrecht, Boston, Lancester: 353 pp.

Hastenrath, S. (2001): Variations of East African climate during the past two centuries. *Climate Change*, 50: p. 209–217.

Hastenrath, S. and Polzin, D. (2004): Volume decrease of Lewis Glacier, Mount Kenya, 1978–2004. *Zeitschrift für Gletscherkunde und Glazialgeologie* 39: p. 133–139.

Hastenrath, S. (2005): *Glaciological studies on Mount Kenya* 1971–2005. University of Wisconsin, Madison, USA: 220 pp.

Hewitt, K. (2005): The Karakoram Anomaly? Glacier expansion and the 'elevation effect', Karakoram Himalaya. *Mountain Research and Development* 25 (4): p. 332–340.

Higuchi, K., Iozawa, T., Fujii, Y. and Kodama, H. (1980): Inventory of perennial snow patches in Central Japan. *GeoJournal* 4 (4): p. 303–311.

Hoelzle, M. and Trindler, M. (1998): Data management and application. In: Haeberli, W. (ed.): Into the second century of world glacier monitoring: prospects and strategies. UNESCO, Paris, 56: p. 53–72.

Hoelzle, M., Haeberli, W., Dischl, M. and Peschke, W. (2003): Secular glacier mass balances derived from cumulative glacier length changes. *Global and Planetary Change* 36 (4): p. 77–89.

Hoelzle, M., Chinn, T., Stumm, D., Paul, F., Zemp, M. and Haeberli, W. (2007): The application of glacier inventory data for estimating characteristics of and regional past climate-change effects on mountain glaciers: a comparison between the European Alps and the New Zealand Alps. *Global and Planetary Change* 56: p. 69–82.

Holmlund, P. and Jansson, P. (2005): A re-analysis of the 58-year mass balance record of Storglaciären, Sweden. *Annals of Glaciology* 42 (1): p. 389–394.

Huggel, C., Zgraggen-Oswald, S., Haeberli, W., Kääb, A., Polkvoj, A., Galushkin, I. and Evans, S.G. (2005): The 2002 rock/ice avalanche at Kolka/Karmadon, Russian Caucasus: Assessment of extraordinary avalanche formation and mobility and application of QuickBird satellite imagery. *Natural Hazards and Earth System Sciences* 5: p. 173–187.

Huggel, C., Ceballos, J.L., Ramírez, J., Pulgarín, B. and Thouret, J.C. (2007): Review and reassessment of hazards owing to volcano-ice interactions in Colombia. *Annals of Glaciology* 45: p. 128–136.

Huss, M., Bauder, A., Funk, M., and Hock, R. (2008): Determination of the seasonal mass balance of four Alpine glaciers since 1865. *Journal of Geophysical Research*, 113, F01015, doi: 10.1029/2007JF000803.

IGOS (2007): *Cryosphere theme report. International global observing strategy for the monitoring of our environment from space and earth*: 100 pp.

Imbrie, J. and Imbrie, K.P. (1979): *Ice ages: solving the mystery*. Macmillan, London.

IPCC (2007): Climate Change 2007: The Physical Science Basis. Contribution of Working Group 1 to the Fourth Assessment Report of the Intergovernmental Panel on Climate Change (eds.: Solomon, S., Qin, D., Manning, M., Chen, Z., Marquis, M.C., Averyt, K., Tignor, M., and Miller, H.L.). Intergovernmental Panel on Climate Change, Cambridge and New York.

Jóhannesson, T., Raymond, C. and Waddington, E. (1989): Time-scale for adjustment of glaciers to changes in mass balance. *Journal of Glaciology* 35 (121): p. 355–369.

Jones, H.G. (2008): From Commission to Association: the transition of the International Commission on Snow and Ice (ICSI) to the International Association of Cryospheric Sciences (IACS). *Annals of Glaciology*, 48: p. 1–5.

Josberg, E.G., Bidlake, W.R., March, R.S. and Kennedy, B.W. (2007): Glacier mass-balance fluctuations in the Pacific Northwest and Alaska, USA. *Annals of Glaciology* 46: p. 291–296.

Kääb, A., Paul, F., Maisch, M., Hoelzle, M. and Haeberli, W. (2002): The new remote-sensing-derived Swiss glacier inventory: II. First Results. *Annals of Glaciology* 34: p. 362–366.

Kääb, A. (2005): Remote sensing of mountain glaciers and permafrost creep. *Schriftenreihe Physische Geographie*, University of Zurich, 48: 266 pp. http://folk.uio.no/kaeaeb/publications/habil_screen.pdf

Kääb, A. , Huggel, C., Fischer, L., Guex, S., Paul, F., Roer, I., Salzmann, N., Schlaefli, S., Schmutz, K., Schneider, D., Strozzi, T., and Weidmann, Y. (2005): Remote sensing of glacier- and permafrost-related hazards in high mountains: an overview. *Natural Hazards and Earth System Science.* 5, 527-554.

Kamb, B., Raymond, C.F., Harrison, W.D., Engelhardt, H., Echelmeyer, K.A., Humphrey, N., Brugman, M.M. and Pfeffer, T. (1985): Glacier surge mechanism: 1982–1983 surge of Variegated Glacier, Alaska, *Science*, 227 (4686): p. 469–479.

Kamb, B. (1987): Glacier surge mechanism based on linked cavity configuration of the basal water conduit system, *Journal of Geophysical Research*, B9: p. 9083–9100.

Kargel, J.S., Abrams, M.J., Bishop, M.P., Bush, A., Hamilton, G., Jiskoot, H., Kääb, A., Kieffer, H.H., Lee, E.M., Paul, F., Rau, F., Raup, B., Shroder, J.F., Soltesz, D., Stearns, L., Wessels, R. and the GLIMS Consortium (2005): Multispectral imaging contributions to Global Land Ice Measurements from Space, *Remote Sensing of Environment* 99 (1/2): p. 187–219.

Karma, Ageta, Y., Naito, N., Iwata, S. and Yabuki, H. (2003): Glacier distribution in the Himalayas and glacier shrinkage from 1963 to 1993 in the Bhutan Himalayas. Bulletin of Glaciological Research 20: p. 29–40.

Kaser, G., and Osmaston, H. (2002): Tropical Glaciers. *UNESCO International Hydrological Series*, Cambridge University Press, Cambridge, UK: 207 pp.

Kaser, G., Fountain, A., and Jansson, P. (2003): A manual for monitoring the mass balance of mountain glaciers with particular attention to low latitude characteristics. A contribution from the International Commission on Snow and Ice (ICSI) to the UNESCO HKH-Friend programme. IHP-VI, *Technical Documents in Hydrology*, No. 59, UNESCO, Paris: 107 pp. + Appendices.

Kaser, G., Cogley, J.G., Dyurgerov, M.B., Meier, M.F. and Ohmura, A. (2006): Mass balance of glaciers and ice caps: Consensus estimates for 1961–2004. *Geophysical Research Letters* 33 (L19501), doi.10.1029/2006GL027511.

Kaufmann, D.S., Porter, S.C. and Gillespie, A.R. (2004): Quaternary alpine glaciation in Alaska, the Pacific Northwest, Sierra Nevada, and Hawaii. In: Gillespie, A.R., Porter, S.C. and Atwater, B.F. (eds.): *The Quaternary period in the United States*. Elsevier, Amsterdam.

Klein, A.G. and Kincaid, J.L. (2006): Retreat of glaciers on Puncak Jaya, Irian Jaya, determined from 2000 and 2002 IKONOS satellite images. Journal of Glaciology 52 (176): p. 65–179.

Klein, A.G. and Kincaid, J.L. (2008): On the disappearance of the Puncak Mandala ice cap, Papua. *Journal of Glaciology* 54 (184): p. 195–197.

Koch, J. and Clague, J.J. (2006): Are insolation and sunspot activity the primary drivers of Holocene glacier fluctuations? PAGES News 14 (3): p. 20–21.

Koerner, R.M. (2005): Mass balance of glaciers in the Queen Elizabeth Islands, Nunavut, Canada. Annals of Glaciology 42 (1): p. 417–423.

Kotlyakov, V.M., Serabryanny, L.R. and Solomina, O.N. (1991): Climate change and glacier fluctuations during the last 1000 years in the southern mountains of the USSR. *Mountain Research and Development* 11: p. 1–12.

Kotlyakov, V.M. et al. (2006): *Glaciation in North and Central Eurasia at present time*. Nauka, Moscow (in Russian with abstract in English).

Kotlyakov, V.M., Osipova, G.B. and Tsvetkow, D.G. (2008): Monitoring surging glaciers of the Pamirs, central Asia, from space. *Annals of Glaciology* 48: p. 125–134.

Kouraev, A.V., Legrésy, B. and Rémy, F. (2008): Northern Novaya Zemlya outlet glaciers: 1990–2000 changes. In: WGMS (2008): *Fluctuations of Glaciers 2000–2005* (Vol. IX). World Glacier Monitoring Service, Zurich.

Kuhn, M. (1981): *Climate and glaciers*. IAHS, 131: p. 3–20.

Kuhn, M., Markl, G., Kaser, G., Nickus, U. and Obleitner, F. (1985): Fluctuations of climate and mass balance. Different responses of two adjacent glaciers. *Zeitschrift für Gletscherkunde und Glazialgeologie* 2: p. 409–416.

Kuhn, M., Dreiseitl, E., Hofinger, S., Markl, G., Span, N. and Kaser, G. (1999): Measurements and models of the mass balance of Hintereisferner. *Geografiska Annaler* A81 (4): p. 659–670.

Kutuzov, S. (2005): The retreat of Tien Shan glaciers since the Little Ice Age obtained from the moraine positions, aerial photographs and satellite images. In: PAGES Second Open Science Meeting 10–12 August 2005, Beijing, China.

LaChapelle, E.R. (1960): Recent glacier variations in western Washington. *Journal of Geophysical Research* 65 (8): p. 2505–2509.

Larsen, C. F., Motyka, R.J., Arendt, A.A., Echelmeyer, K.A. and Geissler, P.E. (2007): Glacier changes in southeast Alaska and northwest British Columbia and contribution to sea level rise. *Journal of Geophysical Research* 112, F01007, doi: 10.1029/2006JF000586.

Li, X., Cheng, G., Jin, H., Kang, E., Che, T., Jin, R., Zongwu, L., Nan, Z., Wang, J. and Shen, Y. (in press): Distribution and changes of glaciers, snow and permafrost in China. Proceedings of workshop on 'Assessment of Snow, Glacier and Water Resources in Asia', Almaty, KZ, 2006. UNESCO.

Lillesand, T.M. and Kiefer, R.W. (1994): *Remote sensing and image interpretation*. 3rd edition, Wiley & Sons, Inc., New York, Chichester, Brisbane, Toronto, Singapore: 750 pp.

Lingle, C.S. and Fatland, D.R. (2003): Does englacial water storage drive temperate glacier surges? *Annals of Glaciology* 36, 1: p. 14–20.

Lliboutry, L. (1974): Multivariate statistical analysis of glacier annual balance. *Journal of Glaciology* 13: p. 371–392.

Luckman, B.H. (2000): The Little Ice Age in the Canadian Rockies, *Geomorphology* 32 (3– 4): p. 357–384.

Luckman, B.H. (2006): The Neoglacial History of Peyto Glacier. In: Demuth, M.N., Munro, D.S. and Young, G.J. (eds.): Peyto Glacier: One Century of Science. *National Hydrology Research Institute Science Report* 8: p. 25–57.

Lythe, M.B., Vaughan, D.G. and the BEDMAP Group (2001): BEDMAP: A new ice thickness and subglacial topographic model of Antarctica. *Journal of Geophysical Research* 106 (B6): p. 11335–11351.

Maisch, M., Wipf, A., Denneler, B., Battaglia, J. and Benz, C. (2000): Die Gletscher der Schweizer Alpen. Gletscherhochstand 1850, Aktuelle Vergletscherung, Gletscherschwund Szenarien. Schlussbericht NFP31. 2. Auflage, VdF Hochschulverlag, Zürich.

McCabe, G. J., Fountain, A.G. and Dyurgerov, M. (2000): Variability in winter mass balance of Northern Hemisphere glaciers and relations with atmospheric circulation. *Arctic, Antarctic and Alpine Research* 32 (1): p. 64–72.

Meier, M.F. (1984): The contribution of small glaciers to sea lever rise. *Science* 226: p. 1418–1421.

Mercanton, P.L. (1930): Rapport sur les variations de longueur des glaciers de 1913 à 1928. Chaîne des Alpes; Scandinavie. *IAHS* 14: 53 pp.

Mercanton, P.L. (1934): Rapport sur les variations de longueur des glaciers de 1928 à 1931. Chaîne des Alpes; Scandinavie. *IAHS* 20: p. 229–250.

Mercanton, P.L. (1936): Rapport sur les variations de longueur des glaciers de 1931 à 1935. Chaîne des Alpes; Scandinavie et Islande. *IAHS* 22: p. 430–456.

Mercanton, P.L. (1948): Rapport sur les variations de longueur des glaciers de 1935 à 1946. Alpes francaises, suisses, italiennes et autrichiennes. Variations des glaciers en Suède, Islande et Norvège. *IAHS* 30: p. 233–256.

Mercanton, P.L. (1952): Rapport sur les variations de longueur des glaciers européens, de 1947 à 1950. *IAHS* 32: p. 107–119 (Paris).

Mercanton, P.L. (1954): Rapport sur les variations de longueur des glaciers européens, en 1950–51, 1951–52, 1952–53. *IAHS* 32: p. 478–490.

Mercanton, P.L. (1958): Rapport sur les variations de longueur des glaciers européens, en 1953/54, 1954/55, 1955/56. *IAHS* 46: p. 358–371.

Mercanton, P.L. (1961): Rapport sur les variations de longueur des glaciers européens, en 1956/57, 1957/58, 1958/59. *IAHS* 54: p. 366–378.

Milana, J.P. (2007): A model of the Glaciar Horcones Inferior surge, Aconcagua region, Argentina. *Journal of Glaciology* 53 (183): p. 565–572.

Milankovitch, M. (1930): Mathematische Klimalehre und astronomische Theorie der Klimaschwankungen, Borntraeger, Berlin.

Molnia, B.F. (2007): Late nineteenth to early twenty-first century behaviour of Alaskan glaciers as indicators of changing regional climate. Global and Planetary Change 56: p. 23–56.

Moore, R.D. and Demuth, M.N. (2001): Mass balance and streamflow variability at Place Glacier, Canada, in relation to recent climate fluctuations. *Hydrological Processes* 15, 3: p. 473–486.

Müller, H. and Kappenberger, G. (1991): Claridenfirn-Messungen 1914–1984. 40, ETH Zürich.

Nakawo, M., Raymond, F.C. and Fountain, A. (2000): Debris-covered glaciers. IAHS publication 264: 288 pp.

Narama, C., Shimamura, Y., Nakayama, D. and Abdrakhmatov, K. (2006): Recent changes of glacier coverage in the Western Terskey-Alatoo Range, Kyrgyz Republic, using Corona and Landsat. *Annals of Glaciology* 43 (6): p. 223–229.

Naranjo, J.L., Sigurdsson, H., Carey, S.N., and Fritz, W. (1986): Eruption of the Nevado del Ruiz Volcano, Colombia, on 13 November 1985: Tephra fall and lahars. *Sience* 233, 4767: p. 961–963.

Naruse, R. (2006): The response of glaciers in South America to environmental change. In: Knight, P.G. (ed.): Glacier Science and Environmental Change. Blackwell, Oxford.

Nesje, A., Lie, O. and Dahl, S.O. (2000): Is the North Atlantic Oscillation reflected in Scandinavian glacier mass balance records? *Journal of Quaternary Science* 15 (6): p. 587–601.

Nesje, A., Bakke, J., Dahl, S.O., Lie, O. and Matthews, J.A. (2008): Norwegian mountain glaciers in the past, present and future. *Global and Planetary Change* 60 (1–2): p. 10–27.

NSIDC (2008): World glacier inventory. Data Set Documentation. World Glacier Monitoring Service and National Snow and Ice Data Center/World Data Center for Glaciology. Boulder, CO. Digital media (last visit on May 12, 2008): http://nsidc.org/data/docs/noaa/g01130_glacier_inventory/.

Nye, J.F. (1960): The response of glaciers and ice-sheets to seasonal and climatic changes. *Proceedings of the Royal Society of London*, A (256): p. 559–584.

Oerlemans, J. (2001): *Glaciers and climate change.* A.A. Balkema Publishers. Lisse, Abingdon, Exton, Tokyo: 148 pp.

Ohmura, A. (2001): Physical basis for the temperature-based melt-index method. *Journal of Applied Meteorology* 40: p. 753–761.

Ohmura, A. (2004): Cryosphere during the twentieth century. In: Sparling, J.Y. and C.J. Hawkesworth (eds.): *The state of the planet: frontiers and challenges in geophysics*. Washington DC, American Geophysical Union: p. 239–257.

Ohmura, A. (2006): Changes in mountain glaciers and ice caps during the 20th century. *Annals of Glaciology* 43: p. 361–368.

Ohmura, A., Bauder, A., Müller-Lemans, H. and Kappenberger, G. (2007): Long-term change of mass balance and the role of radiation. *Annals of Glaciology* 46: p. 367–374.

Østrem, G. and Stanley, A. (1969): *Glacier mass balance measurements. A manual for field and office work.* Canadian Department of Energy, Mines and Resources, Norwegian Water Resources and Electricity Board: 125 pp.

Østrem, G., Haakensen, M., and Melander, O. (1973): Atlas over breer i Nord-Skandinavia. Hydrologisk avdeling, Norges Vassdrags-og Energiverk, Meddelelse, 22: 315 pp.

Østrem, G., Selvig, K.D. and Tandberg, K. (1988): Atlas over breer i Sør-Norge. Oslo, Norges Vassdrags-og Energiverk Vassdragsdirektoret.

Østrem, G. and Haakensen, M. (1993): Glaciers of Norway. In: USGS (in prep.): Satellite image atlas of glaciers of the world. Williams, R.S. and Ferrigno, J.G. (eds.), U. S. Geological Survey. Professional Paper, 1386-E-3: 53 pp.

Østrem, G. and Brugman, M. (1991): Glacier mass-balance measurements: a manual for field and office work. National Hydrology Research Institute Science Report No. 4, Minister of Supply and Service, Canada, Saskatoon: 224 pp.

Padma Kumari, B., Londhe, A.L., Daniel, S. and Jadhav, D.B. (2007): Observational evidence of solar dimming: Offsetting surface warming over India. *Geophysical Research Letters*, 34 (L21810): doi:10.1029/2007GL031133.

Paterson, W.S.B. (1994): *The physics of glaciers.* 3rd edition, Pergamon Press, Oxford: 480 pp.

Patzelt, G. (1985): The period of glacier advances in the Alps, 1965 to 1980. *Zeitschrift für Gletscherkunde und Glazialgeologie* 21: p. 403–407.

Paul, F., Kääb, A., Maisch, M., Kellenberger, T. and Haeberli, W. (2002): The new remote-sensing-derived Swiss Glacier Inventory: I. Methods. *Annals of Glaciology* 34: p. 355–361.

Paul, F., Kääb, A., Maisch, M., Kellenberger, T. W. and Haeberli, W. (2004): Rapid disintegration of Alpine glaciers observed with satellite data. *Geophysical Research Letters* 31, L21402, doi:10.1029/2004GL020816.

Paul, F. and Kääb, A. (2005): Perspectives on the production of a glacier inventory from multispectral satellite data in Arctic Canada: Cumberland Peninsula, Baffin Island. *Annals of Glaciology* 42 (1): p. 59–66.

Paul, F., Kääb, A. and Haeberli, W. (2007): Recent glacier changes in the Alps observed from satellite: Consequences for future monitoring strategies. *Global and Planetary Change* 56 (1–2): p. 111–122.

Pelfini, M. and Smiraglia, C. (1988): L'evoluzione recente del glacialismo sulle Alpi Italiani: strumenti e temi di ricerca. *Bollettino della Societa Geografica Italiana*, 1-3: p. 127- 154.

Peterson, J.A., Hope, G.S., and Mitton, R. (1973): Recession of snow and ice fields of Irian Jaya, Republic of Indonesia. *Zeitschrift für Gletscherkunde und Glazialgeologie* 9, 1-2: p. 73–87.

Podrezov, O., Dikikh, A. and Bakirov, K. (2002): Variability in the climatic conditions and glacier of Tien Shan in the past 100 years. Kyrgyz Russian Slavic University, Bishkek (in Russian).

PSFG (1967): Fluctuations of Glaciers 1959–1965, Vol. I. P. Kasser (ed.), IAHS (ICSI) and UNESCO, Permanent Service on Fluctuations on Glaciers, Paris: 52 pp.

PSFG (1973): Fluctuations of Glaciers 1965–1970, Vol. II. P. Kasser (ed.), IAHS (ICSI) and UNESCO, Permanent Service on Fluctuations on Glaciers, Paris: 357 pp.

PSFG (1977): Fluctuations of Glaciers 1970–1975, Vol. III. F. Müller (ed.), IAHS (ICSI) and UNESCO, Permanent Service on Fluctuations on Glaciers, Paris: 269 pp.

PSFG (1985): Fluctuations of Glaciers 1975–1980, Vol. IV. W. Haeberli (ed.), IAHS (ICSI) and UNESCO, Permanent Service on Fluctuations on Glaciers, Paris: 265 pp.

Rabot, C. and Muret, E. (1911): Les variations périodiques des glaciers. XVIme Rapport, 1910. *Zeitschrift für Gletscherkunde und Glazialgeologie* VI: p. 81–103.

Rabot, C. and Muret, E. (1912): Les variations périodiques des glaciers. XVIIme Rapport, 1911. *Zeitschrift für Gletscherkunde und Glazialgeologie* VII: p. 37–47.

Rabot, C. and Mercanton, P.L. (1913): Les variations périodiques des glaciers. XVIIIme Rapport, 1912. *Zeitschrift für Gletscherkunde und Glazialgeologie* VIII: p. 81–103.

Rabot, C. and Muret, E. (1913): Supplément au XVIIme rapport sur les variations périodiques des glaciers, 1911. *Zeitschrift für Gletscherkunde und Glazialgeologie* VII: p. 191–202.

Radok, U. (1997): The International Commission on Snow and Ice (ICSI) and its precursors, 1984–1994. *Hydrological Sciences* 42 (2): p. 131–140.

Radok, V. and Watts, D. (1975): A synoptic background to glacier variations of Heard Island. *IAHS* 104: p. 42–56.

Rau, F., Mauz, F., De Angelis, H., Jaña, R., Arigony Neto, J., Skvarca, P., Vogt, S., Saurer, H. and Gossmann, H. (2004): Variations of glacier frontal positions on Northern Antarctic Peninsula. *Annals of Glaciology* 39: p. 525–530.

Raup, B.H., Kääb, A., Kargel, J.S., Bishop, M.P., Hamilton, G., Lee, E., Paul, F., Rau, F., Soltesz, D., Khalsa, S.J.S., Beedle, M. and Helm, C. (2007): Remote Sensing and GIS technology in the Global Land Ice Measurements from Space (GLIMS) Project. *Computers and Geosciences* 33: p. 104–125.

Reid, H. and Muret, E. (1904): Les variations périodiques des glaciers. IX^{ème} Rapport, 1903. Extrait des Archives des Sciences physiques et naturelles 109/4 (18), Genève: p. 160–195.

Reid, H. and Muret, E. (1905): Les variations périodiques des glaciers. X^{ème} Rapport, 1904. Extrait des *Archives des Sciences physiques et naturelles* 110/4 (20), Genève: p. 62–74.

Reid, H. and Muret, E. (1906): Les variations périodiques des glaciers. XI^{ème} Rapport, 1905. *Zeitschrift für Gletscherkunde und Glazialgeologie* I: p. 1–21.

Reinwarth, O. and Stäblein, G. (1972): Die Kryosphäre - das Eis der Erde und seine Untersuchung. *Würzburger Geographische Arbeiten* 36: 71 pp.

Reynolds, J.M. (2000): On the formation of supraglacial lakes on debris-covered glaciers. In: *Debris-Covered Glaciers*: p. 153-161.

Richter, E. (1898): Les variations périodiques des glaciers. III^{ème} Rapport, 1897. Extrait des Archives des Sciences physiques et naturelles 103/4 (6), Genève: p. 22–55.

Richter, E. (1899): Les variations périodiques des glaciers. IV^{ème} Rapport, 1898. Extrait des *Archives des Sciences physiques et naturelles* 104/4 (8), Genève: p. 31–61.

Richter, E. (1900): Les variations périodiques des glaciers. V^{ème} Rapport, 1899. Extrait des *Archives des Sciences physiques et naturelles* 105/4 (10), Genève: p. 26–45.

Rignot, E., Rivera, A. and Casassa, G. (2003): Contribution of the Patagonia icefields of South America to sea level rise. *Science* 302: p. 434–437.

Rivera, A., Benham, T., Casassa, G., Bamber, J. and Dowdeswell, J. (2007): Ice elevation and areal changes of glaciers from the Northern Patagonia icefield, Chile. *Global and Planetary Change* 59: p. 126–137.

Rott, H., Rack, W., Skvarca, P. and De Angelis, H. (2002): Northern Larsen Ice Shelf – Further retreat after the collapse. *Annals of Glaciology* 34: p. 277–282.

Ruddell, A. (2006): An inventory of present glaciers on Heard island and their historical variation. In: Green, K. and Woehler, E. (eds.): Heard Island: Southern Ocean Sentinel. Surrey Beatty & Sonse, Chipping Norton NSW: p. 28–51.

Ruddiman, W.F. (2000): Earth's climate: past and future. Freeman, New York.

Ruddiman, W.F. (2003): The anthropogenic greenhouse era began thousands of years ago. *Climate Change* 61 (3): p. 261–293.

Schöner, W., Auer, I. and Böhm, R. (2000): Climate variability and glacier reaction in the Austrian eastern Alps. *Annals of Glaciology* 31 (1): p. 31–38.

Sigurdsson, O., Jónsson, T. and Jóhannesson, T. (2007): Relation between glacier-termini variations and summer temperature in Iceland since 1930. *Annals of Glaciology* 46 (1): p. 170–176.

Shahgedanova, M., Stokes, C.R., Khromova, T., Nosenko, G., Popovnin, V., Narozhny, Y., Aleynikov, A. and Muraveyev, A. (2008): State of glaciers in the Caucasus and southern Siberian mountains and their links with climate oscillations since the 1950s. *Geophysical Research Abstracts*, Vol. 10, EGU2008-A-10158.

Shroder, J., Bishop, M., Haritashya, U., Olsenholler, J., Bulley, H. and Sartan, J. (2006): Glacier Debris Cover Variation in the Hindu Kush and Karakoram Himalaya. American Geophysical Union, Fall Meeting 2006, abstract #H53B-0632.

Shumskii, P.A. (1964): *Principles of structural glaciology*. Translated from the Russian by D. Kraus. Dover Publications Inc., New York: 497 pp.

Shumsky, P.A. (1969): Glaciation. In: Tolstikov, E. (ed.): *Atlas of Antarctica*, Vol. 2, Leningrad: p. 367–400.

Sicart, J.E., Wagnon, P. and Ribstein, P. (2005): Atmospheric controls of the heat balance of Zongo Glacier (16°S, Bolivia). *Journal of Geophysical Research*, 110, D12106, doi:10.1029/2004JD005732.

Skvarca, P. and De Angelis, H. (2003): Impact assessment of regional climatic warming on glaciers and ice shelves of the northeastern Antarctic Peninsula. *Antarctic Research Series* 79: p. 69–78.

Skvarca, P., De Angelis, H. and Ermolin, E. (2004): Mass-balance of „Glaciar Bahiá del Diablo", Vega Island, Antarctic Peninsula. *Annals of Glaciology* 39: p. 209–213.

Solanki, S.K., Usoskin, I.G., Kromer, B., Schüssler, M. and Beer, J. (2004): Unusual activity of the sun during recent decades compared to the previous 11,000 years. *Nature* 431: p. 1084–1087.

Solomina, O. (1996): Glaciers recession in the mountains of the former USSR after the maximum of the Little Ice Age: Time and scale. In: The proceedings of Meeting of the Work Group on Geospatial Analysis of Glaciated Environments. International Union for Quaternary Research, Dublin.

Solomina, O. (2000): Retreat of mountain glaciers of northern Eurasia since the Little Ice Age maximum. *Annals of Glaciology* 31: p. 26–30.

Solomina, O., Haeberli, W., Kull, C. and Wiles, G. (2008): Historical and Holocene glacier-climate variations: General concepts and overview. *Global and Planetary Change* 60 (1-2): p. 1–9.

Stokes, C.R., Popovnin, V., Aleynikov, A., Gurney, S.D. and Shahgedanova, M. (2007): Recent glacier retreat in the Caucasus Mountains, Russia, and associated increase in supraglacial debris cover and supra-/proglacial lake development. *Annals of Glaciology* 46: p. 195–203.

Su, Z. and Shi, Y. (2002): Response of monsoonal temperature glaciers to global warming since the Little Ice Age. *Quaternary International* 97 (98): p. 123–131.

Svendsen, J.I. and Mangerud, J. (1997): Holocene glacial and climatic variations on Spitsbergen, Svalbard. Holocene 7: p. 45–57.

Swithinbank, C. (1988): Satellite image atlas of glaciers of the world. Antarctica. *U.S. Geological Survey, Professional Papers* 1386-B: p. 1–138.

Thost, D.E. and Truffer, M. (2008): Glacier recession on Heard Island, Southern Indian Ocean. *Arctic, Antarctic and Alpine Research* 40 (1): p. 199–214.

Tomlinson, A., and Sansom, J. (1994): Rainfall normals for NZ. For the period 1961 to 1990. *NIWA Science and Technology Series* No. 3.

Trabant, D.C., March, R.S. and Molnia, B.F. (2002): Growing and Advancing Calving Glaciers in Alaska. American Geophysical Union, Fall Meeting 2002, abstract #C62A-0913.

Troll, C. (1973): High mountain belts between the polar caps and the Equator: their definition and lower limit. *Arctic and Alpine Research* 5, 3: p. A19–A27.

UNEP (2007): *Global outlook for ice & snow*. UNEP/GRID-Arendal, Norway: 235 pp.

UNESCO (1970): Perennial ice and snow masses. A guide for compilation and assemblage of data for a World Glacier Inventory, UNESCO/IAHS Technical Papers in Hydrology, Zurich.

USGS (in prep.): Satellite image atlas of glaciers of the world. Williams, R.S. and Ferrigno, J.G. (eds.), U.S. Geological Survey Professional Papers.

Van der Veen, C.J. (1996): Tidewater calving. Journal of Glaciology 42 (141): p. 375–385.

Villalba, R. (1994): Tree-ring and glacial evidence for the Medieval Warm Epoch and the Little Ice Age in southern South America. *Climatic Change* 26: p. 183–197.

Vincent, C. (2002): Influence of climate change over the 20th century on four French glacier mass balances. *Journal of Geophysical Research* 107, No. D19, 4375, doi:10.1029/2001JD000832.

Vincent, C., Le Meur, E., Six, D. and Funk, M. (2005): Solving the paradox of the end of the Little Ice Age in the Alps. *Geophysical Research Lettres* 32, L09706: doi.10.1029/2005GL022552.

Volden, E. (2007): ESA's GlobGlacier project. *Ice and Climate News* 9: p. 5.

Wagnon, P., Ribstein, P., Francou, B. and Sicart, J.E. (2001): Anomalous heat and mass budget of Glaciar Zongo, Bolivia during the 1997/98 El Niño year. *Journal of Glaciology* 47 (156): p. 21–28.

Weidick, A. (1968): Observations on some Holocene glacier fluctuations in West Greenland. *Meddelelser om Grønland* 165 (6): p. 1–202.

Weidick, A. and Morris, E. (1998): Local glaciers surrounding continental ice sheets. In: Haeberli, W., Hoelzle, M. and Suter, S. (eds.): Into the second century of world glacier monitoring – prospects and strategies. A contribution to the IHP and the GEMS. Prepared by the World Glacier Monitoring Service, UNESCO Publishing: p. 197–207.

Wessels, R., Kargel, J.S. and Kieffer, H.H. (2002): ASTER measurements of supraglacial lakes in the Mount Everest region of the Himalaya. *Annals of Glaciology* 34: p. 399-408.

WGMS (1988): *Fluctuations of Glaciers* 1980–1985 (Vol. V). Haeberli, W. and Müller, P. (eds.), IAHS(ICSI)/UNEP/UNESCO, World Glacier Monitoring Service, Paris: 290 pp.

WGMS (1989): *World glacier inventory - status 1988*. Haeberli, W., Bösch, H., Scherler, K., Østrem, G. and Wallén, C. C. (eds.), IAHS(ICSI)/UNEP/UNESCO, Nairobi: 458 pp.

WGMS (1991): *Glacier Mass Balance Bulletin* No. 1. (1988–1989). Haeberli, W. and Herren, E. (eds.), IAHS(ICSI)/UNEP/UNESCO, World Glacier Monitoring Service, Zurich: 70 pp.

WGMS (1993a): *Fluctuations of Glaciers* 1985–1990 (Vol. VI). Haeberli, W. and Hoelzle, M. (eds.), IAHS(ICSI)/UNEP/UNESCO, World Glacier Monitoring Service, Paris: 322 pp.

WGMS (1993b): *Glacier Mass Balance Bulletin* No. 2 (1990–1991). Haeberli, W., Herren, E. and Hoelzle, M. (eds.), IAHS(ICSI)/UNEP/UNESCO, World Glacier Monitoring Service, Zurich: 74 pp.

WGMS (1994): *Glacier Mass Balance Bulletin* No. 3 (1992–1993). Haeberli, W., Hoelzle, M. and Bösch, H. (eds.), IAHS(ICSI)/UNEP/UNESCO, World Glacier Monitoring Service, Zurich: 80 pp.

WGMS (1996): Glacier Mass Balance Bulletin No. 4 (1994–1995). Haeberli, W., Hoelzle, M. and Suter, S. (eds.), IAHS(ICSI)/UNEP/UNESCO, World Glacier Monitoring Service, Zurich: 90 pp.

WGMS (1998): *Fluctuations of Glaciers* 1990–1995 (Vol. VII). Haeberli, W., Hoelzle, M., Suter, S. and Frauenfelder, R. (eds.), IAHS(ICSI)/UNEP/UNESCO, World Glacier Monitoring Service, Paris: 296 pp.

WGMS (1999): *Glacier mass balance bulletin* No. 5 (1996–1997). Haeberli, W., Hoelzle, M. and Frauenfelder, R. (eds.), IAHS(ICSI)/UNEP/UNESCO, World Glacier Monitoring Service, Zurich: 96 pp.

WGMS (2001): *Glacier Mass Balance Bulletin* No. 6 (1998–1999). Haeberli, W., Frauenfelder, R. and Hoelzle, M. (eds.), IAHS(ICSI)/UNEP/UNESCO/WMO, World Glacier Monitoring Service, Zurich: 93 pp.

WGMS (2003): *Glacier Mass Balance Bulletin* No. 7 (2000–2001). Haeberli, W., Frauenfelder, R., Hoelzle, M. and Zemp, M. (eds.), IAHS(ICSI)/UNEP/UNESCO/WMO, World Glacier Monitoring Service, Zurich: 87 pp.

WGMS (2005a): *Fluctuations of Glaciers* 1995–2000 (Vol. VIII). Haeberli, W., Zemp, M., Frauenfelder, R., Hoelzle, M. and Kääb, A. (eds.), IUGG(CCS)/UNEP/UNESCO, World Glacier Monitoring Service, Paris. 288 pp.

WGMS (2005b): *Glacier Mass Balance Bulletin* No. 8 (2002–2003). Haeberli, W., Noetzli, J., Zemp, M., Baumann, S., Frauenfelder, R. and Hoelzle, M. (eds.), IUGG(CCS)/UNEP/UNESCO/WMO, World Glacier Monitoring Service, Zurich: 100 pp.

WGMS (2007): *Glacier Mass Balance Bulletin* No. 9 (2004–2005). Haeberli, W., Hoelzle M. and Zemp, M. (eds.). ICSU(FAGS)/IUGG(IACS)/UNEP/UNESCO/WMO, World Glacier Monitoring Service, University of Zurich: 100 pp.

WGMS (2008): *Fluctuations of glacier*s 2000–2005 (Vol. IX). Haeberli, W., Zemp, M. and Hoelzle, M. (eds.), ICSU(FAGS)/IUGG(IACS)/UNEP/UNESCO/WMO, World Glacier Monitoring Service, University of Zurich.

White, S.E. (2002): Glaciers of México. In: USGS (in prep.): Satellite image atlas of glaciers of the world. Williams, R.S. and Ferrigno, J.G. (eds.), *U.S. Geological Survey Professional Paper* 1386-J-3: p. 383–404.

Wild, M., Ohmura, A. and Makowski, K. (2007): Impact of global dimming and brightening on global warming. *Geophysical Research Letters* 34(L04702): doi:10.10129/2006GL028031.

Williams, R.S. and Ferringno, J.G. (2002): Glaciers of Canada – Introduction. In: Satellite image atlas of glaciers of the world – Glaciers of North America. U.S. Geological Survey Professional Paper 1386-J-1.

Winkler, S. (2004): Lichenometric dating of the 'Little Ice Age' maximum in Mt. Cook National Park, Southern Alps, New Zealand. *Holocene* 14 (6): p. 911–920.

Yablokov, A. (2006): Climate change impacts on the glaciation in Tajikistan. In: Assessment report for the Second National Communication of the Republic of Tajikistan on climate change. Tajik Met. Service, Dushanbe (in Russian).

Zeeberg, J.J. and Forman, S.L. (2001): Changes in glacier extent on north Novaya Zemlya in the twentieth century. *The Holocene* 11 (2): p. 161–175.

Zemp, M., Frauenfelder, R., Haeberli, W. and Hoelzle, M. (2005): Worldwide glacier mass balance measurements: general trends and first results of the extraordinary year 2003 in Central Europe. Data of Glaciological Studies [Materialy glyatsiologicheskih issledovanii], 99, Moscow, Russia: p. 3–12.

Zemp, M., Haeberli, W., Hoelzle, M. and Paul, F. (2006): Alpine glaciers to disappear within decades? *Geophysical Research Letters* 33, L13504, doi:10.1029/2006GL026319.

Zemp, M., Haeberli, W., Bajracharya, S., Chinn, T.J., Fountain, A.G., Hagen, J.O., Huggel, C., Kääb, A., Kaltenborn, B.P., Karki, M., Kaser, G., Kotlyakov, V.M., Lambrechts, C., Li, Z.Q., Molnia, B.F., Mool, P., Nellemann, C., Novikov, V., Osipova, G.B., Rivera, A., Shrestha, B., Svoboda, F., Tsvetkov D.G. and Yao, T.D. (2007a): Glaciers and ice caps. Part I: Global overview and outlook. Part II: Glacier changes around the world. In: UNEP: *Global outlook for ice & snow*. UNEP/GRID-Arendal, Norway: p. 115–152.

Zemp, M., Paul, F., Hoelzle, M. and Haeberli, W. (2007b): Glacier fluctuations in the European Alps 1850–2000: an overview and spatio-temporal analysis of available data. In: Orlove, B., Wiegandt, E. and B. Luckman (eds.): *The darkening peaks: Glacial retreat in scientific and social context*. University of California Press: p. 152–167.

Appendix 1 National Correspondents of the WGMS

List of the national correspondents of the WGMS. A detailed list of the principle investigators of glaciers monitored within GTN-G as well as a list of the supporting agencies are given in the WGMS data publications (WGMS 2005a and earlier volumes).

ARGENTINA/ ANTARCTICA	Lydia Espizua Instituto Argentino de Nivología y Glaciología CONICET (IANIGLA) Casilla de Correo 330 ARGENTINA – 5500 Mendoza E-mail: lespizua@lab.cricyt.edu.ar
AUSTRALIA/ ANTARCTICA	Andrew Ruddell 4/17 Wellington Square North Adelaide AUSTRALIA – South Australia 5006 E-mail: andrew.ruddell@bigpond.com
AUSTRIA	Michael Kuhn Institute of Meteorology and Geophysics University of Innsbruck Innrain 52 AUSTRIA – 6020 Innsbruck E-mail: Michael.Kuhn@uibk.ac.at
BOLIVIA	Javier C. Mendoza Rodríguez IHH (Instituto de Hidráulica e Hidrología) and SENAMHI (Servicio Nacional de Meteorología e Hidrología) P.O. Box 699 BOLIVIA – La Paz E-mail: jmendoza@senamhi.gov.bo jcmendoza@umsa.bo
CANADA	Michael N. Demuth Natural Resources Canada Geological Survey of Canada 601 Booth Street CANADA – Ottawa, ON K1A 0E8 E-mail: mdemuth@NRCan.gc.ca
CHILE	Gino Casassa Centro de Estudios Científicos Av. Prat. 514 CHILE – Valdivia E-mail: gcasassa@cecs.cl
CHINA	Li Zhongqin Tianshan Glaciological Station / Cold and Arid Regions Environment and Engineering Research Institute (CAREERI) Chinese Academy of Sciences (CAS) 260 West Donggang Road P. R. CHINA – 730 000 Lanzhou, Gansu E-mail: lizq@ns.lzb.ac.cn
COLOMBIA	Jair Ramirez Cadenas INGEOMINAS Diagonal 53 No. 34-53 COLOMBIA – Bogota E-mail: jairamir@ingeominas.gov.co
ECUADOR	Bolivar Cáceres INAMHI (Instituto Nacional de Meteorología e Hidrología) and IRD ECUADOR – 16 310 Quito E-mail: bolivarc@inamhi.gov.ec
FRANCE	Christian Vincent Laboratory of Glaciology and Environmental Geophysics (CNRS) P.O. Box 96 FRANCE – 38402 St. Martin d'Hères Cedex E-mail: vincent@lgge.obs.ujf-grenoble.fr
GERMANY	Ludwig Braun Commission for Glaciology Bavarian Academy of Sciences Alfons-Goppel-Str. 11 GERMANY – 80539 München E-mail: ludwig.braun@kfg.badw.de
GREENLAND	Andreas Peter Ahlstrøm Department of Quaternary Geology The Geological Survey of Denmark and Greenland (GEUS) Øster Voldgade 10 DENMARK – 1350 København K E-mail: apa@geus.dk
ICELAND	Oddur Sigurdsson National Energy Authority Hydrological Service Grensásvegi 9 ICELAND – 108 Reykjavik E-mail: osig@os.is
INDIA	C.V. Sangewar Glaciology Division Geological Survey of India Vasundara Complex, Sector E, Aliganj INDIA – Lucknow 226024 E-mail: cvsangewar@rediffmail.com
INDONESIA	see AUSTRALIA
ITALY	Mirco Meneghel Universita di Padua Dipartimento di Geografia Via del Santo 26 ITALY – 35123 Padova E-mail: mirco.meneghel@unipd.it
JAPAN	Koji Fujita Department of Hydrospheric-Atmospheric Sciences (DHAS) Graduate School of Environmental Studies c/o Hydrospheric Atmospheric Research Center, Nagoya University JAPAN – Nagoya 464 8601 E-mail: cozy@nagoya_u.jp

KAZAKHSTAN
Igor Severskiy
Institute of Geography of the
Ministry-Academy of Sciences of the Republic of Kazakhstan
Pushkinstreet 99
KAZAKHSTAN– 480100 Almaty
i_severskiy@mail.kz

MEXICO
Hugo Delgado-Granados
Instituto de Geofísica
Universidad Nacional Autónoma de México
Circuito Exterior, C. U. Coyoacán
MEXICO – México D. F. 04510
E-mail: hugo@geofisica.unam.mx

NEPAL
see JAPAN

NEW ZEALAND/ ANTARCTICA
Trevor J. Chinn
Alpine and Polar Processes Consultancy
Rapid 20, Muir Rd. Lake Hawea
RD 2 Wanaka
NEW ZEALAND – Otago 9192
E-mail: t.chinn@xtra.co.nz

NORWAY
Jon Ove Hagen
Department of Geosciences
Section of Physical Geography
University of Oslo
P.O. Box 1047, Blindern
NORWAY – 0316 Oslo
E-mail: j.o.m.Hagen@geo.uio.no

PAKISTAN
Ali Ghazanfar
Head Water Resources Section
Global Change Impact Studies Centre (GCISC)
61/A, 1st Floor
Jinnah Avenue
PAKISTAN – Islamabad
E-mail: ghazanfar.ali@gcisc.org.pk

PERU
Marco Zapata Luyo
Unidad de Glaciología y Recursos Hídricos
INRENA
Av. Confraternidad Internacional Oeste No. 167
PERU – Huaraz / Ancash
E-mail: glaciologia@inrena.gob.pe
zapataluyomarco@gmail.com

POLAND
Bogdan Gadek
University of Silesia
Department of Geomorphology
ul. Bedzinska 60
POLAND – 41 200 Sosnowiec
E-mail: jgadek@us.edu.pl

RUSSIA
Victor V. Popovnin
Moscow State University
Geographical Faculty
Leninskiye Gory
RUSSIA – 119 992 Moscow
E-mail: po@geogr.msu.ru
begemotina@hotmail.com

SPAIN
Eduardo Martinez de Pisón
Miguel Arenillas
Ingeniería 75, S.A.
Velázquez 87–4° derecha
SPAIN – 28006 Madrid
E-mail: ing75@ing75.com
map@ing75.com

SWEDEN
Per Holmlund
Department of Physical Geography and Quaternary Geology
Glaciology
University of Stockholm
SWEDEN – 106 91 Stockholm
E-mail: pelle@natgeo.su.se

SWITZERLAND
Martin Hoelzle
Department of Geosciences
University of Fribourg
Chemin de musée 4
SWITZERLAND - 1700 Fribourg
E-mail: martin.hoelzle@unifr.ch

USA
William R. Bidlake
US Geological Survey
Washington Water Science Center
934 Broadway - Suite 300
USA – Tacoma, WA 98402
E-mail: wbidlake@usgs.gov

UZBEKISTAN
Andrey Yakovlev
The Center of Hydrometeorological Service (UzHydromet)
72, K.Makhsumov str.
UZBEKISTAN – 100 052 Tashkent
E-mail: andreyakovlev@mail.ru

Appendix 2 Meta-data on available fluctuation data

Overview table on available length change (FV) and mass balance data series (MB) up to the year 2005. Notes: PU: political unit; PSFG: local PSFG key; WGMS ID: internal WGMS key; FirstRY: first reference year; FirstSY: first survey year; LastSY: last survey year; NoObs: number of observations.

Source: Data from WGMS. An update of this list in various digital formats is available on the WGMS website: www.wgms.ch/dataexp.html

PU	PSFG	NAME	WGMS ID	GENERAL LOCATION	SPECIFIC LOCATION	LATITUDE	LONGITUDE	FV FirstRY	FV FirstSY	FV LastSY	FV NoObs	MB FirstRY	MB LastSY	MB NoObs
AQ	27	ADAMS	885	DRY VALLEYS	MIERS VALLEY	-78.10	163.75	1988	1989	1990	2			
AQ		BAHIA DEL DIABLO	2665	ANTARCTIC PENINSULA	VEGA ISLAND	-63.82	-57.43					2002	2005	4
AQ	16	BARTLEY	893	DRY VALLEYS	WRIGHT VALLEY	-77.52	162.23	1983	1984	1995	9			
AQ	9	CANADA	877	DRY VALLEYS	TAYLOR VALLEY	-77.58	162.75	1972	1979	1979	1			
AQ	12	CLARK CPI	894	DRY VALLEYS	WRIGHT VALLEY	-77.42	162.33	1973	1978	1995	9			
AQ	10	COMMONWEALTH	878	DRY VALLEYS	TAYLOR VALLEY	-77.55	163.08	1972	1979	1979	1			
AQ	5	FINGER	873	DRY VALLEYS	TAYLOR VALLEY	-77.70	161.48	1973	1979	1979	1			
AQ	20	GOODSPEED	888	DRY VALLEYS	WRIGHT VALLEY	-77.42	162.38	1985	1986	1989	4			
AQ	19	HART	889	DRY VALLEYS	WRIGHT VALLEY	-77.50	162.35	1985	1986	1995	7			
AQ	3	HEIMDALL	890	DRY VALLEYS	WRIGHT VALLEY	-77.58	162.87	1984	1987	1992	4			
AQ		KALESNIKA	1434			-82.06	-41.41	1966	1967	1970	4			
AQ		KRASOVSKOGO	1079			-71.50	12.46	1965	1971	1973	2			
AQ	7	LA CROIX	875	DRY VALLEYS	TAYLOR VALLEY	-77.65	162.47	1972	1978	1978	1			
AQ	17	MESERVE MPII	892	DRY VALLEYS	WRIGHT VALLEY	-77.55	162.37	1965	1981	1992	9			
AQ	26	MIERS	886	DRY VALLEYS	MIERS VALLEY	-78.08	163.75	1988	1989	1990	2			
AQ	14	PACKARD	880	DRY VALLEYS	VICTORIA VALLEY	-77.33	162.13	1973	1978	1978	1			
AQ	4	SCHLATTER	872	DRY VALLEYS	TAYLOR VALLEY	-77.70	161.43	1973	1979	1979	1			
AQ	8	SUESS	876	DRY VALLEYS	TAYLOR VALLEY	-77.63	162.67	1972	1979	1979	1			
AQ	6	TAYLOR AN	874	DRY VALLEYS	TAYLOR VALLEY	-77.75	162.00	1972	1978	1978	1			
AQ	15	VICTORIA LOWER	881	DRY VALLEYS	VICTORIA VALLEY	-77.37	162.28	1973	1978	1990	2			
AQ	13	VICTORIA UPPER	879	DRY VALLEYS	VICTORIA VALLEY	-77.27	161.50	1972	1978	1992	5			
AQ	18	WRIGHT LOWER	891	DRY VALLEYS	WRIGHT VALLEY	-77.42	162.83	1975	1985	1995	8			
AQ	11	WRIGHT UPPER B	895	DRY VALLEYS	WRIGHT VALLEY	-77.55	166.50	1970	1979	1992	7			
AR	5003	ALERCE	1346			-41.48	-70.83	1944	1953	1975	4			
AR		AZUFRE	2851	CORDILLERA PRINCIPAL	PLANCHON-PETEROA	-35.17	-70.33	1894	1963	2005	6			
AR	5005	BONETE S	1348			-41.45	-71.00	1969	1970	1975	2			
AR	5002	CASTANO OVERO	918	PATAGON.ANDES	NAHUEL HUAPIN.	-41.18	-71.83	1944	1953	1983	5			
AR		DE LOS TRES	1675	PATAGONIA		-49.33	-73.00	1995	1996	2003	4	1996	1998	3
AR	5004	FRIAS	1347			-41.52	-70.82	1944	1953	1986	4			
AR	64	FRIAS	1661	PATAGONIA	S.PAT.ICEFIELD	-50.75	-75.08	1984	1986	1986	1			
AR		GUESSFELDT	2848	CORDILLERA FRONTAL	ACONCAGUA	-32.59	-70.03	1896	1929	2005	10			
AR	5006	HORCONES INFERIOR	919	CENTRAL ANDES	ACONCAGUA	-32.67	-70.00	1963	1976	2005	9			
AR	131	MARTIAL	917	ANDES FUEGUINOS	MONTES MARTIAL	-54.78	-68.42	1898	1943	2003	5	2001	2002	2
AR		MARTIAL ESTE	2000	ANDES FUEGUINOS	MONTES MARTIAL	-54.78	-68.40					2001	2005	5
AR	34	MORENO	920	PATAGONIA	S.PAT.ICEFIELD	-50.50	-73.12	1945	1970	1986	2			
AR		PENON	2850	CORDILLERA PRINCIPAL	PLANCHON-PETEROA	-35.27	-70.56	1896	1963	2005	6			
AR	5001	RIO MANSO	1345			-41.47	-70.80	1944	1953	1975	4			
AR		TUPUNGATO 01	2852	CORDILLERA PRINCIPAL	TUPUNGATO	-33.39	-69.73	1963	1975	2005	6			
AR		TUPUNGATO 02	2853	CORDILLERA PRINCIPAL	TUPUNGATO	-33.37	-69.75	1963	1975	2005	6			
AR		TUPUNGATO 03	2854	CORDILLERA PRINCIPAL	TUPUNGATO	-33.36	-69.75	1963	1975	2005	6			
AR		TUPUNGATO 04	2855	CORDILLERA PRINCIPAL	TUPUNGATO	-33.34	-69.74	1963	1975	2005	6			
AR	33	UPSALA	921	PATAGONIA	S.PAT.ICEFIELD	-50.00	-73.28	1945	1968	1990	8			
AR		VACAS	2849	CORDILLERA FRONTAL	ACONCAGUA	-32.65	-70.00	1896	1929	2005	10			
AT	229	AEU.PIRCHLKAR	504	EASTERN ALPS	OETZTALER ALPS	47.00	10.92	1982	1982	2004	23			
AT	321	ALP.KRAEUL F.	594	EASTERN ALPS	STUBAIER ALPEN	47.05	11.15	1975	1975	1994	19			
AT	307	ALPEINER F.	497	EASTERN ALPS	STUBAIER ALPEN	47.05	11.13	1848	1848	2004	86			
AT	304	BACHFALLEN F.	500	EASTERN ALPS	STUBAIER ALPEN	47.08	11.08	1892	1892	2005	65			
AT	702	BAERENKOPF K.	567	EASTERN ALPS	GLOCKNER GR.	47.13	12.72	1924	1915	2005	46			
AT	308	BERGLAS F.	496	EASTERN ALPS	STUBAIER ALPEN	47.07	11.12	1891	1892	2005	74			
AT	0105C	BIELTAL F E	1453			46.87	10.13	1968	1969	1978	10			
AT	0105B	BIELTAL F W	1452			46.87	10.13	1969	1970	2005	15			
AT	0105A	BIELTAL F.	481	EASTERN ALPS	SILVRETTA	46.88	10.13	1924	1924	2002	65			
AT		BIELTALFERNER MITTE	2674	EASTERN ALPS	STUBAIER ALPS	46.88	10.13	1996	1997	2005	9			
AT	0310B	BILDSTOECKL F.	603	EASTERN ALPS	STUBAIER ALPEN	47.00	11.10	1964	1969	1990	18			
AT	302	BOCKKOGEL F.	502	EASTERN ALPS	STUBAIER ALPEN	47.03	11.12	1892	1898	1994	43			
AT	727	BRENNKOGL K.	528	EASTERN ALPS	GROSSGLOCKNER G	47.10	12.80	1988	1988	2005	18			
AT	0310A	DAUNKOGEL F.	604	EASTERN ALPS	STUBAIER ALPEN	47.00	11.10	1891	1891	2005	89			
AT	220	DIEM F.	513	EASTERN ALPS	OETZTALER ALPEN	46.81	10.95	1871	1848	2005	100			
AT	509	DORFER K.	577	EASTERN ALPS	VENEDIGER GRUP.	47.10	12.33	1896	1891	2003	67			
AT	317	E.GRUEBL F.	597	EASTERN ALPS	STUBAIER ALPEN	46.98	11.23	1891	1892	1994	53			
AT	708	EISER K.	562	EASTERN ALPS	GLOCKNER GR.	47.15	12.68	1961	1955	1989	27			
AT	1301	EISKAR G.	1632	KARNISCHE ALPEN		46.62	12.90	1897	1920	2005	19			
AT	312	FERNAU F.	601	EASTERN ALPS	STUBAIER ALPEN	46.98	11.13	1890	1891	2004	85			
AT	0601B	FILLECK K.	476	EASTERN ALPS	GRANATSPITZ GR.	47.13	12.60					1964	1980	17
AT	320	FREIGER F.	595	EASTERN ALPS	STUBAIER ALPEN	46.97	11.20	1898	1899	2005	38			
AT	706	FREIWAND K.	564	EASTERN ALPS	GLOCKNER GR.	47.10	12.75	1928	1929	2005	54			
AT	507	FROSNITZ K.	579	EASTERN ALPS	VENEDIGER GRUP.	47.08	12.40	1891	1860	2005	66			

Acknowledgements

The scientific authors of this publication are indebted to all the institutes, organisations and the numerous researchers who have been providing important data for many decades. They gratefully acknowledge the efforts made by staff members and temporary assistants of the World Glacier Monitoring Service as well as of its predecessor and partner organisations in order to compile, publish, and make digitally available these important data sets. Gratitude is also extended to the international umbrella organisations for the long-standing support and guidance.

Special thanks associated with the production of the present publication go to Jaap van Woerden for extensive advice and support, to Diana Rizzolio for the great implementation of the design and layout, Susan Braun-Clarke for carefully polishing the English, all the colleagues kindly providing their greatest photo shots, and to the following glaciologists for thoughtful and constructive feedback to a first manuscript (with special focus on one of the macroregions):

- Ian Allison (New Guinea), Antarctic Climate & Ecosystems Cooperative Research Centre, Tasmania, AU
- Maria Ananicheva (Northern Asia), Russian Academy of Sciences, Moscow, RU
- Liss M. Andreassen (Scandinavia), Norwegian Water Resources and Energy Directorate, Oslo, NO
- Ludwig N. Braun (Central Europe), Commission for Glaciology, Munich, DE
- David O. Burgess (Arctic), Natural Resources Canada, Ottawa, CA
- Gino Casassa (South America), Centro de Estudios Científicos, Valdivia, CL
- Trevor Chinn (New Zealand), Alpine and Polar Processes Consultancy, Otago, NZ
- Michael N. Demuth (North America), Natural Resources Canada, Ottawa, CA
- Koji Fujita (Central Asia), Nagoya University, Nagoya, JP
- John E. Gordon (Antarctica), Scottish Natural Heritage, Edinburgh, and University of St Andrews, GB
- Jon Ove Hagen (Arctic), University of Oslo, Oslo, NO
- Stefan Hastenrath (Africa), University of Wisconsin, Madison US
- Victor V. Popovnin (Northern Asia), Moscow State University, Moscow, RU
- Pedro Skvarca (Antarctica), Instituto Antártico Argentino, Buenos Aires, AR

At present, the work of the central office of the WGMS is funded mainly through the Swiss National Science Foundation, the Swiss Federal Office for the Environment and the Department of Geography of the University of Zurich with contributions from the international umbrella organisations and the Swiss Academy of Sciences. The United Nations Environment Programme and the Department of Geography of the University of Zurich have provided additional financial support for the assessment, preparation, and publication of the present publication.

This publication is available online from: http://www.grid.unep.ch/glaciers/

The back cover shows Oberaar Glacier in Switzerland during a field campaign end of June 2003.
Source: M. Zemp, University of Zurich, Switzerland.

www.wgms.ch

World Glacier Monitoring Service
Department of Geography,
University of Zurich, Switzerland
Tel.: +41 44 635 5139
Fax: +41 44 635 6841
e-mail: wgms@geo.uzh.ch
www.wgms.ch

www.unep.org

United Nations Environment Programme
P.O. Box 30552 - 00100 Nairobi, Kenya
Tel.: +254 20 762 1234
Fax: +254 20 762 3927
e-mail: uneppub@unep.org
www.unep.org

UNEP

This publication is about the world's surface ice on land outside the two polar ice sheets. It provides a sound and well illustrated review on the basis of available data, the global distribution of glaciers and ice caps, and their changes since maximum extents of the so-called Little Ice Age. The publication also provides the background knowledge needed to understand the compiled glacier observations in view of the ongoing climate change. It presents the latest state of knowledge on glacier changes in view of the available data sets and the scientific literature, and discusses the challenges of the 21st century for the monitoring of glaciers and ice caps.

The publication was prepared in a joint project of the United Nations Environment Programme (UNEP) and the World Glacier Monitoring Service (WGMS). It was written by the officers of the WGMS and reviewed by scientists from around the world with expertise in the research and monitoring of glaciers and ice caps.

ISBN: 978-92-807-2898-9
Job N°: DEW/1027/GE

Publication 14

Zemp, M., Hoelzle, M. & Haeberli, W. (2009). **Six decades of glacier mass balance observations - a review of the worldwide monitoring network.** Annals of Glaciology, 50(50), 101-111.

Six decades of glacier mass-balance observations: a review of the worldwide monitoring network

M. ZEMP, M. HOELZLE, W. HAEBERLI

World Glacier Monitoring Service, University of Zürich, Winterthurerstrasse 190, CH-8057 Zürich Switzerland
E-mail: michael.zemp@geo.uzh.ch

ABSTRACT. Glacier mass balance is the direct and undelayed response to atmospheric conditions and hence is among the essential variables required for climate system monitoring. It has been recognized as the largest non-steric contributor to the present rise in sea level. Six decades of annual mass-balance data have been compiled and made easily available by the World Glacier Monitoring Service and its predecessor organizations. In total, there have been 3480 annual mass-balance measurements reported from 228 glaciers around the globe. However, the present dataset is strongly biased towards the Northern Hemisphere and Europe and there are only 30 'reference' glaciers that have uninterrupted series going back to 1976. The available data from the six decades indicate a strong ice loss as early as the 1940s and 1950s followed by a moderate mass loss until the end of the 1970s and a subsequent acceleration that has lasted until now, culminating in a mean overall ice loss of over 20 m w.e. for the period 1946–2006. In view of the discrepancy between the relevance of glacier mass-balance data and the shortcomings of the available dataset it is strongly recommended to: (1) continue the long-term measurements; (2) resume interrupted long-term data series; (3) replace vanishing glaciers by early-starting replacement observations; (4) extend the monitoring network to strategically important regions; (5) validate, calibrate and accordingly flag field measurements with geodetic methods; and (6) make systematic use of remote sensing and geo-informatics for assessment of the representativeness of the available data series for their entire mountain range and for the extrapolation to regions without in situ observations; and (7) make all these data and related meta-information available.

INTRODUCTION

The World Glacier Monitoring Service (WGMS) collects and publishes mass-balance data of glaciers obtained by direct glaciological and geodetic methods as a contribution to the Global Terrestrial Network for Glaciers (GTN-G) which is part of the Global Climate/Terrestrial Observing Systems (GCOS/GTOS; GCOS 2004). The GTN-G monitoring strategy uses glacier observations in a system of tiers (cf. Haeberli and others, 2000; Haeberli, 2004). These tiers include extensive glacier mass-balance measurements within major climatic zones for improved process understanding and the calibration of numerical models (tier 2), as well as for the determination of regional volume changes within major mountain ranges using cost-saving methodologies (tier 3). Glacier-front variation and global inventories are further components of the monitoring strategy but are not discussed here. First surveys of accumulation and ablation of snow, firn and ice at individual stakes date back to the end of the 19th century and beginning of the 20th century, for example at Rhone glacier (Mercanton, 1916) and Silvretta glacier (Huss and others, 2008a). Annual glacier mass-balance measurements made by the direct glaciological method (cf. Østrem and Stanley, 1969; Østrem and Brugman, 1991), based on an extensive net of ablation stakes, snow pits and snow probing, were initiated in 1945 at Storglaciären, Sweden (Holmlund and others, 2005). Today, six decades of annual (and partially seasonal) mass-balance data are readily available from the WGMS and have been analyzed in detail by Dyurgerov (2002) and widely used for studies of glacier changes (e.g. Braithwaite, 2002; Dyurgerov and Meier, 2005) and related questions from hydrology (e.g. Braun and others, 2000), climate change (e.g. Oerlemans and Fortuin, 1992; Francou and others, 2003; Ohmura, 2006) or sea-level variation studies (e.g. Kaser and others, 2006; Raper and Braithwaite, 2006; Meier and others, 2007). However, due to the specific foci of these works, a sound and integrative discussion of the basic dataset and related issues is often missed out. Here we aim to give a review of the present monitoring network, a spatio-temporal analysis of the available data and discuss important issues related to the monitoring and interpretation of glacier mass-balance data.

AVAILABLE MASS-BALANCE DATA

The WGMS collects mass-balance data of glaciers annually from the preceding year through its collaboration network of national correspondents and principal investigators. This 1 year retention period allows the investigators time to properly analyze and publish their data before making them available to the scientific community and the wider public. Preliminary data are published annually on the WGMS website (www.wgms.ch) and every 2 years in the *Glacier Mass Balance Bulletins* (WGMS, 2007, and earlier issues) as well as every 5 years, in full detail, in the *Fluctuations of Glaciers* (WGMS, 2008a, and earlier issues). All data are available digitally on request and free of charge. We aim to collect seasonal and annual mass-balance data that are measured according to the direct glaciological method (cf. Østrem and Stanley, 1969; Østrem and Brugman, 1991), i.e. based on a network of ablation stakes and snow pits distributed over the entire glacier, and inter-/extrapolated to the total area of the (same) glacier independently of meteorological or hydrological measurements. Ideally, these mass-balance measurements determined annually are

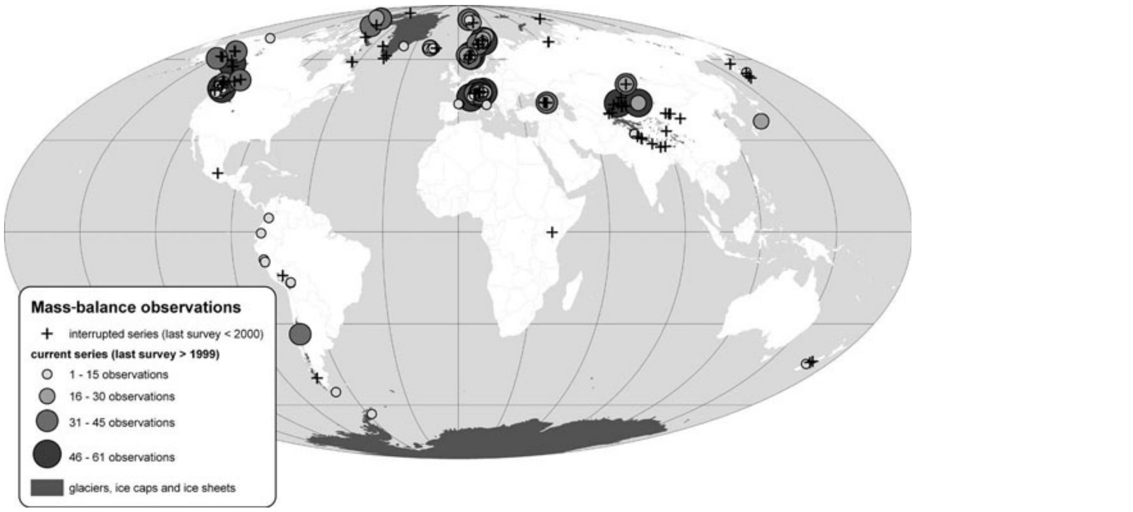

Fig. 1. Global overview of available mass-balance measurements from 1946 to 2006. The current series, sized according to the number of observations, and interrupted programmes are plotted over the global distribution of glaciers, ice caps and the two ice sheets. Note that the data point in Japan refers to the Hamaguri Yuki snowfield. Data sources: mass-balance data from the WGMS, outlines of countries and ice cover from the Environmental Systems Research Institute's Digital Chart of the World.

combined with decadal volume-change assessments from geodetic surveys to reduce method-dependent uncertainties and systematic errors.

For the period 1946–2005, there are 3385 annual mass-balance results from 228 glaciers available through the WGMS (Fig. 1). Additional information on mass-balance vs altitude intervals has been reported for 45% of the annual observations and for 56% of the glaciers. A derived equilibrium-line altitude (ELA) and accumulation-area ratio (AAR) are available for 73% and 82% of the annual values and data series, respectively. Seasonal mass balances have been submitted for 45% of the observation years and for 63% of the glaciers. From the 228 available data series, 120 provide information from the 21st century whereas the remaining data series were interrupted in the past century. The average period of observations per series is 15 years, and 39 glaciers have more than 30 years of measurements. For the hydrological year 2006, preliminary mass-balance data

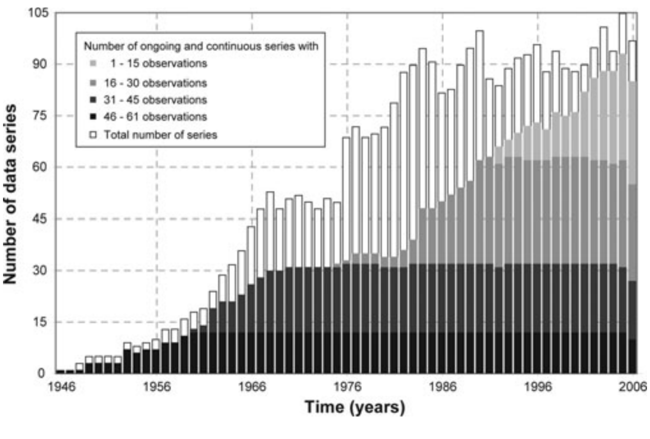

Fig. 2. Temporal overview of available mass-balance series from 1946 to 2006. The total number of reported data series per year is overlaid with the number of ongoing (i.e. last survey after 2003) and continuous (i.e. number of data gaps <20% of observation years) measurement programmes, shaded according to the number of observations per series. Source: data from the WGMS.

have been reported from 97 glaciers. A temporal overview of the number of data series reported to the WGMS is given in Figure 2. The total number of series is shown together with the data series that are ongoing, continuous and consist of up to 15, 30, 45 and 61 observation years. Of the 228 data series, there are just 31 continuous measurement programmes reaching back to 1970, and only 12 back to 1960. Of these glaciers, the *Glacier Mass Balance Bulletin* (WGMS, 2007) lists a set of 30 'reference' glaciers with continuous measurement programmes back to 1976 and earlier (see Appendix).

MASS-BALANCE SERIES VS THE GLOBAL GLACIER DISTRIBUTION

About 90% of the mass-balance series come from the Northern Hemisphere and about 40% from Europe. An overview of the available mass-balance series in comparison with the global distribution of glaciers is given in Table 1. Most with the longest time series are found in the European Alps and Scandinavia, followed by North America and High Mountain Asia, with the earliest observations in the 1940s and 1950s, respectively. In the Canadian Arctic Archipelago and in High Mountain Asia, more than two-thirds of the series were interrupted in the last century. The only long-term observation series from the tropics, at Lewis Glacier (1979–96) on Mount Kenya, results in the high average observation length of the region class 'Africa, New Guinea, Irian Jaya'. Northern Asia and Siberia, South America and the large ice masses around the two ice sheets in Greenland and Antarctica with few and only short-term data series are strongly underrepresented within the network (in respect of their ice cover).

The size and elevation distributions of the glaciers with available mass-balance observations and the glaciers with detailed information in the World Glacier Inventory (WGI; WGMS, 1989) are given in Tables 2 and 3, respectively. The total area covered by the 228 glaciers with mass-balance series is about 10 000 km^2. More than 75% of the glaciers have an area of 0.1–10.0 km^2, covering 2.5% of the total ice

Table 1. Global distribution of glaciers and of mass-balance series. The ice cover of 12 macro-regions is listed with an overview of available mass-balance series including the number of mass-balance programmes, recent observation series and 'reference' glaciers, as well as the first/last survey years and the average duration of the observation series. Information about the ice cover comes from Dyurgerov and Meier (2005) which is based mainly on WGMS (1989). Mass-balance data come from the WGMS

Macro-region	Area km^2	Mass-balance series	Observations >1999	Reference glaciers	First survey	Last survey	Average observation duration
Africa, New Guinea, Irian Jaya	9	1	0	0	1979	1996	18.0
New Zealand	1160	1	1	0	2005	2006	2.0
European Alps, Pyrenees, Caucasus	3785	43	29	10	1948	2006	20.2
Sub-Antarctic Islands	7000	0	0	0	–	–	–
South America	25 000	11	9	1	1976	2006	8.6
Scandinavia, Iceland, West Arctic Islands	50 809	59	40	10	1946	2006	15.7
Northern Asia, Siberia, East Arctic Islands	59 279	9	1	0	1973	2000	6.0
Around Greenland	76 200	5	1	0	1979	2006	3.5
High Mountain Asia, Japan	116 180	40	10	5	1957	2006	15.0
North America (US+CD+MX), Alaska	124 260	45	24	4	1953	2006	16.3
Canadian Arctic Archipelago	151 433	13	4	0	1960	2006	13.3
Around Antarctica	169 000	1	1	0	2002	2006	5.0
Global	**784 115**	**228**	**120**	**30**	**1948**	**2006**	**15.3**

cover with mass-balance observations. About 90% of this ice cover comes from the 15 glaciers which are >100 km^2. The elevation of the terminus of 33%, 60% and 80% of these glaciers is below 1000, 2000 and 3000 m a.s.l., respectively. The glaciers of the WGI, with detailed area information, cover overall about 180 000 km^2 which corresponds to about 23% of the estimated global glacier cover (Dyurgerov and Meier, 2005). About 80% of these glaciers are <1 km^2 and represent 7.5% of the inventoried ice cover, whereas 50% of this ice cover comes from the 235 glaciers >100 km^2. Half of the inventoried glaciers end between 3000 and 5000 m a.s.l., and less than 10% reach below 1000 m a.s.l.

SPATIO-TEMPORAL ANALYSIS OF GLOBAL AND REGIONAL GLACIER MASS CHANGES

The 30 'reference' glaciers (see WGMS, 2007) with (almost) continuous measurements since 1976 show an (arithmetic) average annual mass loss of 0.58 m w.e. for the decade 1996–2005, which is more than twice the loss rate for the period 1986–95 (0.25 m w.e.), and more than four times the rate for the period 1976–85 (0.14 m w.e.). The preliminary value of –1.30 m w.e. for 2006 (based on so far reported values from 27 reference glaciers) seems likely to become a new record loss surpassing the mass-balance values of the years 2003 (–1.24 m w.e.), 2004 (–0.74 m w.e.) and 1998 (–0.71 m w.e.). The apparent advantage of analyzing only continuous mass-balance series comes with the disadvantage of having to deal with a small sample size and shorter data series. As a consequence, the available mass-balance values can be averaged annually, disregarding the completeness and length of the time series, but it is necessary to accept all the problems related to moving sample size (Ohmura, 2004; Cogley, 2005; Dyurgerov and Meier, 2005). A third approach takes into account that the mean of all glaciers is strongly biased by the large proportion of Alpine and Scandinavian glaciers and, hence, calculates the annual mass balance from the (arithmetic) averaged regional mean values (cf. Haeberli and others, 2007). Other ways to correct for the spatial bias of the data are to use regional averages which are weighted by the corresponding glacier area or to apply polynomial spatial interpolation (e.g. Cogley, 2005). Figure 3 shows the cumulative mean (annual) mass balances of: (1) the 30 reference glaciers (and the subsample before 1977); (2) all available glaciers; (3) all available glaciers excluding the reference glaciers; (4) the (subsample of) averages of the 12 macro-regions (Table 1); and (5) the (subsample of) area-weighted averages of the 12 macro-regions (Table 1). The samples used in approaches (1) and (3) are entirely independent; however, (2), (4) and (5) contain the sample from (1). From 1946 to 2006 (i.e. 61 years), the mean of all five approaches shows a cumulative ice loss of 21.2 m w.e., corresponding to an average annual ice loss of 0.35 m w.e. After six decades the difference between the five approaches, i.e. the range between (3) and (5), is 5.14 m w.e. This corresponds to an annual difference of 0.08 m w.e. and is in the same order of magnitude as the mean annual standard errors of the approaches (e.g. (1): 0.19 m w.e.; (2) and (3): 0.12 m w.e.).

Table 2. Size distribution of glaciers. The number and area of glaciers with available mass-balance observation (MB) and detailed inventory (WGI) data are listed according to their size class. Data from the WGMS

	Number of glaciers		Area of glaciers	
Size class km^2	MB	WGI	MB	WGI
<0.1	4%	23%	0%	0%
≥0.1 and <1	45%	56%	1%	7%
≥1 and <10	32%	18%	2%	19%
≥10 and <100	13%	2%	8%	24%
≥100 and <1000	5%	1%	44%	31%
≥1000	1%	0%	45%	19%
Total	**228**	**67 737**	**10 087 km^2**	**179 979 km^2**

Table 3. Elevation distribution of glacier termini. The number of glaciers with available mass-balance observation (MB) and detailed inventory (WGI) data are listed according to the elevation class of the ice front. Data from the WGMS

Elevation class	Number of glaciers	
	MB	WGI
m a.s.l.		
>5999	0%	0%
5000–5999	1%	2%
4000–4999	9%	21%
3000–3999	12%	29%
2000–2999	20%	14%
1000–1999	26%	26%
<1000	32%	8%
Total	**228**	**63 189**

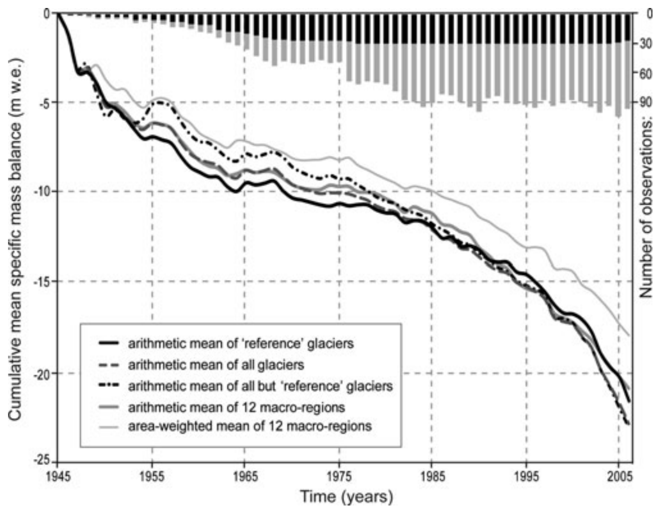

Fig. 3. Global glacier mass changes from 1945 to 2006. The cumulative mean specific mass balance (left *y* axis) of the reference glaciers and of four different sampling/averaging approaches (see text) are shown together with the number of available observations (right *y* axis) from reference (black) and other (grey) glaciers. Source: data from the WGMS.

Regional and individual cumulative mass-balance curves have been shown and discussed in detail, for example by Kaser and others (2006, and references therein) and WGMS (2007). Here, we dissolve the global glacier mass balances, using approach (2), in six macro-regions and six decades (Fig. 4a–f). In addition to the global and regional mass balance, the standard deviation and the number of available observations are given in order to provide a measure for the variance and the observation density, respectively. For the first three decades (1946–75), mass-balance measurements are available only for latitudes higher than 30° N. Later, information becomes available from the regions between 30° N and 30° S. Latitudes below 30° S are covered with observations from South America after 1976, and from the northeastern side of the Antarctic Peninsula and New Zealand in the last decade. The regional data samples higher than 30° N consist of more than 100 observations per decade after 1976, whereas the six regions south of that exceed ten observations only in the case of South America in the last decade and, hence, are to be considered of limited significance.

In the decade 1946–55, observations of the five glaciers in the European Alps and two glaciers in Scandinavia indicate a mass loss of more than 0.4 m w.e., whereas the mean of the two glaciers in North America features a zero balance over the last 3 years of that decade. In the following two decades (1956–75), North America, Europe and Northern Asia show a moderate ice loss, with a mean annual change of –0.10 to –0.25 m w.e. After 1976, the decadal mass losses increase in North America and Northern Asia to mean annual mass balances of –0.65 and –0.43 m w.e., respectively, in the last decade. The decadal mean balances in Europe remain moderately negative between 1976 and 1995, due to the temporal regain in mass of some glaciers, and become strongly negative (–0.72 m w.e.) in the last decade. In South America, positive and close to steady-state balances are reported in the third decade (1976–85) from Quelccaya (PE) and Echaurren Norte (CL), respectively, followed by two decades of average ice losses with values between –0.26 and –0.90 m w.e. from a sample of 12 glaciers (including four observations from Ventorillo (MX)). In Africa, negative mass balances have been reported from Lewis Glacier on Mount Kenya with observations between 1979 and 1996. The three negative decadal balances of Southern Asia come from 11 observations from AX010 and Rikha Samba, Nepal Himalaya, and from Changmekhangpu, Sikkim Himalaya. Furthermore, the average mass loss of Bahía del Diablo on Vega Island, Antarctica, (–0.25 m w.e.) and the 1 year gain of Brewster (NZ) show up in the last decade.

DISCUSSION

Available dataset and 'reference' glacier concept

Unlike meteorological data, which are mainly measured, collected and made available through governmental agencies (GCOS, 2003), glacier mass-balance observations are usually carried out within scientific projects, collected within a cooperation network, and made available by the WGMS. As a consequence, the data collection runs with a very low funding level and depends fully on the cooperativeness of the individual investigators. An exception is Norway where for decades the majority of mass-balance observation programmes (over 40 series) have been run and made available by the Norwegian Water Resources and Energy Directorate. At first glance, the available mass-balance observations seem to be well distributed over the globe. However, looking at the length and continuity, or lack thereof, of the time series it is apparent that the observation network is strongly overrepresented by glaciers located in Europe and North America. Unfortunately, the regions hosting large proportions of the glacier cover of the Earth (e.g. the Canadian Archipelago, Patagonia, the Arctic Islands and the ice bodies around the two ice sheets in Greenland and Antarctica) are greatly underrepresented or even lack any long-term data series. In Asia a large number of observation series have been started but the vast majority were interrupted in the 1980s and 1990s.

With regard to the limited dataset, it is particularly unfortunate that data on mass balance vs altitude have been

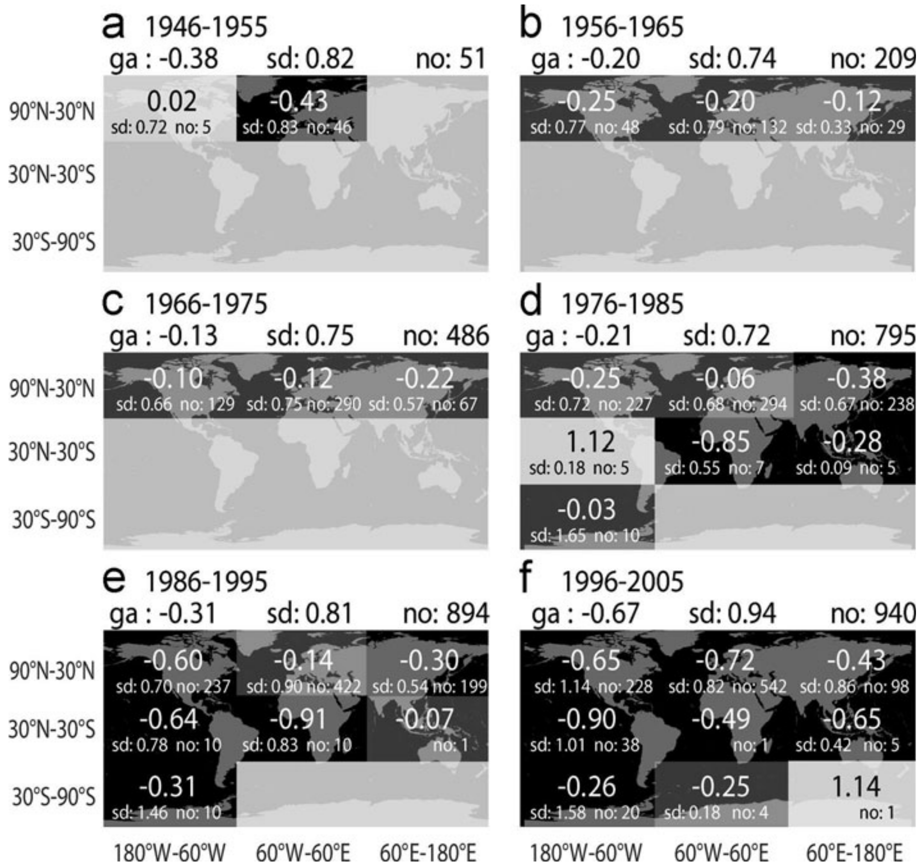

Fig. 4. Spatio-temporal overview of glacier mass changes. The average annual mass balance for nine spatial sectors of the globe is shown for the six decades between 1946 and 2005 (a–f). Sectors with observations are highlighted according to the mean annual mass balance (in m w.e.), with positive balances in white, ice losses up to 0.25 m w.e. in dark grey and ice losses greater than this in black. For each decade the global average (ga), standard deviations (sd) and number of observations (no) are given. Source: figure modified from WGMS (2008b), based on data from the WGMS.

reported for only 45% of the annual measurements and ELA/AAR for only 73%. The seasonal balances were measured at 63% of the glaciers. Mass balance vs altitude and ELA/AAR can, at least in principle, be derived from the existing raw data and would provide valuable information about, for example, mass-balance gradients (e.g. Dyurgerov and Dwyer, 2001), mass turnover (e.g. Dyurgerov, 2002), the glacier climate regime (e.g. Hoelzle and others, 2003) and climate sensitivity (e.g. Oerlemans and Fortuin, 1992). In order to improve the available seasonal dataset, the annual observation programmes need to be extended with seasonal field surveys, although the in situ determination of the winter/wet-season accumulation might be a major challenge. Once available, these data would provide insight into the processes behind the glacier fluctuations (e.g. Dyurgerov and Meier, 1999; Schöner and others, 2000; Ohmura, 2006) and would be of great value for model validation (e.g. Oerlemans, 2001). The observation and standardized compilation of further parameters such as temperature and precipitation at the ELA, ice/firn temperatures or the remaining mean/maximum ice thickness would be of great value for many scientific questions, especially in view of the fast changes in nature.

Trend analyses ideally are based on long-term measurement series. It is for that purpose that the WGMS has introduced the concept of 'reference' glaciers. A mass-balance observation programme is considered to be a 'reference' series if it is ongoing, continuous and long-term (see Fig. 2), with reliable reporting of data and meta-information. At present, a set of 30 reference glaciers in nine mountain ranges (in five of the macro-regions; see Table 1) are listed in the *Glacier Mass Balance Bulletin* series (WGMS, 2007) with (almost) continuous observations since 1976, and for 11 of the reference glaciers observations reach back to 1960 or earlier (see Appendix). The set of reference glaciers is reviewed after each call-for-data and it will help to support the continuation of these unique data series. Further glaciers that could be considered next as reference glaciers include Baby and White (Canadian High Arctic), Peyto (Canadian Rocky Mountains), Helm (Canadian Coast Mountains) and Lemon Creek (US Coast Range).

Uncertainties

Data provided by the WGMS, but also in general, are subject to errors and inaccuracies and, hence, have to be quality-checked against the related literature before being used in further analysis. The measurement and calculation of mass balances contain various sources of systematic and random errors that include: the accuracy of stake readings, snow probing and snow/firn density measurements (Østrem and Brugman, 1991; Jansson, 1999; Østrem and Haakensen, 1999), the distribution of the stake and pit network (Lliboutry, 1974; Cogley, 1999; Fountain and Vecchia, 1999), the method used to interpolate between the measurement points

(Østrem and Brugman, 1991; Kaser and others, 1996; Funk and others, 1997; Hock and Jensen, 1999), the extrapolation for unprobed areas such as crevasse (Karlén, 1965; Jannson, 1999) or debris-covered zones (Nakawo and Rana, 1999, Nakawa and others, 2000), special problems related to internal accumulation (Rabus and Echelmeyer, 1998) and calving (Arendt and others, 2002; Rignot and others, 2003; O'Neel and others, 2005), as well as any changes in the glacier area that are usually not subject to annual measurement (Elsberg and others, 2001). Generally, the accuracy of the results from the summer balance and the ablation area exceeds that of the results from the winter balance and the accumulation zone, as the ablation processes spatially correlate much better than the snow accumulation (Jansson, 1999; Kuhn and others, 1999). The dimensions of the various errors are glacier-specific, and their propagation is hard to quantify. Typical estimates of the annual mass-balance accuracy range lie between 0.1 m w.e. (Jansson, 1999) and 0.6 m w.e. (Funk and others, 1997). Further errors are introduced when comparing mass balances derived from different measurement systems (stratigraphic vs fixed-date systems) or from different hemispheres (i.e. the hydrological years of the two hemispheres are shifted by half a year).

In contrast to the in situ point measurements based on a changing reference (i.e. the previous year's summer surface), geodetic methods have the advantage of providing volume changes over the entire glacier based on a non-changing reference (i.e. the surrounding bedrock), but encounter some problems with (fresh) snow in the accumulation area and density assumption for snow, firn and ice (Krimmel, 1999). A combination of the direct glaciological method with decadal geodetic methods has proven to be an appropriate way to detect systematic biases (e.g. Jansson, 1999; Krimmel, 1999; Kuhn and others, 1999; Bauder and others, 2007). Several studies have shown that other remote-sensing methods are also useful for determining glacier volume changes over longer periods, for example those based on airborne laser altimetry (Arendt and others, 2002) or the differencing of digital elevation models using SPOT5 (Système Probatoire pour l'Observation de la Terre) (Berthier and others, 2007), SRTM (Shuttle Radar Topography Mission) (Rignot and others, 2003; Larsen and others, 2007; Schiefer and others, 2007) or ASTER (Advanced Spaceborne Thermal Emission and Reflection Radiometer) and its optical stereo (Kääb, 2007). Differencing of digital elevation models from spaceborne sensors is, at present, no replacement for such validation purposes, as the resolution and quality is still too low. However, it can already be used to assess the representativeness of available field measurements with respect to long-term glacier volume changes over large areas (e.g. Kääb, 2008).

Given the present state of knowledge, the manifold sources of errors, and the often missing meta-information, it is not possible to quantify the overall error of the available mass-balance data. As an objective measure of uncertainty we, hence, estimate the confidence interval of the here-presented global dataset to be in the magnitude of two standard errors of the reported annual mass-balance data, i.e. between 0.25 and 0.5 m w.e. but increasing with small sample sizes. With an average annual standard deviation of about 0.7 m w.e., the annual signal of the mean mass balances is smaller than the regional variability. However, the change of the cumulative mean mass balances over extended periods is far beyond the estimated uncertainty and, hence, significant. In order to reduce, better understand and quantify these uncertainties, we reiterate the recommendation to validate and calibrate systematically the mass-balance data derived from annual/seasonal field observations with decadal mass/volume changes as assessed from geodetic methods, and to submit also the corresponding meta-information. It is one of the major shortcomings of the available datasets that this information is often missing and, as a consequence, it is difficult to reconstruct whether a mass-balance series is geodetically calibrated or not.

Global and regional glacier changes

The global average cumulative mass balance indicates a strong mass loss in the first decade after the start of the measurements in 1946 (for Europe), slowing down in the second decade (1956–65; based on observations above 30° N only), followed by a moderate ice loss between 1966 and 1985 (with data from the Southern Hemisphere only since 1976) and a subsequent acceleration until the present (2006). Over the six decades the global average ice loss has cumulated to about 21 m w.e., or an average mass balance of –0.35 m w.e. a^{-1}, a dramatic ice loss compared with the global average ice thickness which is estimated (by dividing volume by area) to be between 100 m (Solomon and others, 2007) and about 180 m (personal communication from A. Ohmura, 2008). The vast ice loss since the mid-20th century has already led to the disintegration of many glaciers within the observation network, including Lower Curties and Columbia 2057 (US), Chacaltaya (BO), Carèser (IT), Lewis (KE) and Urumqihe (CN), and presents one of the major challenges for glacier monitoring in the 21st century.

The cumulative mass loss is in the same order for all the sample/methods used for averaging. These methods are: 30 reference glaciers (and subsamples before 1976), all but the reference glaciers, all glaciers, arithmetic and area-weighted average of the regions. In addition, the global result corresponds well with the findings of several approaches as summarized by Kaser and others (2006) and published in Solomon and others (2007). They state an average annual ice loss of 0.283 m w.e. between 1961 and 2004 (in this study, sampling approach (2) gave 0.286 m w.e.). This is not surprising, as both approaches are based mainly on the dataset provided by the WGMS, but Kaser and others (2006) extended about 70 data series which have either not been reported to the WGMS or had to be rejected due to insufficient data quality or to their dependence on hydrological/meteorological measurements. For the last three decades (1976–2006) the strong cumulative changes calculated from a sample of 60–100 glaciers from 8 of the 12 glacierized macro-regions can be considered as representative of the global mass-balance signal, as the mass-balance variability in time is spatially correlated over distances of several hundred kilometres (Letréguilly and Reynaud, 1990; Cogley and Adams, 1998). Some reservation has to be made because of the lack of data series for the glaciers around Greenland and Antarctica as well as in New Zealand, and because the sample of glaciers with mass-balance observations might not be representative, with respect to characteristics (e.g. tidewater, debris cover), ice temperature and hypsometry, of the ice bodies that are major (potential) contributors to sea-level change. Going further back in time, the average is based only on observations from North America, Europe and Asia, increasingly dominated by the sample from Europe. Together with the less pronounced trends, the 'global' average mass balance from this small and regionally biased sample might not be representative anymore for the other regions. Approaches using regional (area-weighted) averaging might reduce this bias but cannot completely overcome the lack of observations.

The regional cumulative mass changes can be considered to be a good first-order index for the glacier changes in these areas over the corresponding period. However, further analysis might have to resample the series according to the focus of the study and have to consider the glacial characteristics of the different geographical regions (Fountain and Vecchia, 1999): mass-balance variability of temperate alpine glaciers in the Northern Hemisphere is mainly driven by accumulation and ablation during winter and summer seasons, respectively (Kuhn and others, 1999). This is not valid for low-latitude glaciers where ablation occurs throughout the year and multiple accumulation seasons exist (Kaser and Osmaston, 2002), monsoonal glaciers of the Himalaya where the accumulation and ablation seasons occur at about the same time (Ageta and Fujita, 1996), and high-altitude and polar glaciers where any season can be the accumulation season (Chinn, 1985). However, annual/net mass balances integrate these seasonal complexities and as such might not be relevant for some analysis. Strongly diverse mass-balance characteristics also exist between glaciers under dry-continental conditions and in maritime regions. The former can be found in northern Alaska, Arctic Canada, sub-Arctic Russia, parts of the Andes near the Atacama Desert and in many central Asian mountain chains. They show low mass turnover, equilibrium lines at high altitudes and firn/ice well below melting temperatures. The latter, glaciers in maritime regions, are found in Patagonia, Iceland, southeast Alaska, as well as in the coastal parts of Norway and New Zealand, and show high mass turnover, low equilibrium lines and firn/ice at melting temperatures (Shumskiy, 1964; Ohmura and others, 1992; Haeberli and Burn, 2002).

For a sound analysis of global or regional glacier changes, results from the valuable but small sample of mass-balance measurements have to be complemented with other glacier observations, such as front variation measurements (available for about 1700 glaciers worldwide; WGMS, 2008, and earlier issues) or investigations of the glacier retreat from the trimlines of the Little Ice Age which can be found around the globe (Grove, 2004). Examples for such integrative analysis for entire mountain ranges are given by Molnia (2007) for Alaska, by Casassa and others (2007) for the Andean glaciers, by Kaser and Osmaston (2002) for tropical glaciers, by Andreassen and others (2005) for Norway, by Zemp and others (2007b) for the European Alps, by Kotlyakov (2006) for Russia, and by Chinn (2001) for New Zealand, as well as by Hoelzle and others (2003), Grove (2004), Zemp and others (2007a), and WGMS (2008b) for a global overview.

Glacier mass balance as a climate proxy

Glacier mass changes are used widely as a climate proxy in many environmental and climate change assessment reports (e.g. Solomon and others, 2007). The mass change of glaciers, which are not influenced by thick debris covers, calving or 'surge' instabilities, is the direct, undelayed reaction of a glacier to climatic forcing. The mass-balance variability in time is well correlated spatially over larger distances (Letréguilly and Reynaud, 1990; Cogley and Adams, 1998) and with climatic parameters such as (seasonal) air temperature, precipitation and sunshine duration (Lliboutry, 1974; Schöner and others, 2000). However, the glacier mass-balance change provides an integrative climatic signal, and the quantitative attribution of the forcing to individual meteorological parameters is not straightforward. The energy and mass balance at the glacier surface is influenced by changes in atmospheric conditions (solar radiation, air temperature, precipitation, wind, cloudiness, etc.). Air temperature thereby plays a predominant role, as it is related to the radiation balance, turbulent heat exchange and solid/liquid precipitation ratio (Kuhn, 1981; Ohmura, 2001). The climatic sensitivity of a glacier not only depends on regional climate variability but also on local topographic effects, which can result in two adjacent glaciers featuring different specific mass-balance responses (Kuhn and others, 1985).

For a temperate glacier, an assumed step-change in climatic conditions would cause an initial mass-balance change followed by a return towards zero values, due to the adaptation of the size of the glacier (surface area) to the new climate (Jóhannesson and others, 1989; Haeberli and Hoelzle, 1995). The observed trend of increasingly negative mass balance over reducing glacier surface areas thus leaves no doubt about the ongoing climatic forcing resulting from the change in climate and possible enhancement mechanisms such as mass-balance/altitude feedback, altered turbulent fluxes due to the size and existence of rock outcrops or changes in the surface albedo. The specific mass-balance data can be compared directly between different glaciers of any size and elevation range. These data series provide a combined hydrological and climatic signal. Glacier contribution to runoff can be calculated very easily by multiplying the specific mass balance with the corresponding glacier area, whereas a climatic interpretation needs to relate the mass changes to a glacier reference extent in order to derive a pure climate signal (cf. Elsberg and others, 2001; WGMS, 2007, and earlier issues).

In order to advance the present mass-balance monitoring, as part of the Global Climate Observing System, it is necessary to continue with the existing data series and to extend the network in respect of the global glacier distribution. Systematic use should be made of remote sensing and geo-informatics for assessing the representativeness of the available in situ observations (e.g. Paul and Haeberli, 2008). Analytical or numerical modelling is needed to quantify the above-mentioned topographic effects as well as to attribute the glacier mass changes to individual meteorological or climate parameters (e.g. Kuhn, 1981; Oerlemans, 2001) and, in combination with measured and reconstructed glacier fluctuations, to compare the present mass changes with the (pre-)industrial variability (e.g. Haeberli and Holzhauser, 2003)

Glacier mass balance and sea-level changes

Measurements from the mass-balance monitoring network are used to estimate the contribution of glaciers to past, present and future sea-level changes (Kaser and others, 2006 and references therein; Raper and Braithwaite, 2006). These estimates are hampered by the fact that: (a) no complete detailed inventory of the Earth's glaciers exists; (b) the estimation of the overall ice volume of glaciers contains large uncertainties; (c) the spatial distribution of the available mass-balance series is disproportionate to the global ice cover; and (d) the small sample of mass-balance observations is (most probably) not representative for the entire sample of glaciers.

Most of the approaches use the regional ice extents of Dyurgerov and Meier (2005 and earlier versions; mainly based on WGMS, 1989) as a baseline inventory to calculate the overall potential sea-level rise equivalent as well as sea-level changes. A detailed inventory, including information on glacier location, size and altitude extent, is only available for about 70 000 glaciers covering about 180 000 km^2. This corresponds to only 43% of the approximate total number and 23% of the overall glacier area based on rough estimates from Meier and Bahr (1996) and Dyurgerov and Meier (2005), respectively. As a further uncertainty factor, the existing inventory contains no information on the proportion of ice below sea level. There are only a few glaciers where thickness measurements have been carried out (so far not compiled by the WGMS). Different approaches exist for estimating the overall ice volume (e.g. Haeberli and Hoelzle, 1995; Bahr and others, 1997), but they all contain a number of uncertainties that could amount to 30–50% of the total ice volume. The latest assessment report of the Intergovernmental Panel on Climate Change (IPCC) (Solomon and others, 2007) quotes the total area and corresponding potential sea-level rise as 510 000–540 000 km^2 and 150–370 mm, respectively. These estimates, as correctly noted in Solomon and others (2007), do not include ice bodies around the ice sheets in Greenland (70 000 km^2 based on Weidick and Morrris, 1998) and Antarctica (169 000 km^2 based on Shumskiy, 1969) and, hence, might considerably underestimate the overall potential sea-level rise due to melting glaciers. As shown above, many of the regions with large ice covers, such as the Canadian Arctic, High Mountain Asia, South America and around the two ice sheets, are not represented by an adequate number of long-term mass-balance measurements. Mass-balance programmes require intensive fieldwork and are usually carried out on glaciers that are easy accessible, safe and not too large. Hence, these glaciers are neither representative of the glacier size distribution nor of the elevation distribution of all glaciers, at least when compared with the presented data of about 70 000 glaciers with detailed inventory information (the data for an exact comparison are not available).

The current first-order estimates of the contribution from glaciers to past, present and future sea-level changes can only be improved significantly by completing a detailed baseline inventory of the Earth's glaciers as well as a review and enlargement of the available (measured) glacier thickness dataset. This would be needed to scale-up the few in situ series that we have to cover all glaciers. It is hoped that internationally coordinated efforts, such as the European Space Agency-funded GlobGlacier project (Volden, 2007) or the Global Land Ice Measurements from Space initiative (Raup and others, 2007), will make major steps in that direction. Furthermore, it is necessary to continue and extend the present mass-balance network in respect of the global distribution of the ice cover and to make systematic use of remote sensing and geo-informatics to assess the representativeness of the available in situ annual mass-balance series (Paul and Haeberli, 2008) as well as of decadal volume changes in ice fields and ice caps that are too large for in situ measurements (e.g. Rignot and others, 2003; Larsen and others, 2007).

CONCLUSIONS AND CONSEQUENCES FOR THE MONITORING OF GLACIERS

During the six decades of glacier mass-balance observation, the WGMS has compiled a dataset of more than 3400 annual mass-balance measurements from 228 glaciers worldwide. The collection and free availability of these data through a purely scientific collaboration network is a great success and, at the same time, one of the reasons why the present monitoring network is unevenly distributed in comparison with the global ice coverage. The 30 reference glaciers with continuous observation series since 1976 show an accelerated thinning, with mean annual ice losses of 0.14 m w.e. (1976–85), 0.25 m w.e. (1986–95) and 0.58 m w.e. (1996–2005), which gives a total average ice-thickness reduction of about 10 m w.e. The available data from the first three decades indicate strong mass losses as early as the 1940s and 1950s, followed by moderate mass losses until the end of the 1970s. The mass-balance data are widely used by the scientific community and represent one backbone of glacier research. Mass balance is recognized as an essential climate variable within the global climate-related observing systems and is, in effect, the largest non-steric contributor to the global sea-level rise at the turn of the century.

In view of the discrepancy between the relevance of glacier mass-balance data and the relatively small set of current long-term observations with a strong bias towards the Northern Hemisphere and Europe, we strongly recommend to:

- continue the work on the glaciers with long-term measurements,
- resume the interrupted long-term series,
- replace vanishing glaciers by starting early with parallel observations on larger or higher-reaching glaciers,
- extend the monitoring network to strategically important regions with few or no series,
- validate and calibrate the field measurements with the results of geodetic methods (and clearly flag such data series),
- make systematic use of remote sensing and geo-informatics for assessment of the representativeness of the field measurements and for (decadal) volume change analysis in mountain ranges lacking such data, and
- make the data and related meta-information readily available to the scientific community and the wider public.

The potential dramatic changes as sketched for the 21st century by the IPCC report (Solomon and others, 2007) require critical reflection and a rigorous implementation of the monitoring strategies for glaciers in order to face the challenges of the fast changes in nature and to bridge the gap between historical observation series and the new technologies.

ACKNOWLEDGEMENTS

We express our gratitude to the National Correspondents, Principal Investigators of the WGMS and all other individuals and institutions for the collection and free exchange of these important data over many years. Sincere thanks go to the field scientists and programme managers of the long-term data series: without their commitment to maintain the observation series through politically and financially difficult times, many of the current insights would not have been possible. We thank F. Paul for thoughtful remarks on a first draft of the manuscript, the two reviewers for constructive feedback, the scientific editor for providing guidance towards the final paper, and I. Woodhatch for polishing the English. This study has been mainly funded by the Swiss National Science Foundation and the Swiss Federal Office for the Environment.

REFERENCES

Ageta, Y. and K. Fujita. 1996. Characteristics of mass balance of summer-accumulation type glaciers in the Himalayas and Tibetan Plateau. *Z. Gletscherkd. Glazialgeol.,* **32**, 61–65.

Andreassen, L.M., H. Elverøy, B. Kjøllmoen, R.V. Engeset and N. Haakensen. 2005. Glacier mass-balance and length variation in Norway. *Ann. Glaciol.,* **42**, 317–325.

Arendt, A.A., K.A. Echelmeyer, W.D. Harrison, C.S. Lingle and V.B. Valentine. 2002. Rapid wastage of Alaska glaciers and their contribution to rising sea level. *Science,* **297**(5580), 382–386.

Bahr, D.B., M.F. Meier and S.D. Peckham. 1997. The physical basis of glacier volume–area scaling. *J. Geophys. Res.,* **102**(B9), 20,355–20,362.

Bauder, A., M. Funk and M. Huss. 2007. Ice-volume changes of selected glaciers in the Swiss Alps since the end of the 19th century. *Ann. Glaciol.,* **46**, 145–149.

Berthier, E., Y. Arnaud, R. Kumar, S. Ahmad, P. Wagnon and P. Chevallier. 2007. Remote sensing estimates of glacier mass balances in the Himachal Pradesh (Western Himalaya, India). *Remote Sens. Environ.,* **108**(3), 327–338.

Braithwaite, R.J. 2002. Glacier mass balance: the first 50 years of international monitoring. *Progr. Phys. Geogr.,* **26**(1), 76–95.

Braun, L.N., M. Weber and M. Schulz. 2000. Consequences of climate change for runoff from Alpine regions. *Ann. Glaciol.,* **31**, 19–25.

Casassa, G. *and 6 others*. 2007. Current status of Andean glaciers. *Global Planet. Change,* **59**(1–4), 1–9.

Chinn, T.J.H. 1985. Structure and equilibrium of the Dry Valleys glaciers. *NZ Antarct. Rec.,* **6**, 73–88.

Chinn, T.J. 2001. Distribution of the glacial water resources of New Zealand. *J. Hydrol. (NZ),* **40**(2), 139–187.

Cogley, J.G. 1999. Effective sample size for glacier mass balance. *Geogr. Ann.,* **81A**(4), 497–507.

Cogley, J.G. 2005. Mass and energy balances of glaciers and ice sheets. *In* Anderson, M.G., *ed. Encyclopaedia of hydrological sciences. Part 14. Snow and glacier hydrology.* New York, Wiley, 2555–2573.

Cogley, J.G. and W.P. Adams. 1998. Mass balance of glaciers other than the ice sheets. *J. Glaciol.,* **44**(147), 315–325.

Dyurgerov, M. 2002. *Glacier mass balance and regime: data of measurements and analysis.* Boulder, CO, University of Colorado. Institute of Arctic and Alpine Research. (INSTAAR Occasional Paper 55.)

Dyurgerov, M.B. and J.D. Dwyer. 2001. The steepening of glacier mass balance gradients with Northern Hemisphere warming. *Z. Gletscherkd. Glazialgeol.,* **36**, 107–118.

Dyurgerov, M.B. and M.F. Meier. 1999. Analysis of winter and summer glacier mass balances. *Geogr. Ann.,* **81A**(4), 541–554.

Dyurgerov, M.B. and M.F. Meier. 2005. Glaciers and the changing Earth system: a 2004 snapshot. 58. Boulder, CO, university of Colorado. Institute of Arctic and Alpine Research. INSTAAR Occasional Paper

Elsberg, D.H., W.D. Harrison, K.A. Echelmeyer and R.M. Krimmel. 2001. Quantifying the effects of climate and surface change on glacier mass balance. *J. Glaciol.,* **47**(159), 649–658.

Fountain, A.G. and A. Vecchia. 1999. How many stakes are required to measure the mass balance of a glacier? *Geogr. Ann.,* **81A**(4), 563–573.

Francou, B., M. Vuille, P. Wagnon, J. Mendoza and J.E. Sicart. 2003. Tropical climate change recorded by a glacier in the central Andes during the last decades of the twentieth century: Chacaltaya, Bolivia, 16°S. *J. Geophys. Res.,* **108**(D5), 4154. (10.1029/2002JD002959.)

Funk, M., R. Morelli and W. Stahel. 1997. Mass balance of Griesgletscher 1961–1994: different methods of determination. *Z. Gletscherkd. Glazialgeol.,* **33**(1), 41–55.

Global Climate Observing System (GCOS). 2003. *The second report on the adequacy of the global observing systems for climate in support of the UNFCCC. GCOS-82.* Geneva. World Meteorological Organization (WMO TD 1143)

Global Climate Observing System (GCOS). 2004. *Implementation plan for the global observing system for climate in support of the UNFCCC. GCOS-92.* Geneva. World Meteorological Organization (WMO TD 1219)

Grove, J.M. 2004. *Little ice ages: ancient and modern. Second edition.* London and New York, Routledge.

Haeberli, W. 2004. Glaciers and ice caps: historical background and strategies of worldwide monitoring. *In* Bamber, J.L. and A.J. Payne, *eds. Mass balance of the cryosphere.* Cambridge, Cambridge University Press, 559–578.

Haeberli, W. and C. Burn. 2002. Natural hazards in forests: glacier and permafrost effects as related to climate change. *In* Sidle, R.C., *ed. Environmental change and geomorphic hazards in forests.* New York, etc., CABI Publishing, 167–202.

Haeberli, W. and M. Hoelzle. 1995. Application of inventory data for estimating characteristics of and regional climate-change effects on mountain glaciers: a pilot study with the European Alps. *Ann. Glaciol.,* **21**, 206–212.

Haeberli, W. and H. Holzhauser. 2003. Alpine glacier mass changes during the past two millennia. *PAGES News,* **11**(1), 13–15.

Haeberli, W., J. Cihlar and R.G. Barry. 2000. Glacier monitoring within the Global Climate Observing System. *Ann. Glaciol.,* **31**, 241–246.

Hock, R. and H. Jensen. 1999. Application of kriging interpolation for glacier mass balance computations. *Geogr. Ann.,* **81A**(4), 611–619.

Hoelzle, M., W. Haeberli, M. Dischl and W. Peschke. 2003. Secular glacier mass balances derived from cumulative glacier length changes. *Global Planet. Change,* **36**(4), 295–306.

Holmlund, P., P. Jansson and R. Pettersson. 2005. A re-analysis of the 58 year mass-balance record of Storglaciären, Sweden. *Ann. Glaciol.,* **42**, 389–394.

Huss, M., A. Bauder, M. Funk and R. Hock. 2008a. Determination of the seasonal mass balance of four Alpine glaciers since 1865. *J. Geophys. Res.,* **113**(F1), F01015. (10.1029/2007JF000803.)

Huss, M., A Bauder and M. Funk. 2008b. Homogenization of long-term mass-balance time series. Ann. Glaciol., **50**

Jansson, P. 1999. Effect of uncertainties in measured variables on the calculated mass balance of Storglaciären. *Geogr. Ann.,* **81A**(4), 633–642.

Jóhannesson, T., C. Raymond and E. Waddington. 1989. Time-scale for adjustment of glaciers to changes in mass balance. *J. Glaciol.,* **35**(121), 355–369.

Kääb, A. 2007. Glacier volume changes using ASTER optical stereo. A test study in Eastern Svalbard. *In Proceedings of the International Geoscience and Remote Sensing Symposium (IGARSS 2007), 23–28 July, 2007. Barcelona, Spain* Piscataway, NJ, Institute of Electrical and Electronics Engineers, 3994–3996.

Kääb, A. 2008. Glacier volume changes using ASTER satellite stereo and ICESat GLAS laser altimetry. A test study on Edgeøya, Eastern Svalbard. *IEEE Trans. Geosci. Remote Sens.,* **46**(10), 2823–2830.

Karlén, W. 1965. Ablation i sprickområden. *In* Pytte, R. and G. Østrem, *eds. Glacio-hydrologiske undersökelser i Norge 1964.*

Oslo, Norges Vassdrags- og Elektrisitetsvesen, 65–66. (NVE Hydrol. Avd. Medd. 14.)

Kaser, G. and H. Osmaston. 2002. *Tropical glaciers.* Cambridge, etc., Cambridge University Press.

Kaser, G., M. Munari, B. Noggler, C. Oberschmied and P. Valentini. 1996. Ricerche sul bilancio di massa del Ghiacciaio di Fontana Bianca (Weissbrunnferner) nel Gruppo Ortles-Cevedale. *Geogr. Fís. Din. Quat.,* **18**(2), 277–280.

Kaser, G., J.G. Cogley, M.B. Dyurgerov, M.F. Meier and A. Ohmura. 2006. Mass balance of glaciers and ice caps: consensus estimates for 1961–2004. *Geophys. Res. Lett.,* **33**(19), L19501. (10.1029/2006GL027511.)

Kotlyakov, V.M., *ed.* 2006. *Oledenenie Severnoj i Central'noj Evrazii v Sovremennuju epochu [Glaciation in north and central Eurasia at present time]*. Moscow, Nauka. [In Russian with English summary.]

Krimmel, R.M. 1999. Analysis of difference between direct and geodetic mass balance measurements at South Cascade Glacier, Washington. *Geogr. Ann.,* **81A**(4), 653–658.

Kuhn, M. 1981. Climate and glaciers. *IAHS Publ.* 131 (Symposium at Canberra 1979 – *Sea Level, Ice and Climatic Change*), 3–20.

Kuhn, M., G. Markl, G. Kaser, U. Nickus, F. Obleitner and H. Schneider. 1985. Fluctuations of climate and mass balance: different responses of two adjacent glaciers. *Z. Gletscherkd. Glazialgeol.,* **21**, 409–416.

Kuhn, M., E. Dreiseitl, S. Hofinger, G. Markl, N. Span and G. Kaser. 1999. Measurements and models of the mass balance of Hintereisferner. *Geogr. Ann.,* **81A**(4), 659–670.

Larsen, C.F., R.J. Motyka, A.A. Arendt, K.A. Echelmeyer and P.E. Geissler. 2007. Glacier changes in southeast Alaska and northwest British Columbia and contribution to sea level rise. *J. Geophys. Res.,* **112**(F1), F01007. (10.1029/2006JF000586.)

Letréguilly, A. and L. Reynaud. 1990. Space and time distribution of glacier mass-balance in the Northern Hemisphere. *Arct. Alp. Res.,* **22**(1), 43–50.

Lliboutry, L. 1974. Multivariate statistical analysis of glacier annual balances. *J. Glaciol.,* **13**(69), 371–392.

Meier, M.F. and D.B. Bahr. 1996. Counting glaciers: use of scaling methods to estimate the number and size distribution of glaciers of the world. *CRREL Spec. Rep.* 96-27. 89–94.

Meier, M.F. *and 7 others.* 2007. Glaciers dominate eustatic sea-level rise in the 21st century. *Science,* **317**(5841), 1064–1067.

Mercanton, P.L., *ed.* 1916. Vermessungen am Rhonegletscher/ Mensuration au glacier du Rhône: 1874–1915. *Neue Denkschr. Schweiz. Naturforsch. Ges.* 52.

Molnia, B.F. 2007. Late nineteenth to early twenty-first century behavior of Alaskan glaciers as indicators of changing regional climate. *Global Planet. Change,* **56**(1–2), 23–56.

Nakawo, M. and B. Rana. 1999. Estimate of ablation rate of glacier ice under a supraglacial debris layer. *Geogr. Ann.,* **81A**(4), 695–701.

Nakawo, M., C.F. Raymond and A. Fountain, *eds.* 2000. *IAHS Publ.* 264 (Workshop at Seattle 2000 – *Debris-Covered Glaciers*).

Oerlemans, J. 2001. *Glaciers and climate change.* Lisse, etc., A.A. Balkema.

Oerlemans, J. and J.P.F. Fortuin. 1992. Sensitivity of glaciers and small ice caps to greenhouse warming. *Science,* **258**(5079), 115–117.

Ohmura, A. 2001. Physical basis for the temperature-based melt-index method. *J. Appl. Meteorol.,* **40**(4), 753–761.

Ohmura, A. 2004. Cryosphere during the twentieth century. *In* Sparling, J. Y. and C.J. Hawkesworth, *eds. The state of the planet: frontiers and challenges in geophysics.* Washington DC, American Geophysical Union, 239–257.

Ohmura, A. 2006. Changes in mountain glaciers and ice caps during the 20th century. *Ann. Glaciol.,* **43**, 361–368.

Ohmura, A., P. Kasser and M. Funk. 1992. Climate at the equilibrium line of glaciers. *J. Glaciol.,* **38**(130), 397–411.

O'Neel, S., W.T. Pfeffer, R. Krimmel and M. Meier. 2005. Evolving force balance at Columbia Glacier, Alaska, during its rapid retreat. *J. Geophys. Res.,* **110**(F3), F03012. (10.1029/ 2005JF000292.)

Østrem, G. and M. Brugman. 1991. *Glacier mass-balance measurements. A manual for field and office work.* Saskatoon, Sask., Environment Canada. National Hydrology Research Institute. (NHRI Science Report 4.)

Østrem, G. and N. Haakensen. 1999. Map comparison or traditional mass-balance measurements: which method is better? *Geogr. Ann.,* **81A**(4), 703–711.

Østrem, G. and A. Stanley, *eds.* 1969. *Glacier mass balance measurements: a manual for field and office work.* Ottawa, Ont., Department of Energy, Mines and Resources; Oslo, Norwegian Water Resources and Electricity Board.

Paul, F. and W. Haeberli. 2008. Spatial variability of glacier elevation changes in the Swiss Alps obtained from two digital elevation models. *Geophys. Res. Lett.* **35**(21). (10.1029/ 2008GL034718.) L21502

Rabus, B.T. and K.A. Echelmeyer. 1998. The mass balance of McCall Glacier, Brooks Range, Alaska, U.S.A.; its regional relevance and implications for climate change in the Arctic. *J. Glaciol.,* **44** (147), 333–351.

Raper, S.C.B. and R.J. Braithwaite. 2006. Low sea level rise projections from mountain glaciers and icecaps under global warming. *Nature,* **439**(7074), 311–313.

Raup, B. *and 11 others.* 2007. Remote sensing and GIS technology in the Global Land Ice Measurements from Space (GLIMS) Project. *Comput. Geosci.,* **33**(1), 104–125.

Rignot, E., A. Rivera and G. Casassa. 2003. Contribution of the Patagonian icefields of South America to sea level rise. *Science,* **302**(5644), 434–437.

Schiefer, E., B. Menounos and R. Wheate. 2007. Recent volume loss of British Columbian glaciers, Canada. *Geophys. Res. Lett.,* **34**(16), L16503. (10.1029/2007GL030780.)

Schöner, W., I. Auer and R. Böhm. 2000. Climate variability and glacier reaction in the Austrian eastern Alps. *Ann. Glaciol.,* **31**, 31–38.

Shumskiy, P.A. 1964. *Principles of structural glaciology.* New York, Dover Publications.

Shumskiy, P.A. 1969. Oledenemie [Glaciation]. *In* Tolstiikov, E.I., *ed. Atlas Antarktiki II [Atlas of Antarctica, vol. II].* Leningrad, Gidrometeoizdat, 367–400. [In Russian]

Solomon, S. *and 7 others, eds.* 2007. *Climate change 2007: the physical science basis. Contribution of Working Group I to the Fourth Assessment Report of the Intergovernmental Panel on Climate Change*. Cambridge, etc., Cambridge University Press.

Volden, E. 2007. ESA's GlobGlacier project. *Ice Climate News,* 9, 5.

Weidick, A. and E. Morris. 1998. Local glaciers surrounding the continental ice sheets. *In* Haeberli, W., M. Hoelzle and S. Suter, *eds. Into the second century of worldwide glacier monitoring: prospects and strategies.* Paris, UNESCO Publishing, 197–207. (Studies and Reports in Hydrology 56.)

World Glacier Monitoring Service (WGMS). 1989. *World glacier inventory – status 1988, ed.* Haeberli, W., H. Bösch, K. Scherler, G. Østrem and C. Wallén. IAHS (ICSI)/UNEP/UNESCO, World Glacier Monitoring Service, Zürich.

WGMS. 2007. Glacier Mass Balance Bulletin No. 9 (2004–2005), *ed.* Haeberli, W., M. Zemp and M. Hoelzle. ICSU (FAGS)/IUGG (IACS)/UNEP/UNESCO/WMO, World Glacier Monitoring Service, Zürich.

WGMS. 2008a *Fluctuations of glaciers 2000–2005 (Vol. IX), ed.* Haeberli, W., M. Zemp, A Kääb, F. Paul and M. Hoelzle. ICSU (FAGS)IUGG (IACS)/UNEP/UNESCO/WMO, World Glacier Monitoring Service, Zürich.

WGMS, 2008b *Global glacier changes: facts and figures, ed.* Zemp, M., I. Roer, A. Kaab, M. Hoelzle, F. Paul and W. Haerberli. UNEP, World Glacier Monitoring Service, Zürich.

Zemp, M., W. Haeberli, M. Hoelzle and F. Paul. 2007a. Glacier fluctuations in the European Alps 1850–2000: an overview and spatio-temporal analysis of available data. *In* Orlove, B., E. Wiegandt and B.H. Luckman, *eds. Darkening peaks: glacier retreat, science, and society.* Berkeley, CA, University of California Press.

Zemp, M. *and 23 others*. 2007b. Glaciers and ice caps. Part I: Global overview and outlook. Part II: Glacier changes around the world. *In* Eamer, J., *ed. Global outlook for ice and snow.* Nairobi, United Nations Environment Programme.

APPENDIX

'Reference' mass-balance programmes. The 30 glaciers with ongoing, continuous and long-term mass-balance series since 1976 are listed with country code (PU), WGMS database ID, coordinates (latitude/longitude), first and last observation years as well as number of mass-balance surveys. In addition, the table lists the last reported area (in km^2), the equilibrium-line altitude (ELA0 in m a.s.l.) and accumulation-area ratio (AAR0 in %) for steady-state conditions as calculated from the linear regression between ELA/AAR and mass balance (Haeberli and others, 2007), as well as the decadal mean mass changes (in m w.e.) for the decades 1976–85, 1986–95 and 1996–2005. Data from the WGMS

PU	Name	WGMS ID	Latitude	Longitude	First obs.	Last obs.	Number of obs.	Area (year)	ELAo	AARo	1976–85	1986–95	1996–2005
AT	Hintereisferner	491	46.80	10.77	1953	2006	54	7.47 (2005)	2906	66	–0.195	–0.861	–0.873
AT	Kesselwandferner	507	46.84	10.79	1953	2006	54	3.90 (2005)	3118	70	+0.085	–0.322	–0.181
AT	Sonnblickkees	573	47.13	12.60	1959	2006	48	1.39 (2005)	2740	60	+0.077	–0.745	–0.638
AT	Vernagtferner	489	46.88	10.82	1965	2006	42	8.36 (2005)	3082	66	–0.066	–0.694	–0.585
CA	Place	41	50.43	–122.60	1965	2006	42	3.17 (2005)	2080	50	–0.843	–1.366	–0.819
CH	Gries	359	46.45	8.34	1962	2006	45	6.19 (2001)	2838	59	–0.207	–0.913	–0.987
CH	Silvretta*	408	46.85	10.08	1960	2006	47	3.01 (2003)	2763	54	+0.270	–0.389	–0.191
CL	Echaurren Norte	1344	–33.58	–70.13	1976	2006	31	0.40 (2000)	n.a.	n.a.	–0.033	–0.310	–0.331
CN	Urumqihe S. No. 1	853	43.08	86.82	1959	2005	47	1.74 (2000)	4025	56	–0.161	–0.265	–0.579
FR	Saint Sorlin	356	45.17	6.16	1957	2006	50	3.00 (2000)	2863	n.a.	+0.143	–0.882	–1.460
FR	Sarennes	357	45.12	6.14	1949	2006	58	0.50 (2000)	n.a.	n.a.	–0.170	–1.187	–1.653
IT	Caresr	635	46.45	10.70	1967	2006	40	2.83 (2005)	3100	44	–0.403	–1.224	–1.618
KZ	Ts. Tuyuksuyskiy	817	43.05	77.08	1957	2006	50	2.53 (2005)	3746	52	–0.731	–0.466	–0.340
NO	Ålfotbreen	317	61.75	5.65	1963	2006	44	4.50 (2005)	1187	57	+0.217	+1.114	–0.520
NO	Austre Brøggerbreen	292	78.88	11.83	1967	2006	40	6.12 (1995)	275	53	–0.449	–0.367	–0.620
NO	Engabreen	298	66.65	13.85	1970	2006	37	39.55 (2005)	1172	60	+0.573	+0.961	+0.276
NO	Gråsubreen	299	61.65	8.60	1962	2006	45	2.25 (2005)	2132	28	–0.358	+0.025	–0.624
NO	Hardangerjøkulen	304	60.53	7.37	1963	2006	44	17.12 (2005)	1679	68	–0.074	+0.800	–0.154
NO	Hellstugubreen	300	61.57	8.43	1962	2006	45	3.03 (2005)	1837	59	–0.456	+0.024	–0.708
NO	Midtre Lovénbreen	291	78.88	12.07	1968	2006	39	5.45 (1999)	293	58	–0.373	–0.304	–0.472
NO	Nigardsbreen	290	61.72	7.13	1962	2006	45	47.82 (2005)	1565	61	+0.009	+1.113	+0.171
NO	Storbreen	302	61.57	8.13	1949	2006	58	5.35 (2005)	1716	59	–0.355	+0.179	–0.610
SE	Storglaciären	332	67.90	18.57	1946	2006	61	3.21 (2005)	1462	45	–0.134	+0.379	–0.390
SU	Djankuat	726	43.20	42.77	1968	2006	39	2.74 (2005)	3189	56	–0.120	+0.180	–0.137
SU	Leviy Aktru	794	50.08	87.72	1977	2006	30	5.95 (2000)	3160	61	–0.090	–0.011	–0.310
SU	Maliy Aktru	795	50.08	87.75	1962	2006	45	2.73 (2000)	3152	70	+0.002	+0.067	–0.269
SU	No. 125 (Vodopadniy)	780	50.10	87.70	1977	2006	30	0.75 (2000)	3203	68	–0.074	+0.020	–0.246
US	Gulkana	90	63.25	–145.42	1966	2005	40	n.a.	1727	63	–0.157	–0.540	–0.880
US	South Cascade	205	48.37	–121.05	1953	2006	53	1.89 (2003)	1899	53	–0.592	–1.150	–0.695
US	Wolverine	94	60.40	–148.92	1966	2004	39	17.24 (1995)	1151	63	+0.525	–0.498	–0.884
	Mean of 30 glaciers		**51.58**	**1.66**	**1962**	**2006**	**45**	**7.25 (2003)**	**2288**	**58**	**–0.138**	**–0.254**	**–0.578**

* Recent comparisons with geodetically derived volume changes have shown that the mass-balance measurements of Silvretta have been systematically too positive by several decimetres w.e. per year (Huss and others, 2008a).